BRITISH COLUMBIA

Ministry of Energy and Mines
Energy and Minerals Division
Geological Survey Branch

GEOLOGICAL FIELDWORK 1999

A Summary of Field Activities and Current Research

PAPER 2000-1

Energy and Minerals Division
Geological Survey Branch

Parts of this publication may be quoted or reproduced if credit is given. The following is the recommended format for referencing individual works contained in this publication:

MacIntyre, D.G. and Struik, L.C. (2000): Nechako NATMAP Project, Central British Columbia - 1999 Overview; *in* Geological Fieldwork 1999, *B.C. Ministry of Energy and Mines*, Paper 2000-1, p. 7-13.

British Columbia Cataloguing in Publication Data
Main entry under title:
Geological Fieldwork: - 1974 -

Annual.
Issuing body varies
Vols. For 1978-1996 issued in series: Paper / British Columbia. Ministry of Energy, Mines and Petroleum Resources; vols for 1997- 1998, Paper / British Columbia. Ministry of Employment and Investment; vols for 1999- , Paper / British Columbia Ministry of Energy and Mines.

Includes Bibliographical references.
ISSN 0381-243X=Geological Fieldwork

1. Geology - British Columbia - Periodicals. 2. Mines and mineral resources - British Columbia - Periodicals. 3. Geology - Fieldwork - Periodicals. 4. Geology, Economic - British Columbia - Periodicals. 5. British Columbia. Geological Survey Branch - Periodicals. I. British Columbia. Geological Division. II. British Columbia. Geological Survey Branch. III. British Columbia. Geological Survey Branch. IV. British Columbia. Dept. of Mines and Petroleum Resources. V. British Columbia. Ministry of Energy, Mines and Petroleum Resources. VI. British Columbia. Ministry of Employment and Investment. VII. British Columbia Ministry of Energy and Mines. VIII. Series: Paper (British Columbia. Ministry of Energy, Mines and Petroleum Resources). IX. Series: Paper (British Columbia. Ministry of Employment and Investment). X. Series: Paper (British Columbia Ministry of Energy and Mines).

QE187.46 622.1'09711 C76-083084-3 (Rev.)

VICTORIA
BRITISH COLUMBIA
CANADA

JANUARY 2000

FOREWORD

This is the twenty-fifth edition of Geological Fieldwork: A Summary of Fieldwork and Current Research. An annual publication, it contains reports summarizing results from B.C. Geological Survey (GSB) projects completed throughout the province during the past year. As well, there are several contributions by associated researchers from the Mines Branch, University of Victoria and The University of British Columbia.

The contents of this volume reflect the emphasis of the Geological Survey Branch's field surveys. Highlights include:

- Initiation of the Ancient Pacific Margin NATMAP project, a joint venture with the Geological Survey of Canada, universities and industry. Bedrock mapping, surficial mapping and geochemical programs demonstrate that favourable Yukon-Tanana stratigraphy, with potential for volcanogenic massive sulphides, extends from the Yukon into British Columbia. Mineral deposit studies in comparable rocks in central British Columbia were also completed.
- Studies started in the southern part of the province used geology and geochemistry to identify regions having potential for plutonic-related gold deposits, such as Pogo and Fort Knox.
- Another new project was started in the Ecstall Belt within the Coast Plutonic Complex with the objective of more clearly identifying the controls on VMS mineralization.
- An innovative provincial assessment to identify potential copper and gold-rich iron oxide deposits in British Columbia, such as Candelaria and Olympic Dam, was conducted.
- Continuing coal quality and washability studies help to understand the nature of coal deposits, the province's most valuable commodity in 1999.
- Gemstone potential within the province continues to be evaluated.
- Mineral occurrences were examined and key areas in the Coast Ranges and Queen Charlotte Islands were covered with regional geochemical sampling programs as a contribution to Land and Resource Management Plans..
- Geologic mapping in the Mt. McCusker-Robb Lake area was completed as part of the GSB commitment to the Foreland Belt NATMAP project.

The GSB continues to work on upgrading provincial geoscience databases, including those for mineral occurrences (MINFILE), assessment report files (ARIS) and regional geochemical samples (RGS). Access to these databases improves with continual revisions and enhancements to the Ministry's internet site.

The Terrain Stability and Soils projects, funded by Forest Renewal BC, continued during 1999. The B.C. Geological Survey Branch audits digital terrain data submitted by forest companies in compliance with the Forest Practices Code and makes this data available over the internet. Terrain and soil maps are increasingly being used in mineral exploration, for example as an aid in interpreting geochemical surveys. These products are also valuable for land-use planning.

Our thanks to all the authors whose professional skills in the field and office make this publication possible. The articles have been edited and improved due to feedback from their colleagues and GSB managers. Special thanks go to Janet Holland and Brian Grant, the Branch's publications staff, who have worked long hours to meet difficult deadlines.

W.R. Smyth
Chief Geologist
B.C. Geological Survey

TABLE OF CONTENTS

MAPPING

D.G. MacIntyre and L.C. Struik: Nechako NATMAP Project, Central British Columbia - 1999 Overview 7

J. Nelson: Ancient Pacific Margin Part I: BCGS Contributions and Collaborative Activities with GSC and Yukon Geology Program 15

J.L. Nelson, M.G. Mihalynuk, D.C. Murphy, M. Colpron, C.F. Roots, J.K. Mortensen and R.M. Friedman: Ancient Pacific Margin Part II: A Preliminary Comparison of Potential VMS-hosting Successions of the Yukon Tanana Terrane, from Finlayson Lake District to Northern British Columbia 19

M.G. Mihalynuk, J.L. Nelson, C.F. Roots, R.M. Friedman and M. de Keijzer: Ancient Pacific Margin Part III: Regional Geology and Mineralization of the Big Salmon Complex 27

A. Dixon-Warren and A. Hickin: Ancient Pacific Margin Part IV: Surficial Mapping and Till Geochemistry in the Swift River Area, Northwestern British Columbia. 47

S.J. Cook and H.E. Pass: Ancient Pacific Margin Part V: Preliminary Results of Geochemical Studies for VMS Deposits in the Big Salmon Complex, Northern British Columbia. 71

J. Nelson: Ancient Pacific Margin Part VI: Still Heading South: Potential VMS Hosts in the Eastern Dorsey Terrane, Jennings River. 107

F. Ferri: Devono-Mississippian Felsic Volcanism Along the Western Edge of the Cassiar Terrane, North-Central British Columbia 127

A.S. Legun: Geology of the Mount McCusker-Robb Lake Area, Northeastern British Columbia 147

S. Israel and L. Kennedy: Geology and Mineralization of the Tchaikazan River Area Southwestern British Columbia 157

L.N. Poznikoff, J.K. Mortensen, R.M. Friedman and J.E. Gabites: Geochronological and Lead Isotopic Constraints on the Age and Origin of the Laidman Gold Prospect, Central British Columbia 173

L.J. Marshall, J.K. Mortensen and J.E. Gabites: Lead Isotope Data From Epigenetic Sulphide Occurrences in the Purcell Supergroup, Southeastern British Columbia, and Implications for Exploration for Sediment-hosted Base Metal Deposits. 185

ECONOMIC GEOLOGY

J.M. Logan: Plutonic-related Gold-quartz Veins in Southern British Columbia. 193

M.S. Cathro and D.V. Lefebure: Several New Plutonic-related Gold, Bismuth and Tungsten Occurrences in Southern British Columbia 207

R. Lett and W. Jackaman: Geochemical Exploration Techniques for Plutonic-related Gold Deposits in Southern B.C. 225

D.J. Alldrick: Exploration Significance of the Iskut River Fault. 237

D.J. Alldrick and C.S. Gallagher: Geology and Mineral Potential of the Ecstall VMS Belt 249

G.E. Ray and D.V. Lefebure: A Synopsis of Iron Oxide±Cu±Au±P±REE Deposits of the Candelaria- Kiruna-Olympic Dam Family 267

G.E. Ray and I.C.L. Webster: The Heff Prospect at Heffley Lake, South-Central B.C. : An Unusual Example of a Mafic-ultramafic-related Cu-Au-REE-Bearing Magnetite Skarn . . . 273

S.L. Bailey, S. Paradis, S.T. Johnston, and T. Höy: Geologic Setting of the Devonian-Mississippian, Rea and Samatosum VMS Deposits of the Eagle Bay Assemblage, Adams Lake Area, South Central British Columbia. 287

T.P. Gleeson, R.M. Friedman and K.Wahl: Stratigraphy, Structure, Geochronology and Provenance of the Logjam Area, Northwestern British Columbia 297

T. Höy, W.R. Smyth and R.E. Lett: Bull River Copper-Silver-Gold Prospect, Purcell Supergroup, Southeastern British Columbia 307

W. Jackaman, S. Cook and R. Lett: B.C. Regional Geochemical Survey: 1999 Field Programs. . . 315

R.H. Pinsent: Mineral Potential of the Northern Coast Belt, Khutze River Area, British Columbia 319

R.H. Pinsent: Mineral Potential of the Southern Coast Belt, Cape Caution Area, British Columbia 325

R.H. Pinsent: Mineral Potential of the Bella Coola Area, Coast Mountains, British Columbia 333

INDUSTRIAL MINERALS AND COAL

G.J. Simandl, C.P. Riveros and P. Schiarizza: Nephrite (Jade) Deposits, Mount Ogden Area, Central British Columbia. 339

G.J.Simandl, D. Marshall and J. Laird: Gem-quality Cordierite Deposits, Slocan Valley, British Columbia 349

B. Ryan and M.Takkinen: In Situ Fracture Porosity and Specific Gravity of Highly Sheared Coals from Southeast British Columbia 359

B. Ryan : A Note on Difficult to Wash Coals from South East British Columbia 373

Nechako NATMAP Project, Central British Columbia - 1999 Overview

D.G. MacIntyre[1] and L.C. Struik[2]

KEYWORDS: *Nechako Natmap, maps, chemistry, mercury, fossils, plutons, geophysics, Quaternary, ice-flow, CD-ROM, isotopes, petrography, terrane, tectonics.*

INTRODUCTION

The Nechako NATMAP project is a joint mapping venture between the Geological Survey of Canada (GSC) and the British Columbia Geological Survey Branch (BCGSB). This was the fifth and final year of the project which encompasses more than 30 000 square kilometres in central British Columbia (Figure 1). The primary objective of the project has been to improve the quality and detail of bedrock and surficial maps to help resolve several geological problems. In particular it addresses the following questions: 1) the extent and nature of Tertiary crustal extension, 2) Mesozoic compression and the manner of accretion of exotic terranes, 3) the geological and geophysical definition of the terranes, 4) the sequence of changing Pleistocene glacial ice flow directions, and 5) the character and dispersion of glacial deposits.

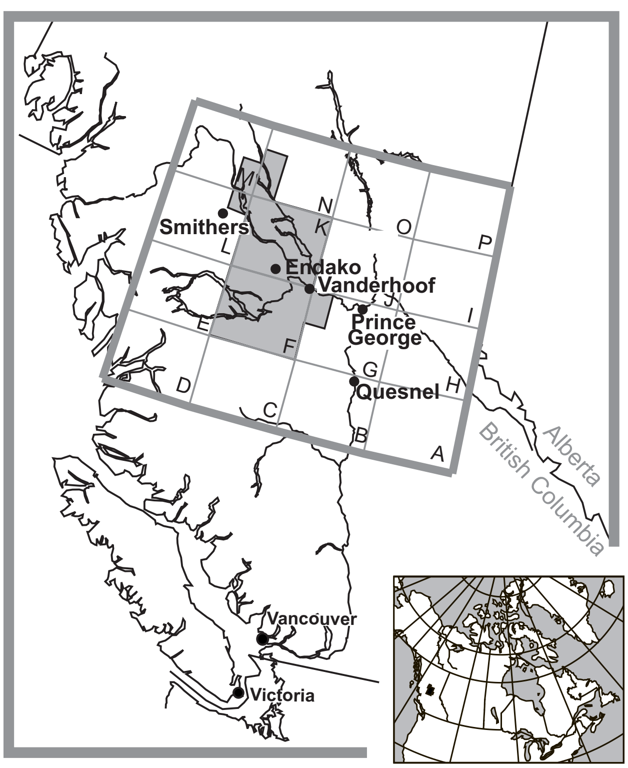

Figure 1. Location of the Nechako NATMAP Project in central British Columbia, as displayed on the Parsnip River NTS map area (93).

This final year of the Nechako NATMAP project was used to research information collected in the field and laboratory, to compile and document the study results through various publications, and to present ideas on the geology at various conferences. In addition we have enhanced our website to include more output from the project including complete published articles, viewable maps and photographic images. The website address is http://www.em.gov.bc.ca/natmap/

As this is the last year of the project and essentially no fieldwork was done, efforts have gone into producing open file and final maps, articles for refereed journals, government bulletins and conference presentations. This article reviews the upcoming products and provides a directory of new and future sources of information on project results.

PROJECT OUTPUT (1999-2000)

Maps

Bedrock, surficial, combined bedrock and surficial, biogeochemistry, and geophysical maps are being completed and will be released as colour open file maps (Figure 2). Drafting of these maps is being done mainly by Steve Williams and Nicky Hastings at the Vancouver office of the Geological Survey of Canada (GSC), Don MacIntyre and Paul Schiarizza at the British Columbia Geological Survey (BCGS), Carmel Lowe at the Pat Bay office of the GSC, and staff of the Geoscience Information Division of Earth Science Sector Ottawa

An annotated lithology map that addresses the relationship between geology and the natural environment has been released for the Fort Fraser map area (93K; Hastings *et al*., 1999). The map, Geoscape Fort Fraser, is 1:250 000 scale, has a pictorial legend and addresses issues such as material properties, molybdenum and mercury in the environment, impact of geology on fish habitat and the dispersion of glacial material.

Several bedrock geology maps have been, or will be, open filed this year. These are summarized in Table 1.

[1] *B.C. Geological Survey Branch*

[2] *Geological Survey of Canada, Vancouver B.C.*

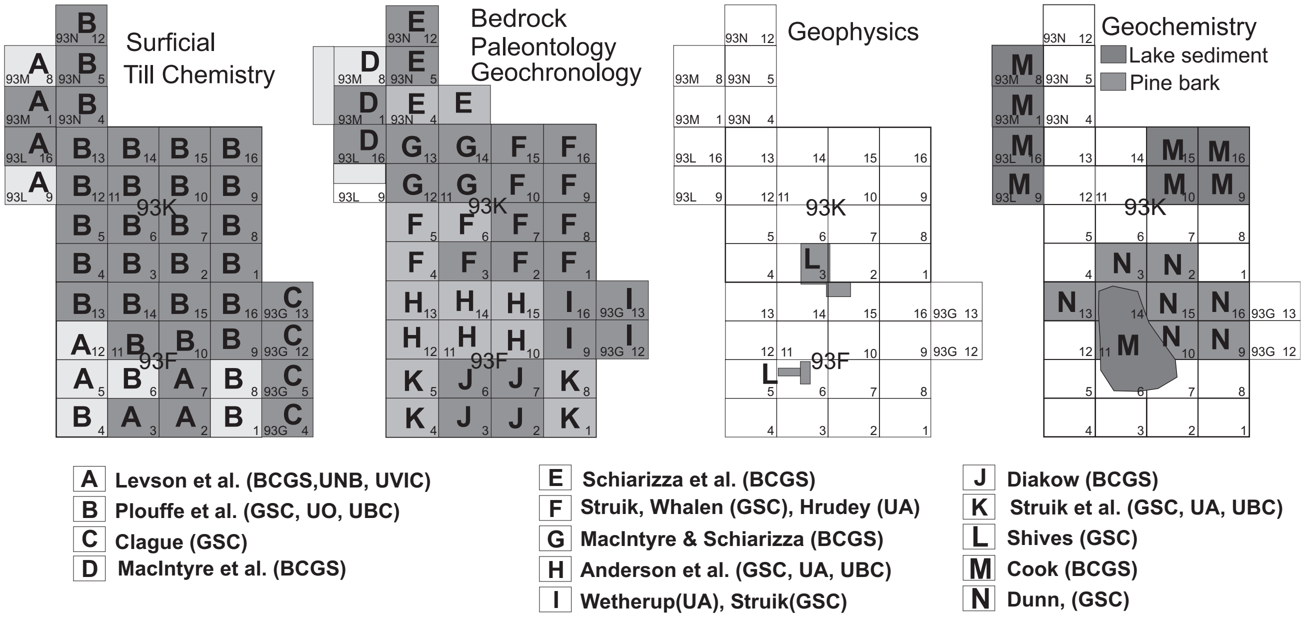

Figure 2. Status of Nechako NATMAP project mapping, displayed on an NTS 1:50 000 scale grid. Maps published as open files or final maps are shown in dark shades and areas mapped and yet to be published are in lighter shades. Unmapped areas are in white.

These maps are being supplemented with data tables that elaborate on fossil sites, isotopic age dates and mineral occurrence information (MINFILE database of the British Columbia Ministry of Energy and Mines). In some cases data tables of lithochemistry will also be included.

Surficial geology maps include that of the 1:50 000 scale Marilla map area (93F/12; Mate and Levson, 1999a), and the 1:100 000 scale Nechako River southeast map area (93F/1, 2, 7, 8; Plouffe and Levson, in prep.)

Maps of biogeochemical survey data have been made available for 2 more areas. The maps include a bedrock geology base of 1:250 000 scale derived from the most current complete compilation, and panels that contain from 6 to 9 maps, each showing the chemical concentrations of a particular element. Areas covered include Nechako River northeast map area (93F/9,10,15,16; Dunn and Hastings, in prep.), and Fort Fraser south-central (93K/2,3; Dunn and Hastings 1999).

Steve Cook (BCGS) is preparing a series of 1:100 000 geochemical compilation maps for the Babine porphyry belt, incorporating available stream sediment, lake sediment, lake water and till geochemical data for the area. Release is tentatively scheduled to coincide with the Minerals North annual meeting in the spring of year 2000.

A number of integrated geological and geophysical images are in preparation and are tentatively scheduled to

TABLE 1
BEDROCK GEOLOGY MAPS SCHEDULED FOR RELEASE IN 1999-2000

be released as open files. These include combined RADARSAT and Digital Elevation Model (DEM) images which provide useful information for analysis of ice flow directions and surficial structures (E. Grunsky, O. Niemann, C. Lowe and V. Levson); artificially-illuminated aeromagnetic base maps with bedrock lithology overlays (C. Lowe, L. Struik, and R. Kung) which provide insight on the shallow crustal structure; and artificially-illuminated aeromagnetic base maps with gravity overlays which emphasize deeper crustal structures (C. Lowe, L. Struik and R. Kung).

Articles

Several manuscripts deal with the economic geology of the region, particularly the Endako molybdenum camp (93K/3). The latter describe the hydrothermal alteration and fluid chemistry (Selby *et al*., 1999), the plutonic geochronology (Villeneuve *et al.,* in prep.) genesis of the Endako Batholith (Whalen *et al*., in prep.), molybdenum distribution in local lake sediments (Cook, in press), and structure of the Endako mine area and batholith using paleomagnetic and aeromagnetic data (Lowe *et al.*, in prep). Work continues on dating molybdenite from the Endako mine and surrounding François Lake Plutonic Suite using the Re-Os technique (D. Selby, personal communication, 1999).

A final report on the Babine Porphyry copper belt (93L/9, 16; 93M/1, 8) will focus on new geochronologic dating and tectonic evolution of the district in Late Cretaceous to Eocene time (MacIntyre *et al.* in prep). A separate article will discuss the economic potential for volcanogenic massive sulphide deposits associated with mid Cretaceous felsic volcanic centers that were identified by geochronologic dating done as part of the Babine project (MacIntyre *et al*., in prep.)

Studies of the chemical patterns within the Pinchi mercury belt (93K/8, 9, 14) have documented the distribution of mercury concentrations in lake sediments (Cook and Jackaman, in prep.) and till (Plouffe, 1999). As well, manuscripts describing the evolution of the Eocene felsic volcanic rocks and associated plutons (Grainger *et al*., in prep.), mafic volcanic rocks of the Endako Group (Anderson *et al.*, in prep.) and Neogene nodule-bearing alkaline basaltic intrusive and volcanic rocks (Resnick *et al*., in prep.) are expected. Lowe *et al.* (in prep.) assess the utility of airborne radiometric data for bedrock and surficial mapping and molybdenum exploration over the Capoose (93F/6) and Endako (93F/15; 93K/2, 3, 4, 5, 6, 7) batholiths.

A summary paleontology article for the Canadian Journal of Earth Science (CJES) is underway as a prelude to a thoroughly documented and fully illustrated GSC Bulletin (M. Orchard, F. Cordey, L. Rui, W. Bamber).

The Quaternary geology of the northern sector of the Nechako River map sheet (93F) is currently being documented (Plouffe, in prep.).

Presentations

Participants of the Nechako NATMAP project presented results of their mapping and research at several conferences and workshops throughout the year (Table 2). Project results will continue to be highlighted in the coming year. In particular, a symposium on the Nechako NATMAP project will be hosted at the Geological Society of America Cordilleran Section meeting to be held in Vancouver, April 27-29, 2000. The symposium is expected to consist of approximately 20 talks and a range of posters on the geological history and in part its metallogenic significance. Papers from the symposium are planned to be compiled and to appear as a special volume of the CJES to be released early in the year 2001.

TABLE 2
PRESENTATIONS MADE AT VARIOUS CONFERENCES APRIL TO OCTOBER 1999

CONFERENCE OR WORKSHOP	PRESENTATION	REFERENCES
19th International Geochemical Exploration Symposium (Vancouver, 04/99)	Talks, posters	Cook, S. (in press); Levson *et al*., 1999b, c; Plouffe, 1999b; Plouffe and Hall, 1999b
Geological Association of Canada Annual Meeting (Sudbury, 05/99)	Talks, posters	Levson *et al*., 1999d; Mate and Levson, 1999b
22nd General Assembly of the International Union of Geodesy and Geophysics	Poster	Anderson, 1999
Canadian Quaternary Association Biannual Meeting (Calgary, 08/99)	Talks, poster	Levson *et al*., 1999e; Mate and Levson, 1999c, d; Plouffe, 1999a; Plouffe and Hall, 1999a
15th Annual International Congress on the Carboniferous-Permian (Calgary, 08/99)	Talks, posters	Orchard *et al*., 1999b
9th International Terrane Conference (Vernon, 09/10/99)	Talks, posters, fieldtrip	Anderson *et al*., 1999b; Lapierre *et al*., 1999; Struik *et al*., 1999a, b

Computer Products

CD-ROM

A CD-ROM product will be used to highlight the geochemical data collected through the Nechako NATMAP project area. All lake, till, biochemical, and MINFILE data have been compiled for the project area. Some of the lithochemical data has also been gathered. Geology base maps for the CD will be at 1:250 000 scale.

Surficial geological maps, reports, and till geochemistry for the Fort Fraser (93K) and Manson River (93N) areas are being compiled onto CD-ROM for interactive use with computers (Plouffe, A. and Williams, S.P., in prep.) The GIS product will include a Windows compatible map and data viewer; the reports are compiled in web browser format.

Internet

Nechako NATMAP project hosts a web site that contains project information and scientific results. The web site was revised this year, and new material and categories of material have been added. The site now hosts scientific reports, project area photographs, some internet viewable maps and updated lists of references to publications derived from the project (Williams and MacIntyre, 1999). The material on the project web site will be transferred to the CORDLink website when all the work on the project is over.

ON-GOING RESEARCH

Several avenues of research are being pursued in the final stages of the project. Each of these is intended to constrain interpretations of the field mapping and to understand the genesis and evolution of the various rock suites. The research includes isotopic chemistry and age dating, combined chemical and petrographic studies, fossil determinations, structural analysis, and ice flow and aquifer characterization.

Isotopic, Chemical and Petrographic Characterization

Several isotopic studies in Nd, Sr, Pb and O concentrations are being used to understand the genesis and sources of the Permian through Eocene magmatic suites (Lapierre *et al.*, 1999; R. Anderson, personal communication 1999; N. Grainger, personal communication,1999). Age dating of these and other plutonic and volcanic suites continues to be used to constrain some of the more apparent critical events (N. Grainger and M. Villeneuve).

Petrographic characterization of the minerals in the Eocene Endako Group (primary and amygdaloidal) has been completed (Barnes and Anderson, 1999).

A detailed study of Eocene volcanic rocks within the Fort Fraser and Nechako River map areas by Nancy Grainger (University of Alberta), has included 4 U-Pb and 7 Ar/Ar ages of units within the Ootsa Lake Group, 25 geochemical analyses, 28 Sm/Nd and Rb/Sr analyses of the Newman volcanics, and Endako and Ootsa Lake groups. An accompanying study of the Oligocene and Miocene volcanic rocks includes 4 Ar/Ar age determinations and Sr and Nd isotopic analyses of basalts and lherzolite xenoliths from three different volcanic centers. Those analyses complement extensive geochemical characterization of the suite and permit comparisons with apparently co-magmatic suites farther south (Resnick, 1999). Ar/Ar and geochemical analytical work was completed at the Geological Survey of Canada (Ottawa) and all other isotopic work was completed at the Radiogenic Isotopic Facility at the University of Alberta. Preliminary data was presented at the Cordilleran Tectonics Workshop (Grainger and Anderson, 1999) and complete data is reported in an unpublished thesis (Grainger, 1999).

A suite of newly recognized Late Cretaceous plutons in southwestern Nechako River map area extends the known distribution of the commonly-mineralized Bulkley plutonic suite farther east than previously known (Billesberger *et al.*, 1999; Friedman *et al.,* 1999)

Paleontology

Subsequent to data published by Orchard *et al.* (1999), an additional 22 conodont microfaunas were recovered from samples collected by Hillary Taylor during the summer of 1998, 6 of them in conjunction with field crews of the BCGS. In addition, BCGS geologists collected samples that added 5 additional conodont faunas. The collections included faunas with Late Carboniferous, Permian and Triassic ages which were not known in this area prior to the Nechako project. Amongst these were Middle to Late Permian conodonts both from Mount Copley, and from recollections in the Leo Creek area. More evidence of both Permian and Triassic conodonts were found in the Necoslie River breccia, and well defined Tethyan fauna were collected from west of Stuart Lake. Well-preserved Late Triassic fauna were recovered from limestone along Pinchi Lake. BCGS collections included new Middle to Late Permian and Late Triassic sites from the south shore of Trembleur Lake.

Preparation of these samples and SEM photography of key elements of the conodont fauna was undertaken during the Spring and a summary of the data was presented at the International Congress on the Carboniferous-Permian, held in Calgary, August 17-21 (Orchard *et al.*, 1999).

Research, evaluation and documentation continues on the radiolaria (Fabrice Cordey), fusulinid (Lin Rui), and coral and brachiopod (Wayne Bamber) collections from the Cache Creek Group of the project area. All the fossil studies will be integrated into an evaluation of the Cache Creek Group paleontological character.

Terrane characterization

As part of research on the Sitlika assemblage of Cache Creek Terrane, Nick Massey and Paul Schiarizza (BCGS) have been interpreting the geochemistry of Sitlika volcanic and plutonic rocks and diabase dikes and gabbros from the adjacent Cache Creek ophiolitic section. Petrography of the sedimentary and volcanic successions is being used to assist in establishing the depositional environments and to differentiate and correlate these successions with those to the southeast.

Tectonics and Structure

Analysis of the structural history and geometry, in combination with the genesis of the various rock suites is being done to further constrain the tectonic evolution of the central Canadian Cordillera. Particular attention has been focussed on the transtensional and magmatic events of the early Eocene, and the Jurassic imbrication of the Quesnel, Cache Creek and Stikine terranes (R.G. Anderson, D.G. MacIntyre, P. Schiarizza, L.C. Struik). Interpretation of paleomagnetic and aeromagnetic data (R.J. Enkin, C. Lowe) are being used to test and constrain the Eocene transtensional model. Cretaceous compression and possibly extension is less well understood due to poor exposure.

Quaternary Geology

Studies of the glacial materials and incorporation of field and high resolution DEM information constraining ice-flow directions are being used to assist in drift prospecting techniques in central British Columbia (V. Levson and A. Plouffe), and to constrain the source areas and distribution of anomalously rich concentrations of cinnabar (A. Plouffe and G. Hall).

Quaternary geology studies conducted by the BCGS in 1999 included the analysis of till geochemical data for the Babine porphyry belt (93 M/1, 2, 7, 8, L/9,16) and the west-central part of the Nechako map area (93F/5, 12). Other work analyses Quaternary stratigraphic data and ongoing landslide hazard studies (*e.g.* Levson, 1999; Levson *et al.,* 1999a; Mate and Levson, 1999a; Stumpf and Broster, 1999a, b, in prep; Stumpf *et al*., in prep a, b).

Recent research has focused on landslide hazard studies including work towards a Ph.D. thesis by Don McClenagan and a M.Sc. thesis by Dave Mate. Both these theses will also contribute to regional Quaternary stratigraphic studies in central British Columbia.

A. Stumpf is completing an investigation of the Fraser Glaciation ice-flow history of west–central British Columbia (Stumpf and Broster, 1999a, b, in prep; Stumpf *et al*., in prep a). New interpretations suggest that during the maximum-phase of glaciation, glaciers moved westward to the Pacific Ocean, and eastward into Alberta from an ice divide/dome situated over the interior of the province. These ice-flow directions are discordant with earlier and later glacier movements; in some areas ice-flow directions shifted by up to 180 degrees). These results are significant, and have applications not only to drift exploration models/techniques, but also to our understanding of subglacial processes, dynamics of large ice sheets, paleoclimatic models, and isostatic tectonics.

D. Mate is currently investigating translational and rotational landslides along the shores of the Nechako Reservoir and banks of the Cheslatta River. Cross-sections compiled for rotational slides along the Cheslatta River show slumps up to 230 m wide and about 25 m high with main scarps as much as 6 m high. The slumps are active and characterized by amphitheatre-shaped main scarps, backward-tilted slump blocks, earthflows, small sag ponds, and slickensided basal slip surfaces in glaciolacustrine sediments (Mate and Levson, 1999d). These slides have been locally reactivated subsequent to logging and road construction (Levson *et al.*, 1999).

Surficial geological mapping of the Marilla map sheet (93F/12) is nearly completed. Compilation of one of the most complete Quaternary sections in the region shows the presence of two exceptionally rare stratigraphic units interpreted as: 1) a till deposited during the penultimate glaciation and 2) nonglacial, organic bearing, lacustrine sediments of probable Middle Wisconsinan age (Mate and Levson, 1999a, b, c). Large-scale troughs oriented transverse to the regional ice flow direction are readily apparent on small scale DEM's and air photos and are associated with ice-parallel, streamlined ridges (crag-and-tail forms) (Mate and Levson, 1999a, c).

In the Fulton River map area, a large area of hummocky moraine and associated incised meltwater channels has been identified (Stumpf, in prep). From the distribution of ice-contact sediments, the orientation of channels, and paleocurrents directions (in some areas evidence of stream piracy and reversals in flow), suggest that an ice lobe stagnated in the central Babine Lake valley during deglaciation (Stumpf in prep.; Stumpf and Broster, in prep.). Also, numerous, sinuous cross-valley ridges identified in the Bulkley River valley, near Smithers are similar to crevasse-squeeze or "De Geer" type moraines, possibly formed during glacier readvance and surging, or massive ice sheet drawdown.

Ten days of fieldwork were completed by A. Plouffe and J. Mayberry in the vicinity of Pinchi and Bralorne-Takla mercury mines, as part of the GSC Metals in the environment initiative. Soils weathering profiles were sampled in detail in the vicinity of both mine sites, but also at sites removed from the mines where mercury concentrations are known to be naturally high and low in till.

A study of the Vanderhoof groundwater aquifer (Jennifer Mayberry of GSC Pacific in Vancouver) will determine the feasibility of making contributions to the understanding of aquifers from existing data sets derived from regional surficial and bedrock mapping and well drilling.

Collaborative research between Andrew Stumpf (UNB) and A.J.T Jull (University of Arizona) was undertaken to date carbonate concretions, sampled from proglacial glacial lake sediments in the Bulkley River valley. Using Accelerator Mass Spectrometry (AMS), ages of these concretions may provide a minimum date for glaciation in central British Columbia.

ACKNOWLEDGMENTS

We would like to thank our colleagues in the Nechako Project for their contribution to this report, and to the project. This project was primarily supported through the GSC NATMAP program, the British Columbia Geological Survey and 11 universities in 4 countries. It received generous scientific and logistical contributions from Placer Dome Ltd., Endako Mines and Cominco Ltd. In addition we developed fruitful scientific connections and joint studies with staff of the British Columbia Ministry of Forests, the British Columbia Environmental Research Institute, Alberta Geological Survey, and the Department of Fisheries and Oceans.

REFERENCES

Cook, S.J., Levson, V.M., Jackaman, W. and Law, D.T. (in prep.): Regional Geochemical Compilation: Babine Porphyry Belt (NTS 93L/9, 16; 93M/1, 2, 7, 8); *British Columbia Ministry of Energy and Mines*, Open File.

Cook, S.J. (in press): Distribution and Dispersion of Molybdenum in Lake Sediments Adjacent to Porphyry Molybdenum Deposits, Central British Columbia*; Journal of Geochemical Exploration*.

Cook, S.J. and Jackaman, W. (in prep.): Geological Controls on the Distribution of Mercury in Lake Sediments, Pinchi Lake Area, Central British Columbia; to be submitted to *Canadian Journal of Earth Sciences*

Dunn, C.and Hastings, N. (1999): Lodgepole pine bark chemistry of the Fraser Lake and Endako map areas, central British Columbia; *Geological Survey of Canada* Open File 3696(a, b, c, d).

Dunn, C. and Hastings, N. (in prep): Lodgepole pine chemistry, Nechako River northeast map area; *Geological Survey of Canada* Open File, 1:250 000 scale maps of 16 elements.

Grainger, N. and Anderson, R.G. (1999): Eocene Ootsa Lake Group volcanics in the northern Nechako River and southern Fort Fraser map sheets, central British Columbia. *in;* SNORCLE and Cordilleran Tectonics Workshop. Lithoprobe Report 69. F. Cook and P. Erdmer (eds). p.263.

Grainger, N. (1999): Geochronology and geochemistry of Middle Jurassic to Miocene igneous rocks within Nechako plateau, central British Columbia: Insight into the nature and origin of Eocene volcanism in central British Columbia. M.Sc. Thesis, *University of Alberta*, Edmonton, Alberta.

Hastings, N.L., Plouffe, A., Struik, L.C., Turner, R.J.W., Williams, S.P., Anderson, R.G., Clague, J.J., Kung, R., and Taccogna, G. (1999): Geoscape, Fort Fraser, central British Columbia; *Geological Survey of Canada*, Miscellaneous Report, 1:250 000 scale map.

Lapierre, H., Tardy, M., Bosch, D., and Struik, L.C. (1999): Is the Cache Creek terrane in southern-central British Columbia (Canada) a remnant of a near-ridge Late Triassic oceanic plateau?; *in* Abstracts and Program of Terran Paths 99 Circum-Pacific Terrane Conference, C.A. Evenchick, G.J. Woodsworth and R. Jongens (eds), *Geological Association of Canada*, Cordilleran Section, Vancouver, British Columbia, p. 46-50.

Levson, V.M. (1999): Till geochemistry and Sampling Techniques in the Canadian Cordillera: *in* Drift Exploration in Glaciated Terrain. 19th International Geochemical Exploration Symposium, Short Course Notes, pages 95-116.

Levson, V.M., Mate, D.J., and Stuart, A.J. (1999a): Quaternary geology and drift prospecting studies in the north central Nechako Plateau (93 F and K): in Geological Fieldwork 1998, *British Columbia Ministry of Energy and Mines*, Paper 1999-1, pages 15-23.

Levson, V.M. Stumpf, A. and Broster, B. (1999b): The influence of glacial flow reversals on geochemical dispersal in the central Canadian Cordillera: 19th International Geochemical Exploration Symposium, *Association of Exploration Geochemists*, W.K. Fletcher and I.L. Elliott, Editors, Symposium Program and Abstracts Volume, pages 32-33.

Levson, V.M., Plouffe, A. Stumpf, A.J., and Cook, S. (1999c): Pleistocene ice flow patterns and dispersal processes in central Stikinia: tools for mineral discovery in till covered areas; 16th Annual Cordilleran Geology and Exploration Roundup*, British Columbia and Yukon Chamber of Mines*, Abstracts volume, pages 4-5.

Levson, V.M., Cook, S.J., Lett, R. and Jackaman, W. (1999d): Geochemical Mapping in the Canadian Cordillera: Recent Developments; *Geological Association of Canada-Mineralogical Association of Canada*, Joint Annual Meeting Program with Abstracts, Volume .

Levson, V.M., Blyth, H. and Seemann, M. (1999e): Slope Stability Mapping in the Canadian Cordillera: A Comparison of Coastal and Interior Systems; *Canadian Quaternary Association and Canadian Geomorphology Research Group*, Joint Annual Meeting, 1999, Calgary Alberta, Abstracts Volume, page 40.

Lowe, C., Enkin, R., Struik, L.C. and Dubois, J. (in prep.): Tertiary extension in the central British Columbia intermontane; magnetic and paleomagnetic constraints from the Endako region; to be submitted to the Canadian Journal of Earth Sciences.

MacIntyre, D.G. and Webster, I. (in prep.) Geology of the Babine Porphyry Belt, (93L/9,16; 93M/1,2,7,8), central British Columbia; *British Columbia Ministry of Energy and Mines*, Open File 2000-2, 1:100 000 scale map.

MacIntyre, D.G. and Schiarizza, P., 1999): Bedrock geology of the Cunnigham Lake map area (93K/11,12,13,14), central British Columbia; *British Columbia Ministry of Energy and Mines*, Open File 1999-11, 1:100 000 scale map.

MacIntyre, D., Villeneuve, M. and Tackaberry, D. (in prep.) Recently discovered mid Cretaceous Rocky Ridge felsic volcanic centers and associated VMS potential, Babine Lake area, Central B.C. to be submitted to the *Canadian Journal of Earth Sciences*.

Mate D. and Levson, V.M. (1999a): Quaternary geology of the Marilla map area (93F/12), British Columbia: in Geological Fieldwork 1998, *British Columbia Ministry of Energy and Mines*, Paper 1999-1, pages 25-32.

Mate D. and Levson, V.M. (1999b): Quaternary Geology of the Marilla Map Sheet, Central, British Columbia; *Geological Association of Canada- Mineralogical Association of Canada*, Joint Annual Meeting Program with Abstracts Volume.

Mate D. and Levson, V.M. (1999c): Quaternary Stratigraphy and Subglacial Landform Studies in Central British Columbia; *Canadian Quaternary Association and Canadian Geomorphology Research Group*, Joint Annual Meeting, 1999, Calgary Alberta, Abstracts Volume, pages 48-49.

Mate D. and Levson, V.M. (1999d): Landslides in Pleistocene Sediments: Examples from the Interior Plateau, British Columbia; *Canadian Quaternary Association and Canadian Geomorphology Research Group*, Joint Annual Meeting, 1999, Calgary Alberta, Abstracts Volume, page 49.

Orchard, M.J., Struik, L.C. and Taylor, H. (1999): Upper Carboniferous-Triassic conodont faunas from the Cache Creek Complex, Nechako Region, Central British Columbia; 15th International Congress on the Carboniferous-Permian, Calgary, Alberta, August 17-21, 1999; Programme with Abstracts, p. 107.

Plouffe, A. (1999a): Deglaciation of central British Columbia with emphasis on the evolution of glacial lakes; *Canadian Quaternary Association and Canadian Geomorphology Research Group*, Joint Annual Meeting, 1999, Calgary Alberta, Abstracts Volume, p. 56.

Plouffe, A. (1999b): Glacial transport and physical partitioning of mercury and gold in till, central British Columbia; in Drift Exploration in Glaciated Terrain. 19th International Geochemical Exploration Symposium, Short Course Notes, p. 329-352.

Plouffe, A. (in press a): Surficial geology, Fort Fraser, British Columbia; *Geological Survey of Canada*, A-series, map scale 1:250 000.

Plouffe, A. (in press b): Surficial Geology, Manson River, British Columbia; *Geological Survey of Canada*, A-series, map scale 1:250 000.

Plouffe, A. (in prep.): Quaternary geology of the northern sector of Nechako River map sheet (93 F), central British Columbia. To be submitted to the *Canadian Journal of Earth Sciences*.

Plouffe, A. and Hall, G.E.M. (1999a): Glacial transport versus anthropogenic signature in the vicinity of a past producing mercury mine, central British Columbia*; Canadian Quaternary Association and Canadian Geomorphology Research Group*, Joint Annual Meeting, 1999, Calgary Alberta, Abstracts Volume, p. 57.

Plouffe, A. and Hall, G.E.M. (1999b): Mercury in humus, B-horizon, and glacial sediments in the vicinity of two past producing mercury mines, British Columbia, Canada; 19th International Geochemical Exploration Symposium, *Association of Exploration Geochemists*, W.K. Fletcher and I.L. Elliott, Editors, Symposium Program and Abstracts Volume, p. 43-44.

Plouffe, A. and Levson, V.M. (in prep.) a: Surficial geology, Euchiniko River, British Columbia (93F/SE); *Geological Survey of Canada*, Open File, 1:100 000 scale map.

Plouffe, A. and Levson, V.M. (in prep.) b: Surficial geology, Entiako Lake, British Columbia (93F/SW); *Geological Survey of Canada*, Open File, 1:100 000 scale map.

Plouffe, A, and Williams, S.P. (in prep.): Quaternary geology, Fort Frase and Manson River map areas, central British Columbia; *Geological Survey of Canada*, Open File, CD-ROM.

Schiarizza, P. (in prep.): Geology, Manson River map area (93N), central British Columbia; *British Columbia Ministry of Energy and Mines*, Open File, and *Geological Survey of Canada* Open File, 1:250 000 scale map.

Schiarizza, P., Massey, N. and MacIntyre, D.G. (in prep.) Bedrock geology, Tsayta Lake map area (93N/SW); *British Columbia Ministry of Energy and Mines* Open File 1999-15, 1:100 000 scale map.

Schiarizza, P. and Payie, G. (in prep.) Bedrock geology, Old Hogem map area (93N/NW); *British Columbia Ministry of Energy and Mines* Open File, 1:100 000 scale map.

Selby, D., Nesbitt, B. E., Muehlenbachs, K. and Prochaska, W., 1999): Hydrothermal Alteration and Fluid Chemistry the Endako Porphyry Molybdenum System, British Columbia: *Economic Geology*, In press (August 1999).

Struik, L.C., Anderson, R.G., Woodsworth, G., MacIntyre, D.G., Gareau, S., and Haggart, J.W. (1999): Terranes and accretion along a central British Columbia transect; Field trip guidebook, 9th Intherantional Terrane Conference, Vernon, British Columbia; Geological Association of Canada Cordilleran Section, Vancouver, British Columbia, 93p.

Struik, L.C, Whallen, J.B., Fallas, K., Hrudey, M., Huscroft, C., and Quat M. (in prep.) Bedrock geology, Burns Lake map area, central British Columbia; *Geological Survey of Canada*, Open File, 1:100 000 scale map.

Struik, L.C., Anderson, R.G., and Diakow, L. (in prep.); Geology, Euchiniko River map area, central British Columbia; *Geological Survey of Canada*, Open File, 1:100 000 scale map.

Struik, L.C., Diakow, L. and Quat, M. (in prep.) Geology; Cheslaslie River map area; *Geological Survey of Canada*, Open File, 1:100 000 scale map.

Struik, L.C., Whalen, J.B., MacIntyre, D.G., Schiarizza, P., Fallas, K., Hrudey, M., Huscroft, C. and Quat, M. (in prep.) Bedrock geology, Fort Fraser map area; *Geological Survey of Canada*, Open File, 1:250 000 scale map.

Stumpf, A.J., (in prep): Surficial geology, Fulton River map area (93 L/NE), British Columbia. *Geological Survey of Canada*, Open File, 1:100 000 scale map.

Stumpf, A.J. and Broster, B.E. in prep: Surficial geology and glacial history of the Fulton River quadrangle (93L/NE), west–central British Columbia; CJES Special Collection, Jan. 2001.

Stumpf, A.J., Broster, B.E., and Levson, V.M. (in prep. a): Multi-phase flow of the Late Wisconsinan Cordilleran Ice Sheet in western Canada; paper submitted to *Geological Society of America Bulletin*

Stumpf, A., Levson, V.M. and Broster, B., and Huntley, D.H.. (in prep b): Late Quaternary stratigraphy and history of the Babine Lake and Bulkley River watersheds, central British Columbia, Canada; paper submitted to *Geographie Physique et Quaternaire*.

Stumpf, A.J. and Broster, B.E. 1999a. Upslope flow and reversals during growth of the Cordilleran Ice Sheet, British Columbia, Canada; *Geological Society of America* (GSA), Annual Meeting and Exposition, Denver, Colorado, USA, October 1999.

Stumpf, A.J. and Broster, B.E. 1999b. Cordilleran ice streaming from north–central interior British Columbia and outlets through the Coast and Rocky mountains; Program with abstracts, 9th Biennial Meeting of the Canadian Quaternary Association, *University of Calgary,* Calgary, AB., August, 1999, p. 76–77.

Stumpf, A., Levson, V.M. and Broster, B. (in prep.): Quaternary Stratigraphy, Glacial Lake History, and Paleogeomorphology of the Babine Lake and Bulkley River Areas, Central British Columbia, Canada; paper submitted to *Geographie Physique et Quaternaire*.

Villeneuve, M., Whalen, J., Anderson, R.G. and Struik, L.C. (in prep.): Episodes of magmatism proximal to Endako porphyry molybdenum mine, north-central British Columbia.

Williams, S.P. and MacIntyre, D.G. (1999): Nechako NATMAP Project web site; http://www.em.gov.bc.ca/natmap; Hosted by the *British Columbia Ministry of Energy and Mines*.

Ancient Pacific Margin Part I: BCGS Contributions and Collaborative Activities with GSC and Yukon Geology Program

By JoAnne Nelson

INTRODUCTION

The Ancient Pacific Margin NATMAP project (Thompson *et al*., 2000) is a collaboration between the British Columbia Geological Survey Branch, the Geological Survey of Canada and the Yukon Geoscience Office. It aims to advance understanding of the Cordillera-long belt of complexly deformed pericratonic rocks that made up the Pacific margin of North America in Paleozoic to early Mesozoic time (Figure 1). This is the first operational year of the joint project.

Beginning in 1994, discoveries of volcanic-associated massive sulphide deposits in the Yukon-Tanana Terrane near Finlayson Lake, Yukon created significant exploration interest in the pericratonic terranes. These deposits, Kudz Ze Kayah, Wolverine, and Fyre Lake, along with Wolf in the nearby Cassiar Terrane, form a mineral camp of previously unsuspected importance (Hunt, 1997, 1998). Provincial and territorial surveys responded to these developments by commencing mapping in the Finlayson Lake belt (Murphy and Timmerman 1997; Figure 1), and by examining possible extensions of favorable stratigraphy along strike in the Yukon (Glenlyon area; Colpron, 1999; Figure 1) and south of the B.C. border (Nelson 1997; Nelson *et al.,* 1998; Mihalynuk *et al.,* 1998; Figure 1). During this time, the Geological Survey of Canada was revising the geology of the Vernon map sheet, which lies within the pericratonic belt of southern B.C., near the Eagle Bay Assemblage with its volcanogenic massive sulphide deposits - Rea Gold, Homestake, and Samatosum (Thompson and Daughtry, 1998).

These physically disparate projects share a conceptual basis: the analysis of the complex and poorly understood assemblages that once represented the active margin of North America. These assemblages include remnants of arcs and marginal basins with the potential to host syngenetic massive sulphide deposits. The Ancient Pacific Margin Project, designed in 1998 and approved in 1999, brings together ongoing work in the pericratonic belt by all three organizations, as well as adding major new initiatives. Geological Survey of Canada contributions to the Ancient Pacific Margin Project are divided geographically into three components, Southern, Central and Northern, along with a belt-long metallogenetic study (Thompson *et al.,* 2000; Figure 1).

BRANCH CONTRIBUTIONS TO THE ANCIENT PACIFIC MARGIN PROJECT

The Central Component included four BCGS contributions in 1999 (Figure 1): geological mapping of the Big Salmon Complex in northern Jennings River map area (Mihalynuk *et al.,* this volume), glacial mapping of the same area (Dixon-Warren and Hickin, this volume), geochemical studies (Cook and Pass, this volume), and geological mapping in the southeastern Dorsey Terrane in south-central Jennings River map area (Nelson, this volume).

Other BCGS contributions to the study of the pericratonic belts and their mineral potential include both regional mapping and detailed deposit studies (Figure 1). Trygve Höy collaborated in 1999 with Suzanne Paradis of the Geological Survey of Canada and others, in continuing analysis of the metallogeny of the Kootenay terrane in southern British Columbia. He coauthored a joint paper on the setting of the Rea-Homestake volcanogenic massive sulphide deposits in the Eagle Bay assemblage (Bailey *et al.,* 2000). His current work focusses on the potential for Broken Hill-type and related massive sulphide deposits in the southern Kootenay Terrane (Höy, 1987).

Fil Ferri investigated extensive rhyolites within the Earn Group in the westernmost Cassiar Terrane of north-central British Columbia (Figure 1; Ferri, this volume). The presence of felsic volcanics interbedded with Mississippian clastic rocks is geologically analogous to the setting of volcanogenic mineralization on Atna Resources' Wolf property in the Pelly Mountains, Yukon (Holbeck and Wilson 1998), except that the volcanic suite there is alkalic.

The Ecstall volcanogenic massive sulphide belt, located in the Coast Mountains near Prince Rupert, is hosted by Devonian volcanic arc strata similar to pericratonic volcanosedimentary sequences of the Yukon-Tanana Terrane such as the Finlayson Lake belt and the Delta VMS district in the Alaska Range. This belt is the subject of a new, multi-year mapping and mineral deposit study led by Dani Alldrick (Figure 1; Alldrick and Gallagher, this volume).

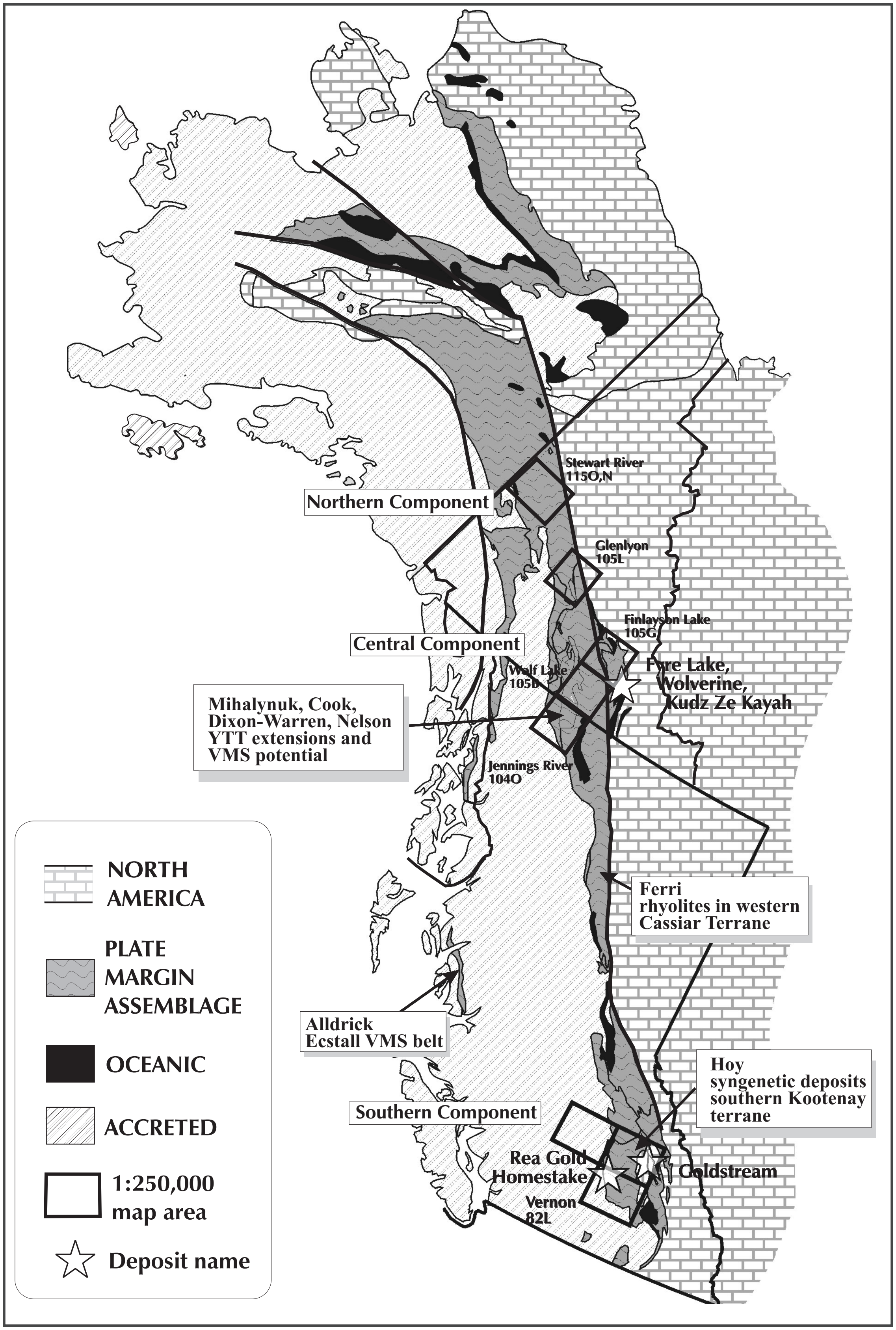

Figure 1. Location map of Ancient Pacific Margin project area.

BRANCH CONTRIBUTIONS TO THE WOLF-JENNINGS PROJECT (CENTRAL COMPONENT)

The largest BCGS contribution to the Ancient Pacific Margin project was to the Central Component in far northern British Columbia, with four interrelated field studies in 1999 (Figure 1). The impetus for this degree of attention comes from interesting discoveries made during recent BCGS mapping of the Big Salmon Complex in northwestern Jennings River map area. In 1997, Mihalynuk and coworkers traced out a metamorphosed silica-(manganese-iron) exhalative unit over 40 kilometres of strike length (Mihalynuk *et al.,* 1998). This unit, the crinkled chert, is regionally anomalous in barium and locally in base metals. In addition, a large pluton, the Hazel orthogneiss, was dated as Devono-Mississippian by U-Pb methods (362.3+7.9/-6.8 Ma, Mihalynuk *et al.,* this volume), and felsic tuffs were dated as late Mississippian **(**325.1±3.0 Ma , Mihalynuk *et al.,* this volume). These positive indicators of a Devono-Mississippian volcanogenic environment reinforced the perceived potential of the area based on extrapolation of known metallotects (Nelson, 1997).

In 1999, geological mapping of the Big Salmon Complex was completed (Mihalynuk *et al.,* this volume); this work resulted in significant increase of the known strike extent of the crinkled chert, and the discovery of several new showings and areas of quartz-sericite schist. A complementary surficial project produced a map of the Big Salmon Complex in British Columbia (Dixon-Warren and Hickin, this volume). The surficial geology map can be used to identify unconsolidated units suitable for geochemical sampling, and as a guide for tracing geochemical anomalies to their bedrock sources. Multimedia geochemical studies focussed on the crinkled chert, RGS anomalies, and known sulphide occurrences, with some regional stream data (Cook and Pass, this volume; Dixon-Warren and Hickin, 2000a, this volume; Dixon-Warren and Hickin, 2000b). The geochemical case studies aim to highlight the potential for VMS mineralization in Yukon-Tanana correlative rocks of the Big Salmon Complex by characterizing the surficial geochemical responses of known VMS prospects and their felsic and mafic volcanic host rocks.

Extensions and possible correlatives of the Big Salmon Complex were the subject of a continuing regional bedrock mapping project in southern/central Jennings River area (Nelson, this volume; Figure 1). Late Mississippian felsic tuffs coeval with those in the Big Salmon Complex, and rocks similar to Big Salmon greenstones near the southern border of the Jennings River area, suggest that the potential Mississippian VMS environment extends well into British Columbia.

The 1999 BCGS program was integrated with a new GSC 1:250 000 mapping project in the Wolf Lake/Jennings River map area, which traced Big Salmon Complex stratigraphy along Hazel Ridge north of the Yukon border (Roots *et al.,* 2000; Figure 1). Continued mapping projects by Don Murphy and Maurice Colpron of the Yukon Geology Program in the Finlayson Lake and Glenlyon map areas in Yukon also form part of the Central Component (Figure 1). In the Finlayson project, Murphy and collaborators have covered the area of the Kudz Ze Kayah and Wolverine VMS properties, providing a preliminary stratigraphic template that is useful for workers in parts of the terrane where volcanogenic potential is less well known (Murphy and Piercey 1999, 2000). Colpron has mapped two areas in the Teslin Zone, the continuation of Yukon-Tanana Terrane southwest of the Tintina Fault (Colpron, 1999, Colpron and Reinecke, 2000).

Collaboration between participants in the Central Component of the Natmap project is already leading to a better understanding of the regional relationships. We are starting to see how stratigraphic sections from different parts of the pericratonic belt from Finlayson Lake to southern Jennings River map area may correlate (Nelson *et al.,* this volume). The geologic history of this region, albeit complex, is decipherable through systematic geological mapping supported by geochronological studies. This is good news for explorationists interested in pursuing the metallogenetic possibilities of the ancient continental margin.

REFERENCES

Alldrick, D.J. and Gallagher, C.S. (2000): Geology and mineral potential of the Ecstall Belt; *in* Geological Fieldwork 1999; *B.C. Ministry of Energy and Mines*, Geological Survey Branch, Paper 2000-1, this volume.

Bailey, S. L., Paradis, S., Johnston, S. T., and Höy, T. (2000): Geological setting of the Devonian-Mississippian Rea and Samatosum massive sulphide deposit, Eagle Bay assemblage, south-central British Columbia; *in* Geological Fieldwork 1999, *B.C. Ministry of Employment and Investment*, Geological Survey Branch, Paper 2000-1.

Colpron, M. (1999): Glenlyon Project: Preliminary stratigraphy and structure of Yukon-Tanana Terrane, Little Kalzas Lake area, central Yukon; *in* Yukon Exploration and Geology 1998; Exploration and Geological Services Division, *Indian and Northern Affairs Canada*, pages 63-72.

Colpron, M. and Reinecke, M. (2000): Glenlyon project: Coherent stratigraphic succession from Little Salmon Range (Yukon-Tanana terrane), and its potential for volcanic-hosted massive sulphide deposits, *in* Yukon Exploration and Geology 1999: Exploration and Geological Services Division, Yukon, *Indian and Northern Affairs Canada*, *in press*.

Cook, S.J. and Pass, H.E. (2000): Ancient Pacific Margin Part V: Preliminary results of geochemical studies for VMS depostis in the Big Salmon Complex, northern British Columbia (104N/9, 16; 104O/11, 12, 13, 14); *in* Geological Fieldwork 1999; *B.C. Ministry of Energy and Mines*, Geological Survey Branch, Paper 2000-1, this volume.

Dixon-Warren, A. and Hickin, A. (2000a): Ancient Pacific Margin Part IV: Surficial mapping and till geochemistry in the Swift River area, northwestern British Columbia; *in* Geological Fieldwork 1999; *B.C. Ministry of Energy and Mines*, Geological Survey Branch, Paper 2000-1, this volume.

Dixon-Warren, A. and Hickin, A. (2000b): Surficial geology of the Swift River area (104N/9, 16; 104O/NW), 1:100,000 scale; *B.C. Ministry of Energy and Mines*, Geological Survey Branch, Open File 2000-5.

Ferri, F. (2000): Devono-Mississippian felsic volcanism along the western edge of the Cassiar Terrane, north-central British Columbia (NTS 93N, 94C and 94D); *in* Geological Fieldwork 1999; *B.C. Ministry of Energy and Mines*, Geological Survey Branch, Paper 2000-1, this volume.

Holbeck, P.M. and Wilson, R.G. (1998): The Wolf discovery: a Kuroko-style volcanogenic massive sulphide deposit hosted by rift-related, alkaline felsic volcanic rocks; *in* Yukon Exploration and Geology 1997, Exploration and Geological Services Division, Yukon, *Indian and Northern Affairs Canada*, pages 115-120.

Höy, T. (1987): Geology of the Cottonbelt lead-zinc-magnetite layer, carbonatites and alkalic rocks in the Mount Grace area, Frenchman Cap Dome, southeastern British Columbia; *B.C. Ministry of Energy, Mines and Petroleum Resources*, Bulletin 80.

Hunt, J. (1997): Massive sulphide deposits in the Yukon-Tanana and adjacent terranes; *in* Yukon Exploration and Geology 1996, Exploration and Geological Services Division, Yukon, *Indian and Northern Affairs Canada*, pages 35-45.

Hunt, J. (1998):The setting of volcanogenic massive sulphide deposits in the Finlayson Lake district; *in* Yukon Exploration and Geology 1997, Exploration and Geological Services Division, Yukon, *Indian and Northern Affairs Canada*, pages 99-104.

Mihalynuk, M.G., Nelson, J.L., and Friedman, R.M. (1998): Regional geology and mineralization of the Big Salmon Complex (104N NE and 104O NW); *in* Geological Fieldwork 1997; *B.C. Ministry of Employment and Investment*, Geological Survey Branch, Paper 1998-1, pages 6-1 - 6-20.

Mihalynuk, M.G., Nelson, J., Roots, C.F. and Friedman, R.M. (2000): Ancient Pacific Margin Part III: Regional geology and mineralization of the Big Salmon Complex (104N/9,10 & 104O/12,13,14W); *in* Geological Fieldwork 1999, *B.C. Ministry of Energy and Mines*, Geological Survey Branch, Paper 2000-1, this volume.

Murphy, D.C. and Timmerman, J.R.M. (1997): Preliminary geology of the northeast third of Grass Lakes map area (105G/7), Pelly Mountains, southeastern Yukon; *in* Yukon Exploration and Geology 1996; Exploration and Geological Services Division, *Indian and Northern Affairs Canada*, pages 62-73.

Murphy, D.C. and Piercey, S.J. (2000): Syn-mineralization faults and their re-activation, Finlayson Lake massive sulphide belt, Yukon-Tanana Terrane, southeastern Yukon, *in* Yukon Exploration and Geology 1998; *Exploration and Geological Services Division, Indian and Northern Affairs Canada*, in press.

Murphy, D.C. and Piercey, S.J. (1999): Finlayson project: Geological evolution of Yukon-Tanana Terrane and its relationship to Campbell Range belt, northern Wolverine Lake map area, southeastern Yukon, *in* Yukon Exploration and Geology 1998; Exploration and Geological Services Division, *Indian and Northern Affairs Canada*, pages 47-62.

Nelson, J.L. (1997): Last seen heading south: extensions of the Yukon-Tanana Terrane into Northern British Columbia; *in* Geological Fieldwork 1996, D.V. Lefebure, W.J. McMillan and J.G. McArthur, editors, *B.C. Ministry of Employment and Investment*, Geological Survey Branch, Paper 1997-1 pages 145-156.

Nelson, J.L. (2000): Ancient Pacific Margin Part VI: Still heading south: Potential VMS hosts in the eastern Dorsey Terrane, Jennings River (104O/1; 7,8,9,10); *in* Geological Fieldwork 1999; *B.C. Ministry of Energy and Mines*, Geological Survey Branch, Paper 2000-1, this volume.

Nelson, J.L., Harms, T.A. and Mortensen, J. (1998): Extensions and affiliates of the Yukon-Tanana Terrane in northern British Columbia; *in* Geological Fieldwork 1997, *B.C. Ministry of Employment and Investment*, Geological Survey Branch, Paper 1998-1, pages 7-1 - 7-12.

Nelson, J.L., Mihalynuk, M. G., Murphy , D. , Colpron ,M., Roots, C. , Mortensen J.K and. Friedman, R. M: (2000): Ancient Pacific Margin Part II: A preliminary comparison of potential VMS-hosting successions of Yukon-Tanana Terrane, from Finlayson district to northern British Columbia; *in* Geological Fieldwork 1999; *B.C. Ministry of Energy and Mines*, Geological Survey Branch, Paper 2000-1, this volume.

Roots, C.F., de Keijzer, M., Nelson, J.L., and Mihalynuk, M.G. (2000): Revision mapping of the Yukon-Tanana and equivalent terranes in northern B.C. and southern Yukon between 131^o and 133^o W; *in* Current Research 2000-A; *Geological Survey of Canada*, in press.

Thompson, R.I. and Daughtry, K.L. (1998): Stratigraphic linkages across Vernon map area, British Columbia; *in* Current Research 1998-A; *Geological Survey of Canada*, pages 181-187.

Thompson, R.I., Nelson, J.L., Paradis, S., Roots, C.F., Murphy, D., Gordey, S.P. and Jackson, L.E. (2000): The Ancient Pacific Margin NATMAP Project: Year One; *in* Current Research 2000-A; *Geological Survey of Canada*, in press.

Ancient Pacific Margin Part II: A Preliminary Comparison of Potential VMS-hosting Successions of the Yukon Tanana Terrane, from Finlayson Lake District to Northern British Columbia*

J.L. Nelson[1] and M.G. Mihalynuk[1], D.C. Murphy and M. Colpron[2], C.F. Roots[3] and J.K. Mortensen and R.M. Friedman[4]

INTRODUCTION

The Yukon-Tanana Terrane of Yukon, Alaska and northern British Columbia consists of poorly understood, lithologically diverse successions of metasedimentary and metavolcanic rocks and voluminous mid- and late Paleozoic granitic metaplutonic bodies (Mortensen and Jilson, 1985; Mortensen, 1992). Significant volcanogenic massive sulphide deposits occur in the terrane in the Delta and Bonnifield districts in Alaska and in the Finlayson Lake belt in southeastern Yukon, and the potential for further discoveries is considered to be high. However, exploration for new deposits has been hindered by the paucity of stratigraphic information from the terrane as a whole.

One of the goals of the Ancient Pacific Margin NATMAP project is to address the deficiencies in stratigraphic information from the Yukon-Tanana Terrane. The Central Component of the Ancient Pacific Margin Project, which spans both Yukon and British Columbia, includes bedrock geological mapping of the Finlayson Lake belt (Murphy and Piercey 1999, 2000; location 1 on Figure 1), the Glenlyon area in central Yukon (Colpron, 1999; Colpron and Reinecke, 2000; locations 2, 3 on Figure 1), the Wolf Lake/Jennings River map area straddling the Yukon/B.C. border (Roots *et al*., 2000; location 4 on Figure 1), the Big Salmon Complex in northern Jennings River map area (Mihalynuk *et al*. this volume; location 5 on Figure 1), and the southeastern Dorsey Terrane in south-central Jennings River map area (Nelson, this volume; location 6 on Figure 1). The Finlayson Lake belt is currently separated from the other areas by the Tintina Fault. Restoration of about 425 kilometres of displacement on the fault (Roddick, 1967; Murphy,Mortensen and Abbott, in prep.) aligns all of these areas in a continuous belt from the Finlayson Lake area to the southern Jennings River (Figure 1). The Yukon-Tanana Terrane along this belt represents a target for volcanogenic massive sulphide deposits that extends over 500 kilometres of strike length.

Sufficient geological mapping and uranium-lead dating have now been done to construct preliminary stratigraphic sections for areas scattered along the extent of the southeastern Yukon-Tanana Terrane (Figure 2). In the Finlayson project, Murphy and collaborators have covered the area of the Fyre Lake, Kudz Ze Kayah and Wolverine volcanogenic massive sulphide deposits. Their work provides a preliminary stratigraphic template that is useful for workers throughout the terrane where the potential for volcanogenic massive sulphide deposits is less well known. This template is used in this paper as a point of comparison for the stratigraphic columns farther south along the restored pericratonic belt. Figure 2 shows fundamental similarities between these areas and the Finlayson Lake district, as well as highlighting significant differences in the ages of volcanism along the belt.

STRATIGRAPHIC SUMMARIES

Finlayson Lake District (Figure 2, Column 1)

Stratified rocks in the Finlayson Lake massive sulphide belt have been subdivided into three first-order successions, each hosting volcanogenic massive sulphide deposits and prospects (Murphy and Piercey, 1999; Figure 2). The lower succession comprises pre-Late Devonian quartz-rich metaclastic rocks, marble and pelitic schist; Late Devonian to early Missisissippian mafic metavolcanic rocks with lesser amounts of carbonaceous metaclastic rocks, felsic metavolcanic and volcaniclastic rocks, and marble; early Mississippian felsic metavolcanic and volcaniclastic rocks and carbonaceous phyllite, and early Mississippian carbonaceous phyllite, quartzite, quartz-feldspar pebble meta-conglomerate and mafic metavolcanic rocks. These units were intruded by early

[1]*B.C. Geological Survey*

[2]*Yukon Geology Program*

[3]*GSC-Yukon*

[4]*UBC Geochronology Laboratory*

[4]*This article also published in Yukon Exploration and Geology, 1999, Exploration and Geological Services Division, Yukon Region, Indian and Northern Affairs, Canada*

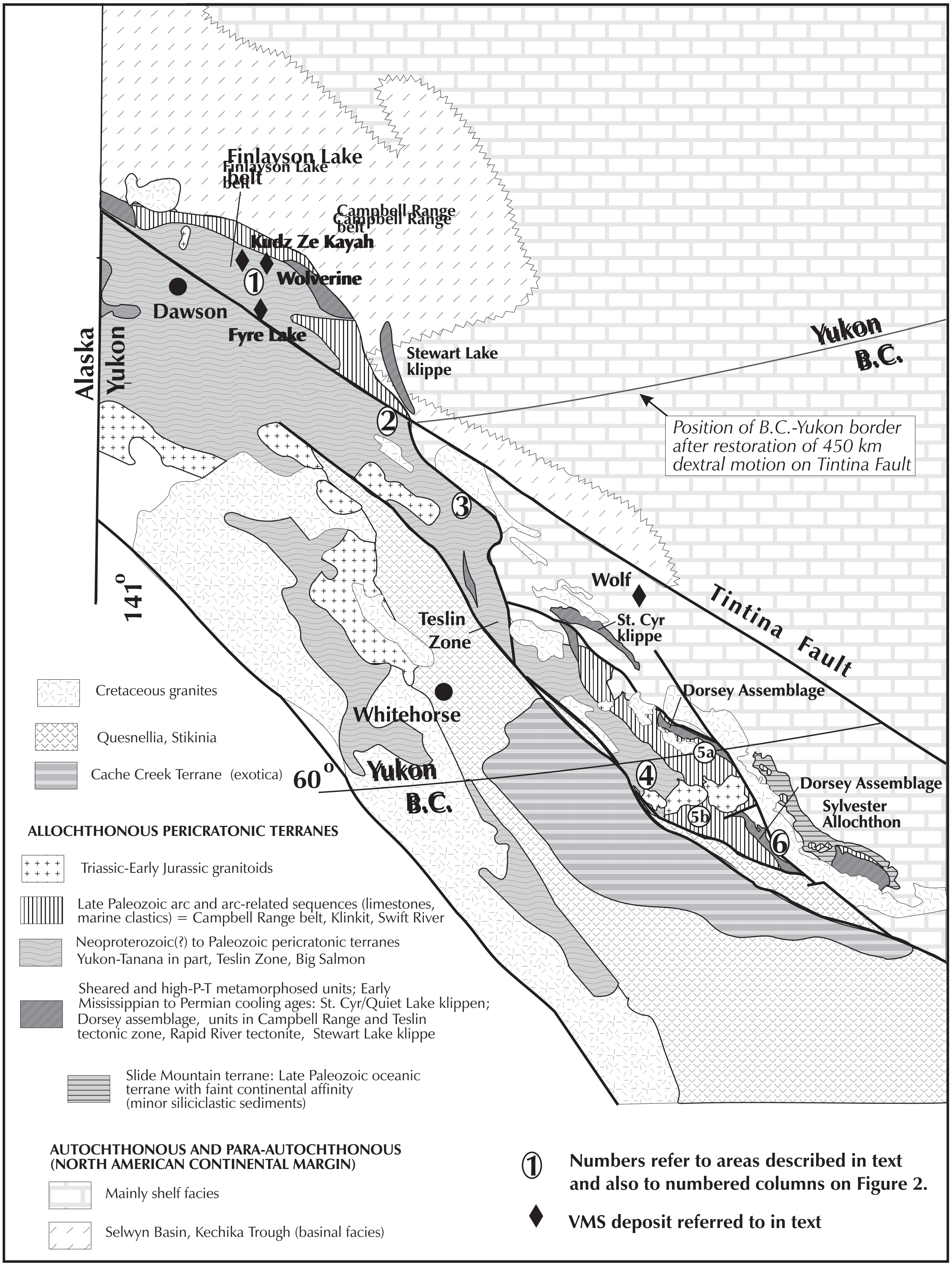

Figure 1. Location map of project area. The 450 km of dextrtal motion on the Tintina Fault has been removed.

Mississippian peraluminous granitic metaplutonic rocks, deformed, and re-intruded by slightly younger, late-kinematic, early Mississippian granitic metaplutonic rocks, before the unconformable deposition of the overlying middle stratigraphic succession. The lower succession hosts both the Fyre Lake Cu-Co-Au deposit and the Kudz Ze Kayah Cu-Pb-Zn-Au-Ag deposit, the former in the Late Devonian to early Mississippian mafic metavolcanic unit and the latter in overlying early Mississippian felsic metavolcanic rocks.

The middle succession, also of probable early Mississippian age, comprises carbonaceous metaclastic rocks, felsic schist and quartz-feldspar metaporphyry of volcanic, volcaniclastic and subvolcanic intrusive protolith. A distinctive, laterally persistent felsic tuff and exhalite unit caps the middle succession. The Wolverine Cu-Pb-Zn-Au-Ag deposit occurs near the top of the unit, just below the tuff/exhalite unit.

The upper succession corresponds to the Campbell Range belt of Mortensen and Jilson (1985). It consists of two intervals of basaltic volcanic and volcaniclastic rocks separated by a lithologically diverse and laterally variable unit of carbonaceous phyllite, greywacke, diamictite, variegated chert, chert-pebble conglomerate and limestone. Mid-Pennsylvanian to Early Permian radiolaria have been obtained from chert in the upper basalt (Harms, in Plint and Gordon, 1997) and Pennsylvanian conodonts were obtained from limestone (M.J. Orchard in Tempelman-Kluit, 1979). The Money occurrence is hosted by the upper Campbell Range basalt and the Ice Cu-Au volcanogenic massive sulphide deposit occurs in lithologically similar rocks about 70 kilometres northwest along strike from the Campbell Range succession.

Glenlyon Area (Figure 2, Columns 2, 3)

Detailed mapping in Glenlyon map area has identified two mid-Mississippian volcanic arc sequences of slightly different ages (Colpron, 1998; 1999a; 1999c; Colpron and Reinecke, 2000). In Little Kalzas Lake area, to the northwest, Early Visean calc-alkaline volcanic and volcaniclastic rocks conformably overlie a thick orthoquartzite unit (location 2 on Figure 1). This sequence was apparently deformed and metamorphosed prior to intrusion of the Tatlmain batholith in mid-Visean time. To the southeast, in Little Salmon Range, mid-Visean (and younger) volcanic and volcaniclastic rocks have mixed calc-alkaline and alkaline affinities (location 3 on Figure 1). The Little Salmon volcanic sequence rests unconformably on two different clastic units, exposed on the east and west limbs of a gentle synclinorium. On the east, it overlies arkosic grit intruded by a 353 Ma-old pluton (Oliver and Mortensen, 1998). On the west, it overlies a heterogeneous sequence of unknown age, which consists of quartzite, psammitic and pelitic schists, marble, greenstone and abundant discontinuous sills of meta-igneous rocks. The Little Salmon volcanic sequence contains Mn chert horizons and hosts a massive sulphide occurrence (Colpron, 1999b).

Northwestern Jennings River (Figure 2, Column 4)

Polydeformed pericratonic and overlying continental arc rocks of the Big Salmon Complex underlie the northwest and northeast corners of the Jennings River (104O/12,13,14W) and Atlin (104N/9E, 16) sheets respectively, and extend northwards into the Yukon (*cf.* Roots *et al.*, 2000). A northwest-trending, amphibolite-grade core zone is flanked by greenschist grade rocks in which protolith textures are locally well preserved.

The inferred oldest unit in the Big Salmon Complex consists of quartz-rich clastic strata, locally with arkosic intervals, thin carbonate layers and, in its upper parts, felsic tuffaceous horizons. It is succeeded by voluminous subaqueous mafic volcanic strata, with structural thicknesses of up to 2 kilometres. Geochemical analyses show that these mafic volcanics formed in a continental arc. They were intruded by the 362 Ma Mt. Hazel body, and are thus dated as Latest Devonian in part. They are overlain by one of three lithologies:

- local felsic meta-volcanics a few metres to perhaps a hundred metres or more thick, commonly with pyritic quartz-sericite schist intervals;
- a regionally extensive chert with exhalative characteristics, known as “crinkle chert” because of its folded habit, is generally 5 to 10 metres thick, to 200 metres where structurally thickened; and
- a quartz-rich conglomeratic and turbiditic unit, known as the “dirty clastics”, that is at least 250 metres thick.

These three units all show evidence of having been deposited during waning of the late Devonian to Early Mississippian arc. Juxtaposition of radically different sedimentary facies calls for isolation of depocentres, probably on a rifted arc substrate. Sulphide lenses within the crinkle chert may be relicts of volcanogenic exhalative accumulations during syn-sedimentary faulting.

Regionally persistent, fossiliferous carbonate deposition above the crinkle chert and felsic volcanic units marks the recovery of reef-forming organisms following their demise in the Late Devonian. Clastic sedimentation appears to have persisted in adjacent basins.

Reefal carbonate deposition is punctuated by one or more conglomeratic horizons, which may represent uplift associated with a mid-Mississippian deformational event that affects the 354 Ma Logjam intrusion (Gleeson *et al.*, 2000). In places, the regional carbonate has been nearly stripped away during uplift. Deformation may have peaked with emplacement of 346 Ma eclogite and blueschist (*cf.* Erdmer *et al.*, 1998) into the Yukon-Tanana Terrane arc complex. The deformation event is recorded in the Big Salmon Complex by folded strata that are cut by ~335 Ma dikes (unpublished data).

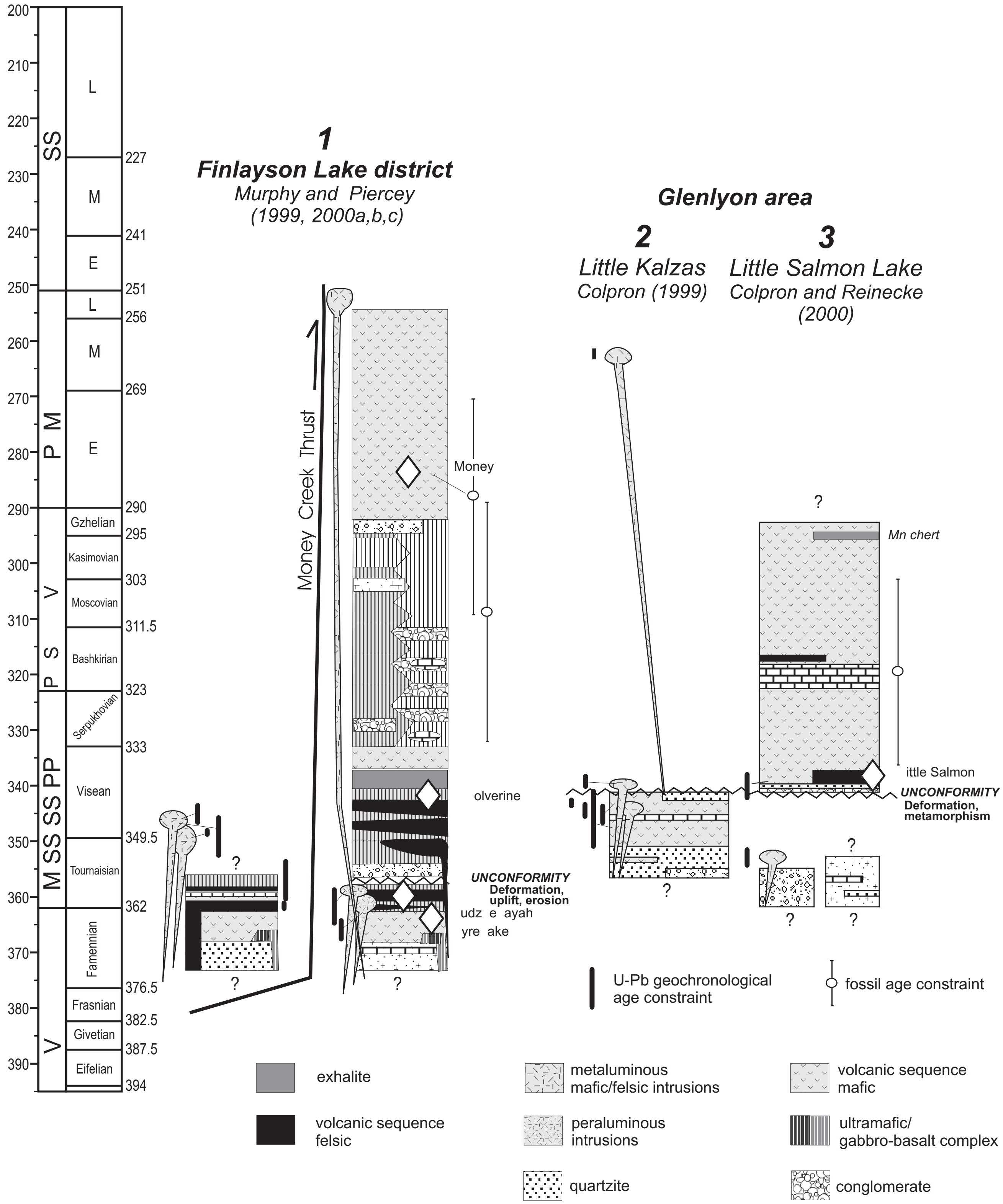

Figure 2. Selected stratigraphic columns from the Yukon-Tanana Terrane, Yukon and Northern British Columbia.

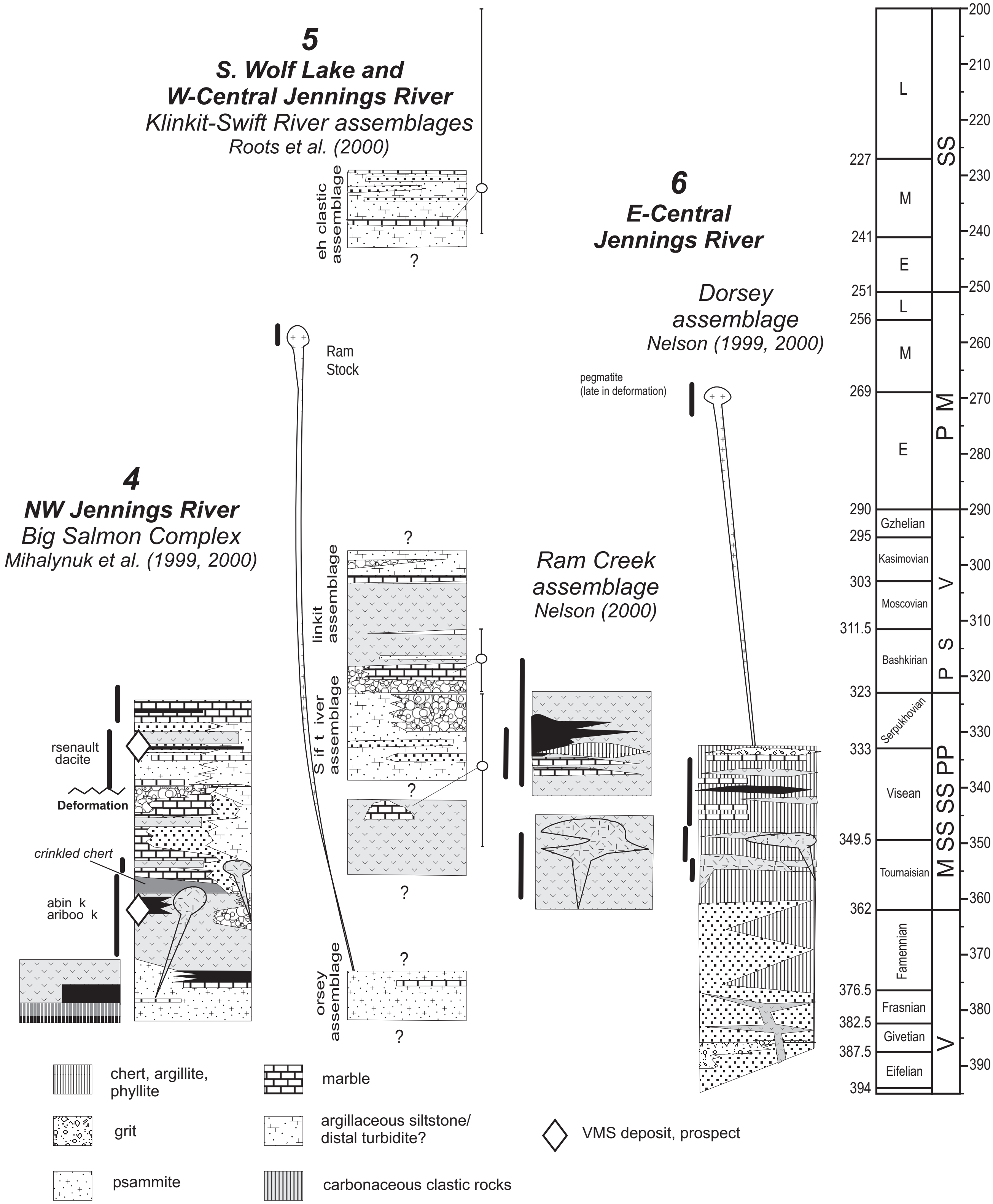

Figure 2. Selected stratigraphic columns from the Yukon-Tanana Terrane, Yukon and Northern British Columbia (continued).

Post-deformational sedimentation is highly varied. Both mafic and felsic distal tuffs and tuffites were deposited in both carbonate and clastic-dominated facies. Pulses of proximal felsic volcanism are recorded by coarse ignimbritic horizons such as those associated with base metal sulphide accumulations at the Arsenault property. A high degree of lithologic variability in the youngest Big Salmon Complex strata makes correlations difficult. However, the youngest dated Big Salmon Complex strata recognized in the Jennings River area are 326 Ma dacitic tuffs in carbonate of the heterolithic succession. No indications of a depositional hiatus exist at this point in the stratigraphy, so it is likely that younger Big Salmon Complex strata exist.

Southern Wolf Lake and West-central Jennings River Area (Figure 2, Column 5)

This section is derived from two areas, one straddling the Yukon/British Columbia border near Swift River (location 5a on Figure 1), and one in the west-central Jennings River map area (location 5b). It spans the Ram Creek, Dorsey, Swift River and Klinkit assemblages (Harms and Stevens, 1996). As suggested by Harms and Stevens, and corroborated in 1999 field mapping (Roots *et al*, 2000), each assemblage consists of related sedimentary and volcanic strata that are mappable and lithologically distinct from adjacent assemblages.

The oldest known rocks are included in the Dorsey assemblage (location 5a, Figure 1), which is exposed as a narrow, elongate strip near the northeastern side of the pericratonic belt. It is a siliceous succession including quartzite and quartzo-feldspathic metasedimentary protoliths, interspersed with quartz-augen felsic meta-tuff and marble layers, as well as foliated, sill-like leucocratic intrusions. It is characterized by a medium- to high-pressure metamorphic mineral assemblage. The Dorsey assemblage in Yukon was deformed prior to the emplacement of the mid-Permian Ram Stock (Stevens and Harms, 1995). Its oldest protoliths are probably pre-Devonian-Mississippian, the age of intrusions in southern Dorsey assemblage in British Columbia (see below).

The Swift River assemblage comprises several hundred metres, in structural thickness, of dark meta-siltstone and argillite with interbeds of quartzite; and thick-bedded, dark-coloured chert. There is no age control, except that a distinctive chert-pebble conglomerate facies at the top interfingers with, and is conformably overlain by Carboniferous (in part lower Pennsylvanian) Screw Creek limestone.

The Screw Creek limestone is white, thick-bedded, and contains abundant macrofossil debris. As mass flow deposits from a reef environment, this limestone is not a direct stratigraphic marker, but the Bashkirian conodonts (Abbott, 1981) provide an approximate age.

The Klinkit assemblage in central Jennings River area (location 5b, Figure 1) contains dark-coloured, thick-bedded chloritic meta-tuffs and breccias, volcanic-derived meta-siltstone and minor mafic flows, light-coloured limestone and siltstone-argillite layers. One or two prominently red quartzite (possible metamorphosed chert) layers lie several tens of metres above the base, which is locally a limestone that contains Carboniferous macrofauna, correlated with the Screw Creek limestone. The top of Klinkit assemblage, as used here, is a variable succession of meta-siltstone through quartzite with chloritic meta-tuff layers of unknown age.

The Triassic succession in west-central Jennings River area (The clastic assemblage; location 5b, Figure 1) consists of interbedded black argillite, meta-siltstone and quartzite, with minor chert, fetid limestone and conglomerate (T. Harms, personal communication, 1999). One limestone bed yielded a single Triassic conodont (M. Orchard, personal communication to T. Harms, 1997). This single age is considered preliminary. Moreover, although rocks that visually resemble this lithologic succession are found in several places in direct contact with Klinkit assemblage, field evidence for their stratigraphic relationship and even their stratigraphic order remains to be found.

East-central Jennings River (Figure 2, Column 6)

In east-central Jennings River area, rocks of the Big Salmon Complex disappear eastwards below less-metamorphosed younger strata of the Klinkit and Swift River assemblages. Possible equivalents, including Mississippian felsic volcanic units, reappear from beneath these to the east. They are assigned to the Dorsey and Ram Creek assemblages (Location 6 on Figure 1). The Dorsey assemblage, also described in the Wolf Lake map area (Location 5a), structurally overlies the Ram Creek assemblage across a post-mid Permian thrust fault (Nelson, this volume). For this reason, sections from these two assemblages are presented separately (Figure 2). The Dorsey assemblage is a metamorphic complex containing a variety of protoliths that range from siliciclastic to basinal sediments and tuffs, with isolated metabasic and ultramafic bodies. It is intruded by early Mississippian deformed granitoids. Early Mississippian intrusions also form part of the underlying Ram Creek assemblage. It is possible that during Mississippian time, the Dorsey assemblage was basement to the Ram Creek magmatic arc (Nelson, this volume). The Ram Creek assemblage contains tracts of mafic to rhyolitic meta-tuffs with local limestone and chert sequences. Two uranium-lead dates from the felsic tuffs are late Mississippian, coeval with tuffs in the Big Salmon Complex (Figure 2, column 4) and Little Salmon Lake sequence (Figure 2, column 3).

CONCLUSIONS

The columns described above demonstrate both the integrity and the variability of the southeastern Yukon-Tanana Terrane. Mafic to felsic arc activity in a pericratonic setting ranges in age from early Mississippian (*circa* 360-350 Ma) to late Mississippian-early Pennsylvanian (*circa* 335-320 Ma). The Finlayson Lake district contains significant volcanogenic massive sulphide deposits associated with the early Mississippian event (Murphy and Piercey, 2000). This syngenetic event is represented in the Big Salmon Complex near the British Columbia-Yukon border by the "crinkle chert", a siliceous meta-exhalite containing anomalous barium and manganese, and by small felsic accumulations with associated base-metal geochemical anomalies (Mihalynuk *et al*., this volume). Late Mississippian felsic tuffs occur in the Ram Creek assemblage, in the upper part of the Big Salmon Complex, and near Little Salmon Lake, where a small massive sulphide showing and cherty exhalite like the "crinkled chert" are also reported (Colpron, 1999b, Colpron and Reinecke, 2000). The late Mississippian volcanic suite, not apparently present in the Finlayson Lake district, represents a new, largely unexplored host for volcanogenic massive sulphide deposits in northern British Columbia and south-central Yukon.

REFERENCES

Abbott, J.G. (1981): Geology of the Seagull Tin District; *in* Yukon Geology and Exploration 1979-1980, *Indian and Northern Affairs Canada*, pages 32-44.

Colpron, M. (1998): Preliminary geological map of Little Kalzas Lake area, central Yukon (NTS105L/13): *Exploration and Geological Services Division, Yukon, Indian and Northern Affairs Canada*, Open File 1998-3, 1:50 000-scale.

Colpron, M. (1999a): Glenlyon Project: Preliminary stratigraphy and structure of Yukon-Tanana Terrane, Little Kalzas Lake area, central Yukon; *in* Yukon Exploration and Geology 1998; *Exploration and Geological Services Division, Indian and Northern Affairs Canada*, pages 63-72.

Colpron, M. (1999b): A new mineral occurrence in Yukon-Tanana terrane near Little Salmon Lake, central Yukon (NTS 105L/2), *in* Yukon Exploration and Geology 1998: *Exploration and Geological Services Division, Yukon, Indian and Northern Affairs Canada*, pages 255-258.

Colpron, M. (1999c): Preliminary geological map of Little Salmon Range (parts of NTS 105L/1, 2 & 7), central Yukon: *Exploration and Geological Services Division, Yukon, Indian and Northern Affairs Canada*, Open File 1999-2, 1:50 000-scale.

Colpron, M. and Reinecke, M. (2000): Glenlyon project: Coherent stratigraphic succession from Little Salmon Range (Yukon-Tanana terrane), and its potential for volcanic-hosted massive sulphide deposits, *in* Yukon Exploration and Geology 1999*: Exploration and Geological Services Division, Yukon, Indian and Northern Affairs Canada*, *in press*.

Erdmer, P., Ghent, E.D., Archibald, D.A. and Stout, M. (1998): Paleozoic and Mesozoic high-pressure metamorphism at the margin of Ancestral North America; *Geological Society of America Bulletin*, Volume 110, pages 615-629.

Gleeson, T. P., Friedman, R.M. and Wahl, K. (2000): Stratigraphy, structure, geochronology and provenance of the Logjam area, northwestern British Columbia (NTS 104O/14W); *in* Geological Fieldwork 1999, *B.C. Ministry of Energy and Mines*, Geological Survey Branch, Paper 2000-1, this volume.

Harms, T.A. and Stevens, R.A. (1996): Assemblage analysis of the Dorsey Terrane; Slave-Northern Cordillera Lithospheric Evolution (SNORCLE) and Cordilleran Tectonics Workshop, Report of the 1996 Combined Meeting; pages 199-201.

Mihalynuk, M.G., Nelson, J.L., and Friedman, R.M. (1998): Regional geology and mineralization of the Big Salmon Complex (104N NE and 104O NW); *in* Geological Fieldwork 1997; *B.C. Ministry of Employment and Investment*, Geological Survey Branch, Paper 1998-1, pages 6-1 - 6-20.

Mihalynuk, M.G., Nelson, J., Roots, C.F. and Friedman, R.M. (2000): Ancient Pacific Margin Part III: Regional geology and mineralization of the Big Salmon Complex (104N/9,10 & 104O/12,13,14W); *in* Geological Fieldwork 1999, *B.C. Ministry of Energy and Mines*, Geological Survey Branch, Paper 2000-1, this volume.

Murphy, D.C. and Piercey, S.J. (1999a): Finlayson project: Geological evolution of Yukon-Tanana Terrane and its relationship to Campbell Range belt, northern Wolverine Lake map area, southeastern Yukon, *in* Yukon Exploration and Geology 1998; *Exploration and Geological Services Division, Indian and Northern Affairs Canada*, pages 47-62.

Murphy, D.C. and Piercey, S.J. (1999b): Geological map of Wolverine Lake area, Pelly Mountains (NTS 105G/8), southeastern Yukon: *Exploration and Geological Services Division, Yukon, Indian and Northern Affairs Canada*, Open File 1999-3, 1:50 000-scale.

Murphy, D.C. and Piercey, S.J. (1999c): Geological map of parts of Finlayson Lake area (NTS 105G/7, 8 and parts of 1, 2, and 9) and Frances Lake (parts of NTS 105H/5 and 12) map areas, southeastern Yukon: *Exploration and Geological Services Division, Yukon, Indian and Northern Affairs Canada*, Open File 1999-4, 1:100 000-scale.

Murphy, D.C. and Piercey, S.J. (2000): Syn-mineralization faults and their re-activation, Finlayson Lake massive sulphide belt, Yukon-Tanana Terrane, southeastern Yukon, *in* Yukon Exploration and Geology 1999; *Exploration and Geological Services Division, Indian and Northern Affairs Canada*, in press.

Nelson, J.L. (2000): Ancient Pacific Margin Part VI: Still heading south: Potential VMS hosts in the eastern Dorsey Terrane, Jennings River (104O/1; 7,8,9,10); *in* Geological Fieldwork 1999; *B.C. Ministry of Energy and Mines*, Geological Survey Branch, Paper 2000-1, this volume.

Oliver, D. H. and Mortensen, J. K. (1998): Stratigraphic succession and U-Pb geochronology from the Teslin suture zone, south central Yukon, *in* Yukon Exploration and Geology 1997: Exploration and Geological Services Division, Yukon, *Indian and Northern Affairs Canada*, pages 69-75.

Plint, H.E. and Gordon, T.M. (1997): The Slide Mountain Terrane and the structural evolution of the Finlayson Lake Fault Zone, southeastern Yukon; *Canadian Journal of Earth Sciences*, Volume 34, pages 105-126.

Roots, C.F., de Keijzer, M., Nelson, J.L., and Mihalynuk, M.G. (2000): Revision mapping of the Yukon-Tanana and equivalent terranes in northern B.C. and southern Yukon between 131° and 133° W; *in* Current Research 2000-A; *Geological Survey of Canada*, in press.

Stevens, R.A. and Harms, T.A. (1995): Investigations in the Dorsey Terrane, Part 1: Stratigraphy, structure and metamorphism in the Dorsey Terrane, Southern Yukon Territory and Northern British Columbia; *Geological Survey of Canada,* Current Research 1995-A, pages 117-128.

Tempelman-Kluit, D.J. (1979): Transported cataclasite, ophiolite, and granodiorite in Yukon: Evidence for arc-continent collision; *Geological Survey of Canada* Paper 79-1427 pages.

Ancient Pacific Margin Part III: Regional Geology and Mineralization of the Big Salmon Complex (NTS 104N/9E,16 & 104O/12,13,14W)

By Mitchell G. Mihalynuk[1], JoAnne L. Nelson[1], Charlie F. Roots[2], Richard M. Friedman[3] and Martin de Keijzer[4]

KEYWORDS: *Regional geology, Big Salmon Complex, Nisutlin Assemblage, Klinkit Assemblage, Swift River Assemblage, Yukon-Tanana Terrane, Kootenay Terrane, Dorsey Terrane, Slide Mountain Terrane, Teslin Fault, volcanogenic massive sulphide, mineralization, Atlin, Teslin, Jennings River.*

INTRODUCTION

Regional geological mapping of the Big Salmon Complex in northwestern British Columbia (104N/09 & 16 and 104O/12, 13 & 14W, Figure 1) was conducted in 1999 under the aegis of the Ancient Pacific Margin National Mapping Program (NATMAP, *cf*. Nelson, *et al.*, 2000, this volume; Roots, *et al.*, 2000). This mapping builds on 1997 reconnaissance mapping (Mihalynuk *et al.*, 1998) that confirmed long-standing correlations between the Big Salmon Complex in British Columbia and the Yukon (*e.g.* Mulligan, 1963; Gabrielse, 1969; Figure 2).

[1]*Geolgical Survey Branch, British Columbia Ministry of Energy and Mines, PO Box 9320 Stn Prov Govt, Victoria, British Columbia V8W 9N3; Email: mitch.mihalynuk@gems5.gov.bc.ca*

[2] *Yukon Geology Program, Canada-Yukon Geoscience Office, 2099-2nd Avenue, Whitehorse, Yukon, Y1A 1B5*

[3] *Department of Earth and Ocean Sciences, University of British Columbia, 6339 Stores Road, Vancouver, British Columbia, V6T 2B4*

[4] *Department of Geology, University of New Brunswick, PO Box 4400, Fredricton, New Brunswick, E3B 5A3*

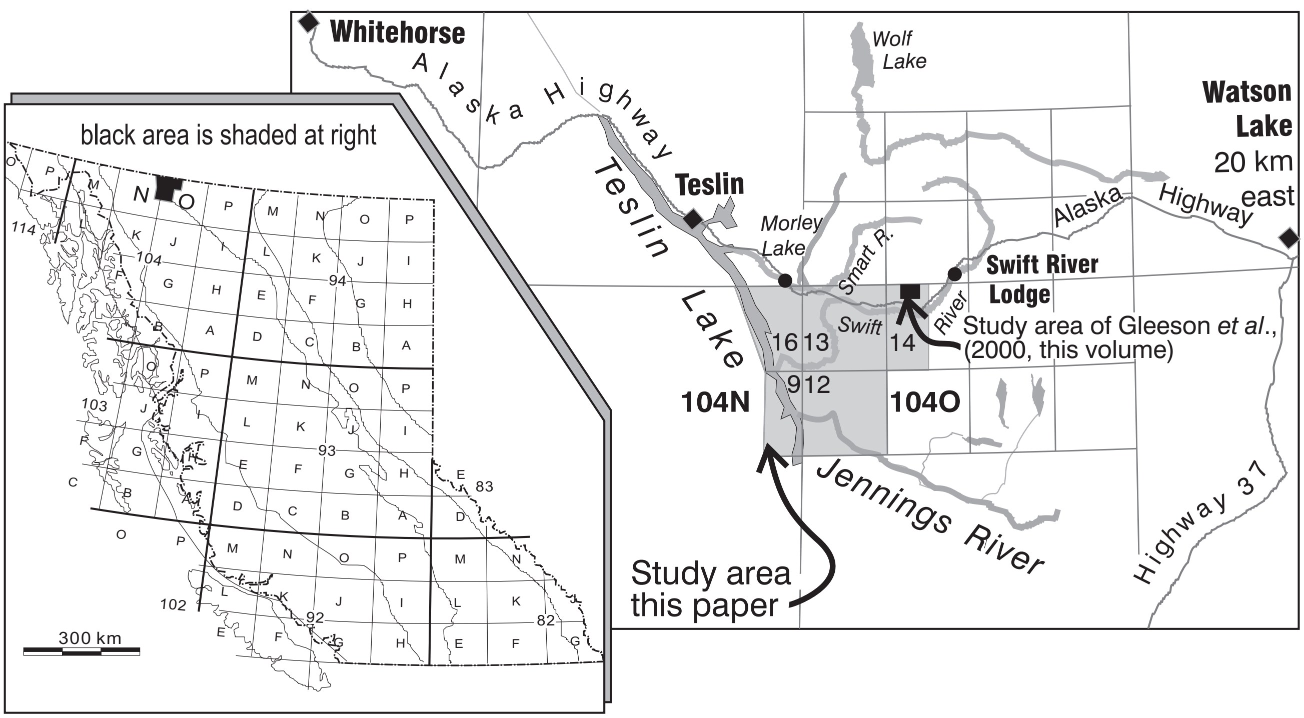

Figure 1. Location map showing the location of the Big Salmon Complex study area in northern British Columbia and southern Yukon (after Roots *et al.*, 2000). The area of Figure 3 is shown by the shading.

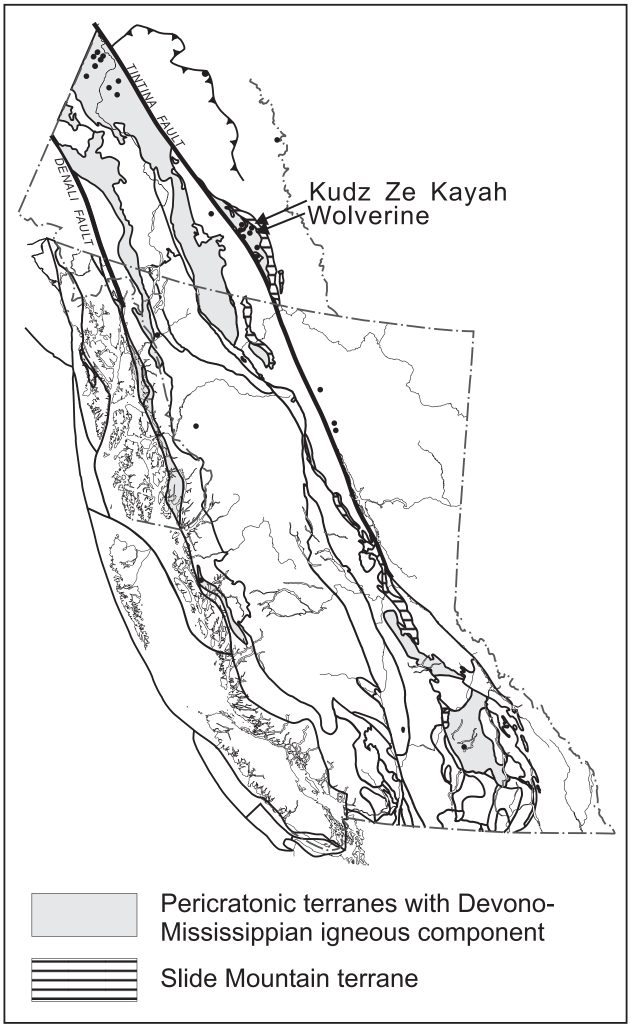

Figure 2. Tectonic assemblage map showing the approximate distribution of Yukon-Tanana and Slide Mountain terranes. Modified after Wheeler *et al*. (1991).

In southern Yukon, Big Salmon Complex rocks have subsequently been included with the Kootenay Terrane (Gordey, 1995) which include the Lower and Middle Units of the Yukon-Tanana Terrane as used by Mortensen (1992). This correlation is important because Yukon-Tanana Terrane rocks, historically ignored by mineral exploration geologists, have been the focus of mineral exploration programs since 1993 with the discovery of mineralized float at what came to be the Kudz Ze Kayah deposit. Other exploration successes include the Wolverine and Fyre Lake volcanogenic massive sulphide deposits.

Highlights of the 1999 field program are reported here together with descriptions of map units and geological relationships, and new insights. Mihalynuk *et al.* (1998) describe units encountered in the 1997 field season and present a structural synthesis, the details of which are not repeated here.

LOCATION AND PHYSIOGRAPHY

During the six week field program (early July to mid-August), mapping concentrated on low-lying, tree or swamp-covered areas (Photo 1) that occupy more than 90% of the area bounded by the British Columbia-Yukon border on the north, Teslin Lake on the west, Mount Charlie Cole to the south and Simpson Peak to the east (Figure 3). Most of the area is covered by fluvial and glacial deposits that attain thicknesses of 40 metres or more (Dixon-Warren and Hickin, 2000, this volume); although, air photo analysis and fixed wing aerial reconnaissance revealed that outcrop is more abundant than indicated on previous maps (Gabrielse, 1969). Reaching the outcrops can, however, be a challenge, usually requiring foot travel between swamps that provide the only helicopter landing spots.

The map area is accessed from the Alaska Highway, which crosses it near the Yukon border, between Watson Lake and Whitehorse (Figure 1). Only three rough secondary roads reach more than a kilometre from the highway. These mineral exploration roads; each extend about 10 kilometres in British Columbia. Two lead into the Yukon, up the west side of Logjam Creek and east side of Smart River valleys. However, washouts on the Smart River Road render it impassable after a few kilometres. Another road, constructed to provide access to the Arsenault property, can only be traveled as far as the Swift River where the bridge has long since washed away. Fuel and rudimentary supplies are available at Swift River and Morley River Lodge, just outside the eastern and western limits of the map area, respectively.

Charter fixed wing aircraft are available year round at Teslin from Teslin Lake or at a converted military gravel strip, both, about 45 kilometres west of the map area. Charter helicopters are available year round from Atlin, about 80 air kilometres west of the map area.

GEOLOGIC FRAMEWORK

Most of the field area is underlain by the Big Salmon Complex (Figure 3). Dominant protoliths are mafic vol-

Photo 1. An aerial view of the low-lying, swamp and tree-covered Nisutlin Plateau near the south end of Teslin Lake.

canic rocks, quartz-rich clastic sediments, and intrusive rocks of diorite, tonalite and leucogranite composition. Felsic tuff, crystalline limestone and chert-exhalite units are volumetrically minor, but conspicuous and mappable units. A lower amphibolite grade "core zone" in which protolith textures are mostly destroyed, is broadly parallel to the northwest trend of the Big Salmon Complex, and is flanked by greenschist grade rocks to both the southwest and northeast in which relict protolith textures may be relatively well preserved. Metamorphosed tonalite, lesser diorite and minor leucogranite, herein called the Hazel orthogneiss, dominate the north-central part of the "core zone" (Figure 3).

Big Salmon Complex rocks are bounded to the southwest by Teslin Lake (Teslin fault, *see* de Keijzer *et al.*, 2000) and Cache Creek Terrane in the Atlin area (Aitken, 1959; Figure 3). They clearly extend northwest into the Yukon (Roots *et al.*, 2000) and are probably equivalent to Mississippian volcanics in the Teslin area (unit Mv of Gordey and Stevens, 1994; Gordey, 2000). Relationships with rocks to the southeast and northeast are less certain (*see* Discussion).

Both Aitken (1959) and Gabrielse (1969) considered the Big Salmon Complex to be at least partly correlative with the Sylvester Group (Slide Mountain Terrane) based upon the abundance of mafic volcanic protoliths, but this assignment is not supported by more recent data. For example, Mihalynuk *et al.* (1998) showed that the Big Salmon Complex greenstones are geochemically like continental arc volcanics, not mid ocean ridge basalts typical of the Slide Mountain Terrane. Along strike in the Teslin zone, Creaser *et al.* (1997) showed that the geochemistry of both sedimentary and volcanic rocks lithologically correlative with the Big Salmon Complex is not permissive of genesis in the Slide Mountain ocean basin because εNd values are strongly negative (+0.5 to –26.2), indicating a significant continental component.

Tempelman-Kluit (1979) interpreted rocks in the Yukon that are equivalent to, and along strike with the Big Salmon Complex as part of a subduction/collisional complex (Teslin suture zone), a contention supported by discovery of relict high pressure metamorphic assemblages including eclogite (Erdmer and Helmstaedt, 1983; Erdmer, 1985; Erdmer and Armstrong, 1989). Working along the western part of the Big Salmon Complex, Hansen (1989, 1992a, 1992b) and Hansen *et al.* (1989, 1991) claimed to outline a fossil Permo-Triassic subduction zone with off-scraped sediments affected by tectonic backflow. More recent work by Stevens (1992, 1994), Stevens and Erdmer (1993), Stevens and Harms (1995), Stevens *et al.* (1996) and Colpron (1999) shows that the Teslin "suture zone" is comprised not of mélange of off-scraped oceanic sediments and subduction zone tectonites, but of continental margin strata (Creaser *et al.*, 1997) with relatively coherent stratigraphic relationships. This coherent stratigraphy has enabled the definition of a polydeformed nappe (deKeijzer and Williams, 1999) within the former Teslin suture zone. Likewise, a persistent stratigraphy can be traced throughout the study area, and none are composed of scaly subduction mélange.

STRATIGRAPHIC FRAMEWORK

A persistent stratigraphy provides the foundation for correlating from one area to another in the Big Salmon Complex. In British Columbia, three distinctive and contrasting units are recognized as forming a marker succession (Mihalynuk *et al.*, 1998; Figure 4). Based on new isotopic and geologic constraints, their stratigraphic order, from oldest to youngest is now known to be:

- 1200 m of tuffite-dominated greenstone;
- 30-150 m of buff to grey weathering limestone with metre-thick tuffaceous and thin centimetre to decimetre quartzite layers;
- 20-50 m of thinly bedded, finely laminated manganiferous crinkle chert/quartzite with muscovite partings;

This marker succession persists in southeast and northwest 104O/13 and south-central 104O/12. In northern 104N/16 a hybrid unit having some characteristics of felsic tuff mixed with crinkle chert occurs in place of the crinkle chert unit.

Two other more broadly defined rock packages are recognized:

- >150 m of dirty clastics: brown to tan wacke, stretched quartzite-pebble and granule conglomerate and slate;
- >1000 m of heterolithic, quartz-rich clastics interbedded with thin limestone and mafic and felsic tuffs.

Lacking age control, Mihalynuk *et al.* (1998) concluded that the "dirty clastics" were considerably younger than the unconformably underlying greenstone unit, because they contained clasts that appeared to be derived from the older polydeformed and polymetamorphic units. And because the "dirty clastics" unit was observed to sit only on the greenstone unit, greenstone was considered the next youngest unit, prompting the conclusion: "A thick greenstone and overlying clastic strata within the Big Salmon Complex of British Columbia have no obvious correlatives within the Yukon-Tanana Terrane and may be considerably younger."

Subsequent petrographic analysis showed that polydeformed phyllite clasts within the "dirty clastics" succession were deformed *in situ*, and were not derived from a previously deformed terrain. Two fabrics shown by the phyllite clasts are seen in thin section to be weakly developed in adjacent, phyllosilicates-poor quartzite clasts (Photo 2). Furthermore, new isotopic age data from samples of the former lower (Mt. Francis dacite at 325 Ma) and upper (Hazel orthogneiss at 362 Ma) parts of the stratigraphy require that the stratigraphy of Mihalynuk *et al.* (1998) is inverted, with important consequences for regional correlations (*see* Geochronology and Discussion). A revised stratigraphy is shown in Figure 4.

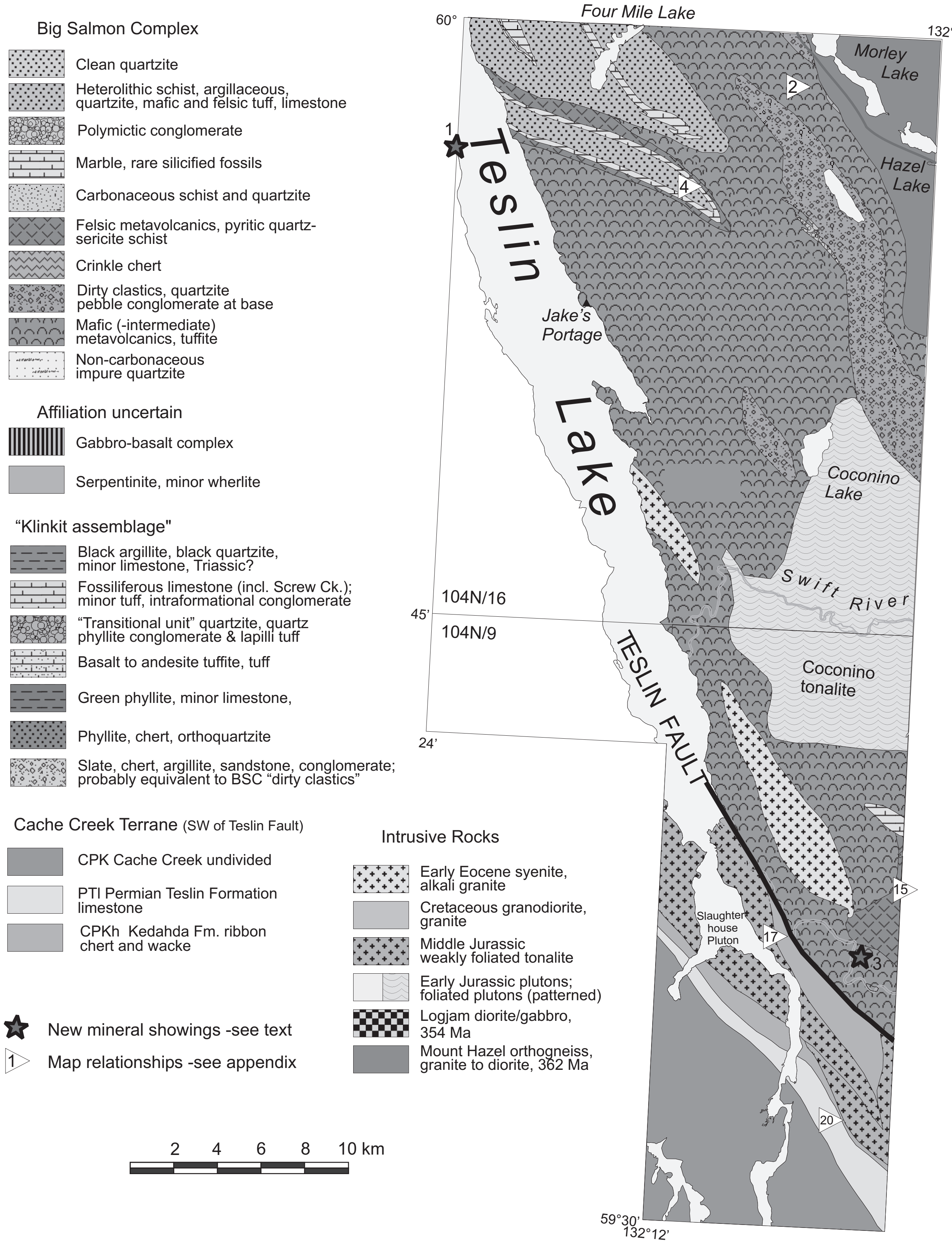

Figure 3. Generalized geology of the map area showing place names, access roads and sample sites referred to in the text.

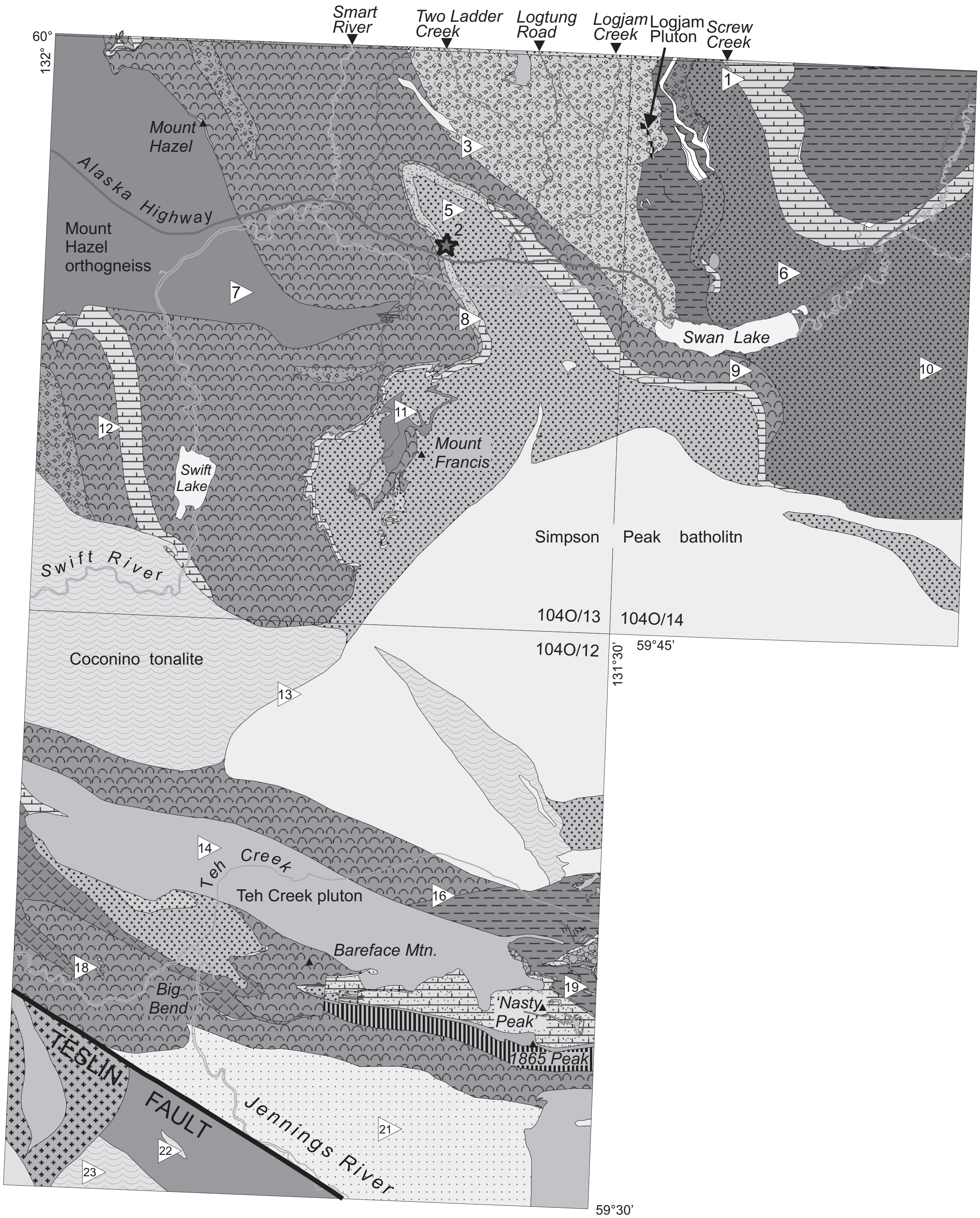

Smart River
Two Ladder Creek
Logtung Road
Logjam Creek
Logjam Pluton
Screw Creek
60°
132°
Mount Hazel
Alaska Highway
Mount Hazel orthogneiss
Swan Lake
Mount Francis
Swift Lake
Simpson Peak batholitn
Swift River
104O/13
104O/14
104O/12
59°45'
131°30'
Coconino tonalite
Teh Creek
Teh Creek pluton
Bareface Mtn.
Big Bend
'Nasty Peak'
1865 Peak
TESLIN FAULT
Jennings River
59°30'
1
2
3
5
6
7
8
9
10
11
12
13
14
16
18
19
21
22
23

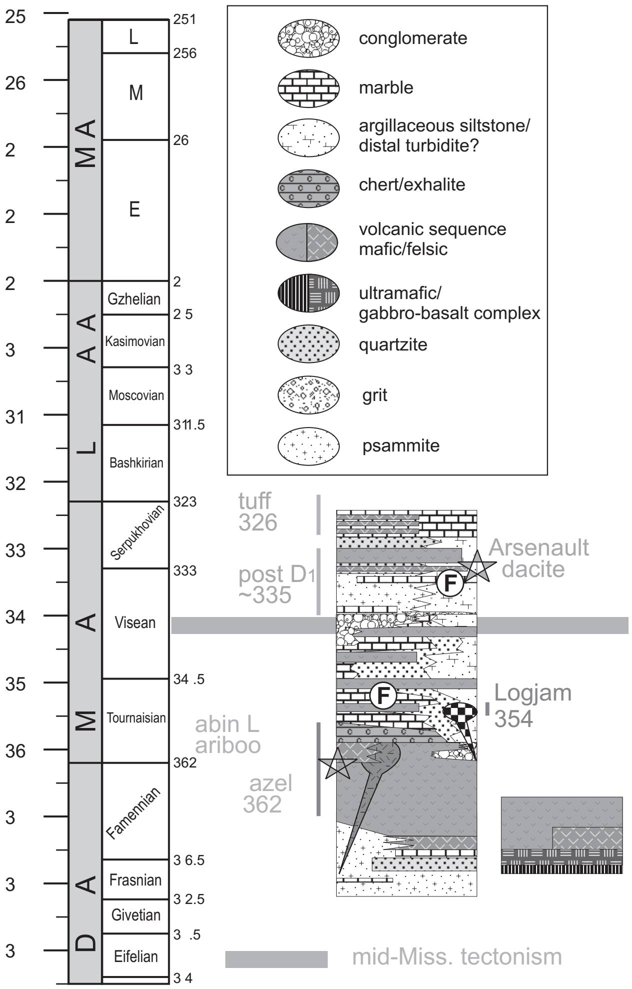

Figure 4. Generalized stratigraphy of the Big Salmon Complex in British Columbia.

Facing indicators are among the textures commonly preserved on the relatively weakly metamorphosed flanks of the Big Salmon Complex. However, unless they can be observed at the interface of the units being compared, they must be considered suspect because isoclinal folds are pervasive. In particular, the “dirty clastics” unit, which displays good graded bedding, is strongly deformed near its contact with the greenstone due to high rheological contrast (Photo 3).

A heterolithic succession, dominated by quartz-rich clastics with minor, grey-weathering carbonate layers 1-10m thick and quartz-phyric volcanic tuff layers up to 40m thick, are now considered to sit near the top of the Big Salmon Complex stratigraphy as they include the 325 Ma dacite layers. A lower quartz and feldspar-rich metaclastic unit that is lithologically similar, but not identical to some metaclastics of the upper unit, apparently underlies the greenstone unit upstream of the Big Bend (104O/12 south). Immediately to the north, a basalt-gabbro-ultramafite succession occurs within the greenstone near Teh Creek, where rock units belonging to the “Klinkit assemblage” are well exposed. Layered and intrusive units not previously described by Mihalynuk *et al.* (1998) are described here, beginning with the oldest layered rocks.

Lower Quartz and Feldspar-Rich Metaclastic Unit

In southern 104O/12, a > 350 m thick (structural) succession dominated by quartz-rich and lesser quartz-feldspar-rich metaclastic rocks lies structurally below the greenstone unit. In order of abundance, the rock types are: muscovite-quartz schist; biotite-muscovite±garnet quartz schist; muscovite-quartz±chlorite±feldspar schist, and biotite-chlorite-feldspar-quartz-schist. Feldspathic schists may be strongly deformed granitoid bodies, but the gradual appearance of feldspar down section from the greenstone argues for a sedimentary source. Sinistral shear bands are well developed in the feldspathic schist; about 2.5 kilometres north of the presumed trace of the Teslin fault (Figure 3).

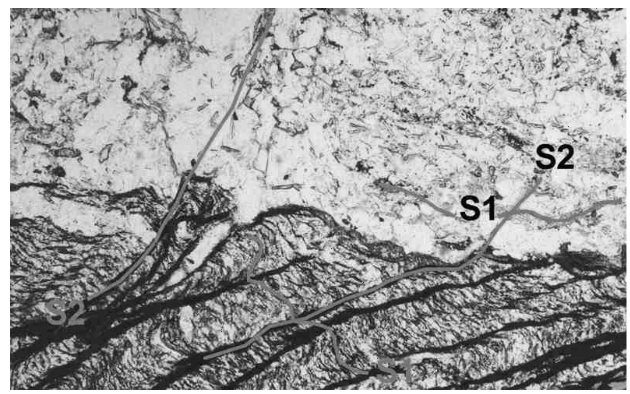

Photo 2. Photomicrograph of stretched quartzite pebble conglomerate of the dirty clastic succession shows that the phyllitic fabric displayed by argillaceous clasts (S1) continues into the adjacent quartzite clasts. A second fabric (crenulation cleavage, S2) is also printed on both phyllite clasts and quartz clasts. Such fabric development demonstrates that the conglomerate was deposited prior to at least two phases of deformation, and that the phyllite clasts need not have been derived from a previously deformed and metamorphosed terrain. Width of the photomicrograph represents 4 mm.

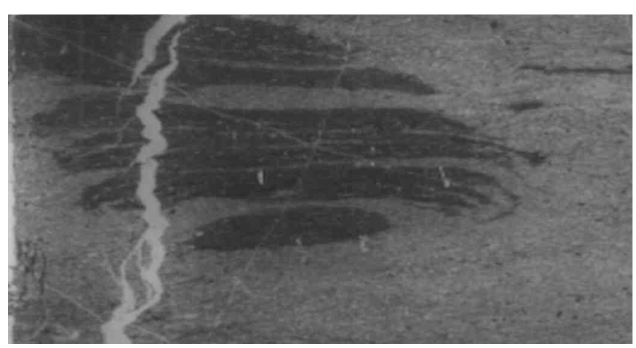

Photo 3. Sheath fold in turbiditic siltstones of the “dirty clastics” unit from within 5 metres of the greenstone contact (8x magnification).

Ultramafite-Gabbro-Basalt-Porphyry

A north to south succession of ultramafite (70-600m), gabbro (150-700m) and basalt (>20-2000m) can be traced for about 13 kilometres (Figures 3 and 4, all thicknesses are structural). It extends from the eastern limit of the map area, the Butsih Creek valley, and extends west almost to Bareface Mountain (informal, on Figure 3) where serpentinite was previously recognized by Gabrielse (1969). Farther west, the serpentinite disappears and the gabbro-basalt complex merges with the Big Salmon Complex greenstone unit. Greenstone with gabbro intervals is well exposed on both the long south ridge and the southwest flank of Bareface Mountain. At the eastern end of the belt, exposures are lost beneath glacial cover of the Butsih Creek valley. The easternmost 2 kilometres of serpentinite outcrops are bordered to the north by distinctive, coarsely porphyritic andesitic volcanic and hypabyssal rocks. All contacts of the ultramafite are faulted; they are either intrusive contacts that have been structurally modified, or original tectonic contacts.

Ultramafite exposures are typically orange, waxy yellow or dark green-black on both weathered and fresh surfaces. They are dominantly strongly foliated serpentinite, but lozenges of less foliated lherzolite are common on "1865m peak" (Figure 3) where the unit is thickest and best exposed. Where first encountered, the lherzolite was described as a wherlite, but geochemical anlaysis shows the rock to be too Mg-rich to support an abundance of clinopyroxene, so the pyroxenes are probably deformed hypersthene. At a locality 1.8 km west of the peak, coarsely crystalline lherzolite cumulate is preserved as a septa bounded to the north and south by gabbro. Exposures are not sufficient to determine whether this relationship is due to structural interleaving or is a relict of an originally intrusive contact. A series of outcrops on the north side of Teh Creek valley displays trains of serpentinized pyroxenes that may be a relict mantle tectonite fabric, but a pervasive late foliation renders this interpretation tenuous. (Harzburgite tectonite erratics are common along the belt. When first encountered, the erratics were suspected to be of local derivation. However, they occur throughout the map area and beyond, and are evidence of a once extensive, preglacial ophiolite terrain.)

The gabbro and basalt comprise an intrusive complex. Gabbro is cut by basalt and basalt is cut by gabbro. At the northern margin of the complex, gabbro predominates and at the southern margin, basalt predominates. Gabbro is white to green on fresh or weathered surfaces, although it can also be ruddy weathering. It is medium to very coarse-grained; locally it is pegmatitic. Plagioclase, pyroxene, and hornblende are epidote- and chlorite-altered and comprise more than 90% of the rock. Pyroxene is probably largely altered to hornblende, but this is not yet confirmed by petrographic analysis. Contacts with the ultramafite are best exposed within 0.5km of "1865 Peak" where they are clearly tectonic. Gabbro grain size is cataclastically reduced from greater than 1 cm to less than 0.01 cm over a width of 4 metres at the ultramafite contact. Shallowly-plunging mineral lineations suggest transcurrent motion, in support of map-scale sinistral shear bands; however, these lineations are folded and macroscopic kinematic indicators are inconsistent or equivocal.

The basalt is dark green weathering, aphanitic or microporphyritic. Flat chlorite disks up to 1 cm across are probably relict amygdales. They may comprise as much as 3% of the rock and are best displayed at one outcrop on the southern flank of "1865 Peak", where they are concentrated in concentric zones in what appear to be stretched pillows (Photo 4).

Basalt outcrops are lost beneath thick colluvial and glacial deposits in the valley south of "1865 Peak". Green-weathering basalt and andesite lapilli tuff dominate the next ridge to the south. They are extensively epidote-chlorite altered, foliated, and plagioclase-phyritic, with locally preserved pyroxene and hornblende phenocrysts. Less abundant, strongly planar beds of dust tuff or tuffite are conspicuous because of alternating, centimetre-thick, lime yellow and dark green bands. Pillowed and subaqueous sheet flows are also locally preserved. Similar units occur within the Big Salmon Complex greenstone unit along strike to the west (Figure 3), where they show higher degrees of strain.

Photo 4. Stretched pillows(?) within the basalt-gabbro-ultramafite complex. If these are pillows, then part of the complex was deposited in a submarine environment.

Coarsely Porphyritic Andesite

A package of distinctive, coarsely porphyritic, green-weathering, volcanic and hypabyssal andesitic rocks underlie most of the northern spur of "1865 Peak" where they are structurally admixed with serpentinite along their southern contact. They are separated from tuffite-dominated succession of "lower Klinkit assemblage" north of the spur by a colluviated valley. A stream occupies the valley bottom 1.6 km to the east where outcrops of dark green, fine-grained tuff are washed clean. In places, the tuff appears autoclastic. Broad zones, tens of metres across, are plagioclase-porphyritic, and in one 20 cm wide zone, flattened pyroxene crystals up to 4 mm across (average 2-3 mm) are preserved. Near the serpentinite, the unit is megaporphyritic. Plagioclases up to 4 cm long are strongly zoned, possibly to K-feldspar. Blocky black hornblendes range up to 2.5 cm long. Both feldspar and hornblende megacrysts are aligned down dip in a green, fine-grained foliated matrix (305°→65° to vertical). Some broken phenocrysts display an asymmetry that suggests north-side-up reverse motion, but most show ambiguous shear sense.

These tuffs could have provided the source for epiclastic deposits in the "lower Klinkit assemblage", although such a contention cannot be proven at this time. Granodioritic intrusives hornfels both porphyritic tuffs and epiclastics and chalcopyrite (<0.25%) is widely disseminated in the porphyritic tuffs.

Klinkit Assemblage

Rocks of the "Klinkit Assemblage" (Stevens and Harms, 1996) crop out in the eastern portions of the map area (104O/12E, 13NE, 14W; Figure 3). Harms mapped much of the "Klinkit assemblage" near Teh Creek (104O/12E, Figure 3; Harms, written communication, 1999) and established a useful subdivision which aided our 1999 mapping in the area. In 104O/13NE and 14W the "Klinkit assemblage" includes a lower unit equivalent to the "dirty clastics" and higher (?) units described by Gleeson *et al.* (2000, this volume; not described here). The fossiliferous Screw Creek limestone apparently sits near the top of the "Klinkit assemblage", although existing age data suggest protracted limestone deposition. Observations from the Teh Creek succession and Screw Creek limestone are presented here, from oldest to youngest.

Tuffite (240 m)

Well-preserved graded planar beds 10 to 100 cm thick of fine-grained tuffiteare characteristic of this unit. Approximately 200 metres of rhythmic deposits consist mainly of sets that average 3 metres thick and grade upwards from massive hornblende-feldspar-phyric lapilli that form 2/3 of their thickness, through fine-grained, planar-bedded ash and into laminated dust tuff. Sets may be capped by cross-stratified volcanic siltstone. Fine-grained detrital hornblende and plagioclase are abundant enough in some layers to produce a felted texture. In some cases, fine mafic grains are equant and may originally have been pyroxene, now replaced by actinolite. Fresh, coarse augite porphyry was observed in talus. Some intervals are very fine grained and cherty, resembling pelagic deposits. They are interpreted as dust tuff layers and may preserve ball and pillow structures. Sparse decimetre-scale calcareous layers are accentuated in thermal aureoles of thick sills and stocks by the development of light-coloured calc-silicates (grossular, diopside, epidote and quartz). One gossanous laminated white calcsilicate is, at a minimum, 6 metres thick.

Exceptionally well-preserved bedding and fine depositional features including cross-stratification, graded bedding, various water escape features, and scours permit assessment of facing directions. The succession is right way up and deformed by upright open to close folds in which foliation is only weakly developed, except for the fold core regions in which protolith textures are in part obliterated. Rhythmic deposits resemble thick turbidites, possibly ABC Bouma sequences; however, the predominance of reverse grading in planar-bedded ash layers suggests water lain tuffs that have not been reworked.

This unit has yielded neither fossil nor isotopic ages from within the map area. Similar tuffite in the Teslin sheet (Gordey, 2000) contain minor interbedded limestones with Middle Mississippian (Viséan) conodonts (M.J. Orchard *in* Poulton *et al*., 1999; *see* Figure 2 in Nelson *et al.*, 2000, this volume). However, the reliability of this distant extrapolation is questionable.

Near both the eastern and western limits of the tuffite displays apparent stratigraphic contacts with overlying conglomerate of the transitional unit.

Transitional Unit(s)

The transitional unit is so named because it marks a distinct change from volcanic to carbonaceous and quartz-rich clastic sedimentation. Two units define this transition: a light grey tuff/tuffite, and a conglomerate with quartz-rich clasts.

A complete section of grey, fine lapilli and coarse ash tuff and tuffite has not been observed. It is probably about 40 metres thick and is partly interbedded with the conglomerate unit. Some tuffaceous layers appear felsic, due to their siliceous nature, however, no quartz phenocrysts have been observed. Tuff is probably subordinate to grey or purple-brown phyllitic siltstone, which in places resembles microdiorite due to thermal alteration and growth of fine biotite. Siltstone is generally very well bedded on millimetre to centimetre scales, and may display cross laminae, but clear way-up indicators are rare, and these show that the unit is isoclinally folded. High strain zones are common and their orientation with respect to strongly transposed bedding indicates that they are axial-parallel and focused at fold hinges. In contrast, later, near-vertical mylonitic zones cut across folded limbs.

Granules to cobbles of quartzite, quartz-rich phyllite and possibly recrystallized chert are the principal components of the conspicuous conglomerate unit (Photo 5) that marks the transitional unit north of "Nasty Peak" (informal, Figure 3). Conglomerate matrix material varies from light grey-green phyllite to grit. Clasts are typically slightly stretched. Structural complexity makes thickness estimates difficult, but it is at least 5 m thick, and probably attains thicknesses of 30 m.

Highly strained, probable equivalents occur 4 km east of Bareface Mountain and on the southern ridge of the mountain. Quartz cobbles are flattened to sub-millimetre thicknesses (Photo 6), but low strain zones show good preservation of grey ash tuff interbeds.

Black Argillite-Quartzite

Rusty, pyritic and locally graphitic black argillite and thinly interbedded siltstone is the most abundant lithology within the black argillite-quartzite unit. Centimetre to decimetre thick beds of vitreous black sandstone are, however, characteristic, and at least one conspicuous, 4-8 m thick layer of tan, carbonate matrix-supported quartz grit occurs near the top(?) of the unit. Total thickness of the unit is difficult to assess due to the affects of at least one phase of isoclinal folding overprinted by upright folds. It is probably in excess of 200 m thick with structural thicknesses of more than a kilometre.

Screw Creek Limestone

One of the most complete sections through the fossiliferous Screw Creek limestone in British Columbia is east of Screw Creek, near the border with Yukon (104O/14W; Figure 3). Along this transect the structurally lowest outcrops are decimetre thick limestone beds with planar, centimetre-thick cherty maroon and green layers, probably silicified tuffs. Facing indicators in these brightly coloured layers are not well preserved, but truncated layering gives the impression that the units are right way up. The next highest unit is calcareous sharpstone conglomerate which are clearly upside-down based on well-developed channel scours and lags (Photo 7a). Intraclasts predominate; they appear to have been derived from the cherty tuff layers. Overlying coralline boundstone is also upside-down as indicated by corals in growth position (Photo 7b). At yet higher elevations a west-closing recumbent fold hinge is traversed and the sharpstone conglomerate is repeated. A third repetition of the sharpstone conglomerate is succeeded by highly fossiliferous limestone indicating a return to inverted stratigraphy. Highest limestone exposures enclose a 2-5 metre thick tuffaceous interval containing 2 – 10 cm thick planar bedded white tuff layers interlayered near the top of the succession with decimetre thick carbonate. These lithologies are joined by black siltstone beds several centimetres thick. The highest carbonate layers contain black phyllitic clasts. Carbonate content diminishes abruptly over several metres until well-bedded black and brown siltstone and feldspathic sandstone predominate.

Photo 5. Conglomerate of the "transitional unit" of the "Klinkit assemblage".

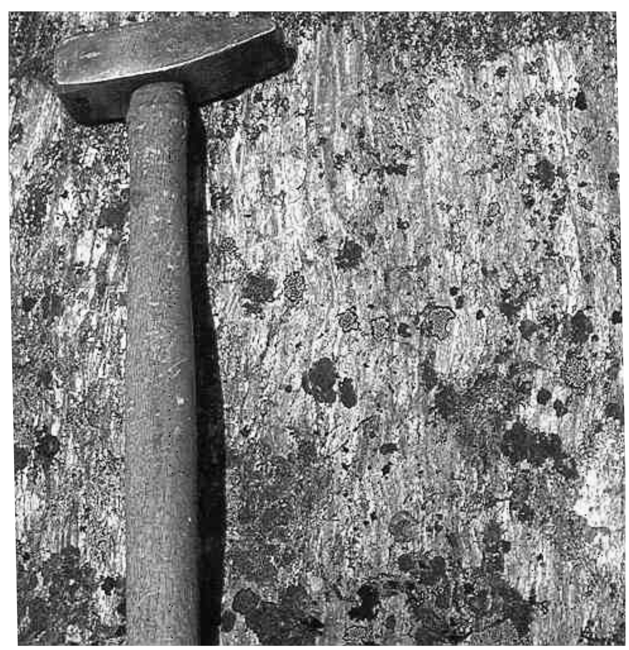

Photo 6. Strongly flattened quartz clast conglomerate, probably the "transitional unit".

Photo 7. Screw Creek limestone: (a) cross stratified overturned sharpstone conglomerate with clasts cannibalized from lower beds, and (b) rugosan boundstone with fossils preserved in overtuned growth position. Both photos are taken on the overturned limb of a regional recumbent fold.

This latter lithology apparently belongs to the "Swift River assemblage" (*see* Nelson *et al.*, 2000). If this is true, then the contact between the lowest Screw Creek limestone ("Klinkit assemblage") and "Swift River assemblage", is gradational.

GEOCHRONOLOGY

Critical age data from two units are presented here. A sample of Hazel orthogneiss was collected near a repeater tower on the south flank of Mount Hazel (located on Figure 3). Hazel orthogneiss occurs within the greenstone unit, which it apparently cuts, thereby providing a minimum age on the greenstone which underlies more than half of the map area.

A second data set is reported for a sample of intermediate to dacitic tuff that is interbedded with limestone on the north flank of Mount Francis (*see* Figure 3). It is believed to occupy one of the highest stratigraphic positions within the Big Salmon Complex (Figure 4).

Mount Hazel Orthogneiss

A sample of a massive to weakly deformed, granite from the Mt. Hazel orthogneiss yielded a modest quantity of cloudy, metamict, to less commonly clear, pale pink prismatic zircon. Eight fractions of the clearest and coarsest grains available all gave discordant results (2-10% discordant), with ellipses aligned in a linear fashion (Figure 5, Table 1). An upper intercept of $362.3^{+7.9}/_{-6.8}$ Ma (eight-point Davis regression) is interpreted as the best estimate for the igneous age of the Mt. Hazel pluton. A well-defined lower intercept of $189^{+16}/_{-17}$ Ma may correspond with the time of Pb loss. Lead loss may be due to a late deformational event which produces a strong fabric in the *circa* 196 Ma Coconino tonalite (Mihalynuk, *et al.*, 1998), whereas the *circa* 185 Ma Simpson Peak batholith (recalculated from Wanless *et al.*, 1970) is mostly undeformed.

Mount Francis Dacitic Tuff

This foliated metadacite yielded a moderate amount of cloudy to rarely clear, pale pink prismatic zircon. Seven strongly abraded fractions of the clearest grains available were analysed (Figure 6, Table 1). All of these likely show the effects of Pb loss, despite the strong abrasion. Four fractions (A, F, G and H) are discordant, and are inferred to contain significant inheritance; they give 207Pb/206Pb ages of ca. 546-1235 Ma. Fractions B and C give $^{207}Pb/^{206}Pb$ ages of about 325 Ma. The weighted average $^{207}Pb/^{206}Pb$ age for these two fractions, 325.1±3.0 Ma, provides the best estimate for the age of the rock. Slightly discordant fraction D is interpreted to contain minor inheritance. Another tuff bed from the same outcrop yields concordant fractions giving the same *circa* 325 Ma age.

PLUTONIC ROCKS

The Coconino tonalite, Simpson Peak batholith, Slaughterhouse quartz diorite, Two Ladder tonalite and Midshore granite bodies (Figure 3) were described previously by Mihalynuk *et al.* (1998). New observations in the Simpson Peak batholith show it to be compositionally and texturally variable, and the Midshore granite is now be-

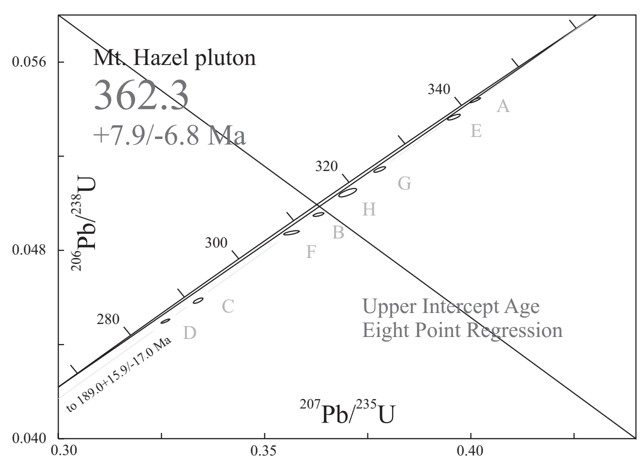

Figure 5. Concordia plot showing isotopic ratios with error estimates for four zircon (A to D) and two titanite (T1, T2) mineral fractions from the Mount Hazel orthogneiss.

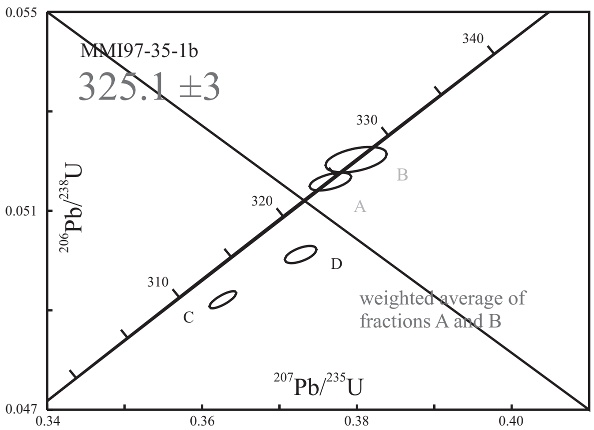

Figure 6. Concordia plot showing isotopic ratios with error estimates for zircon mineral fractions from tuff layers in limestone on the north flank of Mount Francis.

lieved to be part of a syenitic intrusive suite. These observations, together with descriptions of plutons encountered during mapping in 1999, are reported here from presumed oldest to youngest:

Charlie Cole Pluton (EJCg)

A large body of strongly foliated light grey to white-weathering granite underlies Mount Charlie Cole (Gabrielse, 1969), and a few outcrops on its northern flank extend onto southwestern 104O/12 in the present map area. It consists of medium-grained quartz (30%) and plagioclase (30%), with K-Feldspar as phenocrysts (20%) and matrix (10%), and 15% smeared, chloritized mafics (biotite?). S-C fabrics are well developed for nearly a kilometre across strike. They indicate sinistral motion on C-planes (Photo 8), but the fabric appears folded in at least one locality where shear sense switches rapidly. Charlie Cole pluton is 4 kilometres south of the inferred trace of the Teslin Fault, which trends 300°. Orientation of most of the C-planes is 185° to 020° such that

TABLE 1
ISOTOPIC DATA FOR TWO SAMPLES OF THE BIG SALMON COMPLEX

Fraction[1]	Wt (mg)	U[2] (ppm)	Pb*[3] (ppm)	$^{206}Pb/^{204}Pb$ [4]	Pb[5] (pg)	^{208}Pb[6] (%)	Isotopic ratios (1σ,%)[7] $^{206}Pb/^{238}U$	$^{207}Pb/^{235}U$	$^{207}Pb/^{206}Pb$	Apparent ages (2σ,Ma)[7] $^{206}Pb/^{238}U$	$^{207}Pb/^{206}Pb$
Mt. Francis Dacite, MMI97-35-1a: 325.1±3.0 Ma											
A c,N2,p,b	0.067	450	29	11032	10	13.2	0.06041 (0.09)	0.5265 (0.15)	0.06321 (0.08)	378.1 (0.7)	715.2 (3.5)
B m,N2,p,b	0.036	361	16	3496	10	13.6	0.04333 (0.10)	0.3163 (0.18)	0.05294 (0.10)	273.5 (0.5)	326.0 (4.5)
C f,N2,p	0.038	493	26	9843	6	14.5	0.05042 (0.14)	0.3677 (0.19)	0.05290 (0.09)	317.1 (0.8)	324.3 (4.1)
D ff,N2,p	0.010	592	33	5489	4	15.9	0.05248 (0.10)	0.3849 (0.17)	0.05320 (0.11)	329.7 (0.6)	337.4 (4.9)
F m,N2,p	0.007	493	30	2902	4	14.0	0.05577 (0.11)	0.0627 (0.18)	0.08156 (0.11)	349.8 (0.8)	1234.9 (4.4)
G f,N2,p	0.007	470	18	2041	4	10.7	0.03776 (0.14)	0.3042 (0.23)	0.05843 (0.17)	269.7 (1.1)	546.0 (7.3)
H f,N2,p	0.009	490	25	3579	4	13.2	0.04869 (0.15)	0.4661 (0.22)	0.06943 (0.13)	306.5 (0.9)	911.5 (5.4)
Mt. Hazel Pluton, MMI97-29-1: 362.3+7.9/-6.8 Ma											
A m,N2,p	0.037	349	20	7988	6	13.3	0.05438 (0.10)	0.4010 (0.16)	0.05349 (0.09)	349.5 (3.9)	349.5 (3.9)
B m,N2,p	0.025	413	21	1039	32	13.5	0.04952 (0.08)	0.3631 (0.18)	0.05317 (0.14)	336.0 (6.5)	336.0 (6.5)
C f,N2,p	0.016	534	25	6861	4	11.2	0.04586 (0.12)	0.3339 (0.18)	0.05280 (0.12)	320.1 (5.2)	320.1 (5.2)
D m,N2,p,b	0.032	719	33	8566	8	12.4	0.04499 (0.10)	0.3260 (0.16)	0.05254 (0.09)	309.1 (4.0)	309.1 (4.0)
E m,N5,p,s	0.013	599	35	4269	6	16.4	0.05366 (0.11)	0.3959 (0.20)	0.05350 (0.13)	350.2 (5.9)	350.2 (5.9)
F m,N5,p,e	0.014	240	12	1870	6	13.0	0.04875 (0.09)	0.3565 (0.26)	0.05304 (0.21)	330.5 (9.6)	330.5 (9.6)
G m,N5,p,e	0.010	489	27	4429	4	15.1	0.05144 (0.12)	0.3779 (0.19)	0.05328 (0.12)	340.8 (5.5)	340.8 (5.5)
H f,N5,p,b	0.010	560	31	2391	7	16.5	0.05045 (0.18)	0.3701 (0.29)	0.05321 (0.20)	317.3 (1.1)	337.7 (8.9)

[1] Upper case letter = zircon fraction identifier. All zircon fractions air abraded; Grain size, intermediate dimension: c=>134μm, m=<134μm and >104μm, f=<104μm and >74μm, ff <74μm;
Magnetic codes:All zircons are nonmagnetic on Franz magnetic separator at field strength of 1.8-2.0A and a sideslope of 5°. Front slope for all fractions=20°; Grain character codes: e=elongate, p=prismatic, s=stubby.

[2] U blank correction of 1pg ± 20%; U fractionation corrections were measured for each run with a double ^{233}U-^{235}U spike (about 0.005/amu).

[3] Radiogenic Pb

[4] Measured ratio corrected for spike and Pb fractionation of 0.0035/amu ± 20% (Daly collector) and 0.0012/amu ± 7% and laboratory blank Pb of 1-3pg ± 20%. Laboratory blank Pb concentrations and isotopic compositions based on total procedural blanks analy

[5] Total common Pb in analysis based on blank isotopic composition

[6] Radiogenic Pb

[7] Corrected for blank Pb, U and common Pb. Common Pb corrections based on Stacey Kramers model (Stacey and Kramers, 1975) at the age of the rock or the $^{207}Pb/^{206}Pb$ age of the fraction.

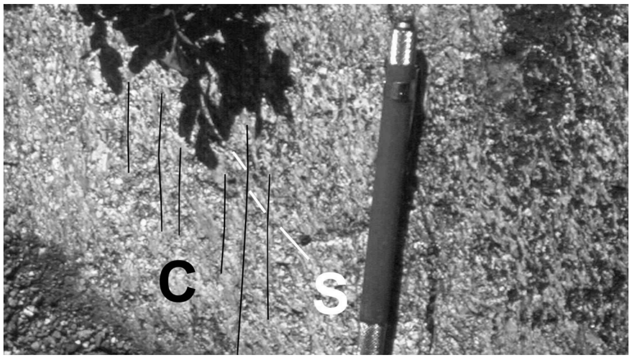

Photo 8. S-C fabrics are well displayed in outcrops on the north flank of Mount Charlie Cole about 4 kilometres south of the Teslin Fault.

their development cannot be attributed to simple kinematic linkage with the Teslin Fault. Because of apparent late folding of the S-C fabrics, their use in constraining any regional structural interpretation would be suspect. However, a sample collected for isotopic age dating should provide a maximum age for this fabric.

Simpson Peak Batholith (EJSg1, 2, 3, EJSgd)

Four lithologies comprise the Simpson Peak batholith. These are described from oldest to youngest based on field relationships:

Hornblende>biotite granite (EJSg1) with flattened pink K-feldspar megacrysts is well foliated, but poorly lineated. This unit was sampled at two localities and vantage point mapping suggests that rocks with similar weathering characteristics crop out in a gently northwest tapering wedge of pluton in northeastern 104O/12.

Medium-grained grey to tan granite (EJSg2) contains white to pink intergrowths of plagioclase and K-feldspar (60%), fresh biotite (10%, or up to 5% chloritized) and coarse smoky quartz (30%). It is blocky weathering with distinctive low angle jointing, and weathers to abundant grus. Joint surfaces may be chlorite coated. Foliation is weak to absent. It is the most abundant unit in the batholith.

Biotite porphyry dominates a gently northwest-dipping tabular complex about 240 metres thick (EJSg3). It is medium-grained,with subequant feldspar and grey quartz phenocrysts and medium to fine-grained rusty biotite, in a tan to flesh coloured, non-foliated, sucrosic siliceous matrix. Numerous 0.5 to 3 metre thick quartz dioritic sills cut the complex, giving it a strongly jointed appearance from a distance. The complex clearly cuts foliated K-feldspar megacrystic granite as do irregular fleshy pink aplitic dikelets interpreted as coeval.

Weakly to non-foliated quartz-diorite to granodiorite (EJSgd) forms medium-grained tabular zones within the batholith, and occurs as fine to medium-grained dikes that cut the sill complex porphyry.

Teh Creek Pluton (KGg)

White hornblende < biotite granodiorite, granite and lesser grey quartz diorite comprise this elongate, west northwest-trending body that stretches across mapsheet 104O/12. Mafics, including about 1% yellow-brown sphene, comprise about 16% of the rock. Slightly porphyritic K-feldspar comprises 10% (to 30% including matrix), plagioclase ~25% and xenomorphic quartz about 30% of the rock.

Originally mapped as belonging to three separate suites, including parts of the Klinkit and Simpson Peak batholiths (Gabrielse, 1969), the Teh Creek pluton is most likely an extension of the Klinkit batholith, a satellite of which is mapped east of upper Butsih Creek (just east of 104O/12). Although, the Klinkit batholith is described as foliated (Gabrielse, 1969), no planar fabric is developed within the map area. Thus, the Teh Creek pluton is treated separately. It appears to have intruded by stoping of blocks controlled by two sets of joints; north and west-northwest sets, resulting in pluton margins that are demarked by sets of orthogonal dikes (*see* headwaters of Teh Creek, Figure 3).

Early Eocene Syenite (EEsy)

Pink, varitextured, unfoliated syenite occurs as two elongate, high-level plutons east of Teslin Lake. The southern body gives way on its southern margin to a sill complex. Xenoliths of complexly folded Big Salmon Complex are common. Textures range from fine-grained, felted intergrowth of feldspar and amphibole in which feldspar phenocrysts may range from a sparse to dominant component. Feldspars are up to 3 centimetres across and are typically zoned; they have white calcic? cores and pink potassic rims. The northern pluton was called the Midshore granite by Mihalynuk *et al.* (1998). A compositionally distinctive zone at its northern end is composed of 75% coarse, zoned feldspar and is pink with tan weathering. Amphiboles are typically acicular. The southern syenite body is reported to contain the sodic pyroxene aegerine (Aitken, 1959). U-Pb isotopic analysis of zircons extracted from the Midshore granite indicate an Early Eocene age (unpublished). A sample collected from the southern body should confirm correlation with the dated pluton to the north.

New Occurrences and Mineral Potential

Several new mineralized zones were discovered during the course of mapping in 1999. They are either intrusion-related gold veins or stratabound copper-rich lenses in crinkle chert. The most prospective examples are reported below together with analytical results where available (analyzed by Instrumental Neutron Activation and Inductively Coupled Plasma Emission Spectroscopy (note that ICP digestion is by aqua regia which is incomplete for most elements); *see* also Table 2). One pyritic sericite schist is geochemically unremarkable, but it is extensive and is included below.

Assay Data from Three Mineralized Zones

West Teslin Lake border area. Along west shore of northern Teslin Lake, 6 km south of the Yukon border (just west of the map area, "1" on Figure 3), a set of moderately to steeply west to northwest dipping brittle shears, spaced about 5-10 metres apart within an Eocene granitoid body, show evidence of west-side-up movement. They are invaded by quartz veins and rusty, pyritic mineralization with rare malachite staining and variably developed alteration envelopes. One 2-3 cm thick vein with a somewhat wider than average 20 centimetre alteration envelope was chip sampled for 2.5 metres along the vein. It returned values of 1320 ppb Au, 0.4% As, and 194 ppm Sb (MMI99-22-3; Table 2; location 1 on Figure 3).

Copper in the Crinkle Chert. Numerous occurrences of minor sulphide mineralization and copper staining were encountered in the crinkle chert unit, further indication of the high mineral content of this unit as previously established by mapping in 1997. Most significantly, a chlorite-porphyroblastic, 6 metre by 0.5 metre lens with disseminated chalcopyrite returned 0.9% Cu; 0.3g Au, 2.9g Ag, 6.8% Fe, and 0.17% Ba from a chip sample across its width (MMI99-27-19, Table 2; location 2, Figure 3).

Jennings River "knee". Pyrite-rich sericite schist crops out at many localities within the map area. Most extensive are those at locality "3" on Figure 3, near the Jennings River "knee". Here it is well developed within a regional quartz-phyric horizon of probable dacite composition. Old claim posts indicate that the mineralization was known previously, but the claims were apparently never registered. The one sample analyzed did not return anomalous metal values (99JN-27-1C, Table 2). Despite scant exposures, the felsic host unit is intermittently exposed for at least 16 km (Location 3 on Figure 3). If it is indeed continuous, it could represent a significant mineralizing system that warrants further work.

DISCUSSION

In southern Yukon and British Columbia, the Big Salmon Complex can be reliably mapped on the basis of the stratigraphy presented herein. In British Columbia, it is possible to walk Big Salmon Complex greenstone from transitional greenschist-amphibolite facies near the core of the Big Salmon Complex, either southeast or northwest into greenschist-grade rocks that display good protolith textures. Stevens and Harms (1996) include the former, relatively high grade rocks with the "Hazel Assemblage", and the latter, lower grade rocks with the "Klinkit assemblage". This raises two questions: what is the usefulness of the term Big Salmon "complex" given that a coherent stratigraphy is present?, and what is the utility of this assemblage given that it is possible to trace units (like the greenstone) from higher grade "Hazel assemblage" to lower grade "Klinkit Assemblage".

Is Big Salmon Complex a Complex?

Use of the term "complex" is recommended in the North American Stratigraphic Code "…where the mapping of each separate lithic component is impractical at ordinary mapping scales. "Complex" is unranked but commonly comparable to suite or supersuite, therefore, the term may be retained if subsequent, detailed mapping distinguishes some or all of the component lithodemes or lithostratigraphic units." (NACSN, 1983, page 861). Clearly, resolution of regionally mappable units within the Big Salmon Complex does not in itself justify abandonment of the name. Future work may demonstrate justification, but in the interim, we have elected to retain the original name of "Big Salmon Complex" rather than adopt the nomenclature of Stevens and Harms (1996). Dual nomenclature is confusing and prone to misleading interpretation especially when the assemblages are implicitly fault-bounded with distinct stratigraphies and structural and metamorphic characteristics (*see* definitions of Stevens and Harms, 1996). Rigorous unit definitions together with reference sections or type localities need to be established in order to address this problem.

Big Salmon Complex-"Klinkit Assemblage" Relationships

Gabrielse (1969) showed the Big Salmon Complex as bounded to the northeast by a belt of Mississippian "Sylvester Group", including massive greenstone, chert, agglomerate and metadiorite which he designated as "unit 7"; and he showed Big Salmon Complex bounded to the southeast by the Simpson Peak batholith and other plutons in the Jennings River area. However, it is now clear that to the northeast, some "unit 7" rocks north of the Alaska Highway belong to the Big Salmon Complex. To the southeast, marker units can be traced to the "Big Bend" of the Jennings River (Figure 3, location 18), and the enclosing strata probably extend an additional 20 kilometres farther east southeast where they apparently merge with the "Klinkit assemblage" of Stevens and Harms (1996). These authors included both "unit 7" as well as the presumably younger "unit 12" chert, argillite, limestone and conglomerate of Gabrielse (1969) and units Mv and Ml of Gordey and Stevens (1994) in their informal "Klinkit assemblage". The age of the "Klinkit assemblage" is constrained by Middle Mississippian (Viséan) conodonts from limestone layers in the volcanic division (unit "Mv" of Gordey, 2000; fossil age compiled by M.J. Orchard in Poulton *et al*., 1999), by Triassic conodonts in the dark clastic division (M. Orchard *in* Harms and Stevens, 1996), and especially by the fossiliferous Screw Creek formation limestone (informal; Poole, 1956) which contains Early to Middle Carboniferous macrofossils (Abbott, 1981), early Pennsylvanian fusulinids (Gabrielse, 1969), and is structurally underlain by thin limestone layers with conodonts of Middle Penn-

TABLE 2
ANALYTICAL RESULTS FROM MINERALIZED ZONES

			Element	Au	Mo	Cu	Pb	Zn	Ag	Co	Fe	Fe	As	As
			Units	ppb	ppm	ppm	ppm	ppm	ppm	ppm	%	%	ppm	ppm
			Method[1]	INA	AICP	AICP	AICP	AICP	AICP	AICP	AICP	INA	AICP	INA
			Lab.[2]	ACT	ACM	ACM	ACM	ACM	ACM	ACM	ACM	ACT	ACM	ACT
			Dect'n Limit	2	1	1	3	1	0.3	1	0.01	0.02	2	0.5
Field No.	Mapsheet	Northing	Easting											
99JN-27-1C	104N/9E	6613006	667397	18	7	32	157	4	0.3	1	1.6	1.7	3	3.5
MMI99-22-3	104N/16	6648136	645330	1320	4	42	< 3	17	0.7	3	1.88	2.01	4420	4290
MMI99-27-19	104O/13E	6646808	349969	311	1	8786	14	155	2.9	24	6.83	8.42	< 2	4.5

			Element	Sb	Sb	Bi	V	P	Mn*	Al	Na	K	Ba	Ba
			Units	ppm	ppm	ppm	ppm	%	ppm	%	%	%	ppm	ppm
			Method[1]	AICP	INA	AICP	AICP	AICP	AICP	AICP	AICP	AICP	INA	AICP
			Lab.[2]	ACM	ACT	ACM	ACM	ACM	ACM	ACM	ACM	ACM	ACT	ACM
			Dect'n Limit	2	0.1	2	1	0	2	0.01	0.01	0.01	50	1
Field No.	Mapsheet	Northing	Easting											
99JN-27-1C	104N/9E	6613006	667397	< 3	0.2	< 3	27	0.023	183	0.57	0.11	0.33	580	88
MMI99-22-3	104N/16	6648136	645330	145	194	8	12	0.038	351	0.95	0.07	0.28	820	94
MMI99-27-19	104O/13E	6646808	349969	< 3	1.6	10	104	0.066	2044	3.99	0.07	0.27	3400	1731

1 Methods: AICP = Inductively coupled plasma, Aqua regia digestion; INA = Instrumental neutron activation

2 Lab.: ACM = Acme Analytical Laboratories Ltd., Vancouver; ACT = Activation Laboratories Ltd., Ancaster, Ontario

sylvanian age (Abbott, 1981). Stevens and Harms (1996) suggest that carbonate units within the “Klinkit assemblage” contain conodonts as young as Early Permian. However, at least part of “unit 12” of Gabrielse (1969) that Stevens and Harms (1996) included in the “Klinkit assemblage” must be older than the Screw Creek limestone based on the findings of Gleeson *et al.* (2000, this volume) who mapped four ridges underlying the northeastern limits of “unit 12”. They report U-Pb isotopic age results that constrain the age of the clastics to between Earliest Mississippian and Silurian, much older than previously expected, and much older than any lithologically comparable units in the “Klinkit Assemblage”. Such fundamental departures from recent stratigraphic interpretation show that our understanding of the Big Salmon Complex is not yet mature and that detailed tectonic syntheses involving the eastern Big Salmon Complex must be considered speculative.

Effects of Structural Complexity

Direct age comparisons are made difficult by isoclinal, mountain scale, south and southwest-verging folds and parasitic folds that exert a fundamental control on the distribution of different units. For example, the new isotopic ages reported here together with structural observations show that substantial parts of the stratigraphy are inverted by large-scale nappes, but even so, some age conflicts cannot be reconciled. Distribution of units is further complicated by both older and younger folding.

Recognition of intense, regional strain partitioning (in part related to nappes) shows that correlations cannot be reliably based on degree of strain, although local differences in metamorphic history may warrant division of units into separate assemblages. An early, nearly layer-parallel fabric is folded by the large scale folds and is commonly overprinted by a second or third schistosity imparted during subsequent deformational events.

A mid-Mississippian deformational event is well documented to the north in the Glenlyon area (M. Colpron *in* Nelson *et al.*, 2000) and in the Finlayson area (Murphy and Piercey, 1999; although it could be slightly older). This same event might have affected the Jennings River area, but the age is less tightly constrained. It is represented by deformational discordance above and below a conglomerate within the regional carbonate unit. A dike cuts folded strata that predate the conglomerate, thus providing an upper constraint on the age of deformation ~335 Ma (unpublished). The conglomerate is interpreted as a post-deformational basal facies. A maximum age limit for early deformation in the area is provided by the 354 Ma Logjam pluton (Gleeson *et al.*, 2000, this volume). This deformation may correspond to a regional collisional event during which blueschist and eclogite facies rocks were emplaced within the Yukon-Tanana Terrane *circa* 346 Ma (Erdmer *et al.*, 1998). As suggested by Murphy and Piercey (1999), this deformational pulse may prove to be a useful feature for regional correlations.

Broader map coverage and new kinematic data show that the deformational history culminated in an important north-south compressional event that affects the southern margin of the Simpson Peak batholith, although this event is not everywhere in evidence. New discovery of superb exposures of the Teslin fault along Jennings River reveal a broad zone of mylonite with sinistral kinematics, overprinted by quasi-ductile dextral fabrics (de Keijzer *et al.*, 2000), but the age and duration of these kinematic events and how they relate to deformational events in the adjacent rocks are unknown.

Stratigraphy Inverted, or Not?

The revised stratigraphy here relies heavily on the intrusive relationship of Hazel orthogneiss into greenstone, providing a minimum age of 362 Ma for the greenstone and underlying rocks. However, the contact relationship between the main body of the Hazel orthogneiss and greenstone has not been unequivocally established. Outcrop patterns support such an interpretation as do thin apophyses of orthogneiss within greenstone, but such apophyses have not been traced back to the main body of Hazel orthogneiss. No such apophysies have been recognized in presumably younger units. Neither are presumably younger units cut by the main body, even though the outcrop pattern on Figure 3 would seem to show this for both the crinkle chert and carbonate units. At three localities, the margin of the Hazel body follows and does not cross-cut crinkle chert (at Mount Hazel, and near localities 2 and 7 on Figure 3), or carbonate (north of locality 12). Where outcrop control is best, from Mount Hazel to the BC-Yukon border, the crinkle chert apparently occurs within a synformal keel immediately northeast of the Hazel orthogneiss. At Mount Hazel a septa of strongly foliated felsic, muscovite- and magnetite porphyroblast-rich tuff (?) or intrusive border phase (not shown on Figure 3) separates the chert from less deformed Hazel pluton.

Syndepositional Faulting?

The "dirty clastics" unit and crinkle chert unit are both observed to record the same deformational events and both rest depositionally atop greenstone. They rest on no other units. Crinkle chert is clearly overlain by limestone and a succession of other lithologies. In contrast, the "dirty clastics" unit is not overlain by other units west of Two Ladder Creek. If the "slate, chert, argillite, conglomerate" unit of the "Klinkit assemblage" that extends eastward from Two Ladder Creek (where it was originally included with the "dirty clastics" unit by Mihalynuk *et al.*, 1998 because of close lithologic similarity) is correlative with the "dirty clastics", then it is overlain by a "phyllite and minor limestone" unit and both are intruded by the 354 Ma Logjam intrusion (Gleeson *et al.*, 2000, this volume). Thus, the crinkle chert may have been deposited at the same time as the conglomeratic "dirty clastics", suggesting that the extents of these contrasting facies were controlled by syndepositional faults. Crinkle chert may have accumulated as mixed hydrothermal and biogenic sediment in a rift graben, protected from the influx of voluminous "dirty clastics". Similar synsedimentary faults are suggested to control mineralization controls at the Fyre Lake and Kudz Ze Kayah deposits (Murphy, personal communication, 1999). This rift event apparently marks a fundamental change in the continental arc in which the greenstone was deposited, because younger volcanic rocks in the Big Salmon Complex are much less voluminous.

An enigmatic basalt-gabbro-ultramafite succession between Teh and Butsih Creeks (southeastern 104O/12) is 2 kilometres thick and 13 kilometres long and enveloped by Big Salmon Complex greenstone. If it is an oceanic crustal fragment, the structure that emplaced it does not appear to extend west of Bareface Mountain, because greenstone crops out over extensive areas both north and south of where such a hypothetical structure should exist. Alternatively, it could have been emplaced during arc rifting and cessation of *circa* 362 Ma volcanism in the continental arc, which led to exhalative contributions and crinkle chert deposition. It does appear to sit near the top (termination?) of the greenstone succession. Alternatively, it may be a differentiated sill that pinches out to the west, in similar fashion to those believed to have been emplaced along syndepositional faults in the Finlayson area (Murphy and Piercy, 1999). In either case, such faults are important conduits for mineralizing fluids and the coincidence of 95th percentile regional geochemical results in this area (Cook and Pass, 2000, this volume) may reflect such a mineralizing system. Geochemical results aimed at this problem are pending.

SUMMARY

U-Pb isotope geochronological data is key to unraveling the stratigraphy and geological history of the Big Salmon Complex and adjacent terrains. Two new age dates are reported here. A 362 Ma age from the Hazel orthogneiss provides a minimum age for the greenstone, which it appears to intrude, and underlying rocks. The other isotopic age is 325 Ma from some of the structurally highest felsic tuffaceous units. These ages require that most of the stratigraphy outlined by Mihalynuk *et al.* (1998) is inverted. Regardless of the stratigraphic younging direction, the greenstone-chrinkle chert-limestone marker succession can be confidently traced throughout the Big Salmon Complex in British Columbia and southernmost Yukon (*cf.* Roots *et al.*, 2000), and a crude metallogenic history can be pieced together.

Vigorous continental arc volcanism in the late Devonian to Early Mississippian (*circa* 370-360 Ma) resulted in the accumulation of voluminous, submarine, dominantly mafic tuff and tuffite on a substrate of pericratonic strata. A pulse of felsic volcanism and arc rifting and probably marks the end of the magmatic cycle and the formation and preservation of a regionally developed exhalative chert horizon known as the "crinkle chert" as well as coeval clastic facies preserved in fault-bounded basins. Felsic volcanic intervals immediately beneath the crinkle chert commonly contain pyritic quartz-sericite schist intervals. These may serve as potential pathways to volcanogenic massive sulphide deposits. Within the crinkle chert, a Cu-Zn-Fe-Mn-Ba-rich lens several metres long points to the potential for volcanogenic exhalative deposits.

Carbonate deposition atop crinkle chert probably marks a rise in carbonate productivity in the Early Mississippian, following the Late Devonian crisis and extinction reef organisms. Thick carbonate banks probably coexisted with basins in which terrigenous clastics were deposited. Complex facies may have been linked by pulses of volcanism and widespread tuff deposition. A mid-Mississippian deformational event (between 354 and 335 Ma) may have peaked with emplacement of 346 Ma eclogite and blueschist (*cf*. Erdmer *et al.*, 1998). It caused uplift and erosion of units and deposition of widespread conglomeratic facies. The ensuing strata display at least as much lithologic variability as do pre-deformation sediments, but felsic volcanism is again proximal as it was at the close of greenstone deposition. Base metal sulphides are associated with these felsic volcanics such as at the Arsenault property.

The youngest Big Salmon Complex strata recognized in the Jennings River area are 325 Ma dacitic tuffs in carbonate. They do not correspond in any way to a clear break in deposition, and much younger Big Salmon Complex strata could exist in other areas. Peak metamorphism predates the 196 Ma Coconino tonalite and may have occurred around 270 Ma when blueschist and eclogites were incorporated into the Yukon Tanana Terrane (Erdmer *et al.*, ibid.). The youngest regional deformational event produced a strong fabric in the ~196 Ma Coconino tonalite, but affected only the southern margin of the *circa* 185 Ma Simpson Peak batholith. Youngest magmatism is Eocene, and one Eocene pluton west of north Teslin Lake hosts a set of veins with elevated gold values. Clearly, the area has a long and complex history and significant mineral potential.

ACKNOWLEDGMENTS

Thanks to Tom Gleeson for top notch field assistance and to Steve Gordey (GSC) and Tekla Harms (Amherst College) for sharing their regional geological insight. Ed Balon and Wojtek Jakubowski of Fairfield Resources provided access to their Cabin Lake property and freely shared their ideas about mineral potential in the Big Salmon Complex. Geoff Bradshaw, James Smith and Terry Tucker of Brett Resources provided access to their Cariboo Creek property and a steady flow of observations (together with hand samples) during their stay in our camp. Retrospective thanks to Andy Page of Fireweed Helicopters who helped to develop both our rapid bush-crash technique and our resilience to thigh-deep swamp water. Flying skills and keen eye of Denny Dennison (Coyote Air) greatly aided our aerial reconnaissance. His air sickness tips were appreciated, if ultimately futile. Our successful field season is owed in part to the hospitable Breeden family at Morley River Lodge. Critical review by Dave Lefebure is gratefully acknowledged.

REFERENCES

Abbott, J.G. (1981): Geology of the Seagull Tin District; in Yukon Exploration and Geology 1979-1980, *Indian and Northern Affairs Canada,* pages 32-44.

Aitken, J.D. (1959): Atlin Map-area, British Columbia; *Geological Survey of Canada*, Memoir 307, 89 pages.

Creaser, R.A., Erdmer, P., Stevens, R.A. and Grant, S.L. (1997): Tectonic affinity of Nisutlin and Anvil assemblage strata from the Teslin Tectonic Zone, Northern Canadian Cordillera: Constraints from neodymium isotope and geochemical evidence; *Tectonics,* Volume 16, pages 107-121.

Colpron, M. (1999): Glenlyon project: Preliminary stratigraphy and structure of Yukon-Tanana Terrane, Little Kalzas Lake area, central Yukon (105L/13); *in* Roots, C.F. and Emond, D.S. (editors), Yukon Exploration and Geology 1998, Exploration and Geological Services Division, Yukon, *Indian and Northern Affairs Canada*, pages 63-71.

Cook, S. and Pass, H. (2000): Ancient Pacific Margin Part V: Preliminary results of geochemical studies for VMS deposits in the Big Salmon Complex, Northern British Columbia, in Geological Fieldwork 1999, *B.C.Ministry of Energy and Mines*, Paper 2000-1, this volume.

deKeijzer, M., Williams, P. and Brown, R.L. (1999): Kilometre-scale folding in the Teslin zone, northern Canadian Cordillera, and its tectonic implications for the accretion of the Yukon-Tanana Terrane to North America; *Canadian Journal of Earth Science*, Volume 36, pages 479-494.

de Keijzer, M., Mihalynuk, M.G. and Johnston, S.T. (2000): Structural investigation of an exposure of the Teslin Fault; in Current Research, *Geological Survey of Canada*, Paper 2000-A, (in press).

Dixon-Warren, A. and Hickin, A. (2000): Ancient Pacific Margin NATMAP Part IV: Surficial mapping and till geochemistry in the Swift River Area, north western British Columbia; in Geological Fieldwork 1999, *B.C. Ministry of Energy and Mines*, Paper 2000-1, (in press).

Erdmer, P. (1985): An examination of cataclastic fabrics and structures of parts of Nisutlin, Anvil and Simpson allochthons, central Yukon: test of the arc-continent collision model; *Journal of Structural Geology*, Volume 7, pages 57-72.

Erdmer, P. and Helmstaedt, H. (1983): Eclogite from central Yukon: a Record of subduction at the western margin of Ancient North America; *Canadian Journal of Earth Sciences*, Volume 20, pages 1389-1408.

Erdmer, P. and Armstrong, R.L. (1989): Permo-Triassic isotopic dates for blueschist, Ross River area, Yukon; *in* Yukon Exploration and Geology, Volume 2: Exploration and Geological Services Division, Yukon, I*ndian and Northern Affairs Canada*, pages 33-36.

Erdmer, P., Ghent, E.D., Archibald, D.A. and Stout, M.Z. (1998): Paleozoic and Mesozoic high pressure metamorphism at the margin of ancestral North America in central Yukon; Geological Society of America Bulletin, Volume 110, pages 615-629.

Gabrielse, H. (1969): Geology of the Jennings River Map-Area, British Columbia (104-O); *Geological Survey of Canada*, Paper 68-55.

Gleeson, T.P., Friedman, R.M. and Wahl, K. (2000): Stratigraphy, structure, geochronology and provenance of the Logjam Creek area, northwestern British Columbia (NTS

104O/14W); in Geological Fieldwork 1999, *B.C. Ministry of Energy and Mines*, Paper 2000-1, (in press).

Gordey, S.P. (1995): Structure and Terrane Relationships of Cassiar and Kootenay (Yukon-Tanana) Terranes, Teslin Map Area, Southern Yukon Territory; *in* Current Research 1995-A; *Geological Survey of Canada*, pages 135-140.

Gordey, S.P. (2000): Geology, Teslin, Yukon Territory (105C); *Geological Survey of Canada,* Open File 2886, scale 1:250 000.

Gordey, S.P. and Stevens, R.A. (1994): Preliminary interpretation of bedrock geology of the Teslin area (105C), southern Yukon; *Geological Survey of Canada*, Open File 2886, scale 1:250 000.

Hansen, V.L. (1989): Structural and kinematic evolution of the Teslin suture zone, Yukon: Record of an ancient transpressional margin; *Journal of Structural Geology*, Volume 11, pages 717-733.

Hansen, V.L., (1992a): P-T Evolution of the Teslin suture zone and Cassiar tectonites, Yukon, Canada: evidence for A- and B-type subduction; *Journal of Metamorphic Geology*, Volume 10, pages 239-263.

Hansen, V.L. (1992b): Backflow and margin-parallel shear within an ancient subduction complex; Geology, Volume 20, pages 71-74.

Hansen, V.L., J.K. Mortensen, and Armstrong, R.L. (1989): U-Pb, Rb-Sr, and K-Ar isotopic constraints for ductile deformation and related metamorphism in the Teslin suture zone, Yukon-Tanana terrane, south-central Yukon; *Canadian Journal of Earth Sciences*, Volume 26, pages 2224-2235.

Hansen, V.L., M.T. Heilzer, and Harrison, T.M. (1991): Mesozoic thermal evolution of the Yukon-Tanana composite terrane: New evidence from 40Ar/39Ar data; *Tectonics*, Volume 10, pages 51-76.

Harms, T.A. and Stevens, R.A. (1996): A working hypothesis for the tectonostratigraphic affinity of the Stikine Ranges and a portion of the Dorsey Terrane; in Cook, F. and Erdmer, P. (compilers), Slave-Northern Cordillera Lithospheric Evolution Transect and Cordilleran Tectonics Workshop Meeting, *University of Calgary*, Lithoprobe Report No. 50, pages 93-95.

Mihalynuk, M.G., Nelson, J. and Friedman, R.M. (1998): Regional geology and mineralization of the Big Salmon Complex (104N NE and 104O NW) in Geological Fieldwork 1997, *B.C. Ministry of Employment and Investment*, Paper 1998-1, pages 157-170.

Mortensen, J.K. (1992): Pre-mid-Mesozoic tectonic evolution of the Yukon-Tanana terrane, Yukon and Alaska; *Tectonics*, 11, pages 836-853.

Mortensen, J. K., Ghosh, D.K. and Ferri, F. (1995): U-Pb geochronology of intrusive rocks associated with copper-gold porphyry deposits in the Canadian Cordillera; in Porphyry Deposits of the Northwestern Cordillera of North America, Schroeter, T.G., Editor, Canadian Institute of Mining, Metallurgy and Petroleum; Special Volume 46, pages 142-158.

Mulligan, R. (1963): Geology of the Teslin Map-Area, Yukon Territory; Geological Survey of Canada, Memoir 326, 96 pages.

Murphy, D.C. and Piercey, S.J. (1999): Finlayson project: Geological evolution of Yukon-Tanana Terrane and its relationship to Campbell Range belt, northern Wolverine Lake map area, southeastern Yukon; in Roots, C.F. and Emond, D.S. (editors.), Yukon Exploration and Geology 1998, Exploration and Geological Services Division, Yukon, Indian and Northern Affairs Canada, pages 47-62.

Nelson, J.L., Mihalynuk, M. G., Murphy, D.C., Colpron, M., Roots, C.F., Mortensen, J.K. and Friedman, R.M. (2000): Ancient Pacific Margin Part II: A preliminary comparison of potential VMS-hosting successions of Yukon-Tanana Terrane, from Finlayson district to northern British Columbia; *in* Geological Fieldwork 1999, *B.C. Ministry of Energy and Mines*, Paper 2000-1, (this volume).

North American Commission on Stratigraphic Nomenclature (1983): North American stratigraphic code; The American Association of Petroleum Geologists Bulletin, Volume 67, pages 841-875.

Poole, W.H. (1956): Geology of the Cassiar Mountains in the vicinity of the Yukon-British Columbia boundary; unpublished Ph.D. thesis, Princeton University, 247 pages.

Poulton, T., Orchard, M.J., Gordey, S.P. and Davenport, P. (1999): Selected Yukon fossil determinations; *in* Yukon digital geology, S.P. Gordey and A.J. Makepeace (compilers), *Geological Survey of Canada*, Open File D3826, *and* Exploration and Geological Services Division, Yukon, *Indian and Northern Affairs Canada*, Open File 1999-1(D).

Roots, C.F., de Keijzer, M., Nelson, J.L. and Mihalynuk, M.G. (2000): Revision mapping of the Yukon-Tanana and equivalent terranes in northern B.C. and southern Yukon between 131° and 132°W; in Current Research, Geological Survey of Canada, Paper 2000-1A, pages (in press).

Stevens, R.A. (1992): Regional geology, fabric and structure of the Teslin suture zone in Teslin map area, Yukon Territory; in Current Research, Geological Survey of Canada, Paper 92-1A, pages 287-296.

Stevens, R.A. (1994): Geology of the Teslin suture zone in parts of Laberge (105E/1), Quiet Lake (105F/4) and Teslin (105C/11, 13, 14) map areas, Yukon Territory; Geological Survey of Canada, Open File 2768.

Stevens, R.A. and Erdmer, P. (1993): Geology and Structure of the Teslin suture zone and related rocks in parts of Laberge, Quiet Lake and Teslin map areas, Yukon; in Current Research, Geological Survey of Canada, Paper 93-1A, pages 22-20.

Stevens, R.A. and Harms, T.A. (1995): Investigations in the Dorsey Terrane, Part 1: Stratigraphy, Structure and Metamorphism in the Dorsey Terrane, Southern Yukon Territory and Northern British Columbia; in Current Research, Geological Survey of Canada, Paper 95-1A, pages 117-128.

Stevens, R.A. and Harms, T.A. (1996): Geology in the vicinity of the Dorsey Range, southern Yukon Territory and northern British Columbia; scale 1:50 000; in Cook, F. and Erdmer, P. (compilers), Slave-Northern Cordillera Lithospheric Evolution Transect and Cordilleran Tectonics Workshop Meeting, University of Calgary, Lithoprobe Report No. 50, pages 222-225.

Stevens, R.A., Erdmer, P., Creaser, R.A. and Grant, L.S. (1996): Mississippian assembly of the Nisutlin assemblage: Evidence from primary contact relationships and Mississippian magmatism in the Teslin tectonic zone, part of the Yukon-Tanana Terrane of south-central Yukon; Canadian Journal of Earth Sciences, Volume 33, pages 103-116.

Tempelman-Kluit, D.J. (1979): Transported cataclasite, ophiolite and granodiorite in Yukon: evidence of arc-continent collision; Geological Survey of Canada, Paper 79-14.

Wheeler, J.O., Brookfield, A.J., Gabrielse, H. Monger, J.W.H., Tipper, H.W. and Woodsworth, G.J. (1991): Terrane map of the Canadian Cordillera; Geological Survey of Canada, Map 1713A.

Appendix I: Notes on Figure 3

Thick Quaternary deposits completely blanket some parts of the map area for tens of square kilometres. These are problem areas in which tenuous extrapolations are required to produce the map of Figure 3. Many extrapolations, if correct, carry important implications. Other extrapolations, drawn to mimic local structural style, imply detailed knowledge of unit distributions that does not exist. Most limitations of Figure 3 will become apparent with future publication of 1:50 000 scale Open File maps which will show inferred contacts and limits of outcrop; however, many of the following remarks are germane to those maps as well. The numbered points below correspond to the numbers, ordered from north to south, enclosed by triangles on Figure 3.

1. Western contacts of the Screw Creek limestone have not been found in the Screw Creek valley bottom. Lowest exposures of limestone are apparently right way up based on poorly preserved grading in siliceous tuffaceous layers. Structurally higher parts of the limestone are clearly upside down (described above).
2. Crinkle chert occurs in the old Alaska Highway road cut, but the area to the west is swamp; no greenstone is mapped.
3. This contact is well constrained between the elongate pluton of presumed Jurassic age and the Alaska Highway, but has not been observed north or south of those points.
4. The syncline is constrained along the shoreline and near "4". However, closure could not be confirmed by mapping. Felsic volcanics on the southern limb are locally very siliceous and might be a volcanic-crinkle chert hybrid.
5. Closure of the fold has not been demonstrated unequivocally. However, all indications point to fold closure: only greenstone is mapped along the Smart River road, both limbs have been mapped to within a couple kilometres of the hinge and layer-cleavage relationships on the limbs are consistent with closure.
6. Mapping of 104O/14W is incomplete. Low outcrops in the downstream stretches of the Screw Creek valley include small areas of limestone, perhaps hinges of folds developed on the lower limb of the Screw Creek limestone.
7. Crinkle chert occurs as a large area of angular boulders atop Hazel orthogneiss where it is assumed to be locally derived. Crinkle chert is known to occur along the contact of the Hazel orthogneiss at location 2 and near the Peak of Mount Hazel.
8. Only small lenses of carbonate are found in the axial zone of the fold. Carbonate on the fold limbs apparently grades laterally into graphitic wacke near the fold core.
9. Only three areas of outcrop constrain the eastern limestone belt south of the Alaska Highway. One is near the north margin of the Simpson Peak batholith another is south of central Swan Lake on Hook Creek (creek not shown on Figure 3), and third is an area of sparse outcrops in the forest west of Swan Lake. At none of these localities is the crinkle chert unit exposed.
10. Geology near "10" and an equal distance due north of the highway has been compiled mainly from vantage point mapping. It requires confirmation by direct observations.
11. Orthogneiss near Mt. Francis is lithologically similar to the Hazel orthogneiss in many respects; however, it apparently cuts younger stratigraphy. It is presumably between 362 and 335Ma, because it is younger than the greenstone, but is overlain by conglomerate believed derived subsequent to a deformational event around 345 Ma. (*see* Discussion).
12. Only scattered outcrops of limestone and greenstone cut by tonalite are present at the southern end of the carbonate belt. More persistent outcrop near the northern end of the belt leads to a map pattern that implies that the Hazel orthogneiss also cuts the limestone, but this is probably not the case. It appears more likely that the limestone belt outlines a tight synformal keel that is bent to the west and extends over the Hazel orthogneiss (*see* location 7). The crinkle chert unit was apparently not deposited at this locality below the limestone.
13. All contacts between Coconino tonalite and Simpson Peak batholith are covered. Since Coconino tonalite is older and more deformed than the Simpson Peak batholith, the interpreted contact configuration is meant to show the former cut by the latter.
14. Teh Creek pluton is shown as an elongate body trending 290°. In fact, most of the central portion traversed by Teh Creek is covered and two separate bodies could be present. However, the plutonic rocks exposed at either end of the body lithologically indistinguishable, and the body is known to continue in similar fashion to the east beneath a carapace of Klinkit assemblage rocks to where it is exposed in the Butsih Creek valley. Several correlated geochemical anomalies coincide with carapace rocks in easternmost 104O/12 (near 19; *see* also Cook and Pass, 2000, this volume).
15. Felsic volcanics are not mapped north of "15", but are shown extending through a covered area to the limestone belt because of their common association with limestone elsewhere.
16. As is the case for locality "14", no outcrop exists to support the interpretation of a continuous septa of greenstone. However, clear relationships occur at both the western and eastern ends of the septa. The contact shown between greenstone and Klinkit argillite is purely conjectural.
17. Teslin fault is beautifully exposed here (*see* deKeijzer *et al.*, 2000).
18. A tight synformal keel of crinkle chert and limestone is enveloped by greenstone. In particular, limestone layers are strongly folded and rodded, producing a "false stretched monomict conglomerate" in which the apparent stretched limestone "cobbles" are actually decapitated, isoclinal interference folds. Protolith textures are destroyed due to the coincidence of interference fold cores; however, good protolith textures are displayed in greenstone where it occurs out along the relatively planar fold limbs.
19. Teh Creek pluton in subsurface produces hornfels and multielement geochemical anomalies in local stream sediments (*see* "14" above and Cook and Pass, this vol-

ume). Roof rocks are cut by abundant thick dikes and the pluton is again exposed in Butsih valley to the east.

20. Cherty argillite believed to be part of the Cache Creek Kedahda Formation is strongly hornfelsed near the intrusive contact.
21. Most of the unit is covered within 5 kilometres of the River. Observations are restricted to within 2 kilometres of the northern contact.
22. A few scattered outcrops of strongly foliated, blue grey limestone occur in the middle of a broad glacial outwash plain east of Kachook Creek. They are included with the Permian Teslin Formation based only upon lithological similarity. Thus, the trace of the Teslin Fault must run to the north, down the Jennings River.
23. Both northwest and northeast contacts of the Charlie Cole pluton are covered.

Ancient Pacific Margin Part III: Regional Geology and Mineralization of the Big Salmon Complex (NTS 104N/9E,16 & 104O/12,13,14W)

By Mitchell G. Mihalynuk[1], JoAnne L. Nelson[1], Charlie F. Roots[2], Richard M. Friedman[3] and Martin de Keijzer[4]

KEYWORDS: *Regional geology, Big Salmon Complex, Nisutlin Assemblage, Klinkit Assemblage, Swift River Assemblage, Yukon-Tanana Terrane, Kootenay Terrane, Dorsey Terrane, Slide Mountain Terrane, Teslin Fault, volcanogenic massive sulphide, mineralization, Atlin, Teslin, Jennings River.*

INTRODUCTION

Regional geological mapping of the Big Salmon Complex in northwestern British Columbia (104N/09 & 16 and 104O/12, 13 & 14W, Figure 1) was conducted in 1999 under the aegis of the Ancient Pacific Margin National Mapping Program (NATMAP, *cf*. Nelson, *et al.*, 2000, this volume; Roots, *et al.*, 2000). This mapping builds on 1997 reconnaissance mapping (Mihalynuk *et al.*, 1998) that confirmed long-standing correlations between the Big Salmon Complex in British Columbia and the Yukon (*e.g.* Mulligan, 1963; Gabrielse, 1969; Figure 2).

[1] *Geolgical Survey Branch, British Columbia Ministry of Energy and Mines, PO Box 9320 Stn Prov Govt, Victoria, British Columbia V8W 9N3; Email: mitch.mihalynuk@gems5.gov.bc.ca*

[2] *Yukon Geology Program, Canada-Yukon Geoscience Office, 2099-2nd Avenue, Whitehorse, Yukon, Y1A 1B5*

[3] *Department of Earth and Ocean Sciences, University of British Columbia, 6339 Stores Road, Vancouver, British Columbia, V6T 2B4*

[4] *Department of Geology, University of New Brunswick, PO Box 4400, Fredricton, New Brunswick, E3B 5A3*

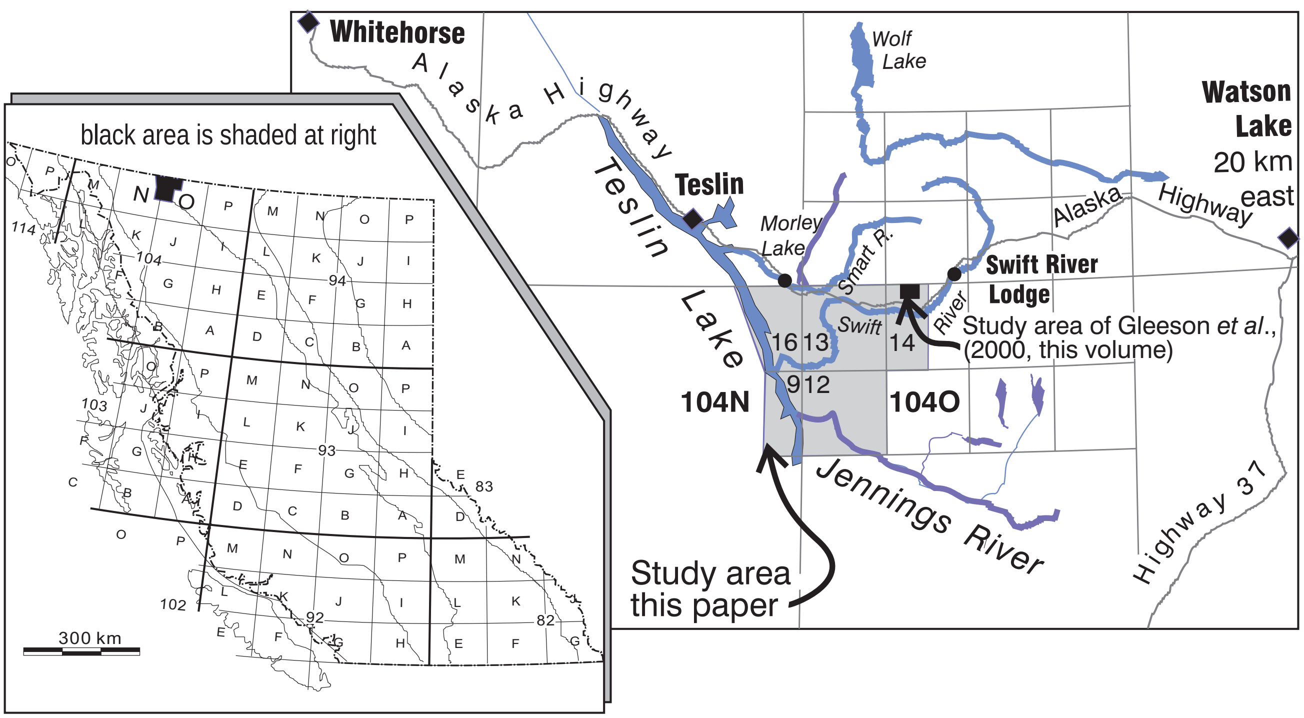

Figure 1. Location map showing the location of the Big Salmon Complex study area in northern British Columbia and southern Yukon (after Roots *et al.*, 2000). The area of Figure 3 is shown by the shading.

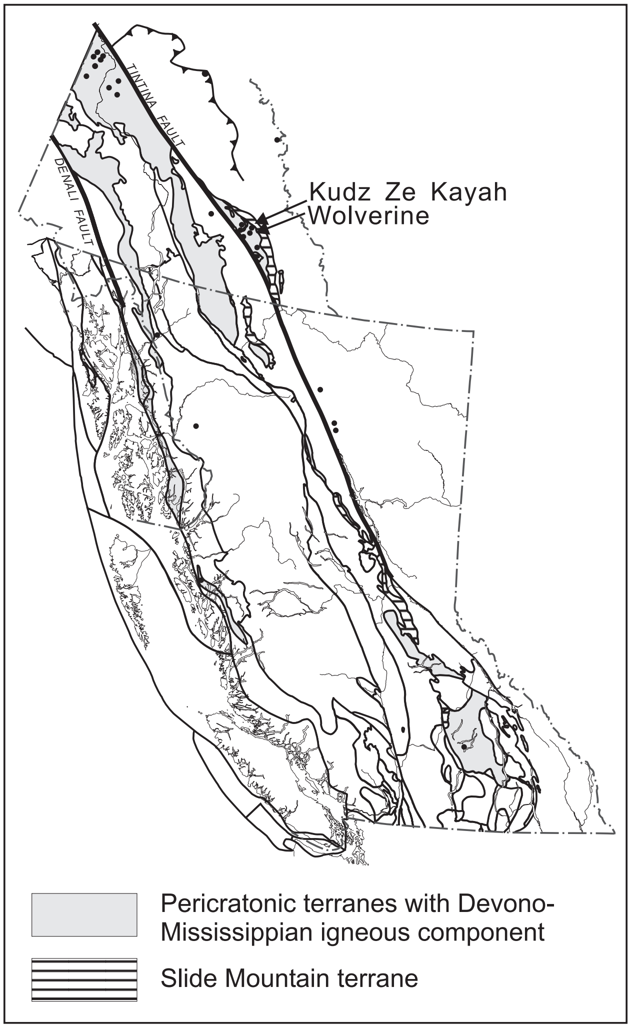

Figure 2. Tectonic assemblage map showing the approximate distribution of Yukon-Tanana and Slide Mountain terranes. Modified after Wheeler *et al*. (1991).

In southern Yukon, Big Salmon Complex rocks have subsequently been included with the Kootenay Terrane (Gordey, 1995) which include the Lower and Middle Units of the Yukon-Tanana Terrane as used by Mortensen (1992). This correlation is important because Yukon-Tanana Terrane rocks, historically ignored by mineral exploration geologists, have been the focus of mineral exploration programs since 1993 with the discovery of mineralized float at what came to be the Kudz Ze Kayah deposit. Other exploration successes include the Wolverine and Fyre Lake volcanogenic massive sulphide deposits.

Highlights of the 1999 field program are reported here together with descriptions of map units and geological relationships, and new insights. Mihalynuk *et al.* (1998) describe units encountered in the 1997 field season and present a structural synthesis, the details of which are not repeated here.

LOCATION AND PHYSIOGRAPHY

During the six week field program (early July to mid-August), mapping concentrated on low-lying, tree or swamp-covered areas (Photo 1) that occupy more than 90% of the area bounded by the British Columbia-Yukon border on the north, Teslin Lake on the west, Mount Charlie Cole to the south and Simpson Peak to the east (Figure 3). Most of the area is covered by fluvial and glacial deposits that attain thicknesses of 40 metres or more (Dixon-Warren and Hickin, 2000, this volume); although, air photo analysis and fixed wing aerial reconnaissance revealed that outcrop is more abundant than indicated on previous maps (Gabrielse, 1969). Reaching the outcrops can, however, be a challenge, usually requiring foot travel between swamps that provide the only helicopter landing spots.

The map area is accessed from the Alaska Highway, which crosses it near the Yukon border, between Watson Lake and Whitehorse (Figure 1). Only three rough secondary roads reach more than a kilometre from the highway. These mineral exploration roads; each extend about 10 kilometres in British Columbia. Two lead into the Yukon, up the west side of Logjam Creek and east side of Smart River valleys. However, washouts on the Smart River Road render it impassable after a few kilometres. Another road, constructed to provide access to the Arsenault property, can only be traveled as far as the Swift River where the bridge has long since washed away. Fuel and rudimentary supplies are available at Swift River and Morley River Lodge, just outside the eastern and western limits of the map area, respectively.

Charter fixed wing aircraft are available year round at Teslin from Teslin Lake or at a converted military gravel strip, both, about 45 kilometres west of the map area. Charter helicopters are available year round from Atlin, about 80 air kilometres west of the map area.

GEOLOGIC FRAMEWORK

Most of the field area is underlain by the Big Salmon Complex (Figure 3). Dominant protoliths are mafic vol-

Photo 1. An aerial view of the low-lying, swamp and tree-covered Nisutlin Plateau near the south end of Teslin Lake.

canic rocks, quartz-rich clastic sediments, and intrusive rocks of diorite, tonalite and leucogranite composition. Felsic tuff, crystalline limestone and chert-exhalite units are volumetrically minor, but conspicuous and mappable units. A lower amphibolite grade "core zone" in which protolith textures are mostly destroyed, is broadly parallel to the northwest trend of the Big Salmon Complex, and is flanked by greenschist grade rocks to both the southwest and northeast in which relict protolith textures may be relatively well preserved. Metamorphosed tonalite, lesser diorite and minor leucogranite, herein called the Hazel orthogneiss, dominate the north-central part of the "core zone" (Figure 3).

Big Salmon Complex rocks are bounded to the southwest by Teslin Lake (Teslin fault, *see* de Keijzer *et al.*, 2000) and Cache Creek Terrane in the Atlin area (Aitken, 1959; Figure 3). They clearly extend northwest into the Yukon (Roots *et al.*, 2000) and are probably equivalent to Mississippian volcanics in the Teslin area (unit Mv of Gordey and Stevens, 1994; Gordey, 2000). Relationships with rocks to the southeast and northeast are less certain (*see* Discussion).

Both Aitken (1959) and Gabrielse (1969) considered the Big Salmon Complex to be at least partly correlative with the Sylvester Group (Slide Mountain Terrane) based upon the abundance of mafic volcanic protoliths, but this assignment is not supported by more recent data. For example, Mihalynuk *et al.* (1998) showed that the Big Salmon Complex greenstones are geochemically like continental arc volcanics, not mid ocean ridge basalts typical of the Slide Mountain Terrane. Along strike in the Teslin zone, Creaser *et al.* (1997) showed that the geochemistry of both sedimentary and volcanic rocks lithologically correlative with the Big Salmon Complex is not permissive of genesis in the Slide Mountain ocean basin because εNd values are strongly negative (+0.5 to –26.2), indicating a significant continental component.

Tempelman-Kluit (1979) interpreted rocks in the Yukon that are equivalent to, and along strike with the Big Salmon Complex as part of a subduction/collisional complex (Teslin suture zone), a contention supported by discovery of relict high pressure metamorphic assemblages including eclogite (Erdmer and Helmstaedt, 1983; Erdmer, 1985; Erdmer and Armstrong, 1989). Working along the western part of the Big Salmon Complex, Hansen (1989, 1992a, 1992b) and Hansen *et al.* (1989, 1991) claimed to outline a fossil Permo-Triassic subduction zone with off-scraped sediments affected by tectonic backflow. More recent work by Stevens (1992, 1994), Stevens and Erdmer (1993), Stevens and Harms (1995), Stevens *et al.* (1996) and Colpron (1999) shows that the Teslin "suture zone" is comprised not of mélange of off-scraped oceanic sediments and subduction zone tectonites, but of continental margin strata (Creaser *et al.*, 1997) with relatively coherent stratigraphic relationships. This coherent stratigraphy has enabled the definition of a polydeformed nappe (deKeijzer and Williams, 1999) within the former Teslin suture zone. Likewise, a persistent stratigraphy can be traced throughout the study area, and none are composed of scaly subduction mélange.

STRATIGRAPHIC FRAMEWORK

A persistent stratigraphy provides the foundation for correlating from one area to another in the Big Salmon Complex. In British Columbia, three distinctive and contrasting units are recognized as forming a marker succession (Mihalynuk *et al.*, 1998; Figure 4). Based on new isotopic and geologic constraints, their stratigraphic order, from oldest to youngest is now known to be:

- 1200 m of tuffite-dominated greenstone;
- 30-150 m of buff to grey weathering limestone with metre-thick tuffaceous and thin centimetre to decimetre quartzite layers;
- 20-50 m of thinly bedded, finely laminated manganiferous crinkle chert/quartzite with muscovite partings;

This marker succession persists in southeast and northwest 104O/13 and south-central 104O/12. In northern 104N/16 a hybrid unit having some characteristics of felsic tuff mixed with crinkle chert occurs in place of the crinkle chert unit.

Two other more broadly defined rock packages are recognized:

- >150 m of dirty clastics: brown to tan wacke, stretched quartzite-pebble and granule conglomerate and slate;
- >1000 m of heterolithic, quartz-rich clastics interbedded with thin limestone and mafic and felsic tuffs.

Lacking age control, Mihalynuk *et al.* (1998) concluded that the "dirty clastics" were considerably younger than the unconformably underlying greenstone unit, because they contained clasts that appeared to be derived from the older polydeformed and polymetamorphic units. And because the "dirty clastics" unit was observed to sit only on the greenstone unit, greenstone was considered the next youngest unit, prompting the conclusion: "A thick greenstone and overlying clastic strata within the Big Salmon Complex of British Columbia have no obvious correlatives within the Yukon-Tanana Terrane and may be considerably younger."

Subsequent petrographic analysis showed that polydeformed phyllite clasts within the "dirty clastics" succession were deformed *in situ*, and were not derived from a previously deformed terrain. Two fabrics shown by the phyllite clasts are seen in thin section to be weakly developed in adjacent, phyllosilicates-poor quartzite clasts (Photo 2). Furthermore, new isotopic age data from samples of the former lower (Mt. Francis dacite at 325 Ma) and upper (Hazel orthogneiss at 362 Ma) parts of the stratigraphy require that the stratigraphy of Mihalynuk *et al.* (1998) is inverted, with important consequences for regional correlations (*see* Geochronology and Discussion). A revised stratigraphy is shown in Figure 4.

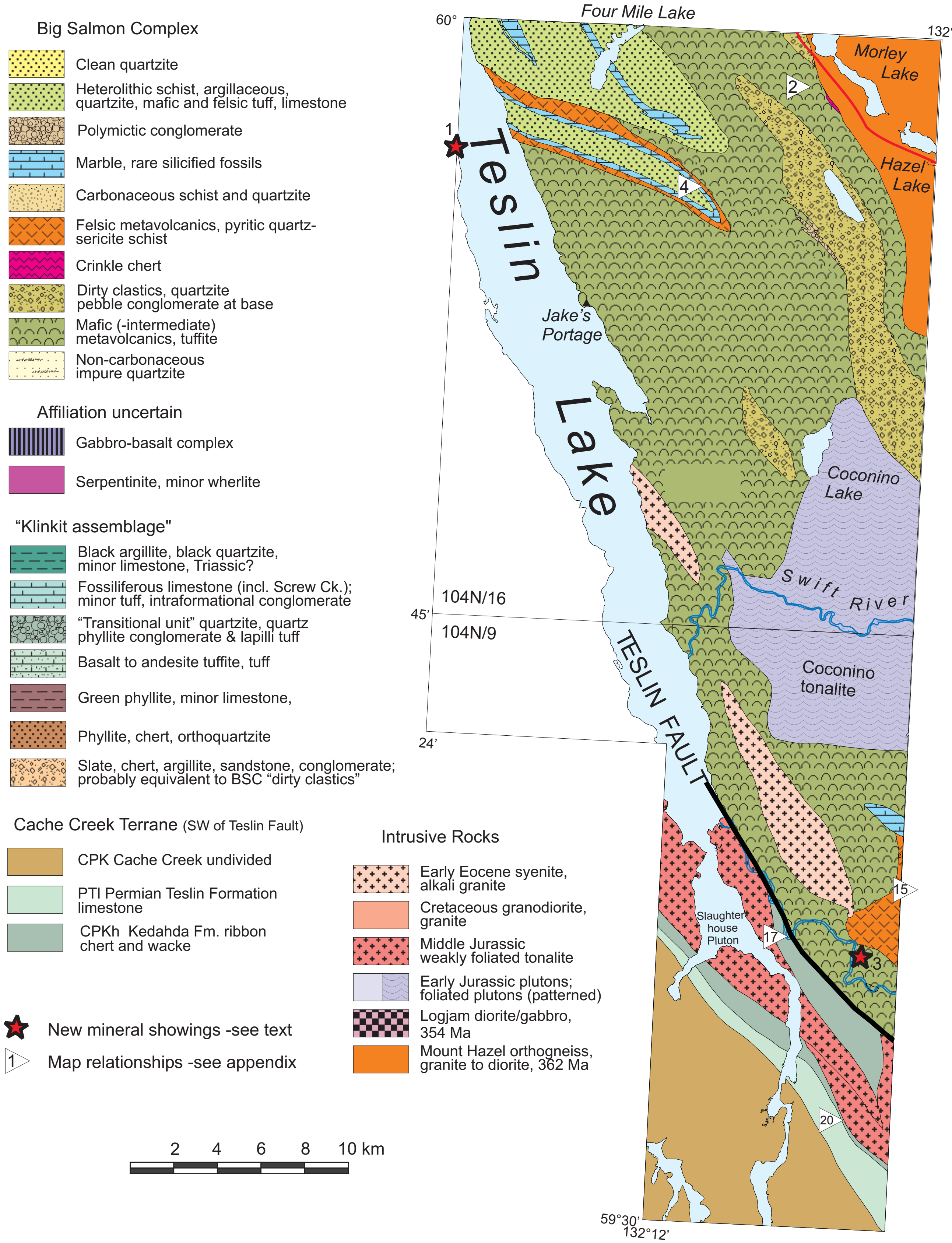

Figure 3. Generalized geology of the map area showing place names, access roads and sample sites referred to in the text.

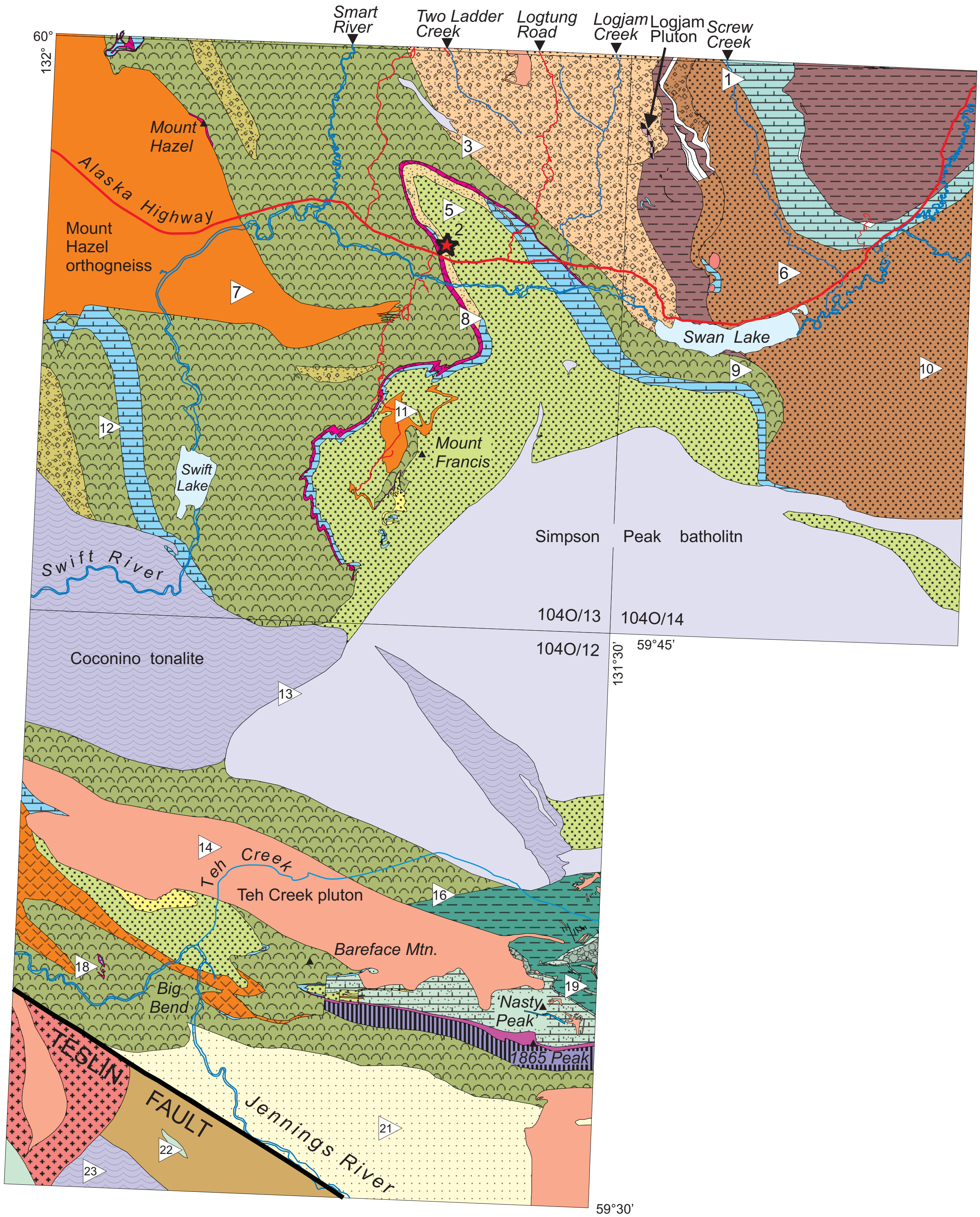

60°
132°
Smart River
Two Ladder Creek
Logtung Road
Logjam Creek
Logjam Pluton
Screw Creek
Mount Hazel
Alaska Highway
Mount Hazel orthogneiss
Swan Lake
Mount Francis
Swift Lake
Swift River
Simpson Peak batholitn
104O/13
104O/14
104O/12
59°45'
131°30'
Coconino tonalite
Teh Creek
Teh Creek pluton
Bareface Mtn.
Big Bend
'Nasty Peak'
1865 Peak
TESLIN FAULT
Jennings River
59°30'
1
2
3
5
6
7
8
9
10
11
12
13
14
16
18
19
21
22
23

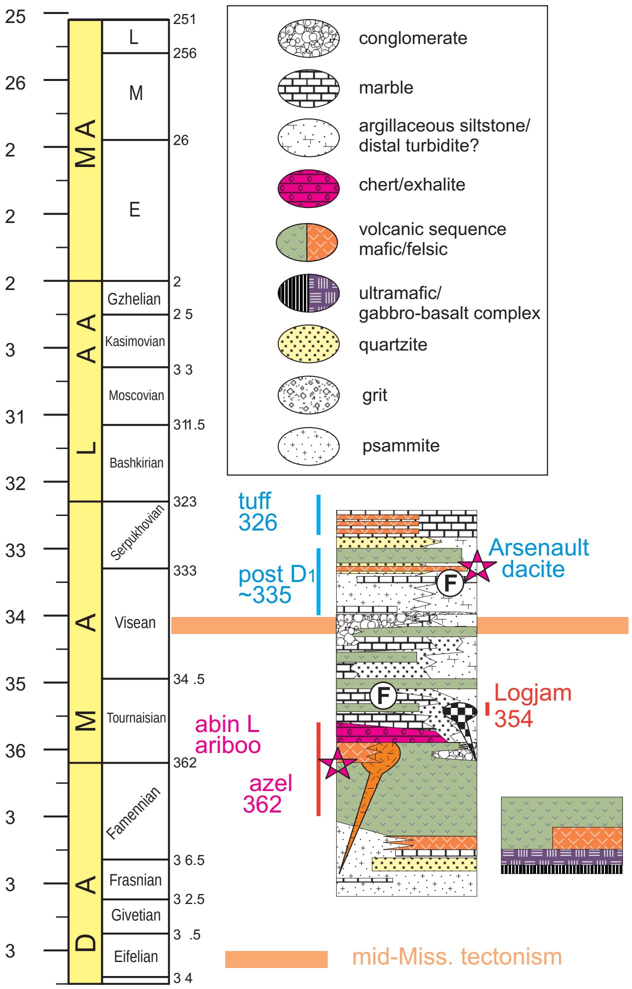

Figure 4. Generalized stratigraphy of the Big Salmon Complex in British Columbia.

Facing indicators are among the textures commonly preserved on the relatively weakly metamorphosed flanks of the Big Salmon Complex. However, unless they can be observed at the interface of the units being compared, they must be considered suspect because isoclinal folds are pervasive. In particular, the “dirty clastics” unit, which displays good graded bedding, is strongly deformed near its contact with the greenstone due to high rheological contrast (Photo 3).

A heterolithic succession, dominated by quartz-rich clastics with minor, grey-weathering carbonate layers 1-10m thick and quartz-phyric volcanic tuff layers up to 40m thick, are now considered to sit near the top of the Big Salmon Complex stratigraphy as they include the 325 Ma dacite layers. A lower quartz and feldspar-rich metaclastic unit that is lithologically similar, but not identical to some metaclastics of the upper unit, apparently underlies the greenstone unit upstream of the Big Bend (104O/12 south). Immediately to the north, a basalt-gabbro-ultramafite succession occurs within the greenstone near Teh Creek, where rock units belonging to the “Klinkit assemblage” are well exposed. Layered and intrusive units not previously described by Mihalynuk *et al.* (1998) are described here, beginning with the oldest layered rocks.

Lower Quartz and Feldspar-Rich Metaclastic Unit

In southern 104O/12, a > 350 m thick (structural) succession dominated by quartz-rich and lesser quartz-feldspar-rich metaclastic rocks lies structurally below the greenstone unit. In order of abundance, the rock types are: muscovite-quartz schist; biotite-muscovite±garnet quartz schist; muscovite-quartz±chlorite±feldspar schist, and biotite-chlorite-feldspar-quartz-schist. Feldspathic schists may be strongly deformed granitoid bodies, but the gradual appearance of feldspar down section from the greenstone argues for a sedimentary source. Sinistral shear bands are well developed in the feldspathic schist; about 2.5 kilometres north of the presumed trace of the Teslin fault (Figure 3).

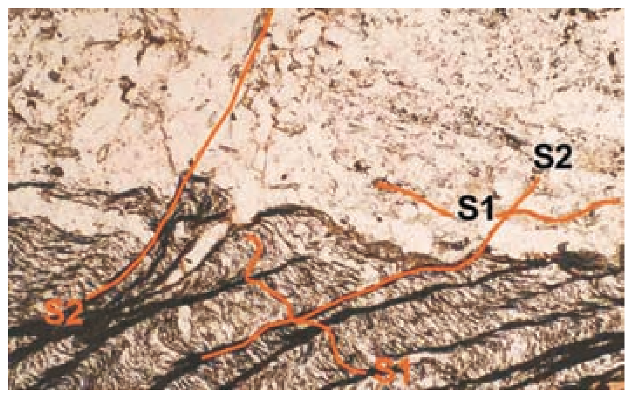

Photo 2. Photomicrograph of stretched quartzite pebble conglomerate of the dirty clastic succession shows that the phyllitic fabric displayed by argillaceous clasts (S1) continues into the adjacent quartzite clasts. A second fabric (crenulation cleavage, S2) is also printed on both phyllite clasts and quartz clasts. Such fabric development demonstrates that the conglomerate was deposited prior to at least two phases of deformation, and that the phyllite clasts need not have been derived from a previously deformed and metamorphosed terrain. Width of the photomicrograph represents 4 mm.

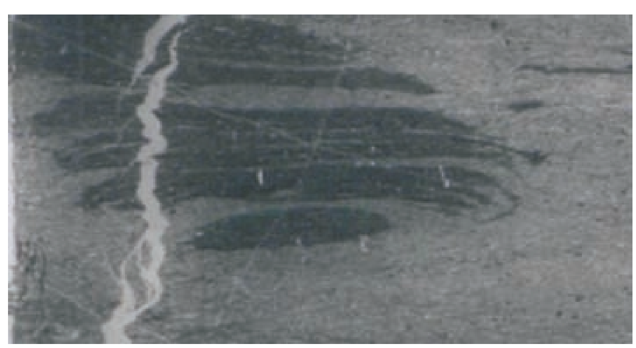

Photo 3. Sheath fold in turbiditic siltstones of the “dirty clastics” unit from within 5 metres of the greenstone contact (8x magnification).

Ultramafite-Gabbro-Basalt-Porphyry

A north to south succession of ultramafite (70-600m), gabbro (150-700m) and basalt (>20-2000m) can be traced for about 13 kilometres (Figures 3 and 4, all thicknesses are structural). It extends from the eastern limit of the map area, the Butsih Creek valley, and extends west almost to Bareface Mountain (informal, on Figure 3) where serpentinite was previously recognized by Gabrielse (1969). Farther west, the serpentinite disappears and the gabbro-basalt complex merges with the Big Salmon Complex greenstone unit. Greenstone with gabbro intervals is well exposed on both the long south ridge and the southwest flank of Bareface Mountain. At the eastern end of the belt, exposures are lost beneath glacial cover of the Butsih Creek valley. The easternmost 2 kilometres of serpentinite outcrops are bordered to the north by distinctive, coarsely porphyritic andesitic volcanic and hypabyssal rocks. All contacts of the ultramafite are faulted; they are either intrusive contacts that have been structurally modified, or original tectonic contacts.

Ultramafite exposures are typically orange, waxy yellow or dark green-black on both weathered and fresh surfaces. They are dominantly strongly foliated serpentinite, but lozenges of less foliated lherzolite are common on "1865m peak" (Figure 3) where the unit is thickest and best exposed. Where first encountered, the lherzolite was described as a wherlite, but geochemical anlaysis shows the rock to be too Mg-rich to support an abundance of clinopyroxene, so the pyroxenes are probably deformed hypersthene. At a locality 1.8 km west of the peak, coarsely crystalline lherzolite cumulate is preserved as a septa bounded to the north and south by gabbro. Exposures are not sufficient to determine whether this relationship is due to structural interleaving or is a relict of an originally intrusive contact. A series of outcrops on the north side of Teh Creek valley displays trains of serpentinized pyroxenes that may be a relict mantle tectonite fabric, but a pervasive late foliation renders this interpretation tenuous. (Harzburgite tectonite erratics are common along the belt. When first encountered, the erratics were suspected to be of local derivation. However, they occur throughout the map area and beyond, and are evidence of a once extensive, preglacial ophiolite terrain.)

The gabbro and basalt comprise an intrusive complex. Gabbro is cut by basalt and basalt is cut by gabbro. At the northern margin of the complex, gabbro predominates and at the southern margin, basalt predominates. Gabbro is white to green on fresh or weathered surfaces, although it can also be ruddy weathering. It is medium to very coarse-grained; locally it is pegmatitic. Plagioclase, pyroxene, and hornblende are epidote- and chlorite-altered and comprise more than 90% of the rock. Pyroxene is probably largely altered to hornblende, but this is not yet confirmed by petrographic analysis. Contacts with the ultramafite are best exposed within 0.5km of "1865 Peak" where they are clearly tectonic. Gabbro grain size is cataclastically reduced from greater than 1 cm to less than 0.01 cm over a width of 4 metres at the ultramafite contact. Shallowly-plunging mineral lineations suggest transcurrent motion, in support of map-scale sinistral shear bands; however, these lineations are folded and macroscopic kinematic indicators are inconsistent or equivocal.

The basalt is dark green weathering, aphanitic or microporphyritic. Flat chlorite disks up to 1 cm across are probably relict amygdales. They may comprise as much as 3% of the rock and are best displayed at one outcrop on the southern flank of "1865 Peak", where they are concentrated in concentric zones in what appear to be stretched pillows (Photo 4).

Basalt outcrops are lost beneath thick colluvial and glacial deposits in the valley south of "1865 Peak". Green-weathering basalt and andesite lapilli tuff dominate the next ridge to the south. They are extensively epidote-chlorite altered, foliated, and plagioclase-phyritic, with locally preserved pyroxene and hornblende phenocrysts. Less abundant, strongly planar beds of dust tuff or tuffite are conspicuous because of alternating, centimetre-thick, lime yellow and dark green bands. Pillowed and subaqueous sheet flows are also locally preserved. Similar units occur within the Big Salmon Complex greenstone unit along strike to the west (Figure 3), where they show higher degrees of strain.

Photo 4. Stretched pillows(?) within the basalt-gabbro-ultramafite complex. If these are pillows, then part of the complex was deposited in a submarine environment.

Coarsely Porphyritic Andesite

A package of distinctive, coarsely porphyritic, green-weathering, volcanic and hypabyssal andesitic rocks underlie most of the northern spur of "1865 Peak" where they are structurally admixed with serpentinite along their southern contact. They are separated from tuffite-dominated succession of "lower Klinkit assemblage" north of the spur by a colluviated valley. A stream occupies the valley bottom 1.6 km to the east where outcrops of dark green, fine-grained tuff are washed clean. In places, the tuff appears autoclastic. Broad zones, tens of metres across, are plagioclase-porphyritic, and in one 20 cm wide zone, flattened pyroxene crystals up to 4 mm across (average 2-3 mm) are preserved. Near the serpentinite, the unit is megaporphyritic. Plagioclases up to 4 cm long are strongly zoned, possibly to K-feldspar. Blocky black hornblendes range up to 2.5 cm long. Both feldspar and hornblende megacrysts are aligned down dip in a green, fine-grained foliated matrix (305°→65° to vertical). Some broken phenocrysts display an asymmetry that suggests north-side-up reverse motion, but most show ambiguous shear sense.

These tuffs could have provided the source for epiclastic deposits in the "lower Klinkit assemblage", although such a contention cannot be proven at this time. Granodioritic intrusives hornfels both porphyritic tuffs and epiclastics and chalcopyrite (<0.25%) is widely disseminated in the porphyritic tuffs.

Klinkit Assemblage

Rocks of the "Klinkit Assemblage" (Stevens and Harms, 1996) crop out in the eastern portions of the map area (104O/12E, 13NE, 14W; Figure 3). Harms mapped much of the "Klinkit assemblage" near Teh Creek (104O/12E, Figure 3; Harms, written communication, 1999) and established a useful subdivision which aided our 1999 mapping in the area. In 104O/13NE and 14W the "Klinkit assemblage" includes a lower unit equivalent to the "dirty clastics" and higher (?) units described by Gleeson *et al.* (2000, this volume; not described here). The fossiliferous Screw Creek limestone apparently sits near the top of the "Klinkit assemblage", although existing age data suggest protracted limestone deposition. Observations from the Teh Creek succession and Screw Creek limestone are presented here, from oldest to youngest.

Tuffite (240 m)

Well-preserved graded planar beds 10 to 100 cm thick of fine-grained tuffiteare characteristic of this unit. Approximately 200 metres of rhythmic deposits consist mainly of sets that average 3 metres thick and grade upwards from massive hornblende-feldspar-phyric lapilli that form 2/3 of their thickness, through fine-grained, planar-bedded ash and into laminated dust tuff. Sets may be capped by cross-stratified volcanic siltstone. Fine-grained detrital hornblende and plagioclase are abundant enough in some layers to produce a felted texture. In some cases, fine mafic grains are equant and may originally have been pyroxene, now replaced by actinolite. Fresh, coarse augite porphyry was observed in talus. Some intervals are very fine grained and cherty, resembling pelagic deposits. They are interpreted as dust tuff layers and may preserve ball and pillow structures. Sparse decimetre-scale calcareous layers are accentuated in thermal aureoles of thick sills and stocks by the development of light-coloured calc-silicates (grossular, diopside, epidote and quartz). One gossanous laminated white calcsilicate is, at a minimum, 6 metres thick.

Exceptionally well-preserved bedding and fine depositional features including cross-stratification, graded bedding, various water escape features, and scours permit assessment of facing directions. The succession is right way up and deformed by upright open to close folds in which foliation is only weakly developed, except for the fold core regions in which protolith textures are in part obliterated. Rhythmic deposits resemble thick turbidites, possibly ABC Bouma sequences; however, the predominance of reverse grading in planar-bedded ash layers suggests water lain tuffs that have not been reworked.

This unit has yielded neither fossil nor isotopic ages from within the map area. Similar tuffite in the Teslin sheet (Gordey, 2000) contain minor interbedded limestones with Middle Mississippian (Viséan) conodonts (M.J. Orchard *in* Poulton *et al*., 1999; *see* Figure 2 in Nelson *et al.*, 2000, this volume). However, the reliability of this distant extrapolation is questionable.

Near both the eastern and western limits of the tuffite displays apparent stratigraphic contacts with overlying conglomerate of the transitional unit.

Transitional Unit(s)

The transitional unit is so named because it marks a distinct change from volcanic to carbonaceous and quartz-rich clastic sedimentation. Two units define this transition: a light grey tuff/tuffite, and a conglomerate with quartz-rich clasts.

A complete section of grey, fine lapilli and coarse ash tuff and tuffite has not been observed. It is probably about 40 metres thick and is partly interbedded with the conglomerate unit. Some tuffaceous layers appear felsic, due to their siliceous nature, however, no quartz phenocrysts have been observed. Tuff is probably subordinate to grey or purple-brown phyllitic siltstone, which in places resembles microdiorite due to thermal alteration and growth of fine biotite. Siltstone is generally very well bedded on millimetre to centimetre scales, and may display cross laminae, but clear way-up indicators are rare, and these show that the unit is isoclinally folded. High strain zones are common and their orientation with respect to strongly transposed bedding indicates that they are axial-parallel and focused at fold hinges. In contrast, later, near-vertical mylonitic zones cut across folded limbs.

Granules to cobbles of quartzite, quartz-rich phyllite and possibly recrystallized chert are the principal components of the conspicuous conglomerate unit (Photo 5) that marks the transitional unit north of "Nasty Peak" (informal, Figure 3). Conglomerate matrix material varies from light grey-green phyllite to grit. Clasts are typically slightly stretched. Structural complexity makes thickness estimates difficult, but it is at least 5 m thick, and probably attains thicknesses of 30 m.

Highly strained, probable equivalents occur 4 km east of Bareface Mountain and on the southern ridge of the mountain. Quartz cobbles are flattened to sub-millimetre thicknesses (Photo 6), but low strain zones show good preservation of grey ash tuff interbeds.

Black Argillite-Quartzite

Rusty, pyritic and locally graphitic black argillite and thinly interbedded siltstone is the most abundant lithology within the black argillite-quartzite unit. Centimetre to decimetre thick beds of vitreous black sandstone are, however, characteristic, and at least one conspicuous, 4-8 m thick layer of tan, carbonate matrix-supported quartz grit occurs near the top(?) of the unit. Total thickness of the unit is difficult to assess due to the affects of at least one phase of isoclinal folding overprinted by upright folds. It is probably in excess of 200 m thick with structural thicknesses of more than a kilometre.

Photo 5. Conglomerate of the "transitional unit" of the "Klinkit assemblage".

Screw Creek Limestone

One of the most complete sections through the fossiliferous Screw Creek limestone in British Columbia is east of Screw Creek, near the border with Yukon (104O/14W; Figure 3). Along this transect the structurally lowest outcrops are decimetre thick limestone beds with planar, centimetre-thick cherty maroon and green layers, probably silicified tuffs. Facing indicators in these brightly coloured layers are not well preserved, but truncated layering gives the impression that the units are right way up. The next highest unit is calcareous sharpstone conglomerate which are clearly upside-down based on well-developed channel scours and lags (Photo 7a). Intraclasts predominate; they appear to have been derived from the cherty tuff layers. Overlying coralline boundstone is also upside-down as indicated by corals in growth position (Photo 7b). At yet higher elevations a west-closing recumbent fold hinge is traversed and the sharpstone conglomerate is repeated. A third repetition of the sharpstone conglomerate is succeeded by highly fossiliferous limestone indicating a return to inverted stratigraphy. Highest limestone exposures enclose a 2-5 metre thick tuffaceous interval containing 2 – 10 cm thick planar bedded white tuff layers interlayered near the top of the succession with decimetre thick carbonate. These lithologies are joined by black siltstone beds several centimetres thick. The highest carbonate layers contain black phyllitic clasts. Carbonate content diminishes abruptly over several metres until well-bedded black and brown siltstone and feldspathic sandstone predominate.

Photo 6. Strongly flattened quartz clast conglomerate, probably the "transitional unit".

Photo 7. Screw Creek limestone: (a) cross stratified overturned sharpstone conglomerate with clasts cannibalized from lower beds, and (b) rugosan boundstone with fossils preserved in overtuned growth position. Both photos are taken on the overturned limb of a regional recumbent fold.

This latter lithology apparently belongs to the “Swift River assemblage” (*see* Nelson *et al.*, 2000). If this is true, then the contact between the lowest Screw Creek limestone (“Klinkit assemblage”) and “Swift River assemblage”, is gradational.

GEOCHRONOLOGY

Critical age data from two units are presented here. A sample of Hazel orthogneiss was collected near a repeater tower on the south flank of Mount Hazel (located on Figure 3). Hazel orthogneiss occurs within the greenstone unit, which it apparently cuts, thereby providing a minimum age on the greenstone which underlies more than half of the map area.

A second data set is reported for a sample of intermediate to dacitic tuff that is interbedded with limestone on the north flank of Mount Francis (*see* Figure 3). It is believed to occupy one of the highest stratigraphic positions within the Big Salmon Complex (Figure 4).

Mount Hazel Orthogneiss

A sample of a massive to weakly deformed, granite from the Mt. Hazel orthogneiss yielded a modest quantity of cloudy, metamict, to less commonly clear, pale pink prismatic zircon. Eight fractions of the clearest and coarsest grains available all gave discordant results (2-10% discordant), with ellipses aligned in a linear fashion (Figure 5, Table 1). An upper intercept of $362.3^{+7.9}/_{-6.8}$ Ma (eight-point Davis regression) is interpreted as the best estimate for the igneous age of the Mt. Hazel pluton. A well-defined lower intercept of $189^{+16}/_{-17}$ Ma may correspond with the time of Pb loss. Lead loss may be due to a late deformational event which produces a strong fabric in the *circa* 196 Ma Coconino tonalite (Mihalynuk, *et al.*, 1998), whereas the *circa* 185 Ma Simpson Peak batholith (recalculated from Wanless *et al.*, 1970) is mostly undeformed.

Mount Francis Dacitic Tuff

This foliated metadacite yielded a moderate amount of cloudy to rarely clear, pale pink prismatic zircon. Seven strongly abraded fractions of the clearest grains available were analysed (Figure 6, Table 1). All of these likely show the effects of Pb loss, despite the strong abrasion. Four fractions (A, F, G and H) are discordant, and are inferred to contain significant inheritance; they give 207Pb/206Pb ages of ca. 546-1235 Ma. Fractions B and C give $^{207}Pb/^{206}Pb$ ages of about 325 Ma. The weighted average $^{207}Pb/^{206}Pb$ age for these two fractions, 325.1±3.0 Ma, provides the best estimate for the age of the rock. Slightly discordant fraction D is interpreted to contain minor inheritance. Another tuff bed from the same outcrop yields concordant fractions giving the same *circa* 325 Ma age.

PLUTONIC ROCKS

The Coconino tonalite, Simpson Peak batholith, Slaughterhouse quartz diorite, Two Ladder tonalite and Midshore granite bodies (Figure 3) were described previously by Mihalynuk *et al.* (1998). New observations in the Simpson Peak batholith show it to be compositionally and

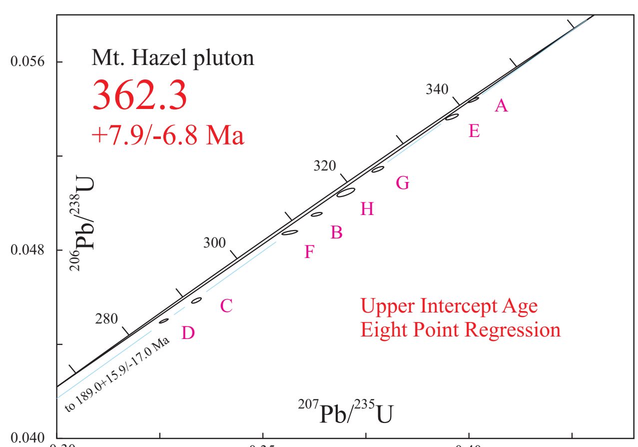

Figure 5. Concordia plot showing isotopic ratios with error estimates for four zircon (A to D) and two titanite (T1, T2) mineral fractions from the Mount Hazel orthogneiss.

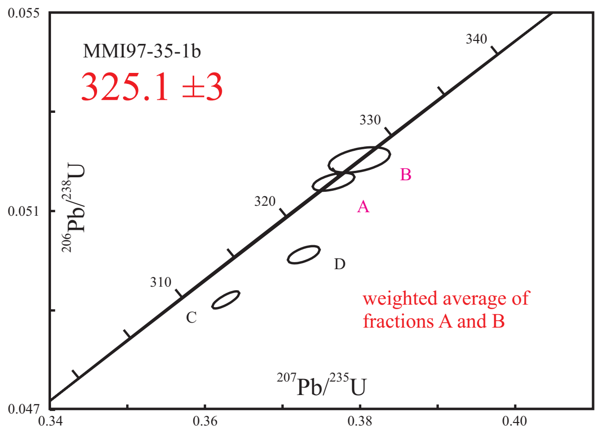

Figure 6. Concordia plot showing isotopic ratios with error estimates for zircon mineral fractions from tuff layers in limestone on the north flank of Mount Francis.

textually variable, and the Midshore granite is now believed to be part of a syenitic intrusive suite. These observations, together with descriptions of plutons encountered during mapping in 1999, are reported here from presumed oldest to youngest:

Charlie Cole Pluton (EJCg)

A large body of strongly foliated light grey to white-weathering granite underlies Mount Charlie Cole (Gabrielse, 1969), and a few outcrops on its northern flank extend onto southwestern 104O/12 in the present map area. It consists of medium-grained quartz (30%) and plagioclase (30%), with K-Feldspar as phenocrysts (20%) and matrix (10%), and 15% smeared, chloritized mafics (biotite?). S-C fabrics are well developed for nearly a kilometre across strike. They indicate sinistral motion on C-planes (Photo 8), but the fabric appears folded in at least one locality where shear sense switches rapidly. Charlie Cole pluton is 4 kilometres south of the inferred trace of the Teslin Fault, which trends 300°. Ori-

TABLE 1
ISOTOPIC DATA FOR TWO SAMPLES OF THE BIG SALMON COMPLEX

Fraction[1]	Wt (mg)	U[2] (ppm)	Pb[*3] (ppm)	$^{206}Pb/^{204}Pb$[4]	Pb[5] (pg)	^{208}Pb[6] (%)	Isotopic ratios (1σ,%)[7] $^{206}Pb/^{238}U$	$^{207}Pb/^{235}U$	$^{207}Pb/^{206}Pb$	Apparent ages (2σ,Ma)[7] $^{206}Pb/^{238}U$	$^{207}Pb/^{206}Pb$
Mt. Francis Dacite, MMI97-35-1a: 325.1±3.0 Ma											
A c,N2,p,b	0.067	450	29	11032	10	13.2	0.06041 (0.09)	0.5265 (0.15)	0.06321 (0.08)	378.1 (0.7)	715.2 (3.5)
B m,N2,p,b	0.036	361	16	3496	10	13.6	0.04333 (0.10)	0.3163 (0.18)	0.05294 (0.10)	273.5 (0.5)	326.0 (4.5)
C f,N2,p	0.038	493	26	9843	6	14.5	0.05042 (0.14)	0.3677 (0.19)	0.05290 (0.09)	317.1 (0.8)	324.3 (4.1)
D ff,N2,p	0.010	592	33	5489	4	15.9	0.05248 (0.10)	0.3849 (0.17)	0.05320 (0.11)	329.7 (0.6)	337.4 (4.9)
F m,N2,p	0.007	493	30	2902	4	14.0	0.05577 (0.11)	0.0627 (0.18)	0.08156 (0.11)	349.8 (0.8)	1234.9 (4.4)
G f,N2,p	0.007	470	18	2041	4	10.7	0.03776 (0.14)	0.3042 (0.23)	0.05843 (0.17)	269.7 (1.1)	546.0 (7.3)
H f,N2,p	0.009	490	25	3579	4	13.2	0.04869 (0.15)	0.4661 (0.22)	0.06943 (0.13)	306.5 (0.9)	911.5 (5.4)
Mt. Hazel Pluton, MMI97-29-1: 362.3+7.9/-6.8 Ma											
A m,N2,p	0.037	349	20	7988	6	13.3	0.05438 (0.10)	0.4010 (0.16)	0.05349 (0.09)	349.5 (3.9)	349.5 (3.9)
B m,N2,p	0.025	413	21	1039	32	13.5	0.04952 (0.08)	0.3631 (0.18)	0.05317 (0.14)	336.0 (6.5)	336.0 (6.5)
C f,N2,p	0.016	534	25	6861	4	11.2	0.04586 (0.12)	0.3339 (0.18)	0.05280 (0.12)	320.1 (5.2)	320.1 (5.2)
D m,N2,p,b	0.032	719	33	8566	8	12.4	0.04499 (0.10)	0.3260 (0.16)	0.05254 (0.09)	309.1 (4.0)	309.1 (4.0)
E m,N5,p,s	0.013	599	35	4269	6	16.4	0.05366 (0.11)	0.3959 (0.20)	0.05350 (0.13)	350.2 (5.9)	350.2 (5.9)
F m,N5,p,e	0.014	240	12	1870	6	13.0	0.04875 (0.09)	0.3565 (0.26)	0.05304 (0.21)	330.5 (9.6)	330.5 (9.6)
G m,N5,p,e	0.010	489	27	4429	4	15.1	0.05144 (0.12)	0.3779 (0.19)	0.05328 (0.12)	340.8 (5.5)	340.8 (5.5)
H f,N5,p,b	0.010	560	31	2391	7	16.5	0.05045 (0.18)	0.3701 (0.29)	0.05321 (0.20)	317.3 (1.1)	337.7 (8.9)

[1] Upper case letter = zircon fraction identifier. All zircon fractions air abraded; Grain size, intermediate dimension: c=>134μm, m=<134μm and >104μm, f=<104μm and >74μm, ff <74μm;
Magnetic codes:All zircons are nonmagnetic on Franz magnetic separator at field strength of 1.8-2.0A and a sideslope of 5°. Front slope for all fractions=20°; Grain character codes: e=elongate, p=prismatic, s=stubby.

[2] U blank correction of 1pg ± 20%; U fractionation corrections were measured for each run with a double ^{233}U-^{235}U spike (about 0.005/amu).

[3] Radiogenic Pb

[4] Measured ratio corrected for spike and Pb fractionation of 0.0035/amu ± 20% (Daly collector) and 0.0012/amu ± 7% and laboratory blank Pb of 1-3pg ± 20%. Laboratory blank Pb concentrations and isotopic compositions based on total procedural blanks analy

[5] Total common Pb in analysis based on blank isotopic composition

[6] Radiogenic Pb

[7] Corrected for blank Pb, U and common Pb. Common Pb corrections based on Stacey Kramers model (Stacey and Kramers, 1975) at the age of the rock or the $^{207}Pb/^{206}Pb$ age of the fraction.

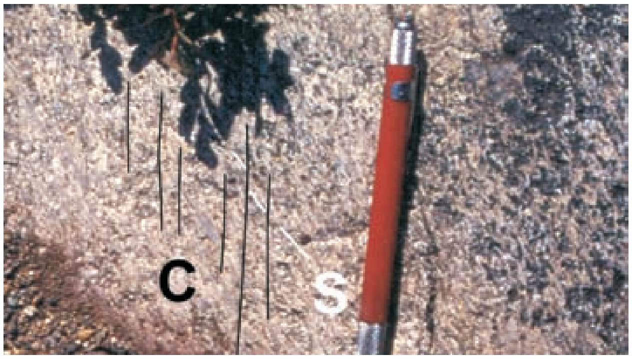

Photo 8. S-C fabrics are well displayed in outcrops on the north flank of Mount Charlie Cole about 4 kilometres south of the Teslin Fault.

entation of most of the C-planes is 185° to 020° such that their development cannot be attributed to simple kinematic linkage with the Teslin Fault. Because of apparent late folding of the S-C fabrics, their use in constraining any regional structural interpretation would be suspect. However, a sample collected for isotopic age dating should provide a maximum age for this fabric.

Simpson Peak Batholith (EJSg1, 2, 3, EJSgd)

Four lithologies comprise the Simpson Peak batholith. These are described from oldest to youngest based on field relationships:

Hornblende>biotite granite (EJSg1) with flattened pink K-feldspar megacrysts is well foliated, but poorly lineated. This unit was sampled at two localities and vantage point mapping suggests that rocks with similar weathering characteristics crop out in a gently northwest tapering wedge of pluton in northeastern 104O/12.

Medium-grained grey to tan granite (EJSg2) contains white to pink intergrowths of plagioclase and K-feldspar (60%), fresh biotite (10%, or up to 5% chloritized) and coarse smoky quartz (30%). It is blocky weathering with distinctive low angle jointing, and weathers to abundant grus. Joint surfaces may be chlorite coated. Foliation is weak to absent. It is the most abundant unit in the batholith.

Biotite porphyry dominates a gently northwest-dipping tabular complex about 240 metres thick (EJSg3). It is medium-grained,with subequant feldspar and grey quartz phenocrysts and medium to fine-grained rusty biotite, in a tan to flesh coloured, non-foliated, sucrosic siliceous matrix. Numerous 0.5 to 3 metre thick quartz dioritic sills cut the complex, giving it a strongly jointed appearance from a distance. The complex clearly cuts foliated K-feldspar megacrystic granite as do irregular fleshy pink aplitic dikelets interpreted as coeval.

Weakly to non-foliated quartz-diorite to granodiorite (EJSgd) forms medium-grained tabular zones within the batholith, and occurs as fine to medium-grained dikes that cut the sill complex porphyry.

Teh Creek Pluton (KGg)

White hornblende < biotite granodiorite, granite and lesser grey quartz diorite comprise this elongate, west northwest-trending body that stretches across mapsheet 104O/12. Mafics, including about 1% yellow-brown sphene, comprise about 16% of the rock. Slightly porphyritic K-feldspar comprises 10% (to 30% including matrix), plagioclase ~25% and xenomorphic quartz about 30% of the rock.

Originally mapped as belonging to three separate suites, including parts of the Klinkit and Simpson Peak batholiths (Gabrielse, 1969), the Teh Creek pluton is most likely an extension of the Klinkit batholith, a satellite of which is mapped east of upper Butsih Creek (just east of 104O/12). Although, the Klinkit batholith is described as foliated (Gabrielse, 1969), no planar fabric is developed within the map area. Thus, the Teh Creek pluton is treated separately. It appears to have intruded by stoping of blocks controlled by two sets of joints; north and west-northwest sets, resulting in pluton margins that are demarked by sets of orthogonal dikes (*see* headwaters of Teh Creek, Figure 3).

Early Eocene Syenite (EEsy)

Pink, varitextured, unfoliated syenite occurs as two elongate, high-level plutons east of Teslin Lake. The southern body gives way on its southern margin to a sill complex. Xenoliths of complexly folded Big Salmon Complex are common. Textures range from fine-grained, felted intergrowth of feldspar and amphibole in which feldspar phenocrysts may range from a sparse to dominant component. Feldspars are up to 3 centimetres across and are typically zoned; they have white calcic? cores and pink potassic rims. The northern pluton was called the Midshore granite by Mihalynuk *et al.* (1998). A compositionally distinctive zone at its northern end is composed of 75% coarse, zoned feldspar and is pink with tan weathering. Amphiboles are typically acicular. The southern syenite body is reported to contain the sodic pyroxene aegerine (Aitken, 1959). U-Pb isotopic analysis of zircons extracted from the Midshore granite indicate an Early Eocene age (unpublished). A sample collected from the southern body should confirm correlation with the dated pluton to the north.

New Occurrences and Mineral Potential

Several new mineralized zones were discovered during the course of mapping in 1999. They are either intrusion-related gold veins or stratabound copper-rich lenses in crinkle chert. The most prospective examples are reported below together with analytical results where available (analyzed by Instrumental Neutron Activation and Inductively Coupled Plasma Emission Spectroscopy (note that ICP digestion is by aqua regia which is incomplete for most elements); *see* also Table 2). One pyritic sericite schist is geochemically unremarkable, but it is extensive and is included below.

Assay Data from Three Mineralized Zones

West Teslin Lake border area. Along west shore of northern Teslin Lake, 6 km south of the Yukon border (just west of the map area, "1" on Figure 3), a set of moderately to steeply west to northwest dipping brittle shears, spaced about 5-10 metres apart within an Eocene granitoid body, show evidence of west-side-up movement. They are invaded by quartz veins and rusty, pyritic mineralization with rare malachite staining and variably developed alteration envelopes. One 2-3 cm thick vein with a somewhat wider than average 20 centimetre alteration envelope was chip sampled for 2.5 metres along the vein. It returned values of 1320 ppb Au, 0.4% As, and 194 ppm Sb (MMI99-22-3; Table 2; location 1 on Figure 3).

Copper in the Crinkle Chert. Numerous occurrences of minor sulphide mineralization and copper staining were encountered in the crinkle chert unit, further indication of the high mineral content of this unit as previously established by mapping in 1997. Most significantly, a chlorite-porphyroblastic, 6 metre by 0.5 metre lens with disseminated chalcopyrite returned 0.9% Cu; 0.3g Au, 2.9g Ag, 6.8% Fe, and 0.17% Ba from a chip sample across its width (MMI99-27-19, Table 2; location 2, Figure 3).

Jennings River "knee". Pyrite-rich sericite schist crops out at many localities within the map area. Most extensive are those at locality "3" on Figure 3, near the Jennings River "knee". Here it is well developed within a regional quartz-phyric horizon of probable dacite composition. Old claim posts indicate that the mineralization was known previously, but the claims were apparently never registered. The one sample analyzed did not return anomalous metal values (99JN-27-1C, Table 2). Despite scant exposures, the felsic host unit is intermittently exposed for at least 16 km (Location 3 on Figure 3). If it is indeed continuous, it could represent a significant mineralizing system that warrants further work.

DISCUSSION

In southern Yukon and British Columbia, the Big Salmon Complex can be reliably mapped on the basis of the stratigraphy presented herein. In British Columbia, it is possible to walk Big Salmon Complex greenstone from transitional greenschist-amphibolite facies near the core of the Big Salmon Complex, either southeast or northwest into greenschist-grade rocks that display good protolith textures. Stevens and Harms (1996) include the former, relatively high grade rocks with the "Hazel Assemblage", and the latter, lower grade rocks with the "Klinkit assemblage". This raises two questions: what is the usefulness of the term Big Salmon "complex" given that a coherent stratigraphy is present?, and what is the utility of this assemblage given that it is possible to trace units (like the greenstone) from higher grade "Hazel assemblage" to lower grade "Klinkit Assemblage".

Is Big Salmon Complex a Complex?

Use of the term "complex" is recommended in the North American Stratigraphic Code "…where the mapping of each separate lithic component is impractical at ordinary mapping scales. "Complex" is unranked but commonly comparable to suite or supersuite, therefore, the term may be retained if subsequent, detailed mapping distinguishes some or all of the component lithodemes or lithostratigraphic units." (NACSN, 1983, page 861). Clearly, resolution of regionally mappable units within the Big Salmon Complex does not in itself justify abandonment of the name. Future work may demonstrate justification, but in the interim, we have elected to retain the original name of "Big Salmon Complex" rather than adopt the nomenclature of Stevens and Harms (1996). Dual nomenclature is confusing and prone to misleading interpretation especially when the assemblages are implicitly fault-bounded with distinct stratigraphies and structural and metamorphic characteristics (*see* definitions of Stevens and Harms, 1996). Rigorous unit definitions together with reference sections or type localities need to be established in order to address this problem.

Big Salmon Complex-"Klinkit Assemblage" Relationships

Gabrielse (1969) showed the Big Salmon Complex as bounded to the northeast by a belt of Mississippian "Sylvester Group", including massive greenstone, chert, agglomerate and metadiorite which he designated as "unit 7"; and he showed Big Salmon Complex bounded to the southeast by the Simpson Peak batholith and other plutons in the Jennings River area. However, it is now clear that to the northeast, some "unit 7" rocks north of the Alaska Highway belong to the Big Salmon Complex. To the southeast, marker units can be traced to the "Big Bend" of the Jennings River (Figure 3, location 18), and the enclosing strata probably extend an additional 20 kilometres farther east southeast where they apparently merge with the "Klinkit assemblage" of Stevens and Harms (1996). These authors included both "unit 7" as well as the presumably younger "unit 12" chert, argillite, limestone and conglomerate of Gabrielse (1969) and units Mv and Ml of Gordey and Stevens (1994) in their informal "Klinkit assemblage". The age of the "Klinkit assemblage" is constrained by Middle Mississippian (Viséan) conodonts from limestone layers in the volcanic division (unit "Mv" of Gordey, 2000; fossil age compiled by M.J. Orchard in Poulton *et al*., 1999), by Triassic conodonts in the dark clastic division (M. Orchard *in* Harms and Stevens, 1996), and especially by the fossiliferous Screw Creek formation limestone (informal; Poole, 1956) which contains Early to Middle Carboniferous macrofossils (Abbott, 1981), early Pennsylvanian fusulinids (Gabrielse, 1969), and is structurally underlain by thin limestone layers with conodonts of Middle Penn-

TABLE 2
ANALYTICAL RESULTS FROM MINERALIZED ZONES

			Element	Au	Mo	Cu	Pb	Zn	Ag	Co	Fe	Fe	As	As
			Units	ppb	ppm	ppm	ppm	ppm	ppm	ppm	%	%	ppm	ppm
			Method[1]	INA	AICP	AICP	AICP	AICP	AICP	AICP	AICP	INA	AICP	INA
			Lab.[2]	ACT	ACM	ACM	ACM	ACM	ACM	ACM	ACM	ACT	ACM	ACT
			Dect'n Limit	2	1	1	3	1	0.3	1	0.01	0.02	2	0.5
Field No.	Mapsheet	Northing	Easting											
99JN-27-1C	104N/9E	6613006	667397	18	7	32	157	4	0.3	1	1.6	1.7	3	3.5
MMI99-22-3	104N/16	6648136	645330	1320	4	42	< 3	17	0.7	3	1.88	2.01	4420	4290
MMI99-27-19	104O/13E	6646808	349969	311	1	8786	14	155	2.9	24	6.83	8.42	< 2	4.5

			Element	Sb	Sb	Bi	V	P	Mn*	Al	Na	K	Ba	Ba
			Units	ppm	ppm	ppm	ppm	%	ppm	%	%	%	ppm	ppm
			Method[1]	AICP	INA	AICP	AICP	AICP	AICP	AICP	AICP	AICP	INA	AICP
			Lab.[2]	ACM	ACT	ACM	ACM	ACM	ACM	ACM	ACM	ACM	ACT	ACM
			Dect'n Limit	2	0.1	2	1	0	2	0.01	0.01	0.01	50	1
Field No.	Mapsheet	Northing	Easting											
99JN-27-1C	104N/9E	6613006	667397	< 3	0.2	< 3	27	0.023	183	0.57	0.11	0.33	580	88
MMI99-22-3	104N/16	6648136	645330	145	194	8	12	0.038	351	0.95	0.07	0.28	820	94
MMI99-27-19	104O/13E	6646808	349969	< 3	1.6	10	104	0.066	2044	3.99	0.07	0.27	3400	1731

1 Methods: AICP = Inductively coupled plasma, Aqua regia digestion; INA = Instrumental neutron activation

2 Lab.: ACM = Acme Analytical Laboratories Ltd., Vancouver; ACT = Activation Laboratories Ltd., Ancaster, Ontario

sylvanian age (Abbott, 1981). Stevens and Harms (1996) suggest that carbonate units within the "Klinkit assemblage" contain conodonts as young as Early Permian. However, at least part of "unit 12" of Gabrielse (1969) that Stevens and Harms (1996) included in the "Klinkit assemblage" must be older than the Screw Creek limestone based on the findings of Gleeson *et al.* (2000, this volume) who mapped four ridges underlying the northeastern limits of "unit 12". They report U-Pb isotopic age results that constrain the age of the clastics to between Earliest Mississippian and Silurian, much older than previously expected, and much older than any lithologically comparable units in the "Klinkit Assemblage". Such fundamental departures from recent stratigraphic interpretation show that our understanding of the Big Salmon Complex is not yet mature and that detailed tectonic syntheses involving the eastern Big Salmon Complex must be considered speculative.

Effects of Structural Complexity

Direct age comparisons are made difficult by isoclinal, mountain scale, south and southwest-verging folds and parasitic folds that exert a fundamental control on the distribution of different units. For example, the new isotopic ages reported here together with structural observations show that substantial parts of the stratigraphy are inverted by large-scale nappes, but even so, some age conflicts cannot be reconciled. Distribution of units is further complicated by both older and younger folding.

Recognition of intense, regional strain partitioning (in part related to nappes) shows that correlations cannot be reliably based on degree of strain, although local differences in metamorphic history may warrant division of units into separate assemblages. An early, nearly layer-parallel fabric is folded by the large scale folds and is commonly overprinted by a second or third schistosity imparted during subsequent deformational events.

A mid-Mississippian deformational event is well documented to the north in the Glenlyon area (M. Colpron *in* Nelson *et al.*, 2000) and in the Finlayson area (Murphy and Piercey, 1999; although it could be slightly older). This same event might have affected the Jennings River area, but the age is less tightly constrained. It is represented by deformational discordance above and below a conglomerate within the regional carbonate unit. A dike cuts folded strata that predate the conglomerate, thus providing an upper constraint on the age of deformation ~335 Ma (unpublished). The conglomerate is interpreted as a post-deformational basal facies. A maximum age limit for early deformation in the area is provided by the 354 Ma Logjam pluton (Gleeson *et al.*, 2000, this volume). This deformation may correspond to a regional collisional event during which blueschist and eclogite facies rocks were emplaced within the Yukon-Tanana Terrane *circa* 346 Ma (Erdmer *et al.*, 1998). As suggested by Murphy and Piercey (1999), this deformational pulse may prove to be a useful feature for regional correlations.

Broader map coverage and new kinematic data show that the deformational history culminated in an important north-south compressional event that affects the southern margin of the Simpson Peak batholith, although this event is not everywhere in evidence. New discovery of superb exposures of the Teslin fault along Jennings River reveal a broad zone of mylonite with sinistral kinematics, overprinted by quasi-ductile dextral fabrics (de Keijzer *et al.*, 2000), but the age and duration of these kinematic events and how they relate to deformational events in the adjacent rocks are unknown.

Stratigraphy Inverted, or Not?

The revised stratigraphy here relies heavily on the intrusive relationship of Hazel orthogneiss into greenstone, providing a minimum age of 362 Ma for the greenstone and underlying rocks. However, the contact relationship between the main body of the Hazel orthogneiss and greenstone has not been unequivocally established. Outcrop patterns support such an interpretation as do thin apophyses of orthogneiss within greenstone, but such apophyses have not been traced back to the main body of Hazel orthogneiss. No such apophysies have been recognized in presumably younger units. Neither are presumably younger units cut by the main body, even though the outcrop pattern on Figure 3 would seem to show this for both the crinkle chert and carbonate units. At three localities, the margin of the Hazel body follows and does not cross-cut crinkle chert (at Mount Hazel, and near localities 2 and 7 on Figure 3), or carbonate (north of locality 12). Where outcrop control is best, from Mount Hazel to the BC-Yukon border, the crinkle chert apparently occurs within a synformal keel immediately northeast of the Hazel orthogneiss. At Mount Hazel a septa of strongly foliated felsic, muscovite- and magnetite porphyroblast-rich tuff (?) or intrusive border phase (not shown on Figure 3) separates the chert from less deformed Hazel pluton.

Syndepositional Faulting?

The "dirty clastics" unit and crinkle chert unit are both observed to record the same deformational events and both rest depositionally atop greenstone. They rest on no other units. Crinkle chert is clearly overlain by limestone and a succession of other lithologies. In contrast, the "dirty clastics" unit is not overlain by other units west of Two Ladder Creek. If the "slate, chert, argillite, conglomerate" unit of the "Klinkit assemblage" that extends eastward from Two Ladder Creek (where it was originally included with the "dirty clastics" unit by Mihalynuk *et al.*, 1998 because of close lithologic similarity) is correlative with the "dirty clastics", then it is overlain by a "phyllite and minor limestone" unit and both are intruded by the 354 Ma Logjam intrusion (Gleeson *et al.*, 2000, this volume). Thus, the crinkle chert may have been deposited at the same time as the conglomeratic "dirty clastics", suggesting that the extents of these contrasting facies were controlled by syndepositional faults. Crinkle chert may have accumulated as mixed hydrothermal and biogenic sediment in a rift graben, protected from the influx of voluminous "dirty clastics". Similar synsedimentary faults are suggested to control mineralization controls at the Fyre Lake and Kudz Ze Kayah deposits (Murphy, personal communication, 1999). This rift event apparently marks a fundamental change in the continental arc in which the greenstone was deposited, because younger volcanic rocks in the Big Salmon Complex are much less voluminous.

An enigmatic basalt-gabbro-ultramafite succession between Teh and Butsih Creeks (southeastern 104O/12) is 2 kilometres thick and 13 kilometres long and enveloped by Big Salmon Complex greenstone. If it is an oceanic crustal fragment, the structure that emplaced it does not appear to extend west of Bareface Mountain, because greenstone crops out over extensive areas both north and south of where such a hypothetical structure should exist. Alternatively, it could have been emplaced during arc rifting and cessation of *circa* 362 Ma volcanism in the continental arc, which led to exhalative contributions and crinkle chert deposition. It does appear to sit near the top (termination?) of the greenstone succession. Alternatively, it may be a differentiated sill that pinches out to the west, in similar fashion to those believed to have been emplaced along syndepositional faults in the Finlayson area (Murphy and Piercy, 1999). In either case, such faults are important conduits for mineralizing fluids and the coincidence of 95th percentile regional geochemical results in this area (Cook and Pass, 2000, this volume) may reflect such a mineralizing system. Geochemical results aimed at this problem are pending.

SUMMARY

U-Pb isotope geochronological data is key to unraveling the stratigraphy and geological history of the Big Salmon Complex and adjacent terrains. Two new age dates are reported here. A 362 Ma age from the Hazel orthogneiss provides a minimum age for the greenstone, which it appears to intrude, and underlying rocks. The other isotopic age is 325 Ma from some of the structurally highest felsic tuffaceous units. These ages require that most of the stratigraphy outlined by Mihalynuk *et al.* (1998) is inverted. Regardless of the stratigraphic younging direction, the greenstone-chrinkle chert-limestone marker succession can be confidently traced throughout the Big Salmon Complex in British Columbia and southernmost Yukon (*cf.* Roots *et al.*, 2000), and a crude metallogenic history can be pieced together.

Vigorous continental arc volcanism in the late Devonian to Early Mississippian (*circa* 370-360 Ma) resulted in the accumulation of voluminous, submarine, dominantly mafic tuff and tuffite on a substrate of pericratonic strata. A pulse of felsic volcanism and arc rifting and probably marks the end of the magmatic cycle and the formation and preservation of a regionally developed exhalative chert horizon known as the "crinkle chert" as well as coeval clastic facies preserved in fault-bounded basins. Felsic volcanic intervals immediately beneath the crinkle chert commonly contain pyritic quartz-sericite schist intervals. These may serve as potential pathways to volcanogenic massive sulphide deposits. Within the crinkle chert, a Cu-Zn-Fe-Mn-Ba-rich lens several metres long points to the potential for volcanogenic exhalative deposits.

Carbonate deposition atop crinkle chert probably marks a rise in carbonate productivity in the Early Mississippian, following the Late Devonian crisis and extinction reef organisms. Thick carbonate banks probably coexisted with basins in which terrigenous clastics were deposited. Complex facies may have been linked by pulses of volcanism and widespread tuff deposition. A mid-Mississippian deformational event (between 354 and 335 Ma) may have peaked with emplacement of 346 Ma eclogite and blueschist (*cf*. Erdmer *et al.*, 1998). It caused uplift and erosion of units and deposition of widespread conglomeratic facies. The ensuing strata display at least as much lithologic variability as do pre-deformation sediments, but felsic volcanism is again proximal as it was at the close of greenstone deposition. Base metal sulphides are associated with these felsic volcanics such as at the Arsenault property.

The youngest Big Salmon Complex strata recognized in the Jennings River area are 325 Ma dacitic tuffs in carbonate. They do not correspond in any way to a clear break in deposition, and much younger Big Salmon Complex strata could exist in other areas. Peak metamorphism predates the 196 Ma Coconino tonalite and may have occurred around 270 Ma when blueschist and eclogites were incorporated into the Yukon Tanana Terrane (Erdmer *et al.*, ibid.). The youngest regional deformational event produced a strong fabric in the ~196 Ma Coconino tonalite, but affected only the southern margin of the *circa* 185 Ma Simpson Peak batholith. Youngest magmatism is Eocene, and one Eocene pluton west of north Teslin Lake hosts a set of veins with elevated gold values. Clearly, the area has a long and complex history and significant mineral potential.

ACKNOWLEDGMENTS

Thanks to Tom Gleeson for top notch field assistance and to Steve Gordey (GSC) and Tekla Harms (Amherst College) for sharing their regional geological insight. Ed Balon and Wojtek Jakubowski of Fairfield Resources provided access to their Cabin Lake property and freely shared their ideas about mineral potential in the Big Salmon Complex. Geoff Bradshaw, James Smith and Terry Tucker of Brett Resources provided access to their Cariboo Creek property and a steady flow of observations (together with hand samples) during their stay in our camp. Retrospective thanks to Andy Page of Fireweed Helicopters who helped to develop both our rapid bush-crash technique and our resilience to thigh-deep swamp water. Flying skills and keen eye of Denny Dennison (Coyote Air) greatly aided our aerial reconnaissance. His air sickness tips were appreciated, if ultimately futile. Our successful field season is owed in part to the hospitable Breeden family at Morley River Lodge. Critical review by Dave Lefebure is gratefully acknowledged.

REFERENCES

Abbott, J.G. (1981): Geology of the Seagull Tin District; in Yukon Exploration and Geology 1979-1980, *Indian and Northern Affairs Canada,* pages 32-44.

Aitken, J.D. (1959): Atlin Map-area, British Columbia; *Geological Survey of Canada*, Memoir 307, 89 pages.

Creaser, R.A., Erdmer, P., Stevens, R.A. and Grant, S.L. (1997): Tectonic affinity of Nisutlin and Anvil assemblage strata from the Teslin Tectonic Zone, Northern Canadian Cordillera: Constraints from neodymium isotope and geochemical evidence; *Tectonics,* Volume 16, pages 107-121.

Colpron, M. (1999): Glenlyon project: Preliminary stratigraphy and structure of Yukon-Tanana Terrane, Little Kalzas Lake area, central Yukon (105L/13); *in* Roots, C.F. and Emond, D.S. (editors), Yukon Exploration and Geology 1998, Exploration and Geological Services Division, Yukon, *Indian and Northern Affairs Canada*, pages 63-71.

Cook, S. and Pass, H. (2000): Ancient Pacific Margin Part V: Preliminary results of geochemical studies for VMS deposits in the Big Salmon Complex, Northern British Columbia, in Geological Fieldwork 1999, *B.C.Ministry of Energy and Mines*, Paper 2000-1, this volume.

deKeijzer, M., Williams, P. and Brown, R.L. (1999): Kilometre-scale folding in the Teslin zone, northern Canadian Cordillera, and its tectonic implications for the accretion of the Yukon-Tanana Terrane to North America; *Canadian Journal of Earth Science*, Volume 36, pages 479-494.

de Keijzer, M., Mihalynuk, M.G. and Johnston, S.T. (2000): Structural investigation of an exposure of the Teslin Fault; in Current Research, *Geological Survey of Canada*, Paper 2000-A, (in press).

Dixon-Warren, A. and Hickin, A. (2000): Ancient Pacific Margin NATMAP Part IV: Surficial mapping and till geochemistry in the Swift River Area, north western British Columbia; in Geological Fieldwork 1999, *B.C. Ministry of Energy and Mines*, Paper 2000-1, (in press).

Erdmer, P. (1985): An examination of cataclastic fabrics and structures of parts of Nisutlin, Anvil and Simpson allochthons, central Yukon: test of the arc-continent collision model; *Journal of Structural Geology*, Volume 7, pages 57-72.

Erdmer, P. and Helmstaedt, H. (1983): Eclogite from central Yukon: a Record of subduction at the western margin of Ancient North America; *Canadian Journal of Earth Sciences*, Volume 20, pages 1389-1408.

Erdmer, P. and Armstrong, R.L. (1989): Permo-Triassic isotopic dates for blueschist, Ross River area, Yukon; *in* Yukon Exploration and Geology, Volume 2: Exploration and Geological Services Division, Yukon, I*ndian and Northern Affairs Canada*, pages 33-36.

Erdmer, P., Ghent, E.D., Archibald, D.A. and Stout, M.Z. (1998): Paleozoic and Mesozoic high pressure metamorphism at the margin of ancestral North America in central Yukon; Geological Society of America Bulletin, Volume 110, pages 615-629.

Gabrielse, H. (1969): Geology of the Jennings River Map-Area, British Columbia (104-O); *Geological Survey of Canada*, Paper 68-55.

Gleeson, T.P., Friedman, R.M. and Wahl, K. (2000): Stratigraphy, structure, geochronology and provenance of the Logjam Creek area, northwestern British Columbia (NTS

104O/14W); in Geological Fieldwork 1999, *B.C. Ministry of Energy and Mines*, Paper 2000-1, (in press).

Gordey, S.P. (1995): Structure and Terrane Relationships of Cassiar and Kootenay (Yukon-Tanana) Terranes, Teslin Map Area, Southern Yukon Territory; *in* Current Research 1995-A; *Geological Survey of Canada*, pages 135-140.

Gordey, S.P. (2000): Geology, Teslin, Yukon Territory (105C); *Geological Survey of Canada,* Open File 2886, scale 1:250 000.

Gordey, S.P. and Stevens, R.A. (1994): Preliminary interpretation of bedrock geology of the Teslin area (105C), southern Yukon; *Geological Survey of Canada*, Open File 2886, scale 1:250 000.

Hansen, V.L. (1989): Structural and kinematic evolution of the Teslin suture zone, Yukon: Record of an ancient transpressional margin; *Journal of Structural Geology*, Volume 11, pages 717-733.

Hansen, V.L., (1992a): P-T Evolution of the Teslin suture zone and Cassiar tectonites, Yukon, Canada: evidence for A- and B-type subduction; *Journal of Metamorphic Geology*, Volume 10, pages 239-263.

Hansen, V.L. (1992b): Backflow and margin-parallel shear within an ancient subduction complex; Geology, Volume 20, pages 71-74.

Hansen, V.L., J.K. Mortensen, and Armstrong, R.L. (1989): U-Pb, Rb-Sr, and K-Ar isotopic constraints for ductile deformation and related metamorphism in the Teslin suture zone, Yukon-Tanana terrane, south-central Yukon; *Canadian Journal of Earth Sciences*, Volume 26, pages 2224-2235.

Hansen, V.L., M.T. Heilzer, and Harrison, T.M. (1991): Mesozoic thermal evolution of the Yukon-Tanana composite terrane: New evidence from 40Ar/39Ar data; *Tectonics*, Volume 10, pages 51-76.

Harms, T.A. and Stevens, R.A. (1996): A working hypothesis for the tectonostratigraphic affinity of the Stikine Ranges and a portion of the Dorsey Terrane; in Cook, F. and Erdmer, P. (compilers), Slave-Northern Cordillera Lithospheric Evolution Transect and Cordilleran Tectonics Workshop Meeting, *University of Calgary*, Lithoprobe Report No. 50, pages 93-95.

Mihalynuk, M.G., Nelson, J. and Friedman, R.M. (1998): Regional geology and mineralization of the Big Salmon Complex (104N NE and 104O NW) in Geological Fieldwork 1997, *B.C. Ministry of Employment and Investment*, Paper 1998-1, pages 157-170.

Mortensen, J.K. (1992): Pre-mid-Mesozoic tectonic evolution of the Yukon-Tanana terrane, Yukon and Alaska; *Tectonics*, 11, pages 836-853.

Mortensen, J. K., Ghosh, D.K. and Ferri, F. (1995): U-Pb geochronology of intrusive rocks associated with copper-gold porphyry deposits in the Canadian Cordillera; in Porphyry Deposits of the Northwestern Cordillera of North America, Schroeter, T.G., Editor, Canadian Institute of Mining, Metallurgy and Petroleum; Special Volume 46, pages 142-158.

Mulligan, R. (1963): Geology of the Teslin Map-Area, Yukon Territory; Geological Survey of Canada, Memoir 326, 96 pages.

Murphy, D.C. and Piercey, S.J. (1999): Finlayson project: Geological evolution of Yukon-Tanana Terrane and its relationship to Campbell Range belt, northern Wolverine Lake map area, southeastern Yukon; in Roots, C.F. and Emond, D.S. (editors.), Yukon Exploration and Geology 1998, Exploration and Geological Services Division, Yukon, Indian and Northern Affairs Canada, pages 47-62.

Nelson, J.L., Mihalynuk, M. G., Murphy, D.C., Colpron, M., Roots, C.F., Mortensen, J.K. and Friedman, R.M. (2000): Ancient Pacific Margin Part II: A preliminary comparison of potential VMS-hosting successions of Yukon-Tanana Terrane, from Finlayson district to northern British Columbia; *in* Geological Fieldwork 1999, *B.C. Ministry of Energy and Mines*, Paper 2000-1, (this volume).

North American Commission on Stratigraphic Nomenclature (1983): North American stratigraphic code; The American Association of Petroleum Geologists Bulletin, Volume 67, pages 841-875.

Poole, W.H. (1956): Geology of the Cassiar Mountains in the vicinity of the Yukon-British Columbia boundary; unpublished Ph.D. thesis, Princeton University, 247 pages.

Poulton, T., Orchard, M.J., Gordey, S.P. and Davenport, P. (1999): Selected Yukon fossil determinations; *in* Yukon digital geology, S.P. Gordey and A.J. Makepeace (compilers), *Geological Survey of Canada*, Open File D3826, *and* Exploration and Geological Services Division, Yukon, *Indian and Northern Affairs Canada*, Open File 1999-1(D).

Roots, C.F., de Keijzer, M., Nelson, J.L. and Mihalynuk, M.G. (2000): Revision mapping of the Yukon-Tanana and equivalent terranes in northern B.C. and southern Yukon between 131° and 132°W; in Current Research, Geological Survey of Canada, Paper 2000-1A, pages (in press).

Stevens, R.A. (1992): Regional geology, fabric and structure of the Teslin suture zone in Teslin map area, Yukon Territory; in Current Research, Geological Survey of Canada, Paper 92-1A, pages 287-296.

Stevens, R.A. (1994): Geology of the Teslin suture zone in parts of Laberge (105E/1), Quiet Lake (105F/4) and Teslin (105C/11, 13, 14) map areas, Yukon Territory; Geological Survey of Canada, Open File 2768.

Stevens, R.A. and Erdmer, P. (1993): Geology and Structure of the Teslin suture zone and related rocks in parts of Laberge, Quiet Lake and Teslin map areas, Yukon; in Current Research, Geological Survey of Canada, Paper 93-1A, pages 22-20.

Stevens, R.A. and Harms, T.A. (1995): Investigations in the Dorsey Terrane, Part 1: Stratigraphy, Structure and Metamorphism in the Dorsey Terrane, Southern Yukon Territory and Northern British Columbia; in Current Research, Geological Survey of Canada, Paper 95-1A, pages 117-128.

Stevens, R.A. and Harms, T.A. (1996): Geology in the vicinity of the Dorsey Range, southern Yukon Territory and northern British Columbia; scale 1:50 000; in Cook, F. and Erdmer, P. (compilers), Slave-Northern Cordillera Lithospheric Evolution Transect and Cordilleran Tectonics Workshop Meeting, University of Calgary, Lithoprobe Report No. 50, pages 222-225.

Stevens, R.A., Erdmer, P., Creaser, R.A. and Grant, L.S. (1996): Mississippian assembly of the Nisutlin assemblage: Evidence from primary contact relationships and Mississippian magmatism in the Teslin tectonic zone, part of the Yukon-Tanana Terrane of south-central Yukon; Canadian Journal of Earth Sciences, Volume 33, pages 103-116.

Tempelman-Kluit, D.J. (1979): Transported cataclasite, ophiolite and granodiorite in Yukon: evidence of arc-continent collision; Geological Survey of Canada, Paper 79-14.

Wheeler, J.O., Brookfield, A.J., Gabrielse, H. Monger, J.W.H., Tipper, H.W. and Woodsworth, G.J. (1991): Terrane map of the Canadian Cordillera; Geological Survey of Canada, Map 1713A.

Appendix I: Notes on Figure 3

Thick Quaternary deposits completely blanket some parts of the map area for tens of square kilometres. These are problem areas in which tenuous extrapolations are required to produce the map of Figure 3. Many extrapolations, if correct, carry important implications. Other extrapolations, drawn to mimic local structural style, imply detailed knowledge of unit distributions that does not exist. Most limitations of Figure 3 will become apparent with future publication of 1:50 000 scale Open File maps which will show inferred contacts and limits of outcrop; however, many of the following remarks are germane to those maps as well. The numbered points below correspond to the numbers, ordered from north to south, enclosed by triangles on Figure 3.

1. Western contacts of the Screw Creek limestone have not been found in the Screw Creek valley bottom. Lowest exposures of limestone are apparently right way up based on poorly preserved grading in siliceous tuffaceous layers. Structurally higher parts of the limestone are clearly upside down (described above).
2. Crinkle chert occurs in the old Alaska Highway road cut, but the area to the west is swamp; no greenstone is mapped.
3. This contact is well constrained between the elongate pluton of presumed Jurassic age and the Alaska Highway, but has not been observed north or south of those points.
4. The syncline is constrained along the shoreline and near "4". However, closure could not be confirmed by mapping. Felsic volcanics on the southern limb are locally very siliceous and might be a volcanic-crinkle chert hybrid.
5. Closure of the fold has not been demonstrated unequivocally. However, all indications point to fold closure: only greenstone is mapped along the Smart River road, both limbs have been mapped to within a couple kilometres of the hinge and layer-cleavage relationships on the limbs are consistent with closure.
6. Mapping of 104O/14W is incomplete. Low outcrops in the downstream stretches of the Screw Creek valley include small areas of limestone, perhaps hinges of folds developed on the lower limb of the Screw Creek limestone.
7. Crinkle chert occurs as a large area of angular boulders atop Hazel orthogneiss where it is assumed to be locally derived. Crinkle chert is known to occur along the contact of the Hazel orthogneiss at location 2 and near the Peak of Mount Hazel.
8. Only small lenses of carbonate are found in the axial zone of the fold. Carbonate on the fold limbs apparently grades laterally into graphitic wacke near the fold core.
9. Only three areas of outcrop constrain the eastern limestone belt south of the Alaska Highway. One is near the north margin of the Simpson Peak batholith another is south of central Swan Lake on Hook Creek (creek not shown on Figure 3), and third is an area of sparse outcrops in the forest west of Swan Lake. At none of these localities is the crinkle chert unit exposed.
10. Geology near "10" and an equal distance due north of the highway has been compiled mainly from vantage point mapping. It requires confirmation by direct observations.
11. Orthogneiss near Mt. Francis is lithologically similar to the Hazel orthogneiss in many respects; however, it apparently cuts younger stratigraphy. It is presumably between 362 and 335Ma, because it is younger than the greenstone, but is overlain by conglomerate believed derived subsequent to a deformational event around 345 Ma. (*see* Discussion).
12. Only scattered outcrops of limestone and greenstone cut by tonalite are present at the southern end of the carbonate belt. More persistent outcrop near the northern end of the belt leads to a map pattern that implies that the Hazel orthogneiss also cuts the limestone, but this is probably not the case. It appears more likely that the limestone belt outlines a tight synformal keel that is bent to the west and extends over the Hazel orthogneiss (*see* location 7). The crinkle chert unit was apparently not deposited at this locality below the limestone.
13. All contacts between Coconino tonalite and Simpson Peak batholith are covered. Since Coconino tonalite is older and more deformed than the Simpson Peak batholith, the interpreted contact configuration is meant to show the former cut by the latter.
14. Teh Creek pluton is shown as an elongate body trending 290°. In fact, most of the central portion traversed by Teh Creek is covered and two separate bodies could be present. However, the plutonic rocks exposed at either end of the body lithologically indistinguishable, and the body is known to continue in similar fashion to the east beneath a carapace of Klinkit assemblage rocks to where it is exposed in the Butsih Creek valley. Several correlated geochemical anomalies coincide with carapace rocks in easternmost 104O/12 (near 19; *see* also Cook and Pass, 2000, this volume).
15. Felsic volcanics are not mapped north of "15", but are shown extending through a covered area to the limestone belt because of their common association with limestone elsewhere.
16. As is the case for locality "14", no outcrop exists to support the interpretation of a continuous septa of greenstone. However, clear relationships occur at both the western and eastern ends of the septa. The contact shown between greenstone and Klinkit argillite is purely conjectural.
17. Teslin fault is beautifully exposed here (*see* deKeijzer *et al.*, 2000).
18. A tight synformal keel of crinkle chert and limestone is enveloped by greenstone. In particular, limestone layers are strongly folded and rodded, producing a "false stretched monomict conglomerate" in which the apparent stretched limestone "cobbles" are actually decapitated, isoclinal interference folds. Protolith textures are destroyed due to the coincidence of interference fold cores; however, good protolith textures are displayed in greenstone where it occurs out along the relatively planar fold limbs.
19. Teh Creek pluton in subsurface produces hornfels and multielement geochemical anomalies in local stream sediments (*see* "14" above and Cook and Pass, this vol-

ume). Roof rocks are cut by abundant thick dikes and the pluton is again exposed in Butsih valley to the east.

20. Cherty argillite believed to be part of the Cache Creek Kedahda Formation is strongly hornfelsed near the intrusive contact.

21. Most of the unit is covered within 5 kilometres of the River. Observations are restricted to within 2 kilometres of the northern contact.

22. A few scattered outcrops of strongly foliated, blue grey limestone occur in the middle of a broad glacial outwash plain east of Kachook Creek. They are included with the Permian Teslin Formation based only upon lithological similarity. Thus, the trace of the Teslin Fault must run to the north, down the Jennings River.

23. Both northwest and northeast contacts of the Charlie Cole pluton are covered.

Ancient Pacific Margin Natmap Part IV: Surficial Mapping and Till Geochemistry in the Swift River Area, Northwestern British Columbia

By Antigone Dixon-Warren[1] and Adrian Hickin[2]

KEYWORDS: *Quaternary, Surficial Geology, Till, Geochemistry, Exploration, Swift River, Teslin Lake.*

INTRODUCTION

An integrated surficial mapping and detailed till geochemistry project was conducted in the summer of 1999 by the British Columbia Geological Survey Branch in northwestern British Columbia. Recent volcanogenic massive sulphide (VMS) discoveries such as Kudz Ze Kayah and Wolverine and intrusive related gold deposits like Pogo within the Yukon-Tanana Terrane have provided an impetus for geological studies to examine similar age rocks in British Columbia. These deposits are an important source of copper, zinc, gold and silver. Previous mapping indicates that the Big Salmon Complex (Mihalynuk *et al*., 1998) and Dorsey Terrane (Nelson, 1999) are Yukon-Tanana equivalent and contain appropriate rocks/stratigraphy to host mineralization. Given the widespread drift cover in the study area and high mineral potential, there was an obvious need to integrate Quaternary studies to develop exploration strategies for new buried targets. This study is a component of the Ancient Pacific Margin NATMAP project and associated work includes bedrock mapping (Nelson, this volume; Mihalynuk *et al*., this volume) and multi-media geochemical surveys (Cook and Pass, this volume).

Surficial mapping was completed over the Big Salmon Complex to understand the local glacial history and aid in the interpretation of geochemical data. Mapping of surficial sediments defines the distribution of preferred sampling media (*e.g.* till) and bedrock exposure. Compilation of ice-flow indicator data enables the reconstruction of local paleo-ice-flow history and can consequently be used to define the methodologies for sampling down ice dispersal patterns. Till sampling assists in defining the size and shape of geochemical anomalies over a known mineral showings as well as select perspective host rocks. Characterization of geochemical signatures and dispersal in the study area will assist in the development of future geochemical exploration projects.

[1]*British Columbia Ministry of Energy and Mines*

[2]*Vanessa Ventures*

The main objectives of the program were to stimulate exploration and economic activity in the area by:

- producing a 1:100 000 surficial geology map, identifying unconsolidated units suitable for geochemical sampling and tracing of mineral anomalies to their bedrock sources;
- collecting and mapping ice-flow indicators (*e.g.* striae, drumlins) to establish paleo-ice-flow directions to assist in the interpretation of geochemical trends;
- conducting till geochemical case studies at known prospects to better develop and refine the geochemical response of mineralization; and
- further defining areas of high mineral potential through till geochemistry.

The results of the surficial mapping component, including an interpretation of surficial deposits, and detailed geochemical studies are briefly described in this paper.

PHYSIOGRAPHIC AND GEOLOGIC SETTING

The study area, covering about 4,000 square kilometres, is located in northwestern British Columbia approximately 100 kilometres north-east of Atlin (Figure 1) and is coincident with NTS map areas 104N/9, 16 and 104O NW. The gently rolling Nisutlin Plateau covers the western half of the area, and the rugged Stikine Range of Cassiar Mountains the eastern margin. Teslin Lake forms the western margin of the area, whereas the northern boundary is shared with the British Columbia-Yukon border. Elevations range from nearly 700 metres to more than 2,100 metres above sea level. Simpson Peak (2,173 metres) is the highest mountain in the region. The Alaska Highway, the primary road access, crosses the northern portion of the area.

The rolling topography of the Nisutlin Plateau is covered by thick glacial sediments. Several bluffs and ridges composed of bedrock are found throughout the plateau, but few rise more than 300 metres above their surroundings. Many lakes occur in the area, most ranging in size from small ponds (10's of metres) to 5 kilometres. Teslin Lake, the largest water body in the study area is nearly

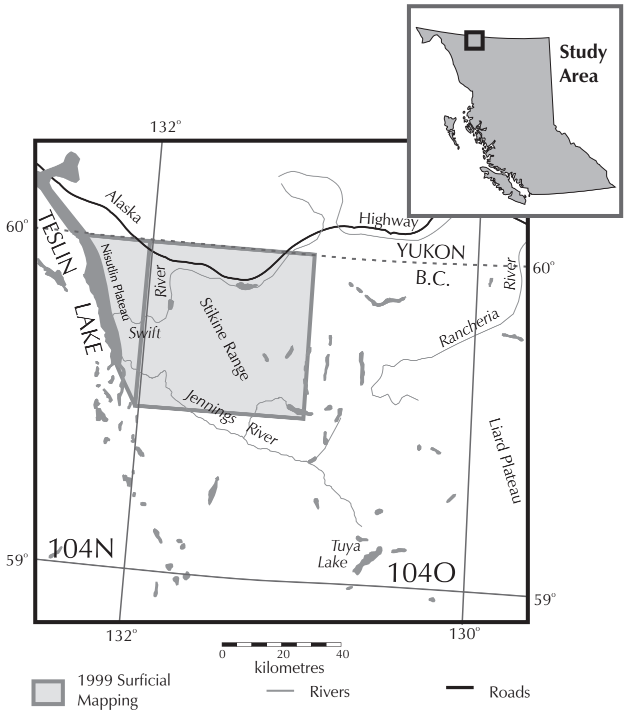

Figure 1. Location of Swift River study area, north western British Columbia.

200 kilometres long. Swamps and marshes cover areas where drainage is poor.

Mountains of the Stikine Range have sharp peaks linked by narrow arêtes. Their scree strewn slopes are generally steep and cut by cirques. Deep, broad north-south trending valleys are filled with thick deposits of glacial sediments which are being reworked by modern fluvial systems. Kettle lakes and moraine dammed lakes are common.

VEGETATION AND CLIMATE

The Swift River area lies within the boreal white and black spruce, spruce-willow-birch, and alpine tundra biogeoclimatic zones (MacKinnon *et al.*, 1992). Winters are long and cold, and summers short, cool and wet. The ground remains frozen for much of the year. Mean annual temperatures are commonly below 0°C and precipitation in the valleys averages 400 to 500 millimetres per year (BC Ministry of Environment, 1978).

The relatively well-drained shores of Teslin Lake and river valleys are covered with trembling aspen and lodgepole pine. Where the topography is flat and poorly drained, the landscape is typically a mosaic of black spruce bogs and white spruce and trembling aspen stands. In the subalpine areas, stands of stunted white spruce and fir grow on the lower slopes. Above treeline (1500 metres), long, cold winters create conditions too severe for the growth of most woody plants. This zone is dominated by dwarf shrubs (*e.g.* birch, willow), herbs, mosses, lichens, and grassland (MacKinnon *et al.*, 1992).

BEDROCK GEOLOGY

Bedrock geology studies were initially completed within the region by Gabrielse (1969), Aitken (1959) and Watson and Mathews (1944). Most recently, detailed mapping has been conducted by Mihalynuk *et al.*, (2000b) in the Big Salmon Complex and by Nelson *et al.* (2000) in the Dorsey Terrane to the southeast. Devono-Mississippian rocks of the Big Salmon Complex underlie much of the study area (Figure 2).

The Big Salmon Complex is a sequence of stratified rocks that have been metamorphosed and undergone several episodes of folding (Mihalynuk *et al.*, 1998; Nelson *et al.*, 1998). From youngest to oldest, stratified units include siliciclastic rocks and interbedded felsic tuffs, limestone, manganiferous chert, quartz-rich greywacke, orthogneiss and greenstone dominated by epiclastics (Mihalynuk *et al.*, 2000).

The Big Salmon Complex rocks have been intruded by Jurassic and Cretaceous granitoids and are overlain by Pleistocene to Recent basalt of the Tuya Formation. The exact age of the basalts is unknown, however, volcanic activity preceded and then continued during a time of glaciation (Gabriesle, 1969). For a complete description of the geology of the Big Salmon Complex, refer to Mihalynuk *et al.* (this volume).

Mineral Showings

The Arsenault copper prospect (MINFILE 104O 011) is the only developed property in the area with potential for hosting VMS mineralization. It is located approximately 14 kilometres south of the Smart and Swift Rivers confluence, on the west side of Mount Francis (Figure 2). Copper mineralization was discovered on the property in the 1940's (Sawyer, 1979) and geological and geochemical work was performed on the property in 1967 (Sawyer, 1967) and 1970's (Sawyer, 1979; Phendler, 1982). Exploration work included trenching, geophysical surveys (airborne EM, magnetometer, induced polarization), soil surveys, geological mapping and diamond drilling.

Host rocks include interbedded metasedimentary and metavolcanic lithologies such as carbonates, quartzite and schist. Mineralization at the surface is best exposed in quartz-rich strata containing disseminated and blebs of chalcopyrite and pyrite with associated epidote, garnet, actinolite, magnetite and wollastonite in contact with carbonate. Sawyer (1979) also reported traces of bornite, molybdenite, piedmontite (manganese-epidote) and spessartine (manganese-garnet).

The type of mineralization forming the Arsenault prospect is poorly understood. Although quartz-carbonate association and calc-silicate mineralogy and textures suggest a skarn association, there are no significant intrusive bodies exposed nearby (Mihalynuk *et al.*, 1998). A volcanogenic origin has also been proposed (Sawyer, 1979) and recent work has centred on the VMS potential of the host rocks in the area (Traynor, 1999). Elevated selenium in soils also supports a syngenetic origin as the

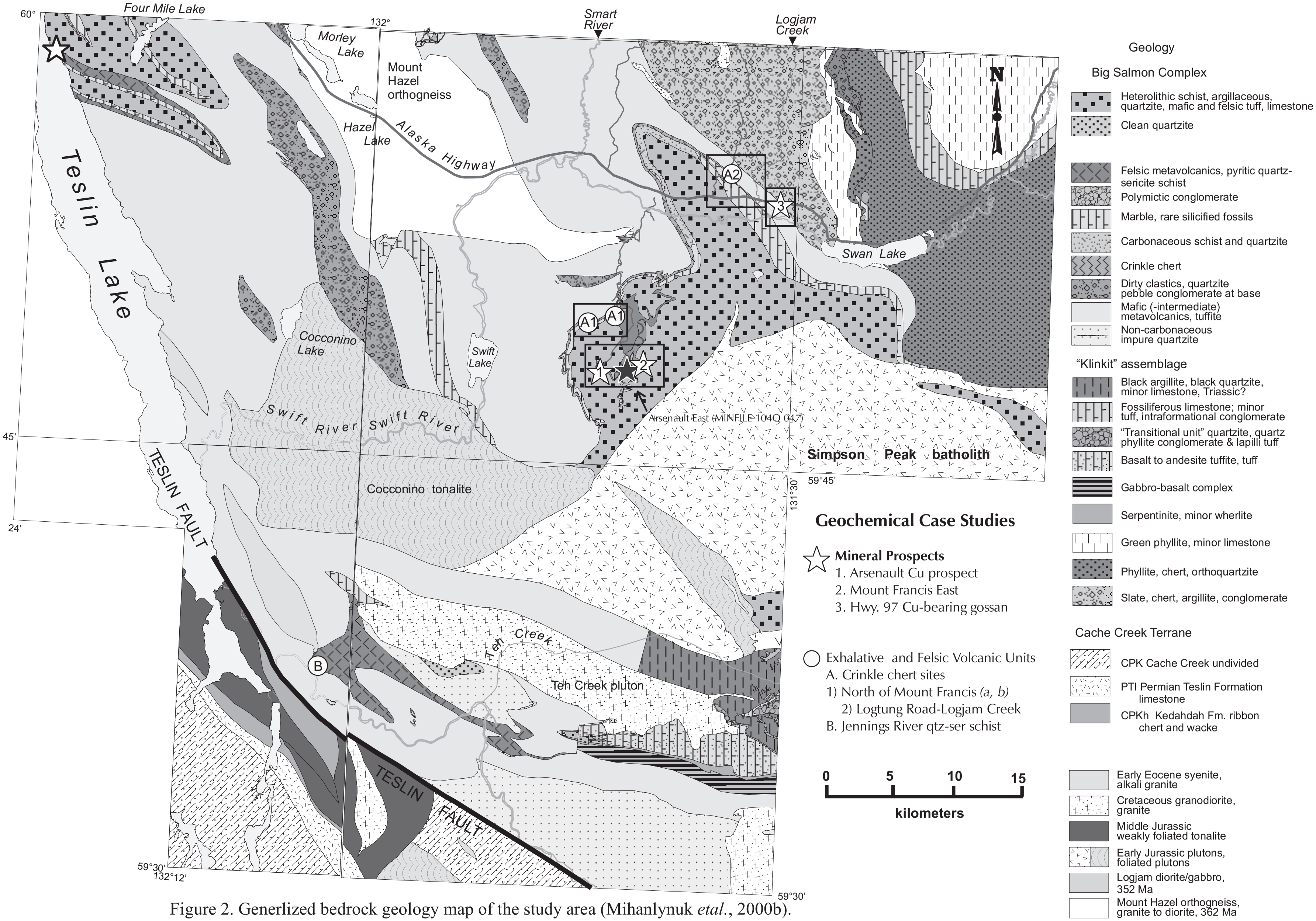

Figure 2. Generlized bedrock geology map of the study area (Mihanlynuk *etal.*, 2000b).

VMS deposits in the Yukon Tanana Terrane (*e.g.* Kudz Ze Kayah and Wolverine) are selenium-rich (Cook and Pass, this volume).

Arsenault East (MINFILE 104O 047), a new mineral occurrence interpreted as occurring in about the same 100 metres stratigraphic interval as the Arsenault prospect, was discovered by Mihalynuk *et al.* (1998) on the east flank of Mount Francis. The showing consists of a 10 metre-long chalcopyrite-bearing vein replacement zone developed in carbonate rocks. Another new mineral occurrence discovered by Mihalynuk *et al.* (1998) includes the Highway 97 Cu-bearing gossum(MINFILE 104O 054; Figure 2).

METHODOLOGIES

During an initial compilation phase, all existing geological and geochemical information for the area was evaluated. Surficial maps of Klassen (1982, 1978) and Morison and Klassen (1997) provided background data on the types of sediments expected. Regional mapping by the Geological Survey of Canada (Gabrielse, 1969) and British Columbia Department of Mines (Watson and Mathews, 1944) provided additional information on the type and distribution of surficial sediments as well as paleo-ice-flow patterns. Regional Geochemical Survey (RGS, 1978, 1979) stream and lake sediment data and property scale geochemical surveys (*e.g.* Sawyer, 1967) provided limited geochemical information for the area.

Airphoto analysis and 'pretyping' followed the terrain classification system of Howes and Kenk (1997). Air photos at a scale of 1:70,000 (flight lines BC88063, BC88080 and BC37067) were used in the map generation. Thirty-three 1:20,000 digital TRIM maps were tiled for the base map, produced at a scale of 1:100,000 (Dixon-Warren and Hickin, 2000). About 20 per cent of the preliminary polygon interpretations were verified through field checking, corresponding to a Terrain Survey Intensity Level D (Resources Inventory Committee, 1996).

Field Methods

Fieldwork was conducted over a four week period during July and August from a base camp on Morley Lake, near the British Columbia-Yukon border. Most fieldwork was helicopter supported. Road access was restricted to the northern portion of the study area along the Alaska Highway (Highway 97) and along spur roads to borrow pits and mineral showings.

At each field verification station some or all of the following was recorded: UTM location, elevation, general slope, type of exposure (*e.g.* road cut, river cut), geographic landforms (*e.g.* terrace, floodplain, ridge), type of bedrock (if present), unconsolidated surface material and expression (terrain polygon designation), and orientation of striations/grooves/stoss and lee forms. Surficial sediments were described and interpreted at relevant stations. Logged information included: number of units, stratification, bedding thickness, sorting, texture, structures, and colour (wet and dry), clay content, clast content (per cent), clast roundness and size, and dominant lithologies.

Forty-five bulk sediment samples (approximately 5 kilograms in size) were collected for geochemical analysis at six sites in the study area. Basal till was the preferred media, although colluviated tills and colluvium were sampled where necessary. Natural exposures and hand excavation were used to obtain samples from undisturbed C horizon material. At each site, the above information was recorded, in addition to: type of exposure (*e.g.* roadcut, rivercut, excavated trench); depth to sample from top of soil; matrix or clast-supported diamicton; consolidation; matrix texture; structures; clast shape, size and lithology; clast percentages; and colour. Table 1 compares some the descriptive properties of each sample collected.

Till samples were submitted to Bondar Clegg-Intertek Laboratories, North Vancouver, for drying and sieving to <63 microns (-230 mesh). A 5 gram and 25 gram portion split were taken from the <63 micron samples. Acme Analytical Laboratories, Vancouver, analyzed the 5 gram split for a suite of trace elements by aqua regia digestion-ICPMS (inductively coupled plasma mass spectroscopy; Table 2) and for major element oxides by lithium metaborate ($LiBO_2$) fusion-ICP (11 oxides, loss on ignition and 7 minor elements; Table 4). The 25 gram split was submitted to Activation Laboratories, Ancaster, Ontario, for thermal neutron activation analysis (INAA) for 35 elements (Table 3). Data for 29 elements (gold, antimony, arsenic, barium, bromine, calcium, cerium, cesium, chromium, cobalt, europium, hafnium, iron, lanthanum, lutetium, molybdenum, neodymium, rubidium, samarium, scandium, selenium, sodium, tantalum, terbium, thorium, tungsten, uranium, ytterbium, and zinc) are reported here. Additional data for six other elements (silver, mercury, iridium, nickel, tin and strontium) are not reported due to factors such as low elemental abundance and inadequate detection limits.

Quality Control

Quality control is important for distinguishing geochemical trends caused by geological features versus those resulting from anthropogenic influences, spurious sampling or analytical errors. In order to evaluate geochemical sampling and analytical variability, field triplicate samples, laboratory duplicate samples and reference standards were incorporated in the sample suites submitted for commercial laboratory analysis. The standards, triplicates and duplicates are inserted into each batch of 20 prepared samples to measure accuracy and precision. Each batch of 20 samples contained sixteen routine till samples, a field triplicate collected adjacent to a routine sample, a blind duplicate sample split from one of the sixteen samples prior to analysis, and a control reference standard containing material of known element concentrations (either Canada Centre for Mineral and Energy Technology certified standard or a Geological Survey Branch 'prepared bulk standard'). Commonly, elements

TABLE 1
DESCRIPTION OF TILL PHYSICAL PROPERTIES

Station	Sample	NTS Mapsheet	UTME[1] (NAD83)	UTMN[1] (NAD83)	Material	Structure	Matrix	Colour	Clast (%)	Clast Range (cm)	X-Size (cm)	Roundness Range	X-Roundness	Sample Depth (m)
Crinkle Chert - North of Mount Francis														
ADW99-120	996025	104 O/13	346065	6636115	M	massive	sdy-cly	Grey	10	<1 - 30	2	A - R	SR	0.45
ADW99-120	996026	104 O/13	346065	6636115	M	massive	sdy-cly	Grey	10	<1 - 30	2	A - R	SR	0.45
ADW99-120	996027	104 O/13	346065	6636115	M	massive	sdy-cly	Grey	10	<1 - 30	2	A - R	SR	0.45
ADW99-105A	996029	104 O/13	348746	6636773	CM	massive	sd	Brown grey	35	<1 - >50	2	VA - WR	SR	0.40
ADW99-106A	996030	104 O/13	348601	6636847	M	massive	cly-slt	Olive grey	10	<1 - 75	0.5	A - R	SR	0.40
ADW99-107	996031	104 O/13	348394	6636795	M	massive	cly-slt	Olive grey	10	<1 - 75	0.5	A - R	SR	0.40
ADW99-108	996032	104 O/13	348444	6636712	M	massive	slty-sd	Brown grey	15	<1 - 10	1	A - R	SR	0.40
ADW99-109	996033	104 O/13	348504	6636553	M	massive	silt-sd	Brown grey	35	<1 - >50	2	VA - WR	SR	0.30
ADW99-110	996034	104 O/13	348635	6636661	CM	massive	slty-sd	Brown grey	35	<1 - >50	2	VA - WR	SR	0.30
ADW99-113	996035	104 O/13	346247	6636142	CM	massive	slty-sd	Tan grey	20	<1 - 5	<1	A - R	SR	0.30
ADW99-114	996036	104 O/13	346247	6636142	CM	massive	slty-sd	Tan grey	20	<1 - 5	<1	A - R	SR	0.30
ADW99-115	996037	104 O/13	346247	6636142	CM	massive	slty-sd	Tan grey	20	<1 - 5	<1	A - R	SR	0.30
ADW99-112	996038	104 O/13	346303	6636214	M	massive	slty-sd	Brown grey	10	<1 - 10	1	SA - SR	SR	0.40
ADW99-118	996045	104 O/13	346137	6636074	M	massive	sdy-cly	Brown grey	15	<1 - 8	0.75	A - R	SR	0.60
ADW99-119	996046	104 O/13	346227	6636128	M	massive	sdy-slt	Brown grey	25	<1 - 12	1	A - SR	SA	0.65
Crinkle Chert - Logtung Road														
ADW99-123	996047	104 O/13	355511	6645963	M	massive	sdy-cly-slt	Tan grey	15	<1 - 10	1	A - SR	SA	0.30
ADW99-124	996048	104 O/13	355421	6645940	M	massive	cly	Olive grey	15	<1 - 6	0.5	A - R	SR	0.40
ADW99-125	996050	104 O/13	355589	6645886	M	massive	cly	Medium grey	10	<1 - 8	0.5	A - R	SR	0.20
ADW99-126	996051	104 O/13	357515	6644440	M	massive	slty-cly	Tan grey	30	<1 - 200	1	A - SR	SA	0.30
Jennings River Quartz-Sericite Schist														
ADW99-116	996039	104 N/9	667150	6612984	M	massive	slty-cly	Olive grey	10	<1 - 30	2	VA - R	SR	0.60
ADW99-117	996042	104 N/9	667080	6612977	M	massive	slty-cly	Dark grey	20	<1 - 30	2	VA - R	SR	0.50
ADW99-117	996043	104 N/9	667080	6612977	M	massive	slty-cly	Dark grey	20	<1 - 30	2	VA - R	SR	0.50
ADW99-116	996044	104 N/9	667150	6612984	M	massive	slty-cly	Olive grey	10	<1 - 30	2	VA - R	SR	0.60
Arsenault Prospect														
ADW99-102	996020	104 O/13	347294	6632957	M?	massive	cly-slt	Olive brown	10	<1 - 8	0.5	A - SR	SA	0.50
ADW99-103	996022	104 O/13	347182	6632718	CM	massive	cly-slty-sd	Grey	15	<1 - 7	0.5	A - SR	SA	0.35
ADW99-104	996023	104 O/13	347391	6632697	CM	massive	sd-cly-slty	Grey	25	<1 - 30	1	A - SR	SA	0.40
ADW99-105	996024	104 O/13	347940	6633436	C	massive	sd	Red brown	40	<1 - 50	2	VA - SR	SA	0.60
ADW99-106	996028	104 O/13	347819	6633485	CM	massive	slty-cly-sd	Grey	15	<1 - 3	0.5	SA - R	SR	0.80
Mount Francis East														
ADW99-091	996008	104 O/13	350388	6633477	CM	massive	slty-sd	Brown	35	<1 - 40	2	VA - R	SA	0.80
ADW99-092	996012	104 O/13	350289	6633424	CM	massive	slty-sd	Brown	35	<1 - 40	2	VA - R	SA	0.50
ADW99-093	996013	104 O/13	350427	6633480	CM	massive	slty-sd	Brown	20	<1 - 25	1	VA - SR	A	0.70
ADW99-094	996014	104 O/13	350735	6633273	CM	massive	sd	Orange brown	15	<1 - 25	2	VA - R	SA	0.80
ADW99-095	996016	104 O/13	350801	6633262	CM	massive	slty-sd	Light grey	20	<1 - 30	2	VA - A	SA	1.00
ADW99-096	996017	104 O/13	350780	6633180	CM	massive	slty-sd	Grey	20	<1 - 25	2	VA - SA	SA	0.20
ADW99-097	996018	104 O/13	351056	6632892	FG?	massive	sdy-cl	Brown grey	20	<1 - 30	1	A - R	SR	0.60
ADW99-098	996019	104 O/13	351018	6632982	FG?	massive	sd	Brown	40	<1 - 25	2	VA - WR	SR	0.50
Highway 97 Prospect														
ADW99-049	996002	104 O/13	359017	6643685	M	massive	slty-sd	Tan brown	10	0.5 - 20	1	SA - R	SR	0.50
ADW99-050	996003	104 O/13	359032	6643716	M	massive	slty-cly	Olive grey	15	<1 - 60	2	A - SR	SA	0.30
ADW99-052	996004	104 O/13	359102	6643685	M	massive	slty-sd	Tan brown	10	<1 - 10	1	A - SR	SA	0.15
ADW99-051	996005	104 O/13	359029	6643772	M	massive	slty-cly	Olive grey	15	<1 - 60	2	A - SR	SA	0.30
ADW99-053	996006	104 O/13	358964	6643682	M	massive	cly-slt	Grey	5	<0.5 - 1	<1	SA - SR	R	0.45
ADW99-054	996007	104 O/13	359102	6643718	M	massive	slty-cly	Olive grey	15	<1 - 60	2	A - SR	SA	0.30
ADW99-055	996009	104 O/13	358959	6643684	M	massive	slty-cly	Olive grey	15	<1 - 60	2	A - SR	SA	0.30
ADW99-055	996010	104 O/13	358959	6643684	M	massive	slty-cly	Olive grey	15	<1 - 60	2	A - SR	SA	0.30
ADW99-055	996011	104 O/13	358959	6643684	M	massive	slty-cly	Olive grey	15	<1 - 60	2	A - SR	SA	0.30

[1] values accurate within 50 metres

Notes

M = basal till	X-Roundness = mean roundness
C = colluvium	WR = well rounded
CM = colluviated till	R = rounded
FG = glaciofluvial	SB = subrounded
cly = clay	SA = subangular
slt =silt	A = angular
sd = sand	VA = very angular
X-Size = mean size	

TABLE 2
DETECTION LIMITS AND GEOCHEMICAL RESULTS FOR INDUCTIVELY COUPLED PLASMA MASS SPECTROSCOPY (ICPMS)

	Element	Mo	Cu	Pb	Zn	Ag	Ni	Co	Mn	Fe	As	U	Au	Th	Sr	Cd	Sb	Bi	V
	Units	(ppm)	(ppm)	(ppm)	(ppm)	(ppb)	(ppm)	(ppm)	(ppm)	(%)	(ppm)	(ppm)	(ppb)	(ppm)	(ppm)	(ppm)	(ppm)	(ppm)	(ppm)
Sample	Detection Limit	0.01	0.01	0.01	0.1	2	0.1	0.1	1	0.01	0.1	0.1	1	0.1	0.5	0.01	0.02	0.02	2
Crinkle Chert - North of Mt. Francis																			
996021	ADUP 996025	0.52	29.36	12.02	47.0	24	28.6	9.3	345	2.39	6.3	0.7	3	4.6	21.6	0.13	0.41	0.16	68
996025	FieldTRIP 1	0.49	27.09	11.76	45.2	41	27.8	9.0	338	2.31	6.4	0.7	3	4.5	21.0	0.08	0.39	0.16	67
996026	FieldTRIP 2	0.45	24.29	11.63	39.7	17	22.1	7.2	295	2.10	5.8	0.8	3	4.7	20.2	0.06	0.38	0.15	59
996027	FieldTRIP 3	0.42	24.51	12.62	40.6	17	22.6	6.9	281	2.19	5.6	0.8	3	4.9	19.6	0.09	0.40	0.16	61
996029		1.80	57.82	13.65	85.0	55	33.0	16.5	375	3.74	42.1	0.9	5	4.5	19.4	0.10	0.83	0.38	74
996030		1.74	56.69	13.79	83.8	48	32.8	15.9	373	3.67	43.7	0.9	4	4.6	19.6	0.09	0.74	0.40	72
996031		1.20	32.87	10.33	62.6	100	25.1	10.6	367	2.85	13.0	0.8	5	2.7	18.8	0.11	0.48	0.29	65
996032		1.56	28.25	12.37	65.4	68	31.1	12.9	456	3.32	41.0	0.6	3	4.6	13.7	0.15	0.77	0.77	66
996033		4.09	32.23	12.39	58.2	51	30.4	13.0	422	2.67	18.3	0.8	73	5.1	13.0	0.12	0.51	0.19	64
996034		10.73	64.65	8.01	88.5	86	22.9	15.1	368	5.09	13.4	0.8	13	5.8	20.0	0.11	0.46	0.13	56
996035		0.65	35.21	11.69	55.9	15	35.0	13.4	500	2.80	12.4	1.6	2	4.7	12.0	0.05	0.39	0.25	75
996036		0.73	41.93	12.68	65.3	10	36.1	14.3	430	3.06	17.7	1.0	2	5.4	11.0	0.12	0.42	0.19	83
996037		0.87	31.95	12.91	60.5	17	33.5	13.9	352	2.98	10.9	0.9	3	4.9	10.6	0.09	0.44	0.16	74
996038		0.58	29.92	8.83	49.7	32	35.4	12.2	392	2.49	6.5	0.6	2	3.6	22.7	0.12	0.35	0.14	69
996045		0.66	38.97	10.25	54.0	18	28.1	12.4	380	2.78	8.7	0.6	3	4.2	14.6	0.06	0.34	0.23	69
996046		0.59	29.10	9.89	50.6	27	38.2	13.7	521	2.53	10.3	0.5	3	3.4	22.1	0.03	0.34	0.14	73
Crinkle Chert - Logtung Road																			
996047		0.91	28.41	10.33	56.1	86	30.5	8.3	345	2.33	9.9	0.9	3	8.7	25.4	0.16	1.06	0.21	46
996048		1.04	39.51	14.12	66.4	130	39.1	10.9	562	2.68	12.8	0.9	3	9.6	30.9	0.41	1.25	0.24	52
996050		1.12	41.76	10.15	70.8	187	40.1	10.4	409	2.78	14.0	0.9	10	9.8	29.2	0.16	1.42	0.24	52
996051		1.00	39.84	14.84	72.3	127	33.1	16.8	1273	2.83	29.9	0.9	4	7.9	53.5	0.37	2.72	0.24	34
996041	ADUP 996051	0.96	37.79	13.16	71.5	126	32.4	16.1	1245	2.74	29.8	0.8	5	7.8	53.9	0.31	2.78	0.42	33
Jennings River Quartz-Sericite Schist																			
996039		5.57	82.57	11.92	104.7	242	88.7	21.0	715	3.97	14.4	1.4	3	2.9	104.0	0.55	1.16	0.23	75
996042		1.49	49.38	6.61	76.7	128	65.7	19.9	666	3.40	7.2	1.2	4	4.5	91.0	0.28	0.48	0.16	69
996043		4.78	74.97	10.05	90.5	242	90.3	23.0	790	3.67	10.4	1.7	4	2.9	106.0	0.47	0.90	0.19	75
996044		4.55	74.44	9.96	96.7	194	85.6	20.7	705	3.74	10.9	1.0	2	3.1	107.4	0.50	0.92	0.45	73
Arsenault Prospect																			
996020		2.44	589.98	13.83	236.2	168	47.7	16.5	647	3.65	15.2	1.0	8	7.8	24.3	2.41	0.52	0.50	75
996022		2.62	387.65	8.54	64.6	90	35.8	13.9	547	3.10	14.3	1.1	7	6.1	24.8	0.22	0.39	0.50	66
996023		2.60	227.26	12.88	71.2	101	38.2	16.1	558	3.21	35.4	1.4	15	8.8	19.0	0.26	0.65	0.33	63
996024		2.39	157.55	20.86	84.8	81	42.2	23.4	978	3.43	32.2	1.3	28	6.4	15.0	0.48	0.60	0.56	58
996028		2.32	104.35	19.44	67.1	66	25.3	13.8	701	3.03	22.8	1.5	2	2.5	28.8	0.21	0.39	0.44	72
Mount Francis East																			
996008		1.74	35.72	11.30	64.8	61	27.6	11.2	485	2.94	25.9	1.4	3	2.8	14.8	0.22	0.61	0.21	49
996012		2.06	93.88	10.14	74.4	130	52.2	15.5	649	2.84	41.1	1.6	2	4.2	16.4	0.27	0.75	0.50	56
996013		2.20	50.09	8.54	56.9	64	38.7	20.3	602	2.90	24.6	1.3	3	4.7	12.0	0.20	0.74	0.21	60
996014		2.12	116.38	11.14	90.1	114	74.0	19.8	537	2.76	54.3	2.0	6	6.2	21.0	0.38	0.63	0.32	47
996016		2.09	132.88	11.52	132.4	458	77.3	13.8	560	2.56	13.4	13.5	11	3.0	28.9	0.36	0.51	0.25	47
996017		2.46	97.23	13.71	116.8	249	49.1	17.5	927	3.19	26.0	3.7	3	3.4	23.5	0.66	0.58	0.29	65
996018		2.14	76.45	11.67	76.4	150	39.7	12.0	595	2.67	40.8	2.8	4	2.6	30.8	0.30	0.56	0.32	58
996019		1.69	39.63	8.50	86.9	117	29.4	10.4	491	2.22	12.2	2.6	2	2.1	35.9	0.26	0.36	0.18	50
Highway 97 Prospect																			
996002		0.72	53.05	11.54	50.4	37	36.9	11.1	361	2.77	13.3	1.3	4	10.1	19.2	0.08	0.95	0.28	61
996003		0.79	55.17	9.67	60.2	50	39.1	10.3	449	2.78	12.3	1.0	4	7.9	22.9	0.08	0.94	0.26	58
996004		0.58	54.01	9.65	57.5	99	35.1	11.7	307	2.72	8.1	0.8	3	6.6	15.7	0.06	0.58	0.21	59
996005		0.58	23.21	9.58	36.8	20	25.2	8.5	303	2.03	9.4	1.0	2	8.1	18.8	0.06	0.63	0.21	44
996006		1.03	24.14	8.60	61.3	54	37.7	13.5	411	2.62	6.4	1.3	3	5.4	33.8	0.11	0.53	0.20	55
996007		0.69	27.81	7.69	42.7	69	28.8	8.1	339	2.24	8.6	1.0	2	7.2	20.2	0.06	0.68	0.19	47
996009	FieldTRIP 1	0.64	22.32	7.90	39.0	42	23.1	7.2	319	1.92	7.7	0.9	< 1	6.9	24.7	0.07	0.62	0.38	40
996001	ADUP 996009	0.67	22.79	7.83	38.8	42	22.7	7.4	322	1.96	7.3	0.9	5	6.7	25.2	0.07	0.68	0.33	40
996010	FieldTRIP 2	0.71	22.62	8.14	39.1	38	24.3	7.6	319	2.02	8.5	1.0	3	7.6	26.6	0.09	0.66	0.24	41
996011	FieldTRIP 3	0.70	20.46	7.72	39.8	41	23.7	7.4	318	1.96	7.7	0.9	10	6.8	25.7	0.06	0.62	0.19	40
	Median	1.56	49.38	11.14	65.4	81	35.8	13.7	485	2.83	13.4	1.0	3	4.7	21.0	0.16	0.60	0.24	63
	Mean	1.95	80.64	11.30	73.9	101	41.1	14.1	525	2.96	19.0	1.5	7	5.4	29.7	0.27	0.70	0.29	61
	Std. dev.	1.86	104.73	2.85	32.9	86	18.0	4.1	203	0.59	12.7	2.0	12	2.2	25.5	0.38	0.41	0.14	11
	Minimum	0.49	22.32	6.61	36.8	10	22.9	7.2	303	1.92	6.4	0.5	<1	2.1	10.6	0.03	0.34	0.13	34
	Maximum	10.73	589.98	20.86	236.2	458	90.3	23.4	1273	5.09	54.3	13.5	73	9.8	107.4	2.41	2.72	0.77	83

TABLE 2 CONTINUED
DETECTION LIMITS AND GEOCHEMICAL RESULTS FOR INDUCTIVELY COUPLED PLASMA MASS SPECTROSCOPY (ICPMS)

	Element	Ca	P	La	Cr	Mg	Ba	Ti	B	Al	Na	K	W	Tl	Hg	Se	Te	Ga	S
	Units	(%)	(%)	(ppm)	(ppm)	(%)	(ppm)	(%)	(ppm)	(%)	(%)	(%)	(ppm)	(ppm)	(ppb)	(ppm)	(ppm)	(ppm)	(%)
Sample	Detection Limit	0.01	0.001	0.5	0.5	0.01	0.5	0.001	1	0.01	0.001	0.01	0.2	0.02	5	0.1	0.02	0.02	0.02
Crinkle Chert - North of Mt. Francis																			
996021	ADUP 996025	0.40	0.065	14.4	47.8	0.82	511.5	0.199	< 1	1.86	0.099	0.10	0.2	0.09	13	0.6	0.06	5.70	<0.01
996025	FieldTRIP 1	0.39	0.063	14.2	46.3	0.82	510.3	0.201	< 1	1.88	0.110	0.09	0.2	0.09	11	0.6	0.07	5.50	<0.01
996026	FieldTRIP 2	0.38	0.063	14.5	38.8	0.70	424.6	0.184	2	1.71	0.088	0.08	0.2	0.08	12	0.6	0.04	4.80	<0.01
996027	FieldTRIP 3	0.38	0.063	14.9	39.4	0.73	440.3	0.192	1	1.82	0.095	0.08	0.2	0.09	18	0.6	0.05	5.20	<0.01
996029		0.29	0.056	15.8	45.7	0.94	210.2	0.155	1	2.43	0.051	0.06	<0.2	0.09	9	1.7	0.32	6.10	<0.01
996030		0.29	0.054	15.8	46.3	0.94	210.2	0.157	< 1	2.44	0.051	0.07	0.2	0.09	11	1.6	0.29	6.10	0.01
996031		0.26	0.057	14.1	41.3	0.73	178.7	0.151	< 1	2.00	0.027	0.09	<0.2	0.09	15	0.9	0.15	6.90	0.01
996032		0.23	0.038	11.0	45.1	0.85	129.3	0.141	1	2.15	0.021	0.13	0.3	0.10	27	0.9	0.14	7.60	0.01
996033		0.18	0.022	11.9	42.6	0.83	132.0	0.141	1	2.28	0.027	0.11	0.3	0.11	25	0.6	0.07	6.40	0.01
996034		0.12	0.058	13.8	22.4	1.29	160.6	0.122	< 1	3.37	0.034	0.22	0.2	0.24	48	1.3	0.11	8.20	0.11
996035		0.16	0.024	8.8	44.4	0.81	251.5	0.173	2	2.66	0.027	0.10	0.2	0.10	34	0.7	0.08	6.50	<0.01
996036		0.16	0.033	9.6	46.2	1.00	303.8	0.177	1	3.18	0.035	0.15	0.2	0.11	39	0.8	0.09	7.50	<0.01
996037		0.16	0.037	8.8	46.5	0.89	308.8	0.154	1	3.23	0.026	0.13	0.2	0.11	39	0.8	0.06	7.20	<0.01
996038		0.30	0.026	11.1	44.2	0.71	210.7	0.192	1	1.75	0.048	0.07	0.2	0.08	20	0.6	0.06	5.10	<0.01
996045		0.28	0.043	8.9	39.0	0.95	336.6	0.158	< 1	2.41	0.048	0.13	0.3	0.08	23	0.6	0.06	7.00	<0.01
996046		0.30	0.022	9.0	44.7	0.81	458.2	0.196	< 1	1.98	0.057	0.09	<0.2	0.09	15	0.7	0.06	5.50	<0.01
Crinkle Chert - Logtung Road																			
996047		0.40	0.059	21.8	36.8	0.58	205.8	0.124	< 1	1.55	0.051	0.13	0.2	0.10	62	0.5	0.05	4.50	<0.01
996048		0.44	0.048	22.3	43.5	0.64	274.9	0.119	1	1.92	0.049	0.21	0.2	0.13	103	0.6	0.07	5.50	<0.01
996050		0.48	0.057	21.5	40.3	0.65	274.2	0.109	1	1.76	0.041	0.19	0.2	0.12	109	0.7	0.06	5.40	0.01
996051		3.09	0.061	18.8	26.5	0.69	232.3	0.070	< 1	1.44	0.017	0.18	0.5	0.06	37	1.1	0.08	3.00	<0.01
996041	ADUP 996051	2.99	0.059	18.4	26.9	0.64	222.0	0.068	< 1	1.38	0.018	0.18	0.5	0.07	42	1.4	0.11	3.20	<0.01
Jennings River Quartz-Sericite Schist																			
996039		2.08	0.085	10.7	73.8	1.45	480.5	0.217	3	1.61	0.059	0.13	<0.2	0.17	180	2.0	0.12	4.80	0.20
996042		1.64	0.085	13.2	56.9	1.44	344.0	0.261	1	1.69	0.090	0.16	<0.2	0.12	81	0.9	0.10	5.30	<0.01
996043		2.28	0.085	10.6	69.6	1.57	477.6	0.215	2	1.70	0.060	0.13	<0.2	0.15	189	1.3	0.12	5.00	0.11
996044		2.04	0.085	11.4	64.9	1.34	464.5	0.205	3	1.57	0.050	0.13	<0.2	0.17	143	1.9	0.13	5.10	0.02
Arsenault Prospect																			
996020		0.62	0.073	19.3	57.5	1.26	263.1	0.202	1	2.24	0.066	0.18	0.3	0.13	29	0.9	0.35	6.80	<0.01
996022		0.58	0.078	18.2	48.3	1.11	182.8	0.196	< 1	1.83	0.076	0.12	0.3	0.09	16	1.0	0.41	5.70	<0.01
996023		0.47	0.065	21.5	49.7	1.13	195.1	0.196	< 1	1.96	0.051	0.15	0.3	0.13	14	0.8	0.21	5.50	<0.01
996024		0.27	0.091	17.7	48.6	0.93	117.5	0.141	< 1	2.32	0.016	0.10	0.3	0.09	55	1.2	0.31	5.60	0.01
996028		0.74	0.056	16.1	56.3	1.52	157.9	0.155	< 1	2.30	0.015	0.08	<0.2	0.07	17	1.1	0.12	9.20	0.03
Mount Francis East																			
996008		0.35	0.042	17.8	38.5	0.53	124.0	0.112	1	1.38	0.011	0.10	0.2	0.07	24	1.0	0.09	6.20	0.02
996012		0.33	0.040	21.3	48.5	0.60	161.1	0.130	1	1.47	0.014	0.10	<0.2	0.08	19	1.3	0.10	5.20	0.02
996013		0.15	0.039	14.3	39.8	0.49	85.5	0.157	1	1.49	0.010	0.06	0.3	0.07	14	0.9	0.12	4.80	0.02
996014		0.41	0.055	23.5	36.2	0.56	118.1	0.108	1	1.27	0.015	0.07	0.2	0.07	18	1.3	0.13	4.30	0.03
996016		0.82	0.085	131.8	49.2	0.64	163.8	0.098	2	1.71	0.019	0.07	0.3	0.09	104	1.1	0.08	3.70	0.05
996017		0.59	0.062	34.8	53.3	0.66	336.9	0.145	1	1.82	0.015	0.13	0.2	0.08	44	1.4	0.11	6.80	0.03
996018		0.78	0.069	25.1	42.5	0.57	202.2	0.108	1	1.81	0.018	0.13	0.2	0.10	39	1.5	0.09	6.00	0.04
996019		0.99	0.076	17.4	39.1	0.47	192.4	0.101	2	1.57	0.019	0.11	<0.2	0.09	48	1.1	0.07	5.60	0.03
Highway 97 Prospect																			
996002		0.30	0.022	18.7	52.8	0.60	278.8	0.128	2	2.33	0.034	0.19	0.3	0.14	78	1.1	0.09	7.50	<0.01
996003		0.30	0.031	18.1	43.4	0.58	286.0	0.137	2	1.74	0.045	0.20	0.2	0.12	78	0.5	0.09	6.00	<0.01
996004		0.27	0.024	11.7	40.5	0.74	298.9	0.139	1	2.61	0.025	0.14	0.3	0.12	18	0.5	0.07	7.20	<0.01
996005		0.22	0.018	17.9	39.2	0.47	310.8	0.115	1	1.79	0.039	0.13	0.2	0.10	44	0.4	0.05	5.50	<0.01
996006		0.56	0.050	13.6	51.5	0.90	261.6	0.202	2	1.98	0.095	0.15	<0.2	0.11	18	0.6	0.06	6.00	<0.01
996007		0.30	0.025	15.6	38.5	0.50	224.8	0.123	1	1.65	0.038	0.13	0.2	0.10	47	0.7	0.06	5.20	<0.01
996009	FieldTRIP 1	0.33	0.018	14.6	32.6	0.45	168.3	0.115	2	1.44	0.041	0.15	0.2	0.10	30	0.6	0.07	4.60	<0.01
996001	ADUP 996009	0.33	0.018	14.3	32.0	0.44	166.4	0.114	2	1.41	0.041	0.15	0.2	0.09	30	0.6	0.06	4.80	<0.01
996010	FieldTRIP 2	0.33	0.018	16.4	31.6	0.47	185.6	0.121	1	1.50	0.043	0.16	0.2	0.10	35	0.8	0.08	5.20	<0.01
996011	FieldTRIP 3	0.33	0.019	14.7	31.7	0.45	171.6	0.115	2	1.46	0.042	0.16	0.2	0.09	27	0.7	0.07	4.90	0.01
	Median	0.33	0.055	15.8	44.7	0.81	224.8	0.145	1	1.83	0.038	0.13	0.2	0.10	34	0.9	0.09	5.60	0.01
	Mean	0.61	0.052	18.8	45.7	0.84	250.8	0.152	1	1.99	0.040	0.13	0.2	0.11	48	1.0	0.12	5.89	0.02
	Std. dev.	0.66	0.022	18.9	9.9	0.31	108.7	0.041	1	0.50	0.024	0.04	0.1	0.03	44	0.4	0.09	1.21	0.04
	Minimum	0.12	0.018	8.8	22.4	0.45	85.5	0.070	<1	1.27	0.010	0.06	<0.2	0.06	9	0.4	0.05	3.00	<0.01
	Maximum	3.09	0.091	131.8	73.8	1.57	510.3	0.261	3	3.37	0.110	0.22	0.5	0.24	189	2.0	0.41	9.20	0.20

Notes:

TABLE 3
DETECTION LIMITS AND GEOCHEMICAL RESULTS BY THERMAL NEUTRON ACTIVATION ANALYSIS (INAA)

	Element	Au	As	Ba	Br	Ca	Co	Cr	Cs	Fe	Hf	Mo	Na	Rb	Sb	Sc
	Units	(ppb)	(ppm)	(ppm)	(ppm)	(%)	(ppm)	(ppm)	(ppm)	(%)	(ppm)	(ppm)	(%)	(ppm)	(ppm)	(ppm)
Sample	Detection Limit	2	0.5	50	0.5	1	1	5	1	0.02	1	1	0.01	15	0.1	0.1
Crinkle Chert - North of Mt. Francis																
996021	ADUP 996025	2	8.1	1400	2.2	2	14	122	2	4.27	6	5	2.05	66	1.1	19.2
996025	FieldTRIP 1	9	7.0	1300	1.6	2	13	118	2	4.31	6	8	2.06	59	1.1	19.0
996026	FieldTRIP 2	4	6.8	1100	2.2	2	10	103	2	3.58	6	5	1.86	53	0.9	16.2
996027	FieldTRIP 3	12	6.7	1100	<0.5	2	11	98	2	3.74	6	8	1.91	50	0.9	16.9
996029		<2	44.3	1100	2.0	2	19	114	2	5.37	6	10	1.52	73	1.5	18.4
996030		<2	44.2	1000	2.4	1	18	114	2	5.24	6	8	1.48	65	1.1	18.2
996031		5	15.2	1000	5.6	2	13	120	3	4.44	6	10	1.45	70	0.9	16.7
996032		<2	42.3	960	6.6	1	16	118	3	5.27	6	9	1.36	66	1.2	16.1
996033		<2	20.4	770	5.7	2	17	113	3	4.47	6	11	1.64	64	1.2	15.8
996034		21	16.1	770	9.5	1	19	54	4	7.45	4	22	0.88	73	0.8	18.9
996035		12	13.2	1300	6.6	1	19	112	2	4.64	5	8	1.59	56	1.1	18.6
996036		7	18.3	850	9.3	2	18	102	2	4.59	5	5	1.57	60	1.0	19.4
996037		4	11.3	790	6.5	2	16	101	2	4.27	4	4	1.47	52	1.0	17.0
996038		4	7.5	790	1.7	2	16	135	2	4.14	5	7	1.83	52	0.8	16.7
996045		4	11.4	920	4.1	1	17	101	2	4.49	5	4	1.82	60	1.0	18.4
996046		6	12.2	1500	2.5	1	19	132	2	4.45	5	6	1.78	56	1.5	18.6
Crinkle Chert - Logtung Road																
996047		<2	10.5	910	2.8	1	10	103	4	3.20	5	8	1.30	105	1.6	12.6
996048		<2	12.6	950	1.8	1	11	96	4	3.48	5	7	1.09	108	2.0	13.2
996050		3	15.0	970	4.1	1	12	113	5	3.93	5	8	1.20	102	2.3	14.5
996051		5	28.0	960	<0.5	4	18	76	3	3.87	5	9	0.69	103	4.1	15.4
996041	ADUP 996051	3	27.6	920	<0.5	4	17	77	2	3.79	5	11	0.66	93	4.0	15.5
Jennings River Quartz-Sericite-Schist																
996039		9	16.0	1400	<0.5	4	26	181	2	5.89	4	13	1.32	51	1.9	17.0
996042		4	8.8	910	3.8	4	26	170	2	5.46	4	8	1.62	54	0.9	17.2
996043		6	12.3	1300	3.2	4	26	181	3	5.54	4	13	1.40	48	1.6	17.1
996044		4	12.2	1300	<0.5	4	24	172	3	5.45	4	12	1.29	53	1.5	16.7
Arsenault Prospect																
996020		11	17.5	890	<0.5	2	20	127	2	5.88	6	8	1.47	78	1.0	19.0
996022		12	14.8	760	<0.5	2	17	123	2	5.11	6	10	1.55	77	0.9	17.3
996023		17	39.4	990	<0.5	2	20	142	2	5.39	7	16	1.34	91	1.2	19.2
996024		10	35.4	690	14.3	2	27	135	2	5.55	6	16	1.14	80	1.1	16.3
996028		14	24.7	640	6.4	2	16	136	2	4.72	6	12	1.09	71	0.8	16.4
Mount Francis East																
996008		<2	27.8	910	10.4	2	13	123	2	4.44	7	11	0.86	95	1.2	13.1
996012		13	42.9	920	13.3	2	19	182	2	4.67	9	15	1.14	72	1.2	16.8
996013		5	26.7	930	4.8	2	23	170	2	5.14	9	14	1.36	73	1.3	15.0
996014		17	55.4	900	5.3	3	24	135	2	4.98	8	18	1.40	64	1.3	15.9
996016		13	16.0	900	14.8	3	17	161	4	4.43	8	23	1.28	71	0.8	20.7
996017		4	27.3	1100	8.4	3	21	151	3	5.01	7	19	1.24	109	1.3	16.4
996018		10	38.3	760	8.5	2	14	121	2	3.94	6	14	1.21	77	1.0	14.0
996019		7	13.0	760	6.4	2	12	104	2	3.54	6	13	1.42	70	0.7	12.7
Highway 97 Prospect																
996002		5	16.1	1100	3.0	1	14	119	4	4.62	5	11	1.32	115	2.0	17.4
996003		8	15.9	1100	2.6	1	13	110	4	4.44	5	12	1.39	99	2.0	16.1
996004		7	9.7	880	3.3	1	14	98	4	4.30	5	9	1.20	69	1.3	13.7
996005		5	11.2	1000	2.7	1	10	91	3	3.42	6	<1	1.36	107	1.3	13.8
996006		<2	8.5	1200	2.3	1	17	128	3	4.29	5	<1	1.54	104	1.3	15.9
996007		<2	11.0	950	2.9	2	10	96	4	3.47	5	<1	1.30	87	1.3	13.7
996009	FieldTRIP 1	<2	8.8	960	2.7	2	10	94	3	3.38	6	6	1.43	109	1.3	12.5
996001	ADUP 996009	<2	7.9	940	2.9	2	10	95	3	3.30	5	10	1.41	102	1.1	12.3
996010	FieldTRIP 2	<2	9.4	920	3.3	2	9	103	3	3.41	6	10	1.44	95	1.2	13.1
996011	FieldTRIP 3	<2	8.3	910	2.5	2	9	95	3	3.22	5	10	1.37	82	1.1	12.1
	Median	5	15.9	950	3.3	2	17	119	2	4.49	6	10	1.36	72	1.2	16.7
	Mean	7	20.5	978	4.8	2	17	124	3	4.65	6	10	1.38	77	1.3	16.4
	Std. dev.	5	12.6	196	3.8	1	5	29	1	0.84	1	5	0.26	20	0.6	2.1
	Minimum	<2	7.0	640	<0.5	1	10	54	2	3.20	4	<1	0.69	48	0.7	12.5
	Maximum	21	55.4	1500	14.8	4	27	182	5	7.45	9	23	2.06	115	4.1	20.7

TABLE 3 CONTINUED
DETECTION LIMITS AND GEOCHEMICAL RESULTS BY THERMAL NEUTRON ACTIVATION ANALYSIS (INAA)

	Element	Se	Ta	Th	U	W	Zn	La	Ce	Nd	Sm	Eu	Tb	Yb	Lu	Mass
	Units	(ppm)	(ppm)	(ppm)	(ppm)	(ppm)	(ppm)	(ppm)	(ppm)	(ppm)	(ppm)	(ppm)	(ppm)	(ppm)	(ppm)	(g)
Sample	Detection Limit	3	0.5	0.5	0.5	1	50	0.1	3	5	0.1	0.2	0.5	0.2	0.05	n/a
Crinkle Chert - North of Mt. Francis																
996021	ADUP 996025	<3	1.6	8.4	2.6	<1	64	30.5	68	29	5.8	1.6	0.6	3.0	0.45	24.45
996025	FieldTRIP 1	<3	1.5	8.1	2.3	<1	112	30.1	64	27	5.6	1.5	0.8	3.0	0.47	24.23
996026	FieldTRIP 2	<3	1.1	7.9	2.4	<1	95	28.0	61	22	5.1	1.3	0.7	2.7	0.40	28.73
996027	FieldTRIP 3	<3	1.3	8.1	2.4	<1	89	28.3	63	24	5.0	1.4	0.6	2.8	0.42	30.44
996029		<3	1.0	8.4	2.5	<1	117	32.2	65	26	5.6	1.4	0.7	3.1	0.46	25.61
996030		<3	0.6	8.5	2.6	<1	124	32.0	64	24	5.5	1.4	0.7	3.1	0.46	26.81
996031		<3	1.7	8.7	2.5	<1	100	30.7	63	25	4.8	1.2	0.7	2.8	0.43	29.21
996032		<3	1.3	8.9	2.5	<1	129	25.8	59	19	4.4	1.1	0.6	2.3	0.36	26.42
996033		<3	1.4	9.7	2.7	2	127	27.3	59	20	4.4	1.2	0.6	2.4	0.37	26.70
996034		<3	1.0	9.8	2.3	1	124	26.2	47	14	3.5	0.9	0.5	2.4	0.36	27.15
996035		<3	1.1	7.7	3.4	2	100	23.5	54	19	3.8	1.1	<0.5	2.2	0.33	29.73
996036		<3	1.2	8.2	2.6	<1	100	21.9	50	16	4.0	1.0	0.7	2.2	0.33	28.10
996037		<3	0.9	7.6	2.4	<1	110	20.2	47	17	3.9	1.0	0.6	2.1	0.33	28.50
996038		<3	0.9	6.3	2.2	1	99	25.7	55	19	4.0	1.2	0.6	2.3	0.35	28.54
996045		<3	1.0	7.0	1.4	2	95	21.2	45	16	3.6	1.1	0.7	2.4	0.36	29.05
996046		<3	0.9	7.2	2.6	<1	92	23.6	50	15	3.9	1.2	0.5	2.5	0.37	27.62
Crinkle Chert - Logtung Road																
996047		<3	1.8	14.2	2.9	<1	82	38.9	80	28	5.0	1.2	0.9	3.3	0.52	27.63
996048		<3	1.2	14.3	2.8	<1	59	38.9	75	30	6.6	1.2	0.8	3.3	0.52	28.80
996050		<3	1.9	15.1	2.5	2	118	39.8	76	27	6.9	1.3	0.9	3.8	0.57	29.14
996051		<3	0.7	10.9	2.1	3	114	35.1	74	25	5.8	1.3	0.8	2.9	0.49	26.48
996041	ADUP 996051	<3	1.0	10.7	2.1	2	96	33.2	71	25	5.3	1.3	0.8	2.8	0.43	29.59
Jennings River Quartz-Sericite-Schist																
996039		<3	0.9	5.4	2.3	<1	156	24.5	52	23	5.1	1.5	0.7	2.7	0.40	25.27
996042		<3	1.2	6.9	2.6	<1	121	25.3	53	19	4.9	1.5	0.7	2.7	0.40	29.64
996043		<3	1.1	5.5	2.6	<1	139	23.5	48	20	4.7	1.5	0.7	2.7	0.39	26.40
996044		<3	1.3	5.3	2.0	<1	130	23.1	49	18	4.8	1.4	<0.5	2.6	0.38	27.79
Arsenault Prospect																
996020		<3	1.8	10.9	3.0	3	285	38.0	75	31	6.4	1.5	0.9	3.4	0.53	28.87
996022		<3	1.6	9.8	3.4	<1	130	37.2	74	28	6.2	1.6	0.8	3.0	0.45	29.88
996023		<3	1.0	13.3	4.0	<1	128	46.9	94	35	7.0	1.6	0.8	3.4	0.50	26.28
996024		<3	1.4	13.6	3.8	2	135	37.4	102	30	6.5	1.6	0.8	3.1	0.46	26.96
996028		<3	1.6	11.1	3.9	<1	109	33.4	74	28	5.4	1.3	0.6	3.2	0.48	27.91
Mount Francis East																
996008		<3	1.6	12.4	4.1	3	114	34.7	76	29	6.3	1.7	0.9	3.6	0.52	27.20
996012		<3	1.7	12.5	4.8	2	138	44.0	147	38	8.0	1.9	0.9	3.8	0.59	29.77
996013		<3	1.7	11.5	4.5	2	127	38.2	83	27	5.7	1.5	0.9	3.3	0.51	29.37
996014		<3	1.7	13.9	4.8	2	161	48.6	124	35	7.7	2.0	0.9	3.9	0.58	27.60
996016		<3	1.8	16.3	19.2	2	233	186.0	113	163	27.9	5.7	3.0	13.3	2.10	25.57
996017		<3	1.9	13.9	6.4	2	173	58.5	120	53	10.9	2.8	1.5	4.6	0.65	26.64
996018		<3	1.4	10.2	4.4	<1	116	41.8	74	30	6.5	1.6	1.0	3.2	0.47	30.58
996019		<3	0.8	8.4	4.2	<1	143	33.0	63	27	5.2	1.3	0.8	2.7	0.43	27.07
Highway 97 Prospect																
996002		<3	1.2	16.1	3.5	2	128	38.2	81	26	5.5	1.2	<0.5	2.7	0.41	25.05
996003		<3	1.7	13.4	2.2	<1	114	37.1	74	31	6.7	1.6	1.0	3.7	0.57	26.29
996004		<3	1.2	10.4	2.6	2	77	25.8	54	20	4.1	0.8	0.5	2.3	0.35	26.48
996005		<3	1.6	13.5	3.2	<1	65	35.4	77	24	5.5	1.2	0.7	3.0	0.46	26.94
996006		<3	1.3	9.2	3.3	<1	136	27.9	61	24	4.9	1.3	0.7	2.4	0.38	25.06
996007		<3	1.9	12.3	3.8	<1	85	30.5	68	22	4.9	1.1	0.6	2.5	0.38	27.30
996009	FieldTRIP 1	<3	1.6	12.4	3.3	<1	100	31.2	74	22	5.0	1.2	0.7	2.5	0.38	27.09
996001	ADUP 996009	<3	1.9	11.8	2.8	<1	97	30.8	69	22	4.9	1.0	0.6	2.7	0.40	27.92
996010	FieldTRIP 2	<3	1.3	12.6	3.4	<1	90	33.1	70	25	5.3	1.0	0.7	2.7	0.41	26.33
996011	FieldTRIP 3	<3	1.5	12.5	2.8	<1	95	30.6	69	20	4.7	1.0	0.7	2.5	0.39	28.01
	Median	3	1.3	10.2	2.8	1	118	32.2	68	25	5.4	1.3	0.7	2.9	0.45	27.20
	Mean	3	1.3	10.5	3.5	1	123	36.4	72	29	6.0	1.5	0.8	3.2	0.48	27.48
	Std. dev.	0	0.4	3.0	2.7	1	40	25.3	23	23	3.8	0.8	0.4	1.7	0.27	1.53
	Minimum	<3	0.6	5.3	1.4	<1	59	20.2	45	14	3.5	0.8	<0.5	2.1	0.33	24.23
	Maximum	3	1.9	16.3	19.2	3	285	186.0	147	163	27.9	5.7	3.0	13.3	2.10	30.58

Notes:

ADUP = analytical duplicate

FieldTRIP = field triplicate

TABLE 4
DETECTION LIMITS AND GEOCHEMICAL RESULTS FOR MAJOR OXIDES BY $LiBO_2$ FUSION INDUCTIVELY COUPLED PLASMA (ICP)

	Element	SiO2	Al2O3	Fe2O3	MgO	CaO	Na2O	K2O	TiO2	P2O5	MnO	Cr2O3	Ba	Ni	Sr	Zr	Y	Nb	Sc	LOI	C/TOT	S/TOT	SUM
	Units	(%)	(%)	(%)	(%)	(%)	(%)	(%)	(%)	(%)	(%)	(%)	(ppm)	(ppm)	(ppm)	(ppm)	(ppm)	(ppm)	(ppm)	(%)	(%)	(%)	(%)
Sample	Detection Limit	0.01	0.01	0.01	0.01	0.01	0.01	0.01	0.01	0.01	0.01	0.001	5	5	5	5	5	10	1	0.1	0.01	0.01	0.01
Crinkle Chert - North of Mt. Francis																							
996021	ADUP 996025	67.26	12.85	5.32	2.24	2.47	2.54	1.48	0.96	0.18	0.07	0.014	1391	36	220	182	22	12	7	4.2	0.22	0.02	99.79
996025	FieldTRIP 1	68.71	12.23	5.07	2.48	2.35	2.31	1.34	1.07	0.19	0.04	0.014	1526	35	241	204	23	14	8	3.6	0.22	<0.01	99.64
996026	FieldTRIP 2	68.85	12.57	4.91	2.14	2.48	2.54	1.49	0.96	0.18	0.05	0.012	1315	26	216	191	21	13	7	3.3	0.24	<0.01	99.69
996027	FieldTRIP 3	68.68	12.94	5.05	2.09	2.49	2.59	1.56	0.95	0.17	0.08	0.012	1293	28	212	179	21	13	7	3.1	0.24	<0.01	99.92
996029		63.36	14.89	7.25	2.28	1.90	2.01	1.76	0.95	0.17	0.07	0.015	1419	45	202	213	23	13	8	4.9	0.54	0.02	99.77
996030		64.17	14.29	6.96	2.26	1.81	1.91	1.66	0.94	0.16	0.07	0.014	1406	36	209	209	24	14	8	5.3	0.54	0.02	99.77
996031		64.49	13.32	5.71	2.03	1.90	1.82	1.70	1.03	0.20	0.08	0.015	1289	28	223	225	21	15	7	7.4	1.63	0.02	99.90
996032		63.07	12.32	6.38	2.27	1.85	1.61	1.59	0.92	0.13	0.06	0.014	1180	34	203	218	16	12	7	9.4	2.41	0.01	99.81
996033		65.94	12.71	5.49	2.39	1.92	1.91	1.36	0.98	0.07	0.07	0.013	967	34	221	214	18	13	7	6.9	1.04	0.01	99.90
996034		53.95	15.25	9.28	2.95	1.57	1.03	1.54	0.84	0.19	0.12	0.007	1133	27	128	157	15	13	9	12.5	2.07	0.12	99.40
996035		61.39	14.90	6.57	2.40	2.10	2.32	1.60	0.94	0.07	0.19	0.013	1553	49	170	164	18	12	8	7.2	0.85	<0.01	99.92
996036		60.44	14.96	6.37	2.48	1.85	2.24	1.55	0.86	0.09	0.12	0.011	1034	37	143	156	17	11	8	8.8	1.04	<0.01	99.92
996037		60.96	14.58	6.12	2.19	1.96	2.15	1.41	0.80	0.10	0.09	0.011	985	38	160	143	16	11	7	9.4	1.27	0.02	99.93
996038		67.10	12.74	5.57	2.09	2.66	2.48	1.35	0.96	0.08	0.12	0.015	994	44	246	157	17	12	7	4.6	0.36	0.01	99.92
996045		63.51	13.92	6.00	2.53	2.29	2.44	1.43	0.83	0.12	0.08	0.011	1098	34	167	134	16	12	7	6.6	0.66	0.01	99.92
996046		66.59	13.09	5.89	2.36	2.50	2.31	1.35	0.95	0.07	0.15	0.015	1738	53	235	140	17	12	7	4.4	0.27	<0.01	99.92
Crinkle Chert - Logtung Road																							
996047		72.66	11.05	4.19	1.50	1.56	1.69	1.87	0.82	0.15	0.06	0.011	1053	31	155	151	27	16	5	4.2	0.36	<0.01	99.93
996048		70.45	11.24	4.61	1.63	1.57	1.38	1.96	0.83	0.13	0.08	0.012	1117	40	147	162	31	17	6	5.6	0.55	<0.01	99.67
996050		68.02	12.13	5.28	1.78	1.70	1.58	2.03	0.84	0.17	0.07	0.013	1220	48	160	163	34	17	6	6.0	0.55	<0.01	99.79
996051		59.59	14.15	5.49	1.58	5.35	0.98	2.98	0.68	0.15	0.16	0.009	1086	38	151	151	23	< 10	6	8.4	1.09	<0.01	99.68
996041	ADUP 996051	61.13	13.38	5.23	1.74	5.07	0.88	2.58	0.76	0.16	0.19	0.009	1195	37	169	172	25	10	7	8.2	1.10	0.02	99.53
Jennings River Quartz-Sericite-Schist																							
996039		59.78	11.22	7.57	3.29	4.85	1.78	1.48	1.05	0.23	0.13	0.020	1614	110	279	116	22	14	7	7.8	0.80	0.25	99.44
996042		60.19	11.67	6.85	3.66	4.96	2.04	1.36	1.28	0.23	0.16	0.020	1240	77	340	146	23	20	7	6.9	0.72	0.01	99.53
996043		58.52	11.43	7.22	3.60	5.20	1.86	1.48	1.07	0.24	0.13	0.023	1563	107	290	116	21	14	7	8.3	1.07	0.16	99.30
996044		59.32	11.49	7.35	3.26	4.80	1.81	1.53	1.06	0.24	0.14	0.020	1629	92	278	114	21	14	7	8.4	0.95	0.02	99.66
Arsenault Prospect																							
996020		60.55	14.07	7.63	3.17	3.18	1.93	1.81	0.95	0.20	0.11	0.016	1029	52	209	183	25	14	8	5.8	0.22	0.02	99.58
996022		64.11	13.16	6.75	3.11	3.32	2.08	1.66	1.02	0.20	0.07	0.016	964	40	238	204	24	15	7	4.2	0.18	0.01	99.85
996023		63.75	13.83	6.38	3.21	2.60	1.57	2.22	1.07	0.18	0.10	0.016	1166	43	199	246	28	16	8	4.6	0.23	<0.01	99.74
996024		55.00	12.35	6.96	3.05	2.44	1.38	1.43	1.04	0.29	0.15	0.018	858	47	206	211	23	16	7	15.5	4.19	0.05	99.75
996028		55.93	12.78	6.26	3.29	2.75	1.45	1.61	1.03	0.25	0.10	0.016	759	27	165	200	21	18	6	14.3	3.83	0.08	99.90
Mount Francis East																							
996008		61.22	12.54	6.14	2.17	2.12	1.12	2.27	1.08	0.20	0.10	0.017	1152	34	158	276	29	16	6	10.6	2.50	0.04	99.78
996012		62.08	13.24	6.35	2.30	2.63	2.14	2.23	1.15	0.16	0.10	0.024	1220	61	186	303	32	19	7	7.1	1.35	0.03	99.73
996013		64.51	11.86	6.77	2.10	2.60	2.30	1.65	1.18	0.13	0.16	0.020	1040	48	195	288	22	22	6	6.4	1.06	0.01	99.88
996014		64.26	11.76	6.15	2.71	3.60	1.69	1.63	1.03	0.17	0.13	0.016	1036	74	266	267	28	17	6	6.4	1.11	0.03	99.75
996016		55.98	11.12	5.66	2.74	3.58	1.59	1.29	1.08	0.35	0.10	0.021	973	88	259	291	126	17	9	16.0	4.35	0.02	99.72
996017		56.86	12.53	6.57	2.24	2.71	1.60	1.84	1.06	0.27	0.15	0.018	1183	53	192	221	44	19	7	13.7	3.56	0.05	99.75
996018		55.97	12.61	5.70	1.97	3.08	1.75	1.74	0.92	0.25	0.10	0.015	1043	45	233	231	28	14	6	15.6	4.38	0.07	99.88
996019		56.42	12.14	4.86	1.60	3.41	2.00	1.55	0.81	0.25	0.08	0.012	1014	28	281	215	22	12	5	16.6	4.83	0.01	99.91
Highway 97 Prospect																							
996002		67.63	12.71	5.63	1.59	1.50	1.57	1.72	0.85	0.07	0.02	0.012	1061	38	134	165	20	14	7	6.3	0.47	<0.01	99.78
996003		68.16	12.32	5.74	1.59	1.63	1.74	1.88	0.78	0.09	0.07	0.013	1191	47	162	155	29	16	6	5.6	0.34	0.02	99.79
996004		65.34	13.46	5.81	1.84	1.87	1.58	1.53	0.85	0.08	0.07	0.012	1079	39	152	143	17	14	5	7.1	0.77	0.03	99.69
996005		71.60	11.54	4.40	1.28	1.43	1.69	1.68	0.77	0.06	0.03	0.011	1148	32	169	170	21	14	5	4.9	0.40	<0.01	99.57
996006		65.43	13.34	5.55	2.28	2.20	1.96	1.95	0.97	0.15	0.07	0.014	1321	42	207	150	18	16	6	5.7	0.56	0.01	99.81
996007		71.01	11.13	4.50	1.39	1.55	1.65	1.67	0.75	0.08	0.07	0.011	1089	31	170	158	19	14	5	5.6	0.65	0.02	99.57
996009	FieldTRIP 1	72.02	10.91	4.13	1.36	1.73	1.75	1.75	0.77	0.06	0.07	0.010	1015	24	168	167	18	14	5	5.0	0.79	<0.01	99.70
996001	ADUP 996009	71.12	11.43	4.36	1.37	1.82	1.85	1.89	0.79	0.06	0.04	0.012	995	35	167	162	18	14	5	4.8	0.77	0.01	99.70
996010	FieldTRIP 2	72.11	11.10	4.23	1.30	1.72	1.79	1.80	0.71	0.06	0.04	0.010	987	23	159	155	19	13	5	4.7	0.62	0.01	99.71
996011	FieldTRIP 3	72.20	10.99	4.17	1.31	1.70	1.76	1.77	0.74	0.06	0.01	0.010	1013	25	164	154	17	14	5	4.7	0.67	0.03	99.58
	Median	63.51	12.61	6.12	2.28	2.29	1.78	1.65	0.95	0.16	0.10	0.014	1117	40	199	167	22	14	7	6.9	0.80	0.01	99.77
	Mean	63.17	12.76	6.08	2.34	2.60	1.81	1.69	0.95	0.16	0.10	0.015	1175	47	202	188	25	15	7	7.9	1.34	0.03	99.75
	Std. dev.	4.99	1.22	1.04	0.65	1.09	0.36	0.32	0.13	0.07	0.04	0.004	222	21	50	50	17	3	1	3.6	1.32	0.05	0.16
	Minimum	53.95	10.91	4.13	1.28	1.43	0.98	1.29	0.68	0.06	0.02	0.007	759	24	128	114	15	<10	5	3.6	0.18	<0.01	99.30
	Maximum	72.66	15.25	9.28	3.66	5.35	2.48	2.98	1.28	0.35	0.19	0.024	1738	110	340	303	126	22	9	16.6	4.83	0.25	99.93

Notes:
ADUP = analytical duplicate
FieldTRIP = field triplicate

of field triplicates display a larger measure of variability as compared to the analytical duplicates as the former represent three different (but adjacent) samples, whereas the latter is two parts of the same original sample. In general, the key elements (*e.g.* copper, cadmium, lead, selenium) showed good reproducibility in field triplicates and analytical duplicates (Table 5). For example, two field duplicates (996009, 996010) reported differences of 1.3 per cent and 0.3 per cent for copper and zinc, respectively. Two analytical duplicates (996001 and 996009) also showed good reproducibility for copper and zinc recording differences of 2.1 per cent and 0.5 per cent, respectively.

Results from the insertion of three CANMET reference material indicate acceptable levels of analytical precision (less than 10 per cent) for key elements in till. For instance, copper and zinc recorded relative standard deviations (RSD) of 1.8 and 2.1 per cent, respectively (Table 5).

GLACIAL HISTORY AND STRATIGRAPHY

Ryder and Maynard (1991) and Clague (1989) provide a limited regional overview of the Quaternary geology of northern British Columbia. Although there is little chronological information for the northern Cordilleran ice sheet available, evidence suggests processes were similar to those in the south of the province (Ryder *et al.*, 1991). Dates collected from lavas flows and organics show multiple glaciations, separated by warmer interglacial periods, occurred during late Pliocene (1.64 to 5.2 Ma) and Pleistocene (0.01 to 1.64 Ma).

TABLE 5
PERCENT DIFFERENCES FOR KEY ELEMENTS FROM ANALYTICAL (996001 AND 996009) AND FIELD (996009 AND 996010) DUPLICATES. RELATIVE STANDARD DEVIATION (%RSD) CALCULATED FROM 3 CANMET REFERENCE STANDARDS

Element		Detect. L. (ppm)	Anal. Dups (%)	Field Dups (%)	%RSD
Silver	Ag	2	0.0	10.0	2.5
Bismuth	Bi	0.02	14.1	45.2	2.0
Cadmium	Cd	0.01	0.0	25.0	5.0
Cobalt	Co	0.1	2.7	5.4	1.8
Copper	Cu	0.01	2.1	1.3	1.8
Manganese	Mn	1	0.9	0.0	1.6
Molybedum	Mo	0.01	4.6	10.4	3.3
Lead	Pb	0.01	0.9	3.0	3.1
Selenium	Se	0.1	0.0	28.6	9.1
Zinc	Zn	0.1	0.5	0.3	2.1

Detect. L. = Detection Limit
Anal. Dups = Analytical Duplicates
Field Dups = Field Duplicates
RSD = Relative Standard Deviation

The Fraser glaciation (late Wisconsinan in age), the last ice advance, largely obscured any evidence of earlier glacial and non-glacial events. For example, reconnaissance work along the Kechika River to the east suggest only one till sheet to be present in exposed settings (Bobrowsky, pers. comm., 1999). Several other authors also noted no evidence of multiple glaciations in northern British Columbia (*e.g.* Watson and Mathews, 1944; Kerr, 1948). Where glacial and interglacial sediments are preserved, dates are obtained only at scattered localities. To the southeast near Finlay River, Bobrowsky and Rutter (1992) collected a series of dates spanning from early Holocene to middle Wisconsinan time (10,000 to 37,190 ka) from multiple glacial and non-glacial sediments. To the east, in the Atlin area, Levson and Blyth (1993) collected radiocarbon dates from organics lying stratigraphically between till and placer gravels. Peat and wood fragments yielded dates of 31ka BP and 36 ka BP (middle Wisconsinan in age). Potassium-argon dates (0.5 to 3.6 Ma) attained from basalts interbedded with the placer deposits indicate some of the gravels are interglacial, although most are preglacial in age. Aitken (1959) also recorded two tills and associated outwash overlying a third till and outwash in a placer camp near Atlin. Peat radiocarbon dates suggest the lowest till may be older than 37,000 years (Miller, 1976), corresponding to a early Wisconsinan glaciation. To the south, Spooner *et al.* (1996) estimated the age of a regional advance, beneath basalt flows in the Stikine River valley. Potassium-argon dates and paleomagnetic analysis imply the sediments to be between 330-360 ka, corresponding to a pre-Illinoian isotope stage 10.

Additional stratigraphic evidence of multiple Cordilleran ice advances, but no absolute dating, has also been noted in northern British Columbia. In the Atlin area, Levson (1992) noted up to three auriferous gravel sequences interbedded with till. In the Omineca Mountains near Uslika Lake, glaciolacustrine silts deposited in a moraine dammed lake are overlain by till (Roots, 1954). In the Dease River valley, two separate ice advances are suggested by a sequence where till is overlain by silts with a superimposed esker complex (Gabrielse, 1969). However, whether these represent two advances of the Fraser Glaciation, as in the two upper tills Aitken's study area (see above), or two distinct glaciations is unclear.

Fraser Glaciation

Earlier workers noted that the development of the last ice sheet appears to have been preceded by an episode of alpine glaciation which was long enough for the development or redevelopment of erosional landforms. Gabrielse (1969) noted rounded spurs and cirque headwalls modified by meltwater erosion in the Cassiar Mountains. Aitken (1959) cited over-ridden cirques and rounded aretes.

In the early phases of glaciation, ice built up due to the growth of cirque and valley glaciers in the Coast Mountains and higher parts of the Skeena Mountains. Alpine glaciers also developed in the Cassiar Mountains and many parts of the Stikine Plateau. Due to the many centres of ice accumulations, ice sheet morphology and flow patterns were complex at the time of coalescence. Local shifts in ice-flow directions did occur due to changes in the relative influence of topographic control on thickening and thinning ice (Ryder and Maynard, 1991).

Advancing glaciers from the local mountains dammed river valleys forming lakes across the region (Ryder and Maynard, 1991). As the ice overrode these areas and thickened, the extensive ice-sheet rose to an elevation of at least 2000 metres as shown by erratics (Watson and Mathews, 1944). Roots (1954) recorded glacial limits up to 2300 metres in the Omineca Mountains whereas Johnston (1926) and Gabrielse (1969) noted heights of 2100 metres in the Cassiar Mountains.

Deglaciation occurred partly by frontal retreat of ice tongues and partly by downwasting of stagnant ice. Paleo-ice-flow directions altered according to increasing topographic control. Widely distributed small bodies of glaciolacustrine sediments indicate that numerous lakes existed during deglaciation. Large esker complexes as well as kames and kettles dot the valley floors, indicating that ice stagnation was the dominant deglacial process in the mountainous areas. Local re-advances or pauses occurred during the late phase of the Fraser Glaciation. Recessional moraines and kame terraces mark ice margins during pauses in ice retreat. Morainal ridges bounding cirques could also be attributed to the growth and decay of alpine glaciers reoccupying cirques after the last ice sheet disappeared (Aitken, 1959).

Since glaciation, previously deposited glaciogenic sediments have been reworked by colluvial processes under paraglacial conditions and resedimented at the base of steep slopes. Similarly, paraglacial alluvial-fan sedimentation was active during deglaciation and has continued until the present. If Holocene glacial activity occurred it was restricted to high cirques in alpine areas. Fluvial terrace, floodplain and active channel deposits have also formed along valley floors during the Holocene.

SURFICIAL SEDIMENTS

The surficial sediments within the study area were deposited during the last cycle of the Fraser Glaciation and ensuing post-glacial activity. At lower elevations, on gentle slopes and plateaus, the bedrock topography is mantled by variable amounts of a massive, matrix-supported diamicton. Deposits range from a thin veneer (<1 metre) to a thick (≈45 metres) mantle. The physical properties of these diamictons suggest they are basal tills derived from lodgement processes (*e.g.* Dreimanis, 1988).

In general, basal till deposits are massive to very poorly-stratified, dark olive grey (or brown) and moderately to highly-consolidated (Photo 1). The matrix is commonly fissile with a high clay content. Deposits are dense, compact, and cohesive. Clast content ranges from 5 per cent to 40 per cent, with a mean of 15 per cent. Clast size ranges from granular (<1 centimetre) to boulder (>1metre), averaging 1 to 2 centimetres. Clasts occur in a range of roundness, but most are subangular. Clast lithologies are variable and include local bedrock. Many clasts (≤25 per cent) are striated and faceted. In some areas, particularly along or at the base of steep slopes, tills are reworked and colluviated.

Lateral and recessional moraines are common in the Cassiar Mountains (Photo 2). Till ridges range from 10's to 100's of meters in length and are no more than 20 metres in width. Moraines mark the location of ice pauses during local glacier retreat. Surficial sediments are commonly dissected by meltwater channels and can be used to establish the sequential positions of the edge of the ice (Photo 3).

Glaciofluvial, glaciolacustrine, modern fluvial and organic materials dominate valley settings. Deposits of massive to well-stratified sand, gravel and silt are evident in upland valley and as terraces throughout the study area. Coarse gravel beds range from open framework clast-supported beds to very well-stratified sands with normal, reverse or no grading (Photo 4). Ripples and cross-stratified beds are common. Load structures are locally preserved. Such sediments likely represent ice-proximal to ice-distal facies deposited during deglaciation. In the

Photo 1. Basal lodgement till exposed in a road cut along the Alaska Highway.

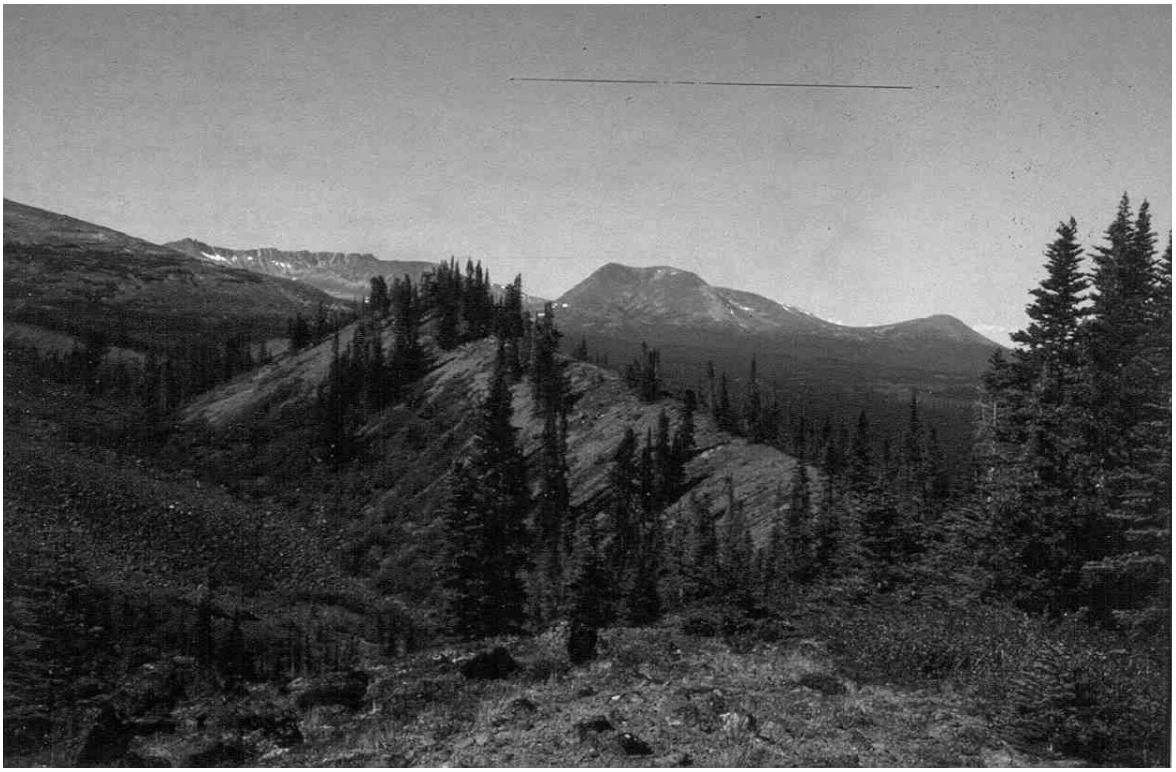
Photo 2. Lateral moraine in the Cassiar Mountains marking the ice margin during glacial retreat.

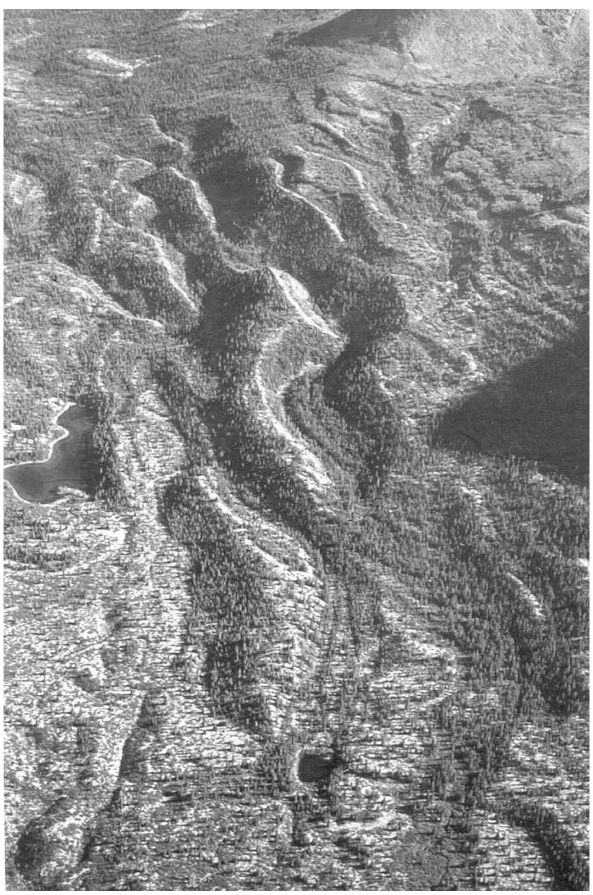
Photo 3. Meltwater channels developed on slope in Cassiar Mountains composed of thick till.


Photo 4. Glaciofluvial gravels exposed along the Jennings River.

deep, broad valleys in the Cassiar Mountains, esker complexes and kame and kettle topography are abundant. Eskers range from 10's to 100's metres in length. Kettles, identified by their circular shape, have formed where abandoned ice blocks were left to slowly ablate while sedimentation occurred around them (Photo 5).

Along the Swift River valley and Teslin Lake, thick sequences of fine sand, silt and clay form terraces above the modern day floodplain. The terraces occur below 900 metres in elevation. Exposures show rhythmically laminated, horizontal, tabular beds. Rip-up clasts and dropstones are common. Individual rhythmites have sharp basal contacts and vary in thickness from a few millimetres to several tens of centimetres. In select areas, glaciolacustrine rhythmites lie stratigraphically between two till layers (Figure 3). Occasionally, thin (<2 metres) sequences of glaciofluvial sands and gravels cap the rhythmites. The contact between the upper till and underlying unit is commonly abrupt and erosive. Rhythmites are often convoluted and contain load structures. The two diamictons exhibit similar physical properties such as colour, texture, and structure. The glaciolacustrine sediments are the remnants of a lake formed by the damming of the Teslin trench by advancing glaciers. Whether the tills are the result of two advances of the same ice sheet, or of two separate glaciations, is unclear without dating.

Modern fluvial, colluvial and organic deposits are found throughout the study area. Large modern floodplains dominate valley settings, with large alluvial fans forming along valley margins. Deposits includes clean, well-sorted and stratified sand and gravel. Clasts are well-rounded and of variable lithologies.

Intense post-glacial erosion within the area has produced widespread colluvial debris. Deposition and accumulation of these sediments result from direct, gravity-induced movement involving no agent of transportation such as water or ice, although the moving material may have contained water and/or ice. Colluvium can be massive to crudely-stratified, poorly-sorted to moderately-sorted, matrix to clast-supported and monolithic to polylithic, depending on source material. Clast size ranges from granular to boulder and shapes are variable. Deposits commonly occur in veneer or blanket accumulations or as large cones along steep valley walls and slopes.

Organic deposits commonly occur in areas of poor drainage such as marshes and swamps. Deposits are common along floodplains, along old meltwater channels, and between drumlinoid features. In areas of higher elevations, including plateaus, organic material accumulates where bedrock topography traps surface water to form bogs.

Photo 5. Eskers and kettle lakes in Cassiar Mountains. Landforms are produced under stagnant ice during glacial retreat.

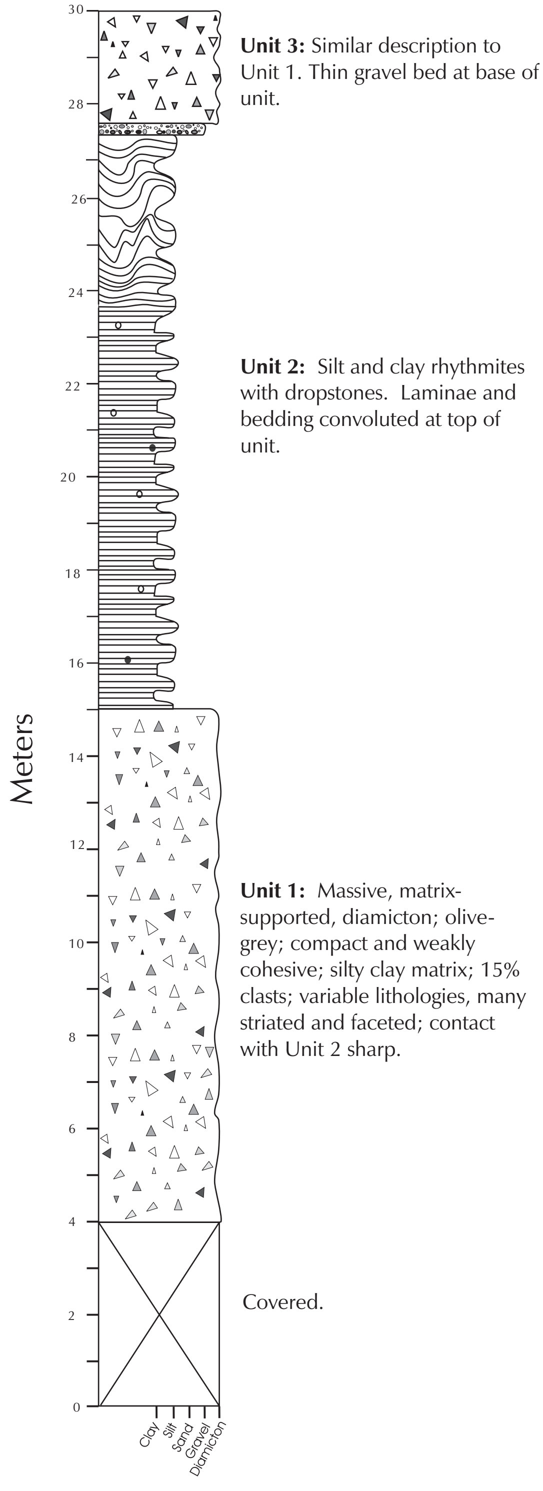

Figure 3. Stratigraphic section of two tills and glaciolacustrine sediments exposed along the Jennings River.

Ice-Flow

Mapping of ice-flow indicators (Photo 6) reveals trends similar to those suggested by other authors (*e.g.* Ryder and Maynard, 1987; Clague, 1989; Jackson, 1994). At the glacial maximum, an ice divide developed over the Cassiar Mountains between the Liard and Teslin Plateaus (Figure 4). Ice flowed westerly from the mountains and upon reaching the Teslin Depression, moved northerly into the Yukon. In contrast, on the east side of the Cassiar peaks, ice flowed northeast toward the Liard plateau and into the Yukon. It is unclear if the Cordilleran Ice sheet was influenced at all times by underlying topography or if a true continental ice sheet, with flow directions independent of underlying topography, developed. However, local flow directions did alter in accordance with increasing topographic control as the ice thinned.

A second set of cross-cutting striae and stoss and lee forms was documented at seven locations along the shore of Teslin Lake and the Alaska Highway corridor. A second, older (?) northeasterly flow event may have occurred across the study area.

TILL GEOCHEMISTRY

Forty-five till samples were collected for geochemical analyses in the area of six geochemical case study locations. The studies focused on sampling till over: 1) exhalative and felsic metavolcanics packages with potential for hosting polymetallic massive sulphide deposits (*e.g.* copper-bearing crinkled chert); and 2) mineral prospects (*e.g.* Arsenault MINFILE 104O 011). The case studies and collected samples are summarized in Table 6. Data listed here complements the work of Cook and Pass (this volume).

Felsic Volcanic and Exhalative Packages

The following case studies were conducted over horizons with perceived potential for hosting base metal mineralization: a) copper-bearing crinkle chert (north of Mount Francis and Logtung Road); and b) Jennings River quartz-sericite schist. Results discussed are based on aqua regia ICPMS determinations unless otherwise stated.

Copper-Bearing Crinkle Chert

Minor sulphide mineralization and copper staining have been found at select sites within a distinct marker horizon of crinkle chert. This unit is characteristically white to pink in colour, thinly bedded to laminated and contorted. Least recrystallized beds have purple-grey to greenish-coloured fresh surfaces comprised of silica, lesser argillite and minor ash tuff. Recrystallized beds are quartzite with white mica. Commonly, piedmontite (manganese-epidote) has coloured the rocks pink and red. Idiomorphic garnet, specular hematite and staurolite are present. The unit is best exposed in the Mount Hazel, Logjam Creek and Mount Francis areas in the Smart River (104O/13) map area (Mihalynuk *et al.*, 1998).

Two bedrock samples collected by (Mihalynuk *et al.*, 1998), have highly anomalous concentrations of barium (average 2254 ppm, INAA) in the chert unit, compared to

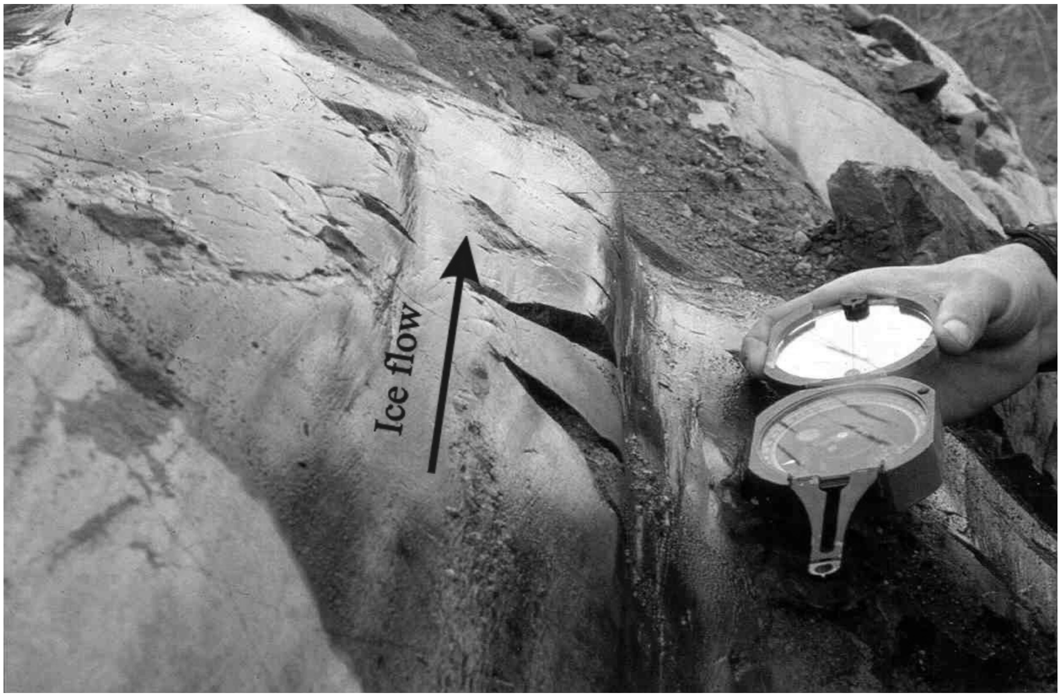

Photo 6. Striated and grooved bedrock surface, exposed along the Alaska Highway. Ice-flow was from east to west.

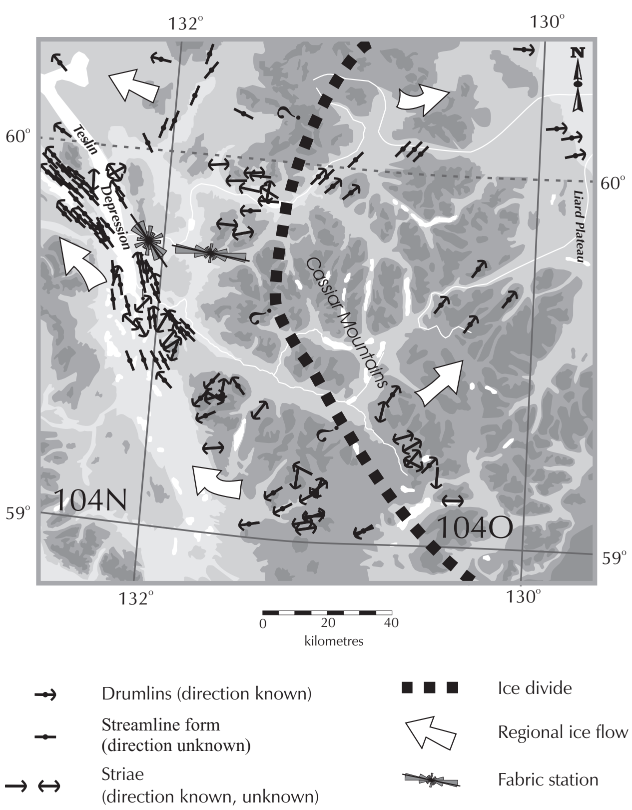

Figure 4. Summary of ice-flow directions for the study area. Position of ice divide is approximate. Data compiled from Dixon-Warren and Hickin (2000), Morison and Klassen (1997), Jackson , L.E. (1994), Klassen (1978), Gabrielse (1968), Watson and Mathews (1944).

many of the other lithologies in the study (average 59 ppm; N=28). Cook and Pass (this volume) also detected anomalous values in 5 chert samples with barium ranging from 1600 to 19,000 ppm (Cook and Pass, this volume; Table 4). Elevated barium levels may be a useful element to distinguish crinkle quartzite from other fine grained quartzites within the study area (Mihalynuk *et al.*, 1998).

1) North of Mount Francis

Two small bedrock knobs, located approximately 2 kilometres apart, are composed of metasedimentary rocks, (east knob), and crinkle chert (west knob; Figure 2). The Arsenault prospect is about 3 kilometres to the south and the Alaska Highway is 9 kilometres to the north. Ten thin (<2 metres thick) till and colluviated till sites were sampled within the area, six on the east knob, four on the west knob (Figure 5). Three samples were also collected from thin (<50 centimetres) colluvial debris directly over bedrock on the west knob. Eight soil profiles were collected in select till pits by Cook and Pass (this volume; Tables 5, 6, and 7). Ice-flow is inferred to be from east to west, as indicated by striae observed within the area.

Samples collected on the east knob have lower barium values (770-1100 ppm, INAA) than samples collected over the chert unit (790-1500 ppm, INAA; Table 7). The east knob is expected to have lower barium concentrations due to its up-ice location from the chert unit. Key base metal concentrations, *e.g.* copper and zinc, were at or near background (median) concentrations for all stations (Table 2). High barium values were detected in both colluvial debris (*e.g.* 996035, 1300 ppm, INAA) over bedrock and till (*e.g.* 996046, 1500pm, INAA) dispersed down-ice

TABLE 6
SUMMARY OF TILL GEOCHEMISTRY
CASE STUDY SAMPLING SITES

Case Study		NTS Mapsheet	MINFILE	Samples
Exhalative:	Crinkle Chert - North of Mount Francis	104O/13	n/a	996029, 996030, 996031, 996032, 996033, 996034, 996025, 996026, 996027, 996035, 996036, 996037, 996038, 996045, 996046
	Crinkle Chert - Logtung Road	104O/13	n/a	996047, 996048, 996050, 996051
Felsic Volcanic:	Jennings River quartz-sericite schist	104N/9	n/a	996039, 996042, 996043, 996044
Mineral Prospects:	Arsenault Prospect	104O/13	104O 011	996020, 996022, 996023, 996024, 996028
	Mount Francis East	104O/13	n/a	996008, 996012, 996013, 996014, 996016, 996017, 996018, 996019
	Highway 97 Prospect	104O/13	104O 054	996002, 996003, 996004, 996005, 996006, 996007, 996009, 996010, 996011

TABLE 7
GEOCHEMICAL RESULTS FOR BARIUM (INAA) AND MANGANESE AT THE CRINKLE CHERT, NORTH OF MOUNT FRANCIS

Sample		Ba (ppm)	Mn (ppm)
East Knob			
996029		1100	375
996030		1000	373
996031		1000	367
996032		960	456
996033		770	422
996034		770	368
West Knob			
996025	Field Trip. 1	1300	338
996026	Field Trip. 2	1100	295
996027	Field Trip. 3	1100	281
996035		1300	500
996036		850	430
996037		790	352
996038		790	392
996045		920	380
996046		1500	521

Field Trip. = field triplicate

of the knob, indicating both sediment types are suitable for sample media.

Although there is no regional till data to compare these results against, several such surveys have been conducted in central and southern British Columbia. Results show median values between 380-850 ppm for barium and 508-805 ppm for manganese (*s*ee Table 8; Cook and Pass, this volume). Thereby, high barium concentrations do appear unique in this area, particularly for the crinkle chert unit. However, manganese concentrations (Table 7) are indistinguishable from background levels in other parts of the province. More information on soil and rock geochemistry collected here is given by Cook and Pass (this volume).

2) Logtung Road

The crinkle chert unit is clearly exposed along Logtung Road, 1.5 kilometres north of the Alaska Highway and 1 kilometres west of Logjam Creek. Three samples were collected along an east-west traverse, parallel to paleo-ice-flow directions (Figure 6). Striated bedrock within the case study area indicate ice-flow was from the east to the west. The sampling medium, inferred to be basal till, was gleyed and moist. At least 10 centimetres of peat overlay the till. No samples were collected to the east, as no suitable sampling media were available. One grab sample (996051) was also obtained from a thick unweathered basal till sequence exposed along the Logjam Creek, 150 metres north of the junction of the Alaska Highway and Logjam Creek (Figure 6). Outcrop, bark and twig, stream sediment and water samples were collected by Cook and Pass (this volume), but results are not yet available.

Base metal values were low in all samples collected west of Logtung Road. Copper and zinc ranged from 28.41 to 41.76 ppm and 56.1 to 70.8 ppm, respectively. Barium, the key signature element for the crinkle chert unit, ranged from 910 to 970 ppm (INAA). Sample 996051, collected from unweathered till, recorded high concentration of barium (960 ppm, INAA), but metal concentrations; *e.g.* copper (39.84 ppm), and zinc (72.3 ppm) were also low (Tables 2 and 3).

Low base metal concentrations may reflect the removal of more mobile metals from till by leaching; although, results could also reflect a lack of mineralization at this location. However, the elevated geochemically less mobile barium values still successfully reflect the

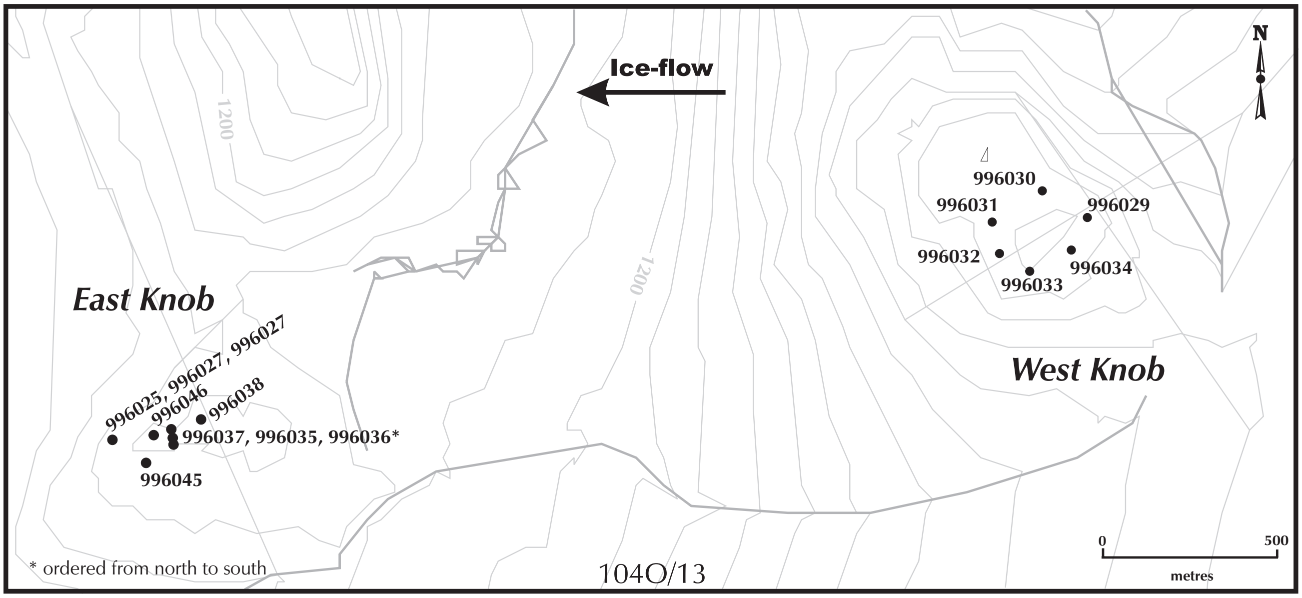

Figure 5. Approximate location of crinkle chert sampling sites, north of Mount Francis. Regional ice-flow was from east to west. Cook and Pass (this volume) summarize soil data collected at this site.

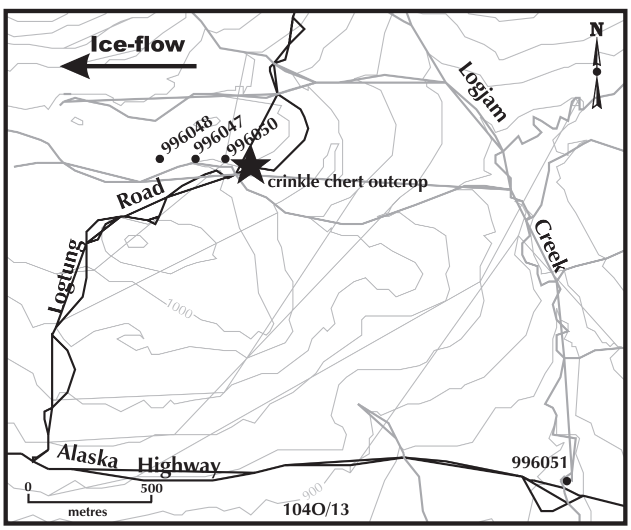

Figure 6. Approximate location of crinkle chert sampling site, Logtung Road. Regional ice flow was from east to west.

proximity of the crinkle chert unit. Elevated barium values recorded at the site adjacent to Logjam Creek suggest that a source area enriched in these two elements lies nearby.

Jennings River Quartz-Sericite Schist

On the north side of the Jennings River, surficial sediments were sampled over a quartz-sericite schist, to test its potential for associated polymetallic mineralization. A composite rock sample (99-SJC-12), collected across a 1.5 metre-wide altered pyritic quartz-sericite schist horizon yielded only background-level concentrations of copper (20 ppm), zinc (17 ppm), cobalt (4.7 ppm) and barium (320 ppm, INAA; Cook and Pass, this volume). The bedrock is overlain by a 12 to 14 metres thick sequence of basal till, and is capped by 2 metres of glaciolacustrine sediments (silt and clay rhythmites). Ice-flow was established to be from the south-east based on ice-flow indicators such as drumlins, striae and stoss and lee forms.

Two till profiles, comprised of two samples each, were collected from the exposure to evaluate the geochemical response to underlying bedrock (Figure 7 and Table 8). Sample 996044, collected within 1 metre of bedrock was situated 3 metres below sample 996039 (Profile A). Sample 996042, collected near the contact of the glaciolacustrine sediments and till units, was sampled approximately 10 metres up section from sample 996043, sampled within 2 metres of bedrock (Profile B). Profile A is 30 metres to the east of Profile B. Cook and Pass (this volume) also collected two soil profile from the overlying glaciolacustrine sediments, to demonstrate the poor geochemical response of this sample media.

Results indicate base metal elements detected in the soils have weaker geochemical signature than in the underlying till. For example, copper and zinc values in the B horizon are 19.17 ppm and 50.7 ppm, respectively, whereas, in the underlying till they are 74.97 ppm and 90.7 ppm (see Table 5 of Cook and Pass, this volume). As basal till is generally a first derivative product of bedrock, it will carry a strong geochemical signature of its parent material and therefore is a preferred sampling media for geochemical exploration (Shilts, 1976). In contrast, glaciolacustrine sediments have been extensively reworked and more distally derived and consequently, tracing an anomaly back to a source area is more complex.

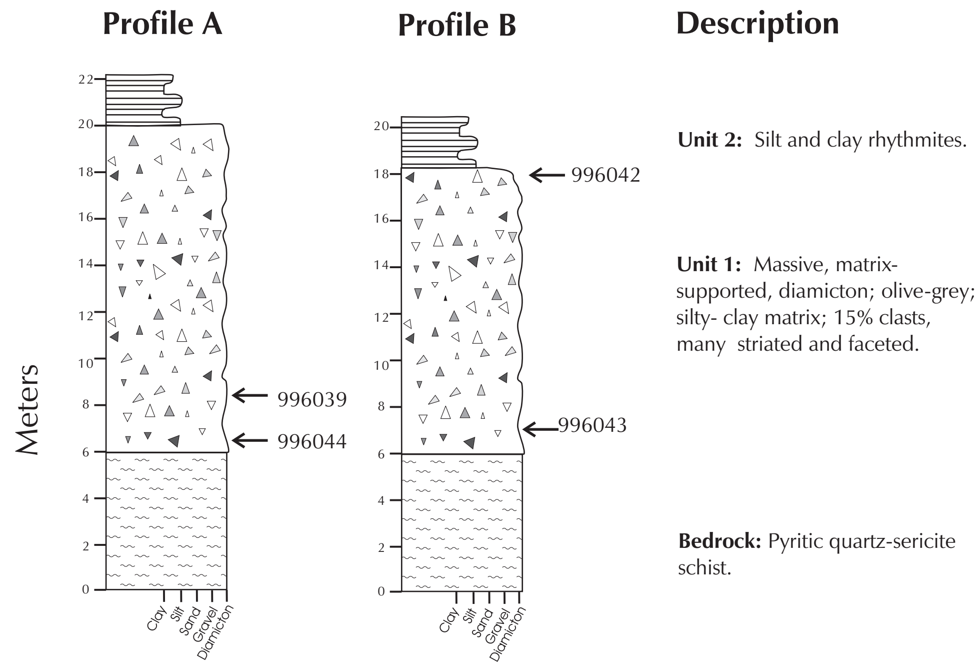

Figure 7. Stratigraphic sections showing sample sites over the pyritic quartz-sericite schist. Cook and Pass (this volume) summarize soil profile data collected at this site.

TABLE 8
CONCENTRATIONS OF KEY ELEMENTS FROM TILL PROFILE DATA COLLECTED OVER THE PYRITIC JENNINGS RIVER QUARTZ-SERICITE SCHIST

Sample	Height[1] (m)	Mo (ppm)	Cu (ppm)	Pb (ppm)	Zn (ppm)	Co (ppm)	Cd (ppm)	Se (ppm)
Profile A								
996039	4	5.57	82.57	11.92	104.7	21.0	0.55	2.0
996044	<1	4.55	74.44	9.96	96.7	20.7	0.50	1.9
Profile B								
996042	10	1.49	49.38	6.61	76.7	19.9	0.28	0.9
996043	2	4.78	74.97	10.05	90.5	23.0	0.47	1.3

[1] measured in metres above bedrock

Tills sampled near bedrock report higher elemental values than those collected up profile (Table 8). For example, elevated copper (74.44-82.57 ppm), zinc (90.5-104.7 ppm), cobalt (20.7-23.0 ppm), cadmium (0.47-0.55 ppm) and selenium (1.3-2.0 ppm) occur in the samples 996039, 996043 and 996044. In contrast, sample 996042 recorded comparatively lower values: 49.38 ppm copper; 76.7 ppm zinc; 19.9 ppm cobalt; 0.28 ppm cadmium; and 0.9 ppm selenium. Close to the bedrock, the geochemical signature from the parent material will be more pronounced in overlying sediments as the source is relatively close. In contrast, sediments higher in the profile have been transported from farther up-ice, and the concentrations detected are lower due to dilution (Miller, 1984). Sample 996039, collected approximately 4 metres above bedrock, has consistently higher elemental concentrations than the two underlying samples. Sediments collected may be part of a metal rich dispersal plume derived from a source, up-ice to the south.

Mineral Prospect Studies

Till sampling was conducted over the Arsenault copper prospect (MINFILE 104O 011) and Highway 97 (MINFILE 104O 054) showing to define their geochemical signatures. Sampling was also conducted on the east side of Mount Francis to further characterize the geochemistry of a RGS anomaly most-likely associated with the mineralized rocks of the Arsenault prospect.

Arsenault Prospect

A previous soil geochemical study conducted by Sawyer (1967) provides an indication to the configuration of dispersal patterns one can expect around the Arsenault prospect (Figure 8). Although ice-flow indicators suggest a westerly regional flow in the area, ice may have been locally deflected southward around the northeast trending Mount Francis. The trend of copper dispersal plumes parallels ice flow, showing a broad discontinuous zone of ribbon-shaped plumes extending southwest. Secondary downslope dispersion has overprinted the original dispersal plumes, attenuating the southern boundaries of the plumes. These results should be cautiously interpreted as no description of type of sediment sampled (*e.g.* B or C horizon, colluvium or till) was provided in the original report.

To further characterize the geochemical signature of the Arsenault showing, samples were collected adjacent to two exploration trenches on a subsidiary western ridge of Mount Francis. Cook and Pass (their Tables 5, 6 and 7;

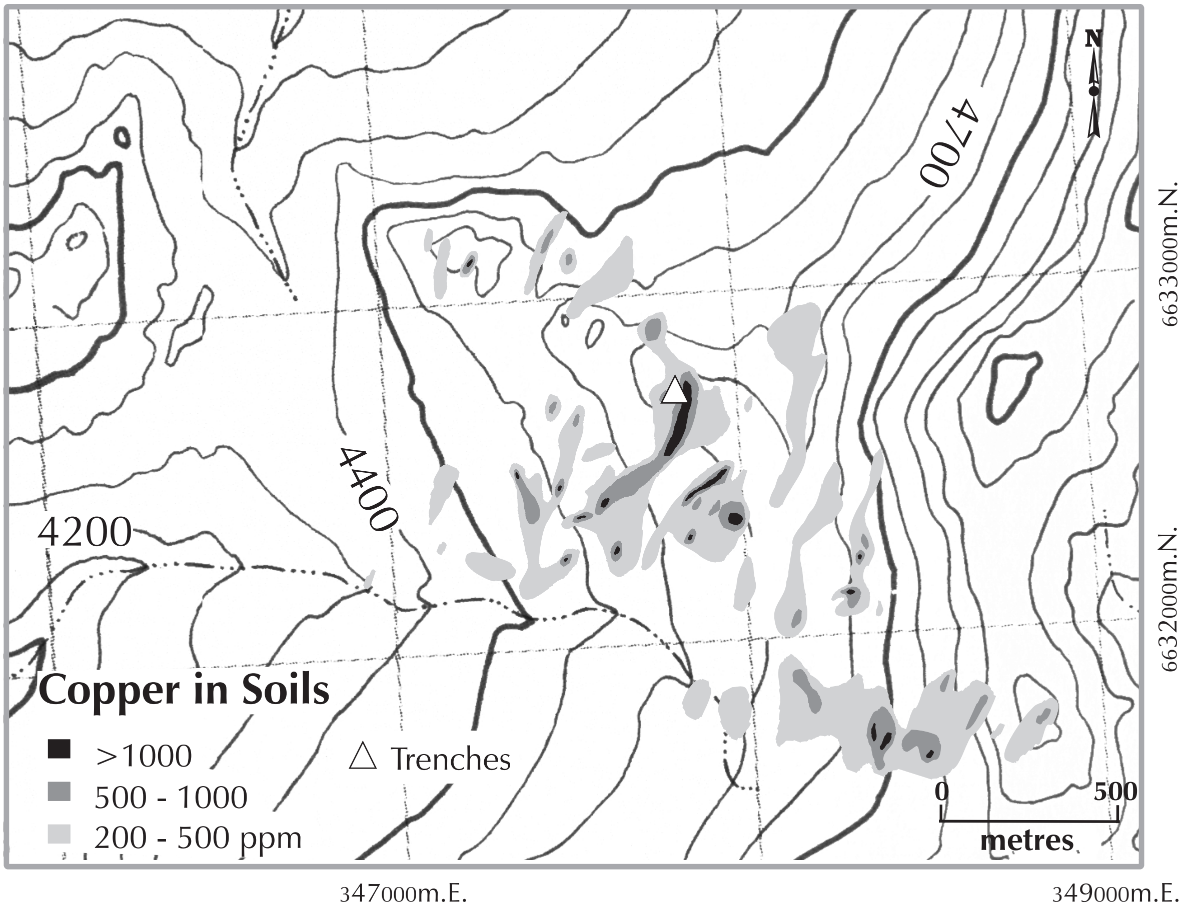

Figure 8. Copper in soils at the Arsenault prospect. Modified after Sawyer (1967).

this volume) sampled two soil profiles here, as well as collected stream sediment and water samples to the northwest. Three till samples were collected 200 metres southwest of the trenches and two samples 200 metres to the northeast (Figure 9). Samples were approximately 100 metres apart along an east-west traverse. Surficial materials were thin (<1 metre), discontinuous and colluviated. Ice-flow was from the east to west, based on the orientation of striae recorded in the area. However, ice may have been locally deflected by topographic influences. Solifluction lobes, resulting from slow downslope movement of unconsolidated surficial material, indicates that surface debris was subject to colluvial processes.

Soil data contained values as high as 4977 ppm copper, 142 ppm molybdenum, 77 ppb mercury and 29 ppm selenium in colluvium (sample 996509) over bedrock (their Table 5, Cook and Pass, this volume). Mineral-rich debris is also detected in the till, resulting in a strong copper-zinc-cadmium-selenium signature (Table 9). Elevated concentrations of copper (104.35-589.98 ppm), zinc (64.6-236.2 ppm), cadmium (0.21-2.41 ppm), and selenium (0.8-1.2 ppm) were recorded in all the samples. Samples collected to the southwest (996020, 996022, and 996023) have higher copper values than the two samples (996024 and 996028) collected northeast of the trenches. These results echo the observations of Sawyer (1967) who recorded anomalous zones (>200 ppm) of copper in soil samples collected to the southwest of the property (Figure 8). The thin, colluviated samples indicate transport distance was limited and the potential source area, associated with the mineralized rocks surrounding this prospect, lies up-slope towards the east.

Mount Francis East

Limited trace element data area available through RGS program for the map area 104O (RGS, 1979). Cook and Pass collected additional samples to verify the original RGS anomalies, identify possible sources and investigate metal speciation (Cook and Pass, this volume; Table 1; RGS, 1979). East of the Arsenault prospect, a RGS stream water sample collected at approximately 1300 metres returned elevated values of copper (104 ppm), zinc (130 ppm) and cobalt (8 ppm). To further define the anomaly and evaluate if high elemental values are reflected in the surficial sediments above and below, eight samples of thin colluviated material were collected along 3 northeast-southwest transects in the drainage basin (Figure 9). Sample spacing was approximately 30 metres, along transects at about 1450 metres, 1300 metres and 1200

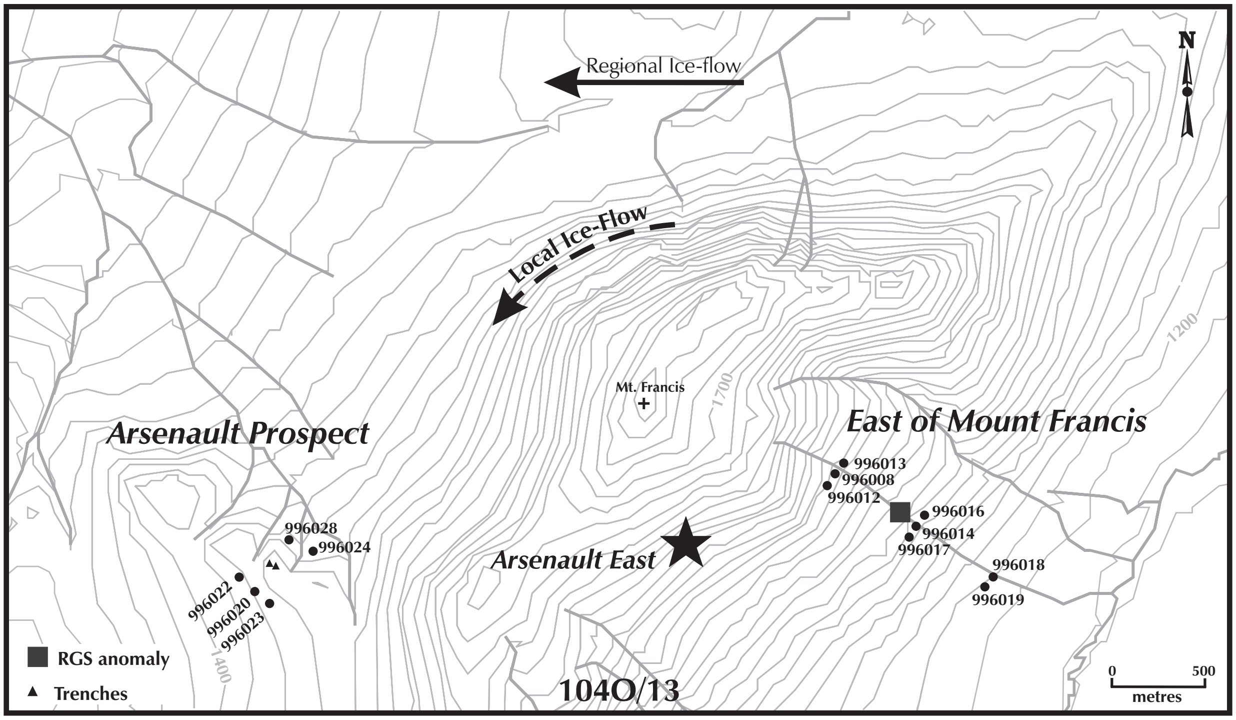

Figure 9. Location of sampling sites at the Arsenault prospect Mount Francis East. Regional ice-flow was from east to west; however, ice was probably locally deflected to the south around Mount Francis. Cook and Pass (this volume) summerize soil profile data collected at the trenches.

TABLE 9
CONCENTRATIONS OF KEY ELEMENTS IN TILLS AT THE ARSENAULT PROSPECT

Sample	Mo (ppm)	Cu (ppm)	Pb (ppm)	Zn (ppm)	Co (ppm)	Cd (ppm)	Se (ppm)
Southwest of Exploration Trenches							
996020	2.44	589.98	13.83	236.2	16.5	2.41	0.9
996022	2.62	387.65	8.54	64.6	13.9	0.22	1.0
996023	2.60	227.26	12.88	71.2	16.1	0.26	0.8
Northeast of Exploration Trenches							
996024	2.39	157.55	20.86	84.8	23.4	0.48	1.2
996028	2.32	104.35	19.44	67.1	13.8	0.21	1.1

metres. Regional ice-flow was inferred to be from the east to the west, however, it was probably deflected to the south by Mount Francis.

Key elements reached anomalous levels the tills (Table 2). Copper concentrations ranged from low (35.72 ppm) to elevated levels (132.33 ppm). Other elements such as zinc (56.9-132.4 ppm), cobalt (10.4-20.3 ppm), arsenic (13.0-55.4 ppm, INAA) and selenium (0.8 to 1.3 ppm) showed similar patterns. More sampling is required to accurately delineate the source area more sampling is required; however, the colluvial nature of the surface material requires that it be northwest, in the upper portion of the drainage basin, along the strike of the slope. It is likely genetically related to the Arsenault and Arsenault East showings.

Highway 97 Prospect

A greenstone unit composed of resistant, dark green to black-weathered basalt and intermediate to mafic tuff lies west of Mount Francis and both east and west of Logjam Creek. Well-bedded, bright green, aphanitic lapilli tuff is the most common lithology, with massive flows equivocally identified in only a few localities.

Along Highway 97, a 3-metre wide gossanous zone, cross-cut by north northwest trending quartz-chlorite-magnetite-pyrite chalcopyrite veins (<30 centimetres thick) was first reported by Mihalynuk (1998) in the greenstone unit 3.5 kilometres west of Swan Lake. Mineralized chips sampled collected returned 0.2 per cent copper, 165 ppm cobalt, 210 ppm arsenic and 45 ppm tungsten (Mihalynuk *et al.*, 1998). This unit stratigraphically underlies the crinkled chert unit.

Till sampling was conducted here to establish the extent of dispersal of mineralized debris from this source. Seven till sites were sampled in area of thin basal till (<2 metres), four to the north of the highway and three to the south (Figure 10). Cook and Pass (this volume) also collected thin oxidized soil (996502) and rubble sample (996503R) over the mineralization as well as a cobble sample (99-SJC-03) at station 996002. Paleo-ice-flow directions are inferred to be from the east to the west based on striae and stoss and lee forms exposed along the Alaska Highway.

Only the rock samples collected by Cook and Pass (this volume) have elevated metal concentrations, (*e.g.* copper 228.92 ppm), whereas the till samples show background (median) or near background concentrations of copper and other base metals (Table 2). Detection of the dispersal plume may have been disrupted during highway construction.

CONCLUSIONS

Surficial mapping and geochemical studies over the Big Salmon Complex and adjacent rocks in northwest British Columbia has shown that:

- basal till, the preferred sampling medium, is abundant on gentle slopes and plateaus at lower elevations
- an ice divide may have existed within the study area between the Nisutlin and Liard plateaus complicating ice-flow patterns;
- till, a first derivative product of bedrock, carries a stronger geochemical signature then other sampling media;
- trace metals commonly associated with massive sulphides, including copper, zinc, and cadmium as well as important pathfinder elements such as selenium and cobalt, detected over favourable host rocks;
- high concentrations of barium were detected in surficial media around the copper-bearing crinkle chert and seems to be a useful pathfinder for the unit; and
- a strong copper-zinc-cadmium signature was detected in surficial media associated with the Arsenault property; elevated selenium was also detected in samples suggesting a VMS origin for the mineralization .

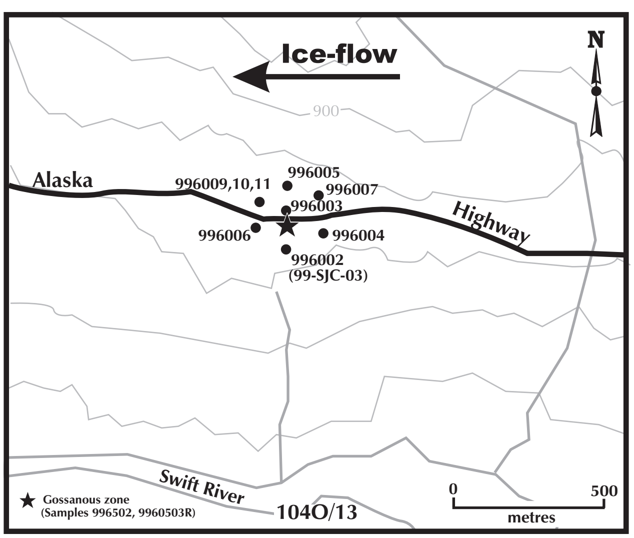

Figure 10. Approximate location of Highway 97 sampling sites. Cook and Pass (this volume) summarize soil profile and rock data collected at this case study.

ACKNOWLEDGEMENTS

This NATMAP project would not of been successful without S. Cook, M. Mihalynuk, and J. Nelson. Our gratitude extends to C. Roots, Geological Survey of Canada, for coordinating camp logistic at Morley Lake and Beth Hunt, the camp cook, for preparing delicious meals. Special thanks to A. Paige, Fireweed Helicopters, and D. Dennison, Coyote Air, whose talented flying ensured we flew all corners of the study area. H. Pass assisted with field sampling and A. Bichler helped with digital map compilation and preparation of figures. Thanks to R. Lett, P. Bobrowsky, S. Cook, M. Mihalynuk and G. McArthur for their comments on early revisions of this manuscript. An extra special thanks to V. Levson who provided insight on the local surficial geology and airphoto interpretation. The supervision of P. Bobrowsky on the project is gratefully acknowledged.

REFERENCES

Aitken, J.K. (1959): Atlin map-area, British Columbia (104N); *Geological Survey of Canada*, Memoir 307, 38 pages.

Bobrowsky, P.T. and Rutter, N. (1992): The Quaternary geologic history of the Canadian Rocky Mountains; *Geographie Physique et Quaternaire*, Volume 46, Number 1, pages 5-50.

British Columbia Ministry of Environment (1978): Soils and landscapes of British Columbia: K.W.G. Valentine, P.N. Sprout, T.E. Baker, and L.M. Lavkulich, Editors, *British Columbia Ministry of Environment*, Resource Analysis Branch.

Clague, J.J. (1989): Cordilleran Ice Sheet; *in* Quaternary Geology of Canada and Greenland, R.J. Fulton, Editor, *Geological Survey of Canada*, Geology of Canada, no.1 (also Geological Society of America, Geology of North America, v.K-1), pages 40-42.

Cook, S. and Pass, H. (2000): Ancient Pacific Margin Natmap Part IV: Preliminary results of geochemical studies for VMS deposits in the Big Salmon Complex, Yukon-Tanana Terrane, northern British Columbia (104N/9, 16; 104O/11, 12, 13, 14); *this volume.*

Dixon-Warren, A. and Hickin, A (2000): Surficial Geology of the Swift River Area (104N/9, 16 and 104O NW), scale 1:100,000; *BC Ministry of Energy and Mines*, Open File 2000-5.

Dreimanis, A. (1988):Till: their genetic terminology and classification; *in* Genetic Classification of Glaciogenic Deposits, R.P. Goldthwait and C.L. Matsch, Editors, Balkema, pages 17-67.

Gabrielse, H. (1969): Geology of the Jennings River map area, British Columbia (104O); *Geological Survey of Canada*, Paper 68-55.

Howes, D.E. and Kenk, E. (1997): Terrain classification system for British Columbia (Version 2); *B.C. Ministry of Environment*, Land and Parks, Survey and Resource Mapping Branch, MOE Manual 10, 102 pages.

Jackson, L.E. (1994): Terrain inventory and Quaternary history of the Pelly River area, Yukon Territory; *Geological Survey of Canada*, Memoir 437, 41 pages.

Johnston, W.A. (1926): The Pleistocene of Cariboo and Cassiar Districts, British Columbia, Canada; *Transactions of the Royal Society of Canada*, Series 3, Volume 20 (4), pages 137-147.

Kerr, F.A. (1948): Lower Stikine and western Iskut River areas, British Columbia; *Geological Survey of Canada*, Memoir 246.

Klassen, R. (1978): Surficial geology, Swift River, Yukon Territory (NTS 104N/16, 104O/13, 14, 105B/3,4 and 105C/1); *Geological Survey of Canada*, Open File 539, scale 1:100,000.

Klassen, R. (1982): Suficial Geology, Wolf Lake, Yukon Territory (NTS 105O); *Geological Survey of Canada*, Preliminary Map 14-1982, 1:250,000.

Levson, V. (1992): Quaternary geology of the Atlin Area (104N/11W, 12E): *in* Geological Fieldwork 1991, *British Columbia Ministry of Energy, Mines, and Petroleum Resources*, Paper 1992-1, pages 375-390.

Levson, V. and Blyth, H. (1993): Applications of Quaternary geology to placer deposit investigations in glaciated areas; a case study, Atlin, British Columbia; *Quaternary International*, Volume 20, pages 93-105.

MacKinnon, A., Pojar, J., and Coupe, R. (1992): Plants of Northern British Columbia; *B.C. Ministry of Forests* and *Lone Pine*.

Mihalynuk, M.G., Nelson, J., R.M. Friedman (1998): Regional geology and mineralization of the Big Salmon Complex (104N NE and 104O NW); *in* Geological Fieldwork 1997, A Summary of Field Activities and Current Research, *Ministry of Employment and Investment*, Paper 1998-1, pages 6-1 to 6-20.

Mihalynuk, M.G., Nelson, J., Roots, C., Friedman, R.M. and de Keijzer, M. (2000a): Ancient Pacific Margin Part III: Regional geology and mineralization of the Big Salmon Complex (104N/9,10 & 104O/12,13,14W); *this volume*.

Mihalynuk, M.G., Nelson, J., Roots, C., Friedman, R.M. and de Keijzer, M. (2000b): Geology of the Smart River area (104O/13); *B.C. Ministry of Energy and Mines*, Open File 2000-6.

Miller, J.K. (1984): Model for clastic indicator trains in till; *in* Prospecting in areas of glaciated terrain-1984, *Institution of Mining and Metallurgy*, London, pages 69-77.

Miller, M.M, (1976): Quaternary erosional and stratigraphic sequences in the Alaska-Canada Boundary Range; *in* Quaternary stratigraphy of North America, W.C. Mahaney, Editor, *Dowden, Hutchinson and Ross, Inc*., Stroudsburg, Pennsylvania.

Morison, S.R. and Klassen, R.W (1997): Surficial geology, Teslin, Yukon Territory; *Geological Survey of Canada*, Map 1891A, scale 1:25 000.

Nelson, J. (1999): Devono-Mississippian VMS project: continuing studies in the Dorsey Terrane, northern British Columbia; *in* Geological Fieldwork 1998, *Ministry of Energy and Mines*, Paper 1999-1, pages 143-156.

Nelson, J. (2000): Ancient Pacific Margin Part VI: Still heading south: continuation and re-evaluation of potential VMS hosts in the eastern Dorsey Terrane, Jennings River (104O/1; 7,8,9,10); *this volume*

Nelson, J., Harms, T., and Mortensen, J. (1998): Extensions and affiliates of the Yukon-Tanana Terrane in northern British Columbia; *in* Geological Fieldwork 1997, *Ministry of Employment and Investment*, Paper 1998-1, pages 7-1 to 7-12.

Nelson, J., Harms, T.A., Zantvoort, W., Gleeson, T. and Wahl, K. (2000): Geology of the southeastern Dorsey Terrrane, 104O/7, 8, 9, 10; *B.C. Ministry of Energy and Mines*, Geological Survey Branch, Open File 2000-4.

Phendler, R.W. (1982): Report on Assessment Work (Diamond Drilling) on the Arsenault #1, #2, and #3 claims, Jennings River Area, Atlin Mining Division, British Columbia, NTS Map 104O; *B.C. Ministry of Energy, Mines and Petroleum Resources*, Assessment Report 10411.

Resource Inventory Committee (1996): Guidelines and Standards to Terrain Mapping in British Columbia. Surficial Geology Task Group, Earth Sciences Task Force, British Columbia, *Resources Inventory Committee*, Publication #12, 216 pages.

RGS (1978): Regional Geochemical Survey, Atlin map area (NTS 104N); *B.C. Ministry of Energy and Mines*, NGR 28.

RGS (1979): Regional Geochemical Survey, Jennings River map area (NTS 104O); *B.C. Ministry of Energy and Mines*, NGR 41.

Roots, E.F. (1954): Geology and mineral deposits of Aiken Lake map-area, British Columbia; *Geological Survey of Canada*, Memoir 274.

Ryder, J.M. Fulton, R.J. and Clague, J.J. (1991): The Cordilleran ice sheet and the glacial geomorphology of southern and central British Columbia, *Geographie Physique et Quaternaire*, 45, pages 365-377.

Ryder, J. and Maynard, D. (1991): The Cordilleran ice sheet in northern British Columbia; *Geographie Physique et Quaternaire*, Volume 45, pages 355-363.

Sawyer, J.B.P. (1967): Geological and Geochemical and Geophysical Report for Assessment Credits on the Top Claim Group; *B.C. Ministry of Energy, Mines and Petroleum Resources*, Assessment Report 1149.

Sawyer, J.B.P. (1979): Report on the 1979 Drilling Program on the Arsenault Claims Copper Prospect, Jennings River Area; *B.C. Ministry of Energy, Mines and Petroleum Resources*, Assessment Report 8022.

Shilts, W.W. (1976): Glacial till and mineral exploration; *in* Glacial Till: An Inter-disciplinary Study, R.F. Legget, Editor, *The Royal Society of Canada Special Publications*, Number 12, pages 205-224.

Spooner, I.S., Osborn, G.D., Barendregt, R., and Irving, E. (1996): A Middle Pleistocene (isotope stage 10) glacial sequence in the Stikine River valley, British Columbia; *Canadian Journal of Earth Sciences*, Volume 33, Number 10,pages 1428-1438.

Traynor, S. (1999): Tanana Exploration update on Southern Yukon/Northern B.C., Bigtop, Arsenault and King Lake Properties; *unpublished promotional report*.

Watson, K and Mathews, W.H. (1944): The Tuya-Teslin Area, Northern British Columbia; *British Columbia Department of Mines*, Bulletin 19, 52 pages.

Ancient Pacific Margin Part V: Preliminary Results of Geochemical Studies for VMS Deposits in the Big Salmon Complex, Northern British Columbia (104N/9, 16; 104O/11, 12, 13, 14)

By Stephen J. Cook and Heidi E. Pass

KEYWORDS: *Geochemistry, soils, till, Big Salmon Complex, Arsenault, copper, VMS, exhalite.*

INTRODUCTION

The Yukon-Tanana Terrane extends southeasterly from eastern Alaska to northern British Columbia. Successful exploration for volcanogenic massive sulphide (VMS) deposits (*e.g.* Kudz Ze Kayah, Wolverine) within this prospective belt of rocks in the southern Yukon has focused attention on the VMS potential of its proposed southern extensions within northern British Columbia. Recent mapping of these Yukon-Tanana correlative rocks just south of the Yukon border, the Big Salmon Complex and the Dorsey Terrane, by Mihalynuk *et al.* (2000; 1998) and Nelson (2000; 1999), identified prospective Devonian-Mississippian stratigraphy and reinforced their potential for hosting VMS deposits. Volcanogenic massive sulphide deposits are a major source of copper, zinc, gold and silver in Canada and British Columbia, and over the period 1995-1998 massive sulphide exploration represented 11.3 to 37.3 per cent of exploration targets in the province each year (*e.g.* Schroeter, 1999). Other than baseline Regional Geochemical Surveys (RGS), no systematic interpretative work or detailed geochemical studies have been conducted in this part of northern British Columbia to characterize element signatures and geochemical dispersal of either VMS deposits or their volcanic host rocks within the surficial environment.

The purpose of this project is to highlight the potential for VMS mineralization in Yukon-Tanana correlative rocks of the Big Salmon Complex by characterizing the surficial geochemical responses of known VMS prospects and their felsic and mafic volcanic host rocks. These results, and those of RGS interpretation studies, will be used to formulate geochemical exploration models for the region. During the 1999 field season, seven geochemical case studies were conducted in the Big Salmon Complex using a variety of surficial media including stream sediments, moss mats, stream waters, soil profiles, vegetation and rock. This paper discusses available RGS data and briefly outlines preliminary geochemical results of the case studies. Only soil profile and rock results were available at the time of writing. Colluvial soil profiles at the Arsenault copper prospect (MINFILE 104O 011), for example, contain highly elevated levels of copper, molybdenum and selenium, among other elements. As well, soils on till and colluvium near exposures of barium-rich exhalative crinkled chert units contain elevated barium concentrations which, in tills, generally increase down profile. Remaining results, including stream water geochemical studies undertaken as part of a University of Victoria B.Sc. thesis (Pass, in preparation) will be presented at a later date.

This project is a component of the Ancient Pacific Margin NATMAP Project, and is being carried out in conjunction with integrated bedrock and surficial geology mapping programs (Mihalynuk *et al*., this volume; Nelson, this volume; Dixon-Warren and Hickin, this volume). It is a northern counterpart to VMS geochemical studies conducted by Lett *et al.* (1999) in comparable rocks of the Kootenay Terrane in southern British Columbia.

PROJECT COMPONENTS AND OBJECTIVES

This project has two components. The first involves office compilation and interpretation of existing RGS data, in both the Big Salmon Complex and adjacent northern British Columbia terranes, to identify those areas potentially favourable for VMS-associated alteration and mineralization. The second involves site-specific field and laboratory studies in the Big Salmon Complex. These field studies, begun in 1999, are the subject of this paper.

Multi-media case study investigations were conducted at regionally-anomalous groups of watersheds in two parts of the Big Salmon Complex in 1999 (Figures 1 and 2). A further five case studies were conducted with Dixon-Warren and Hickin (this volume) at known VMS prospects (*e.g.* Arsenault copper prospect), some recently-mapped felsic and mafic metavolcanic packages, and at barium-manganese-rich chert horizons (Figures 1 and 2). Objectives of these studies are to characterize geochemical signatures and responses of: i) VMS mineralization and associated hydrothermal alteration assemblages, and ii) potential felsic and mafic metavolcanic host units and exhalative horizons, in various surficial media such as soil profiles, tills, stream sediments, moss mats and stream waters to determine which may be suit-

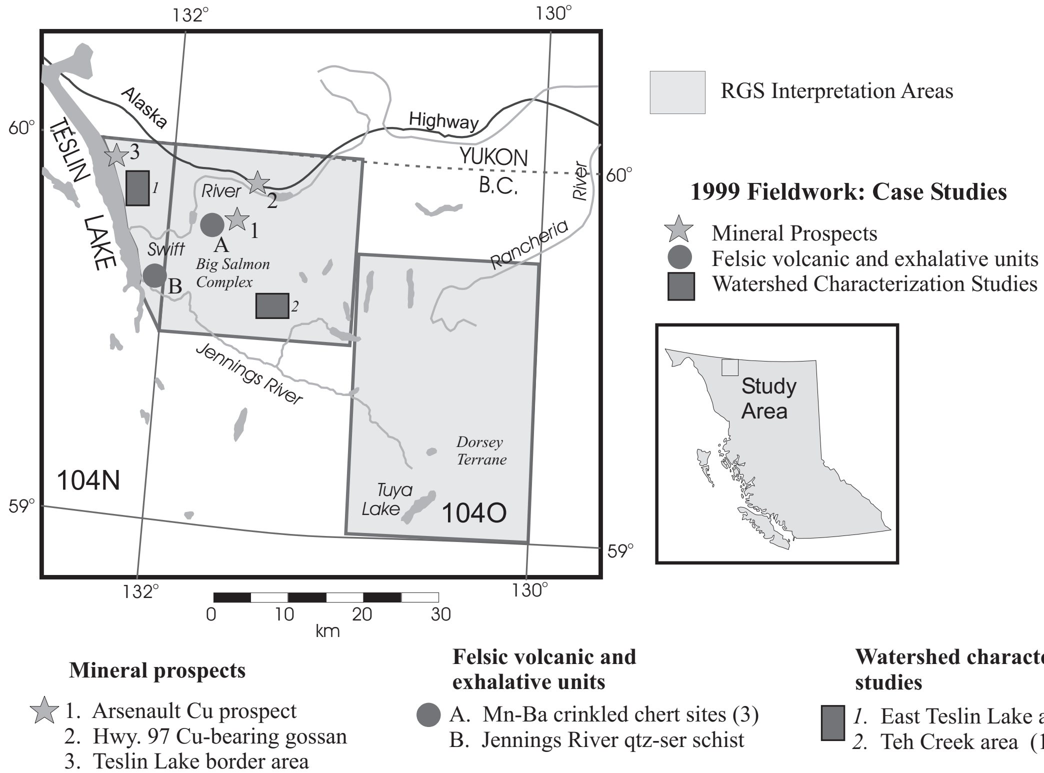

Figure 1. General location map showing 1999 field case study locations.

able for geochemical exploration. Subsequent laboratory studies will focus on size fraction analysis and heavy mineral concentrates of clastic sediments and soils to aid in speciation of the mineralization, alteration and related elements in the weathering environment. Characterization of geochemical signatures and dispersal in this area will aid in further interpretation of regional geochemical data and will help in the development of more effective geochemical exploration methods. Identifying the most effective geochemical exploration methods for VMS deposits is the principal objective of this project.

GEOLOGICAL SETTING AND MINERAL DEPOSITS OF THE BIG SALMON COMPLEX

Bedrock mapping of the Jennings River and Atlin map areas was first carried out at 1:250 000 scale by Gabrielse (1969) and Aitken (1959), respectively. More recently, detailed 1:50 000 scale geological mapping has been conducted by Mihalynuk *et al.* (in press, 2000, 1998) in the Big Salmon Complex and by Nelson (2000, 1999) in the Dorsey Terrane to the southeast. The Big Salmon Complex underlies much of the study area (Figure 2) and is situated east of Teslin Lake in the northwest part of the Jennings River area and the northeast part of the Atlin area. Geology has been described by Mihalynuk *et al.* (this volume, 1998), and the following is taken from those accounts.

The Devono-Mississippian Big Salmon Complex is a sequence of five volcano-sedimentary rock units, all but the oldest of which are correlable with Yukon-Tanana Terrane rocks of the Finlayson Lake belt (Mihalynuk *et al.*, 1998; Nelson *et al.*, 1998). They comprise: i) a variable youngest succession of siliceous clastic rocks and minor carbonates; ii) grey to white limestone with tuff and conglomerate interbeds; iii) thinly bedded to laminated manganiferous ‘crinkled’ chert; iv) a succession of quartz-rich clastic rocks and immature greywacke, and v) a thick oldest succession of greenstone, primarily mafic to intermediate tuffs with lesser basaltic flows. The Early Mississippian Mount Hazel orthogneiss is exposed in the interior of the Big Salmon Complex. Intrusive rocks in the study area include, among others, the Early Jurassic Simpson Peak batholith and Coconino tonalite.

Surficial geology of the study area is described by Dixon-Warren and Hickin (this volume, 2000) and will not be discussed at length here. In general, thick till sequences mantle plateau areas and gentle slopes, with colluvium common on steep slopes and in areas of higher relief. Thick accumulations of fluvial sediments occur in valleys, and pockets of glaciolacustrine material are found along Teslin Lake and the Alaska Highway.

Known mineral occurrences the Big Salmon Complex area include the Arsenault copper prospect (MINFILE 104O 011) and several small copper showings described by Mihalynuk *et al.* (1998, this volume). These are discussed in more detail in the case study sections of this paper, and their locations are shown in Figure 2 and

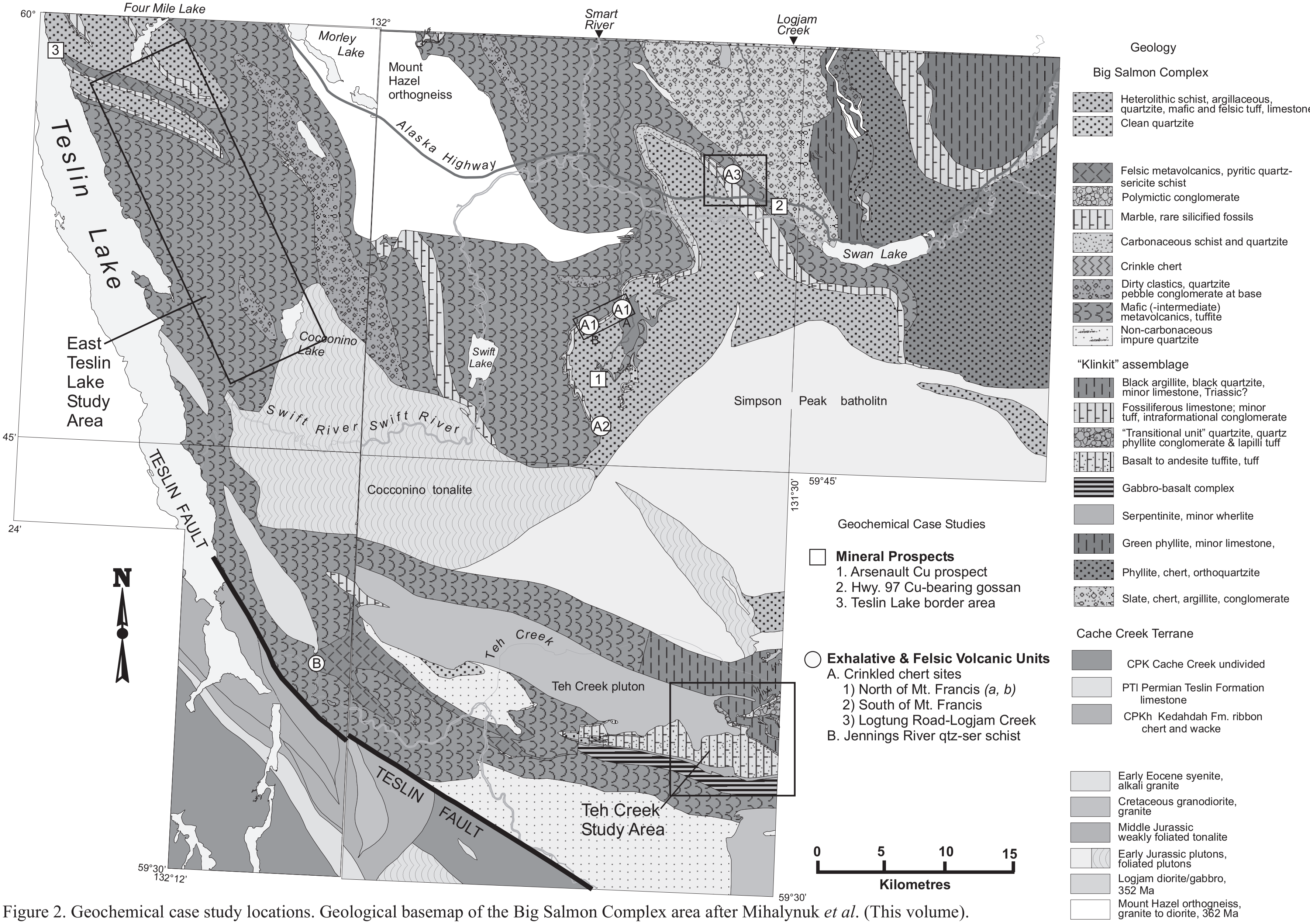

Figure 2. Geochemical case study locations. Geological basemap of the Big Salmon Complex area after Mihalynuk *et al*. (This volume).

on geochemical plot maps (Figures 4-6). For exploration purposes, Mihalynuk *et al.* (1998) suggested two stratigraphic intervals in the Big Salmon Complex as being most prospective for VMS-style mineralization: i) porphyritic blue quartz-eye dacite tuff similar to that at the Arsenault prospect, and ii) barium and manganese-bearing piedmontite schist of the crinkled chert unit, which is interpreted as partly exhalative in origin. Geochemical dispersal studies of the crinkled chert are an important component of this study.

RGS DATA RESULTS IN THE BIG SALMON COMPLEX AREA

The British Columbia Regional Geochemical Survey (RGS) program contains multi-element geochemical data for over 42 000 stream sediment sites covering approximately 65 per cent of the province. RGS stream sediment geochemical data is available for most of north-central and northwestern British Columbia, with the exception of the Dease Lake area (NTS 104J). RGS coverage is available for the Atlin (NTS 104N), Jennings River (NTS 104O) and McDame (NTS 104P) map areas, but is restricted to a small suite of trace elements such as copper, zinc and cobalt determined by atomic absorption spectroscopy (AAS). These are some of the earliest RGS surveys completed in the province. Samples were collected in 1977 and 1978 at a density of one site per 13 square kilometres, and the data was released in the following year (RGS, 1978, 1979). These results, and those of the adjoining Wolf Lake (NTS 105B) map area in the southern Yukon, were also presented graphically by the Geological Survey of Canada (NGR, 1981) as part of the 1:2 000 000 coloured compilation map series. The release of corresponding instrumental neutron activation analysis (INA) stream sediment data for gold, arsenic, antimony, rare earth and other elements in these three areas, reanalyzed by the British Columbia Geological Survey Branch as part of the RGS Archive Program, is scheduled for summer, 2000 (Jackaman *et al.*, this volume; Jackaman, in preparation). Data packages will include the earlier AAS data, and results for all elements will be graphically portrayed using drainage basin geochemical maps.

As part of this study, a subset of 252 stream sediment and 33 lake sediment RGS sites covering all or part of six 1:50 000 map areas east of Teslin Lake (104N/9, 16; 104O/11, 12, 13, 14) was selected for regional data interpretation in the Big Salmon Complex area. Summary statistics and boxplots for zinc, copper, lead, cobalt and additional elements are given in Table 1 and Figure 3, respectively. Geochemical maps showing the regional distribution of copper and zinc are shown in Figures 4 and 5. Numerous stream sediment sites have elevated geochemical signatures, not associated with known showings, which may reflect the presence of buried VMS mineralization. No subdivision of statistics on underlying geology is attempted, as new geological maps of the area are currently being prepared (Mihalynuk *et al.*, 2000) to replace that of Mihalynuk *et al.* (1996; Figures 4 through 6).

The following methods were used for preparation and analysis of RGS stream sediments and lake sediments in the Atlin (RGS, 1978) and Jennings River (RGS, 1979) map areas. Stream sediments were prepared in and analyzed by contract laboratories. They were air-dried, sieved through a -80 mesh (<177 microns) screen, and ball milled prior to analysis for zinc, copper, lead, nickel, cobalt, silver, manganese, iron and molybdenum by AAS following aqua regia digestion. Tin and mercury (NTS 104N only) were also determined with an AAS finish. Tungsten was determined colorimetrically following pyrosulfate fusion and dithiolcarbonate complexing, and uranium was determined by neutron activation. Analytical data for lake sediments, obtained from relatively low-lying areas of the Teslin Lake region in both Atlin and Jennings River map areas, is available for zinc, copper, lead, nickel, cobalt, silver, manganese, iron, molybdenum, mercury (104N only), tungsten and uranium. These were determined by the same methods outlined for stream sediments. In comparison to stream sediments, loss on ignition (LOI) data is available for lake sediments, whereas tin data is not. No INA data will be available for lake sediment sites. Water geochemical data for uranium, fluoride and pH is, however, available for both streams and lakes in these map areas.

Similar sample preparation and analytical methods permit results of older RGS surveys of the late 1970s to be compared to those conducted more recently, despite some minor differences in the element suites. For instance, no data is available in the Atlin and Jennings River areas for LOI in stream sediments, or for sulphate in waters. Tungsten, formerly determined colorimetrically, is now determined by INA. Arsenic and antimony were not determined in the earlier surveys, but are routinely included in both AAS and INA analytical suites. Regional stream sediment geochemical data is also available for adjoining areas of the southern Yukon as Geological Survey of Canada Open File reports, but these are not considered.

DESCRIPTION OF THE STUDY AREAS

Three types of geochemical case study investigations were conducted (Figure 1):

1) Watershed characterization of anomalous areas
2) Prospective felsic volcanic horizons and exhalative units (*e.g.* crinkled chert)
3) Mineral deposit or prospect case studies (*e.g.* Arsenault copper prospect)

Summary data for the number of samples of each of the various sample media collected over the case studies are given in Tables 2 and 3.

TABLE 1
SUMMARY STATISTICS FOR SELECTED ELEMENTS: RESULTS OF RGS STREAM AND LAKE SEDIMENT SURVEYS IN THE STUDY AREA, JENNINGS RIVER AND ATLIN MAP AREAS

Stream Sediments

	Cu (ppm)	Zn (ppm)	Pb (ppm)	Ag (ppm)	Co (ppm)	Fe (%)	Mn (ppm)	Mo (ppm)	Ni (ppm)	W (ppm)	pH
Median	**22**	**54**	**2**	**0.1**	**7**	**1.95**	**410**	**1**	**19.5**	**2**	**7.5**
Mean	29.5	61.7	3	0.13	8.1	2.08	670.7	2	21.6	3.6	7.4
± 1s	30.3	41.5	3.4	0.08	5.3	0.84	1845.2	2.7	15.3	9.5	0.50
Min	4	14	1	0.1	1	0.60	80	1	2	2	5.5
Max	295	475	26	0.7	57	9.10	28500	23	162	120	8.4
C.V.	1.025	0.672	1.109	0.667	0.657	0.402	2.751	1.326	0.705	2.639	0.067
N=sites	*252*	*252*	*252*	*252*	*252*	*252*	*252*	*252*	*252*	*252*	*252*

Lake Sediments

	Cu (ppm)	Zn (ppm)	Pb (ppm)	Ag (ppm)	Co (ppm)	Fe (%)	Mn (ppm)	Mo (ppm)	Ni (ppm)	W (ppm)	pH
Median	**52**	**84**	**2**	**0.1**	**11**	**2.65**	**525**	**8**	**46**	**2**	**8.0**
Mean	60	84.5	2	0.12	11.8	2.81	845.8	10.1	46.8	2	8.1
± 1s	29.4	28.4	1.5	0.07	6.8	1.54	1186.8	8.0	19.9	0	0.32
Minimum	16	22	1	0.1	1	0.30	165	2	12	2	7.3
Maximum	140	152	7	0.4	27	6.65	6550	43	104	2	8.5
C.V.	0.490	0.336	0.734	0.534	0.580	0.550	1.403	0.790	0.426	0.000	0.039
N=sites	*33*	*33*	*33*	*33*	*33*	*33*	*33*	*33*	*33*	*33*	*33*

Watershed Characterization Studies

Watershed characterization studies were conducted in two areas of the Big Salmon Complex with elevated RGS multi-element geochemical signatures: the East Teslin Lake area of the Nisutlin Plateau and the Teh Creek area of the Cassiar Mountains (Figures 1 and 2). They are investigations of the comparative geochemical responses, in several adjoining watersheds, of different types of drainage sediment and water samples in order to quantify differences in geochemical contrast. The two study areas are paired in that they have similar underlying geology but are located in very different physiographic environments. Similar projects to verify original RGS anomalies and identify possible metal sources have also been undertaken elsewhere in British Columbia (Cook *et al.*, 1992; Sibbick and Laurus, 1995; Cook, in preparation).

Area Selection

Element sum ranking of RGS data characteristic of volcanogenic massive sulphide (VMS) deposits was used to select the two areas. Briefly, the method used is as follows: zinc, copper, lead, silver, cobalt and iron data for both RGS stream sediment and lake sediment sites were independently summed using the following algorithm: Zn + Cu + (10*Pb) + (100*Ag) + Co + (10*Fe). Lead and iron results were multiplied by a factor of 10, and silver by 100, to bring all elements to equivalent orders of magnitude, as based on regional median concentrations. The resulting site scores for both streams and lakes were ranked and plotted (Figure 6), and two groups of adjoining watersheds in the upper five percentiles of combined data rankings selected for further study. Similar element combinations (Zn-Cu-Pb-Ag; Zn-Cu-Pb-Ag-Co) yielded comparable results. Neither of the two areas are known to host any VMS or related deposits, and no detailed geological mapping had been conducted here prior to 1997.

Field Methods

A variety of drainage sediment and stream water suites were sampled in each area. Original RGS stream sediment sites in each drainage were resampled, and several additional media including moss mats, bulk sieved (-18 mesh) sediments and moss mats, stream waters and suspended solids were also obtained at most sites. Some adjoining watersheds not included in the prior RGS surveys were incorporated into these studies. The water geochemical component in the two study areas, focusing on the suspended and dissolved loads in stream water, is the object of a B.Sc. Honours thesis by Pass (in preparation) at the University of Victoria.

a) East Teslin Lake Area (NTS 104N/16)

The study area is located in the Gladys River map area (NTS 104N/16) in the Nisutlin Plateau along the east shore of Teslin Lake, immediately south of the British Columbia-Yukon border (Photo 1). The approximately

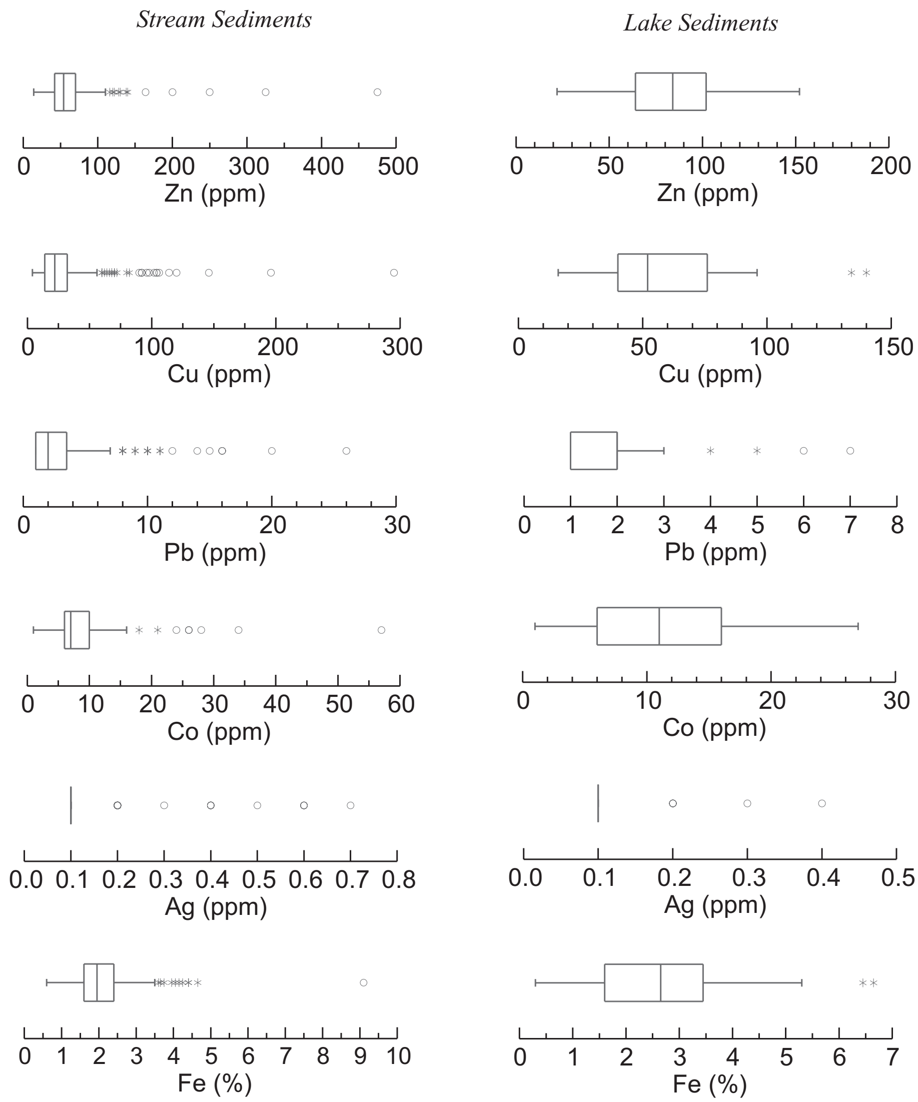

Figure 3. Boxplots showing distribution of zinc, copper, lead, cobalt, silver and iron (AAS) in RGS stream sediments (n=252 sites) and lake sediments (n=33 sites) in the study area. *See* Table 1 for summary statistics.

20 kilometre-long area is heavily drift-covered and extends from Four Mile Lake in the north to Coconino Lake in the south (Figure 2). The plateau area is characterized by rolling till-covered terrain (maximum elevation: 1485 metres) which drops steeply to the southwest within a few kilometres of Teslin Lake, where the adjacent flats (elevation: approximately 700-760 metres) are floored by post-glacial glaciolacustrine silts and till (Dixon-Warren and Hickin, 2000, in press). Numerous small streams drain into small lakes and wetlands in the low-lying base of slope area. The plateau area and wetlands are heavily forested with stands of white and black spruce, respectively. Bedrock geology of this region was mapped as predominantly Mississippian greenstone and chlorite schist by Aitken (1959) and Gabrielse (1969). Recent mapping at 1:50 000 scale (Mihalynuk *et al.*, 1998, in press) shows the area is underlain by mafic volcanic flows and tuffs such as greenstone and chlorite schist, with lesser meta-argillite and marble units, which strike in a northwesterly direction roughly parallel to Teslin Lake. Some felsic volcanics are in the northern part of the study area just south of the Yukon border.

RGS stream sediment geochemical data here between Four Mile and Coconino lakes exhibit an elevated copper-cobalt±iron±manganese trend which, for the most part, is within the upper five percentiles of data for most of these elements in the regional study area. Copper concentrations in three adjoining RGS streams here are in the range 90-114 ppm, approximately 4-5 times the regional median copper concentration (22 ppm). Furthermore, both Four Mile and Coconino Lakes, which bound these stream sediment sites to the north and south, contain elevated sediment Cu concentrations of 104 ppm and 140 ppm, respectively (Figure 4). Other, smaller lakes, in the low-lying area along Teslin Lake which receive drainage from the Nisutlin Plateau also exhibit locally high levels of copper in sediment. In particular, three small lakes northwest and southwest of Coconino Lake contain 54-90

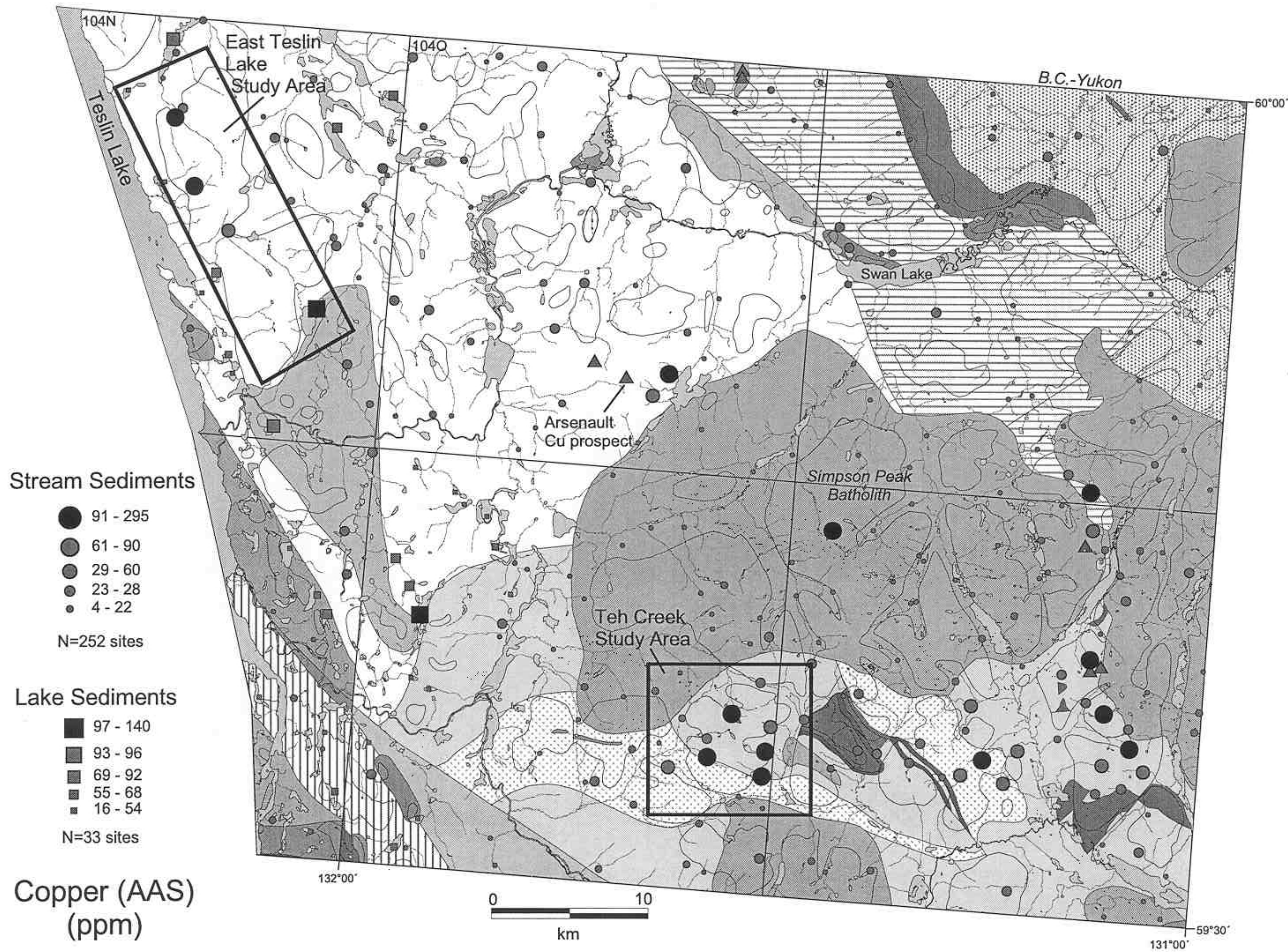

Figure 4. Distribution of copper (ppm) in RGS stream and lake sediments in the study area. Symbol sizes correspond, in each case, to upper limits of the 50th percentile, 70th percentile, 90th percentile, 95th percentile and top 5 percentiles as per standard RGS format. Locations of watershed characterization studies are outlined. Geology from Mihalynuk *et al.* (1996). Minfile locations are shown by triangles.

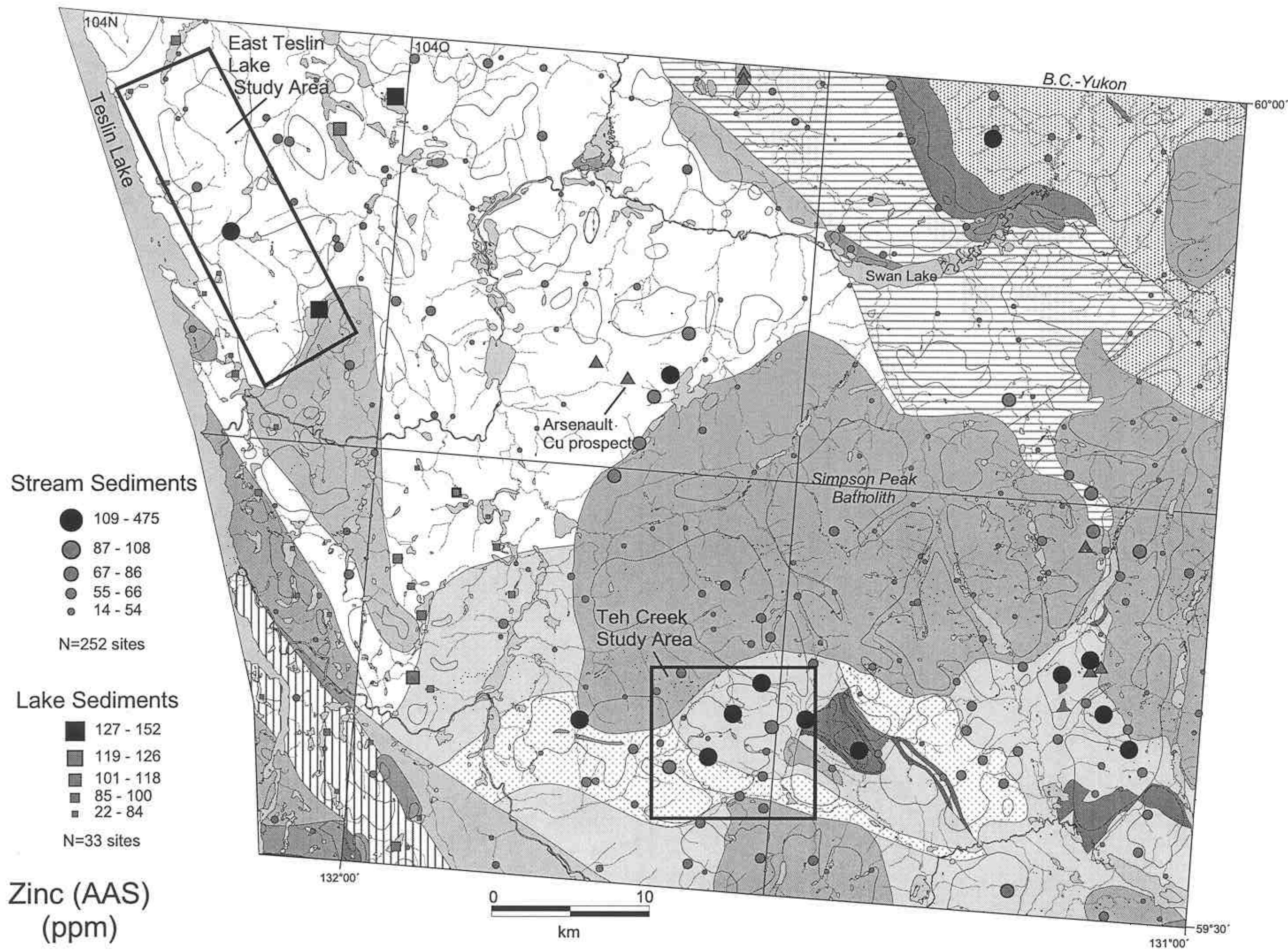

Figure 5. Distribution of zinc (ppm) in RGS stream and lake sediments in the study area. Geology from Mihalynuk *et al.* (1996). MINFILE locations are shown by triangles.

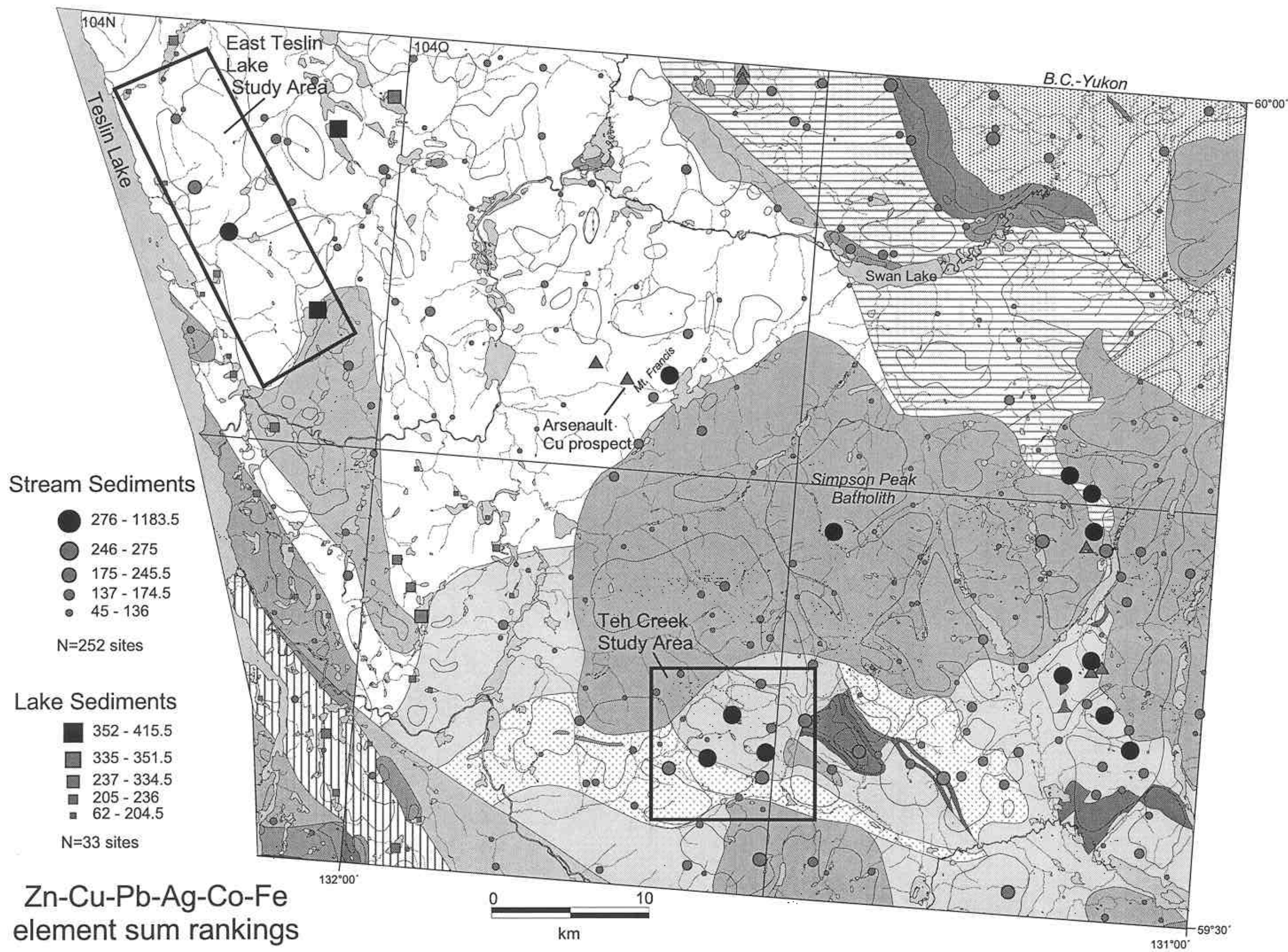

Figure 6. Distribution of Zn-Cu-Pb-Ag-Co-Fe element sum rankings for RGS stream and lake sediments in the study area. Geology from Mihalynuk *et al.* (1996). MINFILE locations are shown by triangles.

TABLE 2
SAMPLE SUMMARY MEDIA: 1999 GEOCHEMIAL STUDIES IN THE BIG SALMON COMPLEX

		Number of Sites **Watershed Studies**		**Stratigraphic Units**		**Cu Prospects**				
		Nisutlin Plateau	Teh Creek area	a	b	1	2	3	***Total Sites***	*Total Samples*
Routine Drainage	Stream sediments	9	10	4	-	4*	-	-	**27**	29
Sediments	Moss mats	8	3	3	-	4*	-	-	**18**	20
Sieved Drainage	Sieved stream sediments	4	7	3	-	2	-	-	**16**	16
Sediments	Bulk moss mats	5	-	-	-	-	-	-	**5**	5
Soil Profiles	*Total No. of Soil Profiles*	-	-	*12*	*2*	*2*	*1*	-	***17***	
	Mineral Soil Horizons**			18	4	4	1	-	**27**	29
	Underlying rock or rubble	-	-	4	-	2	1	-	**7**	7
Waters	RGS-Suite	9	10	5	-	6	-	-	**30**	34
	ICP-MS (cations only)	-	-	5	-	5	-	-	**10**	10
	ICP-MS full package	9	10	-	-	-	-	-	**19**	23
Vegetation	Bark	-	-	3	-	-	-	1	**4**	4
	Twigs	-	-	3	-	-	-	-	**3**	3
Rocks	Outcrop, till pit cobbles, etc.	3	4	8	1	1	2	3	**22**	22

a Crinkle chert localities (*see* Table 3)
b Jennings River qtz-ser schist

1 Arsenault Cu prospect
2 Hwy. 97 Cu prospect
3 Teslin lakeshore Cu prospect

* 6 sites total (sediments and waters)
** figures do not include underlying till samples of Dixon-Warren and Hickin (this volume)

TABLE 3
SAMPLE MEDIA SUMMARY: CRINKLED CHERT STUDY AREAS

		Number of Sites Each Study Area				
		1a	1b	2	3	*Totals*
Routine Drainage	Stream sediments	-	-	-	4*	4
Sediments	Moss mats	-	-	-	3*	3
Sieved Drainage	Sieved stream sediments	-	-	-	3	3
Sediments	Bulk moss mats	-	-	-	-	-
Soil Profiles	*Number of Soil Profiles*	*4*	*4*	*4*	-	*12*
	Mineral Soil Horizons**	5	8	5	-	18
	Underlying rock or rubble	4	-	-	-	4
Waters	RGS-Suite	-	-	-	5	5
	ICP-MS (cations only)	-	-	-	5	5
	ICP-MS full package	-	-	-	-	-
Vegetation	Bark	-	-	-	3	3
	Twigs	-	-	-	3	3
Rocks	Outcrop, till pit cobbles, etc.	1	3	1	3	8

Crinkled chert sites: 1a Mount Francis North (North Arsenault area)
1b Mount Francis North (North Arsenault area)
2 Mount Francis South, southwest of the Arsenault showing
3 Logtung Road-Logjam Creek area

* total of 5 sites
** figures do not include underlying till samples of Dixon-Warren and Hickin (this volume)

ppm copper in sediment. No RGS data were available, prior to this study, for the streams draining the adjacent plateau uplands here. In addition to the foregoing, elevated cobalt concentrations up to 16 ppm in stream sediments and 27 ppm in lake sediments are also present in this anomalous zone. Concentrations of other elements such as zinc, lead and silver which may be constituents of VMS deposits are generally lower. Only a single stream sediment site, for instance, contains elevated zinc up to 325 ppm. Nevertheless, combined Zn-Cu-Pb-Ag-Co-Fe element rankings (Figure 6) also show this trend.

Nine sites were sampled here in 1999. In addition to resampling original RGS sites, infill sampling was conducted north of, south of and between the three anomalous RGS creeks to better define anomalous watershed patterns and their relation to underlying geology. The pattern of elevated copper and other elements is largely restricted to westward or northward-draining watersheds, and background levels of copper in lake sediments, most of which are in the Teslin Lake area, are relatively high (median: 54 ppm) compared to other parts of British Columbia. RGS watersheds east of the plateau ridge axis contain much lower copper concentrations, up to about 36 ppm. No data for the background copper content of the greenstone unit is available.

b) Teh Creek Area (NTS 104O/11, 12)

The study area is located in a rugged area of the Cassiar Mountains (Photo 2), approximately 35 kilometres south of the Alaska Highway, along the border of the Klinkit Lake map area (NTS 104O/11) and another un-

Photo 1. View to the northwest of the Nisutlin Plateau and Teslin Lake, with Dawson Peaks in background.

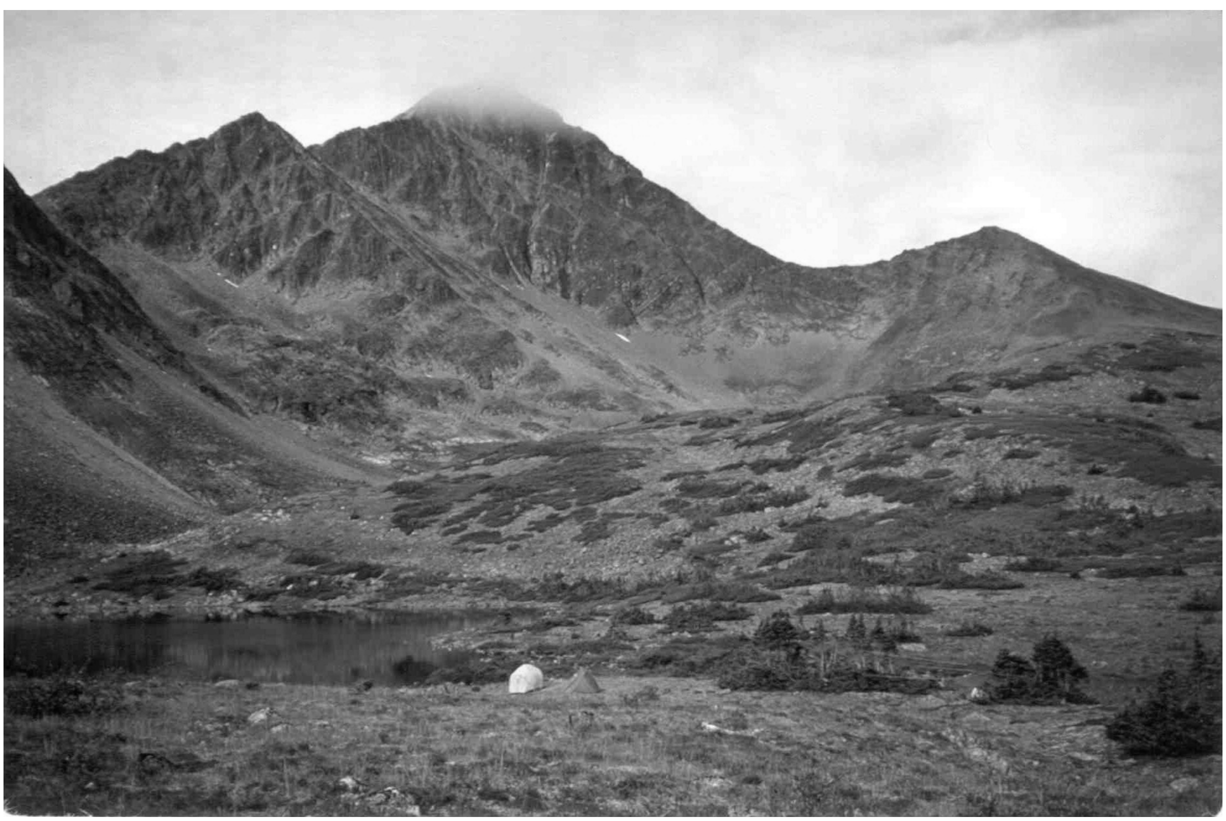

Photo 2. Fly camp in the Teh Creek area of the Cassiar Mountains.

named map area (NTS 104O/12). The area, approximately 7 kilometres by 7 kilometres, is centred on an unnamed mountain southeast of Teh Creek, a tributary of the Jennings River. The geological setting is similar to that of the East Teslin Lake area, but the physiographic setting is different. The area is characterized by steep, roughly east-west trending, ridges (maximum elevation: approximately 1900 metres) separated by tarn-filled cirques (elevation: 1400-1600 metres). Much of the area is above treeline. Extensive talus and colluvium deposits cover the lower slopes. Stream drainage from the cirques flows west and east into wide valleys and then to the Jennings River, in the latter case via Butsih and Klinkit creeks. Bedrock geology of the region, which is directly south of the southern contact of the Simpson Peak Batholith, was mapped as predominantly Carboniferous argillite, volcanic flows and tuffs by Gabrielse (1969). Recent detailed mapping (Mihalynuk *et al.*, 2000) indicates that the northern and central parts of the study area are mainly underlain by argillite and volcanic rocks, respectively, while the southern portion is underlain by newly-recognized gabbroic and ultramafic units.

RGS stream sediment geochemical data in the study area exhibit an elevated copper-cobalt-iron±zinc±nickel trend which is within the upper five percentiles of data for most of these elements in the regional study area. Copper concentrations in four of five adjoining RGS streams at the core of the study area (Figure 4) are in the range 104-196 ppm (regional 95th percentile: 90 ppm), approximately 5-10x the regional median copper concentration (22 ppm). Sediment cobalt concentrations in the same four streams are in the range 13-26 ppm (regional 95th percentile: 14 ppm), and are as high as 28 ppm in other adjoining watersheds. Nickel concentrations are also very high in the southern part of the study area, in the range 44-162 ppm (regional 95th percentile: 42 ppm) in three adjoining watersheds. The elevated nickel and, in part, cobalt content of RGS stream sediments in the south part of the study area are attributed to the serpentinized ultramafic and gabbroic rocks exposed here.

Ten sites were sampled in this area during 1999. The field study area is centred on the copper-cobalt RGS trend and does not encompass all of the anomalous area. Nevertheless two different, and somewhat weaker, element trends are also apparent in watersheds to the east of the immediate study area, neither of which was investigated in the field. First, several watersheds to the immediate northeast and east display elevated element signatures more typical of sedex environments, with elevated zinc concentrations in the range 120-200 ppm (regional 95th percentile: 108 ppm), and silver concentrations locally in the range 0.4-0.7 ppm. By comparison, 86 per cent of the sites in the study region have only 0.1 ppm silver. Secondly, several watersheds located about 10 kilometres east of the present study area contain elevated lead or moderately elevated copper concentrations. Elevated lead concentrations of 11-12 ppm (regional 95th percentile: 10 ppm) are present in two of the watersheds, while moderately elevated copper concentrations of 62-98 ppm occur in five adjacent watersheds. In the latter case, most copper concentrations are within the 90-95th percentile of the regional data set.

Combined Zn-Cu-Pb-Ag-Co-Fe element rankings (Figure 6) appear as a composite of the above copper-cobalt, zinc and copper trends for this area. These rankings are greatest in the core of the study area, where copper-cobalt levels are highest, and progressively decrease eastward in watersheds where zinc-silver, and then copper concentrations, predominate.

Felsic Volcanic and Exhalative Units Case Studies

Case studies were conducted at two horizons with potential for hosting polymetallic VMS deposits, the crinkled chert unit and a quartz-sericite schist unit exposed along the Jennings River.

a) Crinkled Chert (NTS 104O/13)

A unit of crinkled chert occurs widely throughout the northwestern part of the Big Salmon Complex (Mihalynuk, 2000, this volume). The crinkled chert, or crinkle quartzite as it is also known, forms a distinctive marker horizon 25 to 60 metres thick and has been interpreted to have an exhalative origin (Nelson, 1997). It was first described by Nelson (1997) and Mihalynuk *et al.* (1998), and the following description is from those accounts. The crinkled chert unit is white to pink-weathering, thinly-bedded to laminated, and contorted; it has been mapped as metachert, quartz-piedmontite-muscovite schist, and quartz-muscovite schist. It is resistant to weathering and is distinguished by a localized pink to red colour attributed to the presence of piedmontite, a manganese-epidote (Mihalynuk *et al.*, 1998). The most prominent exposures of the crinkled chert unit are in the Mount Hazel, Logjam Creek and Mt. Francis areas in the Smart River (NTS 104O/13) map area (Mihalynuk *et al*., 2000).

The crinkled chert unit was suggested by Mihalynuk *et al.* (1998) to be one of two Big Salmon Complex units most prospective for base metal massive sulphide exploration. An exposure of piedmontite-hematite metachert overlying metarhyolite (quartz-muscovite schist) on Hazel Ridge was reported by Nelson (1997) as analogous to chert iron formation (exhalite?) stratigraphy at the Wolverine deposit in the Yukon, where the mineralized horizon is above quartz-sericite schist and below chert-magnetite iron formation. To investigate surficial geochemical signature and response of these chert units in the Big Salmon Complex, geochemical orientation studies were conducted at three localities (Figure 2) in the Smart River (NTS 103O/13) area where the unit is exposed: i) north of Mt. Francis, ii) the southwest Mt. Francis area, and iii) the Logtung Road-Logjam Creek area. These studies involved mostly soil profiling at the first two sites, and stream sediment, water and vegetation sampling at the latter.

North of Mt. Francis

The study site is located on two small knobs, approximately 2 kilometres apart, situated about 3 kilometres north of the Arsenault property and about 9 kilometres south of the Swift River and the Alaska Highway. A total of eight soil profiles were obtained from the vicinity of crinkled chert exposures here (Mihalynuk, 2000), four on the eastern knob and four on the western knob. Thin colluvial soils and additional tills were also sampled at several locations at the western site (Dixon-Warren and Hickin, this volume).

Southwest Mt. Francis

The study site is situated on a small knob of a ridge on the southwest flank of Mt. Francis, approximately 8 kilometres southeast of Swift Lake. It forms the southernmost segment of a continuous band of crinkled chert mapped by Mihalynuk *et al.* (2000). Thin, mostly colluvial soils were sampled at four profile sites above this unit.

Logtung Road-Logjam Creek area

The study site is located adjacent to the Logtung deposit access road, west of Swan Lake, which joins the Alaska Highway about 3 kilometres west of Logjam Creek. The most comprehensive crinkled chert study was conducted here, where the unit is exposed on either side of the Logtung Road approximately 2.6 kilometres north of the highway. Rock samples were obtained from exposures east and west of the road, and outer bark and twigs of lodgepole pine (*Pinus contorta*) at both localities were also sampled. Outcrop, bark and twig samples were also obtained from a quartzite exposure just west of the 1.2 kilometre point on the Logtung road. Stream sediment and/or water samples were obtained at five sites in the area. Samples were collected from a small eastward-flowing stream draining the immediate area of the crinkled chert exposure, and at its confluence with Logjam Creek about 1.5 kilometres to the east. Sediments and waters were also obtained from Logjam Creek, just upstream of the Alaska Highway, and from an unnamed creek about 4 kilometres west of the Logtung road, opposite the intersection of the Arsenault access road with the highway. This stream catchment area overlies the same crinkled chert unit on the western limb of a regional fold (Mihalynuk *et al.,* 2000).

b) Jennings River quartz-sericite schist (NTS 104N/09)

An exposure of quartz-sericite schist was examined on the north side of the Jennings River, about 4 kilometres east of Teslin Lake. Bedrock here is overlain by till and glaciolacustrine sediments which are exposed on the river bank. Ice flow here is from southeast to northwest (Dixon-Warren and Hickin, this volume). Two till profiles and two soil profiles were sampled above, and down ice of, this exposure, respectively.

Mineral Prospect Case Studies

Case studies were conducted at three potential mineral prospects in the Big Salmon Complex, the Arsenault copper prospect and two lesser showings described by Mihalynuk *et al.* (1998), the Highway 97 copper-bearing gossan and the Teslin lakeshore altered tuff.

a) Arsenault copper prospect (NTS 104O/13; MINFILE 104O 011)

Stream sediments, waters and soil profiles were sampled in several areas near the Arsenault copper prospect (Photo 3), the best-explored mineral prospect in the Big Salmon Complex of British Columbia. The Arsenault prospect (elevation: approximately 1440 metres) is located about 12 kilometres south of the Alaska Highway and 7 kilometres east of Swift Lake (Figure 2). The prospect was discovered in the 1940's and has been described in several assessment reports (*e.g.* Turnbull and Simpson, 1970; Sawyer, 1967, 1979; Phendler, 1982). It consists of stratabound disseminated to layered chalcopyrite, pyrrhotite and pyrite in complexly-deformed amphibolite-grade chlorite-actinolite schist. The mineral assemblage is skarn-like, but no significant plutonic bodies are exposed, and the prospect has been interpreted as initially volcanogenic in origin (Sawyer, 1979; Phendler, 1982; Traynor, 1999). More recent exploration work (Traynor, 1999) has focused on VMS potential of metasedimentary and metavolcanic rocks exposed on the central ridge of the property. Another prospect, the Arsenault East (MINFILE 104O 047), is located on the east slope of Mt. Francis and consists of a 10 metre-long chalcopyrite-bearing vein replacement zone developed in limestone. Mihalynuk *et al*. (1998) interpreted it as occurring in about the same 100 metre stratigraphic interval as the Arsenault prospect; chip sampling across the 2.5 metre width of the skarn-like zone returned copper, zinc and cobalt concentrations of 4.6 per cent, 0.3 per cent and 322 ppm, respectively.

Extensive soil sampling on the Arsenault property (Sawyer, 1967; Turnbull and Simpson, 1970) identified zones of elevated copper concentrations up to 3620 ppm (Figure 5 of Dixon-Warren and Hickin, this volume). In addition, several RGS sites in streams on the eastern and northern flanks of Mt. Francis have elevated copper, zinc or copper-zinc concentrations (Figures 4 and 5). For example, elevated copper concentrations of 70-104 ppm (95^{th} percentile: 90 ppm) are present in two streams draining the eastern flank of Mt. Francis. Elevated zinc concentrations here are more widely distributed, with four sites draining the eastern and northern flanks of the ridge with 100-130 ppm (95^{th} percentile: 108 ppm).

Six additional stream sediment and water sites were sampled in the Mt. Francis area during 1999 to supplement available RGS stream sediment data, including one site which was re-sampled. Four sites were sampled on the eastern flank of Mt. Francis, infilling areas between anomalous RGS streams and encompassing stream drainage from the Arsenault East prospect. Two sites were

Photo 3. Excavating soil profile 2 in a trench at the Arsenault copper prospect.

sampled to the west in intermittent streams draining the area of Arsenault mineralization, where two colluvial soils were profiled in old exploration trenches. Sediment and water geochemical data for this area will be reported at a later date.

b) Highway 97 Copper-bearing Gossan (NTS 104O/13; MINFILE 104O 054)

One soil profile and six till sites were sampled above a copper-bearing gossan exposed along the Alaska Highway (Highway 97) about 3.5 kilometres west of Swan Lake. Tills and soils were sampled north and south of the highway in conjunction with Dixon-Warren and Hickin (this volume) to test the dispersal, if any, of mineralized material from this site. The presence of chalcopyrite-bearing veins in Big Salmon Complex greenstone here was first reported here by Mihalynuk *et al*. (1998), and the following summary is taken from that account. Several north-northwest trending quartz-chlorite-magnetite-pyrite-chalcopyrite veins (maximum thickness: 30 centimetres) occur in a 3 metre wide gossanous zone in the Big Salmon Complex greenstone unit. Mihalynuk *et al.* (1998) reported chip samples taken over a 1.5 metre interval of 80 per cent vein material to contain 0.2 per cent copper, 165 ppm cobalt, 210 ppm arsenic and 45 ppm tungsten.

c) Teslin Lake border area (NTS 104N/16; MINFILE 104N 135)

Limited geochemical sampling was conducted at the Teslin Lake border area occurrence to investigate the distribution of copper and other elements here. The occurrence was described by Mihalynuk *et al.* (1998). It comprises a series of copper-bearing pyritic gossan zones in phyllitic to schistose mafic to felsic tuffaceous rocks, quartz-sericite schists and siltstones which are exposed over approximately one kilometre along the east shore of Teslin Lake. Individual gossanous layers are strongly pyritic (up to 10 per cent), with trace chalcopyrite occurring as clots and stringers. Mihalynuk *et al.* (1998) reported that a single grab sample returned 2.2 per cent copper and 28 ppm silver, but upon repeat sampling equally cupiferous zones could not be located.

No soil profiles or tills were developed or are present over the occurrences, and no active stream drainages occur here. Geochemical sampling was restricted to the outer bark of a single gnarled lodgepole pine (*Pinus contorta*) growing on pyritic bedrock, and to sampling gossanous bedrock.

FIELD SAMPLING, PREPARATION AND ANALYTICAL METHODS

A brief description of field sampling, preparation and analytical methods for various sample media is given below:

Soil Profiles

A total of 17 soil profiles were sampled, mostly near exposures of the crinkled chert unit, to determine the relative distribution of trace elements among various soil horizons. In all, samples were obtained from 27 mineral soil horizons and 7 underlying bedrock or rubble levels (Table 1). Till samples, if present at any given site, were in most cases collected and data reported for by Dixon-Warren and Hickin (this volume) as part of surficial geological studies of the Big Salmon Complex area. Soils in many areas here, particularly those of greater relief, are thin and relatively juvenile due to colluvial movement. Many soil profiles comprise just a thin veneer of colluvium above bedrock.

Soil horizons at profile sites were sampled from pits, or from excavations in trench walls (*e.g.* Arsenault prospect; Photo 3). Horizons were sampled from the bottom up to avoid cross-contamination. Preparation and analytical procedures are identical to those of till samples (Dixon-Warren and Hickin, this volume). Sample preparation was conducted at Intertek Testing Services-Bondar Clegg, North Vancouver. Samples were air-dried and split into two equal parts. One half was archived. The second half was disaggregated and sieved through a -230 mesh (<63 micron) stainless steel sieve until sufficient material was obtained for analysis. Two splits of each sample were taken. One 10 gram split was submitted to Acme Analytical Laboratories Ltd., Vancouver, for two analytical suites: i) analysis of trace elements including zinc, copper, lead, silver, molybdenum, cobalt, iron, manganese and nickel (Table 5) by inductively coupled plasma-mass spectrometry (ICP-MS) and inductively coupled plasma-emission spectroscopy (ICP-ES) techniques following aqua regia digestion, and ii) determination of major element oxides by lithium metaborate ($LiBO_2$) fusion and an ICP-ES finish (Table 7). Loss on ignition (LOI), total carbon and total sulphur were also determined. A second, approximately 30 gram, split of each sample was submitted to Activation Laboratories, Ancaster, Ontario, for analysis of gold and 34 additional elements using thermal instrumental neutron activation analysis (INA). Data for 29 elements (gold, antimony, arsenic, barium, bromine, calcium, cerium, cesium, chromium, cobalt, europium, hafnium, iron, lanthanum, lutetium, molybdenum, neodymium, rubidium, samarium, scandium, selenium, sodium, tantalum, terbium, thorium, tungsten, uranium, ytterbium and zinc) are reported here in Table 6. Data for six other elements (silver, mercury, irridium, nickel, tin and strontium) are not reported due to inadequate detection limits, low element abundance and/or poor precision.

Stream Sediments and Moss Mats

Collection, preparation and analysis of stream sediment and moss mat samples was conducted to the standards of the British Columbia RGS program. Field duplicate samples were obtained in each block of 20 samples. Preparation of sediment and moss mat samples was done at Rossbacher Laboratory, Burnaby, using standard RGS procedures. Stream sediments were air-dried (<35°C) and dry sieved to -80 mesh (< 177 microns) using stainless steel sieves. In preparation of moss mat samples (*e.g.* Gravel and Matysek, 1989), fine sediment is disaggregated from the moss fronds in a ceramic mortar, and passed through a -18 mesh (<1 millimetre) sieve prior to sieving to -80 mesh (<177 microns). Two splits of each sample were taken. One split was submitted to Acme Analytical Laboratories Ltd., Vancouver, for analysis of a suite of trace elements including zinc, copper, lead, silver, molybdenum, cobalt and iron by inductively coupled plasma-mass spectrometry (ICP-MS) and inductively coupled plasma-emission spectroscopy (ICP-ES) techniques following aqua regia digestion. Gold is also determined directly by ICP-MS on the 1 gram sample used in this procedure; depending on sample mineralogy, not all of the gold may be released by the acid. Loss on ignition (LOI) was also determined. A second, approximately 30 gram, split of each sample was submitted to Activation Laboratories, Ancaster, Ontario, for total analysis of gold and 34 additional elements using thermal instrumental neutron activation analysis (INA). Analytical results for stream sediments and moss mats are not included in this paper, and will be released at a later date.

Bulk Drainage Sediments

Bulk stream sediment and moss mat samples were obtained, where possible, to aid in speciation of elements of interest (*e.g.* copper, zinc, barium, manganese) with respect to size and density fractions of the sediment, and to compare results between these two varieties of drainage sediment and routine -80 mesh sediments. Bulk sediments were obtained in the field by wet-sieving sediment material through a Nalgene -18 mesh (<1 millimetre) nylon sieve until a several-kilogram sample was obtained. Owing to the practical difficulties in attempting to wet-sieve fine-grained moss mat material in the field, a bulk moss mat sample was instead collected at these sites, where possible.

Sieved stream sediments were air-dried at the Analytical Science Laboratory of the Geological Survey Branch, Victoria, disaggregated, and mechanically dry-sieved to 5 size fractions (-10+40, -40+80, -80+140, -140+230 and -230 mesh). In the case of bulk moss mats, samples were transferred to large paper bags and air-dried in Victoria, and then submitted to Rossbacher Laboratory, Burnaby, for disaggregation and dry sieving to -18 mesh (<1 millimetre) using a nylon sieve. Prepared samples were returned to Victoria for size-fraction sieving, as above.

In both cases, the resulting sediment and moss mat size fractions were weighed, and representative splits submitted to Acme Analytical Laboratories Ltd., Vancouver, and Activation Laboratories, Ancaster, Ontario for analysis of trace and precious metals corresponding to those of sediments and moss mats outlined in the previous section. In addition, heavy mineral concentrates (HMC) will be prepared from some size fractions using heavy liquid techniques to separate any particulate barite and sulphide grains which may be associated with nearby VMS mineralization.

Stream Waters

At least two paired water samples were obtained at each stream site using high-density polyethylene (HDPE) bottles: i) a raw water sample (250 millilitre) similar to that routinely collected during RGS surveys, and ii) a filtered (45 millimetre, cellulose filter) and acidified water sample (125 millilitre) for major element and trace element analysis. All samples were kept in coolers for preservation. Unfiltered raw stream water samples were not subjected to any additional preparation procedures, and were analyzed for the standard RGS water analytical suite (uranium, fluoride, sulphate, pH) at CanTech Laboratories, Inc., Calgary. An aliquot of unfiltered water was retained for determination of conductivity and total dissolved solids (TDS) using a Corning Checkmate 90 conductivity/TDS meter.

In addition to the foregoing, sampling for anions, cations, dissolved mercury, particulate organic carbon and suspended solids (trace metals) were also conducted as part of watershed characterization studies in the Teslin Lake and Teh Creek areas (Photo 4). These sites are the study of a B.Sc. thesis at the University of Victoria on the geochemistry of dissolved, suspended and bed loads in streams by the junior author (Pass, in preparation). Collection and preparation methods used for these samples, which comprise the majority of stream water sites, are those of Telmer (1997) and are summarized below:

Trace Metals in Suspended load / Stream Water Cations, Anions and Dissolved Mercury

Stream waters at depth were collected in a one litre Nalgene HDPE bottle, and filtered to 0.45 microns using vinyl filter paper (47 millimetre Millipore, HV Filter type) in a Swinnex 47 millimetre filter holder with a 50 millilitre plastic rubber-less syringe. Samples were filtered into a 125 millilitre HDPE bottle for a cation sample, a second 125 millilitre HDPE bottle for an anion sample, and into a 50 millilitre Fisher Brand disposable centrifuge tube for the dissolved mercury sample. Dissolved mercury is defined as all BrCl-oxidizable mercury forms and species in the filtrate of an aqueous solution that has been filtered through a 0.45 micron filter (EPA, 1999). Up to approximately one litre of additional water was filtered, but not retained (exact volume recorded), for the collection of sufficient suspended solid matter for trace metal analysis. The syringe type used was specially chosen as it lacked the black rubber plunger tip, common to most syringes, that could be a source of zinc contamination. Similarly, vinyl filter papers were used here as they are less likely to absorb the dissolved load, have a more repeatable tare and are resistant to acid digestion during analysis (K. Telmer, personal communication, 1999).

The syringe and collection bottle were rinsed three times in stream water prior to use. Cation and anion sam-

Photo 4. Water sampling in the Teh Creek area, Cassiar Mountains.

ple bottles were transported into the field containing deionized water and were only opened and emptied once sampling began on site. These bottles were then rinsed three times with an aliquot of filtered water before sample collection. Prior to placing the filter paper into the filter holder, the latter and a pair of tweezers were generously rinsed with deionized water and the filter paper placed into the holder with tweezers. Subsequent to sampling, the filter paper was removed from the filter holder, using tweezers, and stored in a watertight HDPE scintillation vial (ESBE Scientific, 6.5 millilitre) for storage. After filtration, cation samples were acidified with 0.5 millilitre of Seastar Chemicals concentrated ultra pure nitric acid (HNO_3) at base camp that evening. Filtered water for mercury samples were added to centrifuge tubes containing 0.5 millilitres of bromium chloride (BrCl) (EPA, 1999), added each morning from a stock bottle using a Brinkmann Eppendorf repeater pipette with disposable tip. All samples were kept in a cooler following collection. Solution samples of cations, minor elements, rare earth elements and some major elements, as well as digested suspended solids, were analyzed using a VG Plasmaquad 2S ICP-MS. Dissolved anions and major cations were analyzed using a Dionex DX-120 liquid chromatograph (Isocratic), with a AS-14 ion separation column. Dissolved mercury was analyzed using a Perkin Elmer 50A Mercury Analyzer System (cold vapor flameless atomic absorption). The junior author conducted all analyses at the University of Victoria.

To minimize contamination and maintain sample purity, two bottles of nitric acid and bromium chloride were taken to the field. One set of chemicals was used for the Teslin Lake study area and individual case studies, and the other set for the Teh Creek study area. Chemicals were kept in a separate cooler for storage. Deionized water was transported to the field from the University of Victoria in two ten gallon Nalgene carboys and dispensed as needed into Nalgene LDPE squeeze bottles for daily fieldwork. New syringes and one-litre collection bottles were used as often as possible. To further minimize any potential contamination during transportation and storage, the entire suite of up to 6 samples types were packaged into a large watertight Whirlpak bag at each sampling site.

Particulate Organic Carbon (POC) in the Suspended Load

Stream waters were collected at depth in a one litre Nalgene HDPE bottle in the exact position of the stream in which the above-mentioned trace metal, cation, anion and dissolved mercury samples were collected. The syringe was rinsed three times with stream water before sampling began, while the collection bottle was rinsed three times with steam water before and between samplings. For these samples a 60 millilitre VWR plastic syringe with black rubber plunger tip was used, as these syringes are easier to use and the samples were not analyzed for metal content. Glass fiber filter papers (0.45 micron, 47 millimetre, Millipore Brand) were inserted into the Swinnex 47 millimetre filter holder, pre-rinsed with deionized water, using similarly-rinsed tweezers. Stream water was filtered, although not retained, up to a volume of about one litre (exact volume recorded). Deionized water-rinsed tweezers were then used to place the filter into a watertight HDPE scintillation vial (ESBE Scientific, 6.5millilitre) for storage. The sample was then placed into a watertight Whirlpak bag with the other site samples.

Vegetation

A small number of vegetation samples were obtained, primarily near exposures of the crinkled chert unit along Logtung Road. In all, outer bark and twigs of lodgepole pine (*Pinus contorta*) were obtained at four and three sites, respectively. Sampling procedures were consistent with those of Dunn (1995, 1999). Outer bark samples were collected by vertically scraping the back of hand-held pruning snips along the bark, with the sample collected in a small paper bag held beneath. Twig samples were obtained by snipping about 30-40 centimetres of recent growth from the ends of tree branches, and collected in large paper grocery bags.

Vegetation samples were dried and then ashed at 470^0-500^0C for 24 hours at the Geological Survey of Canada, Ottawa, using a Duncan pottery kiln. Needles were separated from the twigs and ashed separately. Ashed bark, twig and needle samples were submitted to Acme Analytical Laboratories Ltd., Vancouver for analysis of trace and precious elements by ICP-MS/ES techniques as outlined above for sediments and soils. Data will be reported at a later date.

Rocks

No systematic lithogeochemical studies were attempted by the authors, but a small number of outcrop grab samples, stream bed float and till pit cobbles were collected and analyzed for trace and precious elements. Rock samples were split into two bags. One was archived for later reference; the second was crushed and pulverized in the Geological Survey Branch Laboratory, Victoria using a jaw crusher and steel ring mill, respectively. One 10 gram split was submitted to Acme Analytical Laboratories Ltd., Vancouver, for trace element determination by inductively coupled plasma-mass spectrometry (ICP-MS) and inductively coupled plasma-emission spectroscopy (ICP-ES) techniques following aqua regia digestion. A second sample split (30 gram) was submitted to Activation Laboratories, Ancaster, Ontario for INA determination of gold and additional elements. No major element oxide determinations were conducted. Selected ICP and INA rock geochemical data for crinkled chert samples only are given in Table 4.

TABLE 4
SELECTED ROCK GEOCHEMICAL DATA: CRINKLED CHERT

INA

Cr. Chert Study Locality	Field Number	Description	UTM Zone	UTME Nad83	UTMN Nad83	Au (ppb) INA	Au2* (ppb) INA	As (ppm) INA	Ba (ppm) INA	Co (ppm) INA	Cr (ppm) INA	Fe % INA	Na % INA	Rb (ppm) INA	Sb (ppm) INA	Sc (ppm) INA	Th (ppm) INA	U (ppm) INA	W (ppm) INA	La (ppm) INA	Ce (ppm) INA	Nd (ppm) INA	Sm (ppm) INA	Eu (ppm) INA	Tb (ppm) INA	Yb (ppm) INA	Lu (ppm) INA	Mass g
1b	99-SJC-13	till pit cobble**	9	346227	6636128	172	325	9.7	2900	16	196	1.31	0.07	37	0.6	8.6	2.3	0.5	1	6.8	24	7	1.6	0.4	0.5	0.7	0.10	37.63
1b	99-SJC-14	outcrop	9	346245	6636140	1	-	6.9	19000	11	122	0.96	0.07	28	6.5	4.3	1.6	2.3	1	4.8	21	16	0.8	0.2	0.5	0.4	0.07	37.30
	99-SJC-14	*Analytical dup.*				*1*	-	*6.0*	*16000*	*10*	*241*	*0.97*	*0.06*	*21*	*5.3*	*4.0*	*1.6*	*2.3*	*1*	*4.4*	*20*	*12*	*0.8*	*0.2*	*0.5*	*0.3*	*0.06*	*39.43*
1b	99-SJC-15	outcrop	9	346250	6636140	1	-	1.2	2100	5	249	0.54	0.05	21	0.1	2.0	0.5	0.5	1	1.0	4	5	0.2	0.2	0.5	0.2	0.05	35.99
2	99-SJC-11	outcrop	9	347106	6629383	1	-	52.1	2100	39	248	2.06	0.22	30	3.6	11.2	3.6	0.7	1	13.7	41	12	3.0	0.8	0.5	1.8	0.27	33.53
3	99-SJC-16	outcrop	9	355750	6645900	1	-	1.6	1600	21	173	1.61	0.12	56	0.7	9.1	2.9	0.5	1	11.5	36	10	2.3	0.6	0.5	1.2	0.17	34.48
3	99-SJC-17	outcrop	9	355600	6646000	1	-	2.2	2700	22	164	1.69	0.06	44	0.9	8.9	2.8	0.5	1	5.2	24	5	1.2	0.3	0.5	1.2	0.20	35.81

ICP-MS

Study Locality	Field Number	Description		UTME Nad83	UTMN Nad83	Mo (ppm) ICPMS	Cu (ppm) ICPMS	Pb (ppm) ICPMS	Zn (ppm) ICPMS	Ag (ppb) ICPMS	Ni (ppm) ICPMS	Co (ppm) ICPMS	Mn (ppm) ICPMS	Fe (%) ICPMS	As (ppm) ICPMS	U (ppm) ICPMS	Au (ppb) ICPMS	Th (ppm) ICPMS	Sr (ppm) ICPMS	Cd (ppm) ICPMS	Sb (ppm) ICPMS	Bi (ppm) ICPMS	V (ppm) ICPMS
1b	99-SJC-13	till pit cobble**	9	346227	6636128	0.08	30.81	1.49	19.5	2	34.4	9.2	708	0.39	8.2	0.1	1	0.4	19.3	0.01	0.02	0.02	2
1b	99-SJC-14	outcrop	9	346245	6636140	0.06	16.35	7.07	7.9	2	8.7	4.1	853	0.20	6.3	2.0	1	0.9	57.5	0.01	0.4	0.11	2
	99-SJC-14	*Analytical dup.*				*0.15*	*20.71*	*7.56*	*11.6*	*2*	*13.8*	*5.5*	*900*	*0.33*	*5.4*	*2.2*	*2*	*0.9*	*73.3*	*0.01*	*0.43*	*0.12*	*2*
1b	99-SJC-15	outcrop	9	346250	6636140	0.09	11.71	0.56	6.2	2	10.7	2.5	218	0.22	1.0	0.1	1	0.1	18.7	0.01	0.02	0.02	2
2	99-SJC-11	outcrop	9	347106	6629383	0.17	119.9	5.94	45.1	5	51.7	21.7	2595	0.70	22.1	0.6	1	0.8	44.2	0.03	2.38	0.06	13
3	99-SJC-16	outcrop	9	355750	6645900	0.08	0.87	1.6	36.3	2	31.7	15.0	515	0.64	0.7	0.1	7	1	7.7	0.01	0.32	0.03	7
3	99-SJC-17	outcrop	9	355600	6646000	0.08	4.82	1.82	42.3	5	33.8	17.6	612	0.75	1.1	0.1	1	1.6	34.6	0.02	0.35	0.05	5

Study Locality	Field Number	Description		UTME Nad83	UTMN Nad83	Ca (%) ICPMS	P (%) ICPMS	La (ppm) ICPMS	Cr (ppm) ICPMS	Mg (%) ICPMS	Ba (ppm) ICPMS	Ti (%) ICPMS	B (ppm) ICPMS	Al (%) ICPMS	Na (%) ICPMS	K (%) ICPMS	W (ppm) ICPMS	Tl (ppm) ICPMS	Hg (ppb) ICPMS	Se (ppm) ICPMS	Te (ppm) ICPMS	Ga (ppm) ICPMS	S (%) ICPMS
1b	99-SJC-13	till pit cobble**	9	346227	6636128	0.04	0.01	1.2	104.2	0.28	1057.7	0.005	1	0.38	0.008	0.13	0.2	0.04	5	0.1	0.02	1.6	0.01
1b	99-SJC-14	outcrop	9	346245	6636140	0.02	0.006	3.0	59.7	0.10	2648.7	0.003	1	0.14	0.004	0.06	0.2	0.02	5	0.1	0.02	0.6	0.04
	99-SJC-14	*Analytical dup.*				*0.01*	*0.006*	*2.7*	*128.6*	*0.15*	*2719.5*	*0.005*	*1*	*0.26*	*0.009*	*0.11*	*0.2*	*0.04*	*5*	*0.1*	*0.02*	*1.2*	*0.04*
1b	99-SJC-15	outcrop	9	346250	6636140	0.01	0.003	0.5	134.3	0.08	1076.1	0.002	1	0.19	0.007	0.10	0.2	0.03	5	0.1	0.02	0.8	0.06
2	99-SJC-11	outcrop	9	347106	6629383	0.17	0.011	2.8	121.0	0.33	1068.9	0.073	1	0.39	0.009	0.17	0.2	0.09	5	0.1	0.02	3.0	0.03
3	99-SJC-16	outcrop	9	355750	6645900	0.06	0.01	3.7	85.7	0.37	299.1	0.03	1	0.48	0.007	0.19	0.2	0.04	5	0.1	0.02	2.1	0.01
3	99-SJC-17	outcrop	9	355600	6646000	0.05	0.013	1.8	86.4	0.44	1369.1	0.019	1	0.49	0.004	0.12	0.2	0.02	15	0.1	0.02	2.3	0.04

* Au2 determined from a different split of the original pulverized sample pulp, using the same laboratory

** pit cobble sampled from soil profile 1 at this study area. Site corresponds to till sample 996046 of Dixon-Warren and Hickin (this volume)

QUALITY CONTROL PROCEDURES AND RESULTS

Field and analytical duplicate samples were included in the various sediment, soil, water and other analytical suites, along with control reference standards containing appropriate concentration ranges of copper, zinc and other base metals. In the water studies, field blank samples were taken using distilled water to monitor for potential contamination during sampling (Pass, in preparation). Only those results for soil profile and rock analytical suites are discussed here. Refer to Dixon-Warren and Hickin (this volume) for duplicate and triplicate results of associated C horizon till samples.

In the case of soil profiles, field duplicate results, denoted as Rep '10' (original) and Rep '20' (duplicate) samples in Tables 5-7, indicate acceptable levels of combined field, preparatory and analytical precision. For example, two field duplicate pairs returned copper concentrations of i) 1370.2/1258.9 ppm in a colluvial Bm horizon soil at the Arsenault prospect, and ii) 50.3/41.9 ppm in an Ah horizon at crinkled chert locality 1b, indicating that precision is acceptable at both the upper and lower ends of the concentration range. INA barium results for the same two field duplicate pairs are 160/220 ppm and 910/970 ppm, respectively. Interestingly, comparatively elevated and precise INA gold concentrations are also present in these two sample pairs, at 29/23 ppb and 16/20 ppb, respectively.

Results for two analytical duplicate pairs in soils (Tables 5-7) also show acceptable precision. Precision of analytical duplicate results is typically greater than that obtained for field duplicates because they are a measure of analytical precision only. To illustrate, coefficient of variation (CV) between analytical duplicates from the same high-copper soil horizon at the Arsenault prospect (996507) is just 0.8 per cent, compared to 6.0 per cent between the field duplicates mentioned above. Similar results occur for cobalt, manganese, arsenic, gold, molybdenum and numerous other elements, particularly for the aqua regia-ICP suite (Table 5). In the case of rocks (Table 4), a crinkled chert sample (99-SJC-14) from the North Mt. Francis area reported 19000 ppm barium (INA) versus 16000 ppm in a duplicate taken from the crushed field sample. The crinkled chert also returned concentrations of 853 ppm manganese (duplicate: 900 ppm), 11 ppm cobalt (duplicate: 10 ppm) and 6.5 ppm antimony (duplicate: 5.3 ppm).

Insertions of a CANMET certified reference material, soil standard SO-2, and of two internal Geological Survey Branch standards indicate acceptable levels of analytical accuracy for relevant elements in soils. To illustrate, a single insertion of SO-2 returned an INA barium concentration of 870 ppm, marginally lower than the certified value of 966 ± 67 ppm, as well as 134 ppm zinc (certified value: 124 ± 5 ppm) and 5.45 per cent iron (certified value: 5.56 ± 0.16 per cent). Certified values are from Bowman (1994). More control standards results will be provided upon completion of all analytical work.

RESULTS AND DISCUSSION

Only rock (Table 4) and soil profile (Tables 5-7) geochemical data were available at the time of writing. The following results are confined to case studies where several soil profiles were obtained, such as the crinkled chert sites. Drainage sediment, water and vegetation geochemical data obtained for watershed characterization studies in the Teslin Lake and Teh Creek areas will be given at a later date.

Felsic Volcanic and Exhalative Units Case Studies

Crinkled Chert (NTS 104O/13)

Rock and soil geochemical results are reported here for the three crinkled chert study localities: north of Mt. Francis, south of Mt. Francis, and Logtung road. No soil profiles were conducted at Logtung road, where basal tills are poorly distributed (Dixon-Warren and Hickin, this volume), and results here are limited to bedrock geochemical data. Analytical results for a single till pit cobble are also shown, although they are excluded from the summary statistics.

i) Rock Geochemistry

Selected ICP-MS and INA rock geochemical data (Table 4) for five crinkled chert outcrop grab samples show that this unit is characterized by highly elevated barium concentrations (mean: 5500 ppm; median: 2100 ppm) in the range 1600-19000 ppm (INA). They also have moderately elevated, although variable, concentrations of manganese (median: 612 ppm) in the range 218-2595 ppm, and of cobalt (median: 21 ppm INA) in the range 5-39 ppm. Barium is a lithophile element and is most abundant in felsic magmatic rocks (up to 1200 ppm) where it may substitute for K^+. Barium concentrations in sandstones, however, are in the range only 100-320 ppm (Kabata-Pendias and Pendias, 1992), with a reported median concentration of 170 ppm for sandstone and quartzite (Rose *et al.,* 1979). Typical concentration ranges of manganese and cobalt in sandstones are 0.3-10 ppm and 100-500 ppm, respectively (Kabata-Pendias and Pendias, 1992).

One crinkled chert sample (99-SJC-14), from the North Mt. Francis area, returned 19000 ppm (1.9 per cent) barium, suggesting the presence of barite. An analytical duplicate of the same material returned similar barium results (16000 ppm). Results here support those of Mihalynuk *et al.* (1998), who reported the presence of elevated barium concentrations (mean: 2254 ppm; 2 samples) in the crinkled chert unit relative to other sedimentary rocks sampled. Mihalynuk *et al.* (1998) suggested that elevated barium content might be a useful means of distinguishing crinkled chert from other fine-grained quartzites in the Big Salmon Complex. Results here support that assertion. Elevated barium levels are present in crinkled chert samples from all three study areas (Table

TABLE 5
SOIL PROFILE DATA: ICP-MS

Sample	Soil Horizon	Depth (cm)	Material	Rep	UTM Zone	UTME Nad83	UTMN Nad83	Mo (ppm)	Cu (ppm)	Pb (ppm)	Zn (ppm)	Ag (ppb)	Ni (ppm)	Co (ppm)	Mn (ppm)	Fe (%)	As (ppm)	U (ppm)	Au ppb	Th (ppm)	Sr (ppm)	Cd (ppm)	Sb (ppm)
996502	Bm(Ap?)	0-15	disturbed (?) soil		9	358942	6643867	0.65	42.08	11.50	60.0	59	36.0	12.6	589	2.75	12.0	0.9	4	9.0	31.7	0.14	0.92
996503R	R	15-25	py rubble over bedrock					0.50	228.92	4.12	63.3	290	16.0	24.6	631	7.09	70.6	0.2	7	0.8	22.5	0.05	7.58
996504	Bm	0-20	oxidized colluvium		9	347508	6633107	16.93	585.60	15.59	67.4	120	42.3	45.4	778	10.15	39.0	1.2	8	4.2	20.5	0.23	0.59
996505	C	20-50	colluvium					51.85	809.30	23.16	33.5	170	27.3	36.7	1082	16.64	52.8	1.4	25	2.6	14.7	0.35	0.52
996506R	R	50-65	rubbly bedrock					19.03	195.73	13.87	79.4	159	26.4	7.4	221	0.94	7.1	1.1	1	8.8	22.7	0.54	0.30
996507	Bm	0-45	oxidized colluvium	10	9	347433	6633132	53.36	1370.24	13.28	18.4	319	38.5	31.7	1372	22.98	53.5	2.8	26	5.5	7.2	0.22	0.75
996508	*Bm*	*0-45*	*colluvium*	*20*				*61.70*	*1258.87*	*10.88*	*18.4*	*225*	*37.2*	*29.3*	*1327*	*18.99*	*51.1*	*2.2*	*17*	*3.4*	*5.5*	*0.23*	*0.61*
996501			analytical duplicate	*80*				*51.57*	*1354.81*	*13.64*	*16.9*	*306*	*38.2*	*30.7*	*1377*	*22.68*	*53.3*	*2.9*	*22*	*5.3*	*7.0*	*0.25*	*0.80*
996509	C	45-65	colluvium					142.16	4977.16	13.79	17.0	664	69.5	74.4	2869	32.84	48.6	6.5	29	4.5	10.6	0.57	0.33
996510R	R	65-90	rubbly bedrock					114.03	1546.05	4.73	16.8	733	45.0	16.7	678	17.02	8.0	3.4	15	3.5	10.1	0.15	0.28
996034*	C	30-37	till		9	348635	6636661	10.73	64.65	8.01	88.5	86	22.9	15.1	368	5.09	13.4	0.8	13	5.8	20.0	0.11	0.46
996526R	R	>37	rubble					4.39	26.87	4.10	52.1	50	9.7	22.9	306	2.48	0.7	0.9	3	3.7	27.2	0.09	0.09
996511	Bm	0-14	oxidized colluvium		9	348397	6636759	2.74	63.47	14.93	83.3	266	23.2	17.9	317	4.60	99.7	0.7	15	2.9	20.4	0.15	0.80
996512	C	15-30	colluvium					1.43	28.10	10.93	107.6	164	22.3	13.9	271	3.50	23.5	0.5	4	2.6	13.7	0.20	0.55
996513R	R	>30	rubble over bedrock					0.13	28.06	3.38	96.3	38	6.3	9.1	679	3.73	3.5	0.8	1	1.9	19.5	0.06	0.14
996514	Ahe	0 - 8/10			9	348444	6636712	2.48	29.85	10.64	42.3	288	15.3	4.2	115	1.08	6.2	0.9	1	0.1	26.4	0.84	0.39
996515	Bm/BC	8/10-30	oxidized till					1.95	18.47	9.20	61.6	42	24.5	10.9	397	3.39	11.9	0.5	2	4.2	13.5	0.10	0.51
996032*	C	30-45	till					1.56	28.25	12.37	65.4	68	31.1	12.9	456	3.32	41.0	0.6	3	4.6	13.7	0.15	0.77
996517R	R	>45	py rubble					0.84	30.89	14.45	88.3	215	10.6	8.4	437	3.92	3.0	1.0	2	3.5	28.2	0.11	0.15
996518	Bm	5-30			9	348746	6636773	0.76	20.00	8.77	44.3	41	28.6	13.8	333	2.55	6.8	0.6	4	4.2	12.3	0.20	0.52
996029*	C	30-40	till					1.80	57.82	13.65	85.0	55	33.0	16.5	375	3.74	42.1	0.9	5	4.5	19.4	0.10	0.83
996519R	R	40-55	rubble					0.50	74.93	10.42	185.4	83	6.5	23.9	381	6.20	1.8	0.1	1	0.7	18.0	0.10	0.04
996520	Bm/C	0-18	oxidized till		9	347107	6629382	0.96	18.82	10.02	56.3	36	28.3	12.7	451	3.19	3.0	0.6	1	2.5	10.2	0.12	0.26
996522	Bm	0-12	oxidized colluvium (?)		9	347117	6629382	1.28	21.48	11.10	65.1	32	29.1	14.5	625	4.29	2.2	0.7	1	2.9	9.5	0.09	0.32
996523	C	12-32	till					0.83	77.51	8.11	76.2	24	43.6	17.8	521	3.24	2.9	1.0	4	4.1	19.3	0.09	0.40
996524	Bm/C	0-25	oxidized colluvium		9	347157	6629382	1.09	47.10	10.76	70.2	168	46.6	16.2	419	3.18	5.7	0.7	2	4.1	12.3	0.10	0.52
996525	Bm/C	0-35	colluviated till (?)		9	347097	6629382	1.03	29.11	9.68	63.7	30	45.5	16.3	483	3.34	5.0	0.7	2	4.5	15.0	0.23	0.44
996521			analytical duplicate	*80*				*0.91*	*27.59*	*9.22*	*62.7*	*26*	*44.9*	*16.0*	*476*	*3.32*	*5.1*	*0.7*	*3*	*4.3*	*14.4*	*0.24*	*0.40*
996531	Bm	0 - 12/15			9	667080	6612977	1.50	19.17	6.51	50.7	84	35.7	14.0	394	3.06	1.2	0.4	1	2.3	24.1	0.08	0.23
996532	IC	12/15 - 45	glaciolacustrine sediment					0.49	35.20	5.58	48.4	42	46.1	13.6	373	2.98	1.7	1.3	2	4.0	37.5	0.04	0.24
996043*	IIC	10-12m	till					4.78	74.97	10.05	90.5	242	90.3	23.0	790	3.67	10.4	1.7	4	2.9	106.0	0.47	0.90
996533	Ah	0-18			9	667060	6613045	2.28	19.08	2.97	9.2	327	14.5	1.6	113	0.26	0.1	7.7	2	0.1	179.3	0.41	0.77
996534	C	18-50	glaciolacustrine sediment					1.57	46.49	6.44	73.1	105	57.1	15.2	455	3.63	3.9	0.6	3	4.2	60.2	0.13	0.36
996535	Ae	0 - 5/7			9	346227	6636128	0.52	5.49	10.96	27.1	17	5.8	3.7	116	1.33	0.1	0.4	3	2.7	12.7	0.16	0.24
996536	Bf	5/7 - 15						0.76	12.94	9.68	55.6	26	19.8	11.2	283	3.29	6.0	0.4	1	3.2	12.7	0.11	0.32
996537	BC	15-35						0.73	25.65	11.74	52.1	21	43.4	18.1	374	2.91	9.9	0.5	2	3.9	16.5	0.07	0.31
996046*	C	35-65	till					0.59	29.10	9.89	50.6	27	38.2	13.7	521	2.53	10.3	0.5	3	3.4	22.1	0.03	0.34
996538	Bf	2-20			9	346137	6636074	1.09	25.24	12.26	51.3	33	20.6	10.1	292	3.49	6.0	0.6	1	3.8	13.8	0.08	0.36
996045*	C	20-60	till					0.66	38.97	10.25	54.0	18	28.1	12.4	380	2.78	8.7	0.6	3	4.2	14.6	0.06	0.34
996539	Ah	0-12		10	9	346065	6636115	0.28	50.32	9.20	15.4	331	9.8	1.4	23	0.56	0.4	2.6	8	0.1	13.5	0.07	0.42
996540	*Ah*	*0-12*		*20*				*0.38*	*41.87*	*12.74*	*17.0*	*286*	*9.9*	*1.7*	*28*	*0.73*	*0.9*	*2.8*	*7*	*0.1*	*13.8*	*0.05*	*0.45*
996025*	C	16-45	till					0.49	27.09	11.76	45.2	41	27.8	9.0	338	2.31	6.4	0.7	3	4.5	21.0	0.08	0.39
996527	Ae	0-5			9	346303	6636214	0.59	4.80	13.88	17.2	12	4.6	2.6	223	0.93	0.1	0.3	1	1.0	12.4	0.19	0.18
996528	Bf	5-15						1.06	16.92	13.61	52.1	44	32.4	13.9	290	3.63	8.4	0.4	1	3.0	13.3	0.18	0.37
996529	B	15-30						0.82	27.68	14.88	60.0	41	44.8	17.3	400	3.12	9.0	0.5	3	4.2	18.9	0.14	0.40
996038*	C	30-40	till					0.58	29.92	8.83	49.7	32	35.4	12.2	392	2.49	6.5	0.6	2	3.6	22.7	0.12	0.35

TABLE 5 CONTINUED
SOIL PROFILE DATA: ICP-MS

Study Area	Profile	Soil Profile Type	Sample	Soil Horizon	Depth (cm)	Material	Rep	UTM Zone	UTME Nad83	UTMN Nad83	Bi (ppm)	V (ppm)	Ca (%)	P (%)	La (ppm)	Cr (ppm)	Mg (%)	Ba (ppm)	Ti %	B (ppm)	Al (%)	Na (%)	K (%)	W (ppm)	Tl (ppm)	Hg (ppb)	Se (ppm)	Te (ppm)	Ga (ppm)	S (%)
Hwy. 97	1	Orthic eutric	996502	Bm(Ap?)	0-15	disturbed (?) soil		9	358942	6643867	0.34	50	0.65	0.050	21.4	35.5	0.62	249.8	0.126	3	1.66	0.029	0.21	0.2	0.13	81	0.1	0.14	5.3	0.01
Cu Prospect		brunisol	996503R	R	15-25	py rubble over bedrock					2.39	78	0.44	0.052	5.2	70.4	1.28	32.0	0.062	2	2.12	0.047	0.15	5.5	0.03	12	2.5	1.86	8.1	2.06
104O/13																														
Arsenault	1	Orthic eutric	996504	Bm	0-20	oxidized colluvium		9	347508	6633107	1.38	58	1.11	0.078	12.2	34.3	0.62	98.5	0.102	2	1.66	0.013	0.06	0.4	0.08	49	19.3	1.45	5.6	0.05
Cu Prospect		brunisol	996505	C	20-50	colluvium					1.50	37	3.12	0.101	13.5	14.8	0.32	66.9	0.064	2	1.18	0.008	0.02	1.4	0.04	37	18.9	1.68	5.7	0.05
104O/13			996506R	R	50-65	rubbly bedrock					0.16	25	0.82	0.169	16.9	60.0	0.77	51.4	0.120	1	0.99	0.043	0.33	0.3	0.06	8	0.6	0.14	4.0	0.05
	2	Orthic eutric	996507	Bm	0-45	oxidized colluvium	10	9	347433	6633132	3.37	20	1.41	0.078	12.1	9.8	0.15	37.3	0.080	2	0.65	0.008	0.01	1.2	0.03	58	50.8	4.71	3.3	0.11
		brunisol	*996508*	*Bm*	*0-45*	*colluvium*	*20*				*2.26*	*20*	*1.50*	*0.067*	*8.7*	*10.2*	*0.16*	*34.1*	*0.048*	*2*	*0.61*	*0.009*	*0.02*	*1.1*	*0.03*	*44*	*36.1*	*3.21*	*3.1*	*0.09*
			996501			analytical duplicate	*80*				*3.39*	*20*	*1.38*	*0.078*	*11.6*	*8.5*	*0.15*	*37.5*	*0.081*	*3*	*0.65*	*0.008*	*0.01*	*0.8*	*0.03*	*59*	*49.9*	*4.78*	*3.1*	*0.09*
			996509	C	45-65	colluvium					3.49	6	1.02	0.089	18.4	9.3	0.07	70.5	0.018	1	0.37	0.008	0.01	1.1	0.02	77	28.9	5.71	1.3	0.13
			996510R	R	65-90	rubbly bedrock					1.51	10	0.77	0.048	6.9	9.5	0.15	12.6	0.059	1	0.30	0.040	0.01	0.4	0.02	15	22.9	2.26	1.8	0.14
Crinkled Chert	1	brunisol	996034*	C	30-37	till		9	348635	6636661	0.13	56	0.12	0.058	13.8	22.4	1.29	160.6	0.122	1	3.37	0.034	0.22	0.2	0.24	48	1.3	0.11	8.2	0.11
Locality 1a			996526R	R	>37	rubble					0.08	23	0.54	0.065	9.8	67.0	0.82	84.2	0.092	1	2.00	0.148	0.36	0.2	0.23	6	0.3	0.02	6.4	0.32
N of Mt. Francis																														
104O/13	2	Orthic eutric	996511	Bm	0-14	oxidized colluvium		9	348397	6636759	0.40	67	0.13	0.059	8.7	27.1	0.84	131.0	0.084	3	3.22	0.019	0.09	0.2	0.14	121	0.8	0.17	6.8	0.09
		brunisol	996512	C	15-30	colluvium					0.23	69	0.14	0.041	9.9	28.9	0.52	114.3	0.136	2	2.31	0.012	0.08	0.2	0.11	105	0.4	0.07	7.9	0.04
			996513R	R	>30	rubble over bedrock					0.03	92	0.67	0.065	4.1	45.7	1.77	60.8	0.137	1	2.87	0.121	0.07	0.2	0.02	14	0.3	0.04	7.5	0.20
	3	Orthic eutric	996514	Ahe	0 - 8/10			9	348444	6636712	0.21	25	0.65	0.143	12.1	11.4	0.07	198.1	0.015	2	0.71	0.007	0.04	0.2	0.04	143	0.4	0.03	2.6	0.13
		brunisol	996515	Bm/BC	8/10-30	oxidized till					0.22	74	0.25	0.029	12.8	38.7	0.62	114.4	0.178	2	1.66	0.013	0.12	0.2	0.09	34	0.2	0.06	8.7	0.01
			996032*	C	30-45	till					0.77	66	0.23	0.038	11.0	45.1	0.85	129.3	0.141	1	2.15	0.021	0.13	0.3	0.10	27	0.9	0.14	7.6	0.01
			996517R	R	>45	py rubble					0.27	81	1.03	0.089	6.7	95.1	1.21	446.7	0.138	1	2.66	0.063	0.15	0.2	0.05	9	2.0	0.24	6.5	0.16
	4	Eluviated	996518	Bm	5-30			9	348746	6636773	0.26	50	0.17	0.030	12.3	35.5	0.59	129.0	0.123	1	2.33	0.016	0.10	0.2	0.10	62	0.3	0.03	5.2	0.01
		eutric brunisol**	996029*	C	30-40	till					0.38	74	0.29	0.056	15.8	45.7	0.94	210.2	0.155	1	2.43	0.051	0.06	0.2	0.09	9	1.7	0.32	6.1	0.01
			996519R	R	40-55	rubble					0.12	208	0.89	0.048	2.5	45.1	2.95	1122.6	0.214	1	4.38	0.078	1.63	0.2	0.48	7	1.1	0.09	13.4	0.26
Crinkled Chert	1	Orthic eutric	996520	Bm/C	0-18	oxidized till		9	347107	6629382	0.20	65	0.16	0.055	13.0	40.7	0.82	123.5	0.173	2	1.84	0.009	0.15	0.2	0.13	62	0.3	0.04	7.0	0.03
Locality 2		brunisol																												
SW Mt. Francis	2	Orthic eutric	996522	Bm	0-12	oxidized colluvium (?)		9	347117	6629382	0.67	92	0.14	0.053	12.8	55.1	0.79	163.1	0.337	3	2.27	0.010	0.10	0.2	0.17	81	0.4	0.11	11.5	0.03
104O/13		brunisol	996523	C	12-32	till					0.25	81	0.27	0.050	15.1	46.7	0.99	319.9	0.216	2	2.31	0.017	0.13	0.2	0.16	48	0.3	0.08	7.1	0.01
	3	Orthic eutric	996524	Bm/C	0-25	oxidized colluvium		9	347157	6629382	0.24	66	0.14	0.024	13.9	47.9	0.88	204.4	0.156	3	2.35	0.011	0.11	0.2	0.16	43	0.4	0.05	6.4	0.01
		brunisol																												
	4	Orthic eutric	996525	Bm/C	0-35	colluviated till (?)		9	347097	6629382	0.21	67	0.26	0.065	14.6	55.5	1.00	171.4	0.191	3	2.01	0.013	0.13	0.2	0.15	47	0.3	0.06	6.5	0.01
		brunisol	*996521*			analytical duplicate	*80*				*0.17*	*67*	*0.26*	*0.064*	*14.0*	*51.4*	*0.93*	*158.3*	*0.178*	*2*	*1.87*	*0.012*	*0.13*	*0.2*	*0.14*	*43*	*0.2*	*0.07*	*6.1*	*0.01*
Jennings River	1	Orthic eutric	996531	Bm	0 - 12/15			9	667080	6612977	0.14	75	0.38	0.023	7.9	58.6	0.64	263.5	0.221	1	1.97	0.028	0.05	0.2	0.08	23	0.4	0.02	6.1	0.01
qtz-ser schist		brunisol**	996532	IC	12/15 - 45	glaciolacustrine sediment					0.14	67	0.48	0.049	15.9	65.2	0.87	308.9	0.279	1	1.64	0.065	0.07	0.2	0.05	42	0.1	0.05	5.0	0.01
104N/09			996043*	IIC	10-12m	till					0.19	75	2.28	0.085	10.6	69.6	1.57	477.6	0.215	2	1.70	0.060	0.13	0.2	0.15	189	1.3	0.12	5.0	0.11
	2	Orthic melanic	996533	Ah	0-18			9	667060	6613045	0.07	14	4.65	0.056	1.3	4.5	0.46	245.0	0.012	13	0.25	0.013	0.01	0.2	0.02	67	11.1	0.04	0.6	0.36
		brunisol	996534	C	18-50	glaciolacustrine sediment					0.16	69	1.07	0.073	15.8	62.2	1.12	285.3	0.268	4	1.88	0.061	0.17	0.2	0.11	71	0.2	0.06	6.2	0.01
Crinkled Chert	1	Humo-ferric	996535	Ae	0 - 5/7			9	346227	6636128	0.23	46	0.17	0.023	12.9	20.3	0.21	158.2	0.190	1	0.85	0.009	0.03	0.2	0.06	23	0.1	0.03	6.7	0.01
Locality 1b		podzol	996536	Bf	5/7 - 15						0.18	84	0.20	0.052	10.1	31.3	0.72	232.1	0.169	1	2.09	0.018	0.08	0.2	0.07	42	0.1	0.05	7.6	0.01
NW of Mt. Francis			996537	BC	15-35						0.16	74	0.26	0.037	9.0	45.9	0.90	437.4	0.207	2	2.74	0.029	0.10	0.2	0.09	39	0.1	0.07	6.4	0.01
104O/13			996046*	C	35-65	till					0.14	73	0.30	0.022	9.0	44.7	0.81	458.2	0.196	1	1.98	0.057	0.09	0.2	0.09	15	0.7	0.06	5.5	0.01
	2	Humo-ferric	996538	Bf	2-20			9	346137	6636074	0.23	87	0.17	0.024	9.8	41.7	0.74	406.3	0.222	2	2.62	0.016	0.11	0.2	0.10	40	0.2	0.04	10.0	0.01
		podzol**	996045*	C	20-60	till					0.23	69	0.28	0.043	8.9	39.0	0.95	336.6	0.158	1	2.41	0.048	0.13	0.3	0.08	23	0.6	0.06	7.0	0.01
	3	Orthic melanic	996539	Ah	0-12		10	9	346065	6636115	0.12	14	0.14	0.202	13.6	18.7	0.09	702.5	0.008	2	1.68	0.006	0.03	0.2	0.04	320	0.9	0.06	3.6	0.12
		brunisol	*996540*	*Ah*	*0-12*		*20*				*0.17*	*17*	*0.13*	*0.150*	*16.7*	*32.3*	*0.12*	*769.8*	*0.012*	*2*	*1.97*	*0.008*	*0.05*	*0.2*	*0.06*	*363*	*0.9*	*0.05*	*5.0*	*0.10*
			996025*	C	16-45	till					0.16	67	0.39	0.063	14.2	46.3	0.82	510.3	0.201	1	1.88	0.110	0.09	0.2	0.09	11	0.6	0.07	5.5	0.01
	4	Humo-ferric	996527	Ae	0-5			9	346303	6636214	0.20	42	0.15	0.017	10.3	12.2	0.15	134.8	0.169	1	0.65	0.008	0.05	0.2	0.05	33	0.1	0.03	5.7	0.01
		podzol	996528	Bf	5-15						0.17	77	0.21	0.031	8.1	37.2	0.70	185.9	0.179	2	2.49	0.016	0.09	0.2	0.06	34	0.2	0.05	7.1	0.01
			996529	B	15-30						0.22	75	0.27	0.023	10.1	52.2	1.03	289.4	0.210	2	2.96	0.029	0.11	0.2	0.10	33	0.2	0.05	6.4	0.01
			996038*	C	30-40	till					0.14	69	0.30	0.026	11.1	44.2	0.71	210.7	0.192	1	1.75	0.048	0.07	0.2	0.08	20	0.6	0.06	5.1	0.01

* C-horizon tills at 6 soil profiles from those of Dixon-Warren & Hickin (this volume)
One sample (996025) is the first of three triplicate samples. *See* Dixon-Warren and Hickin (this volume) for further details.
** thin Aej horizon present but not sampled

UTM locations accurate to ~ 100 metres
Tentative soil types after Canadian System of Soil Classification (Agriculture Canada, 1987) not included here
Mineral horizons only are shown; LFH horizons (not sampled) are not included here

TABLE 6
SOIL PROFILE DATA: INA

Study Area	Profile	Soil Profile Type	Sample	Soil Horizon	Depth (cm)	Material	Rep	UTM Zone	UTME Nad83	UTMN Nad83	Au (ppb)	As (ppm)	Ba (ppm)	Br (ppm)	Ca (%)	Co (ppm)	Cr (ppm)	Cs (ppm)	Fe (%)	Hf (ppm)	Mo (ppm)	Na (%)	Rb (ppm)
Hwy. 97	1	Orthic eutric	996502	Bm(Ap?)	0-15	disturbed (?) soil		9	358942	6643867	5	11.6	950	1.5	2	12	91	3	3.63	5	1	1.29	90
Cu Prospect		brunisol	996503R	R	15-25	py rubble over bedrock					7	70.5	140	0.5	1	27	120	1	9.15	3	1	3.03	17
104O/13																							
Arsenault	1	Orthic eutric	996504	Bm	0-20	oxidized colluvium		9	347508	6633107	25	35.3	450	5.9	4	40	93	3	12.70	4	13	1.05	45
Cu Prospect		brunisol	996505	C	20-50	colluvium					29	48.0	260	3.1	7	31	52	1	19.90	2	43	0.71	42
104O/13			996506R	R	50-65	rubbly bedrock					1	7.1	470	0.5	5	13	154	1	2.63	4	18	2.37	53
	2	Orthic eutric	996507	Bm	0-45	oxidized colluvium	10	9	347433	6633132	29	50.1	160	6.4	5	27	37	1	27.40	2	44	0.71	15
		brunisol	*996508*	*Bm*	*0-45*	*colluvium*	*20*				*23*	*51.8*	*220*	*5.7*	*6*	*27*	*38*	*1*	*25.20*	*2*	*55*	*0.99*	*30*
			996501			analytical duplicate	*80*				*33*	*51.8*	*120*	*6.6*	*5*	*28*	*37*	*1*	*28.10*	*2*	*47*	*0.74*	*15*
			996509	C	45-65	colluvium					35	45.6	80	6.8	4	61	17	1	34.10	1	114	0.21	15
			996510R	R	65-90	rubbly bedrock					15	11.6	50	1.9	5	21	61	1	27.60	1	102	1.10	15
Crinkled Chert	1	brunisol	996034*	C	30-37	till		9	348635	6636661	21	16.1	770	9.5	1	19	54	4	7.45	4	22	0.88	73
Locality 1a			996526R	R	>37	rubble					4	1.8	260	0.5	3	25	118	2	3.73	4	3	1.53	35
N of Mt. Francis																							
104O/13	2	Orthic eutric	996511	Bm	0-14	oxidized colluvium		9	348397	6636759	27	94.8	880	18.5	1	16	65	2	5.58	4	1	1.19	49
		brunisol	996512	C	15-30	colluvium					10	26.4	680	17.5	1	13	89	2	4.47	6	2	1.32	60
			996513R	R	>30	rubble over bedrock					1	4.8	560	0.5	4	10	96	1	5.74	3	1	1.47	31
	3	Orthic eutric	996514	Ahe	0 - 8/10			9	348444	6636712	1	6.6	720	11.1	1	6	62	3	1.88	4	6	0.79	15
		brunisol	996515	Bm/BC	8/10-30	oxidized till					10	14.5	710	3.8	1	12	103	3	4.36	6	1	1.29	65
			996032*	C	30-45	till					1	42.3	960	6.6	1	16	118	3	5.27	6	9	1.36	66
			996517R	R	>45	py rubble					1	4.1	1100	0.5	4	9	162	2	5.34	4	1	1.01	43
	4	Eluviated	996518	Bm	5-30			9	348746	6636773	1	9.7	750	12.9	2	17	107	3	3.83	6	1	1.46	70
		eutric brunisol**	996029*	C	30-40	till					1	44.3	1100	2	2	19	114	2	5.37	6	10	1.52	73
			996519R	R	40-55	rubble					1	1.6	3100	0.5	2	25	88	5	8.88	2	1	0.70	107
Crinkled Chert	1	Orthic eutric	996520	Bm/C	0-18	oxidized till		9	347107	6629382	1	6.0	820	13.2	1	14	128	5	4.76	7	2	1.07	100
Locality 2		brunisol																					
SW Mt. Francis	2	Orthic eutric	996522	Bm	0-12	oxidized colluvium (?)		9	347117	6629382	3	6.3	830	26.2	1	16	168	4	5.71	6	2	1.26	75
104O/13		brunisol	996523	C	12-32	till					6	6.1	1500	4.7	1	21	118	3	4.54	5	1	1.56	57
	3	Orthic eutric	996524	Bm/C	0-25	oxidized colluvium		9	347157	6629382	3	8.3	1200	11.5	1	19	144	4	4.45	7	1	1.44	81
		brunisol																					
	4	Orthic eutric	996525	Bm/C	0-35	colluviated till (?)		9	347097	6629382	1	8.1	920	7.7	1	19	173	3	4.68	7	3	1.36	61
		brunisol	*996521*			analytical duplicate	*80*				*3*	*9.1*	*900*	*7.6*	*2*	*19*	*179*	*4*	*4.90*	*7*	*1*	*1.41*	*64*
Jennings River	1	Orthic eutric	996531	Bm	0 - 12/15			9	667080	6612977	1	4.4	840	0.5	2	18	150	1	4.30	4	1	1.73	49
qtz-ser schist		brunisol**	996532	IC	12/15 - 45	glaciolacustrine sediment					3	3.7	930	0.5	3	16	155	1	4.38	4	1	1.84	46
104N/09			996043*	IIC	10-12m	till					6	12.3	1300	3.2	4	26	181	3	5.54	4	13	1.40	48
	2	Orthic melanic	996533	Ah	0-18			9	667060	6613045	1	1.7	370	20.0	6	2	17	1	0.62	1	1	0.32	15
		brunisol	996534	C	18-50	glaciolacustrine sediment					3	6.5	830	3.4	3	16	131	2	4.65	4	1	1.43	58
Crinkled Chert	1	Humo-ferric	996535	Ae	0 - 5/7			9	346227	6636128	8	5.6	770	1.5	2	6	96	2	2.52	8	2	1.84	63
Locality 1b		podzol	996536	Bf	5/7 - 15						10	14.5	750	3.7	2	13	88	2	4.77	6	1	1.73	60
NW of Mt. Francis			996537	BC	15-35						6	13.6	980	2.6	3	19	121	2	4.38	4	1	1.49	48
104O/13			996046*	C	35-65	till					6	12.2	1500	2.5	1	19	132	2	4.45	5	6	1.78	56
	2	Humo-ferric	996538	Bf	2-20			9	346137	6636074	2	9.7	880	4.1	1	11	99	2	4.65	5	1	1.47	55
		podzol**	996045*	C	20-60	till					4	11.4	920	4.1	1	17	101	2	4.49	5	4	1.82	60
	3	Orthic melanic	996539	Ah	0-12		10	9	346065	6636115	16	5.3	910	13.3	1	2	42	2	1.10	2	1	0.48	15
		brunisol	*996540*	*Ah*	*0-12*		*20*				*20*	*6.3*	*970*	*12.7*	*1*	*4*	*55*	*2*	*1.37*	*2*	*3*	*0.75*	*32*
			996025*	C	16-45	till					9	7.0	1300	1.6	2	13	118	2	4.31	6	8	2.06	59
	4	Humo-ferric	996527	Ae	0-5			9	346303	6636214	3	3.8	660	1.5	2	5	88	2	2.02	7	1	1.93	89
		podzol	996528	Bf	5-15						4	12.8	770	3.5	2	17	110	2	5.10	5	2	1.63	61
			996529	B	15-30						3	12.2	890	1.3	2	20	124	2	4.52	5	2	1.70	52
			996038*	C	30-40	till					4	7.5	790	1.7	2	16	135	2	4.14	5	7	1.83	52

* C-horizon tills at 6 soil profiles from those of Dixon-Warren & Hickin (this volume)
One sample (996025) is the first of three triplicate samples. *See* Dixon-Warren and Hickin (this volume) for further details.

** thin Aej horizon present but not sampled
UTM locations accurate to ~ 100 metres
Tentative soil types after Canadian System of Soil Classification (Agriculture Canada, 1987)

TABLE 6 CONTINUED
SOIL PROFILE DATA: INA

Study Area	Profile	Soil Profile Type	Sample	Soil Horizon	Depth (cm)	Material	Rep	UTM Zone	UTME Nad83	UTMN Nad83	Sb (ppm)	Sc (ppm)	Se (ppm)	Ta (ppm)	Th (ppm)	U (ppm)	W (ppm)	Zn (ppm)	La (ppm)	Ce (ppm)	Nd (ppm)	Sm (ppm)	Eu (ppm)	Tb (ppm)	Yb (ppm)	Lu (ppm)	Mass (g)
Hwy. 97	1	Orthic eutric	996502	Bm(Ap?)	0-15	disturbed (?) soil		9	358942	6643867	1.4	13.7	3	1.5	11.7	2.4	1	107	32.6	58	23	5.3	0.9	0.6	2.6	0.39	30.24
Cu Prospect		brunisol	996503R	R	15-25	py rubble over bedrock					9.6	17.0	3	0.6	1.6	0.5	9	112	10.0	20	10	3.0	0.9	0.5	2.0	0.28	34.44
104O/13																											
Arsenault	1	Orthic eutric	996504	Bm	0-20	oxidized colluvium		9	347508	6633107	1.0	12.5	16	0.9	8.0	3.0	4	105	24.7	48	17	4.1	1.0	0.6	1.8	0.27	30.56
Cu Prospect		brunisol	996505	C	20-50	colluvium					0.7	7.5	14	0.5	5.5	3.2	3	50	22.3	41	16	3.3	1.0	0.5	2.0	0.30	33.30
104O/13			996506R	R	50-65	rubbly bedrock					0.5	19.6	3	1.2	18.1	4.1	2	123	53.6	92	34	7.8	1.6	0.9	3.4	0.51	41.43
	2	Orthic eutric	996507	Bm	0-45	oxidized colluvium	10	9	347433	6633132	1.0	5.8	44	0.5	7.1	4.5	1	50	19.7	33	14	2.9	0.7	0.5	1.4	0.22	31.07
		brunisol	*996508*	*Bm*	*0-45*	*colluvium*	*20*				*0.8*	*5.8*	*32*	*0.5*	*5.4*	*3.5*	*1*	*55*	*15.4*	*29*	*11*	*2.5*	*0.6*	*0.5*	*1.2*	*0.19*	*33.25*
			996501			analytical duplicate	*80*				*1.0*	*6.0*	*47*	*0.5*	*7.4*	*4.5*	*1*	*64*	*19.9*	*33*	*12*	*3.0*	*0.8*	*0.5*	*1.3*	*0.19*	*32.17*
			996509	C	45-65	colluvium					0.5	3.6	24	0.5	5.0	8.4	2	55	22.6	26	17	3.7	0.9	0.5	2.7	0.40	34.35
			996510R	R	65-90	rubbly bedrock					0.3	6.2	25	0.5	4.0	5.8	1	75	9.6	17	6	2.0	0.6	0.5	1.4	0.21	31.35
Crinkled Chert	1	brunisol	996034*	C	30-37	till		9	348635	6636661	0.8	18.9	3	1.0	9.8	2.3	1	124	26.2	47	14	3.5	0.9	0.5	2.4	0.36	27.15
Locality 1a			996526R	R	>37	rubble					0.2	21.1	3	1.4	6.0	2.5	1	99	35.2	57	17	4.3	0.9	0.7	3.5	0.51	37.22
N of Mt. Francis																											
104O/13	2	Orthic eutric	996511	Bm	0-14	oxidized colluvium		9	348397	6636759	1.5	16.7	3	0.7	6.3	1.4	2	130	17.5	33	11	2.8	0.7	0.5	1.4	0.21	22.91
		brunisol	996512	C	15-30	colluvium					0.9	12.0	3	0.5	6.8	2.1	1	150	20.9	40	15	3.2	0.7	0.5	1.5	0.23	24.86
			996513R	R	>30	rubble over bedrock					1.0	31.0	3	0.9	3.3	2.2	2	138	16.2	30	11	2.5	0.8	0.5	1.6	0.24	33.65
	3	Orthic eutric	996514	Ahe	0 - 8/10			9	348444	6636712	0.5	9.6	3	0.5	5.7	2.8	1	102	25.3	45	22	3.7	0.9	0.5	1.7	0.21	4.22
		brunisol	996515	Bm/BC	8/10-30	oxidized till					1.0	12.4	3	1.4	7.7	1.9	1	103	24.6	45	17	3.8	0.8	0.5	1.8	0.28	25.77
			996032*	C	30-45	till					1.2	16.1	3	1.3	8.9	2.5	1	129	25.8	59	19	4.4	1.1	0.6	2.3	0.36	26.42
			996517R	R	>45	py rubble					0.4	18.8	3	0.8	5.0	2.4	1	129	16.9	30	13	3.2	0.9	0.5	2.2	0.31	28.45
	4	Eluviated	996518	Bm	5-30			9	348746	6636773	1.1	13.3	3	1.8	8.3	1.6	1	132	26.3	52	22	4.0	1.0	0.5	2.0	0.31	27.23
		eutric brunisol**	996029*	C	30-40	till					1.5	18.4	3	1	8.4	2.5	1	117	32.2	65	26	5.6	1.4	0.7	3.1	0.46	25.61
			996519R	R	40-55	rubble					0.3	37.0	3	0.5	1.6	0.5	1	237	12.7	23	12	3.0	0.8	0.5	1.7	0.35	37.39
Crinkled Chert	1	Orthic eutric	996520	Bm/C	0-18	oxidized till		9	347107	6629382	1.0	15.8	3	1.6	9.0	2.4	1	88	35.4	70	27	5.2	1.4	0.6	2.5	0.38	24.46
Locality 2		brunisol																									
SW Mt. Francis	2	Orthic eutric	996522	Bm	0-12	oxidized colluvium (?)		9	347117	6629382	0.9	14.7	3	2.2	8.0	2.8	1	50	30.3	61	20	4.8	1.2	0.5	2.3	0.35	21.93
104O/13		brunisol	996523	C	12-32	till					1.0	19.1	3	1.2	8.4	2.9	3	86	31.5	66	27	5.4	1.4	0.5	2.8	0.46	28.48
	3	Orthic eutric	996524	Bm/C	0-25	oxidized colluvium		9	347157	6629382	1.2	15.6	3	1.6	9.2	2.2	1	126	32.1	64	23	4.8	1.1	0.7	2.5	0.37	29.50
		brunisol																									
	4	Orthic eutric	996525	Bm/C	0-35	colluviated till (?)		9	347097	6629382	1.0	16.7	3	1.6	9.9	2.5	1	104	31.8	65	23	5.0	1.2	0.7	2.5	0.37	28.63
		brunisol	*996521*			analytical duplicate	*80*				*1.1*	*17.5*	*3*	*0.5*	*9.0*	*2.9*	*3*	*161*	*33.7*	*66*	*23*	*5.2*	*1.2*	*0.7*	*2.5*	*0.38*	*28.87*
Jennings River	1	Orthic eutric	996531	Bm	0 - 12/15			9	667080	6612977	0.6	14.0	3	1.5	4.3	1.7	1	123	18.8	31	13	3.3	0.9	0.5	1.7	0.25	27.32
qtz-ser schist		brunisol**	996532	IC	12/15 - 45	glaciolacustrine sediment					0.7	17.0	3	1.5	5.1	2.5	1	128	25.6	37	21	5.3	1.5	0.7	2.1	0.33	28.73
104N/09			996043*	IIC	10-12m	till					1.6	17.1	3	1.1	5.5	2.6	1	139	23.5	48	20	4.7	1.5	0.7	2.7	0.39	26.40
	2	Orthic melanic	996533	Ah	0-18			9	667060	6613045	0.5	2.1	12	0.5	1.3	10.7	1	50	4.4	7	5	0.6	0.3	0.5	0.4	0.06	13.18
		brunisol	996534	C	18-50	glaciolacustrine sediment					0.8	14.9	3	1.3	5.2	1.3	1	114	22.0	33	19	4.3	1.2	0.6	2.1	0.31	31.00
Crinkled Chert	1	Humo-ferric	996535	Ae	0 - 5/7			9	346227	6636128	0.9	11.6	3	1.4	6.7	2.2	1	50	26.3	42	19	4.2	1.1	0.6	2.2	0.33	28.27
Locality 1b		podzol	996536	Bf	5/7 - 15						1.0	15.5	3	1.5	5.2	2.0	1	101	20.3	34	13	3.4	0.8	0.5	1.8	0.27	29.87
NW of Mt. Francis			996537	BC	15-35						1.2	16.2	3	0.5	5.7	2.0	1	104	18.0	30	16	3.3	0.9	0.5	1.6	0.25	29.85
104O/13			996046*	C	35-65	till					1.5	18.6	3	0.9	7.2	2.6	1	92	23.6	50	15	3.9	1.2	0.5	2.5	0.37	27.62
	2	Humo-ferric	996538	Bf	2-20			9	346137	6636074	0.8	13.9	3	1.2	5.2	2.5	1	95	19.0	30	15	3.1	0.8	0.5	1.7	0.26	27.26
		podzol**	996045*	C	20-60	till					1.0	18.4	3	1.0	7.0	1.4	2	95	21.2	45	16	3.6	1.1	0.7	2.4	0.36	29.05
	3	Orthic melanic	996539	Ah	0-12		10	9	346065	6636115	0.7	21.7	3	0.5	7.4	5.4	1	59	20.4	33	13	3.5	0.8	0.5	1.0	0.15	11.63
		brunisol	*996540*	*Ah*	*0-12*		*20*				*1.1*	*20.5*	*3*	*0.9*	*7.7*	*4.6*	*1*	*66*	*23.2*	*35*	*20*	*4.0*	*0.9*	*0.5*	*1.2*	*0.17*	*12.84*
			996025*	C	16-45	till					1.1	19.0	3	1.5	8.1	2.3	1	112	30.1	64	27	5.6	1.5	0.8	3.0	0.47	24.23
	4	Humo-ferric	996527	Ae	0-5			9	346303	6636214	0.8	11.6	3	1.5	5.7	2.4	1	90	22.4	45	14	3.5	0.9	0.5	2.2	0.34	24.21
		podzol	996528	Bf	5-15						1.0	16.6	3	1.3	5.0	1.5	1	102	19.6	41	13	3.4	1.0	0.5	2.1	0.31	27.33
			996529	B	15-30						1.0	17.4	3	0.5	6.1	1.5	1	94	21.2	42	18	3.5	0.9	0.5	2.1	0.31	30.68
			996038*	C	30-40	till					0.8	16.7	3	0.9	6.3	2.2	1	99	25.7	55	19	4.0	1.2	0.6	2.3	0.35	28.54

Mineral horizons only are shown; LFH horizons (not sampled) are not included here

TABLE 7
SOIL PROFILE DATA: MAJOR ELEMENTS

Sample	Soil Horizon	Depth (cm)	Material	Rep	UTM Zone	UTME Nad83	UTMN Nad83	SiO_2 (%)	Al_2O_3 (%)	Fe_2O_3 (%)	MgO (%)	CaO (%)	Na_2O (%)	K_2O (%)	TiO_2 (%)	P_2O_5 (%)	MnO (%)	Cr_2O_3 (%)
996502	Bm(Ap?)	0-15	disturbed (?) soil		9	358942	6643867	68.38	11.59	5.06	1.77	2.22	1.66	2.06	0.77	0.16	0.10	0.029
996503R	R	15-25	py rubble over bedrock					-	-	-	-	-	-	-	-	-	-	-
996504	Bm	0-20	oxidized colluvium		9	347508	6633107	47.56	9.96	18.82	2.40	5.07	1.49	1.15	0.77	0.26	0.17	0.018
996505	C	20-50	colluvium					36.81	6.71	30.30	1.85	10.03	1.09	0.48	0.47	0.31	0.24	0.011
996506R	R	50-65	rubbly bedrock					-	-	-	-	-	-	-	-	-	-	-
996507	Bm	0-45	oxidized colluvium	10	9	347433	6633132	30.37	4.23	40.03	2.03	6.64	0.92	0.26	0.35	0.29	0.31	0.004
996508	*Bm*	*0-45*	*colluvium*	*20*				*34.73*	*4.23*	*35.88*	*2.19*	*8.10*	*1.42*	*0.28*	*0.32*	*0.28*	*0.34*	*0.007*
996501			analytical duplicate	*80*				*30.44*	*4.23*	*40.00*	*2.02*	*6.65*	*0.97*	*0.26*	*0.35*	*0.28*	*0.32*	*0.006*
996509	C	45-65	colluvium					18.81	2.06	54.93	1.29	4.36	0.34	0.05	0.16	0.13	0.52	< .001
996510R	R	65-90	rubbly bedrock					-	-	-	-	-	-	-	-	-	-	-
996034*	C	30-37	till		9	348635	6636661	53.95	15.25	9.28	2.95	1.57	1.03	1.54	0.84	0.19	0.12	0.007
996526R	R	>37	rubble					-	-	-	-	-	-	-	-	-	-	-
996511	Bm	0-14	oxidized colluvium		9	348397	6636759	49.55	15.29	8.24	2.03	1.61	1.69	1.64	0.71	0.16	0.07	0.018
996512	C	15-30	colluvium					57.78	12.13	6.22	1.46	1.65	1.79	1.46	0.87	0.12	0.06	0.027
996513R	R	>30	rubble over bedrock					-	-	-	-	-	-	-	-	-	-	-
996514	Ahe	0 - 8/10			9	348444	6636712	35.86	6.38	2.40	0.49	1.72	1.05	1.05	0.63	0.66	0.04	0.015
996515	Bm/BC	8/10-30	oxidized till					65.14	11.24	6.35	1.90	2.02	1.70	1.84	1.01	0.09	0.09	0.030
996032*	C	30-45	till					63.07	12.32	6.38	2.27	1.85	1.61	1.59	0.92	0.13	0.06	0.014
996517R	R	>45	py rubble					-	-	-	-	-	-	-	-	-	-	-
996518	Bm	5-30			9	348746	6636773	62.78	12.36	5.03	1.82	2.12	1.88	1.67	0.83	0.12	0.08	0.028
996029*	C	30-40	till					63.36	14.89	7.25	2.28	1.90	2.01	1.76	0.95	0.17	0.07	0.015
996519R	R	40-55	rubble					-	-	-	-	-	-	-	-	-	-	-
996520	Bm/C	0-18	oxidized till		9	347107	6629382	58.27	12.62	6.46	2.12	1.57	1.43	2.17	1.08	0.18	0.09	0.031
996522	Bm	0-12	oxidized colluvium (?)		9	347117	6629382	50.29	13.07	7.89	1.99	1.45	1.63	2.13	1.35	0.27	0.11	0.031
996523	C	12-32	till					62.21	13.87	6.38	2.51	2.02	2.14	1.82	1.08	0.19	0.11	0.030
996524	Bm/C	0-25	oxidized colluvium		9	347157	6629382	62.36	13.17	5.96	2.27	1.62	1.86	1.90	0.99	0.09	0.08	0.031
996525	Bm/C	0-35	colluviated till (?)		9	347097	6629382	61.59	12.50	6.55	2.62	2.27	1.91	2.05	1.14	0.19	0.11	0.036
996521			analytical duplicate	*80*				*61.63*	*12.66*	*6.65*	*2.64*	*2.30*	*1.92*	*1.93*	*1.14*	*0.20*	*0.11*	*0.037*
996531	Bm	0 - 12/15			9	667080	6612977	65.91	12.18	5.68	1.91	2.78	2.32	1.25	1.14	0.06	0.08	0.030
996532	IC	12/15 - 45	glaciolacustrine sediment					65.17	12.31	5.83	2.28	3.47	2.55	1.44	1.11	0.16	0.08	0.029
996043*	IIC	10-12m	till					58.52	11.43	7.22	3.60	5.20	1.86	1.48	1.07	0.24	0.13	0.023
996533	Ah	0-18			9	667060	6613045	9.07	2.11	0.74	1.02	8.68	0.37	0.31	0.12	0.20	0.02	0.001
996534	C	18-50	glaciolacustrine sediment					60.57	12.45	6.83	2.91	3.77	2.19	1.51	1.14	0.25	0.09	0.029
996535	Ae	0 - 5/7			9	346227	6636128	72.92	11.14	3.36	1.09	2.02	2.59	1.71	1.13	0.09	0.06	0.032
996536	Bf	5/7 - 15						65.48	12.64	6.42	2.07	2.11	2.46	1.54	0.93	0.16	0.08	0.029
996537	BC	15-35						63.99	13.67	6.49	2.46	2.61	2.25	1.50	1.01	0.09	0.12	0.032
996046*	C	35-65	till					66.59	13.09	5.89	2.36	2.50	2.31	1.35	0.95	0.07	0.15	0.015
996538	Bf	2-20			9	346137	6636074	63.67	13.18	6.65	1.95	1.91	2.19	1.47	1.02	0.06	0.08	0.030
996045*	C	20-60	till					63.51	13.92	6.00	2.53	2.29	2.44	1.43	0.83	0.12	0.08	0.011
996539	Ah	0-12		10	9	346065	6636115	19.61	6.17	1.32	0.29	0.75	0.65	0.53	0.35	0.79	0.01	0.010
996540	*Ah*	*0-12*		*20*				*25.36*	*7.24*	*1.89*	*0.46*	*0.73*	*0.93*	*0.80*	*0.43*	*0.68*	*0.02*	*0.014*
996025*	C	16-45	till					68.71	12.23	5.07	2.48	2.35	2.31	1.34	1.07	0.19	0.04	0.014
996527	Ae	0-5			9	346303	6636214	71.39	11.29	2.76	0.77	1.89	2.68	1.74	1.05	0.13	0.07	0.019
996528	Bf	5-15						62.26	13.40	6.89	1.97	2.24	2.06	1.49	0.88	0.04	0.08	0.020
996529	B	15-30						64.14	14.09	6.07	2.36	2.30	2.22	1.58	0.90	0.09	0.09	0.034
996038*	C	30-40	till					67.10	12.74	5.57	2.09	2.66	2.48	1.35	0.96	0.08	0.12	0.015

* C-horizon tills at 6 soil profiles from those of Dixon-Warren & Hickin (this volume)
One sample (996025) is the first of three triplicate samples. See Dixon-Warren

** thin Aej horizon present but not sampled
UTM locations accurate to ~ 100 metres
Tentative soil types after Canadian System of Soil Classification (Agriculture Canada, 1987)

TABLE 7 CONTINUED
SOIL PROFILE DATA: MAJOR ELEMENTS

Study Area	Profile	Soil Profile Type	Sample	Soil Horizon	Depth (cm)	Material	Rep	UTM Zone	UTME Nad83	UTMN Nad83	Ni (ppm)	Sr (ppm)	Zr (ppm)	Y (ppm)	Nb (ppm)	Sc (ppm)	LOI (%)	C/Tot (%)	S/Tot (%)	Sum (%)
Hwy. 97	1	Orthic eutric	996502	Bm(Ap?)	0-15	disturbed (?) soil		9	358942	6643867	45	184	136	26	10	10	5.8	0.92	0.03	99.76
Cu Prospect		brunisol	996503R	R	15-25	py rubble over bedrock					-	-	-	-	-	-	-	-	-	-
104O/13																				
Arsenault	1	Orthic eutric	996504	Bm	0-20	oxidized colluvium		9	347508	6633107	39	157	128	19	10	10	12.2	2.68	0.03	99.96
Cu Prospect		brunisol	996505	C	20-50	colluvium					32	101	123	20	10	5	11.4	1.93	0.05	99.76
104O/13			996506R	R	50-65	rubbly bedrock					-	-	-	-	-	-	-	-	-	-
	2	Orthic eutric	996507	Bm	0-45	oxidized colluvium	10	9	347433	6633132	46	55	96	15	10	3	14.2	2.34	0.11	99.67
		brunisol	*996508*	*Bm*	*0-45*	*colluvium*	*20*				*42*	*51*	*101*	*13*	*10*	*3*	*11.9*	*2.00*	*0.03*	*99.72*
			996501			analytical duplicate	*80*				*42*	*56*	*110*	*16*	*10*	*3*	*14.3*	*2.32*	*0.06*	*99.87*
			996509	C	45-65	colluvium					67	39	64	33	10	2	16.6	1.38	0.12	99.29
			996510R	R	65-90	rubbly bedrock					-	-	-	-	-	-	-	-	-	-
Crinkled Chert	1	brunisol	996034*	C	30-37	till		9	348635	6636661	27	128	157	15	13	9	12.5	2.07	0.12	99.40
Locality 1a			996526R	R	>37	rubble					-	-	-	-	-	-	-	-	-	-
N of Mt. Francis																				
104O/13	2	Orthic eutric	996511	Bm	0-14	oxidized colluvium		9	348397	6636759	28	148	112	13	10	14	18.7	4.65	0.09	99.86
		brunisol	996512	C	15-30	colluvium					24	173	150	14	10	9	16.2	4.69	0.06	99.90
			996513R	R	>30	rubble over bedrock					-	-	-	-	-	-	-	-	-	-
	3	Orthic eutric	996514	Ahe	0 - 8/10			9	348444	6636712	20	128	130	15	10	7	49.4	21.90	0.18	99.79
		brunisol	996515	Bm/BC	8/10-30	oxidized till					33	199	180	17	10	10	8.4	1.75	0.04	99.95
			996032*	C	30-45	till					34	203	218	16	12	7	9.4	2.41	0.01	99.81
			996517R	R	>45	py rubble					-	-	-	-	-	-	-	-	-	-
	4	Eluviated eutric brunisol**	996518	Bm	5-30			9	348746	6636773	39	214	158	16	10	9	11.1	2.67	0.02	99.96
			996029*	C	30-40	till					45	202	213	23	13	8	4.9	0.54	0.02	99.77
			996519R	R	40-55	rubble					-	-	-	-	-	-	-	-	-	-
Crinkled Chert	1	Orthic eutric	996520	Bm/C	0-18	oxidized till		9	347107	6629382	34	148	174	20	10	10	13.6	4.29	0.05	99.76
Locality 2		brunisol																		
SW Mt. Francis	2	Orthic eutric	996522	Bm	0-12	oxidized colluvium (?)		9	347117	6629382	33	135	196	20	10	10	19.6	6.29	0.07	99.96
104O/13		brunisol	996523	C	12-32	till					51	209	168	25	10	14	7.3	1.19	0.04	99.89
	3	Orthic eutric	996524	Bm/C	0-25	oxidized colluvium		9	347157	6629382	48	181	188	20	10	10	9.3	1.85	0.01	99.82
		brunisol																		
	4	Orthic eutric	996525	Bm/C	0-35	colluviated till (?)		9	347097	6629382	51	193	185	22	10	12	8.8	1.84	0.04	99.92
		brunisol	*996521*			analytical duplicate	*80*				*54*	*195*	*211*	*22*	*10*	*12*	*8.5*	*1.89*	*0.03*	*99.88*
Jennings River	1	Orthic eutric	996531	Bm	0 - 12/15			9	667080	6612977	58	262	125	19	10	12	6.3	1.09	0.01	99.79
qtz-ser schist		brunisol**	996532	IC	12/15 - 45	glaciolacustrine sediment					72	309	116	28	10	15	4.8	0.40	0.02	99.40
104N/09			996043*	IIC	10-12m	till					107	290	116	21	14	7	8.3	1.07	0.16	99.30
	2	Orthic melanic	996533	Ah	0-18			9	667060	6613045	21	257	16	< 10	10	2	77.2	31.80	0.34	99.92
		brunisol	996534	C	18-50	glaciolacustrine sediment					63	275	116	25	10	14	7.7	1.20	0.01	99.62
Crinkled Chert	1	Humo-ferric	996535	Ae	0 - 5/7			9	346227	6636128	23	222	212	19	10	9	3.6	0.77	0.01	99.89
Locality 1b		podzol	996536	Bf	5/7 - 15						24	190	158	18	10	10	5.8	0.87	0.01	99.86
NW of Mt. Francis			996537	BC	15-35						50	219	135	17	10	12	5.5	0.46	0.01	99.91
104O/13			996046*	C	35-65	till					53	235	140	17	12	7	4.4	0.27	0.01	99.92
	2	Humo-ferric	996538	Bf	2-20			9	346137	6636074	31	188	153	17	10	10	7.6	1.16	0.01	99.96
		podzol**	996045*	C	20-60	till					34	167	134	16	12	7	6.6	0.66	0.01	99.92
	3	Orthic melanic	996539	Ah	0-12		10	9	346065	6636115	20	84	51	12	10	15	69.5	36.50	0.16	100.09
		brunisol	*996540*	*Ah*	*0-12*		*20*				*22*	*87*	*64*	*13*	*10*	*14*	*61.3*	*31.90*	*0.15*	*99.97*
			996025*	C	16-45	till					35	241	204	23	14	8	3.6	0.22	0.01	99.64
	4	Humo-ferric	996527	Ae	0-5			9	346303	6636214	33	229	183	20	10	10	5.1	1.37	0.02	99.03
		podzol	996528	Bf	5-15						51	198	139	19	10	14	8.2	1.57	0.01	99.67
			996529	B	15-30						90	212	133	21	10	14	5.4	0.50	0.01	99.43
			996038*	C	30-40	till					44	246	157	17	12	7	4.6	0.36	0.01	99.92

Mineral horizons only are shown;
LFH horizons (not sampled) are not included here

4), but another quartzite otherwiser similar to crinkled chert returned only low barium and manganese concentrations.

No detailed lithogeochemical sampling of crinkled chert units was attempted. With regard to other elements, crinkled cherts here exhibit, in most cases, only background-level concentrations of copper (mean: 30.7 ppm), zinc (mean: 27.6 ppm), lead (mean: 3.4 ppm), molybdenum (mean: 0.10 ppm), selenium (mean: 0.1 ppm) and gold (mean: 1 ppb). However, one dark maroon-coloured sample (99-SJC-11) from the South Mt. Francis area has, in addition to elevated barium (2100 ppm), highest concentrations of copper (119 ppm), manganese (2595 ppm), iron (2.06 per cent INA), cobalt (39 ppm INA), arsenic (52.1 ppm INA) and antimony (3.6 ppm INA) relative to other pink or grey specimens sampled.

ii) Soil Profile Geochemistry

Twelve soil profiles were sampled at crinkled chert localities 1 and 2, in areas to the north and south of Mt. Francis, respectively. Barium concentrations up to 1500 ppm (INA) occur in till and colluvial C-horizon soils sampled at eight profiles (Table 6) north of Mt. Francis area (localities 1a,b). The highest concentrations here are present at site 1b (range: 790 - 1500 ppm) nearer the crinkled chert exposures, while somewhat lower barium concentrations (range: 680-960 ppm) occur in the more distal profiles sampled at site 1a. Similar barium levels (range: 820 - 1500 ppm) are present in thin till and colluvial C-horizon veneer above crinkled chert at site 2 south of Mt. Francis. INA reanalysis of remaining sample material from the horizon with the highest barium content here (996523; 1500 ppm) returned a similar 1600 ppm barium. There is no regional till barium data available for adjacent parts of northern British Columbia with which to compare these results. However, many are elevated relative to publicly-available barium data for regional geochemical surveys of central and southern British Columbia tills (Table 8), for which survey medians are in the range 380-850 ppm barium. Most soil manganese concentrations in this study do not differ appreciably from regional medians, which are in the range 508-805 ppm.

Barium concentrations increase down profile in most crinkled chert-area soils here (Table 6), particularly those in tills. Down profile increases in barium are seen in both till profiles at locality 1a, all four till profiles at locality 1b, and the sole multi-horizon till profile at locality 2. Two examples of relevant profiles, a brunisol and a podzol, from crinkled chert locality 1 are shown in Figure 7. In the first case (locality 1a, profile 3), barium concentrations increase down profile from 720 ppm in the near-surface Ahe horizon, to 960 ppm in C horizon till, and finally to 1100 ppm in underlying bedrock rubble. In the second case (locality 1b, profile 1), barium concentrations double down profile, increasing from 770 ppm in the

TABLE 8
BARIUM AND MANGANESE CONCENTRATIONS (PPM) IN VARIOUS BRITISH COLUMBIA TILLS

	Big Salmon Complex *Dixon-Warren (this volume)**	Babine Porphyry Belt, Nechako Plateau *Levson et al. (2000)*	Fawnie Creek map area, Nechako Plateau *Levson et al. (1994)*	Chedakuz Creek map area, Nechako Plateau *Weary et al. (1997)*	Louis Creek-Chu Chua Creek area Southcentral B.C. *Bobrowsky et al. (1998)*	Adams Lake Plateau Area, Southcentral B.C. *Bobrowsky et al. (1997)*	Northern Vancouver Island *Bobrowsky and Sibbick (1996)*	Total Sites
Ba (ppm)								
Median	**930**	**780**	**660**	**-**	**770**	**850**	**380**	
Mean	942	786.7	677.7	-	773.8	885.5	394.8	
SD	263	153.8	105.9	-	279.0	317.9	167.9	
CV	-	0.195	0.156	-	0.4	0.4	0.4	
Minimum	210	360	430	-	50	260	50	
90th pctile.	-	980	820	-	1000 *(87.3%)*	1100 *(87%)*	600 *(90.6%)*	
95th pctile.	-	1100	850	-	1200 *(95.5%)*	1300 *(94.2%)*	680 *(95.4%)*	
Maximum	1500	1600	960	-	2200	4600	1500	
N=sites	*45*	*937*	*171*	-	*331*	*500*	*434*	***2418***
Mn (ppm)								
Median	**440**	**715**	**508**	**538**	**569**	**733**	**805**	
Mean	513	760.9	535.8	546.4	615.0	812.9	962	
SD	228	380.2	231.0	206	388.7	448.1	699.6	
CV	-	0.500	0.431	0.377	0.6	0.6	0.7	
Minimum	281	70	164	160	106	161	43	
90th pctile.	-	1238	834	786	869	1373 *(90.5%)*	*1775 (90.3%)*	
95th pctile.	-	1422	941	887	991	1773 *(95.2%)*	2320 *(95.2%)*	
Maximum	1273	3664	1259	1156	6061	2759	5041	
N=sites	*45*	*937*	*171*	*151*	*331*	*496*	*435*	***2566***

Determinations made on -230 mesh (<63 micron) fraction of tills

* Not a regional-scale geochemical survey

Barium: total barium determined by INA

Manganese: aqua regia digestion - ICP-ES (ICP-MS for data of Dixon-Warren and Hickin, this volume) surficial Ae horizon of the humo-ferric podzol (Photo 5) through to 1500 ppm in C horizon till. There appears to be a close relationship here between till geochemical results and the type of entrained material. A subangular to angular cobble of pink piedmontite schist (99-SJC-13) from this pit, one of several such clasts uncovered, returned similarly elevated barium and manganese concentrations of 2900 ppm (INA) and 708 ppm, respectively. Interestingly, it also returned 172 ppb gold (INA), whereas the enclosing soil horizons here have relatively low but uniform gold concentrations in the range 6-10 ppb. Subsequent reanalysis of remaining pulverized sample material by INA returned corroborative high barium and gold concentrations of 3300 ppm and 325 ppb, respectively.

There are additional similarities between the two profiles beyond the greater barium concentrations at depth. First, differences in barium concentrations between the two uppermost horizons (*e.g.* Ahe and Bm; Ae and Bf) are minimal compared to the much greater differences between these and the underlying C horizon tills. This relation also holds for the barium distribution in till from some other areas, such as profile 1 at the Jennings River study area (Table 6). Secondly, several other elements also increase down profile. These include manganese, zinc and, generally, iron and arsenic. Manganese concentrations, for instance, in the two C horizon tills (437-521 ppm) are 4 times greater than in the eluviated Ae or Ahe horizons near the surface. Some elements are distributed differently between the two profiles. Copper, for instance, is relatively constant with depth in the brunisol but increases with depth in the podzol. In this case the podzolic Bf horizon (12.94 ppm) has 2 times the copper content of the near-surface Ae horizon (5.49 ppm), but less than half that of C horizon till (29.1 ppm). This is attributed to the characteristically much greater clay content of till relative to near-surface mineral horizons.

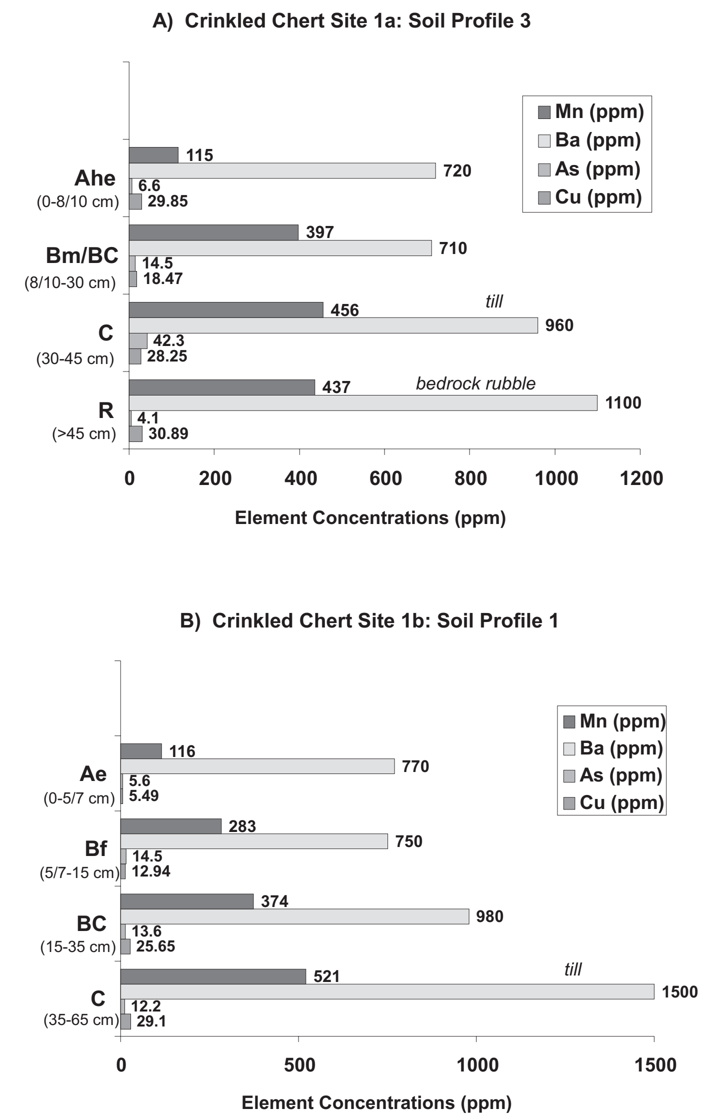

Figure 7. Manganese and copper (ICP-MS) and barium and arsenic (INA) concentrations in A) brunisolic and B) podzolic soil profiles in till at crinkled chert site 1. *See* Tables 4-6 for complete data listings.

Photo 5. Soil profile 1 (humo-ferric podzol) at crinkled chert site 1b northwest of Mt. Francis.

With regard to colluvial soils profiled adjacent to crinkled cherts, most have just a single horizon so there is insufficient data to compare barium distributions in till versus colluvial profiles. However, barium behaves in an opposite manner at one brunisolic profile (2) at locality 1a, decreasing with depth from 880 ppm (colluvial Bm horizon) to 560 ppm in underlying bedrock rubble. This is attributed to the downslope movement of higher-barium colluvial material above bedrock with a lower barium content. Interestingly, the highest gold concentrations in crinkled chert-area soil profiles also occur here. Gold distribution is similar to that of barium, decreasing down profile from 27 ppb in near-surface soil to just 1 ppb in bedrock rubble (Table 6).

Jennings River Quartz-sericite Schist (NTS 104N/09)

A composite rock sample (99-SJC-12) across the approximately 1.5 metre-wide altered quartz-sericite schist horizon exposed on the north side of the Jennings River yielded only background-level metal concentrations of 20 ppm copper, 17 ppm zinc, 4.7 ppm cobalt and 320 ppm barium (INA). The rock outcrop is overlain by 12-14 metres of till and glaciolacustrine sediment, forming a steep riverbank exposure. Irrespective of the low metal concentrations in outcrop, till copper concentrations reported here by Dixon-Warren and Hickin (this volume) are in the range 49-83 ppm, with higher concentrations occurring at higher levels in the till. Till barium (INA) levels are similarly high here, in the range 910-1400 ppm.

Results here provide a good example of how an understanding of surficial materials and Quaternary processes can be applied to interpreting geochemical data. Neither of the two soil pits dug at the top of the riverbank above altered quartz-sericite schist were deep enough to intercept till beneath about 2 metres of exotic glaciofluvial sediment. However, till was sampled at a site (996043) on the steep riverbank about 10-12 metres below soil profile 1, and about 2 metres above the altered horizon. Geochemical results for this composite profile (Tables 5 and 6) provide a good illustration of the potential differences in metal concentrations between surficial materials of varying origins, and of the pitfalls in sampling soils, even when potentially close to mineralization, without understanding their derivation. Differences in metal concentrations between the near-surface brunisolic Bm horizon, and the glaciolacustrine IC horizon from which it developed, are relatively minor when compared to metal concentrations in the underlying till. Till is a first-derivative product of bedrock, and is inferred to have formed here from the up-ice entrainment of relatively locally-derived material. Conversely, low-metal glaciolacustrine sediments have typically been transported great distances and been extensively reworked. Copper concentrations, for example, in the glaciolacustrine Bm and IC horizons (996531 and 996532) are relatively low (19-35 ppm), but are 75 ppm in the underlying till. Similarly, barium (840-930 ppm INA) and mercury (23-42 ppb) levels in the glaciolacustrine soils are considerably less than the corresponding till concentrations of 1300 ppm and 189 ppb, respectively. Similar differences between glaciolacustrine soil horizons and underlying till are also evident for molybdenum, lead, zinc, arsenic, silver and cobalt, among others.

Mineral Prospect Case Studies

Arsenault Prospect (NTS 104O/13; MINFILE 104O 011)

Highly elevated concentrations of copper, molybdenum and several other elements are present in two soil profiles conducted at old exploration trenches at the Arsenault prospect (Figure 8). Both profiles are characterized by brunisolic soils developed in a thin colluvial veneer above bedrock.

Highest metal concentrations are in soil profile 2 (Tables 5-7) in the eastern wall of the westernmost trench. This profile is characterized by a Cu-Mo-Fe-Co-As-Se-Au-Ag-Bi geochemical signature. Elevated copper concentrations increase down profile, from 1370 ppm in the near-surface Bm horizon to 4977 ppm in deeper colluvium (45-65 cm depth). Molybdenum and cobalt levels display similar relations, increasing down profile in the ranges 53-142 ppm, and 31.7-74.4 ppm, respectively. Similar down profile trends are also exhibited by iron (maximum: 32.8 per cent) and manganese (maximum: 2869 ppm). Angular bedrock rubble sampled from the bottom of the soil pit (996510R) contains lower, but nonetheless highly elevated concentrations of copper (1546 ppm), molybdenum (114 ppm) and iron (17.0 per cent).

Profile 1, on the east wall of the easternmost trench, is characterized by a more restricted Cu-Mo-Fe-Co-As-Se-Au geochemical signature. Elevated copper concentrations, although lower than in profile 2, similarly increase down profile, from 586 ppm in the colluvial Bm horizon to 809 ppm in underlying colluvium. Molybdenum, iron and arsenic display similar trends (Tables 5 and 6). As with profile 2, underlying gneissic bedrock rubble (996506R) contains comparatively lower but nonetheless elevated copper (196 ppm) and molybdenum (19 ppm) levels. However, a significant difference here are the lower cobalt, iron, arsenic, manganese, selenium and gold concentrations in rock relative to overlying colluvial soils. For example, rock cobalt content is only 7.4 ppm relative to a range of 36.7 - 45.4 ppm in soils.

Other interesting similarities between the two profiles, beyond their base metal signatures, are elevated concentrations of gold and selenium and relatively low concentrations of zinc and barium. Gold concentrations in the four colluvial soil horizons here (Tables 5 and 6) are

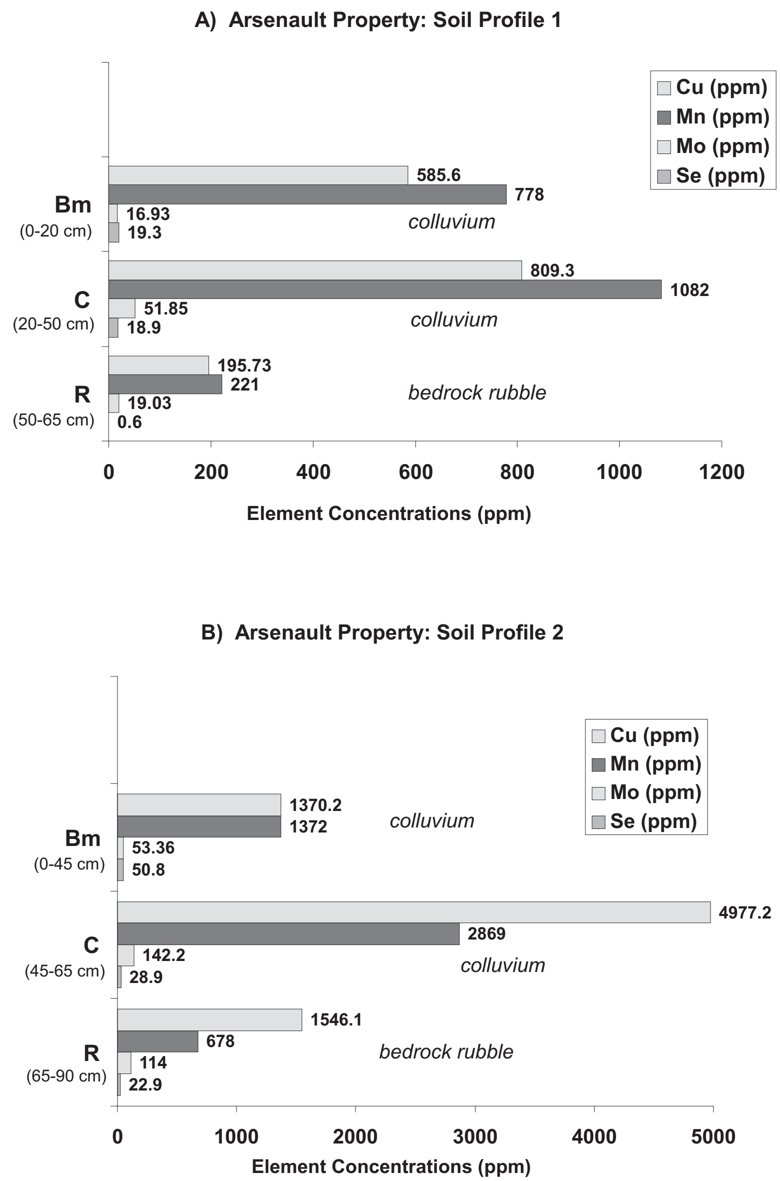

Figure 8. Copper, manganese, molybdenum and selenium concentrations (ICP-MS) in two colluvial soil profiles at the Arsenault copper prospect. *See* table 5 for complete data listings.

in the range 25-35 ppb (INA), and are relatively constant with depth. Selenium levels are high here. They are in the range 18.9-19.3 ppm in profile 1, and in the range 28.9-50.8 ppm in profile 2 where, interestingly, elevated selenium (22.9 ppm) is also present in the underlying rubbly bedrock. In contrast, relatively low zinc and barium concentrations in the mineral horizons do not exceed 67.4 ppm and 450 ppm, respectively.

The range of elements reported here and by Dixon-Warren and Hickin (this volume), although limited to a few sites, is much greater than those from previous soil geochemical surveys of the Arsenault prospect. Soil samples obtained by Sawyer (1967) and Turnbull and Simpson (1970) were collected using hand augers or mattocks, screened to -80 mesh using nylon screens, and analyzed for copper and/or molybdenum using colorimetric or acid digestion-AAS techniques. Turnbull and Simpson (1970) reported that elevated soil copper levels were coincident with known mineralization, particularly in the east-west trending ridge area where skarn-like copper mineralization is exposed at surface. However, no information is given about the types of surficial materials sampled (*e.g.* till versus colluvium) in either survey, which might assist in indicating the glacial or colluvial transport directions (*e.g.* downice or downhill) necessary for effective follow-up of geochemical anomalies. Similarly, there is no indication that any orientation studies were conducted which might indicate the most effective horizons and/or sieve size fractions to sample at this deposit. Soils of Turnbull and Simpson (1970) are reported to have been from the B-horizon, while those of Sawyer (1967) are not specified. Sawyer (1967) stated that sampling was intended to have been from a common horizon, but that the variable soil cover of the area made this difficult to achieve. Property-scale copper results of Sawyer (1967) are reproduced by Dixon-Warren and Hickin (this volume).

Highway 97 Copper-bearing Gossan (NTS 104O/13; MINFILE 104O 054)

A single profile sampled immediately above the gossan exposure, on the south side of the Alaska Highway, comprises a thin oxidized till (996502) above rubbly siliceous pyritic greenstone (996503R; Tables 4 and 5) in the bottom of the pit. Elevated concentrations of copper (229 ppm), cobalt (24.6 ppm), arsenic (70.6 ppm), antimony (9.6 ppm INA) and bismuth (2.39 ppm) are present in the greenstone rubble, but are considerably lower in the overlying soil material, which was likely disturbed and displaced during road construction. Only background levels of copper (42 ppm) are present. As outlined earlier, a similar though more pronounced geochemical signature was reported by Mihalynuk *et al.* (1998) for the gossanous outcrop here.

A similar suite of elevated metal concentrations was also obtained for an angular limonitic cobble (99-SJC-03) sampled from one of the till pits (996002; Dixon-Warren and Hickin, this volume) south of the highway. Elevated levels of copper (132 ppm), cobalt (27.4 ppm) and antimony (24.2 ppm INA) were obtained. Dixon-Warren (this volume) reported only background concentrations of copper in till pits north and south of the highway. Dispersal patterns, if any, of copper-bearing till from this locality may never be conclusively established, as the orientation of the Alaska Highway here is approximately parallel to the glacial transport direction (Dixon-Warren and Hickin, 2000).

Teslin Lake Border Area (NTS 104N/16; MINFILE 104N 135)

Three grab samples of gossanous bedrock (99-SJC-06 to -08) were obtained on the east shore of Teslin Lake. The most interesting results are from a site about 3 kilometres south of the Yukon border, where a grab sample (99-SJC-07) from an approximately 1 metre-wide pyrite-rich zone of altered limonitic schist returned highly elevated concentrations of gold (338 pppb) and arsenic (308 ppm), along with elevated antimony (4.7 ppm) and silver (0.4 ppm). These were determined by INA on a 33.59 gram sample. A comparable result of 309 ppb gold was also determined directly by aqua regia digestion - ICP-MS on a separate 1 gram split, suggesting that the gold present in the rock occurs in a very fine-grained form. No chalcopyrite was observed, as reflected in the very low copper content (7 ppm) of the sample. INA reanalysis of the remaining pulverized sample material (22.46 gram sample) returned corroboratory concentrations of 350 ppb gold, 325 ppm arsenic and 5.7 ppm antimony. A split of the original crushed sample material is presently being reanalyzed by fire assay methods at a second laboratory.

In the remaining cases, a grab sample of pyritic quartz-veined garnet mica schist (99-SJC-06) obtained from the northern end of the lake shore outcrop belt (Mihalynuk *et al.*, 1998) returned moderately high arsenic levels (43.1 ppm INA), but only background concentrations of copper (39 ppm) and cobalt (5.7 ppm). Another grab sample of limonitic rock (99-SJC-08) from the vicinity of a prior assay site of Mihalynuk *et al.* (1998) yielded elevated levels of copper (148 ppm), cobalt (28.1 ppm), silver (0.35 ppm), arsenic (62.8 ppm INA) and antimony (4.6 ppm INA), somewhat lower than earlier-reported results of 2.2 per cent copper and 28 ppm silver. Relatively high levels of cerium (56-105 ppm INA) and lanthanum (31.6-59.4 ppm INA) occur in all three rocks. Barium concentrations are in the range 440-610 ppm (INA).

METALLOGENY OF YUKON-TANANA TERRANE VMS DEPOSITS: APPLICATIONS TO GEOCHEMICAL EXPLORATION IN THE BIG SALMON COMPLEX

Volcanogenic massive sulphide deposits are typically polymetallic and high grade but often areally small. They present a more difficult geochemical exploration target in glaciated regions relative to, for example, porphyry copper deposits, which are associated with large hydrothermal alteration systems. An understanding of the geological and mineralogical characteristics of VMS deposits in general as well as those found elsewhere in the Yukon-Tanana Terrane is a necessary prerequisite for successful geochemical exploration in the Big Salmon Complex. Each deposit type has geochemical signatures related to host rock geology, alteration type and sulphide ore mineralogy which can be used in locating the dispersed remnants of the deposits in the surficial environment. Kuroko-type copper-lead-zinc VMS deposits typically have thin chert or barite exhalative horizons at upper levels and at peripheries, and have footwall alteration zones with quartz, sericite or chlorite zoning outwards to clay minerals, albite and carbonate (Hoy, 1995). They may have multi-element geochemical signatures with elevated levels of copper, zinc, lead, barium, silver, gold and other elements. Cyprus-type copper VMS deposits in mafic volcanics typically show iron and manganese enrichment of footwall stringer zones and may have overlying exhalative horizons of iron-rich mudstone or chert (Hoy, 1995). These deposits may also have a simpler sulphide mineralogy and a more limited copper-zinc geochemical signature.

Metallogeny of Yukon-Tanana Terrane VMS Deposits

Volcanogenic massive sulphide deposits and prospects occur in three main areas of the Yukon-Tanana Terrane other than the Big Salmon Complex (Hunt, 1997): the Finlayson Lake area (YT), the Dawson-Alaska border area (YT) and the Delta district of eastern Alaska. In the latter case, for instance, Devonian metavolcanic and metasedimentary rocks of the Delta district host more than 35 generally Kuroko-type copper-lead-zinc VMS deposits (Lange *et al.,* 1993). During the 1990's, exploration of the Finlayson Lake belt has uncovered several new copper-zinc-lead massive sulphide deposits, including the Kudz Ze Kayah (KZK), Wolverine, Fyre Lake, and Money deposits. Exploration of the Finlayson Lake belt is at a more advanced stage than in the Big Salmon Complex. The following section outlines their distinctive geological features and the geochemical exploration methods used to help discover them, and offers some preliminary suggestions for geochemical exploration in the Big Salmon Complex.

Finlayson Lake belt VMS deposits occur primarily within the 'middle package' of the Yukon-Tanana Terrane: Late Devonian to mid-Mississippian Nasina Assemblage quartzite, schist, marble and metavolcanic rocks and their equivalents, (Hunt, 1997). The two largest, Kudz Ze Kayah (KZK) and Wolverine, are Kuroko-style VMS deposits within Early Mississippian felsic metavolcanic and carbonaceous sedimentary rocks. KZK (11 million tonnes grading 5.9% Zn, 0.9% Cu, 1.5% Pb, 130 grams per tonne Ag and 1.3 grams per tonne Au; Burke, 1999) and Wolverine (6.2 million tonnes grading 12.7% Zn, 1.3% Cu, 1.5% Pb, 371 grams per tonne Ag and 1.76 grams per tonne Au; Burke, 1999) are characterized by relatively fine- to medium-grained pyrite-sphalerite-chalcopyrite-galena massive sulphide mineralization. High silver grades and selenium content are present at Wolverine. The Fyre Lake deposit (Kona deposit) is a Besshi-type copper-cobalt-gold deposit within a chlorite schist host (Blanchflower *et al.*, 1997; Hunt, 1997). Mineralization occurs as massive pyrite-pyrrhotite with subordinate chalcopyrite-sphalerite. The Money copper-zinc prospect is hosted by similar, but less metamorphosed, pillow basalt (Hunt, 1997), and may be either a Besshi or Cyprus-type VMS occurrence. The Eldorado prospect comprises massive sulphides, pyrrhotite-pyrite stringers and quartz-arsenopyrite lenses in black shale, argillite and phyllite (Hunt, 1997). Several additional VMS prospects, Ice, Mamu and Wolf, also occur in the Pelly Mountains volcanic belt (Hunt, 1997), which may be correlative with Yukon-Tanana rocks.

Some Geological Similarities: Host Rocks, Alteration Mineralogy and Ore Geochemistry

A common feature of several Finlayson Lake belt deposits, other than KZK, is their proximity to siliceous iron formation marker horizons interpreted to be exhalative in origin. The Wolverine deposit is associated with a siliceous exhalite and baritic magnetite iron formation (Murphy and Piercey, 1999). At Fyre Lake, massive sulphide float boulders and coincident soil geochemical and geophysical anomalies are spatially associated with several horizons of stratiform iron formation. These horizons, hosted by metamorphosed mafic volcanic and volcaniclastic rocks, have inferred surface traces over 3.2 kilometres in the Kona Creek cirque (Blanchflower *et al.,* 1997). At the Wolf deposit, a semi-massive barite/carbonate exhalite zone occurs stratigraphically just above the overturned massive sulphide zone (Gibson *et al.,* 1999). At Mamu, fragmental felsic metavolcanics contain pyrite-bearing horizons which weather to prominent gossans. The pyritic cherts or tuffs here are also thought to represent exhalative horizons (Doherty, 1997).

Direct comparisons of alteration and sulphide mineralogy between the Finlayson Lake belt and Big Salmon Complex are more difficult to make because of the relatively few prospects known south of the Yukon border. With regard to alteration, Mg-chlorite footwall alteration zones envelope pyrite-chalcopyrite-pyrrhotite stringer mineralization at Wolverine (Tucker *et al.*, 1997). Sulphide ore zones of Finlayson Lake area deposits such as KZK and Wolverine are characterized by high silver and selenium concentrations, and soil profiles at the Arsenault prospect have relatively high levels of selenium.

Geochemical Exploration for VMS Deposits in the Finlayson Lake Belt

Stream sediment and soil geochemical methods together with surface indications of mineralized float played a major role in exploration of the Finlayson Lake belt. The discovery of KZK by Cominco resulted from the follow-up, in 1992 and 1993, of anomalous zinc, lead and copper results from an NGR stream sediment survey which had been conducted by the Geological Survey of Canada in 1988 (Northern Miner, 1997). Elevated soil geochemical results, together with the 1993 discovery of mineralized sulphide float, led to the geophysical and drilling programs which outlined the deposit. Interestingly, an earlier low-density regional stream sediment survey conducted by Cominco in the late 1970's had failed to locate the deposit (Northern Miner, 1997). Initial reconnaissance exploration by Atna Resources, which led to the 1995 discovery of the Wolverine deposit, was also based on government regional geochemical data (Northern Miner, 1995). Drilling of subsequent multi-element soil geochemical anomalies led to the discovery of the deposit (Tucker *et al.*, 1997). NGR stream sediment geochemical signatures around KZK, Wolverine and related deposits were reported by Hunt (1998a).

Soil geochemical results, discovery of surface sulphide float and, in some cases, the position of natural vegetation 'kill zones' (Northern Miner, 1995; Hunt, 1998b) have also been instrumental in the discovery and development of other deposits in the Finlayson Lake belt. Doherty (1997) stated that elevated molybdenum in soils is considered to be an indicator of felsic-hosted VMS mineralization in the area. At Fyre Lake, a large massive sulphide boulder found in 1960 on an esker near the south end of Fire Lake led to the original discovery of outcropping mineralization in Kona Creek (Blanchflower *et al.,* 1997). Massive sulphide float and coincident soil geochemical anomalies here were spatially associated with several horizons of stratiform iron formation (Blanchflower *et al.*, 1997). Ferricrete was also reported from nearby creeks (Hunt, 1997). At the Money deposit, elevated copper (>100 ppm) in soils parallel prospective stratigraphy for several hundred metres, and pyritic sulphide boulders occur as float in adjacent Boulder Creek. According to Hunt (1997), the Cyprus-type Ice property was discovered from a single 2000 ppm copper in soil anomaly.

There is considerable scope for the use of other geochemical methods in the Big Salmon Complex, including lithogeochemistry and vegetation sampling. Lithogeochemical sampling was considered by Sebert and Hunt (1999) to be a useful tool in discriminating chlorite schist hosting mineralization at the Fyre Lake deposit from barren chlorite schist units. They stated that chlorite schist hosting the Kona zones originated from a boninitic protolith, distinctive from the tholeitic nature of other mafic metavolcanics of the area. Relative to other chlorite schist units, the Kona Cirque chlorite schist host exhibits a relatively distinctive major and trace element geochemical signature (higher MgO, SiO_2, Cr; lower TiO_2, Zr) and a distinctive rare earth element (REE) pattern. A more comprehensive lithogeochemical study by Piercey *et al.* (1999), results of which are beyond the scope of this paper, outlined four volcanic rock units in the Finlayson Lake area as being most prospective for hosting VMS mineralization. In contrast to lithogeochemistry, there is little published information on the use of biogeochemical exploration methods in the Yukon-Tanana Terrane. Biogeochemical orientation studies were conducted at two Yukon sites by Hunt *et al.* (1997): Matson Creek, and Bradens Canyon south of Dawson. At Matson Creek, an unglaciated area, black spruce twig geochemical results for copper, zinc, silver, cadmium and lead are generally coincident with B-horizon soil geochemical anomalies associated with known mineralization. At the glaciated Bradens Canyon site, however, twig geochemical results for mostly white spruce were of background levels only. They did not correlate with either paired soil sample results or with anomalous concentrations of lead, zinc, copper and other elements in NGR stream sediments.

Soil geochemistry and surface prospecting have been used successfully in the Finlayson Lake belt, but much of the area where the deposits occur are bedrock-dominated with only thin till and colluvial veneers (Jackson, 1994). Thin soils are more likely to reflect the presence nearby mineralization than are thick tills, where glacial dispersal distances are typically greater. There is little detailed orientation study information available on surficial materials, soil types and glacial dispersal distances here which might be applied to till-covered parts of the Big Salmon Complex.

SUMMARY AND RECOMMENDATIONS

Geochemical studies were conducted in several localities near regionally anomalous RGS watersheds, known mineral prospects and felsic volcanic units during the 1999 field season. Preliminary results are limited here to those obtained for soil profiles and rocks. Colluvial soil profiles at the Arsenault copper prospect contain highly elevated levels of copper, molybdenum and selenium, among other elements. Till and colluvial soil profiles near exposures of barium-rich exhalative crinkled chert units contain elevated barium concentrations which, in tills, generally increase down profile.

Preliminary recommendations are given here for VMS geochemical exploration in the Big Salmon Complex (Table 9). They are based on limited data available at time of writing, and are derived in part from general geological characteristics and geochemical signatures of Kuroko-style VMS deposits (*e.g.* Hoy, 1995), and from those characteristics of the Finlayson Lake belt deposits in particular. Recommendations are modified from those of Allan *et al.* (1972) who, with reference to lake sediment geochemical exploration in the Slave Province, proposed that various scales of geochemical exploration (*e.g.* regional to detailed) for Archean polymetallic massive sulphide deposits in the Canadian Shield follow hierarchical geochemical indicators related to geology, alteration and mineralogy of progressively smaller target areas:

- favourable felsic volcanic belts
- exhalative sedimentary rocks
- VMS alteration assemblages
- VMS sulphide mineral zones

More comprehensive recommendations will be prepared at a later date. Any sampling plan, particularly for regional-scale surveys, should consider the relatively small areal extent of VMS deposits and use a greater sampling density than might be used for, for example, porphyry copper deposit exploration. Modern multi-element analytical techniques such as ICP-MS provide a much wider range of useful elements than were available to explorationists previously, when often only a few elements such as copper and molybdenum were routinely determined.

PROPOSED FUTURE WORK

Future studies and survey work will involve both office and field components, and will focus on i) thematic compilation projects, ii) continued deposit-scale geochemical studies, iii) release of RGS archive data, and iv) collection and release of new RGS data:

i) Continued compilation and interpretation of existing RGS data for adjacent terranes in northern British Columbia, notably a) those parts of the southeastern Dorsey Terrane recently mapped by Nelson (this volume) and, b) those areas underlain by Slide Mountain Terrane and northern Cache Creek Terrane rocks across six 1:250,000 map areas (NTS 104I, K, M, N, O, P). There is considerable potential for new VMS discoveries in these relatively unexplored parts of the province. The Slide Mountain Terrane hosts the Ice deposit in the southern Yukon as well as the Lang Creek showing (MINFILE 104P 008) in northern British Columbia. In the Cache Creek Terrane, Permo-Triassic bimodal mafic-felsic volcanics and subordinate sedimentary rocks host the Kutcho Creek (MINFILE 104I 060) copper-zinc deposit (Childe and Schiarizza, 1997; Barrett *et al.*, 1996). The VMS potential of parts of the Cache Creek Group has also been highlighted by recent mapping of rhyodacite units within the French Range Formation (Mihalynuk and Cordey, 1997). Thematic RGS geochemical maps will be prepared for each terrane to highlight those elements typically associated with VMS deposits and their host rocks.

ii) Continuation of geochemical case studies in the Big Salmon Complex, and new case study investigations of geochemical dispersal at VMS and other prospects in the Dorsey, Cache Creek and Slide Mountain Terranes.

iii) Release of new RGS stream sediment archive data for the Atlin (NTS 104N), Jennings River (NTS 104O) and McDame (NTS 104P) map areas is planned for early summer, 2000.

iv) Stream sediment-lake sediment RGS coverage is proposed for the Dease Lake (NTS 104J) map area, the last remaining unsurveyed area in the region. Completion of RGS coverage there would provide necessary regional data to evaluate the VMS and Pogo-style deposit potential of the area, and allow completion of thematic geochemical maps for the Cache Creek Terrane.

TABLE 9
GEOCHEMICAL EXPLORATION FOR KUROKO-TYPE VMS DEPOSITS (AFTER ALLAN *ET AL*., 1972)

1) Favourable felsic volcanic belts	Elevated K, Si Locally elevated Cu, Zn and related elements Depleted in Mg, Fe, Ti, Ni
2) Exhalative carbonate and iron-rich sediments	Elevated Mn, Ba
3) Alteration zones	Elevated Mg and K, depleted Na and Ca, at quartz-sericite-chlorite-rich cores of footwall alteration pipes
4) Sulphide mineral zones	Elevated Cu, Zn, Pb, Ag, Ba, Fe, As, Se, related elements

ACKNOWLEDGMENTS

The assistance of members of the Ancient Pacific Margin NATMAP Project, particularly A. Dixon-Warren, M. Mihalynuk and J. Nelson of the Geological Survey Branch, is gratefully acknowledged. C. Roots, Geological Survey of Canada, masterminded the logistics of the Morley Lake base camp. A. Hickin assisted with field work and later crushed and pulverized rock samples. Prof. K. Telmer, University of Victoria, provided distilled water for the project, loaned several items of water sampling equipment and supervised the B.Sc. thesis of the junior author. Special thanks are due to A. Paige of Fireweed Helicopters, Whitehorse, for his skillful flying during the course of the project. Vegetation samples were graciously ashed by C. Dunn, Geological Survey of Canada. G. McArthur, R.E. Lett, A. Dixon-Warren and M. Mihalynuk reviewed and commented on earlier versions of the manuscript.

REFERENCES

Agriculture Canada Expert Committee on Soil Survey (1987): The Canadian System of Soil Classification, Second Edition; *Agriculture Canada*, Publication 1646, 164 pages.

Aitken, J.D. (1959): Geology of the Atlin map-area, British Columbia (104/N); *Geological Survey of Canada*, Memoir 307.

Allan, R.J., Cameron, E.M. and Durham, C.C. (1972): Reconnaissance Geochemistry Using Lake Sediments of a 36,000-Square-Mile Area of the Northwestern Canadian Shield; *Geological Survey of Canada*, Paper 72-50.

Blanchflower, D., Deighton, J. and Foreman, I. (1997): The Fyre Lake Deposit: A New Copper-Cobalt-Gold VMS Discovery; *in* Yukon Exploration and Geology 1996, Exploration and Geological Services Division, Yukon, *Indian and Northern Affairs Canada*, pages 46-52.

Barrett, T.J., Thompson, J.F.H. and Sherlock, R.L. (1996): Stratigraphic, Lithogeochemical and Tectonic Setting of the Kutcho Creek Massive Sulfide Deposit, Northern British Columbia; *Exploration and Mining Geology*, volume 5, pages 309-338.

Bobrowsky, P.T., Paulen, R., Little, E., Prebble, A., Ledwon, A. and Lett, R. (1998): Till Geochemistry of the Louis Creek - Chu Chua Area (92P/1E, 92P/8E); *B.C. Ministry of Energy and Mines*, Open File 1998-6.

Bobrowsky, P.T., Leboe, E.R., Dixon-Warren, A., Ledwon, A., MacDougall, D. and Sibbick, S.J. (1997): Till Geochemistry of the Adams Lake Plateau - North Barriere Lake Area (82M/4, 5); *B.C. Ministry of Employment and Investment*, Open File 1997-9.

Bobrowsky, P.T. and Sibbick, S.J. (1996): Till Geochemistry of Northern Vancouver Island Area (92L/5, 6W, 11W, 12); *B.C. Ministry of Employment and Investment*, Open File 1996-7.

Bowman, W.S. (1994): Catalogue of Certified Reference Materials; *Canada Centre for Mineral and Energy Technology*, Natural Resources Canada, CCRMP 94-1E.

Burke, M. (1999): Yukon Mining and Exploration Overview-1998; *in* Yukon Exploration and Geology 1998, Exploration and Geological Services Division, Yukon, *Indian and Northern Affairs Canada*, pages 2-30.

Childe, F.C. and Schiarizza, P. (1997): U-Pb Geochronology, Geochemistry and Nd Isotopic Systematics of the Sitlika Assemblage, Central British Columbia; *in* Geological Fieldwork 1996, *B.C. Ministry of Employment and Investment,* Paper 1997-1, pages 69-77.

Cook, S.J., Jackaman, W. and Matysek, P.F. (1992): Follow-up Investigation of Anomalous RGS Stream Sediment Sites in Southeastern British Columbia: Guide to Potential Discoveries (82E, F, G, J, K, L); *B.C. Ministry of Energy, Mines and Petroleum Resources*, Exploration in British Columbia 1991, pages 51-59.

Cook, S.J., Lett, R.E.W., Levson, V.M., Jackaman, W., Coneys, A.M. and Wyatt, G.J. (1998): Regional Lake Sediment and Water Geochemistry of the Babine Porphyry Belt, Central British Columbia (93L/9, 16; 93M/1, 2, 7, 8); *B.C. Ministry of Employment and Investment*, Open File 1997-17, 31 pages.

Cook, S.J. (in preparation): Follow-up Investigations of Some Anomalous RGS Stream Sediment Sites in Central British Columbia (94L/16; 93N/4); *B.C. Ministry of Energy and Mines*.

Dixon-Warren, A. and Hickin, A. (this volume): Ancient Pacific Margin NATMAP Project Part IV: Surficial Mapping and Till Geochemistry in the Swift River Area, northwestern British Columbia; *B.C. Ministry of Energy and Mines*, Geological Fieldwork 1999, Paper 2000-1.

Dixon-Warren, A. and Hickin, A. (2000): Surficial Geology of the Swift River Area (104N/9, 16; 104O/NW); *B.C. Ministry of Energy and Mines*, Open File 2000-5.

Doherty, A. (1997): Mamu-Bravo-Kulan Claims: A VHMS Exploration Target based on Geochemical and Geophysical Anomalies in Mississippian Volcanics within Cassiar Platform (NTS 105F/7, 8, 9, 10); *in* Yukon Exploration and Geology 1996, Exploration and Geological Services Division, Yukon, *Indian and Northern Affairs Canada*, pages 56-61.

Dunn, C.E. (1995): Biogeochemical Prospecting in Drift-Covered Terrain of British Columbia; *in* Drift Exploration in the Canadian Cordillera, P.T. Bobrowsky, S.J. Sibbick, J.M. Newell and P.F. Matysek, Editors, *B.C. Ministry of Energy, Mines and Petroleum Resources,* Paper 1995-2, pages 229-238.

Dunn, C.E. (1999): Biogeochemical Exploration Methods in the Canadian Shield and Cordillera; *in* Drift Exploration in Glaciated Terrain, *Association of Exploration Geochemists*, Short Course Notes, 19th International Geochemical Exploration Symposium, pages 164-181.

EPA (1999): Method 1631, Revision B: Mercury in water by oxidation, purge and trap, and cold vapor atomic fluorescence spectrometry; *United States Environmental Protection Agency*, internet report EPA-821-R-99-005, May 1999.

Gabrielse, H. (1969): Geology of Jennings River map-area, British Columbia (104O); *Geological Survey of Canada*, Paper 68-55.

Gibson, S.M., Holbek, P.M. and Wilson, R.G. (1999): The Wolf Property - 1998 Update: Volcanogenic Massive Sulphides Hosted by Rift-Related, Alkaline, Felsic Volcanic Rocks, Pelly Mountain, Yukon; *in* Yukon Exploration and Geology 1998, Exploration and Geological Services Division, Yukon, *Indian and Northern Affairs Canada*, pages 237-242.

Gravel, J.L. and Matysek, P.F. (1989): 1988 Regional Geochemical Survey, Northern Vancouver Island and Adjacent Mainland (92E, 92K, 92L, 102I); *in* Geological Fieldwork 1988, *B.C. Ministry of Energy, Mines and Petroleum Resources*, Paper 1989-1, pages 585-591.

Hunt, J.A. (1997): Massive Sulphide Deposits in the Yukon-Tanana and adjacent Terranes; *in* Yukon Exploration and Geology 1996, Exploration and Geological Services Division, Yukon, *Indian and Northern Affairs Canada*, pages 35-45.

Hunt, J.A. (1998a): VMS Exploration in the Yukon-Tanana Terrane; *in* Pathways '98, Extended Abstract Volume, *Society of Economic Geologists*, pages 205-207.

Hunt, J.A. (1998b): The Setting of Volcanogenic Massive Sulphide Deposits in the Finlayson Lake District; *in* Yukon Exploration and Geology 1997, Exploration and Geological Services Division, Yukon, *Indian and Northern Affairs Canada*, pages 99-104.

Hunt, J.A., Dunn, C.E., Timmerman, J.R.M. and Zantvoort, W.G. (1997): Biogeochemical Prospecting in the Yukon-Tanana Terrane, Yukon Territory; *in* Yukon Exploration and Geology 1996, Exploration and Geological Services Division, Yukon, *Indian and Northern Affairs Canada*, pages 74-91.

Hoy, T. (1995): Besshi, Cyprus and Noranda/Kuroko Massive Sulphide Types; *in* Selected British Columbia Mineral Deposit Profiles: Volume 1-Metallics and Coal, D.V. Lefebure and G.E. Ray, Editors, *B.C. Ministry of Energy, Mines and Petroleum Resources*, Open File 1995-20, pages 49-54.

Jackaman, W. (in preparation): Regional Geochemical Surveys of the Atlin, Jennings River and McDame map areas (104N, O, P); *B.C. Ministry of Energy and Mines*, RGS.

Jackaman, W., Cook, S.J. and Lett, R. (2000): Regional Geochemical Survey Program: Review of 1999 Activities; *in* Geological Fieldwork 1999, *B.C. Ministry of Energy and Mines*, Paper 2000-1.

Jackson, L.E., Jr. (1994): Terrain Inventory and Quaternary History of the Pelly River Area, Yukon Territory; *Geological Survey of Canada*, Memoir 437.

Kabata-Pendias, A. and Pendias, H. (1992): Trace Elements in Soils and Plants, Second Edition; *CRC Press*, 365 pages.

Lange, I.M., Nokleberg, W.J., Newkirk, S.R., Aleinikoff, J.N., Church, S.E. and Krouse, H.R. (1993): Devonian Volcanogenic Massive Sulfide Deposits and Occurrences, Southern Yukon-Tanana Terrane, Eastern Alaska Range, Alaska; *Economic Geology*, Volume 88, pages 344-376.

Lett, R.E., Jackaman, W. and Yeow, A. (1999): Detailed Geochemical Exploration Techniques for Base and Precious Metals in the Kootenay Terrane (82L/13, 14; 82M/4, 5; 92P/1); *in* Geological Fieldwork 1998, *B.C. Ministry of Energy and Mines*, Paper 1999-1, pages 297 to 306.

Levson, V.M., Giles, T.R., Cook, S.J. and Jackaman, W. (1994): Till Geochemistry of the Fawnie Creek Map Area (93F/03);

B.C. Ministry of Energy, Mines and Petroleum Resources, Open File 1994-18, 34 pages.

Levson, V.M. and Stumpf, A. (2000): Till Geochemistry of the Babine Porphyry Belt; *B.C. Ministry of Energy and Mines*, Open File 1999-12.

Mihalynuk, M., Nelson, J., Roots, C., Friedman, R.M. and de Keijzer, M. (this volume): Ancient Pacific Margin Part III: Regional Geology and Mineralization of the Big Salmon Complex (104N/9,10 & 104O/12,13,14W); *B.C. Ministry of Energy and Mines*, Geological Fieldwork 1999, Paper 2000-1.

Mihalynuk, M. (2000): Geology of the Smart River Map Area (104O/13); *B.C. Ministry of Energy and Mines*, Open File 2000-6.

Mihalynuk, M., Bellefontaine, K., Brown, D., Logan, J., Nelson, J., Legun, A. and Diakow, L. (1996): Digital Geology, Northwestern British Columbia (94/E, L, M; 104/F, G, H, I, J, K, L, M, N, O, P; 114/I, O, P); *B.C. Ministry of Energy and Mines*, Open File 1996-11.

Mihalynuk, M. and Cordey, F. (1997): Potential for Kutcho Creek Volcanogenic Massive Sulphide Mineralization in the Northern Cache Creek Terrane: A Progress Report; *in* Geological Fieldwork 1996, *B.C. Ministry of Employment and Investment*, Paper 1997-1, pages 157-170.

Mihalynuk, M., Nelson, J.L. and Friedman, R.M. (1998): Regional Geology and Mineralization of the Big Salmon Complex (104N/NE and 104O/NW); *in* Geological Fieldwork 1997, *B.C. Ministry of Employment and Investment*, Paper 1998-1, pages 6-1 to 6-20.

Murphy, D.C. (1998): Stratigraphic Framework for Syngenetic Mineral Occurrences, Yukon-Tanana South of Finlayson Lake: A Progress Report; *in* Yukon Exploration and Geology 1997, Exploration and Geological Services Division, Yukon, *Indian and Northern Affairs Canada*, pages 51-58.

Murphy, D.C. and Piercey, S.J. (1999): Finlayson Project: Geological Evolution of Yukon-Tanana Terrane and its Relationship to Campbell Range Belt, Northern Wolverine Lake Map Area, Southeastern Yukon; *in* Yukon Exploration and Geology 1998, Exploration and Geological Services Division, Yukon, *Indian and Northern Affairs Canada*, pages 47-62.

NGR (1981): National Geochemical Reconnaissance - Southern Yukon Territory and Northern British Columbia (104N, O, P; 105B); *Geological Survey of Canada,* 1:2,000,000 Coloured Compilation Map Series, Open File 733.

Nelson, J.L. (1997): Last Seen Heading South: Extensions of the Yukon-Tanana Terrane into Northern British Columbia; *in* Geological Fieldwork 1996, *B.C. Ministry of Employment and Investment*, Paper 1997-1, pages 145-156.

Nelson, J.L. (1999): Devono-Mississippian VMS Project: Continuing Studies in the Dorsey Terrane, Northern British Columbia; *in* Geological Fieldwork 1998, *B.C. Ministry of Energy and Mines*, Paper 1999-1, pages 143-155.

Nelson, J. (this volume): Ancient Pacific Margin Part VI: Still heading south: continuation and re-evaluation of potential VMS hosts in the eastern Dorsey Terrane, Jennings River (104O/1; 7,8,9,10)*; B.C. Ministry of Energy and Mines*, Geological Fieldwork 1999, Paper 2000-1.

Nelson, J., Harms, T.A., Zantvoort, W., Gleeson, T. and Wahl, K. (2000): Geology of the southeastern Dorsey Terrrane, 104O/7, 8, 9, 10; *B.C. Ministry of Energy and Mines*, Geological Survey Branch, Open File 2000-4.

Nelson, J.L., Harms, T. and Mortensen, J. (1998): Extensions and Affiliates of the Yukon-Tanana Terrane in Northern British Columbia; *B.C. Ministry of Energy and Mines*, Paper 1998-1, pages 7-1 to 7-12.

Northern Miner (1995): 'Kudz Ze Kayah discovery augers well for exploration in Yukon'; *The Northern Miner*, November 27, 1995 issue, pages C1-C4.

Northern Miner (1997): 'Perseverance pays for Cominco in Yukon'; *The Northern Miner*, September 15, 1997 issue, pages B1-B3.

Pass, H.E. (in preparation): Geochemistry of the Suspended and Dissolved Loads in Streams of the Big Salmon Complex, Northern British Columbia; *University of Victoria*, unpublished B.Sc. thesis.

Phendler, R.W. (1982): Report on Assessment Work (Diamond Drilling) on the Arsenault #1, #2, and #3 Claims, Jennings River Area, Atlin Mining Division, British Columbia; *B.C. Ministry of Energy and Mines*, Assessment Report 10411.

Piercey, S.J., Hunt, J.A. and Murphy, D.C. (1999): Lithogeochemistry of Meta-Volcanic Rocks from Yukon-Tanana Terrane, Finlayson Lake Region, Yukon: Preliminary Results; *in* Yukon Exploration and Geology 1998, Exploration and Geological Services Division, Yukon, *Indian and Northern Affairs Canada*, pages 125-138.

RGS (1978): Regional Geochemical Survey, Atlin map area (NTS 104N); *B.C. Ministry of Energy and Mines,* NGR 28.

RGS (1979): Regional Geochemical Survey, Jennings River map area (NTS 104O); *B.C. Ministry of Energy and Mines,* NGR 41.

Rose, A.W., Hawkes, H.E. and Webb, J.S. (1979): Geochemistry in Mineral Exploration, Second Edition; *Academic Press*, 657 pages.

Sawyer, J.B.P. (1967): Geological and Geochemical and Physical Report for Assessment Credit on the Top Claim Group, Swift Lake Area, B.C.; *B.C. Ministry of Energy and Mines*, Assessment Report 1149.

Sawyer, J.B.P. (1979): Report on the 1979 Drilling Program on the Arsenault Claims Copper Prospect, Jennings River Area, Atlin Mining Division, B.C.; *B.C. Ministry of Energy and Mines*, Assessment Report 8022.

Schroeter, T.G. (1999): British Columbia 1998 Mineral Exploration Review; *B.C. Ministry of Energy and Mines*, Information Circular 1999-1, 18 pages.

Sibbick, S.J. and Laurus, K.A. (1995): Investigation of a Natural Acid Rock Drainage and an Anomalous Mercury-Bearing Stream, Northern Vancouver Island (92L/12, 102I/9); *in* Geological Fieldwork 1994, *B.C. Ministry of Energy, Mines and Petroleum Resources*, Paper 1995-1, pages 67-70.

Sebert, C. and Hunt, J.A. (1999): A Note on Preliminary Lithogeochemistry of the Fire Lake Area; *in* Yukon Exploration and Geology 1998, Exploration and Geological Services Division, Yukon, *Indian and Northern Affairs Canada*, pages 139-142.

Telmer, K. (1997): Field and Laboratory Methodology: Ecogeochemistry in the Tapajos River Basin - Canada-Brazil International Cooperation Project; *Geological Survey of Canada*, unpublished internal report.

Traynor, S. (1999): Tanana Exploration update on Southern Yukon/Northern B.C., Bigtop, Arsenault and King Lake Properties; unpublished promotional report.

Tucker, T.L., Turner, A.J., Terry, D.A. and Bradshaw, G.D. (1997): Wolverine Massive Sulfide Project, Yukon; *in* Yukon Exploration and Geology 1996, Exploration and Geological Services Division, Yukon, *Indian and Northern Affairs Canada*, pages 53-55.

Turnbull, I. and Simpson, J.G. (1970): Report on a Geochemical Survey and Physical Work on the Top Claim Group, Atlin Mining District; *B.C. Ministry of Energy and Mines*, Assessment Report 2976.

Weary, G.F., Levson, V.M. and Broster, B.E. (1997): Till Geochemistry of the Chedakuz Creek Map Area, British Columbia (93F/7); *B.C. Ministry of Employment and Investment*, Open File 1997-1

Ancient Pacific Margin Part VI
Still Heading South: Potential VMS Hosts in the Eastern Dorsey Terrane, Jennings River (104O/1; 7, 8, 9, 10)

By JoAnne Nelson

KEYWORDS: *Mississippian, Dorsey Terrane, Yukon Tanana Terrane, northern British Columbia, volcanogenic massive sulphides.*

INTRODUCTION

The goal of this project is to trace out, within central northern B.C., stratigraphy favorable to the formation of Early Mississippian volcanogenic massive sulphide deposits similar to Kudz Ze Kayah, Wolverine, and Fyre Lake, which are hosted by the Yukon-Tanana Terrane in the Finlayson Lake belt of central Yukon. Begun in 1997, the project has focussed on two areas, the eastern Dorsey Terrane near the headwaters of the Cottonwood River in central Jennings River map area (Figure 1; Nelson *et al*., 1998a, Nelson, 1999), and the Big Salmon Complex (Mihalynuk *et al*., 1998 and this volume). Fieldwork in the eastern Dorsey Terrane in 1999 extended the area of coverage south into 104O/1, and taking advantage of the expertise and logistical support provided by the new An-

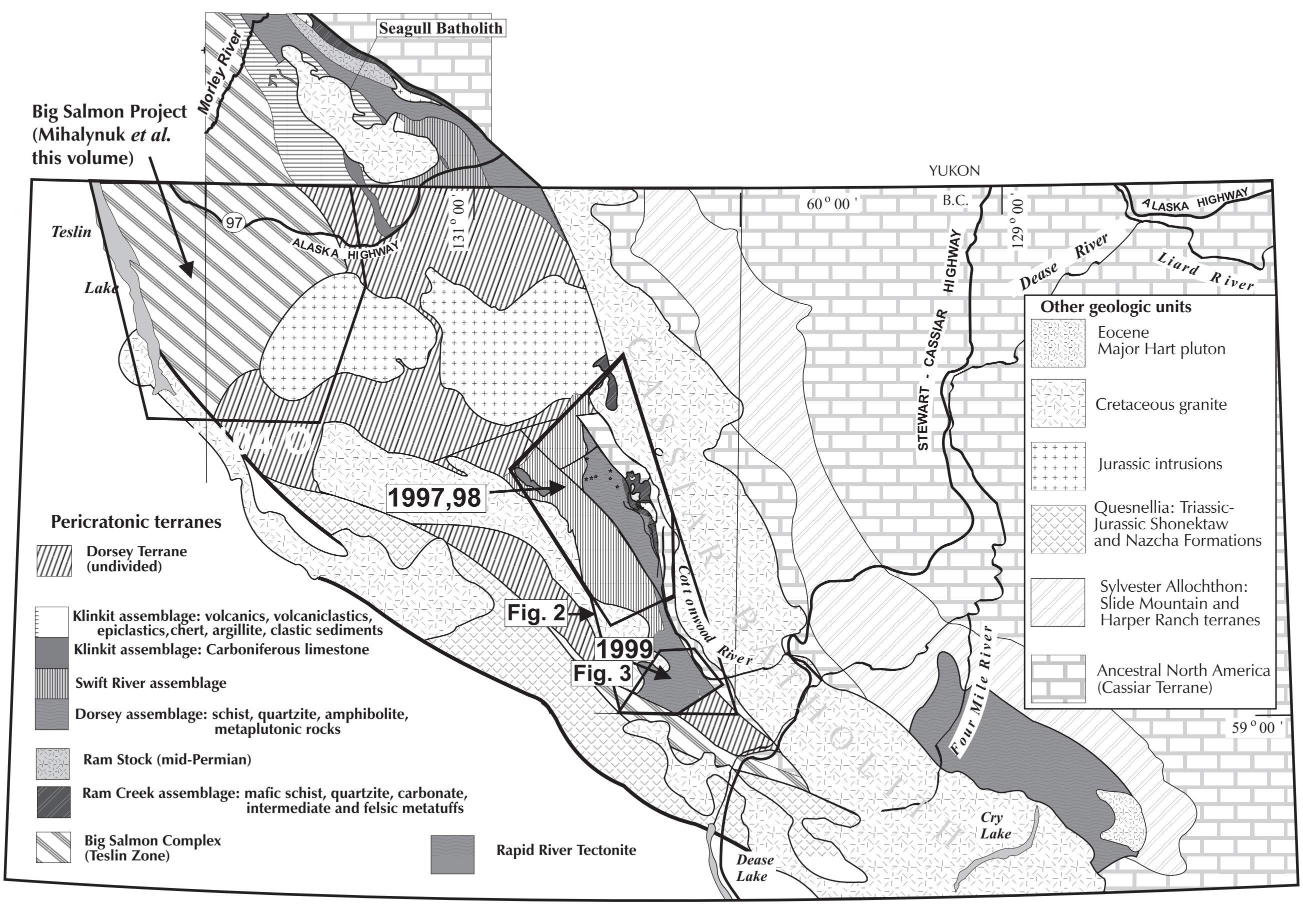

Figure 1. Location and tectonic setting of the southeastern Dorsey Terrane project. Regional geology from Gabrielse (1963, 1969, 1994) and Stevens and Harms (1995).

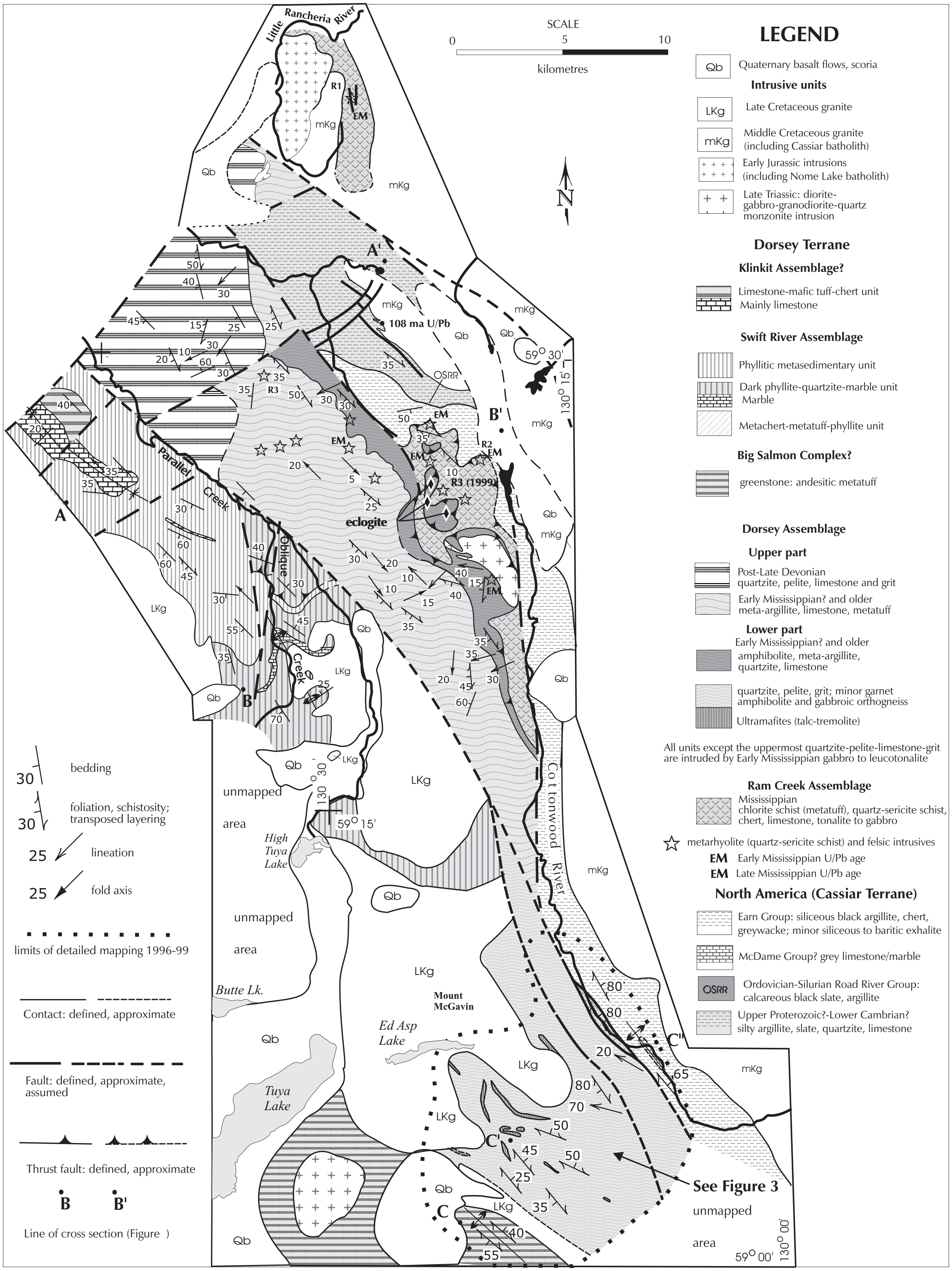

Figure 2. Geology of the area near the headwaters of the Cottonwood River and Parallel Creek (104O/7, 8, 9, 10). Based on 1999 mapping by J. Nelson, M. Mihalynuk, M. DeKeijzer, C. Roots, and P. Erdmer; 1998 mapping by J. Nelson, W. Zantvoort, T. Gleeson and K. Wahl; 1997 mapping by T. Harms, J. Nelson, and M. Mihalynuk; 1996 mapping by J. Nelson; and Gabrielse (1963).

cient Pacific Margin Natmap Project, completed the area covered in 1997-98 with specialized, problem-oriented traverses. A map covering parts of 104O/7, 8, 9 and 10 is now published as an open file (Nelson *et al*., 2000). This report first summarizes the results of a month's new field mapping in 104O/1, and then presents new field and geochronological data that modify and refine geological interpretations from the the 1997-98 map area.

In the central Jennings River map area, the well-exposed basal contact of the Dorsey Terrane rests structurally on metamorphosed basinal strata of the Cassiar Terrane, the western edge of the North American passive continental margin (Nelson *et al*., 1998). Following the usage of Harms and Stevens (1996) the eastern and central Dorsey Terrane has been divided into four assemblages (Figure 2). From most easterly and structurally lowest they are: the Ram Creek, Dorsey, Swift River and Klinkit assemblages. It should be pointed out that the Dorsey Assemblage is a sub-unit of the Dorsey Terrane.

The Ram Creek Assemblage, previously designated the "greenstone-intrusive unit", is confirmed to be of Mississippian age on the basis of three new U/Pb ages on quartz-sericite schist and tonalite. It is interpreted as a Mississippian arc edifice, with a varied volcanic to epiclastic suite ranging from andesite to dacite and rhyolite, accompanied by limestone patch reefs and basinal chert/tuff sequences, all intruded by coeval intermediate plutons. It is comparable to the suite of rocks that hosts VMS deposits in the Yukon-Tanana Terrane near Finlayson Lake, Yukon (Mortensen and Jilson, 1985; Hunt, 1997; Murphy and Piercey, 1999, 2000).

The Dorsey Assemblage, the "metasediment-amphibolite unit", like the Ram Creek Assemblage, is intruded by early Missisippian intermediate to felsic plutons. Unlike the Ram Creek, protoliths and the record of metamorphic/tectonic events in it also predate the early Mississippian. Penetrative ductile fabrics in quartzite and metatuff are cut by the intermediate to felsic intrusions, and eclogite facies metamorphic assemblages are overprinted by those formed at amphibolite grade. The Dorsey Assemblage is overlain structurally by the "metachert-metatuff-phyllite unit", which is assigned to the Swift River Assemblage. This assemblage, which also includes the "dark phyllite-quartzite-marble unit" and the "phyllitic metasedimentary unit" southwest of Parallel Creek (Figure 2), shows lower metamorphic grades and somewhat less intense penetrative deformation than the upper Dorsey assemblage. A large body of limestone and associated mafic metatuff and chert overlies metachert and phyllite of the Swift River Assemblage in the northwestern corner of the map area (Figure 2). This "limestone-tuff-chert unit", considered part of the Klinkit Assemblage, lies on strike with Klinkit limestones north of Klinkit Lake (unit 11g, Gabrielse, 1969).

Mapping in 1999 extended into the southwestern Dorsey Terrane. Greenstones in the mountains southeast of Tuya Lake, tentatively assigned to the Triassic Shonektaw Formation by Gabrielse (1969), strongly resemble metabasalts of the Big Salmon Complex east of Teslin Lake (Mihalynuk *et al.*, this volume). The greenstones near Tuya Lake are separated by a Late Cretaceous granite from lower Dorsey Assemblage metamorphic rocks (Figure 2, 3).

MAPPING IN SOUTHEASTERN JENNINGS RIVER (104O/1)

Mapping of a part of 104O/1 (between the Cottonwood River and Tuya Lake; Figure 3) in 1999 tested strike continuity of units identified in 1997-1998 mapping farther north (Figure 2), and established a partial east-west cross section of the southern Dorsey Terrane. From east to west the following units are exposed: Earn and McDame group equivalents of the westernmost Cassiar Terrane; highly deformed metadiorite; a metamorphic complex of quartzite, grit and pelite with minor ultramafites and metabasites that resembles the lower part of the Dorsey Assemblage; and metabasalts similar to those of the Big Salmon Complex. All of these units are juxtaposed across high-angle faults. In the valley of the Cottonwood River, major northwest-trending faults are accompanied by gently plunging lineations in nearby outcrops. They are probably splays of the Cassiar fault.

North American Marginal Strata (Earn and McDame Groups)

Outcrops along and east of the Cottonwood River are dominated by dark grey to black phyllite and argillite, with lesser dark grey grit and limestone. These rocks are assigned to the Earn Group based on lithologic similarity to its exposures along strike to the north, except for one band of pure grey limestone that may represent the McDame Group. It occurs as a relatively wide, northwest-trending antiformal hinge zone that is best exposed along the banks of the Cottonwood River just below its confluence with Ed Asp Creek (Figure 3). Earn Group exposures typically weather very rusty, due to finely disseminated pyrite. Small grains of andalusite indicate that these rocks have been metamorphosed at low to moderate pressures, like the Earn Group and underlying strata near the headwaters of the Cottonwood River (Nelson *et al*., 1998).

One small subcrop of yellow-white, pyritic chert-barite exhalite was discovered on the northeastern shore of Scaup Lake, a small lake 2 kilometres east of the Cottonwood River (Figure 3). A representative grab sample contains 23,000 ppm (2.3%) barium, along with somewhat anomalous copper (80 ppm) and zinc (154 ppm, INAA; Table 1). The presence of such exhalites allies these rocks with those on the COT claims 5 kilometres south of the Cottonwood River headwaters, where baritic exhalites and anomalous base metals are a recurrent feature within the Earn Group (Nelson, 1997).

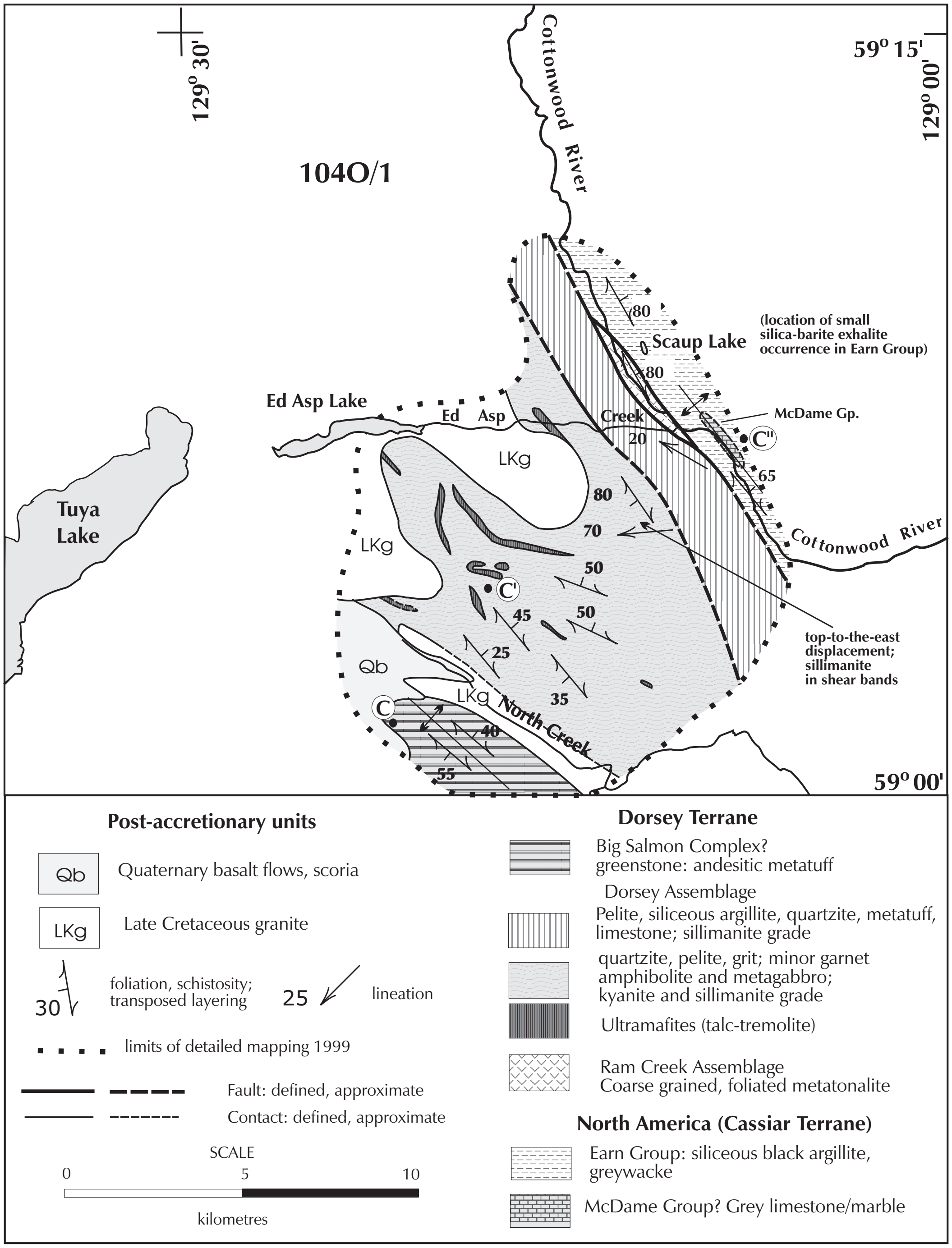

Figure 3. Geology of part of 104O/1. Based on 1999 mapping by J. Nelson and K. Wahl.

Deformed Metadiorite: Ram Creek Assemblage?

Along the Cottonwood River canyon near Ed Asp Creek, Earn Group phyllites and argillites lie in fault contact with a lensoid body of dark green, coarse grained, highly foliated and lineated metadiorite (Figure 3). Its appearance in outcrop is distinctive, with dark green actinolite and biotite streaks standing out in a paler green matrix. This lensoid body can be traced over 5 kilometres in strike length, but is only 500 metres across. Its western contact is a fault against metamorphic rocks of the Dorsey Assemblage. The metadiorite is somewhat variable in texture and composition, ranging from very dark green metagabbro to lighter, more felsic diorite. Mafic minerals have been replaced by elongate smears of actinolite, perhaps due to strike-slip motion on its bounding faults. It resembles metadiorites and metatonalites of the Ram Creek Assemblage near the headwaters of the Cottonwood River.

TABLE 1
ANALYSIS OF ROCK SAMPLE OF SILICA-BARITE EXHALITE, SCAUP LAKE

Element	Au	Ag	Cu	Pb	Zn	Zn	As	Ba	Ca	Co	Cr	Fe	Rb	Sb	Sc	La	Ce
Units	PPB	ppm	ppm	ppm	ppm	PPM	PPM	PPM	%	PPM	PPM	%	PPM	PPM	PPM	PPM	PPM
Method	INA	AICP	AICP	AICP	AICP	INA	INA	INA	INA	INA	INA	INA	INA	INA	INA	INA	INA
Lab.	ACT	ACM	ACM	ACM	ACM	ACT	ACT	ACT	ACT	ACT	ACT	ACT	ACT	ACT	ACT	ACT	ACT
Dect'n Limit	2	0.3	1	3	1	50	0.5	50	1	1	5	0.02	15	0.1	0.1	0.1	3
99JN1-4	**-2**	**1.6**	**80**	**5**	**111**	**154**	**4.2**	**23000**	**5**	**19**	**251**	**3.69**	**98**	**1**	**30.4**	**21.2**	**34**

Notes

Analysis of steel milled @ GSB. Sample. Fe (200-300 ppm) and Cr contamination possible

INA - Thermal neutron activation analysis

ACT - ActLabs, Ancaster, Ontario.

AICP = Aqua regia digestion-ICPES

ACM = ACME Analytical

BAL - Balance

Dorsey Assemblage

Metamorphic rocks occupy most of the mapped area between the Cottonwood River and North Creek (Figure 3). This unit is a fairly monotonous sequence of quartzite, pelite, and grit, including about 2% ultramafite and garnet amphibolite as small lenses and thin tabular bodies (Figure 2, 3). The sequence has undergone Barrovian metamorphism, with biotite-muscovite- plagioclase+ kyanite+sillimanite developed in pelites and quartzites, and coarse tremolite-talc in ultramafites. These thoroughly metamorphosed rocks retain little of their protolith textures, and distinctions between, for instance, granite and grit, are not trivial. All but a possible few of the quartz-plagioclase-mica layers are interpreted as grits, based on the paucity of plagioclase (typically 5-15%), and by their repetitive interlayering with muscovitic quartzite. Photo 1 shows a particularily convincing example of a quartz-pebble conglomerate from the siliciclastic sequence.

Ultramafites and garnet amphibolites form a minor but persistent and characteristic part of the package, occurring as tabular bodies and lenses parallel to layering in the metasediments. The ultramafic bodies are thin but laterally continuous: the longest has a strike length of 3 kilometres. In one ridge-top exposure, ultramafite contains a texturally intact gabbro pegmatite body with comb-textured hornblendes up to 10 cm long. The ultramafites and amphibolites have undergone the same metamorphic and deformational history as the surrounding metasediments; thus their emplacement or juxtaposition must have been a relatively early stage event.

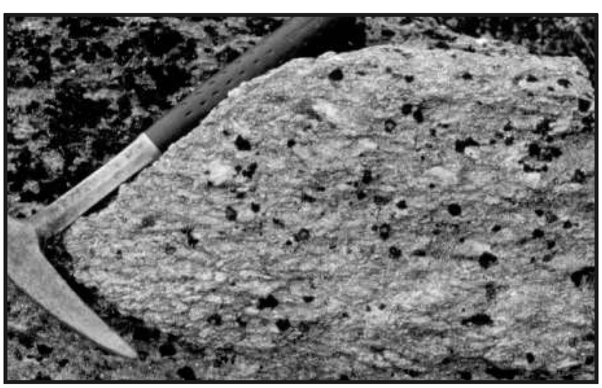

Photo 1. Quartz-pebble conglomerate from a quartzite-grit succession in the Dorsey Assemblage near Ed Asp Lake.

Metamorphism

Garnets are ubiquitous, accompanied by calcic plagioclase (An 30-50), biotite and muscovite in the metamorphosed siliciclastic rocks, and by dark green hornblende±biotite in the garnet amphibolites. Ultramafites are coarse grained assemblages of radiating tremolite and interstitial talc. Bright green actinolite in talc, and massive biotite form discontinuous “blackwall” at their margins.

Kyanite is rare in the metasediments. It forms prisms and, in one sample, strained, recrystallized aggregates with irregular extinction. All kyanite is pre-kinematic, deeply corroded and heavily mantled with muscovite (Photo 2). By contrast, fibrolitic sillimanite grows within syn-kinematic muscovite as well-oriented sheafs and bundles. It also forms sprays of radiating fibres that cut across the foliation. In one key sample, 99JN9-3A, fibrolite is deformed by, and also grows within, top-to-the-east shear bands (Photo 3; location on Figure 3). The succession of kyanite to sillimanite indicates pressure-temperature conditions above the aluminosilicate triple point.

Garnet amphibolites contain pre-kinematic garnet, synkinematic hornblende and in some samples, biotite, plagioclase, and blobby sphenes with tiny relict rutile and ilmenite grains in their cores. In once instance, clinopyroxene is present. These strongly resemble the garnet amphibolites elsewhere in the lower Dorsey Assemblage (Nelson 1999), which are now considered to represent retrograde metamorphism of original eclogite facies assemblages. As is the case farther north, amphibolite-grade metamorphism was complete prior to the juxtaposition of these rocks with the greenschist-grade

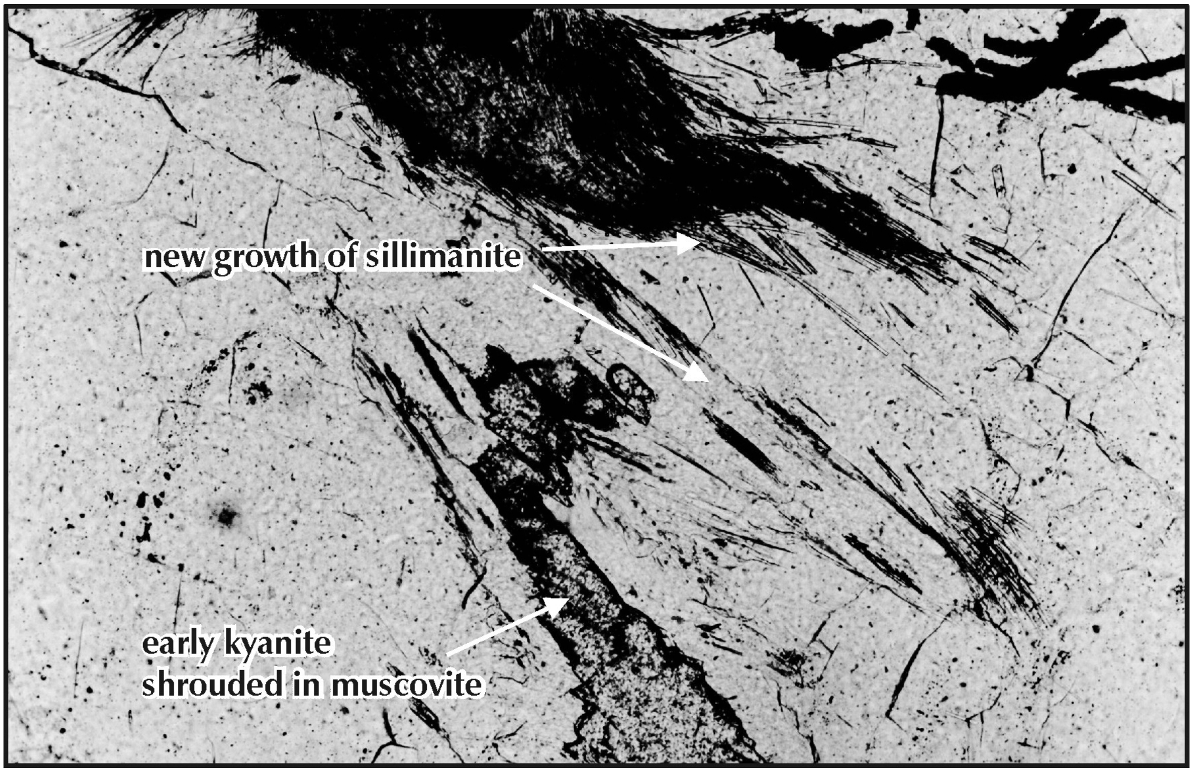

Photo 2. Early kyanite and later sillimanite in metamorphosed impure grit, Dorsey Assemblage near Ed Asp Lake (Field of view 2 X 4 mm).

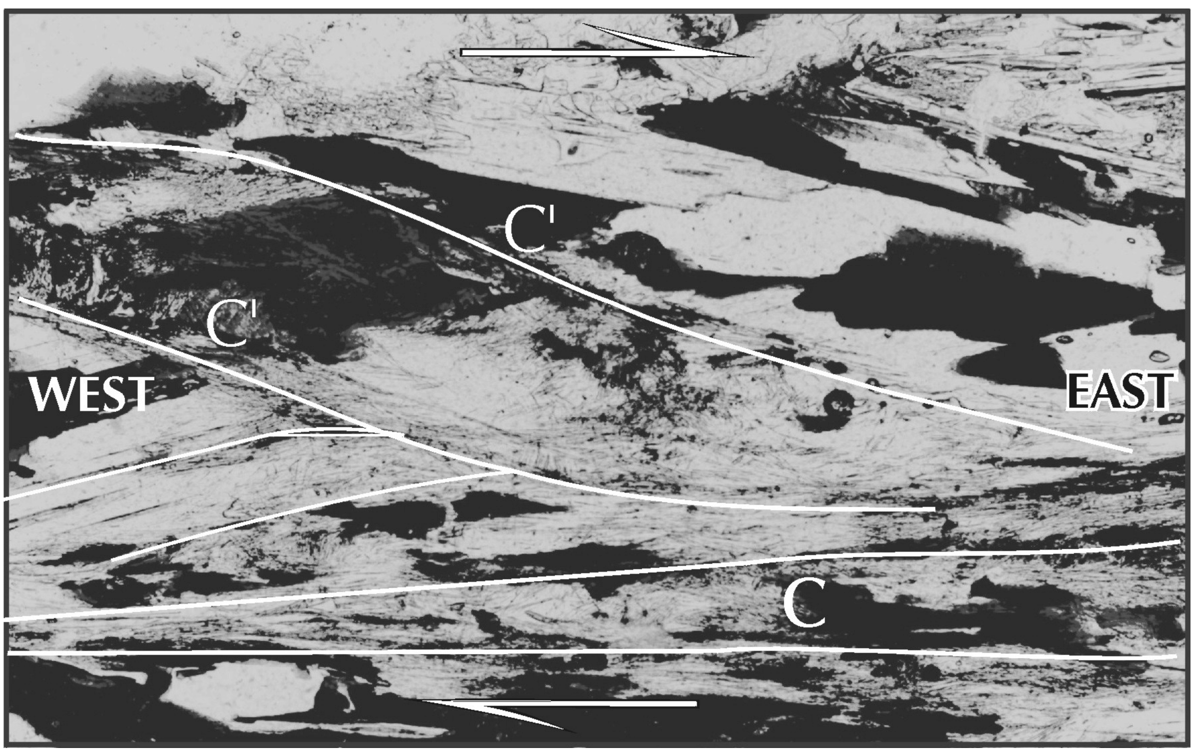

Photo 3. Top-to-the-east shear bands involving metamorphic sillimanite from locality southeast of Ed Asp Lake (Field of view 2 X 4 mm).

metatonalite and the Earn Group, which contains metamorphic andalusite.

Interpretation

The metamorphic sequence in 104O/1 between the Cottonwood River and North Creek is assigned to the lower Dorsey Assemblage, based on its metamorphic grade and the presence of garnet amphibolite and ultramafite. Although minor exposures of pelite and quartzite with garnet amphibolite occur near the base of the Dorsey Assemblage between 3 and 12 kilometres south of the Cottonwood River headwaters, this broad region of dominantly coarse, siliciclastic sediments is unusual in the Dorsey Assemblage and indeed in the Dorsey Terrane as a whole. The area is also anomalous in the widespread preservation of original metamorphic assemblages. The chlorite overprint that is pervasive farther north is not developed here, and thus these rocks provide a window into the early high-grade metamorphic history of the Dorsey Assemblage.

The association of coarse siliciclastic metasediments with minor, thin, layer-parallel ultramafic to mafic bodies poses a conceptual problem. Are the ultramafites and metabasites mantle materials that mark thrust faults? In this case, why does the rock sequence not change across them? What tectonic environment is being telescoped: one of pure quartzite and grit deposited across an ophiolitic basement? Alternatively, could the ultramafites and garnet amphibolites have been sills and dikes within a continental sequence, as described within the Late Proterozoic Horsethief Creek Group by Sevigny (1988)? Petrochemical studies in progress will give clues to the origin of these rocks.

Big Salmon Complex?

Dark green metatuffs on the southwestern side of North Creek are separated from the Dorsey Assemblage by an elongate, northwesterly striking granite body. Although this unit was tentatively assigned to unit 17, the Shonektaw Formation, by Gabrielse (1969), it bears little resemblance either in original volcanic textures and mineralogy, or in metamorphic and structural history to typical Shonektaw exposures. Protoliths for these rocks were a monotonous sequence of laminated tuffs, some with very small plagioclase crystals. Conspicuously absent are the augite phenocrysts so typical of Triassic volcanics of Quesnellia. Layering in the tuffs has been transposed, and the transposition fabric outlined by actinolite, albite, epidote and chlorite is itself refolded. Yellow-green stripes of epidote subparallel to compositional laminations are common.

The metatuffs are intruded by small bodies of gabbro-diorite with highly variable composition and texture. They range from pegmatitic to diabasic, from seriate porphyritic to coarse-grained equigranular, and from hornblende-dominated to equal abundance of hornblende and plagioclase. These variations occur over as little as a few metres. The intrusive rocks are foliated, but they cross-cut the intense transposition fabric of the metatuffs. They in turn are cut by unfoliated, fine grained, acicular hornblende-phyric andesite dikes. The gabbro-diorite and acicular hornblende porphyries are texturally like Triassic and Jurassic intrusive rocks seen elsewhere in the Dorsey Terrane, as well as in Quesnellia. They also resemble gabbros near Logjam Creek in northern Jennings River area, which are now known to be early Mississippian (Gleeson *et al*., this volume). If either correlation is correct, then the metatuffs are most likely Paleozoic, since they were deformed and metamorphosed prior to emplacement of the intrusions.

The laminated and epidote-striped textures of the metatuffs are like those of the greenstone unit of the Big Salmon Complex near Logjam and Two Ladder Creeks (Mihalynuk *et al*., 1998). Mapping in 1999 (Mihalynuk *et al*., 2000) has shown that this unit extends at least as far south as the Jennings River and east to Butsih Creek (latitude 59°30'), roughly on strike with the North Creek metatuffs. It is possible that the greenstone unit lies along the southwestern margin of the Dorsey Terrane throughout the Jennings River map area. In northern Jennings River and Wolf Lake map areas this unit is highly prospective for volcanogenic massive sulphide deposits (Roots *et al*., 2000; Mihalynuk *et al*., this volume). It hosts occurrences of quartz-sericite schist, some accompanied by multi-element soil geochemical anomalies (Ed Balon and Wojtek Jakubowski, personal communication 1998, 1999), and it is directly overlain by manganese-barium-bearing, metamorphosed siliceous exhalite, the crinkled chert unit of Mihalynuk *et al*. (1998).

Although it is now invaded by a Late Cretaceous granite, the precursor contact between the greenschist-facies metatuff unit and the amphibolite grade siliciclastic Dorsey Assemblage is interpreted to have been a steep west-side-down fault.

Late Cretaceous granite

Both the Dorsey Assemblage and metatuff unit are intruded by granitic plutons, apophyses of the Parallel Creek batholith (Gabrielse 1969). This body has yielded a biotite K-Ar age of 78+4 Ma (GSC 67-14). The granite is medium grained, mostly equigranular, with biotite and muscovite. It is unfoliated to very weakly foliated; its apophyses interfinger extensively with the metamorphic country rocks. The granite body at the head of North Creek has a gently convex upper contact that has domed the layered rocks above it (Figure 3 and cross section 4c). Structural attitudes in the Dorsey Asemblage are deflected to northeasterly to the south of this dome, indicating forceful diapiric emplacement of the intrusion.

Structure

The gross structure of 104O/1 differs from that farther north (*see* Nelson, 1999, and discussion in following section of this paper). Near the headwaters of the Cottonwood River, layered rocks overall dip gently to moderately southwest and major thrust contacts are less steep than layering within units (Figure 4 A-A' and B-B'). The Ram Creek and Dorsey/Swift River/Klinkit assemblages form a gently southwest-dipping stack, a geometry that reflects their emplacement as allochthons onto the margin of the Cassiar Terrane. By contrast, layered sequences of Cassiar Terrane and Dorsey Assemblage in 104O/1 form a set of homoclinal, steep northeasterly dipping panels (Figure 4, C-C'-C''). Intact, top-to-the-east shear sense indicators near the base of the Dorsey Assemblage in 104O/1 (Figure 3, photo 3) suggest that this configuration represents the overturning of a once gently-dipping east-verging thrust sequence like that shown in Figure 4, sections A-A' and B-B'.

Minor structures were formed during two phases of deformation. Geometrically these show identical expressions in the North American rocks, the metadiorite, and the Dorsey and Big Salmon(?) assemblages. D_1 created transposition fabrics in all of the units, isoclinal intrafolial folds, and mineral lineations. Although no major D_1 folds are recognized, the great apparent thickness of Dorsey Assemblage metasediments, and converging trends of some of the ultramafic bodies suggest that they are present (Figure 3). Minor linear elements show a contour density peak at 331°/15° and a subsidiary peak of steep westerly plunges at 270°/75 °(Figure 5). Streaky biotite lineations in the sample in which fibrolite displays top-to-the-east shear (Photo 3) belong to the steeply plunging population, with an orientation of 266°/66°.

Actinolite and biotite streaks in the metadiorite exposed along the Cottonwood River (Figures 3 and 5) plunge gently to the northwest. They are geometrically and mineralogically like D_1 linear structures; however their intense development in proximity to cataclastic zones interpreted as major steep faults suggests that they may have developed during late transcurrent motion. No kinematic indicators were observed associated with them.

The second deformational event, D_2, folds the transposition fabrics. Outcrop-scale open to close folds are common in quartzites of the Dorsey Assemblage. A mountain-scale open synform affects the Big Salmon(?) greenstone southwest of North Creek. McDame Group(?) limestone is exposed in an open antiformal culmination cut by the Cottonwood River. Minor folds show a well-developed contour density peak at 322°/06°. Southwesterly

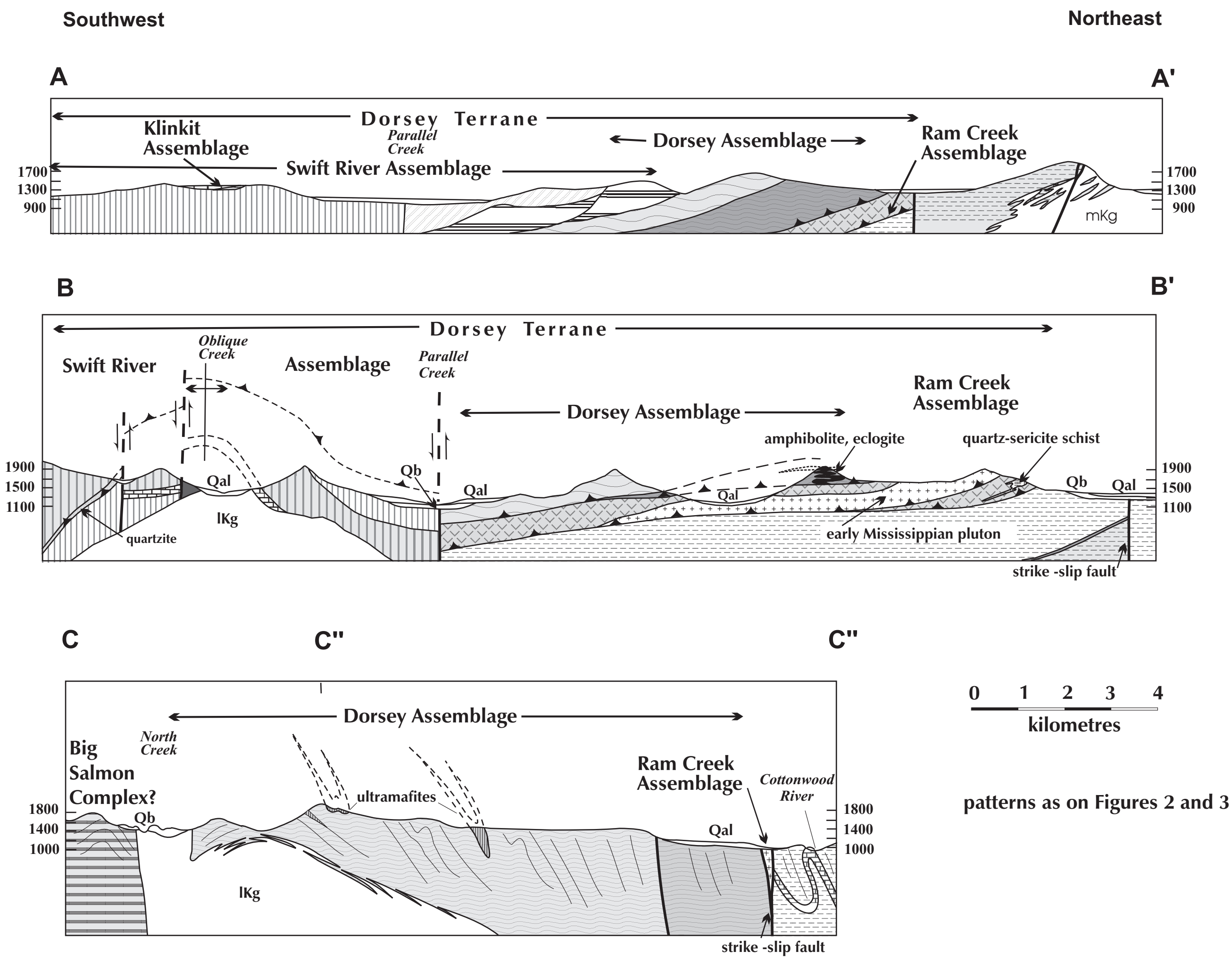

Figure 4. Cross sections of the eastern Dorsey Terrane and western edge of the Cassiar Terrane; locations on Figures 2 and 3.

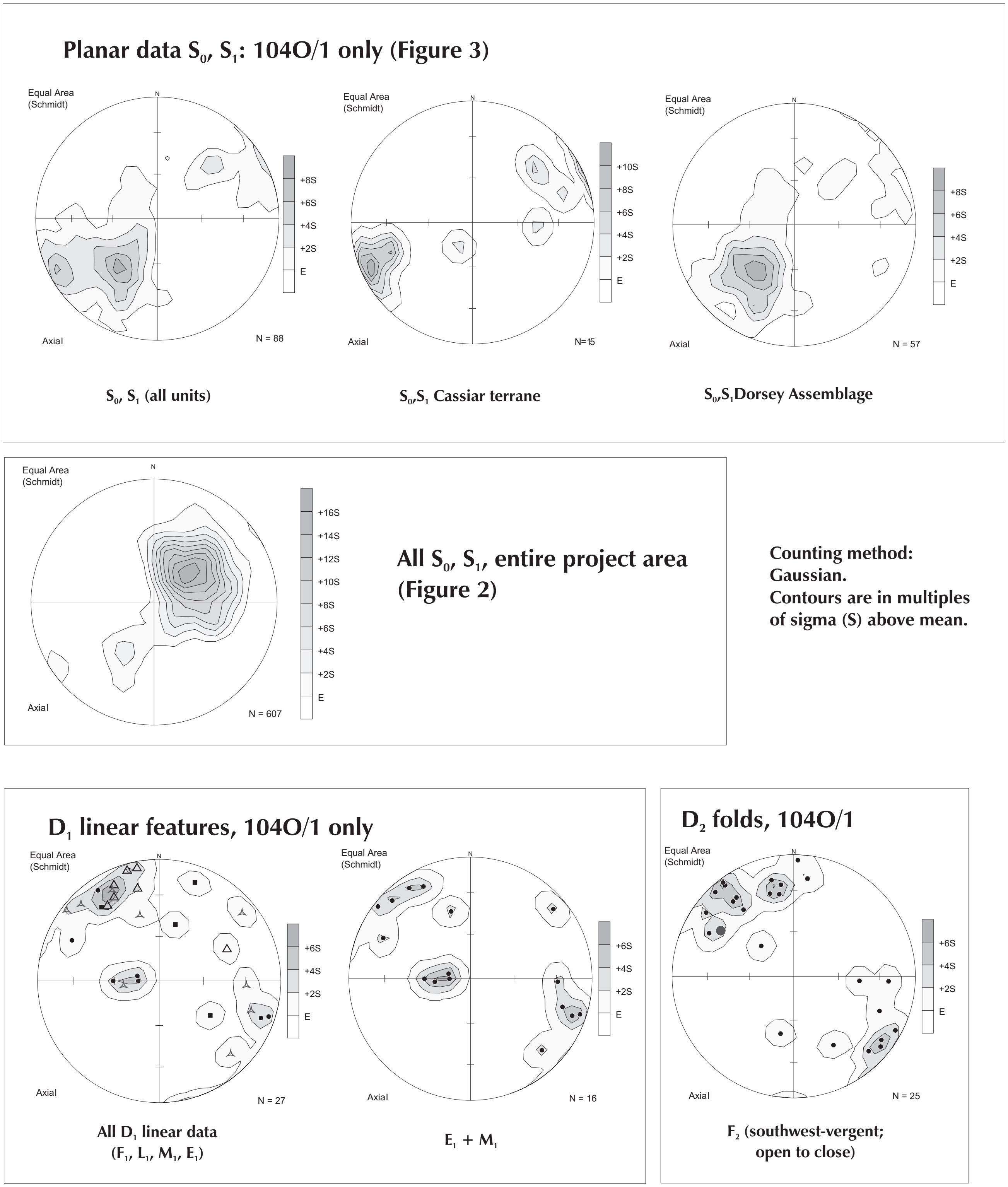

Figure 5. Structural data from 104O/1.

Photo 4. Southwest-verging outcrop-scale fold in Dorsey Assemblage quartzites (D_2).

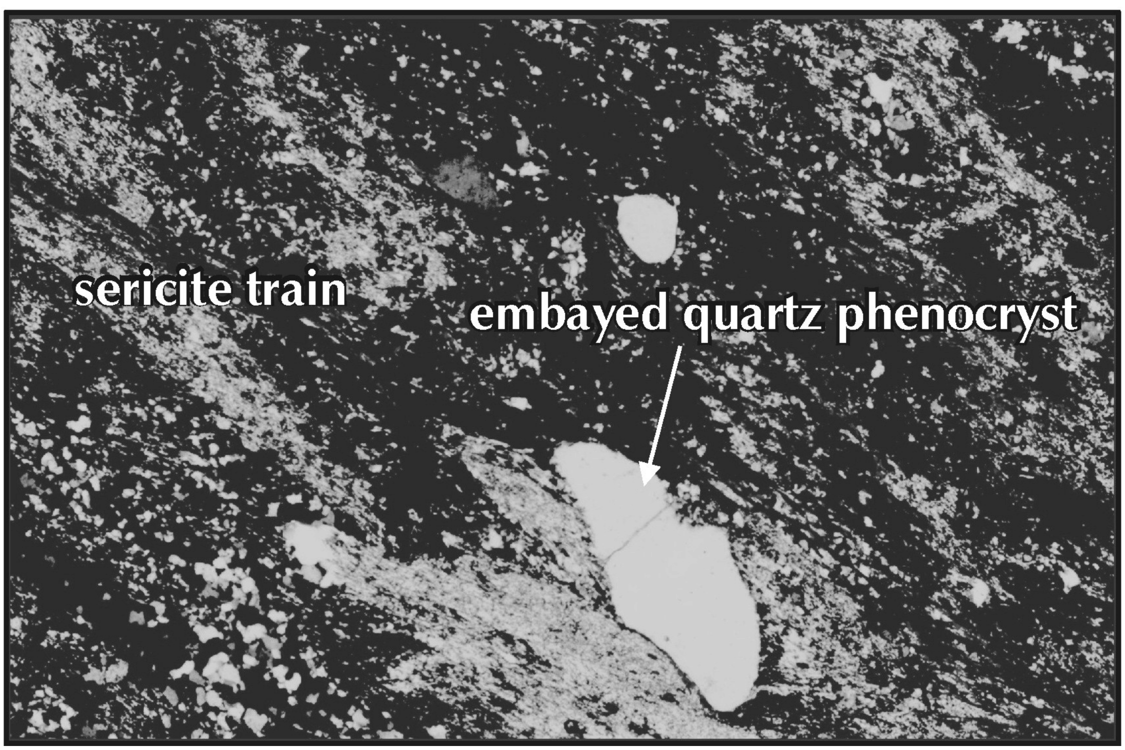

Photo 5. Photomicrograph of quartz-phyric quartz-sericite schist in the upper Ram Creek Assemblage (Field of view 2 X 4 mm).

vergences dominate in the Dorsey Assemblage (Photo 4). Thin, weakly foliated granite sills are affected by the D_2 deformational event. One of them was collected for uranium-lead dating.

D_2 is not recognized along strike farther north along the Cottonwood River. The southwesterly vergences associated with it may relate to the inferred post-accretion southwesterly overturning of the sequence that makes the cross section in this area so different from those farther north (Figure 4). The cause for this difference is unclear. It could have arisen from local transpression related to the regional Cassiar Fault.

NEW DATA AND INTERPRETATIONS RELEVANT TO 1998 MAP AREA (104O/ 7, 8, 9, 10)

The joint field program afforded by the Ancient Pacific Margin Natmap in August 1999 brought a strong scientific team to bear on some of the outstanding geological problems in the 1998 map area. New radiometric data obtained in 1999 have strengthened our interpretations of some of the map units, in particular the potentially economically significant Ram Creek Assemblage. These new results and conceptual advances are summarized here, as an update to Nelson (1999) and accompaniment to the open file map (Nelson *et al*., 2000).

Ram Creek Assemblage

The Ram Creek Assemblage has two main outcrop areas, one south of the bend in the Little Rancheria River at the northern end of the map area, and one immediately west of the lake at the headwaters of the Cottonwood River (Figure 2). Pyritic quartz-sericite schist, with relict quartz and plagioclase phenocrysts, forms a significant part of both of these exposures. Samples were collected by J. Mortensen for uranium-lead dating in 1998. The northern quartz-sericite schist is 320-325 Ma with a maximum probable age of 336±4 Ma; the southern one is 334±6 Ma (Richard Friedman, personal communication 1999). These two dates are essentially coeval, and represent a previously unrecognized late Mississippian felsic volcanic event in the area. This event has several regional parallels, including tuffs near Mt. Francis in the upper part of the Big Salmon Complex (Mihalynuk *et al*., 1998 and this volume), rhyolite bodies that hosts the Tulsequah Chief deposit (Childe, 1995), and felsic volcanic rocks near Little Salmon Lake (Colpron, 2000).

A strongly deformed, well-foliated metatonalite in the Ram Creek Assemblage west of the Cottonwood River headwaters has an early Mississippian U-Pb age of 356.3±6 Ma (R. Friedman, personal communication, 1999). It lies structurally higher than the dated late Mississippian felsic volcanic sequences, but structurally lower than extensive quartz-eye porphyry tuffs and flows/intrusions identified within the upper Ram Creek Assemblage two kilometres west of the Cottonwood headwaters (Photo 5; locality R3 on Figure 2). This indicates that the Ram Creek Assemblage itself is internally imbricated.

The Ram Creek Assemblage contains a record of both early and late Mississippian arc-related igneous activity. This range of igneous ages is like that of the Yukon-Tanana Terrane in the Finlayson belt and central Yukon (Murphy and Piercey, 1999, 2000, Colpron, 2000).

Dorsey Assemblage

The Dorsey Assemblage is a complex of metamorphic and intrusive rocks, including highly deformed Mississippian plutons (349.9±4.2 Ma; Nelson *et al*., 1998a; 355.3±.9; 340.4±5.5 Ma; R. Friedman, personal communication 1999). In its lower part, amphibolite-grade metamorphic assemblages are common. The upper Dorsey Assemblage has been thoroughly metamorphosed at chlorite grade, although relict garnets hint at earlier high-grade metamorphism. The contact between upper and lower parts is transitional, involving the upwards disappearance of metabasites. Metamorphosed granitoids also become rare in the upper Dorsey Assemblage.

The Dorsey Assemblage overlies the Ram Creek Assemblage above a major thrust fault (Figure 4). The interpretation of the Dorsey-Ram Creek contact as a thrust fault is partly based on older-over-younger relationships: the youngest rocks in the underlying Ram Creek Assemblage are late Mississippian; the oldest rocks in the Dorsey Assemblage are pre-Mississippian. Other evidence includes strong shearing near the contact, and emplacement of amphibolite-grade over greenschist-grade rocks. North of the Yukon border, this fault is constrained to be post-mid-Permian because it truncates the Ram Stock (Stevens and Harms 1995), but pre-Jurassic because it is sealed by a (locally undated) pluton of the Early Jurassic suite (Stevens, unpublished mapping; and author's field observations, 1999). Mississippian plutons are a common element that link the Dorsey and Ram Creek assemblages. Therefore the fault that separates the Dorsey from the Ram Creek Assemblage is considered to be a major intra-arc feature, not a terrane boundary.

High P/T Metamorphism in the Dorsey Assemblage

The lower part of the Dorsey Assemblage contains large bodies of garnet amphibolite. Prior to 1999, remnants of eclogite facies metamorphism had been recognized in a single thin section (Philippe Erdmer, personal communication, 1998). Fieldwork by Erdmer in August 1999 resulted in the discovery of two new eclogite outcrops within garnet amphibolite, showing a wider distribution of eclogite than previously recognized. Garnet amphibolites throughout the Dorsey Assemblage contain abundant large titanites with tiny grains of rutile and/or ilmenite in their cores, which may represent the last vestiges of eclogite-grade metamorphism. In general the mineralogy and texture of the amphibolites are identical to those described as retrograde products of eclogites elsewhere on the fringes of the Yukon-Tanana Terrane

(Erdmer 1992) The amphibolites show sharp, unsheared contacts with surrounding schists and quartzites, and are isoclinally interfolded with them. There is no evidence that the eclogites were discrete slivers incorporated into their matrix at a late stage. Rather, it is most reasonable that first eclogite and then garnet amphibolite facies metamorphism affected at least the lower part of the Dorsey Assemblage. This probably requires that the Dorsey Assemblage was partly subducted prior to its residence in a mid- to lower crustal setting.

The garnet amphibolite-facies metamorphism predated the thrusting of the Dorsey Assemblage on top of the greenschist-grade Ram Creek Assemblage, and of the juxtaposition of these with the underlying Cassiar Terrane, which contains andalusite and cordierite as a peak metamorphic assemblage (Nelson, 1998).

The overall thickness of the Dorsey Assemblage, measured from its base to its upper contact with the Swift River Assemblage, is only 1600 metres (Figure 4. Section A-A'). This poses a problem with respect to the high grade metamorphic assemblages in its lower part. What constituted the tectonic load necessary to create high pressures within it? Where are the rocks now, and how were they removed? By erosion? By detachment faulting? When did this occur?

Relationship of the Dorsey and Swift River Assemblages

Unlike its basal thrust fault contact, the nature of the upper contact of the Dorsey Assemblage, and therefore the relationship of the Dorsey to the overlying Swift River assemblage, have not been well described or understood. This problem formed a focus of interest for 1999 field work both here and in the Yukon (Roots *et al*., 2000). During the re-examination the 1997-98 map area, two previously unknown exposures of the Dorsey-Swift River contact were studied.

Regionally, the Dorsey Assemblage contains pre-Mississippian rocks but also a post-Late Devonian grit within the uppermost "quartzite-pelite" unit (Nelson 1999). The overlying Swift River Assemblage has no internal age control. It is probably post-early Mississippian because it is not intruded by this prominent plutonic suite. It is depositionally overlain by late Mississippian to early Pennsylvanian limestone (Nelson, 1997, and 1999 field observations).

The Swift River Assemblage overlies the Dorsey Assemblage on a gently southwest-dipping, foliation-parallel contact. This contact is exposed on a low hill south of the Little Rancheria River in the northernmost part of the map area (Photo 6), and on two ridges northeast of Parallel Creek, where the "metachert-metatuff-phyllite unit" overlies the "quartzite-pelite" and the upper metasedimentary unit of the Dorsey Assemblage (Figure 2). Although regionally there are distinct differences between these units, locally the rock types above and below the contact are not greatly dissimilar. Quartzites, green chloritic metatuffs and metacherts occur in both assemblages. On the more northerly of the two ridges near Parallel Creek, a transitional contact is drawn below the structural level where well-bedded chert and phyllitic argillite become a dominant part of the section. This approximately corresponds to the upper limit of metamorphic garnet, although pre-kinematic garnets are present at scattered localities in the lower Swift River Assemblage.

On the hill near the Little Rancheria River and on the more southerly of the two ridges near Parallel Creek, the Dorsey/Swift River contact is more abrupt. Near Parallel Creek, a steep fault juxtaposes upper Dorsey chlorite-muscovite-garnet phyllite with Swift River dark grey argillite, siltstone and chert. Near the Little Rancheria River, white bedded chert overlies chlorite-muscovite-garnet phyllite and orthoquartzite; rocks near the contact are broken into a series of lensoid packages with strong internal deformation. A series of low angle (normal?) faults is inferred (Photo 6).

The Dorsey/Swift River contact, where not obscured by faults, appears to be a lithologic gradation. Although mappably distinct, the Swift River and upper Dorsey assemblages represent similar depositional environments of basinal sedimentation with periodic influx of distal tuffs and quartz (-plagioclase) sandstones. Unusually

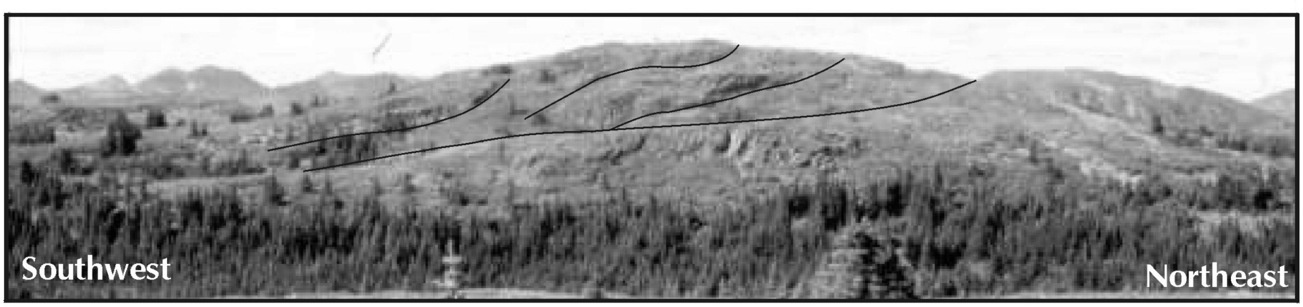

Photo 6. Base of the Swift River Assemblage south of the Little Rancheria River. Strongly deformed quartzite (metachert) is broken into a series of gently southwest-dipping panels. Structures within the panels are steep and discordant with each other. Gently dipping normal faults are inferred between the panels.

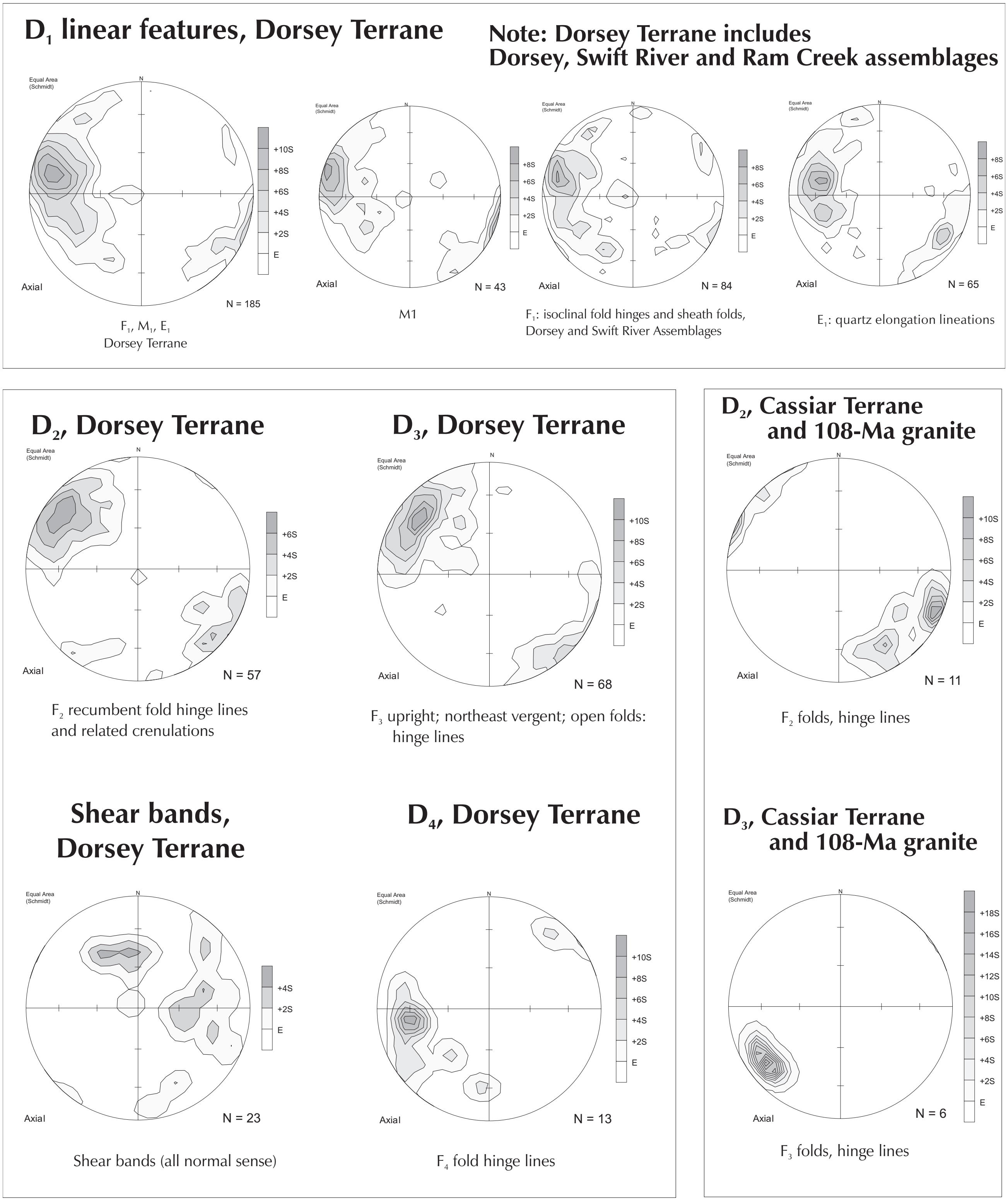

Figure 6. Structural data from 104O/7, 8, 9, 10.

abundant tourmaline is seen in thin sections of metasediments and metatuffs from both assemblages. Their structural histories are similar (*see* below).

Unlike the Dorsey/Ram Creek contact, which is an obvious thrust fault, the contact between the Dorsey and Swift River assemblages is a shear-modified lithologic and metamorphic gradient. It may have been the locus of significant motion, but it does not show the character of a terrane boundary.

Structural History of the Dorsey and Swift River Assemblages

Detailed work by Martin deKeijzer, Mitch Mihalynuk and Charley Roots has improved understanding of the structural history of the Dorsey Assemblage and its relationship to the Swift River Assemblage. The Dorsey Assemblage has undergone a protracted deformation history, from pre-Mississippian to post-Late Triassic (Nelson, 1999). The intensity of the deformation is shown by isoclinal folds at scales ranging from microscopic to mountain-size, refolded isoclines and sheath folds, and mineral and quartz-elongation lineations. Although less metamorphosed, the Swift River Assemblage exhibits a similar structural style. In particular, early southwest-plunging, “downdip” quartz lineations, refolded isoclines and sheath folds have now been observed at several localities in the lower Swift River Assemblage, suggesting that it was affected by the same deformational events as the Dorsey Assemblage.

Figure 6 shows structural data from the combined Dorsey and Swift River assemblages in the central Jennings River map area. The outlined sequence of four structural events is simplified from that in Nelson (1999).

Widespread planar fabrics are assigned to D_1, although scattered remnants hint at an earlier and probably intense deformation history. Very early planar fabrics include those in relict eclogites, foliations preserved within garnets, and foliations cross-cut at a very low angle by sill-like, highly deformed (Mississippian?) granitoids. This early deformation involved layer transposition and thorough development of metamorphic textures not seen in the granitoids.

D_1 includes transposition fabrics, intrafolial isoclines, isoclines that are refolded by other isoclines, sheath folds, and the development of linear fabrics involving amphibole, muscovite, biotite, and quartz. Major isoclinal hinge lines, such as those of folded garnet amphibolite bodies, trend west-northwest. Linear fabrics (fold hinge lines, mineral and quartz lineations) form a girdle from a maximum contoured density of 283°/06° to a subordinate cluster near 230°/40° (Figure 6). Quartz lineations in early Mississippian (349.9±4.2 Ma) metatonalite plot in both clusters. Minor granitoid sills form sheath folds.

D_2 features include recumbent isoclinal folds, isoclines that refold other isoclines, crenulations on S_1, and mineral lineations that involve retrograde minerals such as chlorite or actinolite. Geometrically D_2 linear features are like those of D_1, except that they cluster well with a WNW trend and never show steep southwesterly plunges (Figure 6). D_1 and D_2 were probably part of a single episode of progressive shear deformation.

D_3 features include open, upright and chevron-style folds, and cleavages that are not parallel to the D_1 and D_2 transposition layering. F_3 is coaxial with F_2 (Figure 6), and may represent the waning stages of deformation. Folds with styles like these affect stratified units in the Cassiar Terrane and also apophyses of mid-Cretaceous granite. They are designated F_2, as they only demonstrably fold a single older transposition fabric. They are coaxial with F_3 folds in the Dorsey Terrane (Figure 6), and it is possible that they developed together.

D_4 comprises sporadic west-southwesterly to southwesterly kinks. The hinge lines of F_3 kinks in Cassiar Terrane rocks form a contoured maximum that plots slightly to the southwest (Figure 6).

In the field and microscopically, three shear-sense populations can be distinguished. The first occurs near the base of the Dorsey Assemblage and is associated with down-dip, west to southwesterly-plunging quartz lineations. Top-to-the-northeast and east shear indicators such as muscovite fish, asymmetric pressure shadows, C-S fabrics and C’ shear bands are developed in assemblages that range from peak metamorphic through retrograde conditions. At a locality southeast of Ed Asp Lake (Figure 3), synkinematic sillimanite is deformed by, and also recrystallized into, top-to-the-east shear bands (Photo 3). At the locality described in Nelson (1999), this shear deformation affects an undated, but probably Mississippian, granitic orthogneiss. Mineral assemblages syn-kinematic to the shearing range from muscovite-biotite-clinozoisite-(garnet?) to late sericite-chlorite. One sample from the top of the Ram Creek Assemblage shows the effects of top-to-the-northeast motion. This episode matches D_1 in orientation and style. D_1 sheath folding is probably related to northeasterly transport.

The second shear-sense group, which only involves retrograde assemblages, is more common in the upper part of the Dorsey Assemblage. In samples with well-developed west-northwesterly chlorite and muscovite lineations, top-to-the-west-northwest shear bands and assymmetric pressure shadows around garnet porphyroblasts are seen microscopically (Photo 7). These lineations correspond to the D_2 episode. Perhaps the shear sense is the expression of an orogen-parallel component of motion.

Two sets of steep macroscopic shear bands were seen in mapping in 1999 (Photo 8; Figure 6). They concentrate in the upper Dorsey Assemblage, but are also present in the Swift River, lower Dorsey and even in the Ram Creek Assemblage. They indicate top-down-to-the-southwest and top-to-the-west shear. Development of retrograde chlorite-muscovite in the shear bands suggests that they formed late in the kinematic history. Top-down-to-southwest and west sense of shear would result in the structurally higher, lower grade, and probably younger Swift River Assemblage moving downwards with respect to the

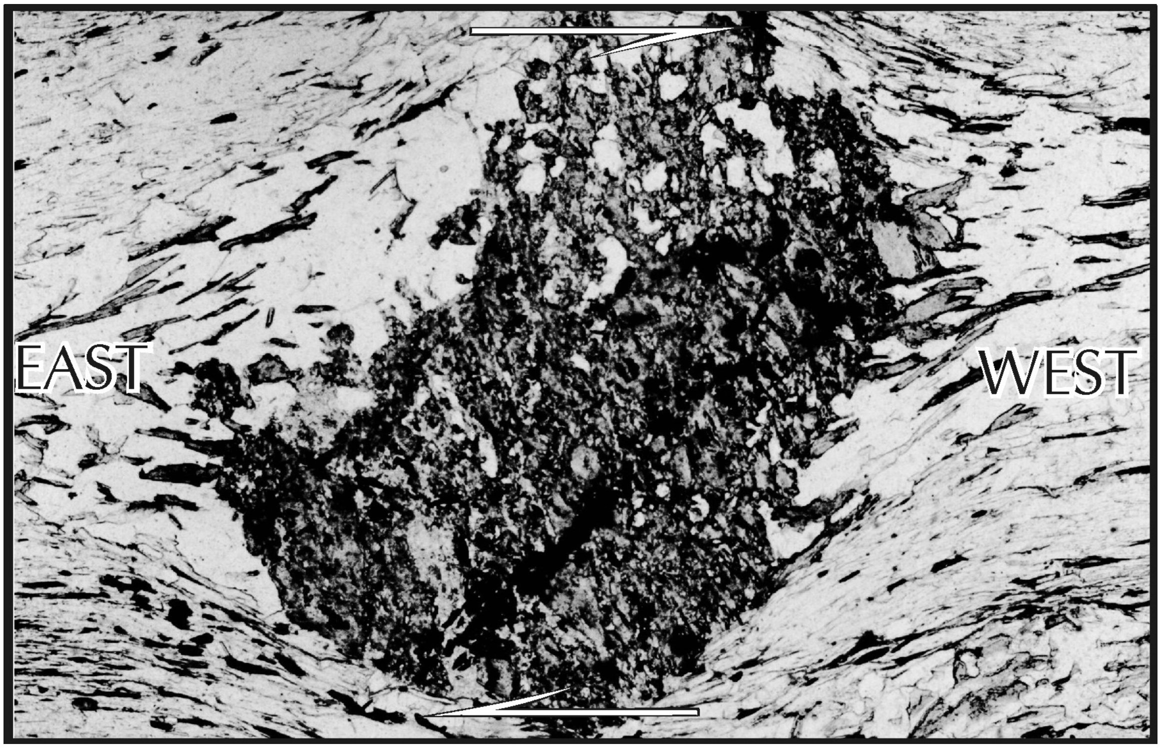

Photo 7. Top-to-the-west shearing shown by assymmetric pressure shadows around retrograded garnet porphyroblast. Retrograde chlorite and sericite participate in this fabric (Field of view 2 X 4 mm).

Photo 8. Macroscopic shear bands show late-stage down-to-the-west-southwest motion in serpentinitized talc schist, base of Dorsey Assemblage.

Dorsey Assemblage; in other words, tectonic denudation. Normal faults at the Dorsey/Swift River contact may have formed during this process. It would explain the otherwise perplexingly condensed metamorphic facies, and the presence of eclogite reverting to garnet amphibolite less than 2 kilometres below purely chlorite-grade rocks. The timing of the denudation event is not well known. It must post-date D_1, which is cross-cut by mid-Permian granites. It could be as old as late Permian or as young as Cretaceous. Future Ar-Ar work by M. Villeneuve is aimed at resolving this important question.

DISCUSSION AND CONCLUSIONS

The eventful geological history of the Dorsey Terrane continues to come to light through the findings of this project and others (Mihalynuk *et al*., 2000, Roots *et al*., 2000), following on the pioneering work of Gabrielse (1969) and Harms and Stevens (1996). The terrane presents a regionally consistent internal anatomy. Its oldest unit is the Dorsey Assemblage, in which eclogite facies was overprinted by amphibolite facies metamorphism, all prior to the emplacement of early Mississippian plutons. Plutons of this age also occur within the Ram Creek Assemblage, an arc edifice that is now known to include late Mississippian felsic to intermediate volcanic rocks.

The overall volcanic-dominated character, early Mississippian plutons and late Mississippian felsic volcanic rocks of the Ram Creek Assemblage suggest that

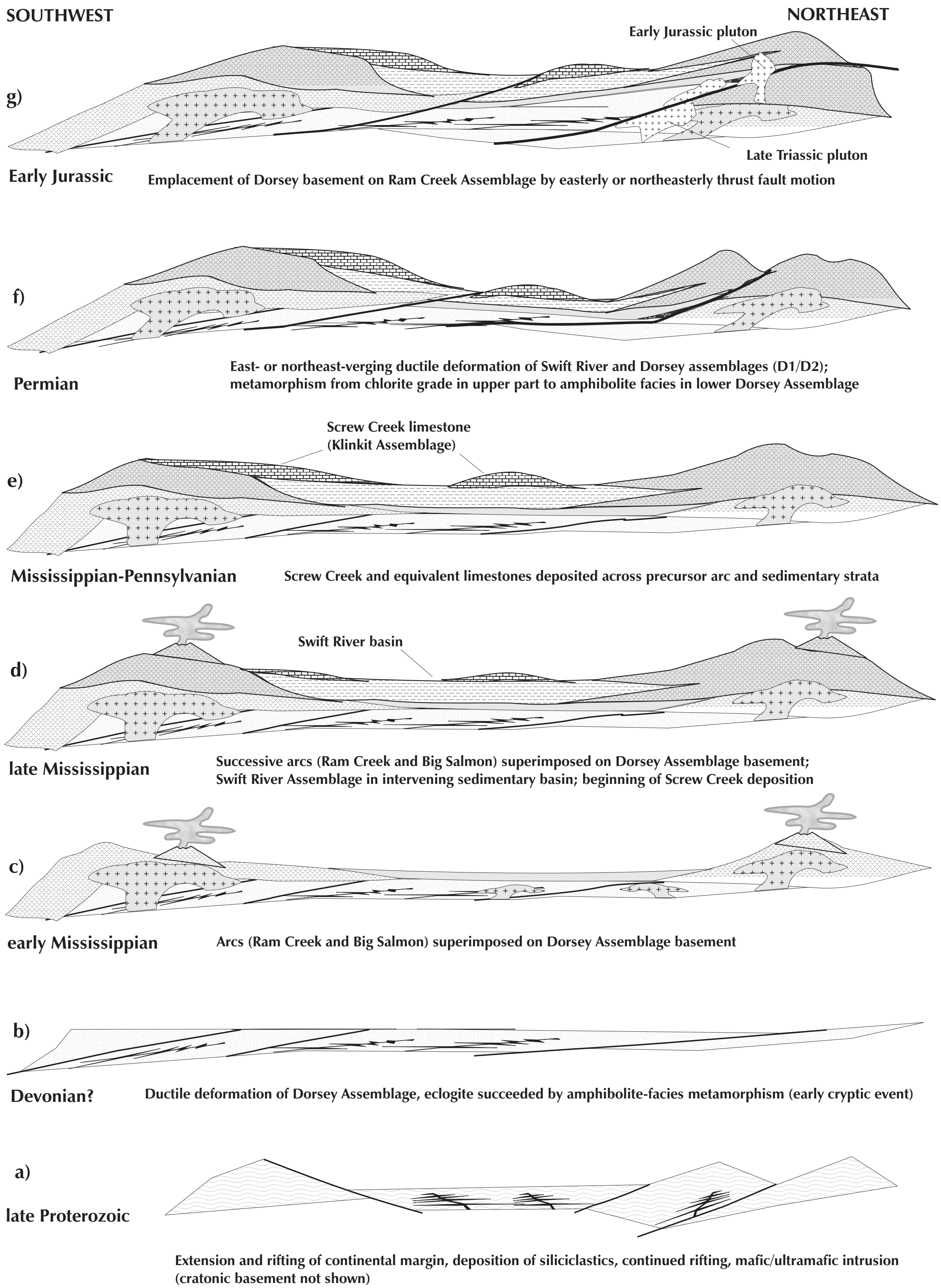

Figure 7. Cartoon evolution of the Dorsey Terrane, from late Proterozoic to Early Jurassic.

they correlate with the Big Salmon Complex on the western side of the Dorsey Terrane. However, intervening major rock sequences complicate this correlation. The Dorsey Assemblage is a likely candidate for basement to the Ram Creek, emplaced on top of it by a thrust fault of post-mid-Permian but pre-Jurassic age (Figure 4). However the Dorsey Assemblage is not overlain by a repeated Ram Creek Assemblage, but instead by basinal sediments, siliciclastic sediments and minor tuffs of the Swift River Assemblage. Very minor quartz-sericite and chlorite-quartz-sericite schist in the upper Dorsey Assemblage could be a distal equivalent to the voluminous Ram Creek igneous suite. In this scenario, a late Mississippian Ram Creek arc to the east would be in part coeval with Swift River sedimentation to the west (Figure 7d).

The external relationships of Big Salmon Complex constitute a major remaining problem in the reconstruction of the Dorsey Terrane. Near Logjam Creek just south of the B.C.-Yukon border, northeasterly-dipping clastic rocks lie structurally above the Big Salmon Complex, but the nature of the contact remains poorly understood (Gleeson *et al*., this volume; Mihalynuk *et al*., this volume). One of the units that overlies the Big Salmon Complex, Unit 3 of Gleeson *et al.,* strongly resembles the "phyllitic metasedimentary unit" southwest of Parallel Creek, which is assigned to the Swift River Assemblage (Figure 2). The base of unit 3 near Logjam Creek is cut by an early Mississippian pluton, which also cuts previously deformed schists that lie structurally below it. Perhaps this contact is analogous to the upper contact of the Dorsey Assemblage with the Swift River Assemblage.

Geologic History in the Regional Context of Southern Yukon and Far Northern B.C.

Pre-Mississippian

New mapping of 104O/1 in the southeastern corner of the Jennings River map area emphasises the variability of the lower Dorsey Assemblage. Pre-Mississippian protoliths are now seen to range from basinal sediments and tuffs in the north, to a thick section of siliciclastic sediments in the south with sparse amphibolite and ultramafite, which strongly resembles relatively coarse sections of the autochthonous Windermere Group. All of these rocks are undoubtedly allochthonous to North America, separated from the Cassiar Terrane by Mississippian arc-related igneous suites. They may be rifted blocks from the North American continental margin, which partly underpin the pericratonic terranes (Figure 7a).

Remnant eclogite in the lower Dorsey Assemblage is believed to record pre-early Mississippian subduction of unknown polarity. Thorough overprinting by Barrovian metamorphism and continued fabric development also predated some of the early Mississippian plutons. A similar geological history, without (so far) documented eclogite metamorphism, characterizes the Rapid River Tectonite in the Sylvester Allochthon (Gabrielse and Harms, 1989), where early Mississippian plutons cross-cut early ductile fabrics in garnet-amphibolite facies rocks, but are themselves in part mylonitized (Nelson *et al*., 1998b and unpublished data; Gabrielse *et al.*, 1993). Eclogites with early Mississippian cooling ages also occur in a klippe near Stewart Lake in the southern Yukon (Erdmer *et al*., 1998).

Other possible correlatives of the Dorsey Assemblage include the Anvil Assemblage in the Teslin Zone near Quiet Lake (deKeijzer *et al*., 1999), and the St. Cyr klippe (Fallas, 1997). However, the Last Peak eclogite in the Teslin Zone has yielded a mid-Permian zircon age (Erdmer *et al*., 1998), and St. Cyr eclogites are show to be mid-Permian by Ar-Ar and possibly U-Pb methods (Fallas, 1997 and personal communication to Erdmer 1998). These are significantly younger than the geologically suggested pre-Mississippian age of eclogite metamorphism in the Dorsey Assemblage. They belong to the Permian tectonic history described below.

Mississippian

Intermediate to felsic plutons of early Mississippian age, and late Mississippian intermediate to felsic volcanics, are now well-documented within the Ram Creek Assemblage. Coeval, cogenetic plutons occur in the Dorsey Assemblage. This age range of arc-related igneous-activity is one of the diagnostic attributes of the Yukon-Tanana Terrane, and also provides the framework for its volcanogenic metallogeny. The Ram Creek Assemblage is a newly-defined piece of the puzzle.

Late Mississippian to Early Permian

Volcanism in the Ram Creek Assemblage is as young as late Mississippian. The Swift River Assemblage structurally overlies the Dorsey Assemblage, and is apparently not cut by Mississippian plutons. Regionally it is depositionally overlain by late Mississippian and early Pennsylvanian limestone. These relationships suggest that the Swift River Assemblage was Mississippian and coeval with Ram Creek volcanism, yet it is dominantly a chert-argillite-quartzite sequence with minor tuffaceous components. A dramatic facies contrast is implied. The facies boundary may have been linked to a through-going crustal break, perhaps the one that later became the thrust fault at the base of the Dorsey Assemblage (Figure 7f,g). Late Mississippian volcanic activity is recorded in the Big Salmon Complex yet farther west. The relationship between these two coeval arc assemblages, separated across the mainly sedimentary Swift River Assemblage, is not known.

Permian

It has been argued in this paper that strong shear deformation affected the Dorsey Assemblage and the overlying Swift River Assemblage together. A minimum age for the deformational event (D_1-D_2) is provided by cross-cutting mid-Permian granite dikes in the lower Dorsey Assemblage (269 Ma; R. Friedman personal communication 1998). Post-kinematic plutons ranging from 262 to 270 Ma occur in the Rapid River Tectonite (Gabrielse *et al.*, 1993), and an undeformed 269 Ma tonalite seals a thrust fault between Mississippian and Pennsylvanian limestone in the panel immediately underlying the tectonite (Harms, 1985; Gabrielse *et al.*, 1993). Perhaps Permian ductile deformation in the Dorsey Assemblage and Rapid River Tectonite culminated in their eastward emplacement onto higher level rocks and generated imbrication of underlying late Paleozoic arc sequences such as the Ram Creek assemblage and Package II of Harms (1985) in the Sylvester Allochthon.

A second episode of eclogite emplacement (exhumation?) accompanied this tectonic event. All of the eclogites of Permian age, except for Last Peak, are exposed on the eastern margin of the Yukon-Tanana Terrane (Erdmer *et al*., 1998). DeKiejzer *et al.* (1999) have reinterpreted Last Peak as lying at the base of a klippe in close proximity to rocks of Ancestral North America. Thus it could occupy a structural position analogous to the others, separating North America and the Slide Mountain Terrane from a combined pericratonic terrane which includes Yukon Tanana, Dorsey, Rapid River Tectonite, Ram Creek Assemblage and upper Paleozoic arc-related strata of Division III of the Sylvester Allochthon (Nelson, 1993).

The movement of structurally higher rocks down to the west and southwest could either have taken place during a late stage of this event, or later during the early Mesozoic.

Mesozoic

In the lower Dorsey Assemblage, a Late Triassic pluton transects the structural fabric and has mildly folded apophyses (Nelson, 1999). Regionally, the Early Jurassic Nome Lake and Simpson Peak batholiths cut all units and post-date most structures in the Dorsey Terrane, although the southern margin of the Simpson Peak batholith is strong foliated with 290°-striking planar fabrics (Mihalynuk *et al*., this volume). Small bodies of granodiorite south of the Little Rancheria River are presumed to be apophyses of the Nome Lake batholith. They are unfoliated and generally cut across structures in the upper Dorsey and lower Swift River assemblages, although a few sills are involved in low-angle shears near the contact.

The plethora of Early Jurassic intrusions in the Dorsey Terrane, compared with their absence in the structurally underlying Cassiar Terrane, is taken as evidence that the allochthonous rocks were not emplaced on the continental margin until after that time. Emplacement-related fabrics appear to be shears restricted to the immediate area of the basal thrust fault that separates the Ram Creek Assemblage from Earn Group equivalents.

Near the headwaters of the Cottonwood River, a strongly foliated pluton, which shows involvement in easterly-verging minor folding and subsequent dextral transport (Nelson *et al*., 1998), has a U-Pb zircon age of 108+3 Ma (R. Friedman, personal communication 1999). This is the inferred age of motion on the dextral Cassiar fault (Gabrielse, 1985). The main strands of the Cassiar fault are mylonite zones within and at the western margin of the batholith. Steep faults in the valleys of the Cottonwood River and Parallel Creek (Figure 2) are probably splays from this system.

Mineral Potential of the Eastern Dorsey Terrane

The preceding discussion of regional tectonics places the local assemblages of the Dorsey Terrane firmly within the broader context of an evolving Yukon-Tanana Terrane. They should not be viewed in isolation, but rather as part of that vast pericratonic terrane with its persistent volcanogenic metallogeny, from the Alaska Range to the Ecstall belt, from the Finlayson Lake district to northern British Columbia. In turn, the Devonian-Mississippian evolution of the Yukon-Tanana Terrane may well have been linked to backarc extension and sedex mineralization in the Earn Group along the western margin of North America. From an economic perspective, the most important achievement of this project has been to document, within a remote area seldom visited by mineral explorationists, arc suites and also autochthonous units that are potential hosts for syngenetic mineralization.

The Ram Creek Assemblage hosts late Mississippian felsic tuffs. This arc assemblage is a likely correlative of the Big Salmon Complex on the western side of the Dorsey Terrane, which similarly hosts quartz-sericite schists and also a regional exhalative unit (Mihalynuk *et al.*, this volume; Roots *et al*., 2000). Some of the Ram Creek felsic tuffs are highly pyritic, and traces of chalcopyrite were discovered within one of them in 1998 (Nelson *et al.*, 1999).

The Earn Group is an interesting metallotect locally as well as regionally, with a new exhalite occurrence at Scaup Lake. This occurrence resembles showings on the COT claims, where previous work has outlined geochemical anomalies in Pb, Zn, and Ba, and disseminated sulphides in black argillite (Gal and Nicholson, 1992; Cathro, 1985). This summer several iron-aluminum oxide seeps were seen in cliff-face exposures of the Earn Group west of the lake that heads the Cottonwood River. Streams draining this area are anomalous in zinc, lead, copper and silver (Regional Geochemical Survey; Geological Survey of Canada, 1978).

In the Yukon-Tanana Terrane in the Finlayson Lake area, southern Yukon, Mississippian meta-rhyolites, marine metasedimentary rocks and intermediate to mafic metatuffs host volcanogenic massive sulphide deposits such as Kudz Ze Kayah, Wolverine and Fyre Lake (Murphy and Piercey, 1999). This assemblage can be traced southwards across a restored Tintina Fault into the Teslin Zone, where Colpron (2000) and Mihalynuk *et al.* (1998, 2000) have identified exhalative occurrences associated with Mississippian volcanic sequences (Nelson *et al*., this volume). These rocks, locally termed the Big Salmon Complex, may extend into far southern Jennings River map area. The Ram Creek and Dorsey Assemblages can be considered a separate eastern extension of this trend. As mapping this year has shown, we have not yet reached the limit of exposure for Yukon Tanana equivalents in northern British Columbia: they are still heading south.

ACKNOWLEDGMENTS

Charlie Roots, Martin de Keijzer, Philippe Erdmer, Mitch Mihalynuk, Jim Mortensen, Mike Villeneuve and Tekla Harms brought significant new perspectives to the project. Richard Friedman has provided over the years a steady supply of high-quality uranium-lead dates without which field investigators of the Dorsey Terrane would have had little traction on the learning curve. I thank Kim Wahl for assistance in the field. Kevin Lohr of Cassiar Stone Outfitting got us there and back. He was aided by Marie, Governor, Sumo, Jenny, Slipper, and Salty - and sometimes by Jess. Mitch Mihalynuk and Dave Lefebure improved the manuscript with careful reviews.

REFERENCES

Cathro, M.S. (1984): A Petrological and Textural Study of the Dakota, Kilt and Maria Stratabound Sulphide Showings, Northern British Columbia; B.Sc., Queen's University.

Childe, F. (1995) Geochronological and radiogenic isotopic investigations of VMS deposits within accreted terranes of the Canadian Cordillera; *in* Third Annual Technical Report, Volcanogenic Massive Sulphide Project, *Mineral Deposits Research Unit*, University of British Columbia, pages 1-1 - 1-56.

Colpron, M. (2000): Glenlyon project: Preliminary stratigraphy and structure of the Little Salmon Range (Yukon-Tanana Terrane), central Yukon; *in* Yukon Exploration and Geology 1998; Exploration and Geological Services Division, Indian and Northern Affairs Canada, in press.

de Keijzer, M., Williams, P.F. and Brown, R.L. (1999): Kilometre-scale folding in the Teslin zone, northern Canadian Cordillera, and its tectonic implications for the accretion of the Yukon-Tanana Terrane to North America; Erdmer, P. (1992): Eclogitic rocks in the St. Cyr klippe, Yukon, and their tectonic significance; Canadian Journal of Earth Sciences, Volume 36, pages 479-494.

Erdmer, P. (1992): Eclogitic rocks in the St. Cyr klippe, Yukon, and their tectonic significance; *Canadian Journal of Earth Sciences,* Volume 29, pages 1296-1304.

Erdmer, P., Ghent, E.D., Archibald, D.A. and Stout, M. (1998): Paleozoic and Mesozoic high-pressure metamorphism at the margin of Ancestral North America; *Geological Society of America Bulletin*, Volume 110, pages 615-629.

Fallas, K.M. (1997): Preliminary constraints on the structural and metamorphic evolution of the St. Cyr Klippe, south-central Yukon; Slave-Northern Cordillera Lithospheric Evolution (SNORCLE) and Cordilleran Tectonics Workshop, Report of the 1997 Combined Meeting, pages 90-95.

Gabrielse, H. (1969): Geology of Jennings River map area, British Columbia (104/O); *Geological Survey of Canada,* Paper 68-55.

Gabrielse, H. (1985): Major dextral transcurrent displacements along the Northern Rocky Mountain Trench and related lineaments in north-central British Columbia; *Geological Society of America Bulletin*, Volume 96, pages 1-14.

Gabrielse, H. (1994): Geology of Cry Lake (104I) and Dease Lake (104J/E) map areas, north central British Columbia; *Geological Survey of Canada;* Open File Map 2779.

Gabrielse, H. and Harms, T.A. (1989): Permian and Devonian plutonic rocks in the Sylvester Allochthon, Cry Lake and McDame map areas, Northern British Columbia; *in* Current Research, Part E. Geological Survey of Canada Paper 89-1E, pages 1-4.

Gabrielse, H., Mortensen, J.K., Parrish, R.R., Harms, T.A., Nelson, J.L., and van der Heyden, P. (1993): Late Paleozoic plutons in the Sylvester Allochthon, northern British Columbia; *in* Radiogenic Age and Isotopic Studies, Report 7, *Geological Survey of Canada*, Paper 93-1, pages 107-118.

Gal, L. and Nicholson, J.A. (1992): Geochemical Assessment Report on the Cot Claims, 30 Kilometres Northwest of Cassiar, B.C., NTS 104O/8; *B.C. Ministry of Energy, Mines and Petroleum Resources,* Assessment Report 22,633.

Gleeson, T. P., Friedman, R.M. and Wahl, K. (2000): Stratigraphy, structure, geochronology and provenance of the Logjam area, northwestern British Columbia (NTS 104O/14W); *in* Geological Fieldwork 1999, *B.C. Ministry of Energy and Mines*, Geological Survey Branch, Paper 2000-1, this volume.

Harms, T.A. (1985): Pre-emplacement thrust faulting in the Sylvester Allochthon, northeast Cry Lake map area, British Columbia, *in* Current Research Part A, *Geological Survey of Canada* Paper 1985-1, pages 301-304.

Harms, T.A. and Stevens, R.A. (1996): Assemblage analysis of the Dorsey Terrane; Slave-Northern Cordillera Lithospheric Evolution (SNORCLE) and Cordilleran Tectonics Workshop, Report of the 1996 Combined Meeting; pages 199-201.

Hunt, J. (1997): Massive sulphide deposits in the Yukon-Tanana and adjacent terranes; *in* Yukon Exploration and Geology 1996, Exploration and Geological Services Division, Yukon, *Indian and Northern Affairs Canada*, pages 35-45.

Mihalynuk, M. Nelson, J.L. and Friedman, R.M. (1998): Regional geology and mineralization of the Big Salmon Complex (104N NE and 104O NW), *in* Geological Fieldwork 1997, *B.C. Ministry of Employment and Investment*, Geological Survey Branch, Paper 1998-1, pages 6-1 - 6-20.

Mihalynuk, M.G., Nelson, J., Roots, C.F. and Friedman, R.M. (2000): Ancient Pacific Margin Part III: Regional geology and mineralization of the Big Salmon Complex (104N/9,10 & 104O/12,13,14W); *in* Geological Fieldwork 1999, *B.C. Ministry of Energy and Mines*, Geological Survey Branch, Paper 2000-1, this volume.

Mortensen, J.K. and Jilson, G.A. (1985): Evolution of the Yukon-Tanana Terrane : Evidence from Southeastern Yukon Territory; *Geology*, Volume 13, pages 806-810.

Murphy, D.C. and Piercey, S.J. (1999): Finlayson project: Geological evolution of Yukon-Tanana Terrane and its relationship to Campbell Range belt, northern Wolverine Lake map area, southeastern Yukon, *in* Yukon Exploration and Geology 1998; Exploration and Geological Services Division, Indian and Northern Affairs Canada, p.47-62.

Murphy, D.C. and Piercey, S.J. (2000): Syn-mineralization faults and their re-activation, Finlayson Lake massive sulphide belt, Yukon-Tanana Terrane, southeastern Yukon, *in* Yukon Exploration and Geology 1998; *Exploration and Geological Services Division, Indian and Northern Affairs Canada*, in press.

Nelson, J. (1993): The Sylvester Allochthon: upper Paleozoic marginal-basin and island-arc terranes in northern British Columbia; *Canadian Journal of Earth Sciences,* Volume 30, pages 631-643.

Nelson, J. (1997): Last seen heading south: extensions of the Yukon-Tanana Terrane into Northern British Columbia; *in* Geological Fieldwork 1996, D.V. Lefebure, W.J. McMillan and J.G. McArthur, editors, *B.C. Ministry of Employment and Investment*, Geological Survey Branch, Paper 1997-1 pages 145-156.

Nelson, J. (1999): Devono-Mississippian VMS Project: Continuing studies in the Dorsey Terrane, northern British Columbia; *in* Geological Fieldwork 1998, *B.C. Ministry of Energy and Mines*, Geological Survey Branch, Paper 1999-1, pages 143-155.

Nelson, J.L., Harms, T.A. and Mortensen, J. (1998a): Extensions and affiliates of the Yukon-Tanana Terrane in northern British Columbia; *in* Geological Fieldwork 1997, *B.C. Ministry of Employment and Investment*, Geological Survey Branch, Paper 1998-1, pages 7-1 - 7-12.

Nelson, J.L., Harms, T.A. and Mortensen, J. (1998b): The southeastern Dorsey Terrane: characteristics and correlations; *in* Slave-Northern Cordillera Lithospheric Evolution (SNORCLE) and Cordilleran Tectonics Workshop, Report of the 1998 Combined Meeting; pages 279-288.

Nelson, J., Harms, T.A., Zantvoort, W., Gleeson, T. and Wahl, K. (2000): Geology of the southeastern Dorsey Terrrane, 104O/7, 8, 9, 10; *B.C. Ministry of Energy and Mines*, Geological Survey Branch, Open File 2000-4.

Roots, C.F., de Keijzer, M., Nelson, J.L., and Mihalynuk, M.G. (2000): Revision mapping of the Yukon-Tanana and equivalent terranes iin northern B.C. and southern Yukon between 131^{o} and 132^{o} W; *in* Current Research 2000-A; *Geological Survey of Canada*, in press.

Sevigny, J.H. (1988): Geochemistry of Late Proterozoic amphibolites and ultramafic rocks, southeastern Canadian Cordillera; *Canadian Journal of Earth Sciences*, Volume 25, pages 1323-1337.

Stevens, R.A. (1996): Dorsey Assemblage: pre-mid-Permian high temperature and pressure metamorphic rocks in the Dorsey Range, southern Yukon Territory; *in* Slave-Northern Cordillera Lithospheric Evolution (SNORCLE) and Cordilleran Tectonics Workshop, Report of the 1996 Combined Meeting, pages 70-75.

Stevens, R.A. and Harms, T.A. (1995): Investigations in the Dorsey Terrane, Part I: Stratigraphy, structure and metamorphism in the Dorsey Range, southern Yukon Territory and northern British Columbia; *in* Current Research, *Geological Survey of Canada* Paper 1995A, pages 117-127.

Devono-Mississippian Felsic Volcanism Along the Western Edge of the Cassiar Terrane, North-Central British Columbia (NTS 93N, 94C and 94D)

By Filippo Ferri

INTRODUCTION

The Late Devonian to Early Mississippian is an important metallogenic epoch within the Canadian cordillera resulting in the production of significant sediment exhalative massive sulphide (SEDEX) and volcanogenic massive sulphide (VMS) mineral occurrences within rocks of cratonic or pericratonic affinity. Major belts include the Late Devonian Earn-hosted SEDEX deposits of the Selwyn and Gataga districts (Tom, Jason, Driftpile Creek, Cirque) and the VMS occurrences within Eagle Bay rocks of the Barriere area (Homestake, Rea). The recent discoveries of the Kudz Ze Kayah, Wolverine, Fyre Lake and Wolf VMS deposits hosted by Devono-Mississippian pericratonic and cratonic rocks of the Yukon-Tanana and Cassiar terranes (Figure 1) again underlines the economic importance of this geologic time interval.

The British Columbia Geological Survey Branch initiated a mapping program focused on a sedimentary sequence with intercalated Devono-Mississippian felsic volcanics in the Johanson Lake area. Previous geologic mapping by the British Columbia Geological Survey Branch between Manson Creek and Aiken Lake delineated a belt of Devono-Mississippian felsic volcanics along the western margin of the Cassiar Terrane (Figure 2; Ferri and Melville, 1994; Ferri *et al*., 1992a, b; 1993a, b). These felsic volcanics, locally termed the Gilliland Tuff, can be traced intermittently for approximately 150 kilometres and can exceed 1000 metres in thickness. They are found within the Big Creek Group, part of the Earn Assemblage, a package which contains both SEDEX and VMS mineral targets. The presence of felsic volcanics within Big Creek rocks may indicate VMS potential.

The objectives of the mapping project were to: 1) evaluate the Omineca Queen bedded barite occurrence and determine its relationship to the felsic volcanism of the Gilliland Tuff; 2) trace these felsic volcanics northward; 3) determine the economic potential of the felsic volcanics and enclosing lithologies for hosting VMS and SEDEX deposits and 4) examine the Lay Range Assemblage, the lower part of which may be equivalent to the Yukon-Tanana Terrane.

This paper summarizes initial results from the mapping program and some key points of the property visit to

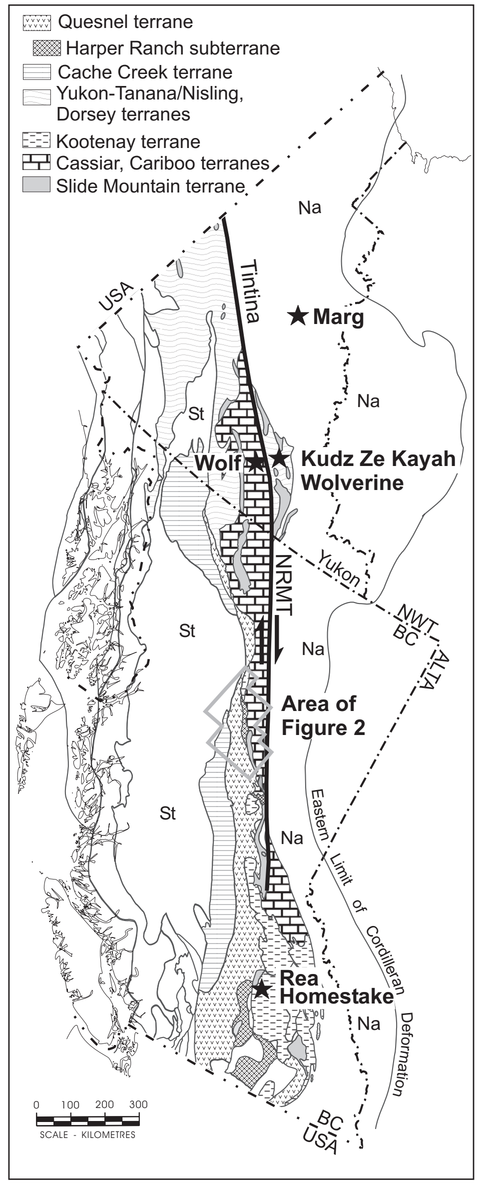

Figure 1. Simplified tectonic assemblage map of the Canadian Cordillera showing the location of the map area with respect to the main terrane assemblages near the contact between Ancestral North American rocks and those of suspect affinity. St: Stikine Terrane, Na: Ancestral North America; NRMT: Northern Rocky Mountain Trench.

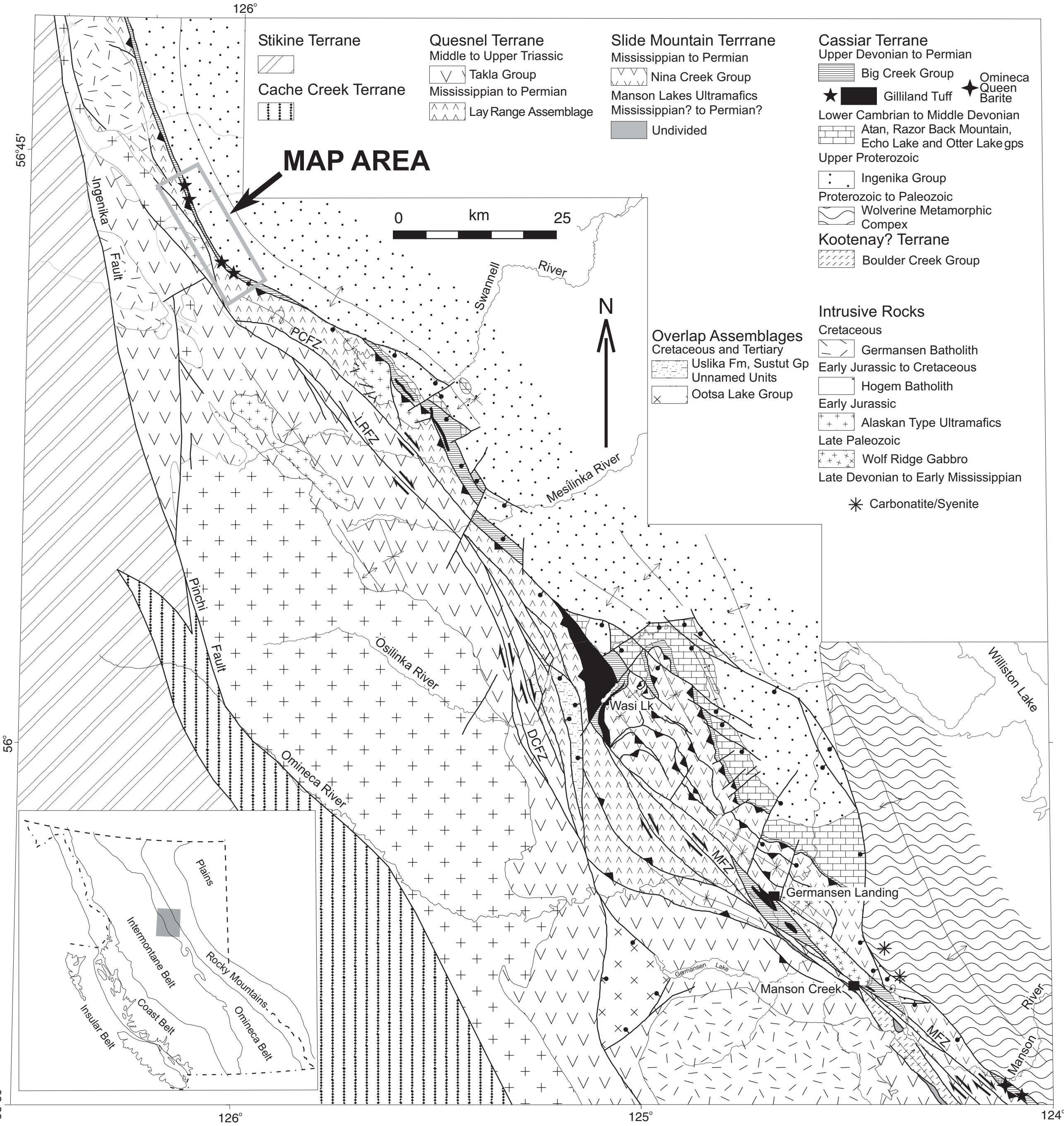

Figure 2. General geology map of the region south of and adjoining the present map area. The bulk of the geology shown is taken from work during the Manson Creek (Ferri and Melville, 1994) and Aiken Lake (Ferri *et al*. 1992a, b and 1993a, b) projects. The area east of the Germansen Batholith is taken from Nelson and Bellefontaine (1996). PCFZ: Polaris Creek Fault Zone. LRFZ: Lay Range Fault Zone. DCFZ: Discovery Creek Fault Zone. MFZ: Manson Fault Zone.

the Omineca Queen barite occurrence. The geology of this property will be reported in greater detail in a later publication.

The map area forms a narrow, northwest-trending belt measuring 5 by 25 kilometres extending from the headwaters of the Swannell River to the Fleet Peak area (Figure 3). The centre of the map area is approximately 15 kilometres northeast of Johanson Lake which is roughly 400 kilometres by road to the towns of Fort St. James or Mackenzie. The area is accessible by helicopter and by foot or pack horse from the Omineca Mining Access Road.

Mapping commenced along the western edge of the Mesilinka River sheet (NTS 94C) and extended northwestward into the McConnell map area (NTS 94D). The southern part of the map area overlaps with a portion

MIDDLE JURASSIC

Jq *Buff-white weathering, white to pale grey, medium grained, equigranular hornblende-bearing quartz monzonite/monzonite/quartz diorite/diorite*

LATE TRIASSIC

Wrede Complex

Twhd *Pale grey to black weathering, fine to coarse grained hornblende diorite or gabbro/clinopyroxene-hornblende diorite or gabbro plagioclase*

Twh *Medium brown weathering, coarse grained hornblende clinopyroxenite*

Twc *Dark to medium grey-green weathering, medium to coarse grained undifferentiated clinopyroxenite, includes hornblende clinopyroxenite, olivine clinopryoxenite and olivine-hornblened clinopyroxenite*

Two *Medium to pale grey-green weathering, medium to coarse grained olivine clinopyroxenite*

Tww *Dark to medium brown weathering, predominantly medium grained or medium to coarse grained wehrlite*

Twd *Pale buff-orange weathering, dark grey to black, fine to medium grained dunite*

Tgh *Rusty weathering, grey-green, biotite-bearing gabbro and grey to orange weathering coarsely crystalline hornblendite*

Takla Group

Tt *Pale to medium grey-green weathering, dark grey-green augite-feldspar bearing volcanic breccia, tuffs and flows*

MIDDLE PENNSYLVANIAN? TO PERMIAN

Lay Range Assemblage

Upper Mafic Tuff Division

PIrua *Grey-geen or maroon weathering, pale to dark green and maroon, feldspar-pyroxene lapilli tuffs volcanic breccia, flows and lesser crystal tuffs. Rare grey limestone*

PIru *Pale greenish grey to green weathering, green to grey green thin to thickly bedded and well laminated tuff. Locally dark green aphanitic basalt with associated lapilli tuff and volcanic breccia.✦ Rare rusty weathering, quartz-bearing tuff to sericite schist*

MPlrll *Grey to buff weathering grey limestone. Massive to platy, locally bioclastic with interlayers of beige to pale grey chert. Locally contains maroon and green siltstone or tuffaceous horizons. Tan to buff weathering, white to cream recrystallized massive dolomite*

MPlrlv *Grey-brown weathering, dark green, aphanitic basalt, lesser volcanic breccia and tuff. Locally spheriolitic. Pale to green, medium to coarsely crysalline gabbro to quartz monzonite, locally foliated*

MPlrl *Thick to massively bedded, beige to brown weathering, tan to greenish brown calcareous sandstone, very fine to granule conglomerate. Interlayered with black argillite, green tuffaceous siltstone, thin bedded whiite to grey chert and brown to orange weathering grey platy limestone*

The region west of 126°W occurs within UTM Zone 9.
The region east of 126°W occurs within UTM Zone 10.
This map is NAD83 Universal Transverse Mercator.

LATE DEVONIAN TO PERMIAN

Big Creek Group

DPbc *Dark grey, dark blue-grey to black slate and thin to moderately bedded argillite. Minor horizons of dark grey to black quartz-chertz wackes, sandstones and lesser granule conglomerate.★ Locally contains thin horizons of light coloured quartz-feldspar-bearing felsic tuff and dark green basalt.*

DMgt *'Gilliland Tuff': Rusty to tan weathering, pale grey to dark grey or greenish grey, quartz-feldspar tuff to lapilli tuff. Sericitic and locally contains pryrite and ankerite porphyroblasts. Minor argillite clasts. Locally contains tan to grey weathering, very fine to medium crystalline diorite or quartz diorite which can be associated with dark green basalt.*

LATE PROTEROZOIC

Ingenika Group

Stelkuz Formation

Pst *Rusty brown weathering, greenish grey slate, lesser thin to massively bedded cream impure quartzite and quartz sandstone and thinly bedded, grey limestone*

Espee Formation

Pes Grey to buff weathering, platy and blocky, finely recrystallized limestone and dolomitic limestone, grey calcareous slate. Cross-cutting zones of orange weathering, coarsely crystalline dolostone are locally present.

Tsaydiz Formation

Pts *Thinly interlayered, grey to orange-brown weathering, grey to green-grey slate, calcareous slate and grey to orange weathering, grey limestone.*

Swannell Formation

Psw *Thickly bedded, grey-green to green, feldspar-bearing quartz sandstone to wacke, quartz sandstone, slate, siltstone, impure quartzite and rare grey limestone. Schistose in its lowest parts, locally containing biotite porphyroblasts.*

Geologic boundary (approximate, assumed):

Thrust Fault (approximate, assumed):

Fault, unknown displacement (approximate, assumed):

Fold axis, overturned (anticline, syncline):

Bedding (tops known-inclined, vertical overturned-inclined vertical, unknown-inclined vertical): 84 30 66

Foliation (first, second generations inclned, vertical): 67 54

Chromite schlieren (inclined vertical) 31

Bedding cleavage intersection: 50

Fold axis: 18

Fold axial plane: 80

Shear zone: ....

Field station: ....

Area of abundant exposure: ....

Geology of the Wrede Complex taken from Nixon et al. (1998).

Figure 3. Geological map of the project area. (a) Southern portion. (b) Northern part. (c) Geological legend to accompany Figures 3(a) and (b). Geology of the Wrede Complex taken from Nixon *et al.* (1998).

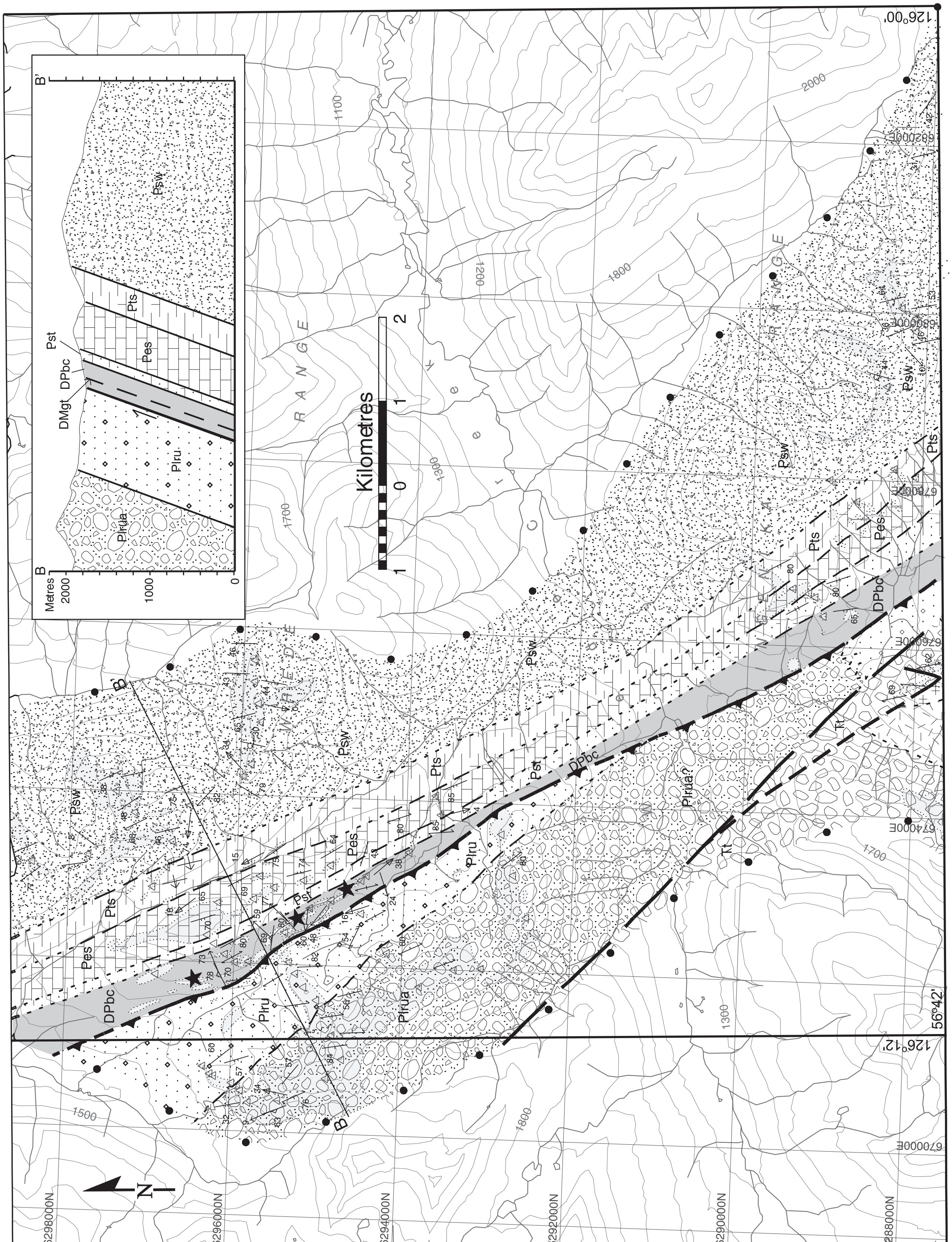
126°00'
126°12'
56°42'
Metres
2000
1000
0
B
B'
Psw
Pts
Pes
Pst
DPbc
DMgt
Plru
Plrua
Plrua?
Tt
Kilometres
1
0
1
2
R A N G E
6298000N
6296000N
6294000N
6292000N
6290000N
6288000N
670000E
674000E
676000E
678000E
680000E
682000E

b

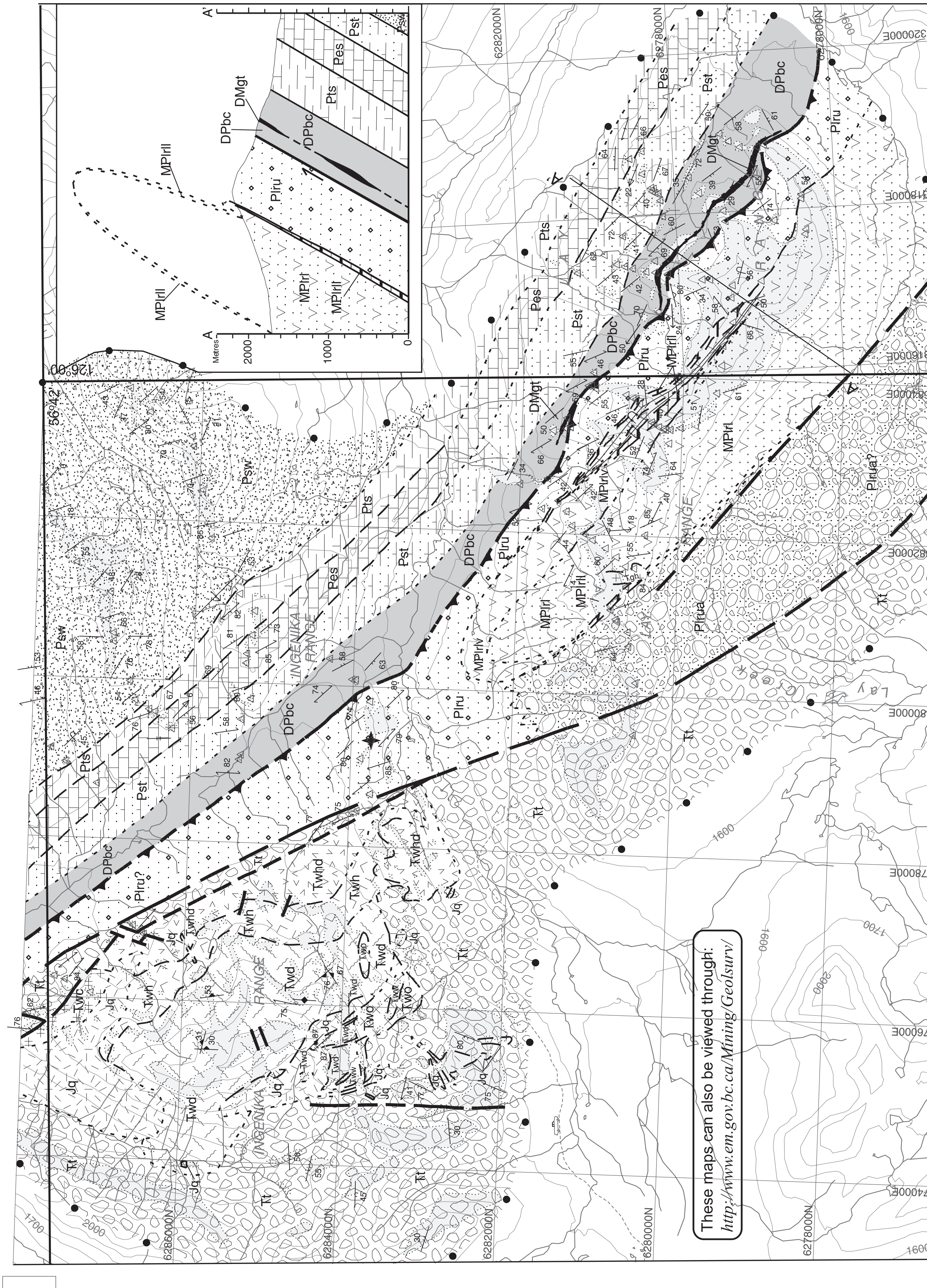
These maps can also be viewed through:
http://www.em.gov.bc.ca/Mining/Geolsurv/
INGENIKA RANGE
Metres
2000
1000
0
A
A'
DPbc
DMgt
Plru
MPlrll
MPlrlt
Pts
Pes
Pst
Psw
Tt
Jq
Twd
Twh
Twhd
Twc
Plrua
126°00'
56°42'

c

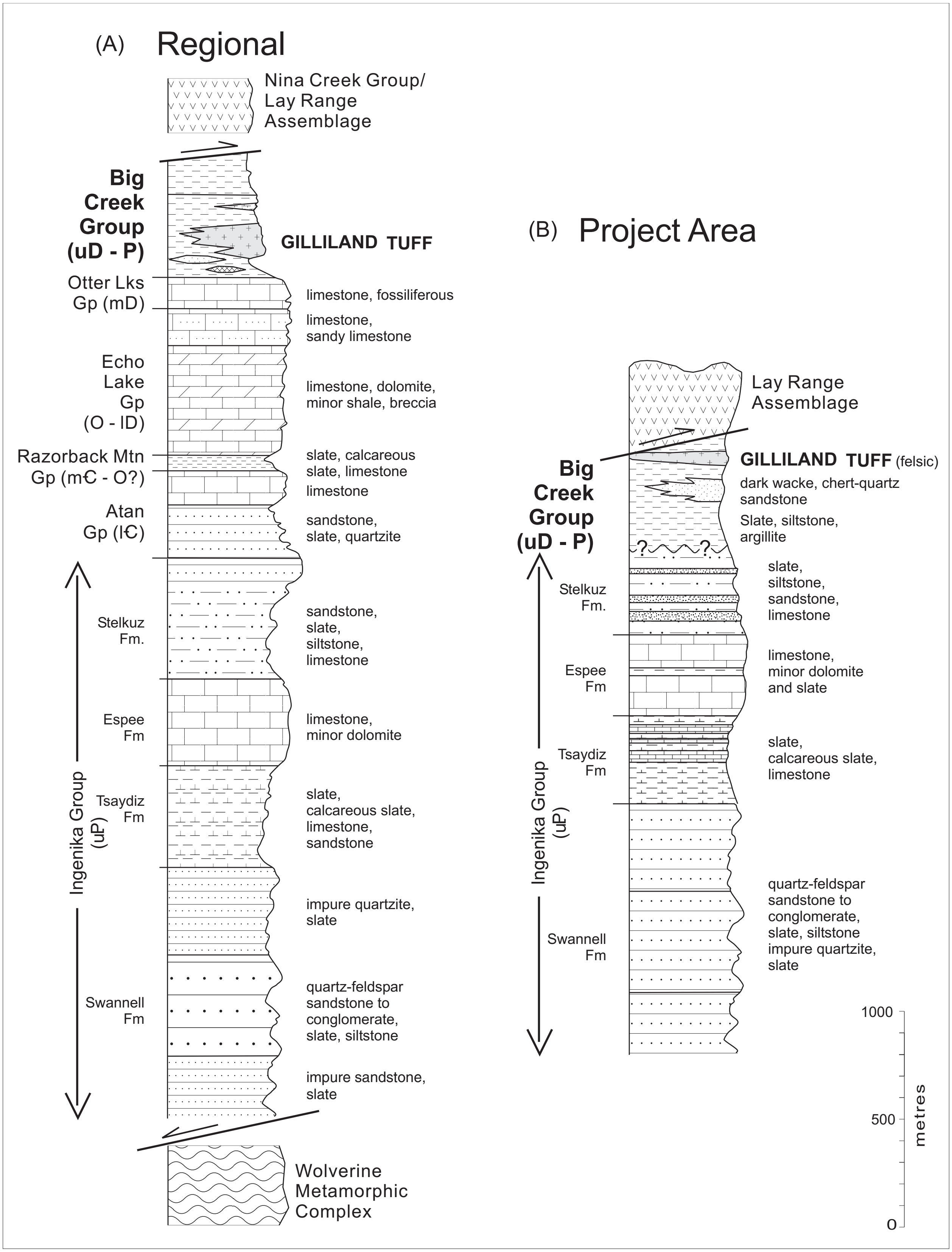

Figure 4. Simplified stratigraphic columns of Ancestral North American stratigraphy. (A) Regional stratigraphy of the Cassiar Terrane between the Omineca and Swannell rivers. (B) Stratigraphic units found in the present map area.

of Open File Map 1993-2 (Ferri *et al*., 1993a, b). The geology in this section of the open file was originally reproduced from unpublished maps and field notes provided by J.W.H. Monger from the Geological Survey of Canada. Some of this information was also incorporated into the present mapping. The opportunity to use this information is gratefully appreciated.

REGIONAL SETTING

The map area straddles the boundary between displaced Ancestral North American rocks of the Cassiar Terrane to the east and volcanic arc and peri-cratonic? rocks of the Quesnel Terrane to the west. In the map area, the Cassiar Terrane is represented by the Ingenika and the Big Creek groups (Figures 2 and 3). The Late Proterozoic Ingenika Group represents a rift to shallow shelf sequence and is subdivided into, from oldest to youngest, rift clastics of the Swannell Formation, upwards shoaling slates and carbonates of the Tsaydiz Formation, shallow carbonates of the Espee Formation and rift-related? clastics and carbonates of the Stelkuz Formation (Mansy and Gabrielse, 1978). Regionally, these rocks are overlain by a carbonate-rich, shallow shelf sequence of Early Cambrian to Middle Devonian in age (Figure 4). These rocks are missing in the map area and the Big Creek Group sits directly atop the Ingenika Group.

The Middle Devonian to Permian Big Creek Group is a dominantly argillaceous sequence. This unit belongs to the Earn Assemblage, a deeper water shale succession. The Earn Assemblage formed, in part, due to the foundering of the ancient carbonate platform which is believed to have occurred in response to rifting in the northern Canadian Cordillera (Gordey *et al*., 1987). The upper part of the Big Creek Group contains a Late Devonian to Early Mississippian calc-alkaline felsic tuff or quartz-feldspar porphyry, locally termed the Gilliland Tuff (Ferri and Melville, 1994).

The Lay Range Assemblage sits structurally above the Big Creek Group, the contact being an easterly directed thrust fault (Ferri *et al*., 1993b; Nixon *et al*., 1993). The Lay Range Assemblage represents a middle to late Paleozoic arc-succession which forms basement to the Late Triassic to Early Jurassic Takla Group volcanics (Ferri, 1997). These rocks have been intruded by the Late Triassic Wrede Creek Alaskan-type ultramafic complex (Nixon *et al*., 1998). To the south, late Paleozoic oceanic volcanics and sediments of the Nina Creek Group, belonging to the Slide Mountain Terrane, sit structurally above rocks of the Big Creek Group (Ferri and Melville, 1994).

Rocks of the Lay Range Assemblage, Takla Group and Wrede Complex, found along the southwest margin of the map area, form rugged alpine areas in excess of 2000 metres. The terrane along the northeastern part of the map area, underlain by rocks of the Swannell Formation, consists of rounded, glaciated peaks approaching 2000 metres in elevation. Recessive rocks of the Big Creek Group, together with those in the upper part of the Ingenika Group, form the subdued region between these two areas. Carbonate of the Espee Formation forms prominent ribs within this subdued area.

STRATIGRAPHY

Ingenika Group

The Late Proterozoic Ingenika Group is a dominantly clastic sequence and is subdivided into four formations which are, from oldest to youngest; the Swannell, Tsaydiz, Espee and Stelkuz formations. Regionally, rocks of the Atan Group sit conformably atop those of the Stelkuz Formation (Mansy and Gabrielse, 1978; Figure 4) and, based on trace fossil evidence, the Cambrian - Precambrian contact is believed to occur in the upper part of the Stelkuz Formation (Gabrielse and Campbell, 1991).

Swannell Formation

The Swannell Formation was examined along ridge tops located north and south of Wrede Creek (Ingenika and Wrede ranges), on the west flank of a broad F_2 or F_3 antiform. These resistive rocks form prominent exposures, particularly on north facing slopes (Photo 1). The Swannell Formation comprises a monotonous package of fine to coarse clastics, probably in excess of 2 kilometres in stratigraphic thickness, although a true measure is difficult to determine due to tectonic thickening.

The Swannell Formation is characterized by thickly bedded, grey-green to green, feldspar-bearing quartz sandstones to wackes, quartz sandstones, slate, siltstone, impure quartzite and rare limestone. These sandstones commonly display graded bedding and are typically coarse grained and locally granule conglomerates. Grains are typically angular resulting in these lithologies being referred to as 'grits' (Mansy and Gabrielse, 1978). Invariably, the sandstones contain a micaceous matrix which varies from 5 to 40 per cent of the rock. Quartz sandstones and quartzites are less common. Feldspar, either plagioclase or microcline, form conspicuous, chalky weathering grains making up to 15 per cent of the sandstone units. Tourmaline is a minor, but prominent accessory mineral. The upper part of the Swannell Formation is dominated by sandstone sections with lesser sequences of interbedded slate. Sections of predominantly grey-green to green slate/schist, with lesser sandstone, up to several hundred metres thick are common lower in the section. Slate is commonly interbedded with sandstone and can contain variable amounts of quartz and feldspar grains. Slates are locally crenulated lower in the stratigraphic section and can contain porphyroblasts of biotite.

Tsaydiz Formation

The Tsaydiz Formation typically forms a poorly exposed, recessive sequence above the Swannell Formation. It is conformable with the underlying Swannell Formation and comprises slate, calcareous slate, limestone and minor sandstone from 175 to 500 metres thick. South

Photo 1. Looking southeast at typical exposure of Swannell Formation within the Wrede Range. This photo shows the monotonous nature of this formation and the prominent ribs formed by the resistive sandstone sequences.

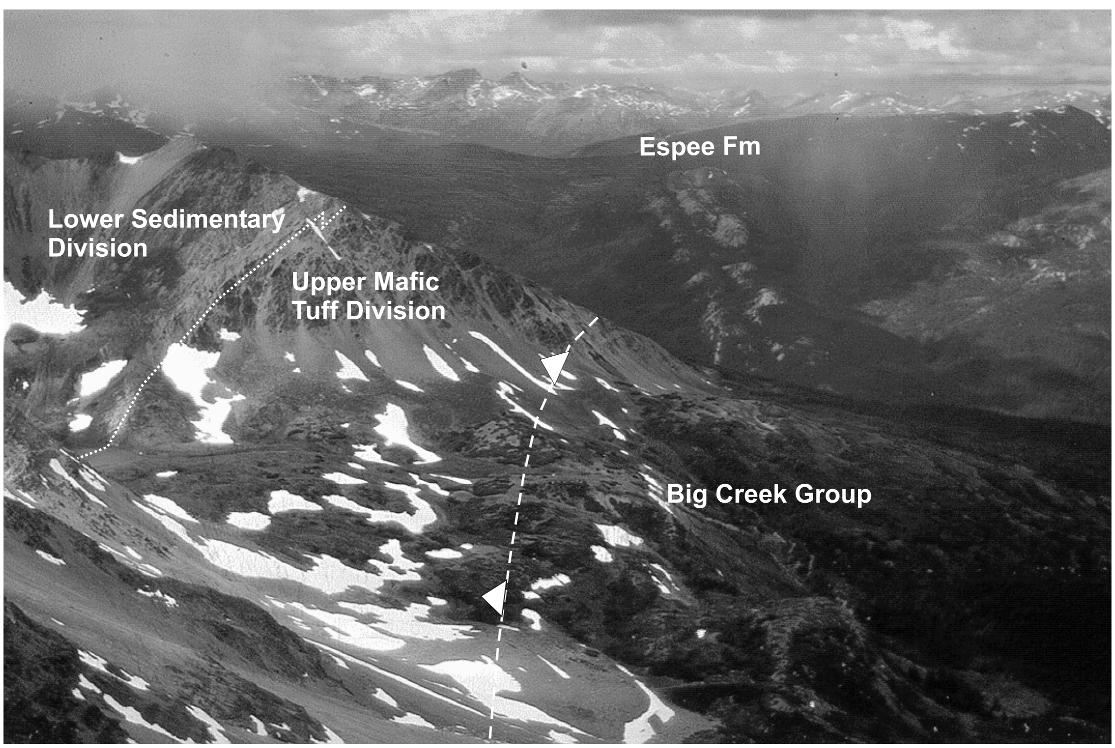

Photo 2. Looking northwest from the northern Lay Range towards the Ingenika Range. The thrust contact between the Lay Range Assemblage and Big Creek Group is shown in the foreground. Rocks of the Lay Range Assemblage are on the overturned eastern limb of an early northeast-verging anticline. The trace of this thrust is shown in the middle ground together with units of the underlying Ingenika Group.

of Wrede Creek, it is characterized by thinly interlayered, grey to orange-brown weathering, grey to green-grey slate, calcareous slate and grey to orange weathering, grey limestone. The amount of limestone diminishes down section resulting in thick sequences of grey, lustrous slate.

To the north, across Wrede Creek, the Tsaydiz Formation contains beds of limestone up to 20 centimetres thick near the Espee contact. In its lower parts, dark grey weathering limestone is from 2 to 5 metres in thickness, comprises up to 30 per cent of the section and locally contains up to 20 per cent dispersed, spherical quartz grains. This limestone is interlayered with typical Swannell sandstone at the base of the formation.

Espee Formation

Limestone of the Espee Formation forms prominent cliffs or ribs between recessive lithologies of the Tsaydiz and Stelkuz formations, and is an excellent marker horizon within the Cassiar Terrane (Photo 2). Structural sections suggest thicknesses between 250 and 450 metres. The unit is characterized by grey to buff weathering, platy and blocky, finely recrystallized limestone and dolomitic limestone. Sections of thinly interlayered limestone and more resistant, orange weathering dolomite or dolomitic limestone are also common. Bedding is typically difficult to distinguish and the grey to buff weathering limestone commonly appears massive. Where visible, beds can be up to a metre thick and are typically discernible through platy, phyllitic partings, as thin grey slaty interlayers, or wispy, darker grey streaks. Grey, calcareous slate in layers 0.5 to 3 centimetres thick is interlayered with the limestone in several localities. Large cross-cutting zones of orange weathering, coarsely recrystallized dolostone can be found within the limestone succession. Up to several per cent dispersed quartz grains were observed within some horizons north of Wrede Creek.

Stelkuz Formation

Regionally, the Stelkuz Formation contains thick sections of sandstone, limestone and slate (Ferri and Melville, 1994; Ferri *et al*., 1993a; Mansy and Gabrielse, 1978). In the present map area it is dominated by rusty brown weathering, greenish grey slate with lesser thin to massively bedded cream impure quartzite and quartz sandstone in sections up to 20 metres thick and thinly bedded, grey limestone. Slate sections can display a distinctive bright green colour typical of the Stelkuz Formation (Ferri *et al*., 1993a). The dominance of slate renders this unit quite recessive and poorly exposed (Photo 2). Structural sections suggest thicknesses between 175 and 550 metres.

Big Creek Group

The Big Creek Group is dominated by dark grey and black slate and argillite with minor quartz-chert wacke, sandstone, felsic and mafic volcanics and limestone. Volcanics towards the top of this unit are locally referred to as the Gilliland Tuff (Ferri and Melville, 1994). Due to the abundance of slate in this unit it is typically very recessive and poorly exposed, occupying valley floors (Photo 2).

The age of the Big Creek Group is thought to be Early Devonian to Early Permian in age (Ferri and Melville, 1994). Generally Late Devonian to Early Mississippian ages are indicated by fossils and U/Pb ages consistent with dates from other members of the Earn Assemblage (Ferri and Melville, 1994). Locally, as in the Nina Lake area, slates in the upper part contain Early Permian fossil assemblages (Ferri and Melville, 1994). In the Aiken Lake area, rocks of the Middle Devonian Otter Lakes Group are not present and slates assigned to the lower Big Creek Group contain conodonts as old as Emsian (Late Early Devonian).

This Big Creek Group is characterized by carbonaceous, dark grey to blue grey weathering, dark grey to black slate which can be interlayered with thinly bedded argillite or siltstone. The blue-grey colour, together with a distinctive yellowish stain on weathered surfaces, is typical of Late Devonian Earn Assemblage rocks found throughout the northern Cordillera. The slate can be quite friable and locally breaks into large, flexible sheets. Slate in the lower part of the unit is more lustrous and has a dark grey-brown colour.

Near the base of the Big Creek Group, rare 1 to 5 metres sections of grey to brown weathering, grey, thinly bedded carbonaceous limestone and argillaceous limestone occur interlayered with slate. Dark grey weathering, platy, recrystallized limestone with slate and silt partings up to 3 metres thick, is sporadically encountered towards the top of the unit.

Coarse Clastics

Lenses of coarse siliciclastics from 5 to more than 40 metres in thickness are found within the upper part of the Big Creek Group and are composed predominantly of chert-quartz wackes to sandstones, conglomerates and siltstones. Although these coarse units comprise only a minor component of the Big Creek Group, their composition has implications for the tectonic evolution of the northern Cordillera. Workers in the northern Cordillera believe that these northerly and westerly derived clastics were shed from uplifted blocks due to a regional rifting event during the Late Devonian (Gordey *et al*., 1987). Mapping in the southern Cordillera, primarily within the Roberts Mountain Allochthon, has shown that contractional deformation was occurring during this time period along the present southwestern margin of Ancestral North America. This has led some to interpret the Earn Assemblage as a foredeep and the associated coarse clastics as representing material shed from easterly thrusted fault blocks (Smith *et al*., 1993).

These coarse clastics form a section over 40 metres thick on the north side of Wrede Creek and are locally graded granule conglomerates. Wackes within these and other sequences contain between 20 to 40 per cent dark

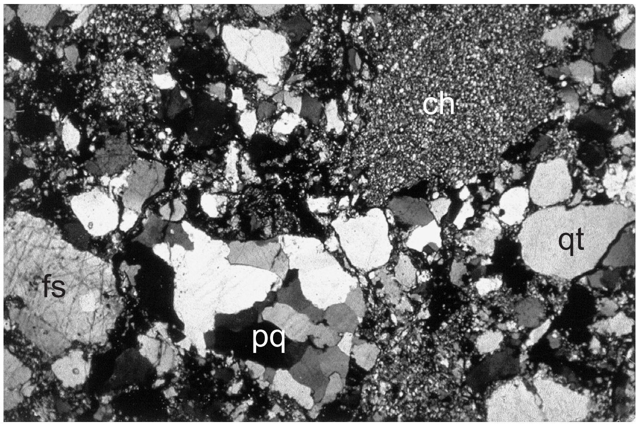

Photo 3. Photomicrograph of coarse clastics within the Big Creek Group. This sample originated from the south end of the Ingenika Range. Width of the photo represents 4.5 millimetres. fs: feldspar, ch: chert, qt: quartz, pq: polygonal quartz.

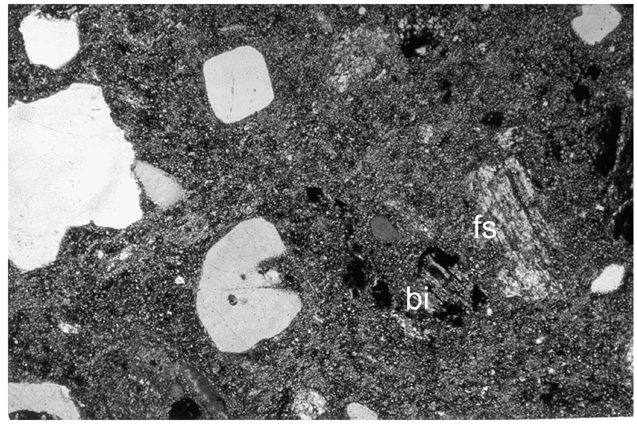

Photo 4. Photomicrograph of felsic volcanics of the Gilliland Tuff from the northern Lay Range. Note the embayed nature of the quartz phenocrysts. Textures visible in outcrop suggest this volcanic is tuffaceous. Cleavage orientation is parallel to the length of the photo. Width of the photo represents 4.5 millimetres. bi: biotite, fs: feldspar.

muddy matrix. Even the 'cleaner' sandstones contain up to 10 per cent dark grey to black argillaceous matrix giving them a dark colour. Clasts can be angular to rounded, although they are typically subangular to subrounded (Photo 3). Quartz, either as single or polygonal grains, usually is the dominant constituent comprising up to 60 per cent of grains and clasts. Light and dark grey to black chert is the next most dominant clast-type forming up to 30 per cent of grains. Minor clasts include siltstone and sandstone (approximately 10 per cent) and plagioclase (1-2 per cent). One section of sandstone contained up to 40 per cent plagioclase and orthoclase? clasts, suggesting it was produced, in part, from the weathering of an igneous protolith.

Volcanics

Felsic and mafic volcanic units from 1 to more than 45 metres in thickness are found stratigraphically above the coarse siliciclastics, within the upper-most part of the Big Creek Group. These are identical to those found regionally within the Big Creek Group and referred to as the Gilliland Tuff (Ferri and Melville, 1994).

Gilliland Tuff

Felsic tuff and massive porphyry (flows or sub-volcanic intrusives) are best developed in the extreme southeastern part of the project area where it forms a sequence over 45 metres thick (Figure 3). The unit is also encountered north of Wrede Creek where it ranges from 1 to 5 metres in thickness (Figure 3). It is typically light grey-green or rusty weathering sericitic quartz-feldspar tuff and/or porphyry. The unit contains sections of lapilli and coarse lapilli tuffs in the southeastern part of the map area (Figure 3). Phenocrysts comprise 5 to 20 per cent of the rock with embayed quartz crystals being the most common followed by plagioclase and poorly preserved accessory minerals. The latter have been altered to chlorite plus opaques, but in several instances residual material, together with pseudomorphs, suggests these were predominantly hornblende. The groundmass consists of sericite, quartz, feldspar plus chlorite, carbonate and opaques. Rip ups of black argillite from the surrounding sediments are locally abundant. Fine grained tuff invariably displays a weak to strong cleavage, although massive porphyry appears relatively undeformed (Photos 4 and 5). Chemical analysis of the tuff collected during the Manson Creek and Aiken Lake projects suggests these rocks are calc-alkaline in composition and are generally rhyolites to rhyodacites, (Ferri and Melville, 1994).

Mafic Volcanics

In the southern part of the map area, basalt and quartz-diorite is exposed at roughly the same stratigraphic horizon as the Gilliland Tuff. Pillowed? or fragmental basalt was observed in one locality and formed lenses and semi-continuous horizons approximately 50 centimetres thick within Big Creek argillites. The massive basalt is dark green and aphanitic with minor

Photo 5. Photomicrograph of felsic volcanics of the Gilliland Tuff from the Wasi Lake area. This sample is very similar to that shown in Photo 4 except that it lacks a penetrative cleavage. Texturally this rock looks like a quartz-feldspar porphyry flow or sub-volcanic intrusion. Width of the photo represents 4.5 millimetres.

calcite veining. Thin section examination reveals a predominance of finely crystalline feldspar together with carbonate, chlorite, sericite and opaques.

A few kilometres southeast of the basalt occurs a horizon of greenish grey quartz-diorite and crowded quartz-feldspar porphyry. The unit is approximately 15 to 20 metres thick and can be traced laterally into dark grey argillites of the Big Creek Group. Green slates are found within the argillites in the vicinity of these mafic rocks. Thin section examination from the periphery reveals it is composed of 30 to 50 per cent coarsely crystalline and sericitized plagioclase, 10 per cent quartz, with the remainder being finely crystalline feldspar, quartz, opaques and up to 30 per cent chlorite. This finer groundmass displays a strong, ductile flattening fabric whereas the large plagioclase phenocrysts behaved brittly and are merely broken. Preliminary lithogeochemical analysis suggests this rock is intermediate in composition.

The precise age of the Gilliland Tuff is poorly constrained. Stratigraphically it is found towards the top the Big Creek Group suggesting it is Mississippian or younger in age. U/Pb geochronology on a zircon collected at the type locality indicated a minimum age of 377±12 Ma (Ferri and Melville, 1994). A sample collected on the west bank of the Osilinka River returned a preliminary minimum age of 342±3 Ma (J. Gabites, personal communication, 1993). The age reported for both samples is based on a least square regression line as there were no concordant fractions in either sample due to inheritance and/or lead loss.

Although this data suggests there may be two periods of volcanism, the similarity between the volcanics suggests otherwise and the discrepancy is probably based on the poor U/Pb systematics within the collected zircons. At present the best estimate on the age of the Gilliland Tuff is Late Devonian to middle Mississippian. More samples were collected this summer in hopes of refining the age of this unit.

Nature of the Big Creek - Stelkuz Contact

In the map area, the Big Creek Group sits directly above the Stelkuz Formation and intervening strata of Early Cambrian to Middle Devonian age are missing (Figure 4). Due to the relatively recessive nature of these two units, the contact was not exposed; no direct observations could be made on the nature of this contact. The possibilities for the lack of intervening stratigraphy include: a steep normal fault; an unconformity or a shale-out of the missing carbonate-dominated stratigraphy.

Mapping in the southern part of the study area initially suggested the presence of a late normal fault offsetting stratigraphy. Although locally this seems possible, the position of the Big Creek above Stelkuz lithologies would require a very persistent normal fault whose stratigraphic and/or structural displacement remains constant over 25 kilometres - a situation that seems rather unlikely.

Missing stratigraphy below the Big Creek Group was also observed in the southern Lay Range during part of the Aiken Lake Project. In this area, rocks of the Echo Lake Group disappear north of the northeast-trending Knoll normal fault, such that Big Creek rocks sit directly above the uppermost Atan Group (Ferri *et al*., 1993a, b). The presence of a normal fault was also postulated by Ferri *et al*. (1993a) in this area, although stratigraphic evidence suggested that the Early Paleozoic carbonate sequence in this area may be shaling out to the north. A more detailed account of this can be found in Ferri *et al*., (1993a).

Although a shale-out of the missing stratigraphy is a possibility, an unconformable contact at the base of the Big Creek Group is presently favoured and is consistent with the present data. In the western Selwyn Basin, rocks of the Earn Assemblage are found unconformably overlying units as old as Late Proterozoic (Gordey and Irwin, 1987), a situation similar to that postulated here.

Extensions of the Big Creek Group Beyond the Map Area

Rocks of the Big Creek Group most likely extend beyond the northern limit of the present mapping project, and are probably traceable up to the Ingenika Fault where rocks of Ancestral North America are juxtaposed against volcanic rocks of Quesnellia (Gabrielse *et al*., 1977). Although Big Creek rocks are not displayed on regional maps of this area (McConnell Creek East-Half; Richards, 1976 and Ware West-Half; Gabrielse *et al*., 1977), the northward continuation of the Stelkuz Formation at the contact with the Lay Range Assemblage, taken in conjunction with the recessive nature of the Big Creek Group, suggests its presence may be masked by overburden. This is supported by the trace of several large creeks which have followed this relatively incompetent horizon.

Southeast of the Manson River, in the Pine Pass map area, Struik and Northcote (1991) traced rocks similar to the Big Creek Group, assigning them to the Earn Group. They also described tuff and minor basalt within this sequence. Struik (1989) also reported felsic tuff up to 300 metres thick within dark grey argillites of Late Devonian age within the McLeod Lake map area. These are found east of the McLeod Lake fault zone and west of the Northern Rocky Mountain Trench fault zone and are probably more akin to the Besa River Formation. Struik (1990) suggests that this block of Ancestral North American stratigraphy is transitional between typical carbonate platform sequences observed to the west and more basinal successions found east of the McLeod Lake fault zone.

Lay Range Assemblage

The Lay Range Assemblage has been subdivided into two broad packages: the Lower Sedimentary Division (LSD) and the Upper Mafic Tuff Division (UMTD) (Ferri, 1997). The LSD is a mixed sedimentary and volcanic sequence whereas the UMTD is almost entirely fine and coarse grained mafic tuffs, volcanic breccia and flows (Figure 5).

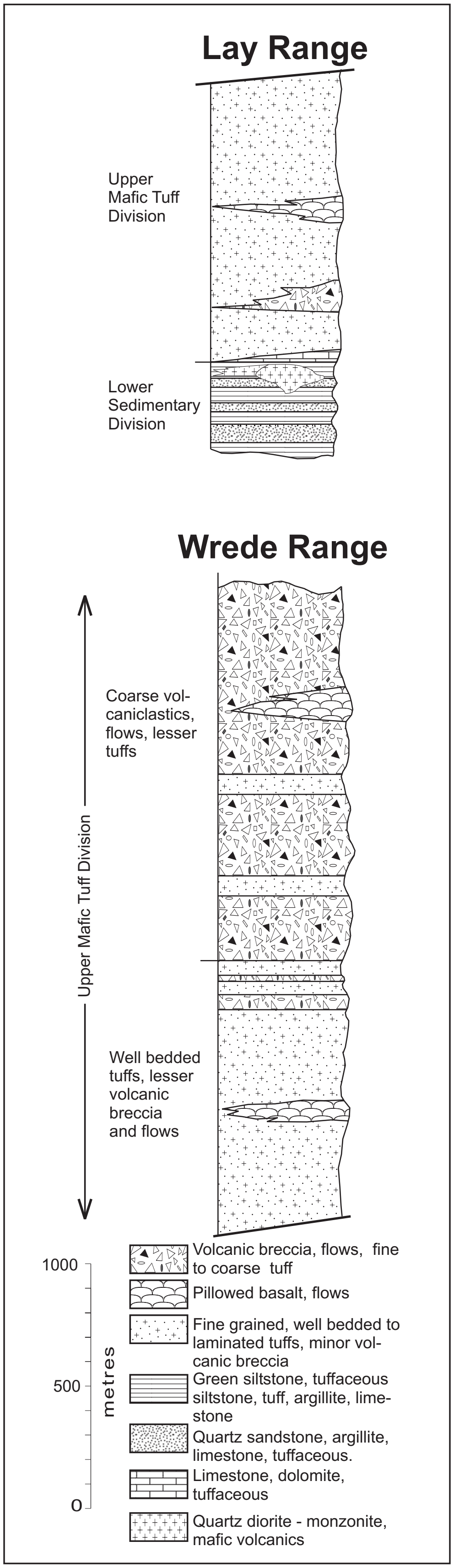

Figure 5. Simplified stratigraphic columns of the Lay Range Assemblage within the map area.

The age of the Lay Range Assemblage is late Mississippian (Namurian) to Permian based on fossil collections made in the southern Lay Range (Ferri, 1997). Conodonts, corals, fusulinids and foraminifera recovered from the LSD suggest a late Mississippian lower age limit and a middle Pennsylvanian upper age limit for limestone at the top of the unit. Radiolarians from chert within the green and maroon siltstone and tuff unit above this limestone have indicated Early Permian ages. Conodonts from the remaining UMTD are broadly Permian in age. In the southern part of the Lay Range tuffs of the UMTD were believed to sit unconformably on the limestone below the green and maroon siltstone suggesting an unconformity of some 13 Ma between the two units (middle Pennsylvanian to Early Permian; Ferri, 1997). Stratigraphic relationships observed within the present map area suggest the limestone and UMTD have a conformable relationship. Although these two interpretations may seem at odds, this is entirely consistent with the variability observed along volcanic arcs.

Lower Sedimentary Division

The LSD is only exposed within the northern Lay Range, in the southeastern portion of the map area (Figure 3) and is restricted to the core of a north-east verging fold (Ferri, 1997). Generally, siliciclastics and carbonates are found within the lower parts of this package with mafic volcanics becoming dominant towards the top. The entire sequence is capped by a limestone up to 50 metres thick.

The lower parts of the LSD are characterized by interbedded quartz sandstone, argillite, siltstone, chert and tuff. Sandstone forms prominent weathering ribs 5 to 15 metres thick within this section and comprises approximately 30 per cent of the sequence. Laterally they appear to pinch out within green siltstone and tuff. Thin to thick or massively bedded sandstone to granule conglomerate is beige weathering and grey in colour. Compositionally it is an impure quartz sandstone and locally contains clasts of feldspar and lithic fragments. The matrix typically is calcareous and greenish, the latter suggesting it is partly of volcanic origin.

Interbedded argillite or slate is dark grey and is associated with platy dark limestone and dark grey to cream, thin to thickly bedded chert. Associated with all these lithologies is green to maroon siltstone grading into tuff which makes up to 50 per cent of the section.

On the eastern limb of the overturned anticline, the upper part of the LSD is intruded by a greenish-grey quartz-diorite to monzonite up to several hundred metres thick. This unit can be spatially associated with grey-brown weathering, dark green aphanitic basalt and brown to orange weathering, green feldspar-pyroxene porphyry. Above these rocks is a distinctive package of interlayered green and maroon siltstone, tuff and jasperoidal chert up to 20 metres in thickness. This unit is commonly associated with limestone and is found at the contact with tuffs of the UMTD. The distinctiveness of this unit and its presence at the LSD - UMTD contact make it a local marker horizon.

Lenses of buff weathering, cream coloured, recrystallized massive dolomite, with layers of green slate, up to 20 metres in thickness is commonly found below the green and maroon siltstone. This dolomite horizon forms a semi-continuous unit which, together with the succeeding limestone, can laterally pinch-out over short distances (Figure 3; Photo 6). Massive to platy grey limestone up to 50 metres thick, with distinctive ribs of beige to light grey wavy chert lenses 1 to 5 centimetres thick can be found stratigraphically above the green and maroon siltstone unit. Although the limestone contains a very strong fabric, textures are preserved locally; some parts are bioclastic with poorly preserved crinoid ossicles and fusulinids (J.W.H. Monger, unpublished notes, 1973). Sections of the limestone are tuffaceous and have a maroon and green colour. Interbeds of green tuff between 10 to 50 centimetres thick are also present. The lower contact of the limestone appears gradational with the underlying green and maroon siltstone. The upper part of the limestone displays a sharp, but interbedded contact with tuffs of the UMTD. This limestone interfingers with tuffs of the UMTD along ridge faces (Photo 6). Its thickness changes drastically to less than a metre in the far southeastern portion of the map area. There, maroon and green siltstone, tuffs and chert are found on either side of the limestone unit, a relationship also observed several kilometres to the north where the limestone thickens to 50 metres.

Two bands of limestone are present along the top of the eastern extent of the LSD. Although they appear to be two separate units, they are remarkably similar and the recurrence of the distinct maroon and green unit, together with the monzonite and tuff, indicates a structural repetition.

Upper Mafic Tuff Division

The UMTD is a relatively homogenous package dominated by thin to massively bedded tuffs with lesser lapilli tuffs, volcanic breccia, basalt, diorite and rare quartz-feldspar tuff or porphyry flows. Thinly bedded tuffs are typically laminated and commonly graded. Rocks of the UMTD are found on either side of the northeast verging, overturned anticline within the northern Lay Range. They can be traced to the north, along the subdued valley east of the Wrede Ultramafic Complex and across Wrede Creek where they form the high ground along the northwestern part of the map area. South of Wrede Creek, graded, well bedded tuffs (Photo 7) are the most common lithology along the east side of the anticline, with massive basalt flows accounting for approximately 10 per cent of the lower and middle section.

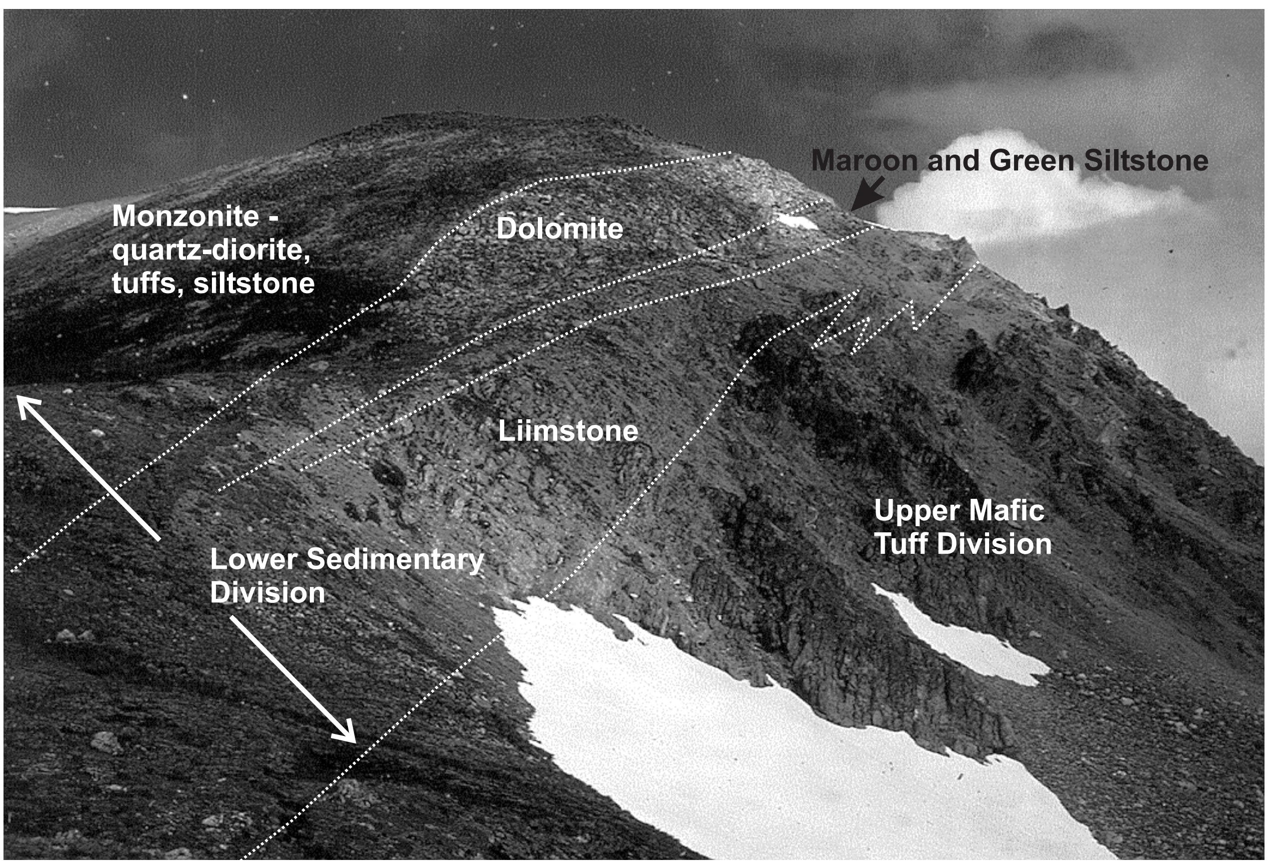

Photo 6. Looking southeast at the contact between the UMTD and LSD of the Lay Range Assemblage along the northern Lay Range. The interfingering between the limestone at the top of the LSD and tuffs of the UMTD has been highlighted. Also shown is the horizon of maroon and green siltstone/tuff which sits stratigraphically below the limestone at this locality but can also be found between it and the UMTD elsewhere, a configuration also observed in the southern Lay Range (Ferri, 1997).

Photo 7. Photograph of typical well bedded and laminated fine grained, graded tuffs of the UMTD. This is the most common lithology observed within the UMTD.

A rare occurrence of rusty weathering, light greenish grey quartz-feldspar sericite schist (originally tuff or porphyry flow), approximately 20 metres thick (*see* Figure 3), was encountered within this unit on the northeast flowing creek immediately north of the Lay Range. This unit was sampled for U/Pb and whole rock analysis. The UMTD is much coarser on the southwest side of the anticline within the Lay Range where it is composed of green and dark green fine to coarse grained lapilli tuffs, volcanic breccias and massive basaltic flows. Volcanic clasts are commonly flattened parallel to cleavage and consist of aphanitic and amygdaloidal basalt. Dark grey and black argillite clasts and quartz grains also form accessories in certain horizons. A rare, small rubbly outcrop of orange-brown coarse grained quartz-feldspar sandstone was observed within this succession.

North of Wrede Creek, the UMTD is found within an upright, steeply southwest dipping panel with the graded, laminated, fine tuffs in the stratigraphically lowest part of the panel (eastern lower slopes) and these are succeeded by lapilli tuffs, volcanic breccias and flows (Photo 8). The contact between the two is gradational with a general coarsening of the volcanic deposits up section until over 50 per cent of the sequence is composed of lapilli tuffs and/or volcanic breccia.

Clasts within the volcanic breccia unit are more diverse than observed south of Wrede Creek. They are typically green to maroon in colour and consist of aphanitic basalt together with fragments of pyroxene and/or feldspar porphyry basalt. Deposits can be monomictic to polymictic and are locally associated, especially towards the top of the ridge, with massive to pillowed basalt of similar composition. Some feldspar porphyry flows are quite distinctive due to the presence of phenocrysts up to several centimetres in size. The coarse volcaniclastics are locally intruded by small bodies of hornblendite and associated gabbro probably related to the Wrede Ultramafic Complex.

Correlations of the Lay Range Assemblage with other packages throughout the Cordillera have been summarized by Ferri (1997). Intermixed sediments and volcanics of the LSD have the greatest potential of being equivalent to rocks of the Yukon-Tanana Terrane which host VMS occurrences. The oldest age known from the Lay Range Assemblage consists of late Mississippian to early Pennsylvanian conodonts recovered from the lower parts of the unit in the southern Lay Range. This is somewhat younger than the Early Mississippian age for quartz-feldspar meta-porphyry associated with the Wolverine deposit (Murphy and Piercey, 1999). As well, the overall character of the LSD is different than that of the Yukon-Tanana Terrane in the Finlayson Lake area. In general, rocks of the LSD and UMTD correlate with the middle and upper parts of the Dorsey Assemblage as de-

Photo 8. Polymictic volcanic breccia of the UMTD. This lithology occurs in the lower part of the UMTD within the Wrede Range and is characterized by maroon and green clasts of aphanitic basalt together with pyroxene and/or feldspar phyric basalt.

scribed by Stevens and Harms (1995) along the B.C. - Yukon border and further south by Nelson (1997).

Takla Group

The Takla Group was observed in only a handful of outcrops south of Wrede Creek. Regionally Takla rocks sit unconformably atop those of the Lay Range Assemblage (Ferri, 1997). A steep fault zone, of possibly strike-slip configuration, separates the two packages within the present map area.

Rocks of the Takla Group consists of augite-feldspar porphyry flows, pyroclastic breccia and tuff, all of which have become sheared and foliated near their contact with the Lay Range Assemblage. Small stocks of beige quartz monzonite locally intrude these volcanics.

The Takla Group is Late Triassic to Early Jurassic in age immediately to the south (Ferri and Melville, 1994; Ferri *et al*., 1992b, 1993b). Augite-plagioclase phyric volcanics observed within the map area belong to a sequence locally referred to as the Plughat Mountain Succession (Ferri and Melville, 1994) which is broadly Late Triassic in age.

Wrede Ultramafic Complex

The Wrede Ultramafic-Mafic Complex is an Alaskan-type body of Late Triassic age intruding rocks of the Takla Group just south of Wrede Creek (Figure 3; Nixon *et al*., 1998). The complex is crudely zoned with a gradation from dunite in the core to gabbro at the margins. These rocks were not examined in any detail; the geology of the complex shown on Figure 3 is taken from Nixon *et al*. (1998). This ultramafic body is most likely related to the Polaris Ultramafic Complex which intrudes rocks of the Lay Range Assemblage within the southern part of the Lay Range (Nixon *et al*., 1998; Ferri *et al*., 1993a, b).

STRUCTURE AND METAMORPHISM

The structural style within the map area is quite variable and is a reflection of the different tectonic terranes present. Generally, the degree of penetrative deformation increases from west to east within the map area. Cleavage is poorly developed or non-existent within coarse volcanic breccias and flows of the UMTD and Takla Group. When present, a weak cleavage within coarse volcaniclastics of the UMTD is one of the criteria used in distinguishing these rocks from similar, but relatively undeformed volcaniclastics in the Takla Group. Commonly a slaty cleavage is present within rocks of the underlying Big Creek Group and the fine tuffs of the UMTD. The intensity of cleavage and metamorphism increases down section, into rocks of the Ingenika Group where well developed, biotite-bearing schists occur in the lower parts of the Swannell Formation. Although biotite porphyroblasts were noted in several localities along the eastern margin of the map area, not enough data points are available to draw a metamorphic isograd. At one locality poikiloblastic biotite porphyroblasts were up to several

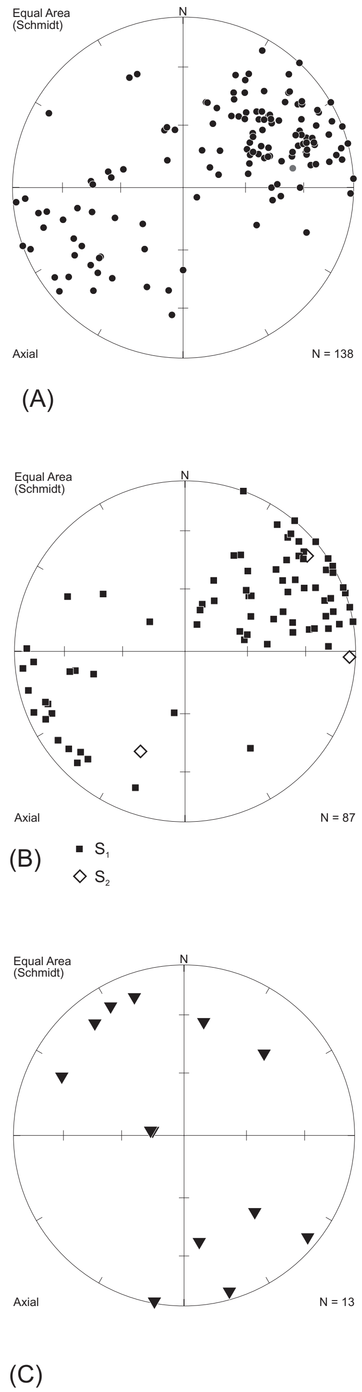

Figure 6. Equal area plots of structural data from the map area. (A) Poles to bedding. (B) Poles to cleavage. (C) Bedding-cleavage intersections.

millimetres in length. Although they grew in a random to semi-random orientation, they were produced near the end of S_1 cleavage development as shown by the slight wrapping of this fabric around the porphyroblasts.

Metamorphism is of regional or Barrovian-type and dating of metamorphic minerals indicates it is Middle Jurassic in age, although mid-Cretaceous and Tertiary cooling ages are also encountered (Ferri and Melville, 1994).

Only one large scale fold was delineated within the map area and consists of a tight, northeasterly overturned structure outlined by the limestone marker between the UMTD and LSD (Figure 3). This large fold is the northward continuation of a structure mapped within the southern Lay Range (Ferri *et al*., 1993a, b). The southwest dipping axial plane of this fold is similar in orientation to the average attitude of cleavage within rocks of the map area (Figure 6). The fold structure is lost north of the Lay Range and only a southwest dipping overturned panel of volcanics belonging to the UMTD occurs north of the Wrede Ultramafic Complex, suggesting the core of the structure is located further to the west. The repetition of the limestone at the top of the LSD along the eastern limb of the structure is believed to be due to small scale folding. Outcrop-scale versions of this large fold were observed primarily within rocks of the Swannell Formation.

Early cleavage, together with the surrounding lithologies, is locally broadly folded and/or crenulated. This folding is best developed within rocks of the Swannell Formation, although the spread of cleavage orientation shown in Figure 6 indicates the entire map area has been affected. This suggests the presence of at least two distinct periods of fold formation. Cassiar rocks within the map area are found on the west flank of a broad antiform similar to others developed within strata of the Ingenika Group (Figure 2). It is not clear if the latter, upright folds within the map area are related to these structures or represent a distinct fold episode. Comparison of bedding-cleavage intersection attitudes and the beta direction for poles to cleavage and bedding within the map area suggest the two fold styles are coaxial.

The large, northeasterly overturned fold within the Lay Range Assemblage is carried in the hangingwall of the major, terrane bounding, northeasterly directed thrust (Swannell Fault; Wheeler and McFeely, 1991), which places rocks of the Lay Range Assemblage above those of the Cassiar Terrane. The thrust is steeply dipping to the southwest and is roughly parallel to bedding in bounding units. This thrust delineates the western boundary of Ancestral North American rocks within this part of the Canadian Cordillera. Although no kinematic indicators were observed in the map area, in the southern Lay Range these display tops to the east directions (Nixon *et al*., 1993; Ferri *et al*., 1993b). It is interesting to note that in the most northern part of the map area folding of the fabric along this zone, in conjunction with brittle pull-aparts, would suggest late strike-slip motion, possibly dextral in nature. The axial planes of these folds are steep and perpendicular to the fault contact and the associated fold axes also exhibit steep plunges. These structural features were localized and their regional significance is presently unknown.

The contact between the Lay Range Assemblage and the Takla Group is marked by a steeply dipping zone of highly sheared volcanics up to 100 metres wide. Regionally, the Lay Range Assemblage has been shown to form the basement to Takla volcanics (Ferri, 1997). The fault zone can be quite narrow, as observed in the northern Lay Range where it is hidden below approximately 10 metres of glacial deposits. Typically the zone is marked by a steep cleavage or schistosity with relic pyroxene, feldspar or lithic clasts. Deformation appears ductile, although certain components, such as feldspar and pyroxene, behaved quite brittly. No kinematic indicators could be discerned where the fault zone was examined in the map area.

In the southern part of the map area the fault zone trends north-northwesterly. It cuts out much of the Lay Range Assemblage as it is traced northwards towards the Wrede Range (Figure 3). It is likely the fault veers more to the west across Wrede Creek due to the increased amount of Lay Range volcanics and the lack of large shear zones within Lay Range rocks.

This steep dipping fault structure probably connects southwards with either the Polaris Creek or Lay Range fault zones, two strike-slip fault zones with several kilometres displacement (Ferri *et al*., 1993b; Ferri, 1997). These faults are part of an en echelon fault array that together with the Manson fault zone and Pinchi and Northern Rocky Mountain Trench systems, record a major period of Late Cretaceous to Early Tertiary dextral motion in this part of the Cordillera.

MINERAL POTENTIAL

The Earn Assemblage, to which the Big Creek Group belongs, is an important metallotect within the Canadian Cordillera. In Selwyn and Kechika basins, it hosts significant SEDEX deposits such as the Tom, Jason, Driftpile Creek, Akie and Cirque. Further west, Earn Assemblage rocks also contain important VMS deposits which include the Marg of northwestern Selwyn Basin and the Wolf deposit found within the northern Cassiar Terrane.

In southeastern British Columbia rocks of similar age to the Earn found within the western Kootenay Terrane, a more distal part of the ancient continental margin, also hosts important VMS deposits such as Rea and Homestake. Finally, Early Mississippian rocks of continental nature, but uncertain affinity within the Yukon-Tanana Terrane, have recently been shown to contain large VMS deposits including the Wolverine, Kudz Ze Kayah and Fyre Lake. As stated earlier, all these occurrences taken together underlines the fact that the Late Devonian to Early Mississippian is an important period of metalliferous deposition.

Major SEDEX mineralization within the Selwyn and Kechika basins are Frasnian and Famennian (Late Devonian) in age (Paradis *et al*., 1998) and found towards the base of the Earn Group. SEDEX occurrences of Early Mississippian age are reported in the MacMillan Pass area of the Selwyn Basin (Irwin and Orchard, 1989). The ore composition of these deposits is simple, being made up of sphalerite and galena (+silver) with pyrite and barite as non-ore components. Barite is an important constituent of these occurrences and is commonly found in distal parts of the deposits or as the primary component of low-temperature systems. The presence of barite by itself within Earn lithologies is important in that it signifies the presence of active exhalative systems.

In the Yukon, VMS deposits within Earn rocks are associated with calc-alkaline and alkaline to calc-alkaline felsic volcanics. The Wolf deposit is found with the alkaline to calc-alkaline Pelly Mountain volcanic belt which is associated with several other VMS occurrences including the MM, Mamu, Bnob, Chezpnough and Tree (Hunt, 1999). Mineralogically these are composed of sphalerite, galena (+silver), minor copper, and with pyrite, pyrrhotite, barite and minor fluorite as accessories. The age of these deposits is uncertain and are broadly Late Devonian to Early Mississippian (Hunt, 1999).

The Marg VMS deposit of northwestern Selwyn Basin is associated with calc-alkaline felsic volcanics of Early Mississippian age (Turner and Abbott, 1990). This is a polymetallic occurrence composed Cu, Zn, Pb, Ag and Au with a sulphide mineralogy made of pyrite, chalcopyrite, sphalerite, galena and minor tetrahedrite and arsenopyrite. Ferroan carbonates and quartz are also important constituents of the ore body. The presence of sericite-carbonate-quartz-pyrite within footwall rocks suggest hydrothermal alteration, a situation rarely seen within the low temperature SEDEX deposits or reported from the Pelly Mountain alkaline occurrences.

Mineral Potential of the Big Creek Group and Gilliland Tuff

Known mineralization within the Big Creek Group is SEDEX in nature although there are anomalous stream sediment and soil geochemistry localities suggesting the potential for mineralization within the Gilliland Tuff. SEDEX mineralization is found at the Omineca Queen bedded barite occurrence and in the Wasi Lake area.

Sedex Mineralization

The Omineca Queen (MINFILE number 093N 087) bedded barite, located near Munro Creek, immediately south of the Manson River, is the only documented SEDEX occurrence within the Big Creek Group (Figure 2; Band, 1970; McCammon, 1975; Craig, 1992). The Omineca Queen consists of up to 7 metres of bedded to massive barite hosted within dark grey argillites and slates. This SEDEX occurrence was visited to examine the mineralization and its possible relationships to the Gilliland Tuff. Old trenches and cat trails are severely overgrown and only two sections of massive to poorly bedded barite up to 3 metres thick were visible. Although no felsic tuff was observed in the area, mapping showed that the barite is found within black, fissile shale to argillite and sits stratigraphically below quartz-chert wackes and sandstone which regionally are below the Gilliland Tuff. This barite mineralization is probably part of the Late Devonian SEDEX event found throughout the Kechika and Selwyn basins of Ancestral North American.

Exploration by Cominco Exploration Ltd. east of Wasi Lake, near the former PAR mineral claims, discovered several other barite occurrences within the Big Creek Group (Bruce Mawer, personal communication, 1993). In this area, Big Creek argillites can be traced around a broad syncline south of the Osilinka River (Figure 2). East of Wasi Lake, anomalous levels of Pb, Zn and Ba in stream silts were reported by Ferri *et al*. (1992a) and from the RGS survey for 94C (Jackaman, 1998). Anomalous stream sediments and soils were also collected on the former RAP mineral claims (Johnson, 1996) which are several kilometres northeast of Wasi Lake. Together, these indicate the potential for SEDEX style mineralization within the Big Creek Group of the Wasi Lake area. Rock geochemistry on several samples of the lower Big Creek Group indicate weakly anomalous Ba levels in one area and elevated levels of Ag (2.6 ppm), Pb (433 ppm) and Ba (1928 ppm) in another area (Johnson, 1996).

Potential for VMS Mineralization

Mapping by the author has traced Gilliland Tuff felsic volcanics from the Manson River area to the Wrede Range, a distance of some 150 kilometres (Figure 2). These volcanics are intermittently present within the upper part of the Big Creek Group and are from several metres to some 50 metres in thickness. Textural features commonly indicate the volcanics are tuffaceous and submarine in nature, being interbedded with fine clastics of the Big Creek Group. Sections in several localities are quite thick and parts of the unit appear to be subvolcanic and texturally resemble a quartz ±feldspar porphyry intrusion. Areas where thick volcanics occur include: the type locality around Germansen Landing; the area south of the Swannell River and the region between the Osilinka River and Wasi Lake where the unit is well in excess of 1000 metres thick. The mapped extent of the volcanics shown in Figure 2 would suggest that a volcanic centre may be present in the Wasi Lake area with subsidiary centres in the Germansen Landing and Swannell River areas. The thin horizons of tuff seen elsewhere within the Big Creek Group would then represent distal deposits produced by these or other volcanic centres.

Although no mineralization has yet been attributed to this unit, several drainages cutting the Gilliland Tuff have returned anomalous stream silt geochemistry and anomalous whole rock geochemistry for the tuff. In the Wasi Lake area, the recent RGS release for NTS sheet 94C (Jackaman, 1998) contains localities with anomalous levels of Pb, Zn, Ba and ±Au for some of the drainages cutting the unit. Rock sampling of carbonaceous breccia or conglomerate from the Gilliland Tuff within the former RAP mineral claims east of Wasi Lake returned anomalous Ag (7.3 ppm) and Ba (greater than 2000 ppm; Johnson, 1996). Gilliland volcanics in the Wasi Lake area locally contain sericite and/or carbonate alteration.

South of Swannell River, several drainages cutting the Gilliland Tuff contain silts with anomalous levels of Cu (24, 104 and160 ppm), Pb (10, 26 and 107 ppm) and Zn (283, 1090 and 1453 ppm; Rhodes, 1994). Silts from several streams cutting the Big Creek Group in the northern Lay Range (Figure 3) contain sediments slightly anomalous in Pb, Zn and Ba (Jackaman, 1998).

The high background level of barium in the Gilliland Tuff, together with the associated barite in some of the VMS occurrences in the Pelly Mountains suggests that this mineral can be, as in the case of SEDEX deposits, a useful indicator of nearby mineralizing systems. Bedded barite of Early Mississippian age is known from the Selwyn Basin and northern Cassiar platform and may be time equivalent to some of the felsic volcanism (Gordey, 1991; Irwin and Orchard, 1990).

SUMMARY

In summary, mapping in north-central British Columbia has delineated the presence of a Late Devonian to Early Mississippian sequence of argillite, slate and sandstone with proven SEDEX potential. The upper part of this succession also contains felsic tuff similar in age and general composition to volcanics in cratonic and pericratonic rocks which are associated with VMS mineralization. These volcanics, locally called the Gilliland Tuff, have been traced from the Manson River area to as far north as Wrede Creek, a distance of some 150 kilometres. Although no direct mineralization was observed within these rocks, anomalous base metals values in silt samples from several drainages cutting these rocks together with elevated base metals in rock analysis suggests the potential for VMS-style mineralization.

Late Paleozoic arc volcanics and pericratonic sediments of the Lay Range Assemblage exposed between the northern Lay Range and Ingenika River, have closer lithologic and age similarities with the middle and upper part of the Dorsey Assemblage than with Yukon-Tanana rocks seen in the Finlayson Lake area of the Yukon.

ACKNOWLEDGMENTS

I would like to thank Pat Johnstone for excellent and cheery assistance, and for teaching me all I know about Formula 1 racing. I would also like to thank Scott Muller for his assistance in expediting our needs in a timely manner this summer. Thanks also to Northern Mountain Helicopters Ltd., Pacific Western Helicopters Ltd. and Interior Helicopters Ltd. for moving may flycamps. I would like to also thank Kim Bellefontaine for reading an early version of this manuscript and Dave Lefebure for making suggestions on later renditions.

REFERENCES

Band, R. (1970): Geochemical Report on Omineca Queen Claims #3 and #4; B.C. Ministry of Energy, Mines and Petroleum Resources, Assessment Report 2636.

Craig, D.L. (1992): Geochemical and Geological Report on the Roe 1-4 Claims; B.C. Ministry of Energy, Mines and Petroleum Resources, Assessment Report 22802.

Ferri, F. (1997): Nina Creek Group and Lay Range Assemblage, North-central British Columbia: Remnants of Late Paleozoic and Arc Terranes; Canadian Journal of Earth Sciences, Volume 34, pages 854-874.

Ferri, F., and Melville, D.M. (1994): Bedrock Geology of the Germansen Landing - Manson Creek Area, British Columbia (93N/9, 10, 15; 94C/2); B.C. Ministry of Energy, Mines and Petroleum Resources, Bulletin 91.

Ferri, F., Dudka, S., Rees, C and Willson, M. (1992a): Geology of the Uslika Lake Area, British Columbia (94C/3,4 and 5); B.C. Ministry of Energy, Mines and Petroleum Resources, Open File 1992-11.

Ferri, F., Dudka, S., and Rees, C. (1992b): Geology of the Uslika Lake Area, Northern Quesnel Trough, B.C. (94C/3,4 and 5); in Geological Fieldwork 1991, B.C. Ministry of Energy, Mines and Petroleum Resources, Paper 1992-1, pages 127-146.

Ferri, F., Dudka, S., Rees, C., and Meldrum, D.G. (1993a): Preliminary Geology of the Aiken Lake and Osilinka River areas, British Columbia (94C/2, 3, 5, 6 and 12); B.C. Ministry of Energy, Mines and Petroleum Resources, Open File 1993-2.

Ferri, F., Dudka, S., Rees, C., and Meldrum, D.G. (1993b): Geology of the Aiken Lake and Osilinka River areas, Northern Quesnel Trough (94C/2, 3, 5, 6 and 12); B.C. Ministry of Energy, Mines and Petroleum Resources, 1992, Paper 1993-1, pages 109-134.

Gabrielse, H. And Campbell, R.B. (1991): Upper Proterozoic Assemblages, Chapter 6 in Geology of the Cordilleran Orogen in Canada, H. Gabrielse and C.J. Yorath (Editors); Geological Survey of Canada, No. 4, pages 125-150.

Gabrielse, H., Dodds, C.J. and Mansy, J.L. (1977): Geological Map of the Ware West Half and Toodoggone River Map Areas; Geological Survey of Canada, Open File 483.

Gordey, S.P. (1991): Devonian-Mississippian Clastics of the Foreland and Omineca Belt, Chapter 8; in Geology of the Cordilleran Orogen in Canada, H.Gabrielse, and C.J.Yorath (Editors); Geological Survey of Canada, Geology of Canada, Number 4, pages 230-242.

Gordey, S.P., Abbott, J.G., Tempelman-Kluit, D.J. and Gabrielse, H. (1987): "Antler" Clastics in the Canadian Cordillera; Geology, Volume 15, pages 103-107.

Gordey, S.P., and Irwin, S.E.B. (1987): Geology, Sheldon Lake and Tay River Map areas, Yukon Territory, Geological Survey of Canada, Preliminary Map 19-1987.

Hunt, J.A. (1999): Preliminary Stratigraphy and Distribution of Devono-Mississippian Massive Sulphide-bearing Volcanic Rocks in the Mount Vermilion (Wolf) Area, Pelly Mountains (105G/5 and G/6), Southeast Yukon; in Yukon Exploration and Geology 1998, C.F. Roots and D.S. Emond (Editors), Indian and Northern Affairs Canada, pages 73-90.

Irwin, S.E.B. and Orchard, M.J. (1989): Upper Devonian - Lower Carboniferous Conodont Biostratigraphy of the Earn Group and Overlying Units, Northern Canadian Cordillera; in Ordovician to Triassic Conodont Paleontology of the Canadian Cordillera, M.J. Orchard and A.D. McCracken (Editors); Geological Survey of Canada, Bulletin 417, pages 185-213.

Jackaman, W. (1998): British Columbia Regional Geochemical Survey, NTS 94C - Mesilinka River, B.C. Ministry of Energy and Mines, BC RGS 47.

Johnson, W. (1996): Geology and Geochemistry RAP 1 and 2 Claims; B.C. Ministry of Employment and Investment, Assessment Report 24352.

Mansy, J.L. and Gabrielse, H. (1978): Stratigraphy, Terminology and Correlation of Upper Proterozoic Rocks in Omineca and Cassiar Mountains, North-Central British Columbia; Geological Survey of Canada, Paper 77-19, 17 pages.

McCammon, J.W. (1975): Omineca Queen, B.C. Ministry of Energy, Mines and Petroleum Resources, Geology, Exploration and Mining in British Columbia 1974, pages 373-374.

Murphy, D.C. and Piercey, S.J. (1999): Finlayson Project: Geological Evolution of Yukon-Tanana Terrane and its Relationship to Campbell Range Belt, Northern Wolverine Lake Map Area, Southeastern Yukon; in Yukon Exploration and Geology 1998, C.F. Roots and D.S. Emond (Editors), Indian and Northern Affairs Canada, pages 47-62.

Nelson, J. (1997): Last Seen Heading South: Extensions of the Yukon-Tanana Terrane in Northern British Columbia; in Geological Fieldwork, D.V. Lefebure, W.J. McMillan and J.G. McArthur (Editors), B.C. Ministry of Employment and Investment, Paper 1997-1, pages 145-156.

Nelson, J. and Bellefontaine, K.A. (1996): The Geology and Mineral Deposits of North-Central Quesnellia; Tezzeron Lake to Discovery Creek, Central British Columbia; B.C. Ministry of Employment and Investment, Bulletin 99.

Nixon, G.T., Archibald, D.A., and Heaman, L.M. (1993): ^{40}Ar-^{39}Ar and U-Pb geochronometry of the Polaris Alaskan-type complex, British Columbia: precise timing of Quesnellia-North America interaction. Geological Association of Canada, Program with Abstracts, page A-76.

Nixon, G.T., Hammack, J.L., Ash, C.A., Cabri, L.J., Case, G., Connelly, J.N., Heaman, L.M., Laflamme, J.H.G., Nuttall, C., Paterson, W.P.E., and Wong, R.H. (1998): Geology and Platinum-Group-Element Mineralization of Alaskan-Type Ultramafic-Mafic Complexes in British Columbia; B.C. Ministry of Energy and Mines, Bulletin 93.

Paradis, S., Nelson, J.L. and Irwin, S.E.B. (1998): Age Constraints on the Devonian Shale-Hosted Zn-Pb-Ba Deposits, Gataga District, Northeastern British Columbia, Canada; Economic Geology, Volume 93, pages 184-200.

Richards, T. (1975): Geology of the McConnell Creek Map-Area (94D/E); Geological Survey of Canada, Open File 342.

Rhodes, D. (1994): 1993 Assessment Report Cygnet/Swan Property; B.C. Ministry of Energy, Mines and Petroleum Resources, Assessment Report 23321.

Smith, M.T., Dickinson, W.R. and Gehrels, G.E. (1993): Contractional Nature of Devonian-Mississippian Antler Tectonism along the North American Continental Margin; Geology, Volume 21, pages 21-24.

Steven, R.A. and Harms, T.A. (1995): Investigations in the Dorsey Terrane, Part I: Stratigraphy, Structure, and Metamorphism in the Dorsey Range, Southern Yukon Territory and Northern British Columbia; in Current Research, Geological Survey of Canada, Paper 1995-A, pages 117-127.

Struik, L.C. (1989): Devonian, Silurian, Cambrian and Precambrian Stratigraphy, McLeod Lake Map Area, British Columbia; Geological Survey of Canada, Paper 89-1A, pages 119-124.

Struik, L.C. (1990): Paleozoic - Triassic Stratigraphy, McLeod Lake Map Area, Central B.C.; Geological Association of Canada, Program with Abstracts, page A126.

Struik, L.C. and Northcote, B.K. (1991): Pine Pass Map Area, Southwest of the Northern Rocky Mountain Trench, British Columbia; Geological Survey of Canada, Paper 91-1A, pages 285-292.

Turner, J.W. and Abbott, G. (1990): Regional Setting, Structure, and Zonation of the Marg Volcanogenic Massive Sulphide

Deposit, Yukon; in Current Research, Part E, Geological Survey of Canada, Paper 90-1E, pages 31-41.

Wheeler, J.O. and McFeely, P. (1991): Tectonic Assemblage Map of the Canadian Cordillera and Adjacent Parts of the United States of America; Geological Survey of Canada, Map 1712A.

Geology of the Mount McCusker-Robb Lake Area, Northeastern British Columbia (94G/4W)

By A.S. Legun

KEYWORDS: *Regional Geology, Paleozoic, , Sidenius thrust, Skoki Formation, Beaverfoot Formation, Nonda Formation, Muncho-McConnell Formation, Mississippi Valley type (MVT) deposits, Robb Lake deposit, lead and zinc mineralisation ,stratiform breccia, Ospika embayment, stratiform sedex potential.*

INTRODUCTION

The Mount McCusker-Robb Lake area of mapping lies near the western margin of the MacDonald platform. This tropical platform extended over much of northeastern B.C. in late Silurian to Devonian time. The western, ocean facing margin of the platform is host to numerous showings and prospects of Mississippi Valley type (MVT) lead-zinc mineralisation. The largest of these is the Robb Lake deposit which has measured geological reserves of six and a half million tonnes at 7.1 per cent combined lead-zinc. Fieldwork in 1999 extended the 1998 mapping southward to the vicinity of the Robb Lake deposit, as well as to the northwest and east. The mapping project is a component of the multidisciplinary National Mapping (NATMAP) Central Forelands Project of the Geological Survey of Canada.

One of the more interesting results of the mapping is indications of sharp breaks in the older Upper Ordovician to Lower Sillurian platform margin. There is some potential for stratiform sedex deposits in the Lower Silurian and Upper Ordovician marine beds of a basinal embayment in the area. A few base metal geochemical highs in host terrain appear to have been ignored, perhaps because the emphasis was to explore using the MVT model.

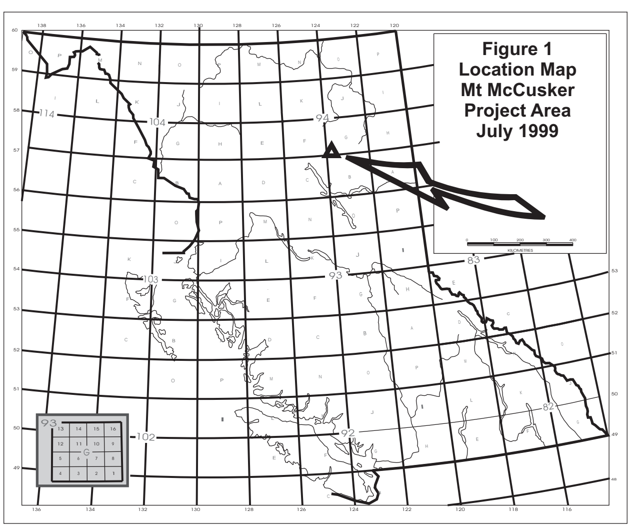

Figure 1. Location of study area.

LOCATION AND ACCESS

The map area lies 80 km due west of the small settlement of Pink Mountain on Highway 97 and 151 km north of Fort St. John. The area is within the eastern Muskwa Ranges, but close to the edge of the Rocky Mountain foothills to the east. The surveyed area lies at an altitude varying from 1250 to 2500 m. It is only accessible by air, but a few trails and seismic lines approach it from the east. The map area is bordered on the north by Colledge Lake and to the east by Mt. Bertha. To the south it extends to the vicinity of the Robb Lake deposit and Mississippi Creek. The main streams within the map area are the upper Sikanni Chief River and Sidenius Creek. Secondary drainages include Bartle, Embree, Gautschi and Colledge Creeks. In the following geological description of the area, major ridges are referenced by using the name of a nearby drainage (Figures 3, 4). For example, the ridge extending south from Sikanni Chief River, drained by Bartle and Embree Creeks, is called Bartle Ridge. Sidenius Ridge is the east-west trending ridge on the north side of the Creek of the same name.

Fieldwork in 1999 involved twenty-one traverses, to cover an area of about 600 square km. with helicopter support provided by the Geological Survey of Canada. The writer was ably assisted by University of Victoria geography co-op student, Panos Skrivanos. Due to foul weather, some areas were not mapped with the desired definition. The work was conducted from two fly camps, one in the northern Gautschi River valley, the second from a tributary on the south side of Sidenius Creek bordering the Robb Lake mapsheet (94B/13), informally named as Flycamp Creek.

PREVIOUS GEOLOGIC MAPPING

Early work in the area dates from the 1960's and focused on the regional stratigraphic and structural framework of the Paleozoic rocks for assessment of oil and gas potential. Mineral exploration received its impetus from active sampling and drilling of the Robb Lake prospect 20 km to the south in the early 1970's. This led to spin-off exploration for Mississippi Valley type deposits along the entire eastern border of the Northern Rockies. In the study area a number of showings were found and several, such as Lad (Williams, 1974a) and Toll (Williams, 1974b) have been drilled.

The area has not been mapped in detail, except for the immediate vicinity of the Lad (Mt. McCusker) prospect at a scale of 1:12000 (McHale and Pearson, 1974). The region is generally covered by a 1:250,000 scale compilation by the GSC (Taylor, 1979). Bob Thompson mapped and compiled the Halfway sheet south of the study area (Thompson, 1989), publishing both 1:50,000 and 1:250,000 scale maps.

GEOLOGIC SETTING

The stratigraphic succession ranges from Ordovician to Devonian. The succession in stratigraphic order (oldest to youngest), comprises the Ordovician Kechika, Skoki and Beaverfoot Formations, an unnamed early Silurian facies, the early Silurian Nonda Formation, a Silurian quartzite marker unit, the Siluro-Devonian Muncho-McConnell Formation, the Devonian Wokkpash, Stone and Dunedin Formations. Dolostones dominate, but there are significant intervals of shale (Figure 2). The lithologies can be ascribed to shelf and slope to basin environments. Biostromal dolostone, algal laminites, reef boundstone, and cross bedded quartzite correspond to the shelf. The offshelf is characterised by calcareous shales with biohermal and bioclastic lenses. The slope to basin facies includes graptolitic shales, quartz turbidites, graded beds with rip-ups and pyritic shale.

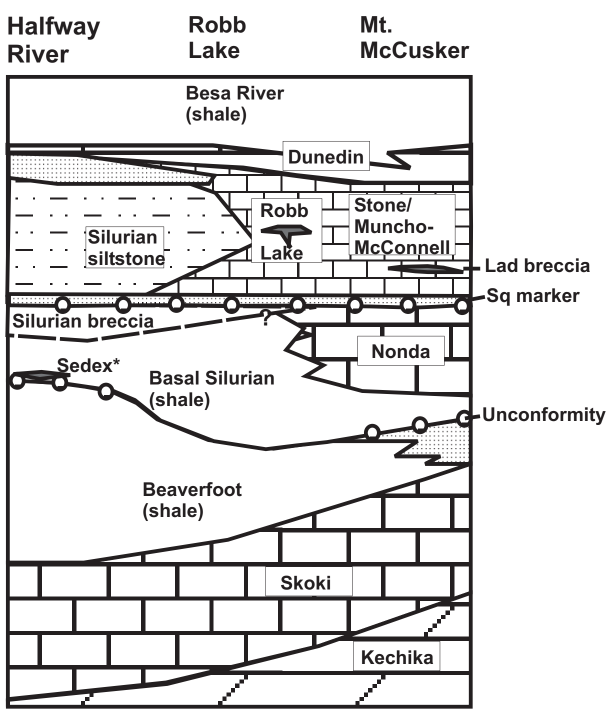

Figure 2. Postulated relationship of stratigraphic units in a general northeast (Mount McCusker) to southeast (Halfway River) transect of map area. * Stratigraphic position of CT, ERN stratiform mineral occurrences in Ware sheet to west (NTS 94F).

Structurally, the area of study lies at the edge of the northern Rocky Mountains at a transformation between a fold and thrust belt characterised by tight overturned folds and ramping thrusts, as at Mt. McCusker or Bartle Ridge, and a belt of more open folds to the east, with fewer and more shallow dipping thrusts such as at Mt. Bertha.

West of the map area in the Ware sheet (NTS 94F) Paleozoic shales dominate from the Ordovician Kechika Group to Devonian Earn Formation in the basin of the Kechika trough. These are described in several reports, including Cecile and Norford (1979), MacIntyre (1998).

The succession at Mt. McCusker preserves deposits of a basinal embayment into the platform in the Ordovician and Silurian called the Ospika embayment (Thompson, 1989). The facies boundary between the Skoki and overlying shales outlines the embayment. The position of the shelf edge in the Trutch and Halfway sheet is illustrated by Thompson (1989, Photo 3). In the study area the basin to shelf transition can be followed via a series of stratigraphic sections from Robb Lake to the Sikanni Chief River.

The stratigraphic succession is broken by two principal unconformities. The oldest lies at the top of the late Ordovician Beaverfoot. The younger unconformity is marked by the base of "Silurian Siltstone" in the basin and the base of the Muncho-McConnell on the platform. Recently the "Silurian Siltsone" has been formally named as the Kwadacha Formation (Pyle and Barnes, in press).

There are other unconformities of more local extent noted by workers, for example, the top of the Stone Formation below the Dunedin (Morrow, 1978).

MT. MCCUSKER AREA STRATIGRAPHY

Kechika Group

The Kechika is an extensive offshelf facies consisting of well recrystallised, thin to medium bedded calcareous shale, limestone and dolostone. Flaggy cleavage plates typically have a slight phyllitic sheen. The Kechika varies little throughout the map area. In some areas (*e.g.* a ridge above Sikanni Chief River east of Gautschi Creek) the uppermost beds below the Skoki are thick bedded. Barnes *et al.* (1998) noted trilobite debris in the Kechika. Work in 1999 delineated the contact of Kechika with Skoki Formation in the cirques northwest of Gautschi valley and in the core of a box-like anticline at Sikanni Chief River.

Skoki Formation

A complete section of Skoki, approximately 500 metres thick, was noted on Sidenius ridge in 1998 (Legun,1999).

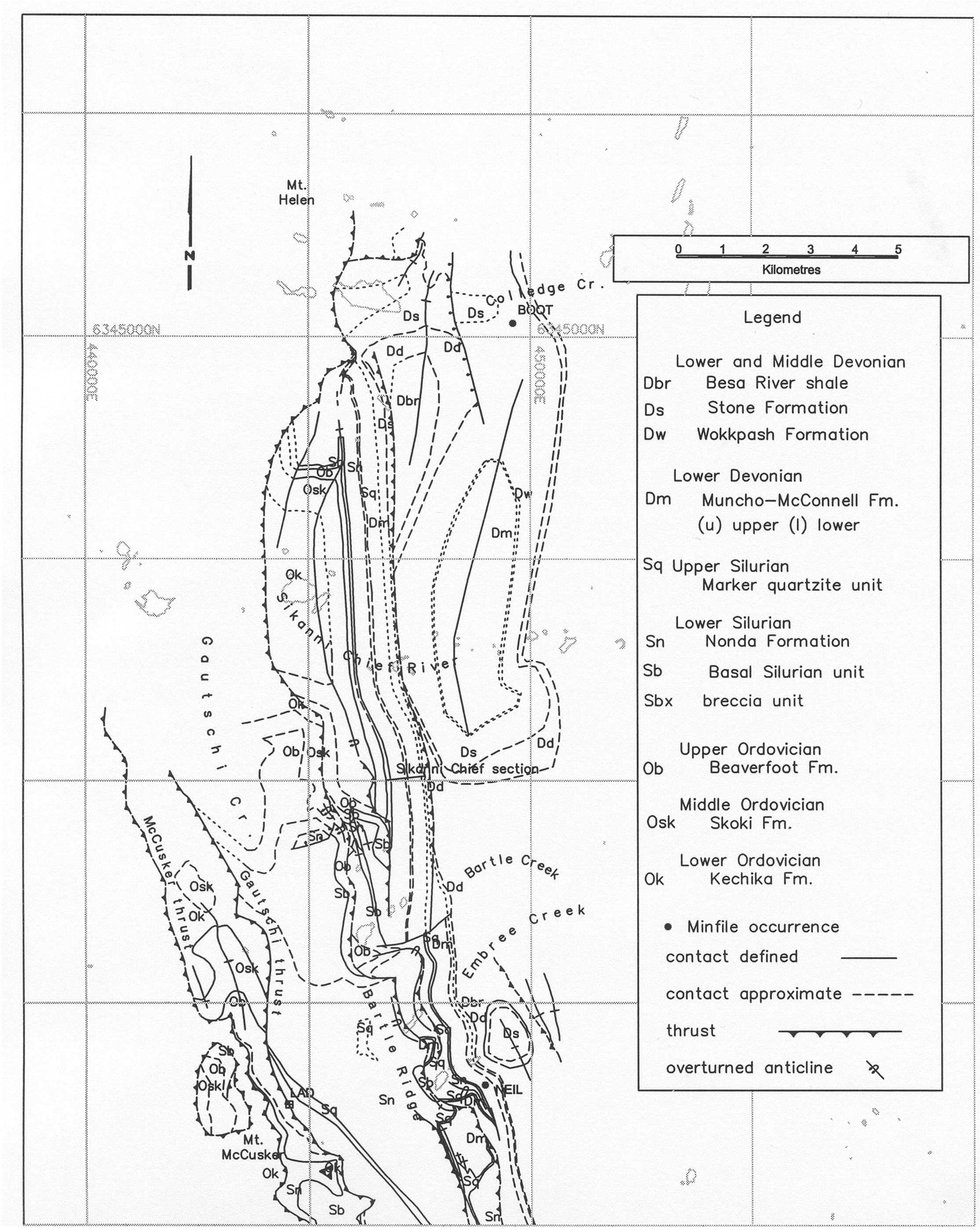

Figure 3. Geology of northern portion of map.

In 1999 the Formation was mapped south of Sidenius Creek. The common oncolitic facies was noted, but the chert facies was not evident. Uppermost beds (100 m or so) show indications of current activity. Bedding surfaces show patches of bioclastic crinoid debris and some beds are rippled and crossbedded. Also evident on bedding surfaces are drapes of reddish mudstone. In several locales near the top of the Formation there are beds with a dense distribution of oncolites cored by brachiopod valves. Macluritid planispiral gastropods are also found in these beds and have been documented elsewhere in the Skoki (Rohr *et al.* 1995).

The interpretation of these upper beds is uncertain, but on the whole, the Skoki does not appreciably change platformal character within the area of study. West of Mt. Kenny in the Halfway sheet it becomes more argillaceous (Thompson, 1989, p. 26). Closer to the Kechika Trough a

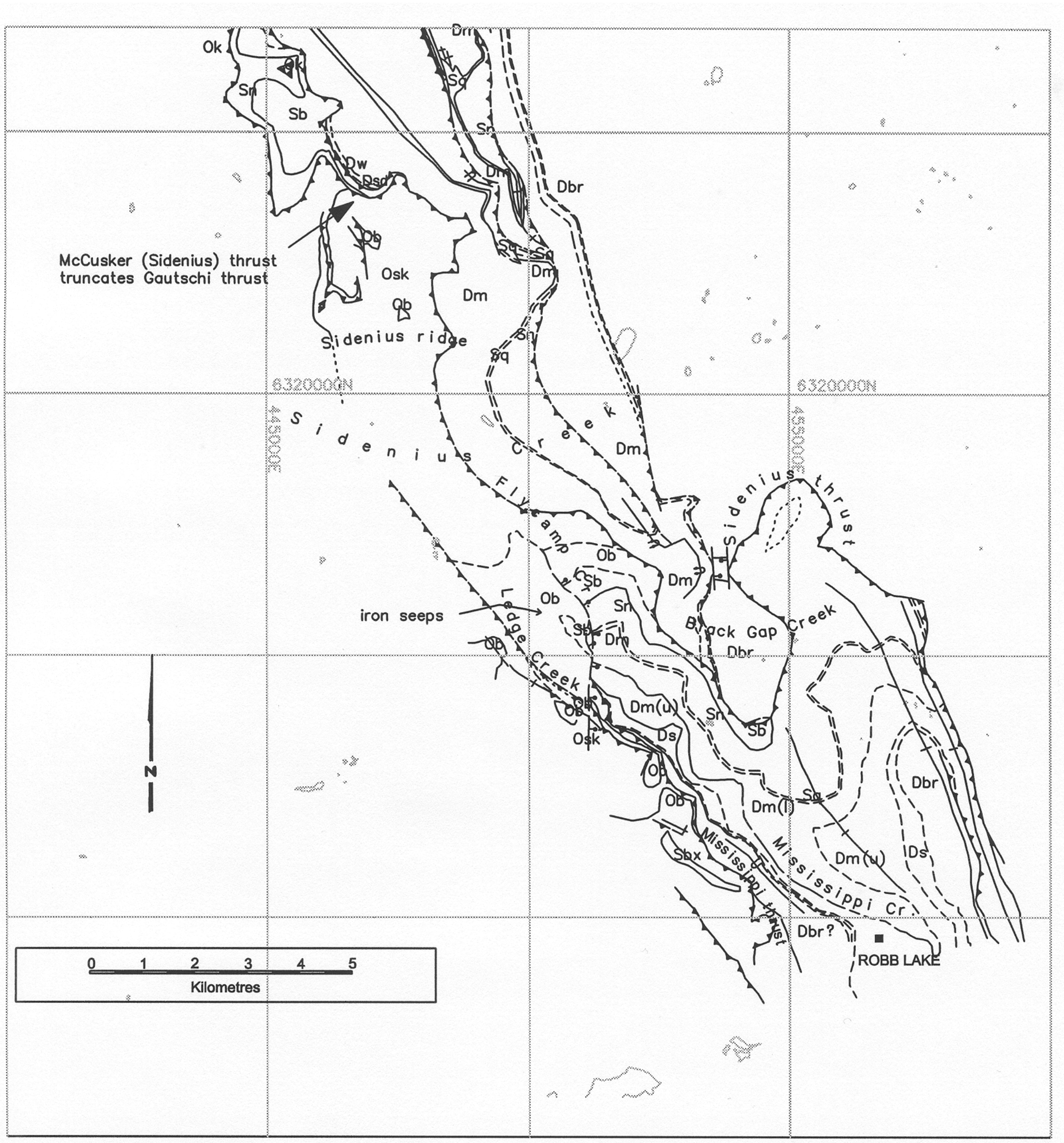

Figure 4. Geology of southern portion of map.

collapsing shelf edge has been described by Cecile and Norford (1979).

Beaverfoot Formation

The Beaverfoot Formation shows a transition from platform to basin depositional setting in the map area. Basically the quartz-dolomite unit of the platform (*ibid.*) was followed into the basin where it corresponds to the brown shale and quartzite unit (Thompson, 1989) near Robb Lake. The writer describes lateral facies within the single nomenclature of Beaverfoot. The quartz dolomite unit, brown shale and quartzite facies of Thompson (1989) are similarly overlain by basal Silurian facies both on the platform and in the basin and are underlain by the Skoki.

The platformal part of the Beaverfoot is well exposed near the Sikanni Chief section of Norford *et al.* (1966) on Bartle Ridge. Here a sequence of reddish (bioturbated) dolomitic siltstones passes upward to laminated and cross-bedded quartz arenite, arenaceous dolostone and orange dolostone. Mudcracks and breccias with ferricrete? nodules are present in the highest beds (Legun, 1999). The sequence, about 200 m thick, indicates an upward shallowing depositional environment.

In the hangingwall of the Gautschi thrust to the west, graded beds and erosional features in arenites together with interbeds of shell coquina suggest a subtidal slope facies. Lithologies include horizontal laminated sandstones, graded dolomitic sandstones with mudstone rip-ups and erosional bases; dolomitic shale (some beds rich in single valve shells); thin (5cm) pyritic beds, fine dolostones, nodular and lensoid breccia, rusty dolomite and sandy dolomite with scattered black chert. The thickness here is on the order of 250 to 300 m. Steep terrain and scree precludes a good section but brownish dolomitic shales are abundant.

Further to the south a nautiloid found in basal beds of the Beaverfoot south on Sidenius ridge (Legun, 1999) confirms open marine conditions at the time of the Ospika Embayment. Dark sandy and shaly calcareous beds lie abruptly on the Skoki. Only about 15m of Beaverfoot is preserved.

On the south side of Sidenius Creek there are several sections of a basinal facies of the marine embayment. In each case there is a sharp contact of very pale dolostones of the Skoki with brownish recessive beds of the Beaverfoot Formation. The lower Beaverfoot at Flycamp Creek (Photo 1) consists of sooty calcareous siltstone and dark shale, brown dolomitic siltstones with intraclasts of chert, and mud rip-ups from underlying beds. At least one thick quartz turbidite with a fluted base is found in the black shale, associated with rusty pyritic shales.

The black shale facies grades upward into a thicker bedded sequence of dolomitic siltstone, variably calcareous dolostone, chert and cherty siltstone. This may correspond to the shallowing up cycle on the platform. There appear to be lateral facies changes with banded cherty siltstones being replaced by calcareous shale, or yellow dolomitic mudstone within a kilometre of each other.

On airphotos and from a distant viewpoint, the transition from Beaverfoot to basal Silurian facies is evident as a change from brownish or paler beds to grey beds. In traverse the brownish or paler beds are a rhythmically banded facies of alternating calcareous dolostone and yellow dolomitic mudstone which develops lenses of limestone and calcareous shale up section. On close examination the calcareous units are bioclastic, either shallow channel bodies of reef detritus or perhaps eroding biohermal mounds. The presence of calcareous beds is a principal feature of the transition zone. This may reflect deepening conditions and other environmental changes.

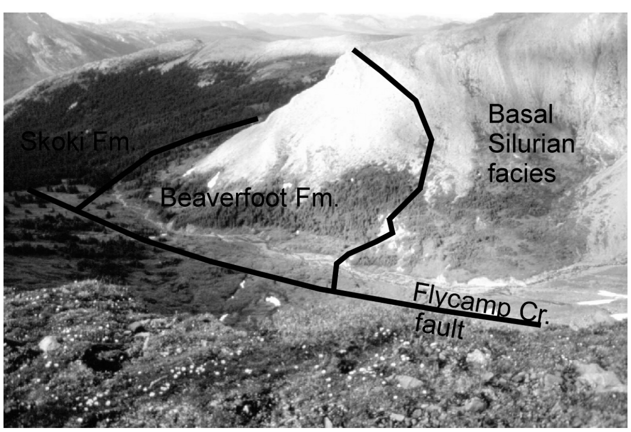

Photo 1. Looking northeast across Flycamp Creek. Ridge section of dipping beds of Beaverfoot Formation (light) to darker basal Silurian facies. Section continues to Nonda shale-out outside of picture to right.

The thickness from bedding dips and elevations at contacts indicates the Beaverfoot is approximately 300 m thick at Flycamp creek.

few kilometres to the south a ridge section exposes strata from the Skoki Formation to a Silurian breccia unit. A resistant bed of quartzite, lieing about 150 m above the base of the Skoki, may be the same bed as mapped to the north. Black shales above it are reported by Pyle (personal communication, 1999) to yield graptolites of the clingani Zone which is Late Ordovician (Caradoc) in age. Lithologically the upper contact of these beds with Lower Silurian shale beds is not clear here. There is minor folding and a fault before the section ends at exposures of Silurian breccia which form a near flat-lying cap to the high part of the ridge.

It is not clear whether in the area south of Sidenius Creek sedimentation was continuous from the Upper Ordovician to Lower Silurian. Ongoing biostratigraphic evaluation by Barnes *et al.* (1999) should provide some answers. In many basinal areas of the northern Cordillera a disconformity is reported (Lenz and McCracken, 1982). In the Halfway River sheet, Thompson (1989) distinguished basinal Lower Silurian beds from Upper Ordovician marine shales (Beaverfoot of this writer).

The disconformity in the basin apparently corresponds to a regionally downcutting unconformity on the platform. Norford (1966) noted that the unconformity cuts down northward such that at 58 latitude the Nonda sits on the Kechika.

Basal Silurian Facies

Basal Silurian beds suggest a transgression occurred at the end of the Ordovician. Basal Silurian calcareous shales, albeit thin, and somewhat oxidised, rest on the quartz dolomite facies of the Beaverfoot and underlie the Nonda Formation. The basal Silurian facies is unnamed on the platform but basinward corresponds to the Carbonaceous limestone unit (Scl) of Thompson (1989) in the Halfway River map sheet.

Norford *et al.* (1966) first recognised a recessive basal Silurian facies. The writer examined Norford's Sikanni Chief section in 1998 and found the recessive beds to be a mappable unit within the area of study.

In the Sikanni Chief section the basal Silurian beds are thin (about 80 m), and comprise yellowish, rubbly, nodular, shaly and calcareous dolostone, grey calcareous shale and dolomitic siltstone. Immediately to the west in the Gautschi valley the section thickens to *circa* 200 m, (see Gautschi Creek section in Barnes *et al.* 1999), and is comprised of a darker flaggy calcareous shale which weathers similar to the Kechika. Further to the west, basal Silurian facies outcrop in the hangingwall of the Gautschi thrust. Exposures are accessible via a cirque at the head of a tributary to Sidenius Creek. The upper contact against the Nonda is sharp, and the base not exposed in the bottom of the cirque. A calculated thickness of 160 m of low dipping beds are present.

The basal Silurian shows an increasing argillaceous character both west and south from the Sikanni Chief section.

Nonda Formation and Basal Silurian Facies

The Nonda is a platformal dolostone, often cherty, with distinct biostromal beds. It is uniform in thickness (about 320 m) and character across the McCusker map area. The westernmost exposures in the Mt. McCusker area are still platformal in character.

South of Sidenius Creek, Riddell (1972) first documented the basal Silurian facies thickening diachronously at the expense of the Nonda. Thompson (1989, Figure 8) described cliff exposures showing tongues of the Nonda pinching into shaly basal Silurian facies. At the shale-out the writer estimates the Lower Silurian to be at least 500 m thick, comprising 200 m of thinning Nonda and 300 m of shale.

South of the shelf break, basal Silurian beds (unit Scl of Thompson, 1989) are overlain by bedded breccias, which have been described as debris flows from a Nonda reef (ibid). Exposures of breccia forming the ridge top west of Mississippi Creek were briefly examined (Photo 4). The breccia consists of medium to dark grey, angular to subangular and subrounded tabular dolostone and “cobbles” of black chert in a grey dolomite cement. The coherence of the fragments suggest a good degree of induration in the host sediment. A discrete bed of breccia is sharply outlined against thin beds of cherty laminated dolostones and brown dolomitic siltstone above and below. Similar brown siltstones occur as clasts. The chert “cobbles” include some elongate pinch and swell shapes suggesting they may be disaggregated nodular beds. The writer noted dark reddish shale clasts, an uncommon lithotype in the Nonda. Nelson *et al.* (1999) noted well preserved fossil fragments of *Halysites*, *Favosites*.

Barnes *et al.* (1999) report that distinctive platform conodonts from the breccias appear to belong to the *Pterospathodus amorphognathoides* Zone, close to the base of the Wenlock. This conodont age is a little younger than the known age of the Nonda (Llandovery). The equivalence of these bedded breccias to the Nonda may need to be re-examined.

The total thickness of the Lower Silurian is reduced in the area where breccia overlies the basal Silurian shales (Thompson 1989, Figure 20). The reason for this is unclear. However the top of the breccia is overlain by Silurian Siltstone facies and the contact is an unconformity. This is further discussed below.

Marker Quartzite

The Silurian marker quartzite marks the top of the Nonda and base of the Muncho-McConnell Formation. Mapping in 1999 confirmed that it extends into the Robb Lake area. It was recognised below Mississippi ridge and in valleys on the south side of Sidenius Creek. At one location it appeared to be missing, represented by a dolomitic breccia with a sandy matrix.

This is the same unit mentioned by other workers in the Robb Lake area. It corresponds to the 60 foot thick quartzite band northeast of Mt. Kenny noted by Riddell (1972, section C-1-72). Thompson (1989, section 3, p. 117) shows a thick orthoquartzite (81 m) at the base of the Muncho-McConnell in the same area. Unit D of Mann (1981) is clearly the same unit.

The quartzite marker may be equivalent to sandstone beds at the base of the brown siltstone unit of Thompson (1989). The brown siltstone facies overlies the breccia facies mentioned above. The quartzite marker and the Silurian breccias may be related. Norford (1990) suggested the Nonda Formation was attenuated by erosion prior to the unconformity. The Silurian breccias may thus represent material that was eroded from subaerially exposed Nonda and carried into the basin, rather than representing debris flows from a reef front.

Thompson (1989) correlates his brown siltstone unit with the Silurian Siltstone facies (SD unit of Cecile and Norford 1979, p.224), also underlain by an unconformity. The base of the SD, brown siltstone, Silurian marker quartzite may represent the same unconformity or fall within a comparable interval of time (?Wenlock sea level low stand of Lenz, 1982). The base of the Muncho-McConnell is reported to be an erosional surface by Norford *et al.* (1966) downcutting eastward. MacIntyre (1998) has suggested the Middle Silurian siltstone facies in the Kechika Trough has its source in the erosion of the eastern portion of the MacDonald platform at this time.

Muncho-McConnell Formation

The Muncho-McConnell Formation consists of pale, fossil-poor, thick to medium bedded dololutites occasionally with discontinuous sand laminae and scattered quartz grains. It includes crinkly beds ascribed to algal mats and scattered quartz ascribed to aeolian sand. MacQueen and Thompson (1978) interpret the Muncho-McConnell as representing dolomitised, high salinity, lagoonal, intertidal, and supratidal carbonates with surfaces of dessication. The Muncho-McConnell thickens towards Robb Lake. It is on the order of 250 m thick near Mt. Helen and over 450 m at Robb Lake.

The Formation has been described in detail by others (*e.g.* Mann, 1981, Nelson *et al.,* 1999). In the Mt. McCusker area it is devoid of fossils. In the Robb Lake area large brachiopods are present which Taylor (1977) linked to the proximity of the Siluro-Devonian facies front. The Muncho-McConnell is replaced by the brown siltstone facies to the south between Robb Lake and Laurier Lake. This is postulated to represent an embayment (MacQueen and Thompson, 1978, p. 1741).

Breccia units within the Muncho-McConnell Formation are described separately under Economic Aspects.

Wokkpash Formation

The Wokkpash was recognised last year in western exposures in the footwall of the Gautschi thrust as a crossbedded dolomitic sandstone unit with scattered gastropods,. It was traceable for a km or so, 10 to 15 m thick, in apparent conformable contact with Muncho-McConnell beds underneath.

The Wokkpash is not a mappable unit on Bartle Ridge but reappears further to the east in a broad anticline in the Sikanni Chief River valley. Here several significant areas of massive quartzite outcrop. They are well jointed but bedding is difficult to discern. They are estimated to be at least thirty m thick. East of that structure Taylor and Mackenzie (1970, table II) measured 63 m (186 feet) in the Mt. Bertha structure.

The Wokkpash is locally mappable in the McCusker area. It represents at least two separate sand bodies.

Stone Formation

The Stone Formation consists of alternations of pale crystalline dolostone and tan dolostones similar to the Muncho-McConnell. The presence of paler (in some cases almost light blue-grey) crystalline dolomites is one of the few features that distinguish it from the more uniform Muncho-McConnell. Where the intervening Wokkpash sandstone is missing, the map contact between Muncho-McConnell and Stone Formations has a low confidence. The upper contact with the Dunedin is fairly sharp.

The Stone is relatively thick (100-150 m) in the broad arch at Sikanni Chief mapped this year. Further to the east at Mt. Bertha, Taylor and Mackenzie (1970) measured 140 m (459 feet). The Stone Formation thickens appreciably northward according to their regional isopach map (ibid.).

To the south Mann (1981) did not recognise the Stone as a mappable unit in the Robb Lake area and incorporated it with the upper member of the Muncho-McConnell. Nelson *et al.* (1999) recognised the facies locally. Thompson (1989, p.117, sections 3,4) noted the sand content of the Stone Formation increases toward the Halfway River. South of Robb Lake he mapped a dolomitic quartz sandstone unit (DqS) which is more or less equivalent to the Stone Formation..

Dunedin Formation

The Dunedin ranges from a few tens of metres to over 100m at Mt. Bertha; but averages 50 to 60 m in the area of study. The Dunedin tends to be poorly exposed and its contact with Besa River shale is often covered. Its continuity is uncertain; for example Thompson (1989) suggests the Dunedin is discontinuous along the edge of the Robb Lake anticline. It is clearly thicker and more continuous in the north part of the map area where new exposures were located in 1999.

The Dunedin is a complex facies spanning reef, shelf and offshelf environments. It includes reef boundstone facies with dark red argillaceous fill (well exposed at Mt. Helen), deeper water crinoid hash facies and sandy zones of uncertain origin. Throughout the area, the lower half of the Dunedin is often a grey, slightly fetid, fossiliferous dolomite with zebra texture and its contact with the Stone Formation is sharp. Its upper facies comprises dark biostromal limestone with abundant fossil debris including *Amphipora*, crinoids and bryozoa. Its contact with Besa River shale can be quite gradational over 10 m or more of dark calcareous shale. The gradational interval locally includes finely laminated, pyritic shale. Areas north of the map area have been subject to detailed study by Morrow (1978).

Tebbut (1970) first described sections from Mt. Helen, Mt. Bertha and Sheep Creek east of Robb Lake. A north to south trending reef front was postulated to lie near Mt. Helen and a thick shelf sequence further to the east at Mt. Bertha (ibid*.)*. Exposures mapped in 1999 around the periphery of an anticlinal arch between Mt. Helen and Mt. Bertha should assist in relating reef facies near Mt. Helen to the shelf at Mt. Bertha.

At Embree Creek the Dunedin is thinner and its fossil content is reduced. A basin re-entrant, postulated by Tebbut (1970), may be present south of Embree Creek. A deep shelf facies of argillaceous crinoidal deposits at Sheep Creek (Tebbut 1970; Thompson 1989), east of Robb Lake, is part of the postulated re-entrant.

Dunedin exposures were found by the writer at the northwest end of the Robb Lake anticline, in stratigraphic continuity with underlying Stone and Muncho-McConnell beds of the anticlinal limb and in the footwall of the Mississippi thrust.

To the south along strike there is a considerable thickness of shale in the footwall of the Mississippi thrust. Is this mostly basal Silurian (Road River) facies as postulated by Nelson *et al.* (1999) or Besa River shale as mapped by Thompson (1989)? Conodont samples at two levels collected by the writer may help clarify the age of calcareous shales and associated crinoid rich bioherms (Dunedin Formation?). Additional thrusts may be present in the tightly folded zone of shale and similar looking shales of varyimg age could easily be juxtaposed. The writer did not cross the stratigraphy further south at Webb ridge.

STRUCTURE

Thrusts

The trace of the McCusker thrust was followed in detail southward and its trace confirmed to coincide at the south end with the Sidenius thrust at Robb Lake. The thrust surface steepens to the west, both at Mt. McCusker and at Robb Lake. At Mt. McCusker the thrust flattens to the east, while at Robb Lake it undulates as a “folded” thrust. The footwall geology has two segments. The thrust appears to truncate the underlying Gautschi thrust at Sidenius ridge, the footwall to the Gautschi thrust then becomes the footwall to the McCusker (Sidenius) thrust. The probable explanation of these relationships is step faulting or ramping. Such step faulting is expected in a sequence of competent and incompetent units such as platformal dolomites with significant intervals of shale. A number of areas of fault rampin have been identified, one is well exposed below the arch of the Sidenius fault arch on the south side of Sidenius Creek (Photo 2).

Normal Faults

A few normal faults of minor displacement were noted in the northern part of the area (Legun, 1999).

The most significant normal fault lies in the south and it truncates the west limb of the Robb Lake anticline. It was mapped as a north-trending, normal fault by Thompson (1989) and the writer has extended its trace north and south via ground observations. The fault has more than one component as a fault wedge of Nonda is preserved against it. Displacement on the fault increases to the south and Dunedin is juxtaposed against Beaverfoot at one point. It appears to truncate the hangingwall Skoki beds of the Mississippi thrust in an area of incomplete exposure. On this basis the fault is mapped as displacing the thrust.

ECONOMIC ASPECTS

The McCusker map area lies along a trend of Mississippi Valley-type (MVT) showings and prospects at the platform edge of Siluro-Devonian rocks. The largest example is the Robb Lake deposit hosted in breccias of the Muncho-McConnell Formation near its shale-out to Silurian Siltstone facies. At Robb Lake the main breccia unit is near the junction of upper and lower members of the Muncho-McConnell, At least 200 m above the base of the Formation.

The Lad (Mt. McCusker) showing is associated with a stratiform breccia situated only about 70 m above the base (top of Silurian marker quartzite). The host Muncho-McConnell is not near any facies front at this location. The breccia is also not related to a nearby thrust as the breccia zone crudely maintains its position relative to the quartzite marker rather than the thrust. A second less well documented breccia near the Neil showing may represent the same stratiform zone as at Lad but on a separate thrust plate.

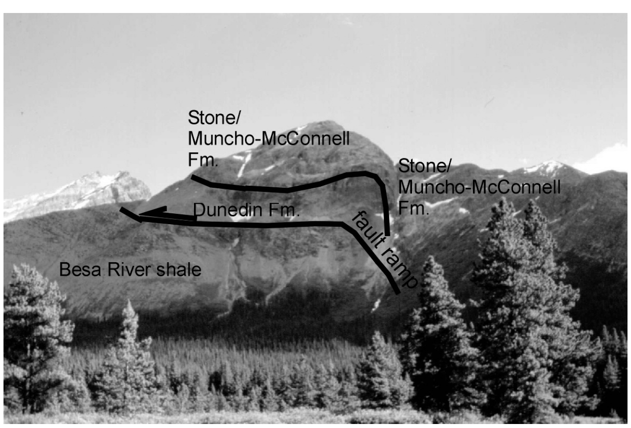

Photo 2. Looking north from Sikanni River along trace of fault ramp below overturned succession of Besa River shale, Dunedin Formation and undivided Stone/Muncho-McConnell Formations.

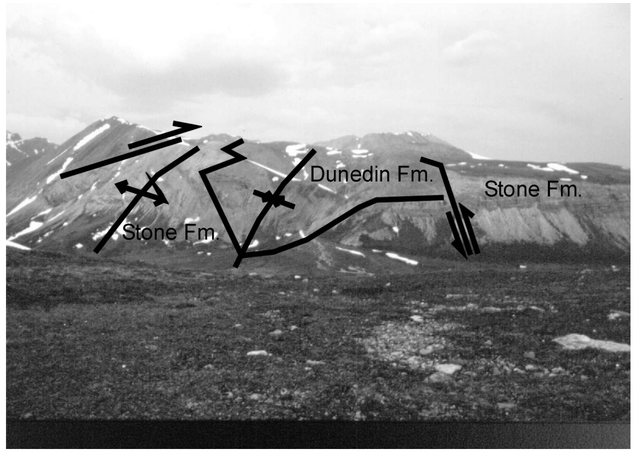

Photo 3. View north across Colledge Creek showing anticline syncline pair exposing Dunedin (dark) and Stone (light) Formations. To the right a normal fault cuts out the Dunedin Formation.

Photo 4. Bed of breccia sharply outlined against evenly bedded cherty dolostones. Photo taken at south end of ridge of Silurian breccia unit (Sbx) in figure 4.

The Lad breccia has some general similarities to Robb Lake breccia (such as irregular vein-like masses with sub-rounded fragments in a crudely stratiform body), but the comminuted “trash breccias” are not apparent.

At Robb Lake no breccia is noted at the Lad and McNeil stratigraphic level. Mann (1981) described a local disconformity known as the ASM or angular sand marker, but at first assessment it appears to lie too high in the stratigraphic section to correlate with the Lad breccia.

A small area of “trash” breccia (after Nelson *et al.,* 1999) occurs within Stone and Dunedin Formations adjacent to the normal fault described in the Structure section. The breccia appears confined to the Stone and Dunedin and is probably cut by the fault. The outcrop may be worth a visit as it does not seem to have been noted previously.

East of the mapped area the Dunedin Formation is prospective for MVT deposits. Minor sphalerite bearing bands are described in Dunedin Formation at Mt. Bertha (Toll showing, Minfile 094G 015). To the north along the same anticlinal structure pods of calcite and barite with minor galena and sphalerite are found (Rb showing, Minfile 094G 004).

The writer suggests the basinal Siluro-Ordovician shales warrant some attention in the area. For that perspective it is necessary to jump west of the map area into the Ware sheet. In the Ware sheet within the Akie River area MacIntyre (1998) notes a few stratiform sedex prospects within basal Silurian units near the shelf margin. The Ern (Minfile 94F 001) is a stratabound sulphide zone in the basal Silurian section, immediately above Ordovician graptolitic black shales. It includes a sulphide bearing quartz breccia, stratiform zone of fine grained pyrite with a silica-barite matrix and minor sphalerite. The CT showing (Minfile 94F 010) is also found in basal Silurian beds interpreted to lie closer to the platform edge. It is essentially a bedded barite layer with zones of pyrite-sphalerite-barite.

Rocks of similar age and character extend to the Robb Lake area by way of marine embayments and re-entrants. A stratabound pyritic zone, associated with a quartzite, and marked by iron oxide seeps along the valley wall, occurs northwest of Robb Lake within the Beaverfoot (Figure 4). One prominent seep is at about UTM easting 450 000, UTM northing 6315700. The valley has not been sampled except at one corner. Four silt samples indicate raised lead (over 500 ppm) and zinc (over 1000 ppm) but disappointing trace metals. There has been no testing for barium. Reconnaissance geochemical sampling is warranted in these valleys.

In the same general area, some high values (4000 ppm zinc, 4000 ppm lead, up to 9 ppm silver and 175 ppm cadmium) are reported from rock and float in the general vicinity of the Nonda shale-out and the normal fault described above (Westoll and Sullivan, 1972). These results were apparently ignored in pursuing younger platformal dolostones. Conceivably the Nonda shale-out marks an old growth fault or is near a basin edge structure.

ACKNOWLEDGMENTS

Many thanks to Mike Cecile and Larry Lane of the Geological Survey of Canada for logistical support and an introduction to the stratigraphic framework of the area. Panos Skrivanos provided helpful assistance and good cheer, particularly when a young bear settled down on the opposite side of the valley. The manuscript benefited from review by Dave Lefebure of the B.C. Geological Survey and Leanne Pyle of the University of Victoria.

REFERENCES

Barnes, C. R. and Pyle L.J. (1998): Lower Paleozoic stratigraphy and conodont biostratigraphy, platform to basin transect, in the Trutch, Halfway River and Ware map areas (94G,B,F); Geological Survey of Canada, Central Forelands Natmap Project Workshop, Technical Program.

Barnes, C. R. and Pyle L.J. (1999): Lower Paleozoic stratigraphy and conodont biostratigraphy, platform to basin transect, in the Trutch, Halfway River and Ware map areas (94G,B,F), northeastern British Columbia; Geological Survey of Canada, Central Forelands Natmap Project 1999 Fall workshop Program and Abstracts, edited by Larry S. Lane.

Cecile, M.P. and Norford, B.S. (1979): Basin to platform transition, lower Paleozoic strata of Ware and Trutch areas, northeastern British Columbia; Geological Survey of Canada, Paper 79-1A, p. 219-226.

Legun A. (1999): Geology of the Mt. McCusker area, northeastern British Columbia (94G/4W); B.C. Ministry of Energy and Mines, Geological Fieldwork 1998, Paper 1999-1, p.115-125.

Lenz, A.C. (1982): Ordovician to Devonian sea-level changes in Western and Northern Canada; Canadian Journal of Earth Sciences, volume 19, p. 1919-1932.

Lenz, A.C., and McCracken, A.D. (1982) The Ordovician-Silurian boundary, northern Canadian Cordillera: graptolite and conodont correlations; Canadian Journal of Earth Sciences, volume 19, pp. 1308-1322.

MacIntyre, D.G. (1998): Geology, Geochemistry and Mineral Deposits of the Akie River Area, Northeast British Columbia; B.C. Ministry of Energy and Mines, Bulletin 103, 91p.

MacQueen , R.W. and Thompson, R.J. (1978): Carbonate-hosted lead-zinc occurrences in northeastern British Columbia with emphasis on the Robb Lake deposit; Canadian Journal of Earth Sciences, volume 15, p. 1737-1762.

McHale, K.B. and Pearson, B.D. (1974): Geological and Geochemical Report McCusker Claim Groups I,II and III, Liard/Omineca Mining Division; B.C. Ministry of Energy and Mines, Mineral Assessment report 4865.

Mann, F.T. (1981): Stratigraphic aspects of the Silurian-Devonian sequence hosting zinc and lead mineralisation near Robb Lake, northeastern British Columbia; unpublished Ph.D. thesis, University of Toronto, Ontario, 252p.

Morrow, D.W. (1978): The Dunedin Formation: a transgressive shelf carbonate sequence; Geological Survey of Canada, Paper 76-12, 35 p.

Nelson, J.L., Paradis, S., Zantvoort, W. (1998): The Robb Lake Carbonate-Hosted Lead-Zinc Deposit, Northeastern British Columbia: A Cordilleran MVT Deposit; B.C. Ministry of Energy and Mines, Geological Fieldwork 1998, Paper 1999-1, p.89-101.

Norford, B.S., Gabrielse, H. and Taylor, G.C. (1966): Stratigraphy of Silurian carbonate rocks of the Rocky Mountains, northern British Columbia; Bulletin of Canadian Petroleum Geology, Volume 14, p. 504-519.

Norford, B.S. (1991): Ordovician and Silurian stratigraphy, paleogeography and depositional history in the Peace River Arch area, Alberta and British Columbia; Bulletin of Canadian Petroleum Geology, v. 38A, p.45-54.

Pyle, J.P. and Barnes, C.R. (in press): Upper Cambrian to Lower Silurian stratigraphic framework of platform to basin facies, northeastern British Columbia; Bulletin of Canadian Petroleum Geology

Riddell, C.H. (1972): Surface Geology, McCusker Area, Northeastern British Columbia; B.C. Ministry of Energy and Mines, Petroleum Assessment report 1761, 51 p.

Rohr, D., Norford, B.S. and Yochelson, E.L. (1995): Stratigraphically significant Early and Middle Ordovician gastropod occurrences, Western and Northwestern Canada; Journal of Paleontology, pp. 1047-1053.

Taylor, A.H. 1977: Carbonate stratigraphy and petrology: Robb Lake zinc-lead property, northeastern British Columbia; unpublished M.Sc thesis, Carleton University, Ottawa, Ontario.

Taylor, G.C. (1979): Trutch (94G) and Ware East Half (94F, E1/2) map-areas, northeastern British Columbia; Geological Survey of Canada, Open File Report 606.

Taylor, G.C. and Mackenzie, W.S. (1970): Devonian stratigraphy of northeastern British Columbia; Geological Survey of Canada, Bulletin 186, 62p.

Tebbut, G.E. (1970): Surface Geology, Trimble Area; B.C. Ministry of Energy and Mines, Petroleum Assessment report 1551.

Thompson, R.I. (1989): Stratigraphy, tectonic evolution and structural analysis of the Halfway River map area (94B), northern Rocky Mountains, British Columbia; Geological Survey of Canada, Memoir 425, 119 p.

Westoll, N. and Sullivan, J. (1972): Mt. Bertha Area Claims, Liard/Omineca Mining Division; B.C. Ministry of Energy and Mines, Mineral Assessment report 4203, 54p.

Williams, M.G. (1974a) Diamond drilling report on the Lad and Lass claim groups, Mt. McCusker area, Mineral Assessment report 5328.

Williams, M.G. (1974b) Geological, Prospecting and diamond drilling report on the Bertha claim groups, Sikanni Chief River, Robb Lake area, B.C. Ministry of Energy and Mines, Mineral Assessment report 5469, 52p.

Williams, M.G. (1975): Geological and geochemical report, LAD, LASS and EL DORADO mineral claims, Liard/Omineca Mining Division; B.C. Ministry of Energy and Mines, Mineral Assessment report 5725, 20p.

Geology and Mineralization of the Tchaikazan River Area Southwestern British Columbia (92O/4)

By Steve Israel and Lori Kennedy
The University of British Columbia

INTRODUCTION

This paper presents preliminary results of bedrock mapping in the Taseko Lakes area. This work represents part of a Master's project funded by International Jaguar Equities (JAG), NWC Exploration Inc. and the University of British Columbia. Fieldwork was completed over two summers; two months of reconnaissance mapping in 1998 and two and a half months of more detailed 1:15 000-scale mapping in 1999. Emphasis was placed upon regional and local structure, their roles in localizing gold and copper mineralization, and their larger scale tectonic significance. More specifically the goals of the 1999 field season were to:

1) work out a coherent stratigraphy for the area and compare this to well-defined stratigraphic sections found to the east of the field area.
2) map the geometry of faults, determine their kinematics, and evaluate their role in the complex tectonic evolution of the region; and
3) identify the structural controls on the Northwest Copper (NWC) Cu-porphyry showing and the Pellaire gold veins and determine if they are temporally linked.

The project area encompasses about 180 square kilometers that is located southwest of upper Taseko Lake and approximately 200 kilometers due north of Vancouver (Figure 1).

It is within the Taseko Management Zone, along the east side of Ts'yl-os Provincial Park. The first geological compilation of the area is that of Tipper (1963), a 1:253 440-scale map covering the Taseko Lakes (92O) sheet. Subsequent work resulted in a more detailed 1:250 000-scale map of the same area (Tipper, 1978). The most detailed map of the project area prior to this study is a 1:100 000-scale map produced by McLaren (1990) as part of a mineral resource assessment of the Chilko Lake Planning Area.

Mineralization within the region includes epithermal and mesothermal veins, porphyry systems and fault-controlled mercury-antimony occurrences (McLaren, 1990). A number of occurrences in advanced stages of exploration are present in and around the project area. JAG has completed a bulk sampling project on the Pellaire gold and silver epithermal veins (MINFILE 092O 045) and is actively exploring the Chita (MINFILE 092O 049) and Northwest Copper (MINFLE 092O 043) occurrences. The Pellaire and Northwest Copper occurrences are found within the project area, whereas the Chita occurrence lies just outside of the project area on the southeast side of upper Taseko Lake. For a more extensive overview of regional mineralization the reader is directed to McLaren (1990).

REGIONAL GEOLOGIC SETTING

The field area is located within the southeastern Coast Belt, which forms part of the boundary between the Intermontane and Insular superterranes (Figure 1; Monger *et al.*, 1982). This highly tectonized belt includes Paleozoic to mid-Mesozoic oceanic and volcanic arc rocks assigned to several different terranes, together with late Middle Jurassic through mid-Cretaceous sedimentary rocks of the Tyaughton-Methow basin, Upper Cretaceous continental arc volcanic rocks of the Powell Creek formation and mid-Cretaceous to Tertiary intrusive rocks of the Coast Plutonic Complex (Schiarizza *et al.*, 1997).

The study area is near the southeast end of a distinctive structural-stratigraphic domain (Eastern Waddington Domain) bounded by the Tchaikazan Fault on the northeast and by mid-Cretaceous to early Tertiary plutons to the southwest (Figure 2).

The oldest rocks within this domain are Upper Triassic volcanic and sedimentary rocks that have been correlated with Stikine Terrane (Mount Moore and Mosley formations of Rusmore and Woodsworth, 1991). These Triassic rocks are imbricated with Lower to Upper Cretaceous volcanic and sedimentary rocks across Late Cretaceous northeast-vergent thrust faults of the eastern Waddington thrust belt (Rusmore and Woodsworth, 1994).

The Tyaughton basin, east of the present study area, is characterized by upper Middle Jurassic to mid-Cretaceous clastic sedimentary rocks that are interpreted to have been deposited above oceanic rocks of the Bridge River Terrane (Schiarizza *et al.*, 1997). Middle Triassic to Middle Jurassic volcanic, plutonic and sedimentary rocks of the Cadwallader arc terrane, which occur mainly east and north of Bridge River Terrane, are likewise overlain by thick Jura-Cretaceous clastic sedimentary rocks comprising the Methow portion of the Tyaughton- Methow basin.

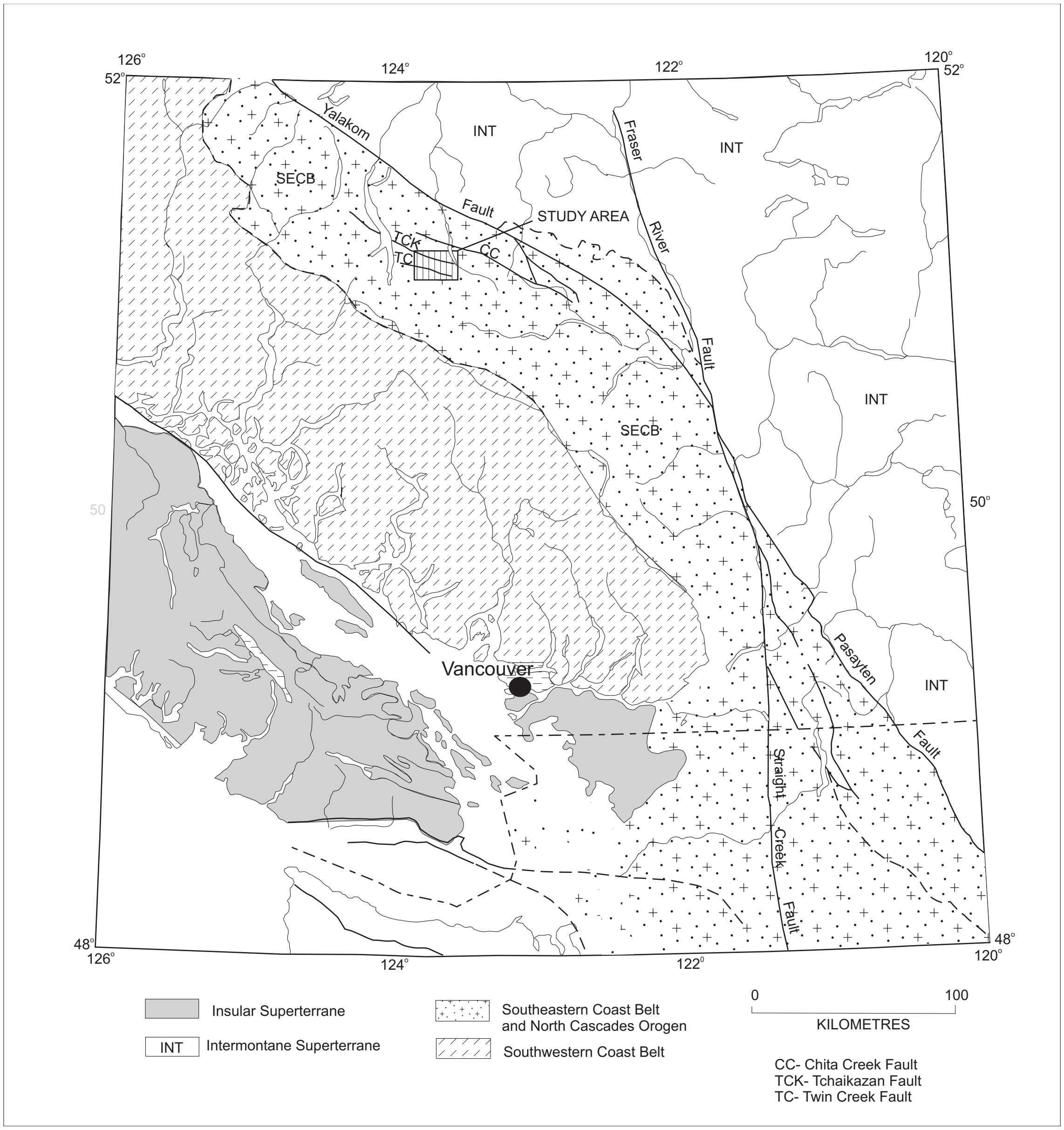

Figure 1. Location of field area, with regional tectonic framework (modified from Schiarizza *et al*., 1997).

Lower Cretaceous rocks on the southwest side of the Tchaikazan fault, including those within the present study area, are in part correlated with the upper Relay Mountain and Taylor Creek groups of the Tyaughton basin to the east. They differ, however, in their more restricted age range (no Jurassic rocks are recognized), and in the predominance of volcanic rocks. In these aspects, they more closely resemble Lower Cretaceous arc volcanic and related sedimentary rocks of the Gambier Group, which are widespread within the southwestern part of the Coast Belt (Monger and Journeay, 1994). Consequently, it has been suggested that this area represents part of the transition from the Early Cretaceous arc of the southswestern Coast Belt to a related back-arc basin, represented by the upper part of the Tyaughton basin (McLaren, 1990; Umhoefer *et al*., 1994). Another interpretation, presented by Monger *et al*. (1994), is that the Tyaughton basin is part of a long-lived accretionary fore-arc complex, and the southwestern Coast Belt arc was emplaced to the west of it by pre-mid-Cretaceous sinistral faulting.

The southeastern Coast Belt had a protracted and complex structural history, extending from at least mid-Cretaceous to Paleogene time, and involving an early phase of contractional deformation followed by dextral strike-slip and locally important extensional faulting (Journeay and Friedman, 1993; Umhoefer and Schiarizza, 1996; Schiarizza *et al*., 1997). The northeast-vergent structures of the eastern Waddington thrust belt, which were active by at least 87 Ma and became inactive before 68 Ma, formed relatively late in the contractional episode, and are interpreted as back thrusts

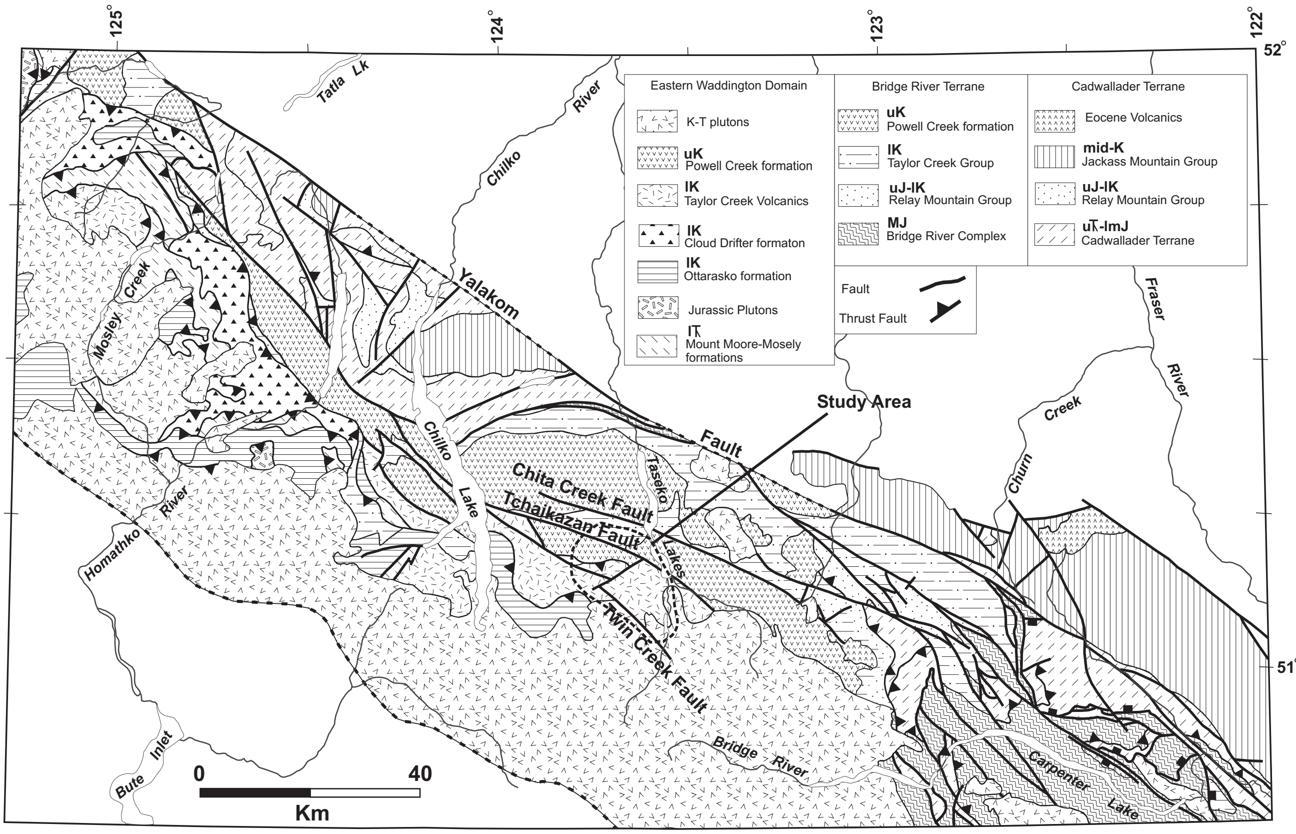

Figure 2. Geologic setting of the project area (based on an unpublished compilation by P. Schiarizza).

within the predominantly southwest-vergent orogen (Rusmore and Woodsworth, 1994).

The dominant regional structures are northwest-striking dextral strike-slip faults (Schiarizza *et al.*, 1997; Journeay *et al*., 1992; Figure 2). These include the Yalakom fault, northeast of the study area (Figure 2), which has a strike length of approximately 300 kilometers, and an estimated 115 kilometers of right-lateral displacement (Riddell *et al.*, 1993). Umhoefer and Schiarizza (1996) suggest that the Yalakom fault system was active from approximately 70 Ma to 40 Ma, with most movement occurring in the early to middle Eocene. Faulting during this latter time period included the development of a series of en echelon left-stepping faults, including the Fortress Ridge and Chita Creek faults, with zones of contraction and uplift in the stepovers (Figure 2). Prominent structures within the present map area, including the Tchaikazan and Twin creek faults, may have formed at the same time and represent a western extension of this left-stepping system (Umhoefer and Kleinspehn, 1995; Figure 2).

STRATIGRAPHY

Volcanic, volcaniclastic and clastic sedimentary rocks of Cretaceous age underlie most of the project area (Figure 3).

These are assigned to the Relay Mountain and Taylor Creek groups and the informal Powell Creek formation . Below we describe the lithologic characteristics of each unit. Emphasis is placed on the Taylor Creek Group as we propose new stratigraphic subdivisions for this thick package of volcanic and volcaniclastic rocks.

Relay Mountain Group (LK_{Rm})

Jeletzky and Tipper (1968) first identified Lower Cretaceous rocks belonging to the Relay Mountain Group in the area southwest of the Tchaikazan fault. These rocks are restricted to two localities mapped by Tipper (1978) and McLaren (1990) on the ridge system northwest of the Tchaikazan River. The eastern locality is in the present map area (north of the Tchaikazan River and the Charlie showing) and is interpreted as a fault-bound lens thrust over the Powell Creek formation and itself overthrust by rocks of the Taylor Creek Group. Here, the Relay Mountain Group consists of dark brown to black shales, interbedded with fine-grained grey to light brown sandstone. Abundant fragments of incoceramid bivalves and

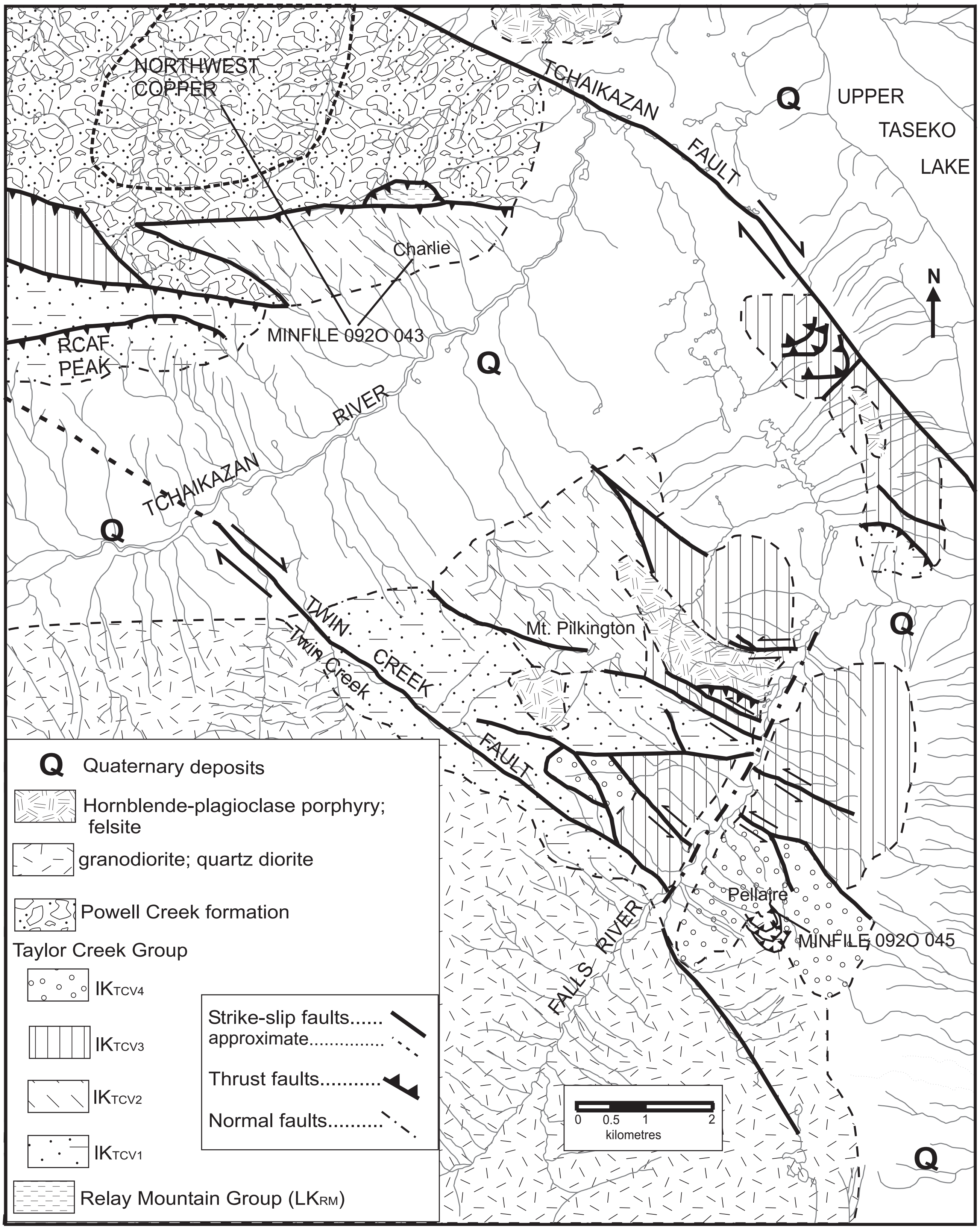

Figure 3. Generalized geology of the project area, showing only large-scale structures.

belemnites are present and a fossil collection from this area was assigned an early Hauterivian age by J.A. Jeletzky (McLaren, 1990).

Taylor Creek Group

In the main part of the Tyaughton basin, east of the field area, mid-Cretaceous rocks of the Taylor Creek Group either rest unconformably above the Bridge River Complex, or disconformably above Lower Cretaceous rocks of the Relay Mountain Group (Schiarizza *et al.*, 1997). Garver (1989) conducted a detailed study of the group in the Big Creek - Bridge River area and subdivided it into four distinct sedimentary units, mostly of mid-Cretaceous (Albian) age. A youngest fission-track peak of 113-114 Ma reported by Garver and Brandon (1994) suggests that the Paradise formation, the lowest within the Taylor Creek Group in the area studied by Garver, is somewhat older (Aptian-Lower Albian). A detailed description of the group is given in Schiarizza *et al*. (1997) where they add the informal Beece Creek succession and a volcanic unit.

Within the field area, the Taylor Creek Group on the southwest side of the Tchaikazan fault comprises more than 2500 metres of dominantly volcanic and volcaniclastic rocks. (Figure 4).

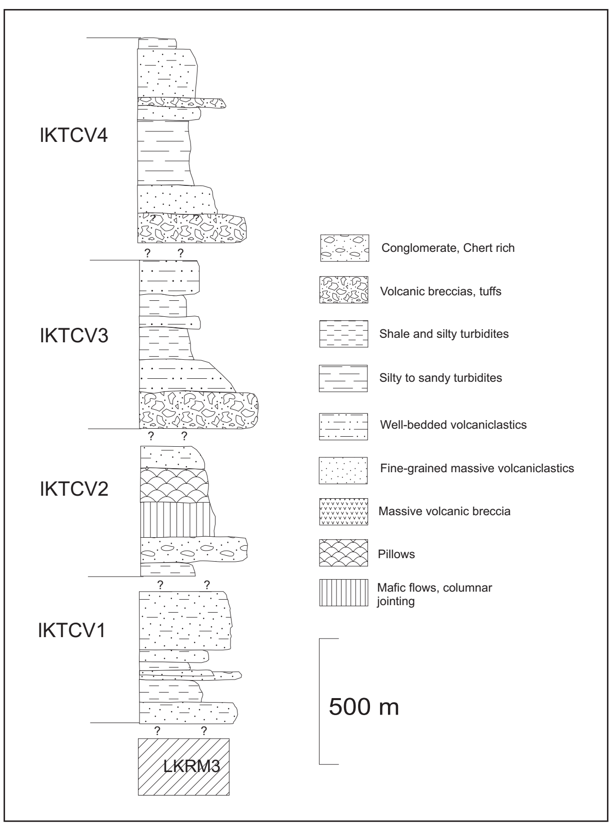

Figure 4. Generalized stratigraphic section from the study area.

We tentatively divide this succession into four separate units based on lithologic characteristics and stratigraphic relationships.

Unit LK_{TCv1}

Unit LK_{TCv1}, the lowest part of the Taylor Creek succession exposed in the project area, is characterized by medium to fine-grained well bedded to massive, green to red volcaniclastics, silty grey to black turbidites and intermediate to felsic tuff horizons. The best section of this unit is found on the south slope of the ridge north of Twin Creek. The unit might continue to the east, towards the Falls River valley where similar felsic and lithic tuff horizons are found (Photo 1).

The lower part of the unit is not well exposed but seems to be characterized by light grey-green to black laminated silty turbidites and black shales. The turbidites occur in beds up to 5m thick with laminations from less than a centimetre to 5 cm. They typically form Tbd and Tcd sequences. The shale is found in beds from one to several metres thick interbedded with the turbidites.

The sediments quickly pass into dark grey volcaniclastic and pyroclastic rocks. The contact with the sediments is gradational. Sedimentary rocks are massive too slightly layered and occur as beds up to 2 metres thick. A distinctive felsic crystal-lithic tuff is present at this level in the unit. It is characterized by fragments composed of dark siltstone and intermediate to felsic volcanic rock within an intermediate to felsic ash matrix. Plagioclase crystals up to 1 millimeter in size occur throughout the bed. This interval has variable thickness, ranging from 1-2 metres in the Twin Creek area to over 20 m farther to the east, just west of the Falls River. A clast-supported conglomerate (1-2 metres thick) is located immediately above the tuff horizon. The clasts are composed of abundant intermediate to felsic volcanic rocks, chert and lesser amounts of siltstone. They are sub-angular to sub-rounded and range from less than 1 cm to 10 cm in size (Photo 2).

This stratigraphic position may be represented to the east where a similar lithic tuff is found. However in that locality the volcaniclastic conglomerate is absent and the lithic tuff horizon is up to 40 metres thick. This may suggest an easterly source for the volcanics, but structural complications in the area still need to be resolved.

Above the conglomerate are alternating, layered green to red volcaniclastics. These make up approximately half of the section totaling 250 metres of semi-exposed outcrop. They occur in well-bedded horizons up to 2 metres in thickness and exhibit normal grading of sub angular to rounded intermediate volcanic pebbles. In places they become more massive and much coarser, composed of angular to rounded intermediate to felsic volcanic fragments in an andesitic volcaniclastic matrix. Large chloritized hornblende crystals up to 1 cm in length occur within these horizons, confined mainly to the fine-grained pyroclastic matrix (Photo 3).

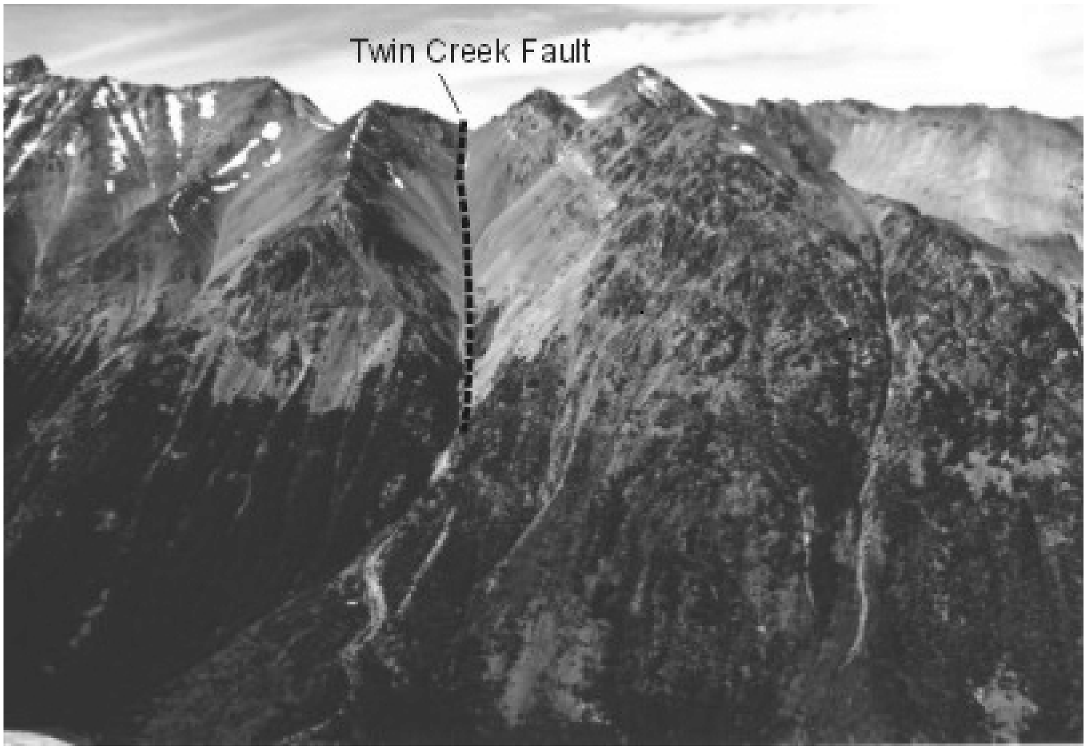

Photo 1. Well-stratified rocks of unit lK_{TCV1}, cut by Twin Creek fault.

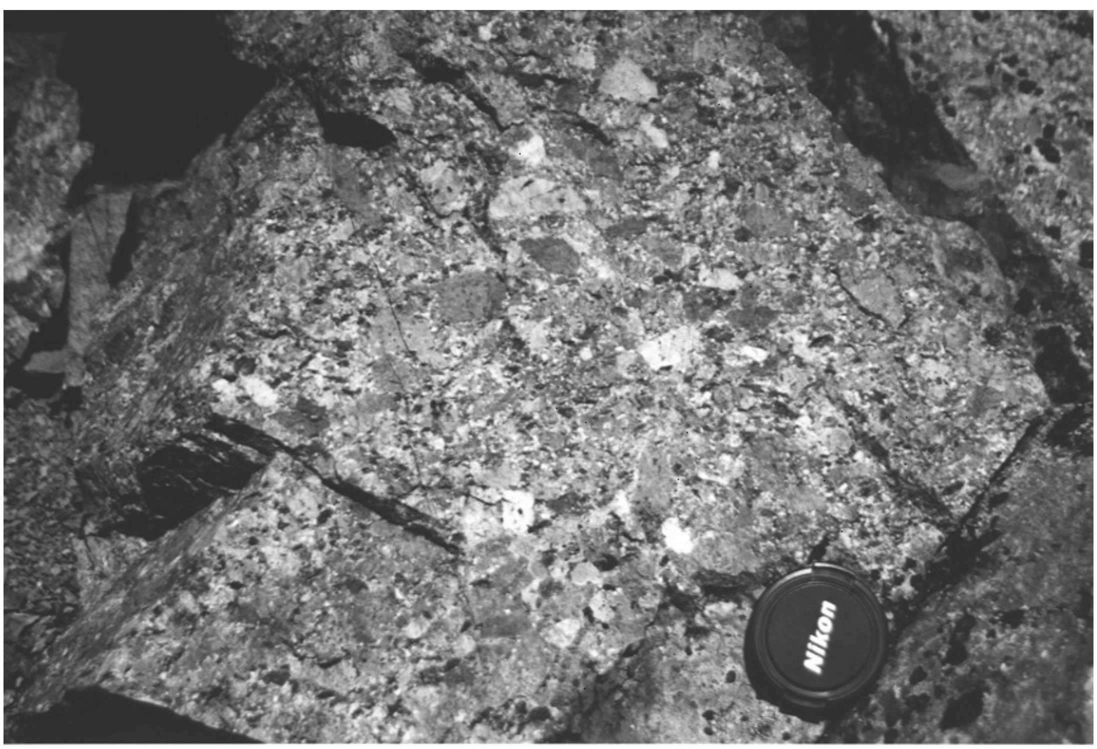

Photo 2. Chert pebble conglomerate found near the middle of unit lK_{TCV1}.

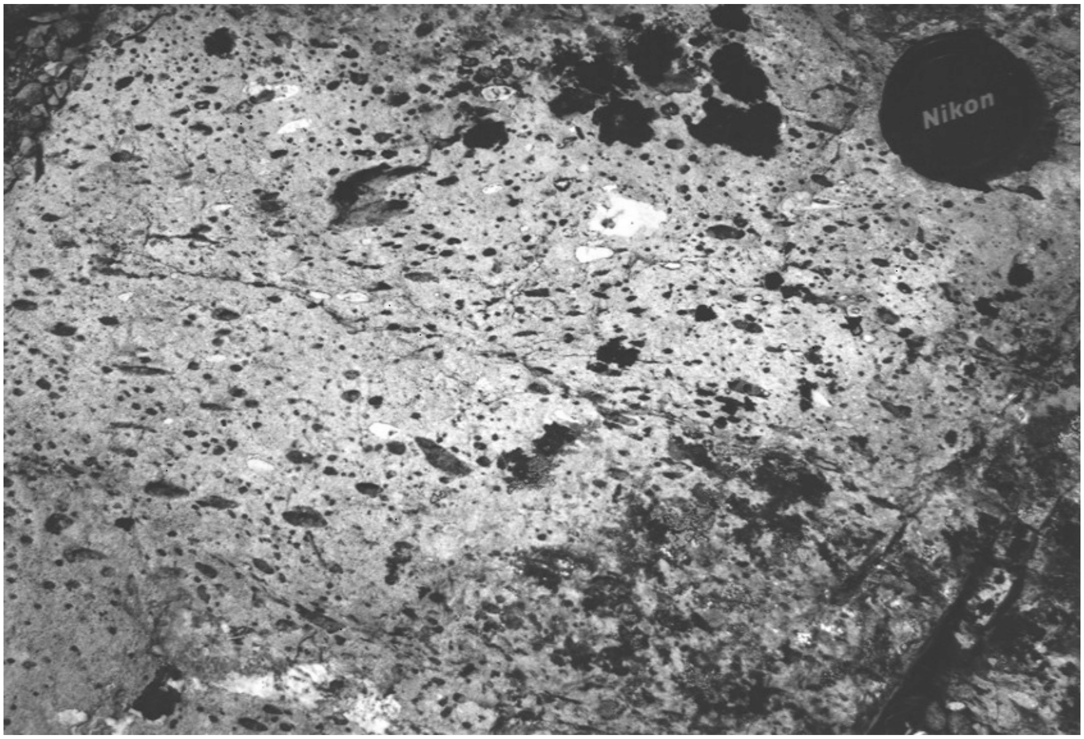

Photo 3. Chloritized hornblende crystals within green volcaniclastics near the top of unit lK_{TCV1}.

Fossils found in this unit consist of non-diagnostic gastropods, belemnites and bivalves in argillites interlayered with volcanic rocks (McLaren, 1990). Based on the presence of the belemnites, McLaren assigned a Hauterivian to Barremian age to the unit. This unit is thought to also occur to the west of RCAF Peak, where it apparently rests stratigraphically above rocks of the Relay Mountain Group (McLaren, 1990).

Unit LK_{TCv2}

The second unit of the volcanic section outcrops on the ridge immediately south of the Tchaikazan River and east of unit LK_{TCv1}, as well as north of the Tchaikazan River east of RCAF Peak. It is characterized by a more mafic succession of volcanic and associated volcaniclastic rocks interbedded with marine sediments. It may also be present in a slightly different form in the northwest portion of the map area, where basaltic flows are interbedded with mafic tuff horizons.

The base of the unit consists of laminated dark grey-green to black turbidites and dark brown shales, which pass upward into a cobble conglomerate consisting entirely of sub-rounded to angular plagioclase-phyric intermediate volcanic clasts within a black shaly matrix. Within this horizon a metre-thick bed of dark brown, mafic pyroclastic rocks are host to a large number of bivalve fossils.

Apparently conformable above the conglomerates is a 50-metre-thick section of columnar jointed mafic to intermediate flows capped by 30 metres of pillowed volcanics (Photo 4).

The columns are roughly 50 cm across but locally reach widths of more than a metre. The pillows become less well defined higher in the section, until they pass into a fine to medium grained, dark green volcaniclastic. Chloritized hornblende crystals occur within the volcaniclastics, similar to those seen in unit LK_{TCv1}.

The stratigraphic position of this unit is somewhat problematic, as the base of it seems to coincide with a steeply dipping fault. However, the bedding dips and facing directions of unit LK_{TCv2} are similar to those within unit LK_{TCv1} and the close proximity to the lower unit could indicate a stratigraphic relationship between the two units. There is no mention of pillows within the Taylor Creek volcanic package by any other worker, suggesting it may just be a small discontinuous unit between LK_{TCv1} and LK_{TCv3}.

Unit LK_{TCv3}

The best exposure of LK_{TCv3} is on the western side of the Falls River valley, directly west of the Pellaire gold deposit. The base of the unit is not well exposed. The top of the unit is involved in a large strike slip fault, but reconstruction along the fault may bring rocks of LK_{TCv4} into place on top of unit LK_{TCv3}. Rocks within this unit are generally volcanic breccias, volcaniclastics and marine turbidites with few beds of tuffaceous sandstone.

Volcanic breccias of LK_{TCv3} consist of large (up to 40 cm) clasts of intermediate to felsic volcanic rocks within

Photo 4. Columnar jointing found in volcanic rocks near the top of unit lK_{TCV2}.

a plagioclase-quartz crystal matrix of similar composition (Photo 5).

The breccias occur at the base of LK_{TCv3} and continue for several tens of metres before grading into well-bedded volcaniclastics of the same material. Beds range from 1 cm to 15 cm in thickness and are commonly graded. Thin, 1 cm, fine-grained ash tuff layers occur throughout this section of the unit (Photo 6).

The volcaniclastics become increasingly sediment-rich higher up stratigraphically, ultimately grading into finely laminated turbidites and shales. The turbidites are dark grey-green to black and commonly show Tab and Tce sequences. Shales are interbedded with the turbidites and are generally massive and black. One, as of yet undated, fossil was found. At the top of the section approximately 30-40 metres of fine-grained grey-green volcaniclastic rock with small (1 mm) hornblende crystals is found interbedded with the sediments.

Unit LK_{TCv4}

The most complete section of LK_{TCv4} is located at the Pellaire occurrence. Here it is roughly 500 metres thick and is composed of volcanic breccias, volcaniclastics and turbidites. It differs from unit LK_{TCv3} in that it does not have shale, has a larger component of turbidites and contains very distinct red jasper within the breccias (Photo 7)

The volcanic breccias of unit LK_{TCv4} are similar to those of unit LK_{TCv3} except that the clasts are more rounded and not as large. The red jasper suggests a difference in the provenance of the breccias. The breccias grade into a fine-grained purple to green massive volcaniclastic, with plagioclase crystals up to 2mm long. West of the Falls River, the same jasper-rich breccias are found to grade into a purple to maroon andesitic flow 30 metres thick, which is overlain by the purple-green volcaniclastics.

Conformably overlying the volcaniclastics is a large package of Tab and Tbc grey-green to black silty turbidites. The package is a monotonous continuation of the same lithology for more than 200 m, eventually grading into more volcaniclastics with slightly larger intermediate to felsic volcanic clasts than seen lower down in the section.

The stratigraphic position of unit LK_{TCv4} is somewhat suspect, but on the west side of the Falls River it apparently overlies unit LK_{TCv3}. However, the actual contact is not exposed making certain interpretation difficult. The lack of shale and higher sandstone content might suggest a change to shallower waters and less volcanic activity.

Beece Creek Succession

The Taylor Creek Group to the east of Taseko Lakes (Figure 2) is dominated by exposures of shale, micaceous sandstone and chert-rich polymictic conglomerate that have been assigned to the informal Beece Creek succession by Schiarizza *et al*. (1997) and Schiarizza and Riddell (1997). The Beece Creek succession forms the upper part of the Taylor Creek Group in this area, and is inferred to represent, at least in part, a distal facies of Garver's (1992) Silverquick conglomerate. Within the present study area, rocks that are confidently assigned to the Beece Creek succession occur as a series of small outcrops near the bridge over the Tchaikazan River, just north of the extent of map in figure 3. These rocks are separated from the volcanic-dominated rocks of the Taylor Creek Group described above by the Tchaikazan fault. However, a mica-rich sandstone found on top of a ridge south of the Tchaikazan fault, near the southwest side of Upper Taseko Lake, may also belong to the Beece Creek succession, although the exposure is limited due to the presence of a felsite intrusion. This observation is significant however, for if this unit is the Beece Creek succession, then it apparently overlies rocks belonging to unit LK_{TCv3}.

The exposures correlated with the Beece Creek succession near the Tchaikazan bridge include chert-pebble

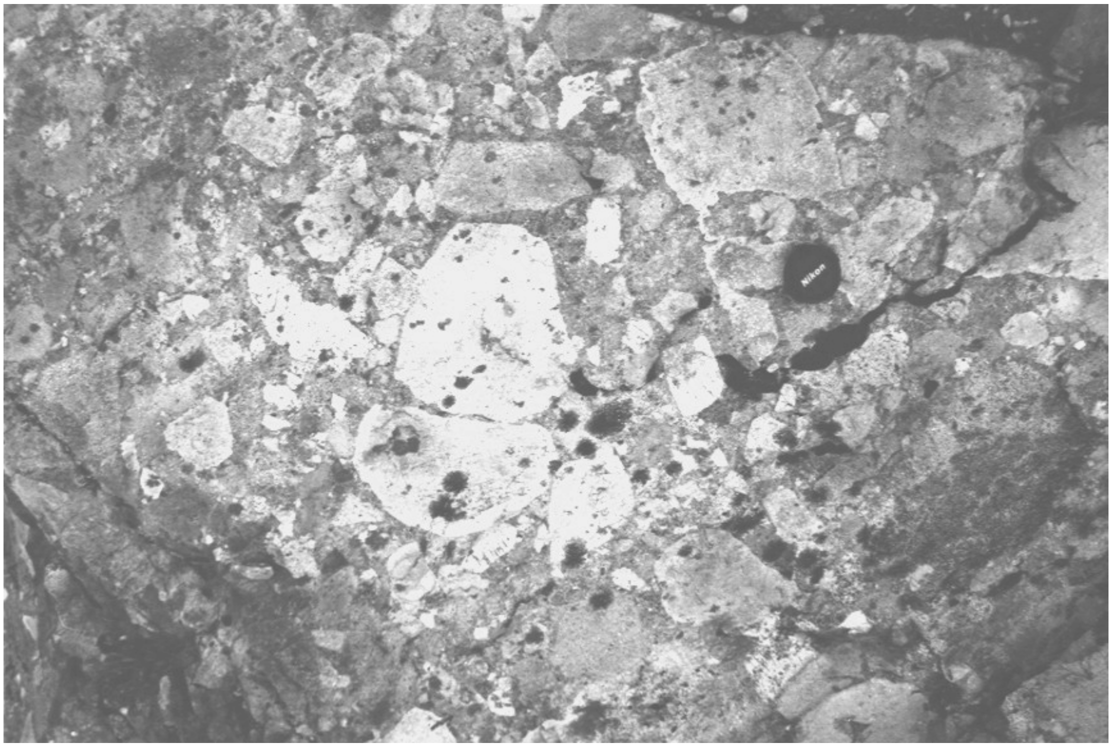

Photo 5. Large clasts of intermediate to felsic volcanic rocks within basal breccia of unit $\mathrm{lK}_{\mathrm{TCV3.}}$

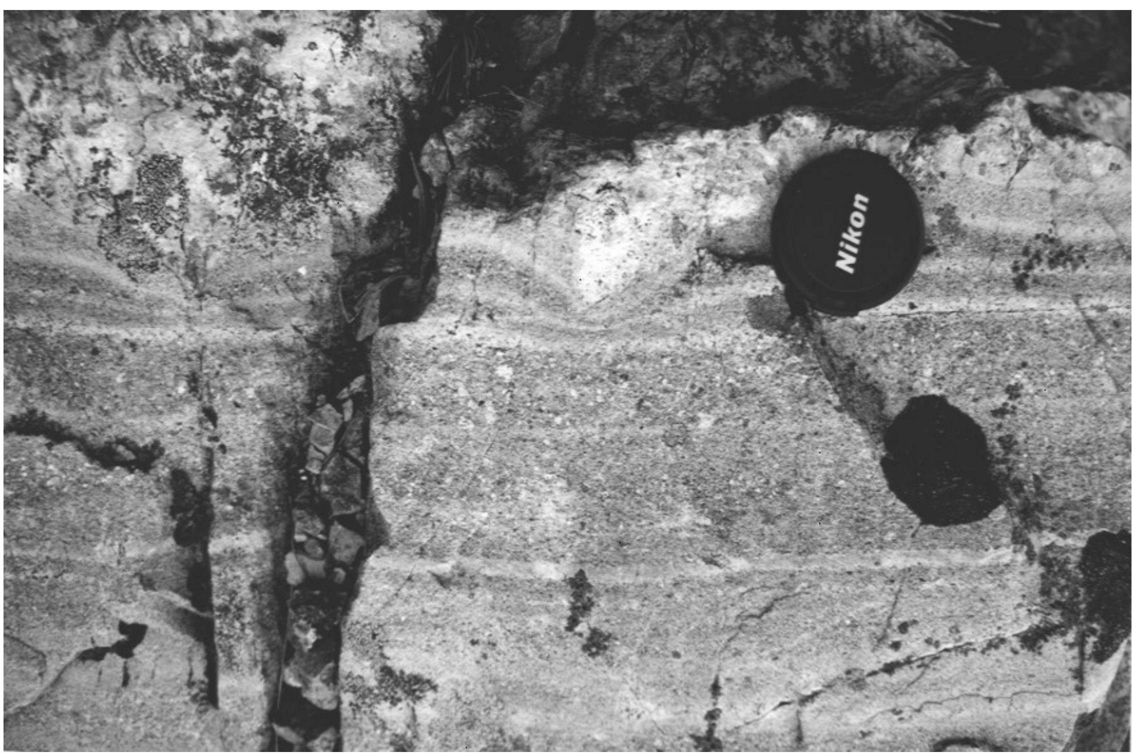

Photo 6. Well-bedded volcaniclastics with thin (1cm)-ash horizons in unit $\mathrm{lK}_{\mathrm{TCV3.}}$

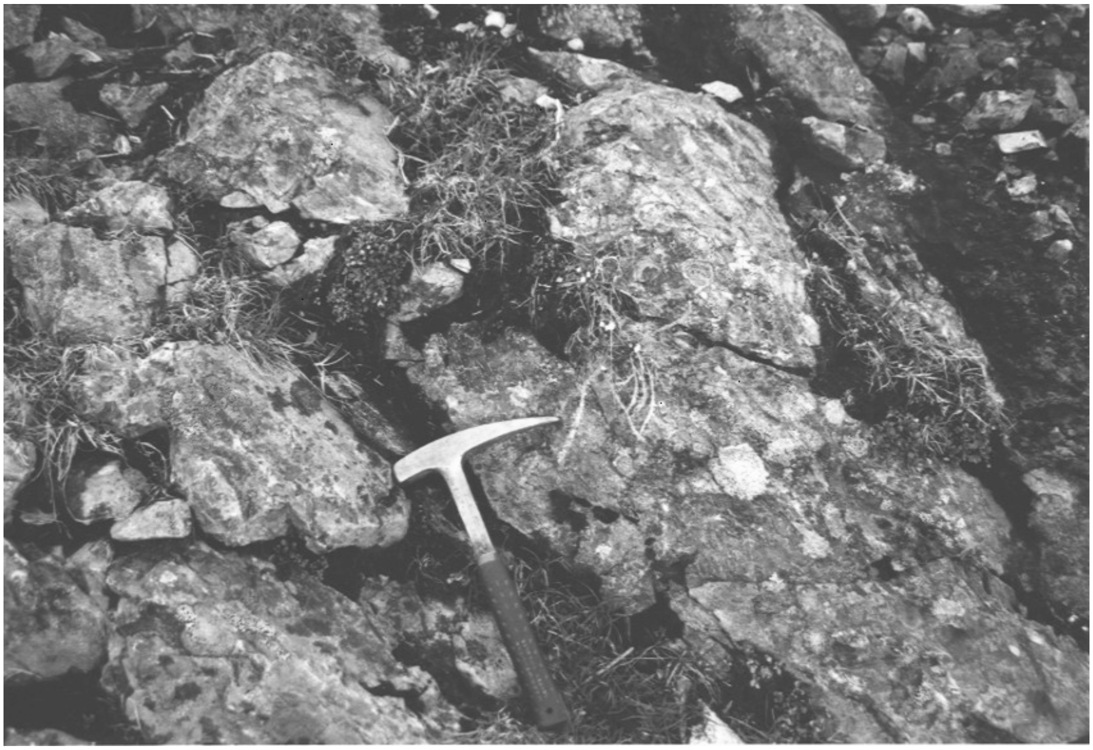

Photo 7. Red jasper within volcanic breccia at base of unit $lK_{TCV4.}$

conglomerate, mica-rich sandstone and shale. The conglomerates are matrix supported and dominated by mottled white-blue-green chert clasts. The chert clasts range from 1 cm up to 7 cm in diameter. Small well-rounded clasts of intermediate to felsic volcanics are rare. The conglomerate package is at least several metres thick, but true thickness is unknown as the top is not exposed.

Sandstones within the Beece Creek succession are characterized by light-grey-weathered, mica-rich, medium-grained beds up to several meters thick, commonly with scour marks. They are interbedded with a dark brown to black sandy shale. A few of the shale horizons host black tabular concretions up to a metre in length.

Taylor Creek Group Correlations

Provenance studies to the east of the project area by Garver (1992) indicate that the lower formations, Paradise and Elbow Pass, of the Taylor Creek Group were derived from a volcanic source to the west. The formations described by Garver have components that are very similar to the units described in this paper. Up to 70% of the clasts found within the coarser sections of the Paradise formation are characterized by green-aphanitic, feldspar-porphyritic and siliceous volcanic rocks (Garver, 1992). Furthermore, a change from a more mafic and intermediate to a clearly andesitic source for the Paradise and Elbow Pass formations, respectively, may reflect a similar change in the project area as one travels up stratigraphic section.

Two U-Pb isotopic dates from intrusive rocks reported here suggest that the age of deposition for the Taylor Creek volcanic rocks in this study area is older than 104 ± 4 Ma, and a Taylor Creek volcanic rock within the eastern Waddington thrust belt to the northwest has yielded a U-Pb zircon date of 107 Ma (Albian; Mustard and van der Heyden, 1997). Fossils described by McLaren (1990) suggest that unit LK_{TCV1} is as old as Hauterivian or Barremian. These dates are compatible with the Barremian to Albian range obtained by fission track dating of detrital zircons from the Paradise formation (Garver and Brandon, 1994).

Figure 5 is a schematic representation of the correlation between rocks found within the study area and rocks found at two localities within the main part of the Tyaughton basin to the east. The rocks found in the study area likely form the western margin of a volcanic sub-marine fan, in which the Paradise and Elbow Pass formations formed the more sediment dominated distal portions of the fan (Garver, 1992). As the basin filled from the west, uplift of the Bridge River complex within the basin to the east reached a sufficient height to initiate deposition of an easterly-derived chert-rich petrofacies, including the Dash formation, Silverquick conglomerate and Beece Creek succession (Garver, 1992; Schiarizza *et al*, 1997) (Figure 5). These chert-rich units are intercalated with arkosic rocks, found mainly in the Lizard formation, which were derived from a continental sediment source still farther east (Garver, 1992). The onset of extensive upper Cretaceous volcanism within the Tyaughton basin,

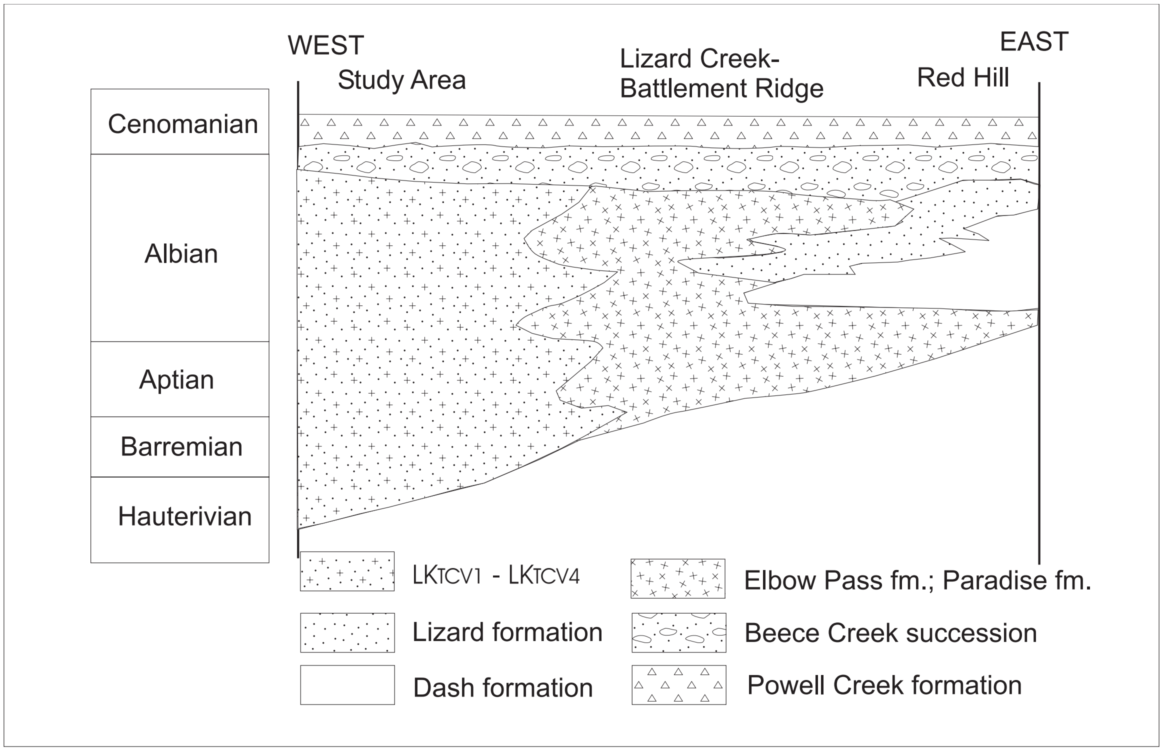

Figure 5. Schematic stratigraphic correlation between the study area, Lizard Creek/Battlement Ridge and Red Hill (after Garver, 1992 and Schiarizza *et al.* 1997).

represented by the Powell Creek formation, reflects an eastward migration of the Cretaceous Coast Belt arc with time (Schiarizza *et al*., 1997).

Garver's interpretation of a western volcanic domain as the source material for the lower formations of the Taylor Creek Group is essentially confirmed by this study. Rocks found within the project area have the right composition and apparently span the appropriate time range to be that domain. The ongoing isotopic and paleontologic work from the study area will help further constrain these ideas.

Powell Creek Formation

An extensive belt of pyroclastic and volcaniclastic rocks crops out in the northwest corner of the map area, directly southwest of the Tchaikazan fault. These rocks were assigned to an unnamed Lower Cretaceous unit by Tipper (1978) and McLaren (1990), but are here correlated with the Upper Cretaceous Powell Creek formation (informal, Schiarizza *et al*., 1997), which overlies the Taylor Creek Group on the northeast side of the Tchaikazan fault, and also occurs as fault bounded lenses along the southwest side of the fault to the northwest of the present study area (Figure 2). This correlation is based on the markedly similar appearance of these rocks to known outcrops of the Powell Creek formation, and similar structural relationships to those shown by Rusmore and Woodsworth (1993) to the northwest, where the Taylor Creek Group is thrust over the Powell Creek formation along the south side of the Tchaikazan fault.

The Powell Creek formation within the study area occurs south of the Tchaikazan fault, just north of RCAF Peak, where it forms the footwall to several large-scale thrust faults which have Taylor Creek and Relay Mountain groups in their hanging walls. It is composed of massive to well-bedded pyroclastic and volcaniclastic rocks of a deep maroon to red colour. Bedded intervals can be as thick as 2 metres, whereas the massive portions are several tens of metres thick. A 20-metre-thick lahar is found on top of an unnamed ridge northeast of RCAF peak and assumed to be part of the Powell Creek formation. It locally has clasts of intermediate volcanic rock several metres in diameter.

INTRUSIVE ROCKS

A large pluton of equigranular granodiorite to quartz diorite crops out extensively in the southern portion of the map area where it intrudes volcanic rocks of the Taylor Creek Group. A preliminary U-Pb zircon analysis from the intrusion at the Pellaire occurrence yielded an age of 104 Ma. Several titanite fractions are currently being selected for analysis to confirm the preliminary zircon data.

Diorite and quartz diorite occur as intrusions scattered throughout the central portion of the map area (McLaren, 1990). These consist of plagioclase and hornblende phenocrysts within a fine-grained matrix of the same material. Quartz is not common but was observed at some localities. Analysis of one of these plutons near Mount Pilkington yielded a conservative U-Pb zircon age of 104±4 Ma. Age similarities between the Pellaire and Mount Pilkington samples suggest a genetic link between the two igneous bodies.

McLaren (1990) mapped a distinctive group of white-weathering, biotite-feldspar porphyries that intrude sedimentary and volcanic rocks of the Taylor Creek Group and the Powell Creek formation. Most of these intrusions are found north of the Tchaikazan fault, with the exception of one that occurs at the southwest corner of Upper Taseko Lake. No geochronological work had been done on these rocks, but Tipper (1978) assigned them an Eocene age.

Dikes of several different compositions are found throughout the area. These include biotite-hornblende to hornblende-biotite-plagioclase porphyries, diabases, aplites and biotite-rich lamprophyres. Diabase, aplite and lamprophyre dikes are most common in the area east of the Tchaikazan River, whereas biotite-hornblende and hornblende-biotite-plagioclase porphyries are found mainly to the west of the river.

STRUCTURE

The map area is extremely dissected by several generations of faults. One of the primary goals of the 1999 field season was to identify fault geometries and kinematics with the aim of unraveling the structural evolution of the study area. Interpretation of kinematically linked faults is on going and, in part, contingent upon isotopic dating (in progress).

The map area is characterized by undeformed panels of rock separated by either thrust/reverse faults or high-angle strike-slip faults. Open folding occurs within the panels but is not common. Metamorphic grade is low to non-existent and cleavage development is localized around high strain zones, near strike slip faults or folds.

Below we describe the fault geometries and kinematics mapped in the field area.

Contractional Faults

Large north-northeast-verging reverse and thrust faults are located in the northwest portion of the map area. They have classic older-over-younger geometry, placing rocks of the Taylor Creek Group over Powell Creek formation. These faults are likely part of the eastern Waddington thrust belt and are interpreted as the oldest structures in the field area. This deformation event was also likely responsible for eastward tilting of most units and large northeast-verging folds within the Taylor Creek Group south of the Tchaikazan River.

Reverse faults at Pellaire deposit host a series of epithermal gold-silver-bearing quartz veins. These faults verge to the southeast and are tentatively interpreted as transfer structures between the Tchaikazan and Twin Creek faults during left-stepping dextral movement (Figure 3). This interpretation is contingent upon further structural analysis and isotopic dating. The reverse faults must be younger than the 104 Ma (U-Pb) granodiorite wall rock.

Several other contractional fault systems of limited extent are found within the field area and are likewise inferred to be linked to movement on the larger strike-slip faults. This is based on the geometry of the thrusts with respect to the strike-slip faults. They have varying vergence, from north to south.

Strike-Slip Faults

The predominant northwest-trending lineaments in the field area are strike-slip faults. Large-scale dextral systems are the most obvious, however, less obvious and possibly older sinistral faults are common.

Sinistral

Sinistral faults with well-developed shear fabrics (Photo 8) are exposed in the southeast portion of the field area (Figure 3).

They are oriented at low-angles to the northwest-striking dextral faults. The strike lengths of the sinistral faults are typically less than one kilometer, and no easy correlation can be made for the faults across the large glacial valleys, suggesting that younger faults offset them.

The sinistral faults are relatively large structures, with the shear zones reaching up to 200 m in width. The shear zones consist of well-developed shear fabrics and associated smaller scale folds and fault arrays. Both brittle and ductile features are present within the fault zones. The absolute timing of these faults is not yet determined, although field relationships indicate that the sinistral faults offset relatively small, north-verging thrust faults. However, the age of these north-verging thrust faults is not yet known; they might be related the eastern Waddington thrust belt, but might be local structures that formed during dextral or sinistral strike-slip faulting. Recrystallized illite from the sinistral fault rock will be dated to constrain timing of deformation.

Dextral

Most of the obvious, continuous lineaments in the field area are interpreted as dextral strike-slip faults. The major strike-slip faults in the field area are the Tchaikazan fault and the Twin Creek fault (Figure 3). Dextral faulting post-dates contractional structures, as exemplified by offsetting relationships (Photo 9).

The Tchaikazan fault, with a strike length of close to 200 km (Figure 2), is the largest of the steeply-dipping faults. It cuts through the northeast corner of the field area with a northwest-southeast strike, although it is very poorly exposed. Mustard and van der Heyden (1994) suggest that the Tchaikazan fault to the west of the project area was the locus of 7 to 8 kilometers of dextral offset. This portion of the fault is inferred to be Eocene in age and

Photo 8. Sinistral shear fabrics from high strain zone, west of Falls River.

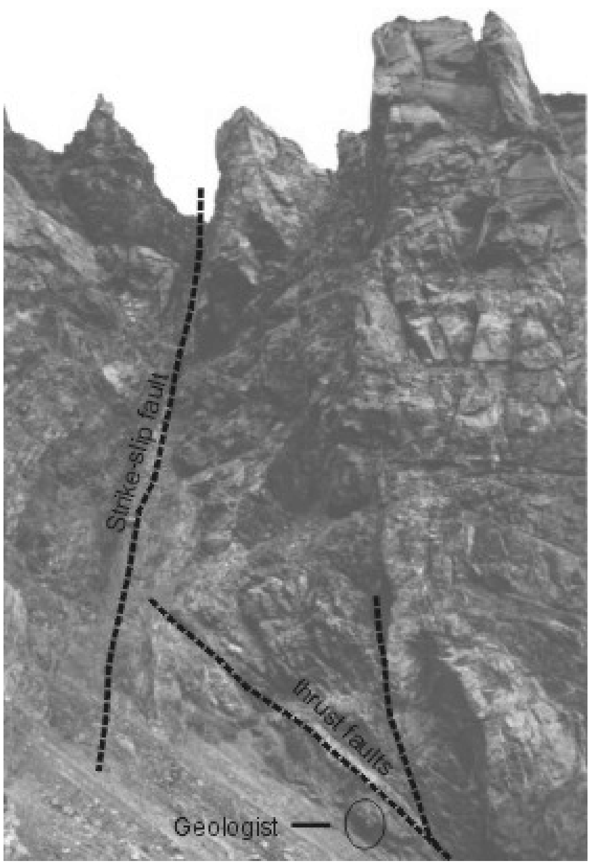

Photo 9. Southwest verging reverse faults crosscut by high angle, strike slip fault.

broadly coeval with the Yalakom fault system to the north (Umhoefer and Kleinsphen, 1995). Schiarizza *et al*. (1997) show the Tchaikazan fault to the southeast being truncated by the 92 Ma Dickson-McLure batholith, however, and suggest that the fault system had a long history of movement that may have included a Late Cretaceous sinistral component.

Within the project area the Tchaikazan fault is exposed near the shore of the Tchaikazan River as a semi-ductile zone within shale at least 300 m wide. Gently-plunging (5^o-15^o) fault groove lineations suggest strike-slip movement, and shear-sense indicators, such as sheared calcareous concretions, indicate dextral movement. The amount and timing of displacement, however, is poorly constrained in the field area.

The Twin Creek fault is located in the southern portion of the field area and extends the length of the mapped region, parallel to the Tchaikazan fault. Dextral movement on this fault is not proven, but is suspected, based partly on its association with mercury showings which elsewhere in the region are along dextral strike-slip faults of the Yalakom system (Schiarizza *et al*, 1997).

Numerous smaller scale structures are interpreted as transfer structures between the Tchaikazan and Twin Creek faults. The reverse and strike slip faults exposed at the Pellaire deposit are interpreted as components to a Reidel geometry. Interpretation assumes left-stepping movement from the Tchaikazan to the Twin Creek fault, setting up a zone of compression where the reverse faults were formed. Ar-Ar dating of syn-tectonic illite associated with the Pellaire thrust faults will place constraints on the timing of deformation of this system. If the structures at the Pellaire occurrence are Eocene and are related to the Tchaikazan, at least a part of the dextral movement along the Tchaikazan must also be Eocene in age.

Extension Faults

Small extensional faults of varying strike occur within the field area, and larger northeast-striking normal faults were mapped by McLaren (1990) to the west of the field area. The smaller normal faults have limited strike length and have little offset associated with them. These are interpreted as accommodation structures related to strike-slip faulting.

Sinistral faults found on either side of the Falls River show apparent dextral offset across a fault that may run through the valley (Figure 3). The actual displacement vector along this fault is unknown, but down-to-the-south displacement with a slight dextral component could account for both the apparent dextral offset and the down-dropping of the jasper rich unit of lK_{TCv4}.

MINERALIZATION

Several mineral occurrences occur within the map area (Figure 3), including copper porphyries and epithermal to mesothermal Au-Ag-bearing quartz veins. The occurrences most actively explored by JAG include Pellaire vein system, Chita Cu-porphyry and Northwest Copper Cu-porphyry. Discussion here is restricted to Pellaire and Northwest Copper.

Pellaire Gold and Silver Bearing Quartz veins (MINFILE 092O 045)

Exploration in the 1930's led to the discovery of gold and silver-bearing veins at Pellaire and subsequent underground exploration. Exploration was initiated again in the late 1980's, leading to further underground work (McLaren, 1990). International Jaguar Equities acquired the property in 1996 and began extensive underground and surface exploration, followed by extraction of a 2000 tonne bulk sample of high-grade ore (34.2 grams per tonne gold and 102.9 grams per tonne silver) from the No. 4 and No. 5 veins (MINFILE 092O 045 report). In 1998 JAG initiated further underground exploration which led to a 10 000 tonne bulk sampling project in 1999.

The Pellaire occurrence is situated near the southeastern corner of the field area at the northern margin of the large granodiorite pluton that occupies the southern part of the map area. It consists of several epithermal to mesothermal, gold-silver bearing quartz veins. The quartz veins are found along steeply dipping, southeast verging reverse faults, that juxtaposes rocks of the Taylor Creek Group against the granodiorite. Extreme sericitic alteration of both the Taylor Creek Group and adjacent granodiorite occurs around the veins and is likely related to vein formation rather than to the intrusion. The faults are found within both units but quartz veins occur only within the granodiorite. Veins attain widths range from 0.3 to 7.5 meters, have sheared margins, and are interpreted as having formed during thrusting. Mafic dikes are found throughout the property and are found to both crosscut and be cut by the veins. Where the dikes crosscut the veins, grade generally increases and rare sulphide mineralization in the form of chalcopyrite occurs. Areas such as the joining of two veins or where the veins change dip are also sites of increased grade.

The veins are post-104 Ma, as indicated by the U-Pb date of the granodiorite. The brittle nature of the structures and the veins suggest they were formed well after the crystallization age of the pluton. The orientation of the thrust faults that host the veins is significantly different than the majority of structures in the project area. As previously described these thrust faults are interpreted as step-over structures related to large strike-slip faults. However, southeast of the field area, mesothermal veins of the Bralorne system are hosted in similar structures that formed late within the major southeastern Coast Belt contractional event (Schiarizza *et al*., 1997). The possibility that the Pellaire veins are also related to this event cannot be ruled out at this time. Isotopic ages from the Pellaire veins are forthcoming and will place timing constraints on mineralization.

Northwest Copper (MINFILE 092O 043)

The presence of the Charlie Cu-Mo-Au prospect (MINFILE 092O 043) found in the Tchaikazan valley south of RCAF Peak led to exploration programs concentrating on the surrounding area. JAG undertook exploration of the area in 1998 based on several copper showings identified by McLaren (1990). The exploration program of 1998 identified a mineralized area of at least 8 square kilometers, which was identified as the Northwest Charlie occurrence and later as Northwest Copper (NWC).

TABLE 1
SELECTED ASSAY RESULTS FROM MAJOR SHOWINGS AT NORTHWEST COPPER
(COURTESY OF JAGUAR EQUITIES)

Showing Name	Au ppb	Ag ppm	Cu ppm
D&O	20	71.2	13200
D&O	10	41	4920
Chikapow	<5	13.4	21100
Chikapow	<5	3.8	8080
Crater	<5	7.2	15800
Crater	<5	1	3960
Far Side	35	110	9310
Far Side	80	234	18000
Far Side	<5	17.8	88100
Leach Cap	10	1.2	13600
Leach Cap	<5	<0.2	320
Leach Cap	90	211	44400
S.Acid Leach	145	90.4	20800
S.Acid Leach	95	125	19100

Subsequent geophysical exploration conducted in the spring of 1999 confirmed a large geophysical anomaly in the area. Several showings within the NWC property were discovered during the field program of 1999. The largest of these include Leach Cap, D and O, Far Side, South Acid Leach, Crater and Chikapow (Table 1).

These showings are all characterized by malachite and azurite with minor native copper (locally found in seams up to 2 cm thick) and chalcopyrite found along fracture planes, associated with quartz-epidote veins. The showings cover and area of roughly 8 square kilometers, with the individual showings only marginally defined.

The Leach Cap is characterized by advanced argillic alteration found in fine-grained tuffs. Drilling in the summer of 1999 has shown that hornblende porphyry intrusive rocks exhibit propylitic (epidote, chlorite, and sericite) alteration in the vicinity of the leach zone. General sequence of alteration seems to be hydrothermal alteration (fracture-controlled quartz-carbonate, chlorite) to argillic to advanced/extreme argillic (kaolinite) alteration as one approaches the leach zone (Andrew Smith, personal communication, 1999). There is abundant iron within the system in the form of hematite, which is found ubiquitously within the volcanic rocks of the Powell Creek formation and may indicate a low sulphur system. This characteristic is confirmed by the lack of pyrite and may also be responsible for the absence of gold mineralization. There is associated silicification in the area around the leach cap, but is likely part of quartz-sericite alteration found within the vertical structures (example the D and O and the south acid leach showings) (Andrew Smith, personal communication, 1999).

Mineralization is thought to be structurally controlled. Mineralized hornblende-porphyry dikes are located in the middle of steeply-dipping shear zones thought to reach a source pluton beneath the Powell Creek formation. The Tchaikazan fault sharply bounds NWC to the northeast, and likely offsets it. Structures splaying off the Tchaikazan may have provided weak areas for intrusion of the dikes.

SUMMARY

The oldest rocks in the map area, Hauterivian shale and sandstone assigned to the Relay Mountain Group, are restricted to a small lens bounded by south-dipping thrust faults. Most of the area is underlain by volcanic, volcaniclastic and associated sedimentary rocks assigned to the Taylor Creek Group. These have been subdivided into four distinct lithologic units. Present constraints suggest they range from Hauterivian-Barremian to Albian age (McLaren, 1990), but paleontologic and isotopic dating in progress may provide tighter constraints on some of the units. Small exposures of conglomerate, sandstone and shale on the northeast side of the Tchaikazan fault are also assigned to the Taylor Creek Group, and correlated with the Albian-Cenomanian Beece Creek succession of Schiarizza *et al.* (1997). An extensive panel of non-marine volcanic and volcaniclastic rocks directly southeast of the Tchaikazan fault, previously assigned to the Lower Cretaceous, is here correlated with the Upper Cretaceous Powell Creek formation, based on lithologic similarity and structural position.

The first deformation event in the area is interpreted as the northeast-directed contraction associated with the eastern Waddington thrust belt. Discontinuous, but well-developed sinistral shear zones crosscut north-verging thrust faults that may be related to eastern Waddington structures. Absolute timing of sinistral movement is not yet known, but likely occurred before dextral movement in the Eocene. Isotopic dating will place constraints on the timing of sinistral movement. The importance of sinistral faulting is not yet known, however, their well-developed shear fabrics and shear zone thickness suggest that these faults accommodated significant displacement. Dextral strike-slip faulting, responsible for the prominent lineaments in the area, is thought to represent the last deformation event. Numerous small-scale thrust faults, normal faults and strike-slip faults are interpreted to have formed during transfer of displacement between the regional dextral strike-slip faults.

Porphyry-style copper mineralization is hosted in rocks of both the Taylor Creek Group and Powell Creek formation associated with hornblende-porphyry intrusions of an unknown age. Epithermal-style gold-silver veins are found along reverse faults within granodiorite of the Coast Plutonic Complex. The faults (and associated mineralization) are suspected to be Eocene in age, an interpretation that will be tested by isotopic dating.

FUTURE WORK

Future efforts will focus on the elucidation of the kinematics and timing of deformation. This requires a more thorough structural analysis and more detailed analyses of fault geometries and kinematics. Both Ar-Ar and U-Pb geochronology will be used to date fabrics within shear zones and to date plutons. Illite from the Pellaire veins and zircon or hornblende from syn-mineralization dikes from NWC will constrain ages of mineralization at each property.

A more robust stratigraphic column will be constructed based on future isotopic dates and fossil identification.

ACKNOWLDGEMENTS

Steve Israel would like to thank: Danny Lilly, Chris Roach and Adrian Garner for excellent assistance in the field; Andrew Smith and Bernie Gaboury for support both in and out of the field. We are grateful to International Jaguar Equities and NWC Exploration Inc. for funding the project. In particular we would like to thank Paul Schiarizza for his endless patience with questions and discussions on the regional geology and taking time to visit the field area. We also thank Paul Umhoefer of Northern Arizona University for sharing his knowledge and ideas of the regional geology. Finally Graeme McLaren for his helpful discussion on the local geology. Project funded by International Jaguar Equities, NWC Exploration Inc. and Collaborative Research and Development Grant (CRD) to Lori Kennedy. We thank Dave Lefebure for helpful editorial comments on an earlier version of the manuscript and Janet Holland for formatting the final version.

REFERENCES

Garver, J.I. (1989): Basin Evolution and Source Terranes of Albian-Cenomanian Rocks in the Tyaughton Basin, Southern British Columbia: Implications for Mid-Cretaceous Tectonics in the Canadian Cordillera; unpublished Ph.D. thesis, *The University of Washington*, 227 pages.

Garver, J.I. (1992): Provenance of Albian-Cenomanian Rocks of the Methow and Tyaughton Basins, Southern British Columbia: a mid-Cretaceous link between North America and the Insular Terrane; *Canadian Journal of Earth Sciences*, Volume 29, pages 1274-1295.

Garver, J.I. and Brandon, M.T. (1994): Fission-track Ages of Detrital Zircons from Cretaceous Strata, Southern British Columbia: Implications for the Baja BC Hypothesis; *Tectonics*, Volume 13, pages 401-420.

Glover, J. K., Schiarizza, P., and Garver, J. I. (1988). Geology of The Noaxe Creek Map Area (92O/2): *in* Geological Fieldwork 1987, *B.C. Ministry of Energy, Mines and Petroleum Resources*, Paper 1988-1, pages 105-123.

Jeletzky, J. A. and Tipper H. W. (1968): Upper Jurassic and Cretaceous rocks of Taseko Lakes map area and their bearing on the Geological History of southwestern British Columbia: *Geological Survey of Canada*, Paper 67-54, 218 pages.

Journeay, J.M. and Friedman, R.M. (1993): The Coast Belt Thrust System: Evidence of Late Cretaceous Shortening in Southwest British Columbia; *Tectonics*, Volume 12, pages 756-775.

Journeay, J. M., Sanders, C., Van-Konijnenburg, J. H., and Jaasma, M. (1992): Fault Systems of the Eastern Coast Belt, southwest British Columbia; *in* Current Research, Part A; *Geological Survey of Canada*, Paper 92-1A, pages 225-235.

McLaren, G.P. (1990): A Mineral Resource Assessment of the Chilko Lake Planning Area; *B.C. Ministry of Energy, Mines and Petroleum Resources*, Bulletin 81, 117 pages.

Monger, J.W.H., Price, R.A. and Tempelman-Kluit, D.J. (1982): Tectonic Accretion and the Origin of the Two Major Metamorphic and Plutonic Welts in the Canadian Cordillera; *Geology*, Volume 10, pages 70-75.

Monger, J.W.H. and Journeay, J.M. (1994): Guide to the Geology and Tectonic Evolution of the Southern Coast Mountains; *Geological Survey of Canada*, Open File 2490.

Monger, J.W.H., van der Heyden, P., Journeay, J.M., Evenchick, C.A. and Mahoney, J.B. (1994): Jurassic - Cretaceous Basins along the Canadian Coast Belt: their Bearing on pre-mid-Cretaceous Sinistral Displacements; *Geology*, Volume 22, pages 175-178.

Mustard, P.S. and van der Heyden, P. (1997): Geology of Tatla Lake (92N/15) and the East Half of Bussel Creek (92N/14) Map Areas; *in* Interior Plateau Geoscience Project: Summary of Geological, Geochemical and Geophysical Studies, Diakow, L.J. and Newell, J.M., Editors, *British Columbia Ministry of Employment and Investment,* Paper 1997-2, pages 103-118.

Mustard, P.S. and van der Heyden, P. (1994): Stratigraphy and Sedimentology of the Tatla Lake - Bussel Creek Map Areas, West-central British Columbia; *in* Current Research 1994-A, *Geological Survey of Canada,* pages 95-104.

Riddell, J., Schiarizza, P., Gaba, R. G., Caira, N. and Findlay, A. (1993): Geology and Mineral Occurrences of the Mount Tatlow Map Area (92O/5,6 and 12); *in* Geological Fieldwork 1992, *B.C. Ministry of Energy, Mines and Petroleum Resources*, Paper 1993-1, pages 37-52.

Rusmore, M.E. and Woodsworth, G.J. (1991): Distribution and Tectonic Significance of Upper Triassic Terranes in the Eastern Coast Mountains and Adjacent Intermontane Belt, British Columbia; *Canadian Journal of Earth Sciences*, Volume 28, pages 532-541.

Rusmore, M.E. and Woodsworth, G.J. (1993): Geological Maps of the Mt. Queen Bess (92N/7) and Razorback Mountain (92N/10) Map Areas, Coast Mountains, British Columbia; Geological Survey of Canada, Open File 2586, 2 sheets, 1:50 000 scale.

Rusmore, M.E. and Woodsworth, G. J. (1994). Evolution of the eastern Waddington Thrust Belt and its relation to the mid-Cretaceous Coast Mountains arc, western British Columbia. Tectonics, Volume 13, pages 1052-1067.

Schiarizza, P., Gaba, R.G., Glover, J.K., Garver, J.I. and Umhoefer, P.J. (1997): Geology and Mineral Occurrences of the Taseko - Bridge River Area; *British Columbia Ministry of Employment and Investment*, Bulletin 100, 291 pages.

Schiarizza, P. and Riddell, J. (1997): Geology of the Tatlayoko Lake - Beece Creek Area (92N/8, 9, 10; 92O/5, 6, 12); *in* Interior Plateau Geoscience Project: Summary of Geological, Geochemical and Geophysical Studies, Diakow, L.J. and Newell, J.M., Editors, *British Columbia Ministry of Employment and Investment*, Paper 1997-2, pages 63-101.

Tipper, H. W. (1963): Geology, Taseko Lakes, British Columbia (92-O); *Geological Survey of Canada*, Map 29-1963

Tipper, H.W. (1978): Taseko Lakes (92O) Map Area; *Geological Survey of Canada*, Open File 534.

Umhoefer, P.J. and Kleinspehn, K.L. (1995): Mesoscale and Regional Kinematics of the Northwestern Yalakom Fault System: Major Paleogene Dextral Faulting in British Columbia, Canada; *Tectonics*, Volume 14, pages 78-94.

Umhoefer, P.J. and Schiarizza, P. (1996): Latest Cretaceous to Early Tertiary Dextral Strike-slip Faulting on the southeastern Yalakom Fault System, southeastern Coast Belt, British Columbia; *Geological Society of America,* Bulletin, Volume 108, pages 768-785.

Umhoefer, P.J., Rusmore, M.E. and Woodsworth, G.J. (1994): Contrasting Tectono-stratigraphy and Structure in the Coast Belt near Chilko Lake, British Columbia: Unrelated Terranes or an Arc - Back-arc Transect?; *Canadian Journal of Earth Sciences,* Volume 31, pages 1700-1713.

Umhoefer, Paul J., Rusmore, M. E. and Woodsworth, G. J. (1994): Contrasting tectono-stratigraphy and structure in the CoastBelt near Chilko Lake, British Columbia: unrelated terranes Or an arc-back-arc transect?: Canadian Journal of Earth Sciences, vol. 31, pages 1700-1713.

Geochronological and Lead Isotopic Constraints on the Age and Origin of the Laidman Gold Prospect, Central British Columbia

By L.N. Poznikoff, J.K. Mortensen, R.M. Friedman and J.E. Gabites
The University of British Columbia

KEYWORDS: *Laidman Lake Batholith, U-Pb age, Pb isotopic analysis, Nechako arch, Stikine Terrane.*

INTRODUCTION

Mineralization at the Laidman Gold Prospect occurs in quartz veins and quartz breccias hosted within granitic rocks of the Laidman Lake batholith (Figure 1). The Laidman property occurs in the general vicinity of several other precious metal epithermal, skarn, and porphyry prospects in the Fawnie Creek map area (Figure 1).

This study focuses on the 110 Zone of the Laidman property where granitic rocks have been affected by an extensive east-west trending zone of sericitic to argillic alteration that hosts locally gold-bearing quartz veins and quartz breccias. The purposes of this study are to describe the different phases within the Laidman property, place constraints on the timing of magmatism and mineraliza-

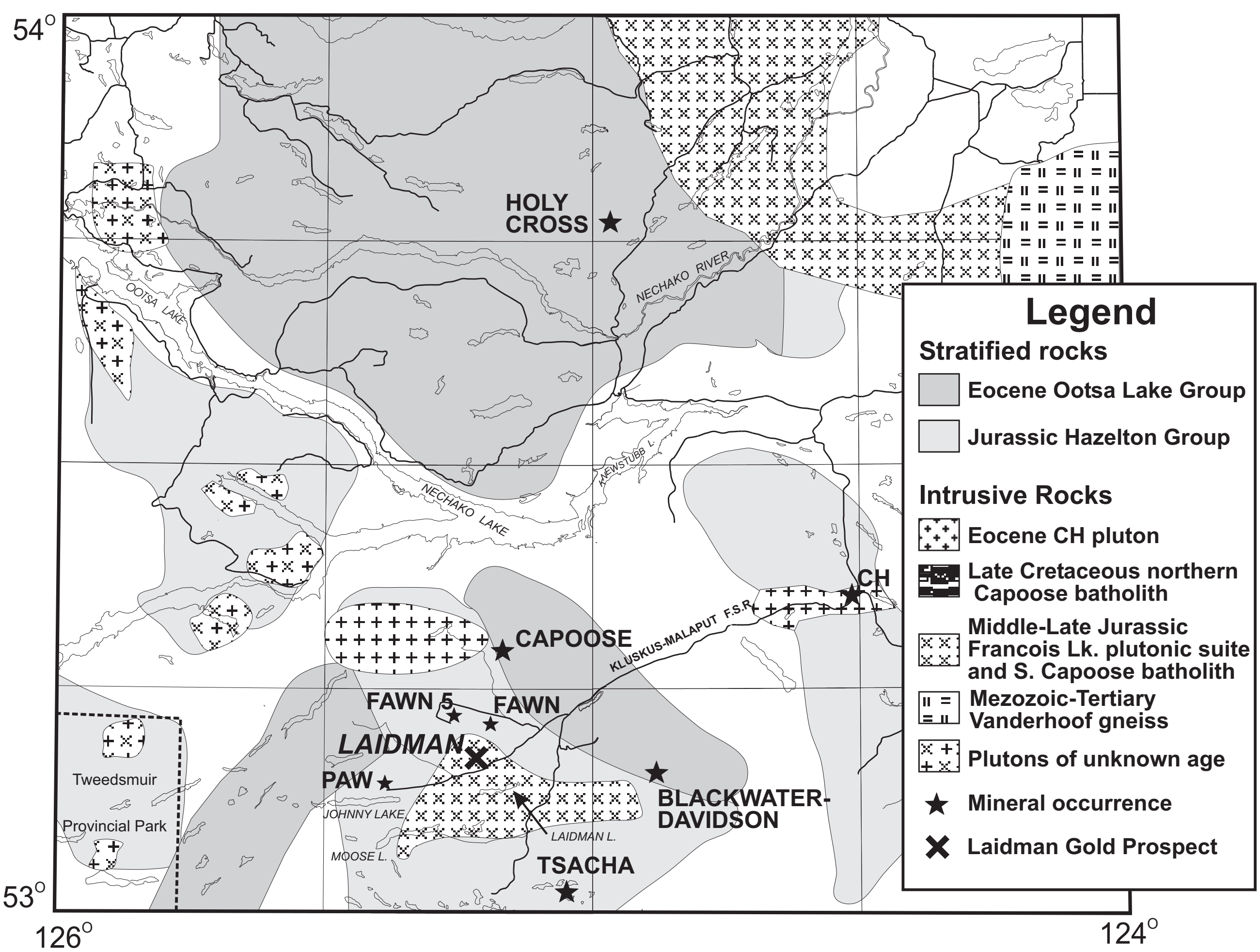

Figure 1. Compilation geological map of the Nechako River map area (93F), modified from Lane and Schroeter (1997), Diakow and Webster (1994), Tipper (1963), and Friedman *et al.* (in prep.).

tion using U-Pb dating and Pb isotopic analyses, and use this data to assess possible relationships with other mineral deposits and occurrences in the region.

Location and Access

The Laidman gold prospect is located on the gently sloping south face of the Entiako Spur, a topographically elevated ridge which intersects the northwest trending Fawnie Range. The claims are within the Fawnie Creek map area (NTS 93 F/3), 155 kilometers southwest of Vanderhoof in the plateau region of central British Columbia. Access to the property from Vanderhoof is via the Kluskus-Ootsa Forest Service road for about 140 kilometers, then southwest along the Kluskus-Malaput Forest Service road for 15 kilometers. Local spur roads built for clear-cut logging purposes and four wheel drive roads to drill sites allow access to the central portion of the claim blocks.

Exploration History

Until recently the Nechako River region has been relatively under-explored although the favourable geology of the area suggests the potential to host many different styles of mineralization. Past exploration efforts were hampered by a lack of bedrock exposure, poor road access, and a generally out-of-date geoscience database (Lane and Schroeter, 1997).

Access to the area has greatly improved since the completion of the Kluskus Forestry road in 1977. As part of the Interior Plateau Project, ongoing geologic mapping, geochemical, geochronological, and metallogenic studies by the British Columbia Geologic Survey Branch and Geologic Survey of Canada has greatly increased the database of knowledge for the interior plateau region of British Columbia. With the release of this new data to the public, a significant increase in staking and exploration has ensued (Lane and Schroeter, 1997). Targets of recent exploration efforts include precious metal-bearing epithermal veins, skarns, and porphyry deposits.

Based on cross-cutting relationships and existing geochronological data associated with specific suites of intrusions, Lane and Schroeter (1997) have recognized three mineralizing events in the interior plateau:

A Late Jurassic-Early Cretaceous event associated with the emplacement of the plutons of the Francois Lake Plutonic Suite which includes the Endako porphyry Mo deposit, the largest molybdenum deposit known in Canada (Woodsworth *et al.*, 1991). Within the Nechako River map area (NTS 93F) Late Jurassic-Early Cretaceous prospects include porphyry (Paw), vein and porphyry related (Laidman), skarn (Fawn 5), and epithermal vein (Fawn) showings (Figure 1);

Late Cretaceous felsic dikes and sills which intrude Hazelton Group rocks are the likely source of mineralization for the Capoose porphyry(?)-related silver (±gold), and the Blackwater-Davidson precious and base metal prospect;

Mineralization of Eocene (or younger) age consists mainly of epithermal precious metal prospects. These include the Wolf, Holy Cross, Trout, Uduk Lake, Loon, and Oboy prospects. Porphyry-style mineralization of Eocene age also occurs at the CH Cu-Au-Mo deposit (Figure 1). The Equity Silver Mine (4.3 million tonnes grading 135 g/t Ag, 0.45 % Cu, and 1.3 g/t Au in Main Zone), 38 kilometers southeast of Houston, B.C., is a classic high sulphidation vein deposit associated with intrusive activity at approximately 60 Ma (Cyr *et al.*, 1984, and Friedman, pers. comm., 1998).

Regional Geology

The Laidman gold prospect lies within the Nechako Arch, a zone of regional uplift in the Stikine terrane near the western margin of the Intermontane Superterrane. Pre-Tertiary rocks exposed in the Nechako Arch include arc-related calc-alkaline volcanic and volcaniclastic rocks of the Middle Jurassic Hazelton Group, and easterly-derived clastic rocks of the Lower Cretaceous Skeena Group. Intrusive rocks include augite porphyry plugs of Middle Jurassic age, likely coeval with similar volcanic rocks of the Hazelton Group, Late Jurassic to Early Cretaceous quartz monzonite to granitic plutons of the Francois Lake Plutonic Suite, and Late Cretaceous quartz diorite and quartz porphyry dikes, plugs, and stocks (Diakow & Webster, 1994).

Rocks of Tertiary and younger age include rhyolitic to dacitic tuff, flows and breccias of the Ootsa Lake Group, and Miocene Chilcotin Group plateau basalt flows (Diakow &Webster, 1994). Tertiary and younger intrusive rocks include the CH granodiorite pluton of Eocene age (Friedman, pers. comm., 1998.).

The oldest rock unit observed in the Fawnie Creek map area (NTS 93 F/3) forms the lowest part of the Hazelton Group. It has been informally named the Naglico formation by Diakow & Webster (1994) and consists of flows and volcaniclastic rocks interbedded with Middle Jurassic sedimentary strata. The Naglico formation underlies the entire Fawnie Creek map area although exposure is less continuous on the Entiako Spur. In this area it comprises a relatively thin blanket of thermally altered rocks in intrusive contact with the Laidman Lake batholith (Diakow & Webster, 1994).

Mesozoic rocks which dominate the Fawnie and Nechako ranges terminate abruptly to the north and south, where younger volcanic successions underlie much of the subdued topography. These dramatic changes in physiography and stratigraphy delineate a broad horst, called the Nechako uplift. The timing of structural uplift may be contemporaneous with Late Cretaceous deformation that imparted a pervasive penetrative cleavage and local mylonitic fabric on Jurassic strata in the Nechako Range. The structural fabric is cut by undated diorite plutons and the Eocene CH pluton (Diakow *et al.*, 1995). Regional metamorphism in the Nechako River map area is limited to low grade greenschist facies (Wetherup, pers. comm., 1998).

PROPERTY GEOLOGY

The western part of the Laidman property is underlain by southwest-dipping sedimentary and volcaniclastic rocks of the Middle Jurassic Naglico formation. Lapillistone and tuff units of the Naglico formation have been intruded and contact metamorphosed by the Laidman Lake batholith, which has converted them to hornfels and local small bodies of skarn (Fox, 1996 unpublished report). During the 1997 field season the author and Steve Wetherup mapped an 800 by 800 metre area surrounding the '110 Zone' on the Laidman property at a scale of 1:2500 (Figure 2). The majority of the 110 Zone map area is underlain by two granite phases of the Laidman Lake batholith. Parallel trending rhyolite and dacite dikes cut the granites and are themselves cut by younger plugs of diorite and monzodiorite. A series of south-facing scarps may be the result of Tertiary extension or movement along the Top Lake lineament immediately north of the Laidman prospect.

Alteration in the 110 Zone map area occurs as extensive east-west trending zones of phyllic to argillic alteration aureoles around quartz veins and stockworks which locally contain chalcedonic quartz and clay-altered feldspar. Quartz veins are white to translucent, massive to vuggy and contain disseminated aggregates of pyrite and arsenopyrite. Rocks within these zones are locally brecciated, containing fragments of granite, dacite, and rhyolite.

Intrusive Phases

Five phases of intrusions were identified during detailed surface mapping and logging of drill core. A suite of least altered samples was collected to determine textural, compositional and petrological variations between phases. Samples were examined petrographically, and a subset of the samples were analyzed for major, trace and rare earth elements (REE).

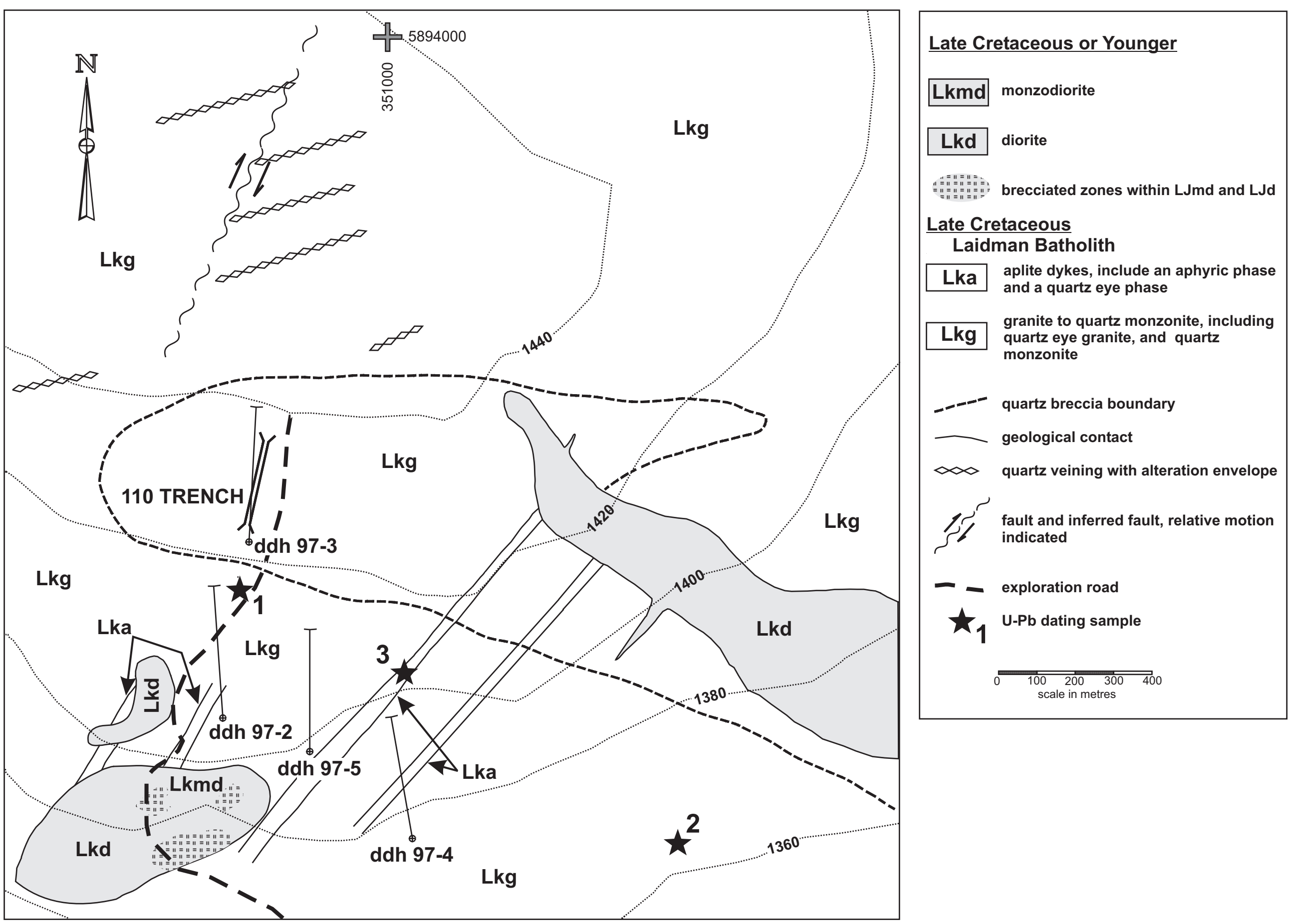

Figure 2. Detailed geology map of the 110 Zone of the Laidman property (after Fox, 1998).

Quartz Eye Granite

The quartz eye granite phase crops out sporadically in the southern portion of the map area . It is light pink where fresh and brown to grey on weathered surfaces. The lack of outcrop in the southern part of the map area obscures the contact relationship with the hypidiomorphic granite phase which surrounds it. The main distinguishing feature of this granite are 2 to 3 mm quartz eyes which occur as agglomeracrysts up to 1.5 cm in size. The agglomeracrysts are surrounded by a hypidiomorphic growth texture of K-feldspar up to 3 mm in size, plagioclase crystals up to 1.5 mm, and quartz grains less than 1 mm in size. The mode of the rock is quartz 35%, K-feldspar 45%, plagioclase 28%, and biotite approximately 2% of the rock. The quartz eye granite ranges from fresh to phyllicly altered, with feldspar minerals partially altered to sericite and biotite partially altered to chlorite.

Granite

The hypidiomorphic granite phase underlies the majority of the map area and surrounds the quartz eye granite phase. The colours of the fresh and weathered surface vary with alteration and proximity to east-west trending quartz veins. Fresh granite is light pink to buff, and weathered surfaces are grey with white plagioclase grains. Where affected by alteration, the feldspars are pale green to chalky white imparting a lighter overall colour to the rock. The modal mineralogy ranges throughout the map area with quartz (up to 3.5 mm in size) 25-35%, K-feldspar (up to 12 mm in size) 40-45%, plagioclase (up to 5 mm) 20-30%, 5-10% biotite, and up to 2% hornblende. Alteration ranges from sericitic to argillic around quartz veins with iron stained argillic alteration prevalent near the monzodiorite plug (see below).

Rhyolitic and Dacitic Quartz-feldspar Porphyry Dikes

Parallel, northeast-trending sets of rhyolite and quartz feldspar porphyry dikes of dacitic composition cross cut the quartz eye granite and hypidiomorphic granite phases (Figure 2). Clasts of both rock types are locally found in quartz breccias and are observed in drill core as xenoliths in the monzodiorite. Relatively fresh rhyolite from drill core is dull grey and aphanitic. Fresh quartz feldspar porphyry dacite from drill core is fine-grained and medium-grey with approximately 20% quartz, 20% K-feldspar, 50% plagioclase, 15% biotite, minor hornblende, and locally up to 5% euhedral pyrite. In thin section the plagioclase crystals show strong zoning, and mafic minerals are partially to completely altered to chlorite.

Hornblende-biotite Diorite

A plug of hornblende-biotite diorite intrudes into the granite and cross-cuts the rhyolite and porphyritic dacite dikes in the central portion of the 110 Zone. The diorite is medium-grained with a salt-and-pepper appearance, with fine-grained border phases near the sharp contact with the granite. Locally the diorite has pervasive carbonate alteration with 1-2 mm calcite veins and is generally weakly to moderately magnetic. Mineral abundances include 15-20% quartz, 10-15% K-feldspar, 45-50% plagioclase, 15% biotite, 10% hornblende and locally up to 10% pyrite. Fresh to weakly chloritized mafic minerals indicate that the diorite has not been extensively altered.

Monzodiorite

Fine to medium-grained olive-coloured monzodiorite occurs as a small plug that intrudes granite in the south-west portion of the map area. The extreme western portion of this plug is similar to the hornblende-biotite diorite unit indicating that there may be a gradational contact between the diorite and the monzodiorite. Breccia zones within the plug contain clasts of granite, quartz monzonite, rhyolite, dacite and diorite surrounded by a monzodiorite matrix. The monzodiorite is fine to medium-grained, and comprises 10-15% quartz, 10-15% K-feldspar, and approximately 45% plagioclase. Mafic minerals include 15% biotite and 10% hornblende with pyrite and other opaque minerals making up the remainder of the rock.

Mineralization

Extensive argillic alteration and quartz stockwork zones were discovered in 1995 along logging roads and within clear-cut blocks. Subsequent work lead to the ‘Discovery Zone’, a zone of quartz veinlets bearing up to 19.6 g/t gold from bedrock and rubble crop exposures. Geochemical soil sampling and prospecting during the 1996 field season defined a continuous gold anomaly (the 110 Zone) with peak gold contents reaching 5640 ppb. Coincident with the gold anomaly are locally high levels of silver, arsenic, and bismuth (up to 23832 ppb Ag, 465 ppm As, and 57 ppm Bi). Initial work indicated that this anomaly coincided with a partially exposed quartz breccia zone which graded up to 1440 ppb (Fox, 1996 unpublished report).

During the 1997 field season, the 110 Zone was mapped at a scale of 1:2500 in preparation for a diamond drill program, which consisted of five holes, totaling 1004.5 metres. Drill hole 97-1 tested mineralization in the original Discovery Zone, and holes 97-2 through 97-5 tested the 110 Zone. The drilling intersected mainly granite and diorite with lesser monzodiorite and dacitic to rhyolitic dikes. The rock were commonly argillic to chloritic altered with local sericitization and silicification. Mineralization consisted of abundant pyrite as disseminations, clots, fracture fillings, and veinlets with rare traces of chalcopyrite and arsenopyrite. Gold content was generally low with the best results from DDH 97-5 where a heavily silicified interval between two dacite dykes averaged 643 ppb gold over 4.1 metres and DDH 97-4 which had an interval of 18 metres averaging 116.7 ppb gold (Fox, 1997 unpublished report).

Polished sections were made from a float sample of quartz breccia with rust coloured granitic fragments (sample LP-203), which assayed 19760 ppb gold, as well as mineralized samples from drill core. Two phases of pyrite are visible in polished section with the first being highly fractured and partially to completely altered to limonite. Less abundant euhedral galena up to 2.5 mm and fine-grained sphalerite are common. The sphalerite has been partially to completely replaced by pyrargyrite which also occurs as fine disseminations in the quartz. Microscopic subhedral to euhedral (cubic) grains of gold are commonly observed in close association with arsenopyrite which has been partially to completely altered to scorodite and limonite. Pyrite from polished section in drill core is euhedral and medium to coarse-grained. Trace chalcopyrite exsolutions from sphalerite are locally observed.

Whole Rock Geochemistry

Whole rock chemical compositions and rare earth element (REE) data for the complete intrusive rock suite are given in Tables 1 and 2 . An Irvine and Barager (1971) plot of Na_2O+K_2O versus SiO_2 is shown in Figure 3. All rocks from the sample suite are calc-alkaline and peraluminous. They plot in the subalkaline field in Figure 3 and define an array with the more felsic rocks having only a slight increase in Na_2O+K_2O with increasing SiO_2. High field strength and rare earth element abundances for rocks in the rhyolite/granite field from Figure 3 were plotted on a normative graph (Figure 4) . All samples follow a similar pattern throughout the element series, plotting for the most part on top of one another. A normative plot of representative samples from each rock type shows a general correlation of peaks and troughs for the element abundances with the exception of Sr which shows a substantial variation within the sample suite (Figure 5).

U-Pb GEOCHRONOLOGY

Studies undertaken by the British Columbia Geological Survey Branch and the Geological Survey of Canada, in conjunction with researchers in universities and industry, have significantly increased the geochronological database for the Nechako River map area. As a result, new intrusive phases and sub-phases have been recognized within the area. Dating of igneous rock units at the Laidman property was undertaken to help determine the relative timing of emplacement of intrusions and allow correlation with other intrusions in the area.

The southern portion of the Capoose batholith, approximately 40 kilometers northeast of the Laidman property, has previously yielded a K-Ar age of 141 Ma (Diakow *et al.*, 1995). A new U-Pb age of 148.1± 0.6 Ma has since been determined (Friedman, pers. comm., 1998) and suggests that the Capoose batholith is age equivalent to the Francois Lake Plutonic suite to the north. The Francois Lake Plutonic suite is interpreted to have crystallized in two main pulses. The Glenannan phase and its subphases were emplaced during the first pulse at 157-154 Ma, and the Endako phase, its subphases, and the Casey phase were emplaced during the second pulse at 148-145 Ma (Whalen *et al.*, 1998).

TABLE 1
RARE EARTH ELEMENT DATA FROM THE LAIDMAN PROSPECT
110 ZONE INTRUSIVE SUITE

Sample Name	Rock Type	Y	La	Ce	Pr	Nd	Sm	Eu	Gd	Tb	Dy	Ho	Er	Tm	Yb	Lu
61266	granite	6.4	12.8	22.7	2.3	8.1	1.3	0.3	0.7	0	0.9	0.2	0.6	0.4	0.7	0
61267	granite	12.1	26.1	48.9	4.7	16.7	2.8	0.4	1.8	0.3	1.6	0.6	1	0.4	1.2	0.2
61268	granite altered	6.4	20.8	33.2	3.2	12.3	1.8	0.4	1	0	0.6	0.4	0.7	0.3	0.6	0
61269	granite	2.3	4.4	9.6	1.1	4.6	0.7	0	0	0	0.3	0	0.6	0.2	0	0
61270	rhyolite	4.2	8.4	14.5	1.4	6.3	1	0.2	0.4	0	0.4	0.2	0.4	0.2	0.4	0
71031	granite	9.6	21.5	40.7	4	14.5	2.2	0.5	1.4	0.3	1.1	0.5	1	0.4	0.9	0.2
71032	diorite	14	23.6	45.1	5.5	22.8	4	1.3	3.2	0.3	1.5	0.8	1.6	0.5	0.9	0.2
71033	diorite	13.1	19.4	38.1	4.6	20.3	3.8	1.3	2.9	0.4	1.5	1	1.4	0.5	0.9	0.2
71034	granite	6.4	22.5	43.9	4	13.3	1.9	0.4	1.1	0.2	0.9	0.4	0.7	0.3	0.6	0
71036	diorite	11.2	23.7	44.6	4.9	20.4	3.4	1.1	2.1	0.3	0.6	0.5	1.3	0.5	0.7	0
71037	dacite altered	10.2	20.8	34.8	4.1	16.8	2.9	1	2.2	0.5	1.2	0.4	1.3	0.5	0.8	0
71038	granite altered	3.3	15.1	23	2.4	8.5	1.3	0.3	0.7	0	0.4	0.3	0.4	0.2	0.4	0
71039	dacite	9.5	23.4	35.8	3.8	15.4	2.5	0.7	1.5	0.2	1.1	0.6	1	0.4	0.9	0.2
71040	rhyolite	4.7	26.2	37.9	3.8	11.4	1.4	0.4	0.8	0	0.6	0.2	0.4	0.3	0.5	0
71041	monzonit	13.8	20.1	44.3	5.8	23.7	4.7	1.6	3.4	0.5	1.6	1	1.8	0.5	0.8	0

TABLE 2
WHOLE ROCK GEOCHEMICAL DATA FROM THE LAIDMAN PROSPECT
100 ZONE INTRUSIVE SUITE

Sample Name	Rock Type	SiO_2	Al_2O_3	Fe_2O_3	MgO	CaO	Na_2O	K_2O	TiO_2	P_2O_5	MnO	Cr_2O_3	Ba	Sr	Zr	LOI	S	SUM
61266	granite	74.92	12.76	1.41	0.38	0.38	3.92	4.71	0.21	0.08	0.01	0.013	962	105	102	1	300	99.74
61267	granite	75.5	12.77	1.41	0.66	0.66	3.76	4.43	0.19	0.06	0.05	0.007	999	87	104	0.7	0	99.92
61268	granite	75.46	12.72	1.55	0.46	0.46	3.43	4.7	0.2	0.07	0.06	0.01	1141	101	82	0.9	0	99.8
61269	altered granite	84.3	2.9	6.35	0.12	0.12	0.16	0.83	0.09	0.28	0.01	0.007	484	31	10	3.2	28900	98.42
61270	rhyolite	75.2	11.81	2.34	0.65	0.65	1.55	5.63	0.19	0.05	0.03	0.01	1344	65	89	1.7	12300	99.52
71031	granite	75.49	12.59	1.75	0.76	0.76	3.74	4.15	0.19	0.03	0.05	0.006	1085	96	111	0.5	0	99.66
71032	diorite	61.1	16.17	6.11	5.02	5.02	4.01	2.63	0.75	0.38	0.13	0.007	1441	857	83	1.2	0	100.5
71033	diorite	61.02	16.23	6.4	5.56	5.56	3.73	2.79	0.78	0.28	0.12	0.01	1544	843	100	0.8	300	100.6
71034	granite	76.08	12.78	1.78	0.34	0.34	3.58	4.56	0.2	0.06	0.02	0.011	1078	105	99	0.9	200	100.6
71036	diorite	56.09	15.96	5.1	5.12	5.12	0.17	5.19	0.65	0.29	0.22	0.004	911	223	113	9.2	1600	100.6
71037	dacite	64.96	14.96	5.51	3.05	3.05	3.39	3.61	0.5	0.23	0.08	0.008	1465	583	104	1.9	6000	100.3
71038	altered granite	80.46	10.61	0.77	0.27	0.27	0.71	4.88	0.12	0	0.02	0.01	842	77	48	1.5	1000	99.62
71039	altered dacite	63.45	14.54	4.91	2.19	2.19	2.9	4.99	0.46	0.22	0.06	0.011	1673	355	133	4.1	24500	99.61
71040	rhyolite	76.82	12.29	1.25	0.07	0.07	1.15	6.27	0.1	0.01	0.01	0.011	1288	116	60	1.2	200	99.62
71041	monzonite	55.75	16.62	7.62	7.39	7.39	4.07	2.22	1	0.43	0.15	0.011	1407	1041	74	1.3	100	100.5

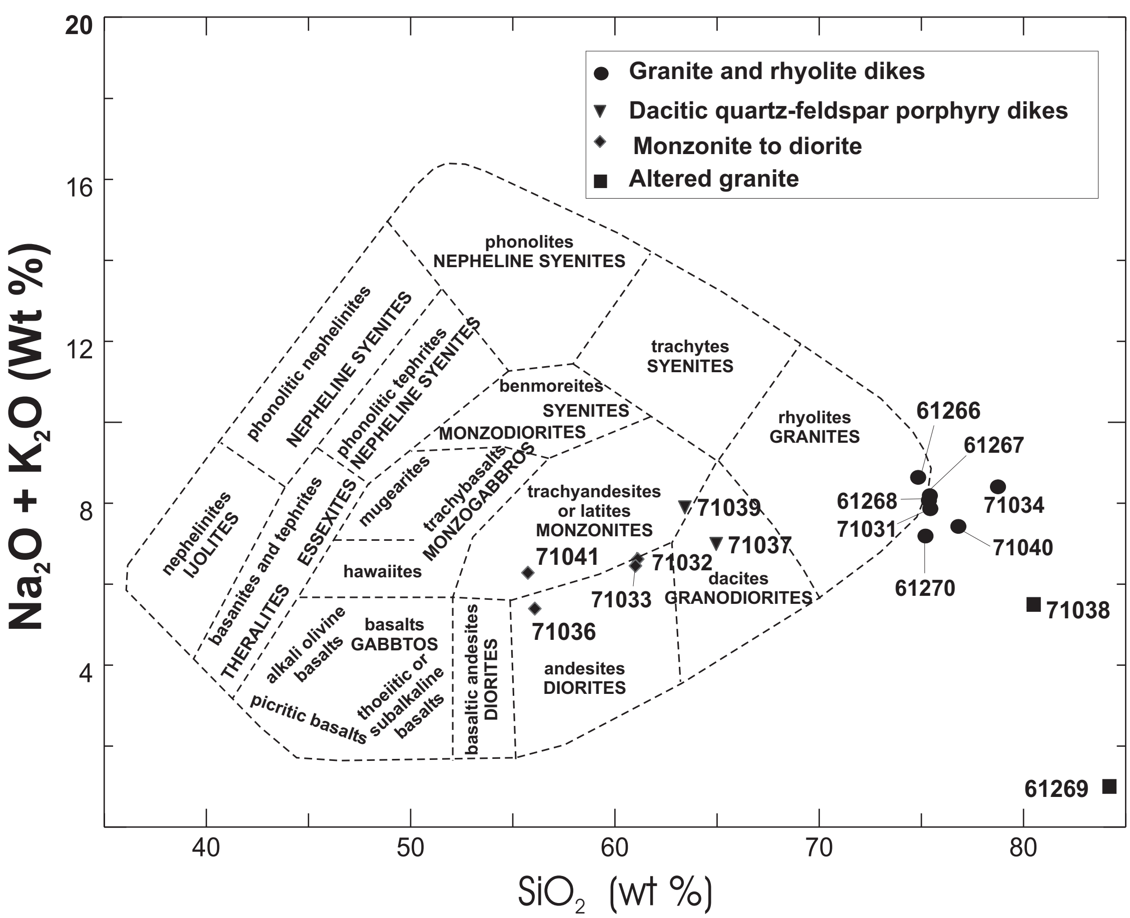

Figure 3. Classification of intrusive rock in the 110 Zone of the Laidman property based on their silica and alkali contents (after Irvine and Barager, 1971 and Cox *et al*., 1979).

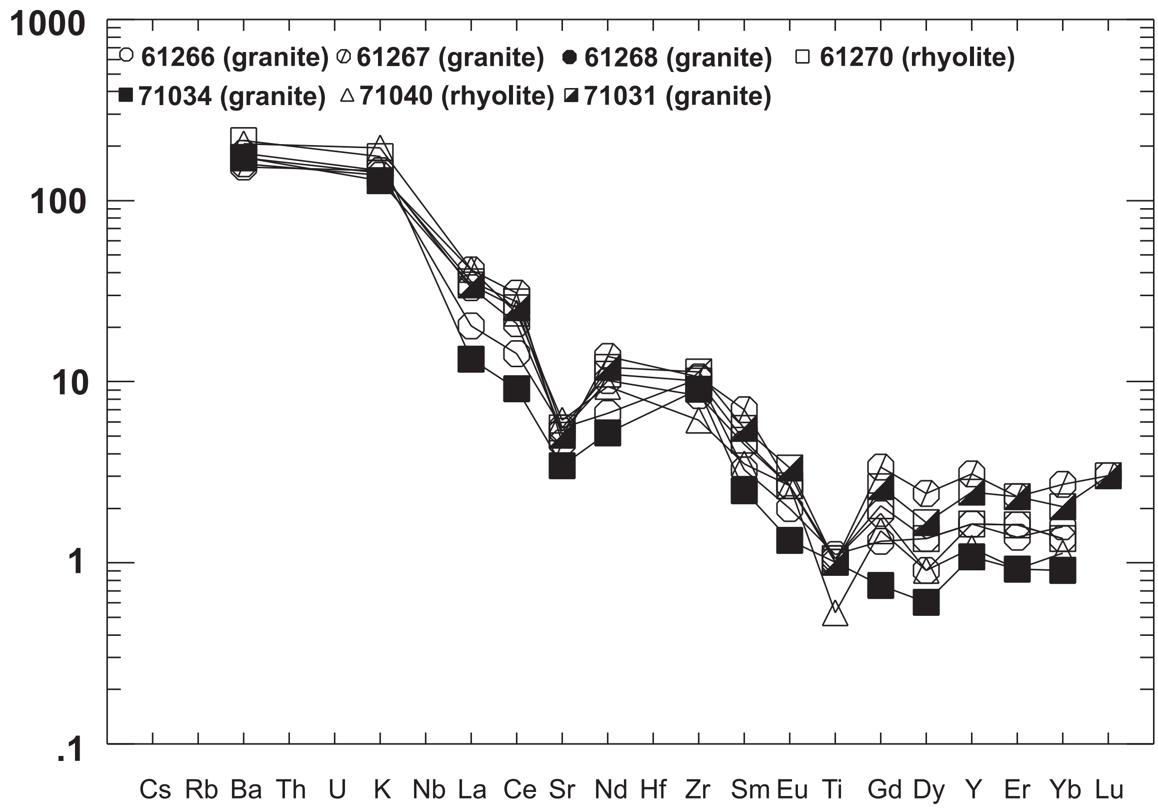

Figure 4. Plot of high field strength and rare earth element abundances normalized to primitive compositions.

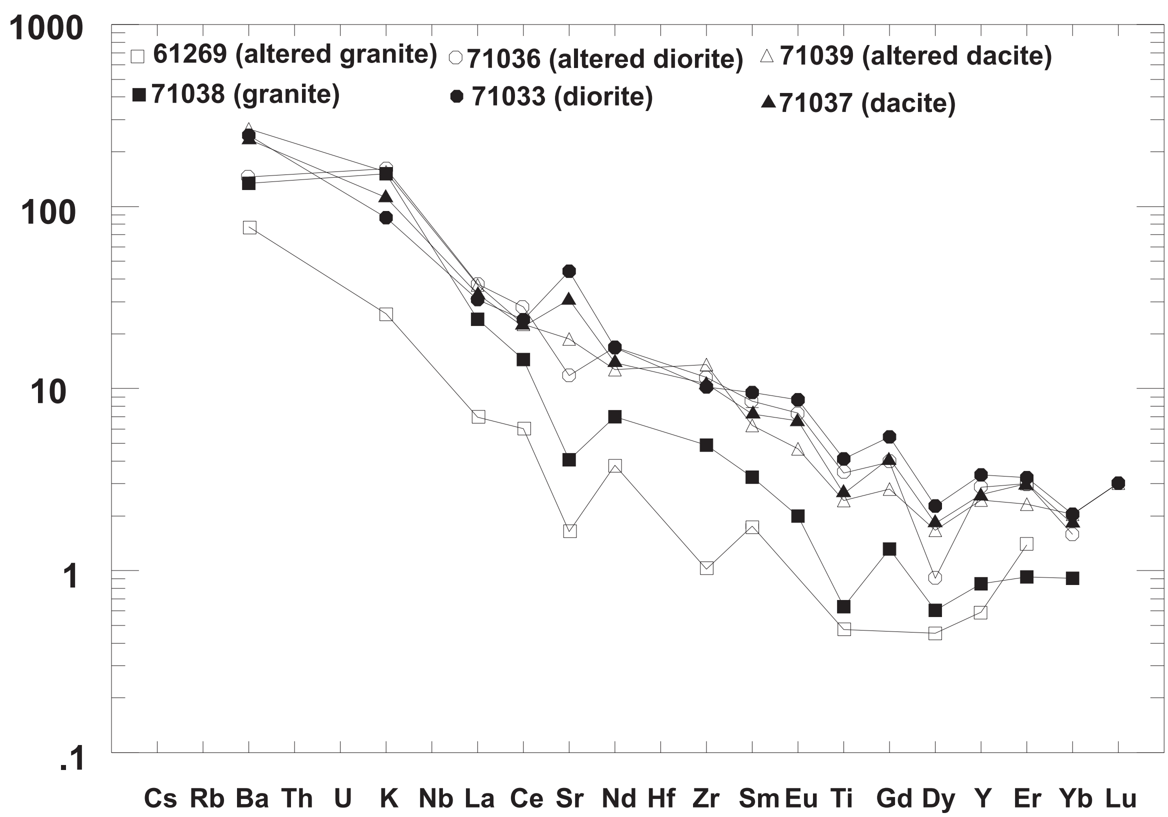

Figure 5. Plot of high field strength and rare earth element abundances normalized to primitive conditions comparing abundances in unaltered and altered rocks.

TABLE 3
U-PB ANALYTICAL DATA

Sample Description	Wt (mg)	U content (ppm)	Pb content* (ppm)	$^{206}Pb/^{204}Pb$ (meas)**	Total Common Pb (pg)	%^{208}Pb***	$^{206}Pb/^{238}U$****	$^{207}Pb/^{235}U$****	$^{207}Pb/^{206}Pb$****	$^{206}Pb/^{238}U$ age***** (Ma)	$^{207}Pb/^{206}Pb$ age***** (Ma)
LP-dacite											
A: N2,+134,abr	0.067	276	5.4	1775	13	12.8	0.02310(0.11)	0.1561(0.25)	0.04899(0.19)	147.2(0.3)	147.4(8.9)
B: N2,+134,abr	0.036	186	4.1	666	13	13.1	0.02031(0.13)	0.1370(0.52)	0.04893(0.46)	129.6(0.3)	144.2(21.7)
C: N2,+134,abr	0.046	152	3.6	806	12	13.7	0.02235(0.14)	0.1510(0.34)	0.04899(0.26)	142.5(0.4)	147.5(12.2)
D: N2,+134,abr	0.04	94	2.2	567	9	15.7	0.02226(0.14)	0.1503(0.58)	0.04899(0.51)	141.9(0.4)	147.4(24.0)
LP-monzonite											
A: N2,+134,abr	0.059	164	3.9	160	100	11.2	.02363(0.27)	0.1638(1.08)	0.05027(0.91)	150.5(0.8)	207.6(42.1)
B: N2,+134,abr	0.024	133	3.3	601	80	16.4	0.02325(0.24)	0.1588(0.82)	0.04954(0.72)	148.2(0.7)	173.4(33.5)
C: N2,+134,abr	0.041	191	4.2	187	62	12.7	0.02151(0.30)	0.1454(1.17)	0.04904(1.01)	137.2(0.8)	149.6(47.2)
D: N2,+134,abr	0.058	189	4.5	853	19	10.9	0.02326(0.10)	0.1572(0.31)	0.04902(0.24)	148.3(0.3)	148.6(11.2)
LP-granite											
A: N1,+134,abr	0.06	262	6.1	2727	8	9.9	0.02317(0.12)	0.1566(0.21)	0.04901(0.15)	147.7(0.3)	148.3(6.9)
B: N1,+134,abr	0.062	220	5.2	3106	6	9.9	0.02337(0.10)	0.1580(0.20)	0.04903(0.14)	148.9(0.3)	149.0(6.6)
C: N1,+134,abr	0.055	132	3.3	1245	9	13.1	0.02330(0.11)	0.1575(0.25)	0.04902(0.18)	148.5(0.3)	148.8(8.4)
D: N1,+134,abr	0.039	93	2.1	894	6	11.5	0.02314(0.14)	0.1563(0.37)	0.04900(0.30)	147.5(0.4)	147.8(14.2)

Footnotes: *N1, N2 = non-magnetic at given degrees side slope on Frantz isodynamic magnetic separator, grain size in microns; **radiogenic Pb, corrected for blank, initial common Pb and spike; ***corrected for spike and fractionation; ****corrected for blank Pb and U and common Pb errors at 1 sigma, *****errors at 2 sigma

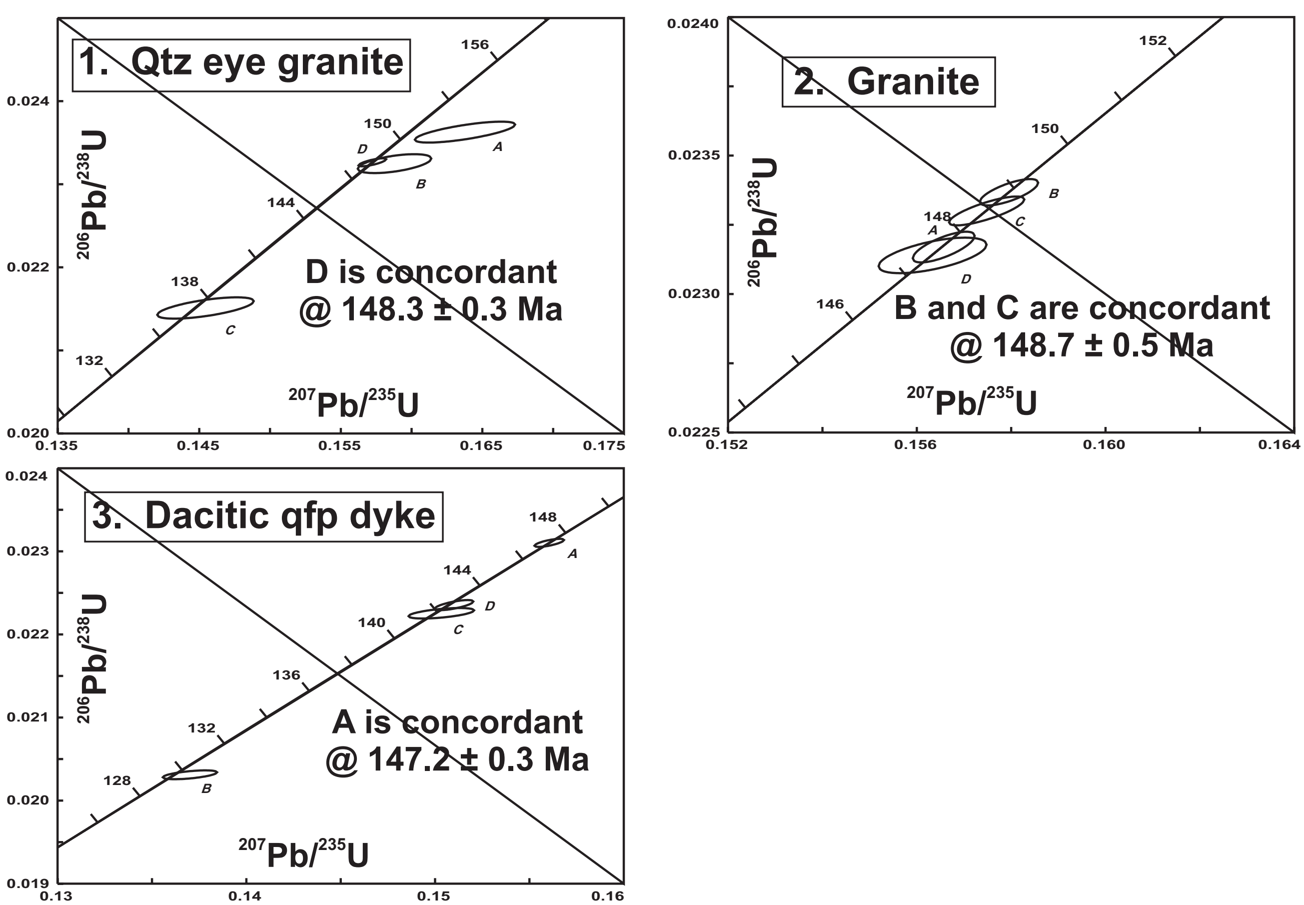

Figure 6. U-Pb concordia diagram for the quartz eye granite, hypidiomorphic granite, and the dacitic quartz-feldspar porphyry.

Molybdenum mineralization at Endako is thought to be associated with the later phase.

Analytical Results

Pb-U zircon ages were determined for the quartz eye granite, hypidiomorphic granite, and dacitic quartz-feldspar porphyry. Mineral separation and isotopic analysis were carried out in the University of British Columbia Geochronology Laboratory, using the methods described in Mortensen *et al.* (1995). Sample locations are indicated on the 110 Zone geologic map (Figure 2), analytical results are shown in Table 3, and a U-Pb concordia diagram for the three samples is shown in Figure 6.

Quartz Eye Granite

Zircons recovered from sample 1 (Figure 2) comprise clear, colourless to pale yellow stubby prismatic grains. No growth zoning or inherited cores were visible. Zircon grains contained rare to abundant bubbles and rod-shaped inclusions. The best quality grains were picked from the coarsest, least magnetic fraction and then strongly abraded. The abraded grains were split into four fractions, from the coarsest, best quality grains (fraction A) to the finest, poorest quality grains (fraction D). All of the analyses are concordant. Fractions B and C yield the oldest ages. The total range of $^{206}Pb/^{238}U$ ages for these two fractions is 148.7± 0.5 Ma which is taken as the best estimate for the crystallization age of the rock. The other two fractions yield slightly younger $^{206}Pb/^{238}U$ ages reflecting minor post-crystallization Pb loss.

Granite

Zircon grains recovered from sample 2 (Figure 2) are very similar in appearance to those in the previous sample. Four abraded zircon fractions were analyzed. Three of the fractions yielded concordant ages. The oldest of these (fraction D) has a $^{206}Pb/^{238}U$ age of 148.3±0.3 Ma which is considered as the best estimate for the crystallization age for this rock. The analysis of fractions B and C reflect minor Pb loss. Fraction A yields a slightly older 207Pb/206Pb age and appears to have incorporated a minor inherited zircon component.

Dacitic Quartz-feldspar Porphyry

Zircons recovered from sample 3 (Figure 2) are similar in appearance to the previous samples. All four fractions of abraded zircons are concordant with the oldest $^{206}Pb/^{238}U$ age at 147.2± 0.3 Ma, which is considered to be the best estimate for crystallization age of the rock. The other three fractions yielded younger $^{206}Pb/^{238}U$ ages reflecting post crystallization Pb loss.

Discussion

The ages of the quartz eye granite and hypidiomorphic granite of the Laidman Lake batholith are similar to the U-Pb age of 148.1± 0.6 Ma for the southern Capoose batholith. The dacite dikes (and presumably the spatially associated rhyolite dikes) are slightly younger than the quartz monzonite and possibly represent a later stage, more differentiated magma, likely derived from the main Laidman batholith.

Pb Isotopic Analysis

Pb isotopic compositions were determined for galena, pyrite, and igneous feldspar, from samples taken from float, outcrop, and drill core. The analytical data from the Laidman property are listed in Table 4 along with Pb isotopic data from other deposits and prospects in the vicinity. The resulting plots of $^{208}Pb/^{204}Pb$ versus $^{206}Pb/^{204}Pb$ and $^{207}Pb/^{204}Pb$ versus $^{206}Pb/^{204}Pb$ are shown in Figure 7 and Figure 8. Several important conclusions may be drawn from the data set:

The Laidman sulphide Pb isotope data plot together in Figure 7 and Figure 8 indicating that the high grade (19760 ppb gold) LP-203 float sample is likely genetically related to mineralization found in drill core.

The quartz eye granite has more radiogenic Pb isotope compositions and likely represents a more evolved intrusive phase relative to the hypidiomorphic granite which plots near the radiogenic end of the Laidman sulphide sample array. The isotopic data is consistent with the source of sulphide Pb being derived from or genetically related to the hypidiomorphic granite phase.

The analyses from the Capoose Creek, Buck (Christmas Cake) and Blackwater-Davidson (PEM) properties give distinctly more radiogenic values relative to the Laidman data and appear to reflect a younger (~70 Ma) mineralizing event (Friedman *et al.*, in prep.). One of the Buck (Christmas Cake) analyses is non-radiogenic compared to the rest of the samples; the reason for this is uncertain.

Galena Pb isotopic data from the Tascha deposit plots with the Laidman data suggesting that it may be of similar age as the Laidman mineralization.

DISCUSSION AND CONCLUSIONS

The presence of vuggy quartz veining, quartz breccias, and extensive alteration of host rocks suggests that mineralization on the Laidman property is associated with a high level porphyry system. U-Pb zircon ages determined for the quartz eye granite, granite, and the dacitic quartz-feldspar porphyry are identical to the U-Pb age of the Capoose batholith approximately 40 kilometers to the north. These dates correspond with the Late Jurassic (148 Ma) Endako phase of the Francois Lake

TABLE 4
LEAD ISOTOPIC COMPOSITIONS FOR SULPHIDES AND FELDSPAR SAMPLES FROM THE LAIDMAN PROPERTY AND OTHER MINERAL OCCURENCES IN THE VICINITY

Laidman Property Samples

Sample Number	Description/Occurrence	Mineral	$^{206}Pb/^{204}Pb$	% error	$^{207}Pb/^{204}Pb$	% error	$^{208}Pb/^{204}Pb$	% error	$^{207}Pb/^{206}Pb$	% error	$^{208}Pb/^{206}Pb$	% error
LP-203	>15g/t quartz breccia float 100m southwest of central 110 zone	galena	18.7711	0.006	15.5529	0.014	38.2857	0.016	0.8286	0.006	2.0396	0.003
LP-204	Coarse-grained pyrite (minor chalcopyrite) mineralization in granitic host (DDH 97-2)	pyrite	18.7812	0.011	15.5655	0.008	38.3114	0.014	0.8288	0.008	2.0399	0.009
LP-208	Medium - grained euhedral pyrite in fractures in a dacitic dike (DDH 97-4) in a dacitic dike (DDH 97-4)	pyrite	18.8268	0.018	15.5962	0.014	38.4193	0.019	0.8284	0.011	2.0407	0.006
LP-57799	Vuggy, quartz breccia with up to 30% pyrite 200 m east of the central 110 zone	pyrite	18.7874	0.053	15.5327	0.053	38.2535	0.053	0.8268	0.007	2.0361	0.005
LP-59888	Vuggy, quartz breccia with up to 30% pyrite 200 m east of the central 110 zone	pyrite	18.8041	0.138	15.5744	0.137	38.3441	0.138	0.8282	0.02	2.0391	0.007
Hypidiomorphic granite	Fresh granite from bulk sample used for U-Pb age dating	feldspar	18.8372	0.0112	15.5877	0.011	38.4069	0.012	0.8275	0.003	2.0389	0.005
Quartz eye granite	Fresh to slightly altered granite from bulk sample used for U-Pb age dating	feldspar	18.9373	0.0075	15.6120	0.006	38.4916	0.008	0.8244	0.004	2.0326	0.003

Deposits and Prospects in the Vicinity of the Laidman Property

Property name	$^{206}Pb/^{204}Pb$	% error	$^{207}Pb/^{204}Pb$	% error	$^{208}Pb/^{204}Pb$	% error	$^{207}Pb/^{206}Pb$	% error	$^{208}Pb/^{206}Pb$	% error
Blackwater-Davidson (PEM)	18.8700	0.010	15.6060	0.010	38.4760	0.020	0.8270	0.000	2.0390	0.010
Blackwater-Davidson (PEM)	18.8590	0.010	15.5890	0.010	38.4210	0.020	0.8266	0.000	2.0373	0.010
Tascha	18.7903	0.008	15.6006	0.006	38.4168	0.009	0.8303	0.005	2.0445	0.005
Buck (Christmas Cake)	18.9157	0.000	15.5973	0.000	38.4798	0.000	0.8245	0.001	2.0341	0.001
Buck (Christmas Cake)	18.6931	0.120	15.4187	0.120	38.0255	0.120	0.8248	0.021	2.0341	0.014
Capoose Creek	18.9030	0.000	15.6010	0.010	38.4820	0.000	0.8253	0.000	2.0358	0.000
Capoose Creek	18.8980	0.000	15.5880	0.010	38.4310	0.000	0.8248	0.000	2.0336	0.000
Capoose Creek	18.9000	0.000	15.5940	0.010	38.4560	0.000	0.8251	0.000	2.0347	0.000
Capoose	18.9070	0.010	15.6030	0.010	38.5060	0.000	0.8253	0.000	2.0367	0.010

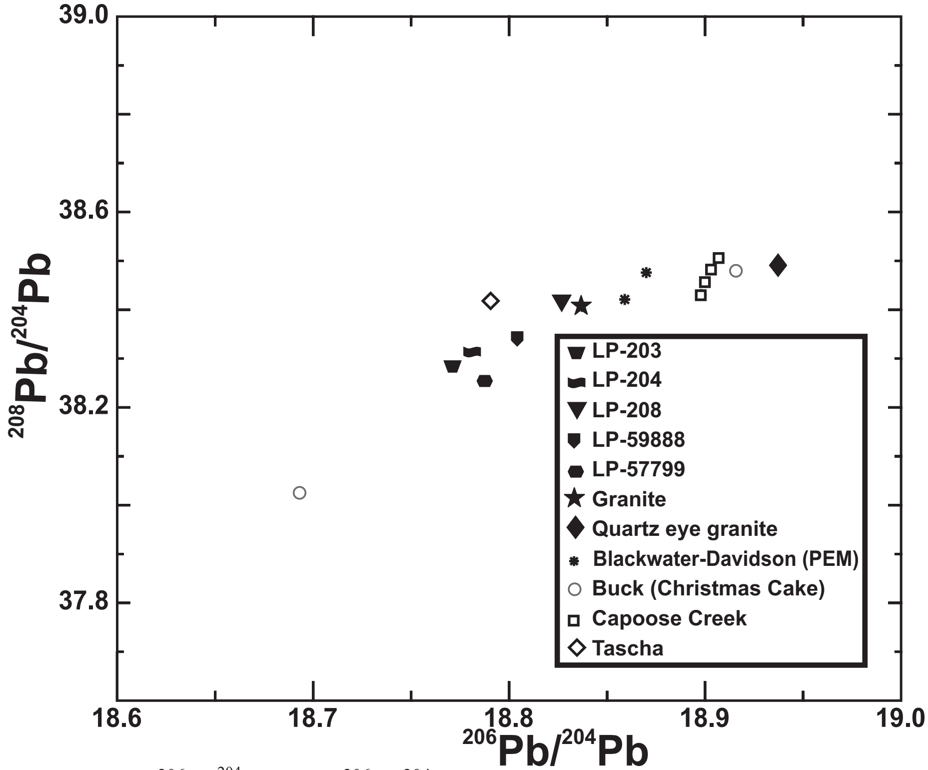

Figure 7. Trace Pb isotope plot of $^{206}Pb/^{204}Pb$ versus $^{206}Pb/^{204}Pb$ with Laidman sulphides, feldspars and Pb isotopic data from other deposits.

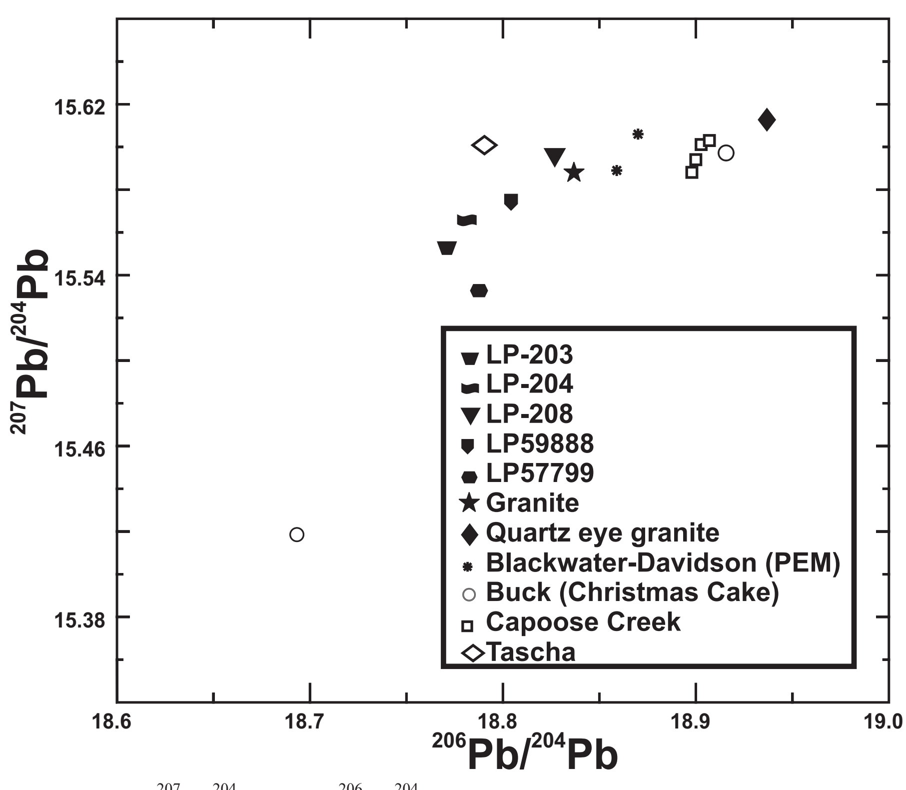

Figure 8. Trace Pb isotope plot of $^{207}Pb/^{204}Pb$ versus $^{206}Pb/^{204}Pb$ with Laidman sulphides, feldspars and Pb isotopic data from other deposits.

Plutonic suite the Late Jurassic to Early Cretaceous mineralizing event in the interior plateau. The Late Jurassic-Early Cretaceous mineralizing event in this area has been suggested to be related to emplacement of plutons of this suite (Lane and Schroeter, 1997).

Pb isotopic data is available from relatively few deposits in the Nechako River map area. Currently, data is available only from the Blackwater-Davidson, Buck, Capoose, and Tascha prospects. Previous work has suggested that the Blackwater-Davidson and Capoose prospects are related to a Late Cretaceous mineralizing event (Friedman, pers. comm., 1998). This is evident on the $^{208}Pb/^{204}Pb$ versus $^{206}Pb/^{204}Pb$ and $^{207}Pb/^{204}Pb$ versus $^{206}Pb/^{204}Pb$ plots where the Late Cretaceous mineralization has more evolved, radiogenic Pb compared to Laidman Pb isotope data. However, the single Tascha galena Pb sample has a similar radiogenic Pb signature as the Laidman data. This suggests that the Tascha and the Laidman mineralization are a result of the Late Jurassic to Early Cretaceous event.

REFERENCES

Bysouth, G.D. and Wong, G.Y. (1995): The Endako molybdenum mine, central British Columbia: An update, *in* Porphyry deposits of the northwestern cordillera of North America, (ed.) Schroeter; *Canadian institute for Mining, Metallurgy and Petroleum*, Special Volume 46, p. 697-703, Part D – Porphyry Molybdenum (±WO_3) Deposits – Paper 52.

Cook, F. and Erdmer, P. (compilers) (1997):Slave – Northern Cordilleran Lithospheric Evolution (SNORCLE) Transect and Cordilleran Tectonics Workshop Meeting (March 7-9), University of Calgary; *Lithoprobe Report* No. 56, 245 pp.

Cyr, J.B., Pease, R.B., and Schroeter, T.G. (1984): Geology and mineralization at the Equity silver mine; *in Economic Geology*, vol. 79, 1984, p. 947-968.

Diakow, L.J., Webster, C.L., Whittles, and Richards, T.A. (1995): Stratigraphic highlights of bedrock mapping in the southern Nechako Plateau, Northern Interior Plateau Region (NTS 93 F/2 and 7); *in* Geologic Fieldwork 1994; *B.C. Ministry of Energy, Mines and Petroleum Resources*, Paper 1995-1, p. 171-6.

Diakow, L.J. and Webster, C.L. (1994): Geology of the Fawnie Creek map area (NTS 93 F/3); *in* Geologic Fieldwork 1993, Grant, B. and Newell, J.M., Editors; *B.C. Ministry of Energy, Mines and Petroleum Resources*, Paper 1994-1, p. 15-26.

Fox, P.E. (1998): Diamond drilling report on the Laidman property; *Internal report for Phelps Dodge Corporation of Canada, Limited*. Dated January 23, 1998.

Fox, P.E. (1996): Geological, geochemical and trenching Report on the Laidman property; *Internal Report for Phelps Dodge Corporation of Canada, Limited*. Dated December 25, 1996.

Gabrielse, H., Monger, J.W.H., Wheeler, J.O., and Yorath, C.J. (1991): Part A. Morphogeological belts, tectonic assemblages, and terranes: in Geology of the Cordilleran Orogeny in Canada; Edited by H. Gabrielse and C.J. Yorath. *Geologic Survey of Canada*, Chapter 2, Geology of Canada, No. 4, p. 15-28.

Lane, R.A. and Schroeter, T.G. (1997): Metallogeny of the Interior Plateau, central British Columbia (Parts of 93B, 93C, and 93F), *in* Interior Plateau Geoscience Project: Summary of Geological, Geochemical and Geophysical studies; Diakow, L.J., Metcalf, P. and Newell, J.M. editors; *B.C. Ministry of Employment and Investment*, Paper 1997-2.

Monger, J.W.H., Wheeler, J.O., Tipper, H.W., Gabrielse, H., Harms, T., Struik, L.C., Campbell, R.B., Dodds, C.J., Gehrels, G.E., O'Brien, J. (1991): Part B. Cordilleran terranes; Upper Devonian to Middle Jurassic assemblages, in Geology of the Cordilleran Orogen in Canada; Edited by H. Gabrielse and C.J. Yorath. *Geologic Survey of Canada*, Chapter 8, Geology of Canada, No. 4, p. 281-327.

Mortensen, J.K., Ghosh, D.K., and Ferri, F. (1995):U-Pb geochronology of intrusive rocks associated with copper-gold porphyry deposits in the Canadian Cordillera; edited by T.G. Schroeter; *in Canadian Institute of Mining, Metallurgy and Petroleum*, Special Volume 46.

Whalen, J.B., Struik, L.C., and Hrudey, M.G. (1998): Bedrock geology of the Endako map area, central British Columbia; *in* Current Research 1998-A; *Geologic Survey of Canada,* p. 113-123.

Woodsworth, G.J., Anderson, R.G., and Armstrong, R.L. (1991): Plutonic regimes, Chapter 15 *in Geology of the Cordilleran Orogen in Canada*, H. Gabrielse and C.J. Yorath (ed.); Geologic Survey of Canada, Geology of Canada, no. 4, p. 491-531.

Lead Isotope Data From Epigenetic Sulphide Occurrences in the Purcell Supergroup, Southeastern British Columbia, and Implications for Exploration for Sediment-hosted Base Metal Deposits

By L.J. Marshall, J.K. Mortensen and J.E. Gabites
The University of British Columbia

KEYWORDS: *Lead isotopes, Purcell Supergroup, Aldridge Formation, Sullivan deposit, St. Eugene deposit, SEDEX deposits.*

INTRODUCTION

This paper investigates Pb isotope and other data from epigenetic base-metal vein occurrences in the Shrink Lake study area, within the Mesoproterozoic Purcell Supergroup in southeastern B.C. The Purcell Supergroup is host to the world renowned Sullivan Pb-Zn deposit, as well as the St. Eugene and other epigenetic vein deposits thought to be of Proterozoic age. The study aims to determine whether Pb isotope data from a number of uneconomic base metal vein occurrences in the area result from remobilization of Pb from large tonnage, sediment hosted Proterozoic base metal deposits that have not yet been discovered.

Field work for this project formed the basis of the principal author's Bachelor's thesis at the University of British Columbia (Marshall, 1999). All field work was supported by Kennecott Canada Exploration Inc..

REGIONAL GEOLOGY

The main supracrustal rocks in the study area consist of Aldridge and Creston formation argillites, siltstones and sandstones that form part of the Mesoproterozoic Purcell Supergroup. The Purcell Supergroup comprises a sequence over 12km thick of siliciclastic and lesser carbonate rocks (Hoy, 1993) that is exposed in a large region in southeastern British Columbia and southwestern Alberta.. The Supergroup is inferred to unconformably overlie Proterozoic and Archean gneissic basement rocks, and is unconformably overlain by Late Proterozoic Windermere Group rocks and Cambrian clastic and carbonate rocks (Hoy, 1993).

The dominantly gabbro and diorite Moyie Sills intrude the lower Aldridge and the lower part of the middle Aldridge formations. The cumulative thickness of the Moyie sills exceeds 2000 meters. Hoy (1993) cites soft sediment deformation, large scale dewatering structures and coarse grained hornblende hornfels as evidence for intrusion of at least some of the sills into wet, unconsolidated sediments. Anderson and Davis (1995) report U-Pb zircon ages of 1468 ±2 Ma for Moyie sills. Gabbro and diorite sills are also present higher in the Purcell stratigraphy, and are believed to be the result of a later magmatic event than that responsible for the Moyie sills (Hoy, 1993).

The White Creek batholith (Reesor, 1958) is one of several middle Cretaceous intrusions that cut the Purcell Supergroup. The most extensive phase of the batholith is a K-feldspar porphyritic biotite quartz monzonite, and Brandon and Lambert (1992) report Rb-Sr whole rock-apatite isochron ages of ~105-115 Ma for the body. The batholith crops out within several kilometers southeast of the study area.

Small biotite lamprophyre dikes (minettes) locally intrude lower Purcell sediments (e.g., McClay, 1983; LeCouteur, 1979; Hoy, 1993). An Early Cretaceous age (~130 Ma) has been assigned to lamprophyres that cut the Sullivan orebody (LeCouteur, op.cit.).

Tectonism

The earliest evidence for tectonism in the Purcell Supergroup is recorded by syndepositional normal block faulting associated with rifting of the Belt/Purcell basin (Hoy, 1993). Evidence for renewed block faulting during deposition of the Sheppard Formation, higher in Purcell stratigraphy, is cited by Hoy (1993).

A Mesoproterozoic tectonic event termed the East Kootenay orogeny has been interpreted by several authors (White, 1959; Leech, 1962; Hoy, 1993) as a compressive event, marked by folding and associated cleavage development. Anderson and Davis (1995), however, suggest that the deformational features observed could have been generated during an extensional event, if deformation had a strike-slip component to generate localized folding. The younger Goat River extensional tectonic event was marked by renewed block faulting, and is thought to mark the initiation of Windermere Group deposition (Hoy, 1993). The Goat River event is placed at approximately 762 Ma (Devlin *et al.*, 1988).

Following these events, the Purcell Supergroup was subject to intermittent periods of extensional tectonism through the Late Proterozoic and Early Paleozoic (Hoy, 1993).

From Late Jurassic to Paleocene time, accretion of tectonostratigraphic terranes to the west produced large scale thrust faulting which led to compression, thickening and eastward displacement of miogeoclinal sedimentary packages along the western margin of North America. The geology of the region is further complicated by syn- to post-thrusting back thrusts and normal faults (Hoy, 1993).

Economic Deposits

The Sullivan deposit (Figure 1) is hosted in the lower Aldridge Formation, at the contact with the middle Aldridge (LMC) (Hoy, 1993; Leitch *et al.*, in prep.). It is a stratiform, sedimentary exhalative (SEDEX) Pb-Zn deposit which contained original reserves of approximately 160 million tonnes of ore, grading 6% lead, 6% zinc, 28% iron and 67 grams per tonne silver (Ransom *et al.*, 1985). Over 125 million tonnes of ore have been extracted from the deposit.

The St. Eugene deposit (Figure 1) consists of epigenetic Ag-Pb-Zn veins that cut middle Aldridge, upper Aldridge and Creston Formation metasediments. Production between 1899 and 1929 produced some 1,475,266 tonnes of ore, with average grades of 7.7% Pb, 1.0% Zn and 124g/tonne Ag and 0.05g/tonne Au (Hoy, 1993). Galena grains found within garnet porphyroblasts in the deposit are interpreted by Beaudoin (1997) to constrain the age of mineralization to prior to East Kootenay metamorphism. The St. Eugene is classified with similar epigenetic deposits of the Coeur d'Alene District, Idaho (Beaudoin, 1997).

LOCAL GEOLOGY

Sedimentary rocks of the middle Aldridge, upper Aldridge and Creston formations crop out in the study area. Contacts between these formations are all conformable, and dip at shallow to moderate angles to the northwest.

The middle Aldridge Formation consists of medium to thickly bedded , siltstones and sandstones, with intermittent thinly bedded argillite layers. Upper Aldridge

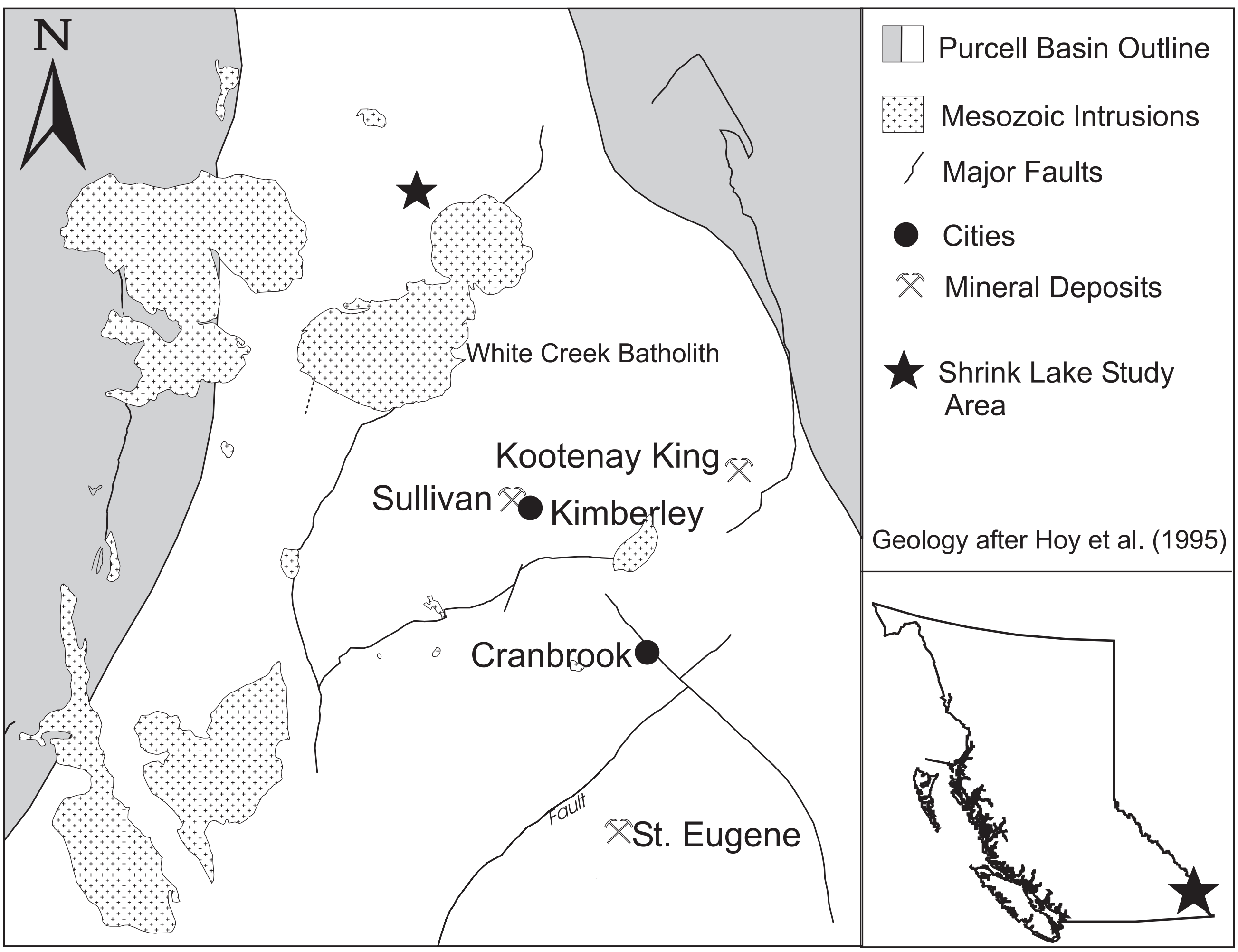

Figure 1. Regional geology, mineral deposits and location of the Shrink Lake study area.

stratigraphy consists dominantly of thinly bedded siltstones and argillites. Strong tourmaline alteration is found locally within the Shrink Lake study area, and is pervasive in the upper Aldridge in the vicinity of the Doc mineral showing, northeast of the study area. The Creston Formation is characterized by green, mauve and grey siltstones and argillites.

Gabbro to diorite sills are present throughout the study area. Within the upper middle Aldridge, upper Aldridge and Creston formations, the intrusions are generally less than 10 meters in thickness, and relatively rare. In the lower middle Aldridge Formation, intrusions are commonly in excess of 100m in thickness, and are relatively abundant.

Small discontinuous lamprophyre dikes were noted at two locations in the study area. One dike was observed to crosscut a gabbroic sill. The mineralogy of these *dike*s is characterized by abundant biotite, lesser quartz and plagioclase and minor calcite.

Numerous small fault zones were noted in the study area. Most faults are moderately to steeply dipping to the west-northwest.

Mineralization

Numerous discontinuous, sulphide-bearing quartz veins are present in the study area. These veins commonly occur along joint sets associated with faults. Veins exhibit a wide variety of textures, degrees of deformation and mineralogy, suggesting multiple veining events. Locations of vein samples for this study are shown in Figure 2. Detailed descriptions of the veins are given by Marshall (1999).

Two mineral occurrences, the Alpine showing (MINFILE 82KSE081) and the Doc showing (MINFILE 82KSE060) are located several kilometres northeast of the study area, within Creston Formation and upper Aldridge Formation stratigraphy, respectively (Figure 2).

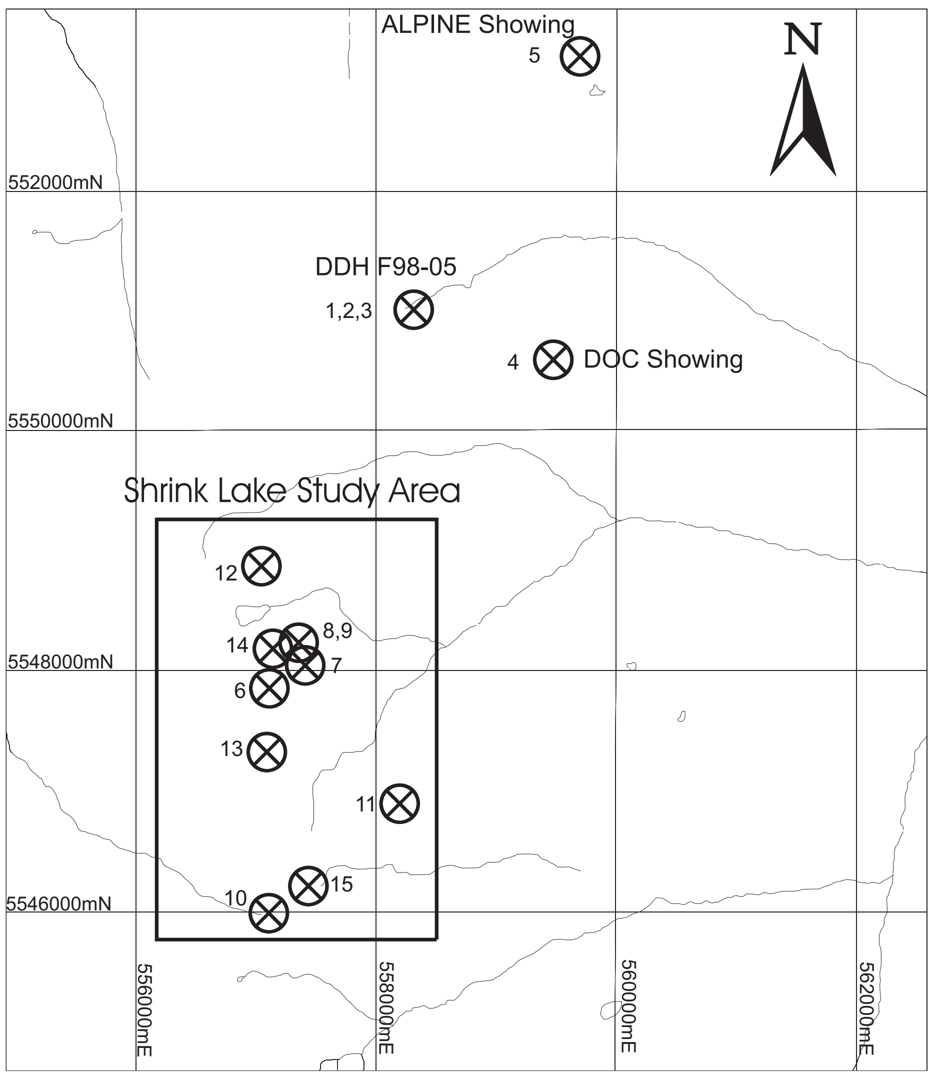

Figure 2. Sample location map.

Stratabound galena mineralization was intersected in 1998 by Kennecott Canada Exploration in DDH F98-05 northeast of the study area (Figure 2). Two samples were obtained from drill core for this study.

The Alpine showing, also referred to as the Rocky Top or Four Tops showing, has been investigated by several companies, including Cominco Ltd. (Mawer, 1986). Disseminated sulphides and high grade bands of pyrite, sphalerite and galena occur within a silicified, albitized and sericitized, shear-controlled alteration zone at the showing. Uneconomic grades of 0.5% Pb and 0.6% Zn across an average width of 3.5m and length of 80m have been previously determined, based on the results of geochemical sampling, geological mapping, bulldozer trenching and diamond drilling (Mawer, op. cit.).

The Doc showing on Tourmalinite Ridge (Figure 2) was first recognized by Kerr Adison Mines in the late 1970's. The showing consists of quartz-galena veins with minor sphalerite, arsenopyrite and chalcopyrite. Veins are exposed in blocky felsenmeer, and are traceable for up to 100m along strike (Brown and Termuende, 1998).

Lead Isotopic Study

A detailed Pb isotopic investigation of mineral occurrences in the study area was undertaken in order to assess the possible sources for Pb, place constraints on the possible timing of mineralization and in particular, determine whether any of the occurrences could represent remobilized, syngenetic mineralization of Sullivan (Mesoproterozoic) age.

Several potential reservoirs from which metals may have been extracted are present in or near the study area, including:

- Lead extracted at different times from Proterozoic metasedimentary rocks of the Purcell Supergroup
- Lead remobilized from Sullivan-type SEDEX deposits contained within the Purcell Supergroup
- Lead remobilized from Proterozoic epigenetic occurrences such as the St. Eugene deposit
- Magmatic Pb from Moyie-type intrusions, Mesozoic granitoids or young lamprophyres.
- Lead introduced from lower crustal and/or mantle reservoirs

Lead remobilized from Pb-rich deposits such as the Sullivan or St. Eugene would be expected to retain the original isotopic composition of those deposits. The isotopic signature of the Sullivan deposit can be approximated by data compiled by Beaudoin (1997) (Figure 3). Beaudoin interprets the distribution of the Sullivan data as a mixing of leads derived from the Lower Aldridge Formation and Precambrian basement gneiss. The St. Eugene Ag-Pb-Zn vein deposit has been classified with deposits of the Coeur d'Alene District, Idaho. Despite being epigenetic, most of these deposits are characterised by Pb isotopic ratios that are less radiogenic than those of the syngenetic Sullivan deposit (Figure 3). Beaudoin (1997) addresses this paradox by attributing the Coeur d'Alene data array to a mixing of upper crustal and mantle Pb. He suggests that mantle Pb was introduced into the Purcell basin environment during intrusion of the Moyie sills.

The expected isotopic composition of Pb extracted from Purcell Supergroup metasedimentary rocks at any particular time can be estimated with some confidence using the "shale curve" (Godwin and Sinclair, 1982), which models the evolution of Pb isotopic compositions in sedimentary strata of the western Canadian miogeocline (Figure 3). The composition of lead derived from Moyie intrusions has been inferred by Andrew *et al.* (1984) from data for epigenetic mineralization thought to be genetically associated with these intrusions (Figure 3). Magmatic Pb from Mesozoic granitoids is expected to have the same isotopic composition as Pb in feldspars contained within the intrusions. Brandon and Lambert (1992) determined Pb isotopic compositions for K-feldspar phenocrysts in each of five major intrusive phases within the mid-Cretaceous White Creek batholith. No constraints are available for the Pb isotopic composition of the young lamprophyres in the study area, although Bevier (1987) reports Pb isotopic compositions for Eocene lamprophyres in the Valhalla complex approximately 100 km west of the study area. Lead introduced from lower crustal and/or mantle reservoirs during or since deposition of Purcell strata can be approximated by the lower crust and mantle curves presented by Zartman and Doe (1981). These curves are estimates made on a global scale and do not account for regional heterogeneity. The possibility of other unrecognized Pb sources for mineralization in the Shrink Lake study area also cannot be ruled out.

Lead isotopic compositions were determined for galena and other sulphide minerals from ten sulphide-bearing samples within the Shrink Lake study area. Additionally, isotopic data was obtained from the Alpine and Doc mineral occurrences in the vicinity of the study area. Two galena samples from a galena rich stratabound horizon intersected in drill core obtained northeast of the study area were also analysed. A K-feldspar phenocryst from the K-feldspar megacrystic quartz monzonite phase of the White Creek batholith was analysed to complement the data from Brandon and Lambert (1992).

From the distribution of Pb isotopic data in Figure 3, the following general observations can be made:

All analyses lie on or near the "shale curve," suggesting that upper crustal rocks represent a major Pb source for the samples analysed.

Some analyses fall significantly below the shale curve suggesting the introduction of at least a minor component of lead from a lower-μ reservoir.

Much of the data forms a roughly linear array, that could represent a single mixing event between a non-radiogenic upper crustal source, and a much more radiogenic upper crustal source. Alternatively, the array may represent complex mixing of Pb from several different sources.

The sample suite likely includes mineralization formed by more than one process, and of more than one age.

TABLE 1
PB ISOTOPIC DATA FROM THE SHRINK LAKE STUDY AREA (SL), STRATABOUND GALENA MINERALIZATION IN THE UPPER ALDRIGE FORMATION (STRAT), THE DOC SHOWING (DOC), THE ALPINE SHOWING (ALPINE) AND THE WHITE CREEK BATHOLITH (WCB)

Sample	Original Sample No.*	Mineral	Location	Pb isotopic data 206/204	207/204	208/204	207/206	208/206
1	zone 2	Galena	STRAT	16.48817	15.42701	36.16196	0.935645	2.193222
2	zone 30	Galena	STRAT	16.51753	15.44671	36.24876	0.935174	2.194578
3	zone 30	Galena	STRAT	16.51894	15.44125	36.21776	0.934764	2.192515
5	LM-058	Galena	ALP	17.72479	15.59184	38.09016	0.879666	2.148992
6	LM-120	Galena	SL	18.52290	15.63239	38.71285	0.843952	2.090014
7	LM-158B	Galena	SL	17.35287	15.52122	37.44653	0.894450	2.157960
8	LM-160	Galena	SL	16.97564	15.49678	36.82133	0.912887	2.169084
9	LM-160	Galena	SL	16.97702	15.50324	36.84027	0.913193	2.170023
10	NT-184a	Galena	SL	17.62106	15.52770	37.74589	0.881204	2.142105
11	VR30307a	Galena	SL	16.52549	15.43508	36.25739	0.934020	2.194044
12	VR30311a	Galena	SL	18.27621	15.60639	38.53895	0.853921	2.108710
13	LM-126	Pyrite	SL	18.44807	15.61731	38.66923	0.846558	2.096128
14	LM-129	Pyrite	SL	18.54023	15.63409	38.73587	0.843255	2.089302
15	LM-139	Pyrite	SL	18.09201	15.59063	38.28208	0.861745	2.115982
16	VR30264	Arsenopyrite	DOC	16.73622	15.45765	36.52043	0.923608	2.182134
17	LM-171	K-Feldspar	WCB	18.50368	15.67265	39.18572	0.847005	2.117741

* (Marshall, 1999)

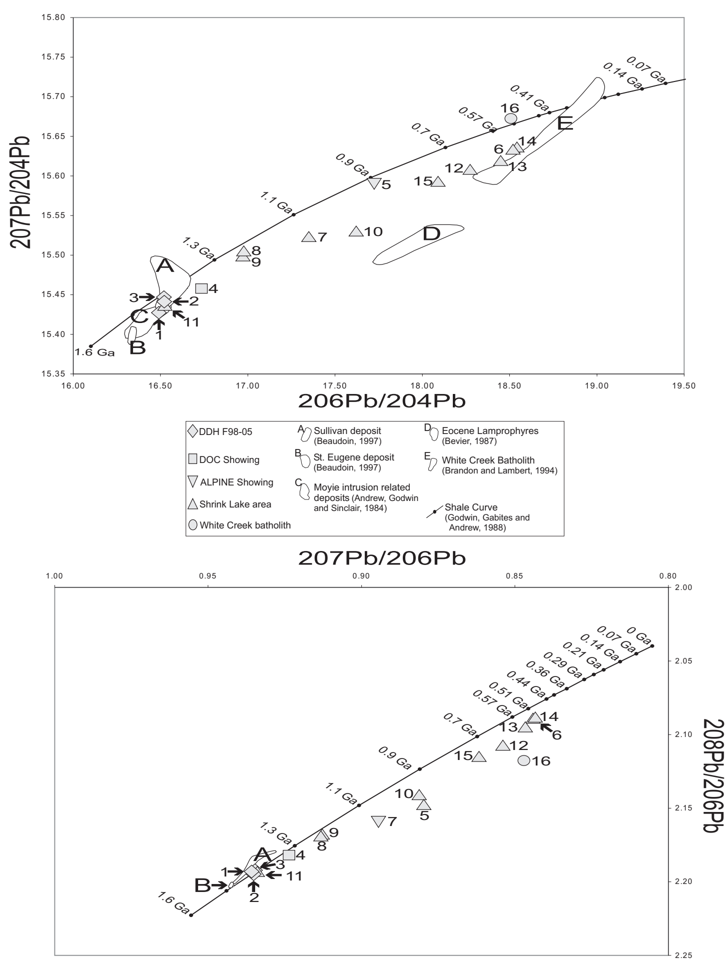

Figure 3. Pb isotopic diagrams for new data from the Shrink Lake study area, DDH F98-05, the Doc showing and the Alpine showing. Previous data for selected reservoirs are shown as fields and model curves.

Finally, some of the epigenetic samples have isotopic compositions that are consistent with remobilization from a Mesoproterozoic base metal deposit.

DISCUSSION

Stratabound Galena Mineralization in the Upper Aldridge Formation

Samples 1, 2 and 3 are galena from mineralized horizons within upper Aldridge sediments. Samples 2 and 3 contain fine grained galena associated with tourmaline rich laminations, in a horizon that has been described as being stratabound and possibly stratiform (Kennecott internal communication, 1998). Sample 1 contains coarse grained galena associated with a siliceous horizon, or a concordant quartz vein (Kennecott internal communication, 1998). Similar mineralization within the same system exhibits irregular vein-sediment contacts that have been interpreted to result from the injection of fluids into wet sediments (Kennecott internal communication, 1999). The isotopic compositions of these samples plots near the intersection of the Sullivan and Moyie arrays (Figure 3), and are therefore consistent with a Mesoproterozoic age of formation. Textural data suggests that this occurrence is epigenetic, but likely formed before consolidation of upper Aldridge sediments, possibly as a result of leaching of Pb from the sediments during basin dewatering (Kennecott internal communication, 1999). Alternatively, Pb in the occurrence may have been remobilized from a syngenetic Sullivan-type deposit, or another Mesoproterozoic base metal deposit. An plutonic-related Pb source is not considered likely, as gabbroic intrusions noted within the upper Aldridge appear to be volumetrically too minor to account for the extent of mineralization.

Doc Showing

Sample 4, from the Doc showing on Tourmalinite Ridge, is slightly more radiogenic than the strongly mineralized samples 1, 2 and 3. This sample was obtained from a quartz-galena-arsenopyrite-chalcopyrite vein within upper Aldridge sediments, at approximately the same stratigraphic level as samples 1, 2 and 3.

The upper Aldridge is a highly permeable formation and is marked by significant geochemical soil anomalies along its strike in the vicinity of Tourmalinite Ridge. These anomalies suggest that the argillites of the upper Aldridge may have acted as a conduit for mineralized fluids at some time. It is conceivable that fluids leached Pb from the nearby stratabound galena occurrence as well as from upper Aldridge sediments, resulting in a shift away from the isotopic ratios characteristic of samples 1, 2 and 3, towards a more radiogenic composition, as seen in sample 4. Alternatively, this shift may be explained by a mixing of Proterozoic Pb with Pb associated with the White Creek batholith, or other as yet unidentified radiogenic Pb sources. Other possibilities for Pb sources for sample 4 include a mixing between upper crustal lead, and Pb derived from either a mantle source, a lower crustal source, or both.

Alpine Showing

Sample 5, from the Alpine Showing, plots immediately adjacent to the shale curve, indicating that all of the lead in this sample may have been leached from lower Purcell sedimentary strata. If this is in fact the case, a model age of approximately 0.9 Ga obtained from the shale curve can be inferred for mineralization at the Alpine showing. Analysis of additional samples from this occurrence would be required to test this hypothesis.

Shrink Lake Study Area Mineralization

Sample 11 is from a quartz-calcite-galena-chalcopyrite vein within a Moyie sill. Isotopic compositions of this sample plot at the intersection of the Sullivan and Moyie arrays. Fluid inclusion studies (Marshall, 1999) indicate that the vein contains very distinct carbonic fluids, inferred to be genetically related to intrusion of the Moyie sills. The isotopic data suggests that Pb in the sample may also be derived from the Moyie sills.

Sample 8 was obtained from within middle Aldridge rocks, near the base of the upper Aldridge, in a fracture filling vein within a well developed joint set. The analyses from this sample can be interpreted in the same way as sample 4. If a mixing of Mesoproterozoic Pb with a more radiogenic Pb source is responsible for the Pb composition of sample 8, a shift towards more radiogenic Pb can be explained by a greater component of Pb leached from Purcell sediments. This could be consistent with a greater distance from the upper Aldridge stratabound galena occurrence. As with Sample 4, this hypothesis is non-unique, and other geologically reasonable explanations are possible.

Interpretations of Pb sources for the remaining samples are more ambiguous. These occurrences likely represent several separate episodes, with Pb being derived from multiple sources. Samples 6, 13 and 14 all plot within the array from the White Creek batholith. As such these veins may represent Pb derived wholly from the intrusion, although this remains unproven. Furthermore, these samples are mineralogically and texturally different, and may not be genetically related to one another.

Samples 7 and 10 plot near the field defined by analyses of lamprophyre dikes from the Valhalla complex. Lamprophyre dikes are also present in the study area, although it is uncertain whether they are related to the dikes in the Valhalla area. The dikes are volumetrically minor, and are not exposed in the vicinity of the sample localities for samples 7 and 10. No veins of any kind were noted in close proximity to the exposed dikes. Omitting the lamprophyre dikes as a possible Pb source, mineralization in samples 7 and 10 likely represents mixing of upper crustal lead with Pb derived from one or more of the White Creek batholith, mantle, lower crustal, Moyie intrusion, and Proterozoic Pb reservoirs.

CONCLUSIONS

Results of this study suggest that mineralization in the study area and in adjacent mineral showings reflects several different mineralizing events. These events may be coincident with tectonic and/or intrusive events that have affected the area. The major interpreted Pb sources include Proterozoic syngenetic or epigenetic deposits, Moyie intrusions, lower Purcell Supergroup sedimentary rocks, and the White Creek batholith.Galena obtained from drill core intersections of galena-rich stratabound horizons within the upper Aldridge Formation contains non-radiogenic Pb. Mineralization is interpreted to be Mesoproterozoic in age, with Pb having been either leached from the Aldridge sediments, or remobilized from a proximal (syngenetic?) base metal deposit.

Lead compositions from an arsenopyrite-bearing quartz vein from the Doc showing are interpreted to represent mixing between a non-radiogenic Pb source and a more radiogenic Pb source. The non-radiogenic Pb source is possibly the stratabound mineralization described above.

If our interpretations of lead sources is correct, Pb isotopic ratios from vein hosted sulphide mineralization can be used as an indicator of remobilization of Pb from potential SEDEX or other Proterozoic base metal targets in the study area, and perhaps elsewhere in the Purcell Supergroup. It is recommended that the analysis of Pb isotopic compositions of vein hosted sulphide mineralization be applied in subsequent exploration for SEDEX mineralization in the region. Interpretation of future data would be greatly enhanced if independent age constraints on mineralizing events are available.

ACKNOWLEDGMENTS

The support and input of Kennecott Canada Exploration Inc. geologists Steve Coombes, Eric Finlayson, Rick Zuran and Nick Thomas is greatly appreciated.

REFERENCES

Anderson, H.E. and Davis, D.W. (1995): U-Pb geochronology of the Moyie sills, Purcell Supergroup, southeastern British Columbia: implications for the Mesoproterozoic geological history of the Purcell (Belt) basin; Canadian Journal of Earth Sciences, v. 32, p. 1180-1193.

Andrew, A, Godwin, C.I. and Sinclair, A.J. (1984): Mixing Line Isochrons: A New Interpretation of Galena Lead Isotope Data from Southeastern British Columbia; Economic Geology, v. 79, p. 919-932.

Beaudoin, G. (1997): Proterozoic Pb Isotope Evolution in the Belt-Purcell Basin: Constraints from Syngenetic and Epigenetic Sulfide Deposits; Economic Geology, v. 92, p. 343-350.

Bevier, M.L. (1987): A Pb isotopic study of the Valhalla complex and its surrounding rocks, southeastern British Columbia: preliminary interpretations; Radiogenic Age and Isotopic Studies: Report 1, Geological Survey of Canada, Paper 87-2, p. 13-20.

Brandon, A.D. and Lambert, R.StJ. (1994): Crustal Melting in the Cordilleran Interior: The Mid-Cretaceous White Creek Batholith in the Southern Canadian Cordillera; Journal of Petrology, v. 35, p. 239-269.

Brown, D.A., Termuende, T. (1998): The Findlay Industrial Partnership Project: Geology and Mineral Occurrences of the Findlay-Doctor Creek Areas, southeastern British Columbia. British Columbia Ministry of Energy and Mines, Minerals Division, Geological Survey Branch, Paper 1998-1, p. 10-1 to 10-9.

Devlin, W.J., Brueckner, H.K. and Bond, G.C. (1988): New Isotopic Data and a Preliminary Age for Volcanics near the Base of the Windermere Supergroup, Northeastern Washington, U.S.A.; Canadian Journal of Earth Sciences, v. 25, p. 1906-1911.

Godwin, C.I. and Sinclair, A.J. (1982): Average Lead Isotope Growth Curves for Shale-Hosted Zinc-Lead Deposits, Canadian Cordillera; Economic Geology, v.77, p. 675-690.

Hoy, T. (1993): Geology of the Purcell Supergroup in the Fernie West-Half Map Area, southeastern British Columbia; British Columbia Ministry of Energy, Mines and Petroleum Resources, Bulletin 84, 110p.

Höy, T., Price, R.A., Legun, A., Grant, B. and Brown, D. (1995): Purcell

Supergroup, southeastern British Columbia; Ministry of Energy, Mines and Petroleum Resources, Geoscience Map 1995-1, 1:250 000 scale.

LeCouteur, P.C. (1979): Age of the Sullivan Lead-Zinc Deposit (Abstract); Geological Association of Canada, Cordilleran Section, Program with Abstracts, p. 19.

Leech, G.B. (1962): Metamorphism and Granitic Intrusions of Precambrian Age in Southeastern British Columbia; Geological Survey of Canada, Paper 62-13, 8p.

Leitch, C.H.B., Turner, R.J.W., Shaw, D.R., Hodgson, C.J., and Brown, T.: Evolution of the vent complex, Sullivan stratiform hosted Zn-Pb deposit: Part 2, wall-rock alteration and sulphide mineralization. Geological Survey of Canada, Mineral Resources Division, Vancouver, B.C., in prep.

Marshall, L.J. (1999); Lead isotope and fluid inclusion study of vein mineralization in the Shrink Lake study area, Purcell Supergroup, British Columbia, Canada; unpublished B.Sc. thesis, *The University of British Columbia*, 91 pages.

Mawer, A.B. (1986): Geological – Soil geochemical report, Alpine Group, Golden Mining Division, Findlay Creek Area; Geological Branch Assessment Report 15,195, 11 pages.

McClay, K.R. (1983): Structural Evolution of the Sullivan Fe-Pb-Zn-Ag Orebody, Kimberley, British Columbia, Canada; Economic Geology, v. 78, p. 1398-1424.

Ransom, P.W., Delaney, G.D. and McMurdo, D. (1985): The Sullivan Orebody. in Stratabound Base Metal Deposits in British Columbia; Geological Association of Canada, Field Trip 11, p. 20-28.

Reesor, J.E. (1958): Dewar Creek Map-area with Special Emphasis on the White Creek Batholith, British Columbia; Geological Survey of Canada, Memoir 292, 78p.

White, W.H. (1959): Cordilleran Tectonics in British Columbia; American Association of Petroleum Geologists, Bulletin, v. 43, p. 60-100.

Zartman, R.E. and Doe, B.R. (1981): Plumbotectonics – The Model; Tectonophysics, v. 75, p. 135-162.

Plutonic-related Gold-quartz Veins in Southern British Columbia

By James M. Logan

KEYWORDS: *Gold, tungsten, plutonic-related, bulk tonnage, mid-Cretaceous intrusions, quartz veins, Cam-Gloria, Valparaiso, Baldy Batholith, Mount Skelly Pluton..*

INTRODUCTION

Extending westerly across the Yukon territory and into Alaska for more than 1000 km is a mid-Cretaceous magmatic belt and associated gold mineralization. This belt of rocks hosts plutonic-related gold deposits, such as Fort Knox (127.5 10^6 g Au), Dublin Gulch (35.7 10^6 g Au), Brewery Creek (28.7 10^6 g Au) and Pogo (162.0 10^6 g Au), and has recently been identified as the Tintina Gold Belt (Figure 1). The intrusions belong to the Tombstone-Tungsten Belt, in Yukon and the Fairbanks intrusions in Alaska.

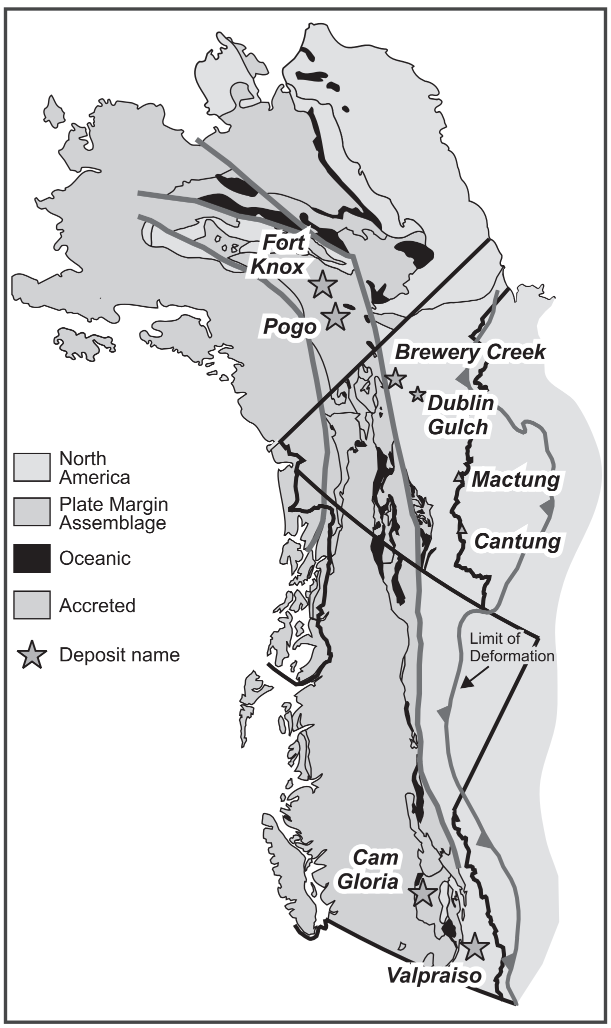

Figure 1. Tectonic assemblage map, after Wheeler and McFeely (1991) showing the distribution of North American, plate margin, oceanic and accreted rocks of the Canadian and Alaskan Cordillera, the location of the Tintina Gold belt and select deposits.

Given the exploration interest in Pogo-type gold mineralization (9.05 million tonnes grading 17.8 g/t Au; Smith *et al*., 1999) and the prospective nature of the province, the British Columbia Geological Survey initiated a field project to provide more information about plutonic-related gold deposits. The Shuswap and Kootenay areas (Figure 1) were selected from the Lefebure *et al*. (1999) data set because they share a number of similarities with the Tintina Gold Belt; including mid-Cretaceous granitic intrusions, solitary, stockwork and sheeted quartz veins with Au-W-Bi metal signatures, and RGS anomalies for pathfinder elements. The Shuswap study focused on the Baldy Batholith area located west of Adams Lake in the Kootenay terrane, where Teck Corporation is evaluating the Cam-Gloria property, while the Kootenay field work concentrated on the Mount Skelly pluton, located north of Creston in North American rocks. These areas were mapped and sampled on a reconnaissance basis to test their potential for Fort Knox and Pogo-style deposits. The results are presented on B.C. Ministry of Energy and Mines Open File maps 2000-7 and 8. In addition, Lett and Jackaman (this volume) carried out multi-media stream sediment sampling to study the geochemical signature of plutonic-related gold mineralization in these areas.

Plutonic-Related Gold-Quartz Deposits

The principal features of plutonic-related gold deposits are reviewed in a number of recent publications, by Baker *et al*. (submitted), McCoy *et al*. (1997), Poulsen *et al*. (1997) and Thompson *et al*. (1999). The major occurrences in the Yukon and Alaska comprise two distinct styles of plutonic-related gold mineralization; the intrusion-hosted low grade, large tonnage sheeted and stockwork low sulphide vein systems at Fort Knox (Bakke, 1995; Bakke *et al*.,1998), Dublin Gulch and Clear Creek, and the high grade quartz veins and bodies that occur proximal to granitoid intrusions on the Pogo claims (Liese Zone) (Smith *et al*., 1999). The main distinguishing factor of this type of gold deposit is the associated metal assemblage of bismuth, tungsten and arsenic and in Alaska and Yukon the association with dikes and cupolas located in or near the apexes of mid-Cretaceous intrusions.

Plutonic-related gold deposits are often associated with a variety of other types of mineralization (Figure 2). For example, peripheral to the sheeted gold-quartz veins in the Eagle Creek Zone of the Dublin Gulch property are gold and tungsten placers, solitary gold-sulphide quartz veins and a tungsten skarn (Hitchins and Orssich, 1995). The tungsten skarn and the gold-sulphide quartz veins are spatially and genetically related to the Dublin Gulch stock (Baker *et al*,. submitted). Further away from the stock are silver-lead-zinc veins which they have interpreted to be distal mineralization related to the intrusion. Similar veins were noted from 2 to 5 kilometres from the source intrusion for other Fort Knox-type deposits by Thompson *et al*. (1999). These associated styles of mineralization provide one of the best methods for identifying areas to prospect for plutonic-related gold deposits.

The key exploration guide for plutonic-related gold deposits is to explore in, and around, highly differentiated granitic intrusions, specifically those intruded in continental marginal settings; a setting shared by tungsten and tin magmatic provinces (Thompson *et al*., 1999). The known prospective areas are underlain by Proterozoic-Paleozoic miogeoclinal rocks of ancestral North America, and the pericratonic Yukon-Tanana and Kootenay terranes. The rocks were deposited along the margin of the North American craton, in shelf and marginal basin environments. Accretion of Quesnellia in the Jurassic led to the deformation, metamorphism and ultimate translation of these rocks along thrust faults onto the craton. These rocks vary from sub-greenschist to amphibolite grade metamorphism. Since the Liese Zone is hosted by gneisses, it is possible that the Pogo-style mineralization is more likely to occur in higher grade metamorphic rocks than typically host other types of gold-quartz lodes.

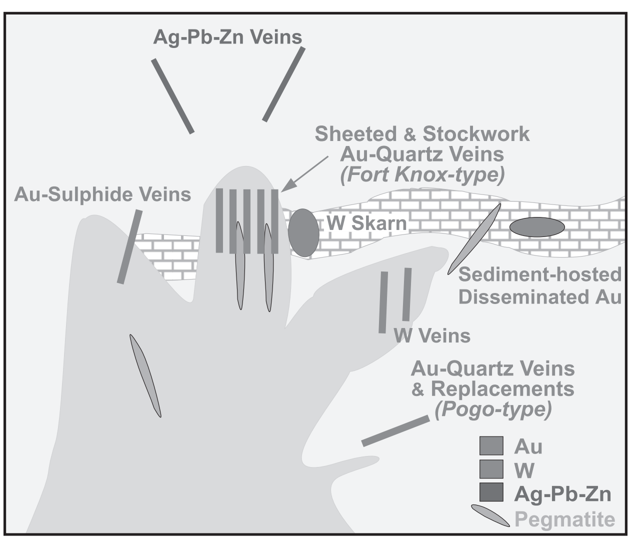

Figure 2. Schematic model of plutonic-related mineral deposits, showing different styles and metal assemblages of intermediate to felsic plutons intruded into continental margin setting (modified from Lefebure and Cathro, 1999).

CORDILLERAN GEOLOGY

The Canadian Cordillera is comprised of five distinct morphogeological belts (Gabrielse *et al.*, 1991). In British Columbia, the Foreland belt is characterized by Proterozoic to Upper Jurassic platformal and miogeoclinal strata that were deposited on the rifted western margin of ancestral North America and then translated northeastward by thin-skinned thrusting and folding to form the Rocky Mountain Fold and Thrust belt. Palinspastic reconstructions indicate at least 200 km of post-middle Cretaceous shortening in the southern foreland belt (Bally *et al.*, 1966; Price and Mountjoy, 1970) and eastward displacement in the north is estimated to be 50 km (Gabrielse *et al.*, 1991). The Omineca belt is the exhumed metamorphic-plutonic hinterland to the foreland belt. In southern BC the Omineca belt consists of the Kootenay terrane and the Barkerville subterrane, which consist of metamorphic rocks probably equivalent to or deposited in proximity with North American miogeoclinal strata (Gabrielse *et al.*, 1991). West of the Omineca belt are the Intermontane, Coast and Insular belts, comprised primarily of Paleozoic to Early Jurassic ocean and island arc terranes. Amalgamation of these terranes and accretion to the western margin of North America occurred in the Middle Jurassic and Early Cretaceous (Monger *et al.*, 1982, Gabrielse and Yorath, 1991). Initial Sr ratios in the Omineca and Foreland belts are commonly greater than 0.705 and those in the western belts commonly less than 0.705 (Armstrong, 1988). The transition between the Omineca and Intermontane belts roughly coincides with the western margin of old radiogenic continental crust and the eastern limit of allochthonous volcanic terranes.

Plutonic rocks comprise a substantial proportion of the Canadian Cordillera, particularly in the Coast and Omineca belts (Figure 3). The mid-Cretaceous plutons of these two belts are markedly different. Those in the Coast belt are primarily I-type, commonly contain hornblende in addition to biotite, and are poor in large-ion lithophile elements (Woodsworth *et al.*, 1991). Those in the eastern belt (Bayonne and Selwyn suites) are S-type, felsic, rich in large-ion lithophile elements and have initial $^{87}Sr/^{86}Sr$ ratios between 0.710 and 0.740 (Anderson, 1988, Armstrong, 1988; Woodsworth *et al.*, 1991). The eastern belt of plutonic rocks intrude North American and marginal assemblage rocks comprising the pericratonic terranes of the northern Cordillera (Figure 1). Molybdenum, tungsten and tin deposits in the northern Canadian Cordillera are related primarily to the mid-Cretaceous (at 110 and 90 Ma) intrusive episodes of the eastern suite (Sinclair, 1995). These include skarn tungsten deposits, such as Cantung and Mactung, and porphyry tungsten-molybdenum deposits at Ray Gulch and Logtung. This tungsten-tin±molybdenum province extends more than 1000 km across the Yukon and into Alaska after restoration of the dextral motion on the Tintina Fault. It also

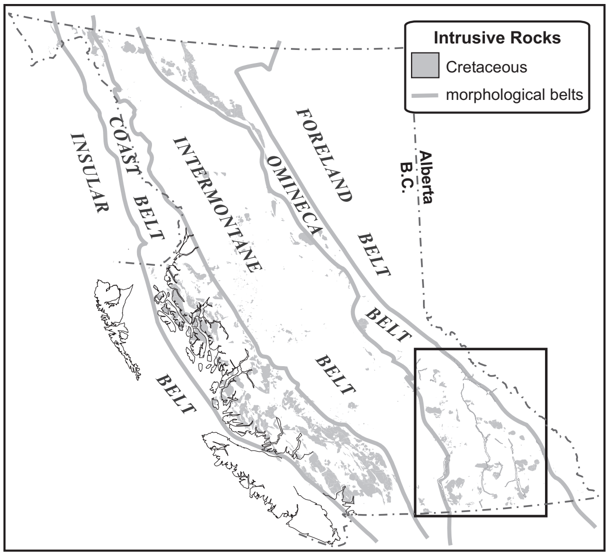

Figure 3. Distribution of Cretaceous plutonic rocks in the Cordillera of British Columbia, showing relationship to the morphogeological belts. Cassiar, Surprise Lake, Cascade and Bayonne suites from Woodsworth *et. al.* (1991).

follows the Omineca Belt southward 1600 km to Salmo near the Canadian-US border.

Bayonne Plutonic Suite of Southeastern British Columbia

In the southeastern Canadian Cordillera, mid-Cretaceous plutons of the Bayonne Suite intrude a wide area extending from North America west across the Omineca and Intermontane belts (Figure 4). Most are post-metamorphic and discordant with the country rocks. They form an arcuate belt of batholiths and stocks, generally composite bodies, comprising several distinctive phases, which follow the eastern edge of the Kootenay Arc and beyond as far northwest as Quesnel Lake. These intrude miogeoclinal rocks of North America affinity. West of the Kootenay Arc, batholiths and large stocks intrude rocks of the Kootenay and Barkerville terranes. North of 51° latitude the batholiths and plutons, such as Baldy and Goldstream, are elongate in an easterly direction.

The mid-Cretaceous suite is comprised of medium to coarse-grained, biotite-hornblende monzogranite to granodiorite and biotite and biotite-muscovite granites. The intrusions are often composite bodies consisting of one or more of these granitoid types and from the available geochemical data there is no simple change from metaluminous to peraluminous along the belt as observed in the Tombstone-Tungsten suite in the Yukon. The Bayonne suite are metaluminous to weakly peraluminous hornblende-biotite granites and strongly peraluminous, 2-mica granites, aplite and pegmatite. Initial Sr and Pb-isotopes suggest an extensive interaction with continental crust. Trace elements (discrimination diagrams of Pearce *et al.*, 1984) are indicative of within-plate tectonic settings for the intrusions cutting North America rocks (Brandon and Lambert, 1993, and this study), but also display volcanic-arc signatures for some of the others (i.e. Goldstream, Honeymoon Bay, Baldy).

At the southern end of the Omineca belt the Bayonne suite intrusions have Sr, Nd and Pb-isotope compositions and REE patterns that can be entirely derived from partial melting of local crustal lithologies (Brandon and Lambert, 1993, Brandon and Smith, 1994). Therefore, these mid-Cretaceous intrusions are likely the result of crustal melting without a mantle derived mafic precursor and were probably generated in response to crustal thickening initiated by thrusting during collapse and obduction of the marginal basin.

REGIONAL GEOLOGY OF SOUTHEASTERN BRITISH COLUMBIA

The present geological architecture of southeastern British Columbia reflects the cumulative effects of Mesozoic accretion of Quesnellia to North America and immediately post-dating compression, substantial extension and exhumation in the Tertiary. Obduction of Quesnellia in the southern Canadian Cordillera began in the earliest Middle Jurassic in response to collision and thrusting of the Intermontane Superterrane over the western margin of North America (Monger *et al.*, 1982; Brown *et al.*, 1986; Murphy *et al.*, 1995). Archibald *et al.* (1983) document Barrovian metamorphism and major deformation *circa* 165-175 Ma in the Kootenay Arc, followed by exhumation and rapid cooling to <300°C prior to the end of the Jurassic. The same Middle Jurassic event was documented in the northern Monashee and Cariboo Mountains (Rees, 1987; Murphy, 1987) and is preserved in the hangingwall rocks of the Eocene extension faults (Johnson, 1994; Parrish 1995). Easterly vergent thrust faults detached the supracrustal rocks from the North America basement and translated them along a major sole thrust, correlative with the Monashee décollement (Brown *et al.,* 1992). Northeast directed motion along the Monashee décollement continued during Cretaceous time, but whether deformation was continuous or episodic is unclear. Contraction caused tectonic wedging that thickened the crust and caused structurally lower rocks to be metamorphosed and the production of anatectic peraluminous melts (in the Cretaceous and Paleocene). In the northern Shuswap, Parrish (1995) evoked a foreland propagating fold-thrust belt to explain the Late Cretaceous to Eocene deformation and metamorphism within the Monashee complex (structurally below the Monashee décollement) and the more varied and long-lived middle Jurassic to Eocene tectonic history of the overlying Selkirk allochthon. This involved westward thrusting of the Monashee complex (basement and sedimentary cover) beneath the hot allochthon in latest Cretaceous to Paleocene. In the allochthon, progressively higher structural levels cross older thrust faults bounding supracrustal rocks with consistently older ages of peak thermal metamorphism. In the southern Kootenay Arc, Leclair *et al.* (1993) provide U-Pb zircon, titanite and allanite dates which constrain penetrative deformation and

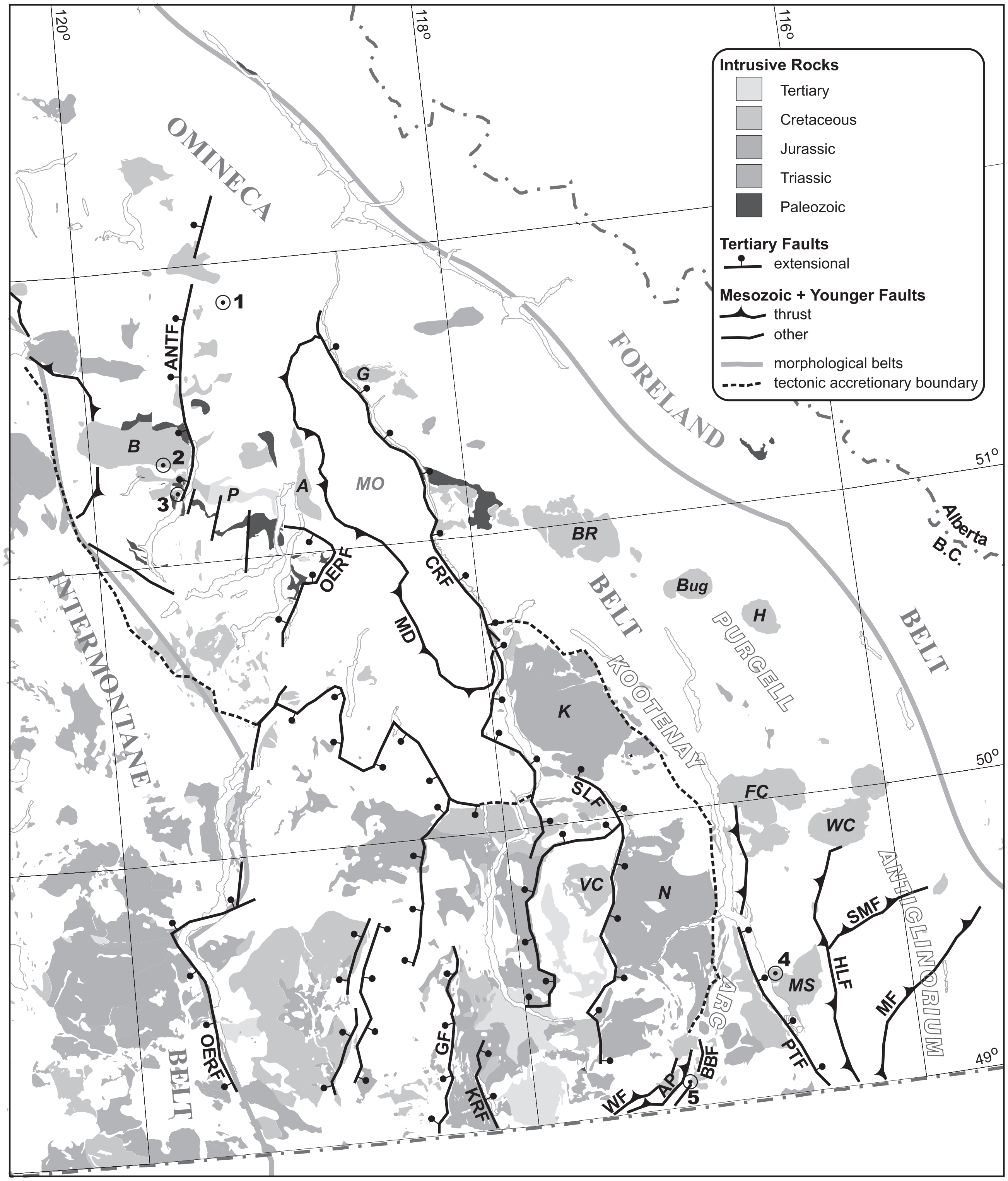

Figure 4. Distribution of Paleozoic, Triassic, Jurassic, Cretaceous and Tertiary plutonic rocks, in southeast British Columbia, also shown are the morphogeological belts and tectonic accretionary boundary. Eocene normal faults (Parrish *et al.*, 1988, Johnson, 1994) bound higher metamorphic grade Shuswap complex rocks, barb on hangingwall side. ANTF=Adams-North Thompson fault, OERF=Okanagan-Eagle River fault, MD=Monashee décollment, MO=Monashee complex, CRF=Columbia River fault, SLF=Slocan Lake fault, VC=Valhalla complex, GF=Granby fault, KRF=Kettle River fault, WF=Wanetta fault, AF=Argillite fault, BBF=Black Bluff fault, PTF=Purcell Thrust fault, HLF=Hall Lake fault, MF=Moyie fault, SMF=St. Mary's fault. Plutonic rocks include; B=Baldy, P=Pukeshun, A=Anstey, G=Goldstream, BR=Battle Range, Bug=Bugaboo, H=Horsethief Creek, K=Kuskanax, FC=Fry Creek, WC=White Creek, N=Nelson, MS=Mount Skelly. Number correspond to mineral occurrences; 1=Bizar, 2=San, 3=Cam-Gloria,4=Valparaiso, 5=Emerald Tungsten.

regional metamorphism to the mid-Cretaceous in amphibolite facies footwall rocks of the Purcell Thrust fault, west of Kootenay Lake (Figure 4). Contraction appears to have continued until the latest Paleocene (Parrish *et al*., 1988; Carr, 1992) at which time the southern Omineca underwent extension. The wide zone of high-grade metamorphic rocks in the southern Omineca belt reflect the substantial amount of extension the area has undergone.

Shuswap Area - Kootenay Terrane Rocks

The Kootenay terrane of the Adams Lake region comprises Proterozoic and Lower Paleozoic sedimentary, volcanic and plutonic rocks and their metamorphic equivalents. Schiarizza and Preto (1987) subdivided the stratigraphy into a lower sequence correlative with Neoproterozoic and Lower Paleozoic ancestral North American miogeoclinal strata and a stratigraphically higher package of Late Paleozoic volcanic arc rocks. West of Adams Lake in the hangingwall of the Eocene Adams-North Thompson Fault (Figure 4), the rocks are chiefly lower greenschist facies, with chlorite to biotite assemblages, but to the east, footwall rocks are higher grade amphibolite facies sillimanite-bearing rocks of the Shuswap metamorphic complex (Read *et al.,* 1991). The Shuswap metamorphic complex is a large, northerly trending metamorphic core complex (Armstrong, 1982). It is bound on its west side, by the west-side-down Okanagan Valley System (Parkinson, 1985; Johnson, 1994) and to the east by the east-side-down Columbia River-Slocan Lake system (Read and Brown, 1981; Parrish, 1984), both outwardly-dipping Eocene normal faults (Figure 4). Adopting the nomenclature of Brown and Carr (1990), the Shuswap complex includes only those high-grade rocks which lie in the footwall of these Eocene extension faults.

The Baldy Batholith is a west-trending, mid- to Late Cretaceous post accretionary intrusive (Schiarizza and Preto, 1987; Calderwood *et al*., 1990). It intrudes Proterozoic to mid-Paleozoic Kootenay terrane metasedimentary and metavolcanic rocks and postdates most of the penetrative deformation in the area; however, its emplacement coincided with some of the latest folding and predated late faults which offset its northern contact (Schiarizza and Preto, 1987). The country rocks host a variety of mineral deposits which predate (mafic VMS, bimodal felsic VMS, disseminated Cu-Mo and stratabound Ag-Pb-Zn) intrusion of the batholith and a wide variety of mineral deposits which may be related to its intrusion (polymetallic base metal veins, porphyry Mo, Au-pyrrhotite veins, Au-quartz veins and W veins).

The Baldy Batholith is a multiphase granite intrusion which covers approximately 650 km^2. The western 2/3rd of the batholith comprises two compositionally similar, but texturally distinct granite phases, a potassium-feldspar megacrystic hornblende-biotite granite to granodiorite and an equigranular biotite monzogranite (Figure 5). The eastern third of the batholith is predominantly a leucocratic biotite-muscovite granite. Muscovite occurs as euhedral and ragged grains associated with biotite. Coarse grained, biotite-muscovite pegmatite and fine grained feldspar-quartz aplite dikes cut all of these phases.

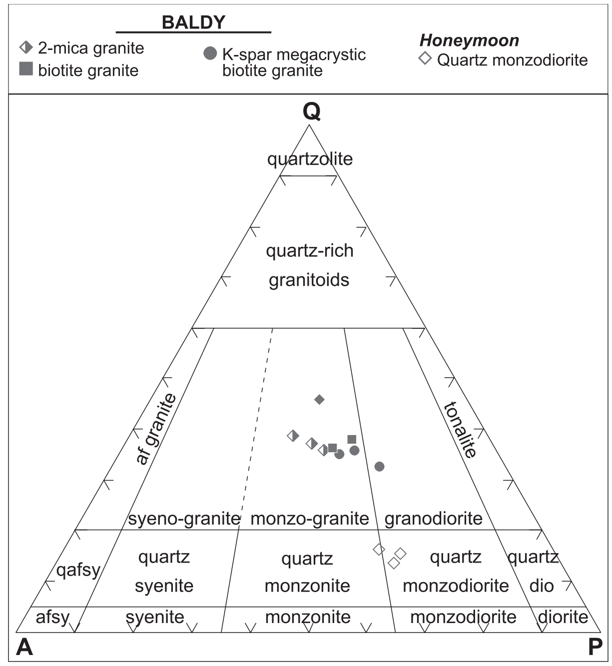

Figure 5. Modal quartz-alkali feldspar-plagioclase feldspar plot for Baldy Batholith and Honeymoon stock. Fields from LeMaitre (1989).

The aeromagnetic survey map for the Adams Lake area distinguishes a weaker magnetic signature for the two-mica granite comprising the eastern end of the batholith, than the two western phases. A ground survey of magnetic susceptibilities of the batholith using a hand held Exploranium KT-9 Kappameter shows the same variation, with distinctive ranges and average values allowing all three phases to be distinguished (Logan and Mann, 2000a).

K-Ar, biotite dates for the Baldy Batholith include the early work by Wanless *et al.* (1966), Kirkland (1971) and Jung (1986) who reported ages of 99±5 Ma; 101±5 Ma and 106±5 Ma; and 104±3 Ma, respectively. These samples provide ages for the north and westernmost biotite ± hornblende granite portion of the Baldy Batholith. A single U-Pb zircon date from this area gave an emplacement age of 115.9±4.6 Ma for the Baldy Batholith (Calderwood *et al*., 1990). K-Ar dates of biotite from gneiss and orthogneisses located south of Baldy Batholith and west of Adams Lake give ages of 129±4 Ma and 99.7±4 Ma (Belik, 1973) and a small quartz monzonite body also from this area (Figure 6), gave a biotite age of 82±6 Ma (Wanless *et al.*, 1966). Schiarizza and Preto (1987) correlate the granitic rocks located south of the main body (*i.e.* Honeymoon stock) with the Baldy Batholith.

South of the Baldy Batholith, between East Barriere and Adams lakes (Figure 6), an irregular east-trending granite body interfingers with Devono-Mississippian orthogneiss and Neoproterozoic to Paleozoic micaceous

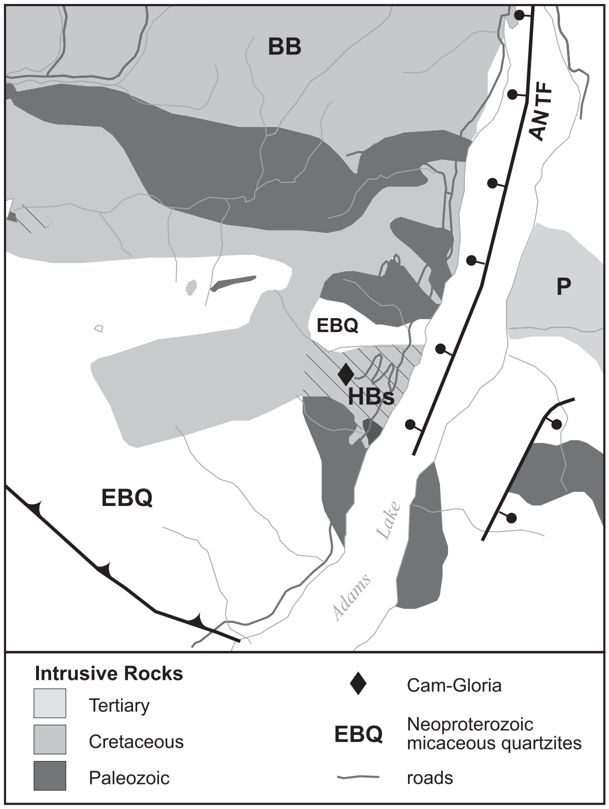

Figure 6. Geology southeastern Baldy Batholith showing location of Honeymoon stock and mineralization at Cam-Gloria. Plutonic rocks include: BB=Baldy, HBs=Honeymoon Bay stock, P=Pukeshun.

quartzites of EBQ (Schiarizza and Preto, 1987). The contacts are irregular and more complex than the steep, clearly crosscutting relationships between the Baldy Batholith and its country rock. Intrusive rocks include hornblende porphyry monzodiorite, biotite-hornblende-epidote quartz monzodiorite and biotite granite. These may represent smaller individual intrusions, but at the present scale of mapping could not be separated. Coarse-grained gneissic units containing sillimanite-staurolite-biotite-hornblende assemblages, calcsilicate gneisses (Schiarizza and Preto, 1987) and rusty-weathering migmatites with felsic leucosomes, pegmatites and sugary-textured aplite dikes host the intrusions in this area. It is not known whether these metamorphic mineral assemblages represent contact or burial metamorphism.

The southeastern-most apophysis of this granitoid body, here called the Honeymoon stock (shaded area in Figure 6), hosts the gold-quartz Cam-Gloria vein. The quartz monzodiorite is typically coarsely crystalline and equigranular (Figure 5). Potassium feldspar megacrysts occur randomly throughout forming as much as 5 % of the rock, but generally few megacrysts are visible in surface outcrops. Major minerals include andesine plagioclase, potassium feldspar, hornblende, biotite, quartz and epidote. Accessories include apatite, sphene, magnetite, and zircon. In thin section euhedral epidote grains, some with amoeboidal intergrowths with plagioclase, are intimately intergrown with hornblende and biotite (Photo 1). The epidote is interpreted as being primary magmatic grains. The mineral assemblage quartz, plagioclase, potassium feldspar, hornblende, biotite, epidote, sphene and magnetite suggest equilibrium pressures of at least 8 kbar (Zen, 1989) and conditions of formation corresponding to greater crustal depths, under fairly oxidizing conditions (Zen and Hammerstrom, 1984). Other intrusions reported to contain magmatic epidote in southeastern British Columbia are middle Jurassic in age and include; the Nelson Batholith (Ghent *et al.*, 1991) and Raft and Mount Toby plutons (Brandon and Smith, 1994). The Honeymoon stock was sampled and submitted to the University of British Columbia, Geochronology Laboratory for mineral separation and U-Pb age-dating.

Mineralization

The Cam-Gloria gold prospect (MINFILE 82M 266) is located three kilometres west of Honeymoon Bay, Adams Lake (Figure 6). The property was staked by prospector Camille Berubé in spring, 1997 following the release of a till geochemical survey (Bobrowsky *et. al.,* 1997) which showed two anomalous sample sites (215 and 43 ppb Au) in the area. The main auriferous quartz vein was discovered on an existing logging road (Photo 2, Cathro, 1998; Lett *et al.*, 1998). The property was optioned to Teck Corporation in early 1999 and surface mapping started during the summer. Initial excavator trenching and diamond drilling were conducted in September-October, 1999.

The Main vein occupies a 35 to 40 metre wide, 700 metre long zone of variable alteration, shearing and quartz veining in quartz monzodiorite of the Honeymoon Bay stock. The alteration zone strikes northeasterly 025 to 045and dips northwest from 45 to 70 and appears to pinch and swell along strike. At the Discovery zone drilling indicates the Main vein is up to 7.3 metres wide. Drilling has intersected two, and in places three, additional (>1 metre wide) veins within the broad alteration zone. Subparallel (sheeted) veins up to 10 cm wide have been encountered over a width of about 20 metres in one drill hole. A second, parallel alteration zone has been discovered by

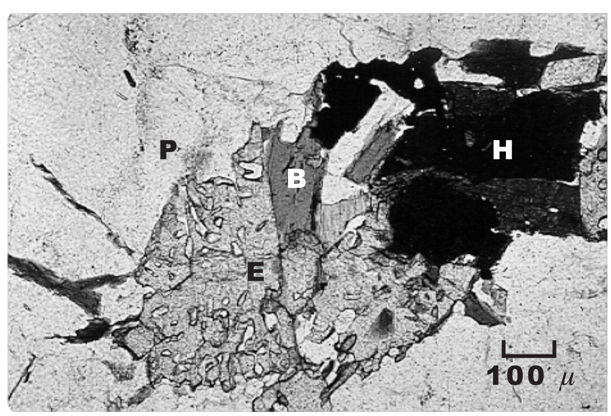

Photo 1. Photomicrograph of Honeymoon Bay - quartz monzodiorite showing typical texture of epidote (E), its euhedral contact with biotite (B) and wormy intergrowths with plagioclase (P).

Photo 2. Large surface exposure of the Main quartz vein at Cam-Gloria gold prospect near Adams Lake, view to the east.

trenching about 100 metres northwest of the main zone. The alteration zones have been affected by moderate to pervasive sericite and clay alteration of feldspars and mafic minerals, and some veins have narrow (2-5 cm) biotite and potassium feldspar selvages. This overprints a low-grade, regional chlorite alteration of the rocks.

The veins contain an average of 1-5 percent, coarse-grained sulphides, mainly pyrite and pyrrhotite, with traces of galena, chalcopyrite, sphalerite and arsenopyrite. Gold values are variable but appear to be associated with galena, fine-grained, bluish-grey sulphides, and local discordant gouge or brecciated zones.

Surface sampling of the Main vein have returned anomalous values in Ag, Bi, Cu, and Pb and weakly anomalous As, Mo, Sb, Te, and W values (Table 1).The highest gold values come from the footwall and hangingwall margins of the vein (samples I, M and J, Table 1). At the southwest end of the Main vein, sericite-altered quartz monzodiorite and vein quartz is exposed in an 8 m trench (sample H). Adjacent to the veins (2 to 8 cm wide), pervasive sericite and coarse muscovite replace feldspars and mafic minerals in the monzodiorite. The footwall zone of the Main vein (exposed north of the road), consists of a 0.2 to 0.5 m thick zone of brecciated vein, flooded by dark grey silica and fine grained sulphides. This is underlain by a variably mineralized, dark grey fault gouge zone which abruptly passes into altered quartz monzodiorite.

Pale green fluorite occurs in the footwall of the Main vein, and as well in several narrow quartz-sulphide veins exposed in road cuts some 100 to 200 metres to the east. The latter (samples A-G) are apparently gold-poor, but do contain locally anomalous Bi , Cu and W values. In addition, float boulders of garnet-pyroxene skarn with traces of pyrrhotite and weakly anomalous Cu and W values have been located on the road about 750 metres northeast of the Main vein.

East of the Cam-Gloria in the higher grade metamorphic rocks of the Shuswap complex prospecting since 1997 has discovered stockwork and sheeted vein, shear zone, manto and skarn showings containing Au, Bi, W, Cu and other metals. The new showings, although gener-

TABLE 1
SELECTED GEOCHEMICAL ANALYSES, MAIN VEIN AND SURROUNDING ZONES, CAM-GLORIA PROPERTY

Au	Ag	As	Bi	Cu	Mo	Pb	Sb	W	Zn	Sample Description
-2	0.1	3.8	0.04	6	<0.2	10.5	0.2	18.7	26	**A**) grab silicified-sericite altered monzonite
17	0.05	2.3	0.13	14	<0.2	9	-0.1	1.7	28	**B**) 25 cm qtz vein, sericite altered HW-FW
-2	0.15	4	0.34	9	<0.2	18	1	3.7	44	**C**) 1 m chip sample across spaced fractures
20	0.25	10.3	398	229	0.2	9	1.1	4.6	18	**D**) 5 cm qtz vein, chlorite + trace po, cpy
6	0.2	6	1.35	31	<0.2	3.5	0.4	0.7	4	**E**) grab 3 sheeted cm-wide quartz veins
13	0.6	108	5.45	676	4.6	25.5	6.7	0.3	6	**F**) 25 cm qtz vein, massive po, trace pyrite
3	<0.05	1.4	0.2	17	<0.2	2	-0.1	0.3	2	**G**) 25 cm wide rusty qtz vein
Main Vein										
20	1.9	5.9	7.7	27	0.2	52.5	0.2	1	4	**H**) grab silicified-sericite altered monzonite
1570	6.6	11.6	17.8	32	1	26.5	0.4	0.4	2	**I**) 3.3 m chip sample starting from the FW
902	9.6	31.4	9.45	49	0.8	169	0.4	1.6	2	**J**) 3.3 m chip from HW side of vein
67	13.2	23.5	31.2	116	0.6	271	0.6	0.3	6	**K**) grab, dissem of po, py, trace cpy, gn
1540	3.15	51.3	30.6	163	1.8	42.5	1.5	0.6	30	**L**) 1.5 m chip sample, SW end of the main vein
18300	15.5	22.5	196	381	3.2	354	2.5	7.8	378	**M**) chip, altered FW-monzonite, brecciated vein
73	11.4	20.8	71.8	251	4	277	2.3	2	526	**N**) 1.5 m chip, coarse and fine grained pyrite
892	60.6	193	240	203	11	1165	1.7	<0.1	576	**O**) grab, fracture filling blebs of po, py, gn

Au, As and Sb by INA; other elements by total digestion-ICP
Au in ppb, rest in ppm

TABLE 2
SELECTED GEOCHEMICAL ANALYSES, GOLDSTRIKE (BIZAR) PROPERTY

Au	Ag	As	Bi	Cu	Mo	Pb	Sb	W	Zn	Sample Description
63	0.05	0.8	77.2	19	76.3	16.5	-0.1	0.5	2	20 cm x-cutting qtz vein, trace py
41400	3.6	5.9	4200	2120	1	6	0.3	<10.0	28	grab, concordant sulphide layer
23400	1.8	3.3	2460	1230	<1.0	12	0.1	<10.0	56	grab, 20 cm massive po+qtz layer
50	0.2	0.7	9.69	383	0.6	0.5	-0.1	0.1	4	x-cutting qtz-plag-andalusite vein
-2	0.3	2	0.9	21	<0.2	16.5	-0.1	0.5	40	x-cutting qtz veins, 1-3 cm
5	1.7	15.2	1.22	393	1.2	24	0.1	4.7	18	grab, py+chlorite in rusty qtz vein
73	0.35	1.2	3.68	39	0.2	14	-0.1	10	12	sericite altered, silicifed bio-schist

Au, As and Sb by INA; other elements by total digestion-ICP
Au in ppb, rest in ppm

ally poorly explored, indicate the potential for plutonic-related gold deposits in the region. Two other new gold prospects with anomalous Bi, Cu, W, Te have been discovered in amphibolite-grade quartzite and schist of the Shuswap complex. The Goldstrike (Bizar) and GQ occurrences are at a very early stage of exploration, but early work by Cathro and Lefebure (this volume) suggests their setting in amphibolite-grade pericratonic rocks with pegmatites is similar to that of the Pogo deposit in Alaska.

The Goldstrike (Bizar) property (MINFILE 82M 267) is located 16 kilometres northeast of the village of Avola (Figure 4). Mineralization consists of semi-concordant and sheeted quartz-sulphide veinlets hosted by amphibolite grade micaceous quartzite and quartz-muscovite-biotite-garnet schist of the Shuswap complex. A semi-concordant layer of auriferous massive pyrrhotite and minor chalcopyrite, up to 20 cm wide, occupies the west end of the Discovery showing. The layer is concordant with dominant synmetamorphic foliation and has been deformed together with the schists into southerly plunging crenulation folds. Tight fractures and narrow centimetre-wide grey quartz veins with limonite selvages trend northerly and dip steeply, crosscutting the micaceous quartzite and schists. Locally as many as 5 veinlets per metre are present, ranging from <1 to 10 centimeters in width. Some high-grade gold assays and anomalous gold values are reported for grab samples from the concordant massive pyrrhotite layers, and quartz veins respectively. Bismuth is particularly enriched and values correlate well with gold values (1:1). In addition anomalous Cu, Ni, Se, Te and W values are present (Table 2). Drilling in October, 1999 intersected narrow zones of quartz sulphide mineralization (*see* Cathro and Lefebure, this volume).

Kootenay Lake Area - North America Rocks

The southern Kootenay Arc coincides with the western margin of the Purcell anticlinorium, a broad, northerly plunging structural culmination of Middle Proterozoic Purcell Supergroup sedimentary rocks. The lower strata consist of the deep water, turbidites of the Aldridge Formation, and extensive Moyie - gabbroic intrusions. Overlying the Aldridge, but beneath the basal unconformity separating the Windermere Supergroup rocks are the fine-grained grey and green clastic quartz-rich rocks of the Creston Formation and fine-grained calcareous rocks of the Kitchener and Dutch Creek formations which underlie the study area. Conglomerates of the Toby Formation, the basal Windermere, unconformably overlie this succession northwest of Sanca stock and define a west-facing succession of North American strata. West of the Purcell Thrust fault are penetratively deformed and metamorphosed Neoproterozoic and Paleozoic rocks of the Kootenay Arc (Figure 4).

The Mount Skelly Pluton (MSP) is a Cretaceous post-accretionary intrusive (Archibald, 1984; Archibald, personal communication). It is another mid-Cretaceous intrusion belonging to the Bayonne Plutonic Suite (Woodsworth *et al.*, 1991; Reesor, 1996). The pluton, located 30 km north of Creston on the east side of Kootenay Lake (Figure 7), trends northeasterly across the structural fabric of Proterozoic Purcell and Windermere supergroup rocks. It consists of three intrusive phases differentiated on the basis of mineralogy, texture, grain size and magnetic signature (Logan and Mann, 2000b). From oldest to youngest, these include a potassium feldspar megacrystic hornblende-biotite granodiorite, a coarse or fine grained biotite granodiorite and a biotite plagioclase porphyritic leucogranite (Figure 8). Fine to medium grained quartz-feldspar-garnet aplite and hornblende-biotite-plagioclase phyric dikes, quartz veins and less commonly, coarse grained pegmatite dikes occur within the plutons, commonly near the margins of the intrusive phases. Biotite porphyry (lamprophyre) dikes occur, locally within and adjacent to mineralized structures. Au quartz veins, W veins and Mo greisen veins are hosted within the multiphase intrusion, while polymetallic base metal veins are found in the surrounding country rocks. Past production of gold is recorded from workings on the Government and Valparaiso crown grants which are hosted in a satellite body of coarse grained, biotite monzogranite located between Sanca and Akokli creeks, two kilometers east of Kootenay Lake (Figure 7).

K-Ar data for biotite and muscovite from the Mount Skelly Pluton and the Sanca Creek stock of the Bayonne Batholith yield conventional dates between 69 and 99 Ma (Archibald *et al.*, 1984; D. Archibald personal communi-

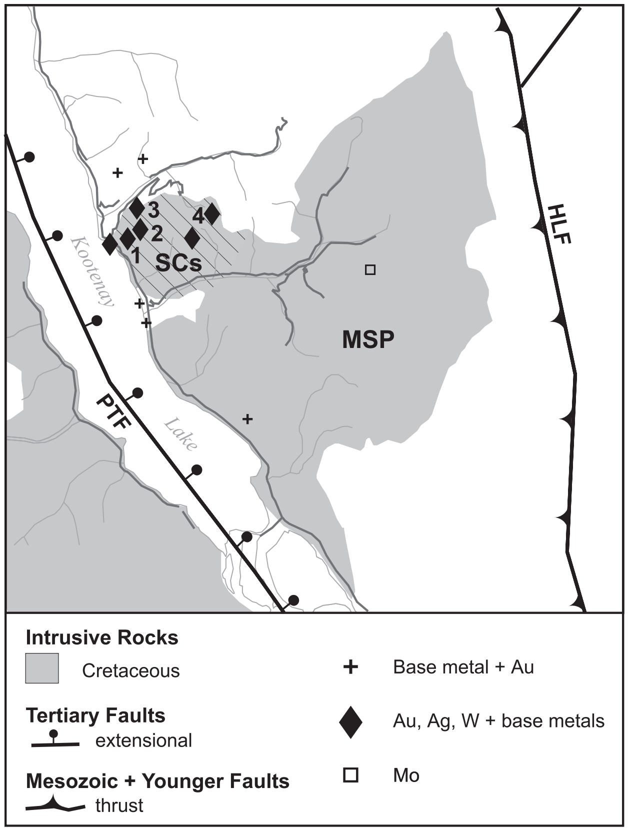

Figure 7. Geology of the Mount Skelly pluton, intrusive phases and mineralization related to the Sanca Creek stock. Mineral occurrences include Au-W deposits; 1=Valparaiso/Government, 2= Sarah, 3= Lost Mine, 4= German Basin, molybdenum and base metal + Au veins.

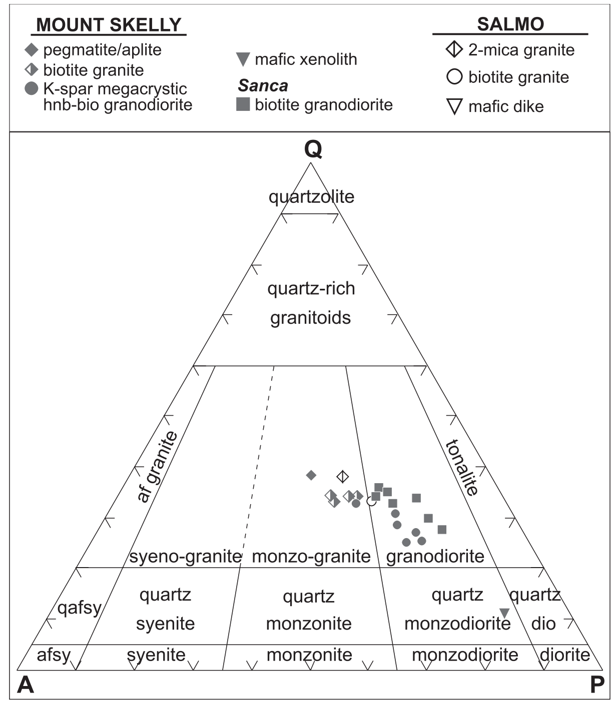

Figure 8. Modal quartz-alkali feldspar-plagioclase feldspar plot for Mount Skelly Pluton (MSP), Sanca Creek stock (SCs) and environs. Fields from LeMaitre (1989).

cation, 1999). The age of the potassium-feldspar megacrystic hornblende granodiorite phase of the MSP is approximately 99 Ma and its southern tail of leucocratic biotite granite averages 70 Ma. Biotite granodiorite of the Sanca Creek stock is approximately 80 Ma. ^{40}Ar-^{39}Ar data yield plateau-shaped age spectra which do not record evidence of a reheating event (Archibald *et al.*, 1984).

The Mount Skelly pluton intruded the Creston Formation and developed a low-pressure, contact-metamorphic aureole. Andalusite and cordierite porphyroblasts overgrow the penetrative fabric in country rock within one kilometre of the northern contact. The presence of adalusite suggests emplacement pressures of less than about 4 kbar. Retrograded garnet-biotite-sericite-cordierite schists are locally present, but for the most part, characteristic pelite mineral assemblages are poorly developed due to the quartzose composition of the Creston Formation. A rusty-weathering, muscovite-biotite, sillimanite-bearing zone of migmatite occupies the innermost zone adjacent to the pluton. The zone is about 100 m wide and comprises ductile deformed, amoeboid-shaped micaceous, quartzose, and calcsilicate country rocks. The zone is cut by tourmaline-muscovite pegmatites and quartz veins. The contact with the intrusion is steep and sharp. The monzonite is neither foliated nor chilled near its margin. The occurrence of sillimanite without kyanite suggests that the pressure did not exceed about 6 kbar (at 600^{o}C).

The majority of the MSP is comprised of a coarse-grained, biotite-hornblende granodiorite characterized by abundant euhedral potassium feldspar megacrysts and rounded mafic xenoliths. Titanite is commonly visible in hand samples of coarse grained varieties, as are trace amounts of magnetite and epidote. The mafic xenoliths are lenticular to rounded, monzodiorite to quartz diorite in composition, consisting mainly of biotite, plagioclase, quartz and titanite. Close to the northwestern margin of the pluton, the inclusions and potassium feldspar megacrysts define a north-trending, east-dipping foliation which parallels the contact. This is the oldest phase in the pluton and has a stronger magnetic signature than the other phases of the MSP.

Fine to medium grained, generally equigranular, biotite granite crops out between Mount Skelly and Jackson Peak in the eastern portion of the pluton and immediately south of Mount Sherman in the west-central portion of the pluton. This phase cuts the main hornblende biotite megacrystic phase. The granite is leucocratic due to the low amount of biotite (~5%). It is fine to medium-grained, equigranular to locally porphyritic, and rarely contains sparse feldspar megacrysts.

The Sanca Creek stock is located northwest of the Mount Skelly Pluton and is separated from the main body by septa of metamorphosed country rock. It stands out as a separate, low to moderate strength magnetic anomaly on the aeromagnetic survey map suggesting the stock is a separate body. It consists of a medium to coarse grained, biotite± hornblende granodiorite with large (up to 1.5

cm), rounded, violet to pale grey quartz grain aggregates or anhedral crystals. Sparse potassium feldspar megacrysts occur locally throughout.

Mineralization

Mineralization is hosted in all intrusive phases of the Mount Skelly Pluton; the main hornblende-biotite potassium feldspar megacrystic granodiorite, the younger biotite granite and the biotite granodiorite of the Sanca Creek. Gold-arsenic mineralized quartz shear zones have been discovered in the oldest phase and sheeted veins of molybdenum mineralization are known from the younger biotite granite, but the majority of gold-tungsten mineralization is contained within the Sanca Creek stock. It hosts the Valparaiso, Government, Sarah, Lost Mine, and German Basin past producing gold mines (Figure 7). The mineral occurrences are hosted in sub-parallel quartz ± pyrite, sphalerite, galena, scheelite, wolframite, gold veins filling prominent north-trending joint and fault structures (Photos 3 and 4).

The Valparaiso-Government (MINFILE 82F 38) vein was discovered in the early 1900's and has received the most exploration and development to date. Shipments of ore are reported for 1900, 1901 and 1933 and tungsten concentrate was produced in 1955. The vein is a well-defined quartz-filled fissure in biotite granodiorite of the Sanca Creek stock. It is exposed over a strike length of 800 metres in various open cuts and developed underground by 160 metres of drifting in the Government workings and 200 metres of drifting in the Valparaiso workings at its north end. The main vein structure strikes northerly and dips eastward at 40 degrees and averages between 1.6 and 2 metres width. Surface sampling of the main and distal parallel veins returned anomalous Au, As, W, Bi, Cu, Pb and Zn. Centimetre to metre wide parallel quartz-filled sheeted fractures are hosted in hangingwall and footwall sections of the main vein-fault. Two footwall-veins are exposed underground in the Valparaiso workings; a 0.12 m scheelite-bearing vein and a 0.45 m sulphide-rich ribboned quartz vein. These underlie the main vein-fault, a 1.1 m oxidized zone comprised of six, 1-3 cm quartz veinlets hosted in sheared hematite and limonite-stained granodiorite. The granodiorite contains discrete, centimetre wide, clay altered shear planes. Sampling indicates gold is associated with the higher sulphide content. Mineralization consists of pyrite, arsenopyrite, wolframite, galena, sphalerite and rare chalcopyrite which occur as streaks, blebs and disseminations irregularly distributed along the vein, but appear concentrated along the vein walls. Gold and silver values are proportional to the amount of sulphides in the vein. A biotite lamprophyre dike occupies the footwall to the vein at the Government.

East of, and 200 m above the Government shaft, are the Imperial-Sarah workings (MINFILE 82F 55), which explore a parallel mineralized quartz vein (Figure 7). Surface cuts expose narrow, north-trending quartz veins hosted by sericite altered biotite granodiorite. A 0.5 m quartz vein with biotite lamprophyre hangingwall is exposed in one trench located north of the caved adit. Mineralization consists of pyrite, arsenopyrite, wolframite, sparse sphalerite and galena and traces of chalcopyrite.

The northern extension of the Valparaiso vein was explored by 40 metres of drifting in the Lost Mine workings (MINFILE 82F 131) located approximately 1000 metres north of the Valparaiso tunnel (Figure 7). Here the structure is comprised of two fractured quartz veins, 0.4 and 0.6 m thick and a narrow footwall gouge zone containing oxidized pyrite.

The German Basin showing (MINFILE 82F 039) is located 3.6 km east of the Vaparaiso-Government high on the ridge between Sanca and Akokli creeks (Figure 7). The vein strikes north, dips west and can be traced on surface for 100 metres. It is developed by two adits and a shaft, as well as numerous open cuts and several raises to surface from the adits. The vein pinches and swells from 2 m at the portal to a minimum width of 0.15 m (Greene, 1981). Adjacent to mineralized structures the granodiorite is altered; biotite is replaced by chlorite and sericite, and feldspars are replaced by sericite. The quartz contains sparse pockets and disseminations of pyrite, sphalerite, galena and rare, orange-coloured scheelite.

Surface drilling to assess the extent of mineralization in the Government showing has been hampered by broken ground conditions which prevented completion of a 1981

Photo 3. Sheeted fractures and quartz veinlets in biotite granodiorite of the Sanca Creek stock.

Photo 4. Parallel quartz vein, mineralized with pyrrhotite and aplite dike hosted by coarse-grained biotite granodiorite of the Sanca Creek stock.

TABLE 3
SELECTED GEOCHEMICAL ANALYSES, MOUNT SKELLY PLUTON
REGIONAL AND PROPERTY SPECIFIC SAMPLES

Au	Ag	As	Bi	Cu	Mo	Pb	Sb	W	Zn	Sample Description
3	0.15	0.8	344	16	3.6	38.5	0.3	8.4	38	spaced fractures-sericite, py, qtz
6	0.25	4.3	2.74	10	1.2	41	3.7	5.2	46	silicified fault zone
-2	0.5	2.2	1.95	3	<0.2	32	0.7	4.7	28	brecciated chalcedony zone
4	0.05	4.6	0.32	3	0.2	26.5	5	1.9	78	0.35 m fault gouge
4	0.05	2.2	0.29	10	<0.2	24.5	0.3	0.7	52	grab silicified fractures
154	1.65	1100	1.98	45	0.6	517	6.8	1.2	478	drusy qtz with botryoidal hematite
247	20.8	38.5	22	765	<1.0	>10000	5.6	<10.0	2590	0.35 m chip alteration+qtz vein
287	>100.0	3	86	320	<1.0	>10000	2.6	<10.0	2000	grab mineralization from trench
3	0.6	2.5	1.56	158	63.9	92.5	0.1	22.4	30	1-2 cm altered fractures, qtz, py
4	0.05	2.1	0.89	12	1.6	43.5	0.1	0.2	14	grab-tight qtz fractures, py, chl
2	<0.20	2	778	24	18	52	0.5	<10.0	30	16 cm drusy qtz vein
21	6.9	32.8	20.4	114	15	490	1.3	3	28	vuggy silicified pyritized intrusive
138	1.2	47.8	2	12	3	86	1.2	10	146	grab - 0.75 m silicifed zone
35	1.3	38.2	1.79	27	1	247	1.6	7.8	116	grab- veins across 16 m zone
German Basin										
954	83.4	13	56.1	211	2.8	7720	0.5	1.3	1780	grab qtz vein, py, sph, galena
Sarah-Imperial										
132	8.9	33.7	0.6	340	0.2	315	1.9	67.4	4460	grab vein, drusy quartz, sph, gal
Valparaiso-Govertment Property										
647	28.3	1470	26.2	718	9	8370	3.1	10.2	1145	5 cm qtz vein, sericite alteration
8	2.3	216	7.66	35	0.8	576	-0.1	96.1	372	0.5m limonitic drusy qtz, traces py
456	9.05	3790	14.85	406	1	441	-0.1	105.5	632	altered monzonite
371	8	10600	8	544	2	1160	2.2	10	730	0.9 m chip, altered-sheared HW
2690	23.6	26200	22	615	5	492	2.2	1150	162	0.50 m chip sample of qtz vein
10	1.2	9600	<2.00	2820	3	210	2.5	40	4050	lamprophyre dike Fw to vein
14400	>100.0	126000	140	8140	<1.0	234	5.2	3160	80	grab, high grade sulphide- in HW
95	3	1110	9.57	124	1.4	1065	3.1	41.7	2520	1.1 m chip granite+qtz veinlets
55	6.6	643	2	140	6	4680	4.1	1810	486	12 cm scheelite-bearing qtz vein
5310	71.8	41400	72	542	11	6350	7.8	7100	354	0.45 m sulphide-rich ribboned vein
1040	12.4	89.3	<2.00	285	4	1630	2.3	2130	16	scheelite, py 3-4 cm qtz vein
2330	24	12.8	0.45	144	12	8420	4	51	568	qtz vein, sericite alteration selvage
28	0.25	9.5	2.29	6	18.8	60.5	0.3	9.4	28	grab 3 veins & alteration selvage
157	3.4	9.3	2.93	21	0.2	113.5	0.2	5.4	18	grab, altered granite + qtz veins
Tungsten Creek vicinity										
1040	12.4	89.3	<2.00	285	4	1630	2.3	2130	16	scheelite, py 3-4 cm qtz vein
2330	24	12.8	0.45	144	12	8420	4	51	568	qtz vein, sericite alteration selvage
28	0.25	9.5	2.29	6	18.8	60.5	0.3	9.4	28	grab quartz veinlets & alteration
157	3.4	9.3	2.93	21	0.2	113.5	0.2	5.4	18	2.5 m sericite-altered qtz veinlets

Au, As and Sb by INA; other elements by total digestion-ICP
Au in ppb, rest in ppm
Sample locations *see* Logan and Mann (2000b).

diamond drill program. Percussion drilling was attempted in 1988 to completed the objectives of the 1981 program but ground conditions again proved insurmountable. The intersection of numerous centimeter to metre wide parallel mineralized and altered fractures, however is encouraging and indicates that mineralization is not restricted to the main zone (Valparaiso fault), but occupies sheeted fractures over a wide vertical range in the intrusive (Greene, 1981). The low-grade bulk-tonnage potential for the showings has not been fully tested.

CONCLUSIONS

The 1999 mapping program carried out reconnaissance mapping, sampling and deposit studies in the vicinity of two mid-Cretaceous Bayonne suite intrusions in southern British Columbia. Results from age-dating, Pb-isotopic studies and geochemistry are pending but field observations and petrography support the permissiveness of the plutonic-related deposit model for gold exploration in British Columbia.

Gold mineralization at Cam-Gloria is associated with Bi, As, Pb, W and Cu metal assemblages in multiple vein structures enclosed by wide pervasive sericite alteration zones. The wide zone of pervasive sericite alteration accompanying quartz veining and mineralization is not a well developed characteristic of Plutonic-related deposits.

Limited past production of gold and tungsten from quartz-filled sheeted veins at the Valparaiso and Government deposits and the distribution of low-grade mineralization throughout the Sanca Creek stock indicate this is a good British Columbia example of a Fort Knox-type of intrusion-hosted, gold-quartz vein deposit. The distribution of low-grade gold mineralization warrants assessment for potential bulk tonnage resources.

This years study focused on intrusion-hosted, gold-tungsten veins of the Fort Knox-type, where a direct relationship between mineralized vein and the pluton is apparent, subsequent work will attempt to establish criteria that recognize areas peripheral to prospective intrusions with Pogo-type potential.

Exploration programs for plutonic-related gold deposits in British Columbia should focus inboard of the accreted terranes in marginal basin rocks of the pericratonic terranes or North American platformal rocks, particularly in, and around, highly differentiated granitic intrusions. As in Alaska and the Yukon, the best targets are mid-Cretaceous plutons and batholiths in structural settings which expose and/or juxtapose deposits formed at different crustal levels. The discovery of the high-grade Pogo gold deposit within amphibolite grade gneisses in Alaska indicates potential in equivalent high grade metamorphic rocks of the Omineca Belt in the Canadian Cordillera.

ACKNOWLEDGEMENTS

I wish to thank Dave Lefebure and Mike Cathro for their enthusiastic introduction to this new gold deposit-type, their logistical help and insightful geological discussions during visits in the field. The author benefited enormously from a field trip to deposits in Alaska and Yukon and would like to thank the following people who spent time touring us there; Thor Bergstrom-Fairbanks Gold Mining, Mike Burke-Yukon Geology Program, Brian Flanigan-Avalon Resources, Rick Diment-Viceroy Resources Ltd., Moira Smith-Teck Corporation and Peggy Young- Kinross Gold.

Richard Mann provided enthusiastic and capable field assistance for the work carried out in southern British Columbia. I thank Teck Corporation and specifically Randy Farmer of Teck Exploration Ltd. for discussions about, and access to the Cam Gloria property. Allan Hilton is thanked for providing a property tour of the Windpass - Sweet Home mines, Linda Dandy for a surface and underground tour of the Jersey Emerald Tungsten and Leo Lindinger for orienting us on the Goldstrike (Bizar) property. I also thank Doug Archibald, of Queen's University for his field visit, discussions and access to unpublished Ar/Ar data.

Dave Lefebure, Mike Cathro and Brian Grant reviewed and improved an earlier version of this manuscript. Verna Vilkos's help with the Figures is much appreciated. This study is part of a larger program investigating the potential for plutonic-related gold deposit in British Columbia.

REFERENCES

Anderson, R.G., 1988, An overview of some Mesozoic and Tertiary plutonic suites and their associated mineralization in the northern Canadian Cordillera: *in* Recent Advances in the Geology of granite-related mineral deposits, ed., R.P. Taylor and D.F. Strong, *The Canadian Institute of Mining and Metallurgy*, Special Volume 39, p. 96-113.

Archibald, D. A., Glover, J. K., Price, R. A., Farrar, E. and Carmichael, D. M. (1983): Geochronology and Tectonic Implications of Magmatism and Metamorphism, Southern Kootenay Arc and Neighbouring Regions, Southeastern British Columbia. Part I: Jurassic to mid-Cretaceous; *Canadian Journal of Earth Sciences*, Volume 20, p. 1891-1913.

Archibald, D. A., Krogh, T.E., Armstrong, R.L. and Farrar, E., 1984, Geochronology and Tectonic Implications of Magmatism and Metamorphism, Southern Kootenay Arc and Neighbouring Regions, Southeastern British Columbia. Part II: mid-Cretaceous to Eocene; *Canadian Journal of Earth Sciences*, Volume 21, pages 567-583.

Armstrong, R. L., 1982, Cordilleran metamorphic core complexes - from Arizona to southern Canada: *Annual Reviews of Earth and Planetary Science Letters*, v. 10, p. 129-154.

Armstrong, R. L., 1988, Mesozoic and Early Cenozoic Magmatic Evolution of the Canadian Cordillera: *in* Processes in Continental Lithospheric Deformation, ed., Clark, S. P., Jr., Burchfield, B. C. and Suppe, J., *Geological Society of America*, Special Paper 218, pages 55-91.

Bally, A.W., Gordy, P.L. and Stewart, G.A, 1966, Structure, seismic data and orogenic evolution of southern Canadian

Rocky Mountains: *Bulletin of Canadian Petroleum Geology*, v. 14, p. 337-381.

Baker, T., Lang, J.R. and Mortensen, J.K., submitted, Characteristics of mineralization associated with intrusions of the mid-Cretaceous Tombstone-Tungsten magmatic belt, Yukon: *Economic Geology.*

Bakke, A., 1995, The Fort Knox 'porphyry' gold deposit - structurally controlled stockwork and shear quartz vein, sulphide-poor mineralization hosted by a Late Cretaceous pluton, east-central Alaska: *in* Porphyry Deposits of the Northwestern Cordillera, *Canadian Institute of Mining, Metallurgy and Petroleum*, Special Volume 46, p. 795 -802.

Bakke, A., Morrell, B. and Odden, J., 1998, The Fort Knox porphyry gold deposit, east-central Alaska: An overview and update: in Porphyry and Hydrothermal Copper and Gold Deposits, Australian Mineral Foundation, Conference Proceedings, November, 1998, p. 89-98.

Belik, G.D., 1973, Geology of the Harper Creek copper deposit: Unpublished M.Sc. thesis, The University of British Columbia, Vancouver, British Columbia, 86 p.

Bobrowsky, P.T., Leboe, E.R., Dixon-Warren, A., Ledwon, A., MacDougall, D. and Sibbick, S.J., 1997, Till Geochemistry of the Adams Plateau-North Barriere Lake Area, 82M/4 and 5: *B.C. Ministry of Employment and Investment*, Open File 1997-9, 262 p.

Brandon, A.D. and Lambert, R.St.J., 1993, Geochemical characterization of mid-Cretaceous granitoids in the Kootenay Arc in the southern Canadian Cordillera: *Canadian Journal of Earth Sciences*, 30, p. 1076-1090.

Brandon, A.D. and Smith, A.D., 1994, Mesozoic granitoid magmatism in southeast British Columbia: implications for the origin of granitoid belts in the North American Cordillera: *Journal of Geophysical Research*, volume 99, p. 11,879-11,896.

Brown, R. L. and Carr, S. D., 1990, Lithospheric thickening and orogenic collapse within the Canadian Cordillera: Australasian Institute of Mining and Metallurgy, 1990 Pacific Rim Congress Proceedings, v. II, p.1-10.

Brown, R. L., Carr, S. D., Johnson, B. J., Coleman, V. J., Cook, F. A. and Varsek, J. L. (1992): The Monashee DQcollement of the Southern Canadian Cordillera: A Crustal-scale Shear Zone Linking the Rocky Mountain Foreland Belt to Lower Crust beneath Accreted Terranes; *in* Thrust Tectonics, McClay, K. R., ed., *Chapman & Hall*, London, pages 357-364.

Brown, R. L., Journeay, M. J., Lane, L. S., Murphy, D. C. and Rees, C. J. (1986): Obduction, Backfolding and Piggyback Thrusting in the Metamorphic Hinterland of the Southeastern Canadian Cordillera: *Journal of Structural Geology*, Volume 8, pages 255-268.

Carr, S.D., 1992, Tectonic setting and U-Pb geochronology of the early Tertiary Ladybird leucogranite suite, Thor-Odin-Pinnacles area, southern Omineca Belt, British Columbia: *Tectonics,* v. 11, p. 258-278.

Calderwood, A.R., van der Hayden, P., and Armstrong, R.L., 1990, Geochronometry of the Thuya, Takomkane, Raft and Baldy batholiths, south-central British Columbia: Geol. Assoc. Can. Mineral. Assoc. Can. Ann. Meet. Programs with Abstr., 15, A19.

Cathro, M.S., 1998, Exploration and Development Highlights in South-Central British Columbia - 1997: *Ministry of Energy and Mines*, Exploration in British Columbia - 1997, p. 33-41.

Cathro, M. and Lefebure, D.V., this volume, Several new intrusive-related gold, bismuth and tungsten occurrences in Southern British Columbia: *British Columbia Ministry of Energy and Mines*, Geological Fieldwork 1999.

Gabrielse, H., and Yorath, C. J., 1991, Tectonic synthesis, Chapter 18, *in* Gabrielse, H., and Yorath, C.J., eds., Geology of the Cordilleran Orogen in Canada: *Geological Survey of Canada*, Geology of Canada, no. 4, p. 677-705 (*also* Geological Society of America, The geology of North America, v. G-2).

Gabrielse, H., Monger, J.W.H., Wheeler, J.O. and Yorath, C. J., 1991, Part A, Morphogeological belts, tectonic assemblage, and terranes, in Chapter 2 of Gabrielse, H., and Yorath, C.J., eds., Geology of the Cordilleran Orogen in Canada: *Geological Survey of Canada*, Geology of Canada, no. 4, p. 15-28 (*also* Geological Society of America, The geology of North America, v. G-2).

Ghent, E.D., Nicholls, J., Simony, P.S., Sevigny, J. and Stout, M., 1991, Hornblende geobarometry of the Nelson Batholith, southeastern British Columbia: tectonic implications: *Canadian Journal of Earth Sciences*, v. 28, p. 1982-1991.

Ghosh, D.K., 1995, Nd-Sr isotopic constraints on the interaction of the Intermontane Superterrane with the western edge of North America in the Southern Canadian Cordillera: *Canadian Journal of Earth Sciences*, v. 32, p. 1740-1758.

Greene, A.S., 1981, Property Evaluation Report, Destiny Bay Properties, Hot Group of Claims, 82F/7: *British Columbia Ministry of Energy, Mines, and Petroleum Resources*, Assessment Report 10811.

Hitchins, A.C. and Orssich, C.N., 1995, The Eagle Zone gold-tungsten sheeted vein porphyry deposit and related mineralization, Dublin Gulch, Yukon Territory: *in* Porphyry Deposits of the Northwestern Cordillera, *Canadian Institute of Mining, Metallurgy and Petroleum*, Special Volume 46, p. 803-810.

Hollister, V.F., 1992, On a proposed plutonic porphyry gold deposit model: *Nonrenewable Resources*, Volume 1, pages 293-302.

Johnson, B.J., 1994, Structure and tectonic setting of the Okanagan Valley fault system in the Shuswap Lake area, southern British Columbia: unpublished Ph.D. thesis, *Carleton University*, 266 pages.

Jung, A., 1986, Geochronometry and Geochemistry of the Thuya, Takomkane, Raft and Baldy batholiths, west of the Shuswap metamorphic complex, south-central British Columbia: Unpublished B.Sc. thesis, *The University of British Columbia*, Vancouver, British Columbia, 140 p.

Kirkland, K.J., 1971, Sulfide deposition at Noranda Creek, British Columbia: Unpublished M.Sc. thesis, *University of Alberta*, Edmonton, Alberta, 107 p.

Leclair, A.D., Parrish, R.R. and Archibald, D.A., 1993, Evidence for Cretaceous deformation in the Kootenay Arc based on U-Pb and 40Ar/39Ar dating, southeastern British Columbia: *in* Current Research, Part A: *Geological Survey of Canada*, Paper 93-1A, p. 207-220.

Lefebure, D.V. and Cathro, M., 1999, Plutonic-related gold-quartz veins and their potential in British Columbia: *in* Short Course on Intrusion-Related Gold- *Kamloops Exploration Group*, p. 185-219.

Lefebure, D.V., Fournier, M.A. and Jackaman, W., 1999, Prospective areas in British Columbia for gold-tungsten-bismuth veins: *British Columbia Ministry of Energy and Mines*, Open File 1999-3, 1:2 000 000 scale map with marginal notes and digital files.

Lett, R.E., Bobrowsky, P., Cathro, M, and Yeow, A., 1998, Geochemical Pathfinders for Massive Sulphide Deposits in the Southern Kootenay Terrane: *B.C. Ministry of Employment and Investment* Geological Fieldwork 1997, p. 15-1-9.

Lett, R.E. and Jackaman, W., this volume, Geochemical Exploration Techniques for Intrusive Hosted Gold Deposits in Southern B.C. (parts of 82M/4, 5, 6 and 82F/7): *in* Geological Fieldwork 1999, *British Columbia Ministry of Energy and Mines,* Paper 2000-1.

Logan, J.M. and Mann, R.K., 2000a, Geology and Mineralization in the Adams -East Barriere lakes area, South-central British

Columbia, 82M/04: *British Columbia Ministry of Energy and Mines*, Open File 2000-7.

Logan, J.M. and Mann, R.K., 2000b, Geology and Mineralization around the Mount Skelly Pluton, Kootenay Lake, Southeastern British Columbia, 82F/07: *British Columbia Ministry of Energy and Mines*, Open File 2000-8.

Logan, J.M., Lefebure, D.V. and Cathro, M., submitted, Plutonic-related gold-quartz veins and their potential in British Columbia: *in* The Tintina Gold Belt Concepts, Exploration and Discoveries, ed., J.L. Jambor, *British Columbia and Yukon Chamber of Mines,* Cordilleran Exploration Roundup 2000, Extended abstracts volume.

Marsh, E.E., Hart, C.J.R., Goldfarb, R.J. and Allen, T.L., 1999, Geology and geochemistry of the Clear Creek gold occurrences, Tombstone gold belt, central Yukon Territory: *in* Yukon Exploration and Geology, *Indian and Northern Affairs, Canada*, Volume 21, p. 185-196.

McCoy, D., Newberry, R.J., Layer, P., DiMarchi, J.J., Bakke, A., Masterman, J.S., and Minehane, D.L., 1997, Plutonic-related Gold Deposits of Interior Alaska: *Economic Geology*, Monograph 9, p. 191-241.

Monger, J.W.H., Price, R.A. and Tempelman-Kluit, D.J. 1982, Tectonic accretion and the origin of the two major metamorphic and plutonic welts in the Canadian Cordillera: *Geology*, Volume 10, pages 70-75.

Mortensen, J.K., Murphy, D.C., Hart, C.J.R. and Anderson, R.G., 1995, Timing, tectonic setting and metallogeny of Early and Mid-Cretaceous magmatism in Yukon Territory: *Geological Society of America*, Abstracts with Programs, v.27, no. 5, p.65.

Murphy, D.C., 1987, Suprastructure-infastructure transition, east-central Cariboo Mountains, British Columbia: geometry, kinematics, and tectonic implications: *Journal of Structural Geology*, No. 9, p. 13-29.

Murphy, D.C., van der Heyden, Parrish, R.R., Klepacki, D.W., McMillan, W., Struik, L.C. and Gabites, J., 1995, New Geochronological constraints on Jurassic deformation of the western edge of North America, southeastern Canadian Cordillera: in Magmatism and tectonics of the North American Cordillera, ed., D.M. Miller and C. Busby, *Geological Society of America*, Special Paper 299, p. 159-171.

Parkinson, D.L., 1985, U-Pb geochronometry and regional geology of southern Okanagan Valley, British Columbia: The western boundary of a metamorphic core complex: Unpublished MSc thesis, The *University of British Columbia*, Vancouver, British Columbia, 149 p.

Parrish, R.R., 1984, Slocan Lake fault: A low angle fault zone bounding the Valhalla gneiss complex, Nelson map area, southern British Columbia: in Current Research, Part A: *Geoogicall Survey of Canada*, Paper 84-1A, p. 323-330.

Parrish, R.R., 1995, Thermal Evolution of the Southeastern Canadian Cordillera: *Canadian Journal of Earth Sciences*, v. 32, p. 1618-1642.

Parrish, , R.R., Carr, S.D. and Parkinson, D.L., 1988, Eocene extensional tectonics and geochronology of the southern Omineca Belt, British Columbia and Washington: *Tectonics*, v. 7, p. 181-212.

Pearce, J.A., Harris, N.B.W. and Tindle, A.G. (1984): Trace element discrimination diagrams for the tectonic interpretation of granitic rocks: *Journal of Petrology*, Volume 25, pages 956-983.

Poulsen, K.H, Mortensen, J.K. and Murphy, D.C., 1997, Styles of intrusion-related gold mineralization in the Dawson-Mayo Area, Yukon Territory: *in* Current Research 1997-A, *Geological Survey of Canada*, p. 1-10.

Price, R.A. and Mountjoy, E.W., 1970, Geological structure of the Canadian Rocky Mountains between Bow and Athabasca rivers - a progress report: in Wheeler, J.O., ed., Structure of the southern Canadian Cordillera: *Geological Association of Canada*, Special Paper 6, p.7-25.

Read, P. B. and Brown, R. L., 1981, Columbia River Fault Zone: Southeastern Margin of the Shuswap and Monashee Complexes, Southern British Columbia: *Canadian Journal of Earth Sciences*, V. 18, p. 1127-1145.

Read, P.B., Woodsworth, G.J., Greenwood, H.J., Ghent, E.D. and Evenchick, C.A., 1991, Metamorphic Map of the Canadian Cordillera: *Geological Survey of Canada*, Map 1714A, scale 1:2 000 000.

Rees, C.J., 1987, The Intermontane-Omineca belt boundary in the Quesnel Lake area, east-central British Columbia: Tectonic implications based on geology, structure and paleomagnetism: Unpublished Ph.D. thesis, *Carelton University*, Ottawa, Ontario, 421 p.

Reesor, J.E., 1996, Geology, Kootenay Lake, British Columbia, *Geological Survey of Canada,* map 1864A, scale 1:100 000.

Schiarizza, P. and Preto, V.A., 1987, Geology of the Adams Plateau-Clearwater-Vavenby area: B.C. *Ministry of Energy, Mines and Petroleum Resources*, Paper 1987-2, 88 p.

Sinclair, W.D., 1995, Molybdenum, tungsten and tin deposits and associated granitoid intrusions in the Canadian Cordillera and adjacent parts of Alaska: *in* Porphyry Deposits of the Northwestern Cordillera of North America: *Geological Society of the Canadian Institute of Mining, Metallurgy and Petroleum*, Special Volume 46, p. 58-76.

Smith, M. , Thompson, J.F.H., Bressler, J., Layer, P., Mortensen, J.K., Abe, I. and Takaoka, H., 1999, Geology of the Liese Zone, Pogo Property, East-Central Alaska, *SEG Newsletter*, No. 38, July 1999 p. 12-21.

Thompson, J.F.H., Sillitoe, R.H., Baker, T., Lang, J.R. and Mortensen, J.K., 1999, Intrusion-related gold deposits associated with tungsten-tin provinces: *Mineralium Deposita*, Volume 34, Number 4, p. 323-334.

Wanless, R.K., Stevens, R.D., Lachance, G.R. and Rimsaite, J.Y.H., 1966, Age Determinations and Geological Studies K-Ar Isotopic Ages, Report 6: *Geological Survey of Canada*, Paper 65-17.

Woodsworth, G.J., Anderson, R.G. and Armstrong, R.L., 1991, Plutonic regimes, Chapter 15: in Geology of the Cordilleran Orogen in Canada: *Geological Survey of Canada*, Number 4, p. 491-531 (also *Geological Society of America*, The Geology of North America, volume G-2).

Zen, E., 1989, Plumbing the depths of batholiths: *American Journal Science*, 289, p. 1137-1157.

Zen, E. and Hammarstrom, J.M., 1984, Magmatic epidote and its petrologic significance: *Geology*, 12, p. 515-518.

Several New Plutonic-related Gold, Bismuth and Tungsten Occurrences in Southern British Columbia

By M.S. Cathro and D.V. Lefebure

INTRODUCTION

Exploration interest in plutonic-related gold deposits in the Cordillera was initially sparked in the 1990s by the discovery and development of the Fort Knox bulk tonnage gold mine located near Fairbanks, Alaska. It has been rejuvenated by the discovery of the high-grade Liese Zone gold deposit (Smith *et al.*, 1999) on the Pogo property in east-central Alaska, with a published resource of 8.89 million tonnes grading 17.83 g/t Au (Teck Corporation Annual Report, 1999). These deposits are part of the "Tintina Gold Belt" and are associated with mid-Cretaceous granitoid rocks of the Tombstone Plutonic Suite. They have a metal assemblage of gold-bismuth-tungsten-arsenic-tellurium-(molybdenum-antimony) and are considered to be plutonic- or intrusion-related deposits, as described in recent review papers by McCoy *et al.* (1997), Poulson *et al.* (1997), Thompson *et al.* (1999), and Baker *et al.* (submitted).

Recent prospecting in the Omineca Belt in southern British Columbia has identified several new plutonic-related gold, bismuth and tungsten occurrences which exhibit similarities to the well studied deposits in Alaska and the Yukon. The potential for plutonic-related gold-quartz veins in B.C. has been discussed by Lefebure and Cathro (1999) and Logan *et al.* (2000) and a compilation map of exploration indicators for these types of deposits was prepared by Lefebure *et al.* (1999).

The showings described here are at an early stage of exploration, with only limited surface mapping, trenching or drilling completed. This paper provides short descriptions, based on brief field visits, of the local geology and exploration history of the showings, along with multi-element geochemical data from grab or chip samples collected by the authors or compiled from other sources. More detailed studies of specific occurrences have been started and the initial results are reported by Logan (this volume), Logan and Mann (2000a) and Logan and Mann (2000b). The results of orientation geochemical surveys conducted near several of the showings are reported by Lett and Jackaman (this volume).

REGIONAL GEOLOGY

The Omineca Belt is a belt of metamorphic, plutonic and sedimentary rocks which separates Proterozoic and Paleozoic sedimentary rocks of the North American miogeocline from Paleozoic and Mesozoic accreted terranes to the west (Monger *et al*., 1982). The belt includes portions of allochthonous terranes and the North American Terrane but is mainly comprised of para-autochthonous terranes such as the Kootenay, Barkerville, Nisling, and Yukon-Tanana Terranes (Monger and Berg, 1984). It has a complex metamorphic, structural and intrusive history which records pre-Paleozoic rifting and deformation, Paleozoic rifting, Devono-Mississippian island arc magmatism, Early-Middle Jurassic to Eocene compression and obduction related to accretion of the Intermontane Superterrane, and Eocene uplift and extension (Monger *et al*., 1982, Parrish *et al*., 1988, Parrish, 1995).

The Omineca Belt in southern British Columbia is comprised of Proterozoic metasedimentary rocks of the Windermere and Purcell Supergroups and Proterozoic and Paleozoic metasedimentary rocks of the Kootenay Terrane. The Omineca Belt here also includes several metamorphic core complexes, such as the Shuswap, Monashee, Okanagan and Valhalla complexes.

Eocene extension in southern British Columbia resulted in exhumation of high-grade metamorphic rocks in domal culminations, such as the Shuswap metamorphic complex, which are bounded by low- to moderate-angle, outward-dipping faults including the Okanagan, Adams-North Thompson and Columbia River-Slocan fault systems (Figure 1, Parrish *et al*., 1988; Johnson, 1994). The Shuswap metamorphic complex has been traditionally understood to include those rocks in the sillimanite zone of regional metamorphism (upper amphibolite facies) as shown on Figure 1 (Okulitch, 1984). Brown and Carr (1990), however, proposed that the term Shuswap complex be used to refer to rocks that lie in the footwall of Eocene extensional faults, which include the Okanagan Valley and Adams-North Thompson faults shown on Figure 1. Johnson (1994) proposed that mylonitized leucogranites of the Pukeashun suite represent the left-stepping "Shuswap Lake transfer zone" which connect the Okanagan- and Adams-North Thompson fault systems.

Granitoid intrusive rocks in the southern Omineca Belt are very common and are mainly Devono-Mississippian, Early Jurassic, Middle Jurassic, middle Cretaceous and Eocene in age. The Middle Jurassic granitoids range in composition from quartz diorite to tonalite to granite, and are thought to have formed as part of a magmatic arc complex formed during accretion and subduction of

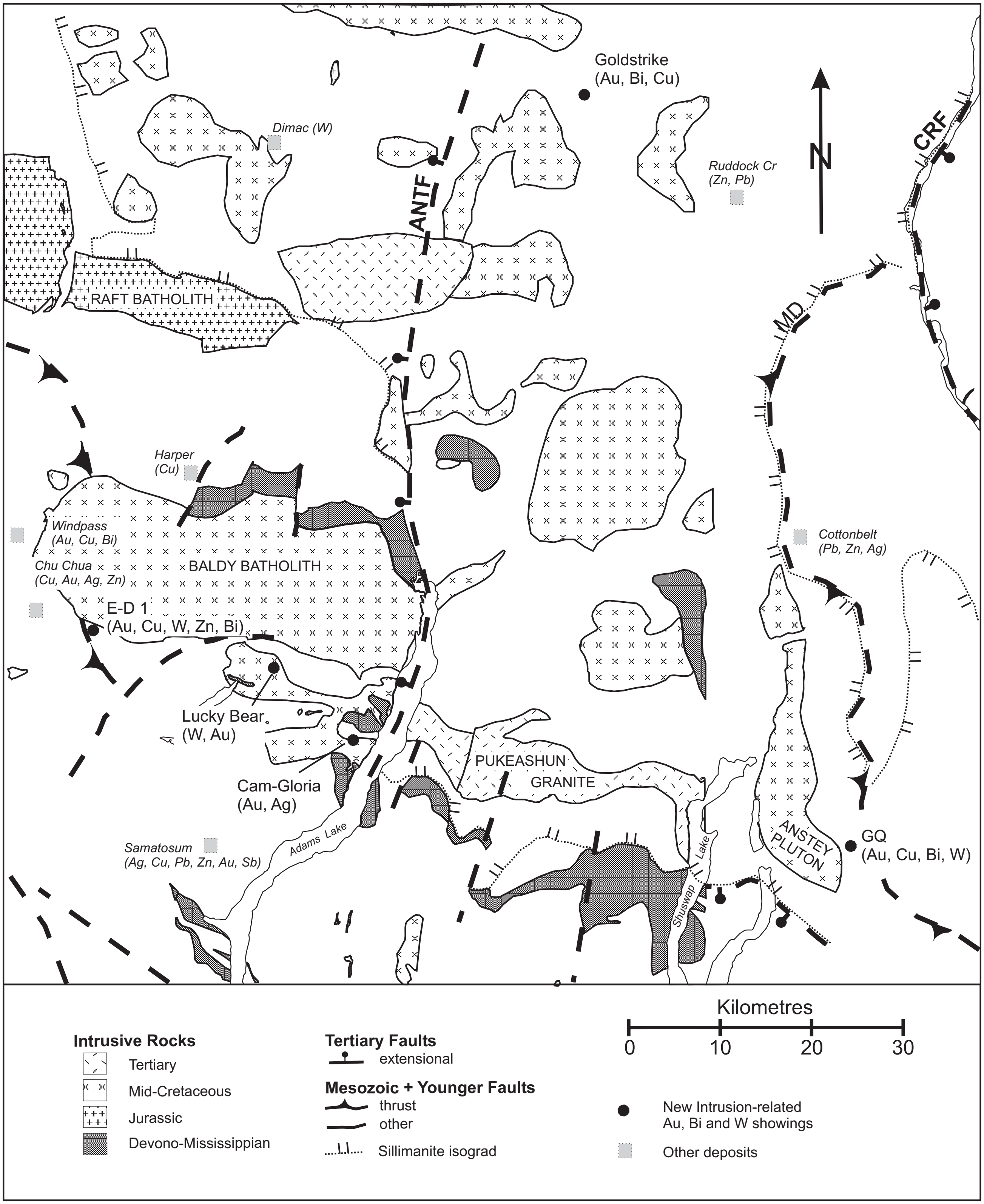

Figure 1. Generalized geology of the Shuswap metamorphic complex and adjacent areas (modified after Wheeler and McFeely, 1991) showing locations of new intrusion-related gold prospects and granitoid intrusions. Adams-North Thompson fault (ANTF), Monashee decollement and Columbia River fault are after Parrish *et al*. (1988) and Johnson (1994). Sillimanite isograd is after Read *et al*. (1991).

allochthonous oceanic terranes (Brandon and Smith, 1994). Mid-Cretaceous intrusions (ca. 100 Ma) are mainly metaluminous to weakly peraluminous hornblende-biotite granites and strongly peraluminous two-mica granites which probably formed by melting of basement gneisses and metapelites in response to crustal thickening (Brandon and Smith, 1994). Trace element plots are indicative of within-plate tectonic settings for inboard intrusions, and volcanic-arc settings for some of the others, such as the Baldy batholith (Logan, this volume).

BALDY BATHOLITH AREA OCCURRENCES

Numerous mid-Cretaceous granitic plutons of the Bayonne suite intrude the Omineca Belt in southern B.C. One of the larger of these is the east-trending Baldy batholith (Figure 1), a multiphase, mid- to Late Cretaceous granitic batholith which intrudes oceanic rocks of the Fennell Formation (Slide Mountain Terrane) and Neoproterozoic to Paleozoic metasedimentary and metavolcanic rocks of the Eagle Bay Assemblage (Schiarizza and Preto, 1987), part of the Kootenay Terrane. Radiometric age dating of the batholith has given a range of 99 +/- 5 Ma to 106 +/- 5 Ma by K-Ar methods, and 115.9 +/- 4.6 Ma by U-Pb methods (summarized by Logan, this volume). Mapping by Logan and Mann (2000a) identified two compositionally similar, but texturally distinct granite phases in the western 2/3 of the batholith, a potassium-feldspar megacrystic hornblende-biotite granite to granodiorite and an equigranular biotite monzogranite. The eastern third of the batholith is predominantly a leucocratic biotite-muscovite granite. Biotite-muscovite pegmatite and aplite dikes cut all the phases (Logan this volume).

South of the main Baldy batholith, between East Barriere and Adams Lake, is an irregular body comprised of hornblende porphyry monzodiorite, biotite-hornblende-epidote quartz monzonite, biotite granite and quartz monzodiorite. It has irregular contacts and intrudes Devono-Mississippian orthogneiss, micaceous quartzite, grit, mica schist, gneissic units containing sillimanite, staurolite, biotite and hornblende assemblages, calc-silicate gneisses and rusty-weathering migmatites (Schiarizza and Preto, 1987; Logan and Mann, 2000a). The southeastern-most apophysis, named the Honeymoon Bay stock (Logan and Mann, 2000a), is comprised mainly of biotite quartz monzodiorite with sparse potassium feldspar megacrysts. Petrographic work by Logan (this volume) suggests that the Honeymoon stock formed at high pressure (>8 kbars) under fairly oxidizing conditions, based on the mineral assemblage epidote, quartz, plagioclase, potassium feldspar, hornblende, biotite, sphene and magnetite.

Cam-Gloria (Honeymoon)

The Cam-Gloria gold prospect (MINFILE 82M 266) is located three kilometres west of Adams Lake (Figure 1). The property was staked by prospector Camille Berubé in spring, 1997 following his discovery of a large auriferous quartz vein on a logging road (Cathro, 1998; Lett *et. al*, 1998). He was following up a British Columbia government till geochemical release by Bobrowsky *et. al* (1997) which showed two sample sites with 215 and 43 ppb gold values, located approximately 300 metres northeast and 1200 metres east of Cam-Gloria, respectively. Berubé optioned the property to Teck Corporation in early 1999. During the summer, Teck staff completed surface mapping, geophysics and excavator trenching. They also drilled 7 holes totaling 835.9 metres in the fall.

The main quartz vein is up to 7.3 metres in width, but locally pinches out or is missing. It occurs within a 35 to 40 metre wide zone of alteration, quartz veining, quartz breccia and minor fault gouge. This zone strikes for 700 metres northeasterly (025 to 045 degrees) and dips steeply northwest (45 to 70 degrees). Drilling has shown that two to three additional large quartz veins (>1 metre wide) also occur within the zone. Subparallel (possibly sheeted) quartz veinlets up to 10 centimetres wide have been encountered over a width of 20 metres in the footwall of the main vein in one drillhole. A second, parallel alteration zone with a narrow quartz vein has been discovered by trenching in one location about 100 metres northwest of the main zone (Randy Farmer, personal communication, 1999). Weak to moderate, pervasive sericite and clay alteration has affected feldspar and mafic minerals in the host quartz monzodiorite. In addition, some veins have narrow (2-5 cm) biotite and k-spar selvages.

The veins typically contain 1 to 5 percent, coarse-grained sulphides, comprising mainly pyrite and pyrrhotite with traces of galena, chalcopyrite, sphalerite and arsenopyrite (Photo 1). Pegmatitic quartz and

Photo 1 Drill core from Hole CG 99-01, Main vein, Cam-Gloria prospect. The grey and white banded material at 44.8 metres is brecciated quartz and fine grained sulphides at the upper (hangingwall) contact. Coarse-grained white quartz is below and sericitized quartz monzodiorite is above.

TABLE 1
SELECTED GEOCHEMICAL ANALYSES OF GOLD, BISMUTH AND TUNGSTEN PROSPECTS IN SOUTH CENTRAL BRITISH COLUMBIA

Property	Showing	Sample #	Au	Ag	As	Bi	Co	Cu	Mo	Ni	Pb	Sb	Se	Te	W	Zn	Comments
Cam-Gloria	Main vein	97RL33	1112	8.6	27.4	55	3	113	11.6	5	420	3.7	<0.3	3.5	n/a	27.1	Grab by R. Lett, GSB; Au by INA; qtz with po, py
	Main vein	CAM-1	3746	61.4	87	56	<2	17	<2	<2	191	<5	n/a	n/a	8	18	Grab by T. Höy, GSB; Au by INA; qtz with po, py
	Main vein	C98-093	10	1.2	31	123	76	794	33	36	60	1.8	0.6	4.1	86	20	Grab; qtz with po, py
Lucky Bear	Water Tank	C99-052	<5	0.2	<5	205	14	30	24	23	18	10	n/a	1.2	4368	1515	Grab; float; garnet-bt-trem-qtz skarn with 1% scheelite
	Little Creek	C99-059	20	<0.2	<5	5	7	18	2	7	6	<5	n/a	0.8	<1	237	Chip; 0-2 m; sheeted qtz vns in gd; trace po and scheelite
	Little Creek	C99-060	20	<0.2	<5	<5	6	22	3	6	6	<5	n/a	1.3	8	95	Chip; 2-4 m; sheeted qtz vns in gd; trace po and scheelite
	Little Creek	C99-061	15	<0.2	10	15	8	23	3	9	6	10	n/a	1.8	<1	95	Chip; 4-6 m; sheeted qtz vns in gd; trace po and scheelite
	Little Creek	C99-062	370	<0.2	<5	35	8	22	3	7	8	<5	n/a	2.5	8	87	Chip; 6-8 m; sheeted qtz vns in gd; trace po and scheelite
	Little Creek	C99-063	5	<0.2	5	10	9	25	3	9	8	<5	n/a	1.2	<1	129	Chip; 8-10.25 m; sheeted qtz vns in gd; trace po and scheelite
	Flat Rock	C99-064	10	<0.2	<5	25	1	46	4	3	<2	<5	n/a	0.3	1480	46	Grab; dump; qtz vn with 1-3% po and trace scheelite
E-D 1	Gossan 1	C98-092	3300	6	4	262	63	1146	26	24	<2	1.8	15	3.1	1487	1320	Grab of limonitic po-cpy manto
	Gossan 1	ED-1	3697	8.7	<5	377	74	1348	2	42	14	5	n/a	n/a	54	55	Grab of limonitic po-cpy manto by T. Höy; Au by INA
	Gossan 1	M1F	2340	7	<5	260	48	1105	19	17	<2	<5	n/a	n/a	280*	1537	Grab of limonitic po-cpy manto by R. C. Wells
Goldstrike	#1 (Bizar)	99607	6000	2.2	<2	300	79	4660	5	60	2	<2	n/a	n/a	<10*	24	DDH 99-02, 59.2-59.4 m; 20 cm qtz vn with 2-3% po, 1% cpy, 2% plag, 1% green sericite and trace pink
	#1 (Bizar)	C98-096	11690	2.2	36	769	318	1939	30	292	<2	2	4.8	1.5	62	24	Grab; 5 cm qtz-po-py-cpy vn
	#1 (Bizar)	C98-097	56800	5.4	6	5271	151	3423	13	140	<2	0.6	11.6	11.8	18	16	Grab; 20 cm wide qtz-po-py-cpy vn; concordant with foliation
	#1 (Bizar)	C99-098	570	<0.2	6	70	6	169	2	8	4	0.4	0.4	0.3	<2	8	Grab; micaceous quartzite with trace FeOx on sheeted fractures
	#2	LBR-99-06	110	<0.2	>10000	<2	44	23	10	20	22	24	n/a	n/a	<10*	<2	Grab by L. Lindinger; 25 cm qtz-aspy vn
	#3 (Road)	LBR-99-32	1710	0.6	466	79	28	361	8	54	<2	2	n/a	n/a	<10*	37	Grab by L. Lindinger; float; bt schist with trace-2% qtz, po and cpy
GQ	SW	WP 023R	1580	1.3	3	225	61.1	305	2.4	38.8	n/a	0.1	n/a	11.2	33.6	72	Grab by W. Gruenwald; 10 cm quartz-po-py-cpy vein
	SW	C99-047	5	<0.2	<5	20	18	44	<1	25	16	<5	n/a	1.7	<20	42	Grab; po-bearing qtz-bt schist
	SW	C99-048	1730	1.8	<5	235	50	389	7	24	40	<5	n/a	5.7	<20	45	Grab; 10 cm qtz-po-py-cpy vn
	SE	WP 025R	115	1.85	<1	11.2	126	992	2.8	43.4	n/a	0.1	n/a	1.35	288	106	Grab by W. Gruenwald; qtz-calc-silicate-po vn/lens adjacent to
	SE	WP 029R	6	<0.2	<1	<2	36	390	3	26	n/a	n/a	n/a	<0.5	1210	90	Grab by W. Gruenwald; calc-silicate-po vn/lens adjacent to pegmatite
	SE	C99-045	15	8.4	5	10	13	47	2	22	34	30	n/a	0.3	<20	35	Grab; po-bearing qtz-bt schist
	SE	C99-058	15	<0.2	<5	<5	16	57	17	33	<2	<5	n/a	1.2	37	340	Grab; 10 cm qtz-po layer at contact between pegmatite and gneiss
	NE	WP 032R	1250	2.1	1	91.2	47.4	510	3.4	33.8	n/a	0.2	n/a	7.25	251	126	Grab by W. Gruenwald; 30 cm po-py-qtz vein/lens
	NE	C99-046	1150	4.2	<5	45	73	734	14	45	12	<5	n/a	6.2	70	40	Grab; 30 cm po-py-qtz vein/lens

plagioclase crystals were noted in the main vein in one of the deeper drill hole intersections. Pale green fluorite is present locally in veins in the footwall of the main vein, as well as in some narrow quartz-sulphide veins in road cuts located some 100 to 200 metres east of the Cam-Gloria discovery outcrop. Limited sampling suggests that the latter are apparently gold-poor, although they do contain locally anomalous Bi (to 1380 ppm), Cu (1198 ppm) and W (48 ppm). In addition, float boulders of garnet-pyroxene skarn with traces of pyrrhotite and weakly anomalous Cu and W values have been found on the road about 750 metres northeast of the Main vein.

Surface grab samples of the main vein have returned gold values varying between trace amounts up to 26.66 g/t (Table 1, Camille Berubé, personal communication, 1997). The vein is also moderately anomalous in Ag, Bi, Cu, and Pb and weakly anomalous in As, Mo, Sb, Te, and W. The gold content is highly erratic, but higher values appear to be associated with galena, fine-grained, bluish-grey sulphides, and local, discordant gouge or brecciated zones. The assay results of the drilling program have not been released by Teck Corporation.

Lucky Bear

Prospecting by Camille Berubé and Dave and Len Piggin has located several new small W-Bi-Zn, W and W-Au showings on the Lucky Bear claim group (Figure 1) near East and North Barriere Lakes. The showings occur about seven kilometres northwest of Teck's Cam-Gloria showing, and are within, or adjacent, to the mid-Cretaceous Baldy batholith.

The "Little Creek" W-Au showing (Figure 1, UTM 11 0314393E 5688542N) is hosted by sericite- and biotite-altered granodiorite. Steeply dipping, north-trending, sheeted quartz veinlets range up to 10 centimetres in width in a 10 metre-wide blasted roadcut exposure (Photo 2). The veinlets contain minor sericite and pyrrhotite. Ultraviolet lamping has identified scheelite grains up to 1.5 centimetres long which occur in scattered patches in the veins, and selected samples collected

Photo 2. Sheeted quartz-sericite-pyrrhotite-scheelite veinlets in mid-Cretaceous granodiorite, "Little Creek" showing, Lucky Bear claims.

by the owners have returned up to 6.15 % W (D. and L. Piggin, written communication, 1999). One chip sample by the senior author contained 370 ppb Au over 2 metres; otherwise the results were not significant for Au, Bi or W (Table 1).

Approximately 500 metres to the east at the "Flat Rock" W showing is an irregular, half-metre-wide quartz vein with 1-3% pyrrhotite and traces of chalcopyrite and scheelite. The vein is hosted by quartz-feldspar-biotite gneiss, part of the Devonian Orthogneiss (Schiarizza and Preto, 1987). A grab sample of the vein taken by the author ran 1480 ppm W and selected samples taken by the owners ran up to 0.39% W, 80 ppb Au, and 135 ppm Bi (L. and D. Piggin, written communication, 1999).

Scheelite-bearing pegmatite and garnet-tremolite-biotite-quartz skarn boulders ranging from 30 centimetres to 1 metre in diameter are found 2 kilometres to the northeast of the Little Creek showing in the "Water Tank' area (UTM 11 0314806E 5690793N). A grab sample of one of the skarn float boulders returned 0.437 % W, 205 ppm Bi and 1515 ppm Zn (Table 1). Although this mineralization has not yet been found in outcrop, the boulders suggest that skarn and pegmatite-hosted tungsten mineralization is associated with the margin of the Baldy batholith.

E-D 1

The E-D 1 claims, owned by Manto Mining Corporation, are located approximately 500 metres south of the southern contact of the Baldy batholith in the headwaters of Birk Creek (Figure 1). The showings were discovered in 1995 by Wayne Tyner, and have received limited mapping, hand trenching, sampling, and geophysical surveys (Wells, 1998). Three holes were drilled in 1997, but no logs or assays are available.

The mineralization occurs at the contact between a grey limestone unit and an underlying green and pink-banded rock, interpreted to be calc-silicate-altered sediments. Regionally, these rocks are mapped as Mississippian-aged Unit EBPl of the Eagle Bay Assemblage (Schiarizza and Preto, 1987) and the faulted contact with basalt of the Fennell Formation (Slide Mountain Terrane) occurs a few hundred metres to the west. The Gossan 1 and 2 showings consist of stratabound pods of partially oxidized, massive pyrrhotite with lesser pyrite, chalcopyrite and sphalerite (Photo 3). They are up to 2 metres thick and several metres in length and dip moderately to the southwest (Wells, 1998). Three surface grab samples indicates that the sulphides contain significant Au (up to 3300 ppb), Bi (up to 377 ppm), Cu (up to 1348 ppm), Zn (up to 1537 ppm), and W (up to 1487 ppm) values and are also weakly anomalous in Ag, Cd, Mo, Se, and Te (Table 1).

The stratabound sulphide mineralization has the appearance and characteristics of a manto-style deposit. The metal assemblage of Au-Cu-Zn-W-Bi with anomalous Te and Mo, combined with proximity to the Baldy batholith and the presence of weakly calc-silicate altered

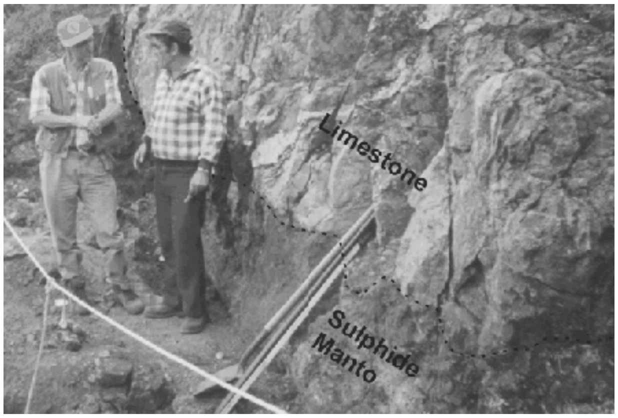

Photo 3. Shallowly west-dipping massive sulphide mineralization containing Au-Cu-Zn-W-Bi at the Gossan 1 showing, E-D 1 claims, Upper Birk Creek area. The mineralization is hosted by Mississippian-aged limestone of the Eagle Bay Assemblage, near the southern contact of the mid-Cretaceous Baldy batholth.

rocks in the footwall suggest that mineralization formed by replacement of limestone adjacent to the batholith.

SHUSWAP AREA OCCURRENCES

Goldstrike (Bizar)

The Goldstrike property is located 16 kilometres northeast of the village of Avola and 2.5 kilometres west of Tumtum Lake in the upper Adams River drainage (Figure 1). Mineralization at the Goldstrike #1 showing (Bizar, MINFILE 82M 267) was discovered and staked by prospector/geologist Leo Lindinger in 1998 and the claims are currently under option to Cassidy Gold Corp. Five short holes were drilled in October, 1999.

The property is underlain by micaceous quartzite and quartz-muscovite-biotite-garnet schist of the Shuswap metamorphic complex (Unit 1c of Campbell, 1963). The foliation in the schist is subvertical and strikes northwesterly at the Bizar showing. Orthogneiss of probable Devonian age outcrops approximately 2.5 kilometres northeast and southwest of the showing. Weakly to moderately sericitized, unfoliated granodiorite of probable mid-Cretaceous age occurs approximately 3.5 kilometres southwest of the showing (L. Lindinger, personal communication, 1999). Boulders of pegmatite float are common throughout the area.

At the Goldstrike #1 showing a partially overgrown roadcut exposes a 20 centimetre wide, strongly contorted, quartz-sulphide band which is conformable with the enclosing schist (Photo 4). This layer contains up to 50% sulphides in places, mainly comprising pyrrhotite and pyrite with minor chalcopyrite and traces of silvery grey, acicular bismuthinite(?). Grab samples of this mineralization returned 11.69 to 56.8 g/t Au, 769 to 5270 ppm Bi and 1939 to 3423 ppm Cu, along with anomalous values of Co, Mo, Ni, Se, Te and W (Table 1). Adjacent to the quartz-sulphide land is a 5 by 25 metre zone of stockwork and locally sheeted, limonite-stained quartz veinlets (Photo 5) which has also returned weakly anomalous Au, Bi, and Cu values (Table 1, Sample C98-098). Up to 5 veinlets per metre are locally present and range from <1 to 10 centimetres in width. Their predominant orientations are 360/30E and 300/40NE to 90.

Additional minor showings were discovered in 1999 but have had only limited sampling and exploration to date. Approximately 1.1 kilometres SSE of Goldstrike #1, a 25 centimetre wide, quartz-arsenopyrite vein dipping 65 degrees to the west, occurs in a roadcut and has returned 110 ppb Au and >10,000 ppm As (#2 showing, Table 1, Gruenwald, 1999). Crenulated biotite schist boulders with semi-concordant layers/veins of quartz, pyrrhotite and minor chalcopyrite have been located 1.5 kilometres SSE of the Goldstrike #1 showing. A grab sample of this float returned 1.71 g/t Au, 466 ppm As, 79 ppm Bi and 361 ppm Cu. These showings contain significantly more arsenic than Goldstrike #1 and may represent a different style or phase of mineralization.

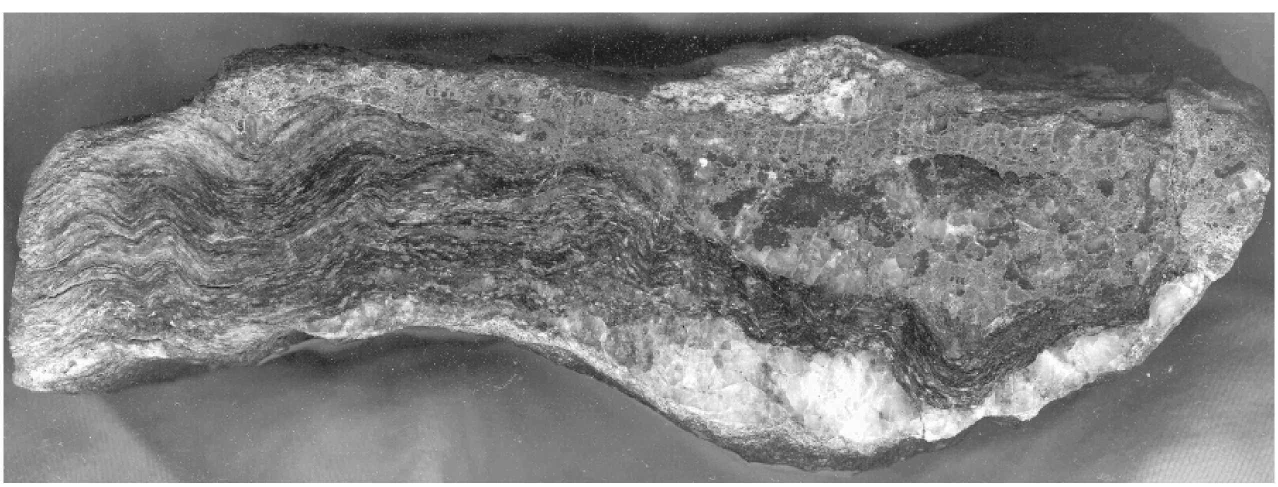

Photo 4. Folded, concordant quartz-pyrrhotite layer with high Au, Bi and Cu values in gneiss, Goldstrike 1 (Bizar) showing.

Photo 5. Goldstrike 1 (Bizar) showing. Sheeted quartz-limonite veins cutting micaceous quartzite of the Shuswap metamorphic complex.

The Goldstrike #1 quartz-sulphide mineralization appears to trend southeasterly for at least 250 metres based on anomalous gold in outcrop, float boulders and soil samples (Gruenwald, 1999). Hole 99-2 was drilled approximately 100 metres southeast of the showing and intersected several narrow, pegmatitic quartz veins with minor sulphides and anomalous Au, Bi and Cu values. The best intersection graded 6 g/t Au over 20 centimetres (Cassidy Gold Corp. news release, December 6, 1999) and comprised a pegmatitic quartz vein with minor pyrrhotite, plagioclase and green sericite and traces of chalcopyrite and pink garnet.

GQ (Second Creek)

Several new pegmatite-related Au-W-Cu-Bi occurrences were discovered northeast of Shuswap Lake in September, 1999 by geologist Warner Gruenwald. He was following up silt samples with anomalous gold values that he had collected during the summer. The showings outcrop on new logging roads in the Second Creek drainage (82M/02), a northwest flowing tributary of the Anstey River. The GQ claims were staked in fall 1999 to cover the area.

Quartz-sulphide zones have been located in outcrop over an area of about 1.5 by 1.5 kilometres on the GQ claims, and anomalous gold values have been encountered at the SW, SE and NE showings (Table 1). The mineralization is hosted by garnet-bearing paragneiss, orthogneiss and quartz-mica schist, and lesser calc-silicate rock, marble and amphibolite of the Shuswap metamorphic complex (Wheeler, 1965). These high-grade metamorphic rocks occur in the hangingwall of the Monashee décollement, to the west of the Frenchman's Cap gneiss dome, part of the Monashee complex (McMillan, 1973). Massive to foliated, granitic intrusive rocks of the mid-Cretaceous Long Ridge pluton (92-94 Ma, U-Pb, Parrish, 1995) occur a few hundred metres to the west of the SW showing. The schist/gneiss package is also intruded by abundant pegmatite dikes, some of which contain tourmaline and minor pyrrhotite.

Mineralization consists of 10 to 30 centimetre wide lenses of quartz, calc-silicate and sulphides which occur along the margins of conformable or slightly discordant, locally tourmaline-bearing pegmatite sills, where they are in contact with marble or schist. Sulphide content ranges from a few percent up to 20-30% in semi-massive pods, consisting mainly of pyrrhotite, minor pyrite and traces of chalcopyrite and scheelite. In all cases, the mineralization has an unusual granular texture with euhedral hexagonal to rounded apatite(?) and quartz grains surrounded by sulphides (Photo 6). In addition to gold values ranging from 115 ppb to 1.73 g/t Au, many of the grab samples from the showings have anomalous geochemical values for Bi (20 to 235 ppm), Cu (305 to 734 ppm), Te (5.7 to 11.2 ppm), and W (33.6 to 1210 ppm).

It is interesting to note that the government Regional Geochemical Survey (RGS) had no sample sites in the Second Creek drainage, and that those few samples in the general GQ property area showed low gold values. Nevertheless, Gruenwald's detailed stream sediment sampling in this area identified several anomalous drainages, including one very strong Au, W, Bi anomaly in a drainage where no mineralization has yet been found. This case highlights the problem in relying on widely spaced government RGS data for gold exploration, and demonstrates the effectiveness of detailed stream sediment sampling and roadcut prospecting.

NELSON-SALMO AREA OCCURRENCES

There are a wide variety of mineral deposits and occurrences and mid-Cretaceous and Middle Jurassic intrusions in the West Kootenays region. An evaluation of British Columbia for the potential for intrusive-related, gold-tungsten-bismuth quartz veins (Lefebure *et al.*, 1999) identified several prospective areas in the

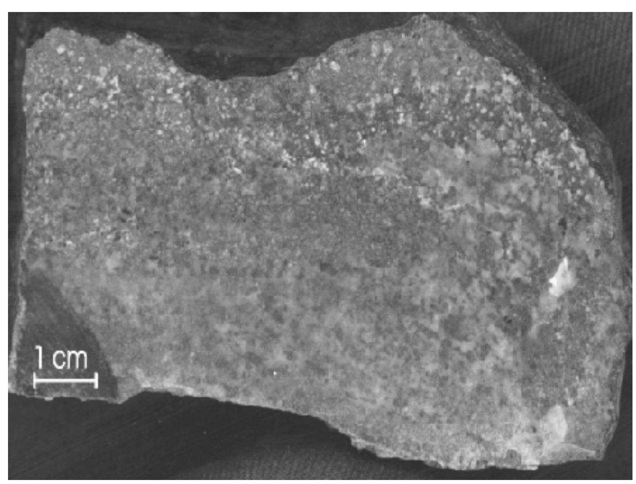

Photo 6. Auriferous quartz-sulphide layer with anomalous Bi, Cu, Te and W from the SW showing, GQ claims. Note granular texture with euhedral hexagonal to rounded apatite(?) and quartz grains surrounded by "net-textured" pyrrhotite.

TABLE 2
POSSIBLE PLUTONIC-RELATED GOLD OCCURRENCES IN THE NELSON-SALMO AREA

Name	Status	Commodities
ALPINE GOLD	Past Producer	Au, Ag, Pb, Zn, Mo, W
VALPARAISO	Past Producer	Zn, Pb, W, Au, Ag, Cu
GOLD BASIN	Prospect	Pb, Cu, W, Au, Ag
SARAH 2ND	Past Producer	Ag, Au, Pb, W, Cu, Zn
BUNKER HILL (L.2939)	Past Producer	Au, Ag, W, Mo
EMERALD TUNGSTEN	Past Producer	W, Mo, Bi, Au
DODGER (L.12083)	Past Producer	W, Mo, Au
KOOTENAY BELLE	Past Producer	Au, Ag, Pb, Zn, W
KENVILLE	Past Producer	Ag, Au, Pb, Zn, Cu ,Cd
VENANGO (L.4757)	Past Producer	Au, Ag, Pb, Zn, W
ROYAL CANADIAN (L.633)	Past Producer	Au, Ag, Zn, Pb, W
ATHABASCA (L.1569)	Past Producer	Au, Ag, Pb, Zn, Cu, W

Kootenays, including the Salmo Mining Camp, Bayonne batholith and parts of the Nelson batholith. The same study identified a number of occurrences in the region with some of the characteristics of plutonic-related gold deposits (Table 2).

In drawing comparisons to the Tintina Gold Belt in Yukon and Alaska, the most promising targets are the Cretaceous granitic intrusions, such as the Bayonne batholith and the Wallack, Lost Creek, Salmo and other smaller stocks in the Salmo mining camp. Initial investigations of the Bayonne batholith by Logan (this volume) and Lett and Jackaman (this volume) have produced more evidence for plutonic-related gold mineralization associated with particular phases. In the Salmo mining camp at the southern end of the Kootenay Arc, bismuth-gold zones near the mid-Cretaceous stocks have been identified and are described in the following section.

Other plutonic-related gold occurrences identified by Lefebure *et al.* (1999) are associated with phases of the Middle Jurassic Nelson batholith. One of these, the Rozan (Figure 2), is also discussed below.

Bismuth-Gold Zone (Jersey Emerald Property)

Lead-zinc-silver, tungsten and gold mineralization occurs on the Jersey Emerald property which is located approximately 10 kilometres south of Salmo (Figure 2). The first claims on the property were staked in 1896 on a high grade gold showing called the Emerald located in the general vicinity of the Emerald tungsten deposit. Subsequent prospecting found lead-rich mineralization in 1906 at the Emerald lead deposit (082FSW310, Figure 3) which produced more than 25 850 tonnes of ore containing 6 788 936 kilograms of lead, 705 292 grams of silver, and 19 771 kilograms of zinc by 1925 (MINFILE). In 1938, skarn tungsten and molybdenum mineralization was discovered in the area of original staking for gold. This became the Emerald tungsten mine which was operated by a Federal Government Agency from 1942 until 1944 and from 1947 until 1958 by Canadian Exploration Ltd. The Emerald deposit (082FSW010) provided the majority of the ore (about 74 %) with the rest coming from the Feeney (082FSW247), Invincible (082FSW218) and Dodger (082FSW011) deposits. Aggregate production totaled 1.45 million tonnes of ore grading 0.76 % WO_3 (Troup, 1994). Canadian Exploration Ltd. discovered the Jersey zinc-lead deposit (082FSW009) and mined it from 1949 to 1970. It produced 7.23 million tonnes grading 1.95% Pb and 3.83% Zn with minor silver (Troup, 1994).

The oldest rocks on the property are micaceous quartzites and quartzites of the Cambrian Reno Formation which outcrop southeast of the Jersey mine (Fyles and Hewlett, 1959). Most of the Jersey Emerald property is underlain by sedimentary rocks of the Cambrian Laib Formation which conformably overlies the Reno Formation and has been subdivided into Lower and Upper parts by Fyles and Hewlett (1959). The Lower Laib is composed of three members - the Truman, Reeves and Emerald, while the Upper Laib is not subdivided because it lacks well-defined marker beds. It consists of green phyllite and micaceous quartzite with minor beds of argillaceous limestone. The Truman Member is a sequence of phyllite, argillite and minor limestone which is primarily brown argillites on the property. The Reeves Member consists of the calcareous rocks, typically grey and white or black and white, fine to medium-grained limestone. It has gradational contacts with the bounding units so the basal contact is defined as the uppermost argillite or phyllite of the Truman Member, while the upper contact is placed at the lowest argillaceous bed of the overlying Emerald Member. The limestone is locally altered to dolomite which is believed to be due to epigenetic replacement associated with Pb-Zn mineralization (Fyles and Hewlett, 1959). Black argillites and phyllites make up the Emerald Member. On the eastern side of the property, the Ordovician Active Formation outcrops as black argillite and slate with minor limestone and dolomite. The sedimentary units have been complexly deformed; Fyles and Hewlett (1959) have identified three phases of folding and thrust and high-angle faults. The principle structure on the property is a north-northeast trending anticline called the Jersey anticline (Figure 3) which has complex recumbent isoclinal folding and thrust faulting (Thompson, 1974).

The layered units are cut by the informally named Dodger and Emerald biotite granite stocks of mid-Cretaceous age. The granitic stocks are coarse to medium grained and cut by aplite or felsite dykes. Pegmatite occurs as small patches (< 0.5 m) in some places in the granite; the Dodger stock has a 4 by 5 metre quartz pegmatite outcrop exposed at the south end of the stock, near the north adit. A potassium-argon biotite age from the Dodger stock yielded 100.0 +/- 3.0 Ma (Dandy, 1997). Underground workings and drillholes show the Dodger and Emerald stocks are joined at depth (Lawrence, 1997). Other intrusive phases are a two-mica granite of possible Cretaceous age that outcrops near the Jersey open pits and Tertiary augite monzonite stocks of the Coryell suite (Figure 3).

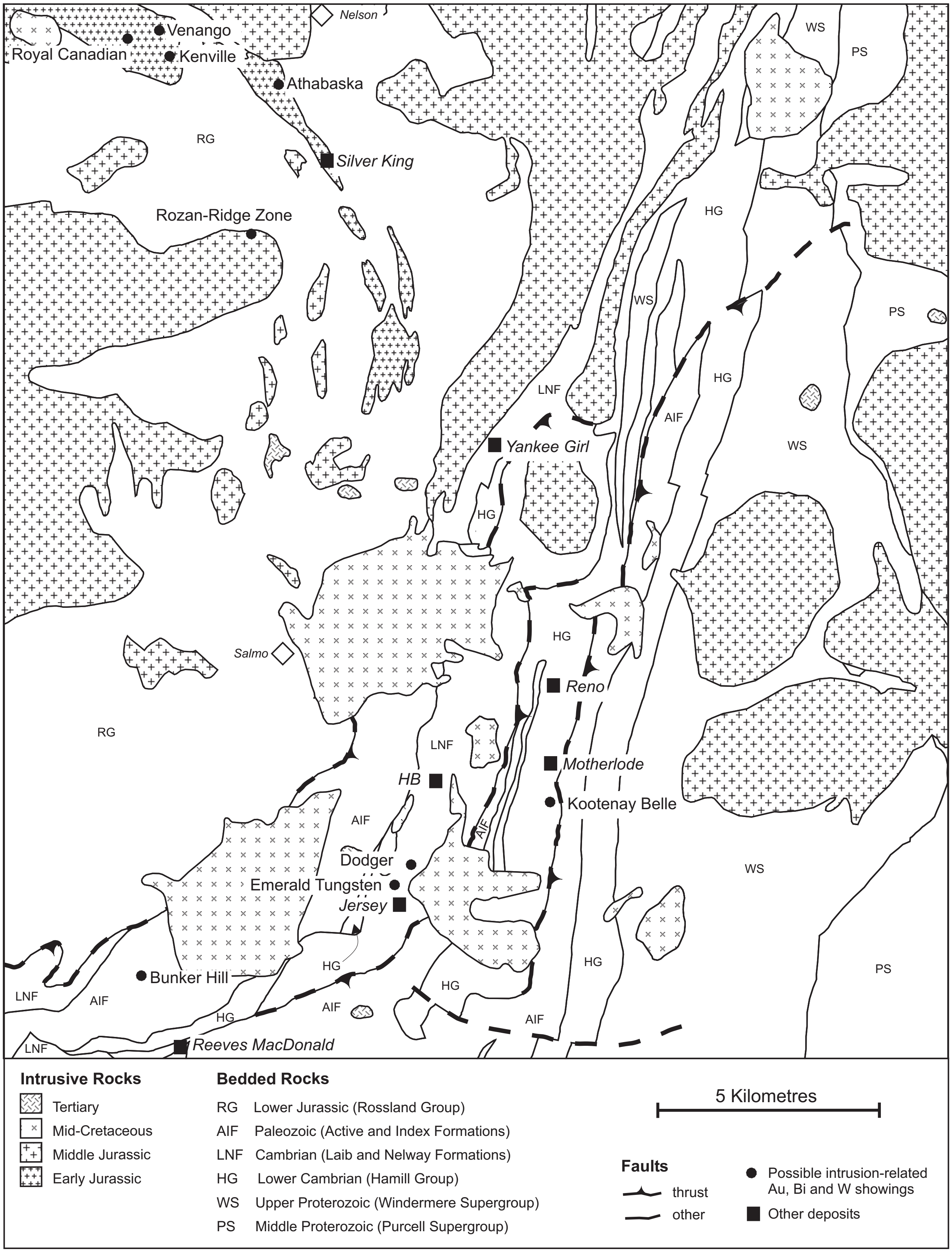

Figure 2. Generalized geology of the Nelson-Salmo area (modified after Wheeler and McFeely, 1991 and Höy and Andrew, 1989b) showing locations of intrusion-related gold prospects and granitoid intrusions.

On the Jersey Emerald property the lead-zinc, tungsten and gold mineralization are hosted largely by calcareous rocks of the Laib Formation. The Jersey lead-zinc deposit has generally been interpreted as either syngenetic sedex (Höy, 1982) and/or Irish-type replacement mineralization (Nelson, 1991), although Dawson (1996) believes it is a distal lead-zinc skarn related to the tungsten skarns. The ore occurs as five bands hosted by dolomitic limestone near the base of the Reeves Member. Dolomitic Reeves limestone also hosts similar base metal deposits, including the HB to the north and Reeves MacDonald to the south (Fyles and Hewlett, 1959) which have no associated skarns. The tungsten skarn mineralization at Jersey Emerald occurs as disseminated scheelite with small amounts of powellite, rare wolframite and scattered flakes of molybdenite (Rennie and Smith, 1957; Fyles and Hewlett, 1959) replacing both Reeves Member limestone immediately adjacent to the granite stocks (*e.g.* Emerald, Feeney, Invincible and Dodger 4400 orebodies), or as replacement zones in limy argillite of the Truman Member close to the intrusions (*e.g.* East Dodger; Lawrence, 1997). Typically the skarn is a green and brown banded rock containing diopside, garnet and calcite. The skarns are believed to be mid-Cretaceous in age and younger than lead-zinc mineralization (Thompson, 1974). The Bismuth Gold, Emerald and Leroy gold zones occur near, or at, the base of the Reeves limestone. Both the Bismuth Gold and Emerald zones are found within tens of metres of tungsten skarns and mid-Cretaceous intrusions (Dandy, 1997).

Canadian Exploration Ltd., while drilling off the Jersey lead-zinc deposit in the 1940s and 1950s, intersected a pyrrhotite-rich zone in several holes overlying the lead-zinc mineralization (George Cross News Letter No.27, February 7, 1997). The zone had a low base-metal content and was not followed-up at that time, although in 1994 it was recognized to be part of the Bismuth Gold zone (Sultan Minerals Inc. Annual Report, 1995). In 1963, Canadian Exploration Ltd. assayed four samples from a native bismuth-arsenopyrite zone. These contained up to 3.4 g/t Au (Troup, 1994); however, they did not follow this up because of low gold prices. In 1983 Lloyd Addie and Bob Bourdon, both of Nelson, panned fine particles of free gold from the tungsten tailings and eventually identified three parallel gold-bearing zones over the Dodger, Emerald and Leroy occurrences (Figure 3; Troup, 1994). Sultan Minerals Inc. optioned the property in late 1993. Since that time they have investigated both the gold and base metal potential of the property with a combination of surface exploration and drilling. The following description of the Bismuth Gold and Leroy-Tungsten Gold zones is based largely on work by staff of Sultan Minerals Inc.

The Bismuth Gold Zone is located on the east side of the Jersey anticline and immediately east of the underground workings of the Jersey lead-zinc deposit (Figure 3). The mineralization is at the contact between the limestone and dolomite of the Reeves Member and is not exposed on surface. The zone varies from 1.2 to 18.0 metres thick and averages approximately 75 metres in width, although it can be up to 200 metres wide (Linda Dandy, personal communication, 1999). It roughly parallels and overlies part of the east limb of the Jersey lead-zinc orebody (Figure 4).

The Bismuth Gold zone contains pyrrhotite, arsenopyrite, quartz, native bismuth and stibnite (Troup, 1994) It is exposed in the Jersey mine workingsnear the east end of the Dodger cross cut (Figure 3). Two grab samples from underground exposures returned assays of 3.43 and 5.49 g/t Au across 4.0 and 1.0 metres respectively with 0.26% and 0.14% tungsten (Troup, 1994). Two drill holes in 1996 by Sultan Minerals Inc. intersected a pyrrhotitic horizon up to 9 metres thick with gold grades ranging from 2.0 to 8.3 g/t Au, including intersections of 2.0 metres grading 8.33 g/t Au and 3.0 g/t Ag in DDH G96-5 and 9.4 metres grading 3.23 g/t Au and 22.9 g/t Ag in underground drillhole 1-96 (Sultan Minerals Inc. press releases, October 10, 1996 and January 10, 1997). Sultan Minerals Inc. traced the zone in four drill holes for a distance of 200 metres, and correlate it with Canadian Exploration Ltd. drill intersections which would extend it another 1100 metres to the south (Dandy, 1997).

Pyrrhotite is typically the most abundant sulphide in the Bismuth Gold zone, however, there are areas where arsenopyrite and bismuth minerals are more common, including several underground exposures in the Jersey mine. There is no visible gold in the zone; no petrographic work has been done to identify the location of the gold. Microprobe analyses of the pyrrhotite, arsenopyrite and quartz mineralization from the Bismuth Gold zone from site A by Ray and Webster (page 60, 1997) identified other minor to trace minerals, including Mg-rich sideritic carbonate, bismuth tellurides (tetradymite, pilsenite and joesite-B), bismuthinite and bismuth selenides. Their analyses also showed that the mineralization is anomalous for Ag, Cu, As, Sb, Bi, Te, Se and Be (Table 3).

On the west limb of the Jersey anticline, Sultan Minerals Inc. has defined two other gold zones, called the Emerald and Leroy (Figure 3). The Emerald zone is coincident with the Emerald Tungsten skarn deposit workings, although the gold mineralization is a separate body. The horizon may be represented by bismuth-rich sulphides (site B, Table 3) and/or a quartz zone hosted by argillite in the south end of the Emerald open pit. The latter grades 5.39 g/t Au and 22 g/t Ag over a 1 metre width (Linda Dandy, personal communication, 1999). It is believed that the same zone is exposed as 1 to 2 metre wide, massive pyrrhotite band in trenches and old pits which follow the Reeves limestone and Emerald argillite contact for over 300 metres south of the open pit (Dandy, 1996). It was also intersected in two drill holes located 300 and 600 metres south of the Emerald pit; the latter hole intersected 0.9 metres grading 27.3 g/t Au and 34.4 g/t Ag (October 10, 1996 press release).

The Leroy zone is exposed in a series of old trenches and crosscut by a short adit. It consists of a quartz band, sometimes with marginal pyrrhotite and minor pyrite mineralization, that is well exposed on surface for 250 metres and may correlate with exposures in pits extending another 450 metres (Dandy, 1996). The quartz/pyrrhotite

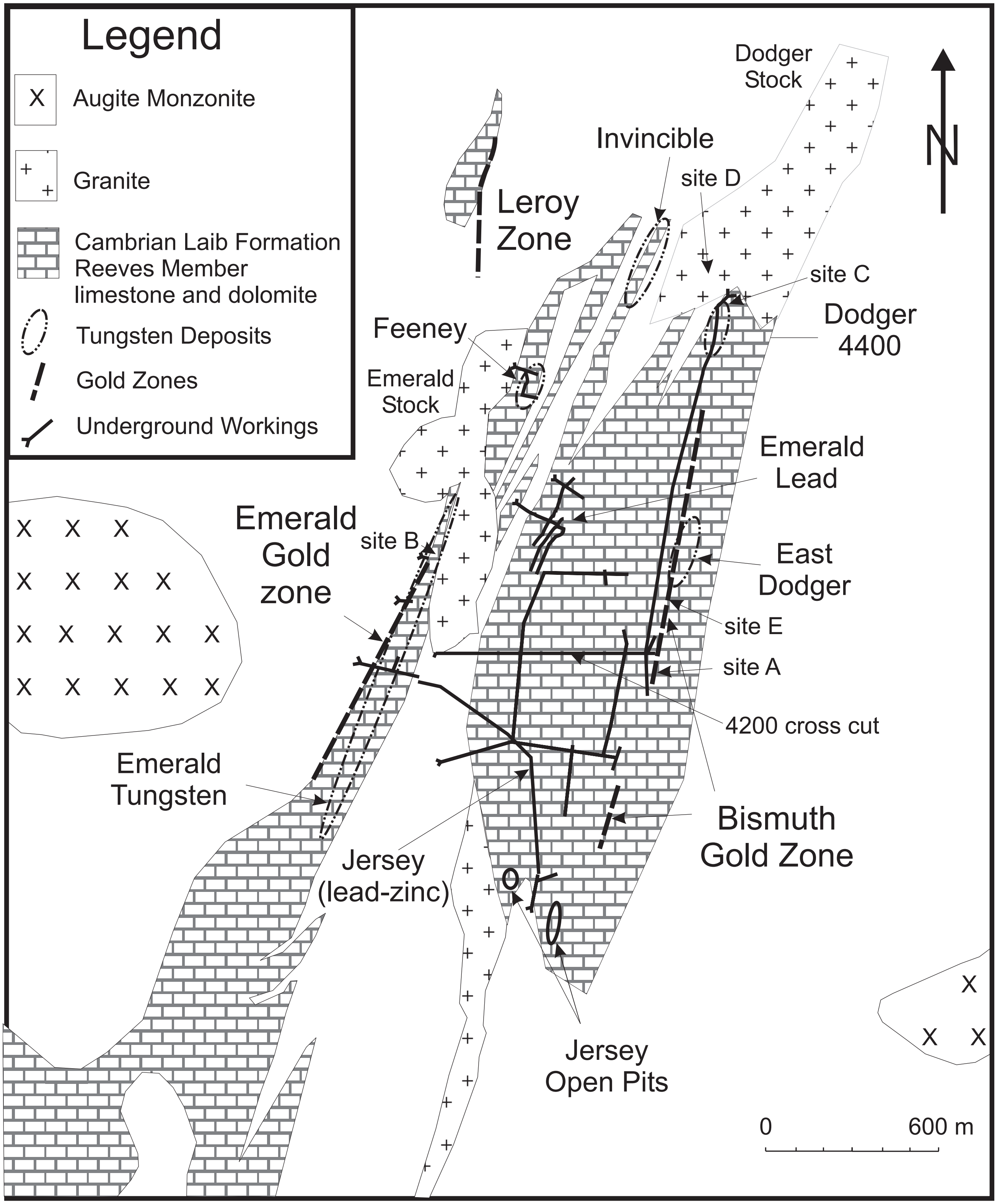

Figure 3. Mineral occurrences of the Jersey Emerald property (derived from Fyles and Hewlett, 1959 and Webster, Ray and Pettipas, 1992).

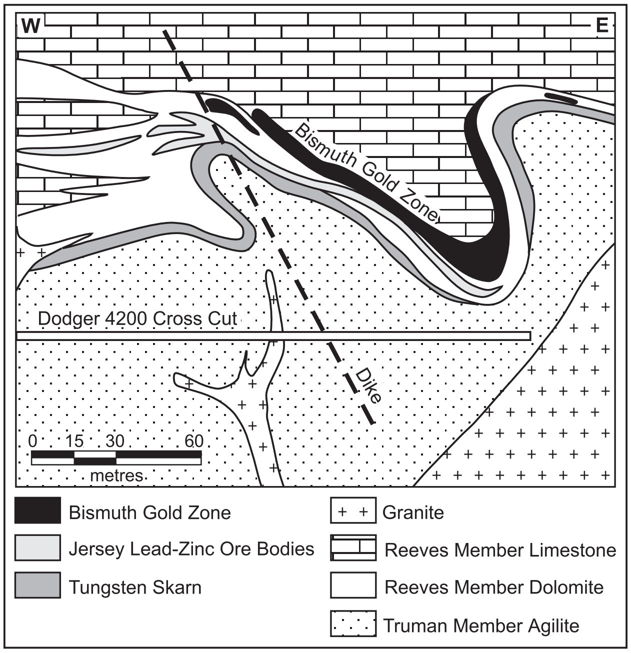

Figure 4. Schematic cross section of the Bismuth Gold zone near the Dodger 4200 crosscut (from Sultan Minerals Inc. 1995 annual report).

band is at the contact between the Reeves limestone and Emerald argillite, the same stratigraphic position as the Emerald gold zone. There are no intrusive rocks or skarn exposed in the immediate area. The quartz band is generally about one metre wide, although locally it is up to 3 metres, with generally less than a couple of percent of arsenopyrite. The veins contain native bismuth which correlates with the best gold values in the quartz (Dandy, 1996). Sulphides can occur over widths of up to a metre on either, or both margins, of the quartz band. Grab sample assays from the Leroy Zone vary from below detection limits up to 30.8 g/t Au and 9256 ppm Bi (Dandy, 1996). A two metre chip sample along the wall of the adit of both host rock and pyrite and pyrrhotite with quartz stringers from the Leroy zone, contained 0.37 g/t Au, 7.4 g/t Ag, 106 ppm Cu, 163 ppm Bi and 100 ppm W (Dandy, 1997).

The importance of stratigraphic position in determining the location of the gold mineralization has been noted by Troup (1994). The two favourable horizons occur in the basal Reeves limestone (Bismuth Gold zone) or at the Reeves limestone and overlying Emerald argillite contact (Emerald and Leroy zones).

More work needs to be done to properly define the characteristics of the three gold zones on the Jersey Emerald property. Obvious common features are:

TABLE 3
SELECTED GEOCHEMICAL ANALYSES OF GOLD-BISMUTH PROSPECTS IN THE NELSON-SALMO AREA, BRITISH COLUMBIA

Property	Showing	Sample #	Au	Ag	As	Bi	Co	Cu	Mo	Ni	Pb	Sb	Se	Te	W	Zn	Comments
Rozan	Ridge Zone	PD-55131	3100	1.4	1.9	14.2	3	18.1	1.9	2	8.7	0.2	1	11.3	40*	10.3	Phelps Dodge sample, Ridge zone
		PD-55132	253	2.5	4.5	4.2	12	29.5	204	4	16.9	<1	<1.5	1.5	9*	3.4	Phelps Dodge sample, Ridge zone
		DVL98-126	305	0.6	1.4	23.5	6	80	80	10	<2	0.2	0.2	21.1	2*	<1	Grab; moly and py on fracture in qtz vn from Main vein dump, Site A, Fig.
		DVL98-127	15	<0.2	1.7	0.4	7	2	2	7	6	0.2	0.2	0.2	5	13	Grab; pegmatitic qtz veinlet (80%) cutting granodiorite (20%), Site B,
		DVL98-128	5	<0.2	0.9	0.2	4	2	2	8	4	0.1	0.1	<0.2	<2	37	Grab; bt qtz diorite with scattered qtz pheno's up to 1 cm, Site C, Fig. 5
		DVL98-129	5	<0.2	1.7	0.1	5	6	6	10	<2	0.1	0.1	<0.2	<2	7	Grab by D. Lefebure; laminated 2 cm qtz vn - 5-10% dilution, Site D, Fig. 5
		DVL98-130	10	<0.2	2.8	0.6	6	3	3	8	4	0.8	0.8	<0.2	<2	15	Grab; sheeted white qtz vns, up to 3 cm wide, trace py, Site D, Fig. 5
		DVL98-131	5	<0.2	1.8	0.3	10	2	2	8	6	0.2	0.2	<0.2	<2	40	Grab; sheeted qtz veinlets, Site D, Fig. 5
Jersey Emerald	Emerald Gold?	GR94-170	3510	4.7	250	823	200	838	55	52	6	7.3	0.1	25	8100	45	Grab, collected by G. Ray, bismuth-rich sulphides, Site B, Fig. 3
	Bismuth Gold	GR94-171	2390	18.1	310	658	11	259	2	16	79	76	2.4	19	8	38	Grab; G. Ray, aspy-po-bismuthinite sample, underground, Site A, Fig. 3
		GR94-172	7630	43.2	160000	2159	45	22	2	9	459	520	12.8	0.3	10	26	Grab; G. Ray, aspy-quartz zone underground, Site A, Fig. 3
		GR94-173	9820	467	140000	9362	110	62	7	12	1651	740	24	6.7	10	45	Grab; G. Ray, aspy-quartz zone underground, Site A, Fig. 3
	Dodger 4400	IWE91-59	1380	19	17800	5	140	720	10	27	51	185	11	14	820	45	Grab; I. Webster, massive po-aspy, portal, Dodger 4400 adit, Site C, Fig.
		DVL98-138	10	0.4	42.9	2.8	2	5	10	23	4	0.3	0.1	0.2	<2	6	Grab; on road; 10 cm qtz vn with vugs, Site D, Fig. 3
	East Dodger	DVL98-136	10	<0.2	12.6	1.5	2	5	1190	11	4	0.7	0.2	0.2	<2	<1	Grab; qtz vn with py, moly; 140' on Dodger ramp, Site E, Fig. 3
		DVL98-137	855	2.6	9910	15.2	10	12	23	8	152	25.3	0.1	0.2	2	799	Grab; py in white quartz vein, 52' on Dodger Ramp, Site E, Fig. 3

Notes:
All values in ppm except Au in ppb
Samples collected by authors unless otherwise noted
All elements by ICP except Au (fire assay with AA finish), unless otherwise noted. GR and IWE samples - Au, As and W by neutron activation, Se and Te by hydride AAS
W by total digestion/ICP except: * by aqua regia (partial) digestion/ICP
n/a not available

- a generally conformable nature with stratigraphy;
- an association with contacts with Reeves Member limestone;
- absence of faults and shears controlling ore lenses;
- the presence of pyrrhotite and arsenopyrite with bismuth minerals (usually native bismuth);
- the existence of both sulphide and quartz-rich zones that appear to grade from one to the other along strike;
- generally similar mineralogy and geochemistry to sulphide-rich tungsten skarn mineralization, although certain minerals and elements are restricted to one style;
- unpredictable anomalous gold values, unless bismuth minerals are present; and
- anomalous bismuth, antimony, arsenic, copper, molybdenum, silver, tellurium and tungsten values.

These features and the close spatial association of the Bismuth Gold and Emerald gold zones with granitic intrusives and tungsten skarns have led Sultan Minerals Inc. staff and Ray and Webster (1997) to interpret the Bismuth Gold zone as skarn-type replacement mineralization. Given the lack of calc-silicate minerals and blanket-like nature of the mineralization, these gold zones could also be called mantos. Mantos are known to occur much further from their related intrusives than skarns, which may explain why the Leroy zone occurs a considerable distance from any known skarn or intrusive. It would also increase the exploration potential of the property distal from intrusions.

The Jersey Emerald property exhibits many of the characteristics of the geological environment of the Tintina Gold Belt in Alaska and the Yukon, including mid-Cretaceous granitic intrusions with associated pegmatites and aplites cutting continental margin host rocks. The presence of tungsten and gold-bismuth replacement zones is a positive metallogenetic indication that the southern Kootenay Arc is prospective for plutonic-related gold-quartz veins similar to deposits found in the Tintina Gold Belt.

Rozan - Ridge Zone

The Rozan property (082FSW179) is located near the summit of Red Mountain, 10 kilometres south-southwest of Nelson (Figure 2). The first claim, called the Golden Eagle, was surveyed on the lower slopes of Red Mountain in 1899. However,serious exploration only began in 1928 when prospector Bill Rozan was attracted to the area because of placer gold in nearby Hall Creek. Rozan searched the mountainside for lode sources of the placer gold for more than 40 years. He started on the lower slopes and eventually discovered several gold-quartz veins, including the Main vein, near the headwaters of Rozan Creek (Figure 5). Following Bill Rozan's death in 1972, Eric Denny of Nelson and Frank Cameron of North Vancouver purchased the property. Since then they have explored the property and optioned it at various times to Harrison Drilling, Hiawatha Resources Inc. and Yukon Revenue Mines Ltd. who completed surface mapping, sampling and trenching on the property (Sevensma, 1988; Craig, 1997).

The region has been mapped by Höy and Andrew (1989a) who show that the area is underlain by argillite and siltstone of the Archibald Formation and andesitic tuff and lapilli tuff of the Elise Formation, both of the Lower Jurassic Rossland Group. These have been intruded by granodiorite and quartz monzonite which is believed to belong to the Middle to Late Jurassic Nelson batholith (Höy and Andrew, 1989b). The biotite granodiorite on the property has sparse quartz and plagioclase phenocrysts up to 1 centimetre in length. It is strongly magnetic and has a pronounced contact metamorphic aureole with disseminated pyrrhotite in hornfelsed sediments that weather a distinctive reddish-brown colour (hence the name Red Mountain). Later minor lamprophyre dykes of probable Cretaceous age (Höy and Andrew, 1989b) cut the property. There are minor aplite, pegmatite and lamprophyre dykes on the property that cut both the Elise Formation tuffs and the granodiorite (Figure 5).

Gold in quartz veins has been the focus of all exploration on the Rozan property. Until recently, the larger solitary quartz veins have attracted the prospecting and development activity. Gold assays and small shipments from the solitary quartz veins vary dramatically from traces to more than 90 grams per tonne gold. The quartz veins have associated minor pyrite and rare visible gold, molybdenum, sphalerite, galena and chalcopyrite. The Main vein, hosted by granodiorite (Figure 5), produced 104 tonnes of hand-selected ore grading 38 g/t Au, 42 g/t Ag, 1.95 % Pb and 1.04 % Zn (MINFILE) between 1928-1958 (Sevensma, 1988). It has been followed for approximately 90 metres underground and is typically 10 to 30 centimetres wide, although it reaches more than a metre in one location (mapping by Santos in Sevensma, 1988). Striking generally north, the Main vein dips from 54 to 70 degrees to the east. A grab sample of quartz from the Main vein dump returned anomalous Au, Bi, Mo, and Te values (Table 3). A number of other solitary quartz veins on the property have been trenched or pitted; although none have produced any ore. The largest is the West vein, located approximately 200 metres west of the Main vein and exposed in several trenches.

The current interest was sparked by the discovery of a more than 1 kilometre-long gold-in-soil anomaly (>30 ppb Au with large areas with >90 ppb Au) with associated anomalous tungsten and copper values (Sevensma, 1988). It extends southeastward from the western boundary of the property along the southern side of Red Mountain and covers most of the area shown in Figure 5, the principle exception being the northeastern corner. Some of the samples within the gold anomaly are also weakly anomalous for bismuth (Jack Denny, personal communication, 1998). Ron Granger of Yukon Revenue Ltd. identified the Ridge zone of auriferous, sheeted quartz veinlets on a ridge near the northeastern limit of the

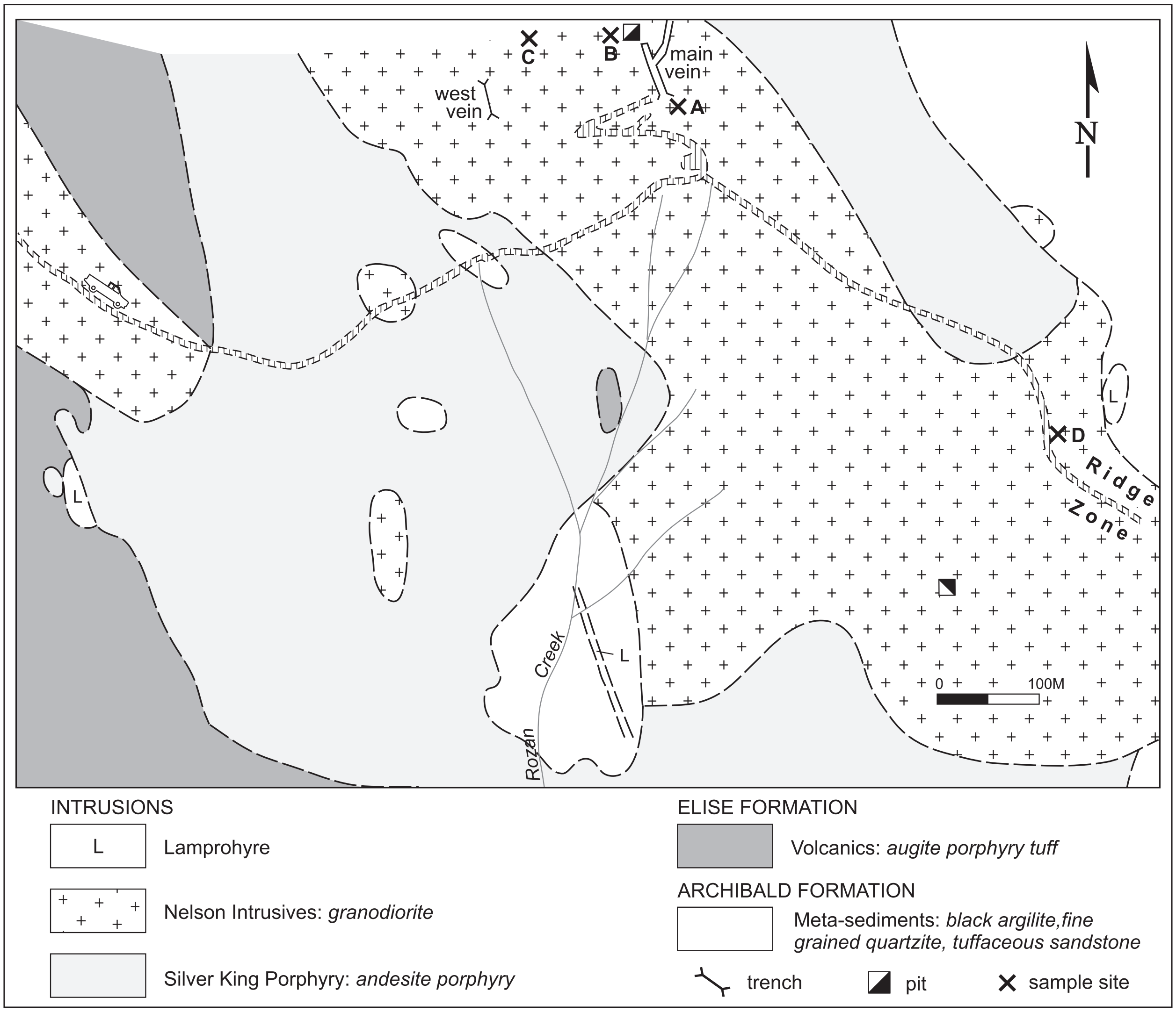

Figure 5. Geology of the central part of the Rozan property (from Sevensma, 1988).

anomaly (along and near the road, southeast of sample site D, Figure 5). Craig (1997) panned three soil samples on the ridge; two showed fine gold dust and small grains of scheelite in two samples. The grey to white veinlets are up to 3 centimetres wide (Photo 7) and generally occur in parallel or sheeted sets with numerous veinlets visible over a 1 to 2 metre wide outcrop. Several sets trend from 140 to 178 degrees with steep dips. There are no obvious wall rock alteration selvages on the veins, although all the feldspars in the granodiorite hosting the veins appear to be weakly altered to clay(?). Trace pyrite grains occur in some veinlets, but not in the host rock. The veinlets are typically featureless, although one quartz veinlet was banded with grey and white quartz.

Seven of twelve samples by collected by Phelps Dodge in 1997 from the Ridge zone carried more than 34 ppb Au and two contained 3604 and 5450 ppb Au with anomalous Bi, Cu and W values (two anomalous samples shown in Table 3). Chip sampling in trench #2, located

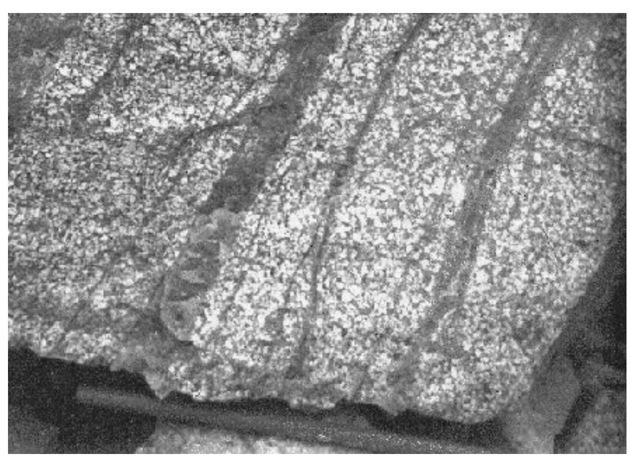

Photo 7. Sheeted quartz veinlets hosted in granodiorite from the Ridge zone of the Rozan property. Field of view is 15 centimetres.

just west of the road along the Ridge zone and approximately 25 metres south of site D, returned 0.93 g/t over 17 metres, including a section with 2.37 g/t Au over 4.5 metres (unpublished report by Yukon Revenue Ltd., Eric Denny, personal communication, 1999). The difficulty in macroscopic identification of auriferous quartz veinlets is shown by sampling at site D. These veinlets appear to be identical to others on the ridge, however, the 3 samples collected here do not contain anomalous Au values (Table 3).

The sheeted auriferous quartz veinlets of the Ridge Zone on the Rozan property look identical to low grade mineralization at the Fort Knox mine in Alaska and Dublin Gulch property in the Yukon. The intrusive host, lack of alteration selvages, low sulphide contents and anomalous Bi, Mo and Te values are consistent with these types of plutonic-related gold deposits.

DISCUSSION AND CONCLUSIONS

Several new showings of gold or tungsten mineralization, with or without associated bismuth, copper, molybdenum, arsenic and tellurium values have been found in southern British Columbia in recent years. In most cases, these showings occur within, or have a close spatial relationship, to mid-Cretaceous intrusive rocks. The exception is the Rozan which is hosted by the Middle Jurassic Nelson batholith. Preliminary work by Logan (this volume) and Logan *et al.* (2000) suggests that some of the mid-Cretaceous intrusions in southern B.C. have broad similarities in age, petrochemistry and depth of emplacement with the prospective Tombstone Plutonic Suite in Alaska-Yukon, which is associated with significant gold deposits such as Fort Knox and Pogo.

The styles of mineralization represented by the new showings include intrusion-hosted solitary veins (Cam-Gloria), intrusion-hosted sheeted veinlets (Rozan, Cam Gloria and Little Creek), skarn (float in "Water Tank" area, Lucky Bear claims), manto? (Bismuth-Gold and E-D 1), and quartz-sulphide layers/veins in upper amphibolite grade metamorphic rocks (Goldstrike and GQ). This array of styles is broadly consistent with proximal to distal portions of plutonic-related gold systems as described by McCoy *et al.* (1997), Thompson *et al.* (1999) and Baker *et al.* (submitted).

The showings described in this paper are mainly gold or tungsten prospects with anomalous values for some or all of the following elements: bismuth, arsenic, copper, molybdenum, lead, zinc and tellurium. The geochemical association of gold with tungsten, bismuth and tellurium in the new B.C. occurrences is a key similarity with the well known deposits in Alaska and Yukon. One important geochemical difference, however, is the relatively high copper content (100 to 1000 ppm) and low arsenic content (<100 ppm) of the B.C. showings relative to the "Tintina Gold Belt" deposits. The exceptions are the arsenopyrite-rich Jersey-Emerald gold occurrences and two minor showings on the Goldstrike property. The genetic significance of this geochemical difference is not understood at this time.

The new discoveries provide useful insights into successful exploration strategies. The importance of using new deposit models to search for gold mineralization on known properties is aptly demonstrated at the Rozan and Jersey Emerald properties. In both cases, continued exploration on well known properties identified new gold zones with many of the characteristics of plutonic-related gold deposits.

In addition, several showings described here were found by conventional prospecting in poorly explored, plutonic and metamorphic terranes. Cam-Gloria was found by follow-up of anomalous gold values in a government till survey, however, several of the other occurences (Goldstrike, GQ, Lucky Bear) were found in areas with no regional geochemical anomalies. This may reflect the poor reliability of gold and tungsten values in silt samples, lack of availability of data for the pathfinder elements bismuth and tellurium, and wide sample spacing and large stream size of conventional government regional geochemical stream sediment surveys. Significantly, the Cam-Gloria and Goldstrike occurrences could have easily been found some time ago as they are both on partially overgrown logging roads.

Conventional grassroots prospecting should focus on locating quartz zones with associated anomalous Au, Bi, Te, W values, in and around mid-Cretaceous plutons, with abundant pegmatite and aplite dikes. Intrusions of Middle Jurassic age (*e.g.* Nelson batholith) also have Au-Bi-W showings (*e.g.* Rozan, Alpine Gold) and should not be ignored. Finally, high-grade metamorphic terranes, such as the Shuswap metamorphic complex, contain multiple ages of intrusive rocks and are under-explored for gold in southern British Columbia. These belts may be worthy of prospecting for deposits similar to multi-million ounce gold, high-grade Liese zone on the Pogo property, Alaska.

ACKNOWLEDGMENTS

This study has benefited from our property visits and the generous sharing of data and ideas by numerous prospectors, geologists, consultants and property owners including Camille Berubé, Linda Dandy (Sultan Minerals Ltd.), Eric and Jack Denny, Graeme Evans and Randy Farmer (Teck Corporation), Jim Gillis (Cassidy Gold Corporation), Warner Gruenwald, Leo Lindinger, Len and Dave Piggin, Wayne Tyner and Ron Wells. In addition, our knowledge of plutonic-related gold deposits was improved by excellent tours of Alaska-Yukon deposits by Thor Bergstrom and Peggy Young (Kinross Gold Corp.), Mike Burke (Northern Affairs Program), Rick Diment and Beth Scott (Viceroy Resource Ltd.), Brian Flanigan (Avalon Development Corp.) and Moira Smith (Teck Corporation). Jim Logan is thanked for reviewing the article and for his patient answers to our many questions on regional geology and tectonics. Bruce Madu and Verna Vilkos assisted in the production of figures.

REFERENCES

Baker, T., Lang, J.R. and Mortensen, J.K. (submitted): Characteristics of mineralization associated with intrusions of the mid-Cretaceous Tombstone-Tungsten magmatic belt, Yukon; *Economic Geology*.

Bobrowsky, P.T., Leboe, E.R., Dixon-Warren, A., Ledwon, A., MacDougall, D. and Sibbick, S.J. (1997): Till Geochemistry of the Adams Plateau-North Barriere Lake Area (82M/4 and 5; *B.C. Ministry of Employment and Investment*, Open File 1997-9, 262 pages.

Brandon, A.D. and Lambert, R.St.J. (1993): Geochemical characterization of mid-Cretaceous granitoids in the Kootenay Arc in the southern Canadian Cordillera; Canadian Journal of Earth Sciences, Volume 30, pages 1076-1090.

Brandon, A.D. and Smith, A.D. (1994) Mesozoic granitoid magmatism in southeast British Columbia: implications for the origin of granitoid belts in the North American Cordillera; *Journal of Geophysical Research*, Volume 99, pages 11,879-11,896.

Brown, R. L. and Carr, S. D. (1990): Lithospheric thickening and orogenic collapse within the Canadian Cordillera; *Australasian Institute of Mining and Metallurgy*, 1990 Pacific Rim Congress Proceedings, Volume II, pages 1-10.

Campbell, R.B. (1963): Adams Lake Map-area, British Columbia, *Geological Survey of Canada*, Map 48-1963, 1:250,000.

Cathro, M.S. (1998): Exploration and Development Highlights in South-Central British Columbia - 1997; *B.C. Ministry of Energy and Mines*, Exploration in British Columbia - 1997, pages 33-41.

Craig, L.O. (1997): Geochemical and Geological Report, Rozan Property; *B.C. Ministry of Energy and Mines*, assessment report 24,843, 18 pages.

Dandy, L. (1996): Geological, geochemical and geophysical report on the Jersey-Emerald and Posie properties; B.C. Ministry of Energy, Mines and Petroleum Resources, assessment report # 24531, 40 pages.

Dandy, Linda (1997): Geological, Geochemical and Diamond Drill Report on the Jersey-Emerald property; *B.C. Ministry of Energy and Mines*, assessment report 24,910, 57 pages.

Dawson, K.M. (1996): Skarn zinc-lead-silver; *in* Geology of Canadian Mineral Deposit Types, O.R. Eckstrand, W.D. Sinclair and R.I. Thorpe, Editors, *Geological Survey of Canada*, Geology of Canada, Volume 8, pages 448-459.

Fyles, J.T. and Hewlett, C.G. (1959): Stratigraphy and structure of the Salmo lead-zinc area, British Columbia; *B.C. Ministry of Energy, Mines and Petroleum Resources*, Bulletin 45, 92 pages.

Gruenwald, W. (1999): Summary Report on the Goldstrike Property; Internal Company Report for Cassidy Gold Corp., 18 pages.

Höy, T. (1982): Stratigraphic and structural setting of stratabound lead-zinc deposits in southeastern B.C.; Canadian institute of Mining and Metallurgy, Bulletin 75, pages 114-134.

Höy, T. and Andrew, K. (1989a): Geology of the Nelson Map Area, Southeastern British Columbia; *B.C. Ministry of Energy, Mines and Petroleum Resources*, Open File 1989-11.

Höy, T. and Andrew, K. (1989b): The Rossland Group, Nelson map Area, Southeastern British Columbia; *B.C. Ministry of Energy, Mines and Petroleum Resources*, Geological Fieldwork 1988, paper 1989-1, pages 33-44.

Johnson, B.J. (1994): Structure and tectonic setting of the Okanagan Valley fault system in the Shuswap Lake area, southern British Columbia; unpublished Ph.D. thesis, *Carleton University*, 266 pages.

Lawrence, E.A. (1997): Diamond Drilling Report on the Jersey Property, Nelson Mining Division, Salmo, B.C.; *B.C. Ministry of Energy and Mines*, assessment report 25,349, 39 pages.

Lett, R.E., Bobrowsky, P., Cathro, M, and Yeow, A. (1998): Geochemical Pathfinders for Massive Sulphide Deposits in the Southern Kootenay Terrane; *B.C. Ministry of Employment and Investment* Geological Fieldwork 1997, pages 15-1-9.

Lett, R.E. and Jackaman, W. (this volume): Geochemical Exploration Techniques for Intrusive Hosted Gold Deposits in Southern B.C. (parts of 82M/4, 5, 6 and 82F/7); *in* Geological Fieldwork 1999, *B.C. Ministry of Energy and Mines,* Paper 2000-1.

Lefebure, D.V., Fournier, M.A. and Jackaman, W. (1999): Prospective areas in British Columbia for gold-tungsten-bismuth veins; *B. C. Ministry of Energy and Mines*, Open File 1999-3, 1:2 000 000 scale map with marginal notes and digital files.

Lefebure, D.V. and Cathro, M. (1999): Plutonic-related gold-quartz veins and their potential in British Columbia; *in* Short Course on Intrusion-Related Gold, *Kamloops Exploration Group*, p. 185-219.

Logan, J.M. and Mann, R.K. (2000a): Geology and Mineralization in the Adams -East Barriere lakes area, South-central British Columbia, 82M/04; *B.C. Ministry of Energy and Mines*, Open File 2000-7.

Logan, J.M. and Mann, R.K. (2000b): Geology and Mineralization around the Mount Skelly Pluton, Kootenay Lake, Southeastern British Columbia, 82F/07; *B.C. Ministry of Energy and Mines*, Open File 2000-8.

Logan, J., Lefebure, D., and Cathro, M. (2000): Plutonic-Related Gold-Quartz Veins and their Potential in British Columbia; *in* J.L. Jambor, Editor, The Tintina Gold Belt: Concepts, Exploration and Discoveries, *British Columbia and Yukon Chamber of Mines*, Special Volume 2.

McCoy, D., Newberry, R.J., Layer, P., DiMarchi, J.J., Bakke, A., Masterman, J.S., and Minehane, D.L. (1997): Plutonic-related Gold Deposits of Interior Alaska; *Economic Geology*, Monograph 9, pages 191-241.

Monger, J.W.H. and Berg, H.C. (1984) Lithotectonic terrane map of western Canada and southeastern Alaska; *in* Lithotectonic Terrane Maps of the North American Cordillera, N.J. Siberling and D.L. Jones Editors, *United States Geological Survey*, Open File Report 84-523.

Monger, J.W.H., Price, R.A. and Tempelman-Kluit, D.J. (1982): Tectonic accretion and the origin of the two major metamorphic and plutonic welts in the Canadian Cordillera; *Geology*, Volume 10, pages 70-75.

McMillan, W.J. (1973): Petrology and Structure of the West Flank, Frenchman's Cap Dome, Near Revelstoke, British Columbia; *Geological Survey of Canada*, Paper 71-29, 88 pages.

Nelson, J.L. (1991): Carbonate-hosted lead-zinc (± silver, gold) deposits of British Columbia*; B.C. Ministry of Energy, Mines and Petroleum Resources*, paper 1991-4, pages 71-88.

Okulitch, A.V. (1984): The role of the Shuswap Metamorphic Complex in Cordilleran Tectonism, a review; *Canadian Journal of Earth Sciences*, Volume 16, pages1171-1193.

Parrish, R.R. (1995): Thermal Evolution of the Southeastern Canadian Cordillera; *Canadian Journal of Earth Sciences*, Volume 32, pages 1618-1642.

Parrish, , R.R., Carr, S.D. and Parkinson, D.L. (1988): Eocene extensional tectonics and geochronology of the southern Omineca Belt, British Columbia and Washington; *Tectonics*, Volume 7, pages 181-212.

Poulsen, K.H, Mortensen, J.K. and Murphy, D.C. (1997): Styles of intrusion-related gold mineralization in the Dawson-Mayo

Area, Yukon Territory; *in* Current Research 1997-A, *Geological Survey of Canada*, pages 1-10.

Ray, G.E. and Webster, I.C.L. (1997): Skarns in British Columbia; *B.C. Ministry of Energy and Mines*, Bulletin 101, 131 pages.

Read, P.B., Woodsworth, G.J., Greenwood, H.J., Ghent, E.D. and Evanchick, C.A. (1991): Metamorphic Map of the Canadian Cordillera, *Geological Survey of Canada*, Map 1714A, scale 1:2 000 000.

Rennie, C.C. and Smith, T.S. (1957): Lead-zinc and tungsten orebodies of Canadian Exploration Limited, Salmo, B.C.; *Canadian Institute of Mining*, Structural Geology of Canadian Ore Deposits, Volume II, pages 116-124.

Schiarizza, P. and Preto, V.A. (1987): Geology of the Adams Plateau-Clearwater-Vavenby area; *B.C. Ministry of Energy, Mines and Petroleum Resources*, Paper 1987-2, 88 pages.

Sevensma, P.H. (1988): Geological and Geochemical Report, Rozan Property*; B.C. Ministry of Energy, Mines and Petroleum Resources*, assessment report 18,188, 10 pages.

Sevigny, J.H., Parrish, R.R., Donelick, R.A., and Ghent, E.D. (1990): Northern Monashee Mountains, Omineca Crystalline Belt, British Columbia: Timing of metamorphism, anatexis and tectonic denudation; *Geology*, volume 18, pages 103-106.

Smith, M. , Thompson, J.F.H., Bressler, J., Layer, P., Mortensen, J.K., Abe, I. and Takaoka, H. (1999): Geology of the Liese Zone, Pogo Property, East-Central Alaska; *SEG Newsletter*, No. 38, July 1999 pages 12-21.

Thompson, J.F.H., Sillitoe, R.H., Baker, T., Lang, J.R. and Mortensen, J.K. (1999): Intrusion-related gold deposits associated with tungsten-tin provinces; *Mineralium Deposita*, Volume 34, Number 4, pages 323-334.

Thompson, R.I. (1974): Invincible, East Dodger; *British Columbia Department of Mines and Petroleum Resources*, Geology, Exploration and Mining In British Columbia, pages 54-57.

Troup, A.G. (1994): Geophysical, Geochemical and Core Research on the Jersey property, Nelson Mining Division, Salmo, B.C.; *B.C. Ministry of Energy, Mines and Petroleum Resources*, assessment report 23486, 26 pages.

Webster, I.C.L., Ray, G.E., and Pettipas, A.R. (1992): An Investigation of Selected Mineralized Skarns in British Columbia; in Geological Fieldwork 1991, *B.C. Ministry of Energy, Mines and Petroleum Resources,* Paper 1992-1, pages 235-252.

Wells, R.C. (1998): An Evaluation of Mineral Potential on the E-D 1 Property; internal company report for Manto Mining Corporation.

Wheeler, J.O. (1965): Big Bend Map-Area, British Columbia, 82M (East Half); *Geological Survey of Canada*, Paper 64-32, 37 pages.

Wheeler J.O. and McFeely, P. (1991): Tectonic Assemblage Map of the Canadian Cordillera and adjacent parts of the United States of America*; Geological Survey of Canada*, Map 1712A, scale 1:2 000 000.

Geochemical Exploration Techniques for Plutonic-related Gold Deposits in Southern B.C. (NTS 82M/4, M/5, M/6 and 82F/7)

By Ray Lett and Wayne Jackaman

KEYWORDS: *Plutonic-related gold deposits, moss mat sediment, stream sediment, Regional Geochemical Surveys.*

INTRODUCTION

Discovery of the Liese Zone on the Pogo property in Alaska (containing an estimated 9.98 million tons of ore grading 0.52 oz gold/ton) where gold-arsenic-copper-bismuth mineralization occurs in gneiss-related quartz bodies close the margin of a Cretaceous batholith (Smith *et al.,* 1999) has stimulated exploration for similar plutonic-related gold deposits in British Columbia. The Pogo property was discovered by follow-up of a subdued (35 ppb) stream sediment geochemical gold anomaly (Robertson, 1998). Similarly, only 15 ppb gold was detected by a regional stream survey in a sediment sample collected from a creek draining the Cam-Gloria mineral occurrence (MINFILE 82M 266), a gold-bismuth-lead mineralized, granite-hosted quartz vein, in southern B.C. (Matysek *et al.,* 1991). This occurrence was found in 1997 by prospecting after anomalous gold values were identified in a regional till sample close to the mineralized vein (Bobrowsky *et al.,* 1997).

There is presently limited published information about the geology or the application of geochemistry for plutonic-related gold deposits in British Columbia. These deposits may be difficult to find by traditional stream sediment surveys because the gold and associated pathfinder elements such as tin, bismuth and tungsten are relatively immobile and tend to be erratically distributed in the sediment. Drainage sediments in British Columbia are also prone to dilution by barren glacial material (unlike the non-glaciated area in Alaska where the Pogo property is located) and therefore gold anomaly contrast may be more subdued. In general, gold anomaly contrast can be improved using more appropriate sample media such as moss mat sediment or a heavy mineral fraction (Matysek and Day, 1987).

A study was carried out in August 1999 by the authors to compare the geochemical response of intrusive-related gold mineralization in different reconnaissance scale sample media such as stream sediment, moss mat sediment and heavy mineral concentrates. The study is part of a Geological Survey Branch initiative to examine the potential for intrusive-related gold deposits in the Province. Results of the geological component are described by Logan, 2000, Geological Fieldwork 1999, Paper 2000-1, this volumes). Geochemical samples were collected in two areas of southern British Columbia, one near Adams Lake and the other east of Kootenay Lake.

Objectives of this study were to 1) develop a better understanding of the stream geochemical response of plutonic-related mineralization; 2) compare the merits (cost effectiveness) of different stream sampling, sample preparation and analytical methods to improve the ability of stream sediment geochemistry to detect plutonic-related gold mineralization; 3) add value to the current RGS database to stimulate future mineral exploration and; 4) evaluate other factors such as element backgrounds in different sample media and bedrock types for improving methods of geochemical data interpretation.

This paper describes the survey areas, sampling technique, the sample preparation and analytical methods used and discusses preliminary geochemical results.

ADAMS LAKE SURVEY AREA DESCRIPTION (NTS 82M/4, M/5, M/6 and 92P/8)

Location

Detailed stream geochemical studies in parts of NTS map sheet 82M/4, M/5 and M/6 focused on the area around the Cam-Gloria Gold occurrence (MINFILE 82M 266) located west of Honeymoon Bay on Adams Lake. Regional stream sampling covered a larger 350 square kilometre area to the west and north-west. Three sites were also sampled within the Newhykulston Creek watershed in NTS 92P/8 (Figure 1).

Physiography and Climate

The survey area is within the Shuswap Highlands, a region of broad forested mountains of moderate to high relief (Holland, 1976). The region bounded by Gollen Creek, Adams Lake, Fennel Creek and the East Barriere River is a dissected plateau with an undulating surface averaging 1700 metres above sea level and with hill tops reaching 1800 metres. Principal drainage is by the west

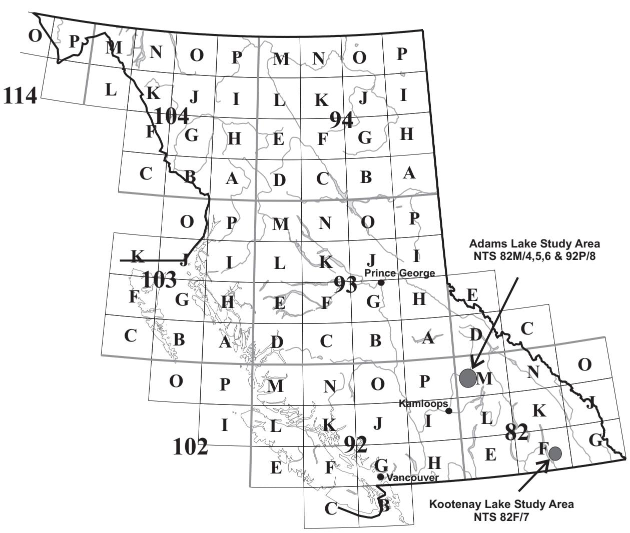

Figure 1. Location of survey areas.

flowing Fennel Creek, East Barriere River and Bendelin Creek and to the east by Spapilem, Fisher, Stratton and Gollen Creeks. The creeks draining into Adams Lake typically have steep gradients (10-15 degrees), are fast flowing and follow steep-sided, deep valleys. The two tributaries of Newhykulston Creek, where samples were collected, join to flow west into the North Thompson River from a rolling plateau that has an average elevation of 1700 metres above sea level.

The climate of the area is moist and temperate. Winter temperatures typically range from - 10 to -15 ^{o}C, summer temperatures can reach 30^{o}C. Annual precipitation averages 417 mm (measured at Vavenby) falling as snow in the winter months and as rain mainly between June and July. The spring freshet occurs between mid May and late June.

Bedrock Geology

The survey area is partly underlain by Cambrian to Mississippian rocks of the Eagle Bay Assemblage and Fennell Formation and by the mid-Cretaceous Baldy Batholith. The Eagle Bay Assemblage, part of the Kootenay Terrane, was originally deposited along the ancestral margin of North America. Older Eagle Bay rocks range from quartzites, quartz-rich schists and limestone. These are overlain by grit, phyllite and quartz mica schist and coarse grained clastic metasediments interbedded with felsic volcanic rocks. Above the metasedimentary rocks are limestone and calcareous phyllite, calcsilicate schist and skarn, pillowed greenstone and chlorite-sericite-quartz schist of felsic origin. At the top of the sequence are slates and siltstone. The Fennell Formation is a Devonian to Permian sequence of oceanic bedded cherts, gabbro, diabase, pillow basalt, sandstone, quartz-porphyry rhyolite and conglomerate that forms part of the Slide Mountain Terrane and has a thrust contact with Eagle Bay Assemblage. The mid-Cretaceous Baldy Batholith is predominantly massive light-grey, coarse-grained quartz monzonite. Xenoliths of country rock are common close to the contact of the Batholith with the Eagle Bay Assemblage. The eastern and northern margins of the Batholith are marked by medium-grey biotite and muscovite Devonian orthogneiss. In addition to the Baldy Batholith there are several smaller satellite intrusive granitic bodies and one of these has been mapped close to the headwaters of Newhykulston Creek (Schiarriza and Preto, 1987).

Surficial Geology

The uplands are mainly covered by till, colluvium, and glaciofluvial deposits, whereas fluvial, glaciofluvial and glaciolacustrine sediments have accumulated in the valleys. These sediments were deposited initially by a predominately northwest to southeast ice advance followed by deglaciation processes during the late Wisconsin. There are two types of basal till deposited in the area, each reflecting a different bedrock source. South of the survey area where geology is dominated by metavolcanic and metasedimentary rocks basal till is massive to poorly stratified with a sandy silt to silty clay texture. In most of the stream survey area, however, the basal till is sandier and light to medium grey in colour reflecting a granitic bedrock source. Boulder fields and massive clast-supported ablation till covers bedrock and basal till on the plateau. The ablation till is generally less compact, dense and cohesive and the sandy matrix is poorly consolidated. Clast content is higher than basal till (up to 45 per cent) and clast size ranges from granule to boulder. Clast lithologies are almost entirely of Baldy Batholith rocks (Dixon-Warren *et al.,* 1997).

Mineral Occurrences

The principal mineral occurrence in the survey area is the Cam-Gloria Gold property (MINFILE 82M 266) discovered in 1997 by follow-up of a regional till geochemical anomaly (Bobrowsky *et al*, 1997). The "discovery" occurrence is a large, rusty auriferous quartz vein located on the north fork of the Grizzly Creek Forest Service road, approximately 3 kilometres west of the Honeymoon Bay campsite on Adams Lake. The vein strikes at 50 degrees, dips steeply northwest and is up to 10 metres wide and roughly 200 metres in length. Pyrite, galena and minor chalcopyrite occur in the quartz and samples of the sulphide-rich vein material contain 1.38 ppm gold, 7.8 ppm silver, 55 ppm bismuth, 430 ppm lead, 118 ppm copper and 21 ppm molybdenum (Lett *et al.,* 1998). Within one kilometre of the auriferous quartz vein there are several narrow monzonite-hosted quartz-fluorite veins and a 30 centimeter wide quartz-pyrite-pyrrhotite vein.

Two other documented mineral occurrences within or close to the Baldy Batholith are the NSP (MINFILE 82M 127) near the headwaters of Spapilem Creek where chalcopyrite occurs as disseminations and in thin quartz stringers in quartz-biotite gneiss and the SAN (MINFILE 82M 135) between North Barriere and Saskum Lakes where pyrite, galena, sphalerite and chalcopyrite occur in a granite hosted, sheared quartz vein.

KOOTENAY LAKE SURVEY AREA DESCRIPTION (82F/07)

Location

The geochemical survey covered roughly 150 square kilometre southeast of Boswell on Kootenay Lake within the watersheds of Akokli, Sanca and Skelly Creeks (Figure 1). Stream sampling included creeks draining known mineral occurrences on Mount Sherman and Mount Dickson.

Physiography and Climate

The survey area is located in the southern Purcell Mountains. Elevations range from 550 metres on the shore of Kootenay Lake to 2700 metres on the peak of Haystack Mountain. Principal watersheds are of those Akokli and Sanca Creeks and east flowing Skelly Creek. The height of land between Akokli and Sanca Creeks is very rugged and the highest elevation (2700 metres) on this ridge is Mount Sherman. South of Sanca Creek the topographic relief is more subdued and above 1700 metres the land surface is a rolling, forested plateau.

Climate of the area is moist and temperate. Winter temperatures average - 6^{o}C and in summer reach 30^{o}C. Annual precipitation averages 580 mm (measured at Bonners Ferry) falling mainly as snow at higher elevations in the winter months. The spring freshet occurs between mid-May and late June.

Bedrock Geology

Most of the survey area is underlain by rocks of the Cretaceous Bayonne Batholith. This Batholith comprises white to light-grey, medium to coarse-grained biotite granite and quartz monzonite. These rocks intruded siltstones and quartzites of the Creston Formation which forms the lower part of the Proterozoic Purcell Supergroup. The contact between the Creston Formation and Bayonne Batholith is located just south of Akokli Creek and trends northwest to southeast (Borovic, 1987).

Surficial Geology

Glacial and recent surficial deposits range from talus and colluvium above timber line and on steep slopes to basal till at lower elevations. Thick glaciofluvial, glaciolacustrine and fluvial deposits fill the major valleys and the Kootenay Lake basin. The till, deposited by a predominately north to south ice advance parallel to Kootenay Lake during the Fraser Glaciation is sandy textured reflecting a predominantly granite source rock (Fulton and Smith, 1978). Glacial and inter-glacial deposits from earlier Wisconsinian glaciations including Okanagan Centre till, paleosol and Bessette sediments have been recognised at the north end of Kootenay Lake (Alley *et al.*, 1986).

Mineral Occurrences

Mineral occurrence in the survey area are typically polymetallic gold-silver-lead-zinc-tungsten veins and mineralized quartz vein stockworks hosted by the granite and quartz monzonite. The Valparaiso occurrence (MINFILE 82FSE 038), located north of Ginol Creek and south of Akokli Creeks is a quartz-filled fissure containing pyrite, arsenopyrite, wolframite, galena, sphalerite and chalcopyrite in granite and granodiorite locally altered to chlorite and sericite. Gold and silver are disseminated in the quartz. The German (Gold) Basin showing (MINFILE 82FSE 039) is also a gold mineralized quartz vein in granodiorite at an elevation of 2133 metres located on the western slope of Mount Sherman. The vein contains scattered irregular bands and patches or pyrite, galena, chalcopyrite and scheelite. Typical metal concentrations of the vein material are 39.7 percent lead, 366 grams per tonne silver and 3.4 grams per tonne gold. The Elmo showing (MINFILE 82FSE 137), located in a cirque west of Mount Dickson, is a stockwork of quartz-muscovite veinlets in medium grained, equigranular and coarse- grained to porphyritic quartz monzonite phases of the Bayonne Batholith. Within the stockwork are scattered molybdenite, scheelite, fluorite, magnetite, pyrite and chalcopyrite grains.

SAMPLING TECHNIQUES

An objective of the study was to compare the geochemical response from plutonic-related gold mineralization in different sample media at an average density of 1 sample per 12 kilometres typical of a routine regional stream geochemical survey. Samples were taken from larger, first and second order creeks draining catchments covering 10 - 15 square kilometres and especially creeks where previous regional stream sediment and till surveys had detected anomalous gold levels. More detailed stream sampling at a higher density was attempted around known gold occurrences. Samples were collected in August, 1999 following the spring freshet. The number and type of samples collected in each are summarized in Table 1.

A total of 68 stream water, 74 stream sediment and 74 moss mat samples (including field duplicates) were collected from 40 sites in 82M/4, 82M/5 and 82M/6 (Adams Lake area), 3 sites in 92P/8 (Newhykulston Creek) and 25 sites in 82F/7 (Kootenay Lake area). In addition 25 bulk screened sediment samples were taken from selected sites for analysis of gold and other elements in a -150 (<100 micron) mesh heavy mineral fraction. The bulk samples were collected from the higher energy environment corresponding to a coarse gravel deposit in the stream channel by wet-sieving sufficient material through an 18 mesh (<1 millimetre) nylon screen to recover 10 kilograms of <1 millimetre sized sediment. Wet

TABLE 1
SUMMARY OF SAMPLES COLLECTED

Element	82M/4,5,6	92P/8	82F/7	Total
Stream Sediment	42	4	28	74
Moss Mat Sediment	42	4	28	74
Bulk Sediment	17	2	6	25
Water	40	3	25	68
Water Filter	17	2	6	25
Rock	16	0	1	17

sieving typically needed one hour to obtain 10 kilograms of the <1 millimetre fraction and the material was then stored in a heavy-duty plastic bag.

Fine textured sediment, typical of material routinely collected during a regional survey was also taken, generally from the sandy part of a bar in the stream channel, and stored in a high wet strength Kraft paper bag. Live moss containing trapped sediment, collected from the surface of boulders or logs in the active stream above the water level, was also stored in Kraft bags. Abundant moss occurred at almost all of the stream sites and was only sparse in areas disturbed by logging. Water samples were collected by filling a 125 millilitre high-density polyethylene bottle after previously rinsing the bottle with the stream water. A two litre bulk water sample was collected at selected sites (generally where a bulk sediment was taken) and later filtered through a 0.45 micron filter to recover the suspended sediment.

Considerable effort was made to chose sample sites upstream of known anthropogenic disturbances such as bridges or culverts or logged areas. This was often difficult in practice because of extensive logging in both survey areas. In fact, detailed stream sediment sampling around the Cam-Gloria occurrence was limited because of poorly developed primary drainages and considerable surface disturbance of stream channels by logging. During regional sampling where a stream flowed through an obviously disturbed area every effort was made to locate the sample site in a undisturbed riparian zone or where secondary timber growth had stabilized the terrain. Field observations about sample media, sample site, local terrain and float geology were recorded and an aluminum tag inscribed with the sample identification number was fixed to a permanent object at each sample site.

SAMPLE PREPARATION

Sediment and moss mat samples were prepared by Eco-Tech Laboratories Ltd. (Kamloops, B.C). The samples were air dried and the - 80 ASTM mesh (<177 micron) fraction recovered by disagregating the sediment or pounding the moss and then dry sieving through a stainless steel screen. Control reference material and analytical duplicate samples were inserted into each analytical block of twenty sediment samples at the Geological Survey Branch Laboratory in Victoria. Any remaining - 80 mesh sediment was archived for future analyses.

The <1 millimetre fraction of bulk stream sediments were processed by C.F.Minerals Research Ltd. (Kelowna, B.C.) to recover heavy minerals. Samples were wet sieved into the following size fractions: - 20+35, - 35 +60 and - 60 mesh and after drying, the - 60 mesh fraction was slowly fed into the middle of a column of tetrabromomethane (TBE), with a specific gravity of 2.96. The resultant heavy minerals that settled to the bottom of the TBE column were then further separated by methylene iodide (MI), with an effective specific gravity of 3.27. The minerals with a specific gravity above 3.27 are called the heavy (H) fraction. The - 60 mesh heavy fraction was then further sieved into - 60 +150 and - 150 (<100 micron) mesh fractions. A Frantz electromagnetic separator was use to generate distinct -150 mesh, heavy fractions based on variations in magnetic susceptibility, as follows: magnetic (M), paramagnetic (P) and nonmagnetic (N). The - 150 mesh, heavy, nonmagnetic fractions (-150HN) were placed in vials for neutron activation analysis.

SAMPLE ANALYSIS

The prepared stream sediment, moss mat sediment and quality control samples were analysed for bismuth by aqua regia digestion - hydride generation atomic absorption spectroscopy (AAS-H) and for cadmium, cobalt, copper, iron, lead, manganese, nickel, silver and zinc by aqua regia digestion - flame atomic absorption spectroscopy (AAS). Background corrections were made for lead, nickel, cobalt and silver. The analytical methods are described in more detail by Matysek *et al.,* 1991. Fluorine content of samples was determined by the sodium carbonate-nitric acid fusion-fluoride ion electrode method (FION) described by Ficklin (1970). The samples were also analysed for molybdenum and vanadium by an aqua regia digestion and atomic absorption spectroscopy using a nitrous oxide acetylene flame. Aluminium chloride solution was added to the digested sample solution as a releasing agent before the determination of molybdenum and vanadium by atomic absorption. Mercury was determined by aqua regia digestion - flameless atomic absorption (AAS-F) using the method described by Jonasson *et al*. (1973). Samples were analysed for tin by ammonium iodide fusion, trioctylphosphine oxide - methyl iobutyl ketone extraction and flame atomic absorption spectrometry (NAIAA) as described by Moldan *et al.* (1970). Loss on ignition of sediment and moss mat samples (GRAV) was determined by ashing the material at 500^{o}C for three hours and then weighing the residue. All of the atomic absorption, fluorine and tin analyses were carried out by CanTech Laboratories (Calgary, Alberta). Reported detection limits for the elements determined by atomic absorption, fluoride and loss on ignition are given in Table 2.

A representative split of each sediment, rock and heavy mineral sample was analysed for antimony, arsenic, barium, bromine, cerium, cesium, chromium, cobalt, gold, hafnium, iron, lanthanum, lutetium, nickel, rubidium, samarium, scandium, sodium, tantalum, terbium,

TABLE 2
REPORTED DETECTION LIMITS

Element	N	Mthd	D.L.	Unit
Antimony	Sb	INA	0.1	ppm
Arsenic	As	INA	0.5	ppm
Barium	Ba	INA	50	ppm
Bromine	Br	INA	0.5	ppm
Calcium	Ca	INA	1	%
Cerium	Ce	INA	3	ppm
Cesium	Cs	INA	1	ppm
Chromium	Cr	INA	5	ppm
Cobalt	Co	INA	1	ppm
Europium	Eu	INA	2	ppm
Gold	Au	INA	2	ppb
Hafnium	Hf	INA	1	ppm
Iron	Fe	INA	0.01	%
Lanthanum	La	INA	0.5	ppm
Lutetium	Lu	INA	0.05	ppm
Neodymium	Nd	INA	5	ppm
Rubidium	Rb	INA	15	ppm
Samarium	Sm	INA	0.5	ppm
Scandium	Sc	INA	0.1	ppm
Sodium	Na	INA	0.01	%
Tantalum	Ta	INA	0.5	ppm
Terbium	Tb	INA	0.5	ppm
Thorium	Th	INA	0.2	ppm
Tungsten	W	INA	1	ppm
Uranium	U	INA	0.5	ppm
Ytterbium	Yb	INA	0.2	ppm
Bismuth	Bi	AAS-H	0.2	ppm
Cadmium	Cd	AAS	0.2	ppm
Cobalt	Co	AAS	2	ppm
Copper	Cu	AAS	2	ppm
Iron	Fe	AAS	0.02	%
Lead	Pb	AAS	2	ppm
Loss on Ignition	LOI	GRAV	0.1	%
Mercury	Hg	AAS-F	10	ppb
Manganese	Mn	AAS	5	ppm
Molybdenum	Mo	AAS	1	ppm
Nickel	Ni	AAS	2	ppm
Silver	Ag	AAS	0.2	ppm
Tin	Sn	NAIAA	1	ppm
Vanadium	V	AAS	5	ppm
Zinc	Zn	AAS	2	ppm
Fluoride (waters)	FW	ION	20	ppb
pH (waters)	pH	GCE		
Sulphate(waters)	$S0_4$	TURB	1	ppm
Uranium (waters)	UW	AAS	0.05	ppb

thorium, tungsten, uranium, ytterbium and zinc using thermal, instrumental neutron activation analysis (INAA) by Activation Laboratories (Ancaster, Ontario). Instrumental neutron activation analysis involves irradiating the sediment samples, which range from 1 to 46 grams for 30 minutes with neutrons (flux density of $7x10^{11}$ neutrons/cm^2/second). After approximately 1 week, the gamma-ray emissions for the elements are measured using a gamma-ray spectrometer with a high resolution, coaxial germanium detector. Counting time was approximately 15 minutes per sample. Table 2 lists the detection limits reported for elements determined by this method.

Water samples were analysed for pH, sulphate, fluoride and uranium by CanTech Laboratories (Calgary, Alberta). Detection limits for each element are listed in Table 2. The pH of water samples was measured using a combination glass-reference electrode (GCE). Sulphate was determined by a barium sulphate suspension turbidimetric method (TURB). Water samples were analysed for fluoride by mixing an aliquot of the sample with an equal volume of total ionic strength adjustment buffer (TISAB II solution) and measuring fluoride ion content using a Corning 101 meter with an Orion fluoride electrode (ION). Uranium in waters was determined by laser-induced fluorescence analysis (LIF) with a Scintrex UA-3 uranium analyzer.

PRELIMINARY RESULTS

Neutron activation data for stream sediment and moss mat sediment samples are discussed in this paper. Because of the small number of drainage samples collected only six field duplicate moss mat sediment and eight analytical duplicate samples were analysed. The R^2 correlation coefficients are greater than +0.9 for most elements in the field duplicate sample pairs and in the analytical duplicate sample pairs. This demonstrates good sampling and analytical reliability. An exception is the poor correlation (R^2 coefficient + 0.227) between gold values for moss sediment field duplicate samples (Table 3). This large variation between duplicate samples has been observed by Matysek, Gravel and Jackaman, (1988) and is believed to reflect local differences affecting the entrapment and sorting of sediment by the moss.

Statistics (mean, median, standard deviation, maximum value, minimum value) for gold, loss on ignition and 39 other elements in stream sediment and moss mat sediment samples are listed in Tables 4 and 5. Data from both survey areas was combined to calculate the statistics. The majority of elements demonstrate higher mean, median and maximum concentrations in moss mat sediments compared to stream sediments. Most notable is gold that exceeds 1000 ppb in moss mat sediment from two sites, but only reaches 59 ppb in stream sediments.

TABLE 3
ARITHMETIC CORRELATION COEFFICIENTS FOR ANALYTICAL AND FIELD DUPLICATE SAMPLES

Element	Analytical Duplicates	Field Duplicates
Gold	R^2 = 0.998	R^2 = 0.227
Arsenic	R^2 = 0.983	R^2 = 0.987
Chromium	R^2 = 0.984	R^2 = 0.968
Tungsten	R^2 = 0.955	R^2 = 0.973

TABLE 4
STATISTICS FOR MOSS MAT

Element	Unit	Mthd	N	Mean	Med	Std Dev	Min	Max	> D.L.
Antimony	ppm	INA	68	0.4	0.3	0.3	0.1	1.6	45
Arsenic	ppm	INA	68	3.9	2.6	3.9	0.5	18.2	60
Barium	ppm	INA	68	665	650	213.05	50	1300	67
Bromine	ppm	INA	68	9.3	6.8	11.11	0.5	67.2	62
Calcium	%	INA	68	2.63	2	1.72	1	7	44
Cerium	ppm	INA	68	201	165	125.2	50	575	68
Cesium	ppm	INA	68	4	4	1.99	2	11	68
Chromium	ppm	INA	68	48	34	45.62	5	208	67
Cobalt	ppm	INA	68	9	8	5.61	2	27	68
Europium	ppm	INA	68	2.2	1.9	1.12	0.9	6	26
Gold	ppb	INA	68	41	2	188.16	2	1140	28
Hafnium	ppm	INA	68	35	20	39.49	3	177	68
Iron	%	INA	68	4.26	3.83	2.24	1.4	11	68
Lanthanum	ppm	INA	68	132.5	104	87.45	24.8	463	68
Lutetium	ppm	INA	68	1.06	0.78	0.67	0.36	2.96	68
Neodymium	ppm	INA	68	65	53	36.37	24	160	68
Rubidium	ppm	INA	68	89	87	46.93	15	204	61
Samarium	ppm	INA	68	13.1	11	6.44	5.5	28	68
Scandium	ppm	INA	68	12.3	10.7	7.05	3.6	34.6	68
Sodium	%	INA	68	2.25	2.36	0.47	0.77	3.21	68
Tantalum	ppm	INA	68	7.6	5.9	6	0.5	28.2	62
Terbium	ppm	INA	68	1.6	1.5	0.9	0.5	3.8	57
Thorium	ppm	INA	68	67.8	35.9	65.21	6.1	278	68
Tungsten	ppm	INA	68	19	4	51.5	1	402	42
Uranium	ppm	INA	68	37.3	21.9	37.4	1.5	150	68
Ytterbium	ppm	INA	68	6.8	5.2	4.18	2.3	17.9	68
Bismuth	ppm	AAS-H	69	1.9	0.4	3.65	0.2	22	49
Cadmium	ppm	AAS	69	1.3	0.3	3.6	0.2	24.3	44
Cobalt	ppm	AAS	69	6	5	2.76	2	14	67
Copper	ppm	AAS	69	19	12	29.27	6	244	69
Iron	%	AAS	69	1.3	1.3	0.37	0.6	2.2	69
Lead	ppm	AAS	69	11	7	14.4	2	117	67
LOI	%	GRAV	69	7.8	6.6	6.42	1.1	45.6	69
Mercury	ppb	AAS-F	69	32	30	20.86	10	170	65
Manganese	ppm	AAS	69	433	295	345.85	126	2020	69
Molybdenum	ppm	AAS	69	3	2	4.47	1	33	38
Nickel	ppm	AAS	69	8	5	6.29	2	27	61
Silver	ppm	AAS	69	0.3	0.2	0.25	0.2	1.9	12
Tin	ppm	NAIAA	69	1	1	0.28	1	2	6
Vanadium	ppm	AAS	69	28	27	11.68	11	60	69
Zinc	ppm	AAS	69	45	39	25.17	17	155	69

TABLE 5
STATISTICS FOR STREAM SEDIMENT SAMPLES

Element	Unit	Mthd	N	Mean	Med	Std Dev	Min	Max	> D.L.
Antimony	ppm	INA	68	0.3	0.2	0.3	0.1	1.6	39
Arsenic	ppm	INA	68	3.9	2.4	3.81	0.5	19.3	63
Barium	ppm	INA	68	636	600	153.9	300	990	68
Bromine	ppm	INA	68	8.4	5	10.64	0.5	65	59
Calcium	%	INA	68	2	2	3.04	1	25	38
Cerium	ppm	INA	68	135	99	91.13	29	401	68
Cesium	ppm	INA	68	5	4	2.1	1	12	67
Chromium	ppm	INA	68	38	23	38.22	5	178	64
Cobalt	ppm	INA	68	9	8	5.5	2	25	68
Europium	ppm	INA	68	1.7	1.4	1.05	0.2	5.5	14
Gold	ppb	INA	68	4	2	7.46	2	59	17
Hafnium	ppm	INA	68	15	8	18.92	1	84	67
Iron	%	INA	68	3.25	2.83	1.85	1.03	11.9	68
Lanthanum	ppm	INA	68	85.5	69.8	52.04	18.8	211	68
Lutetium	ppm	INA	68	0.69	0.48	0.5	0.24	2.24	68
Neodymium	ppm	INA	68	45.5	36	31.68	14	165	68
Rubidium	ppm	INA	68	96	90	45.72	15	234	66
Samarium	ppm	INA	68	9.2	7.2	5.66	3.4	29.7	68
Scandium	ppm	INA	68	10.7	9.6	6.44	2.5	31.1	68
Sodium	%	INA	68	2.29	2.39	0.54	0.65	3.19	68
Tantalum	ppm	INA	68	4.8	3	4.31	0.5	15.5	56
Terbium	ppm	INA	68	1.1	1	0.69	0.5	3.5	51
Thorium	ppm	INA	68	37.2	24.4	35.5	2.3	158	68
Tungsten	ppm	INA	68	9	1	17.42	1	77	32
Uranium	ppm	INA	68	27.6	11.4	35.35	1.4	155	68
Ytterbium	ppm	INA	68	4.5	3.4	3.21	1.5	14.2	68
Bismuth	ppm	AAS-H	69	1.1	0.3	1.59	0.2	7.5	43
Cadmium	ppm	AAS	69	1.2	0.3	4.2	0.2	25.6	37
Cobalt	ppm	AAS	69	6	5	2.76	2	14	68
Copper	ppm	AAS	69	19	12	29.36	6	233	69
Iron	%	AAS	69	1.24	1.2	0.43	0.5	2.4	69
Lead	ppm	AAS	69	10	7	7.83	2	38	68
LOI	%	GRAV	69	6.6	4.4	6.85	0.6	38.2	69
Mercury	ppb	AAS-F	69	29	30	19.86	10	150	63
Manganese	ppm	AAS	69	394	289	311.6	89	1800	69
Molybdenum	ppm	AAS	69	3	2	4.79	1	34	43
Nickel	ppm	AAS	69	9	6	7.19	2	32	62
Silver	ppm	AAS	69	0.3	0.2	0.16	0.2	1.2	10
Tin	ppm	NAIAA	69	1	1	0.12	1	2	1
Vanadium	ppm	AAS	69	29	25	12.66	11	65	69
Zinc	ppm	AAS	69	46	38	26.18	17	167	69

Tungsten, iron and tantalum are also enhanced in moss mat samples relative to the stream sediments suggesting that the moss preferentially captures heavier minerals (Matysek, Gravel and Jackaman, 1988). Other elements such as antimony, arsenic and cobalt have almost identical mean, median and maximum concentrations in both sample types or in the case of rubidium and sodium are lower in the moss mat sediments. This difference could be explained by the different hydraulic behaviour of individual minerals *(e.g.* gold, scheelite) as opposed to rock grains (containing varying sodium and rubidium) when these are transported by stream water. The relationship between gold, arsenic and tungsten in moss sediment and stream sediment is also demonstrated by the scatter plots shown in Figure 2 where element concentration in moss sediment is plotted as a function of element concentration in stream sediment for samples collected at the same site.

The distribution of gold in moss mat sediment samples from the Adams Lake and Newhykulston Creek survey areas is shown in Figure 3. The highest gold (1140 ppb) detected in the survey area is in moss mat sediment from a small stream flowing from the north into the headwaters of Spapilem Creek. Duplicate moss mat samples from this site have 1140 ppb and 159 ppb gold, respectively, illustrating the potential for high variability of gold in moss sediment. Sediment from the Spapilem Creek headwaters stream only has 7 ppb gold by comparison to 1140 ppb in the moss mat sediment (Figure 4). A gold concentration of 1080 ppb was found in a moss sediment sample near the mouth of the creek over 6 kilometres downstream from the headwaters. Stream sediment gold levels only reach 18 ppb at this site. By contrast to the high values in Spapilem Creek, 35 ppb gold occurs in the moss sediment from a small stream draining the area around the Cam-Gloria occurrence. No gold was detected in stream sediment. Moss mat sediment from Grizzly Creek draining a larger watershed just north of Cam-Gloria has 25 ppb gold, but the sediment only contains 5 ppb gold (Figure 4). A previous regional stream sediment surveys (RGS) reported by Matysek *et al.,* (1991) found a similar, low level of gold (15 ppb) in the stream sediment from Grizzly Creek.

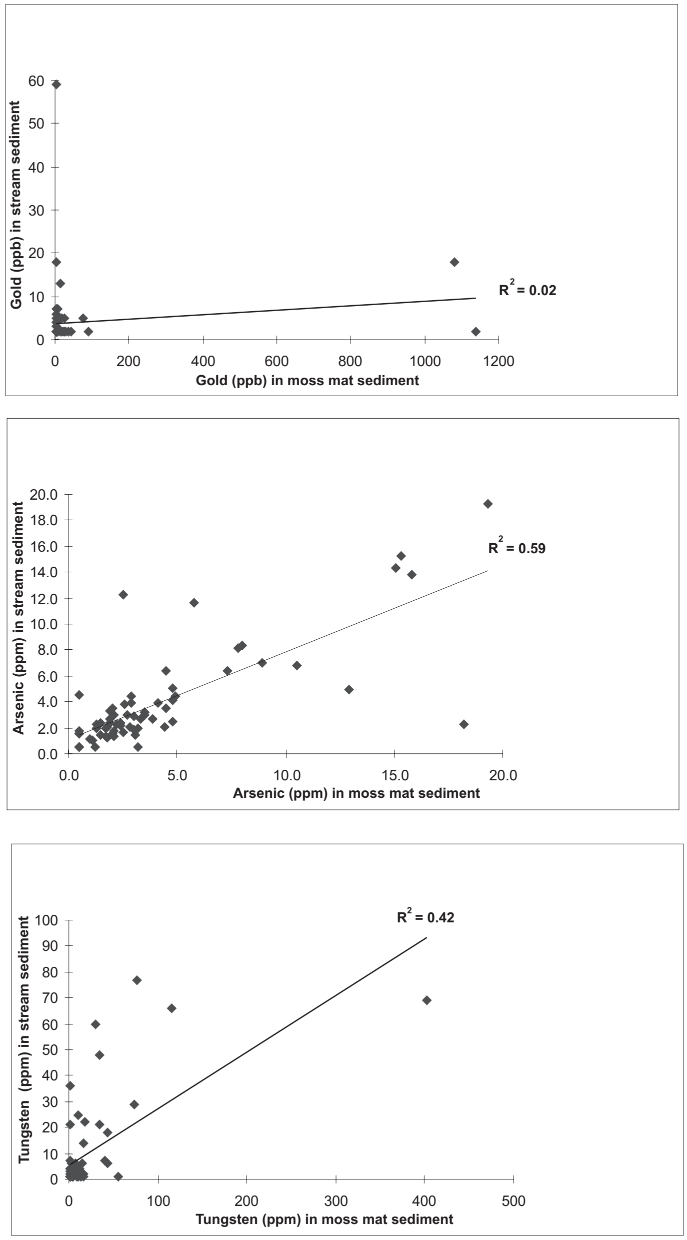

Figure 2. Scatter plots for elements in stream and moss mat sediment.

A moss mat sediment sample from a branch of Newhykulston Creek has 223 ppb gold, and values to 45 ppb could be detected 5 kilometres downstream. Only 5 ppb gold occurs in the stream sediment. However, moss sediment and stream sediment have almost identical arsenic levels reaching 15.3 ppm. The headwaters of Newhykulston Creek are underlain by a small granite intrusive and up to 51 ppb gold has been found in till down-ice of the granite (Bobrowsky *et al.*, 1998).

A moss mat sediment sample from a stream flowing north into Gollen Creek (82M/5) has 92 ppb gold in the moss sediment. Fisher and Stratton Creeks located to the south have over 20 ppb gold in the moss sediment, but only just detectable gold in the stream sediment (Figure 4). Stratton Creek water also contains 41 ppm sulphate and 550 ppb fluoride. The combination of enhanced gold in the moss sediment and anomalous water chemistry suggest a sulphide-fluorite mineralized source in the watershed of Stratton Creek. The distribution of tungsten in moss sediment is shown in Figure 7 and the highest value (40 ppm) found in the area occurs in a north branch of Bendelin Creek. There is only a weak spatial correlation between moss sediment gold and moss sediment tungsten anomalies.

Gold content in moss sediment samples from the Kootenay Survey area is lower than in the Adams lake

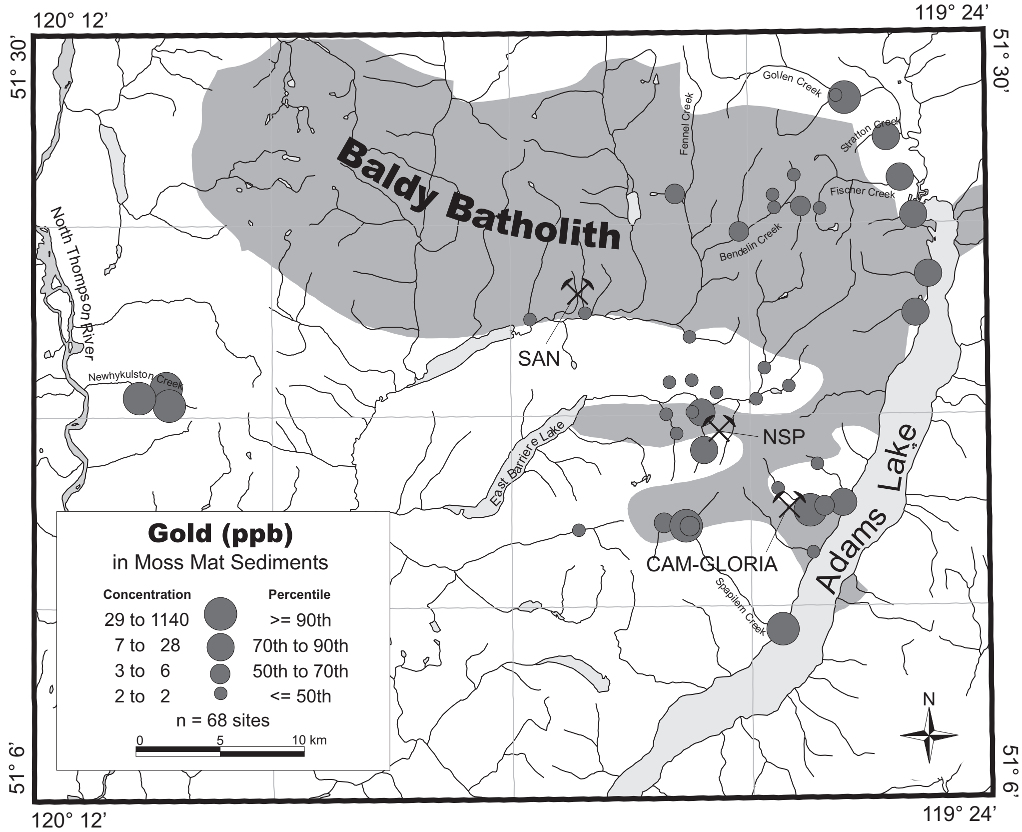

Figure 3. Gold in moss mat sediments, Adams Lake area.

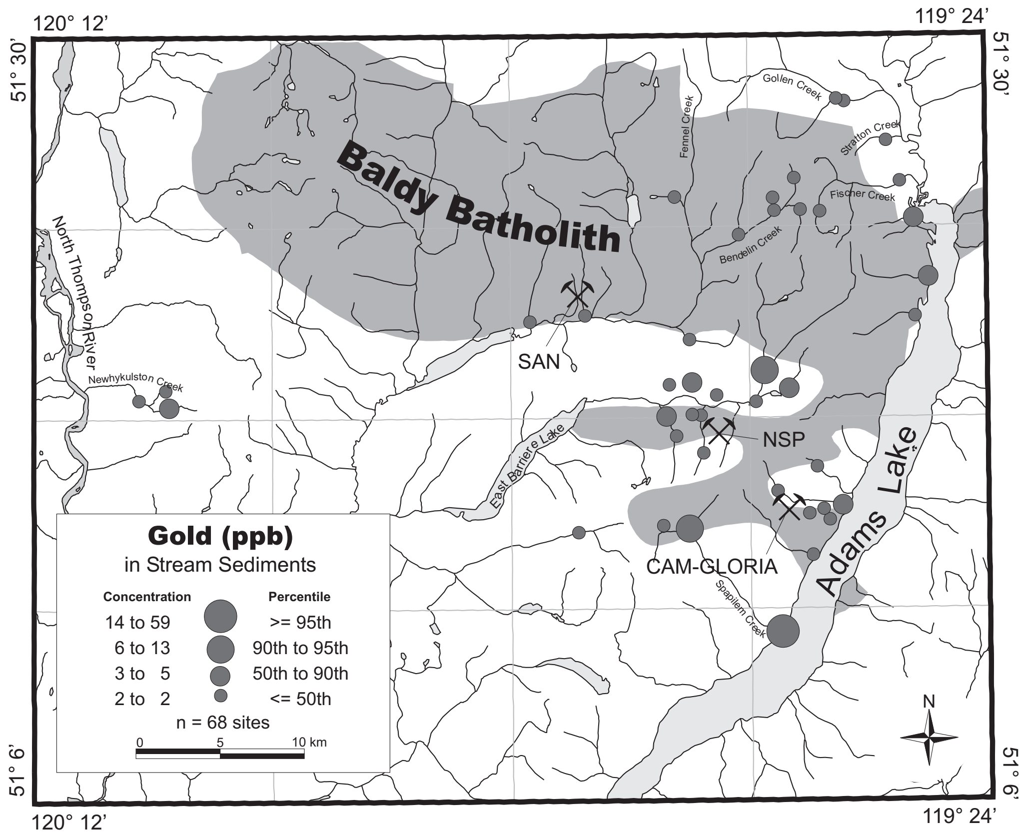

Figure 4. Gold in stream sediments. Adams Lake area.

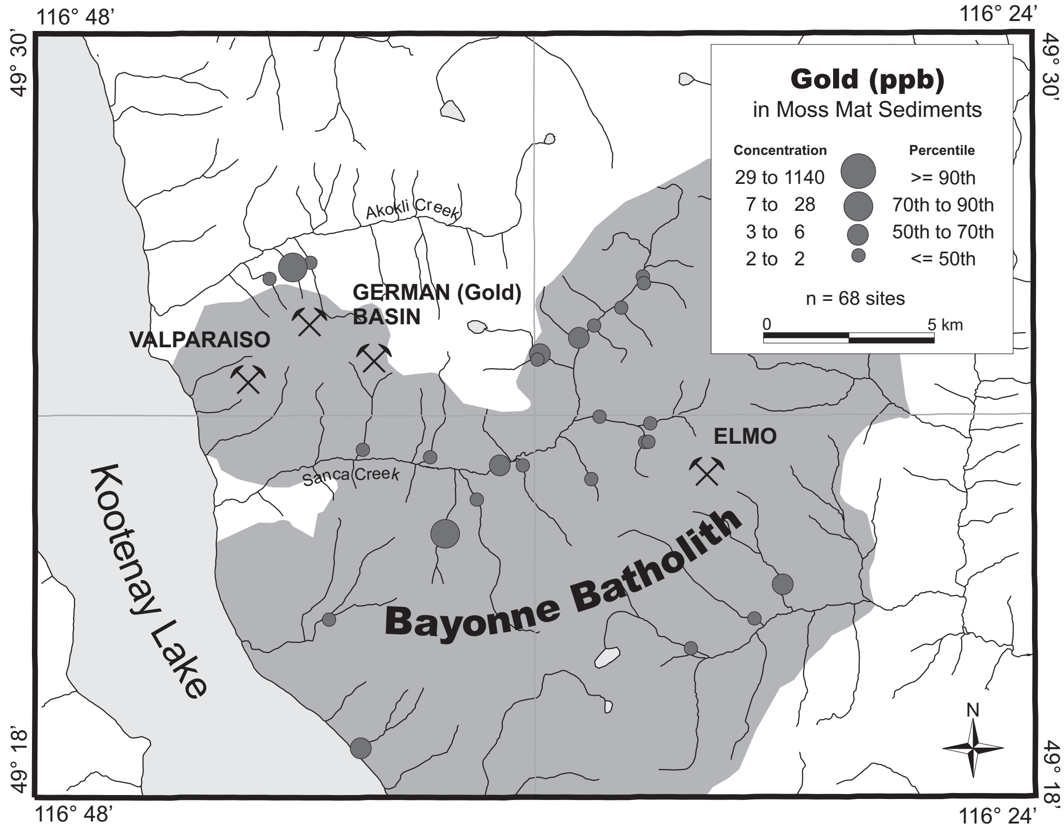

Figure 5. Gold in moss mat sediments, Kootenay Lake area.

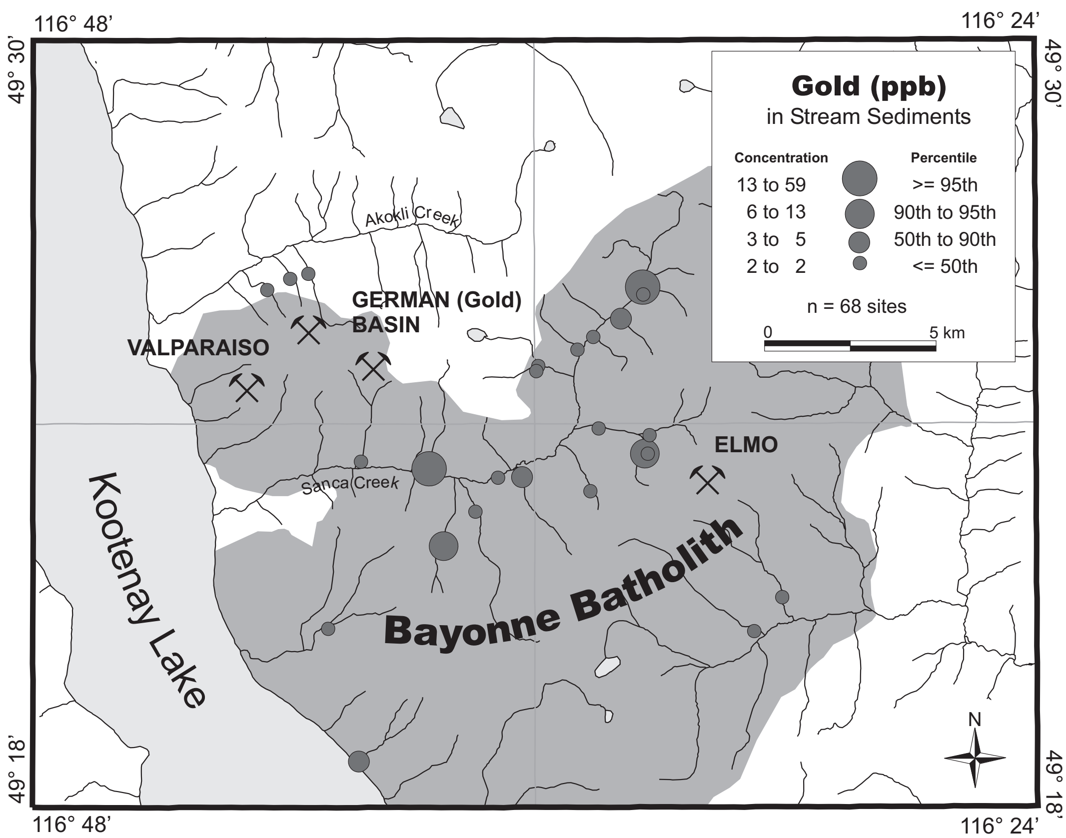

Figure 6. Gold in stream sediments, Kootenay lake area.

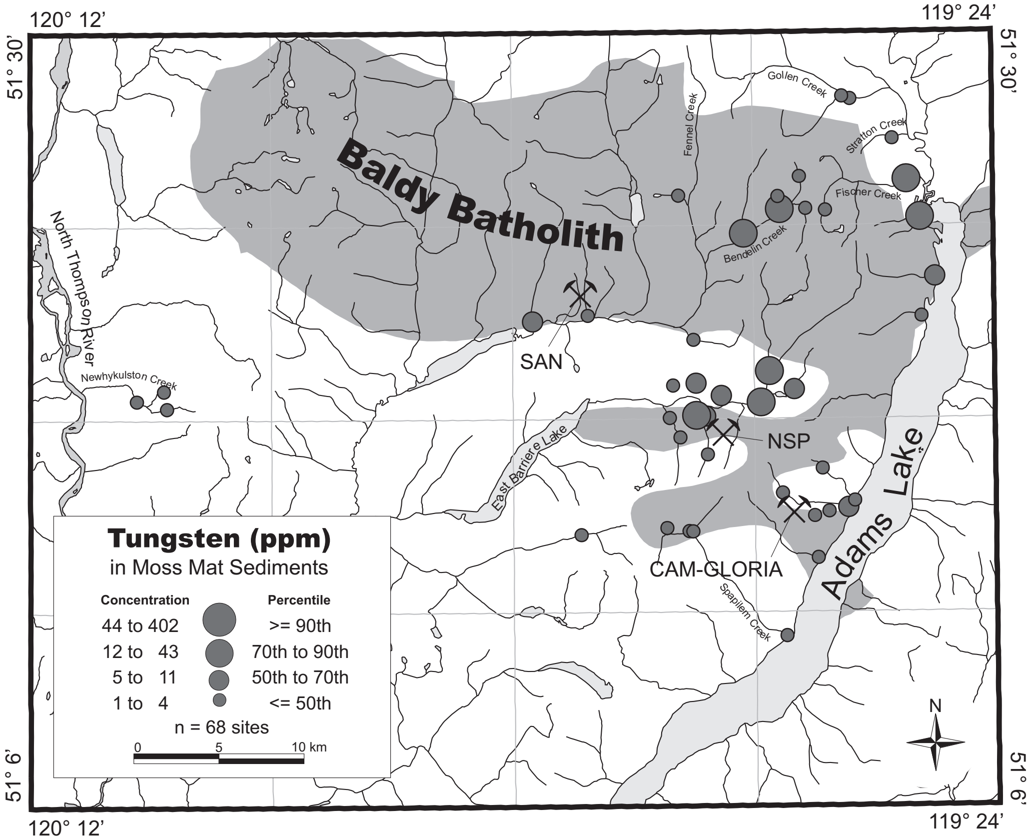

Figure 7. Tungsten in moss mat sediments, Adams Lake area.

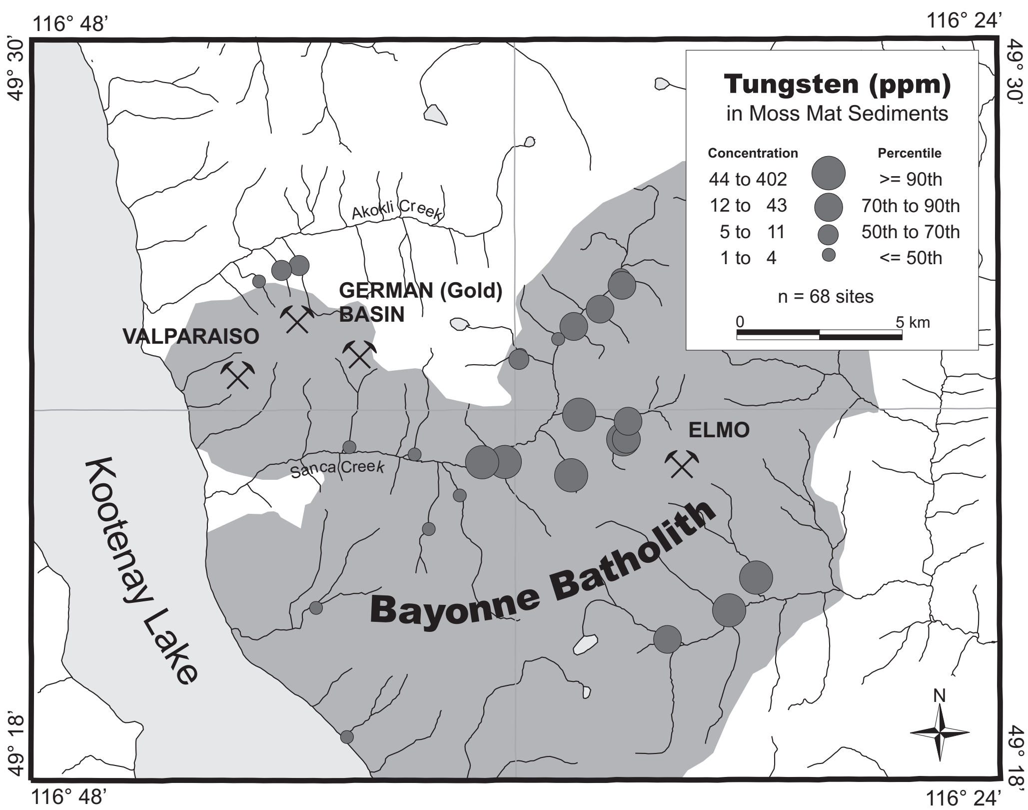

Figure 8. Tungstein in moss mat sediments, Kootenay Lake area.

area and the highest value (34 ppb) occurs in stream flowing into Akokli Creek from the German (Au) Basin showing on the north west side of Mount Sherman (Figure 5). No gold was detected in sediment from this stream although 59 ppb occurs the sediment from a creek draining the south side of Mount Sherman into Sanca Creek (Figure 6). Tungsten levels (Figures 7 and 8) are typically higher in the Kootenay area moss mat sediment samples and the highest value (402 ppm) occurs in moss sediment from a creek flowing from the watershed containing the Elmo occurrence. Almost no (less than 10 ppm) tungsten is present in moss sediment and stream sediment from creeks draining the German (Gold) Basin Showing on south side of Akokli Creek (including "Tungsten" Creek).

CONCLUSIONS

Preliminary results for the Adams Lake area reveal that the gold content of moss mat sediment is much higher than stream sediment collected at the same sample site. However, gold is highly variable in duplicate moss sediment samples. This pattern of gold enhancement and high variability is consistent with the results of previous geochemical studies where both sample media were compared (Matysek and Day, 1987). Other elements such as tungsten and chromium are also enriched in the moss sediment relative to stream sediment, but element variability between field duplicate samples is smaller. In the Kootenay Lake area the highest gold value occurs in stream sediment rather than moss mat sediment. However, the gold anomalous stream sediment and moss mat sediment samples are from different streams. Tungsten values are much higher in moss mat sediment from the Kootenay area and levels, to some extent, reflect known tungsten mineral occurrences.

Further work to complete this study will involve: 1) comparison of gold and other element values in heavy mineral concentrates, stream sediments, suspended sediments and moss mat sediments. The heavy mineral samples are intended to assess the ability of streams to concentrate gold and other high density minerals in stream-bed sediment; 2) evaluation of stream and moss sediment data for other pathfinders (e.g. tin, bismuth, fluorine) for intrusive related gold mineralization; 3) comparison of aqua regia digestion - atomic absorption spectrometry and aqua regia digestion - inductively coupled plasma mass spectrometry analysis of selected samples for gold and pathfinder elements and; 4) field follow-up to establish if the gold anomalies do indeed reflect intrusive related or other styles of gold mineralization.

ACKNOWLEDGEMENTS

The authors appreciate help from M. Cathro with the interpretation of the geochemical data and reviews of this paper by G. McArthur and S. Cook. Richard Mann is thanked for assistance with sample preparation and with compilation of the field data.

W. Gilmour and K. Daughtry, Discovery Consultants, are especially thanked for their advice on sample collection for heavy mineral preparation.

REFERENCES

Alley, H.F., Valentine, K.W.G., and Fulton, R.J. (1986): Paleoclimatic implications of middle Wisconsinian pollen and a paleosol from the Purcell Trench, south central British Columbia; *Canadian Journal of Earth Sciences*, Volume 23, Number 8, pages 1156-1168.

Borovic, I., (1987): Report on the mineral exploration of the Totem Gold property, NTS 82F/7E; *B.C. Ministry of Energy, Mines and Petroleum Resources*, Assessment Report Number 17527, pages 4-8.

Bobrowsky, P.T., Leboe, E.R., Dixon-Warren, A., Ledwon, A., MacDougall, D. and Sibbick, S.J. (1997): Till Geochemistry of the Adams Plateau - North Barriere Lake Area (82M/4 and 5). *B.C. Ministry of Employment and Investment*, Open File 1997-9.

Bobrowsky, P.T., Paulen, Little, E., Prebble, A. and Ledwon, A., (1998): Till Geochemistry of the Louis Creek-Chu Chua Area (92P/1E and 92P/8E). *BC Ministry of Energy and Mines*, Open File 1998-6.

Dixon-Warren, A., Bobrowsky, P.T., Leboe, E.R. and Ledwon, A. (1997): Eagle Bay Project: Surficial Geology of the Adams Lake Plateau (82M/4) and North Barriere Lake (82M/5) map areas; *in* Geological Fieldwork 1996, Lefebure, D.V., McMillan, W.J. and McArthur, G., Editors, *B.C. Ministry of Employment and Investment*, Paper 1991-1, pages. 405-411.

Ficklin, H.E. (1970): A rapid method for the determination of fluorine in rocks and soils using an ion selective electrode; *U.S. Geological Survey*, Paper 700C, pages 186-188.

Fulton, R.J. and Smith, G.W. (1978): Late Pleistocene stratigraphy of south-central British Columbia; *Canadian Journal of Earth Sciences*, Volume 15, pages 971-980.

Holland, S.S. (1976): Landforms of British Columbia, a physiographic outline; *B.C. Ministry of Energy, Mines and Petroleum Resources*, Bulletin 48.

Jonasson, I.R., Lynch, J.J. and Trip, L.J. (1973): Field and laboratory methods used by the Geological Survey of Canada in geochemical surveys: No. 12, Mercury in ores, rocks, soils, sediments and water; *Geological Survey of Canada*, Paper 73-21.

Lett, R.E., Bobrowsky, P.,Cathro, M. and Yeow, A. (1998): Geochemical pathfinders for massive sulphide deposits in the southern Kootenay Terrane; *B.C. Ministry of Employment and Investment*, Geological Fieldwork 1997, Paper 1998-1, pages 15-1 - 15-9.

Logan, J.M. (1999): Plutonic-related gold-quartz veins in Southern British Columbia; *in* Geological Fieldwork 1999; *B.C. Ministry of Energy and Mines*, Geological Survey Branch, Paper 2000-1, this volume.

Matysek, P.F., Jackaman, W., Gravel, J.L., Sibbick, S.J. and Feulgen, S. (1991): British Columbia Regional Geochemical Survey, Seymour Arm (NTS 82M); *B.C. Ministry of Energy, Mines and Petroleum Resources*, RGS 33.

Matysek, P.F., Gravel, J.L. and Jackaman, W.(1988): British Columbia Regional Geochemical Survey, Alert Bay/Cape Scott (NTS 82L/102I); *B.C. Ministry of Energy, Mines and Petroleum Resources*, RGS 23.

Matysek, P.F., and Day, S. J.,(1987): Geochemical orientation surveys: Northern Vancouver Island, Fieldwork and preliminary results; *B.C. Ministry of Energy, Mines and Petroleum Resources*, Geological Fieldwork, 1987, Paper 1988-1, pages 493-502.

Moldan, B., Rubeska, I., Mikovsky, M. and Huka, M. (1970): Determination of tin in geological materials by atomic absorption spectrometry. *Analytica Chimica Acta*., Volume 52, pages 91 - 99.

Robertson, R. (1998): Pogo property in Alaska the latest feather in Teck's cap; *The Northern Miner*, Volume 84, No. 23, pages 1-2.

Schiarizza, P. and Preto, V.A. (1987): Geology of the Adams Plateau-Clearwater-Vavenby area; *B.C. Ministry of Energy, Mines and Petroleum Resources*, Paper 1987-2.

Smith, M., Thompson, J.F.H., Bressler, J., Layer, P., Mortensen, J.K., Abe, I. and Takaoka, H. (1999): Geology of the Liese Zone, Pogo Property, East-Central Alaska; *Society of Economic Geologists Newsletter*, Number 38, July 1999, pages 11 to 21.

Exploration Significance of the Iskut River Fault

By Dani J. Alldrick

KEYWORDS: *Regional mapping, structure, Iskut River, Pitman fault, Iskut River fault, mineral exploration, Eskay Creek.*

SUMMARY

Large-scale aeromagnetic lineaments reveal major faults that cut across northern British Columbia, extending from the Coast Plutonic Complex in the west to the northern Rocky Mountain Trench in the east. These faults are significant because:

- they are part of the record of Tertiary regional-scale tectonic readjustments within the Canadian Cordillera
- they characteristically occur as a set of parallel faults
- they have a predictable orientation, sense of offset, and amount of offset
- they pass near major mineral deposits, offsetting prospective strata. Determination of fault offset allows focused exploration efforts on the offset block.

INTRODUCTION

An aeromagnetic map of northern British Columbia (Figures 1 and 2), contoured and enhanced by low-angle oblique illumination, was prepared by RGI (Resource Geoscience and Imaging) in Vancouver. This map highlights two 500-kkilometre-long east-trending magnetic lineaments that transect the Canadian Cordillera. Along most of its length, the northern magnetic lineament coincides with a mapped fault, the Pitman fault (Figure 3), however, the extent of the coincident aeromagnetic anomaly indicates that the Pitman fault continues westward well beyond its mapped limits. A fault corresponding to the southern magnetic lineament (Figures 2 and 3), the Iskut River fault, is documented for the first time in this paper.

PITMAN FAULT

The Pitman fault is located along latitude 57º 50' N (Figures 2 and 3). There is 3 kilometres of left-lateral offset along the fault, measured where it offsets the Thudaka and Kutcho faults (Gabrielse, 1985). Vertical offset is minor with a small amount of north-side-down offset recorded along the western part of this fault. Movement oc-

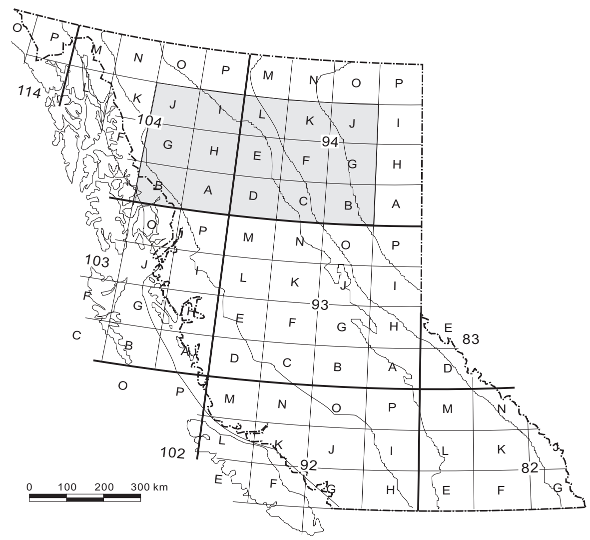

Figure 1. Location of this study. Shading corresponds to the area of Figures 2, 3, 7 and 9.

curred during Eocene to Oligocene time. The sinistral offset along the Pitman fault and the angular relationship (~75º) between the Pitman fault and dominant northwest-striking dextral faults (Kechika, Finlay, Ingenika, Northern Rocky Mountain Trench) are consistent with the interpretation that this is an antithetic fault associated with the continental-scale displacement along the Northern Rocky Mountain Trench (Gabrielse, 1985). Antithetic faults characteristically occur in parallel sets, and there are other faults in the region with similar orientation, attitude, and offset, including a set of subparallel faults that trend east from the north end of Dease Lake (Gabrielse, 1985).

ISKUT RIVER FAULT

The southern magnetic lineament is located along latitude 56º 40' N (Figures 2 and 3). The possibility of a fault lying along the lower (west-flowing) section of the Iskut River has been debated for several years. Features favouring the existence of an east-striking fault are the linearity of the river valley, and it's abrupt dogleg turn from southwest-flowing to west-flowing at the junction with Volcano (Palmière) Creek (Figures 4 and 5). However, arguments for existence of a fault have been difficult to support because there is no unequivocal evidence for offset of lithologic units across the lower Iskut River.

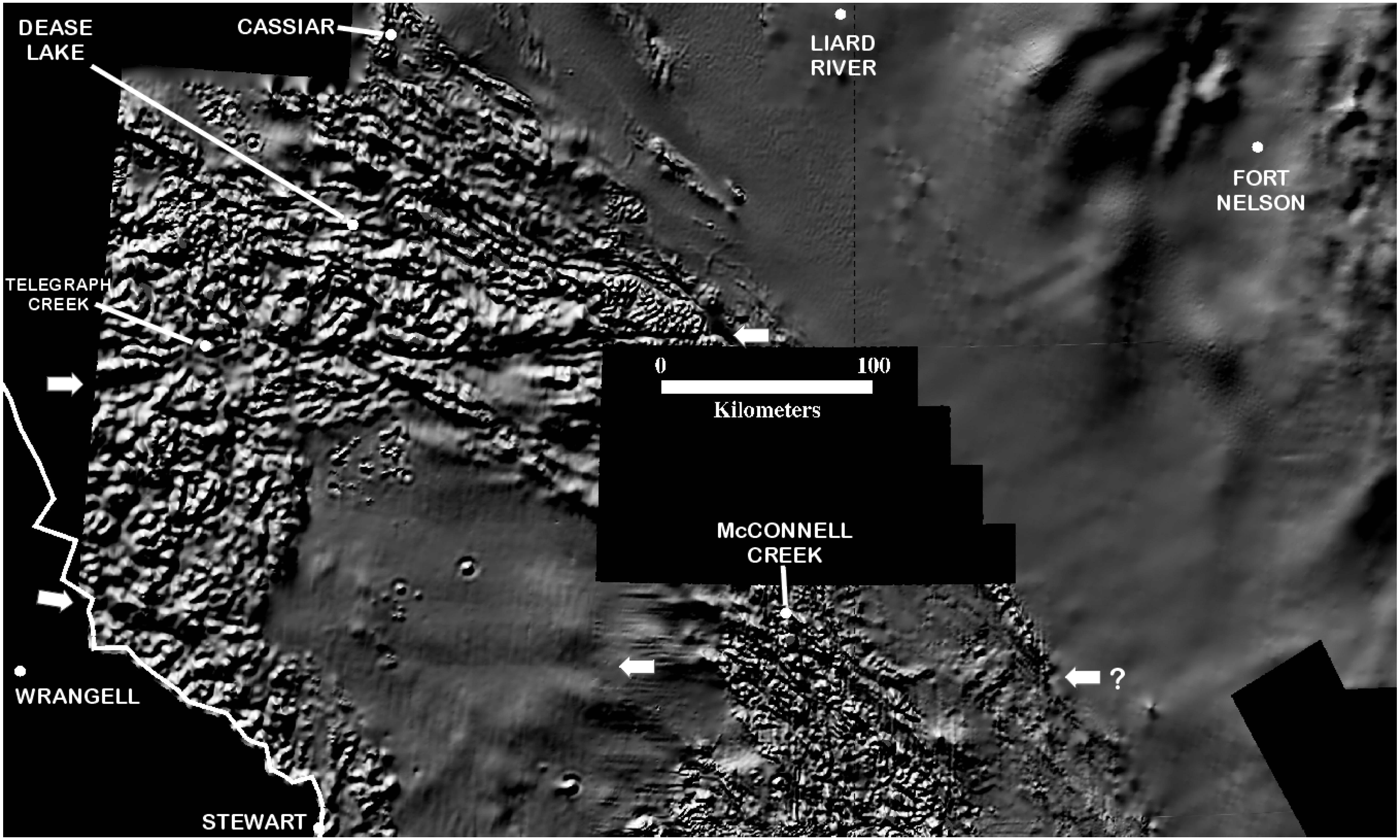

Figure 2. Contoured aeromagnetic map enhanced by low-angle oblique illumination. The two sets of opposing arrows mark the ends of the magnetic anomalies correlated with the Pitman fault (northern set of arrows) and the Iskut River fault (southern set of arrows).

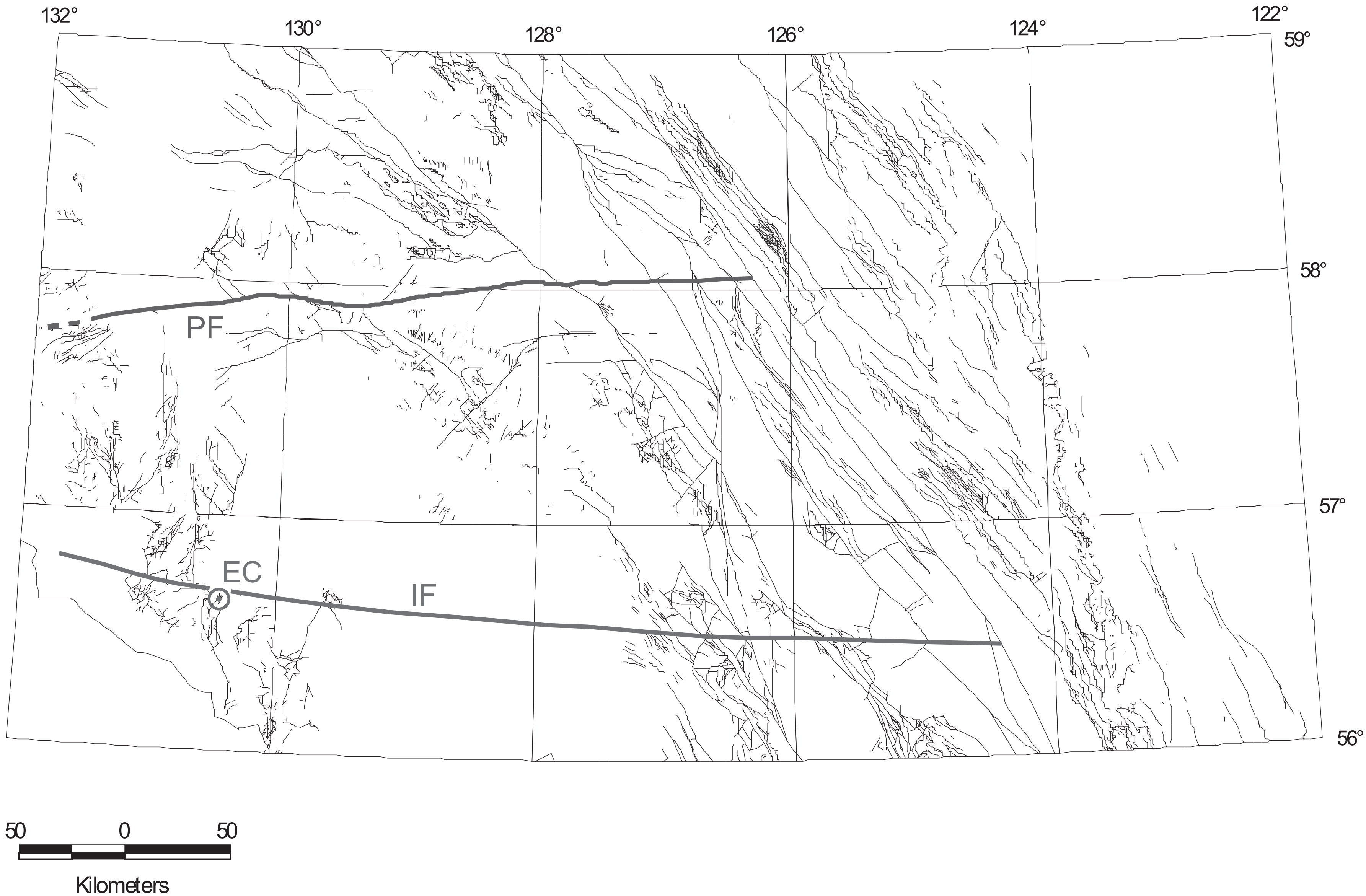

Figure 3. Major faults of north central British Columbia (complied from the maps of the British Columbia Mineral Potential Project). This map matches the area and map projection of Figure 2. PF is the mapped Pitman Fault. IF is the interpreted location and extent of the Iskut River Fault. EC is the Eskay Creek minesite.

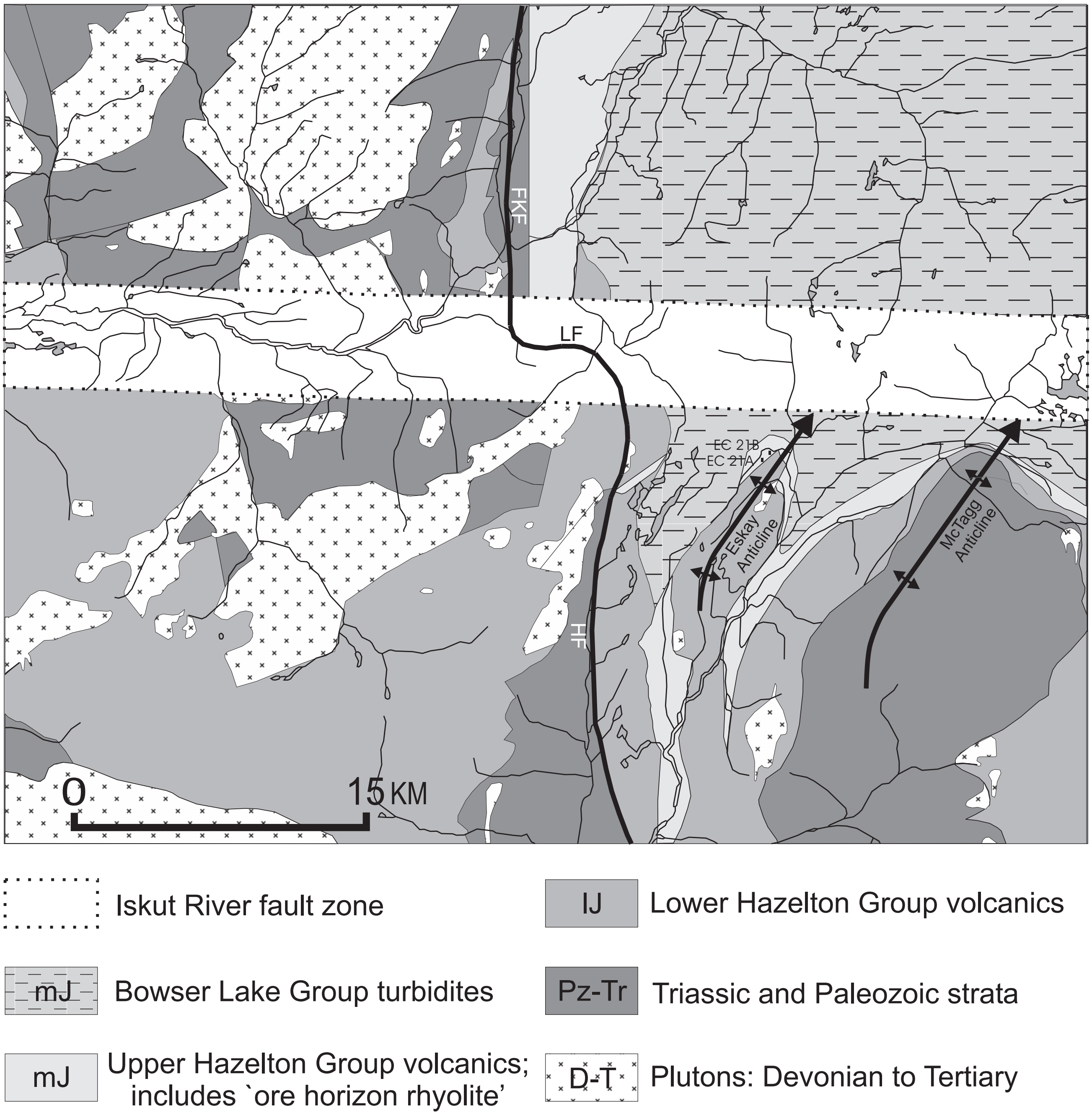

Figure 4. Simplified geology of the Eskay Creek mine area (adapted from Alldrick and Britton, 1992; Lewis, 1996; Logan and Drobe, 1997 and Read *et al.*, 1989). Note abundance of west- and east-flowing streams within the Iskut River fault zone in contrast to surrounding territory. **EC21B**-Eskay Creek 21B zone; **EC21A**-Eskay Creek 21A zone. **FKF-LF-HF** = Forrest Kerr-Leroy Creek-Harrymel Creek faults. All other faults and Pleistocene-Holocene lava flows have been removed.

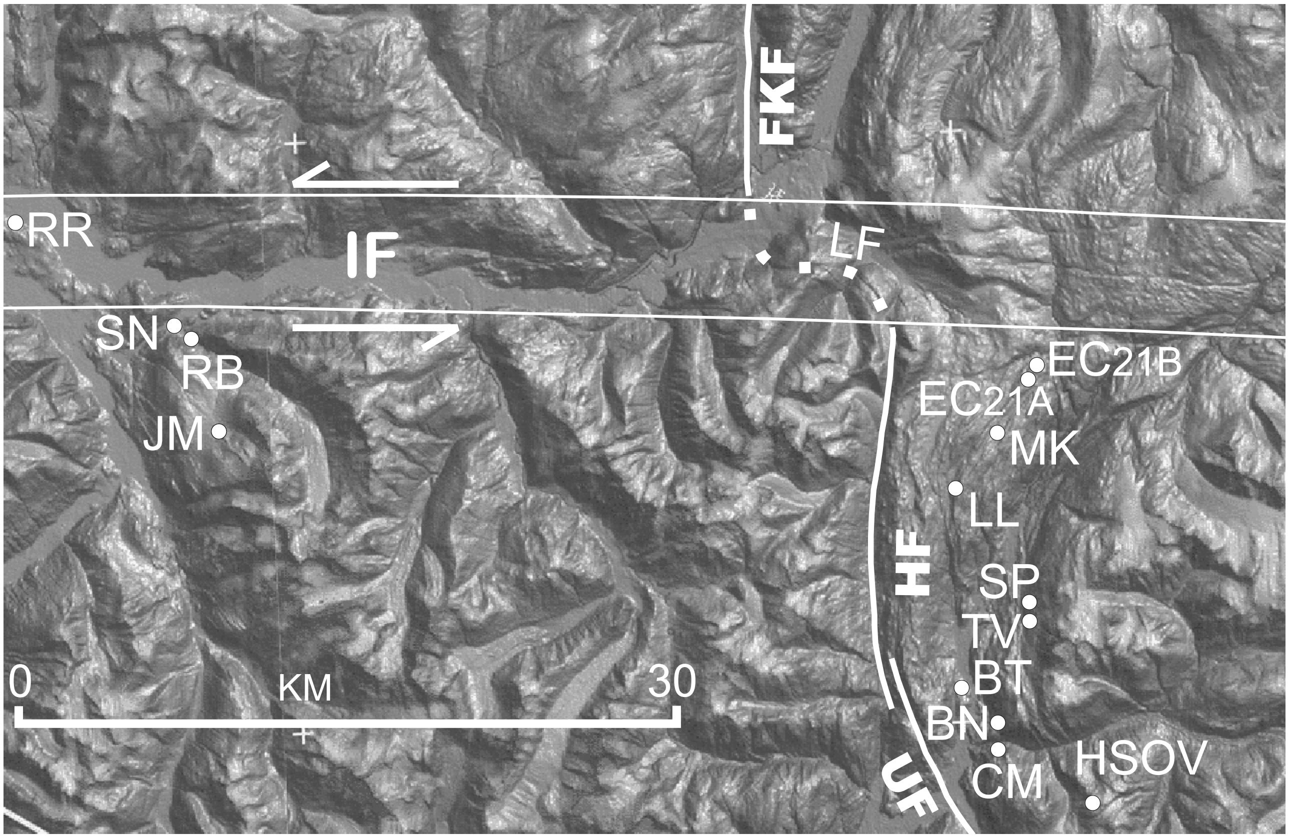

Figure 5. Trace of the Iskut River fault zone in the Eskay Creek mine area plotted on a contoured DEM (topo) map from Resource Geoscience and Imaging, Vancouver. Width of indicated fault zone exaggerated here by 20% to avoid obscuring east-trending topographic lineaments with linework. Left-lateral movement along the Iskut River fault is interpreted from the 6 kilometre offset of the Forrest Kerr fault (FKF)-Leroy Creek fault (LF)-Harrymel Creek fault (HF)-South Unuk River fault (UF) trend. Mineral deposits: RR-Rock and Roll; SN-Snip; RB-Red Bluff; JM-Johnny Mountain; EC21B-Eskay Creek 21B zone; EC21A-Eskay Creek 21A zone; MK-Mackay adit; LL-Lulu; SP-Springer; TV-TV zone; BT-Battlement; BN-Bench; CM-Cumberland; HSOV-HSOV zone.

Three factors have made these apparent contradictions difficult to resolve:

1. An expectation that any fault that localizes a major topographic depression such as the Iskut River valley must have major offset;
2. The 1.8-kilometre-wide gravel-filled valley floor for the lower Iskut River inhibits recognition and documentation of fault offsets; and
3. East of the broad Iskut River valley, the fault trace cuts through the extensive, monotonous turbidite succession of the Bowser Lake Group, where recognition of this fault is difficult.

Several features support the interpretation of an east-striking, left-lateral fault extending along the lower Iskut River valley and continuing eastward:

- A prominent, coincident east-trending linear negative magnetic anomaly that extends from the Stikine River (western limit of aeromagnetic coverage) to the northern Rocky Mountain Trench (Figure 2).
- Development of two major river valleys (the Iskut River and an unnamed western tributary of Ketchum Creek) along this easterly trend is in sharp contrast to the regional drainage directions (Figures 4 and 5).
- Left-lateral offset of the Forrest Kerr and Melville Glacier-Harrymel Creek fault zones, two offset segments of a single major north-striking normal fault (Figures 4 and 5)
- Features such as the sinusoidal Leroy Creek fault are consistent with left-lateral offset (Figures 4 and 5)
- Within terrain underlain by Bowser Lake Group strata, drainage directions are strongly influenced by the inclined bedding of variably weathering siltstone and sandstone. However, within the Iskut River fault zone there are several minor, deeply-incised, straight, east-trending gullies which contrast with local drainage directions (Figure 5).
- Similar magnetic signature, orientation, sense of offset, and scale of offset as the mapped Pitman fault, 130 kilometres to the north (Figures 2, 3 and 8).
- When placed in a tectonic context, the fault displays the characteristic features of an antithetic fault (Figures 6 and 7). The existence of additional, parallel antithetic faults distributed along the entire

length of the continental-scale Kaltag-Tintina-Rocky Mountain Trench fault system is predicted by the tectonic model for formation of these structures.

The Iskut River fault (Figures 2, 3, 4 and 5) is a four-kilometre-wide zone that displays features suggesting periods of both ductile and brittle offset. The distinctive s-shaped outcrop pattern of the Leroy Creek fault (Figures 4 and 5, and Alldrick and Britton, 1992) that trends between the southern end of the Forrest Kerr fault and the northern end of the Harrymel Creek fault demonstrates ductile deformation (Davis, 1984, p.228-230; Hodgson, 1989; Ramsay, 1980; Simpson, 1986). Several narrow, east-trending gullies are evident on the DEM and Landsat images in the area lying between the Unuk and Iskut rivers (northwest of the Eskay Creek mine, Figures 5 and 10). These suggest additional parallel linear breaks indicative of brittle deformation. The offset of the Forrest Kerr and Harrymel Creek faults indicates that the total left-lateral offset is 6 kilometres across the 4 kilometre width of the Iskut River fault zone. Incremental offset within this broad fault zone is illustrated schematically in Figures 5 and 10.

North of this study area, a twin for the unusually shaped Leroy Creek fault has been documented near Telegraph Creek. The northward continuation of the Forrest Kerr fault is called the Mess Creek fault zone (Figure 7). Combined, these two north-trending co-linear structures extend 130 kilometres from the Iskut River fault to the Pitman fault. South of the village of Telegraph Creek, Souther (1972) mapped a curved fault trace (Figure 8) where the younger Pitman fault cuts across the older Mess Creek fault. This small fault segment is similar in scale, shape and sense of offset to the outcrop pattern of the Leroy Creek fault, and is interpreted as a drag-folded (ductily deformed) segment of the Mess Creek fault zone that was deformed during left-lateral offset along the Pitman fault. The postulated north-striking continuation of the Mess Creek fault, on the northern side of the Pitman

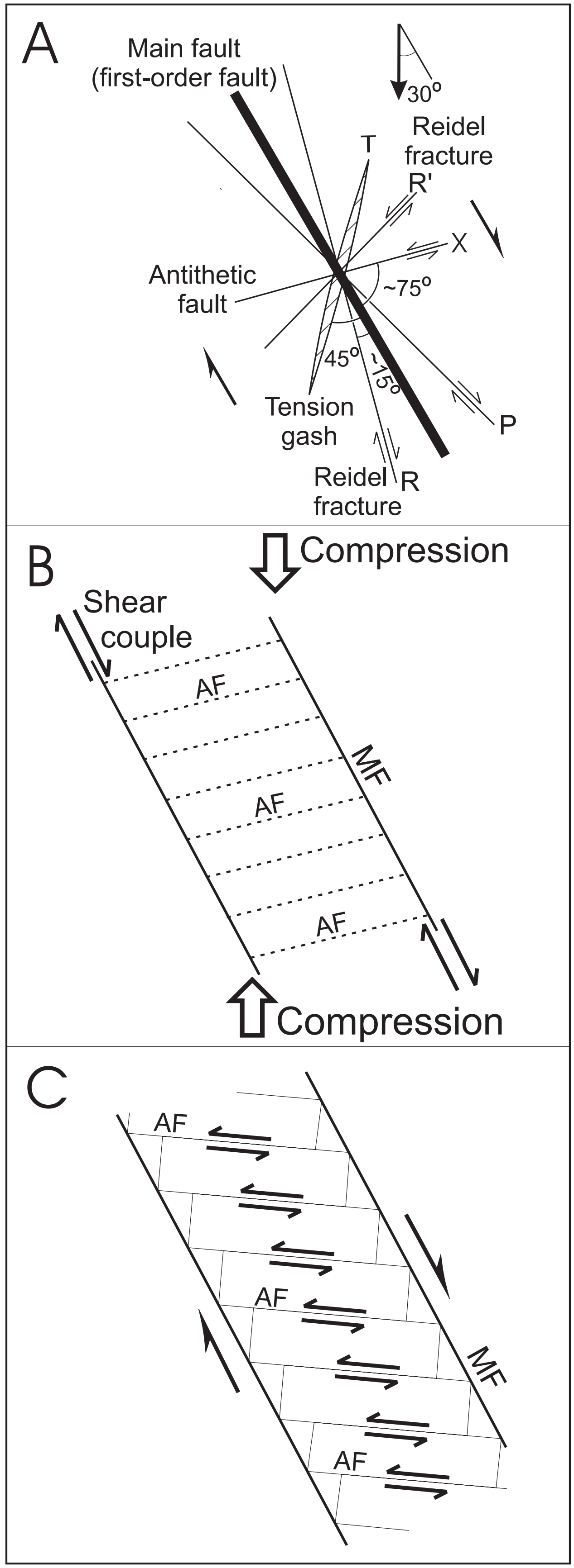

Figure 6. Physics and mechanics of antithetic faults (adapted from Nicolas, 1987; Wilson, 1982; and McClay, 1987). 6a: Geometric relationships between first-order and second-order fractures in a compressional regime. These different fractures are not all activated at the same time. P, T and X fractures develop if the stress on the main fault plane is relatively small, due to low confining pressure (shallow depth), low effective pressure (high fluid pressure), or if the fault follows a pre-existing plane of anisotropy at a low angle to the direction of compression. In contrast, Reidel fractures R and R' predominate in deep or dry faults or where the angle between the fault plane and the direction of compression is large (Nicolas, 1987). 6b: Geometric relations at the moment of failure. Sets of antithetic faults (AF) develop at an angle of 75º to the main fault (MF). 6c: Sense of movement along antithetic fault sets. The amount (distance) of fault offset along antithetic faults is always minor compared to that of the main fault. The individual fault blocks (`dominoes') pivot around at their point of contact with the wall of the main fault, so the absolute amount of movement depends upon the amount of rotation of the blocks and the distance between the antithetic faults.

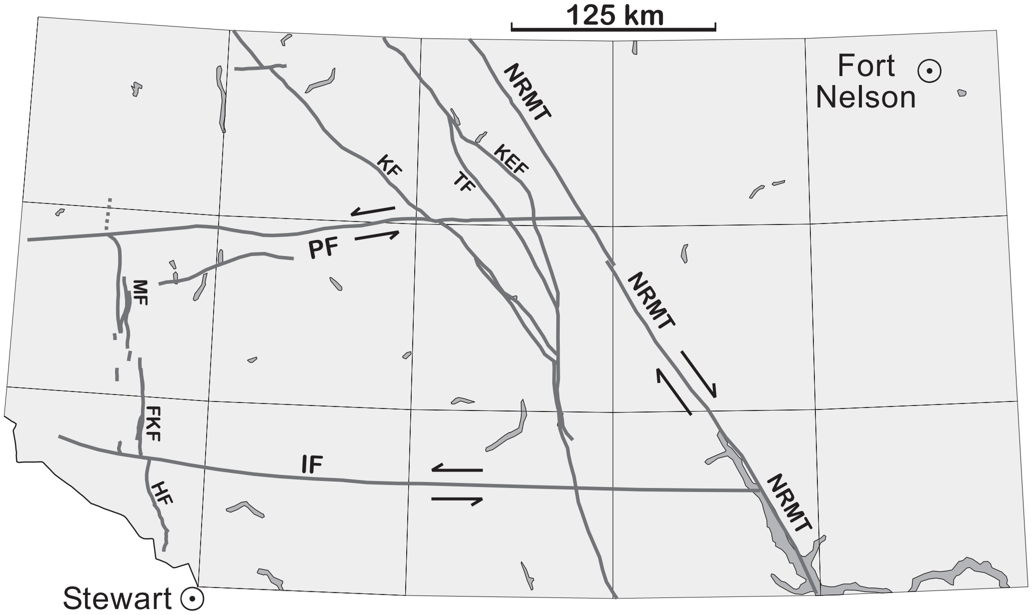

Figure 7. Major faults of north-central British Columbia, simplified from Figure 3, showing their angular relationships and the relatively minor, sinistral offset along the Pitman (PF) and Iskut River (IF) faults. MF-Mess Creek fault zone; FKF-Forrest Kerr fault; HF-Harrymel Creek fault; KF-Kutcho fault; TF-Thudaka fault; KEF-Kechika fault; NRMT-Northern Rocky Mountain Trench.

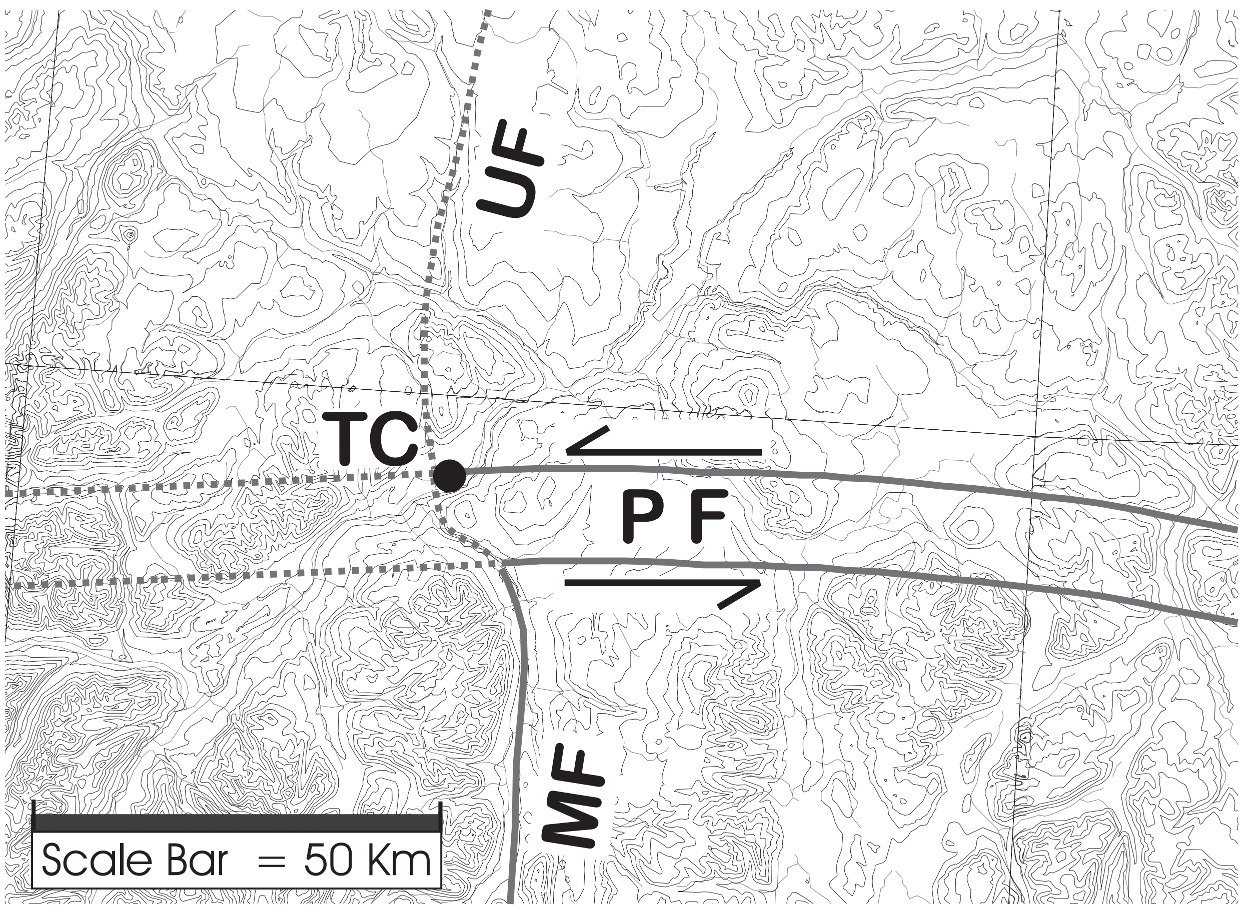

Figure 8. Simplified fault relationships near the village of Telegraph Creek (TC), showing the Mess Creek fault (MF) offset by the younger Pitman fault (PF). The stippled northern continuation of the Mess Creek fault (UF for `unmapped fault') and the western continuation of the Pitman fault have not been identified in the field.

Fault, has not been identified in the field. The westward continuation of the Pitman fault, to the west of Telegraph Creek, has not been mapped either, but this trend coincides with a strong west-trending magnetic anomaly (Figure 2).

TECTONIC SIGNIFICANCE

Both the Pitman and Iskut River faults display the angular relationships, direction of offset, and amount of offset that are consistent with their development as antithetic faults associated with major dextral fault offset during a compressional regime (Figure 6).

Anithetic faults are minor, subsidiary faults which form adjacent to larger faults that have developed due to oblique compression or `transpression' (Figure 6a). The amount of displacement along an antithetic fault is always minor compared to the displacement along the main fault; this difference can be an order of magnitude or more. Antithetic faults typically occur as sets of parallel faults (Figure 6b). The terms `tiling' and `domino effect' have been applied to describe the sense of movement and the accompanying minor block rotation (Nicolas, 1987; McClay, 1987).

The conceptual models for antithetic fault geometry and sense of movement shown in Figure 6 can be compared to the actual fault patterns documented in north-central British Columbia (Figure 7). The models (Figures 6b and 6c) predict that, outside the present study area, there should be additonal east-trending antithetic faults crossing the Canadian Cordillera.

EXPLORATION SIGNIFICANCE

Knowledge of these faults can be applied to mineral exploration work:

- Faults that pass near mineral deposits offset prospective terrain. Determination of the direction and amount of fault offset will enable exploration efforts to focus on the offset block.
- North of the study area, east-striking faults are loci for gold-quartz veins. This suggests that similar Tertiary age structures elsewhere may be prospective for precious metal mineralization.

Fault Offset of Prospective Geology

Figure 9 shows the distribution of mineral occurrences that lie near the trace of the Pitman and Iskut River faults. For stratabound deposits like the Eskay Creek (MINFILE 104B 008) and the Rock and Roll (MINFILE 104B 377) volcanogenic massive sulphide deposits (Figure 5), calculation of the direction and amount of fault offset will permit re-location of faulted-off favourable stratigraphy. For other deposit-types, resolution of fault displacement will allow investigations to continue within the offset segment of favourable geologic tracts.

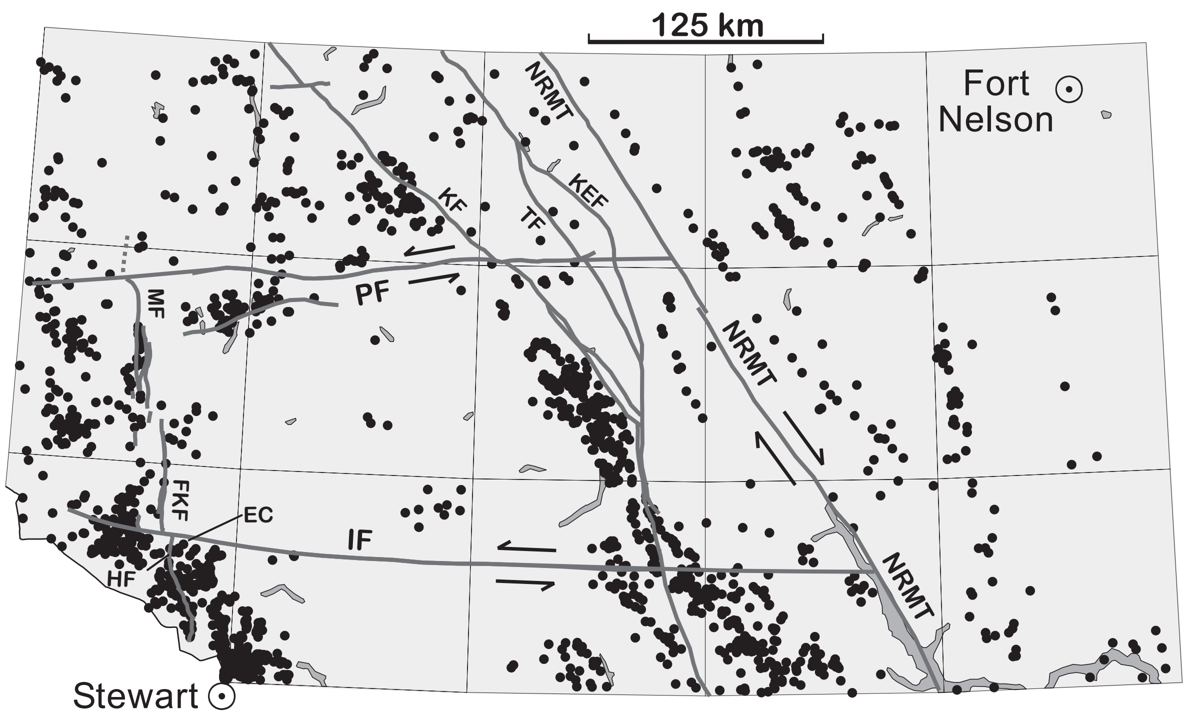

Figure 9. Mineral occurrences (from BC MINFILE) and major faults of north-central British Columbia. EC-Eskay Creek minesite; PF-Pitman fault; IF- Iskut River fault; MF-Mess Creek fault zone; FKF-Forrest Kerr fault; HF-Harrymel Creek fault; KF-Kutcho fault; TF-Thudaka fault; KEF-Kechika fault; NRMT-Northern Rocky Mountain Trench.

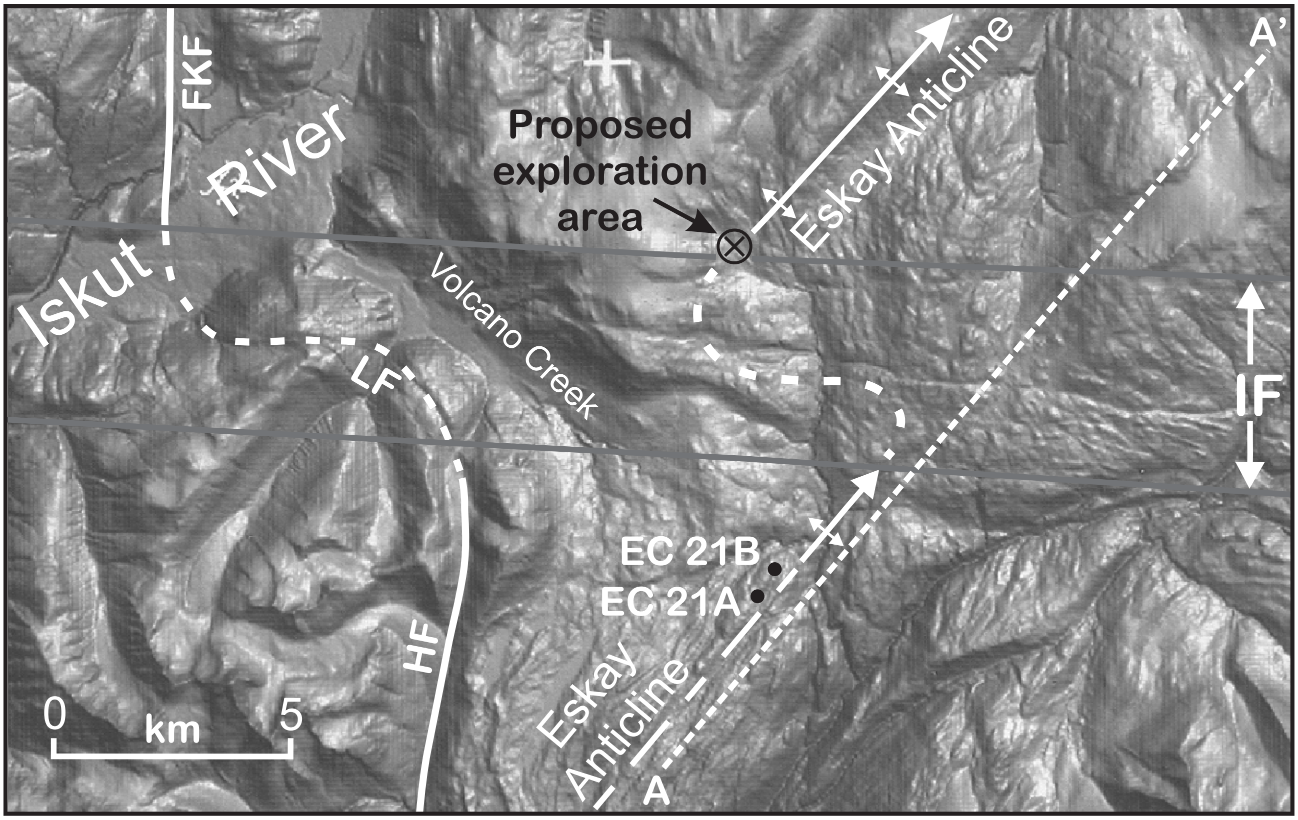

Figure 10. Close up of Figure 5 around the Eskay Creek mine, showing the interpreted sinistral offset of the Eskay Anticline along the Iskut River fault zone and a recommended exploration area. Cross-section A-A' is shown in Figure 11. Width of indicated fault zone exaggerated here by 10% to avoid obscuring east-trending topographic lineaments with linework. FKF-Forrest Kerr fault; LF-Leroy Creek fault; HF-Harrymel Creek fault; IF-Iskut River fault zone; EC 21B- 21B orebody at Eskay Creek mine; EC 21A - 21A deposit at Eskay Creek mine.

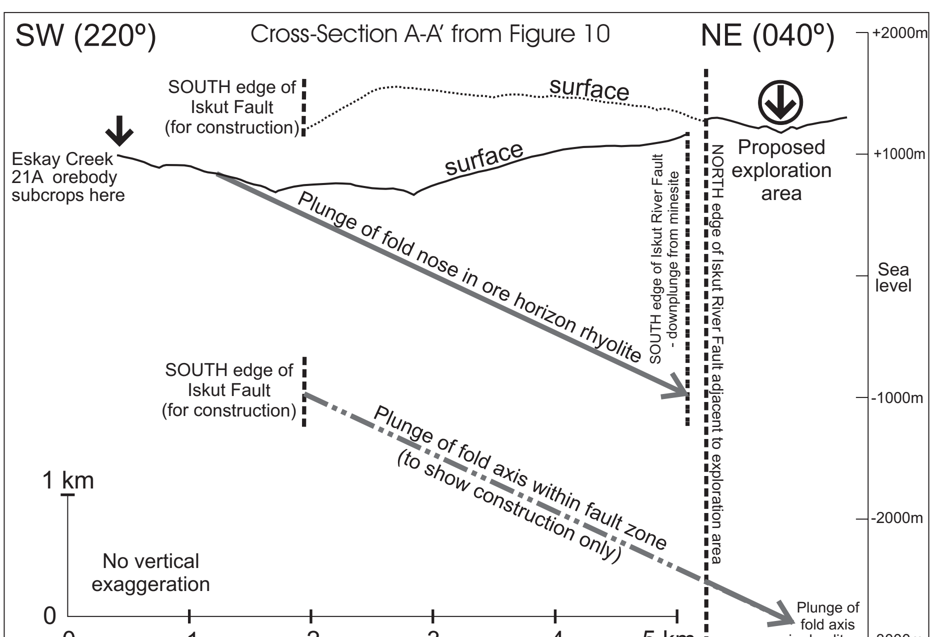

Figure 11. Cross-section along the fold axis of the Eskay anticline, looking WNW (310º). Two separate, overlapping, cross-sections are projected onto this diagram (see Figure 10), showing the plunge of the fold nose within the ore horizon rhyolite down-plunge from the mine area (a) on the south side of the Iskut River fault zone, and (b) on the north side of the Iskut River fault zone. These two lines of section are separated by 6 kilometres of sinistral offset at an oblique angle to the line of section. Some construction lines are shown.

Exploration Example - Eskay Creek Camp

At the Eskay Creek minesite, the 21A deposit subcrops at an elevation of 1000 metres. The Eskay Creek precious-metal-rich ore deposits lie along the western limb of a flat-lying to northeasterly-plunging anticline, the Eskay anticline (Figures 4 and 10). In the mine area this anticline plunges 25º on an azimuth of 040º. With this plunge, the depth to the `ore horizon rhyolite' increases by about 450 metres for every additional kilometre of horizontal distance (Figure 11).

If these angular relationships remain constant, the anticline would be cut by the Iskut River fault zone 4.0 kilometres down-plunge to the northeast of the minesite, at a depth below surface of about 2200 metres (Figures 10 and 11). Assuming the width of the Iskut River fault zone as 4 kilometres based on the interval of the Leroy Creek fault that is drag-folded (*see* Figure 10), and allowing for a progressive (incremental) left-lateral offset totalling 6 kilometres across this fault zone based on the measured offset between the Harrymel and the Forrest Kerr faults, the northeastward projection of the Eskay Creek anticline is predicted to exit the northern side of the Iskut River fault zone underneath a steep east-facing slope located 7000 metres north of the 21A zone on a bearing of 354º (Figures 10 and 11). Surface elevation at this point is 1300 metres - well above treeline. Just 600 metres northeasterly from this point, along the projected 040º trend of the Eskay Creek anticline, the topography drops down into a stream drainage which offers exposure of stratigraphically lower units.

At this point the distance from surface to the projected depth of the fold nose within the ore horizon rhyolite along the crest of the Eskay anticline is about 4000 metres (Figure 11). A program of mapping, deep-penetration geophysics and mercury geochemistry in this area could provide information necessary to justify an exploration drill program to a maximum depth of 4000 metres. However, this calculated depth is too great for routine exploration drilling and too great for all but the deepest mining scenarios. The two following arguments are presented in favour of conducting exploration work on this hillside:

1. The Eskay anticline plunges northeastward at 25º in the immediate mine area. South of the mine area the fold axis flattens abruptly and the Eskay anticline is flat-lying for more than 30 kilometres to the southwest (Lewis, 1996; Alldrick and Britton, 1992; Alldrick *et al.*, 1989). If the fold axis of this anticline also rolls flat down-plunge to the northeast of the minesite, then the depth to the ore horizon rhyolite will be substantially less than 4000 metres.
2. In the immediate mine area, the down-plunge extensions of the orebodies have been tested by an extensive grid drilling program. This work revealed that there are a series of minor southward-verging thrust faults to the north of the mine that lift the ore horizon slightly closer to surface than predicted by calculations based solely on the measured plunge of the fold axis (T. Roth, pers. comm., 1999).

Either or both of these situations would place the ore horizon at a shallower depth below the proposed exploration area than the depth of 4000 metres calculated in this study.

Fault-Hosted Mineralization

Tertiary antithetic faults like the Iskut River and Pitman faults may be prospective for precious-metal mineralisation. East-trending faults to the north of the study area are loci for gold-quartz veins (Mihalynuk *et al.*, 1994, p.192; Smith *et al.*, 1993, Smith and Mihalynuk, 1992, p.141). The western part of these structures, closer to the Tertiary Coast Range batholith and its satellite plutons, will be more prospective.

CONCLUSIONS

Low-angle oblique illumination of contoured federal government aeromagnetic maps has revealed anomalies that coincide with mapped regional-scale geologic structures. Faults identified in this study are key components of the structural and tectonic history of the Canadian Cordillera.

In the Iskut River area, these faults offset highly prospective strata. Resolution of the direction and amount of fault offsets enables focused, property-scale exploration work to continue onto the offset block. Fault zones may also be a locus for precious-metal mineralisation.

ACKNOWLEDGMENTS

Thanks to Margaret McPherson at Resource Geoscience and Imaging (RGI) and to Sarah Maxwell, Mike Fournier and Ward Kilby at the British Columbia Geological Survey for their careful help with figure preparation. The manuscipt was improved by reviews from Derek Brown, Jim Logan and Brian Grant, BCGS.

REFERENCES

Alldrick, D.J. and Britton, J.M. (1992): Unuk River Area Geology, BC Ministry Of Energy Mines and Petroleum Resources, Open File Map 1992-22, Scale 1:20 000.

Alldrick, D.J., Britton, J.M., Webster, I.C.L. and Russell C.W.P. (1989): Geology and Mineral Deposits of the Unuk Area, BC Ministry of Energy, Mines and Petroleum Resources, Open File Map 1989-10, Scale 1:50 000.

Davis, G.H. (1984): Structural Geology; John Wiley and Sons, New York, 492p.

Gabrielse, H. (1985): Major dextral transcurrent displacements along the Northern Rocky Mountain Trench and related lineaments in north-central British Columbia: Geological Society of America Bulletin, v. 96. p. 1-14.

Hodgson, C.J. (1989): The structure of shear-related, vein-type gold deposits: a review; Ore Geology Reviews, v.4, p.231-273.

Lewis, P.J. (1996): Regional geological map set - Iskut River project; in Final Report - Geological Data Sets - June, 1996, The Mineral Deposit Research Unit, The University of British Columbia.

Logan, J.M. and Drobe, J. (1997): BC Ministry Of Energy Mines and Petroleum Resources, Geoscience Map 1997-3, Scale 1:100,000.

McClay, K.R. (1987): The Mapping of Geological Structures, Geological Society of London, Handbook Series, 161 p.

Mihalynuk, M.G., Smith, M.T., Hancock, K.D. and Dudka, S. (1994): Regional and Economic Geology of the Tulsequah River and Glacier Areas; BC Ministry of Energy, Mines and Petroleum Resources, Geological Fieldwork 1993, Paper 1994-1, p. 171-197.

Nicolas, A. (1987): Principles of Rock Deformation; D. Reidel Pub. Co., Dordrecht, Holland, 208 p.

Ramsay, J.G. (1980): Shear zone geometry: a review; Journal of Structural Geology, v.2, p.83-99.

Read, P.B., Brown, R.L., Psutka, J.F., Moore, J.M., Journeay, M., Lane, L.S. and Orchard, J.J. (1989): Geology of More and Forrest Kerr Creeks, Northwestern British Columbia; Geological Survey of Canada, Open File Map 2094, Scale 1:50,000.

Silva, J.B., Oliveira, J.M., Matos, J. and Leitão, J.M. (1997): Aljustrel and the central Iberian Pyrite Belt; in Geology and VMS Deposits of the Iberian Pyrite Belt, Society of Economic Geologists, Guidebook Series Volume 27, p. 73-124.

Simpson, C. (1986): Determination of movement sense in mylonites; Journal of Geological Education, v.34, p.246-261.

Smith, M.T., Mihalynuk, M.G. and MacIntyre, D.G. (1993): Deformation and Structural Styles; Tatshenshini Project; BC Ministry of Energy, Mines and Petroleum Resources, Geological Fieldwork 1992, Paper 1993-1, p. 203-216.

Smith, M.T. and Mihalynuk, M.G. (1992): Tulsequah Glacier: Maple Leaf; in Exploration in Exploration in British Columbia 1991, BC Ministry of Energy, Mines and Petroleum Resources. p. 133-142.

Souther, J.G. (1972): Telegraph Creek map-area, British Columbia. Geological Survey of Canada, Paper 71-44, 38 p.

Wilson, G. (1982): Introduction to Small-Scale Geological Structures, George Allen & Unwin Ltd., London, U.K., 128 p.

Geology and Mineral Potential of the Ecstall VMS Belt (NTS 103H, 103I)

By D.J. Alldrick and C.S. Gallagher

KEYWORDS: *Economic geology, mineral potential, geologic mapping, Central Gneiss Complex, Coast Belt, VMS, sulphide, metavolcanic, greenstone, Devonian, Scotia, Ecstall, Packsack, Prince Rupert.*

INTRODUCTION

The mid-coast region of British Columbia, extending between Prince Rupert and Bella Coola, hosts 31 volcanogenic massive sulphide (VMS) deposits (BC MINFILE; Massey, 1999). A multi-year project will investigate the geologic setting of many of these prospects, starting in the Ecstall VMS belt near Prince Rupert (Figure 1). The Ecstall belt is part of the Central Gneiss Complex, an anastomosing network of high-grade metamorphic rocks enclosed by younger granitoid rocks of the Coast Plutonic Complex (Figure 2).

The Ecstall belt extends 80 kilometres from the estuary of the Skeena River to the Douglas Channel fiord (Figures 2 and 3); width of the belt varies from 3 to 20 kilometres. The belt is equidistant from the northern communities of Prince Rupert, Terrace and Kitimat (Table 1). In addition to its proximity to tidewater and to these communities, the Ecstall belt is close to the Yellowhead Highway, the Skeena Railway line of VIA Rail and the national

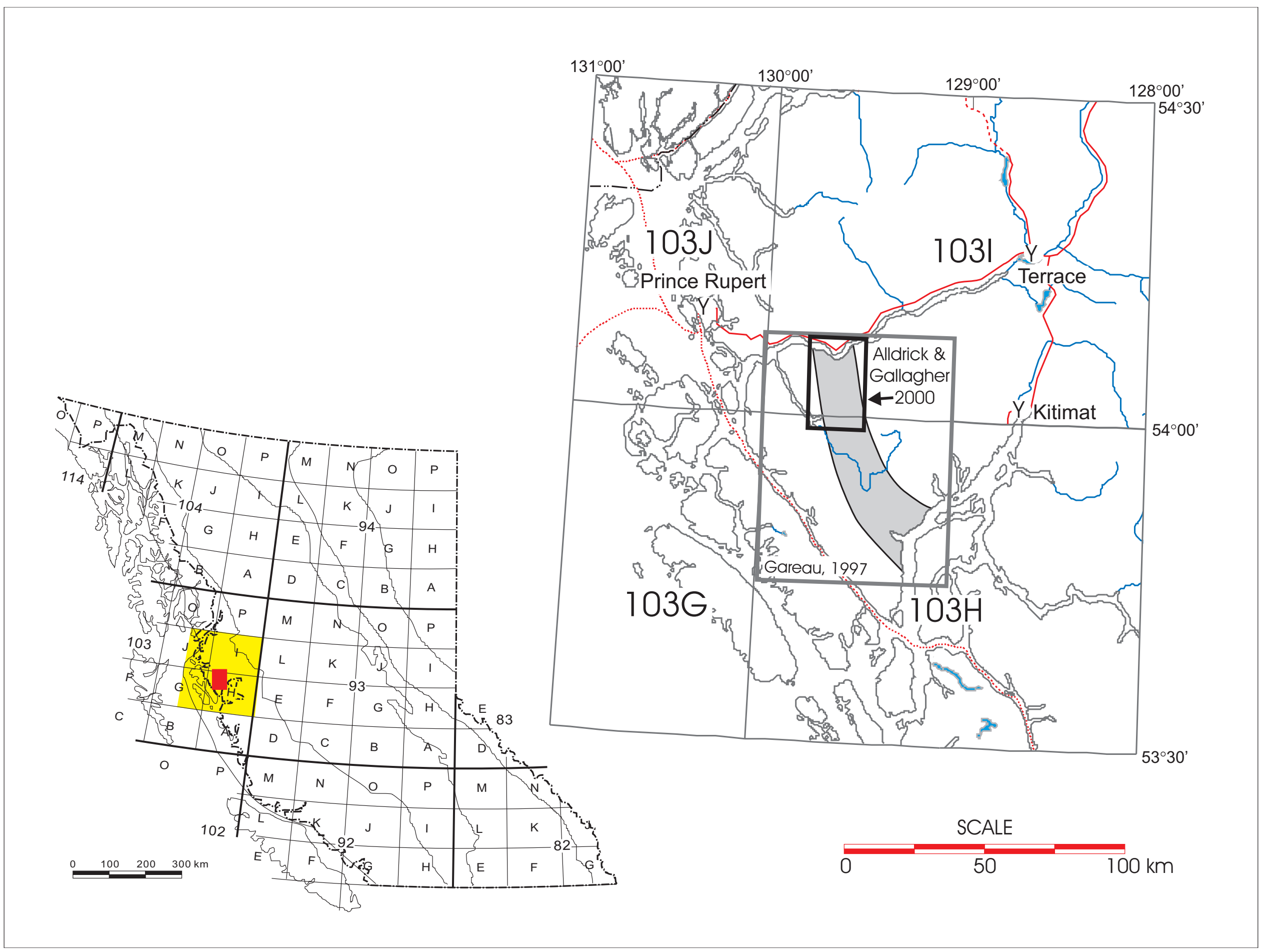

Figure 1. Location of the Ecstall belt in British Columbia.

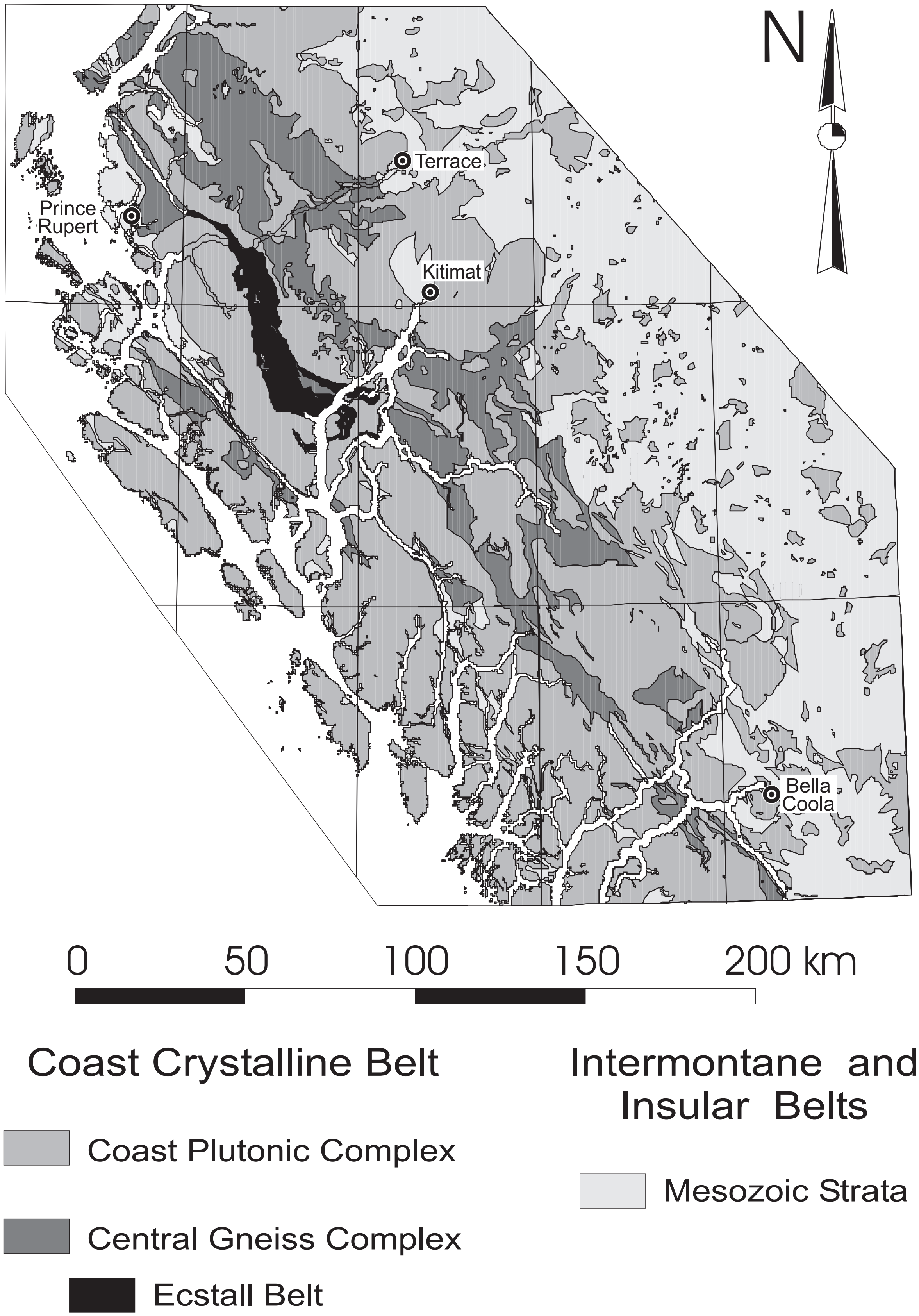

Figure 2. Geology of the mid-coast region of British Columbia, highlighting the location of the Ecstall metavolcanic belt within the Central Gneiss Complex and the Coast Plutonic Complex.

TABLE 1
KEY DISTANCES FOR DEPOSITS IN THE ECSTALL BELT

Deposit:	Scotia	Ecstall	Packsack
Elevation	758 m	182 m	242 m
Distance to:			
Ocean	27	24	18
Estuary / Tidewater	15	6	15
Hydro Powerline	10	19	29
Highway	15	39	49
Railway	15	39	49
Prince Rupert	49	72	82
Kitimat	67	60	59
Terrace	84	93	98

power grid. The northern and southern ends of the belt have established networks of logging roads.

Elevation ranges from sea level to 1760 metres. Smooth undulating ridgecrests are flanked by steep slopes characteristic of glaciated valleys. Despite this precipitous terrain, it is possible to traverse the entire belt from north to south without exceeding 125 metres elevation by traveling up the Scotia River valley and through the pass at Big Falls Lake, then up the Ecstall River valley and through the pass at Ecstall Lake and finally down the Quaal River valley.

Rainfall is heavy; average annual precipitation at Prince Rupert is 244 centimetres (96 inches). The combination of low elevation and proximity to the coast leaves the valley bottoms free of snow through most of the year. Dense coastal rainforest covers all but the steepest slopes where bedrock is exposed in cliffs or along avalanche shoots. Ridgecrests above 1100 metres elevation are free of trees and shrubs.

In the late 1890s local Indians lead prospectors to the exposed sulphide lenses of the Ecstall deposit in Red Gulch Creek. This deposit was investigated intermittently from 1900 to 1952 by a variety of companies. A regional exploration program conducted by Texasgulf Inc. in 1958 discovered the Scotia and Packsack deposits and the Horsefly showing. For the last 20 years there has been continuous exploration work on the properties in this belt, carried out by a series of companies. Discovery of the 14 other sulphide occurrences in the Ecstall belt are the result of these recent exploration efforts.

Regional scale mapping in this area was conducted by the Geological Survey of Canada from 1962 to 1966 (Roddick 1970a, 1970b; Hutchinson 1970, 1979, 1982) and from 1987 to 1989 (Gareau, 1991a,b,c, 1997). Woodsworth, Crawford and Hollister (1983) produced a geological field trip guidebook for the Terrace - Prince Rupert corridor.

University research projects within, adjacent to and along strike from the Ecstall belt have investigated a wide variety of geological features. These studies are reported in theses by Padgham (1959), Money (1959), Eldridge (1983), Krage (1984), van der Heyden (1989), Heah (1991) and Gareau (1991a) as well as in published reports by Hutchinson (1970), Brew and Ford (1978), Crawford and Hollister (1982), Sutter and Crawford (1985), Rubin *et al*. (1990), Heah (1990), Crawford and Crawford (1991), McClelland *et al*. (1991a), McClelland *et al*. (1991b), Gehrels *et al*. (1991a), Gehrels *et al*. (1991b), Gehrels *et al*. (1991c), Samson *et al*. (1991), Gareau (1991c), Drinkwater *et al*. (1993), Dusel-Bacon *et al*. (1996), Gehrels and Kapp (1998), Gehrels and Boghossian (in press) and Boghossian and Gehrels (in press).

Regional scale studies of VMS deposits have recently been completed by Newberry *et al*. (1997) and Massey (1999). Property scale maps and reports prepared by industry geologists between 1912 and 1999 are listed with the individual property descriptions in the BC MINFILE database.

Objectives of the current mapping program include: establish a more detailed lithological breakdown within the four stratigraphic packages documented by Gareau (1997), study the relationships between this detailed lithostratigraphy and the many mineral occurrences of the belt, trace out prospective felsic volcanic strata, and investigate a possible coeval relationship between the Big Falls orthogneiss and the metavolcanic package. In the 1999 field season, three weeks mapping was completed by a team of two. Work concentrated on mapping rock-cuts along the extensive logging road network at the north end of the Ecstall belt and along the Yellowhead Highway and Skeena Railway.

REGIONAL GEOLOGIC SETTING

The geologic setting of the Ecstall belt is shown in Figures 2, 3, 4 and 5. The Ecstall metamorphic belt is part of the Central Gneiss Complex, an anastomosing network of high-grade metamorphic rocks enclosed by younger granitoid rocks of the Coast Plutonic Complex (CPC; Figure 2). Together, these two complexes comprise the Coast Belt. The following summary is adapted from Greenwood *et al*. (1992) and Woodsworth *et al*. (1992).

Plutonic rocks make up more than 80% of the Coast Belt; the remainder is granitoid gneiss, metasediments and metavolcanics. Plutonic rocks of the CPC range in age from Late Silurian to Eocene. In general the oldest plutons are exposed along the western edge of the CPC and the ages of plutons young progressively to the east. Rocks range in composition from granite to gabbro, but 70% of all plutonic rocks lie within the compositional range of tonalite-quartz diorite-diorite. Among the circum-Pacific plutonic terranes, the CPC is the largest, the most mafic, and the most deficient in K-feldspar.

In the Prince Rupert - Terrace region, intrusions of different ages have extensive flat-lying `sills' developed along their eastern margins (Figure 4). In the Ecstall belt north of Big Falls Creek and on Hawkesbury Island, these sill-like apophyses are preserved as erosional remnants

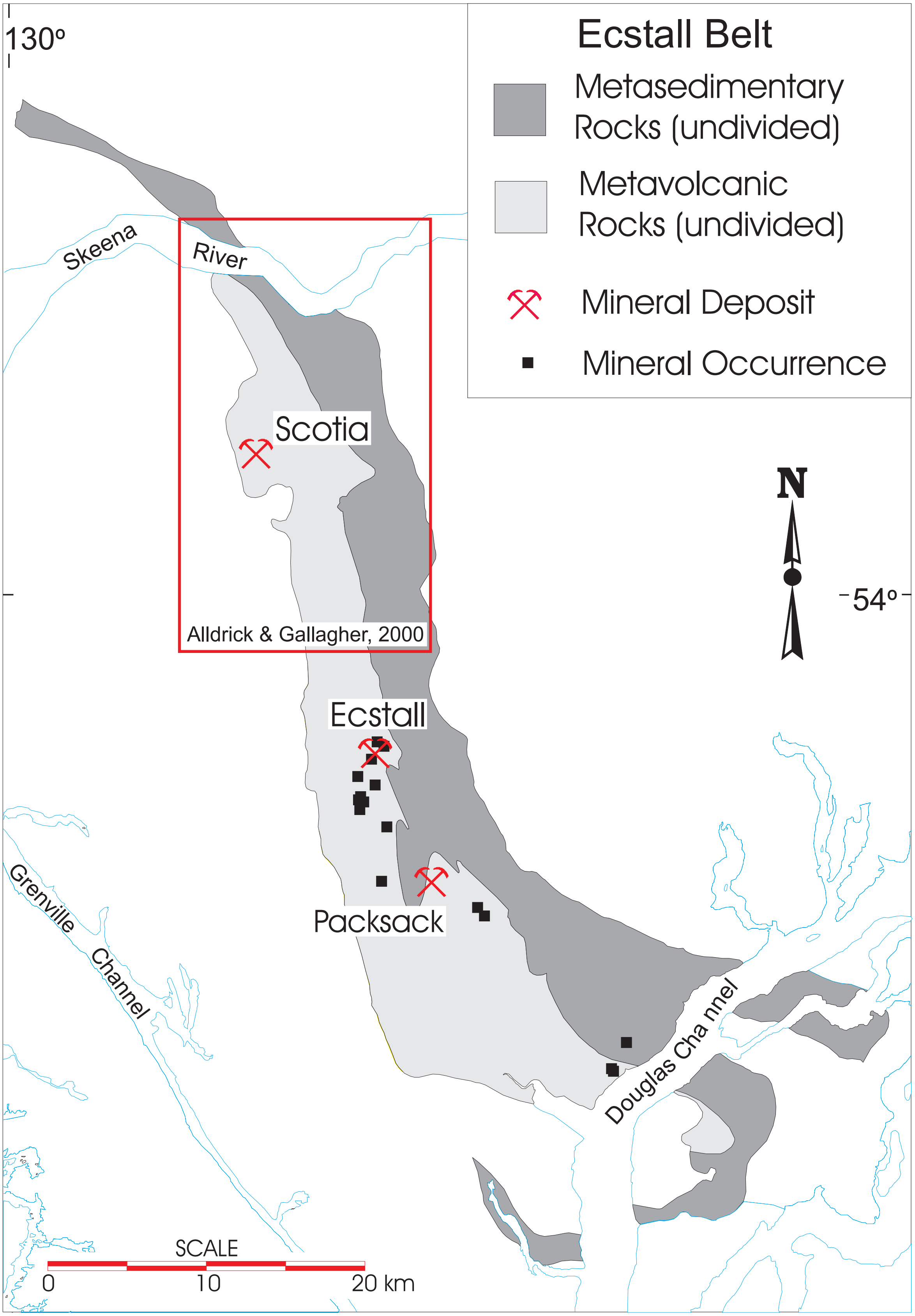

Figure 3. Geology and volcanic-associated massive sulphide occurrences of the Ecstall belt (simplified from Gareau, 1997).

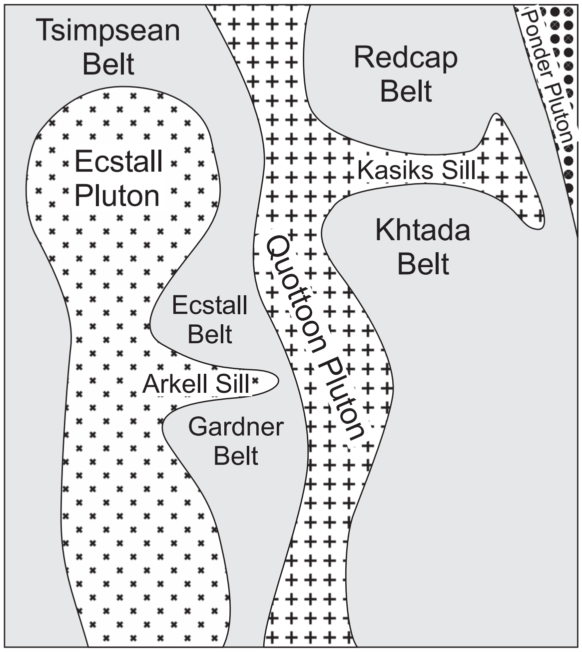

Figure 4. Schematic section showing the relationships between intrusive rocks of the Coast Plutonic Complex and metamorphic rocks of the Central Gneiss Complex in the Ecstall area.

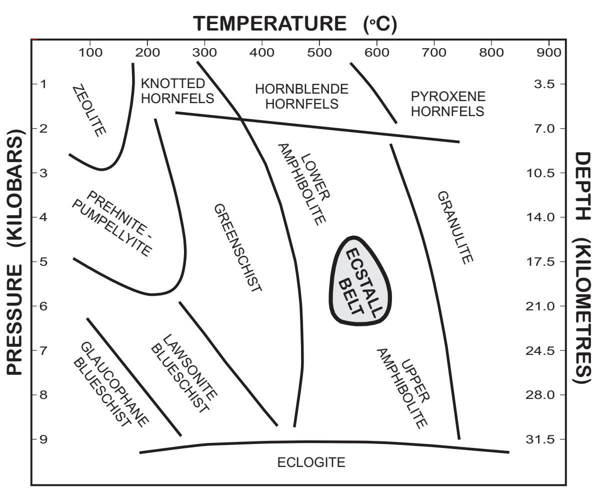

Figure 5. Metamorphic pressure-temperature conditions in the Ecstall belt (modified from Greenwood *et al*., 1992 and Gareau, 1991c).

on hilltops and ridgecrests (Gareau, 1997), where they overlie and obscure prospective metavolcanic strata.

Metamorphic rocks of the Coast Belt typically occur as screens or pendants surrounded or intruded by the plutonic rocks (Figure 2). The Central Gneiss Complex is composed of rocks ranging and age from Proterozoic through Paleozoic. Remnants of Paleozoic metamorphism are preserved locally, while most regional metamorphic overprints are Mesozoic and early Tertiary in age. Intense Cretaceous and early Tertiary metamorphism, deformation and plutonism have obscured evidence of earlier events in many places. Most metamorphic effects can be attributed to regional metamorphism, but contact metamorphism from the adjacent plutons can also create a late metamorphic overprint.

The Prince Rupert - Terrace corridor is the most extensively studied and best understood area of the Coast Belt**.** This is the most deeply exhumed part of the Coast Plutonic Complex, and metamorphic grades range up to kyanite-amphibolite, sillimanite-amphibolite and granulite facies in different parts of this area. Within the Ecstall metavolcanic belt, Gareau (1991a,c) has documented a southwest to northeast progression from lower amphibolite facies to granulite facies, with most rocks falling within the kyanite amphibolite (upper amphibolite) facies (Figure 5).

The Devonian volcanic arc that evolved into the Ecstall metamorphic belt likely developed in a similar pericratonic tectonic setting as the extensive volcanosedimentary rocks of the Yukon-Tanana terrane (Gareau, 1991a,c). The regional geologic history of the Ecstall belt is summarized in Figure 6; Devonian volcanism and sedimentation and comagmatic intrusions, are followed by three poorly-constrained phases of deformation and four well-dated plutonic episodes. The Jurassic to Eocene plutonic and metamorphic history of the CPC is consistent with a model of east-dipping subduction beneath a single, allocthonous Alexander-Wrangellia-Stikinia superterrane, emplaced against North America in Middle Jurassic time (van der Heyden, 1989).

GEOLOGY OF THE NORTHERN ECSTALL BELT

Mapping in the 1999 field season covered road networks within the area outlined on Figure 3. Figure 7 shows the simplified geological map and legend.

Stratified Rocks

Unit 1 - Metavolcanics

Metavolcanic rocks of the Ecstall belt host all the known mineral occurrences (Figure 3). This sequence is the largest unit defined by Gareau (1991a), and extends the entire length of the belt, averaging four kilometres in thickness. Metavolcanic rocks are in gradational contact with the Big Falls orthogneiss (Unit C) and with metasedimentary rocks; contact relationships with other units were not determined. The metavolcanic unit is heterogeneous. Biotite schist, hornblende-biotite schist and semi-schist comprise 70% of the unit. Interlayered with these lithologies are 100-metre-thick heterogeneous lenses of pyrite-quartz-sericite schist, amphibolite, quartzite and calcareous muscovite-biotite schist. The continuity of these smaller lenses has not been confirmed, but they may extend along strike for several kilometres.

Unit 1a - Mafic Metavolcanics

The hornblende-biotite schist is a black to greenish black recessive rock that is fissile and commonly highly

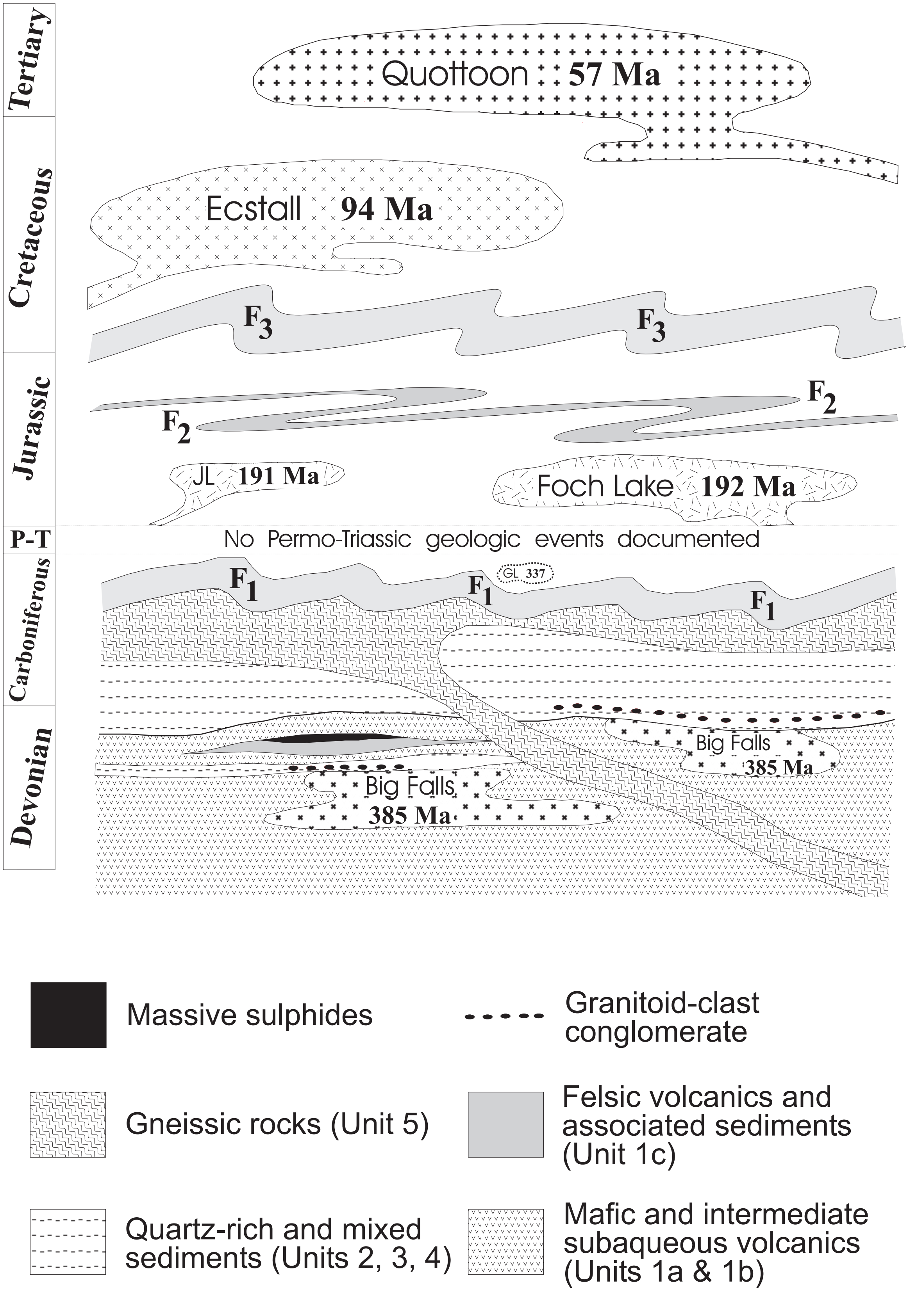

Figure 6. Geologic history of the Ecstall belt. F-1, F-2 and F-3 are successive episodes of folding. JL is the Johnson Lake stock; GL is the Gareau Lake stock (adapted from Gareau, 1991a,b,c and 1997).

weathered. It is the thickest of the metavolcanic units, averaging several hundred meters thickness, and displays gradational boundaries with surrounding metavolcanic and metasedimentary lithologies. Also present within the mafic metavolcanics are lenses of resistant, homogeneous, black to rusty-coloured, garnet-hornblende amphibolite interlayered on a 5 to 20 metre scale.

Compositional layering is typically non-existent, or is very weak and defined by discontinuous millimetre-thick laminae. The rock contains more than 50% medium-grained biotite and 10% to 20% hornblende. Granular, fine to medium grained plagioclase comprises up to 20% of the rock and is typically polygonal. Disseminated pyrite locally constitutes up to 5% of the rock and accessory skeletal garnet porphyroclasts are preserved. Euhedral titanite, that makes up to 10% of some thin sections, is a common mineral associated with sulphide grains. Titanite occurs as well defined layers, as radial masses cored by pyrite, or as interstitial clusters or individual grains. Epidote-hornblende knots or pods are common within this unit; when present these knots make up 5% to 15% of the rock. The schist locally displays discontinuous, orange, medium-grained, calcareous lenses that are highly recessive.

The abundance of hornblende and biotite and the lack of quartz is consistent with a mafic volcanic protolith. The lithologic heterogeneity observed in the unit suggests a highly dynamic depositional environment. Discontinuous carbonate lenses appear to be primary and are indicative of a subaqueous environment.

Unit 1b - Intermediate Metavolcanics

Hornblende-diopside-biotite-quartz-plagioclase semi-schist is common along the east side of the Scotia Main logging road (Unit 1b in Figure 7). The unit has a minimum structural thickness of 200 metres and unknown contact relationships with surrounding lithologies. Gareau (1991a) concluded that this is the dominant lithology in the northern part of the Ecstall belt. Semi-schist is fine to medium grained, granular, well indurated and weathers dark grey to black.

This quartz-plagioclase rock has medium-grained biotite partings spaced 1 to 5 centimetres apart. Plagioclase and diopside microlithons have 5% to 10% interstitial biotite. Titanite occurs as euhedral interstitial grains making up less than 2% of the rock. Fine to medium grained prismatic hornblende, ranging from 5% to 10% by volume, is concentrated along biotite parting surfaces.

The presence of biotite semi-schist members within the mafic metavolcanic schists marks a decrease in mafic minerals, and an increase in quartz from near zero to 10% to 20%. This mineral assemblage suggests that the protolith was a metamorphosed intermediate volcanic rock, or a volcaniclastic sedimentary rock.

Unit 1c - Felsic Metavolcanics

This heterogeneous unit is composed of pyritic quartz-muscovite schist interlayered with 10 to 20 metre thick bands of muscovite-bearing quartzite and hornblende-biotite schist. The unit is shown in Figure 7 as two discontinuous lenses a few hundred metres in thickness that have gradational boundaries with the surrounding metavolcanic unit. These two lenses are roughly on strike with one another and may be a continuous layer. Contacts with adjacent lithologies are typically sharp but may be gradational over half a metre to a metre. Both bands of felsic metavolcanics lie well east of the Scotia VMS deposit; however, the southern lens of this unit is host to the Friday the 13th showing.

Quartz-muscovite schist is a medium to coarse-grained rock with significant sulphides, containing on average 10% to 15% pyrite. These rocks also locally display relict clastic or fragmental volcanic textures. Primary compositional layering, on a 1 to 10 centimetre scale, is defined by alternating quartz and phyllosilicate layers. Pyrite seams or layers, up to 4 millimetres thick, are concordant with compositional layering and characterize the lithology. Subhedral garnet, with an average diameter of 5 millimetres, is commonly associated with the sulphides, as is biotite. Chlorite can be seen in handsample surrounding the garnet porphyroblasts. Quartz-rich metasediments associated with the felsic metavolcanic rocks are similar in composition and relationships as those described in Unit 2.

Pyritic quartz-sericite schists are interpreted as metamorphosed felsic volcanic flows, tuffs and fragmental rocks associated with subaqueous extrusion. Local thin units (1 to 5 metres) of thinly laminated (1 to 2 centimetres) quartz-rich rock that grades into the sericite schist likely share a volcanic origin and are likely metamorphosed chert.

Unit 2 - Quartzite and Quartz Schist

Metasedimentary rocks mapped in this study consist dominantly of muscovite-bearing quartzite. This unit may be correlative with the quartzite of Gareau (1991a,b,c; 1997), shown as Unit 3 in Figure 7. The unit rarely exceeds 200 metres thickness, but attains a maximum structural thickness of one kilometre in one location. Quartzite is in gradational contact with the surrounding metavolcanic unit.

Quartzite contains greater than 95% quartz and is very well indurated, resistant, homogeneous, light to medium grey, and fine to very fine grained. The rock typically weathers light grey, but is rusty red when pyrite is present. The unit locally contains lenses of matrix-supported conglomerate composed of stretched metatonalite and other granitoid cobbles with an aspect ratio of 10:2:1 or more. Finely laminated compositional layering is defined by light grey quartz-rich layers alternating with dark grey to black layers of quartz, biotite and graphite(?). Pyrite commonly occurs along partings as dissemi-

LEGEND

STRATIFIED ROCKS

PALEOZOIC (Devonian?)

GNEISS

5 — Mafic to intermediate gneiss. Biotite epidote hornblende mafic gneiss. Resistant, black to greenish black rock. Commonly migmatitic in northern areas. Medium grained, granular. Locally contains pyrite-, garnet- and diopside-rich boudins and lenses. Medium grained, granular, light grey weathering biotite q-f gneiss is present in southern portions of unit.

METASEDIMENTARY ROCKS

4 — Mixed metasedimentary rocks of the Khtada Lake area. Not mapped in this study. See Hollister (1977, 1982) for description.

3 — Quartzite Unit of Gareau (1997). Not mapped in this study. May be correlative with unit 2.

2 — Quartzite and Quartz Schist: Quartzite is a light grey, resistant rock, >95% quartz. Fine grained to very fined grained. Laminations of muscovite with trace to minor pyrite. Interlayered with garnet-biotite-quartz schist in the southern map area

METAVOLCANIC ROCKS

1c — Felsic Volcanic Rocks: Pyritic quartz-muscovite schist to semi-schist; ± biotite, ± garnet. Fissile and recessive. Forms prominent gossans which can be traced across terrain. Commonly associated with quartz-rich metasedimentary members within the metavolcanic unit: garnet-biotite-quartz schist to phyllite, and muscovite quartzite interlayered on the 5-to-10 metre scale with mafic and felsic metavolcanic rocks.

1b — Intermediate Volcanic Rocks: Hornblende biotite quartz feldspar semi-schist ± epidote. Dark grey to black medium grained rock. Resistant. Hornblende biotite rich partings on cm-

1a — Mafic Volcanic Rocks: Hornblende biotite plagioclase schist ± pyrite ± garnet; dark black to rusty red recessive and commonly fissile, rare discontinuous carbonate lenses, homogeneous on outcrop scale, locally displays relict volcaniclastic tecture.

INTRUSIVE ROCKS

TERTIARY - 56.8 +6/-0.1 Ma (Late Paleocene)

C — **Quottoon Pluton**: hornblende ± biotite tonalite to quartz diorite with abundant screens of gneiss and common rafts of metasedimentary rock. Medium to coarse grained. Strongly foliated throughout and locally lineated along western margin.

CRETACEOUS - 93.5 ± 1 Ma (early Late Cretaceous)

B — **Ecstall Pluton**: Epidote hornblende biotite metadiorite (**Bd**) to metaquartzdiorite (**Bqd**) and granodiorite, with minor biotite hornblende quartz diorite. Medium to coarse grained. Moderately foliated. Up to 5% fine to medium grained epidote is a characteristic feature.

DEVONIAN - 385 ± 4 Ma (Middle Devonian)

A — **Big Falls Orthogneiss**. Biotite hornblende meta-tonalite/trondhjemite ± garnet ± epidote. Light grey, fine to medium grained. Texture varies from plagioclase augen gneiss to fine grained plagioclase porphyritic gneiss to mylonite. Probably co-magmatic with the volcanic

Highway

Synform Axis

Logging Road

Antiform Axis

Mountain Peak

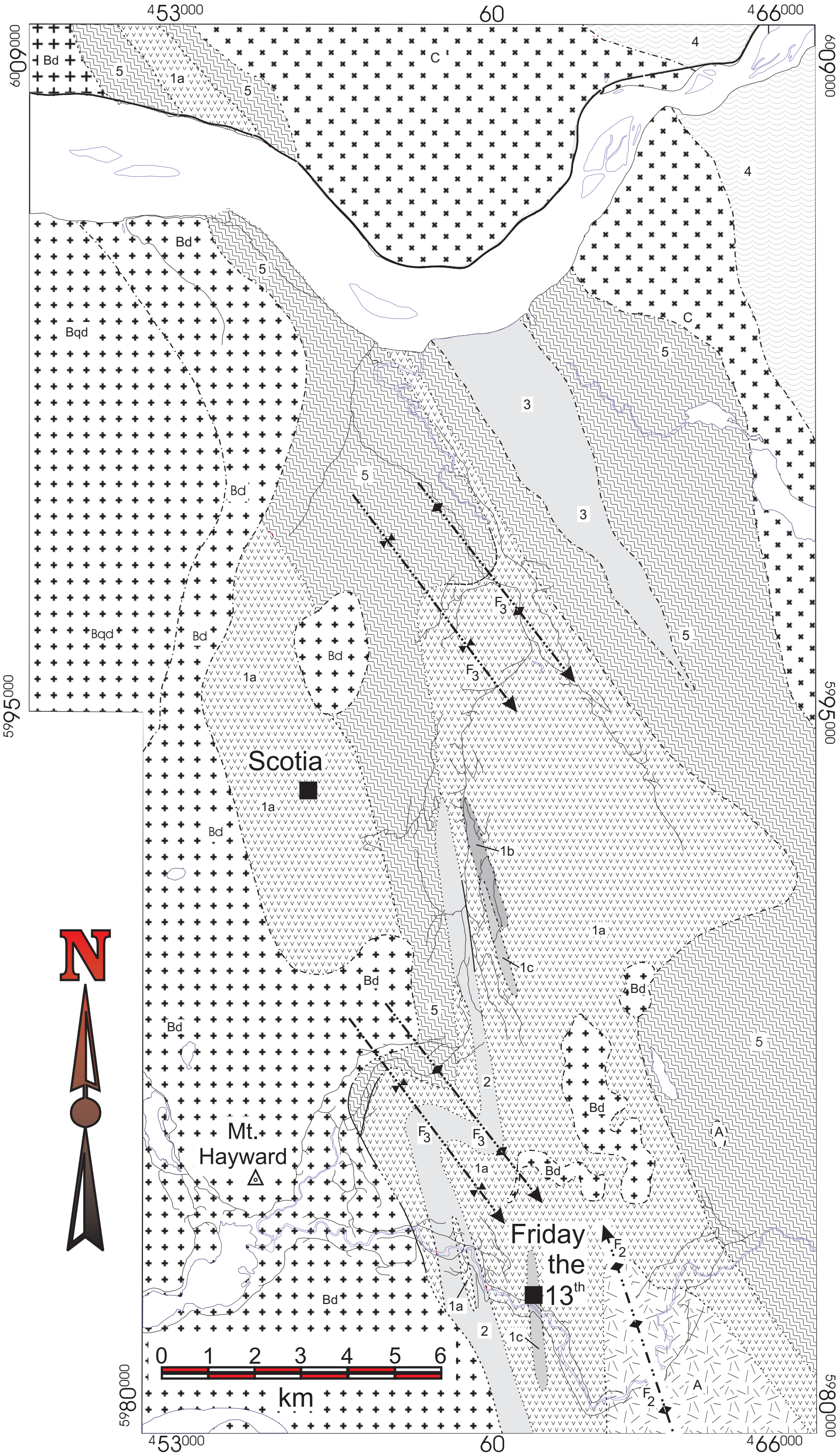

Figure 7. Geology of the northern Ecstall belt.

nations or semi-continuous laminae, not exceeding 5% of the rock.

South of Big Falls Creek, quartzite is interlayered with lenses of fine to very fine grained garnet-biotite-quartz schist. The gradational contact between the quartzite and schist is marked by quartz-rich rock with partings of medium-grained biotite and rare subhedral garnets ranging from 0.3 to 1.0 centimetres in diameter..

Unit 3 - Quartzite unit (from Gareau, 1991a)

This unit crops out northeast of the 1999 map area (Figure 7). The quartzite is a large lens, up to two kilometres thick, hosted entirely within the gneissic unit (Unit 5). Quartzite is in sharp contact with the surrounding gneissic rocks. The map unit is described as a “white to grey, locally pyritic quartzite, interlayered with lesser amounts of biotite-hornblende gneiss, fissile mica schist, black phyllite to meta-argillite, semi-pelite to pelite and marble” (Gareau, 1991a, p.14). The quartzite is a granoblastic rock; biotite is present in thin layers or partings less than 1 millimetre thick, or as minor interstitial grains. Accessory minerals are plagioclase, zoisite, cummingtonite, muscovite and carbonate. Gareau (1991a, p.14) concluded that these potassium and calcium-rich accessory minerals are consistent with a protolith of quartz arenite rather than chert.

Unit 4 - Metasedimentary rocks

Intensely deformed (Crawford *et al.*, 1987) high-grade metasedimentary rocks of the Khtada Lake area have been metamorphosed to granulite facies (Kenah and Hollister, 1983). These are the highest grade metamorphic rocks of the Central Gneiss Complex (Greenwood *et al.*, 1992). No stratigraphic correlation has been proposed for these rocks.

Unit 5 - Gneiss

A substantial belt of gneissic and locally migmatitic rocks are exposed along the western margin of the Ecstall metamorphic belt. Composition varies from buff weathering, grey, quartz gneisses in the south to migmatitic biotite-hornblende mafic gneisses in the north. Transition between the two lithologies is gradational over 300 metres.

Intermediate Gneiss

These light grey, well indurated and resistant gneisses are most common in the central western portion of the mapped area, northeast of Mt. Hayward. They occur as a north-northwest-trending belt with a maximum structural thickness of one kilometre.

Gneissic layering is defined by alternating medium grey and light grey layers averaging 10 centimetres thickness. Medium grey layers consist of medium grained, granular quartz-plagioclase matrix with substantial biotite and chlorite that make up 40% of the rock by volume. Light grey layers consist of approximately 60% quartz and minor plagioclase with up to 30% interstitial biotite. Sparse pyritic laminae are associated with the light grey layers.

Mafic Gneiss

Homogeneous, black to greenish black biotite hornblende plagioclase gneiss occurs as a northwest-trending belt with an average thickness of two kilometres. Along the southern bank of the Skeena River an extensive exposure of mafic gneiss is intruded by a swarm of discordant pegmatite dikes and sills (Woodsworth *et al.*, 1983, p.27-29).

Gneissic layering is well defined and typically 10 to 15 centimetres thick, with sharp boundaries. Compositional layering alternates between mafic biotite-diopside-hornblende to felsic biotite- quartz-plagioclase layers. Mafic layers consist of medium grained hornblende rock (60% amphibole) with interstitial plagioclase and minor biotite and garnet porphyroblasts. Light grey layers consist of 20% quartz, 60% plagioclase with interstitial biotite and hornblende. Minor bands and pods of hornblendite and epidote-garnet-pyrite-diopside and bands of migmatite were also noted. Hornblende amphibolite (hornblendite) layers, averaging 30 centimetres thick, consist entirely of medium to coarse grained, black, subhedral hornblende. Locally present are discontinuous pods of pyrite, garnet, epidote and diopside, typically 10 to 15 centimetres thick. Light grey to white migmatitic layers, several centimetres thick, occur as wavy discontinuous bands within the gneiss and consist of coarse to very coarse grained plagioclase and quartz.

The gneissic rocks lack relict igneous textures, such as flow banding and porphyroclasts, that would indicate an igneous protolith. The mineral assemblage of plagioclase, biotite, hornblende and minor quartz is consistent with a protolith of intermediate to mafic volcanic rock or immature volcanic sediment.

Intrusive Rocks

Ponder Pluton

The Ponder Pluton crops out to the northeast beyond the study area, but it is shown schematically in Figure 4. This is a mid-Eocene (47 Ma) hornblende-biotite granite to granodiorite, that may have been emplaced at a relatively high level (Hutchison, 1982; Sisson, 1985).

Unit A - Quottoon Pluton

This major pluton was mapped north of the Skeena River along the Yellowhead Highway. It is a long narrow body that extends north through southeastern Alaska, where it is called the “foliated tonalite sill” (Brew and Ford, 1978; Gehrels *et al.*, 1991a). The Quottoon Pluton is a medium to coarse grained hornblende quartz diorite to tonalite and is intensely foliated close to its contact with the gneissic rocks of the Ecstall belt. Age determinations from this extensive pluton span Late Cretaceous (80 Ma) to mid-Eocene (43 Ma) time (van der Heyden, 1989, p.158-160), with Gareau's (1991a, p.184-185) age of 56.8 Ma collected from a site closest to the present study area.

Unit B - Ecstall Pluton

The Ecstall pluton is the largest of a series of magmatic-epidote-bearing plutons (Zen and Hammarstrom, 1984; Zen, 1985) in the western Cordillera called the Ecstall Suite (Woodsworth *et al.,* 1992, p.518-519). Along the western margin of the map area (Figure 7), the early Late Cretaceous Ecstall pluton is a large homogeneous biotite-hornblende diorite to quartz diorite. Age determinations span 98 Ma to 64 Ma (Gareau, 1991a, Figure 3-1) with the six most recent analyses averaging 93.5 Ma (unpublished data from van der Heyden, 1991, cited in Gareau, 1991a, p.161-164). The rock is weakly foliated, medium to coarse grained and weathers to a black and white, granular-textured surface. Foliation is defined by preferentially oriented biotite and hornblende. The rock is commonly equigranular, but locally displays plagioclase porphyroclasts. Prominent crystals and aggregates of magmatic epidote comprise 5% of the rock and are associated with knots of biotite. Dark grey to black mafic schlieren are common and parallel the foliation within the rock. Medium grained, euhedral, transparent titanite is also present. Contacts are sharp and discordant to the foliation. The eastern contact of the pluton is also discordant to the regional trend of map units. No chilled margin or contact metamorphic aureole was noted.

Unit C - Big Falls Orthogneiss

The Big Falls Orthogneiss is a Middle Devonian (385 Ma; Gareau, 1991a) medium to coarse grained epidote-biotite-hornblende metatonalite exposed in the southeastern corner of the mapped area. It crops out as homogeneous and resistant light grey rock with a maximum structural thickness of 3.5 kilometres. The unit is in gradational contact with the surrounding metavolcanic unit. This contact zone is several hundred metres wide and characterized by decreasing grain size and increasing biotite content outward from the orthogneiss.

Textural variations range from gneissic to porphyroclastic to mylonitic. Gneissic zones are tens of metres thick with 5 to 10 centimetre bands of alternating quartz-plagioclase and biotite-hornblende layers. Porphyroclastic orthogneiss consists of 0.5 to 1 centimetre diameter plagioclase porphyroclasts in a medium grey fine to medium grained matrix consisting of biotite, hornblende, quartz and plagioclase. Minor epidote pods and layers are common. Up to 2% garnet is locally present. A 20-metre-thick mylonite zone crops out south of Big Falls Creek. Within this zone, millimetre-scale plagioclase porphyroclasts are set in a very fine grained matrix.

The composition, homogeneity, and presence of clear, colourless, euhedral zircons led Gareau (1991a) to conclude that this tonalite orthogneiss is an intrusion. The gradational contacts, showing a variation from medium to fine grainsize, and incorporating an exposure of fragmental volcanic rock at one location, are consistent with a large coeval subvolcanic pluton which fed the surrounding and overlying volcanic pile.

Structure

Rocks of the Ecstall belt are highly deformed and characterized by a northwest-striking, steeply dipping to vertical, transposition foliation that is defined by near-parallel compositional layering and cleavage. Coaxial, map-scale, upright, F_1 and F_2 isoclinal folds and upright to inclined F_3 open folds are identified in the belt. Hornblende mineral lineations and stretching lineations are steeply northwest to southeast plunging and have been rotated through the vertical. Stereographic projections of structural data collected during the 1999 field season are plotted in Figure 9. The relative timing of thermal and dynamic metamorphic events deduced from analysis of textures and mineralogy are shown in Table 2.

Foliation

The oldest foliation preserved is S_0, defined by sub-centimetre to centimetre scale compositional layering that is interpreted to be primary. Within metasedimentary and metavolcanic units, S_0 is characterized by quartz-plagioclase layers alternating with phyllosilicate layers. Within intrusive bodies, S_0 is locally preserved as alternating centimetre-scale mafic and felsic layering (interpreted as primary flow-banding), mafic schlieren and rafts or sheets of country rock.

S_1 foliation is a penetrative cleavage defined by preferentially oriented biotite, muscovite and possibly chlorite within metasedimentary and metavolcanic rocks and by preferentially oriented biotite within intrusive rocks. S_1 cleavage is axial planar to F_1 isoclinal folds and therefore is parallel to S_0 compositional layering in F_1 limbs, but S_1 cleavage remains at a high angle to S_0 within F_1 hinge areas (Figure 8).

Together these two foliations define a composite transposition foliation known as S_t (Figure 8). This transposition foliation is defined by near-parallel S_0 and S_1 foliations, and by centimetre-scale intrafolial isoclinal F_1 folds. Transposed metatonalite dikes, epidote-diopside seams and pods, and sulphide seams also define S_t. S_t is the northwest-trending regional foliation observed in the belt, characterized by near-vertical to steeply southeast or steeply northwest dips (Figure 9a). Along the Skeena River, this regional foliation swings to a west-northwest trend.

An S_2 crenulation cleavage, defined by biotite and minor chlorite, is observed in thin section in the hinges of F_2 minor folds. This cleavage is not visible in handsample (or is not distinguishable from S_t in handsample) and is not considered to be regionally significant.

The youngest foliation identified in the map area, S_3, is a local, medium grained, crenulation cleavage axial

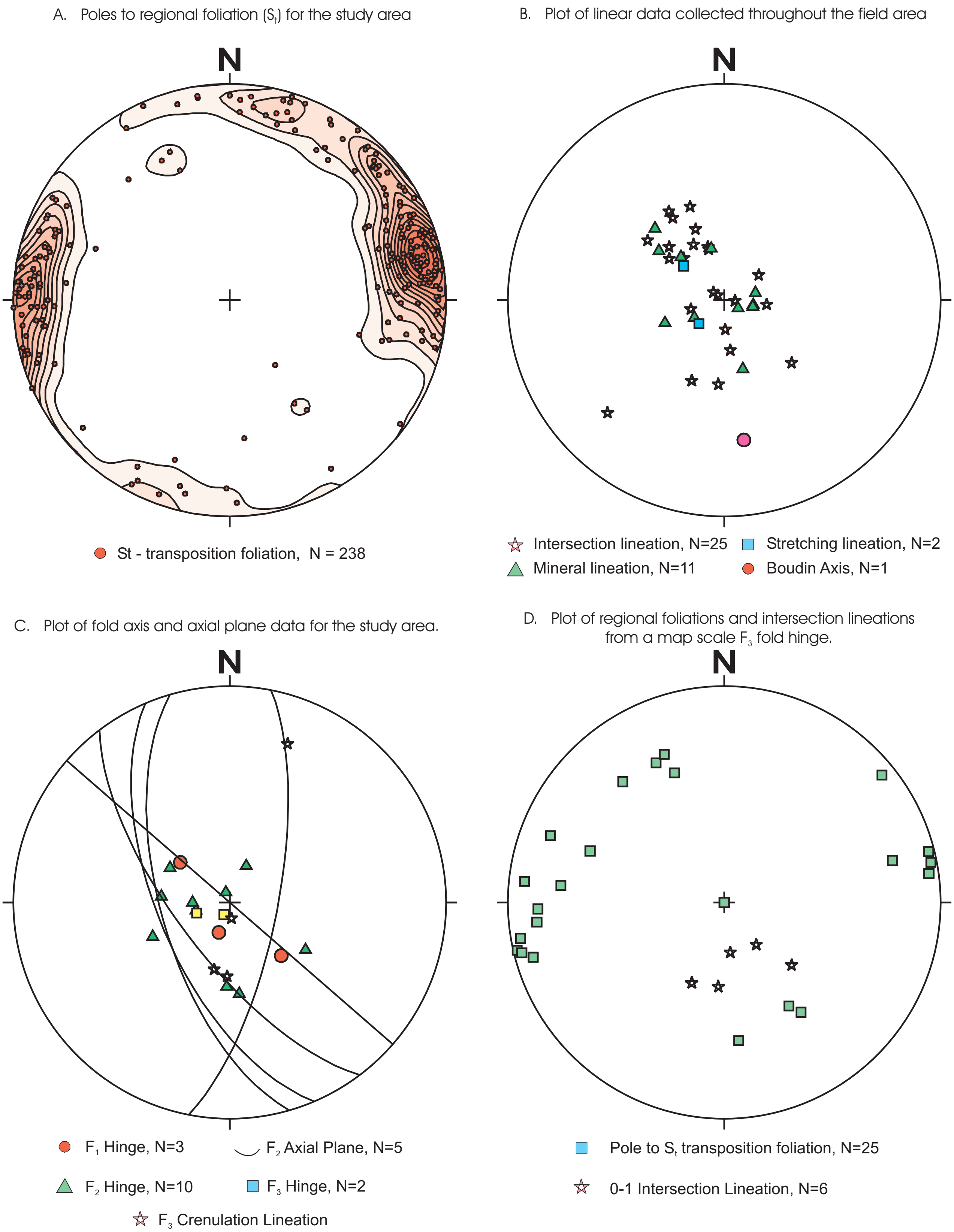

Figure 9. Stereonet plots for the northern Ecstall belt

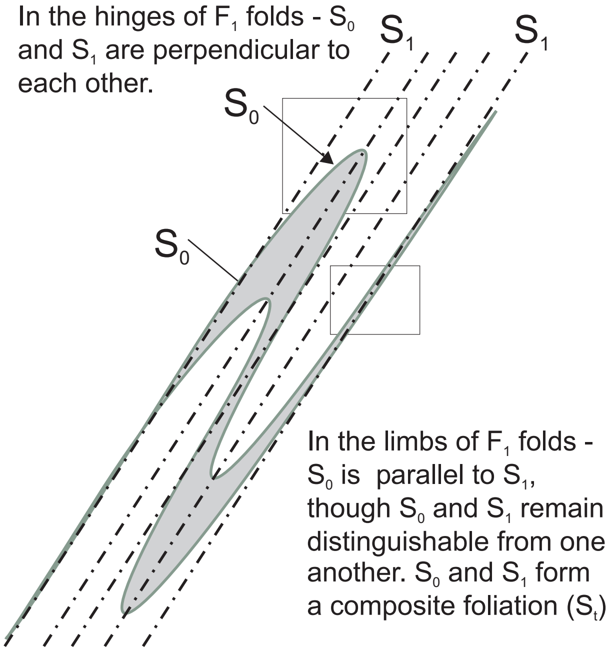

Figure 8. Geometric relationships between S_0, S_1, and S_t in an F_1 isoclinal fold.

TABLE 2
RELATIVE TIMING OF METAMORPHIC EVENTS

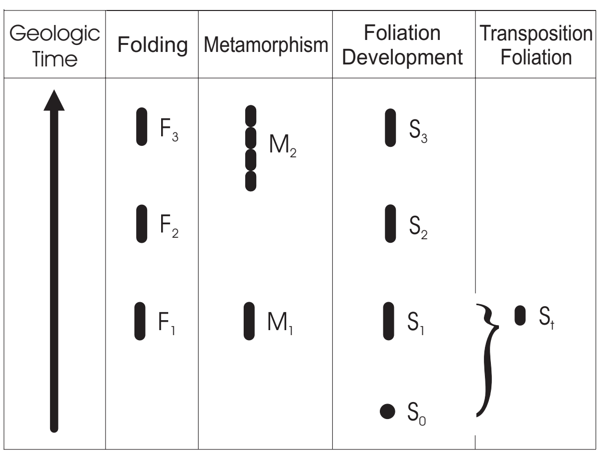

planar to F_3 crenulations. This foliation was only identified in outcrops of quartz muscovite schist (felsic metavolcanics) near the Friday the 13th showing in the southern portion of the map area (Figure 7). S_3 is defined by preferentially oriented muscovite and minor biotite with an average spacing of 1 to 2 centimetres.

Folds

Minor Folds

F_1 minor folds are preserved as rare, rootless, intrafolial, isoclinal hooks and sheared hinges that fold S_0 compositional layering. They are near-vertical upright folds with steeply northwest-plunging hinge lines and near-vertical northwest-striking axial planes (Figure 9c). These folds are subtle and are most readily observed on highly weathered surfaces, or on folded veins or dikes. S_1 cleavage is axial planar to these folds.

F_2 minor folds are the most common folds recorded and are preserved as near-vertical, upright, tight to isoclinal folds with a one centimetre to half-metre wavelength. They fold S_t (both S_0 compositional layering and S_1 cleavage) and have steep northwest-plunging hinge lines and steep west-dipping to vertical axial planes (Figure 9c). F_2 folds differ from F_1 folds by the lack of axial planar cleavage in the F_2 hinge zones at outcrop or handsample scales.

F_3 minor folds occur as open to tight, asymmetric, parallel folds that fold S_t and the axial planes of F_2 folds. The scale of these folds ranges from 15 centimetres to several metres. Hinge lines of the F_3 folds are vertically plunging (Figure 9c) with near-vertical axial planes that are oblique to the regional foliation trend.

Major Folds

Vergence reversals of both F_1 and F_2 minor folds are consistent with major folds. Two upright, steeply north-plunging kilometre-scale F_2 closures have been outlined in the southern part of the map area near Big Falls Creek (Figure 7). Half-kilometre scale F_3 folds are well documented throughout the study area. These folds define a fold belt of northeast-vergent tight to open folds with an average wavelength of 500 metres. They are upright to inclined folds with moderately southeast-plunging hinge lines and moderately northeast-dipping axial planes. Hinge zones of these folds are characterized by moderately southeast-dipping S_t foliations and common F_3 m-folds (Figure 9d). These folds are responsible for the shifts in the northwest-striking regional foliation.

Lineations

Intersection lineations within the belt are preserved as S_0-S_1 bedding-cleavage lineations that are interpreted to be parallel to F_1 hinge lines. They are typically steeply northwest plunging, but do shallow up and plunge moderately to the north-northwest in the northern section of the map area (Figure 9b). Intersection lineations appear to be folded by F_3 map-scale folds in hinge areas.

Mineral lineations are the second most common lineation. These are best displayed in the metavolcanic unit where hornblende is abundant. These lineations are defined by fine to medium grained elongate to prismatic hornblende present on biotite partings and on S_t surfaces. The orientation of these lineations tends to mimic that of the intersection lineations (Figure 9b).

Stretching lineations are recorded from elongate clasts in the metasedimentary and metavolcanic units near Big Falls Creek. The near-vertical clasts have a minimum aspect ratio of 10:2:1. Stretched clasts illustrate the high degree of strain that these rocks have undergone. It is unlikely that stretching lineations defined by individual minerals could have survived the annealing that these rocks have undergone.

Faults

Northwest-striking faults with relative sinistral offset have been identified in a few outcrops. These exposures lie along northwest-trending linear topographic depressions that are readily evident on airphotos and which divert sections of stream drainages. There are many more northwest-trending topographic lineaments that have no confirmed association with faults, but these lineaments are suspected to be localized along similar northwest-striking sinistral faults.

Metamorphism

Evidence for two metamorphic episodes has been documented (Table 2). The peak M_1 mineral assemblage within mafic rocks consists of garnet, biotite, hornblende and titanite. Plagioclase compositions range from An_{40} to An_{45}. Siliceous and metasedimentary rocks have an M_1 mineral assemblage of muscovite, biotite and garnet. Kyanite and cordierite were identified in one pelitic layer within the metavolcanic unit. These assemblages are consistent with peak metamorphic conditions of upper amphibolite facies (Figure 5).

A regional retrograde metamorphic event (M_2), is interpreted from microscopic textures. Biotite is typically surrounded by wispy, fine grained, randomly oriented chlorite; remnant skeletal garnet porphyroblasts commonly display rims of matted chlorite.

Matrix grains of quartz and plagioclase lack any sub-grains and undulatory extinction within quartz is rare. Plagioclase feldspar noticeably lacks polysynthetic strain twins in thin section. Triple-point boundaries are common in quartz and plagioclase grains. Hornblende also displays polygonal grain boundaries in one section. The presence of polygonal matrix grains and the absence of microstructures indicating ductile deformation is consistent with a strong annealing event. This metamorphic event is most likely Cretaceous to Eocene in age, synchronous with intrusion of the Ecstall pluton or Quottoon pluton.

Relative timing of metamorphic and deformation events are constrained by an array of textural features. In the hinges of F_1 folds, M_1 biotite and muscovite grains are undeformed and are preferentially oriented parallel to F_1 axial planes. In F_2 hinges, the same mineral assemblage is kinked and has been rotated parallel to F_2 axial planes. Relative timing of garnet growth with respect to S_1 cleavage development remains ambiguous; garnets are observed truncating S_1 foliation, although S_1 foliation most commonly wraps around garnet porphyroblasts. Skeletal garnets also commonly display sinusoidal inclusion trails consisting of titanite and quartz grains.

Retrograde chlorite is randomly oriented. Chlorite is also common on brittle fault surfaces suggesting that late faulting occurred at greenschist facies conditions. The exact relationship between retrograde chlorite growth and D_2 and D_3 deformation could not be determined.

MINERAL DEPOSITS

Six styles of sulphide mineralisation were noted during this initial field season:

- volcanogenic massive sulphide deposits: VMS lenses, footwall stockworks and distal exhalite horizons have been described in the Ecstall belt
- felsic metavolcanics: pyritic quartz-muscovite schist
- pyritic cert
- quartzite: greater than 95% granoblastic quartz, with minor pynated along muscovite partings
- intrusive contacts: disseminated pyrite is distributed for a few to hundreds of metres into country rock
- faults: minor pyrite is commonly disseminated for 1 to 3 metres into the wallrock trace to minor disseminated pyrite is typical of most lithologies. In gneissic rocks, sulphides are concentrated in bands or boudins

In addition to these types of sulphide occurrences, some potential may exist for intrusion-related gold veins (Au-lithophile element deposits; Pogo - Fort Knox type deposits) associated with the mid-Cretaceous plutons and plugs that intrude the Ecstall belt at several locations (Gareau, 1997).

There are 18 mineral occurrences identified within Ecstall belt rocks; three of these are deposits with reserves. Seventeen of these are described in MINFILE, the remaining showing was discovered by Bishop Resources Ltd. during the 1999 field season. Industry geologists have classified all these occurrences as volcanogenic massive sulphides or related deposits such as footwall stockwork zones or distal exhalite horizons. These occurrences are spread over a 42 kilometre strike length, but all lie within the metavolcanic rock sequence of the Ecstall belt (Figure 3, and Unit 1 of Figure 7).

The following descriptions of the three largest deposits are summarized from MINFILE; reserves for these deposits are summarized in Table 3.

TABLE 3
RESERVES FOR ECSTALL BELT DEPOSITS

PROPERTY	SIZE (mT)	Cu %	Pb %	Zn %	Ag g/T	Au g/T
Scotia	1,240,000	0.1	0.4	3.8	13.0	0.25
Ecstall	6,349,700	0.6		2.5	20.0	0.5
Packsack	2,700,000	0.5	0.01	0.2	34.0	0.3
TOTAL RESOURCE	10,289,700	0.5	0.05	2.1	22.8	0.4

Scotia (103I 007)

The Scotia property is underlain by felsic gneiss, mafic gneiss and amphibolite. Deformed Zn-Ag-Pb-Au volcanogenic massive sulphide mineralization occurs in three stacked lenses extending over a 230-metre strike length, mainly within felsic gneiss. These three lenses may lie within parallel limbs of an overturned isoclinal fold. Massive sulphide widths range up to 11 metres. The sulphide zones strike 160 degrees, dip 40 degrees southwest and plunge 9 degrees south. Exposed in a south-facing cliff, the deposit is open along strike to the northwest and down dip to the southwest. Sulphide minerals include sphalerite, galena, pyrite, pyrrhotite, bornite and chalcopyrite.

Ecstall (103H 011)

The Zn-Cu-Ag-Au Ecstall deposit occurs in hydrothermally altered metavolcanic rocks. Two tabular, concordant, en echelon bodies, the North Lens and South Lens, consist of pyrite with minor chalcopyrite and sphalerite and lesser pyrrhotite, marcasite and galena. The two lenticular bodies of massive pyrite strike north, dip steeply east and plunge steeply south. The North Lens measures 300 x 150 x 30 metres. The South Lens measures 400 x 360 x 7 metres. A smaller deposit occurs 760 metres north of the North Lens, where a 30 x 2.4 metre lens of massive pyrite is exposed.

Property-scale exploration by Falconbridge in 1986 indicated significant stockwork copper mineralization in felsic rocks south of the Ecstall River in the Thirteen Creek area. This stockwork mineralization was interpreted as a possible feeder zone to a volcanogenic massive sulphide deposit.

Packsack (103H 013)

Two massive sulphide bodies, 170 metres apart along strike, occur within quartz-sericite schist associated with a 30-metre-wide shear zone. Disseminated pyrite is common throughout the quartz-sericite schist which has been traced continuously for 600 metres along strike. The deposits average 4 metres in thickness. The southern lens, up to 6 metres thick and traced for 365 metres, consists of massive pyrite with minor chalcopyrite, chalcocite and sphalerite. The northern lens is up to 0.6 metres thick

EXPLORATION AND MINERAL POTENTIAL

All eighteen VMS prospects of the Ecstall belt crop out. These showings have been located despite the fact that rock exposure throughout this belt is limited, thus the potential for discovery of additional deposits in the overburden-covered areas of this highly prospective belt are excellent. All discoveries have been achieved without the aid of regional-scale geological maps, geophysical surveys or geochemical surveys - standard exploration tools which have been particularly successful in the search for blind (subcropping or deeply buried) VMS deposits elsewhere.

Most showings have been discovered over the last 15 years from follow-up of property-scale stream sediment geochemical surveys. These geochemical surveys have not yet covered the whole of the prospective metavolcanic rocks of the belt. Moss-mat geochemical surveys conducted for the past three years have returned superior results compared to duplicate samples collected from stream sediments (A. Birkeland, Arnex Resources Ltd, personal communication).

Geological reconnaissance work and prospecting programs by companies have been intermittent and cover only portions of the belt. This point is exemplified by the Friday the 13th Zn-Cu showing, discovered this season during follow-up of stream sediment and moss-mat survey anomalies. The prospect was located in an eight-year-old logging road-cut where it is exposed as a 50-metre-long highly gossanous band, now heavily overgrown by roadside brush. For most of the last decade the three major deposits and adjacent ground have been held by three separate, competing companies and no comparison or synthesis of the detailed geological information collected around each deposit has been attempted. A company program designed to trace prospective pyritic quartz-sericite units through the central and northern parts of the belt commenced this season, but has limited funding.

No reference to chert has been found in geologic reports reviewed to date, yet two exposures were identified during the short 1999 field season - both exposures were strongly (> 5%) pyritic and part of the felsic metavolcanic package. These units record periods of prolonged exhalative activity in quiescent conditions and deserve careful follow-up.

Recent global research into the geologic setting of VMS deposits have stressed the importance of subvolcanic plutons of tonalite/trondhjemite as the heat source which concentrates VMS deposits at the overlying paleosurface (Galley, 1996; Large, 1996). An exploration program could be designed to investigate Gareau's (1991a,c) conclusion that the major Middle Devonian tonalite/trondhjemite pluton within the Ecstall belt, the Big Falls orthogneiss, is the coeval subvolcanic magma chamber that fed the volcanic pile.

Ground electromagnetic (EM) surveys carried out over known deposits generate clear anomalies that have been used to guide drilling on the prospects. This confirms that regional airborne geophysical surveys can also be effective in this belt, in contrast to many of the VMS districts of the Cordillera where highly conductive carbonaceous sedimentary rock masks the expected responses from sulphide accumulations.

Deposits discovered to date have significant tonnage but overall low base metal grades (Table 3). However, the higher grade section of the Scotia deposit has reserves of 224,000 tonnes grading 12.2% Zn, 1.2% Pb, 0.2% Cu, 23 g/t Ag and 0.55 g/t Au, indicating good potential in this belt for VMS deposits of economic size and grade.

CONCLUSIONS

The Ecstall metavolcanic belt is a classic VMS-rich greenstone belt. This Devonian age volcano-sedimentary complex is clearly underexplored with excellent potential for discovery of additional prospects and good potential for discovery of economic Zn-Cu-Ag-Au VMS deposits. With regional exploration work still at a relatively early stage, exploration success can be expected from programs ranging from prospecting, to regional stream geochemistry, to airborne geophysics, to regional-scale and property-scale geologic mapping. Despite its location in the heart of the rugged Coast Mountains the district has admirable access and proximity to infrastructure.

ACKNOWLEDGMENTS

Thanks to Arne Birkeland of Arnex Resources Limited and the management of Bishop Resources Limited for sharing their data and ideas developed over many years of work in the district. We appreciate the good care and cooperation from the staff and management of Bear Creek Contracting Limited who provided accommodation and logistical support during the 1999 field season.

REFERENCES

Boghossian, N.D. and Gehrels, G.E. (in press): Nd isotopic signature of metasedimentary pendants in the Coast Mountains between Prince Rupert and Bella Coola, British Columbia; in Tectonics of the Coast Mountains, southeastern Alaska and coastal British Columbia, *Geological Society of America*, Special Paper.

Brew, D.A. and Ford, A.B. (1978): Megalineament in southeastern Alaska marks southwest edge of Coast Range batholithic complex; Canadian Journal of Earth Sciences, V. 15, p. 1763-1772.

Crawford, M.L. and Crawford, W.A. (1991): Magma emplacement in a convergent tectonic orogen, southern Revillagigedo Island, southeastern Alaska; *Canadian Journal of Earth Sciences*, V. 28, p. 929-938.

Crawford, M.L. and Hollister, L.S. (1982): Contrast of metamorphic and structural histories across the Work Channel lineament, Coast Plutonic Complex, British Columbia; *Journal of Geophysical Research*, V. 87, p. 3849-3860.

Crawford, M.L., Hollister, L.S. and Woodsworth, G.J. (1987): Crustal deformation and regional metamorphism across a terrane boundary, Coast Plutonic Complex, British Columbia; Tectonics, V. 6, N. 3, p. 343-361.

Drinkwater, J.L., Brew, D.A. and Ford, A.B. (1993): Chemical characteristics of major plutonic belts of the Coast Plutonic-Metamorphic Complex near Juneau, southeastern Alaska; *in* Geological Studies in Alaska by the U.S. Geological Survey, 1993, *United States Geological Survey*, p. 161-172.

Dusel-Bacon, C., Brew, D.A. and Douglass, S.L. (1996): Metamorphic facies map of southeastern Alaska - distribution, facies and ages of regionally metamorphosed rocks; United States Geological Survey Professional Paper 1497-D, 42 p., 2 map sheets.

Galley, A.G. (1996): Geochemical characteristics of subvolcanic intrusions associated with Precambrian massive sulfide deposits, *in* Wyman, D. A., editor, Trace Element Geochemistry of Volcanic Rocks: Applications for Massive Sulfide Exploration, Mineral Deposits Division, *Geological Association of Canada*, p. 239-278.

Gareau, S.A. (1991a): Geology of the Scotia-Quaal metamorphic belt, Coast Plutonic Complex, British Columbia; unpublished Ph.D. thesis, Carleton University, 390 p.

Gareau, S.A. (1991b): Geology of the Scotia-Quaal metamorphic belt, Coast Plutonic Complex, British Columbia; *Geological Survey of Canada*, Open File Map 2337, scale 1:50 000, 4 sheets.

Gareau, S.A. (1991c): The Scotia-Quaal metamorphic belt: a distinct assemblage with pre-early Late Cretaceous deformational and metamorphic history, Coast Plutonic Complex, British Columbia; *Canadian Journal of Earth Sciences,* V.28, p. 870-880.

Gareau, S.A., compiler (1997): Geology, Scotia-Quaal metamorphic belt, Coast Plutonic Complex, *British Columbia; Geological Survey of Canada*, Map 1868A, scale 1:100 000, 1 sheet.

Gehrels, G.E. and Boghossian, N.D. (in press): Reconnaissance geology and U-Pb geochronology of the west flank of the Coast Mountains between Bella Coola and Prince Rupert, coastal British Columbia; *in* Tectonics of the Coast Mountains, southeastern Alaska and coastal British Columbia, *Geological Society of America,* Special Paper.

Gehrels, G.E. and Kapp, P.A. (1998): Detrital zircon geochronology and regional correlation of metasedimentary rocks in the Coast Mountains, southeastern Alaska; *Canadian Journal of Earth Sciences*, V. 35, p. 269-279.

Gehrels, G.E., McClelland, W.C., Samson, S.D., Jackson, J.L. and Patchett. P.J. (1991a): U-Pb geochronology of two pre-Tertiary plutons in the Coast Mountains batholith near Ketchikan, southeastern Alaska; *Canadian Journal of Earth Sciences*, V.28, p. 894-898.

Gehrels, G.E., McClelland, W.C., Samson, S.D. and Patchett, P.J. (1991b): U-Pb geochronology of Late Cretaceous and Early Tertiary plutons in the northern Coast Mountains batholith; *Canadian Journal of Earth Sciences*, V. 28, p. 899-911.

Gehrels, G.E., McClelland, W.C. Samson, S.D. and Patchett, P.J. (1991c): U-Pb geochronology of detrital zircons from a continental margin assemblage in the northern Coast Mountains, southeastern Alaska; *Canadian Journal of Earth Sciences*, V. 28, p. 1285-1300.

Greenwood, H.J. Woodsworth, G.J., Read, P.B., Ghent, E,D, and Evenchick, C.A. (1992): Metamorphism; Chapter 16 *in* Geology of the Cordilleran Orogen in Canada, *Geological Survey of Canada*, Geology of Canada, N.4, p. 533-570.

Heah, T.S.T. (1990): Eastern margin of the Central Gneiss Complex in the Shames River area, Terrace, British Columbia; *in* Current Research, Part E, *Geological Survey of Canada*, Paper 90-1E, p. 159-169.

Heah, T.S.T. (1991): Mesozoic ductile shear and Paleogene extension along the eastern margin of the Central Gneiss Complex, Coast Belt, Shames River area, near Terrace, British Columbia; unpublished M.Sc. thesis, *University of British Columbia*, 155 p.

Hutchinson, W.W. (1970): Metamorphic framework and plutonic styles in the Prince Rupert region of the Central Coast Mountains, British Columbia; *Canadian Journal of Earth Sciences*, V. 7, p. 376-405.

Hutchinson, W.W. (1979): Geology of the Prince Rupert-Skeena map area, British Columbia; Geological Survey of Canada, Map 1472A, scale 1:250 000.

Hutchinson, W.W. (1982): Geology of the Prince Rupert-Skeena map area, British Columbia; *Geological Survey of Canada*, Memoir 394, 116 p.

Kenah, C. and Hollister, L.S. (1983): Anatexis in the Central Gneiss Complex, British Columbia; *in* Migmatites, Melting and Metamorphism, Proceedings of the Geochemical Group of the Mineralogical Society, p. 142-162.

Krage, S.M. (1984): Metamorphic and fluid inclusion study of amphibolite grade rocks, West Scotia, British Columbia; unpublished M.A. thesis, *Bryn Mawr College*, Philadelphia, 98 p.

Large, R.R., Doyle, M., Raymond, O., Cooke, D., Jones, A., and Heasman, L., 1996, Evaluation of the role of Cambrian granites in the genesis of world class VHMS deposits in Tasmania: *Ore Geology Reviews*, V. 10, p. 215-230.

Massey, N.W.D. (1999): Volcanogenic massive sulphide deposits of British Columbia; *British Columbia Ministry of Energy and Mines*, Geological Survey, Open File Map 1999-2, scale 1:2 000 000, 2 sheets.

McClelland, W.C., Anovitz, L.M. and Gehrels, G.E. (1991a): Thermobarometric constraints on the structural evolution of the Coast Mountains batholith, central southeastern Alaska; *Canadian Journal of Earth Sciences*, V. 28, p. 912-928.

McClelland, W.C., Gehrels, G.E., Samson, S.D. and Patchett, P.J. (1991b): Protolith relations of the Gravina Belt and Yukon-Tanana terrane in central southeastern Alaska; *Journal of Geology*, V. 100, p. 107-123.

Money, P.L. (1959): Geology of Hawkesbury Island, Skeena Mining Division, British Columbia; unpublished M.Sc. thesis, *University of British Columbia*, 159 p.

Newberry, R.J., Crafford, T.C., Newkirk, S.R., Young, L.E., Nelson, S.W. and Duke, N.A. (1997): Volcanogenic massive sulphide deposits of Alaska; *in* Mineral Deposits of Alaska, *Economic Geology Publishing Company,* Economic Geology Monograph number 8, p. 120-150.

Padgham, W.A. (1958): The Geology of the Ecstall-Quaal Rivers area, British Columbia; unpublished M.Sc. thesis, *University of British Columbia*, 202 p.

Roddick, J.A. (1970a): Douglas Channel - Hecate Strait map area, British Columbia; *Geological Survey of Canada*, Paper 70-41, 56 p.

Roddick, J.A. (1970b): Douglas Channel - Hecate Strait map area, British Columbia; *Geological Survey of Canada*, Preliminary Map 23-1970, scale 1:250 000.

Rubin, C.M., Saleeby, J.B., Cowan, D.S., Brandon, M.T. and McGroder, M.F. (1990): Regionally extensive mid-Cretaceous west-vergent thrust system in the northwestern Cordillera: implications for continent-margin tectonism; *Geology*, V.18, p. 276-280.

Samson, S.D., Patchett, P.J., McClelland, W.C. and Gehrels, G.E. (1991): Nd and Sr isotopic constraints on the petrogenesis of the west side of the northern Coast Mountains batholith, Alaskan and Canadian Cordillera; *Canadian Journal of Earth Sciences*, V.28, p. 939-946.

Sisson, V.B. (1985): Contact metamorphism and fluid evolution associated with the intrusion of the Ponder Pluton, Coast Plutonic Complex, British Columbia, Canada; unpublished Ph.D. thesis, *Princeton University*, New Jersey, 345 p.

Sutter, J.F. and Crawford, M.L. (1985): Timing of metamorphism and uplift in the vicinity of Prince Rupert, British Columbia and Ketchikan, Alaska; *in* Geological Society of America, Cordilleran Section, Program with Abstracts, p. 4 11.

van der Heyden, P. (1989): U-Pb and K-Ar geochronometry of the Coast Plutonic Complex, 53ºN to 54ºN, British Columbia, and implications for the Insular-Intermontane superterrane boundary; unpublished Ph.D. thesis, *University of British Columbia*, 392 p.

Woodsworth, G.J., Anderson, R.G. and Armstrong, R.L. (1992): Plutonic Regimes; Chapter 15 *in* Geology of the Cordilleran Orogen in Canada, *Geological Survey of Canada*, Geology of Canada, N. 4, p. 491-531.

Woodsworth, G.J., Crawford, M.L. and Hollister, L.S. (1983): Metamorphism and Structure of the Coast Plutonic Complex and adjacent belts, Prince Rupert and Terrace areas, British Columbia; *Geological Association of Canada Annual Meeting* - Victoria 1983, Field Trip Guidebook No.14, 62 p.

Zen E. and Hammarstrom, J.M. (1984): Magmatic epidote and its petrologic significance; Geology, V. 12, p.5 15-518.

Zen, E. (1985): Implications of magmatic epidote-bearing plutons on crustal evolution in the accreted terranes of northwestern North America; *Geology,* V. 13, p. 266-269.

A Synopsis of Iron Oxide ± Cu ± Au ± P ± REE Deposits of the Candelaria-Kiruna-Olympic Dam Family

By Gerald E. Ray and David V. Lefebure

KEYWORDS: *Economic geology, mineral deposit model, Olympic Dam, Candelaria, Kiruna, iron oxide, magnetite, hematite, copper, apatite, deep-seated structures.*

INTRODUCTION

The Fe oxide-rich family summarized in this synopsis includes a wide spectrum of deposits whose only major common characteristic is the presence of abundant hematite and/or low Ti-bearing magnetite. These deposits exhibit highly varied styles of mineralization, alteration and chemistry, and they occur in geological settings that range from rifted continental crust to volcanic-arc environments. Consequently the validity of the family as a deposit classification is still controversial. It could be argued, for example, that the Australian Cu-U-Au-Ag Olympic Dam deposit is so unique that it has little in common with the sulphide-poor, magnetite-only deposits such as El Romeral in Chile. Conversely, like the well-known skarn family which also includes a spectrum of equally diverse deposits, the Fe oxide family may prove to be a valid grouping, as advocated by Hitzman *et al* (1992), Williams (1999) and other workers. It is hoped that this synopsis will, among other things, stimulate debate on this question.

SYNONYMS

Synonyms for this class of mineral deposits include: Olympic Dam, Kiruna, Ernest Henry or Candelaria types; iron oxide breccias and veins; apatite iron ore; volcanic-hosted magnetite; iron oxide-rich deposits; Proterozoic iron oxide (Cu-U-Au-REE) deposits.

COMMODITIES

The important economic commodities in these deposits are Fe, Cu, Au, Ag, U and P. There is also a potential for byproduct REE's, Ba, Mo and Co.

EXAMPLES

Olympic Dam (Gawler district, South Australia); Ernest Henry, Osborne (Cloncurry district, Australia); Kiirunavaara (Kiruna district, Sweden); Candelaria, Punta del Cobre, El Algarrobo, Boqueron Chanar, Manto Verde and El Romeral (Chilean Iron Belt); Monterrosas, Eliana, Raul, Condestable, Marcona (Peru); Cerro de Mercado (Durango district, Mexico); Pea Ridge, Pilot Knob and Boss-Bixby (Missouri, USA); Sue-Dianne and Great Bear (Northwest Territories, Canada); Wernecke Breccias (Yukon, Canada); Iron Range (082FSE014 - 028, British Columbia); Vergenoeg (South Africa); Mangula (Zimbabwe); Shimyoka, Kantonga, and Kitumba prospects (Mumbwa district, Zambia); Bafq (Iran).

Other possible examples include the Heff prospect (092INE - 096, British Columbia), Salobo and Igarape Bahia (Carajas district, Brazil), and the Bulagidun prospect (North Sulawesi, Indonesia).

CAPSULE DESCRIPTION

Hydrothermal hematite and/or low-Ti magnetite-rich mineralization which may be hosted by sedimentary, igneous or metamorphic rocks. These deposits exhibit a wide range of morphologies, including multiphase breccia pipes and sheets, veins, stockworks, diatremes and both concordant and crosscutting tabular bodies. Mineralization varies from sulphide-poor magnetite±apatite ore bodies (*e.g.* Kiirunavaara, El Algarrobo, El Romeral) to more sulphide-rich hematite±magnetite deposits±Cu±Au±Co±U±REE's (*e.g.* Olympic Dam, Ernest Henry and Candelaria).

TECTONIC SETTING

Proterozoic deposits are found in rifted cratonic settings whereas many Phanerozoic examples lie close to major linear structures in an Andean, continental margin, volcanic arc setting.

DEPOSITIONAL ENVIRONMENT/ GEOLOGICAL SETTING

The depth-range in which these deposits form is uncertain. Some deposits (*e.g.* Salobo) may have developed in a very shallow, possible exhalite environment; others (*e.g.* Olympic Dam; Cerro de Mercado) formed at near surface levels <1 km), whilst depths down to 6 km are speculated for some magnetite-albite dominated systems (Oreskes and Hitzman, 1993). Deposits are commonly associated with long-lived brittle-ductile fractures, narrow grabens or rifts that may, in part, be coeval with host-rock deposition.

AGE OF MINERALIZATION

Proterozoic to Tertiary. Many of the better known deposits are mid-Proterozoic (1.2 to 1.9 Ga). However, the Chilean and Peruvian Iron Belt examples are of Cretaceous age.

HOST/ASSOCIATED ROCK TYPES

The Fe oxide mineralization crosscuts, or is conformable with, a wide variety of sedimentary, igneous and metamorphic rocks, including mafic flows, felsic volcanic breccias, tuffs, clastic sedimentary rocks, granites, gabbros, diorites, granodiorites and syenites. Prograde garnet-pyroxene±scapolite skarn mineral assemblages may develop where the fluids are Ca-rich and high temperature, or where reactive calcareous host-rocks are present. Some deposits are associated with very coarse grained actinolite-apatite veins and breccias (crystals >3 cm long), and large volumes of sediment-hosted hematite-rich "ironstone" or iron oxide-bearing volcanic rocks.

DEPOSIT FORM

Highly variable. Sub-horizontal to steeply inclined, discordant to concordant pod-like zones, dike-like veins, lenses, tabular bodies, pipes and stockworks. The iron-rich veins and tabular zones may reach hundreds of metres in width and have a strike length of many kilometres.

TEXTURE/STRUCTURE

The Cu-Au mineralization may be hosted in the Fe oxide matrix as disseminations, micro-veinlets and as rare mineralized clasts. Textures indicating replacement and microcavity filling are common (*e.g.* tuff lapilli may be selectively replaced by iron oxides). Intergrowths between minerals are noted. Hematite and magnetite may display well developed crystals, interlocking mosaics, and tabular or bladed textures. Hematite varies from specular to massive to botryoidal (kidney ore). Some deposits are characterized by matrix-supported hydrothermal, polymictic and multiphase breccias. Breccia textures are highly variable; they may grade from core zones containing 100% Fe to weakly fractured and Fe-veined host-rock on the margins. Breccias may be difficult to recognize in hand sample as the same apparent Fe oxide phase may comprise both the fragments and matrix. Many breccias contain clasts of magnetite, hematite, fresh to altered country rock, quartz, calcite and older breccia material supported in a matrix of younger iron oxides and /or calcite. If Ca-rich host-rocks are present, fragments of garnet-pyroxene±scapolite skarn overgrown by iron oxides may be seen. Breccia fragments are generally angular to sub-angular although rounded and mechanically milled clasts are not uncommon. They range up to >10 m in diameter, but tend to be <15 cm wide. Contacts with the unbrecciated host-rocks are frequently gradational over scale of centimetres to metres. Hematite breccias often display a diffuse wavy layered texture of red and black hematite, and some microbreccias have thin, hair-like veins of hematite. Replacement (pseudomorphing) of early magnetite by hematite (martite) may be a common feature.

ORE MINERALOGY

These vary from low sulphide-bearing magnetite-apatite deposits with actinolite±pyroxene (*e.g.* Kiirunavaara, El Romeral) to more sulphide-rich, polymetallic hematite-magnetite deposits (e.g. Olympic Dam, Candelaria). The principal ore minerals are hematite (includes specularite, botryoidal hematite and martite), low-Ti magnetite, bornite, chalcopyrite, chalcocite and pyrite. Subordinate minerals include digenite, molybdenite, covellite, native copper, carrolite, cobaltite, Cu-Ni-Co arsenates, pyrrhotite, pitchblende, uraninite, coffinite, autunite, brannerite, bastnaesite, monazite-xenotime, florencite, native silver and gold and silver tellurides. At Olympic Dam, the native gold, uraninite, coffinite, bastnaesite and florencite are very fine grained; gold is disseminated either in the breccia matrix or as inclusions in the sulphides whereas bastnaesite and florencite occur in the matrix as grains, crystals and crystal aggregates.

GANGUE MINERALOGY

Gangue is intergrown with ore minerals as veins, as clasts in breccias or as disseminations. Principal gangue minerals include albite, K-feldspar, sericite, carbonate, chlorite, quartz, amphibole, pyroxene, massive silica, biotite and apatite. Lesser amounts of fluorapatite, fluorite, barite, epidote, rutile, titanite, monazite, ilvaite, tourmaline and allanite may also occur. The amphiboles include hastingsite and tschermakitic varieties as well as Cl-rich hornblende. Hematite breccias are frequently cut by veins, up to 10 cm wide, containing fluorite, barite, siderite, hematite and sulphides.

ALTERATION MINERALOGY AND ZONING

Hitzman *et al*. (1992) note that at greater depths, alteration in these systems comprises large (>1 kilometre wide) zones of Na-Fe metasomatism (early albite-actinolite-magnetite, apatite and late epidote); if Ca-rich host-rocks are present, Fe-rich garnet-clinopyroxene ±scapolite skarn assemblages may form (*e.g.* Heff prospect, British Columbia; Candelaria, Chile; Kiruna, Sweden; Shimyoka and Kantonga prospects, Zambia).

Overlying the Na-Fe alteration, at intermediate depths, are extensive haloes of K-Fe-rich alteration (K-feldspar, secondary biotite, sericite, magnetite, actinolite, chlorite); intense chloritization may result in almost total destruction of the hydrothermal biotite. The upper parts of the hydrothermal systems tend to be marked by lower temperature Si-Fe-K assemblages (massive silica-quartz-sericite-specular hematite-chlorite).

Olympic Dam has intense sericite and hematite alteration with increasing hematite towards the centre of the breccia bodies at higher levels. Close to the deposit, the sericitized feldspars are rimmed by hematite and cut by hematite veinlets. Adjacent to hematite breccias the feldspar, rock flour and sericite are totally replaced by hematite. Chlorite or K-feldspar alteration predominates at depth. Quartz, fluorite, barite, carbonate, rutile, orthoclase and epidote are also present.

The Kiruna orebodies contain scapolite and albite with actinolite-epidote alteration in the mafic wallrocks; up to 20 wt % apatite is also reported. Some Chilean and Peruvian Phanerozoic examples contain tourmaline (*e.g.* Manto Verde, Monterrosas) and this mineral also occurs at Kiirunavaara and Olympic Dam.

WEATHERING

In certain weathering environments, pervasive kaolin-clay alteration may develop as well as some supergene alunite veins. In arid environments, a blanket containing secondary Cu, Cu-Mn and U phosphates, oxides, sulfates and chlorides may be present (*e.g.* turquoise, torbernite, brochantite, antlerite, atacamite). Supergene enrichment of Cu and U is possible; examples include the pitchblende veins in the Great Bear Magmatic Zone.

ORE CONTROLS

There are strong structural ore controls in most deposits although in some (*e.g.* Candelaria) stratigraphy also plays an important role. Deposits are hosted by rocks adjacent to brittle-ductile fractures or narrow grabens that have undergone repeated transcurrent and extensional movement. They may cluster along linear arrays more than 100 km long and >10 km wide and be spaced 10-30 km along the trend. Many older deposits (*e.g.* Kiirunavaara, Olympic Dam, Ernest Henry) are hosted by mid-Proterozoic continental crustal rocks and past exploration has focused largely on fractures that cut these packages. However, recognition of younger deposits (*e.g.* Bafq, Chilean and Peruvian Iron Belts) demonstrates that fault zones in Phanerozoic volcanic arcs are also important exploration targets.

GENESIS

Recent work (*e.g.* Oreskes and Einaudi, 1990; Hitzman *et a*l., 1992; Oreskes and Hitzman, 1993; Borrok *et al*., 1998; Gow *et al*., 1994) suggests that these deposits are hydrothermal in origin. However, there is disagreement about this interpretation and whether or not these diverse orebodies should be grouped as a single deposit type. Barton and Johnson (1996) suggest that evaporites provided a source for chlorides and the sodium alteration in some deposits; this involves a process of non-magmatic fluids circulating through evaporites, and being drawn into an intrusion-centered hydrothermal system. A magmatic-volcanic (syngenetic) versus epigenetic origin of the Kiruna (Sweden) and El Laco (Chile) magnetite mineralization is still hotly debated (*e.g.* Parak, 1975; Nystrom and Henriquez, 1994). In some cases the mineralization appears to be younger than, and unrelated to the hosting igneous rocks (*e.g.* Ernest Henry, Candelaria), but recent studies at Olympic Dam (Johnson and Cross, 1995; Campbell *et al*., 1998) suggest that the hosting granite is only slightly older (*circa* 8 Ma) than the mineralization. Sm-Nd data from Olympic Dam (Johnson and McCulloch, 1995) indicate a mantle-derived origin for the mineralization. However, many examples lack an identifiable plutonic source; hence the origin of the hydrothermal fluids and composition of the assumed parent magmas are unknown.

ASSOCIATED DEPOSIT TYPES

On a wide district scale, these Fe oxide± Cu±Au±REE deposits may be associated with volcanic-hosted U orebodies, alkaline and calc-alkaline porphyry Cu-Au deposits, supergene U and/or Cu blankets or veins, and hematite-rich massive iron-stones. Some sedex-type Pb-Zn-Ag deposits are found in the same geological setting as Fe oxide deposits, although there is no proven genetic relationship. Examples of this broad regional association include Broken Hill and Olympic Dam, Mount Isa and Ernest Henry (Australia), Kabwe and the Shimyoka, Kantonga, and Kitumba prospects (Zambia), and Sullivan and the Iron Range prospect (British Columbia). In the latter case, however, the age of the Iron Range prospect relative to the Sullivan deposit is unknown.

COMMENTS

Hitzman *et al*. (1992) note that the magnetite in these deposits is generally low in Ti (<0.5% TiO_2), in contrast to the magnetite associated with anorthosites, gabbros and layered mafic intrusions. Some carbonate-hosted Fe oxide-Cu-Au±REE deposits with a skarn gangue resemble calcic island-arc Fe skarns; both deposit types contain low-Ti magnetite, Fe-rich and Mn-poor garnets and hedenbergitic clinopyroxenes, and sporadic Cu, Au and Co geochemical anomalies. Also, both types tend to have early albitic alteration, sporadic younger K-feldspar development and similar textures (hydrothermally brecciated magnetite and magnetite veins and dikes). Unlike Fe oxide-Cu-Au deposits, however, island-arc Fe skarns are strongly controlled by pluton margins, they contain relatively little hematite and lack anomalous REE's and U.

GEOCHEMICAL SIGNATURE

Anomalously high values for Fe, Cu, U, Au, Ag, Co, REE's (Ce, La, Nd, Pr, Sm, Gd)±P±F±B±Mo±Y±As ±Bi ±Te±Mn ±Se and ±Ba in associated rocks and in stream sediments. The light REE's tend to be concentrated in minerals such as allanite, epidote, bastnaesite, florencite, monazite, xenotime or apatite.

GEOPHYSICAL SIGNATURE

Large positive gravity anomalies related to the Fe oxides. Regional aeromagnetic anomalies related to magnetite and/or coeval igneous rocks. Radiometric anomalies (detectable by ground and airborne gamma-ray spectrometer surveys) occur with polymetallic deposits containing U mineralization or K alteration. IP was a useful tool in exploring the Candelaria deposit (Ryan *et al*., 1995).

OTHER EXPLORATION GUIDES

Promising areas are those with narrow rift structures and deep-seated brittle-ductile fault zones. Favorable features along such structures include the presence of: (1) extensional or trans-tensional movement, (2) zones of albite, K-feldspar, sericite, chlorite, apatite, epidote, tourmaline, fluorite, actinolite, garnet±pyroxene±scapolite skarn or silica-rich alteration, (3) Fe oxides, particularly in breccias, stockworks and veins, (4) sodic or potassically-altered intrusions, (5) U oxides and/or REE-enriched alteration, and (6) secondary Cu phosphates. The favorable linear belts may exceed 100 kilometres in length and be tens of kilometres wide.

TYPICAL GRADE AND TONNAGE

Deposits may exceed 1000 Mt grading >20 % Fe. Reserves for the following deposits are:

- Olympic Dam - 2000 Mt grading 1.6% Cu, 0.06% U_3O_8, 3.5 g/t Ag and 0.6 g/t Au with a measured and indicated resource in a large number of different ore zones of 450 Mt grading 2.5% Cu, 0.08 % U_3O_8, 6 g/t Ag, 0.02% Co and 0.6 g/t Au with ~2000 g/t La and ~3000 g/t Ce (Reeves *et a*l., 1990);
- Ernest Henry - 166 Mt averaging 1.1 % Cu and 0.5 g/t Au (quoted in Williams, 1999);
- Sue-Dianne - 8.16 Mt averaging 0.8% Cu, up to 150 ppm U and locally significant gold (Gandhi, 1989);
- Kiruna district - > 2000 Mt grading 50-60% Fe and an average apatite content of 0.9 % (quoted in Williams, 1999);
- Candelaria - 366 Mt averaging 1.08 % Cu, 0.26 g/t Au and 4.5 g/t Ag (Ryan *et al*., 1995).

ECONOMIC LIMITATIONS

The larger, sulphide-poor Fe oxide deposits are a potential economic source for Fe and P in areas with easy access and existing infrastructure. However, the more sulphide-rich Fe oxide deposits with Cu-Au-Ag mineralization are currently more attractive economically.

IMPORTANCE

These deposits continue to be significant producers of Fe and represent an important source of Cu, Au, P, U and possibly REE's.

ACKNOWLEDGEMENTS

Many people contributed ideas that were used to complete this synopsis. Their opinions on the validity of this family of deposits were as varied as the individual deposits described in this profile! Thanks are expressed to the following: John Allen, consultant, New Zealand; Bill Chavez, New Mexico School of Mines; Larry Dick, Ralph Fitch, Rodrigo Arcos and Dan Maus, General Minerals Corporation, Denver, Colorado; Tony Floyd, Inca Pacific Resources Inc., Vancouver; Sunil Gandhi, Geological Survey of Canada; Murray Hitzman and Kari Fox, University of Colorado; Jay Hodgson, Barrick Gold Corporation, Toronto; Rod Kirkham, consultant, Vancouver; James Macdonald, David First, Gavin Whitfield and Dave Sleigh, Billiton International Metals; Stefan Nicolescu, Washington State University; Waldo Cuadra, Noranda Chile S.A.; Phil Seccombe, The University of Newcastle, Australia; Tom Setterfield, consultant, Ottawa; Dick Sillitoe, consultant, London, UK; John Thompson and Jeff Toohey, Teck Corporation, Vancouver; Cesar Vidal, Cia. De Minas Buenaventura S.A.; and Pat Williams, James Cook University, Australia.

BIBLIOGRAPHY

Barton, M.D., and Johnson, D.A. (1996): Evaporitic-source model for igneous-related Fe oxide-(REE-Cu-Au-U) mineralization; *Geology*, Volume 24, Number 3, pages 259-262.

Bookstrom, A.A., (1977): The magnetite deposits of El Romeral, Chile; *Economic Geology*, Volume 72, pages 1101-1130.

Borrok, D.M., Kesler, S.E., Boer, R.H., and Essene, E.J. (1998): The Vergenoeg magnetite-fluorite deposit, South Africa: Support for a hydrothermal model for massive iron oxide deposits; *Economic Geology*, Volume 93, Number 5, pages 564-586.

Campbell, I.H., Compston, D.M., Richards, J.P., Johnson, J.P., and Kent, J.R. (1998): Review of the applications of isotopic studies to the genesis of Cu-Au mineralization at Olympic Dam and Au mineralization at Potgera, the Tennant Creek district and Yilgarn Craton; A*ustralian Journal of Earth Sciences*, Volume 45, pages 201-218.

Cox, D.P. (1986): Descriptive model of Olympic Dam Cu-U-Au; In Mineral Deposit Models, Cox, D.P., and Singer, D.A., Editors, *U.S. Geological Survey*, Bulletin 1693, 379 pages.

Johnson, J.P., and Cross, K.C. (1995): U-Pb geochronological constraints on the genesis of the Olympic Dam Cu-U-Au-Ag deposit, South Australia; *Economic Geology*, Volume 90, Number 5, pages 1046-1063.

Johnson, J.P., and McCulloch, M.T. (1995): Sources of mineralizing fluids for the Olympic Dam deposit (South Australia): Sm-Nd isotopic constraints; *Chemical Geology*, Volume 121, pages 177-199.

Gandhi, S.S. (1989): Rhyodacite ignimbrites and breccias of the Sue-Dianne and Mar Cu-Fe-U deposits, southern Great Bear Magmatic Zone, Northwest Territories; *in* Current Research, Part C, *Geological Survey of Canada*, Paper 89-1C, pages 263-273.

Gandhi, S.S. (1994): Geological setting and genetic aspects of mineral occurrences in the southern Great Bear Magmatic Zone, Northwest Territories; *in* Studies of Rare-metal Deposits in the Northwest Territories, Sinclair, W.D., and Richardson, D.G., Editors, *Geological Survey of Canada*, Bulletin 475, pages 63-96.

Gow, P.A., Wall, V.J., Oliver, N.H.S., and Valenta, R.K. (1994): Proterozoic iron oxide (Cu-U-Au-REE) deposits: further evidence of hydrothermal origins; *Geology*, Volume 22, pages 633-636.

Hansgeorg, H., and Jafarzadeh, A. (1994): The Bafq mining district in central Iran: a highly mineralized Infracambrian volcanic field; E*conomic Geology*,. Volume 89; Number 8, pages 1697-1721.

Hauck, S.A. (1990): Petrogenesis and tectonic setting of Middle Proterozoic iron oxide-rich ore deposits; An ore deposit model for Olympic Dam type mineralization; *in* The Midcontinent of the United States - Permissive Terrane for an Olympic Dam Deposit?, Pratt, W.P., and Sims, P.K., Editors, *U. S. Geological Survey,* Bulletin 1932, pages 4-39.

Hildebrand, R.S. (1986): Kiruna-type deposits: Their origin and relationship to intermediate subvolcanic plutons in the Great Bear Magmatic Zone, Northwest Canada; *Economic Geology,* Volume 81, pages 640-659.

Hitzman, M. W., Oreskes, N., and Einaudi, M.T. (1992): Geological characteristics and tectonic setting of Proterozoic iron oxide (Cu-U-Au-REE) deposits; *Precambrian Research*, Volume 58, pages 241-287.

Laznicka, P., and Gaboury, D. (1988): Wernecke Breccias and Fe, Cu, U mineralization: Quartet Mountain-Igor Area (NTS 106E); *in* Yukon Exploration and Geology, Exploration and Geological Services Division, *Yukon, Indian and Northern Affairs*, pages 42-50.

Marschik, R., and L. Fontbot (1996): Copper (-iron) mineralization and superposition of alteration events in the Punta Del Cobre belt, northern Chile; *in* Andean copper deposits: new discoveries, mineralization, style and metallogeny, *Society of Economic Geologists*, Special Publication Number. 5, Camus, F., Sillitoe, R.H., and Peterson, R., Editors, pages 171-190.

Nystrom, J.O., and Henriquez, F. (1994): Magmatic features of iron ore of the Kiruna type in Chile and Sweden: Ore textures and magnetic geochemistry; *Economic Geology*, Volume 89, pages 820-839.

Oreskes, N., and Einaudi, M.T. (1990): Origin of rare earth-enriched hematite breccias at the Olympic Dam deposit, Roxby Downs, South Australia; *Economic Geology*, Volume 85, Number 1, pages 1-28.

Oreskes, N., and Hitzman, M.W. (1993): A model for the origin of Olympic Dam-type deposits; *in* Mineral Deposit Modeling, Kirkham, R.V., Sinclair, W.D., Thorpe, R.I. and Duke, J.M., Editors, *Geological Association of Canada*, Special Paper 40, pages 615-633.

Parak, T. (1975): Kiruna iron ores are not "Intrusive-magmatic ores of the Kiruna type"; *Economic Geology*, Volume 68, pages 210 -221.

Ray, G.E., and Webster, I.C.L. (2000, this volume): The Heff Prospect at Heffley Lake, south-central B.C. (092INE096): An unusual example of a mafic-ultramafic-related Cu-Au-REE-bearing magnetite skarn; *British Columbia Ministry of Energy and Mines*, Geological Fieldwork 1999, Paper 2000-1 (this volume).

Reeves, J.S., Cross, K.C., Smith, R.N., and Oreskes, N. (1990): Olympic Dam copper-uranium-gold-silver deposit; In Geology of the mineral deposits of Australia and Papua New Guinea, *The Australasian Institute of Mining and Metallurgy*, Hughes, F.E., Editor, pages 1009-1035.

Ryan, P.J., Lawrence, A.L., Jenkins, R.A., Matthews, J.P., Zamora, J.C., Marino, E.W., and Diaz, I.U. (1995): The Candelaria copper-gold deposit, Chile; *in* Porphyry Copper Deposits of the American Cordillera, Pierce, F.W. and Bolm, J.G., Editors, *Arizona Geological Society Digest*, Volume 20, pages 625-645.

Stinson, P., and Brown, D.A., (1995): Iron Range deposits, southern British Columbia (82F/1); *British Columbia Ministry of Energy, Mines and Petroleum*, Paper 1995-1, pages 127-134.

Vidal, C.E., Injoque-Espinoza, J., Sidder, G.B., and Mukasa, S.B. (1990): Amphibolitic Cu-Fe skarn deposits in the central coast of Peru; *Economic Geology*, Volume 85, pages 1447 -1461.

Vila, T., N. Lindsay., and R. Zamora. (1996): Geology of the Manto Verde copper deposit, northern Chile: A specularite-rich, hydrothermal-tectonic breccia related to the Atacama Fault Zone; *in* Andean copper deposits: new discoveries, mineralization, style and metallogeny, *Society of Economic Geologists*, Special Publication Number 5, Camus, F., Sillitoe, R.H., and Peterson, R., Editors, pages 157-170.

Williams, P.J. (1998): Metalliferous economic geology of the Mount Isa Eastern succession, northwest Queensland; *Australian Journal of Earth Sciences*, Volume 45, pages 329-341.

Williams, P.J. (1999): Fe oxide-copper-gold deposits. Shortcourse notes, *James Cook University,* Economic Geology Research Unit and Mineral Deposits Research Unit, *The University of British Columbia., Vancouver, 11th March 1999.*

The Heff Prospect at Heffley Lake, South-Central B.C. (092INE096): An Unusual Example of a Mafic-ultramafic-related Cu-Au-REE-Bearing Magnetite Skarn

By G.E. Ray and I.C.L. Webster

KEYWORDS: *Heff Prospect, Heffley Lake, Magnetite-Cu-Au-REE skarn, Garnet-pyroxene skarn, Alaskan-type mafic-ultramafic pluton, Heffley Creek Pluton, Candelaria-Ernest Henry-Fe oxide deposits, Geochemistry, Economic geology.*

INTRODUCTION AND LOCATION

The Heff prospect (also known as Iron Range, Hal and Mesabi claims, B.C. MINFILE No. 092INE096) is located on the north side of Heffley Lake, approximately 26 kilometres northeast of Kamloops. It lies within the Intermontane Belt and is hosted by calcareous metasediments of the Quesnel Terrane (Figure 1) and younger mafic intrusive rocks. The road between the township of Heffley Creek and the Sun Peaks ski resort passes immediately south of the property (Figure 2).

In the summer of 1999 the authors spent 15 days mapping and sampling the property and its surrounding area (Figure 2). Previous sampling had revealed anomalous quantities of REE's in the Heff magnetite skarn (Ray and Webster, 1997); the recent seasons' study was part of a program to investigate the potential for Fe-oxide-Cu-Au-REE mineralization of the Candelaria-Ernest Henry types (Hitzman *et al.*, 1992; Ryan *et al.*, 1995; Marschik and Fontboté, 1996; Williams, 1999; Ray and Lefebure, 2000) in British Columbia. Work included geological mapping at 1:5 000 scale of a 2.5 km^2 area containing the skarn alteration and mineralization, using a previously cut exploration grid. In addition, a 30 km^2 area surrounding the property was mapped at a scale of 1:20 000 (Ray and Webster, 2000)

This report presents the preliminary conclusions of the mapping program together with assay results of mineralization and whole rock chemical data of some intrusive rocks. An Alaskan-type mafic-ultramafic pluton and several Cu occurrences were discovered (Figure 2; Ray and Webster, 2000). The results of on-going work to extract conodont microfossils from the limestones and complete microprobe analyses of the skarn mineralization and alteration will be published at a later date.

PREVIOUS WORK

Past exploration and drilling have been concentrated in a poorly exposed area that lies at the base of a series of northwest trending limestone cliffs, immediately north of Heffley Lake (Figure 2). Since the early part of this century the property has undergone several name changes, and there are discrepancies in the records regarding some past exploration and drilling.

Copper mineralization was first noted in 1915 (MMAR, 1916) when the lake was then known as "Hefferly Lake". The Lake View and Monarch claims were staked and trenched, and samples containing up to 51 percent Fe and trace Cu and Au were noted. By the 1940's, more trenches had been cut on the "Iron Range Group" property. In the early 1960's the prospect was known as the HAL group. At least four diamond drillholes totalling 250 metres were completed in 1966 but only one hole was reportedly sampled and assayed (Casselman, 1980; Arseneau, 1997). Two additional holes apparently did not hit bedrock and were abandoned. The drilling intersected over 10 metres of massive magnetite and another 4.5 metres thick zone of semi-massive magnetite with chalcopyrite; the latter zone graded 1.67 percent Cu and 0.48 g/t Au. From this work, a resource of 63 Mt grading 30 percent Fe was calculated (Northern Miner, 1967; B.C. MINFILE). Federal Government records also note that in 1976 (when the property was registered as the Freda 1 claim), diamond drilling totalling 72 metres was completed in deepening a pre-existing drillhole.

In 1980, Cominco conducted a mapping and soil sampling program over the "Heff Lake" property (Casselman, 1980). This identified a broad, 600 metres-long Cu soil anomaly but no samples were apparently assayed for Au (Arseneau, 1997). In 1985, a single 58 metres long hole intersected 16 metres of semi-massive magnetite, one 6 metre interval of which assayed 25 percent Fe and 0.5 g/t Au (Arseneau, 1997).

In 1994, the property was sampled as part of a project to examine skarn occurrences throughout British Columbia (Ray and Webster, 1997). This work revealed that the Heff magnetite skarn, unlike the large Fe skarn deposits on the west coast of British Columbia, contained anomalous quantities of REE's (up to 570 ppm La and 490 ppm Ce). Subsequently, Echo Bay Mines optioned the claims in 1997 (which they called the Mesabi property). A geophysical and soil sampling program was conducted over east-west orientated grid lines spaced 100 metres apart. This outlined several magnetic anomalies with coinci-

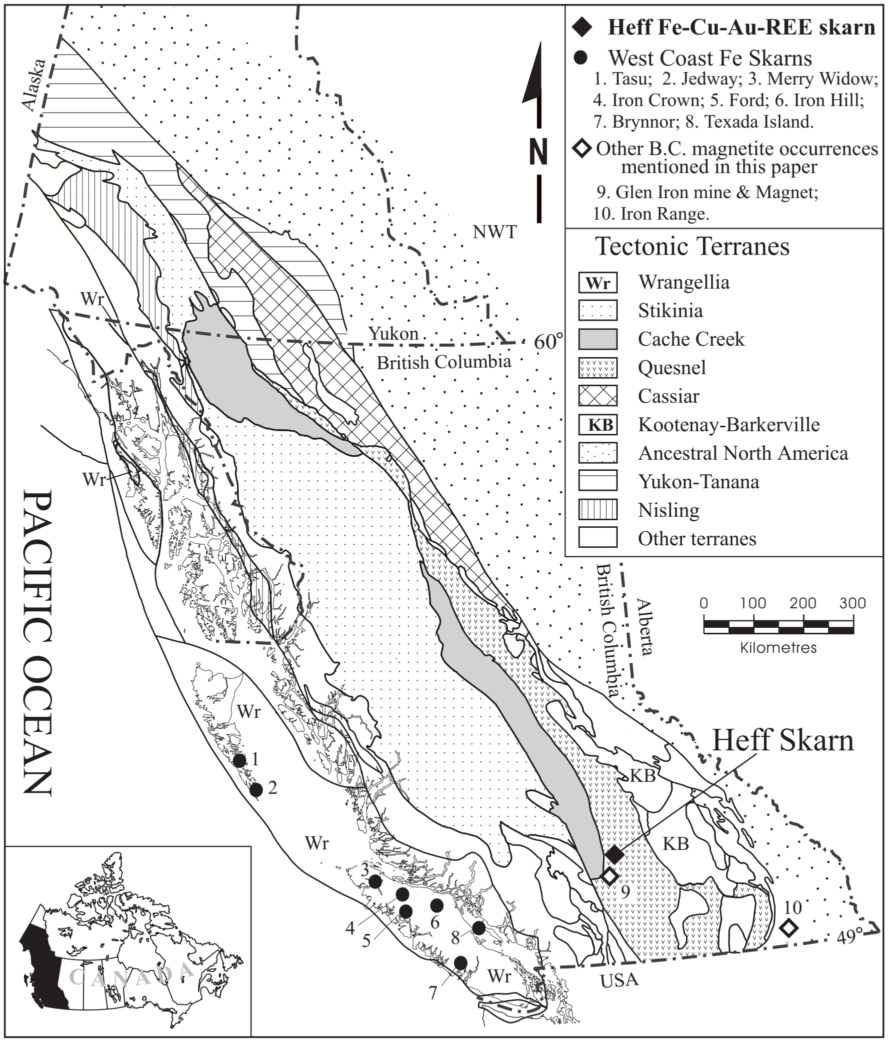

Figure 1. Simplified terrane map of the Canadian Cordillera showing the locations of the Heff skarn and some other Fe-oxide-rich properties in British Columbia. Terrane map modified after Wheeler *et al.* (1991).

dent soil geochemistry marked by values exceeding 1200 ppm Cu and 1000 ppb Au; these anomalies lay adjacent to magnetite-rich skarn. Drilling was recommended but not completed (Arseneau, 1997).

In 1999, whilst this mapping was in progress, a magnetometer and VLF geophysical survey was completed by one of the present property owners.

Previous government mapping of the area includes early work by Cockfield (1944, 1947) and, more recently, a 1:250 000 scale geological map of the district has been published (Monger and McMillan; 1989).

GENERAL GEOLOGY OF THE HEFFLEY LAKE AREA

Stratified Rocks

The 30 km^2 area mapped is extensively covered with superficial glacio-fluvial deposits and is estimated to have < 1 percent rock exposure. The stratified rocks were originally mapped as Cache Creek Group (Cockfield, 1944, 1947) but more recently they are considered to belong, in part, to the Harper Ranch Group of the Quesnel Terrane (Monger and McMillan, 1989). They mainly comprise steeply dipping, northwest striking argillites and calcareous siltstones with lesser andesitic ash and lapilli tuff and some limestone. These rocks were intruded by the Heffley Creek Pluton and then folded and overprinted by lower to sub-greenschist metamorphism producing slatey and phyllitic fabrics. Bleached marbles and calc-silicate-rich metasediments are developed where hydrothermal or thermal alteration has occurred. The magnetite-bearing garnet-pyroxene skarn alteration comprising the Heff property is hosted by calcareous metasediments and a suite of dioritic minor intrusions; it is best exposed in a number of overgrown trenches that lie 200 to 300 metres north of the Heffley Creek-Sun Peaks road (Figure 2).

The southern part of the area includes units of blue-grey crinoidal limestone and black argillites whilst

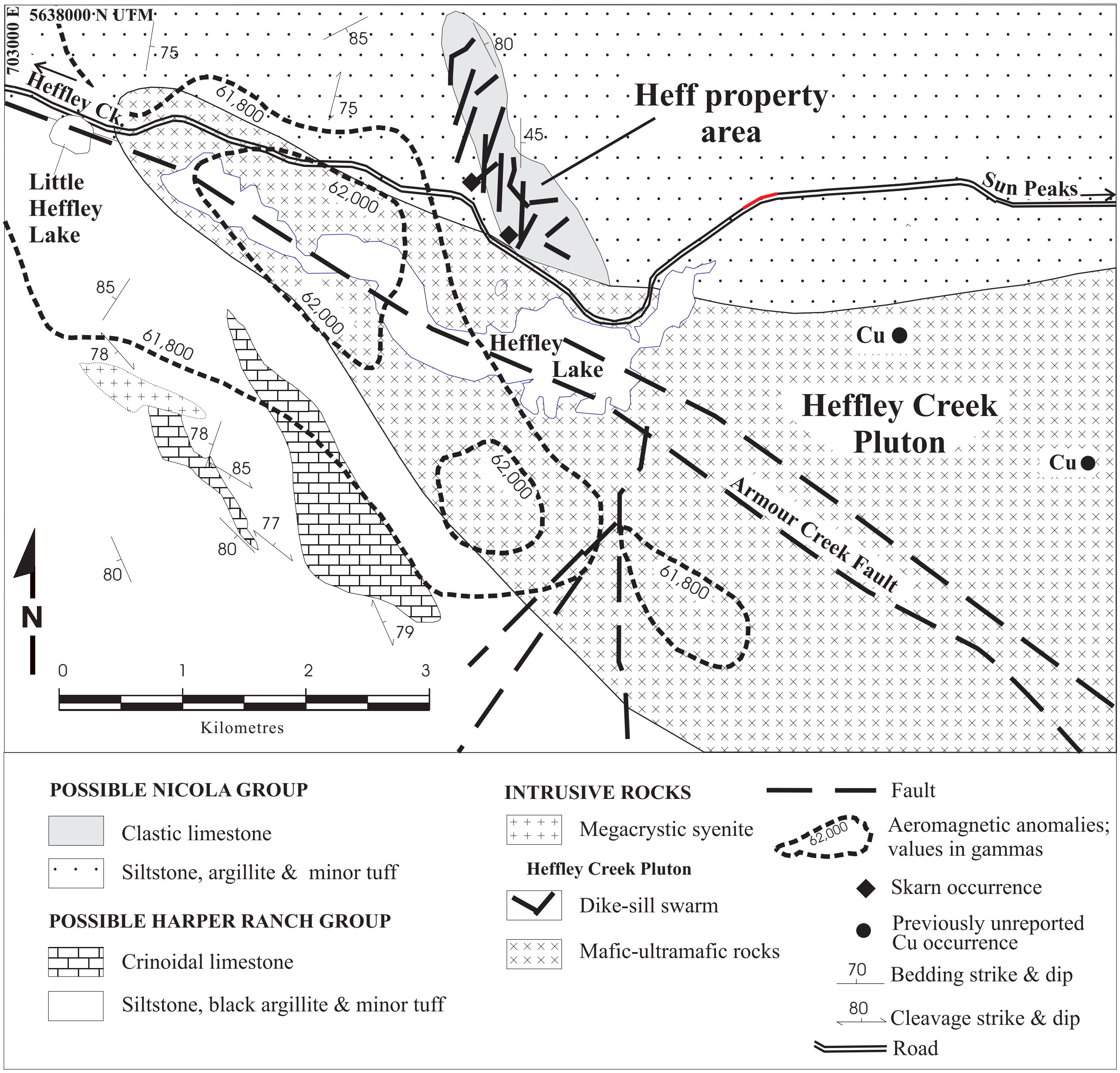

Figure 2. Geology of the Heffley Lake area, south central British Columbia.

the coarsely clastic to conglomeratic limestones in the vicinity of the Heff skarn, north of Heffley Lake, lack crinoids and the argillites are less organic-rich. This and other lithological differences suggest that the supracrustal rocks may be separated into northern and southern packages; these are tentatively believed to represent the Nicola and Harper Ranch groups respectively. The northwest trending contact between these packages is thought to pass under the Heffley lakes and continue south-eastwards along Armour Creek. This original stratigraphic contact has been intruded by the mafic-ultramafic Heffley Creek Pluton and has subsequently been the locus of brittle movement along the Armour Creek Fault (Figure 2).

INTRUSIVE ROCKS

Introduction

Two intrusive phases are recognised. The oldest, largest and most economically important of these is the Heffley Creek Pluton and its marginal dike-sill swarm (Figure 2), which is genetically related to the Heff skarn. This either predates or was coeval with the district-wide folding, and it was also affected subsequently by younger brittle movement along the Armour Creek Fault. A younger generation, which post-dates the folding, resulted in bodies of distinctive megacrystic, feldspar-porphyry syenites; these occur mainly 2 km southwest of Heffley Lake (Figure 2).

Heffley Creek Pluton and its Related Dike-Sill Swarm

Most of the pluton lies south and southeast of Heffley Lake, where small, scattered outcrops of the intrusion are traceable over a 10 km^2 area. The true size and shape of the pluton are unknown because its southern, eastern and north-western margins have not been fully mapped (Figure 2). The pluton probably forms an elongate body that intruded the Nicola and Harper Ranch groups. It contains a variety of rock types, including early ultramafics, younger mafic and felsic gabbros, diorites and quartz diorites, and minor amounts of late leucocratic monzodiorite. In addition, a strongly altered swarm of sills and dikes on the Heff property, north of Heffley Lake, is probably related to both the pluton and the magnetite skarns.

The ultramafic rocks, which include pyroxenites and hornblendites, appear to lie in the central part of the pluton They are dark, coarse grained (up to 0.5 centimetres) and massive rocks that commonly contain up to 2 percent disseminated pyrite and up to 10 percent disseminated magnetite. The latter mineral produces an elongate magnetic anomaly outlined by a 1:25 000 scale government aeromagnetic survey (Map 4411G) that extends 6 km south-eastwards from Little Heffley Lake (Figure 2).

The late felsic monzodiorite is an extremely minor part of the pluton. It forms irregular and narrow dikes, between 1 cm and 1.5 metres wide, that cut the ultramafics to produce intrusive breccias comprising sharply angular clasts of ultramafite in a matrix of felsic monzodiorite.

Thin sections reveal that the ultramafic rocks are dominated by either cumulate clinopyroxene or inter-cumulate hornblende, both of which are variably altered to chlorite or light coloured secondary amphibole. The pyroxene includes both colourless and highly pleochroic varieties. Minor amounts of highly altered olivine were tentatively identified in a few outcrops but its presence has not been verified in thin section. Other cumulate minerals include sphene and euhedral to subhedral crystals of magnetite. Secondary minerals include chlorite, epidote, pyrite, phlogopite, talc and trace serpentine, chalcopyrite and plagioclase.

Major and trace element analytical data for the various rock types in the Heffley Creek Pluton are presented in Table 1 and the chemical plots are shown in Figure 3. The data can be subdivided into four compositional groups, namely the ultramafic rocks, the gabbroic to quartz-dioritic intrusives, the late felsic monzodioritic phase, and the swarm of strongly altered sills and dikes on the Heff skarn property. The two ultramafic samples (GR99-30A and 51) are notable for their high Fe, Ca and Mg contents, and one of these magnetite-bearing samples contains more than 23 percent total iron (Table 1). The gabbroic and dioritic samples from the main body range from highly altered microdiorite on the margin of the pluton (GR99-24A), to felsic quartz diorite (GR99-27A) to more mafic gabbro-diorite (GR99-26A and 29A). The total alkali content of the latter group indicates a weak alkalic affinity (Figure 3A). However, other plots, including ones using less mobile trace elements (Figure 3D and E) suggest that these rocks are calc-alkaline and that their higher alkali content is due to hydrothermal alteration. The relatively low Fe and high Ca and Na contents of the one felsic monzodiorite sample (GR99-52; Table 1) reflects the plagioclase-rich nature of this rock-type.

The limestone unit exposed in cliffs on the Heff property are cut by a variety of minor intrusives, the most common and economically important of which occur as a swarm of strongly altered dioritic sills and dikes (Figure 2). Individual bodies are usually less than 10 metres wide but a few exceed 50 metres in thickness. Due to the ubiquitous presence of up to 6 percent disseminated, fine-grained pyrite, these rocks are rusty-weathering. However, fresh samples are generally light grey coloured and are weakly to moderately enriched (Table 1) in Si, Ca and Na which reflects silicification with carbonate and albitic plagioclase alteration. The relatively high loss on ignition content also reflects the presence of carbonate in these rocks.

Hydrothermal alteration in the sills and dikes varies in intensity over short distances; some bleached and strongly altered dikes contain rounded small (less than 1m diameter) remnants of dark coloured and less altered igneous rock. The widespread overprinting has caused difficulties in identifying the original composition of these minor intrusions which, due to their siliceous appearance, have been mapped previously as "dacites" (Arseneau, 1979). However, plots using immobile trace elements (Figure 3D and E) show they are dioritic in composition; they are believed to be related to both the Heffley Creek Pluton and the hydrothermal event that produced the Heff Fe-Cu-Au-REE skarn.

The dike-sill swarm includes equigranular and porphyritic varieties; the latter are more common and contain euhedral to anhedral, corroded phenocrysts of plagioclase, clinopyroxene and hornblende up to 0.5 centimetres long. The north to north-northwest trending swarm can be traced for 2 kilometres on the Heff property (Figure 2). These intrusions are much more common in the limestones than in the adjoining tuffaceous and siltstone-argillite units. Most of the sills and dikes strike north to northeast, but some of the more irregularly orientated intrusions bifurcate or intersect one another. Their margins are lobate and highly irregular, and many dikes are folded and overprinted by a fracture cleavage. Whilst the hosting limestones have undergone ductile deformation, boudinage has produced brittle rupturing in the more competent intrusions.

Megacrystic Syenite

These are the youngest intrusives in the area and they are believed to post-date the major folding event, although they have undergone brittle faulting. They are best seen south of Heffley Lake; in this area a single, 500

TABLE 1
MAJOR AND TRACE ELEMENT ANALYSES OF THE HEFFLEY CREEK PLUTON, HEFFLEY LAKE, B.C.

	Altered pyritic dikes & sills				Samples from the main pluton						
Sample	GR99	GR99	GR99	GR99	GR99	GR99	GR99	GR99	GR99	GR99	GR99
No.	24	46	47	48	24A	26A	27A	29A	30A	51	52
SiO_2	57.50	57.11	46.61	49.32	49.76	58.12	63.19	49.57	47.07	40.13	55.57
TiO_2	0.59	0.55	0.81	0.78	1.00	0.83	0.34	0.78	0.61	1.29	0.46
Al_2O_3	17.46	15.87	15.71	14.74	18.51	16.23	16.61	16.91	4.61	5.25	17.58
Fe_2O_3	5.66	6.11	9.24	8.36	7.95	7.44	3.73	9.26	10.14	23.47	4.57
MnO	0.06	0.05	0.09	0.12	0.17	0.14	0.09	0.15	0.14	0.19	0.10
MgO	1.92	2.44	5.50	6.24	3.48	2.57	1.21	5.15	14.87	10.06	2.13
CaO	5.72	5.14	11.35	10.83	11.71	5.99	3.95	8.02	20.13	16.82	9.28
Na_2O	4.34	5.40	2.02	3.09	3.89	4.47	4.69	3.69	0.26	0.33	6.05
K_2O	2.23	3.84	3.13	2.09	1.09	2.74	4.17	1.77	0.10	0.16	0.75
P_2O_5	0.18	0.29	0.35	0.30	0.30	0.21	0.16	0.44	0.03	0.04	0.32
LOI	3.66	1.98	3.83	2.68	1.21	0.60	1.12	2.88	1.05	1.33	2.48
TOTAL	99.32	98.78	98.64	98.55	99.07	99.34	99.26	98.62	99.01	99.07	99.29
K2O/Na2O	0.51	0.71	1.55	0.68	0.28	0.61	0.89	0.48	0.38	0.48	0.12
Ba	1300	1665	1865	1030	310	1415	1890	760	75	140	495
Rb	56	66	80	64	28	56	100	46	12	16	18
Sr	588	1040	846	1025	842	650	966	630	38	980	1020
Nb	8	8	2	6	8	10	8	6	4	6	18
Zr	96	111	63	78	84	132	105	60	27	51	90
Y	20	24	20	18	22	24	20	20	12	8	12
F	270	460	1300	1200	640	300	410	500	50	80	170
Hg (ppb)	50	10	10	<10	10	<10	10	10	<10	<10	<10
Rb/Sr	0.10	0.06	0.09	0.06	0.03	0.09	0.10	0.07	0.32	0.02	0.02
Ba/Sr	2.21	1.60	2.20	1.00	0.37	2.18	1.96	1.21	1.97	0.14	0.49

Oxides in percent; Hg in ppb; other trace elements in ppm.

Sample description:

GR99-24 & 46	Moderately silicified, rusty weathering, pyritic and albite-altered intrusion.
GR99-47 & 48	Pyritic and carbonate-altered intrusion.
GR99-24A	Altered, hornblende-microdiorite with minor pyrite.
GR99-26A	Medium grained gabbro with 60% mafics and 2% pyrite.
GR99-27A	Felsic diorite with 12% mafics and 1% pyrite. Minor quartz veining.
GR99-29A	Coarse, horblende porphyry gabbro with 15% mafics and 1% pyrite.
GR99-30A	Coarse grained pyroxenite with 5% magnetite & trace pyrite.
GR99-51	Coarse grained hornbende-pyroxene ultramafic with 10% magnetite.
GR99-52	Pale, feldspathic monzodiorite agmatite cutting ultramafics.

Analyses completed at Chemex Labs Ltd., 212 Brookbank Ave., North Vancouver, B.C.
Methods: Major & minor oxides = XRF; Au = Fire assay and AA finish;
Ba, Rb, Sr, Nb, Zr, Y = XRF; Hg = Atomic Absorption Specroscopy (AAS)
F = Specific Ion Electrode

metre-long syenitic body has been inferred from the sporadic small outcrops (Figure 2). However, north of Heffley Lake, the limestones and the altered dioritic dike-swarm are cut by a few syenitic dikes that are generally less than 3 metres thick.

These syenites appear as leucocratic, buff coloured rocks; some contain up to 7 percent remnant mafic amphibole and biotite, both of which are extensively chloritized, as well as trace to minor glassy quartz. Many outcrops are cut by parallel veins of white quartz up to 1 cm thick. The syenites are characterised by abundant (up to 30 percent) elongate euhedral to subhedral feldspar laths that are generally between 2 and 4 cm long, although some crystals exceed 15 cm in length. Some of these pale brown phenocrysts have thin, light coloured margins and are partially resorbed. Many crystals show a pronounced parallel orientation due to igneous flow. Intrusive contacts between the syenites and the sedimentary country rocks were seen both north and south of Heffley Lake. No chilled margins were observed, although thin (less than 0.5 m wide) zones of silicification and hornfels occur adjacent to some dikes.

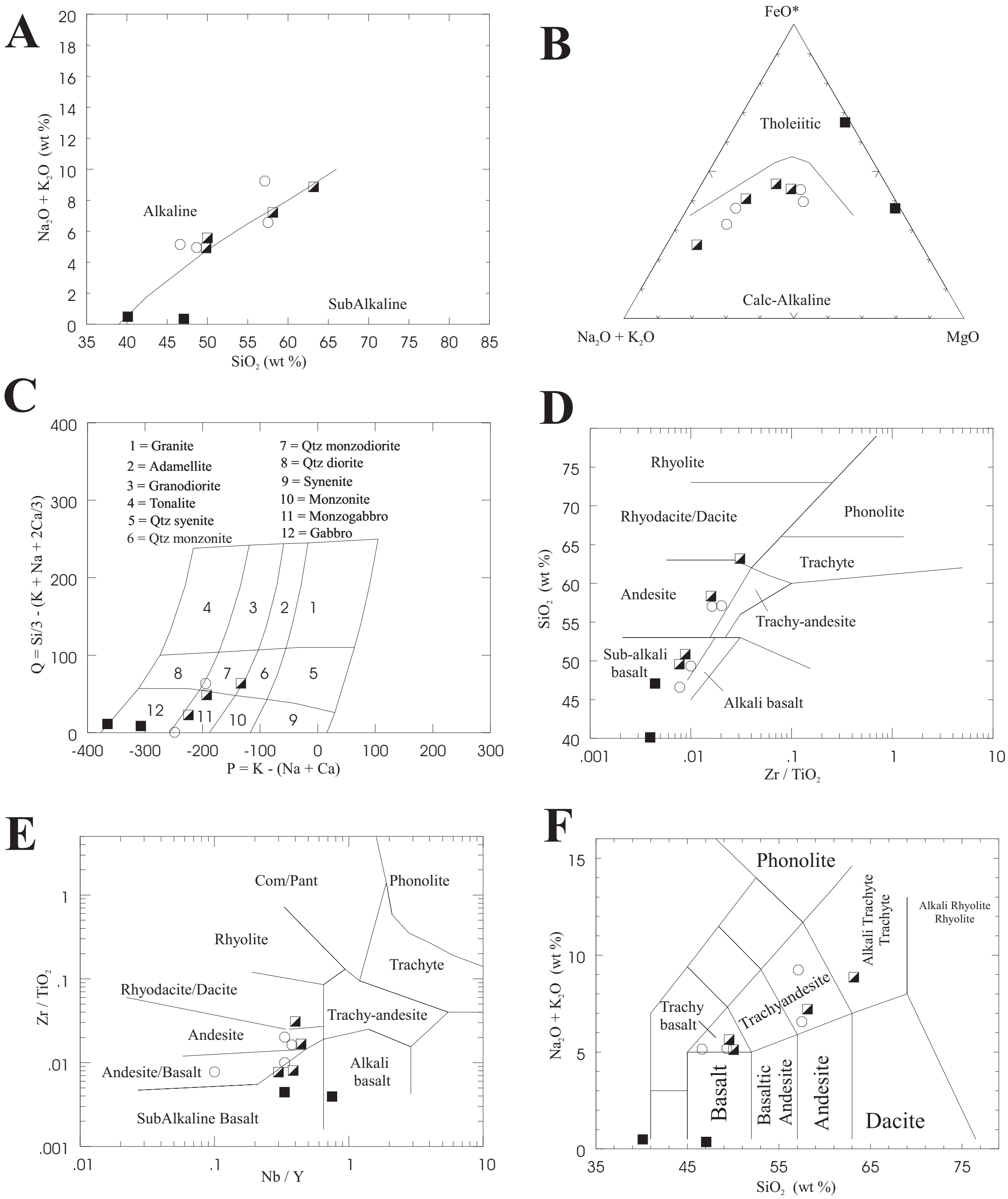

■ Pyroxene-hornblende ultramafic rocks

◩ Gabbro-diorite-quartz diorite

○ Altered pyritic dike-sill-swarm intruding limestones north of Heffley Lake

Figure 3. Plots showing the major and trace element geochemistry of the Heffley Creek Pluton.

(A) Alkali-silica plot (after Irvine and Baragar, 1971

(B) AMF plot (after Irvine and Baragar, 1971)

(C) Q - P plot (after Debon and Le Fort, 1983)

(D) Silica versus Zr/titanium plot (after Winchester and Floyd, 1977)

(E) Zr/titanium versus Nb/Y plot after Winchester and Floyd, 1977)

(F) Alkali versus silica plot (after Le Maitre *et al*., 1989).

ALTERATION RELATED TO THE HEFF SKARN

Most of the limestones on the Heff property show little or no signs of thermal or hydrothermal overprinting, despite the presence of the pervasively altered dike-sill-swarm. Varying degrees of pyritic, albitic, carbonate and silica alteration are seen in all the dioritic dikes and sills on the Heff property and this alteration overprints the intrusions for at least 1.5 km north of the Heff skarn occurrences. There is a progressive southerly change in the intensity and style of alteration in the dikes, and, to a lesser extent, in the limestones. This change reflects increasing proximity to the mineralised Heff skarn occurrences and the northern margin of the Heffley Creek Pluton, which is presumed to either underlie Heffley Lake or its northern shore (Figure 2).

In the north part of the Heff property grid, the sills and dikes are characterised by up to 3 percent by volume pyrite, which is fine grained and disseminated. Further south, however, in the vicinity of line 6700N and 6800E (this and the following locations refer to the cut grid illustrated in Map 1, Arseneau, 1997), the pyrite content increases; in addition to the disseminated sulphide, the margins of some sills and dikes contain haloes, up to 7 centimetres thick, of massive, coarse grained pyrite. Still further south (close to line 6400N and 6950E), endoskarn alteration is first recognised; the dikes are still pyritic but they also contain trace amounts of magnetite together with pyroxene, epidote and silica. The limestones in this area have also undergone a recognisable colour-change. To the north they are unaltered and dark to medium grey in colour but further south they become pervasively paler. Coinciding with the first southern appearance of pyroxene-endoskarn, the pale grey limestones are cut by irregular veins and stringers, up to 4 centimetres thick, of white marble. These fracture-controlled bleached veins in the limestones represent the more distal effects of hot, metal-poor fluids from the Heff skarn hydrothermal system.

Immediately to the south of this area, on line 6400N and 6850E, coarse garnet-dominant skarn is first recognised with massive to semi-massive magnetite and lesser pyroxene and pyrite and trace chalcopyrite. Some of this garnet-rich alteration appears to be endoskarn, although in the majority of cases the alteration is so intense that the protolith is unidentifiable. In this area, the fracture controlled bleaching in the carbonates is so intense that some rocks comprise mostly white, fine grained marble that enclose small dark relicts of original limestone. In the coarser skarns, the euhedral garnet crystals are intergrown with calcite. Thin section studies show that the garnets are moderately birefringent and they form anhedral to euhedral crystals up to 1 centimetre in diameter. Many contain small inclusions of pyroxene, calcite and opaque Fe oxides; some garnet crystals are skeletal, consisting of alternating growth zones of garnet-rich and calcite-rich material. Other minerals identified in thin section in the skarns include epidote, chlorite, quartz, albitic plagioclase, zoisite and ilmenite.

MINERALIZATION AND GEOCHEMISTRY

At least two types of Cu-bearing mineralization are recognised in the area. These are: (1) magnetite-rich chalcopyrite ± Au ± REE garnet-pyroxene skarns which occur on the Heff property north of Heffley Lake, and (2) disseminations and veins of chalcopyrite ± magnetite-pyrite mineralization in the Heffley Creek Pluton south of Heffley Lake (Figure 2).

Unlike the Cu-showings in the Heffley Creek Pluton, the Heff skarns have had a long history of exploration. The more extensive pyroxene ± garnet skarn horizons reach up to 50 metres thick but most are generally less than 2 metres wide. Surface mineralization in the skarn consists of pods and massive lenses of magnetite with lesser amounts of pyrite and pyrrhotite and trace of chalcopyrite. The sulphides occur as disseminations and veinlets, and pyrite is generally dominant to pyrrhotite. Magnetite lenses up to 1 metre wide crop out on surface but massive magnetite zones over 10 metres thick have been intersected by drilling (Casselman, 1980). Mineralization occurs locally in the intrusions and in what is believed to be the adjacent exoskarn. On a local scale, many of the calc-silicate layers are mineralogically zoned with a central core of coarser grained garnet-dominant skarn and a wider outer halo of finer grained pyroxene-dominant skarn. Magnetite-sulphide mineralization tends to be better developed in the garnet-dominant skarn.

Assay results of grab samples of mineralised Heff property skarn are shown in Table 2. Many samples contain > 25 percent Fe which reflects the abundant magnetite, and some are weakly anomalous in Au (up to 445 ppb), Cu (up to 1195 ppm), Co (up to 467 ppm) and Mo (up to 14 ppm) as well as being sporadically enriched in REE's (up to 490 ppm Ce and 570 ppm La) and P (up to 1560 ppm).

Assay data for pyrite-bearing grab samples from the Heffley Creek Pluton and its dike-sill swarm are presented in Table 3. Two samples of magnetite-bearing ultramafic pyroxenite were assayed for PGE's but they contained only 15 ppb Pt and 4 ppb Pd. However, there are unconfirmed reports that Pt geochemical soil anomalies are present in the area (Roed, 1988).

Samples collected from the altered pyritic dike-sill swarm on the Heff property contain no economic quantities of Cu and Au, although one sample (GR99-24; Table 3) is weakly anomalous in Au (145 ppb) and some are moderately anomalous in F (up to 1300 ppm F; Table 1). Disseminated cumulate magnetite is common throughout the main Heffley Creek Pluton but locally some pyrite ± chalcopyrite ± secondary Cu oxides are also seen. Many of these sulphide-rich zones are characterised by silicification and plagioclase veining and they appear to be fault-related. One chalcopyrite-malachite-K feld-

TABLE 2
ASSAY RESULTS OF MINERALIZED SKARN, HEFF PROPERTY, HEFFLEY LAKE, B.C.

SAMPLE No.	GR94-217	GR94-219	GR94-220	GR94-223	GR94-224	GR99-19	GR99-25A	GR99-27	GR99-28	GR99-29	GR99-32A	GR99-32	GR99-33	GR99-34	GR99-37	GR99-40	GR99-42
Au	96	55	49	176	445	36	<5	75	160	55	20	35	25	40	205	20	25
Hg	15	10	15	20	25	<10	40	<10	60	10	50	<10	10	<10	20	10	50
Sb	3.1	0.1	1.5	1	1.4	1.3	0.7	7	0.5	0.9	0.7	1.2	1	0.6	0.5	2.1	0.8
Ba	>10	>10	>10	61	92	270	170	560	<10	30	10	<10	50	40	60	70	60
Be	1	4	1	4	1	0.35	9.65	0.85	<0.05	0.3	0.4	0.55	1	0.4	0.5	0.4	0.25
Bi	<4	<4	<4	<4	<4	0.13	0.16	1.5	0.91	0.07	0.19	0.1	0.14	0.75	0.14	0.18	0.15
Cd	0.8	3	3.2	3.2	1.2	0.1	0.22	0.22	0.02	0.02	0.06	0.02	0.02	0.1	0.22	0.08	0.3
Ce	9	490	86	6	6	1.41	13.7	62.4	0.62	6.26	2.2	1.58	1.03	0.75	1.15	12.65	3.92
Cs	>1	>1	>1	1	1	5.1	0.2	0.25	<0.05	0.7	0.35	0.15	0.9	3.95	5.8	2.2	0.75
Cr	130	48	38	120	120	30	71	61	3	27	54	16	23	7	27	35	80
Co	79	63	45	54	48	67	77.1	68.3	467	40.2	61.6	44.6	46.8	135	33.8	68.5	42.4
Cu	511	769	393	495	352	392	754	439	243	350	718	377	363	822	679	905	1195
Ga	-	-	-	-	-	12.7	7.2	11.4	0.4	14.3	10.1	9.1	15.4	9.4	6.7	8.9	6.1
Ge	-	-	-	-	-	0.6	3.2	1.2	0.3	0.6	0.9	0.7	1	0.8	0.5	1	0.9
La	7.2	570	100	2.8	2.9	0.5	6.5	47.5	<0.5	6	1.5	1	0.5	<0.5	0.5	9.5	2.5
Pb	4	4	4	4	4	3.5	20	8.5	6.5	3	3	2.5	6.5	5	2	3.5	2
Li	-	-	-	-	-	0.6	23	2.4	<0.2	1.2	1.6	1.6	0.8	1.6	1	1.2	1
Mn	2738	571	896	2456	2721	1530	2730	1245	180	890	1770	1045	1560	1355	1205	2080	3060
Mo	8	2	2	10	14	0.2	0.6	0.4	0.4	<0.2	0.2	<0.2	0.2	0.2	1.6	<0.2	0.6
Ni	43	25	21	48	53	16.8	32.8	75.3	144.5	13.2	27.6	14	21.2	57.5	19.6	32.2	20
Nb	4	2	2	2	3	0.6	13.8	1.6	<0.2	0.2	0.8	0.2	0.4	0.2	<0.2	0.8	1.2
P	1500	700	300	1200	1000	670	760	1210	120	420	910	700	890	800	570	730	1560
Rb	>5	7	10	>5	8	14.8	25.4	9.4	0.2	2.2	1	0.8	3.8	23.2	18.6	5.2	2.2
Ag	0.3	0.3	0.3	0.3	0.3	0.75	0.95	0.5	2.25	0.45	0.9	0.4	0.85	0.85	0.9	1	1.3
Sr	42	50	31	52	146	174.5	474	605	8.8	29.6	86.5	30.6	41.8	65.6	77.5	55.9	110.5
Ta	-	-	-	-	-	<0.05	0.05	0.05	<0.05	<0.05	<0.05	<0.05	<0.05	<0.05	<0.05	0.05	0.05
Te	0.3	0.4	0.2	0.3	0.2	0.2	0.05	0.15	4.15	0.25	0.55	0.3	0.3	0.75	0.3	0.35	0.4
Tl	-	-	-	-	-	0.02	0.14	0.08	<0.02	<0.02	0.02	<0.02	0.02	0.18	0.16	0.08	0.02
Th	1	1.4	0.6	1	1.1	0.6	0.8	2.4	<0.2	<0.2	0.2	0.2	<0.2	0.2	0.4	0.8	0.4
W	8	2	>1	>1	>1	1.1	0.2	0.8	0.1	0.3	1.8	0.3	1	0.3	0.1	0.9	2.7
U	2.8	0.5	2.3	3.6	3.8	1	3.8	2.6	<0.2	0.8	1.2	0.4	0.8	0.4	0.6	1.4	1.8
V	134	37	40	95	112	80	151	233	3	71	92	57	65	59	155	164	109
Y	18	4	3	13	15	5.1	12.3	10.7	0.3	2.8	7.5	1.3	2.4	2.4	1.6	9.5	13.9
Zn	24	31	30	30	20	20	126	36	<2	26	24	28	32	16	32	30	32
As	6.4	28	8	6.6	9.1	9	<1	79	<1	<1	<1	<1	<1	<1	2	<1	2
F	500	240	210	270	260	100	240	360	40	100	150	160	170	260	140	180	270
Total S	5.5	3.75	3.46	3.14	3.82	-	-	-	-	-	-	-					
Al	3.32	0.7	0.7	2.62	2.76	1.88	2.34	8.05	0.21	0.95	1.78	0.75	1.38	0.79	1.09	2.5	3.41
Ca	14.27	3.53	5.07	12.43	15.94	7.93	10.25	11.95	0.75	3.85	11.7	6.77	6.84	5.35	3.39	9.19	17.75
Fe	16.3	49.5	39.5	28	18.1	>25.0	15.9	7.2	>25.0	>25.0	>25.0	>25.0	>25.0	>25.0	>25.0	>25.0	13.85
Mg	1.09	1.31	2.61	1.1	1.16	0.53	1.49	2.73	0.14	0.55	1.48	2.81	1.51	1.23	1.04	1.2	1.93
K	0.07	0.07	0.1	0.07	0.09	0.32	1.54	0.69	0.06	0.15	0.08	0.11	0.11	0.53	0.59	0.22	0.11
Na	0.06	0.1	0.12	0.05	0.05	0.24	1.73	0.89	0.15	0.23	0.09	0.18	0.13	0.17	0.19	0.15	0.11
Ti	0.18	0.04	0.05	0.12	0.12	0.07	0.14	0.42	<0.01	0.07	0.11	0.05	0.06	0.05	0.05	0.13	0.2

Au and Hg in ppb

Total S, Al, Ca, Fe, Mg, K, Na, & Ti in wt %

Other elements in ppm

Analyses completed at Chemex Labs Ltd., 212 Brookbank Ave., North Vancouver, B.C.

Methods:

Au = Fire assay and AA finish; F = Specific Ion Electrode; As = AAS; other elements = ICP-MS

TABLE 2 CONTINUED
ASSAY RESULTS OF MINERALIZED SKARN, HEFF PROPERTY,

For sample locations *see* Ray and Webster (2000)	
GR94-217, 219 & 220	Garnet-pyroxene-magnetite skarn with pyrite and trace chalcopyrite
GR94-223 & 224	Drill core: magnetite-garnet skarn with pyrite and trace chalcopyrite
GR99-19	Pyroxene-magnetite-pyrite skarn; UTM 10 7067 80E; 56 365 18N
GR99-25A	Magnetite-pyrite-garnet skarn
GR99-27	Ganet-pyroxene skarn with pyrrhotite, pyrite and trace chalcopyrite
GR99-28 & 29	Pyrite-magnetite skarn with trace garnet and chalcopyrite
GR99-32A	Magnetite-garnet-proxene skarn
GR99-32	Magnetite-pyroxene skarn with pyrite and trace chalcopyrite
GR99-33	Magnetite skarn with trace garnet, pyrite and chalcopyrite
GR99-34	Magnetite vein with minor pyrite
GR99-37	Massive magnetite with pyrite and trace garnet
GR99-40	Magnetite-garnet-pyrite skarn with trace chalcopyrite
GR99-42	Garnet-pyroxene-pyrite skarn with minor chalcopyrite

spar-bearing occurrence was seen in a new road cut at NAD 83, UTM location 11 2 89 285E; 56 34 320N. A grab sample from this occurrence (sample GR 99-53; Table 3) contained 0.8 percent Cu as well as anomalous Mo, Co and Ag. This sample also contained the highest quantity of Hg (250 ppb) recorded during this survey. The pyritic mineralization in both the pluton and its related dike-sill swarm are weakly anomalous in P and possibly Ce (Table 3).

THE HEFF SKARN COMPARED TO OTHER Fe SKARNS IN B.C.

In some respects, the Heff skarn resembles the calcic Fe skarns on the west coast of British Columbia, such as the Merry Widow, Tasu and Texada Island deposits (Sangster, 1969; Meinert,1984; Ray 1995; Ray and Webster, 1997). Similarities include:

(a) the presence of abundant massive magnetite with variable amounts of Fe sulphides that are associated with sporadic Cu and Au-rich mineralization;

(b) the presence of dark-coloured (probably Fe-rich) garnet and pyroxene assemblages; and,

(c) the proximal development of magnetite skarn in calcareous rocks adjacent to mafic, Fe-rich intrusions.

However, the Heff mineralization is significantly different from that in the west coast deposits which suggests it is not a typical island arc Fe skarn. These differences include:

(a) its location in the central part of the province where it is hosted by Quesnel Terrane rocks whereas the major Fe skarn deposits lie further west in Wrangellia (Figure 1);

(b) unlike the west coast Fe skarns, the Cu-Au mineralization at the Heff skarn lacks enrichment in Co, Ni, and As (Table 2);

(c) the Heff mineralization contains more Ti, REE's, P, Sr and Ba than the west coast Fe skarns (Figs. 4A, B and C); the higher P content is probably related to the presence of apatite, although this mineral has not been identified on the Heff property;

(d) unlike the west coast Fe skarns, there are positive correlations between Ti and P, Ba and Sr, and La and Ce in the Heff mineralization (Figure 4); the latter has a higher average Cu content (Figure 4D) but contains less Ag (Figure 4E and F); and,

(e) there is a moderate to good positive correlation between Cu and Ag in the west coast Fe skarns (Ray and Webster, 1995); this correlation is less obvious at the Heff property (Figure 4E).

DISCUSSION

Previously, the Heff mineralization has been considered to be either a skarn or to have resulted from syngenetic submarine fumerolic activity (Casselman, 1980). We believe it is a skarn that formed by the infiltration of hydrothermal fluids from the Heffley Creek Pluton. The latter probably represents an Alaskan-type intrusion, similar to the Tulameen body and other late Triassic to Jurassic mafic-ultramafic complexes that intrude rocks of the Quesnel and Stikinia terranes elsewhere in British Columbia (Taylor, 1967; Nixon *et al.*, 1997).

The Heffley Creek Pluton is one of several major Fe-rich intrusive bodies in the district that include the alkalic and dioritic Iron Mask Batholith, located 33 km southwest of Heffley Lake. The batholith is related to the Ajax and Afton Cu-Au porphyry deposits (Ross *et al.*, 1995) and, like the Heffley Creek Pluton, it is controlled along a southeast trending structure (Carr and Reed, 1976). Parts of the batholith contain detectable amounts of Pd (Kwong, 1987) as well as some magnetite-apatite vein mineralization, as seen

TABLE 3
ASSAY RESULTS OF MINERALIZED INTRUSIVE ROCKS, HEFFLEY LAKE, B.C.

	Altered pyritic dikes & sills			Heffley Creek Pluton		
SAMPLE No.	GR99-23	GR99-24	IW99-9	GR99-28A	GR99-30A	GR99-53
Au	<5	145	5	<5	8	15
Sb	1.3	0.9	2.2	1.8	0.3	1.8
Ba	230	430	290	300	20	150
Be	0.5	0.7	1.2	0.75	0.1	0.8
Bi	0.2	0.06	0.12	0.28	<0.01	0.52
Cd	0.02	0.08	0.1	0.16	0.08	1.3
Ce	16.85	17.45	24	22.9	5.44	21.3
Cs	1.1	0.6	0.8	0.45	0.1	0.6
Cr	162	40	43	116	556	65
Co	21.8	21.4	30.6	26	46	83.8
Cu	116	85	141	144	<1	8230
Ga	12.5	14.7	20.6	13.4	7	12.6
Ge	1.3	1.2	1.5	1.5	1.5	0.8
La	7.5	8	10.5	9.5	1.5	10.5
Pb	3.5	5	7	8.5	2	9.5
Li	10.8	4.2	12.4	6.6	7.6	5.2
Mn	830	365	690	1525	875	300
Mo	1.4	0.6	2	20.2	<0.2	16.8
Ni	29.8	6.6	26	27.6	85.2	5.2
Nb	1.6	2.8	2.6	1	<0.2	3.8
P	1130	760	1460	1630	80	1170
Rb	34.2	37	64	25.6	1.2	100
Ag	0.95	0.65	0.5	0.45	0.2	14.4
Sr	811	591	789	834	58.8	331
Ta	0.05	0.2	0.05	0.05	<0.05	0.05
Te	0.2	0.15	0.2	0.05	<0.05	0.6
Tl	0.42	0.26	0.36	0.18	<0.02	0.54
Th	2	2.6	2.6	1.4	<0.2	2.6
W	0.7	1.1	1.6	0.9	0.1	22.5
U	1	1.2	1.6	0.8	<0.2	1.8
V	274	121	232	356	215	121
Y	12.3	11.9	16.3	17.8	7.7	11.4
Zn	30	16	22	64	30	122
As	1	1	6	20	1	20
F	930	270	550	480	50	310
Hg	<10	50	<10	<10	<10	250
Al	7.09	8.76	9.1	6.41	2.1	5.98
Ca	7.37	4.06	6.67	7.07	11.2	0.83
Fe	5.79	3.62	5.05	7.46	5.5	5.49
Mg	3.64	1.1	2.55	3.95	7.81	0.83
K	1.46	1.7	2.08	0.82	0.05	3.25
Na	1.53	3.27	2.06	1.47	0.2	1.43
Ti	0.49	0.32	0.42	0.47	0.33	0.2

Au and Hg in ppb
Al, Ca, Fe, Mg, K, Na, & Ti in wt %
Other elements in ppm
Analyses completed at Chemex Labs Ltd., 212 Brookbank Ave., North Vancouver, B.C.
Methods:
Au = Fire assay and AA finish; F = Specific Ion Electrode; As = AAS; other elements in ICP-MS

Sample Descriptions, Heff Skarn
GR99-23 2m wide pyrite-bearing dike, 7100N-6775E
GR99-24 5m wide pyritic and sicified dike adjacent to garnet-pyroxene skarn, 5700N-7600E
IW99-9 15 cm-wide hornblende-pyroxene-porphyry dike with pyrite-pyrrhotite veinlets.
GR99-28A Altered, silicified mafic diorite with 10% pyrite and quartz veins.
GR99-30A Dark, clinopyroxenite with 5% cumulate magnetite and trace pyrite.
GR99-53 Silicified, altered and malachite-stainedgabbro with pyrite & chalcopyrite. UTM 11 2 89 285E; 56 34 320N
GR99-51 Dark, pyroxene-hornblende ultramafic with 10% cumulate magnetite and trace pyrite. UTM 10 7 08 482; 56 33 287

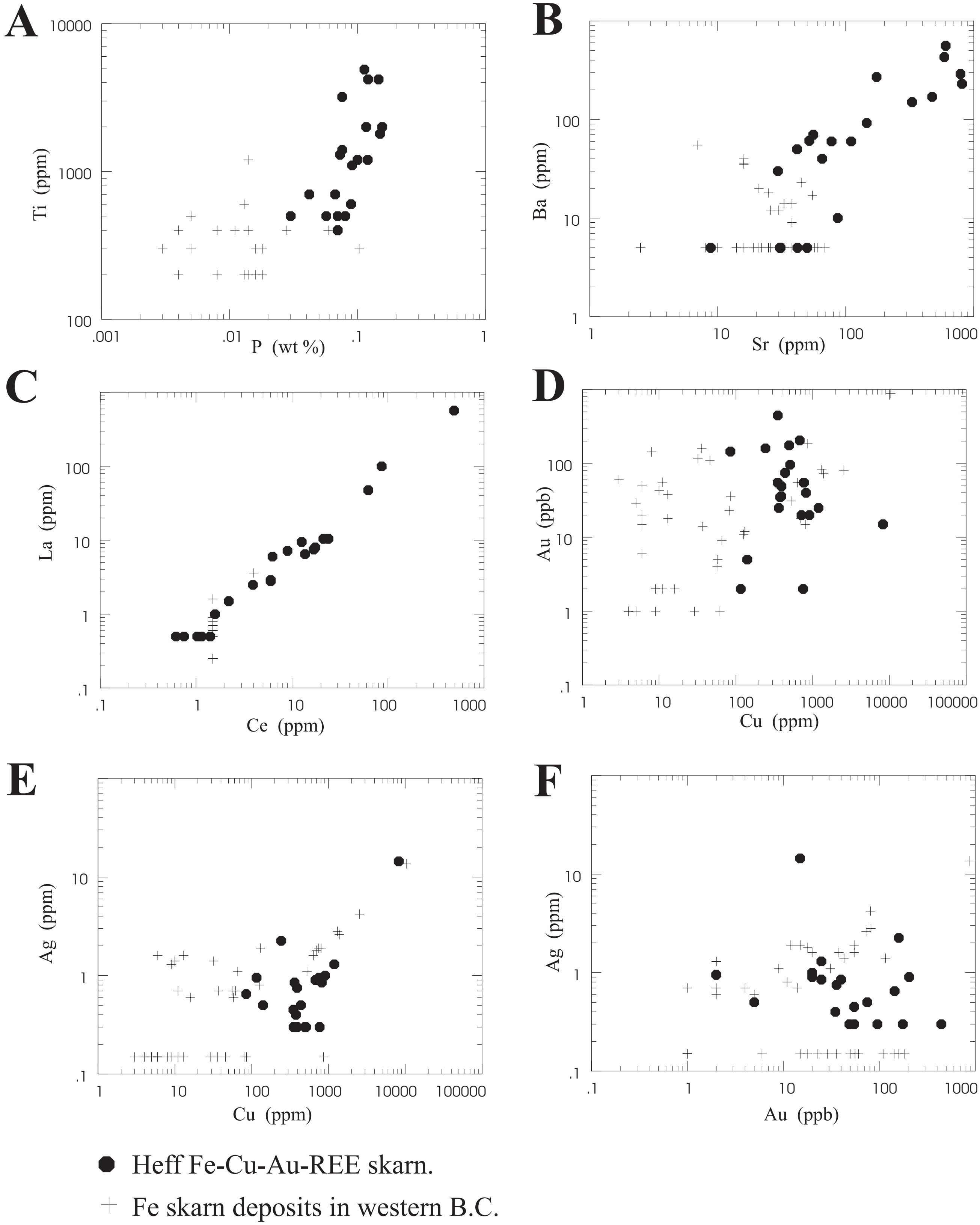

Figure 4. Plots comparing the chemistry of magnetite-rich mineralization at the Heff property with the Fe skarn deposits in western British Columbia. The plots include 21 samples from the Heff skarn and a total of 43 samples from the Merry Widow, Texada Island and Iron Crown deposits (*see* Figure 1).

at the Glen Iron mine and the Magnet occurrence (Figure 1; MINFILE Nos. 092INE 025 and 022 respectively; Hancock, 1988). The latter includes several south-east-trending veins of massive magnetite that reach up to 10 metres in thickness and 400 metres in strike length. The coarse crystalline magnetite is intergrown with coarse pale apatite crystals up to 3 centimetres long; some veins also include very coarse amphibole crystals over 5 centimetres in length. A magnetite-apatite-rich grab sample from the Magnet occurrence contained low quantities of Au, Cu and Ag, but the mineralization is anomalous in P (over 1 percent) and some REE's and trace elements, containing 172 ppm Ce, 20 ppm Ga, 76 ppm La, 57 ppm Y and 1775 ppm V.

A few REE ± U-rich skarns have been identified in the Yukon (e.g. Yukon MINFILE Nos. 116B 056 and 117A 020), but skarns containing both magnetite and anomalous quantities of REE's similar to the Heff property are extremely rare in the Canadian Cordillera. One exception is the Guano skarn (Yukon MINFILE 105F 081), a magnetite-U-REE-F-bearing occurrence. The Heff skarn may have resulted from an Fe-oxide-Cu-Au-REE-P-rich hydrothermal system similar to those responsible for deposits in the Ernest Henry (Australia)-Kiruna (Sweden)-Candelaria (Chile)-Wernecke Breccias (Canada) spectrum. These systems, which have been described by Laznicka and Gaboury (1988), Einaudi and Oreskes (1990), Hitzman *et al.* (1992), Oreskes and Hitzman (1990; 1993), Bookstrom (1977, 1995), Ryan *et al.* (1995), Jenkins *et al.* (1998), Williams (1998; 1999) and Ray and Lefebure (2000), have the following characteristics, some of which are seen at the Heff property:

(a) they are associated with large volumes of pervasive, massive hematite and/or magnetite; the latter mineral tends to have a lower Ti content than primary magmatic-related magnetite;

(b) they occur along major, long-lived brittle structures that were deep enough to tap mantle-derived intrusions;

(c) they occur in a variety of tectonic environments and rock types, ranging from rifts in intercratonic granitic basement (e.g. Olympic Dam) to mafic volcanic arcs (e.g. the Chilean Fe belt examples, including the Candelaria deposit);

(d) the orebody-morphology is highly variable; mineralization may occur as veins, breccia sheets, breccia pipes, tabular bodies or stockworks. Structure is the dominant regional and local control, but mineralization may also be strongly influenced by stratigraphy and host-rock lithology;

(e) they range in age from Proterozoic (e.g. Ernest Henry) to Cretaceous (e.g. Candelaria) (Marschik and Fontboté, 1996; Marschik *et al.*, 1996; Jenkins *et al.*, 1998; Williams, 1998; 1999);

(f) they may contain elevated values of U, REE's and trace elements (La, Ce, Nd, Pr, Sm, Y, Gd); the latter elements are commonly concentrated in mineral phases such as allanite, monazite or epidote;

(g) many represent low-sulphur Fe-oxide systems and are uneconomic for base metals. However, deposits such as Olympic Dam, Ernest Henry and Candelaria are more sulphide-rich and are an economic source of Cu and Au;

(h) the intrusions may be a critical source of the heat, fluids and metals in these systems (Oreskes and Hitzman, 1993), but in many deposits there is a poor spatial relationship between the deeper-level plutons and the mineralization, which tends to form at higher structural levels;

(I) where associated plutons are identified, they range in composition from syenite to granodiorite to mafic gabbro-diorite; and,

(J) many of these deposits world-wide lack skarn. However, where calcareous protoliths are present (e.g. Candelaria in Chile, Osborne and Mount Elliot in Australia), garnet-pyroxene-scapolite skarn assemblages may develop (Ryan *et al.*, 1995; Adshead *et al.*, 1998; Garrett, 1992; Williams, 1999).

CONCLUSIONS AND RECOMMENDATIONS

The Heffley Lake area contains two types of chalcopyrite-bearing mineralization, namely: (1) magnetite-rich garnet-pyroxene skarns on the Heff property, and (2) pyrite ± magnetite disseminations and veins south of Heffley Lake in the Heffley Creek Pluton.

The Heff skarn represents an unusual Cu ± Au ± REE ± P-bearing magnetite skarn whose location and distinctive chemistry (Figs. 1 and 4) suggests it differs from the typical Fe skarns occurring along the west coast of British Columbia. It possibly resulted from a Fe-oxide ± Cu ± Au ± REE ± P-bearing hydrothermal system similar to those responsible for deposits in the Ernest Henry-Candelaria-Wernecke Breccias spectrum. Structurally-controlled Fe oxide mineralization of this type is recorded at the Iron Range occurrences east of Creston, British Columbia (Figure 1; MINFILE Nos. 82FSE 014-028; Brown *et al.*, 1994; Stinson and Brown, 1995). However, the Heff skarn lacks the extensive brecciation and widespread Na ± K metasomatism that characterises many deposits of the Ernest Henry-Candelaria-Wernecke Breccias spectrum.

The Heff skarn is genetically related to the Heffley Creek Pluton, a pyroxene and magnetite-bearing mafic-ultramafic body that exceeds 10 km^2 in outcrop area. The pluton, which contains several Cu occurrences, is thought to represent an Alaskan-type body, similar to the Tulameen and other Triassic-Jurassic complexes in British Columbia.

A proposed model for the Heff skarn involves the emplacement of the elongate Heffley Creek pluton and the related skarns along a structure that may have marked the original Harper Ranch-Nicola unconformity. Subsequently, large-scale folding resulted in the north-easterly tilting of the skarn, the pluton, and its hostrocks. No skarns or minor intrusions are seen along the southern border of the pluton, perhaps because this was the basal margin of the body. Instead, late, Fe-rich hydrothermal fluids from the pluton were channelled upwards along a swarm of minor intrusions into overlying Nicola Group limestones. Thus, the skarns and the dike-sill swarm seen north and northeast of Heffley Lake are believed to have formed along, and close to, the upper margin of the pluton. The dominance of pyrite over pyrrhotite and the abundance of magnetite suggests the presence of an oxidised, low sulphur hydrothermal system.

Recommendations for further work in the area include:

(a) map the remainder of the Heffley Creek Pluton to accurately determine its distribution and margins;

(b) prospect the interior of the Heffley Creek Pluton for Cu, Au, Cr and PGE mineralization, and explore its margins for Cu-Au-REE skarns similar to the Heff property;

(c) future exploration for blind skarn orebodies on the Heff property should include a geophysical survey along the presumed margin of the Heffley Creek Pluton, in the poorly exposed area immediately north of, and under Heffley Lake. The southerly change in mineral alteration recognised in this survey, supported by the very high Au and Cu soil anomalies previously outlined, suggests that an economic skarn orebody could underlie Heffley Lake and its alluvium-covered northern shore;

(d) the Heff skarns and their host rocks are strongly folded; thus, future exploration for orebodies on the property should commence with an attempt to determine the structural controls; and finally,

(e) the recognition of a large Alaskan-type pluton in this highly accessible part of southern British Columbia indicates that the entire district needs to be re-mapped and evaluated for its skarn, porphyry and PGE-potential.

ACKNOWLEDGMENTS

The ideas and scientific opinions of the following persons were helpful to this program: D. A. Brown, M.S. Cathro, D.V. Lefebure, R.H. McMillan, G.T. Nixon, and V.A.G. Preto.

REFERENCES

Adshead, N.D., Voulgaris, P., and Muscio, V.N. (1998): Osborne copper-gold deposit, NW Queensland; *Australasian Institute of Mining and Metallurgy,* Monograph 22, p. 793-798.

Arseneau, G.J. (1997): Geological, geochemical and geophysical report on the 1997 field work, Mesabi property; Unpublished report for Echo Bay Mines, October 1997, *B.C. Ministry of Energy, Mines and Petroleum Resources*, Assessment Report 25203, 79 pages.

Bookstrom, A.A., (1977): The magnetite deposits of El Romeral, Chile, *Economic Geology*, Volume 72, pages 1101-1130.

Bookstrom, A.A. (1995): Magmatic features of iron ores of the Kiruna type in Chile and Sweden; ore textures and magnetite geochemistry; discussion. *Economic Geology*. 90; 2, Pages 469-473.

Brown, D.A., Bradford, J.A., Melville, D.M., Legun, A.S., and Anderson, D. (1994): Geology and mineral deposits of the Purcell Supergroup in the Yahk map area, south-eastern British Columbia (82F/1); *B.C. Ministry of Energy, Mines and Petroleum Resources*, Geological Fieldwork 1993, Paper 1994-1, pages 129-151.

Carr, J.M., and Reed, A.J. (1976): Afton; *In* Porphyry deposits of the Canadian Cordillera. (A. Sutherland Brown, ed.). *Canadian Institute of Mining and Metallurgy;* Special Volume 15, pages 376-387.

Casselman, M.J.(1980): Assessment report of line-cutting and geological, soil geochemical and magnetometer surveys on the Heff Lake Property; *Cominco Limited*.

Cockfield, W.E. (1944): Nicola map area, British Columbia, Paper 44-20. Map with descriptive notes, *Geological Survey of Canada*, Ottawa, 1944.

Cockfield, W.E. (1947): Nicola, Kamloops and Yale districts, British Columbia, *Geological Survey of Canada*, Map 886A, scale 1:253 440.

Debon, F., and Le Fort, P., 1983, A chemical-mineralogical classification of common plutonic rocks and associations: *Royal Society of Edinburgh*, Transactions, Earth Sciences 73 (for 1982), p. 135-149.

Einaudi, M.T., and Oreskes, N. (1990): Progress towards an occurrence model for Proterozoic iron oxide deposits - a comparison between the ore provinces of South Australia and southeast Missouri. *In* The Mid-continent of the United States - Permissive Terranes for an Olympic Dam Deposit?, *U.S. Geological Survey,* Bulletin 1392.

Garrett, S.J.M. (1992): The geology and geochemistry of the Mt. Elliott Cu-Au deposit, northwest Queensland; Unpublished MSc thesis, Hobart, *University of Tasmania*.

Hancock, K.D. (1988): Magnetite occurrences in British Columbia; *B.C. Ministry of Energy, Mines and Petroleum Resources*, Open File 1988-28, 153 pages.

Hitzman, M.W., Oreskes, N., and Einaudi, M.T. (1992): Geological characteristics and tectonic setting of Proterozoic iron oxide (Cu-U-Au-REE) deposits; *Precambrian Research*, Volume 58, pages 241-287.

Irvine, T.N., and Baragar, W.R.A. (1971): A guide to the chemical classification of the common volcanic rocks; *Canadian Journal of Earth Sciences*, Volume 8, pages 523-547.

Jenkins, R.A., Leveille, R.A., and Marin, W. (1998): Discovery and geology of the Candelaria deposit, Chile. Pathways '98, extended abstract volume*, B.C. & Yukon Chamber of Mines and Society of Economic Geologists*. Pages 78-79.

Kwong, Y.T.J. (1987): Evolution of the Iron Mask Batholith and its associated copper mineralization; *B.C. Ministry of Energy, Mines and Petroleum Resources*, Bulletin 77, 55 pages.

Laznicka, P., and Gaboury, D. (1988): Wernecke Breccias and Fe, Cu, U mineralization: Quartet Mountain-Igor area (NTS 106E); *in* Yukon Exploration and Geology, *Exploration and Geological Services Division, Yukon, Indian and Northern Affairs Canada*, pages 42-50.

Le Maitre, R.W., Bateman, P., Dudek, A., Keller, J., Lameyre, J., Lebas, M.J., Sabine, P.A., Schmid, R., Sorensen, H., Streckeisen, A., Woolley, A.R., and Zanettin, B., Eds., (1989): A classification of igneous rocks and glossary of terms: recommendations of the International Union of Geological Sciences Subcommission on the systematics of igneous rocks, *Oxford Blackwell Scientific Publications*, 193 pages.

Marschik, R., and L. Fontboté (1996): Copper (-iron) mineralization and superposition of alteration events in the Punta Del Cobre Belt, northern Chile; *In* Andean copper deposits: new discoveries, mineralization, style and metallogeny, *Society of Economic Geologists Special Publication No. 5*, Camus, F., Sillitoe, R.H., and Peterson, R., eds. 1996, pages 171-190.

Marschik, R., Singer, R., Munizaga, F., Tassarini, C., and Fontbote, L. (1996): Age of the Cu(-Fe) mineralization and Cretaceous to Paleocene thermal evolution of the Punta del Cobre district, northern Chile. *In* Proceedings of the XXXIX Brazilian Geological Congress, Bahia. Anais 7, pages 306-309.

Meinert, L.D., 1984, Mineralogy and petrology of iron skarns in western British Columbia, Canada: *Economic Geology*, v. 79, p. 869-882.

MMAR (1916): Hefferly Lake, Minister of Mines, *Province of British Columbia*, Annual Report for the Year Ended 31st December 1915, page K222.

Monger, J.W.H. and McMillan, W.J. (1989): Geology, Ashcroft, British Columbia*; Geological Survey of Canada,* Map 42-1989, sheet 1, scale 1:250 000.

Nixon, G.T., Hammack, J.L., Ash, C.H., Cabri, L.J., Case, G., Connelly, J.N., Heaman, L.M., Laflamme, J.H.G., Nuttall, C., Paterson, W.P.E., and Wong, R.H. (1997): Geology and platinum-group element mineralization of Alaskan-type ultramafic-mafic complexes in British Columbia; *B.C. Ministry of Energy, Mines and Petroleum Resources*, Bulletin 93, 142 pages.

Oreskes, N. and Einaudi, M.T. (1990): Origin of rare earth-enriched hematite breccias at the Olympic Dam deposit, Roxby Downs, South Australia; *Economic Geology*, Volume 85, Number 1, pages 1-28.

Oreskes, N., and Hitzman, M.W., (1993): A model for the origin of Olympic Dam-type deposits. *In*, Mineral deposit modeling: *Geological Association of Canada*, Special Paper No. 40, pages 615-633.

Ray, G.E. (1995): Fe skarns; *In* Selected British Columbia Mineral Deposit Profiles, Volume I - Metallics and Coal, editors D.V. Lefebure and G.E. Ray. *B.C. Ministry of Energy, Mines and Petroleum Resources*, Open File 1995-20, pages 63-65.

Ray, G.E. and Webster, I.C.L. (1995): The geochemistry of mineralized skarns in British Columbia; Geological Fieldwork 1994, *B.C. Ministry of Energy, Mines and Petroleum Resources*, Paper 1995-1, pages 371-383.

Ray, G.E. and Webster, I.C.L. (1997): Skarns in British Columbia, *B.C. Ministry of Employment and Investment, Geological Survey Branch,* Bulletin 101, 260 pages.

Ray, G.E. and Lefebure, D.V. (2000): A synopsis of iron oxide-Cu-Au-U-P-(REE) deposits of the Candelaria-Kiruna-Olympic Dam Family; *B.C. Ministry of Energy and Mines*, Paper 2000-1 (this volume).

Ray, G.E. and Webster, I.C.L. (2000): Geology and mineral occurrences in the Heffley Lake Area, south-central B.C.; *B.C. Ministry of Energy and Mines,* Open File Map.

Roed, M.A. (1988): Geological exploration of the Hawk 1 to 4 mineral claims, 1987, Heffley Lake, B.C.; Unpublished report for Redbird Gold Corp., *B.C. Ministry of Energy, Mines and Petroleum,* Assessment report 17147, 40 pages.

Ross, K.V., Godwin, C.I., Bond, L., and Dawson, K.M. (1995): Geology, alteration and mineralization of the Ajax East and Ajax West copper-gold alkalic porphyry deposits, southern Iron Mask batholith, Kamloops, British Columbia; *In* Porphyry Deposits of the Northwest Cordillera of North America. (T.G. Schroeter, ed.). *Canadian. Institute of Mining, Metallurgy and Petroleum.* Special volume 46, pages 565-608.

Ryan, P.J., Lawrence, A.L., Jenkins, R.A., Matthews, J.P., Zamora, J.C., Marino, E.W. & Diaz, I.U. (1995): The Candelaria copper-gold deposit, Chile; *In* Porphyry Copper Deposits of the American Cordillera, editors Pierce, F.W. and Bolm, J.G, *Arizona Geological Society Digest*, 20, 625-645.

Sangster, D.F. (1969): The Contact metasomatic magnetite deposits of British Columbia; *Geological Survey of Canada*, Bulletin 172, 85 pages.

Stinson, P, and Brown, D.A., (1995): Iron Range Deposits, southern British Columbia (82F/1); *B.C. Ministry of Energy, Mines and Petroleum,* Paper 1995-1, pages 127-134.

Taylor, H.P., Jr. (1967): The zoned ultramafic complexes of southeastern Alaska; *In* Ultramafic and related rocks, editor Wyllie, P.J., *John Wiley and Sons Inc*., New York, pages 97-121.

Wheeler, J.O., Brookfield, A.J., Gabrielse, H., Monger, J.W.H., Tipper, H.W. and Woodsworth, G.J. (1991): Terrane map of the Canadian Cordillera; *Geological Survey of Canada,* Map 1713a, Scale 1:2 000 000.

Williams, P.J. (1998): Metalliferous economic geology of the Mount Isa Eastern Succession, northwest Queensland. *Australian Journal of Earth Sciences*, Volume 45, pages 329-341.

Williams, P.J. (1999): Fe oxide-copper-gold deposits. Shortcourse notes, *James Cook University Economic Geology Research Unit and Mineral Deposits research Unit*, University of B.C., Vancouver, 11 th March 1999.

Winchester, J.A., and Floyd, P.A. (1977): Geological discrimination of different magma series and their differention products using immobile elements. *Chemical Geology*, Volume 20, pages 325-343.

Geologic Setting of the Devonian-Mississippian, Rea and Samatosum VMS Deposits of the Eagle Bay Assemblage, Adams Lake Area, South Central British Columbia

Sean L. Bailey[2], Suzanne Paradis[3], Stephen T. Johnston[2], and Trygve Höy[4]

ABSTRACT

Highly deformed, low-grade metasedimentary and metavolcanic rocks of the Eagle Bay Assemblage host the volcanogenic (?) massive sulphide Twin Mountain and Rea deposits, and the Samatosum vein deposit. The Twin Mountain deposit consists of sulphide-bearing quartz-carbonate-barite lenses hosted by sericitized and silicified schists of volcanic origin. The Rea deposit consists of at least two massive sulphide lenses. The Samatosum deposit is a stratabound sulphide-rich quartz vein system that could be interpreted as a stockwork zone. The Rea and Samatosum deposits occur within an overturned metasedimentary sequence of sericitized and silicified argillites structurally overlain by mafic volcaniclastic rocks and flows. The stratigraphic sequences at Rea and Samatosum are very similar and we suggest that structural repetition by faulting occurred, and that the sedimentary and volcanic succession is of Devonian-Mississippian age.

INTRODUCTION

Highly deformed Cambrian to Mississippian metasedimentary and metavolcanic rocks of the Eagle Bay Assemblage in the Adams Lake area host numerous polymetallic sulphide deposits. The region has long been recognized as favorable for various types of sulphide deposits, and is still today a prospective "ground" for mineral exploration. The Homestake barite-sulphide deposit was discovered in 1893. Since then numerous sulphide occurrences have been found in the district. Some of these, including Samatosum, Rea and Homestake, have had limited production, and others, such as Twin Mountain, have had extensive exploration work over the years.

This paper briefly describes the Samatosum, Rea, and Twin Mountain sulphide deposits located in the Adams Lake area of south central British Columbia, approximately 80 kilometers northeast of Kamloops (Figure 1). It defines their geological settings, and addresses some fundamental structural and stratigraphic problems in the region. This study was initiated during the summer of 1999 as the M.Sc. project of the first author (Sean L. Bailey) and included 1: 5000 scale regional mapping of an approximately 30 km^2 area conducted over a 7 week period. It is part of the Ancient Pacific Margin NATMAP metallogenic study of syngenetic sulphide deposits of the Kootenay Terrane and the correlative Yukon-Tanana Terrane in northern British Columbia and Yukon.

The area is dominated by dense vegetation, thick till coverage, and steep mountainous terrane. A series of logging and drill roads allow good access to the plateau of Samatosum mountain, with the best exposures found along roadcuts, clearcuts, trenches remaining from past exploration, and creeks.

EXPLORATION HISTORY

The first documented discovery of sulphide occurrence in the Adams Lake area dates back to 1893 with the discovery of the Homestake barite-sulphide deposit. The Homestake mine was worked intermittently between 1893 and 1984. In the 1920s, numerous sulphide occurrences were found in the Birk Creek and Harper Creek areas. In 1978, the Chu Chua massive cupriferous pyrite deposit was discovered in basalts of the Fennell Formation. However, none of these discoveries resulted in significant production.

In 1983, A. Hilton and R. Nicholls discovered the Rea massive sulphide deposit. They optioned it to Rea Gold Corporation who in turn optioned it to Corporation Falconbridge Copper (presently Inmet Mining Corporation). Drilling carried out by Corporation Falconbridge Copper in the 1980s outlined two small but fairly high-grade massive sulphide lenses (known as the "Discovery zone" or the "Rea horizon"). The most recent published estimate of the mineralization was 376,000 tonnes grading 0.33 percent copper, 2.2 percent lead, 2.3 percent zinc, 6.1 grams per tonne gold, and 69.4 grams per tonne silver (Northern Miner – November 30, 1987).

[1]*Contribution to the Ancient Pacific Margin NATMAP Project*

[2]*School of Earth and Ocean Sciences, University of Victoria, P.O. Box 3055, STN CSC Victoria, British Columbia V8W 3P6*

[3]*Geological Survey of Canada, Mineral Resources Division, P.O. Box 6000, Sidney, British Columbia V8L 4B2*

[4]*B.C.Geological Survey Branch, Ministry of Energy and Mines, Victoria*

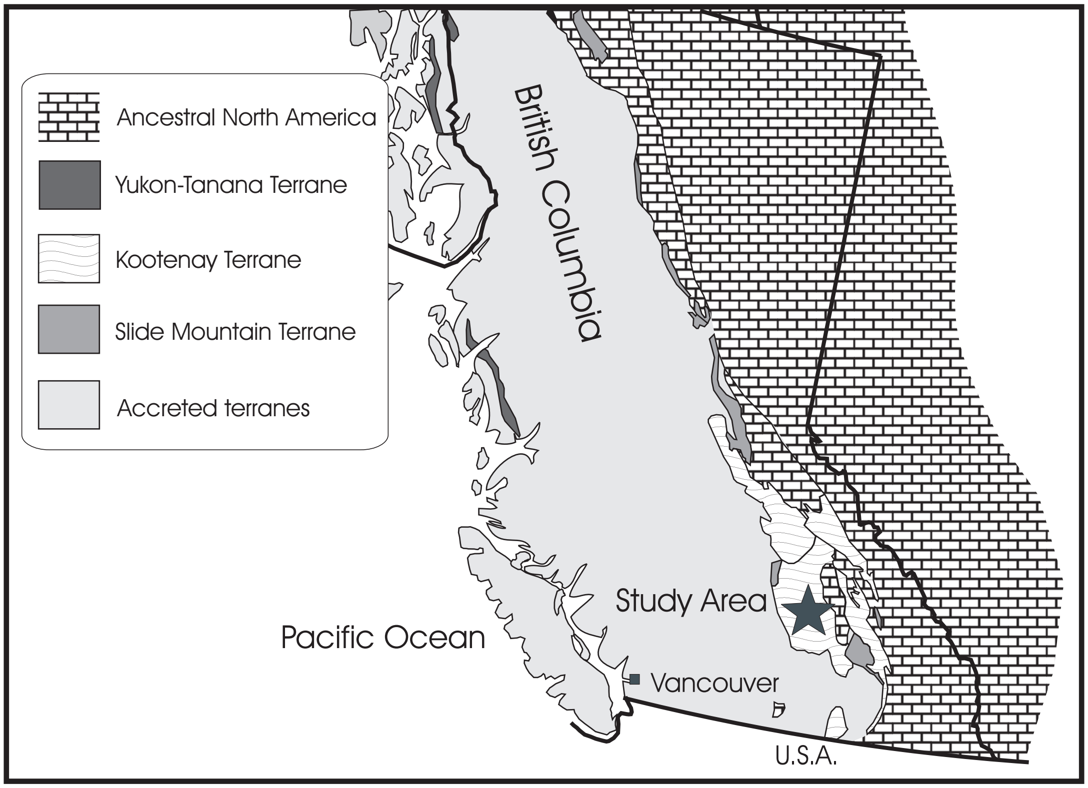

Figure 1. Location of the study area, within the Kootenay Terrane of central British Columbia (modified after Wheeler and Mcfeely, 1991).

Mapping in 1984 and 1985 by Corporation Falconbridge Copper produced a general understanding of the stratigraphy and structure in the area. In addition, horizontal-loop electromagnetic (HEM) surveys defined several long stratiform conductors. By early 1986, a new mineralized horizon (the "Silver zone") was found, and this was immediately followed by the discovery of the Samatosum deposit.

Regional Geology

Metavolcanic and metasedimentary rocks of the Eagle Bay Assemblage of the Kootenay Terrane host the Rea and Twin Mountain sulphide deposits and the Samatosum vein deposit. The Kootenay Terrane and correlative rocks of the Yukon-Tanana Terrane farther north comprise dominantly Paleozoic sedimentary and volcanic rocks that are inferred to have been deposited on the distal western edge of ancestral North America. The successions of the Kootenay Terrane include the Lardeau Group, the Eagle Bay Assemblage, eastern assemblages of the Late Paleozoic Milford Group, and equivalent rocks within the Shuswap metamorphic complex (Höy, 1999).

The Eagle Bay Assemblage, described by Schiarizza and Preto (1987), comprises Lower Cambrian to Mississippian rocks that are intruded by Late Devonian orthogneiss and Jurassic-Cretaceous granodiorite and quartz monzonite of the Raft and Baldy batholiths. Within the study area, the Eagle Bay Assemblage is contained within four west-directed thrust slices. The assemblage consists of clastic metasedimentary rocks (units EBH and EBQ Schiarizza and Preto 1987), mafic metavolcanic rocks and limestone (unit EBG), and structurally overlying clastic metasedimentary rocks, with minor carbonate and volcanic rocks (unit EBS), all of which are interpreted as Cambrian in age. These are in turn overlain by Devonian-Mississippian mafic to intermediate metavolcanic and metasedimentary rocks (units EBA and EBF, respectively), which are overlain by metaclastic rocks (unit EBP).

Numerous volcanogenic sulphide occurrences of the Eagle Bay Assemblage, including Rea, Homestake, Samatosum and Twin Mountain are within mafic to intermediate metavolcanic and metasedimentary rocks of units EBA, EBF, and EBG (Figure 2). Regional mapping by Schiarizzia and Preto (1987) and this study indicate that units EBA, EBF, and EBP between the Samatosum and Homestake deposits are apparently right-way-up regionally but locally overturned (Figure 2). These are structurally overlain by mafic metavolcanic rocks of EBG and the Tshinakin Limestone Member which is assigned a Lower Cambrian age (Schiarizza and Preto, 1987). These stratigraphic and structural relationships led to the inference by Schiarizza and Preto (1987) of the Haggard Creek Thrust Fault, which places Cambrian rocks on Devonian–Mississippian rocks. The Samatosum and Rea deposits are located near the inferred trace of this fault, and controversy exists over which package(s) of rocks hosts

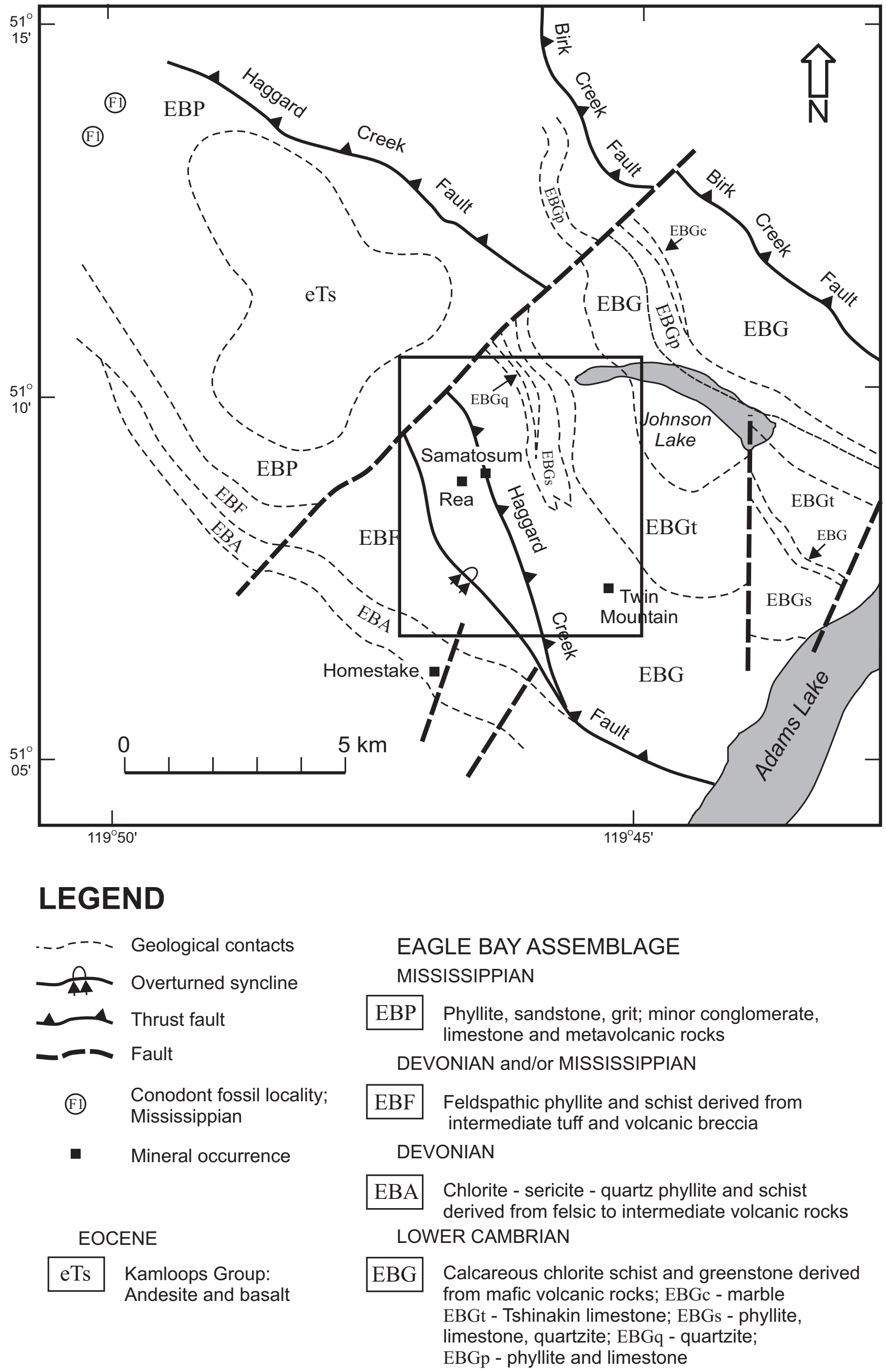

Figure 2. Geological map of the Johnson Lake area, modified after Schiarizza and Preto (1987)

the deposits and whether or not a major thrust fault exists. This study will attempt to resolve these matters.

Local Stratigraphy

The main stratigraphic units encountered in the area of the deposits are described below and their distribution illustrated in Figure 3. An interpreted SW-NE cross-section through the Rea and Samatosum zones is shown in Figure 4. Lack of age control makes our interpretation somewhat preliminary and hence other scenarios are possible.

Fossil archaeocyathids were found within limestone at a single locality 50 kilometers north of the study area in a different fault panel. Correlation of this limestone with the Tshinakin limestone member at Johnson Lake sug-

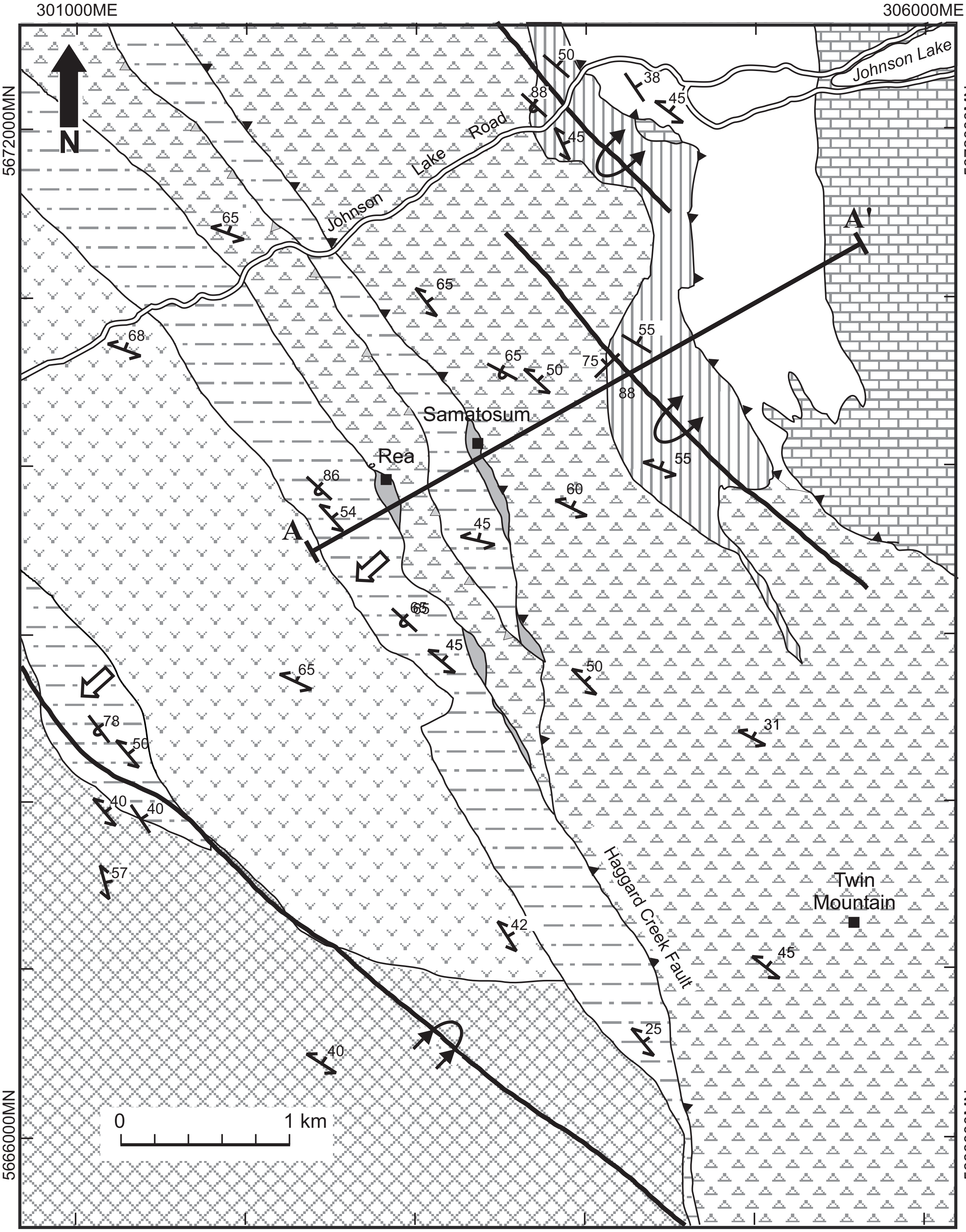

Figure 3. Preliminary geological map of the Johnson Lake area.

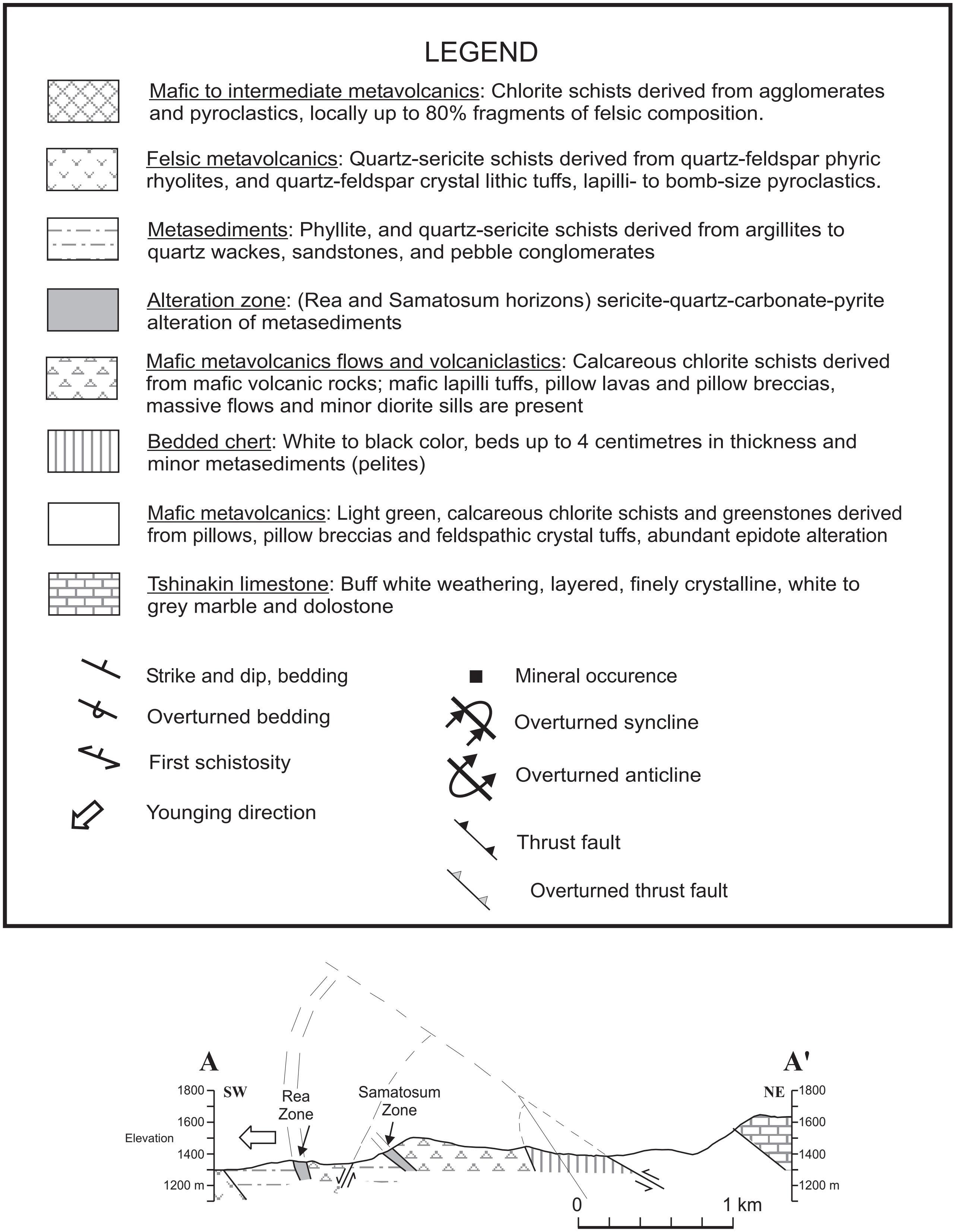

Figure 4. SW-NE cross section through the Rea and Samatosum zones, no vertical exaggeration.

gests an Early Cambrian age for this unit (Schiarizza and Preto, 1987). Mafic volcanic rocks are locally interbedded with the limestone and consequently are interpreted to be Early Cambrian (Schiarizza and Preto, 1987). U-Pb zircon age dates of 387 Ma (*i.e.*, Middle Devonian) have been obtained from felsic metavolcanics of unit EBA on the east shore of Adams Lake (Preto, 1981; Preto and Schiarizza, 1985). Felsic to intermediate rocks of unit EBF are interpreted to be younger (*i.e.*, Devonian and/or Mississippian), as they are stratigraphically above rocks of unit EBA and below rocks of unit EBP, which contains Mississippian conodonts (Schiarizza and Preto, 1987).

The deposit area is underlain by northeast-dipping metasedimentary and metavolcanic rocks that, based on well developed graded beds (Höy and Goutier, 1986; and this study), display an overall younging direction structurally down-section and toward the west (Figure 4). Hence, much of the stratigraphy within this region is overturned. From oldest to youngest, the stratigraphy includes the Tshinakin limestone, mafic metavolcanic rocks, bedded cherts, mafic metavolcanic flows and volcaniclastic rocks, metasediments, and mafic to intermediate metavolcanic rocks.

Tshinakin Limestone

The Tshinakin limestone outcrops in the eastern portion of the map area (Figure 3) and is best exposed in the cliffs above Johnson Lake. It consists dominantly of finely crystalline white to grey marble with minor dolostone, which display a buff white to grey weathered surface. It is usually massive; however, laminations defined by light and dark bands are locally observed (Figure 5A). It is interbedded with calcareous chlorite schist at other locations, such as nearby Adams Lake (Schiarizza and Preto, 1987).

Mafic Metavolcanics

This unit is composed of greenstones and chlorite schists derived from pillows, pillow breccias and feldspathic crystal tuffs. Pillows locally exceed one meter or more in length. The metavolcanics have a light green color due to abundant epidote, and commonly have a white or grey weathered surface. Tuffs contain crystals of feldspar less than 1 mm in diameter.

Bedded Chert

A bedded chert unit occurs between two distinct mafic volcanic packages (Figure 3). The chert is light grey-white to black in color, locally graphitic, and has well defined bedding (Figure 5B). Minor amounts of pelites occur, which locally contain particles up to sand size and display a c-s fabric along the contact with the structurally overlying pillow breccias.

Mafic Metavolcanic Flows and Volcaniclastics

The mafic metavolcanic rocks in the central portion of the map area are dominated by calcareous chlorite-sericite-quartz schists and chlorite schists derived from mafic volcanic rocks. Abundant volcaniclastic rocks and rare mafic massive flows and pillow basalts and breccias are also present. The most common rock type is a lapilli-tuff with average fragment size of approximately 4-5 centimeters. The lapilli are commonly bleached and are thought to be of similar composition to the matrix. Locally, the fragments are up to bomb size (Figure 5C) as exposed at the Samatosum mine site. Fine-grained chlorite schists are abundant throughout the unit. The massive flows contain calcite and quartz amygdules. Pillows are approximately 1 meter in size, are amygdaloidal, and have been flattened in the penetrative foliation plane. These display an outer non-vesicular 2 to 3 centimeters rim. The entire unit is calcareous, and locally contains disseminated pyrite.

Major and trace element analysis of these mafic units, indicate that they are dominantly alkali, within-plate basalts (Höy, 1987). As most of the Devonian-Mississippian volcanic rocks of the Eagle Bay Assemblage are calc-alkaline it was suggested that the Rea and Samatosum stratigraphy represented deposition in a rifted volcanic arc (Höy 1987).

Diorite sills or dikes were observed within this unit and may have played a role in sulphide mineralization. The Twin Mountain sulphide deposit occurs within pyritic, calcareous chlorite-sericite-quartz schists and chlorite schists derived from mafic volcanic rocks.

Metasediments

The metasediments are phyllites and quartz-sericite schists thought to have originally been fine-grained argillites and quartz wackes. A quartz-lithic pebble conglomerate at the stratigraphic top of this sequence is composed of clasts (commonly 2-3 centimeters in diameter) of chert, chlorite schist, and vein quartz. This conglomerate has been traced to the northwest, extending beyond the map area where it appears to thicken.

Near the Samatosum and Rea deposits, the metasediments are part of a structurally complex sequence called the “Mine Series”. The Samatosum and Rea deposits are located within the metasediments near the contact with the structurally overlying mafic volcanic rocks. Here, the metasediments are highly strained and altered (*i.e.*, sericitized ± clay, silicified, and carbonatized). They consist of carbonaceous black argillites, sericitized yellowish argillites containing chert lenses, and pyrite-rich silicified greyish argillites. Some of the beds show graded bedding and rip-up clasts. Locally distributed massive to brecciated chert within the metasediments appears to be spatially associated with base-metal sulphides.

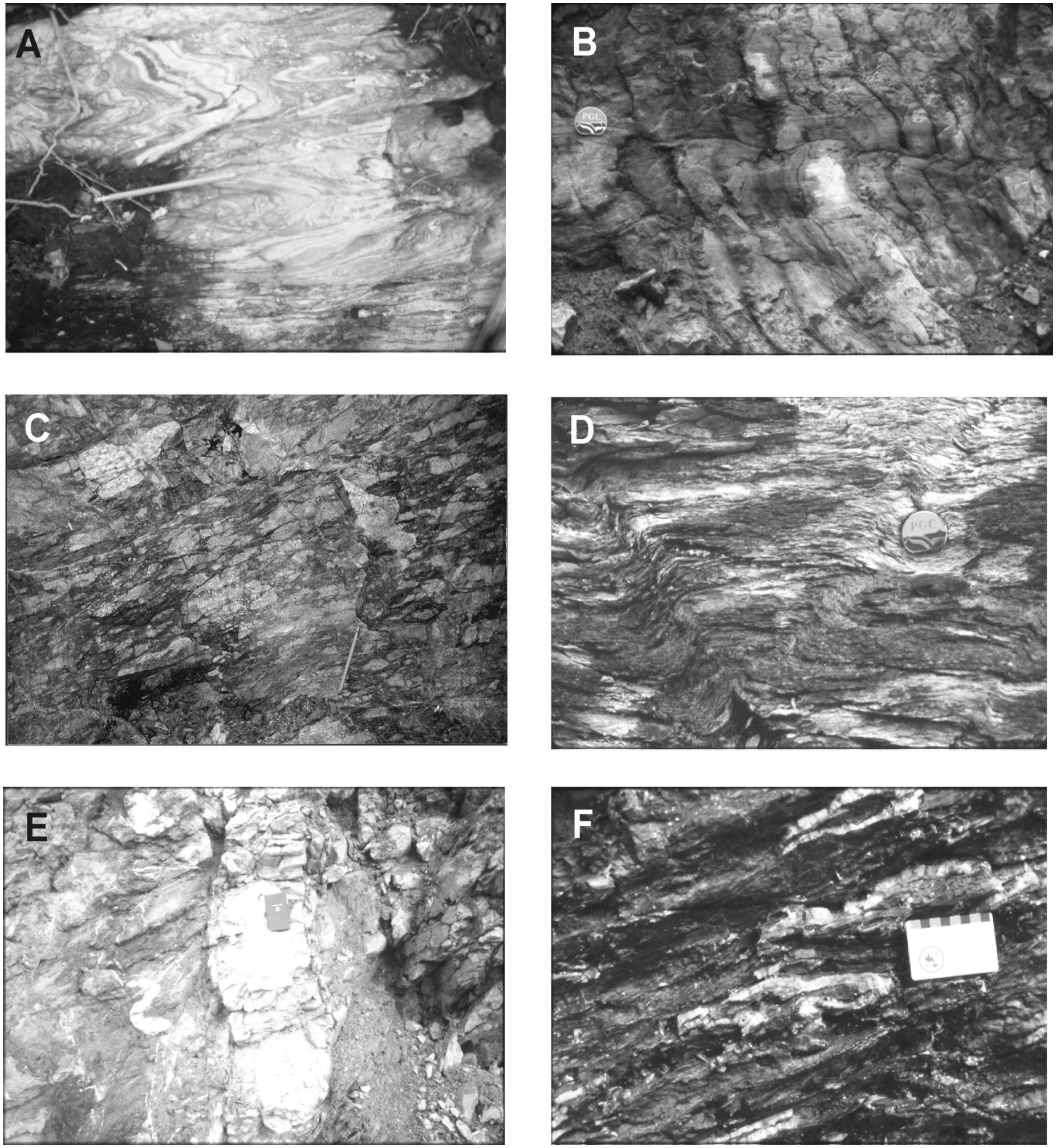

Figure 5. A.) Parasitic folding of layers in Tschinikan Limestone. B.) Bedded chert, (Pin for scale is 3 centimeters in diameter). C.)Mafic flow breccia, fragments are bleached, and range from bomb to lapilli size. D.) Kink bands and reverse kink bands in mafic tuff. E.) Mineralized quartz veins at the Samatosum deposit. F.) Quartz veins,(2 centimeters thickness) which have been folded by, and transposed into the penetrative foliation, hosted within sericitized-silicified sediments, Samatosum deposit.

Felsic Metavolcanics

The felsic metavolcanic unit is composed of white weathering, beige quartz-sericite schists derived from quartz-feldspar porphyritic rhyolite, quartz-feldpar-crystal-lithic tuffs and pyroclastics. The feldspar component of this unit is mainly albite. The volcanics are bounded to the east by quartz-lithic pebble conglomerate and appear to be interlayered with phyllite and quartz wackes, which commonly contain several percent euhedral pyrite.

Mafic to Intermediate Metavolcanics

Chlorite schists derived from mafic volcaniclastic rocks are located in the western part of the map area. The most common rock type is mafic volcanic breccia containing 30-centimetre fragments. However, in the eastern most section of this unit, the metavolcanics include fragments of felsic volcanic rocks that locally account for 65 to 80 percent of the rock.

STRUCTURE AND METAMORPHISM

The structure of the area is dominated by a series of northwest trending, shallow dipping, tight overturned folds, with penetrative axial planar cleavage defined by lower to middle greenschist metamorphic minerals. These folds are west-verging, have parallel axial traces to, and are likely related to a series of southwest-directed thrust faults (Schiarizza and Preto, 1987). Bedding-cleavage relationships and stratigraphic top determinations indicate that the western limbs of these folds are overturned. Parasitic folds plunge at shallow to moderate angles to the northwest.

The penetrative cleavage is crenulated by a second cleavage. The crenulation lineation trends northeast, and appears to have formed in conjunction with northeastward trending low amplitude folds (Schiarizza and Preto, 1987).

Graded beds are the most commonly observed indicators of stratigraphic tops. They are a series of fine sandy layers, which abruptly overlie muddy layers, and grade up into mud. In the coarser units, this gradation proceeds from pebble conglomerate to coarse sand. Rare sedimentary features such as rip up clasts, and scour-and-fill structures were also observed. Höy (1987) interpreted this as a turbidite sequence developed on the distal continental margin in deep marine conditions during rifting.

MINERALIZATION

Prospectors and geologists have long recognized the Johnson-Adams Lake area as a favourable region for base-metal sulphide deposits. Several significant mineral occurrences including Samatosum, Rea, and Twin Mountain are located within the map area (Figure 3). These deposits have been suggested to be volcanogenic sulphide deposits (Höy and Goutier, 1986). The Twin Mountain deposit consists of sulphide-bearing quartz-carbonate-barite lenses hosted by sericitized and silicified schists derived from mafic volcanic rocks (unit EBG of Schiarizza and Preto, 1987). The Rea deposit consists of volcanogenic massive to semi-massive sulphide lenses, whereas the Samatosum deposit may be a stockwork system related to stratabound volcanogenic sulphide lenses.

The Samatosum and Rea deposits are within a similar overturned sequence of greenschist metamorphic grade sericitized, silicified and carbonaceous argillites that are structurally overlain by mafic volcaniclastics and flows. We suggest that the sulphide mineralization at Samatosum and Rea occur within a fault repetition of the same stratigraphic sequence. Alternatively, two distinct but similar stratigraphic sequences may host the deposits. Lead isotopes from the Rea deposit suggest a Late Devonian age (Goutier, 1986), supporting the speculation that rocks hosting the Rea and Samatosum deposits belong to the Devonian-Mississippian succession of the Eagle Bay Assemblage.

Rea

The Rea deposit was discovered in 1984 by local prospectors, Alex Hilton and R. Nicholl, who optioned it to Corporation Falconbridge Copper. Subsequent exploration revealed two massive sulphide lenses, named RG8 lens and L100 lens. The RG8 lens is the southernmost and has a surface strike of 75 metres with a downdip extension of 80 metres. The northern lens (L100) or discovery zone has a surface strike of 50 meters and a down dip extension of at least 120 meters.

Combined reserves for the two massive sulphide lenses totaled 376,000 tonnes grading 0.33 percent copper, 2.2 percent lead, 2.3 percent zinc, 6.1 grams per tonne gold, and 69.4 grams per tonne silver (Northern Miner – November 30, 1987). Sulphides are pyrite, sphalerite, galena, arsenopyrite, chalcopyrite, and tetrahedrite. These are fine to medium grained with banded to breccia texture in the massive sulphide lenses. Gold and silver are associated with massive sulphide and barite.

Rea has been examined in considerable detail by Höy and Goutier (1986) and Höy (1987; 1991. The deposit occurs on the overturned eastern limb of a northwest-trending syncline. The stratigraphic footwall of the deposit consists of metamorphosed mafic tuffs and chert, which show sericite-quartz-carbonate alteration, likely representing footwall alteration of a mafic volcanic precursor. The two massive sulphide lenses, one of which contains a barite cap (RG8), are stratigraphically above this horizon and overlain by a thin mafic tuff. These are then stratigraphically overlain by a several hundred meter-thick sequence of argillites and minor tuffs, which grades into a quartz pebble conglomerate at the top.

Subsequent exploration of the Rea zone has shown that it can be traced along strike for seven kilometers and hosts at least five volcanogenic massive sulphide lenses (Carmichael, 1991).

Samatosum

The Samatosum Ag-Pb-Zn-Cu deposit originally contained 634,984 tonnes of ore containing 1.9 grams/tonne Au 1,035 grams/tonne Ag, 1.2 percent Cu, 1.7 percent Pb and 3.6 percent Zn (Pirie, 1989). It was mined by Inmet Mining Corporation between 1989 and 1992.

The deposit consists of a highly deformed quartz vein system containing massive to disseminated tetrahedrite, sphalerite, galena, and chalcopyrite. It lies within altered and deformed metasediments close to the contact with structurally overlying mafic volcaniclastic rocks. According to Pirie (1989), structural evidence indicates that the sequence is inverted and that the deposit is on the overturned limb of a recumbent syncline.

The sequence is called the "Mine Series" by the mining companies. Metasediments consist of carbonaceous black argillites, sericitized yellowish argillites containing chert lenses, and pyrite-rich silicified greyish argillites. Some of the beds show grading and rip-up clasts. The metasediments are heavily strained and highly altered; they display pervasive quartz-pyrite-sericite-fuchsite-carbonate alteration, which is most intense along the metasediment-metavolcanic contact. The protolith of these rocks is difficult to recognize because of intense alteration, deformation, and mineralization. Future geochemical and petrographic studies will try to resolve this issue.

Mafic volcaniclastic rocks structurally overlying the sediments are most commonly tuffaceous to lapilli in texture. Some pillowed flows are present. Folded and brecciated mineralized quartz veins crosscut the metasediments and the metavolcanics in the vicinity of the deposit (Figures 5E and F).

Twin Mountain

The Twin Mountain occurrence consists of galena, sphalerite, chalcopyrite, and pyrite mineralization within carbonate-quartz veins, and sulphide barite lenses. The host rock consists of sericitized and silicified schists derived from mafic volcanic flows and volcaniclastic rocks. The property was explored by Camoose Mines Ltd. during the 1950's, and was reexamined during the 1980's by Corporation Falconbridge Copper. A drill hole intersected 2.37 meters assaying 10.6 grams per tonne gold, 335.3 grams per tonne silver, 3.13 percent zinc, 2.74 percent lead and 0.55 percent copper (George Cross Newsletter #237, 1987).

DISCUSSION

The stratigraphic and structural setting of the metasedimentary and metavolcanic rocks of the Eagle Bay Assemblage in the Johnson Lake-Adams Lake region has important implications for understanding the genesis of the sulphide mineralization.

Schiarizza and Preto (1987) inferred a major thrust fault, the Haggard Creek Fault, between the structurally overlying Cambrian mafic volcanic rocks (unit EBG of Schiarizza and Preto, 1987) and the underlying Devonian-Mississippian metasedimentary rocks (units EBF, EBA and EBS). This thrust fault trends roughly along the Samatosum and Rea horizons, *i.e.*, along a package of overturned metasedimentary-metavolcanic rocks referred to as the "Mine Series". The Rea deposit was interpreted to be within the Devonian-Mississippian volcano-sedimentary sequence, whereas the Samatosum deposit was interpreted as hosted in Devonian-Mississippian strata with Cambrian volcanics in thrust contact.

The stratigraphic sequences at Rea and Samatosum are very similar. Moreover, the deposits have similar alteration and mineralogy. At Rea, the contact between the mafic volcaniclastic rocks and the underlying metasediments is a stratigraphic one (Höy and Goutier, 1986). These factors suggest that the stratigraphic sequence is the same for both deposits and is repeated by faulting. It also suggests that the sedimentary and volcanic succession hosting Rea, Samatosum, and possibly Twin Mountain, is Devonian-Mississippian in age.

At Samatosum, the presence of quartz and carbonate veins in the structural hanging wall (*i.e.*, mafic volcanic rocks) and the presence of stratiform mineralization within the metasediments, along with pervasive sericite-quartz-carbonate-pyrite alteration of both metasediments and metavolcanics, seems to indicate a stratigraphic rather than structural contact between these two units. This may be verified by geochemical studies, now in progress. At the present, we have inferred the presence of an overturned thrust fault (Figure 4.) to repeat this stratigraphy. In the cross section (Figure 4) this appears to be a normal fault. However the surface trace of the fault appears to strike parallel to the penetrative cleavage (Figure 3) and cleavage does not appear to vary across the fault, which indicates that the fault predates folding and subsequent overturning of the units. Thus, the fault would have been formed during early compression, and rotated into its current orientation as the units were overturned.

Schiarizza and Preto (1987) have noted that Devonian-Mississippian strata unconformably overlie Lower Cambrian rocks at other localities within the Eagle Bay Assemblage. It is possible that this relationship may apply here, although based on the overall regional stratigraphy (Figure 2), a thrust fault seems most likely. Further work will attempt to date stratigraphic units and determine their tectonic settings and geochemical signatures.

ACKNOWLEDGEMENTS

The authors are very grateful to Bob Friesen of Teck Exploration Ltd. for providing pertinent information on the Samatosum deposit. Inmet Mining Corporation gave us access to the Samatosum property and the help of John and Charlene Froese, Dick Ross, and Brent Hamblin of Inmet Mining Corporation was very appreciated. Jack Marr of Geodex Minerals Ltd. and David Wilder of

Remedios and Company also provided maps, plans and sections necessary to conduct this study. We are grateful to Jennifer Porter who provided capable field assistance.

The authors would like to thank Ken Daughtry for discussions regarding the geology of this area. Vic Preto graciously gave us a regional geological tour.

The following people from the British Columbia Geological Survey are thanked for their helpful suggestions: George Simandl, Jim Logan, and Michael Cathro. Paul Schiarizza and Derek Brown reviewed the manuscript; their suggestions and comments are very much appreciated.

REFERENCES

Carmichael, R.G. (1991): 1991 Final Report on the Kamad Property, *Kamad Silver Co Ltd.*, unpublished company report, 28 pages.

Goutier, F.G. (1986):Galena Lead Isotope Study of Mineral Deposits in the Eagle Bay Formation, Southeastern British Columbia; unpublished M.Sc. thesis, *The University of British Columbia*, 152 pages.

Höy, T., and Goutier, F. (1986): Rea Gold (Hilton) and Homestake Volcanogenic Sulphide–Barite Deposits, Southeastern British Columbia (82m/4W); *in* Geological Fieldwork 1985, British Columbia Ministry of Energy, Mines and Petroleum Resources, Paper 1986-1, p. 59-68.

Höy, T. (1987): Alteration, Chemistry and Tectonic Setting of Volcanogenic Massive Sulphide-Barite Deposits At Rea and Homestake, Southeastern British Columbia; *in* Exploration in British Columbia 1986, B.C. Ministry of Energy, Mines and Petroleum Resources, p.B7-B19.

Höy, T. (1999): Massive sulphide deposits of the Eagle Bay Assemblage, Adams Plateau, South Central British Columbia (082M 3, 4); *in* Geological Fieldwork 1998, *British Columbia Ministry of Energy and Mines*, Paper 1999-1, p. 223-245.

Pirie, I. (1989): The Samatosum Deposit; The Northern Miner Magazine, June 1989, p. 15-18.

Preto, V.A. (1981): Barriere Lakes – Adams Plateau Area (82L/13E; 82M/4, 5W; 92P/1E, 8E); *in* Geological Fieldwork 1980, B.C. Ministry of Energy, Mines and Petroleum Resources, Paper 1981-1, p. 15-23.

Preto, V.A. and Schiarizza, P. (1985): Geology and Mineral Deposits of the Adams Plateau-Clearwater Region; *in* Field Guides to Geology and Mineral Deposits in the Southern Canadian Cordillera, edited by D.J. Tempelman-Kluit, *Geological Society of America,* Cordilleran Section Annual Meeting, Vancouver, B.C., p. 16.1-16.11.

Schiarizza, P. and Preto, V.A. (1987): Geology of the Adams Plateau-Clearwater-Vavenby Area; *British Columbia Ministry of Energy, Mines and Petroleum Resources,* Paper 1987-1, 88 pages.

Wheeler, J.O., and Mcfeely, P. (1991): Tectonic Assemblage Map of the Canadian Cordillera and Adjacent Parts of the United States of America, *Geological Survey of Canada,* Map 1712A, Scale 1: 2 000 000.

Stratigraphy, Structure, Geochronology and Provenance of the Logjam Area, Northwestern British Columbia (NTS 104O/14W)

Thomas P. Gleeson[1], Richard M. Friedman[2], and KimWahl[1]

INTRODUCTION

The Logjam area covers four parallel ridges oriented nearly perpendicular to the regional structural fabric between Screw Creek and Logjam Creek, approximately 300 km east of Whitehorse. The Logjam area is 30 km from the Logtung deposit and ninety percent of the area is above treeline (Figure 1). This area has been interpreted as straddling the contact of the Big Salmon Complex (Gabrielse, 1969) and the Klinkit Assemblage (Harms and Stevens, 1996) and therefore is of key geological importance (regional geology map in Mihalynuk *et al*., 2000, this volume). In contrast to the schistose, commonly greenschist facies rocks of the Big Salmon Complex immediately to the west, the Logjam area is underlain mostly by phyllitic metasedimentary rocks with a small outcrop area of schists in the northwest (Figure 2). Mapping was conducted during a ten-day period in September 1998, to gain a better understanding of the stratigraphy, structure, age and tectonic affinity of this poorly known package and its relationship to the Big Salmon Complex.

Field work focused on the documentation of stratigraphic and structural features within the study area and on the collection of key rock samples for isotopic and microfossil age determination. A U-Pb zircon age of a foliated tonalite and detrital zircon ages from a pebble conglomerate were determined. Provenance determinations were made from point-counts of greywacke, grit and pebble conglomerate samples.

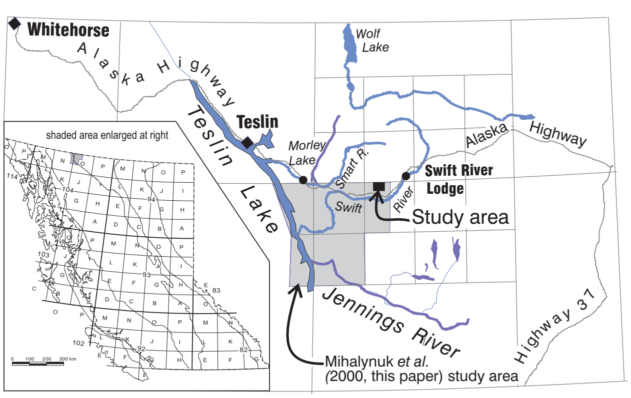

Figure 1. Location of study area; the Logjam area (Figure 2) is highlighted.

REGIONAL GEOLOGY

The Logjam area lies within the belt of pericratonic terranes that extends the length of the Canadian Cordillera and is situated between North American miogeoclinal rocks to the east and accreted terranes to the west. The recognition of pericratonic assemblages and changes in terrane nomenclature of northern British Columbia and southern Yukon are convoluted. Gabrielse (1969) included these rocks in his unit 12, which he divided into three members. The lower member (unit 12a) consists of quartzite, argillite, slate, ribbon chert, and discontinuous grey limestone. The middle member (unit 12b), laminated to thickly bedded limestone with Pennsylvanian fusilinids, is best exposed east of Screw Creek. Poole (1956) described some of the conglomerate in the 'Screw Creek' limestone as red or green chert pebbles in a limestone matrix. Facing indicators in the limestone, including channel scours and corals in growth position demonstrate that the limestone is repeated by recumbent, isoclinal folds (Mihalynuk *et al*., 2000, this volume).

Monger *et al*. (1991) considered the Logjam area to be part of the Dorsey Terrane, a succession of Upper Paleozoic sedimentary rocks that are not readily correlative with assemblages elsewhere in the Cordillera. Harms and Stevens (1996) subdivided the Dorsey Terrane into Dorsey, Swift River and Klinkit assemblages. The Logjam area was considered part of the Klinkit assemblage which has three informal units, from oldest to youngest: 1) Pennsylvanian Screw Creek limestone, 2) Butsih volcanics, 3) Triassic Teh clastics (T. Harms, personal communication, 1999). This assemblage was described as lithologically heterogeneous such that individual beds or composite horizons could not be followed along strike for more than a few kilometres (Stevens and Harms, 1995). Geochronological constraints, discussed below, preclude correlation of layered units with the Klinkit assemblage.

[1]*School of Earth and Ocean Sciences, University of Victoria, BC.*

[2] *Department of Earth and Ocean Sciences, TheUniversity of British Columbia, BC.*

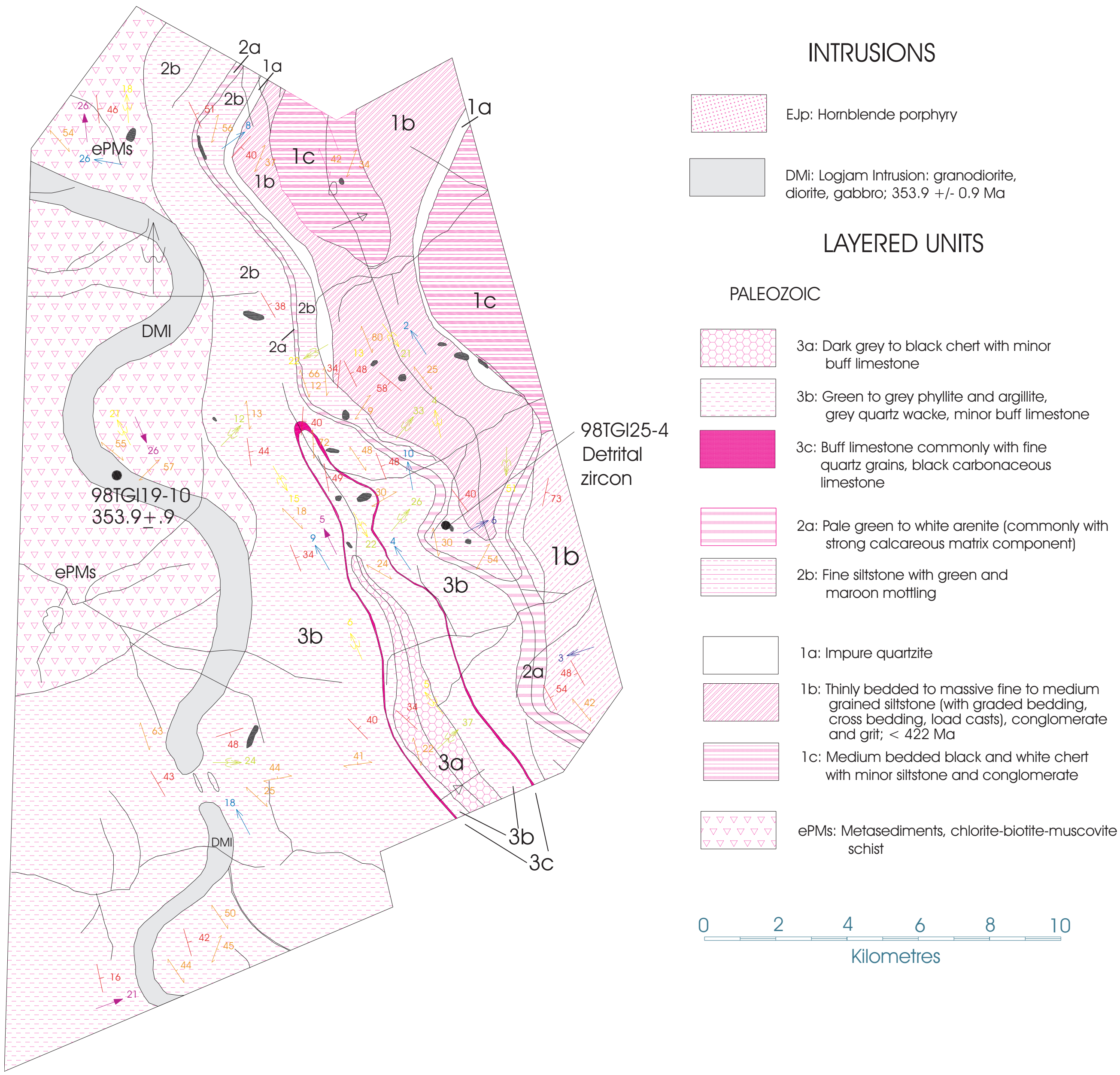

Figure 2. Regional geology map of the Logjam area with U-Pb sampling sites highlighted.

LAYERED UNITS

Three mappable and divisible stratified rock units are recognized in the Logjam area (Figure 2). In ascending stratigraphic order they are: 500 metres of brown, thinly bedded to massive siltstone, chert and impure quartzite (unit 1); 200 metres of green and maroon to white siltstone to sandstone (unit 2); and 300 metres of grey-black to green phyllite, wacke and limestone (unit 3; Figure 3). Insert Figure 3 here. Unit ePms is biotite schist with unknown stratigraphic relations. Contrary to the description of Stevens and Harms (1995), these units were found to be laterally continuous and were traced for more than 20 km across the study area. Relative age assignments are based on preserved way-up indicators within the brown siltstone unit and the position within a regionally significant anticline-syncline pair. U-Pb ages reported below indicate that units 1b to 3b were deposited between middle Silurian and earliest Mississippian (Claoué-Long *et al*., 1992).

Brown Siltstone, Chert and Impure Quartzite (Unit 1)

Rusty brown siltstone and black chert of unit 1 underlie most of the two northernmost ridges of the Logjam

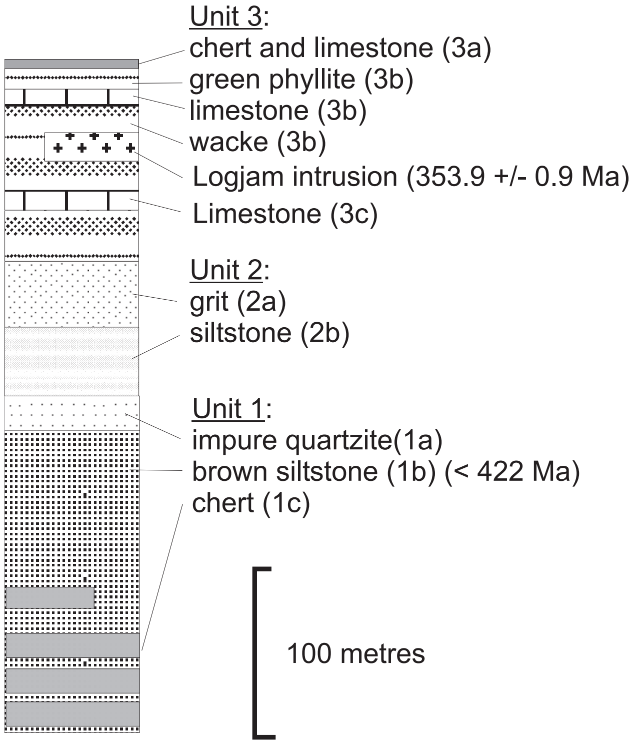

Figure 3. Stratigraphy of Logjam area with approximate lithological thicknesses.

area. They are interbedded on the metre- to outcrop-scale but can be separated at map scale into dominantly (>80%) chert (unit 1c) or dominantly (>90%) siltstone (unit 1b). A third subunit (unit 1a) consists of fractured, impure quartzite. Unit 1c is characterized by 1 to 20 metre thick beds of massive black and white chert interlayered with 1 to 4 metre thick beds of laminated to massive siltstone. Unit 1b consists of rusty orange to brown siltstone with scarce 0.5 to 3 metre thick beds of conglomerate, dolostone and chert. Thinly bedded to laminated siltstone of this unit contains primary sedimentary structures including graded bedding, channel scours, cross bedding and soft-sediment deformation features. At higher stratigraphic levels, the siltstone of unit 1b is commonly black and massive with a slightly calcareous matrix. A distinctive, 1 to 3 metre thick, grit to pebble conglomerate bed sits in unconformable sedimentary contact with siltstone within unit 1b at roughly the same stratigraphic level. A sample of grit from this dominantly conglomeratic horizon was collected for detrital zircon analysis. A single, thin interbed of green tuff containing mafic clasts (?) and chlorite- muscovite partings provides the only evidence within this unit for a distal volcanic source. A fractured, impure quartzite (unit 1a) above unit 1b has sharp (unconformable?) contacts with units 2b and 1b.

Green and Maroon to White Siltstone and Sandstone (Unit 2)

Unit 2 consists of quartz-rich siliciclastics which have been subdivided into members on the basis of colour and grain size. This map unit is differentiated petrographically from unit 1 by coarser, more rounded grains. Unit 2b varies between siltstone to fine grained sandstone with bright olive green and maroon irregular patches that cut bedding planes at random. These are probably diagenetic. Unit 2b siltstone grades into coarser unit 2a, which is a white to light green or pink arenite, commonly with a calcareous matrix. Unit 2a fines upwards into beds of wacke and impure arenite that comprise the basal portion of unit 3b.

Phyllite-Greywacke-Limestone-Chert Unit (Unit 3)

The phyllite-greywacke-limestone-chert unit is lithologically diverse. Unit 3c is a 5 to 10 m thick marker unit of tan, carbonaceous limestone within the compositionally variable package of phyllite, greywacke and limestone (unit 3b). Stratigraphically higher, in the core of a south plunging syncline, is a distinctive unit of black chert and buff limestone (unit 3a). Like unit 2, sedimentary grains in unit 3 are coarser and more rounded than in unit 1. However, unit 3 is differentiated petrographically from unit 2 by a higher matrix component and detrital biotite. Unit 3 is characterized by a muscovite-chlorite phyllitic cleavage but is differentiated from unit 1 and 2 by poorly developed biotite schistosity and epidote alteration. Metamorphic grade is unknown because both greenschist and sub-greenschist metamorphic assemblages are incomplete.

Two limestone beds, one black and the other tan-to-buff coloured, (unit 3c) provide excellent markers within unit 3b. The buff to orange massive limestone is <1.5 m thick with disseminated, rounded, medium-sized quartz grains (<5%). The black, massive to medium bedded limestone is 1.5 - 2.5 m thick and is gradationally interbedded above and below with thin phyllite or argillite horizons. The two carbonates are separated by up to 4 m of clastic sediments.

The siliciclastic component of unit 3b is green to grey to black phyllite and argillite and grey to black quartz wacke interbedded on the decimetre- to outcrop-scales. Lenses (<3m) of grey, massive limestone are common throughout unit 3b. Unit 3a is a distinct association of grey to buff thick bedded limestone and black and white, massive chert. Chert layers are up to ten times more abundant than carbonate and interbedded on decimetre- to metre-scale. Chloritic (tuffaceous?) phyllite is also characteristic of unit 3a.

Quartz-Biotite Schist (Unit ePms)

Quartz-biotite schist is structurally lower than most of units 1-3. Moderately to well developed schistosity, totally recrystallized quartz, and abundant metamorphic biotite (often retrograded to chlorite) differentiate these rocks from those described above. Chloritoid, a defining component of the meta-pelitic upper greenschist assemblage, was not observed so the metamorphic grade is uncertain. Most of the quartz domains are quartz segregations but some may be strained, coarse quartz grains suggesting a protolith of variable grain size. Metre-scale layers of grey-orange marble are inferred to be former carbonate horizons in a dominantly siliciclastic package. Unit ePms is a mappable unit but the protolith may be similar to unit 3. Outcrops of schists are mostly at higher elevations than the Logjam intrusion (described below). One outcrop downslope of the Logjam intrusion is marble and argillite; this is inferred to be part of unit ePms. The contact of unit ePms cuts across the strike of the units 1-3 so it may represent a disconformity or a fault surface but there are no demonstratable difference in metamorphic grade or degree of deformation across the contact. Unit ePms may be representative of the Big Salmon Complex.

INTRUSIVE ROCKS

Three plutons are found in the Logjam area. The largest intrusion is a moderately foliated tonalite and gabbro body informally called the Logjam intrusion. Foliated tonalite occurs as irregular fingers and pods in a more extensive and equally foliated gabbro body. Mutually cross-cutting intrusive relationships between tonalite and gabbro suggest that these phases are the same age and are possibly comagmatic. Variability in grain size and fabric intensity in the gabbro may be due to magmatic fluid enrichment and strain partitioning. The gabbroic body intrudes both unit ePms and unit 3b. On two ridges, it has a similar width and crops out at a similar altitude suggesting it is a continuous, slender body. The intrusive contact with unit 3b does not crop out but wacke flanks gabbro on both sides. A structural discontinuity seems unlikely because foliations do not change from one side of the body to the other. The foliation present in both plutonic phases is interpreted to record post-crystallization (solid-state)

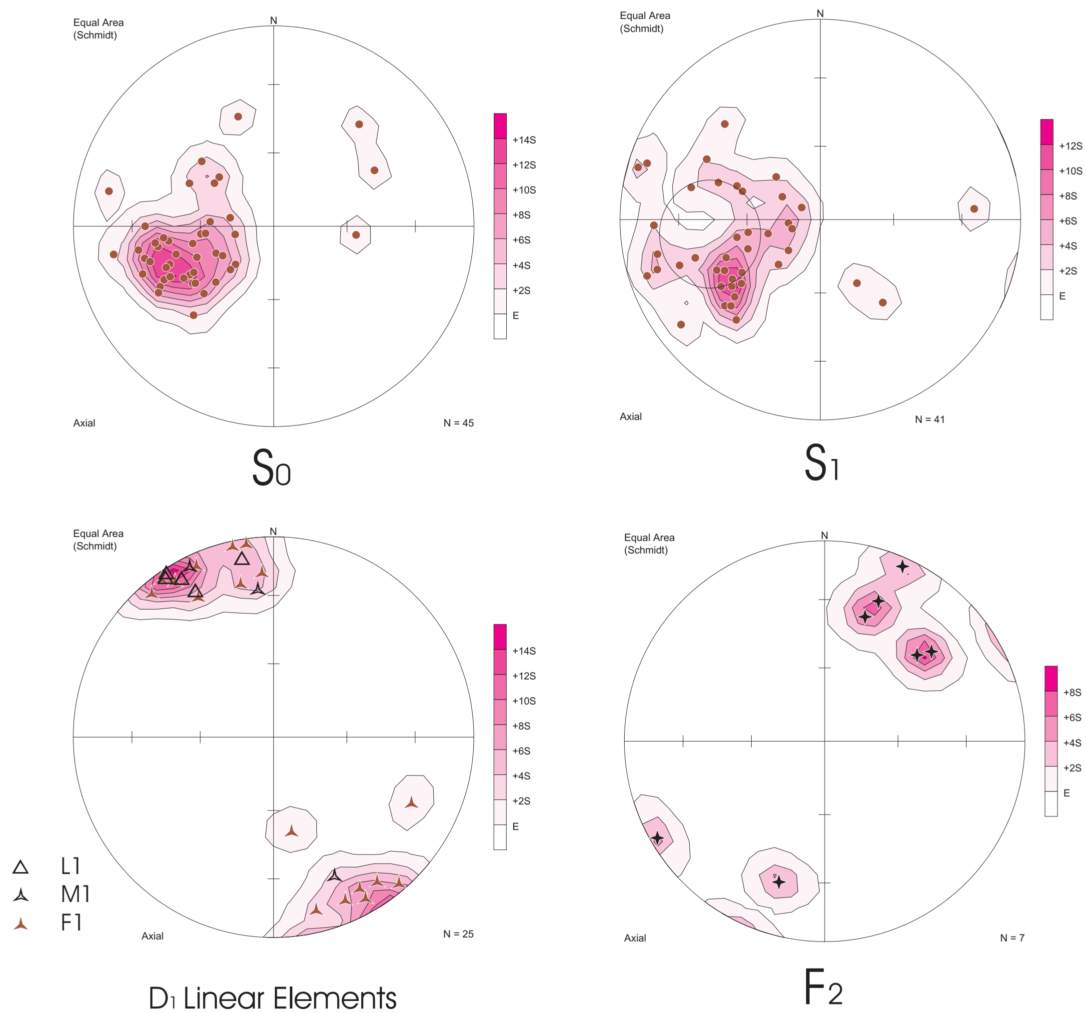

Figure 4. Schmidt equal area stereographic projections showing contoured poles to (a) bedding - S_0), and (b) foliation (S_1) and contoured plots of (c) intersection lineations - L_1, mineral lineations - M_1, and fold axes - F_1, and (d) later fold axes - F_2. Data contoured by Gaussian counting using a weighting function equivalent to a fractional counting area of 0.01. Contour intervals are 2, 4, 6, 8, 10, 12 &14 sigma.

deformation. The foliation is less intense than the schistosity in unit ePms suggesting that the intrusion is late synkinematic. Both units show evidence for later brittle microfractures (*i.e.* offset micas in unit ePms).

Two fine grained, unfoliated hornblende-porphyritic gabbroic intrusions cut all stratigraphic units and deformation fabrics. These intrusions exhibit medium grey fresh surfaces and rusty orange weathering surfaces; in the field they can be distinguished by the presence or absence of plagioclase phenocrysts. Trace element geochemical analysis will be conducted in attempt to further distinguish them and determine their tectonic affinity.

STRUCTURE

The Logjam area is a northeast-dipping homocline (units 1-3) flanked by the structurally lower ePms unit to the northwest. Although development of schistosity varies, fabric elements indicate the entire map area experienced the same deformational regime. The phyllite-wacke-limestone unit (unit 3), interpreted as higher in the stratigraphy, appears structurally lower than units 1 and 2 because it is the most pervasively deformed and is the only unit displaying quartz rodding and boudinage. Relatively intense foliation development in unit 3 can be explained by strain partitioning, or because a more suitable composition for phyllosilicate growth, or both.

Evidence of the earliest deformation (D_1) is a set of NNW and SSE trending folds (F_1) and related phyllitic axial planar cleavage (S_1; Figure 4). Insert Figure 4 here. The phyllitic cleavage is nearly parallel to compositional layers interpreted as transposed bedding (S_1 within 10 degrees and commonly within 3 degrees of S_0; Figure 4). Such widespread near bedding-parallel foliation is due either to transposition or to original high amplitude, isoclinal folding. Large-scale isoclinal folds probably mimic millimetre to metre-scale isoclinal F_1 folds. These folds are inclined to recumbent, and subhorizontal to shallowly plunging. S_0 and S_1 are asymmetric (Figure 4) suggesting a southwestern vergence for F_1. Strong coaxial quartz rodding lineations and stretched pebbles (5:1 aspect ratio) are interpreted as the transport lineations parallel to F_1 axis (Figure 4). All beds must be considered potentially transposed because of the presence of attenuated isoclinal folds. However, the local consistency of facing directions and their limb position suggest these data are significant. Metamorphism was likely to be roughly coeval with D_1 since metamorphic minerals such as chlorite are axial planar to F_1 folds.

Regionally important, kilometre-scale folds have been identified in the Logjam area by recognition of unit repetitions and a facing direction reversal. These folds are close to isoclinal and plunge gently to the southeast. Similar folds are observed in F_1 microstructure (Figure 4), although plunges to the southeast are more common. Units 3a and 3c appear to be cut off as they strike toward the north into this anticline (Figure 2); these units may be truncated by a fault that cuts up section to the north or may be folded within a south-plunging anticline. The latter possibility is favored, as it is supported by the repetition of unit 3c.

Second phase folds (F_2) are commonly at centimeter- to decimetre-scales. They are open to close, upright to inclined and shallowly to moderately plunging (Figure 4). Crenulated foliation surfaces are very common. D_2 crenulations deform tight centimetre-scale F_1 folds, providing age relations for these events. Rarely, later crenulations deforms D_2 crenulations folds. These suggest a later deformational event (D_3?), or more likely these are a product of progressive D_2 deformation because the crenulations have similar geometry. No mineral lineations accompany F_2 folds. Although northeast-striking phyllitic fabrics were identified in the field as S_2; these are never axial planar to F_2. An S_2 fabric that overprints S_1 fabrics was only observed in one outcrop, but even here the relationship was not clear. These observations and the fact that the style of fabric is indistinguishable suggest that S_2 may actually be a folded S_1. When all foliation fabrics are plotted together they outline a small circle suggesting that S_1 is folded by a moderately to weakly conical folds that are coaxial with F_2 (Figure 4). Therefore, phyllitic fabrics with northeastern orientations are considered to be S_1 surfaces folded by outcrop scale F_2 folds.

Late-stage brittle kinks were observed on bedding planes. A fault which juxtaposes units across a minor creek on the north-central ridge is intruded by a hornblende porphyry dike, characteristic of late dikes that crosscut all deformational features.

U-Pb GEOCHRONOLOGY

Three samples from the Logjam area were collected for U-Pb dating: a deformed tonalite from the Logjam intrusion, an undeformed hornblende-phyric intrusion and grit from the conglomeratic facies of unit 1b. The sample from a hornblende-phyric pluton (98TGL17-2) yielded no minerals datable by the U-Pb method. Zircon and titanite concentrates from the other two localities were prepared from representative ca. 10-20 kg samples using conventional crushing, grinding, Wilfley table, heavy liquid and magnetic separation techniques. The methodology for zircon grain selection, abrasion, geochemical preparation and mass spectrometry are described by Mortensen *et al*. (1995). U-Pb analyses were done at The University of British Columbia (Table 1, Figures 5, 6). Insert Table 1 and figures 5 and 6 here. Errors attached to individual analyses were calculated using the numerical error propagation method of Roddick (1987). The decay constants were those recommended by Steiger and Jäger (1977).

Analytical Results

(1) Logjam intrusion deformed tonalite: 98TGL-19-10

A representative sample of foliated tonalite from the Logjam intrusion yielded abundant, high quality, clear, colourless to pale pink zircons. Five analysed zircon frac-

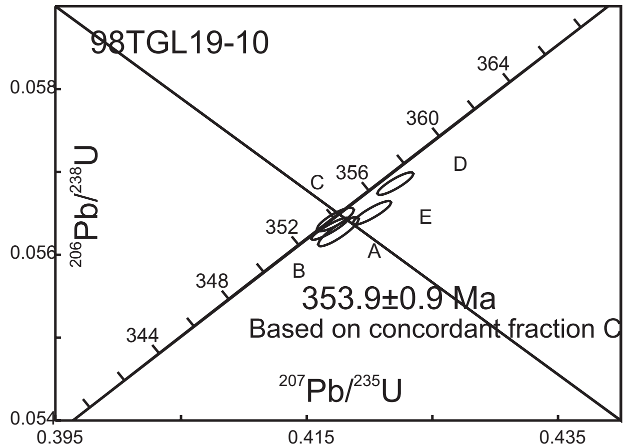

Figure 5. Standard concordia plot for deformed tonalite of the Logjam intrusion (98TGL19-10). Error ellipses are plotted at the 2 sigma level of confidence. U-Pb data are listed in Table 1.

tions cluster on and off of concordia between about 353 Ma and 358 Ma (*et al*). An assigned crystallization age of 353.9 ± 0.9 Ma is based on the $^{206}Pb/^{238}U$ age for concordant fraction C. Discordant fractions A, D and E give older 207Pb/206Pb ages (Table 1) and are inferred to contain minor inherited zircon.

The above age demonstrates that the Logjam intrusion is the product of Devono-Mississippian magmatism, which has been well documented throughout the pericratonic terranes in the Yukon and British Columbia (Murphy and Piercey, 1999; Mortensen, 1992). The Logjam tonalite intrudes unit 3b and its crystallization age thus constrains the minimum depositional age for unit 3b and stratigraphically lower units, and a maximum age for deformation in the area . The unfoliated Nome Lake batholith to the south, with a K-Ar age of ca. 180 Ma (Wanless *et al*., 1970), provides a mid-Jurassic minimum age constraint on deformation.

(2) Unit 1b grit detrital zircon analyses: 98TGL25-4

A grit sample from the conglomerate bed of unit 1b yielded abundant detrital zircons which vary from clear, colourless, well-faceted euhedral prismatic crystals to deep purple, naturally abraded ellipsoidal grains. Ten single grains selected from euhedral and rounded populations gave $^{207}Pb/^{206}Pb$ ages of 2777 Ma to 422 Ma. The $^{207}Pb/^{206}Pb$ ages for six concordant or nearly concordant analyses (2.0-0.1% discordant; Table 1, Figure 6) are interpreted as crystallization ages for these grains . The youngest concordant grain, (J), at 422 Ma, defines a maximum age for deposition of the conglomeratic facies of unit 1b and all stratigraphically higher units. These age constraints suggest that units between 1b and 3b are constrained to between Middle Silurian (*ca.* 422 Ma) and earliest Mississippian (*ca.* 354 Ma). Implications of the detrital zircon data set are further discussed below.

BIOCHRONOLOGY

Fourteen conodont samples were collected from limestone and dolostone beds and interbeds. All samples were barren of conodonts and other microfossils, providing no chronological constraints (M. Orchard, personal communication, 1999).

Provenance

To better constrain the evolution and provenance of units 1 to 3, a point count study was undertaken. Detrital

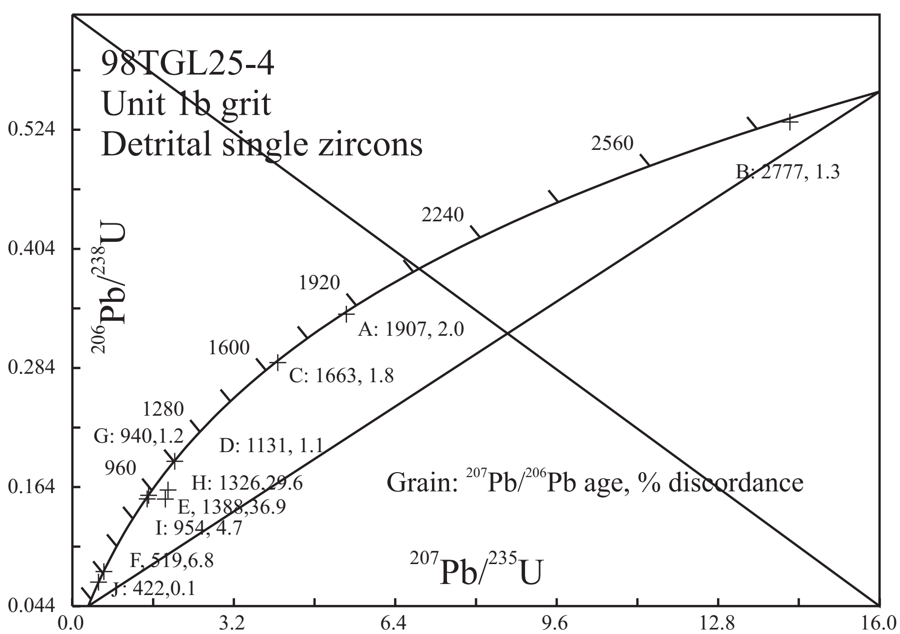

Figure 6.Standard concordia plot for detrital zircon grains in a grit sample from unit 1b (98TGL25-4). Error ellipses are plotted at the 2 sigma level of confidence; $^{207}Pb/^{206}Pb$ ages and discordancies are listed for each fraction on plot and in Table 1.

TABLE 1
U-PB ANALYTICAL DATA FOR THE LOGJAM AREA

Fraction[1]	Wt mg	U[2] ppm	ppm	^{206}Pb[4] / ^{204}Pb	Pb[5] pg	^{208}Pb[6] %	Isotopic ratios (1s,%)[7] ^{206}Pb/^{238}U	^{207}Pb/^{235}U	^{207}Pb/^{206}Pb	Apparent age (2s,Ma)[7] ^{207}Pb/^{206}Pb	%Discordant[8] (to origin)
98TGL19-10 deformed tonalite of Logjam intrusion: 353.9±0.9 Ma											
A p,eu	0.104	347	19	27055	5	6.1	0.05628 (0.16)	0.4175 (0.19)	0.05381 (0.10)	362.9 (4.3)	
B p,eu	0.11	371	20	10304	14	6.8	0.05631 (0.12)	0.4168 (0.18)	0.05368 (0.08)	357.8 (3.8)	
C p,eu	0.092	172	10	9150	6	8.2	0.05643 (0.13)	0.4173 (0.18)	0.05363 (0.10)	355.8 (4.6)	
D p,eu	0.112	281	16	17969	6	7.9	0.05686 (0.12)	0.4221 (0.17)	0.05384 (0.09)	364.2 (4.0)	
E p,eu	0.094	165	9	8110	7	8.5	0.05651 (0.13)	0.4202 (0.18)	0.05393 (0.09)	368.2 (4.2)	
98TGL25-4 Unit 1b grit: detrital single grain zircon analyses											
A c,vp,r	0.032	167	67	17985	6	18.5	0.33743 (0.11)	5.4315 (0.17)	0.11674 (0.07)	1907.0 (2.6)	2
B c,vp,r	0.016	228	144	19970	6	13.7	0.53135 (0.11)	14.2203 (0.16)	0.19410 (0.07)	2777.2 (2.3)	1.3
C c,pp,r	0.015	179	56	7732	6	11.7	0.28915 (0.12)	4.0719 (0.17)	0.10213 (0.08)	1663.3 (3.1)	1.8
D c,pp,r	0.016	643	123	16785	7	8	0.18955 (0.11)	2.0221 (0.16)	0.07737 (0.08)	1130.8 (3.1)	1.1
E c,y,r	0.007	58	9	699	6	10.8	0.15168 (0.15)	1.8460 (0.36)	0.08826 (0.29)	1388 (11)	36.9
F c,y, eu,pr	0.011	570	44	4181	7	7.2	0.07810 (0.16)	0.6214 (0.26)	0.05771 (0.18)	518.6 (8.0)	6.8
G c,pp, eu,pr	0.011	276	41	2353	12	4.7	0.15512 (0.17)	1.5056 (0.25)	0.07040 (0.15)	940.0 (6.1)	1.2
H c,y, eu,pr	0.007	171	32	2002	6	20.6	0.16075 (0.13)	1.8941 (0.21)	0.08546 (0.12)	1326.0 (4.7)	29.6
I c,y, eu,pr,b	0.01	311	45	4491	7	3.3	0.15205 (0.12)	1.4863 (0.18)	0.07089 (0.11)	954.3 (4.3)	4.7
J c,pp, eu,pr,s	0.007	792	57	1892	12	14.3	0.06761 (0.15)	0.5150 (0.27)	0.05524 (0.19)	422.0 (8.4)	0.1

[1] Upper case letter = zircon fraction identifier; All zircon grains >134mm, air abraded, and nonmagnetic on Franz magnetic separator at 2.0A° fieldstrength and 1° sideslope; Grain description codes: b= broken grain, c=clear, cls=colourless, e=elongate, eu=euhedral and faceted, g=grey, pp=pale, pr=prismatic, r=rounded and frosted, s=stubby, t=turbid; vp=vivid pink; y=yellow.
[2] U blank correction of 1pg ± 20%; U fractionation corrections were measured for each run with a double 233U-235U spike (about 0.005/amu).
[3] Radiogenic Pb
[4] Measured ratio corrected for spike and Pb fractionation of 0.0035/amu ± 20% (Daly collector) and 0.0012/amu ± 7% and laboratory blank Pb of 1-3pg ± 20%. Laboratory blank Pb concentrations and isotopic compositions based on total procedural blanks analysed throughout the duration of this study.
[5] Total common Pb in analysis based on blank isotopic composition
[6] Radiogenic Pb
[7] Corrected for blank Pb, U and common Pb. Common Pb corrections based on Stacey Kramers model (Stacey and Kramers, 1975) at the age of the rock or the 207Pb/206Pb age of the fraction.
[8] Detrital zircon analyses only; 207Pb/206Pb ages interpreted as crystallization ages for fractions 2% or less discordant.

grain abundances help discriminate between possible tectonic settings. Petrographic work was complimented by U-Pb detrital zircon ages which give Early Paleozoic and Precambrian crystallization ages (Table 1). The tectonic setting exerts a primary control on sandstone compositions, although relief, climate, transport mechanism, depositional environment and diagenesis all can be important secondary factors (Dickinson, 1985). The point counting methodology of Dickinson and Suczek (1979) was followed. Ten greywacke, grit and coarse siltstone samples, each representative of a unit, were point-counted with more than 300 points per slide at a spacing of 1 mm. Efforts were made to minimize uncertainty presented by differentiating matrix, identifying feldspars, metamorphism and diagenesis (Dickinson, 1970); difficult grains were counted as 'undifferentiated' which is not part of the tectonic discrimination. The detrital zircon grit sample was counted and compared with other samples, even though its grain size is an order of magnitude larger.

All three stratified units (1, 2 and 3) plot in the continental block or recycled orogen provenance on selected ternary tectonic discriminate diagrams (Figure 7). Insert figure 7 here. The total quartz-feldspar-lithics plot (Figure 7) best shows that each unit has a slightly different provenance with unit 3 in the continental block field and unit 1 and unit 2 in the recycled orogen field. The recycled orogen field includes deformed and uplifted supracrustal strata, dominantly sedimentary but also volcanic in part (Dickinson, 1985; Dickinson and Suczek, 1979). Continental block provinces include both stable cratons and basement rifts which yield arkosic sands. The grit of unit 1b plots well away from all other samples (Figure 7). This may show that the methodology is grain-size dependent because the provenance of a thin bed should compare to the provenance of the rest of the unit. The grit has little matrix and coarse sub-angular grains which suggest an alluvial setting and a proximal source.

Detrital zircon ages are also useful provenance indicators (Table 1; Figure 6). Six of ten analysed grains are concordant or nearly concordant (<2% discordance; Table 1). ^{207}Pb/^{206}Pb ages for these analyses are interpreted as crystallization ages of 2777, 1907, 1663, 1131, 940, and 422 Ma. Reliable age interpretations are not possible for the four more discordant analyses, especially highly discordant grains E and H. The paucity of usable data prevents meaningful statistical analysis. However, the six grains that provide reliable age information allow us to draw conclusions relevant to the geologic evolution of the Logjam area, and more generally to strata of the pericratonic terranes of the northern Cordillera.

Concordant ages of single grain zircons and the age constraints on the strata, allow comparison of unit 1b to the reference Devonian miogeoclinal sections of Gehrels *et al*. (1995; Silurian clastic sedimentary rocks are rare or absent in the miogeocline and not represented in reference sections). Gehrels *et al.* (1995) showed that age distributions of detrital zircons characterize different latitudes of the Cordilleran miogeocline. The ages of grains A and B (2.78 Ga and 1.91 Ga, respectively) are consistent with detrital ages that are common in Canadian and Alaskan reference miogeoclinal sections and rare or absent in Nevadan and Sonoran sections (Gehrels *et al*., 1995). Detrital zircons with similar ages, from pericratonic strata in the Yukon-Tanana Terrane in Yukon (Mortensen, 1992) and a correlative assemblage in the Coast Mountains of northwestern British Columbia, have been interpreted as consistent with derivation from northwestern North American cratonic sources (Gehrels and Kapp, 1998). The 1.66 Ga age for fraction C is consistent with derivation from recycled Belt Supergroup sediments in southern British Columbia and Montana (Ross *et al*., 1992). Gehrels and Kapp (1998) suggested this source for metasedimentary assemblages in the Coast Mountains of British Columbia with detrital zircons of a similar age. However, Gehrels *et al*. (1995) also suggested that grains of this age might have latitudinal significance for Nevada and Sonora. Grenvillian-aged grains (fraction C; ca.1.13 Ga), occur in Paleozoic sedimentary rocks younger than ca. 450 Ma throughout North America (Patchett *et al*., 1999), and are thus not latitudinally significant. The 940 Ma age for detrital grain G has not been previously encountered in Paleozoic strata of the miogeocline (Gehrels *et al*., 1995), and possible sources within the North American craton have yet to be identified. Finally, the age of 422 Ma (fraction J) matches detrital ages in Alaskan and to a lesser extent the southern British Columbian miogeoclinal reference sections (Gehrels *et al*., 1995) and the Alexander terrane of southeastern Alaska (Gehrels *et al*., 1996).

In summary, the ages of most detrital zircons from the Logjam area are consistent with detrital ages from other pericratonic terranes of the northern Canadian Cordillera and with those from Devonian reference sections of the North American miogeocline in Alaska and British Columbia. This suggests that strata from the Logjam area and northern pericratonic terranes was likely derived from the northwestern North American craton and Pre-

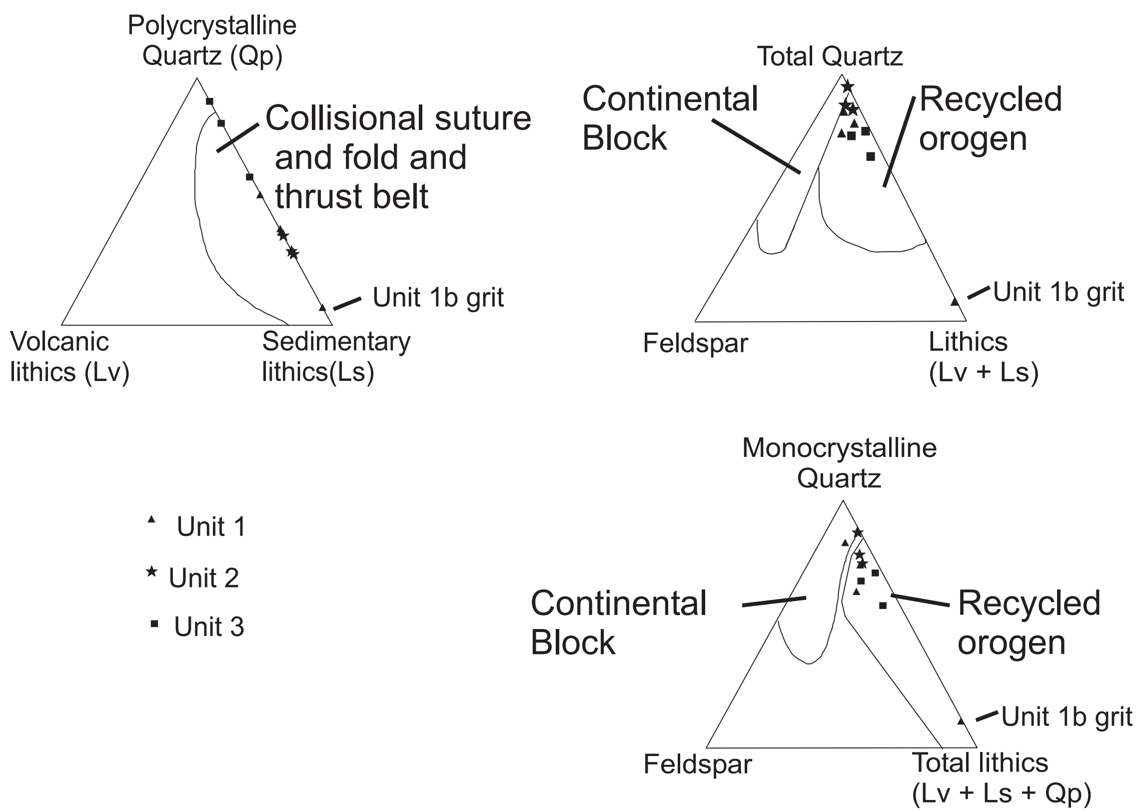

Figure 7.Ternary plots of point-count data from Units 1, 2 and 3; provenance fields after Dickinson (1985).

cambrian to Lower Paleozoic rocks of the northern miogeocline. The recycled nature of the grit from unit 1b is further confirmed by its recycled orogen provenance (Figure 7) and its primary constituent (sedimentary lithics). These conclusions should be considered preliminary until further detrital zircon ages are determined for the Logjam area and pericratonic terranes in general.

DISCUSSION

Mapping between Screw and Logjam Creeks produced a reliable local stratigraphy of three units: brown siltstone and chert (unit 1); green and maroon to white siltstone and sandstone (unit 2); and phyllite, wacke, and limestone (unit 3). Geochronologic constraints suggest that these units were all deposited in Middle Silurian to latest Devonian and subsequently deformed by two Mississippian to Middle Jurassic deformational events. Strata of this age are quite uncommon among pericratonic assemblages. Two examples are the Nasina quartzite within the Yukon-Tanana Terrane and an Upper Devonian siliciclastic unit within the Harper Ranch subterrane of the Quesnellia Terrane (Fritz *et al*., 1991). Mid-Paleozoic age constraints preclude correlation to the Triassic Teh clastics of the Klinkit assemblage roughly along regional strike 30 km to the south. Another possible correlation is with the units directly east of Screw Creek from the Logjam area. The black chert pebble conglomerate and red and green argillite that lie below the Screw Creek limestone may be correlative with the green and maroon siltstone (unit 2b). In this case, both green and maroon lithologies that were deposited between mid-Silurian and Devonian and units above unit 2b (unit 2a and 3) on the Screw Creek ridge must have then been removed by a pre-Pennsylvanian erosion event represented by the conglomerate lowest in the Screw Creek limestone. Although the Logjam area has a consistent stratigraphy and structure, the lack of protolith age constraints and equivocal regional stratigraphic correlations preclude a reliable assemblage assignment.

Relationships between units 1-3 and unit ePms, to the east, and the Big Salmon Complex, to the west, remain enigmatic. The contact between unit ePms schist and units 1, 2 and 3 might be due to compositional differences or strain partitioning. The outcrop distribution of ePms is not reconcilable with the geometry of fault emplacement. Although unit ePms displays a more developed schistosity than units 1-3, it may be the same metamorphic grade (all metamorphic assemblages are incomplete). Unit 3b may be a protolith for unit ePms; the relationship between the schist and the less deformed metasediments is the topic of an ongoing study. Deposition of units 1 to 3 might in part be coeval with the deposition of the lowest greenstone unit of the Big Salmon Complex (which is older than the ca. 366 Ma Mt. Hazel orthogneiss; Mihalynuk *et al*. 2000, this volume). Future work should be directed towards constraining protolith age, perhaps from the tuffaceous rocks, and dynamothermal events by dating the cross-cutting hornblende porphyry dikes.

ACKNOWLEDGEMENTS

We are grateful to: JoAnne Nelson for conceiving, organizing, and funding this project through the Devono-Mississippian VMS Project; Mitch Mihalynuk and JoAnne for passing on some of their skills and passion for field geology to Gleeson and Wahl and for years of advice, answers, and serious editing. Stephen Johnston, Tekla Harms, and Chris Suczek are thanked for helpful discussions. Dave Lefebure and Charlie Roots are also thanked for editing. Family and friends, especially Colleen Cote, were essential to comprehending U-Pb systematics and mineralogical fractionation in provenance studies. Structural data was plotted and analysed with SpheriStat^{TM}2 by Pangaea Scientific; ternary diagrams were plotted using Triplot 3.0 and digital map was produced by using AutoCad 14.0.

REFERENCES

Claoué-Long, J.C., Jones, P.J., Roberts, J., and Maxwell, J. (1992): The numerical age of the Devonian-Carboniferous boundary; *Geological Magazine*, Volume 129, pages 281-291.

Dickinson, W.R. (1970): Interpreting detrital modes of graywacke and arkose; *Journal of Sedimentary Petrology*, Volume 40, pages 695-707.

Dickinson, W.R. (1985): Interpreting provenance relations from detrital modes of sandstones; *in* Provenance of arenite, Zuffa, G.G., Editor; *D.Reidel Publishing Company*, Norwell, MA, pages 333-361.

Dickinson, W.R. and Suczek, C.A. (1979): Plate tectonics and sandstone compositions; *American Association of Petroleum Geologists Bulletin*, Volume 63, pages 2164-2182.

Fritz, W.M., Cecile, M.P., Norford, B.S., Morrow, D., and Geldsetzer, H.H.J. (1991): Cambrian to Middle Devonian assemblages, Chapter 7 *in* Geology of the Cordilleran Orogen in Canada, Geology of Canada, Volume 4, edited by H. Gabrielse and C.J. Yorath, *Geological Survey of Canada,* pages 151-220..

Gabrielse, H. (1969): Geology of Jennings River Map Area, British Columbia (104/O): *Geological Survey of Canada;* Paper 68-55.

Gehrels, G.E. and Kapp, P.A. (1998): Detrital zircon geochronology and regional correlation of metasedimentary rocks in the Coast Mountains, southeastern Alaska; *Canadian Journal of Earth Science*, Volume 35, pages 269-279.

Gehrels, G.E., Dickinson, W.R., Ross, G.M., Stewart, J.H., and Howell, D.G. (1995): Detrital zircon reference for Cambrian to Triassic miogeoclinal strata of western North America; *Geology*, Volume 23, pages 831-834.

Gehrels, G.E., Butler, R.F., and Bazard, D.R. (1996): Detrital zircon geochronology of the Alexander Terrane, southeastern Alaska; *Geological Society of America Bulletin*, Volume 108, pages 722-734.

Harms, T.A. and Stevens, R.A. (1996): Assemblage analysis of the Dorsey Terrane; Slave-Northern Cordillera Lithospheric Evolution (SNORCLE) and Cordilleran Tectonics Workshop, Report of the 1996 Combined Meeting, pages 199-201.

Mihalynuk, M.G., Nelson, J., Roots, C.F., and Friedman, R.M. (2000, this volume): Regional geology and mineralization of the Big Salmon Complex (104N N/9,10 & 104O/12, 13, 14W), *in* Geological Fieldwork 1999*, B.C. Ministry of Employment and Investment*, Geological Survey Branch, Paper 2000-1.

Monger, J.W.H., Wheeler, J.O., Tipper, H.W., Gabrielse, H, Harms, T., Struik, L.C., Campbell, R.B., Dodds, C.J., Gehrels, G.E., and O'Brien, J. (1991): Cordilleran Terranes; Chapter 8 *in* Geology of the Cordilleran Orogen in Canada, Geology of Canada, Volume 4, edited by H. Gabrielse and C.J. Yorath, *Geological Survey of Canada*, pages 281-327.

Mortensen, J.K. (1992): Pre-Mid-Mesozoic tectonic evolution of the Yukon-Tanana Terrane, Yukon and Alaska; *Tectonics,* Volume 11, pages 836-853.

Mortensen, J. K., Ghosh, D.K. and Ferri, F. (1995): U-Pb geochronology of intrusive rocks associated with copper-gold porphyry deposits in the Canadian Cordillera; *in* Porphyry deposits of the northwestern Cordillera of North America, Schroeter, T.G., Editor, *Canadian Institute of Mining, Metallurgy and Petroleum*, Special Volume 46, pages 142-158.

Murphy, D.C., and Piercey, S.J. (1999): Finlayson project: geological evolution of Yukon-Tanana Terrane and its relationship to Campbell Range belt, northern Wolverine Lake map area, Southeastern Yukon; *in* Yukon Geology and Exploration 1998, edited by C.F. Roots and D.S. Emond, *Department of Indian and Northern Affairs*, pages 47-62.

Patchett, P.J., Ross, G.M., and Gleason, J.D. (1999): Continental drainage in North America during Phanerozoic from Nd isotopes; *Science*, Volume 283, pages 671-673.

Poole, W.H. (1956): Geology of the Cassiar Mountains in the vicinity of the Yukon-British Columbia Boundary, unpublished Ph.D thesis, Princeton University.

Roddick, J.C.(1987): Generalized numerical error analysis with application to geochronology and thermodynamics; *Geochimica et Cosmochimica Acta*, Volume 51, pages 2129-2135.

Ross, G.M., Parrish, R.R., and Winston, D. (1992): Provenance and U-Pb geochronology of the Mesoproterozoic Belt Supergroup (northwestern United States): implications for age of depositions and pre-Panthalassa plate reconstructions; *Earth and Planetary Letters*, Volume 113, pages 57-76.

Stacey, J.S. and Kramers, J.D. (1975): Approximation of the terrestrial lead isotope evolution by a two stage model: *Earth and Planetary Letters*, Volume 26, pages 57-76.

Steiger, R.H.J. and Jäger, E. (1977): Subcommission on Geochronology: Convention on the use of decay constants in geo- and cosmochronology; *Earth and Planetary Science Letters*, Volume 36, pages 359-362.

Stevens, R.A. and Harms, T.A. (1995): Investigations in the Dorsey Terrane, Part 1: stratigraphy, structure and metamorphism in the Dorsey Range, southern Yukon Territory and northern British Columbia; *in* Current Research, *Geological Survey of Canada* Paper 1995A, pages 117-127.

Wanless, R.K., Stevens, R.D., Lachance, G.R. and Delabio, R.N. (1970): Age determinations and geological studies, K-Ar isotopic ages, Report 9, *Geological Survey of Canada*, Paper 69-2A, 78 pages.

Bull River Copper-Silver-Gold Prospect, Purcell Supergroup, Southeastern British Columbia

Trygve Höy, W.R. Smyth and Ray E. Lett
British Columbia Geological Survey, Ministry of Energy and Mines, Victoria, B.C.

INTRODUCTION

The Bull River deposit (also called the Dalton Mine or the Gallowai Bul Mine) is a past producer of copper, silver and gold. It is located approximately 30 kilometres due east of Cranbrook on the eastern side of the Rocky Mountain trench (Figure 1). It was operated by Placid Oil Co. from 1971 to 1974, producing 7256 tonnes of copper, 126 kilograms of gold and 6354 kilograms of silver from 471 899 tonnes of milled ore (B.C. MINFILE).

The property and surrounding area, collectively referred to as the Gallowai Bul River claims, was acquired by R.H. Stanfield in 1976. The Bull River mine is jointly owned by Gallowai Metal Mining Corporation and Bul River Mineral Corporation Ltd. It has undergone extensive exploration by these companies since that time. This exploration includes underground work, considerable sampling, geological mapping, geophysical surveys and more than 59 000 metres of percussion and diamond drilling. Exploration in 1998 included advancement of a decline 1100 metres and level advancement of 725 metres, 6508 metres of underground diamond drilling, 1144 metres of surface diamond drilling and 367 metres of percussion drilling. Ongoing work in 1999 mainly involved extending the decline by 554 metres, 1424 of level development and 11 169 metres underground drilling, as well as considerable sampling and anayltical work (Photo 1).

In 1998, the Stanfield Mining Group's Consultant and Project Engineer released to the Ministry estimates of the measured and indicated, mineral resource of the Gallowai Bul River as 5.3 million tonnes containing 2.25 percent copper, 1.06 oz/tonne (36 grams/tonne) silver and 0.35 oz/tonne (12 grams/tonne) gold (de Souza, 1998). This resource was quoted in Ministry publications (Schroeter, 1999, Wilton, 1999).

This study, based on a brief visit to the property in June, 1999, was undertaken to better understand the geology of the deposit and to attempt to verify reported resource grades.

REGIONAL GEOLOGY

The Bull River deposit is located in the Rocky Mountain trench just east of the inferred trace of the Rocky Mountain trench fault, a west-side-down Tertiary normal fault with at least 5 kilometres of vertical displacement. The area is within the Hosmer thrust sheet, the structurally highest thrust package in the Western Ranges of the Rocky Mountains (Benvenuto and Price, 1979). Broad, open east-plunging folds dominate the structures in the immediate area.

The deposit is within the Aldridge Formation, a thick succession of mainly sandy turbidites and interbedded laminated siltites and argillites that forms the basal part of the Middle Proterozoic Purcell Supergroup (Höy, 1993). A number of extensive gabbroic sills and less commonly dikes, collectively referred to as the Moyie sills, intrude this turbidite package. These rocks are overlain to the east by mainly argillites and siltites of the upper Aldridge. Several percent of finely disseminated pyrite and pyrrhotite in the Aldridge result in typically rusty-weathering outcrops.

The Creston Formation, a shallow water platformal succession of mainly quartzites and siltites, is exposed east and upslope of Aldridge exposures. To the southeast, on the south side of the Bull River, the Creston Formation is overlain by tan-weathering carbonate rocks of the Kitchener Formation.

A number of small Cretaceous monzonite stocks intrude rocks of the Purcell Supergroup as well as younger Paleozoic platformal rocks. One of these is exposed just west of the Bull River deposit, intruding mainly carbonate rocks of the Devonian Fairholme Group.

BULL RIVER DEPOSIT (082GNW002)

The Bull River deposit is the largest and probably most important known mineralized zone on property of the Stanfield Holdings. It is described as a massive chalcopyrite vein and replacement deposit in a quartz-siderite gangue (B.C. MINFILE). Placid Oil Co. estimated total underground ore reserves, based on a cut-off grade of 1.0 percent copper and minimum thickness of 1.2 metres, as 664 000 tonnes containing 1.94% copper (Chiang, 1973). These reserves were concentrated in two main zones, the A zone with a strike length of 275 metres and a down dip extent of 90 to 175 metres, and the E zone, 150 metres in strike length and up to 275 metres dip extent. Neither gold nor silver content were reported in these reserve estimates.

The deposit includes a number of quartz-carbonate-sulphide veins in shear or breccia zones that generally trend easterly and dip steeply to the south (Photo 2).

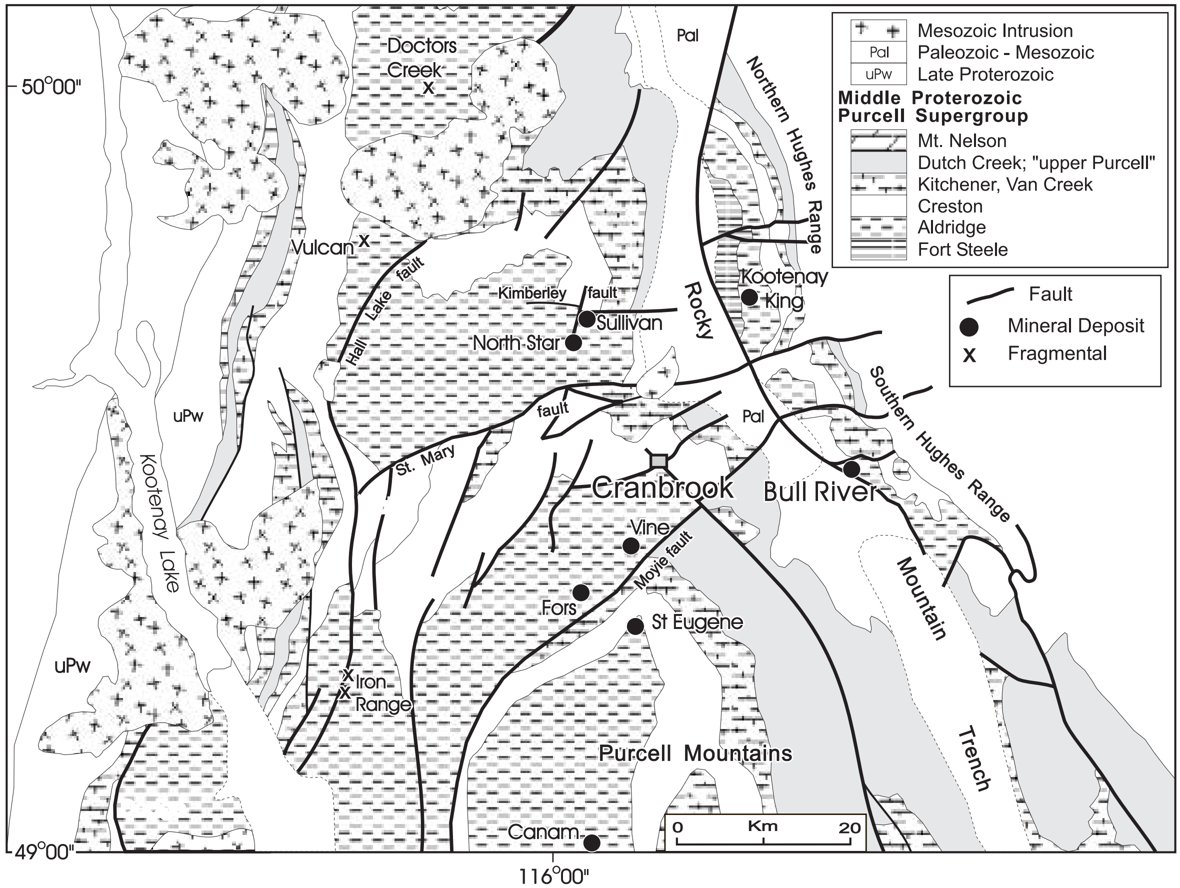

Figure 1. Regional geological map showing the location of the Bull River deposit, and other mineral deposits in the Middle Proterozoic Purcell Supergroup, southeastern British Columbia (base map after Höy *et al.*, 1995, in press)

TABLE 1
DESCRIPTION OF SELECTED SAMPLES, BULL RIVER DEPOSIT

Drill core	Lab no.	Location (depth)	Sample type	Description
BRU-99-11	54661	51.2 - 51.8 m	0.6 m split core	massive argillite, cut by thin qtz-cc veinlets
BRU-99-11	54662	51.8 - 52.6 m	0.8 m split core	vein breccia, with cp, po in qtz-sid gangue
BRU-99-11	54663	52.6 - 53.4 m	0.8 m split core	semi-massive po + cp in qtz-sid gangue; brecciated
BRU-99-11	54664	53.4 - 54.0 m	0.6 m split core	massive siltstone, with thin qtz-sid + po, cp veinlets
BRU-99-11	54665	81.5 - 82.0 m	0.5 m split core	massive cp-po with qtz-carb gangue
BRU-99-11	54666	82.0 - 82.5 m	0.5 m split core	massive cp-po with qtz-carb gangue; late sid veinlets
BRU-99-11	54667	83.1 - 83.7 m	0.6 m split core	semi-massive po + cp in qtz-sid gangue
BRU-99-11	54668	84.7 - 85.2 m	0.5 m split core	sericite-altered siltstone, cut by thin cp veinlets
BRU99-16	54669	37.3 - 37.8 m	0.5 m split core	altered quartzite?, cut by qtz-carb veinlets
BRU99-16	54670	37.8 - 38.5 m	0.7 m split core	massive qtz-sid vein, with po and cp
BRU99-16	54672	38.9 - 39.4 m	0.5 m split core	brecciated vein with cp, cut by carb veinlets
BRU99-16	54673	39.4 - 39.8 m	0.4 m split core	argillaceous quartzite, with minor blebs of po
BRU99-16	54674	122.8 - 123.1 m	0.3 m split core	qtz vein cut by po-cp veinlets
98L3-2	54650	91.1 - 91.7 m	0.6 m split core	massive qtz vein, with patchy cp-po
98L3-2	54651	100 - 100.4 m	0.4 m split core	massive cp, minor po in brecciated qtz vein
98L3-2	54653	98.6 - 99 m	0.4 m split core	argillaceous siltstone, with minor qtz-carb-cp veinlets
98L3-2	54654	100.9 - 102.0 m	1.1 m split core	massive cp, minor po; barite and qtz gangue
Underground samples				
BR-UG-1	54655	Level 3, west wall	grab	semi-massive, brecciated po-cp-carb vein
BR-UG-2	54656	Level 3, Stn 189, -3m	grab	semi-massive, brecciated po-cp-carb vein
BR-UG-3	54657	Level 3, Stn 189, -5m	grab	semi-massive, brecciated po-cp-carb vein
BR-UG-4	54658	Level 3, Crosscut	grab	semi-massive, brecciated po-cp-carb vein
BR-UG-5	54659	Level 5, Crosscut	grab	semi-massive, brecciated po-cp-carb vein

Abbreviations: qtz - quartz; cc - calcite; cp - chalcopyrite; po - pyrrhotite; sid - siderite; do - dolomite; carb - carbonate

Photo 1. A) Photo showing one of the open pits developed during mining of the Bull River deposit by Placid Oil Co. from 1971 to 1974.
B) Portal for underground development, Bull River deposit.

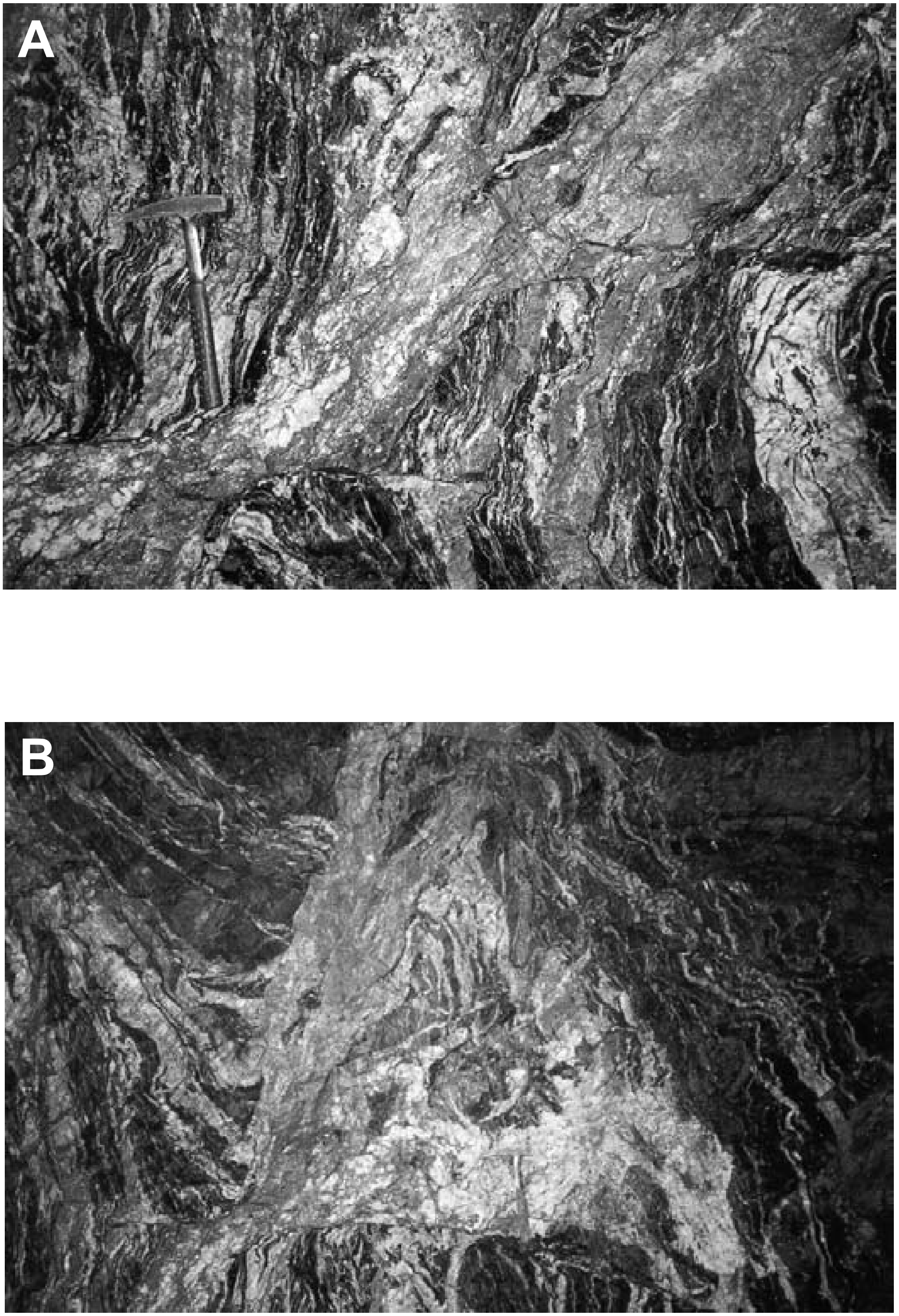

Photo 2. A) Semi-massive chalcopyrite-pyrrhotite vein, Bull River deposit; note multiple vein episodes, with quartz-carbonate gangue, and early ductile folding of veins followed by brittle deformation. Host is dark siliceous argillite of the Middle Proterozoic Aldridge Formation. B) Similar intense brittle deformation of chalcopyrite-pyrrhotite vein; note rock hammer scale.

Widths of these brecciated vein zones vary from a few centimetres to greater than ten metres, and are continuous for several hundred metres in strike length. Common sulphides include chalcopyrite, pyrite and pyrrhotite, with variable but generally minor galena and arsenopyrite, and trace tetrahedrite and interstitial native gold. The sulphides range from massive, irregular bodies within the vein system, to thin discontinuous veins and veinlets, and disseminations in host rocks. Secondary malachite and azurite occur locally. The main gangue minerals are quartz, siderite and dolomite. Sericite, quartz and chlorite alteration occurs within and adjacent to many of the sulphide veins.

SAMPLING AND ANALYTICAL PROCEDURES

Samples from four drill holes, shown by the Company logs to have intersected mineralized vein structures, and from mineralized zones underground were collected. Visible inspection of all samples, summarized in Table 1, confirmed that they are typical of the vein mineralization of the Bull River deposit.

Samples were crushed, split and pulverized in the Ministry of Mines' laboratory in Victoria, and sent to Chemex Laboratories, Vancouver, for gold assay by fire assay-atomic absorption spectrometry finish, and for copper and silver assay by aqua regia digestion-atomic absorption spectrometry. Several randomly selected samples, including a duplicate and a CANMET standard, were also sent to Loring Laboratories, Calgary, for gold by fire assay-atomic absorption spectrometry finish and to Activation Laboratories Ltd. Ancaster, Ontario for thermal neutron activation analysis. The Loring analyses are comparable to those reported by Chemex Laboratories. Thermal neutron activation gold values are similar to those obtained by five assay-atomic absorption spectrometry finish.

TABLE 2
ASSAYS OF MINERALIZED AND HOST ROCK SAMPLES FROM DRILL CORE AND UNDERGROUND, BULL RIVER DEPOSIT

		Chemex Lab			Loring Lab	Act Labs
	GSB Lab No	Au-FAA (g/t)*	Ag-ARAA (g/t)**	Cu-ARAA (%)**	Au-FAA (g/t)***	Au-INA (g/t)****
Drill hole samples	54662	0.030	4.8	0.45		0.048
	54663	0.145	7.5	0.72		0.171
	54665	0.440	102.5	16.95		0.551
	54666	0.180	55.8	8.75		0.305
	54667	0.960	97.2	13.85	0.650	0.650
	54670	0.070	9.3	0.55		
	54672	0.070	12.6	1.33		
	54650	0.390	18.0	2.41		0.445
	54651	0.550	65.4	8.01		0.630
	54654	4.770	161.5	13.00		4.690
	range	0.030-4.77g/t	4.8-161.5 g/t	0.45-16.95 %		
	median value	0.285 g/t	36.9	5.21		
Underground samples	54655	1.045	34.5	4.53	1.250	
	54656	0.160	18.0	2.61		
	54657	1.135	95.4	9.24		
	54658	0.290	26.7	2.92	0.291	
	54659	0.710	13.2	1.17		
	range	0.16-1.135 g/t	13.2-95.4 g/t	1.17-9.24 %		
	median value	0.71 g/t	26.7 g/t	2.92		
Table 2b: Assays of immediate host rock samples						
	54653	0.060	13.2	1.47		
	54661	<0.005	<0.3	0.01		
	54664	0.010	0.6	0.11		
	54668	0.010	2.4	0.37		
	54669	<0.005	0.3	<0.01	0.005	
	54673	<0.005	<0.3	0.01		
	54674	0.055	2.4	0.30	0.055	

Notes:
Preparation: Samples jaw-crushed, split and ring-mill pulverized at the Geological Survey Laboratory, Victoria.
*Au-FAA=Fire Assay-AAS Finish at Chemex Ltd. , Vancouver.
** Ag and Cu assay by aqua regia digestion-atomic absorption spectrometry at Chemex Ltd., Vancouver.
*** Au FAA Fire Assay finished at Loring Laboratory, Calgary.
****Au-INA Thermal Neutron Activation Laboratories Ltd., Ancaster, Ontario.

Results

Assay results from Chemex Laboratories are given in Table 2. Gold content in the 10 mineralized samples from drill core ranged from 0.030 to 4.77 grams/tonne, with a median value of 0.285 grams/tonne. The best intersection, a 1.1 metre interval of massive to semi-massive chalcopyrite and pyrrhotite, with barite and quartz gangue, contained 4.77 grams/tonne gold, 161.5 grams/tonne silver and 13 percent copper. Gold content in the five samples collected underground ranged from 0.16 to 1.135 grams/tonne, with a median of 0.71 grams/tonne. Silver content in these samples ranged from 13.2 to 95.4 grams/tonne and copper, from 1.17 to 9.24 percent.

A number of samples of host rocks immediately adjacent to the sheared and brecciated veins were also analyzed, in an attempt to determine if these contained finely dispersed gold. Although thin quartz-siderite-sulphide veins, minor disseminated sulphides and some vein alteration were apparent in these samples, gold content was low (Table 2). Sample 54653 contained 0.06 grams/tonne gold, probably concentrated mainly in a thin quartz-carbonate vein that contained visible chalcopyrite.

The correlation between gold and copper content, and the essential restriction of gold values to vein structures that contained visible chalcopyrite, suggest that gold is largely restricted to these veins.

CONCLUSIONS

The Bull River deposit is a brecciated and sheared copper-gold-silver prospect in the Middle Proterozoic Aldridge Formation in southeastern British Columbia. Mineralization appears to be restricted to a series of essentially east-trending, steep south-dipping veins just east of the Rocky Mountain trench. The veins vary from mainly massive chalcopyrite and pyrrhotite, to brecciated or sheared quartz-dolomite-siderite veins with variable sulphide content.

In 1998, a measured and indicated, mineral resource for the Bull River deposit of 5.3 million tonnes containing 2.25 percent copper, 36 grams/tonne silver and 12 grams/tonne gold was reported to the Ministry (de Souza, 1999). This resource calculation was based mainly on a volume of the exploration block, which contains both mineralized veins and host rock.

Assays of selected hand samples from underground and drill core, collected during this study, returned variable copper and silver content and trace to minor gold. Copper in these samples are comparable to those in original reserve calculations of Placid Oil Co. Gold values in the mineralized veins ranged from 0.03 grams/tonne to a maximum of 4.77 grams/tonne for a sample collected across 1.1 metres of core. These gold values are in the same order of magnitude as those recovered during the mining life of the deposit in the early 1970s. This brief study, using standard fire assay techniques with atomic absorption spectrometry finish, does not confirm the gold grades reported by the company for the Bull River deposit. Further and more detailed study, using standard techniques, would be necessary to confirm what grades are in fact present.

In summary, the Bull River deposit is fairly typical of the Cu±Ag quartz vein deposit class (I06; Lefebure, 1996). These veins are typically fault-controlled, commonly continuous for several hundred metres, and contain variable copper and silver content, with trace to minor gold.

ACKNOWLEDGEMENTS

We would like to acknowledge the cooperation of personnel of Gallowai Metal Mining Corp. and Bul River Minerals Corp. Ltd. while on a visit to the property in June, 1999.

REFERENCES

Chiang, M.C. (1973): A report on underground ore reserve estimation, Bull River Mine; internal report, *Placid Oil Company*, 16 pages.

Benvenuto, G.L. and Price, R.A. (1979): Structural evolution of the Hosmer thrust sheet, southeastern British Columbia; *Bulletin of Canadian Petroleum Geologists*, volume 27, pages 360-394.

de Souza, P. (1998): Stanfield Group-British Columbia Mineral Exploration Review 1998, *in a letter from Precious and General Metals, Calgary, December 1998.*

Grieve, D.A. (1980): Base metal deposits in the Libby Pondage Reserve area*; B.C. Ministry of Energy, Mines and Petroleum Resources*; Geological Fieldwork 1979, Paper 1980-1, pages 115-117.

Höy, T. (1993): Geology of the Purcell Supergroup in the Fernie west-half map area, southeastern British Columbia; *B.C. Ministry of Energy, Mines and Petroleum Resources*, Bulletin 84,157 pages.

Höy, T., Price, R.A., Legun, A., Grant, B., and Brown, D.E. (1995): Purcell Supergroup, southeastern British Columbia, compilation map, scale 1:100 000; *B.C. Ministry of Energy, Mines and Petroleum Resources*, Geoscience Map 1.

Höy, T., Anderson, D., Turner, R.J.W. and Leitch, C.H.B. (in press): Tectonic, magmatic and metallogenic history of the early synrift phase of the Purcell basin, southeastern British Columbia; *in* The Sullivan Deposit and Its Geological Environment, J.W. Lydon, T. Höy, M. Knapp, and J.F. Slack, Editors, Sullivan Volume; *Geological Association of Canada / Mineral Deposit Division,* Special Publication No. 1..

Lefebure, D.V. (1996): Cu ± Ag quartz veins (I06); *in* Selected British Columbia Mineral Deposit Profiles, Lefebure, D.V. and Höy, T., Editors, *B.C. Ministry of Energy and Mines*, Open File 1996-13, pages 71-73.

Schroeter, T.G. (1999): British Columbia 1998 Mineral Exploration Review; *in* Exploration and Mining in British Columbia 1998; *B.C. Ministry of Energy, Mines and Petroleum Resources,* pages 1-17.

Schroeter, T.G., Cathro, M., Lane, B., Pinsent, R., Ryan, B., Simandl, G., Wilton, P. and Wojdak, P. (2000): British Columbia Mineral Exploration Review 1999; *B.C. Ministry of Energy, Mines and Petroleum Resources,* Information Circular 2000-1.

Wilton, H.P. (1999): Kootenay Region; *in* Exploration and Mining in British Columbia 1998; *B.C. Ministry of Energy, Mines and Petroleum Resources,* pages 65-75.

B.C. Regional Geochemical Survey: 1999 Field Programs

By Wayne Jackaman, Stephen Cook and Ray Lett

KEYWORDS: *Applied geochemistry, mineral exploration, drainage sediments, orientation studies, Regional Geochemical Surveys.*

INTRODUCTION

The Exploration Services and Information Section of the British Columbia Geological Survey Branch is responsible for administering the Regional Geochemical Survey (RGS) program and providing complimentary research and orientation studies designed to promote the effective use of exploration geochemistry by industry. Results are used by industry to pinpoint exploration opportunities and by government for resource management, land-use planning and environmental assessments. The section's contribution of applied geochemical information to the exploration community during the 1999 field season is summarized in this paper.

REGIONAL GEOCHEMICAL SURVEY PROGRAM (RGS)

RGS Archive Program

Since 1975, over 45,000 drainage sediment and water samples have been collected and analyzed by the RGS Program. Starting in 1991, the RGS Archive program has routinely upgraded the RGS database with previously unavailable analytical information. Sediment samples saved from surveys conducted from 1976 to 1985 have been re-analysed by instrumental neutron activation analysis (INAA) for gold and twenty-five other metals not included as part of the original data releases. To date, the RGS Archive Program has compiled and published this new data for over 18,735 samples covering 15-1:250 000 NTS map sheets. The most recent data release included results from 1235 sediment samples collected during a 1979 Quesnel Lake (NTS 93A) RGS Program. New analytical data plus original field and analytical results were published in June, 1999 (Jackaman, 1999). RGS archive gold data for Atlin (NTS 104N), Jennings River (NTS 104O) and McDame (NTS 104P) 1:250 000 survey areas are scheduled for release in the summer of 2000 (Jackaman, in preparation).

Drainage Sediment and Water Surveys

Four reconnaissance-scale drainage sediment and water surveys were conducted in the Central Coast and Queen Charlotte Islands during 1999 (Figure 1). Lake sediment and water samples were collected from 133 sites covering an area of over 700 square kilometres near Cape Caution (92L/14, 92M/3,4). In the Khutze River area (103H/1,2,7), sediment and water samples were collected from 111 sites covering an area of around 800 square kilometres. Moss sediment and water samples were collected from 94 sites covering an area of approximately 800 square kilometres south of Bella Coola (93D/1,2,7,8). On the Queen Charlotte Islands, moss sediment and water samples were collected from 184 sites covering an area of over 1700 square kilometres (103F/1, 103G/4, 103F/7,8,9,10).

These surveys are designed to provide baseline regional geochemical data that can be used in the evaluation of the mineral potential of the target areas. Funded under the government's Corporate Resource Inventory Initiative (CRII), these surveys are part of the Ministry of Energy and Mines' contribution to the Central Coast and Queen Charlotte Island Land Resource Planning process (Pinsent, this volume). The projects are also an extension of the RGS program, and the data would be incorporated into any future surveys conducted in these regions. Results are expected to be published early in 2000.

GEOCHEMICAL RESEARCH AND ORIENTATION STUDIES

Ancient Pacific Margin NATMAP Project

Exploration successes for volcanogenic massive sulphide (VMS) deposits in Yukon-Tanana Terrane *(e.g.* Kudz Ze Kayah, Wolverine) and Slide Mountain Terrane (*e.g.* Ice) rocks of the southern Yukon have focused attention on the possible VMS potential of correlative rocks of the Big Salmon Complex in northern British Columbia. As no detailed geochemical studies had been previously conducted in this area to characterize the element signatures and geochemical dispersal of either VMS deposits or their felsic volcanic host rocks, preliminary field studies were initiated here during the summer of 1999 as part of the Ancient Pacific Margin NATMAP Project (Cook and Pass, this volume). A series of additional papers describing results of NATMAP bedrock and surficial geology mapping programs conducted in this area are also found in this volume.

The geochemical studies project has two components: interpretation of available RGS data for the study area and for adjacent terranes, and geochemical case

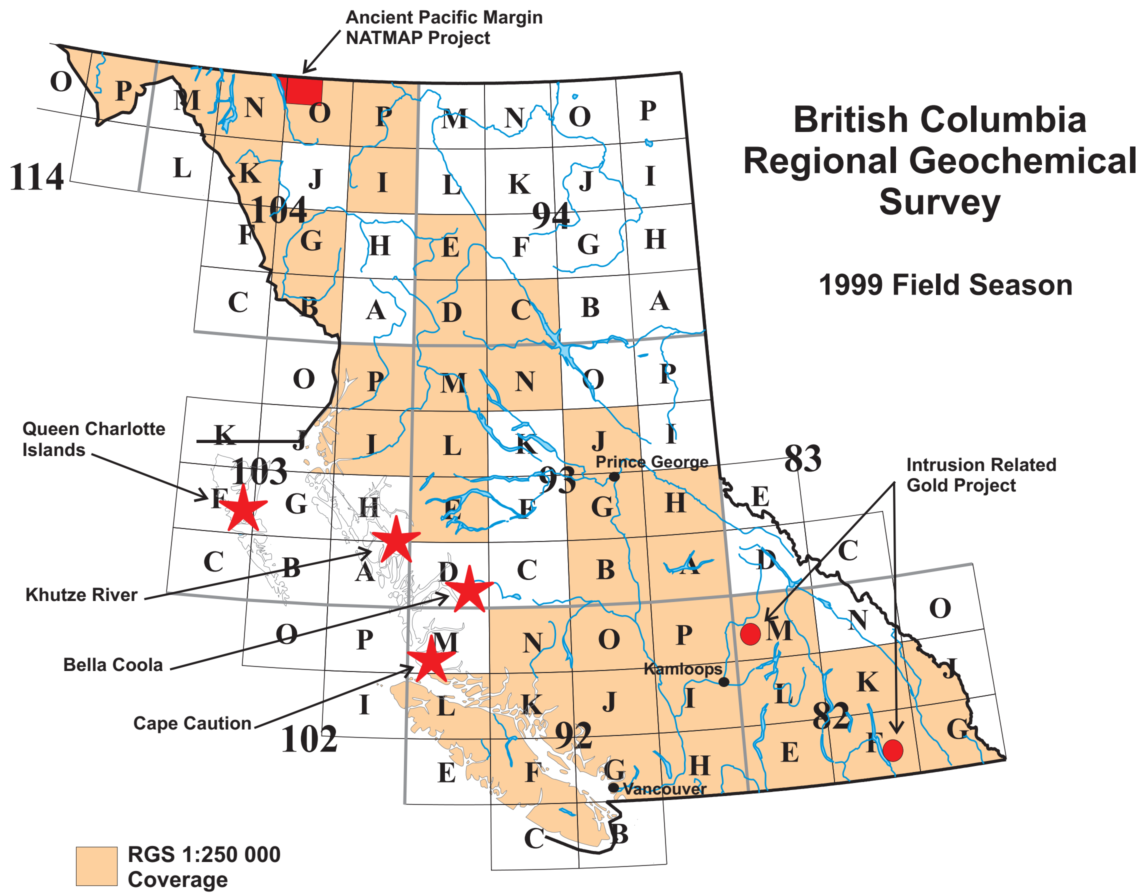

Figure 1. Location map of RGS and related projects.

studies. Both interpretive and field studies concentrate on that part of the Atlin (NTS 104N) and Jennings River (NTS 104O) map areas immediately east of Teslin Lake and just south of the Yukon border, where most of the 1999 NATMAP bedrock and surficial geology mapping programs were conducted. RGS stream sediment and lake sediment data is available for both the Atlin and Jennings River areas, and some preliminary interpretive results are shown by Cook and Pass (this volume). The objective of the case studies is to characterize the geochemical responses of known VMS showings and felsic metavolcanic packages in the area. Case studies were conducted in several areas, notably in the vicinity of meta-exhalative crinkled chert units identified by Mihalynuk *et al.* (1998), the Arsenault copper prospect (MINFILE 104O 011), and several small copper showings. A variety of surficial media were collected here, including stream sediments, moss mat sediments, stream waters, soil profiles, vegetation and rock, in an attempt to characterize the geochemical signature and dispersal of VMS-related metals at these sites. Case studies were also conducted in groups of adjoining watersheds in two parts of the Nisutlin Plateau and Cassiar Mountains which have anomalous RGS Zn-Cu-Pb-Ag-Co-Fe results. The geochemistry of stream waters and suspended stream sediments in these areas is the object of a University of Victoria B.Sc. thesis by Heidi Pass.

Cook and Pass (this volume) provide a brief outline of some preliminary geochemical results for soil profiles and rock samples. Geochemical data for other sample media are pending, and will be published as it becomes available In addition, Dixon-Warren and Hickin (this volume) provide geochemical results for a suite of till samples. The development of recommendations as to the most effective geochemical exploration methods for VMS deposits in the Big Salmon Complex area will be an important outcome of this project.

Intrusion Related Gold Project

Discovery of gold mineralized quartz veins related to Cretaceous granitic intrusions in Alaska and the Yukon has generated new exploration interest for similar deposits in British Columbia. Deposits of this type are difficult to locate using traditional stream sediment surveys because associated metals such a gold, tin, bismuth and tungsten are relatively immobile and tend to be erratically distributed in the sediment. In addition, the metal anomaly contrast may be subdued because of dilution from barren glacial material. Stream geochemical studies carried out to better understand this type of deposit in B.C. are described by Lett and Jackaman (this volume).

ACKNOWLEDGMENTS

Excellent assistance and program support were provided by Gary Payie and Travis Ferbey.

REFERENCES

Cook, S.J. and Pass, H.E. (2000): Preliminary Results of Geochemical Studies for VMS deposits in the Big Salmon Complex, Yukon-Tanana Terrane, Northern British Columbia (104N/9, 16; 104O/11, 12, 13, 14); *in* Geological Fieldwork 1999, *B.C. Ministry of Energy and Mines*, Paper 2000-1, (this volume).

Dixon-Warren, A. and Hickin, A. (2000): Surficial Mapping and Till Geochemical Studies in the Jennings River Map Area, Northwestern British Columbia; *in* Geological Fieldwork 1999, *B.C. Ministry of Energy and Mines*, Paper 2000-1, (this volume).

Jackaman, W. (1999): British Columbia Regional Geochemical Survey - Quesnel Lake (93A), *B.C. Ministry of Energy and Mines*, BC RGS 50.

Jackaman, W. (in preparation): British Columbia Regional Geochemical Survey - Atlin (104N), *B.C. Ministry of Energy and Mines*, BC RGS 51.

Jackaman, W. (in preparation): British Columbia Regional Geochemical Survey - Jennings River (104O), *B.C. Ministry of Energy and Mines*, BC RGS 52.

Jackaman, W. (in preparation): British Columbia Regional Geochemical Survey - McDame (104P), *B.C. Ministry of Energy and Mines*, BC RGS 53.

Lett, R.E. and Jackaman, W. (2000): Geochemical Exploration Techniques for Intrusive Hosted Gold Deposits in Southern B.C. (parts of 82M/4, 5, 6 and 82F/7); *in* Geological Fieldwork 1999, *B.C. Ministry of Energy and Mines,* Paper 2000-1, (this volume).

Mihalynuk, M., Nelson, J.L. and Friedman, R.M. (1998): Regional Geology and Mineralization of the Big Salmon Complex (104N/NE and 104O/NW); *in* Geological Fieldwork 1997, *B.C. Ministry of Employment and Investment*, Paper 1998-1, pages 6-1 to 6-20.

Pinsent, R.H. (2000): Mineral Potential of the Southern Coast Belt, Cape Caution Area, British Columbia (92L, 92M); *in* Geological Fieldwork 1999, *B.C. Ministry of Energy and Mines,* Paper 2000-1, (this volume).

Pinsent, R.H. (2000): Mineral Potential of the Northern Coast Belt, Khutze River Area, British Columbia (103H); *in* Geological Fieldwork 1999, *B.C. Ministry of Energy and Mines,* Paper 2000-1, (this volume).

Mineral Potential of the Northern Coast Belt, Khutze River Area, British Columbia (103H)

By R.H. Pinsent

KEYWORDS: *Economic geology, structure, intrusion-related, shear-hosted vein, gold, silver, copper, staking records, Khutze River, Aaltanhash River, regional stream sediment survey, Surf Inlet, Hunter, Western Copper.*

INTRODUCTION

This report discusses the geology and mineral potential of a segment of the Coast Mountains, east of Princess Royal Island (in NTS area 103H) termed the Khutze River area. The information presented is based on public domain reports and old staking records. In 1999, a regional stream sediment survey was conducted in the area by the Ministry of Energy and Mines. The results of the geochemical survey will be reported separately. The project was funded under the Provincial Government's Corporate Resource Inventory Initiative (CRII), as part of the Ministry's contribution to the Central Coast Land and Coastal Resource Management (CCLCRMP) planning process.

The area is approximately 150 kilometres south of the community of Terrace and includes the Khutze and the Aaltanhash river drainages (Figure 1). The terrain is varied and locally, exceedingly rugged. It includes mountain peaks, alpine glaciers, wooded slopes and flat bottomed valleys. Elevations range from sea level to 1500 metres. Although the coastal portion is readily accessible by boat or float plane, much of the area is accessible only by helicopter.

PREVIOUS WORK

Ministry records indicate that there was a considerable amount of exploration and mine development along the British Columbia coast in the late 1800s and early 1900s. This is best illustrated by the work carried out before the Second World War at the Surf Inlet and Pugsley mines (MINFILE 103H 027) located west of the Khutze River area, on Princess Royal Island. The combined operation is reported to have produced 918 128 tonnes of quartz vein material containing 12 095 368 grams of gold, 6 258 235 grams of silver and 2 834 461 kilograms of copper between 1902 and 1943.

The Khutze River area, on the east side of Graham Reach was mapped at 1:250 000-scale by the Geological Survey of Canada in the mid 1960s as part of its Coast Mountain Project (Roddick *et al*., 1965; Roddick, 1970). This was well after the main period of exploration on the coast, which was conducted without the benefit of good quality maps.

GEOLOGY

The simplified geological map of the Khutze River area shown in Figure 1 is based on government mapping as shown on The MapPlace website (Bellefontaine and Alldrick, 1994). The area is underlain by plutonic rocks and by pendants of deformed and metamorphosed volcanic and sedimentary rocks. Although it has not been mapped in detail, the geology appears to be fairly typical of the core region of the Coast Mountains.

The stratabound rocks occur in two northwesterly-trending belts. One belt comprises a minor amount of thinly laminated micaceous quartzite, crystalline limestone, skarn, and greenstone and schist of possible Paleozoic age (OTrAs). The greenstone and schist is intimately associated with a gneissic and dioritic migmatite complex (MKdn) near the mouth of Khutze Inlet. The other belt is a broad zone of "granitoid gneiss" that includes gneissic quartz diorite, rusty fine-grained gneiss and schist. It is well exposed in the mountains at the head of the Khutze River (PTcg). Some of the more schistose components of the "granitoid gneiss" are clearly sedimentary as they include a recognizable band of thick-bedded recrystallized limestone (PTcs).

The plutonic rocks include the migmatite unit (MKdn) found in the complex referred to above and also broad, northwesterly trending zones of hornblende biotite-rich quartz diorite (MKqd and ETqd), biotite hornblende-rich granodiorite (MKgd) and both biotite quartz rich and leucoquartz monzonite (MKqm, LKqm). Although many of the plutonic rock ages are uncertain, contact relationships suggest the early formation of a central belt of quartz diorite followed by later intrusion of granodiorite and a still later intrusion of quartz monzonite. Most of the plutonic rocks to the southwest of the granitoid gneiss unit are reported to be Middle Cretaceous in age. Those to the northeast may be Tertiary (Roddick, 1970).

The rock units display a broad northwesterly trend and the western contact of the "granitoid gneiss" unit appears to be defined by a major northwesterly-trending fault (Figure 1). North to northeasterly trending faults have not been mapped in the area; however, lineaments

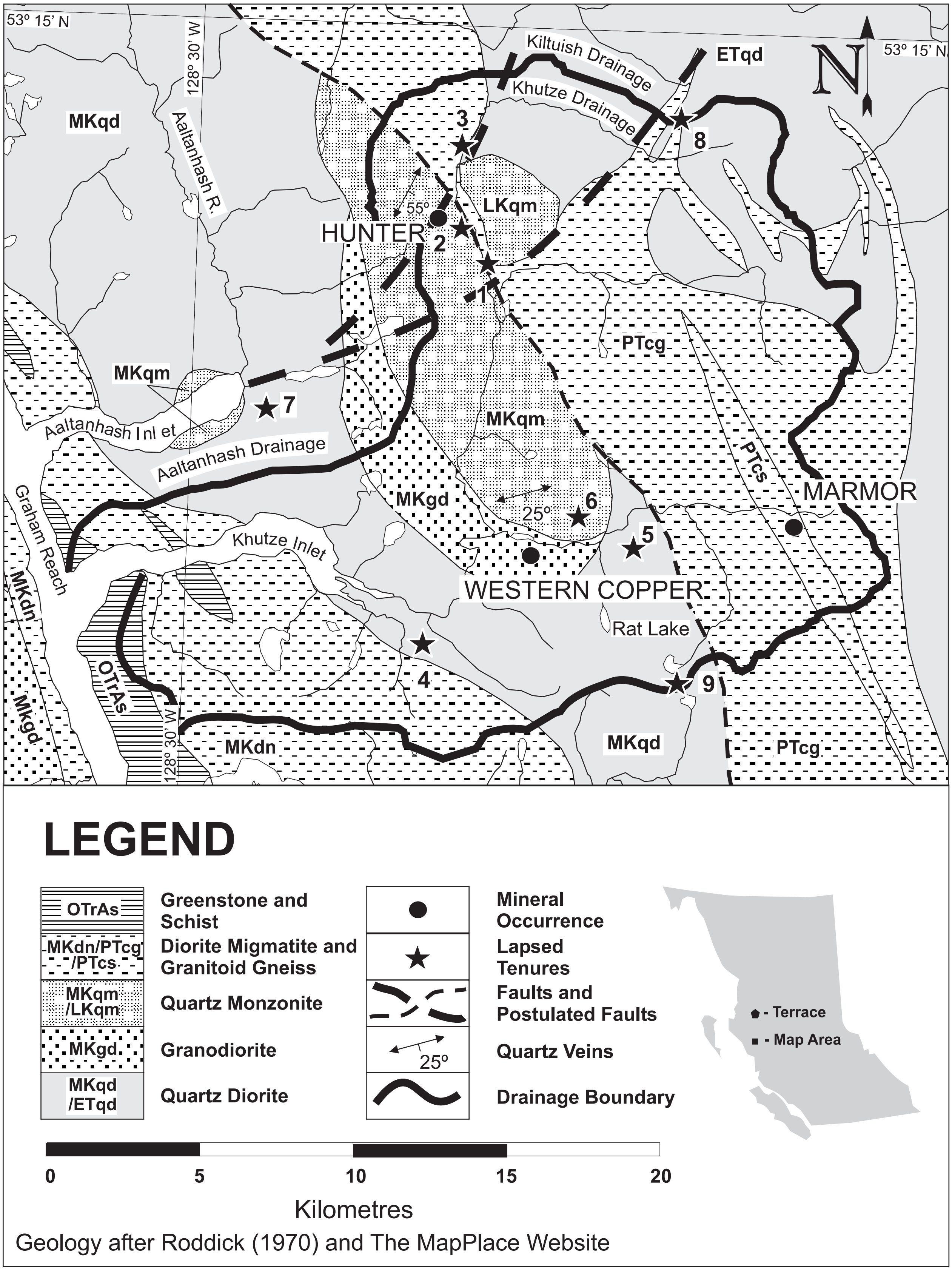

Figure 1. Generalized geology of the Khutze River area showing the location of mineral occurrences and lapsed tenure sites.

and contact relations suggest that there may be several within the map area.

MINERALIZATION

There are three occurrences in the Khutze River drainage listed in the Ministry's MINFILE database (Figure 1). Two are metallic mineral occurrences (Western Copper, 103H 033 and Hunter, 103H 034), and one is a limestone deposit (Marmor, 103H 063). Figure 1 also shows nine "areas of past exploration interest". These are sites that are known to have been staked at some point over the past seventy years but are now lapsed and are no longer located on tenure maps. In most instances, there is insufficient information available on the site to warrant its inclusion as an occurrence in the Ministry's MINFILE database.

The present report is primarily concerned with the two metallic prospects, both of which show enrichment in copper, gold and silver.

Hunter (MINFILE 103H 034)

The Hunter gold deposit (latitude 53º 11″ 39′ N, longitude 128º 23′′ 06′ W) is on the north fork of the Khutze River approximately 22 kilometres from tidewater, at the head of Khutze Inlet, 150 kilometres from Terrace. The deposit is covered by crown granted mineral claims located in the early 1900s.

The Hunter deposit consists of shear-hosted quartz veins which were located in 1927 and prospected and trenched in the late 1920s and early 1930s. The first underground development took place in 1940. The then owners drove a decline for 47 metres into the River vein and drifted along it for a further 57 metres. The following year, they drove an adit for 144 metres on the "Main" vein. The old workings were rehabilitated and the veins were sampled in 1980. Arnhem Resources Inc. further explored the property in 1983. The company mapped the area, resampled the veins and conducted geochemical surveys (Scott, 1984a). It continued the program the following year, diamond drilling seven holes for an aggregate depth of 737 metres (Scott, 1984b).

The Hunter property straddles the north fork of the Khutze River in the floor of a deep, northerly to northwesterly trending, "U"-shaped valley formed along the trace of a section of the possible fault on the southwestern side of the granitoid gneiss (PTcg) unit. The property straddles a contact between quartz monzonite (MKqm) and "granitoid gneiss" (PTcg) (Figure 1).

The geology is described by Mandy (1932) and by Scott (1984a,b). The principal feature is a north to northwesterly trending pendant (or tectonic sliver) of biotite gneiss that underlies the floor of the valley. The biotite gneiss pendant appears to be largely metavolcanic in origin, although it is highly deformed and displays a pronounced north to northwesterly trending foliation. The pendant hasn't been fully delineated, but it is about 700 metres wide. It is bounded by granitic gneiss and is cut by a variety of plutonic rocks, including foliated quartz diorite and quartz monzonite, and non-foliated aplite and pegmatite.

The mineralized quartz veins are markedly discordant to the foliation in the pendant and the foliated plutonic rock. The veins display north to northeasterly strikes and steep to moderate easterly dips. For example, the "Main" vein is reported to have a strike of between 20 and 35 degrees and a dip of 55 to 70 degrees to the southeast. The cluster of veins, as a whole, also displays a pronounced northeasterly trend. It has been traced intermittently for a distance of approximately 1.5 kilometres from the "Main" zone, which cuts granite gneiss on the west side of the Khutze River, to the River zone which cuts biotite gneiss on the east side. Several veins are, at least in part, located in or along narrow pegmatitic dikes (Scott, 1984a,b).

The Hunter veins pinch and swell along strike, but rarely attain widths in excess of 0.25 metre. Some of the veins display minor amounts of wall-rock alteration. Adjacent host rocks are bleached and enriched in pyrite, chlorite, sericite, carbonate and clay. The veins are composed of milky-white, massive quartz, a variable amount of pyrite and lesser amounts of chalcopyrite. The gold content of the veins appears to increase with an increase in the pyrite content. The higher values, in the order of several tens of grams per tonne gold, are most commonly found in sections of vein that contain semi-massive to massive sulphides. These appear to be best developed near flexures in the vein system (Scott, 1984a,b). Mandy (1932) indicates that gold to silver ratios increase with an increase in elevation. The River vein has a ratio of approximately 1:0.5. The "Main" vein, higher up the valley wall, has a ratio of approximately 1:1.5. A three-tonne sample, collected from an open cut on the River vein in 1933, yielded 933 grams of gold, 373 grams of silver and 40 kilograms of copper.

In 1984, Arnhem Resources Inc. established a resource of 94 338 tonnes grading 12 grams per tonne gold, at a mine width diluted to 1.2 metres (MINFILE).

Western Copper (MINFILE 103H 033)

The Western Copper gold deposit (latitude 53º 05″ 49′ N, longitude 128º 20″ 06′ W) crops out on a precipitous mountain side on the east fork of the Khutze River, approximately eight kilometres from the head of Khutze Inlet and 160 kilometres south of Terrace. It is covered by a cluster of Crown Granted and reverted Crown Granted mineral claims.

The property was located in 1908 and saw considerable development over the next few years and again in the mid-1920s. The work included construction of a narrow-gauge railway from the head of the inlet to the property, construction of camps connected by tramways and ladder-assisted trails at three elevations. Also included was the driving of approximately 370 metres of drifts and crosscuts and 245 metres of shafts and raises. This early work was followed by more limited development in the early 1930s (Mandy, 1932). After a prolonged break, Noranda Exploration Company Limited examined the property and carried out a stream sediment survey in the area in 1987 (Maxwell, 1987).

The Western Copper deposit is a vein occurrence in a biotite, hornblende granodiorite intrusion (MKgd) that is cut by aplite and pegmatitic dikes. The principal vein occupies a joint in a shear zone that strikes 070 degrees and dips at 20 to 30 degrees to the south, into the north-facing wall of the Khutze River canyon. The vein has been traced for approximately 1200 metres along strike. It pinches and swells, and locally attains a maximum width of approximately 2.0 metres. The wall-rocks locally exhibit minor amounts of quartz and sericite alteration (Mandy, 1932).

The vein is described as being "of pegmatitic affinity" (Mandy, 1932). It contains quartz, feldspar and variable amount of sulphides. Discrete zones of massive sulphides, predominantly pyrite and chalcopyrite with lesser chalcocite and covellite, grade outward into zones of increasingly more sparsely disseminated mineralization. These zones are separated by sections of quartz vein that contain intermittent narrow streaks of high-grade mineralization. Although these streaks produce values of many tens of grams of gold and silver per tonne and several percent copper, they are commonly only a few centimetres in width. According to Mandy, the mineralization may be zoned. Streaks of sulphide found at the west end of the vein contain more chalcopyrite than those at the east end. The latter are more pyritic but are equally enriched in gold and silver. The richest lens, so far identified, has a strike length of 10 metres and a width of approximately 1.5 metres. Its down dip extent has yet to be determined (Mandy, 1932).

According to MINFILE, a small, 215 - tonne bulk sample, collected in 1928 and 1929, yielded 5319 grams of gold, 45 193 grams of silver and 30 812 kilograms of copper.

Lapsed Tenures

In addition to the MINFILE occurrences, Figure 1 shows the location of nine lapsed claim groups. Three were staked by C.W. and J.M. Meldrum between 1931 and 1940, while Meldrum and Associates were working on the Hunter property. They include two (1, 2) that follow the trace of the main northwesterly trending structure to the southeast of the Hunter prospect and one (3) that straddles a possible north-northeasterly trending fault contact a short distance to the northeast of the deposit (Figure 1).

Although there is no record of work conducted on the Western Copper deposit in the 1960s, staking records indicate that Mr. C. W. Hunt staked claims to the west (4) and east (5) of the main block of Western Copper crown grants in 1968. At the time, the south side of the Khutze River was covered by claims for over ten kilometres, from south of the head of Khutze Inlet in the west to well beyond Rat Lake in the east. At the same time, Mr. Hunt staked another block (6) on the mountain across the east fork of the Khutze River from Western Copper (Figure 1).

In 1928, Mr. E. C. Brooke staked three units (7) immediately to the southeast of the head of Aaltanhash Inlet. The tenures indicate no apparent relation to known mineralization, however they display an easterly to northeasterly trend and they appear to be approximately on strike with the Hunter vein system. They are also close to a small plug of probably post-tectonic, leucocratic monzonite or granite (Figure 1).

An eighth group (8) was staked by United Pacific Gold Limited in 1988. It covers the ridge that separates the headwaters of the north fork of the Khutze River from the headwaters of the Kiltuish drainage. The tenures cover a postulated faulted contact between "granitoid gneiss" and quartz diorite. The location and size of the tenure group suggests staking in response to anomalous results in a stream geochemical survey.

The ninth lapsed tenure (9) was also staked by J. M. Meldrum in 1931. It straddles the height of land between two small lakes on the southern boundary of the Khutze drainage.

STREAM GEOCHEMISTRY

In July, 1999, the Geological Survey Branch conducted a stream sediment and water sampling survey in the Khutze River area. It sampled 111 sites over an area of approximately 800 square kilometres including the Khutze and adjacent Aaltanhash River drainages. The program is described by Jackaman *et al*. (1999), this volume.

SUMMARY AND CONCLUSION

The Hunter and Western Copper deposits are post-tectonic, shear-hosted vein deposits that formed in approximately northeasterly trending fractures that are markedly discordant to the regional trend of the plutonic and metamorphic rocks in the area. They are both associated with aplitic and pegmatitic dikes and both contain copper, gold and silver. In each case, the wall-rocks exhibit minor amounts of propylitic alteration. The deposit style and composition is consistent with intrusion-related vein-type mineralization.

Although major northeasterly trending faults have not yet been mapped in the Khutze River area, topographic and geological relations suggest that there may be a significant, post-orogenic, north-northeasterly to northeasterly trending fault and fracture system crossing the drainage. This may have influenced the location of mineralized veins, such as those found at the Hunter and Western Copper occurrences (Figure 1). The fault and fracture directions are found in the regional drainage pattern and in the contact relations displayed between the granitoid gneiss unit and the adjacent quartz diorite and quartz monzonite plutons. Figure 1 illustrates two postulated faults that may have influenced the distribution of rock types and mineralization in the Khutze and Aaltanhash River drainages.

Although the aplitic and pegmatitic dikes found at the two showings have yet to be age-dated, they are described as being undeformed. They are postulated to be relatively young, possibly reflecting intrusion of felsic rocks within broad north-northeasterly to northeasterly trending zones of weakness underlying the drainage. The small leucocratic quartz monzonite pluton that straddles Aaltanhash Inlet may be a late-stage, high-level intrusion emplaced along similar, easterly to northeasterly trending structures.

There is no way of knowing why the lapsed claim groups in the area were staked, but it is interesting to note that several fall on, or are close to, postulated structures (Figure 1). This may reflect a prospector interest in similar style mineralization.

The style and composition of the mineralization at the Hunter and Western Copper occurrences suggest that they are probably related to high-level, Tertiary intrusions. If they are, the geology of the Khutze River area would appear to indicate considerable potential for additional quartz vein-hosted gold deposits and possibly also for porphyry copper-style deposits.

ACKNOWLEDGMENTS

The author acknowledges the help and assistance of numerous ministry staff including, Tom Schroeter, Ward Kilby, Rolf Schmitt , Wayne Jackaman, Dorthe Jakobsen and Brett Gilley in the development of this report.

REFERENCES

BCGSB, The MapPlace.Http://www.em.gov.bc.ca/geology

Bellefontaine, K. and Alldrick, D. (1994): Geological Compilation of the Mid-Coast Area, Southwestern British Columbia; B.C. Ministry of Energy Mines and Petroleum Resources, Open File 1994-17.

Jackaman, W., Cook, S.J. and Lett, R.E. (1999): B.C Regional Geochemical Survey: 1999 Field Programs; in Geological Fieldwork 1999, B.C. Ministry of Energy and Mines, Paper 2000-1, (this volume).

Mandy, J.T. (1932): Northwestern Mineral Survey District (No. 1); Lode-gold Deposits of British Columbia; British Columbia Department of Mines Bulletin #1, pp. 14-42.

Maxwell, G. (1987): Geochemical Orientation Survey, Western Copper Group, Skeena Mining Division; B.C. Ministry of Energy and Mines, Assessment Report #15 886, 8 pages, plus maps.

MINFILE 103H, Jones, L.D. and Duffett, L.L. (1989): Douglas Channel Map Area; B.C. Ministry of Energy, Mines and Petroleum Resources, MINFILE, release Sept. 1989.

Roddick, J.A., A.J. Baer, and W.W. Hutchison (1965): Coast Mountain Project; British Columbia; Geological Survey of Canada, Paper 66-1, Report of Activities May to October, 1965, pp. 80-85.

Roddick, J.A. (1970): Douglas Channel and Hecate Strait; Geological Survey of Canada, Map 23 - 1970, Paper 70-41.

Scott, T.C. (1984a): Geological and Geochemical Assessment Report on the Hunter Property, Skeena Mining Division; B.C. Ministry of Energy and Mines, Assessment Report #11 937, 32 pages, plus maps.

Scott, T.C. (1984b): Geological Assessment of the Main Vein area, Hunter Property, Skeena Mining Division; B.C. Ministry of Energy and Mines, Assessment Report #13 398, 23 pages, plus maps.

Mineral Potential of the Southern Coast Belt, Cape Caution Area, British Columbia (092L, 092M)

By R.H. Pinsent

KEYWORDS: *Economic geology, shear-hosted, quartz vein, gold, lead, zinc, silver, Cape Caution, regional stream sediment survey, Drury Inlet, Nugent Queen, Nugget Queen/Bobmac, Bonanza.*

INTRODUCTION

This report discusses the geology and mineral potential of a segment of the southern Coast Mountains, near Cape Caution (straddling NTS areas 092L, 092M). The information presented is based on field visits, public domain reports and old staking records. The area was covered by a Ministry of Energy and Mine's lake sediment survey in 1999. The program is discussed in Jackaman *et al*. (1999), this volume. The project was funded under the Provincial Government's Corporate Resource Inventory Initiative (CRII) as part of the Ministry's contribution to the Central Coast Land and Coastal Resource Management (CCLCRMP) planning process.

The Cape Caution area covers approximately 1200 square kilometres of Hecate Lowland on the northeast side of Queen Charlotte Strait, 20 kilometres northeast of the northern-most tip of Vancouver Island (Figure 1). It is low-lying (less than 700 metres elevation) but highly irregular in topography and, locally, extremely rugged. The terrain is glaciated and over-deepened valleys have been flooded to create a patchwork of steep-sided marine sounds, inlets, peninsulas and islands.

The area is readily accessible by boat, float plane or helicopter from Port Hardy or Port McNeill; however, the bush is thick over much of the area and there are few helicopter landing sites. There has been a considerable amount of logging in the Mount Bullock area, at the north end of Drury Inlet and in the Bamford Lagoon area. These areas are readily accessible by road from ocean-based forestry load-out sites. Road construction has, exposed a considerable amount of rock.

PREVIOUS WORK

Ministry records, including Annual Reports, indicate that there was a considerable amount of exploration interest in the southern coastal region in the late 1800s and early 1900s. This is best exemplified by the work carried out on the Doratha Morton, Alexandria and other Crown Granted mineral claims in the Loughborough Inlet area, approximately 150 kilometres to the southeast of Cape Caution.

Much of the early exploration in the area was carried out without the benefit of geological maps. The Geological Survey of Canada carried out reconnaissance surveys along the coast in the early 1900s and produced a brief description of the geology of the Cape Caution area in 1909 (Graham, 1909). It did not map the area in any detail until the 1960s, when it was covered by the Coast Mountain Project (Roddick and Hutchison, 1967). The geology of the southern part of the area (Alert Bay Map Sheet 092L) is described at 1:125 000-scale by Roddick (1980) and the northern part (Rivers Inlet Map Sheet 092M), is described at 1:250 000-scale by Roddick (1996). Access to the inland portion of the map area was exceedingly difficult in the 1960s and Roddick (1980) notes that individual map units commonly include a variety of other rock types. Despite their common provenance, there are significant inconsistencies in nomenclature between the two maps covering the northern and southern parts of the area.

GEOLOGY

A simplified geological map of the Cape Caution area and adjacent parts of Vancouver Island taken from government and industry mapping (Bellefontaine and Alldrick, 1994) is shown in Figure 1. The mainland portion is underlain by stratabound rock pendants, diorite complexes and cross-cutting plutonic rocks.

The Cape Caution area is underlain by subparallel belts of pendant rocks, diorite complex material and massive to foliated intermediate plutonic rocks. Together, they define a broad regional fabric with a well-defined northwesterly trend. The rocks display both tectonic and intrusive contacts.

A major northeasterly dipping thrust fault that extends from Drury Inlet in the south to Belize Inlet in the north, a distance of approximately 50 kilometres, is shown in Figure 1. The Nenahlmai thrust has juxtaposed a five-kilometre wide package of interleaved pendant, diorite complex and younger plutonic rock against a large body of locally schistose footwall granodiorite and quartz diorite of the Burnett Bay Pluton (Roddick, 1996).

Locally, the rocks in the Cape Caution area display a pronounced northeasterly to easterly fracture set that is subparallel to a dominant set of local lineations. The

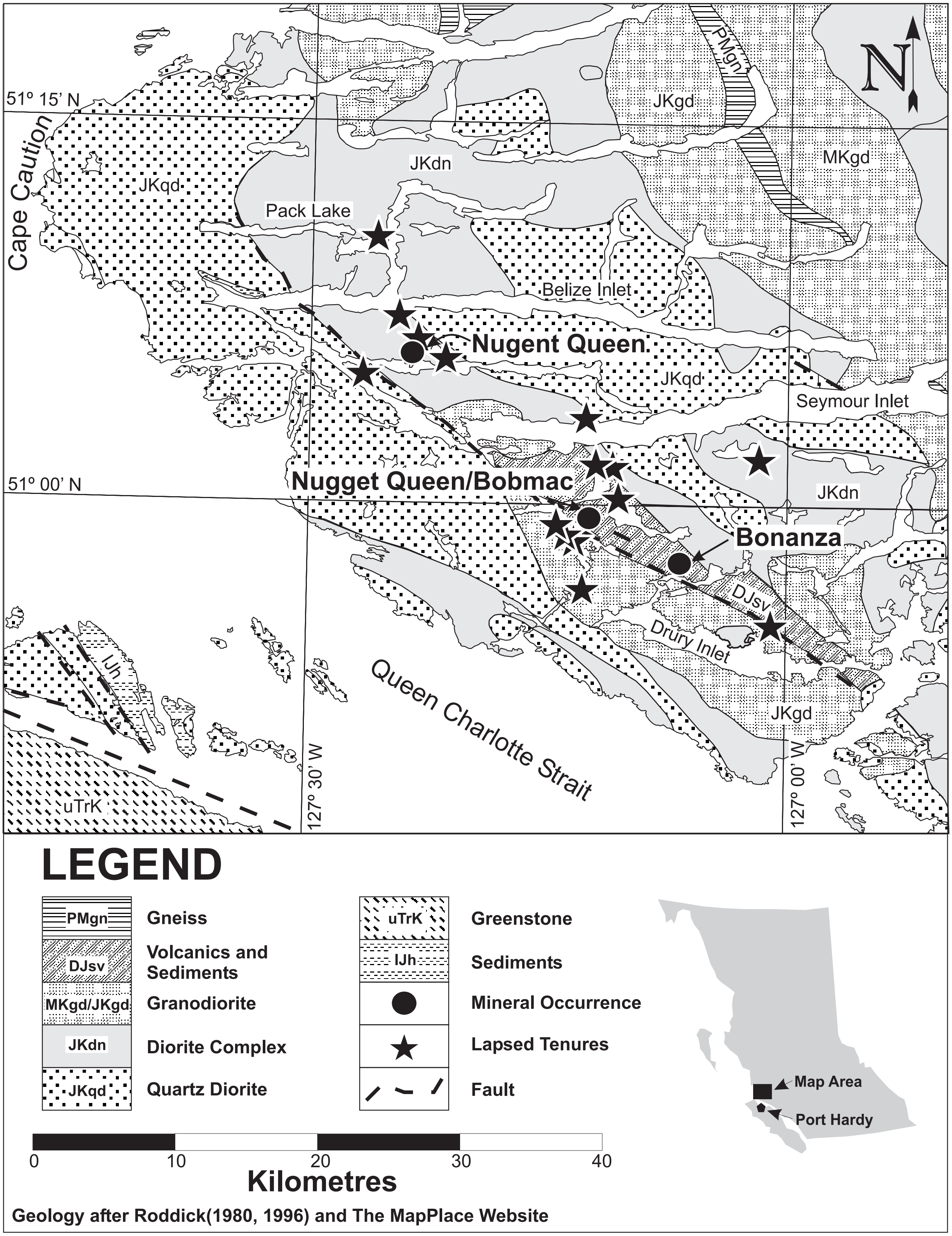

Figure 1. Generalized geology map of the Cape Caution area showing precious metal occurrences and lapsed tenure sites.

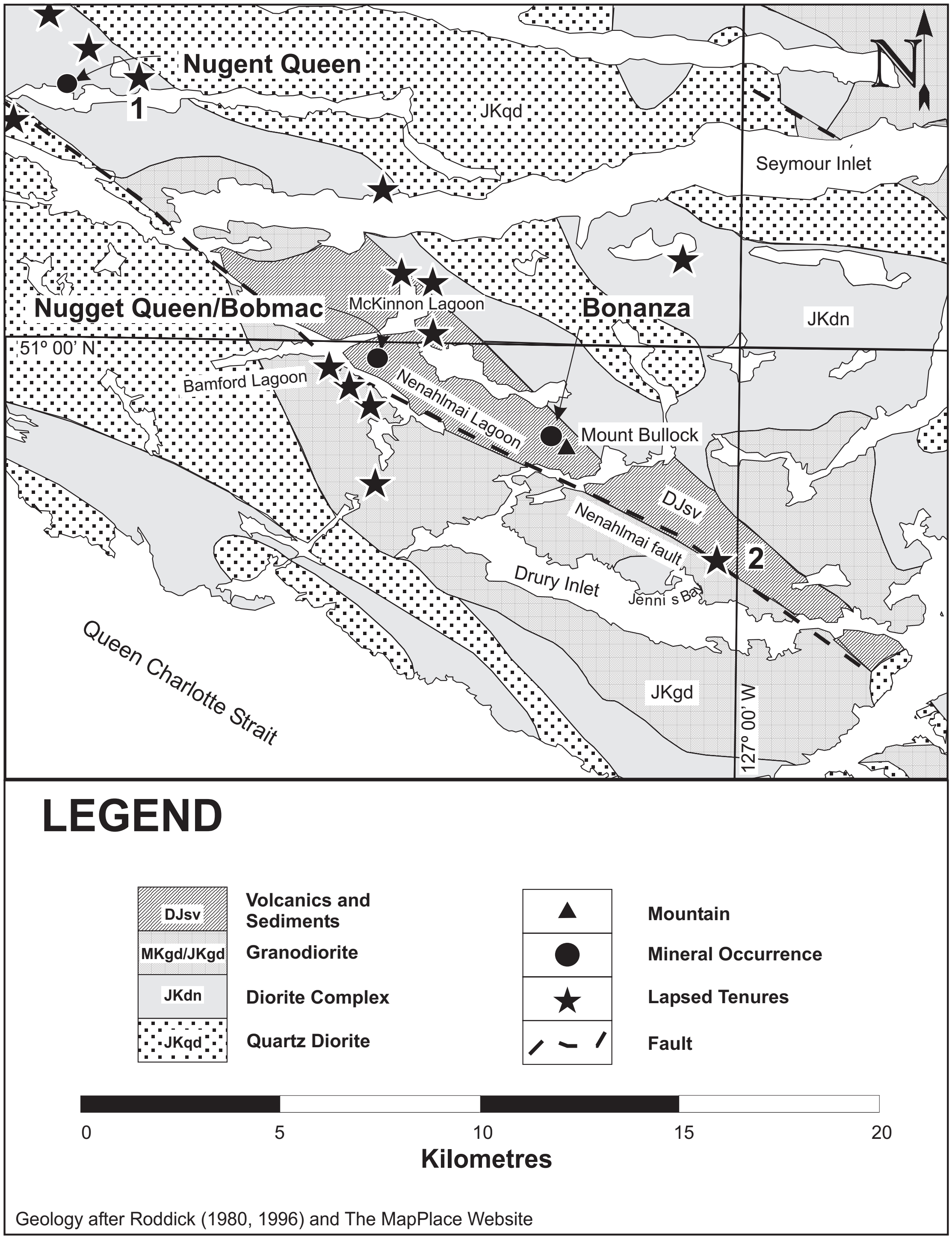

Figure 2. Generalized geology map of the Drury Inlet area showing the location of the Nenahlmai fault and related mineral occurrences.

structures are related to late faults, although there is little evidence of disruption on the Nenahlmai thrust.

The pendants are fragments of weakly to strongly metamorphosed volcanic and sedimentary strata of probable Devonian to Cretaceous age (PMgn, DJsv). They include both relatively undeformed and more schistose and gneissic varieties of greenstone, amphibolite, tuff, argillite, chert and limestone. Many of the pendants are spatially but probably not genetically related to "diorite complexes" (JKdn). These are composed of intermixed agmatite, gneiss and amphibolite of mainly gabbro to diorite composition but which show local gradation to quartz diorite and tonalite. Diorite complexes contain slivers of pendant rock but, according to Roddick (1996), they are commonly too low in metamorphic grade to be anything other than tectonically interleaved with the diorite. The diorite complexes may be Jurassic and/or Cretaceous in age. They are cut by coeval to younger Jurassic and Early Cretaceous quartz diorite (JKqd) and granodiorite (JKgd) plutons.

MINERALIZATION

There are four hard-rock MINFILE occurrences in the survey area (Nugget Queen, 092L 178; Bobmac #6, 092L 179; Bonanza, 092L 292 and Nugent Queen, 092M 005) as shown in Figure 1. They appear to be shear-hosted, gold-bearing quartz vein prospects, although there is very little data available on the Nugent Queen occurrence and, as noted below, some of that may be suspect. In addition, the figure shows numerous “lapsed tenures”. These are small sites that are known from old staking records to have been staked at some point over the past 70 years but for which there is insufficient information to warrant inclusion as a mineral occurrence in the Ministry’s MINFILE database. The rationale behind the staking isn’t known but, in most cases, the locator is likely to have been a prospector who found traces of mineralization.

The distribution of MINFILE showings and “lapsed tenures” suggests considerable potential for gold mineralization in the hanging wall of the Nenahlmai thrust.

Nugget Queen (MINFILE 092L 178) and Bobmac (MINFILE 092L 179)

The Nugget Queen and Bobmac gold prospects (latitude 50º 59’ N and longitude 127º 12’ W) are separate occurrences in MINFILE but they cover a single cluster of quartz veins near a pendant contact on the east side of Nenahlmai Lagoon (Figure 2) approximately 36 km northeast of Port Hardy.

Between them, the two prospects include eight veins, seven of which were known in the 1930s. According to information in the Ministry’s Property File, they were extensively explored and trenched by the Mining Company of Canada Limited, in 1938. The eighth vein was located by Solaia Ventures Inc. in 1996.

Most of the veins are in a narrow, 200-metre wide band of slaty, pyritic argillite that is intercalated with basalt near the western margin of a pendant which is bounded by weakly foliated granodiorite and quartz diorite. Some of the veins are subparallel to bedding and display a northwesterly strike and a steep to vertical northeasterly dip. Others are markedly discordant and fill east-southeasterly trending structures in the argillite and adjacent meta-basalt. The discordant veins are also either vertical or they dip steeply to the northeast. Most of the exploration to date has been focused on six of the veins. However, there are two lesser known outliers, an occurrence in basalt close to the pendant contact near the shore of McKinnon Lagoon and a showing in granodiorite a short distance to the south.

The veins are contained in silicified shear zones. They are discontinuous, pinch and swell and reach a maximum width of approximately 2.0 metres. They are comprised of milky white, partially strained and recrystallized breccia-type, quartz with a trace amount of sericite, carbonate and, locally, angular fragments of country rock argillite. They also contain variable amounts of disseminated to semi-massive, blebby and stringer sulphide, principally galena, sphalerite, chalcopyrite and lesser bornite intermixed with pyrrhotite and pyrite. In most of the veins, there is a positive correlation between sulphide and gold content. Sulphide-rich samples commonly contain in excess of thirty grams per tonne of gold (Grove, 1996; Yacoub and Young, 1997).

The Mining Company of Canada stripped, trenched and sampled several of the veins. One of the east-southeasterly trending veins was exposed over a strike length of approximately 76 metres. The company sampled the vein at 1.5 metres intervals and, based on 43 samples, calculated a weighted grade of 5.69 grams per tonne gold over an average width of 0.7 metre (Yacoub and Young, 1997).

There was no recorded production from 1938 but ministry records indicate that a private individual shipped 604 tonnes of “higher-grade” material, taken from a 15-metre long, 5-metre deep surface cut along one of the northwesterly trending veins, to the Tacoma smelter in 1940/1941. A further 5 tonnes were shipped from the “main” vein in 1949. According to MINFILE, the samples yielded 20 869 grams of gold, 44 758 grams of silver, 1755 kilograms of copper, 10 188 kilograms of lead and 234 kilograms of zinc.

In 1972, Q.C. Explorations Ltd. conducted a limited VLF-EM geophysical survey in the vicinity of the producing vein (Allen, 1972) and in 1980, Frank Beban Logging Limited undertook additional geophysical and regional mapping programs (Brownlee *et al*., 1980). Three years later, it drilled five short winkie drill holes for a total depth of 157 metres to test the previously sampled vein immediately to the west of the old sample site. The results were disappointing as the holes encountered argillite and quartz but returned low gold values (Soltermann, 1983).

More recently, in 1995, Solaia Ventures Inc. optioned the property and commissioned Ashworth Explorations Limited to conduct a variety of grid-based and other exploration programs. The next two years, Ashworth re-sampled the old trenches, collected stream sediment samples, conducted magnetometer and VLF-EM geophysical surveys over the main vein cluster, implemented both wide spaced and in-fill soil geochemical surveys and hand trenched and sampled several areas of anomalous soil geochemistry (Grove, 1996; Yacoub and Young, 1997).

The soil survey located a pronounced polymetallic (gold, lead, zinc and arsenic) soil geochemical anomaly coincident with a newly discovered quartz vein, approximately 80 metres to the south of the “main” vein. The anomaly displays an east-southeasterly trend and extends for a minimum strike length of 225 metres (Yacoub and Young, 1997). It has not been drill tested.

Bonanza (MINFILE 092L 292)

The Bonanza gold prospect (latitude 50º 58' N and longitude 127º 07' W) is located on the north side of Mount Bullock (Figure 2), approximately 38 km north-east of Port Hardy. The area has recently been opened up for forest harvesting and the property is currently accessible by road from tidewater.

The Bonanza deposit is a shear-hosted quartz vein prospect, similar to the Nugget Queen/Bobmac occurrence. It has a similar structural setting within the same sedimentary and volcanic pendant. It is approximately seven kilometres to the southeast. There is very little known about the prospect's early history other than that it was hand trenched in 1945. The trenches were reopened in 1979, and Cominco Limited acquired the area in 1980. The trenches exposed a mineralized quartz vein in a northwesterly trending, steeply, possibly northeasterly, dipping shear zone in a narrow band of deformed graphitic argillite in the pendant. The pendant, at this latitude, is bounded by granodiorite and/or quartz diorite to the southwest of the Nenahlmai fault and by gneissic quartz diorite to the northeast. The sediment band is interbedded with basalt and it is cut by a large number of basalt sills (Dawson, 1987).

The mineralized shear zone is concordant with bedding. It is silica flooded and contains mineralized quartz veinlets, veins and boudins with disseminated to massive sulphides including pyrite, sphalerite, galena and lesser chalcopyrite and bornite. Most of the higher gold values correlate with high levels of lead and zinc and with zones of intense silicification (Dawson, 1987). The trenched section of the vein is between one and two metres wide. It displays an average width of 1.55 metres over a strike length of approximately 280 metres. Surface samples indicated an average grade of 3.39 grams per tonne gold (Wiley, 1981). However, selected sulphide-rich samples are reported to be appreciably higher in grade.

Cominco constructed a small grid and conducted detailed magnetometer and VLF-EM geophysical surveys over the trenched section of the vein (Jackisch, 1981). It also diamond drilled seven angled holes from three sites on the northeast side of the structure, looking for continuity of grade to depth. The results were disappointing. The holes encountered argillite with less quartz than found on surface. Locally the core contained traces of sulphide but the best drill intercept assayed 3.77 grams per tonne gold over 0.3 metre (Wiley, 1981).

American Bullion Minerals Limited examined the property in 1987 and concluded that, given the degree of flexure exhibited by the vein, Cominco's drill holes may not have been deep enough to intersect the main part of the vein system. The company acquired the property, constructed a 32-line kilometre grid and extended the earlier magnetometer and VLF-EM geophysical surveys. It identified a linear magnetic low over the argillite band hosting the vein and a coincident electromagnetic conductor, which was attributed to either graphite in the shear zone or sulphide in the vein. The anomalies were traced for a minimum 1.7 kilometres along strike beyond the trenched section (Dawson, 1987), but they were never drilled.

Nugent Queen (092M 005)

The Nugent Queen gold prospect (latitude 51º 5.39' N and longitude 127º 23.22' W) is described in MINFILE as being on the north shore of Nugent Sound, 5.5 km east of the entrance to Seymour Inlet (Figure 1). However, its precise location is uncertain. It may be marked by the O.K. claims (locality 1, Figure 2) which were staked by Mr. R. D. Smith as an agent for Mr. R.C. McCorkell in July, 1938. If so, it is located between the southeast point of Boydell Lake and Nugent Sound, approximately 45 kilometres north-northeast of Port Hardy.

The property is poorly documented and there are no detailed geological descriptions. However, the O.K. claims can be shown to have straddled a contact between diorite complex rocks and quartz diorite.

The Minister of Mines Annual Report for 1939 documents that a bulk sample, comprised of three small test lots from the Nugent Queen property, was processed in Prince Rupert. The samples had an aggregate dry weight of 0.867 tonne and an average grade of 48.7 grams per tonne gold, 121 grams per tonne silver, 0.46 percent copper, 3.2 percent lead and 0.9 percent zinc.

It is worth noting that the metal ratios are similar to those obtained from bulk samples taken from the Nugget Queen/Bobmac property a few years later, and there is a possibility that the samples came from the latter property. Mr. McCorkell had interests in both properties and data in the Ministry's Property File suggests that there may have been confusion between the two properties as early as the early 1940s.

Lapsed Tenures

With the exception of one site, the lapsed tenures shown in Figures 1 and 2 are known only from staking records. The ministry has old claim records which document where the claims were staked, when and by whom but not why. Nevertheless, their distribution is informative.

The known site was staked by Mr. L. L. King to the north of Jennis Bay on Drury Inlet in 1967 (locality 2, Figure 2). He staked ten, two-post, (Jay Bee) claims along a section of the Nenahlmai fault covering similar rocks to those found on the Bonanza property, approximately eight kilometres to the northwest. The site was covered by an expanded claim group in the 1970s; however, the tenures had lapsed by 1976.

Two lines of evidence suggest the presence of gold-bearing quartz vein mineralization on the property. American Bullion Minerals Limited indicates the presence of a gold occurrence in the area on a regional map

(Dawson, 1987), and a regional geochemical silt sample collected from a stream cutting the property and listed in MEMPR BC RGS 23, 1988 (Sample # 887133) contains 12 parts per million lead and 32 part per billion gold.

Most of the remaining lapsed tenures cover pendant or diorite complex rocks in the hanging wall of the Nenahlmai fault. They include several sites that were staked in the 1930s in the same geological environment as the O. K. tenures mentioned previously. They cover a contact between diorite complex rocks and quartz diorite (Figure 1). There are also four sites covering granodiorite on the footwall side of Nenahlmai fault. Most of these are close to the fault and may reflect prospector interest in splays emanating from it.

LAKE GEOCHEMISTRY

In June, 1999, the Geological Survey Branch collected 157 lake sediment and lake water samples over an area of approximately 1200 square kilometres, between Pack Lake and the south end of Drury Inlet (see Figure 1). The samples were collected to test for mineralization along the trace of the Nenahlmai fault and elsewhere in the Cape Caution region. The program is discussed in Jackaman *et al*. (1999), this volume.

Preliminary data indicate that a few of the sediment samples are weakly to strongly anomalous in one or more element, including molybdenum, lead, arsenic and zinc. Some lake water samples are enriched in flourine and/or sulphate. Although most of these samples are isolated, spot occurrences, many are located close to the Nenahlmai fault.

SUMMARY AND CONCLUSIONS

Two of the three known mineral occurrences in the Cape Caution area, the Nugget Queen/Bobmac and Bonanza prospects are polymetallic, gold-bearing, mesothermal quartz veins that have a common setting. They are located in sheared argillite in a large pendant in the hanging wall of the Nenahlmai fault. The third occurrence, the Nugent Queen prospect may be similar in type but it is poorly described and may be spurious.

Assessment report and other data suggest the presence of another mineralized site, near Jennis Bay, on Drury Inlet. The data indicates intermittent mineralization within the pendant over a minimum distance of approximately 15 kilometres.

The mineralization appears to be related to the Nenahlmai fault, a major, deep-rooted, structure that can be traced for approximately 50 kilometres. The known showings are restricted to the southern part of the structure, but the same style of mineralization may continue to the north. This concept was recently tested by means of a lake geochemical survey. Although the results are far from conclusive, spot anomalies are consistent with local mineralization along the fault.

The results suggest potential for mesothermal vein-type gold deposits in pendant rocks in the hanging wall of the Nenahlmai fault, and possibly also for similar deposits in the hanging wall of other deeply rooted thrusts in the southern Coast Mountains.

ACKNOWLEDGMENTS

The author acknowledges the help of numerous ministry staff including Tom Schroeter, Ward Kilby, Rolf Schmitt, Stephen Cook, Dani Alldrick, Dorthe Jakobsen and Brett Gilley in the development of this report.

REFERENCES

Allen, A. (1972): Electromagnetic Survey on the Q.C. Group, Seymour Inlet Area, Vancouver Mining Division; B.C. Ministry of Energy and Mines, Assessment Report #4252, 8 pages, plus maps.

BCGSB, The MapPlace. Http://www.em.gov.bc.ca/geology

Bellefontaine, K. and Alldrick, D. (1994) Geological Compilation of the Mid-Coast Area, Southwestern British Columbia; B.C. Ministry of Energy, Mines and Petroleum Resources, Open File 1994-17.

Brownlee, D.J., Shore, G.A. and Nevin, A.E. (1980): Geological and Geophysical Report on the Whelakis Property, Vancouver Mining Division; B.C. Ministry of Energy and Mines, Assessment Report #7991, 12 pages, plus maps.

Dawson, G. (1987): Geological, Geophysical and Geochemical Report for the Bonanza 1 and 2 Claims, Vancouver Mining Division; B.C. Ministry of Energy and Mines, Assessment Report #17 049, 17 pages, plus maps.

Graham, R.P.D. (1909): On a preliminary survey of the geology of the British Columbia Coast from Kingcome Inlet to Dean Channel, including adjacent islands; in Summary Report of the Geological Survey Branch of the Department of Mines, for the calendar year 1908, Ottawa, pp. 38-40.

Grove, E.W. (1996): Geological Report and Work Proposal on the Nugget Queen Claims, Seymour Inlet Area, Vancouver Mining Division; B.C. Ministry of Energy and Mines, Assessment Report #24 334, 26 pages, plus appendices and maps.

Jackaman, W., Cook, S.J. and Lett, R.E. (1999): Applied Geochemistry Section: 1999 Fieldwork Programs; in Geological Fieldwork 1999, B.C. Ministry of Energy and Mines, Paper 2000-1, (this volume).

Jackisch, I. (1981): Geophysical Survey on the Bonanza Property, Vancouver Mining Division; B.C. Ministry of Energy and Mines, Assessment Report #9237, 2 pages, plus maps.

MINFILE 092L, W.S. Vanderpoll, N.J. Hulme and Duffett L.L. (1989): Alert Bay Map Area; B.C. Ministry of Energy, Mines and Petroleum Resources, MINFILE, released June, 1989. MINFILE data revised June, 1996.

MINFILE 092M, Rees, C.J. and Fischl, P.S. (1992): Rivers Inlet Map Area Map; B.C. Ministry of Energy, Mines and Petroleum Resources, MINFILE, released May 1992.

Roddick, J.A. and W.W. Hutchison (1967): Coast Mountains Project, British Columbia; Geological Survey of Canada, Paper 68-1, Part A, Report of Activities pp. 37-40.

Roddick, J.A. (1980): Geology of Northeast Alert Bay Map Area, British Columbia; Geological Survey of Canada, Open File 722, Scale 1:125 000.

Roddick, J.A. (1996): Geology, Rivers Inlet - Queens Sound, British Columbia (092M), (102P); Geological Survey of Canada, Open File 3278, Scale 1:250 000.

Soltermann, M.W. (1983): Drilling and Physical Work on the Whelakis Claims, Vancouver Mining Division; B.C. Ministry of Energy and Mines, Assessment Report #11 283, 12 pages.

Wiley, W.E. (1981): Diamond Drilling, Bonanza Claim, Drury Inlet Area, Vancouver Mining Division; B.C. Ministry of Energy and Mines, Assessment Report #9303, 2 pages, plus appendices and maps.

Yacoub, F.F. and Young, J. (1997): Geological and Geochemical Report on the Nugget Queen Claim Group, Seymour Inlet Area, Vancouver Mining Division; B.C. Ministry of Energy and Mines, Assessment Report #24 958, 50 pages, plus maps.

Mineral Potential of the Bella Coola Area, Coast Mountains, British Columbia (093D)

By R.H. Pinsent

KEYWORDS: *Economic Geology, intrusion-related, skarn, shear-hosted vein, gold, copper, molybdenum, staking records, Bella Coola, Mount Saugstad, Smitley River, Smitley-Oly, regional geochemical survey.*

INTRODUCTION

This report reviews the geology and metallic mineral potential of a segment of the Coast Mountains south of the Bella Coola River (in NTS area 093D). It is based on public domain reports and old staking records. In 1999, a regional stream sediment survey was conducted in the area by the Ministry of Energy and Mines. The program is described by Jackaman et al. (1999), this volume. The Bella Coola project was funded under the Provincial Government's Corporate Resource Inventory Initiative (CRII), as part of the Ministry's contribution to the Central Coast Land and Coastal Resource Management (CCLCRMP) planning process.

The area studied includes the communities of Bella Coola and Hagensborg. It is bounded by the Bella Coola River valley in the north, the Noeick and Nusatsum Rivers in the south and east and by South Bentinck Arm in the west (Figure 1). The area is extremely rugged and mountainous and it is noted for sharp rocky peaks, alpine glaciers and snow fields, wooded lower slopes and flat bottomed valleys. Elevations range from sea level to 2908 metres (Mount Saugstad).

Unlike most of the Central Coast, the Bella Cool area is linked by road to the interior of the province. It has limited logging road access through the Bella Coola River valley and through a coastal load-out facility at the south end of South Bentinck Arm. Otherwise, access is by helicopter or by boat.

PREVIOUS WORK

Although there has been exploration in the Bella Coola area for over a century, it has been intermittent and much of it has been focused on a few known occurrences north of the Bella Coola River. The Ministry's MINFILE database describes work on the Bella Coola Chief (093D 009) property, the Nifty (093D 006) and adjacent Keen (093D 007) occurrences, the Sure Copper (093D 010) prospect and around the Burnt Bridge (093D 030) showing.

The Bella Coola Chief is an intrusion-related copper deposit developed in the early 1900s and explored intermittently to the late 1980s. The Nifty and adjacent Keen occurrences are volcanogenic massive sulphide showings that were explored in the 1970s and 1980s and are still of interest today. The Sure Copper prospect is a shear or fracture-hosted copper occurrence explored in the early 1900s and the Burnt Bridge prospect is a molybdenum showing located in the 1960s.

The first three occurrences are reasonably well described in public domain reports. However, the others are less well documented. There is relatively little information available on mineral occurrences south of the river.

The Geological Survey of Canada studied the geology of the Central Coast intermittently in the late 1800s and early 1900s and the coastal geology around Bella Coola is described by Dolmage (1925). The Geological Survey of Canada conducted a 1:250 000-scale mapping program in the Bella Coola area in the early to mid 1960s as part of its Coast Mountain Project. The rocks are described by Baer (1967, 1973) and van der Heyden (1990).

GEOLOGY

The simplified map of the Bella Coola area, shown in Figure 1, is based on mapping on the MapPlace website (Bellefontaine and Alldrick, 1994). The area is underlain by a variety of stratabound and intrusive rocks of predominantly Mesozoic and younger age. It is on the eastern flank of the Coast Mountains and it is bounded on the west by a major fault that underlies South Bentinck Arm. Rocks to the west of the fault include undifferentiated paragneiss (PPn), schistose metasediment (PPsm) and mafic orthogneiss and migmatite (PMdn) typical of the core region of the Coast Mountains. Layered rocks to the east of the fault are less highly deformed and metamorphosed. They comprise two major units. One is an older, Jurassic and/or Cretaceous "greenstone" (JKv) that contains a minor amount of intercalated sediment (JKs) and is mapped as being widespread within the area studied (Figure 1). The other is a younger, Lower Cretaceous (lKG) volcanic and sedimentary unit that is mapped on the eastern border of the study area (van der Heyden, 1990; Bellefontaine and Alldrick, 1994).

The "greenstone" (JKv) comprises weakly to strongly deformed, greenschist facies, andesitic to basaltic metavolcanic rocks that are locally cut by abundant

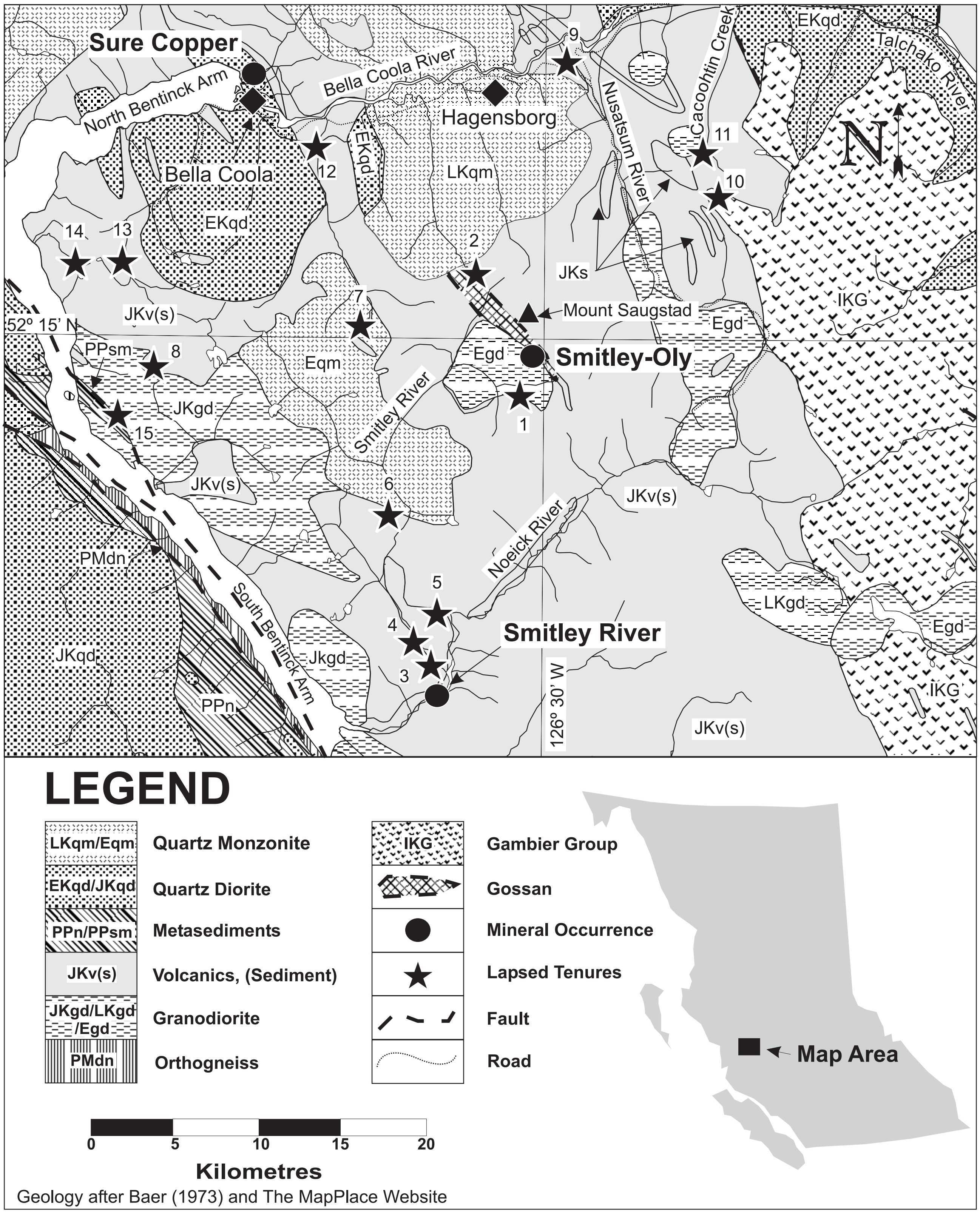

Figure 1. Generalized geology of the Bella Coola area, showing the location of metallic mineral occurrences and lapsed tenure sites.

mafic dikes. The rocks grade into foliated diorite that is, locally, difficult to distinguish from plutonic rock (Baer, 1973). The sedimentary component (JKs) consists of black slate, argillite, conglomerate and limestone. Figure 1 shows that they are well exposed in the Nusatsum River area, where they appear to occur near the base of the overlying volcanic package (Baer, 1973). They are also mapped around the margins of several plutons.

The upper volcanic and sedimentary unit (lKG) is largely undifferentiated but it contains basaltic andesite, dacitic and rhyolitic tuff and breccias, and local intercalations of slaty argillite (van der Heyden, 1990). It is less deformed and metamorphosed than the underlying "greenstone" and it may have been deposited on an eroded basement that contains an abundance of plutonic rock. According to van der Heyden (1990), much of the "greenstone" (JKv) that Baer (1973) mapped along the upper reaches of the Bella Coola and Talchako rivers is granitoid plutonic rock intruded by mafic dikes. These rocks may have contributed to the clasts he reports finding in conglomerates near the base of the upper volcanic unit. Although the age of the underlying "greenstone" (JKv) unit is uncertain, it may be stratigraphically equivalent to the Hazleton Group in Central British Columbia (Baer, 1973). The upper volcanic and sedimentary unit (lKG) is thought to correlate with Gambier Group strata in southern British Columbia (van der Heyden, 1990; Bellefontaine and Alldrick, 1994).

The stratabound rocks in the Bella Coola area are intruded by several phases and ages of intrusion. They include granodiorite (JKgd, LKgd and Egd), quartz diorite (JKqd, Ekqd) and quartz monzonite (LKqm, Eqm). The older phases are commonly weakly to strongly foliated; however, the younger quartz monzonite plutons are more massive.

Although the "greenstone" unit (JKv) is locally strongly deformed and is reported to have a northwesterly trending, moderate to steep northeasterly dipping foliation throughout the Bella Coola area (Baer, 1973), the only mapped faults are in the vicinity of South Bentinck Arm (Figure 1). There may be other significant structures in the area; lineaments and contact relations suggest the presence of several north to northwesterly and northeast to easterly trending structures.

MINERALIZATION

The Ministry's MINFILE database describes two metallic mineral deposits south of the Bella Coola River. The Smitley River (093D 013) occurrence is a polymetallic prospect near the south end of South Bentinck Arm and the Smitley-Oly (093D 022) occurrence is a precious metal-bearing quartz vein system on Mount Saugstad (Figure 1).

Although there has been exploration elsewhere in the area, it has not been described in the public domain. Staking Affidavits filed with the Ministry of Energy and Mines show that at least fifteen localities have been staked at one time or another over the past seventy years. However, most of these tenures have lapsed and are no longer located on tenure maps. In most instances, there is insufficient geological information to warrant the sites inclusion in the Ministry's MINFILE database.

Smitley River (MINFILE 093D013)

The Smitley River silver, copper, lead, zinc occurrence (latitude 52º 03′ 25′′ N; longitude 126º35′ 29″W) is close to the junction of the Noeick and Smitley Rivers, approximately seven kilometres upstream from the south end of South Bentinck Arm. It is known from a single reference in the Ministry of Energy and Mines Annual Report for 1926. The report describes the staking of claims and plans to follow up a sample that was reported to have contained 891 grams per tonne silver, 3 percent copper, 12 percent lead, 10 percent zinc and a trace of gold. The type of mineralization is unknown. The prospect has been staked several times over the years. It was covered by the Nomack claims in 1944, the Lead and Copper claims in 1956 and the TK claims in 1984.

Smitley-Oly (093D022)

The Smitley-Oly gold, silver, copper occurrence (latitude 52º14′11′′ N; longitude 126º 31′ 34′′ W) was staked by Noranda Exploration Limited following a stream sediment geochemical survey in 1980. It staked two tenure blocks close to a granodiorite stock on the west side of Mount Saugstad. The Smitley Group (1) was staked over a precious-metal bearing quartz-carbonate vein system and the Snootli Group (2) was located over hornfels enriched in precious metals, copper and molybdenum (Price, 1985). The company revisited the area but allowed the tenures to lapse. The Smitley showing was restaked as the Patch Group by Queenstake Resources Limited in 1982 (Price, 1985) and both showings were included in the Aleeta, Bas and Nus tenures in 1984. They too were allowed to lapse; United Pacific Gold Limited staked the Oly claims over the Smitley showing in 1987 (Twyman and Forgeron, 1988).

The Smitley (1) showing is comprised of a system of sub-parallel, northwesterly to westerly trending quartz veins that crop out on both sides of a westerly flowing tributary to the Smitley River. The vein system straddles an easterly trending intrusive contact that crosses the floor of a cirque.

The main vein cuts silicified "greenstone" on the cirque wall on the south side of the creek. It has been traced for a minimum of 1500 metres but is open-ended, as it disappears under ice and moraine. It is 2.0 to 5.0 metres wide, has a westerly strike and a moderate to shallow southerly dip. The vein is composed of rusty quartz and carbonate with local, but erratic, concentrations of coarse pyrite and chalcopyrite. It is difficult to get at and it has not been systematically sampled. Price (1985) refers to a sample, collected in 1982, containing 14.0 grams per tonne gold, 118.3 grams per tonne silver and 0.15 percent copper over 1.5 metres. However, he also notes that none of the samples collected from the east end of the vein in 1984 were so enriched in precious metals. The highest assay obtained at that time was 6.2 grams per tonne gold, 59 grams per tonne silver and 3.79 percent copper from a sulphide-rich sample of quartz float (Price, 1985). United Pacific Gold also had difficulty getting access to the vein. It reports locating one sample containing 4.55 grams per tonne gold and 62.0 grams per tonne silver (Twyman and Forgeron, 1988).

United Pacific Gold explored a more accessible quartz vein system in the floor of the cirque. It mapped and sampled a quartz-carbonate vein stockwork in a sheared, silicified and carbonatized pendant in granodiorite on the north side of the tributary. The pendant is bounded by northwesterly trending quartz veins that contain trace amounts of gold (Twyman and Forgeron, 1988).

The Snootli (2) occurrence is in a pronounced linear gossan that can be traced from the head of Snootli Creek, where it appears to terminate against a quartz monzonite pluton, for a distance of approximately 9.0 kilometres across the summit of Mount Saugstad where it is adjacent to a granodiorite intrusion (Figure 1). The underlying unit is mapped by Baer (1973) as hornfelsed grey/black siliceous argillite but Price (1985) considers it to be a silicious contact phase of the "greenstone". The unit contains well-defined lenses of pyrite and epidote as well as pods and veins of quartz that are locally enriched in gold, silver, copper and molybdenum (Price, 1985). Noranda identified a chalcopyrite and molybdenite occurrence in a cliff face at the north end of the belt, near the head of Snootli Creek (Figure 1).

Lapsed Tenures

Based on the distribution of lapsed tenures, there would appear to have been considerable prospector interest over the years in the ground along the Smitley River and between the Smitley and Noeick Rivers. The three lapsed tenure sites (3,4,5) were probably located to cover or tie on to the Smitley River showing (Figure 1).

The rationale for staking the Chang claims (6), approximately 15 kilometres up the Smitley River, is unknown. The tenures were located in 1959 as a narrow, two-unit wide, north-south trending, claim group that crosses a northwesterly trending contact between quartz monzonite and "greenstone" (Figure 1).

Noranda Exploration Limited is known to have staked the Smitley (1) and Snootli (2) tenures as a result of stream sediment survey conducted in 1980 (Price, 1985) and it is possible that several of the other tenure blocks were staked as a result of similar surveys. They include tenures staked over a metasedimentary rock pendant in quartz monzonite on Big Snow Mountain (7) and over a granodiorite-greenstone contact at the head of Clayton Falls Creek (8).

The lapsed tenure site (9) near the mouth of Nusatsum River, upstream from the Bella Coola River junction (Figure 1), may have been located as a result of prospecting. It was staked as the Bella property in 1970 and was known as the Brimstone occurrence in the early the 1980s. The tenures covered a strongly pyritic, hornfelsed argillite unit close to the contact of a quartz monzonite pluton (Morton, 1983). The argillite is intruded by dikes of quartz feldspar porphyry and rhyolite breccia and is described as being cut by sulphide-bearing quartz-eye breccia veins. Morton conducted a limited soil geochemical survey on the property in 1983 and obtained erratic, weakly elevated, values of copper and zinc.

The two lapsed tenure sites (10,11) on the divide between the Nusatsum River and Cacoohtin Creek (Figure 1) could be either prospecting or stream sediment sampling discoveries. The Jingle (10) tenures were staked at the head of Cacoohtin Creek and the Nusatsum (11) tenures were staked on the west flank of the creek. Both cover a complex area of "greenstone", metasediment and granodiorite close to the postulated unconformity beneath the upper volcanic unit (Figure 1).

Three of the remaining sites are road accessible. The Doris tenures (12) were staked to cover a granodiorite contact with "greenstone" near the mouth of Thorsen Creek, and the CFC (13) and Jay Group (14) tenures, near the head of Clayton Falls Creek, were staked to cover minor quartz veins in outcrop along a logging road. They are mapped as being underlain by "greenstone". However, prospecting reports by Krusche (1993a & b) suggest that both are underlain by a mixture of "greenstone" and granodiorite.

The Goman tenures (15) covered a linear depression marking the trace of a fault that may be related to the major structure that underlies South Bentinck Arm. They cover a sliver of schistose metasediment that appears to have been tectonically emplaced in a diorite pluton (Figure 1).

Stream Geochemistry

In September, 1999, the Geological Survey Branch conducted a stream sediment (moss mat) and water sampling survey in the Bella Coola area. It sampled 94 sites over an area of approximately 1200 square kilometres. The program is described by Jackaman *et al.* (1999), this volume.

SUMMARY AND CONCLUSION

Although, there are only two metallic MINFILE occurrences in the area south of Bella Coola, old staking records show several areas of past exploration interest that are not sufficiently well documented to warrant inclusion in the MINFILE database.

The best described showings are on the Smitley-Oly (093D 022) property on Mount Saugstad. Price (1985) and Twyman and Forgeron (1988) describe a precious-metal bearing quartz-carbonate vein system on the lapsed Smitley (1) tenures and Price (1985) describes a possible skarn or intrusion-related copper and molybdenum occurrence on the lapsed Snootli (2) claims (Figure

1). There may be other intrusion or skarn-related occurrences in the area, as Morton (1983) documents an occurrence of this type near the mouth of Nusatsum Creek (9) and other tenures were staked over rocks mapped as metasediment. The geological setting appears to be similar to that of the Bella Coola Chief (093D 009) prospect, where andesite, rather than sediment, has been hornfelsed, brecciated, intruded by felsic porphyry dikes and cut by veins containing irregular pods and masses of chalcopyrite and pyrite (Krueckl, 1985).

The Smitley River (093D 013) showing is too poorly described to determine its style of mineralization, but it is located along a prominent topographic lineament and it may be structurally controlled. Similarly, the Goman tenure (15) is poorly documented but was most likely staked to cover mineralization along a splay from the main South Bentinck Arm fault.

The lapsed tenure sites south of the Bella Coola River are poorly documented and in most cases one can only guess as to why the tenures were staked. However, some may have been located as a result of stream geochemical surveys and the Ministry's moss mat survey (Jackaman *et al.*, 1999) may provide insight into the significance of some of the showings.

ACKNOWLEDGMENTS

The author acknowledges the help and assistance of numerous Ministry staff including Tom Schroeter, Ward Kilby, Rolf Schmitt, Wayne Jackaman, Stephen Cook, Larry Jones, Dorthe Jakobsen and Brett Gilley in the development of this report.

REFERENCES

Baer, A.J. (1967): Bella Coola and Laredo Sound Map-Areas, British Columbia, 93D and 103A; *Geological Survey of Canada,* Paper 66-25, 13 pages, plus maps.

Baer, A. J. (1973): Bella Coola-Laredo Sound Map Areas, British Columbia; *Geological Survey of Canada*, Memoir 372, 119 pages, plus maps.

Dolmage, V. (1925): Tatla-Bella Coola area, Coast District, British Columbia; *Geological Survey of Canada*, Summary Report for 1925, pt. A, p. 155-163.

Jackaman, W., Cook, S.J. and Lett, R.E. (1999): B.C. Regional Geochemical Survey: 1999 Field Programs; in Geological Fieldwork 1999, *B.C. Ministry of Energy and Mines*, Paper 2000-1 (this volume).

Krueckl, G. P. (1985): Report on the Bella Coola Chief Mineral Claim Group, Skeena Mining Division; *B.C. Ministry of Energy and Mines*, Assessment Report #14 674, 12 pages, plus appendix.

Krusche, J.B. (1993a): Geological Survey and Comments on the Gold Potential of the CFC Group of Claims, Skeena Mining Division; *B.C. Ministry of Energy and Mines*, Assessment Report #23 297, 55 pages, plus maps.

Krusche, J.B (1993b): Geological Survey and Comments on the Jay Group of Claims, Skeena Mining Division; *B.C. Ministry of Energy and Mines*, Assessment Report #23 298, 51 pages, plus maps.

Morton, J.W. (1983): Geochemical Soil Survey of the Brimstone Claims, Skeena Mining Division; *B.C. Ministry of Energy and Mines*, Assessment Report #11 609, 6 pages, plus maps.

Price, M. G. (1985): Geology and Mineralization of the Aleeta Claims, Skeena Mining Division; *B.C. Ministry of Energy and Mines*, Assessment Report #14 278, 8 pages, plus maps.

Twyman, M. and Forgeron, F. D. (1988): The Geology and Gold Potential of the Oly 1-4 Claims, Skeena Mining Division; *B.C. Ministry of Energy and Mines*, Assessment Report #18 006, 18 pages, plus maps.

van der Heyden, P. (1990): Eastern Margin of the Coast Belt in west-central British Columbia; in Current Research, Part E, *Geological Survey of Canada*, Paper 90-1E, pp. 171-182, 1990.

Nephrite (Jade) Deposits, Mount Ogden Area, Central British Columbia (NTS 093N 13W)

G.J. Simandl[1], C.P. Riveros[2] and P. Schiarizza[1]

KEYWORDS: *Nephrite, jade, gemstones, industrial minerals, garnetite, serpentinite, economic potential, tile-making grade.*

INTRODUCTION

Jade

Jade is a commercial term encompassing green, white, black or yellow-brown jadeitite or nephrite. Jadeitite is a rock that consists essentially of jadeite (Na-rich pyroxene), whereas nephrite consists of prismatic to acicular amphiboles of the tremolite-actinolite series forming bundles that are randomly oriented and interlocked. The density of British Columbia nephrite varies from 2.95 to 3.01 g/cm^3 (Leaming, 1978). Jadeitite is slightly denser and harder than nephrite (7 compared to 6.5 on the Mohs scale) Nephrite is tougher (harder to break) than jadeitite. Its fracture strength is about 200 MN/m^2 whereas that of jadeitite is about 100 MN/m^2.

Nephrite and jadeitite are used in jewellery as gemstones and as carving and ornamental stones. The world market for jade, both nephrite and jadeitite is estimated at 300 tonnes per year, and three quarters of this originates in British Columbia (Scott, 1996). Nephrite accounts for all of the current British Columbia production. The price of raw jade varies from less than Can $10.00 to $100.00 per kilogram on the retail scale, depending on the quality and importance of the transaction. In general, jadeitite commands a higher price than nephrite.

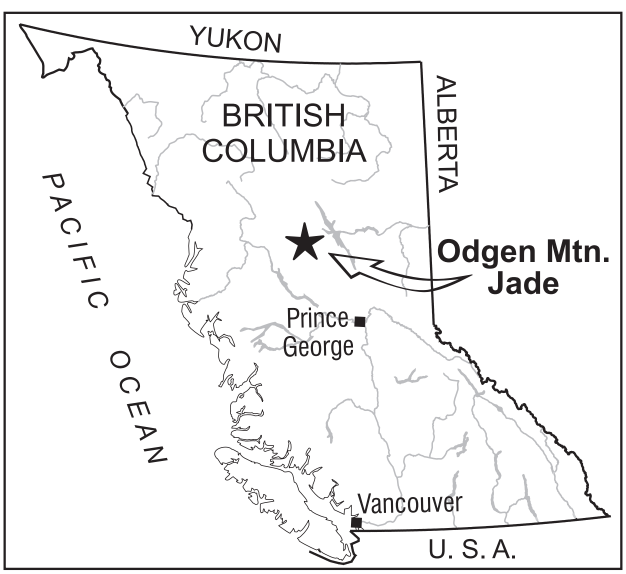

Figure 1. Location of the nephrite (Jade) camp in the Mount Ogden area, central British Columbia.

The Mount Ogden occurrences are located in central British Columbia (Figure 1) on the southwestern slopes of Mount Ogden, approximately 40 kilometres north-northeast of Takla Landing (MINFILE No. 093N 165). The main objective of this paper is to document two of these deposits which were examined during a two-day visit in 1999. The main aspects covered are geological setting, deposit controls, lithological relationships, petrology and mineralogy. The nephrite and nephrite schist samples that are described in this study are low grade. The best material, which has been described as 99% nephrite was previously extracted from the pits. The potential use of industrial grade nephrite which was stockpiled on the site for tile-making is also of interest.

Jade in British Columbia

In western North America, a belt favourable for jade exploration extends intermittently from Alaska through British Columbia and California to Mexico (Leaming, 1995). In British Columbia, the nephrite occurs as individual blocks, boulder fields, talus blocks and in situ occurrences. There are over 50 known nephrite deposits and occurrences in British Columbia.

The in situ deposits of nephrite occur at, or near the contact of ultramafic/mafic rocks (mainly serpentinites) with cherts, and other metasedimentary rocks of Mississippian to Jurassic oceanic terranes such as Cache Creek and Slide Mountain. There are at least 17 occurrences located in southern British Columbia along the Coquihalla River, Fraser River, Hozameen and Bridge River areas, in Shulaps and Cadwalder Range. Important commercial activity took place in Central British Columbia in the Mount Ogden camp (Figure 1), where at least 9 occurrences were located and to a lesser extent, in the Mount Sidney Williams area. Cry Lake and Dease Lake areas, where 22 nephrite occurrences were reported, and the

[1] *British Columbia Geological Survey, Victoria, British Columbia, Canada*

[2] *Riveros Geological Services*

Cassiar Mine are the most productive camps of northern British Columbia. Most of the known occurrences are described by Leaming (1978), and all of these are contained in "BC MINFILE" (www.em.gov.bc.ca/mining/geolsurv/MINFILE).

British Columbia deposits occur mainly along tectonic inclusions of country rocks, dikes and mafic rock layers within serpentinites, or at the contact of sepentinite with the country rock, as described in other parts of the world by Coleman (1967). Tectonic and lithological contacts seem to be predominant ore controls. Where the nephrite is found in situ, it may be separated from the country rocks by a "white rock" or it may contain irregular zones of such a rock. In the literature, the "white rock" is commonly described as rodingite or calcsilicate rock containing hydrogarnet, diopside, wollastonite and tremolite (Coleman, 1967 and Leaming, 1978). In the field, the British Columbia prospectors also use this term to describe white-colored post-nephrite selvages and alteration zones which are fabric-controlled.

Good quality nephrite is a nearly monomineralic rock consisting of very fine and interlocked bundles of acicular tremolite crystals. It commonly contains small concentrations of spinel group minerals (chromite, magnetite, picotite), diopside, uvarovite, titanite, chlorite and talc. Bright green specs of chrome diopside are characteristic, but not restricted to Cassiar nephrite.

GEOLOGICAL SETTING OF MOUNT OGDEN DEPOSITS

The Mount Ogden nephrite camp is located near Fort St. James, in the northwest corner of the area described by Armstrong (1949). The area was also studied by Paterson (1974), and more recently by Schiarizza and Payie (1997) and Schiarizza *et al.* (1997). It is situated within the Cache Creek Terrane of the central Intermontane Belt. At this latitude the Cache Creek Terrane includes the Sitlika assemblage in the west and the Cache Creek Complex to the east. The Sitlika assemblage consists of Permo-Triassic bimodal volcanic rocks overlain by Upper Triassic to Lower Jurassic clastic sedimentary rocks. This assemblage is in fault contact with a poorly dated, but partially age-equivalent ophiolitic sequence that forms the western part of the Cache Creek Complex. Eastern elements of the Cache Creek Complex include a Permian to Lower Jurassic succession of predominantly pelagic metasedimentary rocks and thick Pennsylvanian - Permian carbonate sequences associated with ocean island basalts.

The earliest deformation documented within the Cache Creek Terrane in central British Columbia is related to subduction, probably beneath adjacent magmatic arc rocks of the Quesnel Terrane, as indicated by local exposures of blueschist facies rocks that yield Late Triassic K-Ar and Ar-Ar cooling dates (Paterson and Harakal, 1974; Paterson, 1977; Ghent *et al*., 1996). Subsequent uplift of Cache Creek Terrane is recorded by chert-rich clastic detritus that was shed westward into the basal part of the Bowser Lake Group in late Middle Jurassic to Late Jurassic time. This uplift may be related to a deformational episode that generated greenschist facies metamorphism and penetrative deformation within the Cache Creek Terrane and the Sitlika assemblage, and ultimately resulted in Cache Creek Terrane being thrust westward over Stikine Terrane (Monger *et al*., 1978). Younger deformation in the region involved Late Cretaceous(?) to early Tertiary dextral strike-slip and related extension, in part, along major structures such as the Pinchi and Takla faults (Gabrielse, 1985; Struik, 1993; Wetherup and Struik, 1996).

The nephrite occurrences in the Mount Ogden area occur within a belt of ultramafic rocks and serpentinite melange (Figure 2) that was informally referred to as the Cache Creek ultramafic unit by Schiarizza and Payie (1997). These rocks are part of an extensive belt of ultramafic and related rocks that were referred to as Trembleur intrusions by Armstrong (1949), who interpreted them as intrusive bodies cutting Cache Creek volcanic and sedimentary rocks. More recently, these rocks have been interpreted to be tectonically emplaced upper mantle and lower crustal portions of dismembered ophiolite sequences (Whittaker, 1983; Ash and Macdonald, 1993; Schiarizza and MacIntyre, 1999). In the Mount Ogden area, the ultramafic unit is characterized by serpentinite melange comprising serpentinite and serpentine-carbonate-talc schists containing abundant knockers and fault-bounded lenses of greenstone, amphibolite and metasedimentary rocks. Greenstone was in part derived from mafic volcanic rocks, but also includes a large proportion of diabasic to gabbroic rocks, locally grading to weakly to moderately foliated amphibolite. Metasedimentary rocks include bedded chert, quartz phyllite and limestone.

The eastern margin of the ultramafic unit is an east-dipping thrust fault. An assemblage of mainly metasedimentary rocks forms the hangingwall of the fault (Figure 2). This sedimentary unit is dominated by light to dark-grey, platy quartz phyllites, but also includes metachert, cherty argillite, slate, limestone, metabasalt and metasandstone. Farther to the east, this unit includes thick bodies of light-grey weathered limestone that contain fusulinids of early Late Permian age (Paterson, 1974).

To the west of the ultramafic unit is an extensive belt of metasedimentary rocks dominated by slate, siltstone and sandstone, with local conglomerate (Figure 2). These rocks belong to the Upper Triassic to Lower Jurassic clastic sedimentary unit of the Sitlika assemblage (Paterson, 1974; Schiarizza and MacIntyre, 1999). The contact between the two units is not exposed in this area. Regionally, it is an east-dipping thrust fault (Schiarizza and MacIntyre, 1999), but where observed about 10 kilometres south of the present study area it is marked by a younger dextral strike-slip fault (Schiarizza and Payie, 1997).

An elongate stock of coarse grained, biotite±muscovite granodiorite cuts through the eastern to central part of

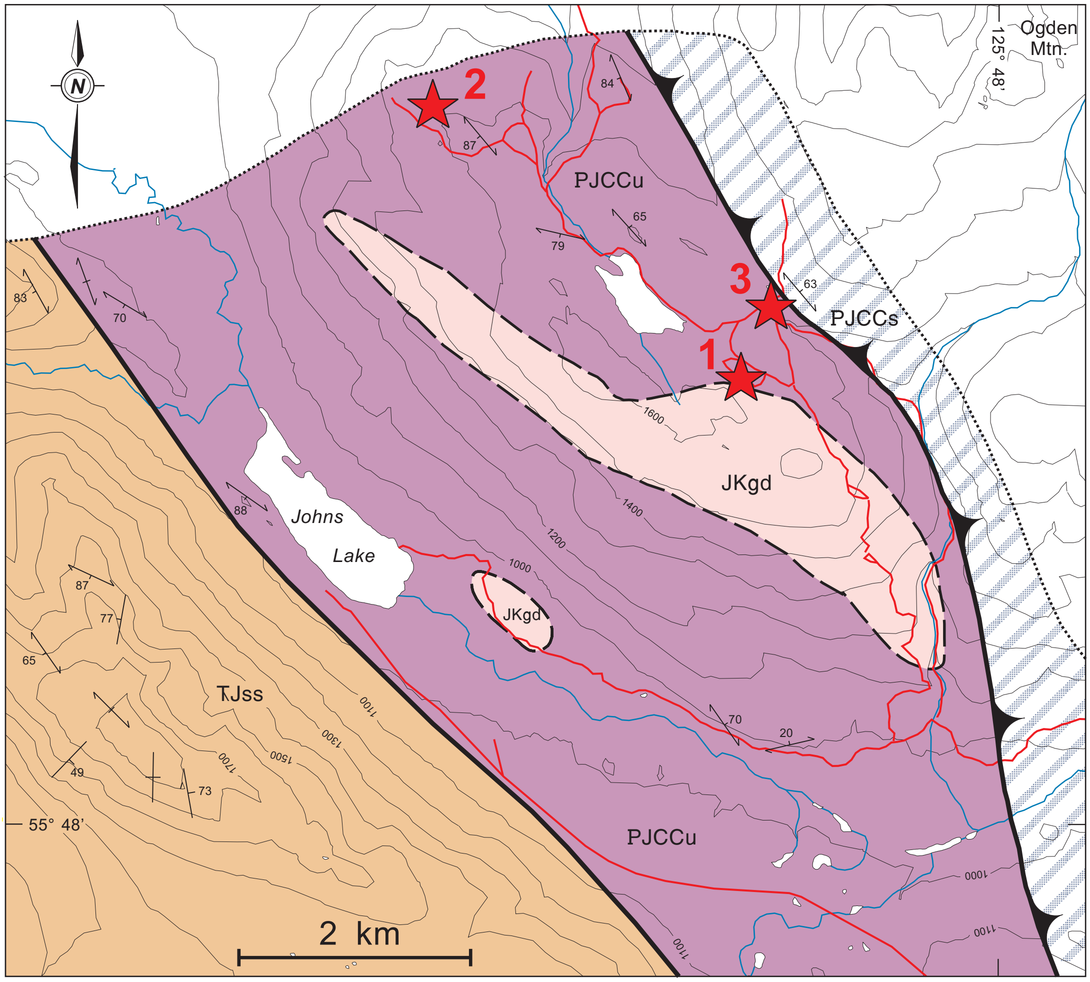

Source: Schiarizza, et al., 1997.

Jurassic or Cretaceous(?)

JKgd — Medium to coarse grained biotite granodiorite

SITLIKA ASSEMBLAGE

Triassic to Jurassic(?)

TJss — Eastern clastic unit: variably foliated siltstone, sandstone and conglomerate containing felsic volcanic clasts; medium to dark grey slate and phyllite; locally includes foliated limestone, limestone conglomerate and green chloritic phyllite.

CACHE CREEK COMPLEX

Pennsylvanian to Lower Jurassic

PJCCs — Sedimentary unit: light to medium grey quartz phyllite, platy quartzite and metachert; lesser amounts of recrystalized limestone, dark grey phyllite, massive to pillowed greenstone and chlorite schist; minor amounts of metasandstone.

PJCCu — Ultramafic unit: serpentinite, serpentinized ultramafite and serpentine-magnesite-talc schist; sepentinite melange containing knockers of greenstone, diabase, amphibolite, chert and limestone; locally includes mariposite-quartz-magnesite-altered rock (listwanite), rodingite and nephrite.

77 80 Foliation, bedding
Limit of mapping
Geological Contact
Fault
Thrust fault
Roads
Contours
Rivers
Lakes
1 Nephrite

Fig 2 Mtogden Map.cdr

Figure 2. General geology of the Mount Ogden area (modified from Schiarizza *et al*., 1997).

the ultramafic unit (Figure 2). Similar granodiorite forms a small plug 2 kilometres southwest of the main stock, and occurs as dikes and pods elsewhere in the ultramafic unit. These rocks are undated, but are suspected to be Early Cretaceous in age, based on their lithologic similarity to parts of the Early Cretaceous Mitchell batholith, which cuts the Cache Creek Complex and Sitlika assemblage 50 kilometres to the south (Schiarizza and MacIntyre, 1999).

GEOLOGY OF THE NEPHRITE DEPOSITS

The three in situ, past producing deposits located within the study area (Figure 2) are identified as (1), (2) and (3). Deposit 1 is located at the contact of a granodiorite pluton which forms a prominent knob with a low relief ultramafic unit. The ultramafic unit consists of serpentinites, serpentine-carbonate-talc schists and melange containing knockers of greenstone, diabase, amphibolite, chert and limestone. Deposit 2 is located approximately 3.5 kilometres northwest of deposit 1. At the scale of figure 2, deposit 2 seems to be located entirely within the same ultramafic unit as deposit 1. Deposit 3 is located about 800 metres northeast of deposit 1, along a fault contact between the ultramafic unit and the sedimentary unit. The sedimentary unit consists mainly of phyllites, quartzites, metacherts, marble, and chlorite schists. Deposit 3, also referred to as “main showing” by Leaming (1978), was not studied because of flooding of the pit and lack of good exposure. The cross section of this deposit was published and described by Leaming (1978). The nephrite lens in deposit 3 was 50 metres long, 3 metres wide and 5 metres high, with the total estimated tonnage of 2250 tonnes (Leaming, 1978). Most of the material was probably industrial grade. Deposits 1 and 2 are described below in more detail.

Deposit 1

Deposit 1, which was referred to as the “new showing” by Leaming (1978) is now almost completely mined out (Photo 1), but a large quantity of industrial grade nephrite is stockpiled at the site. The pit that contained the deposit is oriented approximately 120º and is over 250 metres along strike. Along the nearly vertical wall, the excavation is in places more than 18 metres high and 5 metres wide. The exposed footwall is arcuate and follows roughly topographic contours and the contact of granodioritic pluton with the ultramafic unit (Photo 1). The possible reserves before mining were estimated at 500 to 1000 tonnes. Probable reserves were estimated at 50 tonnes (Leaming, 1978). At this stage it is impossible to determine what was the total tonnage extracted from

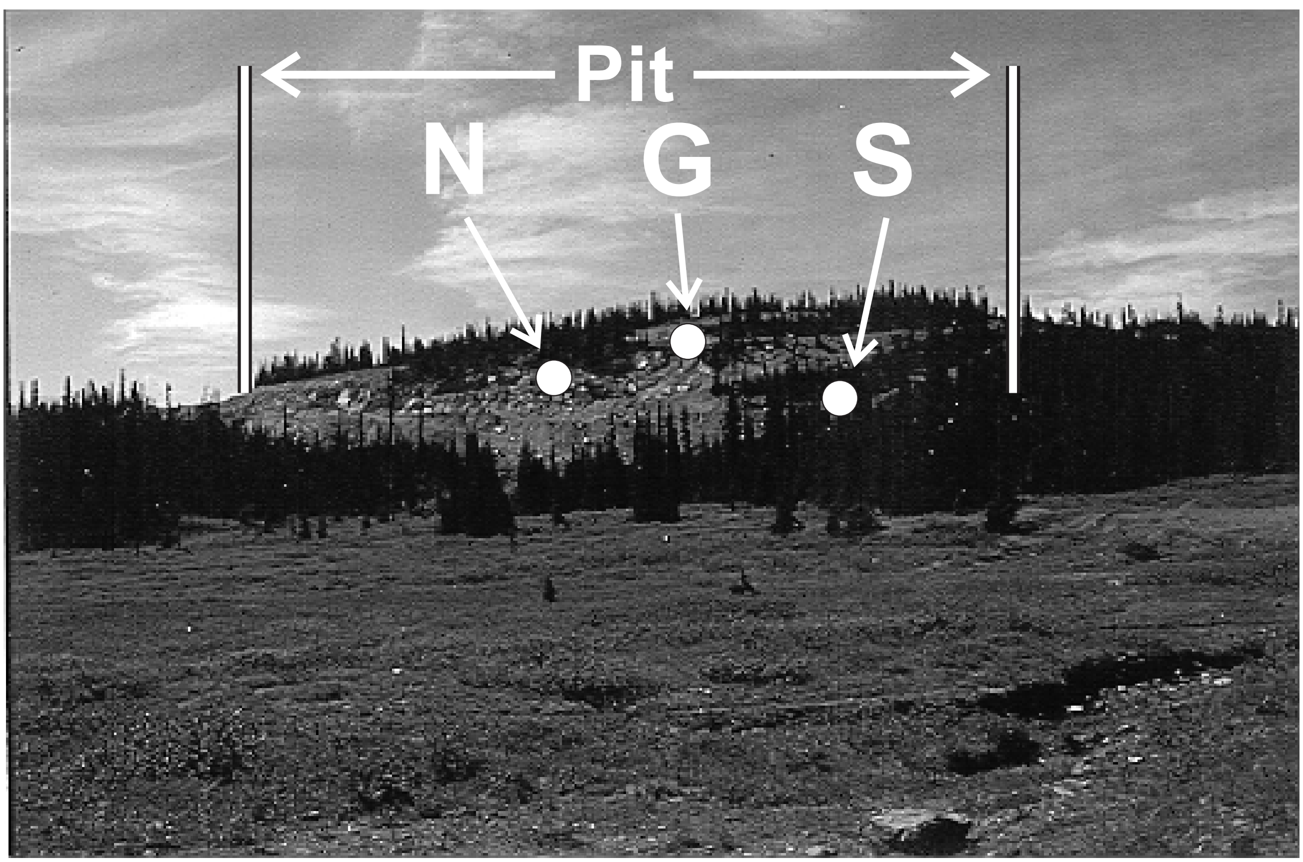

Photo 1. Deposit 1, Mount Ogden area: granodiorite-diorite (G), nephrite (N) and serpentinite (S). The excavation is approximately 250 metres along strike.

this deposit and if any metasediments were originally present within the pit limits.

Granodiorite Pluton

The granodiorite-diorite pluton is about 6.5 kilometres in length and more than one kilometre in width. It is a gray, pink or beige, medium-grained, equigranular rock consisting of 29.6 % quartz, 20.4 % orthoclase, 41.1% oligoclase-andesine, 6.7 % chlorite and minor titanite and apatite (Armstrong, 1949). A sample of the pluton near its southwest extremity collected during earlier mapping, shows relatively fresh biotite and muscovite instead of chlorite. The plutonic rock, exposed less than 10 metres from the pit, is strongly altered and crosscut by closely spaced sets of centimetre-scale thick fractures, in-filled by a fine grained siliceous phase containing quartz (65-70%), feldspar (15-20%), epidote group minerals (10-15%), sericite (15%) and chlorite (3%). The altered pluton consists of feldspar (75%), epidote (12-15%), zoisite (3-5%), chlorite (6-7%), limonite (<1%), and carbonate and titanite in trace amounts.

White Rock

The main lithology exposed within the wall is a white, hard, massive, granular, macroscopically homogeneous rock. Microscopically, this rock is quite heterogeneous consisting mainly of zoisite/clinozoisite (15-50%), serpentine (1-40%), epidote (1-60%), and other minerals which are locally important such as tremolite, wollastonite(?), carbonate and minor constituents such as talc, chlorite, titanite, apatite and pyrite.

Nephrite

There is currently no in situ nephrite exposed, with the exception of three small remnants of nephrite, probably less than 30 centimetres thick and 2 metres along the wall of the pit. Good quality nephrite from one of the remnants is very hard, dark green semitransluscent, and consists mainly of actinolite-tremolite microfibers (>90%), serpentine (<10%), talc (6%), spinel group minerals (<1%), and traces of titanite, ilmenite and hematite. Lower quality nephrite is dark green, greenish-grey, schistose and consists of larger proportions of serpentine or talc and opaques. Leaming (1978) indicates that chlorite was also present. Backfill or debris covers the bottom of the pit, and no in situ rocks that formed the hangingwall of the deposit are observed within the excavation.

Nephrite-Host Rock Relationship

Several of the fresh and angular blocks near the excavations were examined. Two representative examples that show the relation of lower quality nephrite and country rock are shown below. The first example shows irregular contacts of nephrite (N) with the country "white rock" (Photo 2). Nephrite (N) is aphanitic, compact, deep green, vitreous and moderately schistose, comprised mainly of tremolite (48-52%), serpentine (48-50%), and less amounts of limonite, chromite and locally uvarovite (1.5-2%) which forms bright green rims around chromite. The country rock is pale greenish-pinkish white, equigranular, very hard and massive. The coarse grained "white rock" (CW) contains mainly epidote group minerals (74-80%), serpentine (13-15%) and titanite (7-9%). The fine grained "white rock" (FW) also consists mainly of epidote group minerals (84-90%), in addition to carbonates (13-15%), titanite (1-3%) and serpentine (1.5-2%). Microscopic observations show that both the coarse grained (CW) and fine grained "white rock" (FW) are generally fine grained (less than 1 mm), however, interlocking aggregates of epidote group minerals in combination with the serpentine content results in a coarser and more granular texture on the weathered surface.

The inferred lithologies that probably formed the footwall of the pit are strongly serpentinized ultramafic rocks that are now exposed in the southern part of the excavation. These rocks are almost black to yellow green, aphanitic and consist mainly of serpentine (30- 85%), talc (<15%) and opaques (<30%, locally <18% magnetite).

The second example shows the nephrite-serpentine contact (Photo 3). Good quality, massive, deep green, semitranslucent nephrite, comprised of tremolite-actinolite (90-95%), serpentine (5-10%) and chromite (1-1.5%), grades sharply into schistose, dark greenish-greyish-white and mottled semi-nephrite (SN). Semi-nephrite contains fine grained tremolite (50-52%), serpentine (28-30%), talc (16-18%) and traces of limonite, and grades progressively into serpentinite (S). Serpentinite (S) comprises a dark green, fissile rock, of mainly fine grained serpentine (88-90%), tremolite (8-10%), magnetite (1.5-2%), ilmenite (1%) and traces of titanite. Centimetre thick, anastomosing, fibrous white to pale green tremolite veins cut, and are most abundant in, the semi-nephrite, but extend into serpentinite, where they pinch out gradually. These veins are thickest at the semi-nephrite - nephrite contact, where they terminate abruptly at high angles to the contact (Photo 3).

Deposit 2 (Far North)

On the regional scale, deposit 2, also refered to as the "Far North deposit" is located entirely within the ultramafics (Figure 2), however detailed investigation (Figure 3) indicates that the nephrite follows the northwest-trending contact of ultramafic rocks (in this case serpentinite) with garnetite**.** The excavation trends 125º and is approximately 100 metres long by 5-15 metres wide, and less than 5 metres deep (Figure 3). It contained approximately 500 tonnes of high quality nephrite (Kirk Maakeppeace, Jade West).

The excavation area consists of a steeply northeast-dipping lithological sequence comprising serpentinite, nephrite, nephrite schist, chlorite schist, garnetite, blue marble and metavolcanics / metasediments (in geographic order from south to north). No lithological contacts between nephrite or nephrite schist with serpentinite

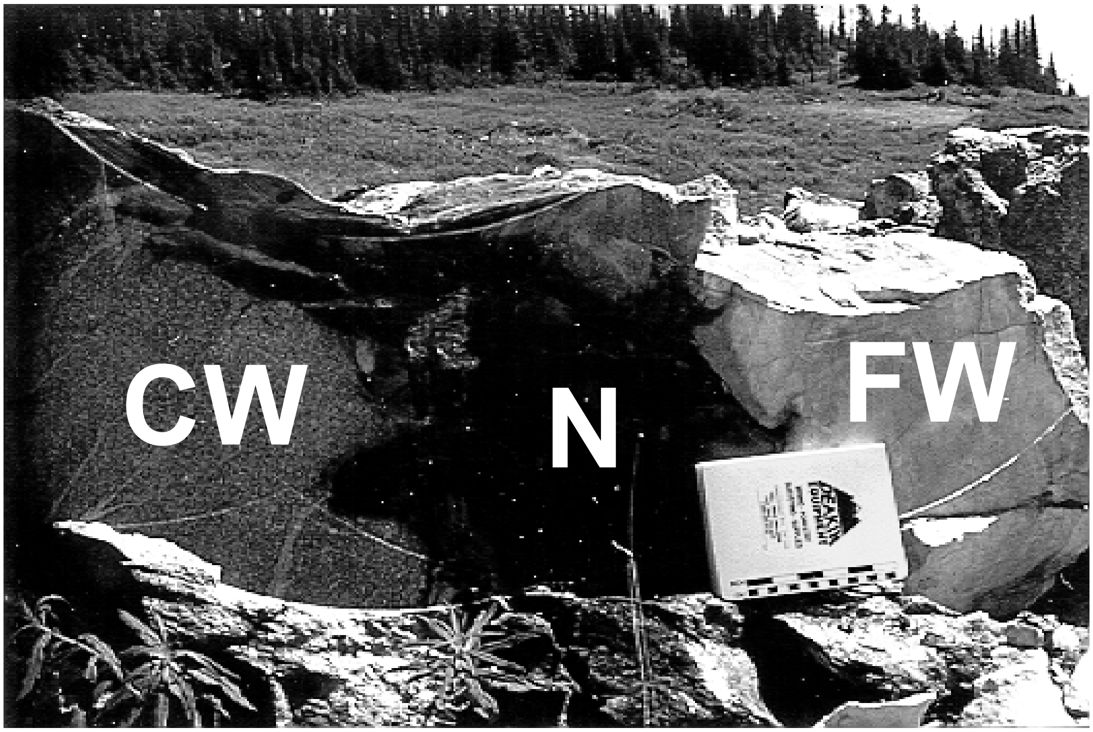

Photo 2. Nephrite in sharp contacts with fine grained "white rock" and coarse grained "white rock"; deposit number 1, Mount Ogden area. Nephrite (N) contains mainly tremolite and serpentine and less amounts of limonite, chromite and uvarovite. The fine grained "white rock" (FW) consists mainly of clinozoisite, carbonate and some titanite; the coarse grained "white rock" (CW) consists mainly of zoisite and epidote and less amounts of serpentinte, titanite and clinozoisite.

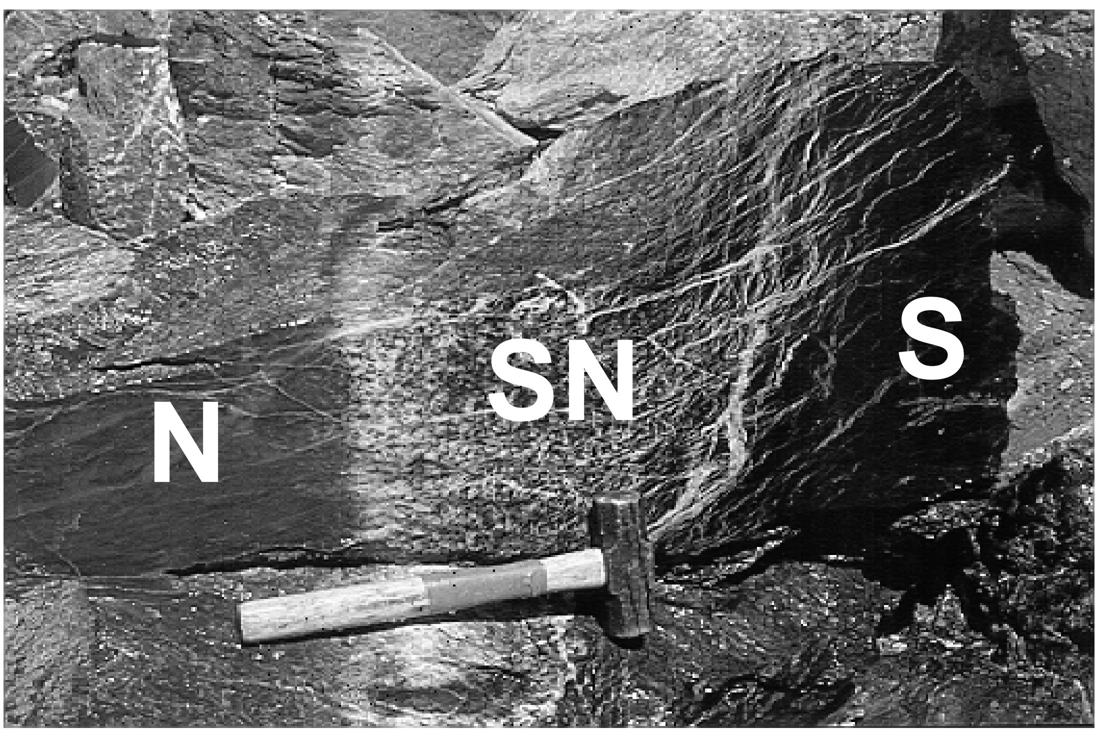

Photo 3. Nephrite - serpentinite contact, Jade West stockpile, Mount Ogden area (hammer handle is 25 cm in length). Coarse, anastomosing, white to pale green tremolite veins cross cut the semi-nephrite (SN) and serpentinite (S). Nephrite (N) is massive and comprised mainly of tremolite and less amounts of serpentine and chromite; semi-nephrite (SN) contains mainly tremolite, serpentine and talc and traces of limonite; serpentinite (S) contains mainly serpentine and less amounts of tremolite, magnetite, ilmenite and titanite.

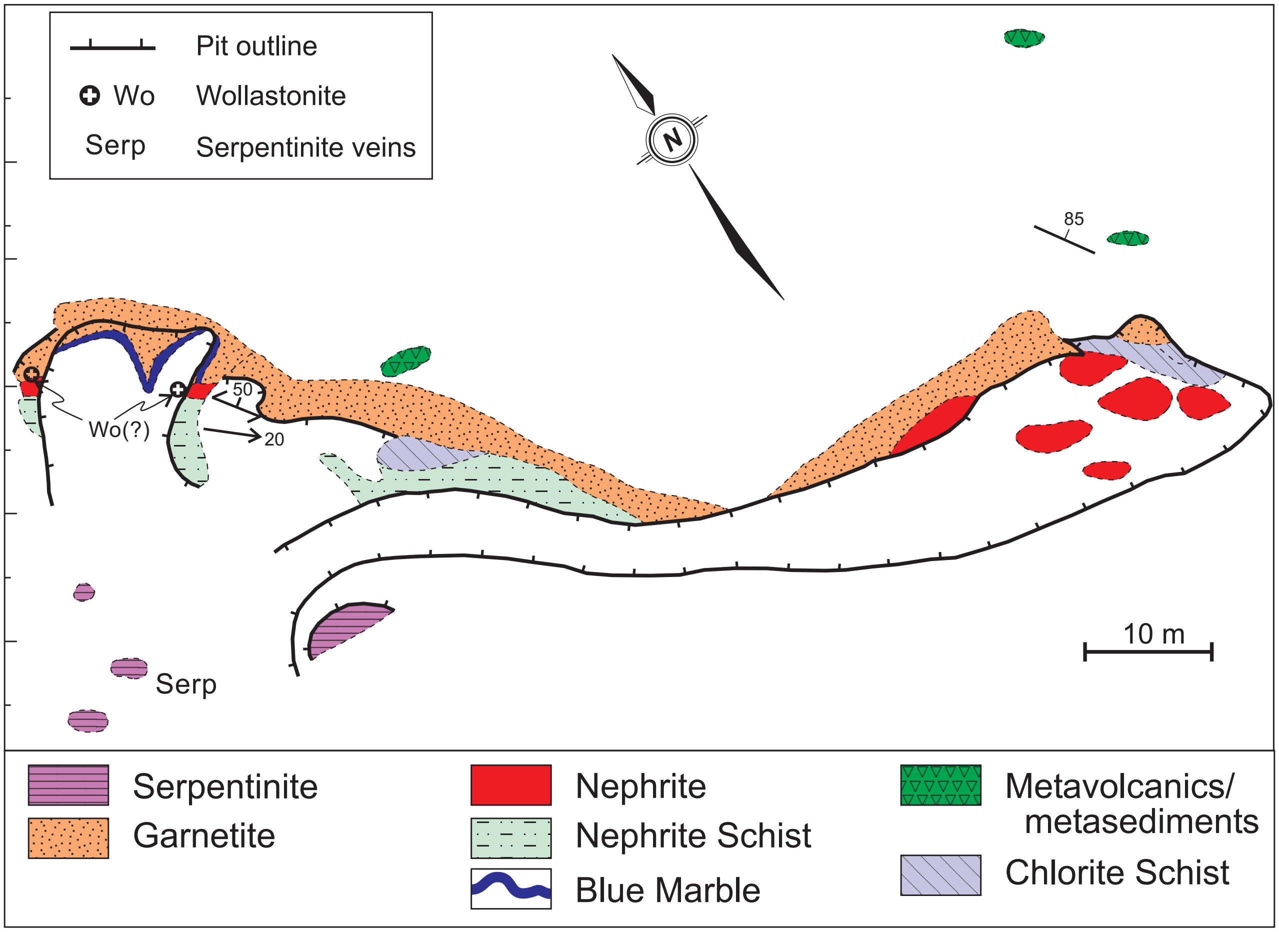

Figure 3. Geology of deposit number 2, Mount Ogden area.

are observed because of the backfill and grading of the pit floor. In the western portion of the pit, a less than 20 centimetre thick vein of fibrous mineral, tentatively identified as wollastonite, separates nephrite schist from the garnetite. All other lithological contacts are sub-parallel or parallel to the regional fabric (Figure 2), to the schistosity within the pit, and to the pit outline (Figure 3). The contact between marble and garnetite is sharp and irregular, and appears to be folded in the western portion of the excavation. The orientation of the axis of this partially exposed decametre-scale fold is expected to be collinear with minor fold axes observed within the pit, which plunge 20º towards 125º.

Nephrite/Nephrite Schist

No gem quality, and little good quality ornamental grade nephrite remains in the pit. Most of the nephritic rock exposed in the pit is a nephrite schist, characterized by a green-grey colour and foliation parallel to lithological contacts. Nephrite schist is generally aphanitic, comprising mainly of 50-55% interlocking subhedral tremolite-actinolite fibres (0.03 mm), acicular prisms (up to 0.4 mm long) and blades, and 35-40% fibrous and prismatic serpentine aggregates. The rock also contains actinolite (3-5%), carbonate (5-7%), limonite (8-10%), hematite (1.5-2%), pyrite (trace-0.5%), traces of chalcopyrite and spinel, and 0.5% of an unknown mineral. Carbonate forms in veins and pods parallel to the schistosity.

Chlorite Schist

Aphanitic, greyish-green chlorite schist is softer and more fissile than the nephrite schist. It contains chlorite (40-45%), serpentine (40-45%), clinozoisite (10-12%), limonite (10-12%) and traces of magnetite and apatite. The schist lenses are cut by folded carbonate veins and are in contact with garnetite, which forms the northern wall of the excavation.

Garnetite

Garnetite macroscopically resembles the “white rock” in deposit number 1. It is the most prominent, homogeneous and continuous lithology exposed within the pit wall, characterized by a white colour, rugous feel, massive appearance and reacts weakly with HCl. The rock is hard, fine to medium grained, equigranular, and comprised mainly of garnet (probably hydrogarnet; 65-80%), carbonate (probably calcite; 15-25%), quartz

(5%), and traces of talc, epidote, clinozoisite and apatite. Carbonate forms mainly in garnet interstices and in garnet fractures. Garnetite separates the nephrite from marble.

Blue Marble

Blue marble is distinctively dark bluish-grey, medium grained, equigranular and massive. It reacts moderately to strongly with HCl. The rock is a nearly monomineralic and consists mainly of carbonate (96-98%), limonite (2-3%), and traces of pyrite and hematite. Carbonate grains have folded twin lamellae and wavy to embayed contacts.

Serpentinite

The serpentinite forms the footwall of the excavation and is characterized by fine to medium grained, strongly schistose and fissile rocks ranging from dark greenish-grey serpentinite (94-97% serpentine), to banded pale greenish-greyish-white talc schist. The talc schist contains up to 55% talc, serpentine (30-35%) and chlorite (7%). Both serpentinite and talc schist contain traces to minor amounts of garnet, pyrite, chromite and oxidized magnetite. Serpentinite is cut by a hatch pattern of fibrous and prismatic serpentine veins. Talc schist is cut by anastamosing, fibrous talc and lesser serpentine veins that are parallel to the schistosity and make up to 45% of the rock.

Metavolcanics/Metasediments

Centimetricaly banded dark grey to pale grey, medium grained and schistose metavolcanics / metasediments within the hangingwall of the excavation, were not observed in direct contact with nephrite. Metavolcanics / metasediments contain plagioclase (53-55%), serpentine (in veinlets 33-35%), biotite (5-6%), epidote group minerals (3-4%), and traces of garnet and apatite. The unit also contains an unknown mineral, tentatively identified as anthophyllite (5-6%). Fine grained plagioclase and epidote veinlets cut the serpentine-rich veinlets.

Origin

A variety of origins were proposed to explain nephrite deposits (Leaming, 1978). It is believed that most of the British Columbia nephrite occurrences formed by contact metasomatic exchange between serpentinized ultramafics and country rocks (commonly metasediments).

There is a wealth of published data on the stability field of tremolite in marbles and to lesser extent in ultramafic rocks. The common range of PT conditions where tremolite-actinolite amphiboles are reported extends from less than 1 kilobar at 300°C (contact metamorphism) to over 6 kilobars at 700°C (relatively high-grade regional metamorphic environments). These limits are reasonable for most geological situations where metamorphic fluids are internally buffered, and thermodynamic equilibrium is attained within carbonate or other homogeneous protolith. The processes responsible for the formation of the British Columbian nephrite deposits were probably externally buffered, because of the association between nephrite and faults. The relative spatial distribution of the serpentinite, "white rocks", nephrite and metasediments is typical of metasomatic reaction zones, and in most cases, thermodynamic equilibrium at the scale of the deposit was probably not attained. Furthermore, good quality nephrite rocks are nearly monomineralic, therefore tremolite is expected to remain stable to higher temperatures. The granodiorite was traditionally considered as unrelated to the formation of nephrite (Leaming, 1978), but more work is required to validate this statement.

Exploration Potential

The Mount Ogden area still has good economic potential for the discovery of extensions to the existing deposits or new nephrite deposits, despite the extensive overburden and repeated coverage in past years by traditional prospecting. The three deposits within the study area trend approximately northwest and are parallel to the dominant regional fabric; potential new discoveries are expected to have the same orientation.

The main nephrite controls appear to be the contact between the granodiorite pluton and ultramafic unit and major tectonic contacts between metasedimentary / metavolcanic rocks and the ultramafic unit. It is possible that VLF would turn out to be an efficient geophysical tool to outline the controls described above. The "white rock" in outcrops or boulder trains is itself an indirect nephrite indicator.

Economic Potential

British Columbia is renowned for its nephrite production. The value-added processing, which resides mainly in carving and jewelry is also well established. To sustain this industry, new high quality nephrite discoveries are needed.

Nephrite tile making offers an other opportunity. A number of the nephrite mining camps, such as those of the Mount Ogden area, were exploited by surface mining. As a result, important quantities of industrial grade nephrite, suitable for tile making, were left as stockpiles at the sites. While nephrite tiles would not be able to compete with the main-stream granite or marble tiles in terms of cost per unit, they will represent an upscale niche product. Furthermore, preliminary examination of the "white rock" samples adjacent to nephrite deposit number 2, in the Mount Ogden area, indicates that white garnetite or hydrogarnetite zones may occur in close proximity to the nephrite material and marble. Some applied research is justified to determine if this unusual (hydro-) garnet rich rock has any industrial applications.

ACKNOWLEDGEMENTS

We thank Jade West Group of Companies, for authorizing the access to their properties. We would like to thank K. Makepeace, president of the company, for sharing their experience and hands on approach. The paper was reviewed and improved by comments from Derek Brown from the British Columbia Geological Survey, Suzanne Paradis from Geological Survey of Canada, and Dan Marshall from Simon Fraser University. Drafting was done by Mike Fournier from the British Columbia Geological Survey.

REFERENCES

Armstrong, J.E. (1949): Fort St. James Map-Area, Cassiar and Coast Districts, British Columbia; *Geological Survey of Canada*, Memoir 252, 210 pages.

Ash, C.H. and Macdonald, R.W.J. (1993): Geology, Mineralization and Lithogeochemistry of the Stuart Lake Area, Central British Columbia (Parts of 93K/7, 8, 10 and 11); *in* Geological Fieldwork 1992, *British Columbia Ministry of Energy, Mines and Petroleum Resources*, Paper 1993-1, pages 69-86.

Coleman, R. (1967): Low-Temperature Reaction Zones and Alpine Ultramafic Rocks of California, Oregon and Washington. U.S. Geological Survey Bulletin 1247, 49. Pages.

Gabrielse, H. (1985): Major Dextral Transcurrent Displacements along the Northern Rocky Mountain Trench and Related Lineaments in North-central British Columbia; *Geological Society of America Bulletin*, Volume 96, pages 1-14.

Ghent, E.D., Erdmer, P., Archibald, D.A. and Stout, M.Z. (1996): Pressure - Temperature and Tectonic Evolution of Triassic Lawsonite - Aragonite Blueschists from Pinchi Lake, British Columbia; *Canadian Journal of Earth Sciences,* Volume 33, pages 800-810.

Leaming, S.F. (1995): Jade in North America, in: Roger Keverne editor; Jade; Annes Publishing Limited, London; pages 298-315.

Leaming, S.F. (1978): Jade in Canada; *Geological Survey of Canada*, Paper 78-19, 59 pages.

Monger, J.W.H., Richards, T.A. and Paterson, I.A. (1978): The Hinterland Belt of the Canadian Cordillera: New Data from Northern and Central British Columbia; *Canadian Journal of Earth Sciences*, Volume 15, pages 823-830.

Paterson, I.A. (1974): Geology of Cache Creek Group and Mesozoic Rocks at the Northern End of the Stuart Lake Belt, Central British Columbia; *in* Report of Activities, Part B, *Geological Survey of Canada*, Paper 74-1, Part B, pages 31-42.

Paterson, I.A. (1977): The Geology and Evolution of the Pinchi Fault Zone at Pinchi Lake, Central British Columbia; *Canadian Journal of Earth Sciences*, Volume 14, pages 1324-1342.

Paterson, I.A. and Harakal, J.E. (1974): Potassium-Argon Dating of Blueschists from Pinchi Lake, Central British Columbia; *Canadian Journal of Earth Sciences*, Volume 11, pages 1007-1011.

Schiarizza, P. and MacIntyre, D. (1999): Geology of the Babine Lake - Takla Lake area, central British Columbia (93K/11, 12, 13, 14; 93N/3, 4, 5, 6); *in* Geological Fieldwork 1998, *British Columbia Ministry of Energy and Mines*, Paper 1999-1, pages 33-68.

Schiarizza, P. and Payie, G. (1997): Geology of the Sitlika Assemblage in the Kenny Creek - Mount Olson Area (93N/12, 13), Central British Columbia; *in* Geological Fieldwork 1996, *British Columbia Ministry of Employment and Investment*, Paper 1997-1, pages 79-100.

Schiarizza, P., Payie, G., Holunga, S., and Wright, D. (1997): Geology, Mineral Occurrences and Geochemistry of the Kenny Creek - Mount Olson Area (93N/12, 13), British Columbia; *British Columbia Ministry of Employment and Investment*, Open File 1997-2.

Scott, A. (1996): Jade a Mystical Mineral: Equinox, No.89, pages 64-69.

Struik, L.C. (1993): Intersecting Intracontinental Tertiary Transform Fault Systems in the North American Cordillera; *Canadian Journal of Earth Sciences*, Volume 30, pages 1262-1274.

Wetherup, S. and Struik, L.C. (1996): Vanderhoof Metamorphic Complex and Surrounding Rocks, Central British Columbia; *in* Current Research 1996-A, *Geological Survey of Canada*, pages 63-70.

Whittaker, P.J. (1983): Geology and Petrogenesis of Chromite and Chrome Spinel in Alpine-type Peridotites of the Cache Creek Group, British Columbia; unpublished Ph.D. thesis, *Carleton University*, 339 pages.

Gem-quality Cordierite Deposits, Slocan Valley, British Columbia (NTS 82F/12E)

By George J.Simandl[1], Dan Marshall[2] and James Laird[3]

KEYWORDS: *Economic Geology, Cordierite, Iolite, Anthophyllite-gedrite, Gemstone, Sapphirine, Valhalla Complex, Passmore Dome.*

INTRODUCTION

Cordierite is typically an orthorhombic magnesium-iron aluminosilicate and its high temperature form, indialite (alpha-cordierite), is isostructural with beryl (Deer *et al*.,1963). It has the formula $X_{0-1}M_2T_9O_{18}$ where X=H_2O, CO_2, Ar, Xe, Na and K may be present within channels parallel to the c axis. M= Mg^{2+}, Fe^{2+} and possibly Li^+. T=Al_4Si_5 and possibly Be^{2+}. Cordierite is a common constituent in contact metamorphosed argillaceous or arenaceous sediments and in regionally metamorphosed settings where it occurs only in high grade gneiss (Deer *et al*., 1963; Nathan *et al*., 1995; Nicollet, 1985; Lal, 1997). Cordierite-anthophyllite assemblages or their granulite facies equivalents have been identified and described from many localities including the famous West Uusinaa Complex, Finland (Escola, 1915). A number of these localities are closely associated with base metal deposits, and this assemblage is considered an indirect prospecting tool for volcanogenic massive sulphide deposits in highly metamorphosed terrains (Schreurs and Welstra, 1985; Robinson *et al*., 1982). Cordierite also occurs in a variety of intrusive rocks, including granites, pegmatites, norites (Deer *et al*., 1963; Heinrich, 1950), where critical parameters controlling its stability field are low temperature and pressure, high Mg^{2+} and Fe^{2+}, A/CNK, aAl_2O_3, and fO_2 (Clarke, 1995).

Cordierite is commonly used by geologists as a metamorphic index mineral, but its stability field on petrogenetic grids remains controversial because of uncertainties in its thermodynamic properties (Gunter, 1977; Skippen and Gunter, 1996; Lal, 1997). Cordierite may also have a potential as a CO_2-H_2O sensor for fluids and melts (Visser *et al*., 1994; Harley, 1994; Carrington and Harley, 1996).

Iolite, dichroite and "water sapphire" are the names used to designate the gem-quality cordierite in the gem trade.

Gem-quality cordierite is much less common than its rock forming equivalent. It is transparent to translucent with vitreous to greasy luster and comes in a variety of colours, mainly in shades of blue or violet, greenish, yellowish, or colorless. It is strongly pleochroic making cutting more challenging. No matter the shape of the rough, iolite crystals have to be oriented exactly to take advantage of the most desirable color and consequently the weight of stone may be severely reduced during the cutting. It is a hard mineral (7 to 7.5 on the Moh's hardness scale) with conchoidal fracture and one moderately well-developed cleavage direction. This cleavage makes it less durable than sapphire. Its density varies from 2.53 to 2.78 g/cm^3. The main sources of gem-quality cordierite are Sri Lanka, Mozambique, Madagascar, Burma and India. Other sources are Tanzania, Namibia, Canada and USA.

In Canada, gem-quality material and excellent specimens have been extracted from number of areas (Wight, 1999), including the Geco Mine (Ontario), Great Slave

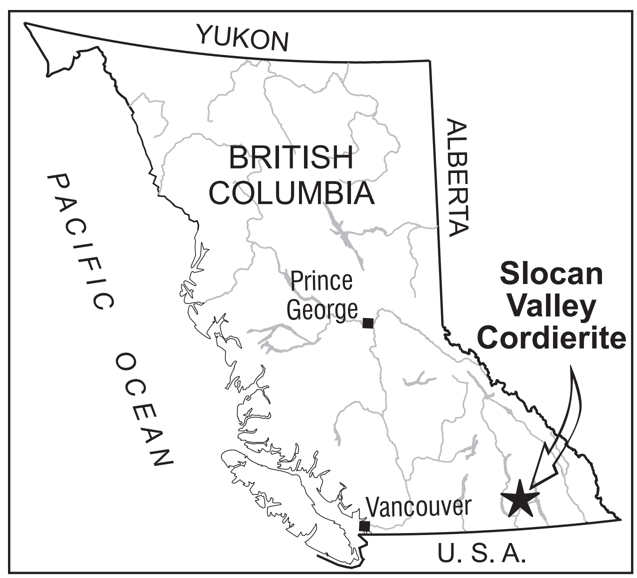

Figure 1. Location of Slocan Valley cordierite occurrences.

[1]*Geological Survey Branch, Ministry of Energy and Mines, 5th Floor 1810 Blanshard St, Victoria, BC*

[2]*Earth Sciences Department, Simon Fraser University, 8888 University Dr. Burnaby, BC. V5A 1S6*

[3] *Former Exploration Manager for Anglo Swiss Resources Inc. Currently Consultant, Laird Exploration Ltd., 21004 Stonehouse Ave., Maple Ridge, B.C. V2X 8C5*

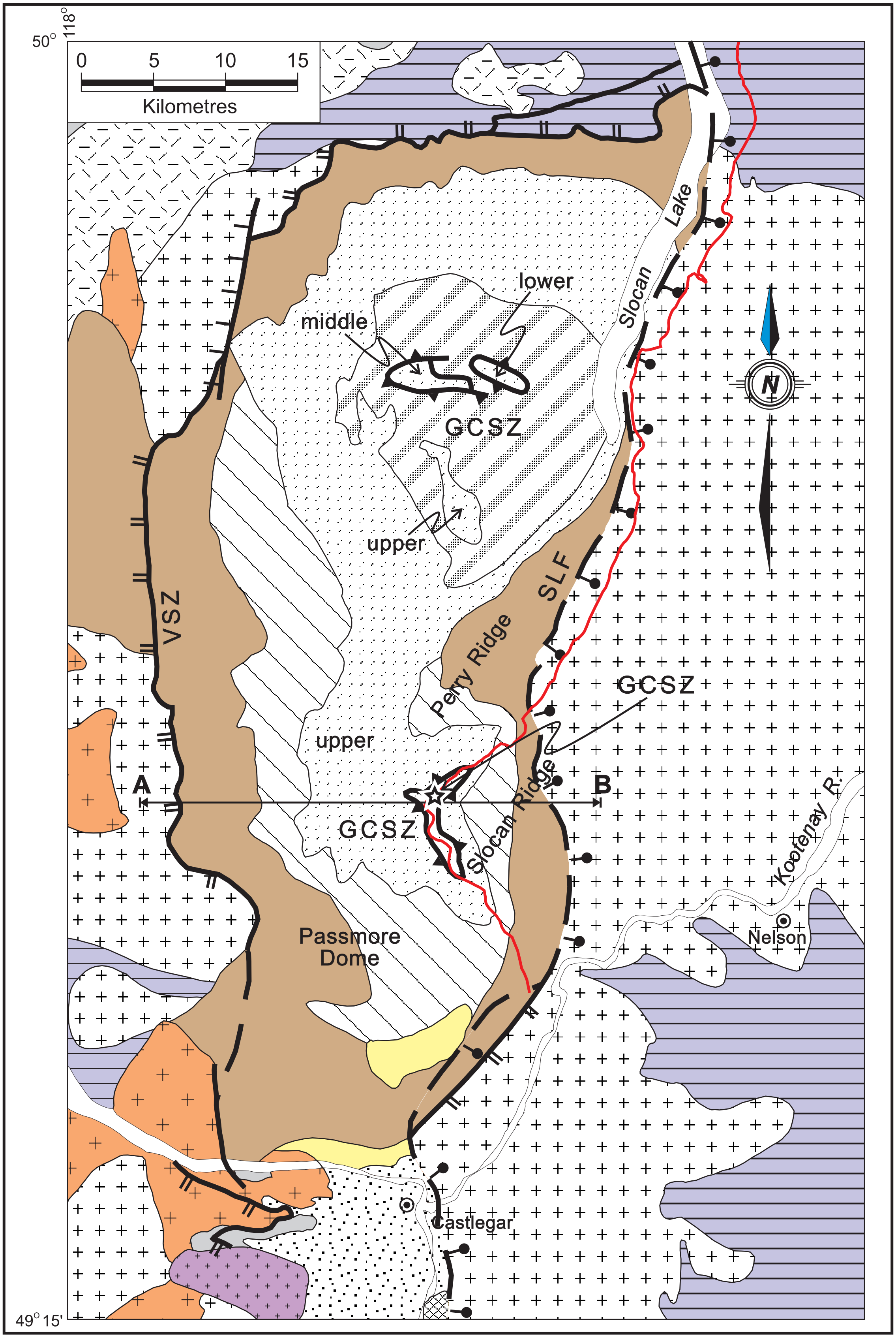

Figure 2. The geological setting of the Slocan Valley and cordierite occurrences (from Schaubs and Carr (1998). SLF: Slocan Valley Fault, VSZ: Valkyr Sheer Zone, GCSZ: Gwillim Creek Shear Zone.

LEGEND

Upper Plate

Middle Eocene Coryell syenite, granite

Eocene College Creek granite

Late Cretaceous granitic rocks

Middle Jurassic granitic rocks

Middle Paleozoic - Early Mesozoic allochthonous Quesnelia

Valhalla complex (Lower Plate)

Early Eocene Ladybird granite

Paleocene Airy Quartz Monzonite

Late Cretaceous Mulvey granodiorite

Late Cretaceous Kinnaird Gneiss

Middle Devonian Trail Gneiss

Metasedimentary rocks

Castlegar Gneiss

Thrust fault

Steep normal fault

Slocan Lake fault

Valkyr shear zone

Cordierite Occurrences

Lake and Ghost Lake areas (Northwest Territories), Snow Lake area (Manitoba) .

Other blue minerals, well established in the gemstone trade, are sapphire, benitoite, spinel and tanzanite (a variety of zoisite). Gem-quality cordierite, currently available on the market, is considered as a moderately priced stone. It is marketed and promoted as an affordable substitute for tanzanite, benitoite or blue sapphire. According to Wight (1999): "Iolite is not seen frequently in jewelry, but it is not rare except in sizes over 30 carats". This perception is now deeply anchored within the colored stone industry and may be difficult to change. As with other gemstones, exceptional stone quality in combination with highly effective marketing programs may enhance the price.

Gemstone Evaluation - General Comments

Conceptual and market studies by independent specialists should be done in the first stages of gemstone deposit evaluation. Such studies are essential to determine if any follow-up work leading to the pre-feasibility stage (including the grade and tonnage estimates) is warranted. The grade and tonnages of hard rock gemstone deposits are difficult to predict. A single large, high quality stone may double cash flow of a mid-size gemstone mining operation, when diamonds, emeralds, sapphires or other high-value stones are involved. Bulk sampling and sorting of the stones into facet, cabochon and specimen grades provide the basis for grade estimates, evaluation of potential product, recovery rate evaluation and the material for test marketing. Bulk sampling also provides a useful check on mining and gemstone extraction cost estimates. The extraction of gemstones from small, "hard rock" deposits tends to be relatively costly, technically demanding and/or labour intensive because care must be taken to minimize gemstone fracturing.

Location and History

The gem-quality cordierite in the Slocan Valley occurrences in southeastern British Columbia, were first reported by Jim Laird, while working for of Anglo Swiss Resources Inc. The occurrences were discovered during the exploration for star corundum and are located on the Blu Starr property (Minfile number 082FNW259) that belongs to Anglo Swiss Resources Inc., approximately 25 kilometres west of Nelson and 30 km south of Slocan near highway 6 (Figure 1).

REGIONAL GEOLOGY

The cordierite occurrences are located within the Omineca Belt and more precisely within the Valhalla metamorphic core complex (Reesor, 1965) which is characterized as a structural culmination with outward-dipping metamorphic layering and foliation (Schaubs and Carr, 1998; Simony and Carr, 1996). The complex consists of the Valhalla and Passmore domes and is delineated by ductile Valkyr shear zone to the north, west and south and Slocan Lake fault to the east. The Valhalla complex forms the footwall of the Valkyr and Slocan Lake shear zones (legend of Figure 2 and Figure 3). It consists of Castlegard Gneiss, metasedimentary rocks, Middle Devonian Trail Gneiss, Late Cretaceous Kinnaird Gneiss, Late Cretaceous Mulvey granodiorite, Paleocene Airy Quartz monzonite and Early Eocene Ladybird granite (Legend of Figure 2). The complex contains three sheets of supracrustal rocks identified as upper, middle and lower. The upper sheet consists of the "Valhalla assemblage" metasedimentary rocks sandwiched between Paleocene granitoids and the Mulvey granodiorite (Figures 2 and 3). The middle sheet and upper portion of the lower sheet are interlayered with Mulvey granodiorite (Figure 2).

The hanging wall of the Valkyr and Slocan Lake shear zones (so called upper plate, legend of Figure 2) consists of Middle Paleozoic to Early Mesozoic rocks of allochtonous Quesnelia, Middle Jurassic and Late Cretaceous granitic rocks, Eocene College Creek granite and Middle Eocene Coryel syenite and granite.

In the Passmore dome area, metasedimentary rocks within the upper sheet are overlain by Airy quartz monzonite (Figure 3) and are interpreted to be underlain by Mulvey granodiorite gneiss (Schaubs and Carr, 1998). The cordierite-bearing lenses lie within or near the mylonites of the Gwillim Creek Shear Zone (GCSZ) which separates the metasediments of the upper sheet from the lower sheet (Figure 2).

The lenses occur within the metasedimentary sequence, described by Schaubs and Carr (1998) as consisting of pelitic schists (biotite>50%, quartz, feldspar, sillimanite and garnet), semipelitic schists (biotite <50%, quartz, feldspar ± sillimanite and garnet) and psammitic gneiss (mainly quartz and feldspar, with minor biotite) and at least one quartzite layer more than 1 metre thick. Mafic and ultramafic rocks form lenses. Most of these lenses can be described as amphibolites with or without garnet. Peak metamorphic assemblages in pelitic schists contain garnet, sillimanite, alkali feldspar and melt indicating temperatures over 800±20ºC and pressure of 8±1kb (Spear,1994). Further thermal history of the complex is discussed by (Parish, 1995). Structural geology of the metasedimentary rocks in the Passmore dome area, where the cordierite deposits are located is covered in detail by Schaubs and Carr (1998). These authors describe metasedimentary rocks displaying nearly flat lying subhorizontal transposition foliation and strong east or west plunging stretching lineation, rootless folds with strongly sheared limbs and sheet folds. All these features were also observed during our visit at the deposit scale.

Geology of the Slocan Valley Cordierite Occurrences

Three cordierite-bearing lenses are reported in the area, however only two of these were examined during our short visit. Both visited occurrences are exposed on

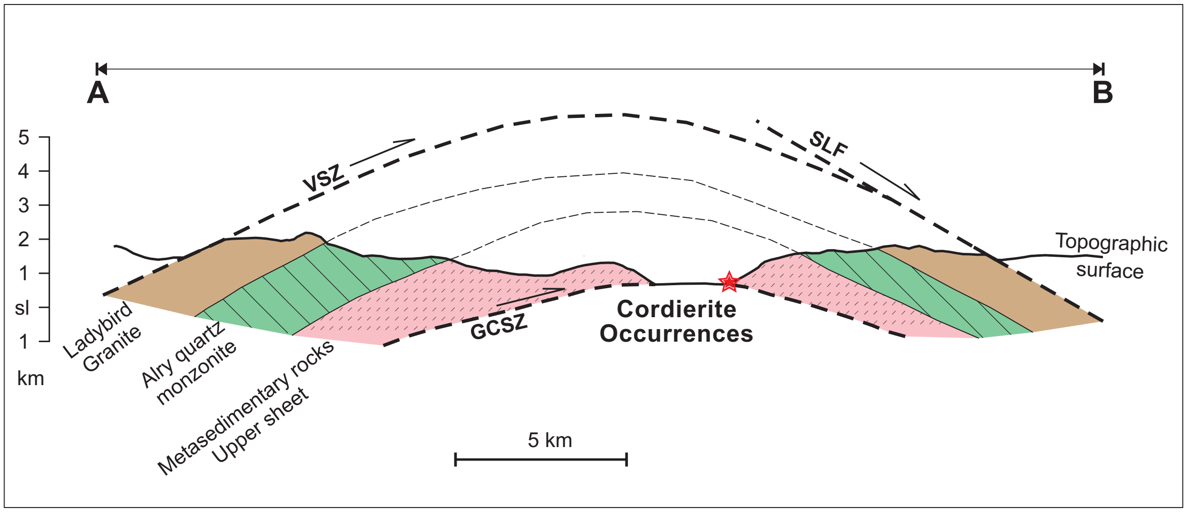

Figure 3. Cross section of the Passmore dome in the area of cordierite occurrences (modified from Schaubs and Carr (1998). For location, *see* Figure 2.

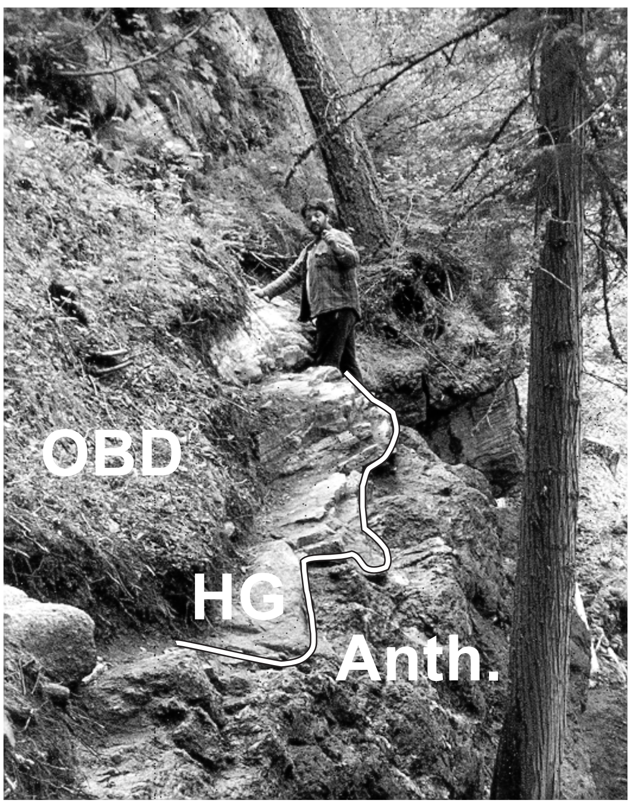

Photo 1. The main cordierite-bearing, anthophyllite rock lense, Slocan Valley; HG: hangingwall gneiss; Ant: anthophyllite-rich rock; OBD: overburden. For approximate location, *see* Figure 2.

the cliff faces approximately one kilometre apart. Lenses are located within or near the Gwillim sheer zone (Figure 3).

Both lenses are located in or near noses of folds that have subhorizontal fold axes plunging 65 to 85°E. The long dimension of the lenses is expected to be collinear with the fold axis and mineral lineations. The larger of the lenses is only partially exposed for nearly 20 metres along strike (Photo 1 and Figure 4). Its maximum exposed thickness is nearly 6 metres with its extent in the third dimension unknown. The smaller lens is exposed for greater than 10 metres along the cliff side and its maximum thickness exceeds 2 metres (Figure 5). The contacts between the lenses and the surrounding gneiss are sharp and irregular or sheared.

Cordierite-bearing, anthophyllite lenses have characteristic rough hummocky appearance. The lenses are brown to dark green on weathered and dark green on fresh surfaces. They are coarse grained, typically 0.5 to 2 centimetres and characterized by interlocking blades of gedritic anthophyllite and irregularly distributed heavily included garnet porphyroblasts up to 5 centimetres in diameter. The mineralogy is approximately gedritic-anthophyllite (55 % or more), quartz (20%), garnet (0 -15%), biotite (0-90%) generally restricted to quartz vein or pegmatite contacts with anthophyllite-rich rock, plagioclase feldspar (5%) with minor clino-amphiboles and cordierite (0-25%). Potassic feldspar may be also present.

The lenses of anthophylite rock are cut by tourmaline-bearing pegmatites, quartz veins and garnet-bearing feldspar veins (Figure 4), fractures and irregular zones consisting mainly of coarse-grained biotite are found adjacent to pegmatite and quartz veins or controlled by the same fractures. Coarse cordierite occurs mainly within quartz veins, along the contact of these veins with the host anthophyllite lens, or in biotite zones. The cordierite crystals are completely embedded in the host rock. Cordierite crystals, in many cases partially or entirely converted to pinite may measure up to 10 centimetres in length. There is a transition from transparent, blue or gray cordierite in the unaltered core of the crystal to pale green translucent to opaque aphanitic rim entirely consisting of pinite.

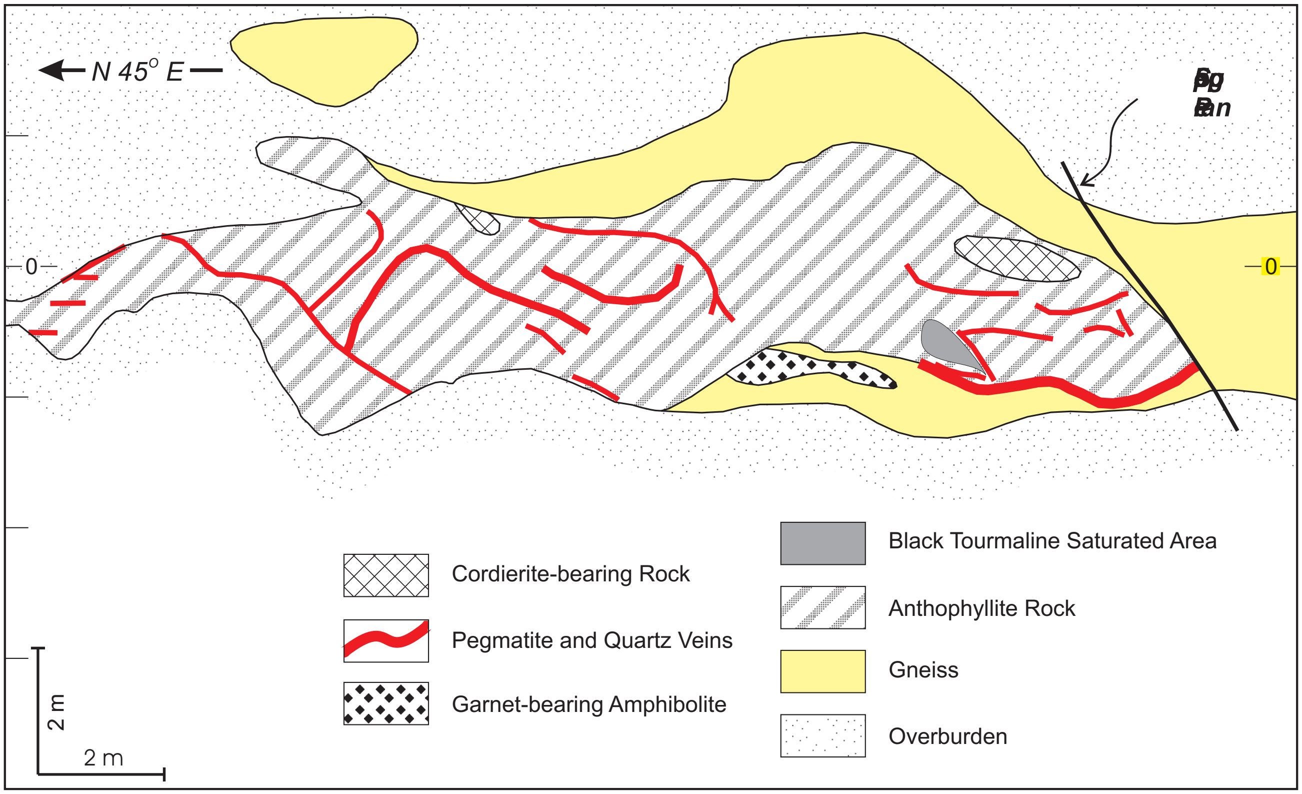

Figure 4. Idealized vertical section along the main cordierite-bearing cliff face (main outcrop).

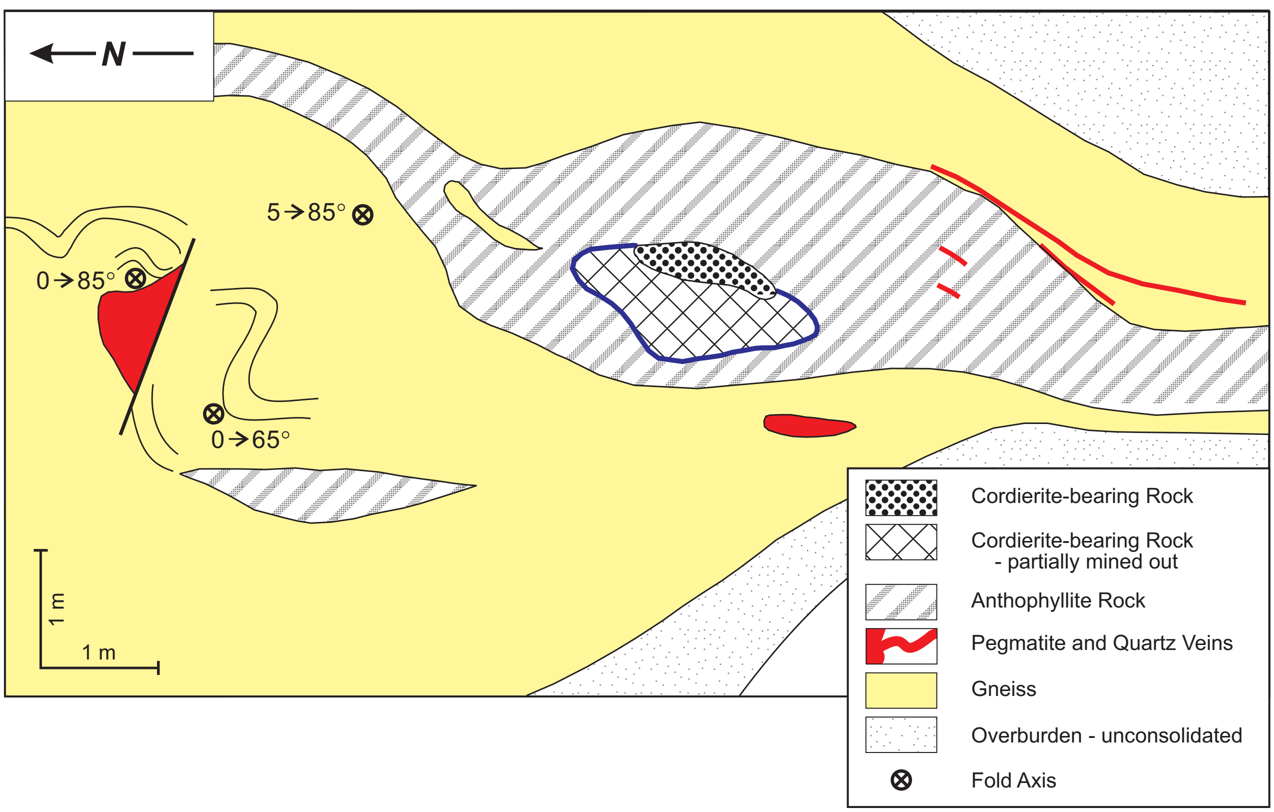

Figure 5. Idealized vertical section, along cliff exposure of the second cordierite-bearing lens, located approximately 1km south from the main outcrop. For approximate location, *see* Figure 2.

TABLE 1
ELECTRON MICROPROBE ANALYSES OF CORDIERITES FROM THE SLOCAN VALLEY

SAMPLE	SiO_2	Al_2O_3	TIO_2	Cr_2O_3	FeO	MgO	MnO	CaO	K_2O	Na_2O	Total
Cord 99-2-10	49.53	35.07	0.03	0.01	3.16	11.96	0.13	0.03	0.00	0.13	100.05
Cord 99-2-10	49.20	34.86	0.09	0.00	3.25	11.73	0.12	0.07	0.01	0.13	99.46
Cord 99-2-10	49.17	35.03	0.09	0.00	3.19	11.78	0.04	0.04	0.00	0.14	99.48
Cord 99-2-19	50.84	33.62	0.00	0.02	3.64	11.33	0.05	0.03	0.02	0.25	99.80
Cord 99-2-19	50.46	33.88	0.00	0.01	3.69	11.45	0.00	0.02	0.00	0.27	99.78
Cord 99-2-19	50.41	33.25	0.04	0.01	3.57	11.53	0.00	0.02	0.01	0.22	99.06
Cord 99-2-19	50.84	33.57	0.10	0.01	3.36	11.56	0.04	0.04	0.01	0.26	99.79

The intensity of the replacement decreases progressively from the crystal edges inward. The cores are commonly clear, blue or bluish gray in color, but fracture networks reduce the maximum size of the stones suitable for cutting. As a result, the majority of the cordierite exposed at the site in July 1999 were of specimen quality. Few stones up to 5 mm in longest dimension, of gem or near-gem quality were extracted during our visit. Table 1 shows results of the microprobe analyses of the iolite. Photo 2 shows an enlarged finished stone from this property.

Terminated amethystine and colorless transparent quartz and tourmaline crystals occur in cavities within the anthophyllite rock and elsewhere on the property.

The gneiss, country rock to the lenses, is characterized by folds with severed limbs and centimetre- to metre-scale layering. The leucosomes are thicker and more continuous than melanosomes. Mineralogy is variable, consisting of quartz (60%), green or brown biotite (20%), plagioclase (8%), potassic feldspar (2%) and sillimanite, titanite, cordierite, garnet (~10%). Melanosomes are composed of quartz (30%) plagioclase (30%), biotite (30%), potassic feldspar (7%), and garnet (3%). The gneiss also contains centimetre to metre thick lenses of clinoamphibolites that may also contain garnet. Representative mineral analyses are given in Table 2.

Photo 2. Raw and cut iolite from the Slocan Valley occurrences, the faceted stones (from left to right) weight 0.5, 0.5, 0.5 and 0.6 carat respectively (courtesy of Anglo Swiss Resources Inc.).

TABLE 2
REPRESENTATIVE MICROPROBE ANALYSES OF MINERALS WITHIN THE ANTHOPHYLLITE LENSES AND COUNTRY GNEISS

Sapphirine	SiO_2	Al_2O_3	TiO_2	Cr_2O_3	FeO	MgO	MnO	CaO	K_2O	Na_2O	Total			
Cord 99-2-10	11.45	65.23	0.03	0.26	9.02	14.93	0.16	0.03	0.00	0.00	101.11			
Cord 99-2-10	11.01	65.17	0.06	0.32	9.04	14.94	0.09	0.10	0.00	0.00	100.73			
Ortho-Amphibole	SiO_2	Al_2O_3	TIO_2	Cr_2O_3	FeO	MgO	MnO	CaO	K_2O	Na_2O	NiO	Cl	F	Total
Cord 99-2-4	48.38	11.86	0.29	0.04	14.64	19.90	0.37	0.75	0.00	0.77	0.00	0.02	0.05	97.07
Cord 99-2-4	47.61	11.92	0.40	0.11	14.54	19.63	0.39	0.70	0.00	0.84	0.00	0.01	0.02	96.17
Cord 99-2-4	47.70	11.89	0.22	0.05	14.57	19.79	0.48	0.69	0.00	0.83	0.00	0.04	0.01	96.27
Clino-Amphibole														
Cord 99-6 #6	41.44	13.18	1.53	0.05	18.50	8.88	0.12	10.86	0.79	1.41	0.00	0.00	0.10	96.86
Cord 99-6 #7	41.50	13.31	1.43	0.05	18.66	8.68	0.11	10.97	1.03	1.33	0.00	0.00	0.05	97.12
Cord 99-6 #8	42.92	12.21	0.91	0.04	18.69	9.17	0.13	11.05	0.58	1.35	0.00	0.01	0.15	97.21
Cord 99-6 #9	42.99	12.44	0.96	0.04	18.34	9.19	0.12	11.00	0.55	1.34	0.00	0.01	0.12	97.10
Garnet	SiO_2	Al_2O_3	TIO_2	Cr_2O_3	FeO	MnO	MgO	CaO	Total					
Cord 99-2-1	38.58	21.75	0.00	0.00	27.02	0.88	9.46	1.63	99.32					
Cord 99-2-10	40.71	22.77	0.00	0.08	18.35	0.73	13.60	3.13	99.37					
Cord 99-2-10	40.71	22.78	0.00	0.07	18.34	0.79	13.63	3.30	99.62					
Cord 99-5 #3	37.66	21.00	0.02	0.04	26.85	1.29	2.90	10.06	99.82					
Cord 99-5 #5	38.53	20.51	0.00	0.05	24.09	1.91	2.68	11.93	99.70					
Cord 99-5 #6	38.58	19.98	0.00	0.04	22.97	2.71	1.92	12.79	98.99					
Cord 99-2-8	39.76	22.67	0.00	0.15	19.85	0.38	14.01	2.42	99.24					
Biotite	SiO_2	Al_2O_3	TIO_2	Cr_2O_3	FeO	MnO	MgO	CaO	K_2O	NiO	Na_2O	BaO	Cl	F
Cord 99-2-10	37.91	18.18	1.59	0.11	10.89	0.01	17.22	0.03	8.85	0.00	0.47	0.05	0.09	0.11
Cord 99-2-10	38.17	18.20	1.75	0.09	10.36	0.03	17.45	0.03	8.83	0.00	0.50	0.00	0.08	0.13
Cord 99-2-1	37.97	16.32	1.42	0.07	12.74	0.08	16.02	0.01	8.23	0.00	0.43	0.00	0.02	0.18
Cord 99-2-6	37.96	16.45	1.37	0.07	13.39	0.07	16.07	0.01	8.29	0.00	0.41	0.00	0.04	0.10
Cord 99-2-8	37.78	17.88	1.69	0.13	9.85	0.06	18.41	0.00	8.51	0.00	0.58	0.00	0.08	0.14
Cord 99-5	36.62	15.97	3.00	0.05	20.24	0.15	10.34	0.02	8.66	0.00	0.37	0.54	0.11	0.22
Cord 99-2-19	38.08	16.89	1.93	0.05	11.59	0.05	16.60	0.00	8.85	0.00	0.47	0.01	0.08	0.17
Cord 99-6 #10	36.62	15.22	2.79	0.04	19.17	0.04	12.14	0.04	8.82	0.00	0.32	0.00	0.03	0.23
Cord 99-2-8	38.43	17.98	1.48	0.15	9.54	0.08	18.48	0.02	8.67	0.00	0.55	0.08	0.07	0.22
Feldspar	SiO_2	Al_2O_3	K_2O	CaO	Na_2O	FeO	Total							

Exploration Potential

The Slocan Valley occurrences are the first discoveries of gem-quality cordierite in British Columbia. It is probable that future prospecting activity within the Passmore or Valhalla dome areas, or similar geological environments elsewhere in British Columbia, will result in new iolite discoveries. Non-gem quality cordierite is also present in the country gneiss that contains iolite-bearing lenses. Cordierite-orthoamphibole assemblages were also reported within Thor-Odin gneiss dome (Smith and Duncan), 1995.

As far as the two occurrences described here, the cordierite occurs mainly in association with quartz veins and pegmatite contained within the anthophyllite lenses. Quartz veins, pegmatites and cordierite bearing zones represent probably about 10% of the exposed face (surface) of the lens. The face of the main lens is still not fully exposed. To evaluate the cordierite content of the lenses, bulk sampling would be required. Small panel samples, if taken adjacent to quartz vein may result in unrealistic high cordierite content. Only a small proportion (<3%) of the recovered cordierite is expected to be suitable for faceting. At this stage it is impossible to estimate what the cut stone to rough ratio will be. The largest faceted stone from this property (Photo 2) is reported to have a weight of 0.6 carats (Anglo Swiss Resources Inc., personal communication). Less clear stones may be cut “en cabochon” (an unfaceted, domed, smoothly polished stone). The largest cabochon from this property weights 1.5 carat (Anglo Swiss Resources Inc., personal communication). Wight (1999) reports that cordierite cut in cabochons from these occurrences display asterism (stars).

Constraints on the Origin

Peak metamorphic conditions are represented by garnet-hornblende-quartz-plagioclase and cordierite-sapphirine-corundum-garnet-plagioclase and shown approximately on Figure 6. Relative topology of the high temperature equilibria shown on Figure 6 is correct, however, reactions make take place at slightly lower temperatures. Until the problems highlighted by Gunter (1977), Skippen and Gunter (1996) and Lal (1997) are addressed the temperatures shown on Figure 8 are approximate.

These assemblages are consistent with peak metamorphic conditions in excess of 900°C and 9 kilobars, but slightly higher than those reported by Spear and Parrish (1996). This temperature is a maximum temperature for cordierite stability in the study area, and possibly corresponds to the highest temperature metamorphic rocks ever reported in British Columbia. Geothermometry of garnet-biotite pairs confirms post-peak reequilibration at

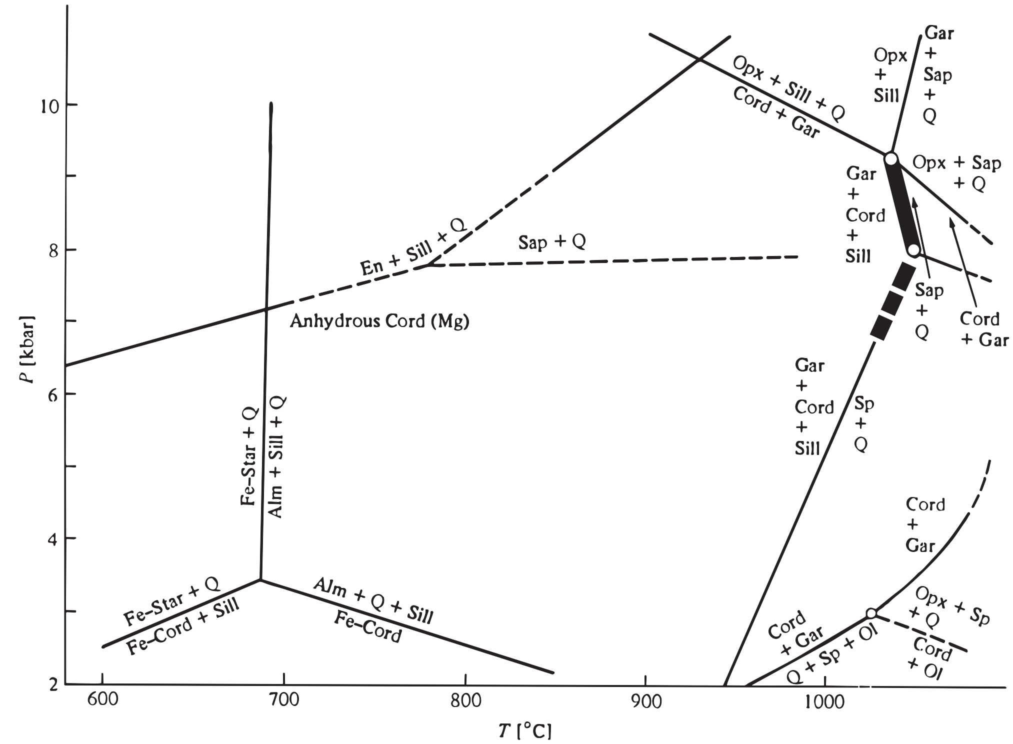

Figure 6. Equilibria involving cordierite in granulite facies (after Muller and Saxena, 1977). Opx; orthopyroxene; Sap: sapphirine; Q: quartz, Cord: cordierite; Gar: garnet; Sill: sillimanite, Sp: spinel; Ol: olivine, En: enstatite. Prograde and retrograde assemblages are shown by heavy solid and heavy doted lines respectively. P total = PH_2O, however PH_2O<P total above 900^oC.

the deposit scale, previously documented on the regional scale by Spear and Parrish (1996). Based solely on the spatial association of iolite with pegmatite, quartz veins and coarse biotite selvages , we can say that anthophyllite lithologies are an important ore control and that gem-quality cordierite is metasomatic or pegmatite-related. Abundant alteration and replacement of coarse euhedral cordierite crystals suggest a retrograde reequilibraion.

ACKNOWLEDGMENTS

We would like to thank to Anglo Swiss Resources Inc. for the permission to visit the property and for providing us with the photographs of cordierite specimen and finished cut stones. Microprobe analyses were done at Carleton University by Peter Jones. Derek Brown and David Lefebure from the B.C. Geological Survey, and Len Danard from Anglo Swiss Resources Inc. improved earlier versions of this manuscript.

REFERENCES

Carrington, D.P and Harley, S.L. (1996): Cordierite as a monitor of fluid and melt H_2O contents in the lower crust; an experimental calibration. Geology, v. 24, n. 7, p. 647-650.

Clarke, D.B. (1995): Cordierite in felsic igneous rocks; a synthesis. Mineralogical Magazine, v. 59, n. 2, p. 311-325.

Deer, W.A. , Howie, R.A. and Zussman, J. (1963): Cordierite; in: Rock Forming Minerals, Volume 1, pages 269-299.

Escola, P. (1915): On the Relation Between the Chemical and Mineralogical Composition in the metamorphic rocks of Orijärvi Region. Bull. Comm. Geol. Finlande No. 44.

Gunter, A.E. (1977): An experimental study of synthetic cordierites. Unpublished M.Sc. Thesis, Carleton University, Ottawa, Ontario, Canada.

Harley, S.L. (1994): Cordierite as a Sensor of Fluid and Melt Distribution in Crustal Metamorphism (extended abstract), Mineralogical Magazine, v. 58A, p. 374-375.

Heinrich, E.W.M. (1950): Cordierite in Pegmatite near Micanite, Colorado. American Mineralogist, Volume 35, pages 173-184.

Lal, R.K. (1997): Internally consistent Calibration or Geothermobarometry of High-grade Mg-Al Rich Rocks in the System $MgO-Al_2O_3-SiO_2$ and their application to Sapphirine-spinel Granulites of Eastern Ghats, India and Enderby Land, Antarcktica. Proceedings of Indian Academy of Science, Vol.106, No.3., pages 91-113.

Muller, R.F. and Saxena, S.K. (1997): Chemical Petrology. Springer-Verlag , New York, 394 pages.

Nathan, N. P., Raghavan, S., Natarajan, V. and Raman, R. Petrography and petrochemistry of the cordierite bearing metapelites of Nartamalai area, Pudukkottai District, Tamil Nadu. (1995): Journal of the Geological Society of India, v. 46, n. 5, p. 477- 483.

Nicollet, C. (1985): Les Gneiss Rubanés à Cordierite et Grenat d'Ihosy: Un Marqueur Thermo-barometrique dans le Sud de Madagascar; Precambrian Research, Volume 8, pages 175-185.

Parrish, R.R. (1995): Thermal Evolution of the Southern Canadian Cordillera; Canadian Journal of Earth Sciences, Volume 32, pages 1618-1642.

Reesor, J.E. (1965): Structural evolution and plutonism in Valhalla gneiss complex. Geological Survey of Canada, Bulletin 129, 128 p.

Robinson , P., Spear F. Schumacher, J.C., Laird, J., Klein, C., Evans, B.W., and Doolan, B. (1982): Phase Relations of Metamorphic Amphiboles: Natural Occurrences and Theory; *In*: D.R. Veblen and P.H. Ribbe (Editors), Amphiboles, Petrology and Experimental Phase Relations. Mineralogical Society of America, Washington DC, Reviews in Mineralogy, No. B.

Schaubs, P.M. and Carr, S.D. (1998): Geology of Metasedimentary Rocks and Late Cretaceous deformation History in the Northern Valhalla Complex, British Columbia; Canadian Journal of Earth Sciences, Volume 35, pages 1018-1036.

Simony, P. S. and Carr, S.D. (1996): Large Lateral Ramps in the Eocene Valkyr Sheer Zone: Extensional Ductile Faulting Controlled by Plutonism in Southern British Columbia, Journal of Structural Geology, Volume pages 769-784.

Schreurs, J. and Welstra, L. (1985): Cordierite-orthopyroxene rocks: The Granulite Facies Equivalents of the Orijärvi Cordierite-anthophyllite rocks in West Uusimaa, Southwest Finland; Lithos, Volume 18, Pages 15-228.

Skippen, G.B and Gunter, A.E. (1996): The thermodynamic properties of H_2O in magnesium and iron cordierite. Contributions to Mineralogy and Petrology, v. 124, n. 1, p. 82- 89.

Smith, B.M.L. and Duncan, I.J. (1995): Petrography and Metamorphism of Cordierite-Orthoamphibolite Assemblages, Thor-Odin Gneiss Dome, Shushwap metamorphic complex, British Columbia. in: 1995 GSA Abstracts with Programs, Southeastern Section, page 38.

Spear, F.S. (1994): P-T-t evolution of the Vahalla Complex, British Columbia, Canada. Mineralogical Magazine, Volume58, pages 868-869.

Spear, F.S. and Parrish, R.R. (1996): Petrology and cooling rates of the Valhalla Complex, British Columbia, Canada. Journal of Petrology, v. 37, n. 4, p. 733-765.

Visser, D. Kloprogge, J.T. and Maijer, C. (1994): An Infrared Spectroscopic (IR) and Light Element (Li, Be, Na) Study of Cordierites from the Bamble Sector, South Norway. Lithos, Vol.32, pages 95-107.

Wight, W. (1999): Garnet and Iolite in the Slocan Valley, British Columbia. Canadian Gemmologist, Vol XX, page 18.

In Situ Fracture Porosity and Specific Gravity of Highly Sheared Coals from Southeast British Columbia (82G/7)

By Barry Ryan[1] and Mike Takkinen[2]

KEYWORDS: *Coal density, specific gravity, fracture porosity, tonnage reconciliation, petrography.*

INTRODUCTION

Converting *insitu* volumes to tonnages available for processing is an important step in coal reserve calculation and in reconciling tonnages predicted to exist *insitu* with those that arrive at the wash plant. An important first step in the process is to assign a density or specific gravity (SG) to the *insitu* volume. Coal companies use a number of empirical equations, which provide SG values based on air-dried ash contents, to convert *insitu* volumes into *insitu* tonnages. Unfortunately many of these equations predict SG values as measured in the laboratory and not that of the *insitu* material. The problem is further compounded when coal seams are effected by folding or shearing, which are suspected of increasing the fracture porosity of the coal and decreasing its effective *insitu* specific gravity (ISG). Papers by Smith (1989) and Ryan (1991) use a more theoretical approach. The paper by Ryan (1991) generated an equation, that in contrast to some equations, predicts SG using the amount of mineral matter, coal, free moisture and void space making up the solid. This equation can therefore respond to changes in a wider range of coal properties than empirical equations and can predict ISG values effected by increased shearing within coal seams.

The process of reconciliation involves the careful consideration of many mining factors that influence the amount of coal delivered to the wash plant. These factors, such as, out-of-seam dilution (OSD), coal loss and breaker rejects, are difficult to quantify accurately. Often reconciliation is achieved by picking values for these factors that are within acceptable ranges and fit with the general perception of the mining operation. Thus, if less coal is reporting to the plant than is predicted by the *insitu* volumes in the pit, coal loss or breaker rejects can be increased to account for the difference. However, when the mining parameters appear to be outside the range accepted by mining experience, one has to question the accuracy of *insitu* tonnage calculations, which means questioning the volume determination, assigned ash content, or SG values used to convert *insitu* volumes to tonnages.

This paper uses the Ryan equation, and a data set of ash *versus* SG measurements for coal from a mine in southeast British Columbia, to derive an ash *versus* SG relationship. The equation provides a good fit to the data and allows terms for SG ash-free coal, SG mineral-matter-free, moisture and void porosity to be derived. This allows the SG used in the reconciliation calculation to be checked for credibility. The data set includes measurements of ash and SG on an air-dried basis using 60 mesh (0.25 millimetre) sized fragments. The SG measured in this way is not a true specific gravity because the coal grains contain some void porosity that is not penetrated by the liquid (kerosene) used in the SG measurement. The SG measured is therefore referred to as an apparent specific gravity (ASG). However in that these micro fractures are too small to be penetrated by ground water, ASG is a good starting point for calculations of ISG and there is no need to attempt to determine the SG of the coal solid minus all porosity. The validity of this assumption was checked by analyzing the ASG of 60 and 200 mesh samples. The petrography of some samples was measured to see if varying percentages of inert macerals produced measurable changes in SG.

It is difficult to measure *insitu* specific gravity (ISG), but there are some approaches that may help derive approximate values of ISG. Useful data can be extracted from washability data and from comparison of air-dried and as-received moisture contents of samples.

A "reconciliation" excel spread sheet is constructed to compare the effects of a number of parameters on the tonnage and the ash content of the coal delivered to the plant. Though the maths involved in this exercise is not complex, care has to be taken over a number of points, in particular, in converting tonnages to different water bases, and in recognizing when percentages are referring to volumes or weights.

SPECIFIC GRAVITY DATA

Proximate and SG analyses were performed on 28 air-dried raw coal samples from the mine (Table 1). The ASG (apparent SG on air-dried samples) was measured using the ASTM D167 test on 60 mesh coal (0.25 milli-

[1]*Geological Survey Branch*

[2]*Fording Coal Limited*

TABLE 1
MINE 1 RAW SG DATA

Sample	as-received M %	Air-dried M %	VM %	Ash %	FC %	SG (60)	SG (200)
1	3.4	0.5	20.0	16.6	62.9	1.42	
3	5.8	0.4	24.0	10.3	66.4	1.38	
5	3.9	0.4	21.7	15.2	62.7	1.4	
7	2.0	0.4	21.1	13.4	65.1	1.38	1.38
9	1.9	0.4	14.4	56.4	28.8	1.84	1.82
11	2.9	0.4	20.9	15.2	63.5	1.41	
13	2.3	0.3	21.3	14.0	64.5	1.38	
15	2.8	0.4	20.7	12.9	66.1	1.37	
17	3.8	0.3	22.0	23.8	53.9	1.46	1.44
19	1.8	0.3	19.6	38.3	41.9	1.64	1.55
21	2.0	0.5	15.1	61.9	22.6	2.02	
23	3.8	0.3	20.1	33.2	46.4	1.6	
25	3.3	0.4	20.7	10.2	68.8	1.4	
27	2.9	0.5	22.6	28.0	48.9	1.54	1.51
29	5.3	0.4	23.5	21.2	54.9	1.45	
31	2.2	0.4	19.7	37.2	48.8	1.63	
33	3.8	0.3	23.3	24.4	52.0	1.46	
35	2.4	0.3	19.1	38.6	42.0	1.64	
37	3.1	0.4	21.7	11.3	66.6	1.38	
39	4.7	0.5	20.2	19.5	59.8	1.45	
41	5.7	0.4	20.2	17.8	61.6	1.44	
43	4.3	0.5	20.2	21.1	68.4	1.46	
45	4.8	0.4	20.2	21.1	68.4	1.46	
45a	2.2	0.3	20.0	38.0	41.7	1.63	
47	1.6	0.3	16.8	58.3	24.6	1.92	
49	1.7	0.3	16.1	61.6	22.0	1.98	
51	3.3	0.2	20.8	30.7	48.2	1.54	1.52
53	3.9	0.4	22.8	20.6	56.2	1.44	
M=moisture 200 and 60 refer to mesh size							

metre) and in addition the ASG values of 6 samples were measured using the ASTM test on 200 mesh coal (0.075 millimetre). Washability tests were performed on 5 samples and the ASG measured on a number of air-dried washability increments to provide an additional 20 samples (Table 2). A single bulk sample from another mine, (Mine 2) with similar rank but different petrography from the first mine, was collected. Six washability increments of this sample were analyzed (Table 2). Specific gravity data from a previous study on the Telkwa deposit (Ryan, 1991) were also used.

A number of different equations were fitted to the mine data set. It was found that an equation of the form Y=1/(A-B*ash) fitted the data very well with an R^2 value of about 0.99 indicating that an equation of this form provides a very good representation of the data. The Ryan

TABLE 2
MINE 1 AND 2 SG DATA FROM WASHED SAMPLES

Sample	Fraction	Weight %	Air-dried M %	VM %	Ash %	FC %	SG (60)
6	1.4 float	49.5	0.3	22.4	7.0	70.2	1.36
6	1.4-1.6	27.3	0.4	21.4	18.6	59.7	1.44
6	1.6-1.8	12.0	0.5	18.8	38.0	42.7	1.64
6	1.8 sink	11.3	0.6	14.6	64.5	20.4	2.02
16	1.4 float	54.6	1.1	24.0	6.7	68.2	1.34
16	1.4-1.6	29.5	0.9	21.4	15.8	61.9	1.42
16	1.6-1.8	6.7	0.8	18.5	37.4	43.3	1.64
16	1.8 sink	9.2	0.6	14.8	63.5	21.1	2.01
26	1.4 float	40.3	0.5	26.5	9.4	63.7	1.33
26	1.4-1.6	43.4	0.7	21.4	21.1	56.9	1.47
26	1.6-1.8	14.3	0.5	19.3	35.6	44.7	1.66
26	1.8 sink	1.9	0.6	16.2	51.4	31.8	1.92
36	1.4 float	49.3	0.7	24.3	6.5	68.5	1.35
36	1.4-1.6	28.3	0.7	21.3	19.1	59.0	1.45
36	1.6-1.8	8.9	0.5	19.4	37.9	42.2	1.67
36	1.8 sink	13.5	0.4	15.3	72.4	11.9	2.24
44a	1.4 float	19.0	0.4	26.3	8.3	65.0	1.33
44a	1.4-1.6	18.8	0.9	22.9	19.8	56.4	1.48
44a	1.6-1.8	16.3	1.5	20.4	36.6	41.5	1.66
44a	1.8 sink	45.9	1.2	15.7	65.2	17.9	2.09
A	1.4 float	59.7	0.4	22.7	7.5	69.4	1.33
A	1.4 1.5	27.2	0.4	20.3	23.7	55.6	1.48
A	1.5 1.6	7.1	0.3	20.1	27.1	52.5	1.52
A	1.6 1.7	3.1	0.3	19.7	37.1	42.9	1.61
A	1.7 1.8	0.7	0.3	18.6	45.4	35.7	1.73
A	1.8 sink	2.1	0.4	16.0	68.7	14.9	2.13

equation also has the form ASG=1/(A-B*ash) and in this case constants represent real terms:

A=1/DC where DC is the ASG of ash-free coal (air-dried basis);

B=wtlos*(DMM-DC)/(DMM*DC) where DMM is the ASG of mineral matter adb (air-dried basis);

wtlos is the ratio of mass of mineral matter divided by mass of ash;

The constant B does not provide unique solutions for either DMM or wtlos though if one is assumed the other can be calculated.

The Ryan equation was fitted to the data sets and values of A, B and DC derived (Table 3, Figure 1). It is apparent that there is very little difference in the clean coal ASG values predicted for raw 60 mesh (0.25 millimetre) samples and the raw 200 mesh (0.075 millimetre) samples and both predict clean coal ASG values of about 1.28. The 200 mesh ASG data do however, predict a lower ASG for mineral matter and the reason for this is not clear. In

TABLE 3
CONSTANTS DERIVED BY CURVE FITTING TO THE SG DATA SETS FROM MINE 1, MINE 2 AND TELKWA

constants	Mine 1 data				Mine 2	Telkwa
	SG60 all	SG60 raw	SG60 wash	SG200 raw	SG60 wash	SG60 raw
A	0.778	0.778	0.776	0.784	0.786	0.763
B	-0.0045	-0.0044	-0.0046	-0.0040	-0.0046	-0.0046
DC	1.285	1.285	1.288	1.276	1.273	1.311

ASG=1/(A-B*ash)

A=1/DC B = wtlos*(DMM-DC)/(DMM*DC)

DC = ASG of ash-free coal (air-dried basis)

DMM = ASG of mineral matter (air-dried basis)

wtlos = ratio weight mineral matter / weight ash

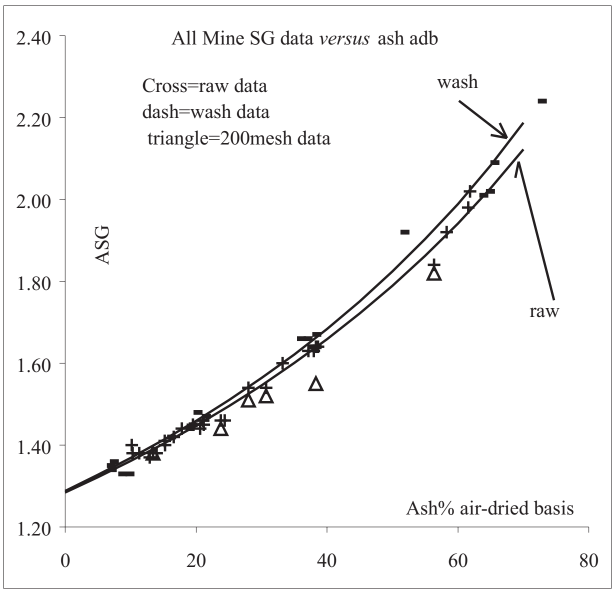

Figure 1. Plot of Raw ASG data *versus* ash % adb, Mine 1; triangles represent 200 mesh data the rest is 60 mesh data with the dashes being washed and the crosses being raw data.

general it appears that crushing the coal to a finer size has not destroyed any of the micro porosity in the coal, which if destroyed would cause an increase ASG for the smaller sized ash-free coal. Therefore, the 60 mesh analyses provide a reliable measurement of ASG on an air-dried basis and any gas filled microporosity must exist on a scale finer than the 60 to 200 mesh size.

Sometimes it is difficult to collect samples with a wide range of ash concentrations required to establish good ash *versus* SG curves. Incremental samples of different specific gravities (washability increments) overcome this problem but may not be representative because of variations in petrography or ash chemistry of the samples. A number of mine samples were separated into a number of SG increments and the ASG of each increment sample determined. The data define a similar ash *versus* ASG relationship as the raw data (Table 3, Figure 1) indicating that reasonable ash *versus* SG relationships can be established from a limited number of samples subdivided into a number of SG splits.

Having established that washed incremental samples provide reliable ASG data, the Ryan equation was fitted to the raw and wash data sets from the mine and the smaller 200 mesh data set (Figure 1). The values of A and B were derived and the clean coal ASG values calculated (Table 3). The clean coal ASG values for the mine coal (1.285) and for coal from the second mine (1.27) are similar and both somewhat lower than the Telkwa data suite (1.31; Ryan, 1991). Coal from the second mine has similar petrography and rank to the first mine samples indicating that there are no marked differences between the ASG values of coals of similar rank and petrography from the two mines.

The wtlos factor and DMM have to be picked based on the most likely paired values as they can not be determined independently. It appears that wtlos varies from 1.09 to 1.15 and DMM from 2.66 to 2.74 (Table 4). Higher wtlos factors are associated with mineral matter enriched in carbonates and this will also increase the value of DMM. The wash data has higher values because the carbonate material is concentrating in the higher SG wash increments.

TABLE 4
REFLECTANCE AND PETROGRAPHY OF MINE 1 AND MINE 2 SAMPLES

	Rmmax%	liptinite	telinite	telocollinite	desmocollinite	detrovitrinite	total reactives	semifusinite	fusinite	macrinite	inertodetrinite	total inerts	mineral matter	ash
17	1.1	3.3	3.7	21.7	22.3	5.7	56.7	11.0	1.0	8.7	7.3	28.0	15.3	23.3
39	1.2	2.3	8.3	12.7	26.0	0.7	50.0	19.0	0.3	14.3	6.7	40.3	9.7	15.5
44a 1.4f		2.7	5.0	34.7	25.7	0.3	68.3	13.3	0.3	7.0	7.3	28.0	3.7	6.2
44a 1.4-1.6		2.7	4.7	13.7	30.3	4.7	56.0	17.7	0.3	7.7	11.0	36.7	7.3	12.0
44a 1.6-1.8		1.0	2.3	5.0	23.0	14.7	46.0	8.0	0.0	5.7	10.7	24.3	29.7	40.1
A	1.3	1.3	8.7	14.0	24.7	2.7	51.3	17.3	0.3	16.0	13.7	47.3	1.3	2.3

TABLE 5
VALID VALUES OF WTLOS AND DMM FOR RAW, WASH AND 200 MESH

B=(DMM-DC)/(DMM*DC)*wtlos DC=1/A				ASG=1/(A+B*ash)	
	Mine 1 raw	Mine 1 wash	mine 1 all data	Telkwa	Mine 1SG200
A	0.77849	0.77629	0.77629	0.7629	0.78361
B	-0.00439	-0.00456	-0.00449	-0.00457	-0.00403
DC	1.285	1.288	1.288	1.311	1.276
wtlos	DMM raw	DMM wash	DMM all	DMM Telkwa	DMM SG200
1.08	2.69	2.82	2.77	2.94	2.44
1.09	**2.66**	2.79	2.74	2.91	2.42
1.1	2.64	2.76	2.72	2.88	2.40
1.11	2.61	2.74	2.69	2.85	2.38
1.12	2.59	2.71	**2.66**	2.82	2.36
1.13	2.56	2.68	2.64	2.79	2.34
1.14	2.54	**2.66**	2.61	2.76	2.33
1.15	2.52	2.63	2.59	**2.74**	2.31
1.16	2.50	2.61	2.57	2.71	2.29

wtlos = wt mineral matter/wt ash

DC = SG ash-free coal DMM = SG dry mineral matter

PETROGRAPHY AND RANK OF SAMPLES

The mean maximum reflectance (Rmmax%) of two samples from the mine (1.11% and 1.12%) and one from the second mine (1.13%) are similar (Table 5). Data were obtained using the procedure of Kilby (1988), which allows the shape of the optical indicatrix to be obtained. The two samples are biaxial positive and the sample from the other mine is biaxial negative. The Telkwa data have Rmmax values that average 0.95% and range from 0.9% to 0.98%.

The petrography of five mine samples and one from the other mine were estimated using 300 point counts. The petrography of the six samples are similar, all containing moderate organic inert contents. Three samples were SG splits of a single sample and these revealed interesting changes in maceral composition as the SG increases. Reactives are concentrated in the low SG fractions mainly as vitrinite A or telinite and telocollinite. Semifusinite is concentrated in the intermediate SG increments and in high SG increments, desmocollinite intermixed with ash predominates. These trends in petrography are similar to those seen by Bustin (1982).

EFFECT OF MACERAL COMPOSITION ON COAL SPECIFIC GRAVITY

The SG of individual pure macerals varies as rank increases. The SG of vitrinite is about 1.4 to 1.5 at lignite rank and decreases to the range 1.25 to 1.35 for medium and low-volatile bituminous ranks, before increasing to over 1.6 in anthracite (Taylor *et al.,* 1998). The SG varies because of devolatilization and changes in the chemical structure and amount and type of micro porosity. The SG of fusinite is high, probably greater than 1.5 in most coals, though it may increase with rank as the original organic texture is destroyed. The SG of semifusinite will be in between that of vitrinite and fusinite and will depend on the amount of fusinization or increase in reflectance experienced.

The ASG of clean coal will be a minimum at medium-volatile bituminous rank (Taylor *et al.,* 1998). The higher ASG at zero ash (1.31) for the Telkwa data compared to the mine (1.285) is probably caused by the lower rank of these coals (Rmmax about 0.95%). The difference in clean coal ASG values may also reflect higher micro porosity in the more deformed coals in southeast British Columbia.

At any rank, SG will vary based on the relative amounts of inert and reactive macerals in the coal. Maroto-Valor *et al.* (1998) demineralized a medium volatile (Rmmax=1.14%) coal and separated enriched maceral fragments (0.075 millimetres) into various SG splits. It is possible to use their data to estimate the ASG values of the pure maceral types vitrinite, semifusinite and fusinite. The best fit with the washability ASG increments was achieved by assigning ASG values of 1.265 to vitrinite, 1.33 to semifusinite and 2.2 to fusinite. Based on these values the predicted DC value for the coal is 1.36. This value is higher than that calculated for the mine data (1.285) and may reflect slightly higher rank or lower micro porosity.

Bustin (1982) studied the washing characteristics and petrography of sheared and non sheared coals sized less than 12.5 mm. It is possible to use his data to estimate the difference in SG between the reactive and non reactive macerals. Composite SG values were calculated for each SG washability split by assigning SG values to three components (mineral matter, reactive and non reactive macerals). The assigned SG values were adjusted until the predicted SG value for each sample fell within the SG bracket for that split (Figure 2). The calculated SG of mineral matter is in the range 2.55 to 2.4, that of reactives is in the range 1.19 to 1.22 and inerts in the range 1.3 to 1.38. It also appears that compared to unsheared samples, mineral matter and reactives have lower SG values and inerts higher SG values in sheared samples. Possibly shearing has mineralized inert macerals, increasing their SG and introduced some additional micro porosity into the reactive macerals, thus reducing their effective SG. The lower SG values calculated from the Bustin (1982) data compared to those calculated using the Maroto-Valer *et al.* (1998) may reflect the difference in size of the two sample sets and increased porosity in the coarser Bustin samples.

The procedure described above does not provide unique solutions for the SG of reactive and inert macerals and mineral matter, but it does provide a rough estimate of

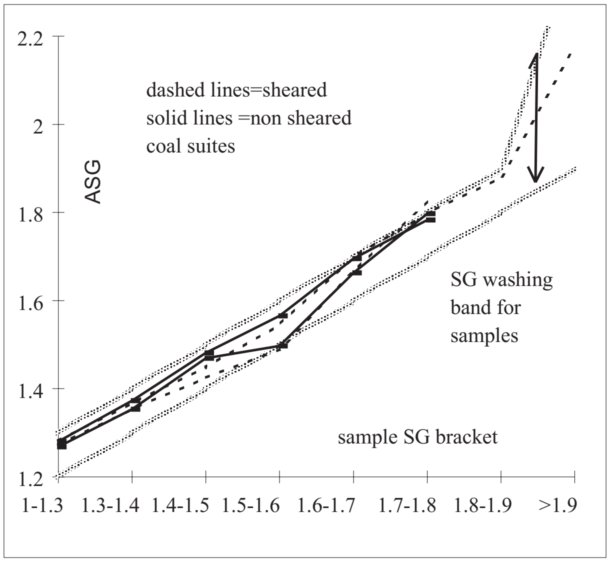

Figure 2. Plot of calculated ASG values for each SG washability increment versus SG increment; data from Bustin (1982).

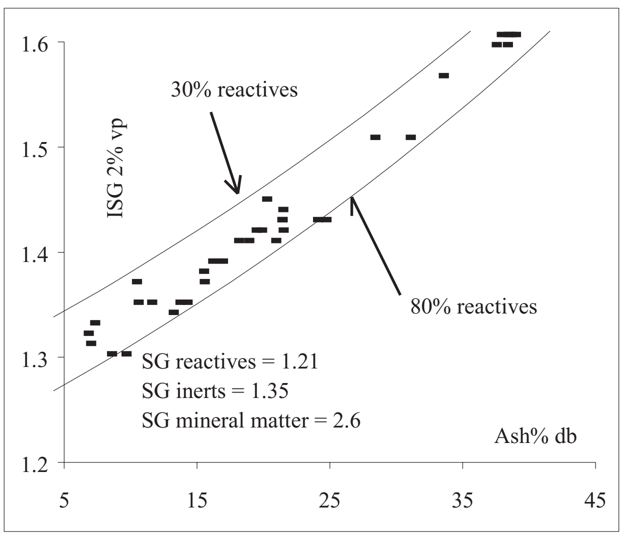

Figure 3.Plot of ISG (2% vp) *versus* ash % dry-basis (db) (Mine 1 data) illustrating possible effects of varying the reactives/inerts ratio in samples.

the difference in SG values between reactives and inerts of about 0.5 to 0.1 for the Bustin coal with a rank in the range Rmmax=1.35% to 1.4% and for the Maroto-Valer *et al.* coal with a rank of Rmmax=1.14%. Based on the difference in SG values and the ranges in reactives/inerts ratios found in Mist Mountain Formation coals, it is possible to construct a plot that illustrates the possible SG values for samples with varying reactives/inerts ratios (Figure 3).

The ASG values for the macerals in the Bustin study seem to be low and this is probably because the heavy liquid, used to wash the < 12.5 mm sized air-dried coal particles, does not penetrate air filled fractures in the particles. This means that in an ash *versus* SG plot, a band representing a petrography variation from 30% reactives to 80% reactives on a mineral free basis, appears to be low when compared to the mine data, which was crushed to <0.25 millimetres. However, when the mine data are corrected for 2% air filled fracture porosity, the data scatters within the 30% to 80% envelope (Figure 3), calculated by assigning SG values of 1.21 to reactives, 1.35 to inerts and 2.6 to mineral matter. Apparently a lot of the scatter seen in Figure 1can be explained by changes in the reactives/inert ratio of the samples. Also the increased size of the air-dried Bustin samples may be responsible for an additional 2% porosity not penetrated by the heavy liquids.

The effect of petrography on the SG of five mine samples was checked by posting the values of the reactives/inerts ratios of samples against their plotted position in an ash *versus* SG plot (Figure 4). It is apparent that samples with high reactives/inerts ratios tend to plot below the curve defined by all mine samples.

PRELIMINARY DETERMINATION OF FRACTURE POROSITY IN COAL

It is exceedingly difficult to measure the *insitu* fracture porosity of a coal seam. Ideally if one could cut out a cubic metre of a seam, seal the sides and measure the weight, then this might provide an answer. A more practical approach involves using well calibrated geophysical density logs to provide the *insitu* specific gravity of a coal seam (ISG). By matching core from a seam to the log pattern for the seam, ash concentrations corresponding to geophysical log densities can be determined. The ASG of the coal at the measured ash concentrations can be determined by laboratory measurement or by using the Ryan Equation. It is then possible using Figure 5 and the values of ISG and ASG to determine possible combinations of volume of water, weight of water, and void volume in the coal. Generally the method is difficult to apply because

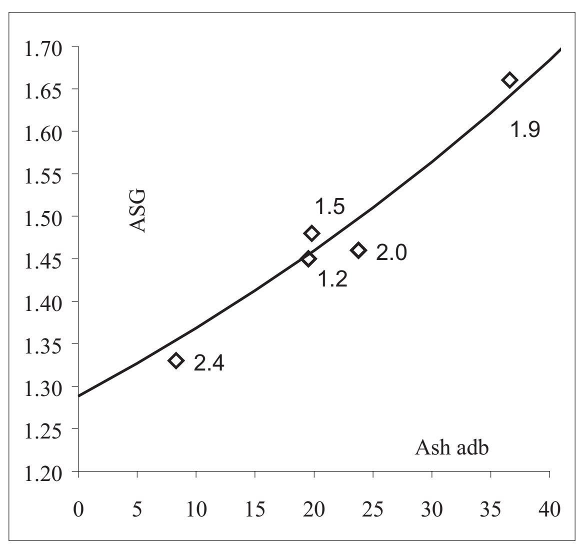

Figure 4. Plot of ash *versus* SG with values of reactives/inerts ratios of samples posted.

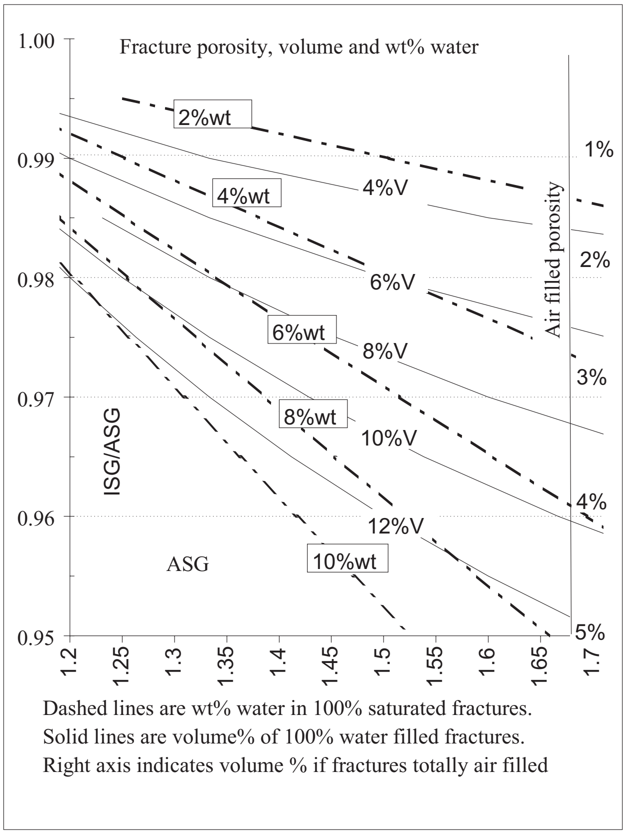

Figure 5. Relationship of SG to void or water filled fracture porosity.

calibration of geophysical logs is not good enough and core recovery of less than 100% introduces uncertainties into the ash determination. The method does however offer the possibility of estimating *insitu* fracture volume at depth. Long spaced density logs can be well calibrated and the density scale linearized. Short spaced density logs are difficult to calibrate and the scale is not linear, however it is possible in some cases to use a combination of long and short spaced logs to determine the density of quite thin coal layers.

Other types of logs can provide relative estimates of fracture porosity. Resistivity of coal seams decreases markedly as the water content increases so that a combination of density logs to identify coal seams and resistivity logs to identify water content can indicate areas in seams of increased fracture porosity. Edwards and Banks (1978) describe a way of using density and resistivity logs to determine volumes of coal, water and wet ash. A resistivity *versus* apparent density plot provides the apparent density of dry ash-free coal and the resistivity of wet mineral matter. These data and data from the resistivity and density logs are used in calculations of water volume. The paper provides data on a 6 metre coal seam, in which the calculated average water volume is 9.5%. The approach is interesting because it does not require core, but it does require an open hole for the resistivity log. Once the volume of water is determined it is easy to use the value to, either calculate ISG based on measured values of ASG, or to calculate the in place tonnage of coal minus free moisture. In general neutron logs are not useful for detecting changes of moisture content in coal seams.

Generally, in the 1980's and 1990's coal geophysical logging concentrated on determining seam thickness and general lithology and not many attempts were made to determine *insitu* seam porosity. However, based upon the recollections of Keith Banks of Roke Logging (personal communication, Banks, 1999) the *insitu* fracture porosity of coals in southeast BC is probably in the range of 4% to 7% and higher at a number of locations. At Sage Creek, coal was carefully cut from an adit and immediately weighed and then weighed after drying. The difference in weights implied an *insitu* porosity of over 20%. In Alberta, near Grande Cache, geophysical logging provided estimates of *insitu* fracture porosity of 15% and in a thrust zone the porosity was estimated to be 32% to 38%. It appears that in deformed coals the *insitu* fracture porosity is increased and can be much greater than 7%.

At depth, increase in fracture porosity in coal generated by shearing may survive because hydrostatic pressure is similar to lithostatic pressure (over pressuring), which is probably a requirement for thrust movement. As the depth of cover decreases and over pressuring disappears the fracture porosity may decrease. This means that in some cases coal volumes calculated at considerable depth may be greater than the volume eventually exposed at surface and that fracture porosity at surface may be less than that which existed at depth. This does not appear to be the case at the mine.

It maybe possible to estimate fracture porosity in laboratory samples using washability and SG data, as illustrated using data in Bustin (1982). The SG for clean coal air-dried basis (adb) with average petrography is about 1.26, which is lower than that predicted by direct measurements for the mine data (1.28). The difference may be explained by the higher rank of the Bustin samples (Rmmax=1.35% to 1.4%) compared to the mine samples (Rmmax=1.12%). The increase in rank moves the Bustin samples closer to the minimum vitrinite SG on the SG *versus* rank relationship described by Taylor *et al.* (1998). Another explanation may be that the mine ASG measurements were made by immersing 60 mesh air-dried samples in kerosene, which penetrates fractures in the air-dried 60 mesh samples more than the heavy liquids, used in washability tests, penetrated the fractures in <12.5 millimetre sized air-dried samples. In fact, by comparing the SG values determined by two approaches it may be possible to calculate the volume of fractures in the washability samples.

The Bustin samples were crushed to minus 12.5 millimetres and immersed in heavy liquids whereas the mine samples were crushed to minus 0.25 millimetres and immersed in kerosene. Based on the difference in estimated SG values for clean coal (1.28 =ASG for the mine and 1.255=ISG for the Bustin samples) this could indicate, if water was removed from the fractures by air drying, an increase in volume of void porosity of 2%, or if the

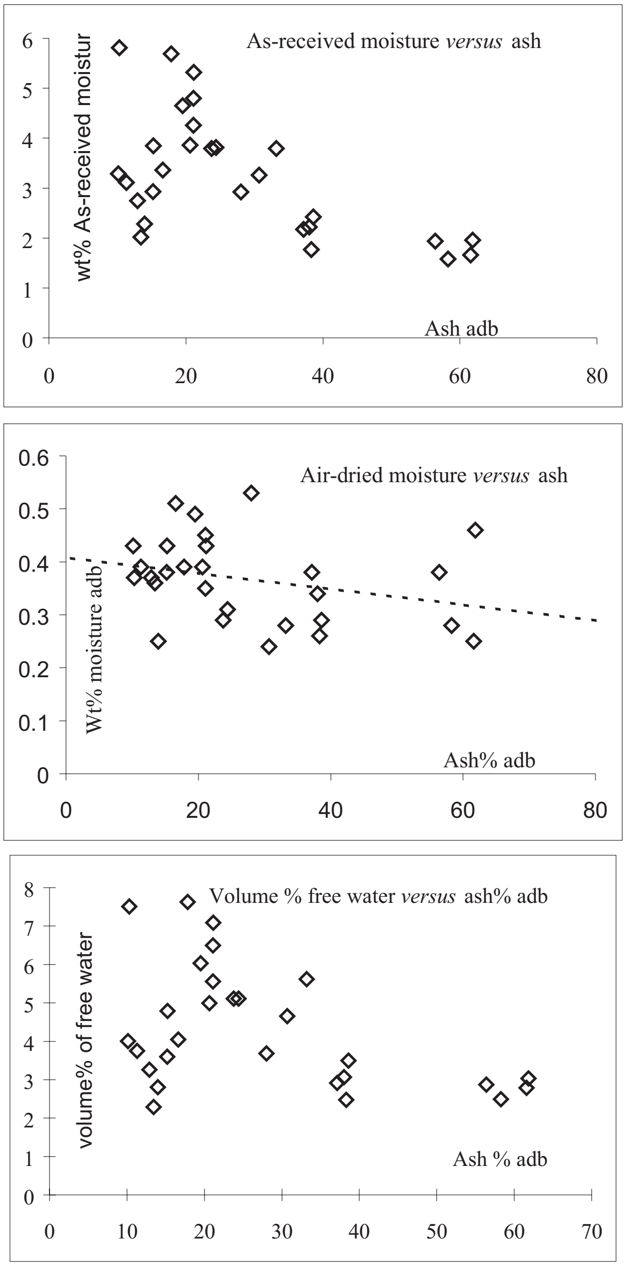

Figure 6. Plots of as-received and air-dried moisture contents *versus* ash contents.

fractures remained filled with water an increase in weight of free water of 7% equivalent to a water filled volume of about 9% (Figure 5). It is apparent that, even if ISG is only slightly less than ASG, this may still indicate quite a large volume of fracture porosity, if it is water filled. In this case, the argument is confused by the rank difference between the Bustin samples to the mine samples.

Washability analyses of samples from the Telkwa property were performed on suites of samples ranging in size from 0.3 millimetres to plus 25 millimetres (Ledda, 1992). As sample size increases the ash content in each SG increment increases, probably in part because preservation of fractures decreases the effective SG of the air-dried samples. The clean coal SG with no fractures is 1.31 (from Ryan, 1991); the SG for 0.3 to 2.0 millimetre material appears to be about 1.26 to 1.28 and for the coarser sized material, it decreases to 1.24 to 1.26. These values were derived by assigning SG values to the coal and mineral matter and attempting to calculate a combined SG that fitted into the SG wash increments. The difference in SG values implies an increase in air filled fracture porosity from zero at SG=1.31 to 5.3% for the coarse sized wash material with an SG of 1.24. This assumes that the differences in SG derive from the fact that the heavy liquids used in the washability analysis do no penetrate air filled fractures in the larger sized air-dried samples and in the smaller sized coal most of the fractures are destroyed. If the fractures remained water filled then the difference in SG would imply a water filled volume of 18%, which appears to be too high.

A volume percent porosity of 5.3% if water filled would be equivalent to 4.3% weight of water. The total water in the coal would therefore be 4.3% plus air-dried moisture for a total of about 5% to 6%. This estimate is similar to estimates of *insitu* water estimates and the average as-received moisture for Telkwa coal (Ryan, 1991). The SG of the mineral matter in the Telkwa coal is estimated to be between 2.4 and 2.5 from the washability data and, as with the coal SG, appears to decrease as the size consist increases. The estimated SG mineral matter from the SG data (Ryan, 1991) is 2.7 this would imply a void porosity of about 9% if air filled.

Using a combination of washability data, sized from 25 or 50 mm to 0.3 mm, and ASG data derived from 0.25 mm sized samples, it is possible to estimate fracture porosity in the coarsest size washed coal based on a number of assumptions. That it is possible to estimate the SG of the wash samples in each SG increment: that variations in the estimated clean coal SG of washed samples are caused by the varying ability of the heavy liquids to penetrate fractures in the coal and by the progressive destruction of these fractures in finer sized coal: that the fractures in the coarser sized fragments are devoid of water because the samples were air-dried.

Another method of estimating minimum fracture porosity from laboratory samples involves using the difference between as-received and air-dried moisture contents. If samples are collected from fresh outcrops, in which the coal still contains most of its *insitu* moisture, then the as-received moisture content is higher than the air-dried moisture in part because fracture spaces in the coal still contain free water. Air drying the samples removes this water and therefore the difference between as-received and air-dried moisture contents may be a minimum estimate of the weight of free water in small fractures. The volume occupied by the free water is given by:

Volume = weight percent free water x ASG

The as-received moisture content of samples decreases as the ash content increases. This appears to indicate that the fracture porosity in high ash or rock samples is much less than in low ash samples. However the data is

TABLE 6
RECONCILIATION CALCULATION SPREADSHEET

Enter data in shaded boxes only. Spread sheet calculates ROM, plant and insitu data depending on inputs.

SG CONSTANTS
set for all calculations

wtlos	DC	DMM	adm
1.09	1.285	2.66	0.4

SG EQUATIONS
ASG =1/(A-B*wt%MM)
wt% MM = wtlos*ash/100
SGfw=ASG/(1-wt%fw+wt%fw*ASG)
ISG = SGfw*(1-vp)
A = 0.778 A=1/DC
B = 0.402 B=(DMM-DC)/(DMM*DC)

DEFINITION OF TERMS
ASG = SG at adm, no fractures no free water
MM = mineral matter wtlos = MM / ash
SGfw = SG corrected for free water (fw) no void porosity
ISG = SG of coal with free water and air filled fractures (vp)
DC = SG of zero ash coal at adm
DMM = SG of mineral matter at adm
OSD = out-of-seam dilution
adm = air-dried moisture
adb = air-dried basis
bcm = bank cubic metres
lcm = loose cubic metres

Ash db = Ash adb /(100-adm)
Volume% water=wt% water x SGfw
Ash ROMm = Ash adb/(100-adm)* (100-ROMm)
constants to convert tonnes from different water bases
wt ratio adb/ROM and adb/insitu = insitu to plant 0.954 0.944
plant to insitu 0.954 0.944

in seam loss % of insitu volume with same free	OSD at adm volume% of total insitu volume	OSD ash at adm	total insitu moisture WT%	free moisture wt% not quite the same as total insitu -	air filled void porosity Volume%	ROM moisture wt%	swell factor as bulk porosity calc using ROM coal+rock adb	truck capacity (lcm)	reject ash at breaker adb	Breaker reject wt% of ROM tonnes at ROM moist	
20	8	65	6	5.62	0	5	10	110	65.7	9.5	**insitu**
20	8	65	6	5.62	0	5	10	110	65.7	9.5	**plant**

		from insitu to plant	from plant to insitu		DESCRIPTION
Insitu fracture vol		**8.44**	**8.44**		**percent volume occupied by free water+void porosity**
INSITU		100000.0	100000.0		insitu coal volume bcm with free water and void porosity
		30.00	30.00		insitu ash adb
		1.546	1.546		ASG of insitu coal at adm no free water no void porosity
		1.500	1.500		SGfw = SG of insitu coal with free moisture no void porosity
		1.500	1.500		ISG = SG of insitu volume with free water and void porosity
		8435.42	8435.42		weight of free water equivalent to volume of free water
		150029.90	150029.90		insitu coal tonnes with free moisture
		141594.48	**141594.48**		**insitu coal tonnes at adb**
		28318.90	28318.90		in seam tonnes mining losses at adb
		91564.58	**91564.58**		**bcm insitu coal adb (no void porosity or free water)**
		20000.00	20000.00		bcm loss of in seam volume
		18312.92	**18312.92**		**volume of coal lost at adb**
RUN OF MINE		2.028	2.028		SG OSD rock at adb
		8000.00	**8000.00**		**volume of OSD at adb added as is to insitu volume**
		16220.55	**16220.55**		**tonnes OSD rock at adb**
		129496.1	**129496.1**		**ROM tonnes coal+rock at adb**
		135766.5	135766.5		ROM tonnes coal+rock at ROM moist
		34.38	34.38		ROM ash adb
		1.594	1.594		SG ROM coal and rock all at adb
		81251.7	81251.7		volume of coal+rock at ROM moisture no void porosity
TRUCKS		90279.6	90279.6		lcm=bcm ROM coal+rock adb corrected for swell factor
		14811	14811		Number of trucks
		110.0	110.0		truck capacity
		6.1	6.1		truck load lcm
BREAKE		**12302.13**	**12302.13**		**breaker reject tonnes at adb**
		2.040	2.040		ASG of breaker reject at adb
		6029.67	**6029.67**		**breaker reject volume at adb**
PLANT		**117194.0**	**117194.0**		**plant delivered tonnes at adb moisture**
		75222.0	**75222.0**		**plant delivered volume at adb**
		122868.7	122868.7		**plant delivered tonnes at ROM**
		31.10	31.10		**plant delivered ash adb**

NOTES FOR TABLE 6

	check reconciliation	
	tonnages adb	volumes adb
insitu	141594	91565
minus lost	28319	18313
plus dilution	16221	8000
minus rejects	12302	6030
equals plant	117194	75222
check	117194	75222

bcm = bank cubic metres ie volume as measured in bank before consideration of swell factor caused by mining and breakage.
bcm contains the fracture volume calculated on the first line of the spread sheet
lcm=insitu air-dried volume with a swell factor added to account for additional breakage during mining.
when swell factor =fracture volume then lcm=bcm with dilution
Solid is assumed to be coal+mineral matter+adm.
Non coal space is occupied by volume of free water plus volume of void porosity
void porosity = fracture or pore space not filled with water (fas filled) it does not include microporosity, which is factored into ASG.

Water is weight percent and porosity is volume percent.
To calculate total non coal space one must convert water wt% to V% in some calculations
It is assumed that adb moisture is an inherent component of coal and ASG. It does not add to coal volume
It does not effect non coal volume which is composed of free moisture and void porosity
The insitu volume available for mining is fixed by the value entered on line 1.
The volume% of non coal space (i.e free water volume+void porosity) depends on values of wt% insitu water and volume% void porosity entered in the appropriate boxes at the top of the sheet. The actual percent total non coal space is calculated in the spread sheet

The basic SG equation for a mixture of coal+mineral matter is ASG=1/(1/DC-(DMM-DC)/(DMM*DC)*MM)
DC=SG pure coal at adm DMM=SG rock at adm MM= wt of mineral matter at adm
MM is converted to ash using wt ash=wt MM x wtlos where wtlos=wt MM / wt ash

The basic SG equation must be adjusted for free water (fw) and void porosity (pv)
SG=Mass /Vol (M/V). After adding water as wt fw% new wt is Mw and Mw=M / (1-fw) Mw-M=M x fw/(1-fw)
Note that fw is not a volume % but Mw is set to 100gm then fw is equivalent cc
SGfw=M/(1-fw%) / (V+M*fw/(1-mf)) but V=M/SG
SGfw=1/((1-fw)/SG+fw) or SGfw=SG/(1-fw+fw x SG)

To handle void porosity
SG=M/V new volume Vn has void porosity Vp Vn=V/(1-vp) ISG=M/Vn=M/(V/(1-vp)) ISG=SGfw x (1-vp)

To convert wt% water to volume% water
SGfw=Mw/Vw mass of water =Mw x fw% is equivalent to cc water therefore volume% water =fw% x Mw / Vw =fw x SGfw

Dilution: Because dilution is added on an ai-dried basis to coal that is at insitu moisture when the volume of dilution material is recalculated to an insitu or ROM water basis its volume relative to that of coal increases
this means that it no longer is in the volume% given as the OSD% and the volume of ROM coal+rock at ROM moisture will not equal insitu volume -loss% + OSD%

ROM volumes: the usefulness of ROM volumes is limited because in reality there is always added porosity or swell generated when the coal is mined and moved. The concept is useful for estimating the size of truck loads.
The most important thing is to compare insitu volumes to tonnes adb delivered to the plant

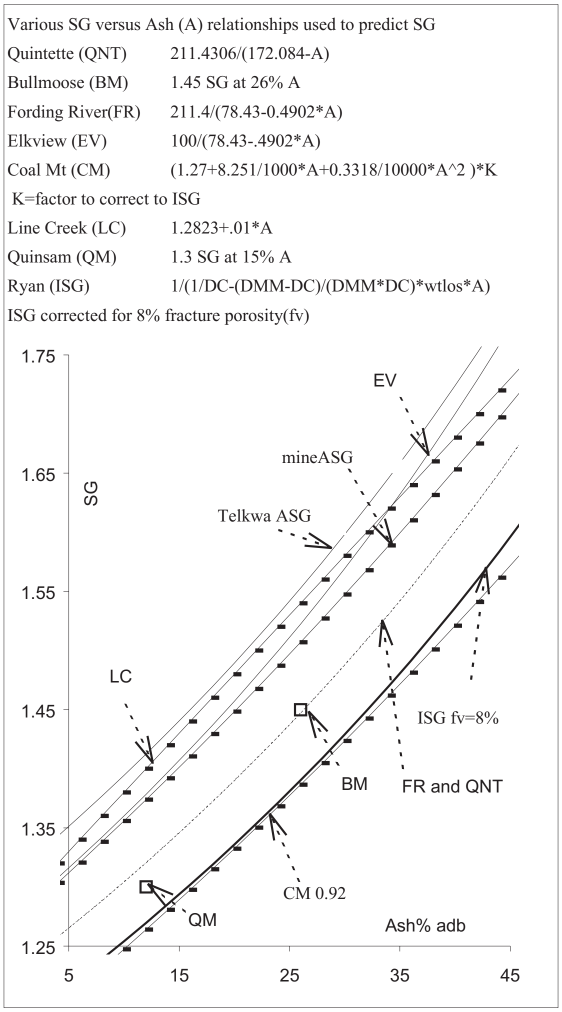

Figure7. Various SG *versus* ash equations used by BC coal mines

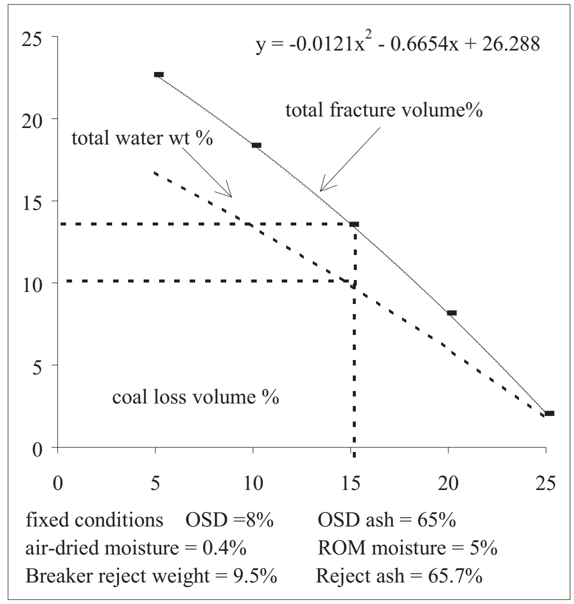

Figure 8. Plot of coal loss *versus* total fracture volume and total weight water.

somewhat deceptive because the effect of a decrease in weight of water is partially offset by an increase in ASG as the ash content of the samples increases. Therefore, a smaller weight percent water can account for the same volume as calculated in low ash samples. The mine as-received moisture data show a moderate trend towards lower values at higher ash contents whereas the air-dried moisture content is almost independent of ash content (Figure 6). By subtracting the as-received moisture from the air-dried moisture and converting the weight percent free water to a volume percent based on using the ASG of the sample, it is possible to estimate the fracture porosity of the samples and illustrate how it changes with increasing ash (Figure 6). At low ash values the porosity is variable ranging from 2% to a high of 8%. At high ash contents the variability seems to decrease and the average volume is about 3%.

RECONCILIATION

Coal reserves are measured in the ground as a volume but the coal is sold as washed tonnes. It is therefore necessary to be able to convert *insitu* volumes into *insitu* tonnes on an air-dried basis and to track these tonnes as they are mined, transported, crushed and washed. Once the *insitu* tonnage on an air-dried basis has been calculated it is necessary to estimate a number of mining factors such as coal loss, out of seam dilution (OSD) and breaker rejects before estimating tonnage delivered to the plant. Conversely, if plant tonnage is accurately known, then by adding back the breaker rejects and coal loss and removing the OSD from the tonnage or volume delivered to the plant it should be possible to calculate the *insitu* tonnage or volume. The calculated value should match or reconcile with that estimated by the mine plan as long as all the calculations are done at the correct water bases.

A detailed excel reconciliation spread sheet (Table 6) was constructed to illustrate the effects of changing coal and mining related parameters on coal tonnage delivered to the plant. A number of definitions and equations are included in the Table. The spread sheet uses the Ryan equation to calculate the SG values of tonnages under *insitu* or air-dried conditions and adjusts tonnages and volumes based on *insitu*, air-dried and ROM moisture contents. The procedure does not involve elaborate mathematics but does require a good understanding of the mining process.

The value of air-dried moisture used in Table 6 is determined from data in Table 1. The values of wtlos, DC and DMM were determined by curve fitting to the mine

ASG *versus* ash data and deriving the constants A and B for the raw wash and combined data (Table 3). Valid combinations of DMM and wtlos are provided in Table 4.

The reconciliation process starts with estimates of *insitu* volume, ash and ISG. When there is sufficient drilling, estimates of *insitu* volume should be good, assuming that the computer model used is appropriate for the type of geology. These data are used to provide a value of the *insitu* fracture volume either directly by comparing ASG, ISG and ash or indirectly by using the weight of *insitu* water and void porosity to calculate the total fracture porosity. The spread sheet uses estimates of total *insitu* moisture and void porosity to calculate total fracture porosity. *Insitu* tonnage on an air-dried basis is then calculated by using the appropriate SG and *insitu* volume. The key to converting *insitu* volume to *insitu* tonnes adb is to know the fracture volume at depth and whether it is filled with water or air. The ISG used must take into account the fracture volume and the degree to which it is water filled. The weight of coal adb is calculated using:

weight of coal adb = ISG* *insitu* volume - weight of free water

Alternatively the weight of coal adb can be derived from:

weight of coal adb = ASG adb* (1-fv) * *insitu* volume; where fv is the total *insitu* fracture volume. The spread sheet (Table 6) displays the total *insitu* fracture volume and allows for variable filling of the fracture volume with water before performing the calculations.

If it is difficult to reconcile tonnages delivered to the plant with estimates of *insitu* volume, then the temptation is to decrease the available tonnage by decreasing the value of SG used. However, it must be kept in mind that, if the SG value is multiplied by *insitu* volume then the implication is that:

SG=ASG * (1-fv);

This assumes a value of fracture porosity that must be credible and that tonnages are calculated on an air-dried basis.

The SG value is derived from a number of SG *versus* ash relationships (Figure 7). Ash *versus* ASG curves were established for Telkwa and the mine coal by analyzing a number of air-dried samples. Ash *versus* ASG curves for the Line Creek and Elkview mines plot close to the mine data line indicating that these relationships are probably modeling coal on an air-dried basis. Using these SG *versus* ash relationships will tend to cause an over estimation of raw coal reserves by about 5% if the ASG value for adb coal is multiplied by the total *in situ* volume, which includes the total fracture porosity present in *in situ* coal.

The Fording River, Quintette and Bullmoose data sets predict lower ASG values for the same ash than the air-dried mine data (mine ASG Figure 7), and therefore, appear to be adjusted to provide ISG values. Compared to mine adb data, the Fording River and Quintette data are compatible with an air-filled fracture volume of 4% that is ISG=ASG*(1-0.04) (Table 6), or if these values of ISG are multiplied by *in situ* volume the result is an estimate of tonnage at adb assuming a 4% *in situ* fracture porosity. Alternatively, the SG values could be lower because higher rank coals up to medium-bituminous rank have lower SG values at similar ash contents. Coal Mountain Operations predicts an ISG based on an 8% air filled porosity. Quinsam uses a fixed SG of 1.3, which unless the raw ash concentration is very low probably under estimates *in situ* tonnage.

Depending on the mining conditions the coal may be above or below the water table when mined. This means that the coal may be completely or only partially saturated. Measurements of ISG at depth derived from geophysical logs can be used, in conjunction with lab measurements of ASG, to calculate the fracture volume, usually assumed to be completely water filled (Figure 5). By the time mining has exposed the coal, some of the water may have drained or additional water added to the fractures. The change in fracture volume does not matter because the ISG value is multiplied by the *insitu* volume measured at depth.

At Mine 1 attempts to reconcile *insitu* volumes with the tonnages delivered to the wash plant have generally required low SG values, implying high fracture porosities, and high coal loss values. In order to keep the coal loss values within an acceptable range, a fracture porosity of 8% has to be assumed. Based on conversations with Keith Banks, a fracture porosity of 8% is probably a conservative value for the mine considering the amount of shearing in the coal. The empirical curve (CM .92) predicts SG values very close to those predicted by the Ryan equation based on the mine data and 8% air filled fracture porosity. It does not model ISG *versus* ash as well if the fracture volume is water filled except at the ash content of about 25%. This does not matter as long as it is assumed to be providing values of ASG*(1-fv) and not values of actual ISG for the total *insitu* volume.

The spread sheet (Table 6) can model an 8% fracture porosity by setting the total moisture equal to the air-dried moisture and the void porosity to 8%, in which case the spread sheet then makes no deduction for weight of free water from the *in situ* tonnage, which is calculated on an air-dried basis. Alternatively, the *in situ* moisture could be set to 6 weight %, which provides about the same fracture volume if the *in situ* ash content is about 25%, and the spread sheet then subtracts the weight of free water before calculating the *insitu* tonnage on an air-dried basis.

Coal losses can be expressed as a percent of tonnage mined, as an absolute thickness of the hangingwall and/or footwall of the seam, or as a percentage of *insitu* volume. In situations where the coal is highly deformed such as at the mine it is probably better to use a percentage of *insitu* volume, though this tends to under estimate actual loses for thin seams and over estimate them for thicker seams. A 10% loss of volume is equivalent to a 10% loss of tonnage whether the tonnage is calculated on an as-received basis or air-dried basis.

Coal loses should be apparent somewhere in the mine (probably waste rock dumps). If high coal losses are suspected, but the lost coal can not be located, then maybe part of the solution is in increasing the estimate of fracture porosity in the *insitu* coal, especially if there is evidence of severe deformation. Increasing the fracture porosity in the *insitu* coal decreases the tonnage delivered to the plant by decreasing the amount of coal in the ground. A plot of total fracture volume *versus* coal loss (Figure 8) illustrates the relationship between these factors, based on fixing the other mining parameters at realistic constant values. If the *in situ* fracture volume is 5% then the coal loss has to be 22.6% (Figure 8). However, when the *insitu* fracture volume is increased to 15% the coal loss decreases to 13.6%, which is intuitively more reasonable. The total *insitu* moisture is 10% in this example. A large fracture volume could in part result from shearing or underground mining in the area.

Ash is usually determined by analyzing chip samples. In some instances fine coal is lost and the reported ash analyses are high and in other cases erosion of fine coal surrounding the hole can result in additional coal being recovered and the analyzed ash values being low. If the ash concentration assigned to the *insitu* volume is too high then *insitu* tonnage estimate will be high and there will be a tendency to correct this by assuming a coal loss value that is too high. However, this will result in the ash concentration of the coal reporting to the plant being lower than predicted. As an example, using spread sheet (Table 6), if the predicted *insitu* ash content adb is 30% (true value 25%), then in order to explain the tonnage reporting to the plant a coal loss of 17% must be assumed as opposed to a true value 14.5% and the predicted ash content of the coal reporting to the plant is 31.1% as opposed to the actual value 26.3%. The actual over estimation of *insitu* tonnage is about 3%. Obviously, if the predicted coal loss and plant ash values seem high then the error is probably in estimating the *insitu* ash content.

Out-of-seam dilution (OSD) is extraneous rock that is incorporated in the coal as it is mined and is not considered when the *insitu* ash of the coal is calculated. It can be defined as a thickness or as a percent of the *insitu* coal volume. In the spreadsheet (Table 6) it is assumed that the OSD has no free moisture or fracture porosity and is added to the coal as rock on an air-dried basis. Alternatively, it could be assumed that the OSD has the same moisture and fracture porosity as the coal. However, fracture volume appears decrease as ash content increases as indicated by the calculation of fracture volume using as-received moisture (Figure 6). The more conservative assumption, which has the effect of increasing percentage dilution, is to assume that OSD is added on an air-dried basis.

Because the coal in most BC mines is soft, rotary breakers are effective at removing rock fragments, which are mainly introduced as OSD. It is difficult to estimate the relative tonnage or volume of breaker rejects, but generally the percentage of material is low and it has a high ash content. It can be expressed as a percentage of the tonnage or volume presented to the breaker. Usually it is expressed as a tonnage, in which case it will be a percent of ROM tonnage at ROM moisture.

The spreadsheet (Table 6) can be used to check various combinations of parameters to see how they effect reconciling *insitu* volume and ash content with tonnage and ash content of the material delivered to the plant. Generally, predicted plant tonnage is reduced by increasing either fracture volume in the *insitu* coal or coal loss. The effect of OSD and breaker rejects will tend to cancel out especially in the situation at the mine where the coal is very friable. As OSD increases so will breaker rejects if they do cancel out then the ash at the plant will be the same as *insitu* ash. If the ash concentration at the plant is higher than *insitu* ash, then OSD is adding more ash than the breaker is removing. This means that:

the value tonnes OSD x ash is greater than the value tonnes breaker reject x ash.

It should be noted that, if breaker reject ash is low and OSD ash high, then plant ash will be increased, and at the same time, tonnage decreased by the net effect of adding OSD and removing breaker rejects.

CONCLUSIONS

It is possible to derive an SG equation that fits laboratory data and provides the opportunity to vary input parameters such as weight of free water and volume of void porosity. Fracture volume is the volume occupied by the free water and void porosity. Fractures in the coal range in size from those that can be penetrated by kerosene in 60 mesh sized particles to major fractures in the coal face. They do not include the micro fractures that may be gas filled but whose effect is incorporated in the calculation of ASG.

The equation can be used to calculate *insitu* tonnages on an as-received or air-dried basis. By increasing the void porosity the equation can be used to help determine tonnages in stock piles. Using differences in ASG and ISG it is possible to estimate the volume of fractures (fv) in *insitu* coal. This is important because to calculate tonnages on an air-dried basis from *insitu* volume requires the values fv and ASG. If the fracture volume is not considered, then *insitu* tonnages will be over estimated by an amount equal to the volume of the fracture porosity.

Some indications of fracture volume can be gained from washability data, which indicates volumes of about 5%. Another way is to use the difference between as-received and air-dried moisture measurements of fresh samples. Both these methods probably under estimate fracture volume. Geophysical logging has indicated fracture porosities of over 20% is some situations. These high porosities survive at depth because hydrostatic pressure equals lithostatic pressure.

The SG of vitrinite decreases from sub-bituminous coal to medium-volatile coal and then increases as the rank increases to anthracite. The SG of inert macerals is higher than that of vitrinite and is probably proportional to reflectance. This means that at a fixed rank and ash content the SG of coal varies depending on maceral composition. Also ash *versus* SG relationships at constant petrographic composition must be established for each rank of coal.

The process of reconciliation and prediction of tonnes and ash content of coal delivered to a plant does not require complex mathematics but it has to be thought out carefully, otherwise mistakes will be introduced that will mask the use of inappropriate values of some of the mining constants.

The mine coal is highly deformed and at depth may have a high fracture porosity of 10% to 20%. It is the volume at depth with the high fracture porosity that is used to calculate *insitu* tonnes so that the ISG used must be corrected for a fracture porosity, that may appear to be too high based on outcrop observations.

ACKNOWLEDGEMENTS

A special thanks is extended to Brad Pisony who collected many of the samples.

REFERENCES

Bustin, R.M. (1982): The Effect of Shearing on the Quality of some Coals in the Southeastern Canadian Cordillera; *Canadian Institute of Mining and Metallurgy bulletin*, Volume 75, pages 76-83.

Edwards, K.W. and Banks, K.M. (1978): A Theoretical approach to the Evaluation of In-situ Coal; *Canadian Mining and Metallurgy Bulletin*, Volume 71 , pages 124-131.

Kilby, W.E. (1988): Recognition of Vitrinite with Non-uniaxial Negative Reflectance Characteristics; *International Journal of Coal Geology*, Volume 9, pages 267-286.

Ledda, A. (1992): Telkwa Exploration Report; Coal Assessment Number 828, Report on file *Ministry of Energy and mines.*

Maroto-Valer, M., Mercedes, Taulbee, Darrel, N. Andresen, John, M. Hower, James, C. and Snape, Colin, E. (1998): The Role of Semifusinite in Plasticity Development for a Coking Coal; *Energy and Fuels*, Volume 12, pages 1040-1046.

Ryan, B.D. (1991): Density of Coals from the Telkwa Coal Property, Northwestern British Columbia; (93L/11); in Geological Fieldwork 1990, *B.C. Ministry of Energy, Mines and Petroleum Resources*, Paper 1991-1, pages 399-406.

Smith G. G. (1989): The Required Use of Coal Density Values for Calculating Average Composition of In situ Coals; Contributions to Canadian Coal Science, *Geological Survey of Canada*; Paper 89-8, pages 131-136.

Taylor, G.H., Teichmuller, M., Davis, A., Diessel, C.F.K., Littke, R. and Robert, P. (1998): Organic Petrography; page 522. *Gebruder Brorntraeger*, Berlin-Stuttgart.

A Note on Difficult to Wash Coals from Southeast British Columbia (82G/7)

By Barry Ryan

KEYWORDS: *Coal washing, ash chemistry, carbonate contents, vitrinite reflectance, SEM on coal, petrography.*

INTRODUCTION

Some coal seams in southeast BC are characterized by fine size consist and a moderate amount of inherent ash. Mining strategies and wash plants are designed to handle these coals but sometimes seams are mined, that are unusually difficult to clean. Samples of a number of such coals were acquired and studied. Samples come from a mine and an adjacent property (samples GC in tables) near Sparwood in southeast British Columbia. Two in-pit samples of coal were collected the mine from areas where the seam was known to wash easily and one sample from an area where it was known to be difficult to wash. A bulk sample of coal from a property near then mine was test washed at the mine wash plant and found to be difficult to wash and a sample of this coal was studied. Occasionally fine coal in the froth floatation circuits in the mine wash plant is difficult to wash. Raw, clean and reject samples of this material were collected. All samples were subjected to a range of chemical analyses, petrographic analysis and in some cases scanning electron microscope (SEM) analysis.

DATA

The three samples collected from the mine pit were crushed and screened at 10 x 0.6, 0.6 x 0.15 and minus 0.15 millimetres (Table 1). The coarser size consists were washed using four SG increments. Oxide analyses (Table 2) were performed on some of the samples to provide an indication of how mineralogy varies between the easy and more difficult to wash samples. Sample 1980-69 was collected from an area where the coal was known to be difficult to wash. Samples 1968-east1 and 1968-east2 were collected from areas where the coal has normal washing characteristics.

The coal from the property is located in the hanging wall of a fault. The seam is thickened and crushed by the fault. A bulk sample of the coal was mined and test washed in the mine wash plant. Washing results and indications of potential coking quality were disappointing, so a sample was collected for further analysis. The sample was screened at 0.6 millimetres and the 0.6 x 0.0 milli-

TABLE 1
WASHABILITY DATA FOR THREE IN PIT SAMPLES

size mm	SG	wt	adm	VM	Ash	FC	Cash	Cwt
Sample 1968-east1								
10x0.6		81.9	0.6	20.7	30.4	58.3	30.4	81.9
0.6x0.15		13.3	0.5	20.7	26.7	52.1	29.9	95.2
< 0.15		4.8	0.5	20.5	33.4	45.6	30.1	100
10x0.6	1.4F	41.5	0.1	22.5	6.8	70.6	6.8	41.5
10x0.6	1.4x1.6	15.9	0.2	21.1	20.3	58.4	10.5	57.4
10x0.6	1.6x1.8	6.6	0.3	19.7	40.8	39.3	13.7	64.0
10x0.6	1.8S	36.0	0.4	12.7	77.1	9.9	36.5	100
0.6x0.15	1.4F	54.8	1.0	24.3	4.9	69.8	4.9	54.8
0.6x0.15	1.4x1.6	15.5	0.6	21.0	17.4	61.0	7.7	70.4
0.6x0.15	1.6x1.8	4.9	0.8	19.8	36.9	42.6	9.6	75.3
0.6x0.15	1.8S	24.7	0.7	13.2	75.2	10.9	25.8	100
Sample 1968-east2								
10x0.6		80.5	0.6	20.1	21.4	57.9	21.4	80.5
0.6x0.15		13.2	0.7	20.6	14.3	64.4	20.4	93.7
< 0.15		6.3	0.7	20.4	17.1	61.7	20.2	100
10x0.6	1.4F	55.6	0.2	21.6	6.5	71.7	6.5	55.6
10x0.6	1.4x1.6	26.3	0.2	20.4	18.2	61.2	10.3	81.9
10x0.6	1.6x1.8	5.4	0.3	20.2	37.3	42.3	11.9	87.3
10x0.6	1.8S	12.7	0.7	14.9	77.9	6.4	20.3	100
0.6x0.15	1.4F	61.1	1.1	23.1	5.0	70.8	5.0	61.1
0.6x0.15	1.4x1.6	27.3	1.2	19.7	15.4	63.7	8.2	88.4
0.6x0.15	1.6x1.8	4.2	0.8	19.7	34.3	45.3	9.4	92.5
0.6x0.15	1.8S	7.5	0.5	17.2	69.7	12.6	13.9	100
Sample 1980-69								
10x0.6		67.9	0.5	17.6	44.9	37.0	44.9	67.9
0.6x0.15		20.8	0.6	20.6	27.9	51.0	40.9	88.7
< 0.15		11.3	0.7	20.3	27.1	51.9	39.3	100
10x0.6	1.4F	26.5	0.2	25.8	7.0	67.1	7.0	26.5
10x0.6	1.4x1.6	11.2	0.3	21.6	21.9	56.2	11.4	37.7
10x0.6	1.6x1.8	18.1	0.3	18.9	41.0	39.8	21.0	55.8
10x0.6	1.8S	44.2	0.3	11.0	74.3	14.4	44.6	100
0.6x0.15	1.4F	44.8	1.3	26.3	6.2	66.2	6.2	44.8
0.6x0.15	1.4x1.6	22.7	1.0	22.0	18.0	59.0	10.1	67.5
0.6x0.15	1.6x1.8	10.0	1.3	19.3	38.1	41.4	13.8	77.5
0.6x0.15	1.8S	22.5	1.4	12.8	68.7	17.1	26.1	100

Cash=cumulative ash%   Cwt=cumulative weight %

TABLE 2
OXIDE DATA FOR INCREMENTAL WASHABILITY SAMPLES

millimetres		Ash	SiO_2	TiO_2	Al_2O_3	Fe_2O_3	MgO	CaO	Na_2O	K_2O	P_2O_5	Ba
1980-69												
10x0.6	1.8sink	74.3	68.8	1.3	23.2	1.04	0.5	0.3	0.1	1.9	0.1	0.1
10x0.6	1.8-1.6	41.0	64.8	1.7	28.5	0.83	0.3	0.2	0.2	0.6	0.1	0.1
10x0.6	1.6-1.4	21.9	65.5	1.7	28.7	0.57	0.3	0.1	0.2	0.9	0.1	0.1
10x0.6	1.4float	7.0	58.2	3.0	28.4	1.67	0.4	0.7	0.6	0.7	0.7	0.6
0.6x0.15	1.8sink	68.7	65.7	1.3	26.4	1.57	0.4	0.2	0.2	1.5	0.1	0.1
0.6x0.15	1.8-1.6	38.1	64.2	1.6	28.6	0.81	0.3	0.2	0.3	1.1	0.1	0.1
0.6x0.15	1.6-1.4	18.0	62.5	1.8	29.2	0.97	0.3	0.3	0.3	0.8	0.2	0.2
0.6x0.15	1.4float	6.2	57.9	3.8	28.8	1.48	0.4	0.7	0.6	0.9	0.8	0.6
1968-east2												
10x0.6	1.8 sink	77.9	54.8	1.8	38.6	0.57	0.4	1.3	0.1	0.3	0	0.1
10x0.6	1.8-1.6	37.3	55.1	3.0	26.5	2.27	2.4	5.6	0.2	0.2	0.1	0.1
10x0.6	1.6-1.4	18.2	56.1	2.2	27.3	3.33	1.7	3.7	0.2	0.2	0.2	0.2
10x0.6	1.4float	6.5	52.1	2.5	26.2	6.19	1.4	3.1	0.7	0.3	0.9	0.7
0.6x0.15	1.6-1.4	15.4	59.5	2.6	27.3	2.78	0.9	2.2	0.3	0.3	0.3	0.3
0.6x0.15	1.4float	5.0	54.7	4.3	26.9	3.35	0.9	2.3	0.6	0.4	0.9	0.7

TABLE 3
ANALYTICAL DATA FOR SCREENED FRESH AND ACID LEACHED SAMPLES, PROPERTY SAMPLES

			arm	adm	VM	VM daf	Ash	FC	FSI
GC1		fresh	4.9	0.7	23.8	31.7	25.0	50.5	4.0
		leached		0.3	23.4	30.2	22.7	53.6	2.0
sample	size mm		wt						
GC2	>0.6	fresh	46.5	0.6	20.6	31.7	34.9	43.9	2.5
GC3	0.6 x 0.0	fresh	53.5	0.7	25.4	30.7	17.2	56.8	5.0
GC2	>0.6	leached		0.3	20.1	31.3	35.8	43.8	1.5
GC3	0.6 x 0.0	leached		0.3	24.4	29.5	17.4	57.9	2.5
screened samples		fresh							
GC4	0.6 x 0.0	1.4F	64.8	1.2	27.9	29.5	5.3	65.6	5.5
GC5	0.6 x 0.0	1.4x1.6	14.1	1.4	25.8	29.7	13.2	59.6	1.0
GC6	0.6 x 0.0	1.6x1.8	7.7	1.4	24.0	34.5	30.7	44.0	0.5
GC7	0.6 x 0.0	1.8S	13.4	0.8	16.8	56.0	70.0	12.4	0.0
screened samples		leached							
GC4	0.6 x 0.0	1.4F		0.7	30.9	32.4	4.7	63.8	4.5
GC5	0.6 x 0.0	1.4x1.6		1.2	26.4	30.0	11.9	60.6	1.0
GC6	0.6 x 0.0	1.6x1.8		1.0	23.6	33.0	28.6	46.8	0.5
GC7	0.6 x 0.0	1.8S		0.6	13.7	47.0	70.8	14.9	0.0

arm = as-received moisture adm = air-dried moisture
F=float S=sink leached=leached in 2 molar HCl to remove carbonate

metre material washed using four SG increments (Table 3). Oxide analyses were performed on the various splits (Table 4) and X ray diffraction analysis was used to identify the major minerals present in the ash. The samples have moderately high CaO contents and X ray diffraction indicates that this is present mainly in calcite. To see if the calcite effected the rheological properties of the samples they were leached in 2 warm molar HCl and then re analyzed (Table 4).

Samples of froth floatation coal were collected to see if there was any obvious reason why it is sometimes difficult to produce a low-ash clean product from this material. Clean, feed and reject samples were analyzed for proximate values (Table 5) and subsequently studied using a Scanning Electron Microscope.

The reflectance of a number of samples was measured. The equipment at the Geological Survey Branch has not been routinely used for some time so a number of duplicate measurements were made. Reflectance standards were checked for internal consistency and then five samples previously analyzed at another lab were analyzed (Table 6). Reflectance analyses were performed on two different microscopes (Leitz ortho plan pol and Leitz MPV3). The measurement procedure involves measuring the maximum reflectance on three standards then on 10 tellinite or telocollinite grains of the sample. The procedure is repeated 5 times to provide 50 measurement of sample grains and 18 measurements of standards. Individual reflectance measurements are corrected for time drift and scaling using the 6 sets of three standard measurements. The 1 sigma SD of the mean for all samples is less than 0.01.

The petrographic composition of some samples was estimated using a counting stage to count 300 grains. The continuous variation from telinite or telocollinite and

TABLE 4
OXIDE ANALYSIS FOR PROPERTY DATA, FRESH AND LEACHED SAMPLES

			Ash db	SiO_2	TiO_2	Al_2O_3	Fe_2O_3	MgO	CaO	Na_2O	K_2O	P_2O_5	Ba
raw samples													
GC2	>0.6mm	fresh	35.2	66.9	0.86	19.6	3.18	1.52	4.24	0.01	2.30	0.19	0.15
		leached	35.9	71.5	0.90	21.4	1.89	0.59	0.21	0.03	2.40	0.18	0.17
GC3	<0.6mm	fresh	17.3	58.5	1.16	24.6	2.36	0.90	7.04	0.01	1.66	0.39	0.29
		leached	17.4	66.5	1.26	26.8	1.63	0.51	0.32	0.15	1.89	0.38	0.33
washed <0.6mm samples													
GC4	1.4F	fresh	5.4	52.2	2.45	30.5	2.95	0.92	5.96	0.18	1.16	1.17	0.83
		leached	4.7	55.9	2.63	34.0	2.05	0.34	0.71	0.18	1.28	1.14	0.87
GC5	1.4-1.6	fresh	13.3	54.6	1.40	30.6	2.63	1.00	5.74	0.08	1.16	0.88	0.55
		leached	12.0	59.1	1.53	33.3	1.53	0.41	0.38	0.20	1.27	0.89	0.63
GC6	1.6-1.8	fresh	31.1	57.7	1.05	27.5	2.23	0.92	6.86	0.01	1.46	0.36	0.24
		leached	28.9	63.4	1.14	30.7	1.31	0.44	0.21	0.07	1.60	0.39	0.29
GC7	1.8S	fresh	70.6	62.5	0.74	21.6	2.21	0.85	7.83	0.01	1.96	0.10	0.10
		leached	71.2	69.3	0.82	24.4	1.79	0.53	0.32	0.07	2.14	0.09	0.12

Data are corrected for loss on ignition, unleached samples have about 5-8% loss and leached samples have 1.5-2.5% loss.
oxides that increase in % indicate no loss. They increase because there is a loss of other oxides
oxides that decrease in % have been removed by leaching

TABLE 5
ANALYTICAL DATA FOR FROTH FLOTTION (FF) SAMPLES

sample	yield	adm	VM	Ash	FC
ff feed	100	0.57	22.11	17.15	59.65
ff clean	75.5	0.89	22.59	12.9	63.62
ff reject	24.5	0.52	20.91	30.25	48.32

Y=yield calculated from
100*17.15=(100-Y)*30.25+Y*12.9 Y=75.5%
carbon recovery=CR calculated from
CR=(1-12.9/100*1.2)/(1-17.15/100*1.2)*75.5 = 80%
weight mineral matter/ash=1.2 assumed

TABLE 6
REFLECTANCE MEASUREMENTS, MINE AND PROPERTY AND INTERNAL AND EXTERNAL DUPLICATES

Sample	Rmmax	bif	mic
1968-east1 1.4float	1.14	0.05	k
1968-east1 1.4float dup	1.14	0.07	g
1968-east1 1.4-1.6	1.14	0.11	k
1968-east1 1.4-1.6 dup	1.14	0.08	g
1968-east2 1.4 float	1.17	0.07	g
1968-east2 1.4-1.6	1.19	0.18	k
1968-east2 1.4-1.6 dup	1.18	0.09	g
1980-69 1.4 float	1.07	0.07	g
198- 69 1.4-1.6	1.12	0.10	g
1980-69 1.6-1.8	1.19	0.08	g
ff clean	1.01	0.07	g
GC 1.4 float	1.08	0.07	g

lab	GSB	Other
sample 1	1.6	1.65
2	1.59	1.58
3	1.09	1.09
4	1.04	1.00
5	1.04	1.03

dup=duplicate ff=froth floatation bif=bireflectance
mic=microscope
g=Leitz orthoplan pd k=Leitz MPV3

from semifusinite to macrinite makes it difficult to produce consistent results in terms of maceral composition. The process, despite the best efforts of the various classification schemes is very subjective. Attempts were made to differentiate between inert plus semi inert macerals and reactive macerals and to differentiate between macerals retaining some original structure (semi fusinite and tellinite) and those retaining no original structure (macrinite and collinite).

DISCUSSION

Coals may be difficult to clean for a number of reasons, but first it is important not to confuse washing difficulty with problems caused by size consist. Coals difficult to clean in wash plants have large amounts of near gravity material in a particular size range. This material can easily be miss placed with higher ash content grains ending up in the clean coal stream and lower ash content grains ending up in the reject stream. The result is a decrease in yield, an increase in wash ash content and an increase of carbon in the reject stream. Also when evaluating laboratory wash data it should be appreciated that the average ash content of particles in the specific gravity (SG) split can vary by about 10% for a 0.1 change in SG and therefore in an SG bracket from 1.4 to 1.5, the ash content of particles can range from about 18% to 28%.

Difficult to wash coals contain a large number of particles with SG values in the range of 1.4 to 1.5 and the ash content of these particles is maximized. There have been a number of papers suggesting ways of measuring washing difficulty prior to cleaning coals in a wash plant (Sanders and Brookes, 1986, and Ryan, 1992). They generally emphasize the importance of measuring the amount and ash content of near gravity material and attempt to reduce washing difficulty to a single number. This is a bit simplistic but it does provide a useful empirical scale for comparing coals.

The method introduced by Ryan (1992) uses ash analyses on head and wash samples and is therefore a simple and rapid way of estimating relative washing difficulty of samples. Data for the three in-pit samples are in Figure 1, which contains iso washing difficulty lines. The Figure clearly separates the 3 samples (1980-69, 1968-east1 and 1968-east2) based on their washing difficulty in agreement with the way they washed in the wash plant. It also indicates that finer material is more difficult to wash than coarse material. Sample 1980-69 is more difficult to wash in both size ranges than the other two samples and it contains more minus 0.6 millimetre material than the other two samples. Plant recovery will be lower when washing 1980-69 type coal because of the finer size consist and increased washing difficulty. There is a rough correlation of raw ash with washing difficulty. The difference in washing difficulty does not appear to be caused by oxidation as the three samples 1968-east1, 1968-east2 and 1980-69 all have percent transmittance values of 99%.

The oxide data for samples 1968-east2 and 1980-69 (Figure 2) can be used to illustrate possible mineral dif-

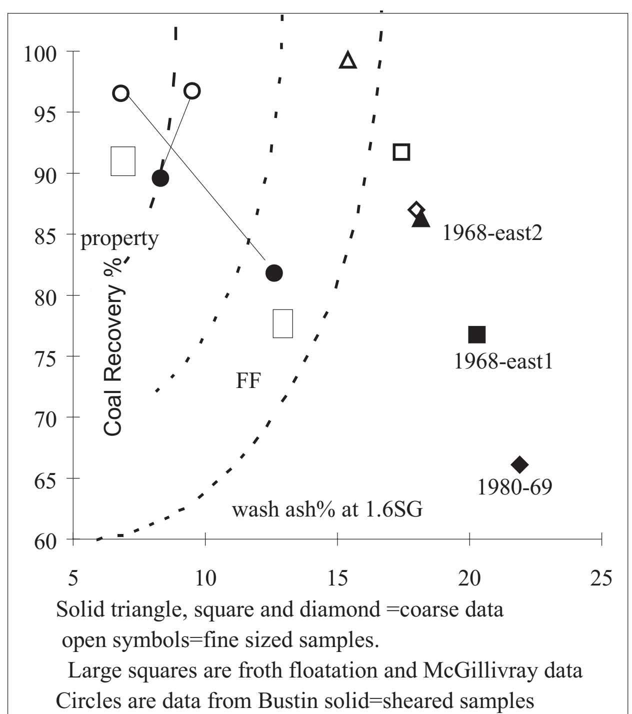

Figure 1. Washing difficulty for samples. X axis is wash ash at 1.6 SG. Y axis is calculated carbon recovery.

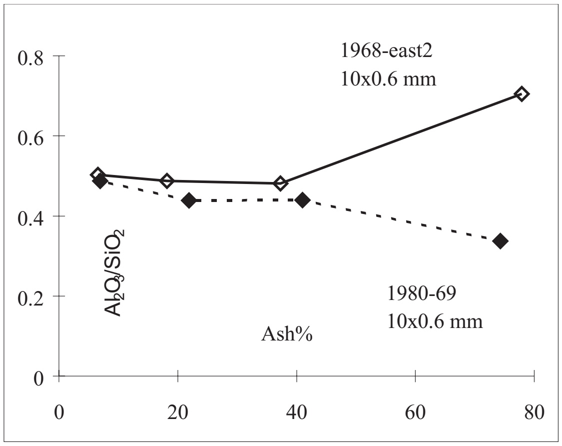

Figure 2. Al_2O_3/SiO_2 ratio versus ash % for samples 1968-east2 and 1980-69.

ferences between the two samples. The Al2O3/SiO2 ratios probably indicate the proportion of clays to free quartz in the sample. The ratio tends to increase at lower ash concentrations because of a tendency for vitrinite to contain more dispersed kaolinite than inertinite. Often washing difficulty is related to clay content. In this case the difficult to wash sample 1968-69 appears to show more of a tendency for the ratio to increase as ash decreases than the easier to wash sample 1980-east2 (Figure 2) but there is not a marked difference. Varying clay contents probably do not fully explain the difference in washing difficulty.

Calcium oxide concentrations in the property samples are quite high and are substantially reduced by acid leaching (Table 4). This indicates the presence of a carbonate, which was confirmed using XRD (Table 7). It is possible to estimate the amount of carbonate in total or in the ash component of samples by assuming, either that all the Ca, Fe and Mg is in carbonate (maximum estimate) or that only the Ca is in carbonate (minimum estimate). This is done by calculating the elemental content of Ca, Mg and Fe and then recalculating the molar content of these elements as X,CO3 either in the total sample or in the ash (Table 8, 9 and 10). Obviously this assumes that all the Ca is in carbonate when in fact some is combined with phosphorus in apatite and also that all the Fe is in carbonates where as a small proportion is combined with sulphur in pyrite. The carbonate and calcite concentrations for the three samples (property sample, 1968-east2 and 1980-69)

TABLE 7
X-RAY DIFFRACTION RESULTS FOR 2 PROPERTY SAMPLES

sample		Ash	Minerals detected
GC-2	>0.6 mm	37.7	abundant quartz, moderate kaolinite minor mixed clays moderate calcite and dolomite
GC-7	<0.6mm 1.8S	75.6	abundant quartz, moderate kaolinite significant calcite some gypsum

TABLE 8
CUMULATIVE OXIDE AND CARBONATE CALCULATIONS FOR THE PROPERTY

	plus0.6mm	minus0.6mm	float1.4	1.4x1.6	1.6x1.8	1.8sink
ash	35.15	17.26	5.33	9.62	17.54	33.43
SiO_2	66.90	58.50	52.20	52.63	53.08	54.34
Al_2O_3	19.60	24.60	30.50	30.52	30.25	29.09
Fe_2O_3	3.18	2.36	2.95	2.89	2.83	2.75
TiO_2	0.86	1.16	2.45	2.26	2.15	1.97
P_2O_5	0.19	0.39	1.17	1.12	1.05	0.92
CaO	4.24	7.04	5.96	5.92	6.00	6.25
MgO	1.52	0.90	0.92	0.93	0.93	0.92
MnO	0.01	0.01	0.01	0.01	0.01	0.01
Na_2O	0.01	0.01	0.18	0.16	0.15	0.13
K_2O	2.30	1.66	1.16	1.16	1.19	1.29
BaO	0.15	0.29	0.83	0.78	0.73	0.65
LOI	5.03	5.28	8.06	7.01	5.86	5.80
B/A	0.17	0.21	0.23	0.23	0.22	0.22
alkalinity	0.06	0.04	0.01	0.02	0.04	0.07
wt% CB TS	5.23	3.03	0.89	1.59	2.89	5.52
wt% C TS	2.66	2.17	0.57	1.02	1.88	3.73
CO2 addition	2.37	1.35	0.39	0.70	1.28	2.48
mm/ash	1.07	1.08	1.07	1.07	1.07	1.07
wt% C in ash	7.57	12.56	10.64	10.57	10.72	11.15
wt% CB in ash	15.36	17.87	16.84	16.72	16.78	17.07

LOI = loss on ignition B/A = base acid ratio
Alkalinity = B/A ratio x ash%
CB = total carbonates C = calcite TS = total sample

are estimated using the oxide data calculated for cumulative rather than incremental wash samples. The first two samples (property sample and 1968-east2), which wash easily have high carbonate contents where as 1980-69, which does not wash easily has a low content.

Carbonate in the property and 1968-east2 samples appears to be concentrated in the ash (Figure 3). Contents calculated on a total sample basis increase as ash increases and contents calculated on an ash base are relatively constant at about 15% carbonate in the ash. Under the microscope there does not appear to be much calcite associated with the coal and most found occurs as discrete grains (Photo 1). In general it is difficult to locate the amount of carbonate indicated in the oxide analysis and it must be finely dispersed in the ash. In sample 1980-69 carbonate contents are low and when calculated on an ash base tend to increase as ash decreases indicating in part a coal association for the carbonate material (Figure 3). Carbonate in this sample occurs as small blebs in desmocollinite (Photo 2).

TABLE 9
CALCULATED CUMULATIVE OXIDE DATA AND CARBONATE CONTENTS FOR 1968-EAST 2

	10x0.6 mm 1.8 sink	10x.6 1.8-1.6	10x0.6mm 1.6-1.4	10x0.6mm 1.4float	0.6x0.15mm 1.6-1.4	0.6x0.15mm 1.4 float
ash	20.3	11.9	10.3	6.5	8.2	5.0
SiO_2	53.7	53.5	53.4	52.1	56.2	54.7
Al_2O_3	28.1	26.5	26.5	26.2	27.0	26.9
Fe_2O_3	4.51	5.09	5.27	6.19	3.17	3.35
TiO_2	2.38	2.47	2.44	2.53	3.80	4.32
P_2O_5	0.59	0.67	0.71	0.93	0.68	0.87
CaO	3.16	3.43	3.29	3.10	2.30	2.34
MgO	1.40	1.55	1.49	1.41	0.89	0.88
MnO	0.01	0.01	0.01	0.01	0.01	0.01
Na_2O	0.44	0.49	0.51	0.67	0.54	0.64
K_2O	0.23	0.23	0.23	0.25	0.34	0.37
BaO	0.45	0.50	0.53	0.68	0.57	0.72
LOI	5.03	5.28	8.06	7.01	5.86	5.80
B/A	0.19	0.17	0.21	0.24	0.14	0.15
alkalinity	0.039	0.021	0.022	0.015	0.011	0.008
wt% CB TS	3.02	1.98	1.69	1.13	0.86	0.54
wt% calcite TS	1.14	0.73	0.60	0.36	0.34	0.21
CO_2 addition	1.32	0.86	0.73	0.48	0.37	0.23
mm/ash	1.06	1.07	1.07	1.07	1.05	1.05
ash	20.3	11.9	10.3	6.5	8.2	5.0
wt% C in ash	5.60	6.09	5.85	5.52	4.09	4.17
wt% CB in ash	15.13	16.74	16.64	17.46	10.57	10.88

TABLE 10
CALCULATED CUMULATIVE OXIDE DATA AND CARBONATE CONTENTS FOR 1980-69

	10x0.6mm 1.8sink	10x0.6mm 1.8-1.6	10x0.6mm 1.6-1.4	10x0.6mm 1.4 float	0.6x0.15mm 1.8 sink	0.6x0.15mm 1.8-1.6	0.6x0.15mm 1.6-1.4	0.6x0.1mm 1.4 float
ash	44.6	21.0	11.4	7.0	26.1	13.8	10.1	6.2
SiO_2	64.9	61.8	60.3	58.2	61.3	60.1	59.5	57.9
Al_2O_3	26.1	28.5	25.3	28.4	28.3	28.9	28.9	28.8
Fe_2O_3	1.12	1.18	0.92	1.67	1.32	1.24	1.31	1.48
TiO_2	1.83	2.29	1.42	2.96	2.53	2.89	3.08	3.75
P_2O_5	0.26	0.38	0.09	0.72	0.41	0.50	0.57	0.76
CaO	0.36	0.42	0.23	0.70	0.45	0.53	0.58	0.73
MgO	0.42	0.34	0.41	0.43	0.36	0.36	0.37	0.41
MnO	0.01	0.01	0.01	0.01	0.01	0.01	0.01	0.01
Na_2O	0.27	0.41	0.14	0.64	0.43	0.50	0.53	0.63
K_2O	1.24	0.73	1.42	0.74	1.06	0.93	0.90	0.93
BaO	0.22	0.34	0.08	0.60	0.33	0.40	0.45	0.58
LOI	5.03	5.28	8.060	7.010	5.860	5.80	5.03	5.03
B/A	0.06	0.04	0.053	0.082	0.065	0.07	0.07	0.08
alkalinity	0.02	0.01	0.006	0.006	0.017	0.01	0.01	0.01
wt% CB TS	1.38	0.66	0.296	0.318	0.901	0.48	0.37	0.44
wt% C TS	0.28	0.16	0.047	0.087	0.211	0.13	0.10	0.13
CO_2 addition	0.60	0.28	0.130	0.135	0.385	0.20	0.16	0.19
mm/ash	1.01	1.01	1.011	1.019	1.015	1.01	1.02	1.03
ash	44.6	21.0	11.4	7.0	26.1	13.8	10.1	6.2
wt% C in ash	0.64	0.74	0.416	1.249	0.809	0.94	1.03	2.14
wt% CB in ash	3.13	3.16	2.608	4.571	3.471	3.49	3.70	7.07

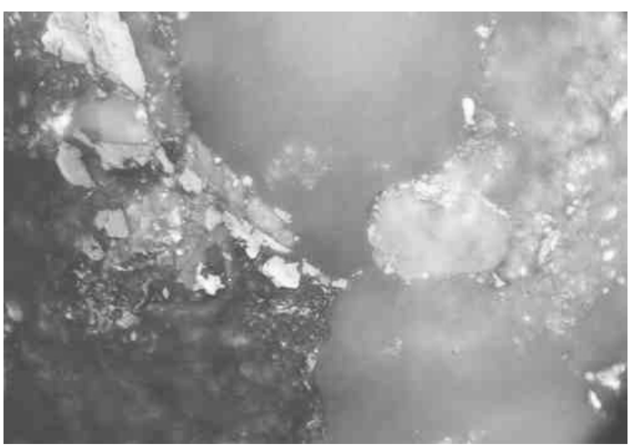

Photo 1. Calcite in property sample; field of view is about 0.25 millimetres.

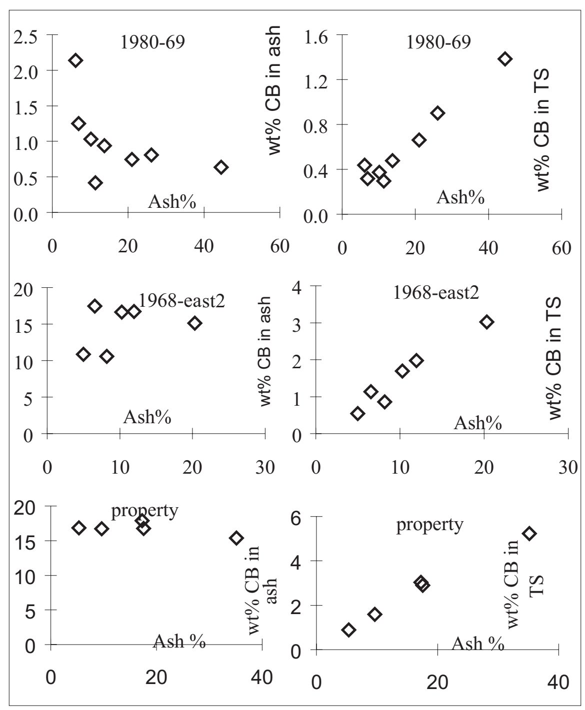

Figure 3. Carbonate (CB) versus ash % for mine samples 1980-east2, 1968-69 and property sample. Data presented on an ash basis and on a total sample (TS) basis.

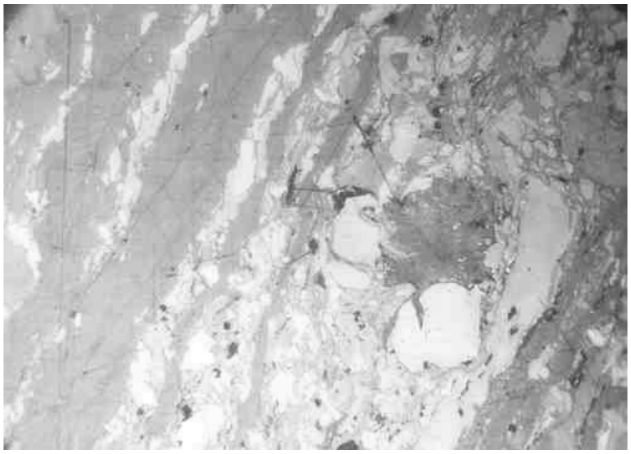

Photo 2. Calcite in 1980-69 occurring as small blebs in desmiocollinite; field of view 0.25 mm.

TABLE 11
LEACHING RESULTS (WARM 2 M HCl), PROPERTY SAMPLES

	fresh Fe_2O_3	leach Fe_2O_3	loss %	fresh MgO	leach MgO	loss %	fresh CaO	leach CaO	loss %
>0.6mm	3.18	1.89	40.5	1.52	0.59	61.1	4.24	0.21	95.0
<0.6mm	2.36	1.63	31.1	0.90	0.51	43.3	7.04	0.32	95.5
1.4 Float	2.95	2.05	30.4	0.92	0.34	63.4	5.96	0.71	88.1
1.4-1.6	2.63	1.53	42.1	1.00	0.41	59.3	5.74	0.38	93.4
1.6-1.8	2.23	1.31	41.3	0.92	0.44	52.7	6.86	0.21	96.9
1.8 Sink	2.21	1.79	19.0	0.85	0.53	37.8	7.83	0.32	96.0
Average %			34.1			52.9			94.2

If the carbonate material is associated with the ash, then this will tend to increase the SG of ash and make it easier to remove. When the carbonate material is associated with the coal, for example occurring as blebs in desmocollinite or on cleats, it will tend to be washed out attached to coal fragments in intermediate SG increments. This will cause loss of coal and deteriorate washing characteristics. Part of the reason for the increased washing difficulty of sample 180-69 may be small amounts of carbonate (calcite) associated with the coal.

The mode of occurrence of carbonate minerals in samples has important implications for coke quality as influenced by base/acid ratio and alkalinity (base/acid ratio times ash content). When carbonate is in the ash base/acid ratios remain constant but alkalinity decreases as ash is removed from the sample. This means that properties such as CSR (coke strength after reaction) improve markedly as a coal is cleaned. On the other hand if the carbonate is associated with the coal part of the sample either as cleat filling or impregnating one of the macerals then as ash is removed carbonate content increases and both base/acid ratio and alkalinity increase. This causes CSR either to deteriorate or not improve as much as expected based on reducing the ash concentration. For the three samples discussed here, alkalinity decreases markedly at low ash for the property and 1968-east2 samples but is only moderately effected by decreasing the ash content in sample 1980-69 (Figure 4).

The presence of carbonate minerals in the property sample was also confirmed by leaching samples in warm 2 molar HCl. The oxide analyses before and after the leaching (Tables 4 and 11) indicate removal of 95% of CaO, 55% of MgO and 35% of Fe2O3 . The carbonate contains some iron and magnesium though leaching does not remove all the Fe and Mg indicating the presence of non carbonate hosts for these elements. About 5% of the Ca remains in the samples probably associated with apatite.

The property coal has unexpected variations in quality that do not appear to be related to oxidation. The FSI values for the fresh and leached samples were measured to see if high carbonate content effects FSI (Table 3). In most cases, leaching out the carbonate reduced the FSI (Figure 5). The leaching was performed using dilute warm HCl and it is assumed that this alone did not deteriorate FSI. If this is the case, then possibly the CO2 emitted when the FSI sample is heated to a temperature of 820(C and the carbonate breaks down, helps maintain the FSI

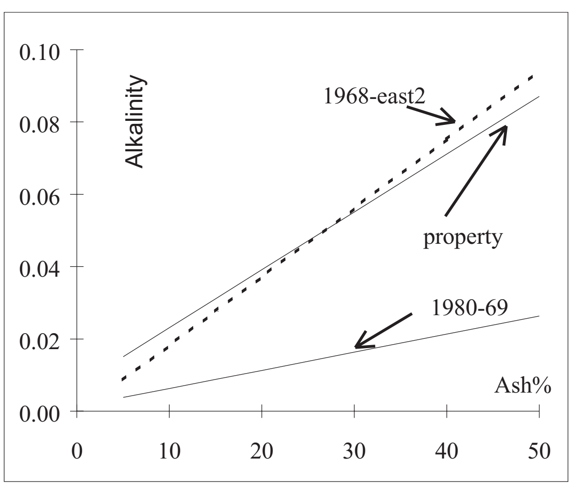

Figure 4. Alkalinity versus ash % for mine samples 1968-east2, 1980-69. and property sample.

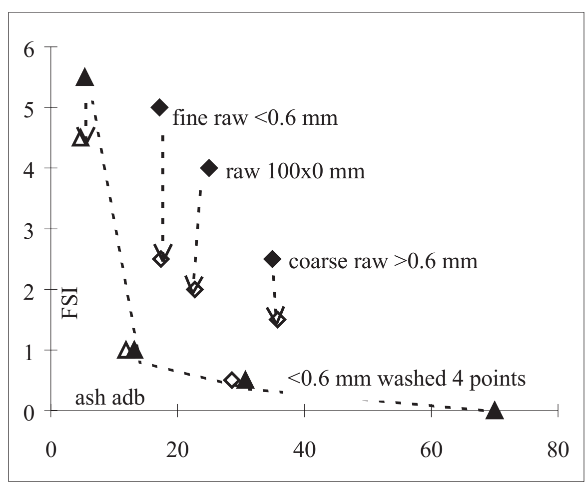

Figure 5. FSI versus ash % adb for property samples before and after leaching in warm dilute HCl.

button. Certainly in most cases the volatile matter content decreased after leaching and removal of the carbonate. If the FSI values are artificially high, then this could lead to an initial deceptively good estimation of coking quality.

Despite the intense shearing, the prpoerty sample appears to wash very well (Figure 1) and the main problem with the bulk sample is one of size consist. A very high proportion of the coal is minus 0.6 millimetres. The apparent low FSI of two of the wash samples may be caused by clay coating fine coal particles. An effect apparently seen in the SEM work and discussed later.

Bustin (1982) investigated the effect of shearing on coal washability. In part he concluded that the main effect was to increase the raw ash content of a seam by mixing hanging and foot wall material into the seam and generally making the ash more difficult to remove. Data for the sheared and non sheared samples of the two seams studied by Bustin are plotted in Figure 1. In one case shearing has increased washing difficulty and in the other it appears to have had little effect. Shearing has had the effect of increasing the ash content of the material in each SG increment. This may be because shearing has decreased coal density by introducing micro fractures and therefore allowed more ash to be attached to each coal particle within an SG increment. Alternatively shearing may have skewed the distribution of particles in each SG increment towards the high SG end. In general the main effects of shearing are to incorporate extra ash into the seam and decrease the over all size consist.

SCANNING ELECTRON MICROSCOPE STUDIES AND PETROGRAPHY OF SAMPLES

Feed, clean and reject froth floatation samples were studied using a petrographic microscope and a scanning electron microscope(SEM). Generally the froth floatation feed (0.15 x 0.0 mm material) can be washed to less than 10% ash in froth floatation circuits. Some mine froth floatation feed washes to a significantly higher ash, in this case about 13% (Table 5). Based on the feed, wash and reject ash contents the yield from the circuit is estimated to be about 75.5% with about an 80% carbon recovery. The circuit is not loosing a significant amount of coal but the coal floating is still associated with a moderate amount of ash.

Generally there is very little well preserved semifusinite seen in the samples when studied using a reflecting microscope. The semifusinite that does occur has very flattened cell structure nearly always mineralized with kaolinite. A lot of the mineral matter occurs as fine grains of quartz or kaolinite coating coal grains. The total reactives content (vitrinite macerals only) (Table 12) on a mineral matter free basis is slightly higher for the difficult to wash sample 1980-69. This is mainly because of an increase in detrovitrinite in the high ash vitrain lithotype. The total reactives contents for these samples range from 52% to 77%. The property samples have higher reactive maceral contents than the mine samples.

**TABLE 12
ESTIMATED PETROGRAPHY OF SOME SAMPLES.
MINERAL MATTER FREE BASIS**

sample	liptinite	telinite	telo collinite	desmo collinite	detro virinite	semi fusinite	fusinite	macrinite	micrinite	inerto detrinite	total reactives	total inerts
ff feed	3	9	24	24	4	10	0	17	0	9	64	36
ff clean	3	7	23	31	7	6	1	16	0	6	70	30
ff reject	3	8	17	35	5	12	1	10	0	9	68	32
1968-east1 1.4-F	6	7	16	21	2	18	0	23	0	7	52	48
1968-east 1 1.4-1.6	8	7	10	24	4	21	0	18	0	8	53	47
1968-east 2 1.4-F	2	15	13	33	0	15	0	16	0	6	63	37
1968-east 2 1.4-1.6	6	11	7	31	2	12	0	24	0	6	58	42
1980-69 10x.6 1.4-F	4	7	21	26	0	19	0	16	0	6	59	41
1980-69 1.4-1.6	7	7	13	25	25	10	0	6	0	7	77	23
GC grab	4	0	28	39	5	8	0	11	0	5	76	24
GC 1.4-F	4	11	29	30	1	9	0	10	1	4	76	24

The fine grain size and continuous variation between vitrinite and semifusinite makes it difficult to get reproducible petrographic data for the samples. There is considerable subjective judgment in separating semifusinite from telinite and macrinite from semifusinite. Some small vitrinite grains were observed in the petrographic microscope and SEM to have high reflecting or high atomic density rims characteristic of high temperature oxidation (Photo 3). It is unlikely that the rims were formed by the pellet making process because the rims were also found in a pellet was made at lower temperature. The grains were seen in feed and wash samples so the effect is not related to froth floatation. Most of the grains were small and contained complete high reflecting rims indicating that either only small grains were effected or the effect post dates tectonic shearing or crushing at the

Photo 3. High reflecting rim to vitrinite grain; field of view 0.25 mm.

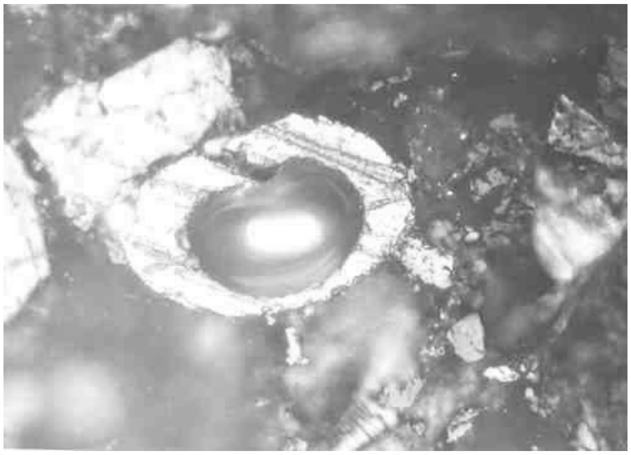

Photo 4. Apparent vesicle in altered vitrinite grain; field of view 0.25 mm.

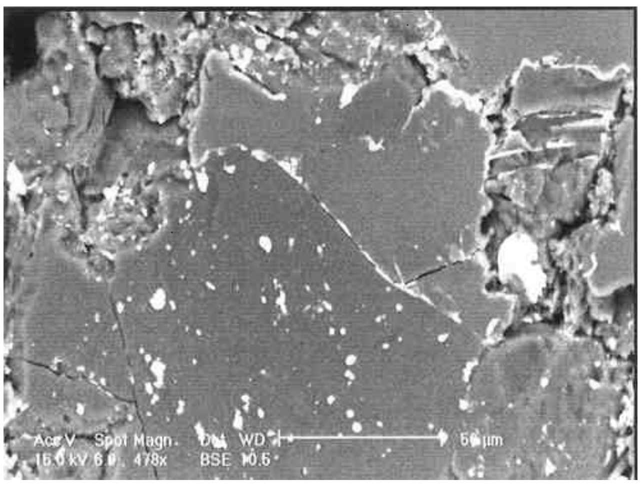

Photo 5. Fine kaolinite coating to coal grains; scanning electron microscope image.

plant. Some of the grains appeared to be partially coked and to contain vesicles (Photo 4). The origin of these grains is not clear; they may have been altered by fires associated with underground mining that occurred prior to 1950. If the coal contained a lot of these grains it would increase the inert content of the coal and probably decrease its coking ability.

In the SEM it appears that many coal grains are coated by very fine kaolinite flakes (Photo 5). Brecciation of semifusinite, which contains kaolinite cell filling, appears to release fine kaolinite, that coats coal fragments making them hard to separate in froth floatation and increasing their ash contents. This also makes it difficult to pelletize the samples because kaolinite also coats the transoptic grains and they do not fuse very well. Semifusinite is more brittle than the reactive macerals and more likely to respond to shearing by brecciation rather than flow. There is no indication that the coal has a high ash content. It appears that shearing has dispersed the kaolinite. This means that whereas before shearing a few large fragments rich in kaolinite would be removed from the clean coal, after shearing kaolinite is finely dispersed partially coating coal grains that may remain with the clean coal. If kaolinite completely coats coal grains, then the effect would be to decrease yield and have marginal effect on clean coal ash. If kaolinite partially coats coal grains, then they may still be recovered with clean coal and the effect is to increase clean coal ash and have marginal effect on yield. The dispersal of the kaolinite associated with tectonic shearing obviously predates the coal entering the wash plant. The coating of the grains with kaolinite may occur before or during crushing, screening and washing the coal.

Generally the mineral matter in semifusinite is predominately kaolinite. When a seam rich in inertinite is deformed there is an increased release of fine kaolinite which is subsequently very difficult to wash out because it partially coats coal particles and ends up in with the clean coal. The average raw ash content of the seam does not change. The liberation of kaolinite, from mineralized semifusinite, that would otherwise be removed in the washing process appears to increase the amount of difficult to remove ash and to increase the wash ash content of the froth product by about 3%.

WASHING DIFFICULTY AND PETROGRAPHY

Washing difficulty increases the more the coal macerals are intermixed with mineral matter. There are a number of ways mineral matter can be included in macerals, but they all relate to processes that occurred in the coal swamp or during diagenesis. The formation of semifusinite and fusinite by fire leaves the cells intact and empty. They are often later filled by mineral matter during diagenesis. In fact, if the cells in semifusinite are not filled, then they will probably be collapsed later when the coal seam is deformed. Fusinite is probably stronger and more likely to survive with or without mineralized cells. The presence of semifusinite or fusinite therefore implies a certain amount of inherent ash, usually kaolinite. Massive vitrinite (telinite or telocollinite) generally does not contain much mineral matter, though sometimes cells in telinite are mineralized with kaolinite. Desmocollinite indicates a moderate amount of "soft sediment deformation" in the coal seam and as it forms, fragments of inert macerals and mineral matter may be included in a vitrinite ground mass. This is apparent in sample 1980-69, which has a lot of heavily mineralized desmocollinite, that also contains a lot of detrovitrinite. Fine mudstone bands may also be incorporated into the macerals. The amount of clay material entering the swamp and the amount of soft sediment deformation during diagenesis influences the amount of near gravity material formed (Ryan, 1996).

Early deformation in coal seams is apparent from the rounding and compaction around macrinite grains embedded in vitrinite (Photo 6). The cell structure in some semifusinite grains is deformed and appears to have experienced simple shear (Photo 7). Higher reflecting

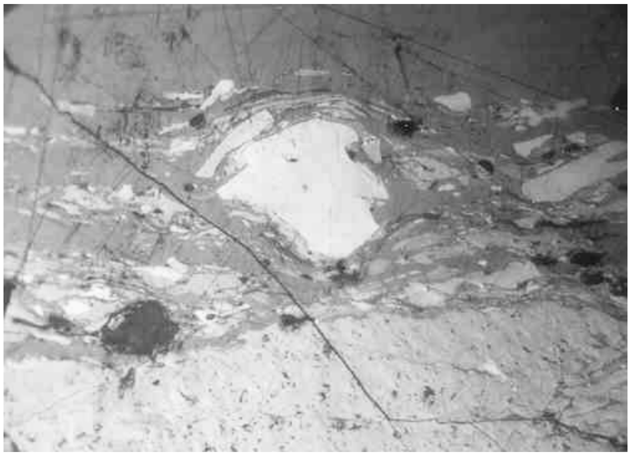

Photo 6. Rounding and compaction around a macrinite grain; field of view 0.25 mm.

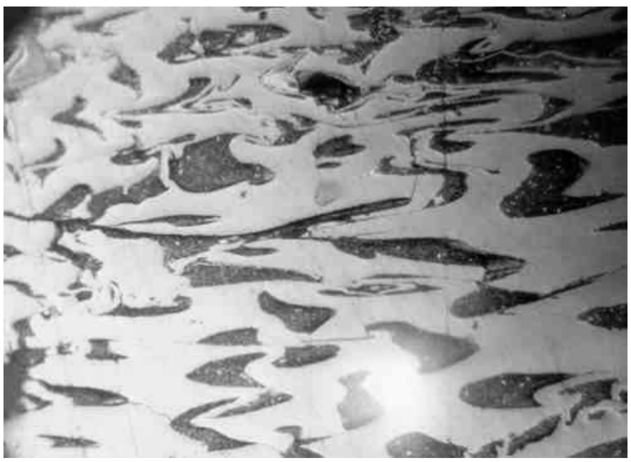

Photo 7. Deformation of semifusinite; field of view 0.25 mm.

semifusinite generally deforms brittlely breaking into shards that may be dispersed as inertodetrinite in desmocollinite.

Tectonic shearing produces brittle deformation and therefore reduces the size consist but does not produce middlings material. However it does appear to be selective in how it breaks fragments in the coal seam producing more very fine telinite particles and possibly releasing kaolinite from semifusinite. Shearing and dispersing fine clay bands through the coal seam can increase the washing difficulty and wash ash content with out increasing the amount of ash in the seam.

VITRINITE REFLECTANCE

The Rmmax values of the washed splits of the three mine pit samples and the froth floatation samples were measured (Table 6). The reflectance increases with washing ease for the three pit samples but there is no obvious reason why rank should effect washing difficulty. The rank and bireflectance also tend to increase as the SG of the wash increment increases. At higher SG values the vitrinite appears more likely to contain finely dispersed micrinite, which increases its SG and reflectance. This effect is probably restricted to coals of intermediate rank, in which micrinite is just starting to form.

CONCLUSIONS

Many washing problems are caused by excessive amount of fines. Though mining methods can reduce fines generation a highly sheared coal will generate fines how ever it is handled. It is probably possible to estimate fines potential by looking at coal faces in the pit or to design a simple in pit attrition test. The as-received water content of samples may also be an indication of the friability of the coal. In that the more fractured the coal the more surface area available for wetting.

Coals are difficult to wash in any size consist when there is an excessive amount of near gravity material. This can originate from processes in the coal swamp and during diagenesis of the coal or from shearing. Turbulence and introduction of clay into the coal swamp can result in a lot of mineralized desmocollinite as in sample 1980-69. A combination of fires to produce semifusinite and fusinite in the coal swamp and diagenetic in filling of cells with kaolinite can increase the mineral matter content of the inert macerals, which tend to concentrate in the intermediate SG increments.

Shearing can increase washing difficulty. It appears to do it by generating fine kaolinite probably in part by breaking mineralized semifusinite grains and releasing the kaolinite contained in the cells. This material then coats vitrinite grains making them difficult to float and increasing their ash content. Shearing can also increase the raw ash content of a seam by incorporating hangingwall or footwall rock into the seam.

The association and amount of carbonate in coals can effect washing difficulty. If the carbonate is associated with ash it will probably help with ash removal. If it is associated with the coal it will cause loss of coal in intermediate SG increments and in crease the ash and Ca content of the clean coal.

It is possible using ash chemistry data to estimate the amount and location of carbonate minerals in the coal. In the easy to wash samples from the property and 1968-east2, the carbonate mineral is calcite or dolomite and is associated with the ash making up about 16% of the ash. In that the carbonate correlates with the ash and not the total sample it is probably not related to fracturing associated with faulting. Its amount may relate to environmental conditions in the coal swamp, which also influence the amount of inherent ash.

The difficult to wash sample (1980-69) contains less carbonate material, which is partially associated with the coal and makes up about 3% of the sample. It might be that for these coals there is a correlation between the amount of carbonate and ease of washing in which case a simple acid test for the presence of carbonate in the coal may indicate whether the coal will be easy or difficult to wash.

ACKNOWLEDGEMENTS

The X-Ray diffraction analyses were performed by Jim McLeod of Cominco labs in Vancouver and the leaching was performed by Arno Hoogveld (Loring Laboratories Calgary).

REFERENCES

Bustin, R.M. (1982): The Effect of Shearing on the Quality of some Coals in the Southeastern Canadian Cordillera; Canadian Institute of Mining and Metallurgy bulletin, Volume 75, pages 76-83.

Ryan, B.D. (1992): Estimation of Coal Washability Using Small Samples; Journal of Coal Quality, Volume 11, pages 13-19.

Ryan, B.D. (1996): Controls on Coal Washing Difficulty, (82G/15 93L/11); in Geological Fieldwork 1995, B.C. Ministry of Energy, Mines and Petroleum Resources, Paper 1996-1, pages

Sanders, G.J. and Brookes, G.F. (1986): Preparation of the Gondwana Coals; 1. Washability Characteristics; Coal Preparation, volume 3, pages 105-120.